P

Peptide Library

Masahiko Sisido
Department of Bioscience and Biotechnology,
The Graduate School of Natural Science and
Technology, Research Core for Interdisciplinary
Sciences, Okayama University, Okayama,
Kita-ku, Japan

Synonyms

Peptide; Peptide drugs; Polymer beads; Polymer supports; Polypeptide; Screening; Solid-phase synthesis

Definition

Peptide library is an assembly of a large number of peptides with different amino acid sequences of 10 to 10^9 or more.

Background

Peptide libraries are usually exploited to discover a single or a group of peptides that bind specifically to a target protein and other biological molecules or to target cells in a dish as well as those inside the living body. The selected peptides are potential candidates as the probing molecules with fluorescent or radioactive labels or as the carrier molecules that deliver drugs to the target cells in vivo.

Building Up of Peptide Library

Peptide library can be built up simply by mixing different peptides of equal or sometimes different amounts. Although the simple mixing method appears too tedious to be practical, it is advantageous in keeping high quality of library, provided that the component peptides have been isolated and purified before mixing. With the use of automatic synthesizers designed for that purpose, up to 384 different peptides may be synthesized on one stage. Then, the peptides are mixed altogether after purification.

Peptide library can be prepared in one pot by using a mixture of Fmoc-amino acids at each elongation step of the peptide synthesis [1]. Care has to be taken, in this case, however, the percentage of each amino acid unit incorporated into library may be different from the percentage of each component in the Fmoc-amino acid mixture, because of different reactivities of Fmoc-amino acids. Roughly speaking, peptide libraries of short peptides of less than 10 amino acids may be synthesized in one-pot synthesis with good enough quality, but those of longer than 15 amino acids have to be built up by mixing isolated and purified peptides.

The component amino acids are selected from naturally occurring 19 amino acids excluding Cys because it leads to intramolecular as well as intermolecular disulfide linkages. Instead, several nonnatural amino acids, like hydrophilic/hydrophobic, fluorescent, biotinated, and even radioactive amino acids, are incorporated depending on the final purpose of the library.

If a mixture of 14 different Fmoc-amino acids was used at each elongation step, the diversity of the final peptide library of eight residue peptides, for instance, will be $14^8 = 1.5 \times 10^9$. This demonstrates how easily a library of large enough diversity can be built up by the mixed Fmoc-amino acid technique.

No matter how the peptide library was built up, the most serious problem remains in the solubility of the component peptides, especially if the library was intended to be in contact with living cells in vitro and in vivo. Peptide components that contain high percentage of Val, Leu, Ile, Met, and Phe tend to precipitate or form aggregates in aqueous media. Even if a specific peptide component itself is water soluble, it may often form insoluble aggregates when it was mixed with other peptide component(s). So, if no precaution has been taken, hydrophobic peptides often precipitate or form aggregates on cell surfaces. Under this condition, peptides screened are biased to highly hydrophobic ones that had been nonspecifically bound onto cell surfaces. To avoid the solubility problem and the nonspecific binding problem, several attempts have been made: incorporation of very hydrophilic components, like oligoethyleneglycol units, as the fixed ingredient works to ease the insoluble problem. Also, biased amino acid populations to decrease percentages of hydrophobic amino acids introduced may be effective.

Easy biodegradation is the second major problem of peptide libraries, when they were screened under cultivated cells on dishes or in the animal body. Some peptides are known to have their lifetimes of less than 10 min under such conditions. Incorporation of D-amino acids or other nonnatural components is the current strategy to avoid this problem.

One-Bead-One-Peptide Library

Usually, peptides are synthesized on small plastic beads of diameters less than 0.1 mm (sold-phase peptide synthesis). Peptide library can be built up on the beads with a single type of peptide on a single bead, i.e., "one-bead-one-peptide (OBOP)" strategy [2]. The library is prepared following the steps as illustrated in Fig. 1a.

First, a whole bunch of the beads on which peptides will be elongated are split into several groups (five groups in the case of Fig. 1a). Then, different amino acids are attached onto different bead groups in separate reaction tubes. After the elongation reaction, the five bead groups are mixed together thoroughly and then split again into five groups. By repeating the (splitting → separate elongation → remixing) cycle, until the peptides attain desired length, an assembly of beads was obtained on which a single type of peptide is linked on a single bead and another type on another bead.

The peptides on beads are utilized for the screening without isolating the peptides from the beads. Typical screening process is as follows (Fig. 1b): First, a solution of target protein labeled with a fluorescent tag was prepared. The library on beads was immersed into the protein solution for a while and then washed to remove temporarily attached proteins. The beads that bind to the labeled protein were detected on a fluorescent microscope. The amino acid sequence of the peptide on the single bead can be identified by using a highly sensitive peptide sequencer.

Although the library building up and the screening along OBOP strategy appear very simple and easy, its limitation is obvious. Since the screening is carried out with the peptides linked to beads, the peptides selected are not always effective when they are liberated from the beads, because of possible changes of peptide conformations and other factors.

Characterization of Peptide Library

Quality of peptide library is a crucial factor for the successful screening. The quality of library
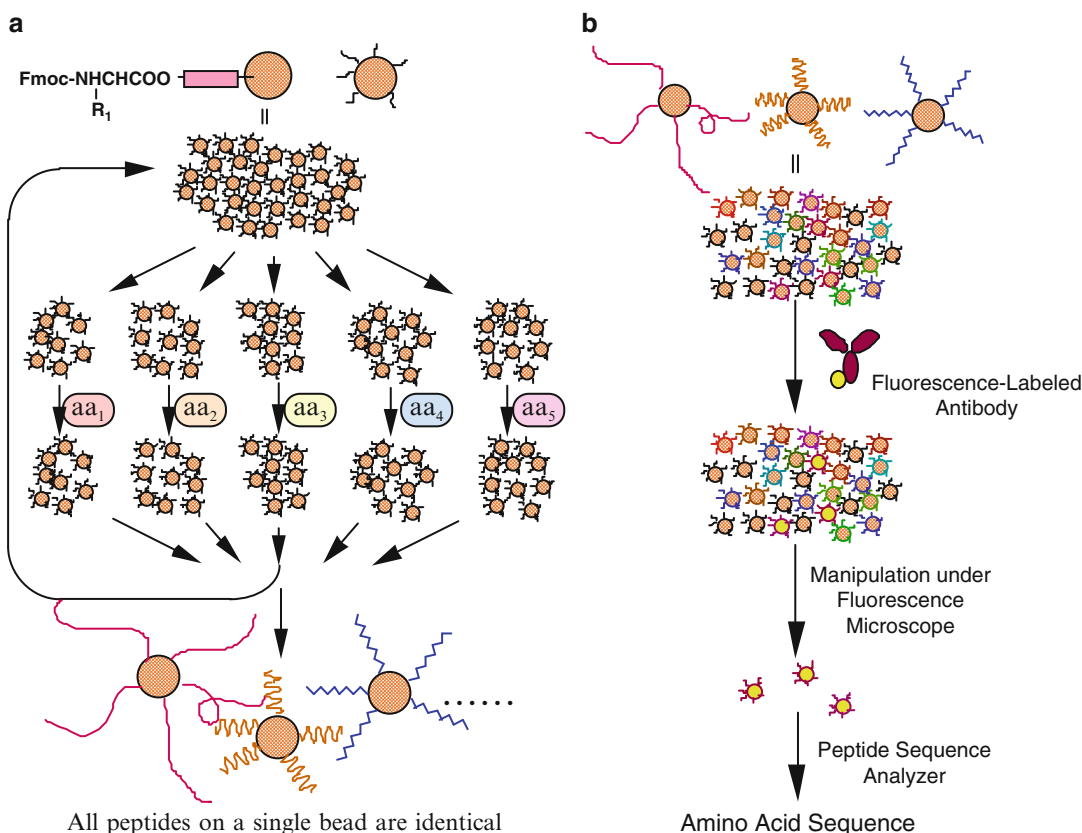
Peptide Library, Fig. 1 (**a**) Buildup of peptide library for "one-bead-one-peptide" strategy. (**b**) Screening of the beads using fluorescently labeled target protein

stands for several factors: First, the expected peptide components should be contained in the library in expected quantities; second, no debris components should be contained; and third, no aggregation of component peptides should be formed. If the library was built up by mixing isolated and purified peptides, the first and the second concern can be avoided.

It had been very difficult to examine those factors after building up the library. Recently, advanced liquid-chromatogram mass spectroscopy (LCMs) instruments become available for the library characterization. As an example, an LCMS chart of a library, H-Lys-Ser-NH$(CH_2CH_2O)_6$-CH_2CH_2CO-xaa-his-xaa-xaa- Sar$_3$-NH$_2$ is shown in Fig. 2.

The peptide library has been built up through one-pot synthesis using mixtures of 14 Fmoc-D-amino acids (xaa's). Since the peptide consists of three xaa units, the total number of peptides will be $14^3 = 2,744$. In the LCMS chart, 1,032 different peaks were identified; each peak showing reasonable matching to one of the molecular weights of peptides expected in the library. At this point, however, all the identified peaks cannot be assigned to peptides, because there are a large number of debris peaks that are not shown on the chart and there remains a possibility that some of debris peaks accidentally show matched molecular weights.

Krokhin et al. proposed a linear relationship between the retention times and the types of amino acids included in the peptides [3]. According to the relation, the retention time, Rt, of a peptide is expressed as the sum of the retention coefficients, Rcs, that are assigned to specific types of amino acids included in the peptide, plus base retention time Rt_0. In the case of the above
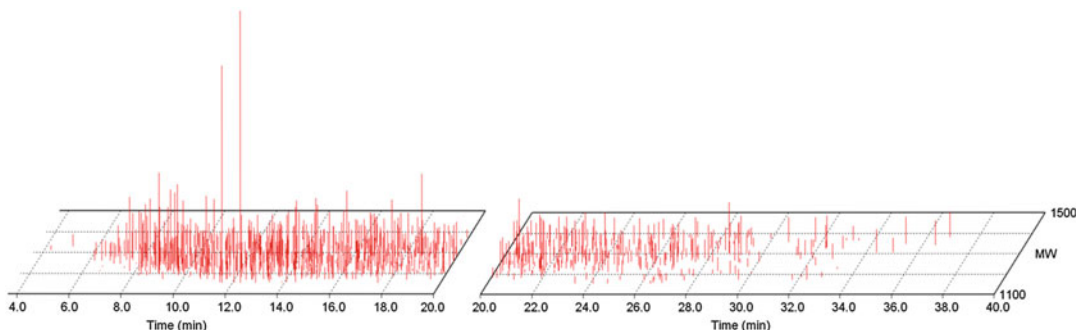
Peptide Library, Fig. 2 LCMS chart of a peptide library, H-Lys-Ser-NH(CH$_2$CH$_2$O)$_6$- CH$_2$CH$_2$CO-xaa-his-xaa-xaa-Sar$_3$-NH$_2$ (xaa = ala, val, leu, met, ser, thr, arg, asp, asn, his, phe, tyr, trp, pro; the small three-letter codes indicate D-amino acids). The sticks on the chart indicate peaks whose molecular weights show reasonable matching to those of the expected peptides

peptides that consist of three mixed amino acid units, (fixed part)-aa$_1$-aa$_2$-aa$_3$-(fixed part), the linear relationship is

$$Rt(aa_1, \ aa_2, \ aa_3) = Rc(aa_1) + Rc(aa_2) \\ + Rc(aa_3) + Rt_0. \quad (1)$$

The parameters, Rcs for all amino acids involved and Rt_0 depend on the LC column and other elution conditions; therefore, they must be determined by a least-squares fitting that optimizes 14 Rc values and Rt_0 to give the best linear relationship. The results for the 1,032 peaks of H-Lys-Ser-NH(CH$_2$CH$_2$O)$_6$-CH$_2$CH$_2$CO-xaa-his-xaa- xaa-Sar$_3$-NH$_2$ peptides in Fig. 2 are shown in Fig. 3a. The retention times of a major portion of the matched peaks are resting close to the diagonal line, indicating that the retention times calculated using the least-squares Rc values are in agreement with observed values. However, a significant number of the peaks are deviated from the linear relationship. The deviated peaks may be assigned to peptides of extraordinary conformations, to peptides temporarily associated with other peptides, or to other debris peaks from unsuccessful synthesis or from the environment. In any case, peaks close to the diagonal line can no doubt be assigned to peptides that are expected in the library.
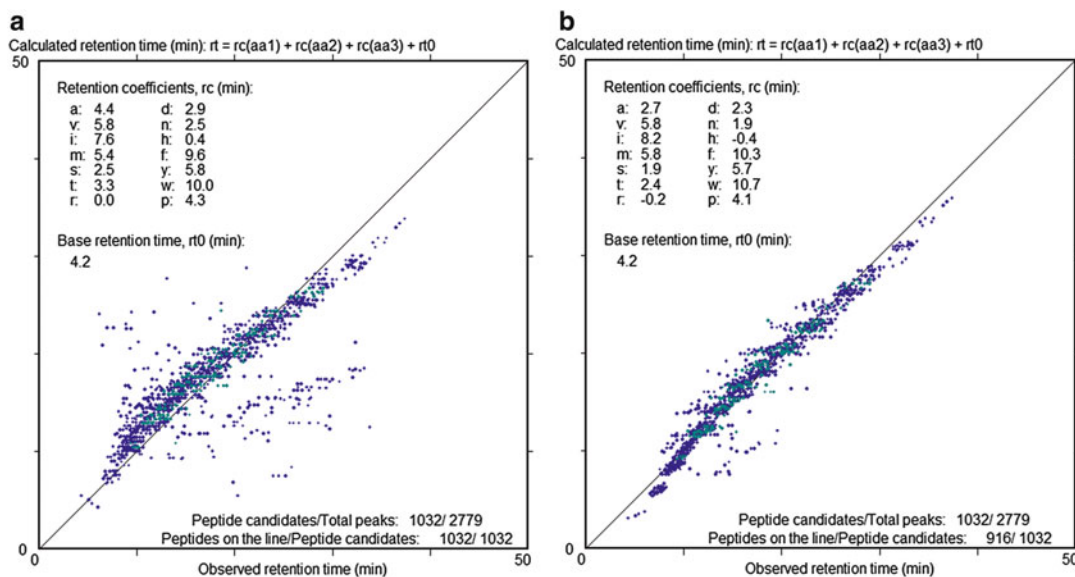
If the peaks deviated from the diagonal line were excluded from the least-squares calculation to optimize Rcs and Rt_0, a more clear relationship is observed between observed and calculated retention times (Fig. 3b).

One of the advantages of the above analysis is that amino acid pairs of equivalent molecular weights, like (Ala + Tyr)/(Ser + Phe), (Val + Glu)/(Leu + Asp), etc., may become distinguished in this way.

Although LCMS technique is very powerful for the identification of peptide components in a library, it has some limitations. First, it will not tell anything about the order of amino acids in a peptide. Second, as described above, there are amino acids and amino acid pairs that cannot be distinguished only by their molecular weights. Leu/Ile are isomers to each other and Gln/Lys have very close molecular weights that are difficult to distinguish. Seventeen amino acid pairs like (Gly + Leu)/(Ala + Val) have the same molecular weights. To compromise this complexity, exclusion of several amino acids from the amino acid ingredients is recommended. For example, if Gly, Leu, Cys, Lys, Glu, and Gln were excluded from the amino acid components, only three pairs are remained to have equivalent molecular weights: (Ala + Tyr)/(Ser + Phe), (Val + Thr)/(Ile + Ser), and (Asn + Trp)/(His + Tyr).

The third limitation is that the sensitivity of mass detector sharply depends on the types of amino acids included in a peptide. Peak intensities in the LCMS chart in Fig. 2, for example, do not necessarily reflect the amounts of the

a

Calculated retention time (min): rt = rc(aa1) + rc(aa2) + rc(aa3) + rt0

b

Calculated retention time (min): rt = rc(aa1) + rc(aa2) + rc(aa3) + rt0

Peptide Library, Fig. 3 (**a**) Correlation between observed retention times and those calculated from Eq. 1, using retention coefficients that give the best fit between the retention times. All peaks that show reasonable matching to the molecular weights of expected pept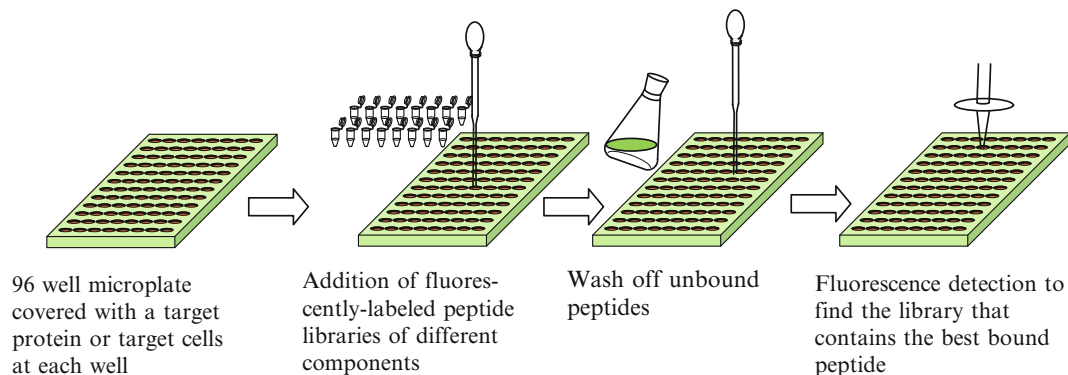ides are plotted. (**b**) Correlation between observed retention times and those calculated from Eq. 1, using retention coefficients that give the best fit between the retention times. Peaks that deviate from the relationship are excluded from the least-squares optimization of Rcs and Rt_0

corresponding peptide components included in the library. Moreover, some types of peptides cannot be even detected. Unfortunately, there seems no reliable theory that predicts the sensitivity of LCMS for a given amino acid sequence. However, roughly speaking, hydrophilic peptides are more sensitively detected than hydrophobic ones. Increase of the population of hydrophilic amino acids during library synthesis may improve this difficulty, but it will introduce a serious bias in the screening result, because hydrophilic amino acids are often ionic ones. Instead, the author recommends the reader to introduce oligosarcosine (Sar) as the fixed C-terminal unit of peptides. Sarcosine (Sar = N-methylglycine) is nonionic and its oligomer unit adds excellent solubility to the peptide. Moreover, oligosarcosine units do not take specific conformation, like α-helix or β-sheet, because the N-methylamide linkage takes both cis and trans configurations almost equally. In short, oligosarcosine unit at the C-terminal will not seriously alter the peptide property.

In Vitro Screening of Peptides Using Peptide Library

Peptide libraries are exploited for efficient discovery of a peptide or a group of peptides that specifically bind to target proteins or target cells. The discovery process usually consists of several screening steps, at each step contracting the diversity of peptide library. The techniques used for peptide screening are divided into several classes, depending on the form of peptide library. If the library is provided as one-bead-one-peptide form, the screening will be made with peptides linked onto beads as illustrated in Fig. 1b. Because peptides are hanging on plastic beads, the screening of OBOP library cannot be done in vivo. Peptides selected by the OBOP strategy must be reexamined or rescreened after liberating peptides from the beads.

If the library is provided as fluorescently labeled free peptides, screening will be made on microplates with a fluorescence detector (microplate reader). Peptide libraries of different

| 96 well microplate covered with a target protein or target cells at each well | Addition of fluorescently-labeled peptide libraries of different components | Wash off unbound peptides | Fluorescence detection to find the library that contains the best bound peptide |

Peptide Library, Fig. 4 Screening of fluorescently labeled library on a microplate covered with a target protein or with target cells

peptide components are screened by the amounts of bound peptides as detected by their fluorescence (Fig. 4).

The screening on microplate can be automated and is practical enough to find candidate peptides. One of the advantages of this method is that peptides are served in solution and, contrary to the case of OBOP strategy, peptides bind onto target proteins or cells in their intact form. This advantage has to be somewhat reserved, however, if the peptides are applied to final uses after removing the fluorescence labels.

If the library is provided as non-labeled free peptides, LCMS is the only technique available for detecting and identifying peptides. The screening procedure currently employed in the author's laboratory is illustrated in Fig. 5. Following this procedure, peptides that are lightly attached onto surfaces of target cells are discarded and only those penetrated into cytosol are selected.
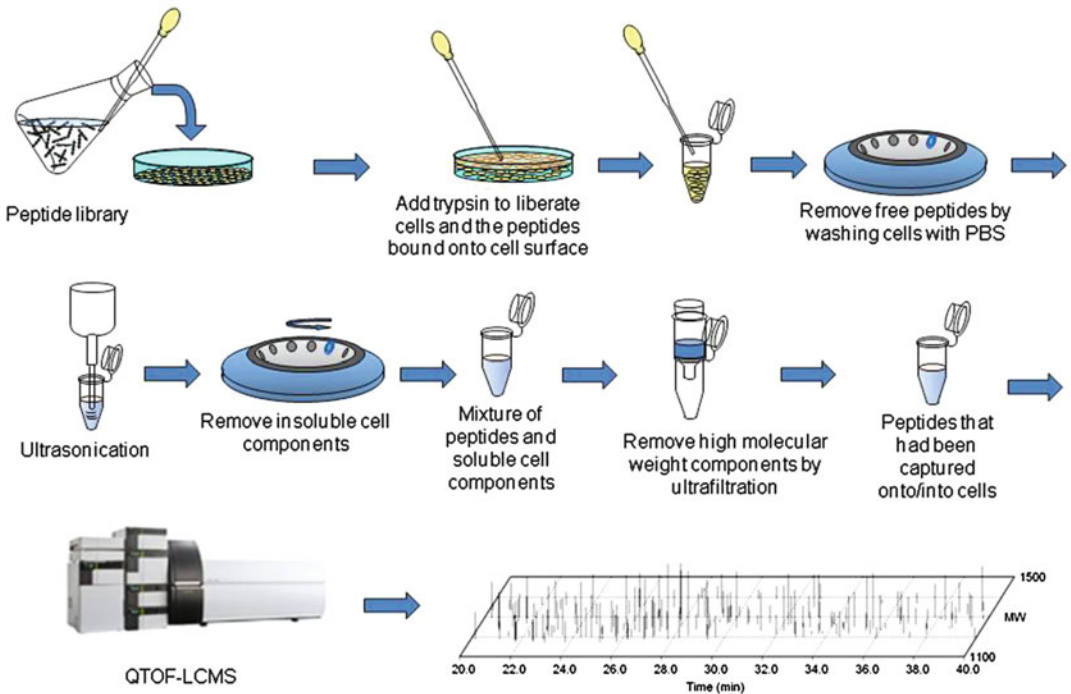
In Vivo Screening of Peptide Library

If one is looking for peptides that bind to target cancer cells inside the human body, in vivo screening of free peptides in cancer-cell-implanted mice is currently the shortest approach. But the shift of the screening process from in vitro to in vivo requires several factors that have to be taken into consideration. First, peptides must not be linked to insoluble supports

and must be well soluble by themselves in aqueous media; otherwise, they will stick onto veins or other organs and will not be delivered to target cells. In some cases, however, serum albumin in blood will take up hardly soluble peptides and possibly transport them around the whole body. The latter possibility may depend on a very subtle balance between the solubility of a peptide and the uptake ability of albumin, making prediction of in vivo results difficult.

Second, as described above, biodegradability is a crucial factor in determining in vivo activity of peptides. Introduction of D-amino acids and/or non-amide backbone is a current strategy to avoid this problem. Third, in vivo experiments are often difficult to reproduce, because of the difficulties in controlling animal conditions, in controlling target (cancer) cell conditions, and in controlling conditions for peptide injection. Those complexities, however, may be averaged off or, at least, compromised by doing in vivo experiments under competitive circumstance. For example, in the author's in vivo screening process, as illustrated in Fig. 6, peptides are screened in competition between different peptides and in competition between different cancer cells.

First, seven different peptide libraries were labeled with seven different fluorescence probes. The libraries were mixed together and injected into a mouse that was implanted with two different cancer cells (e.g., A431 and MCF7). The peptides compete with each other toward the cancer cells in the mouse body. The amount of

Peptide Library, Fig. 5 Screening of non-labeled peptide library on target cancer cells by using LCMS as a detector

P
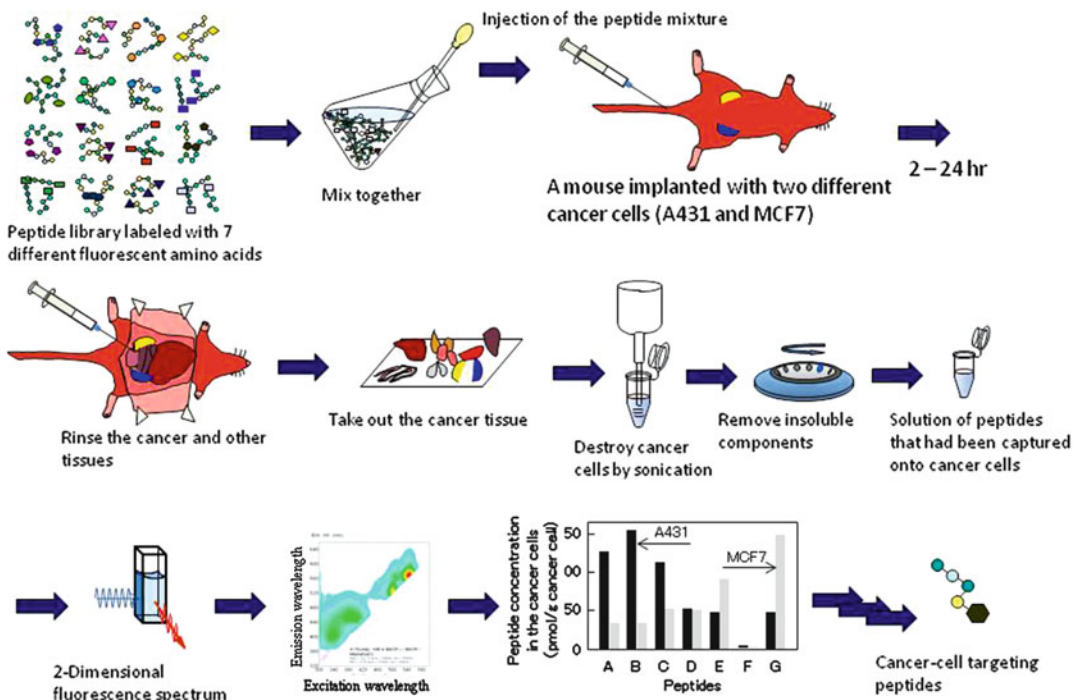
Peptide Library, Fig. 6 Double competitive in vivo screening of peptide libraries labeled with different fluorophores against different target cancer cells, by using two-dimensional fluorescence spectroscopy

each peptide library taken into the cancer cells was evaluated after the mouse was sacrificed and the cancer cells were taken up. The amounts of peptides were evaluated by using two-dimensional fluorescence spectroscopy that enables to quantify concentrations of the seven fluorophores independently by single measurement. The competition between peptides makes the in vivo results much more reliable than the results obtained by injecting a single type of peptide to multiple numbers of implanted mice, because the relative binding or incorporation efficiencies of seven peptide libraries are insensitive to mice conditions, although absolute values vary significantly from mouse to mouse.

As illustrated in Fig. 6, two different cancer cells were implanted into a mouse body, introducing competition between different cancer cells to attract peptides. The dual implant allows to evaluate peptide affinities toward different cancer cells. In the author's experience, the double competitive in vitro screening gives currently the best reliable results, with some reservation that removal of fluorescence labels after screening may change the binding properties of selected peptides.

Future Prospective

Peptide library technique has long been known and applied by many workers. Yet, only a few successful peptides have been found. The most serious problem is their biodegradability. Introduction of nonnatural amino acids and/or D-amino acids may suppress the degradability as described above. Another serious problem is the lack of reliable technique applicable to in vivo screening. In this section, the author described what we believe as the best technique currently available in vivo by using advanced tools, like library synthesizers, LCMS machines, and 2D fluorescence spectrometers. Although the methods described here are not yet very common yet, the author wishes this section will attract attention of young workers who reconsider peptide library as the best shortcut to target drug carriers or target probe molecules.

Related Entries

▶ Polymeric Drugs
▶ Proteins as Polymers and Polyelectrolytes
▶ Vaccine

References

1. Chan W, White P (1999) Fmoc solid phase peptide synthesis: a practical approach, Oxford University Press
2. Lam KS, Salmon SE, Hersh EM, Hruby VJ, Kazmierski WM, Knapp RJ (1991) A new type of synthetic peptide library for identifying ligand-binding activity. Nature 354:82–84
3. Krokhin OV, Craig R, Spicer V, Ens W, Standing KG, Beavis RC, Wilkins JA (2004) An improved model for prediction of retention times of tryptic peptides in ion pair reversed-phase HPLC: its application to protein peptide mapping by off-line HPLC-MALDI MS. Mol Cell Proteomics 3:908–919

Pervaporation Membranes

Tadashi Uragami
Functional Separation Membrane Research
Center, Suita, Osaka, Japan

Synonyms

Liquid permeation

Definition

Pervaporation (PV) membranes are generally composite structures which are consisted of a dense layer (active or permselective layer) and a porous layer (support layer). Those membranes are effective for separation of organic liquid mixtures with high osmotic pressure, can be applied to the separation and concentration of azeotropic mixtures, close-boiling-point mixtures, and structural isomers, and can be used for the removal of certain components in equilibrium reactions.

Pervaporation Membranes, Fig. 1 Principle of pervaporation ((T. Uragami) pervaporation membranes)
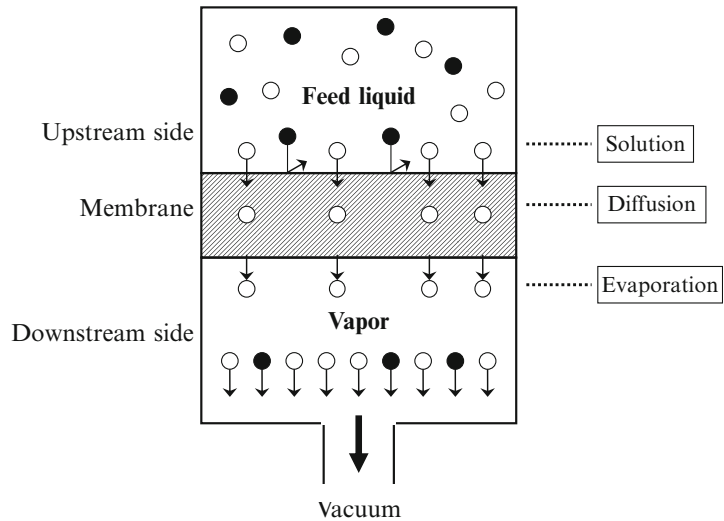
Pervaporation Principle

Pervaporation (PV) was coined as a term for the combination of the *permeation* of the permeate through the membrane and its *evaporation* into the vapor phase based on the two basic steps of the process.

The principle of PV is shown in Fig. 1. In this separation process, when a liquid mixture is fed to the upstream side of a membrane and the downstream side is evacuated, a component in the feed mixture can preferentially permeate through the membrane. In a PV process, differences in the solubility of permeants in the membrane, the diffusivity of permeants in the membrane, and the relative volatility of permeants can influence the permeability and selectivity [1–4]. In general, PV exhibits the following characteristics [5–7]:

1. Selective transport across a non-porous membrane is achieved by a three-step process consisting of solution, diffusion, and evaporation.
2. Because the driving force for permeation is the vapor pressure for each component rather than total system pressure, this process is effective for separation of organic liquid mixtures with high osmotic pressure.
3. PV can be applied to the separation and concentration of mixtures that are difficult to separate by distillation. For example, it is useful for the separation of azeotropic mixtures, close-boiling-point mixtures, and structural isomers.

4. PV can be used for the removal of certain components in equilibrium reactions.
5. Polymer membrane compaction, a frequent problem in high-pressure gas separations, is not encountered in PV because the feed pressure is typically low.

This PV process can be applied to the dehydration of organic liquids, concentration of alcohols, removal of volatile organic compounds (VOCs) in aqueous solutions, separation of organic/organic mixtures, facilitation of chemical reactions such as esterification, and analysis of liquid materials.

Fundamental Permeation Equation

The permeation rate, Q_i, of component i is expressed by Fick's first law as follows [6, 7]:

$$Q_i = -D(C_i)dC_i/dx, \tag{1}$$

where $D(C_i)$ is the diffusion coefficient, C_i is the concentration of component i in the membrane, and x is the distance from the membrane/feed-solution interface.

Fick's second law of diffusion is:

$$dC_i/dt = D(C_i)d/dx(dC_i/dx)$$
$$= D(C_i)(d^2C_i/dx^2) \tag{2}$$

where $D(C_i)$ is given by the following equation:

$$D(C_i) = D_0\exp(\gamma C_i) \qquad (3)$$

Here, D_0 is the infinite dilution diffusion coefficient, and γ is a measure of membrane plasticization that is dependent on temperature.

At steady-state permeation, the boundary conditions are dC_i/dt, $C_i = C_1$ at $x = 0$, $C_i = C_2$ at $x = l$. When Eq. 3 is inserted in Eq. 2 and is integrated, Eq. 4 is obtained.

$$Q_i = (D_0/\gamma l)\,(\exp\gamma C_1 - \exp\gamma C_2) \qquad (4)$$

The concentration distribution is expressed as follows:

$$C_i = (1/\gamma)\ln\{\exp C_1 - x/l(\exp\gamma C_1 - \exp\gamma C_2)\} \qquad (5)$$

If the concentration at the boundary of the feed solution and the membrane is equilibrated thermodynamically, the following equations hold:

$$C_1 = C^*(p^0) \qquad (6)$$

$$C_2 = C^*(p_2) \qquad (7)$$

where C^* is a pressure dependent function, p^0 is saturated vapor pressure, and p_2 is the vapor pressure on the down-stream side of the membrane.

Using these expressions, Eqs. 4 and 5 may be rewritten with p^0 and p_2. At the same time, the permeability, P_i, is derived as follows:

$$P_i = Q_i l/\Delta p = (D_0/\gamma\Delta p)\,(\exp\gamma C_1 - \exp\,\gamma C_2) \qquad (8)$$

where $\Delta p = p^0 - p_2$. When Eqs. 6 and 7 obey Henry's law, $C^*(p) = SP$, and Eqs. 4, 5, and 8 are easily expressed as a function of p^0 and p_2.

$$Q_i = (D_0/\gamma l)\,(\exp\gamma Sp^0 - \exp\gamma Sp_2) \qquad (9)$$

$$C_i = (1/\gamma)\ln\{\exp\gamma Sp^0 - x/l(\exp\gamma Sp^0 - \exp\gamma Sp_2)\} \qquad (10)$$

$$P_i = (D_0/\gamma\Delta p)\,(\exp\gamma Sp^0 - \exp\gamma Sp_2) \qquad (11)$$

Solution-Diffusion Model

When a similar treatment is applied to gas or vapor permeation, the following equations are obtained [1, 8]:

$$Q_i l = \int_{C_1}^{C_2} D(C_i)dC_i \qquad (12)$$

$$Q_i = P_i(p_1 - p_2)/l, \qquad (13)$$

where p_1 and p_2 are the vapor pressures on the high concentration side and low concentration sides of the membrane, respectively.

Combining Eqs. 12 and 13 yields the following:

$$P_i = \left\{\int_{C_1}^{C_2} D(C_i)dC_i\right\}(p_1 - p_2) \qquad (14)$$

Rearrangement gives:

$$Q_i l = R = P_i(p_1 - p_2) = \int_{C_1}^{C_2} D(C_i)dC_i, \qquad (15)$$

where R is the normalized permeation rate. When the concentration-averaged diffusion coefficient, D_i, is defined as in Eq. 16, P_i and R are expressed as in Eqs. 17 and 18, respectively.

$$\overline{D_i} = \int_{C_1}^{C_2} D(Ci)dCi/(C_1 - C_2) \qquad (16)$$

$$P_i = \overline{D_i}\{(C_1 - C_2)/(p_1 - p_2)\} \qquad (17)$$

$$R = \overline{D_i}(C_1 - C_2) \qquad (18)$$

If the diffusion coefficient is not dependent on permeant concentration then D_i equals D. In PV, the downstream pressure is much lower than the upstream pressure ($p_1 \gg p_2$). Hence, Eqs. 16, 17, and 18 can be represented as follows:

$$\overline{D_i} = \int_{C_1}^{C_2} D(Ci)dCi/C_1 \qquad (19)$$

$$P_i = \overline{D_i}(C_1/p_1) \qquad (20)$$

$$R = \overline{D_i} \, C_1, \qquad (21)$$

where $C_1/p_1 = S_1$, which is the pseudo solubility coefficient. Under these conditions P_i may be expressed by:

$$P_i = \overline{D_i} \, S_1. \qquad (22)$$

Separation Factor

The separation factor is represented by the ratio, θ, of the overall permeation rate for the mixed solution, Q^p, and the sum of the permeation rate of each component in the mixture, Q^c.

$$\theta = Q^p/Q^c \qquad (23)$$

The permeation ratio in the A and B binary system, Q_i is defined as follows:

$$Q_A = q_A^p/q_A^c, \quad Q_B = q_B^p/q_B^c, \qquad (24)$$

q^p_i and q^c_i, correspond to the component Q^p and Q^c, respectively.

In an ideal system in which there is not an interaction between the components in the mixed solution, θ is 0. In general, when $\theta > 1$, the permeation rate is larger than that in an ideal system, when $\theta < 1$, it is less than that in an ideal system.

Quantitative Treatment of Separation Factor

When the permeation rates for A and B components in the binary system are q^p_A and q^p_B, respectively, the overall permeation rate, Q, is as follows:

$$Q = q_A^p + q_B^p. \qquad (25)$$

In an ideal state in which there is not an interaction between the components,

$$q_A^p = X_A \, q_A^c, \quad q_B^p = X_B \, q_B^c, \qquad (26)$$

where X_A and X_B are the weight fraction or mole fraction of the components A and B in the upstream side, respectively.

The overall permeation rate in an ideal system, Q^c, is as follows:

$$Q^c = X q_A^c + (1 - X_A) q_B^c. \qquad (27)$$

When the weight fractions or mole fractions of A and B components in the downstream side in PV are Y_A and Y_B, respectively,

$$q_B^p/q_A^p = Y_B/Y_A \qquad (28)$$

The separation factor, $\alpha_{B/A}$, represented by the component fractions in the feed solution and permeate is as follows:

$$\alpha_{B/A} = (Y_B/Y_A)/(X_B/X_A) \qquad (29)$$

By using Eqs. 26, 27, and 28:

$$\begin{aligned}
\alpha_{B/A} &= (Y_B/Y_A)/(X_B/X_A) \\
&= Y_B(1 - X_B)/X_B(1 - Y_B) \\
&= q_B^p/q_A^p = (X_B q_B^c)X_A/(X_A q_A^c)X_B \\
&= q_B^c/q_A^c.
\end{aligned} \qquad (30)$$

The separation factors in the ternary component are as follows:

$$\begin{aligned}
\alpha_{B/A} &= (Y_B/Y_A)/(X_B/X_A), \\
\alpha_{C/A} &= (Y_C/Y_A)/(X_C/X_A), \\
\alpha_{C/B/} &= (Y_C/Y_B)/(X_C/X_B)
\end{aligned} \qquad (31)$$

$$\begin{aligned}
\alpha_{A/total} &= \{Y_{A/}(Y_A + Y_B + Y_C)/X_{A/}(X_A + X_B + X_C)\} \\
&= (Y_A/\Sigma Y i)/X_A/\Sigma X i.
\end{aligned} \qquad (32)$$

In PV, the separation factor, $\alpha_{B/A}$, a relative measure for the degree of separation, can be represented by the component mole fractions in the feed and permeate as follows:

$$\alpha_{B/A} = (Y_B/Y_A)/(X_B/X_A), \qquad (33)$$

where X_A and X_B are the weight fraction or mole fraction of A and B components in the upstream-side, respectively. Y_A and Y_B are the weight fraction or mole fraction of A and B components in the downstream side, respectively.

P

PV Membranes for Separation of Organic Liquid Mixtures

Dehydration PV Membranes

Dehydration PV Membranes for Alcohols

Water/alcohol selective PV membranes are effective for the following scenario. For example, when an aqueous solution of dilute ethanol (about 10 wt%) produced by the bio-fermentation is concentrated by distillation, since an aqueous solution of 96.5 wt% ethanol is an azeotropic mixture, ethanol cannot be concentrated any more by distillation, and consequently ethanol is concentrated by azeotropic distillation with the addition of benzene. If membranes that can preferentially permeate only water at 3.5 wt% in an azeotropic mixture of aqueous ethanol solution can be developed, significant energy savings would be achieved. The separation of permeants in PV depends on the differences in the solubility and diffusivity of the permeants in the feed mixture. When structures of water/alcohol and water/organic liquid for selective PV membranes are domically designed, hydrophilic materials can be recommended as membrane materials. Therefore, an increase in the solubility of water molecules into the membrane during the solution process can be expected. In order to raise the affinity of membranes for water molecules, membranes with dissociation groups introduced into their structure are used for dehydration from organic solvents.

Hydrophilic organic–inorganic hybrid membranes were prepared from hydrophilic quaternized chitosan (q-Chito) and tetraethoxysilane (TEOS) by a sol–gel process, in order to minimize the swelling of the q-Chito membranes. When an azeotrope of ethanol/water was permeated through their q-Chito/TEOS hybrid membranes during PV, the q-Chito/TEOS hybrid membranes showed high H_2O/EtOH selectivity. However, the H_2O/EtOH selectivity of the membranes decreased slightly with increasing TEOS content over 45 mol% [9, 10]. To control the swelling of sodium carboxymethylcellulose (CMCNa) membranes, mixtures of CMCNa and glutaraldehdde (GA) and mixtures

of CMCNa as an organic component and tetraethoxysilane (TEOS) as an inorganic component were prepared, and CMCNa/GA cross-linked membranes and CMCNa/TEOS hybrid membranes were formed. In the separation of an ethanol/water azeotrope by PV, the effects of the GA or TEOS content on the water/ethanol selectivity and permeability of these CMCNa/GA cross-linked and CMCNa/TEOS hybrid membranes were investigated. Cross-linked and hybrid membranes containing up to 10 wt% GA or 10 wt% TEOS exhibited higher water/ethanol selectivity than CMCNa membrane without any cross-linker. This resulted from both increased density and depressed swelling of the membranes by the formation of a cross-linked structure [11]. Zeolite-embedded hybrid membranes are manufactured by using a casting machine with polyester nonwoven fabric as the supporting layer, polyacrylonitrile (PAN) as the porous backing layer, and PVA as the active separating layer. Experimental results show the H_2O/EtOH selectivity has been greatly improved after adding zeolite 4A and that reasonably high separation factor can be achieved for feed ethanol concentration of above 80 wt%, probably due to the superior molecular sieving effect of added zeolite 4A on the water/ethanol system. By incorporation of zeolite, apparent Arrhenius activation energy significantly decreased for water but obviously increased for ethanol. Water molecules require much less energy whereas ethanol molecules need much more energy to transport through the membrane because of the hydrophilic characteristics of zeolite 4A.

Dehydration PV Membranes for Organic Liquids

Water/organic selective PV membranes are effective for the dehydration of water/organic mixtures. The dehydrated organic solvents can be useful as industrial reaction solvents, washing solvents, and analytical solvents.

PVA-based nanocomposite membranes were prepared by coprecipitation of different amounts of Fe(II) and Fe(III) taken in an alkaline medium and their PV performances were investigated to dehydrate from aqueous solutions of 10–20 wt% 2-propanol and 1,4-dioxane and 5–15 wt%

tetrahydrofuran. Thin layer membranes were cast on polyester fabric cloths as support layers to improve their PV separation performances for all three mixtures over that of the pristine cross-linked PVA membrane. In particular, the composite membrane prepared by taking 4.5 wt% of iron oxide showed an improved selectivity with a slight sacrifice in the permeation rate compared to membranes containing lower contents of iron oxide as well as the pristine cross-linked PVA membrane. The permeation rate decreased with increasing content of iron in the PVA matrix, while the selectivity increased systematically. Dense polymer membranes were made by mixing aqueous solutions of hydrophilic polymers PVA and PEI for investigating the separation of an azeotrope of tetrahydrofuran (THF)/water (94 wt% THF) by PV. The membranes were found to have good potential for breaking an azeotrope of THF. An increase in PVA content in the blend caused a decrease in the permeation rate and an increase in selectivity. The blend membrane of PVA/PEI of 5/1 showed the highest separation factor for H_2O/THF selectivity of 181.5 and the permeation rate of 1.28 kg $(m^2h)^{-1}$ for an azeotropic mixture, respectively. Zeolite K-LTL-loaded NaAlg-mixed matrix membranes were prepared by solution casting and cross-linked with GA. The PV dehydration of 2-propanol, 1,4-dioxane, and tetrahydrofuran was tested at 30–70 °C as a function of membrane thickness and feed compositions. These membranes showed enhancement in both the permeation rate and water selectivity in azeotropic mixtures. These results were due to the addition of K-LTL particles in NaAlg matrix. The permeation rate and selectivity to water were higher for water/1,4-dioxane azeotrope than those of water/2-propanol and water/tetrahydrofuran azeotropic mixtures. Molecular sieving effect based on uniform distribution of K-LTL zeolite particles showed that in NaAlg matrix its hydrophilicity and hydrophilic NaAlg gave higher membrane performance than pristine cross-linked NaAlg membrane.

Membranes constructed from pure poly (4-methyl-1-pentene) (TPX) 4-vinylpylidine (4-VP) and modified TPX (TPX/P4-VP) membranes were prepared for PV. The introduction of a hydrophilic 4-VP monomer into the TPX matrix was done by free radical polymerization to form the TPX/P4-VP membrane. The separation factor for H_2O/CH_3COOH selectivity and permeation rate of the TPX/P4-VP membranes were higher than those of the unmodified TPX membranes for the PV of an aqueous acetic acid solution. Acrylnitrile (AN) and hydroxyl ethylmetacrylate (HEMA) were grafted onto PVA using cerium(IV) ammonium nitrate as initiator at 30 °C. The PVA-*g*-AN/HEMA membranes were prepared by a casting method, and used in the separation of acetic acid/water mixtures by PV. PVA-*g*-AN/HEMA membranes gave separation factors for H_2O/CH_3COOH selectivity of 2.26–14.60 and permeation rates of 0.18–2.07 kg $(m^2h)^{-1}$. Grafted membranes gave lower permeation rates and greater separation factors for H_2O/CH_3COOH selectivity than PVA membranes [12]. Novel hydrophilic polymer membranes based on cross-linked mixtures of poly(allylamine hydrochloride)-PVA have been developed. The high selectivity and permeation rate characteristics of these membranes for the dehydration of organic solvents are evaluated using PV technology and are found to be very promising when compared to existing membranes.

Organic Selective PV Membranes for Aqueous Solutions
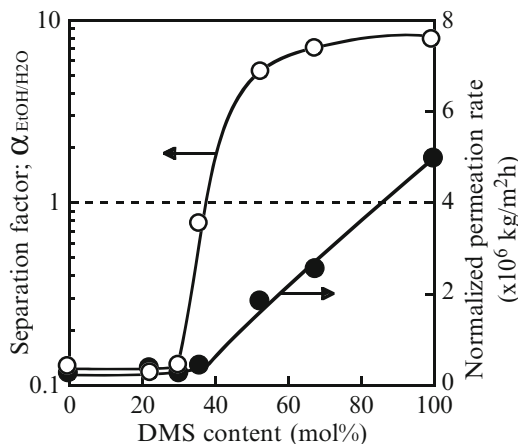
Alcohol Selective Membranes
Cross-linked PVA composite membranes have been used in commercial PV plants for dehydration of ethanol beyond the azeotrope. However aqueous ethanol solutions that can be produced by bio-fermentation are dilute (about 10 wt%). Therefore, if ethanol/water (EtOH/H_2O) selective membranes with high efficiency can be prepared, the distillation process in the first stage to obtain an azeotrope can be replaced which is very advantageous for reduction of energy cost. There are fewer reports on EtOH/H_2O selective membranes compared with those of H_2O/EtOH selective membranes. One reason why the development of efficient high-performance EtOH/H_2O selective membranes is difficult can be attributed to the

P
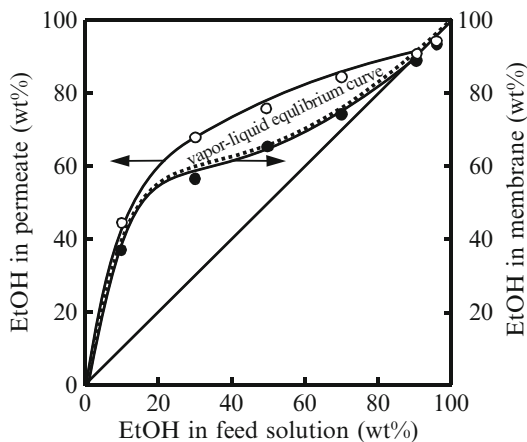
Pervaporation Membranes, Fig. 2 Permeation and separation characteristics of aqueous ethanol solutions through a PDMS membrane during PV ((T. Uragami) pervaporation membranes)

Pervaporation Membranes, Fig. 3 Effects of the DMS content on the normalized permeation rate (○) and separation factor (●) through the PMMA-*g*-PDMS membrane during PV. Feed: aqueous solution of 10 wt% ethanol. *Dashed line* is the feed composition ((T. Uragami) pervaporation membranes)

fact that ethanol has a larger molecular size than water and must be preferentially permeated through the membrane. In fact, permeation and separation in a PV process through dense membranes is based on the solution-diffusion mechanism [1, 8]. Therefore, when it is required that ethanol molecules with larger molecular size preferentially permeate from an aqueous ethanol solution, it cannot be expected to be separated by the diffusion process. Consequently, only a difference of solubility selectivity in the solution process in which both ethanol and water components are dissolved can contribute to the separation. Figure 2 shows the ethanol concentration in the permeate through a poly(dimethylsiloxane) (PDMS) membrane during PV and the amount sorbed into a PDMS membrane. These results support the hypothesis that the difference in the solubility of the permeants contributes to the EtOH/H$_2$O selectivity. PDMS membranes show high EtOH/H$_2$O selectivity, but their mechanical strength is weak, and it is difficult to prepare thin membranes from PDMS. In order to obtain both EtOH/H$_2$O selectivity and mechanical strength, graft copolymers composed of PDMS macromonomer and vinyl monomers were synthesized.

Graft copolymer membranes, which were either ethanol- or water-selective, were prepared by copolymerization of an oligo-dimethylsiloxane (DMS) monomer with methyl methacrylate (MMA) [7]. Transmission electron micrograph (TEM) demonstrated that the PMMA-*g*-PDMS membranes showed microphase-separated structures. When an aqueous solution of 10 wt% ethanol was permeated through the PMMA-g-PDMS membranes by PV, the ethanol concentration in the permeate and the permeation rate increased drastically with the DMS content in the copolymer. In particular, at a DMS content of less than 40 mol%, water permeates preferentially from an aqueous solution of 10 wt% ethanol, whereas membranes with more than about 40 mol% of DMS are EtOH/H$_2$O selective, as shown in Fig. 3. The change in the EtOH/H$_2$O selectivity of the PMMA-*g*-PDMS membranes can be explained by a microphase-separated polymer structure using Maxwell's model and a combined model consisting of both parallel and series expressions. Furthermore, image processing of TEMs allowed the determination of the percolation transition of the PDMS phase at a DMS content of about 40 mol%. These results suggest that the continuity of the PDMS phases in the microphase-separated PMMA-*g*-PDMS membranes directly affects their EtOH/H$_2$O selectivity for aqueous ethanol solutions [7].

It is well known that poly[1-(trimethylsilyl)-1-propyne] (PTMSP) membranes show high EtOH/H$_2$O selectivity [13]. In order to enhance the EtOH/H$_2$O selectivity of PTMSP membranes, surface-modified PTMSP membranes were prepared by adding a small amount of a polymer additive, a graft copolymer (PFA-g-PDMS) consisting of poly(fluoroacrylate) (PFA) and PDMS, in the casting solution of PTMSP. Modified PTMSP membranes were cast on glass plates and the contact angles of water on the membrane surfaces exposed to the air-side and the glass-side, respectively, were measured. The contact angle for water on surface-modified PTMSP membranes was significantly different on the air-side versus that on the glass side; the contact angles on the air-side were more hydrophobic. Furthermore, the contact angle for water increased in hydrophobicity with additional amounts of PFA-g-PDMS. The high hydrophobicity of the membrane surface on the air-side and the increase in hydrophobicity with additional amounts of polymer additive were also confirmed by X-ray photoelectron spectroscopy. The permeation rate for an aqueous solution of 10 wt% ethanol in PV experiments using surface-modified PTMSP membranes decreased slightly. However, the EtOH/H$_2$O selectivity increased considerably with increasing amounts of PFA-g-PDMS [13].

Organic Selective Membranes

Organic liquid/water selective PV membranes are effective for the removal of organics in water and recovery of organic solvents from water. These membranes can contribute to the environmental problem and effective use of organic solvents.

Novel cross-linked hydroxyterminated polybutadiene based polyurethane urea-poly (methyl methacrylate) (PMMA) interpenetrating network (IPN) membranes were developed for the selective removal of chlorinated volatile organic compounds (VOCs) such as 1, 1, 2, 2-tetrachloroethane (TCEN), CHCl$_3$, carbon tetrachloride (CCl$_4$), TCET in water in very low concentration by PV. IPNs of different PMMA content and also different cross-linking density

were used. Since the selective permeation and diffusion of the VOCs through the membrane are dependent on their interaction with the membrane material, their sorption and diffusion behaviors through the membrane were also investigated by swelling the membrane in pure VOCs. The sorption and diffusion behaviors were explained with the help of their solubility parameter data and calculated interaction parameter data of the membrane polymers with the VOCs. All three IPN membranes showed excellent separation performances of the chlorinated VOCs from water. One IPN containing PMMA of 26 % produced TCET of 88.7 % in the permeate and resulted in the permeation rate of 0.2 kg (m^{2}h)$^{-1}$ and a separation factor of 7,842 for 0.1 % aqueous feed at 30 °C. All three IPN membranes of different compositions showed the separation performances, viz., permeation rate and separation factor in the order of TCEN $<$ CCl$_4$ $<$ CHCl$_3$ $<$ TCET.

Fundamental model experiments revealed that very small amounts of VOCs, which are toxic substances, could be removed effectively from water by polymer membranes containing an environmentally friendly ionic liquid (green sustainable reagent) using a PV process. The removal of VOCs is required for the purification of contaminated water as a possible source for drinking water. This removal is very significant for the security of the scarce drinking water supply around the world. To be concrete, a block copolymer membrane composed of poly(styrene) (PSt) and PDMS, which has a PDMS continuous phase in the microphase separated structure in the PSt-b-PDMS membrane, containing an ionic liquid (IL) having high affinity for VOCs and low affinity for water was applied to the removal of VOCs from aqueous solutions of dilute VOCs by pervaporation. The membranes with different IL contents showed high VOC/water selectivity and high permeation rate.

In Table 1, the permeation and separation characteristics of various polymer membranes consisting of the PDMS components are compared under the same PV condition: feed solution, an aqueous solution of 0.05 wt% benzene; permeation temperature, 40 °C; pressure of

P

Pervaporation Membranes, Table 1 Performance for Bz/H_2O of various membranes containing PDMS component [7]

Various PDMS membranes[a]	α_{sep}. Bz/H_2O	α_{sorp}. Bz/H_2O	α_{diff}. Bz/H_2O	NPR[b]	PSI[c]
PMMA	53	422	0.13	0.29	16
PMMA-g-PDMS[d]	620	739	0.86	0.13	226
CA/PMMA-g-PDMS[e]	1,772	1,267	1.40	0.71	1,240
PFA-g-PDMS/PMMA-g-PDMS[f]	4,492			0.64	2,879
PDMSDMMA-DVB[g]	3,171	1,436	2.21	1.46	4,629
PDMSDMMA-DVS[h]	2,886	1,270	2.46	1.96	5,656
PDMSDMMA-DVF[i]	4,316	1,804	2.49	1.72	7,423
CA/PDMSDMMA-DVB[j]	4,021	1,689	2.18	1.75	7,037
CA/PDMSDMMA-DVS[k]	3,866	1,620	2.39	1.97	7,616
CA/PDMSDMMA-DVF[l]	5,027	1,998	2.52	1.86	9,350

[a]PV experimental conditions: feed solution, an aqueous solution of 0.05 wt% benzene; permeation temperature, 40 °C; pressure of permeation side, 1×10^{-2} Torr (1.33 Pa)
[b]Normalized permeation rate [10^{-5} mkg (m^{2}h)$^{-1}$]
[c]PV separation index (NPR $\times \alpha_{sep}$. Bz/H_2O)
[d]PDMS content, 74 mol%
[e]PDMS content, 74 mol%; CA content, 40 mol%
[f]PDMS content, 74 mol%; PFA-g-PDMS content, 1.2 wt%
[g]DVB content, 80 mol%
[h]DVS content, 90 mol%
[i]DVF content, 90 mol%
[j]DVB content, 80 mol%; CA content, 0.5 wt%
[k]DVS content, 90 mol%; CA content, 0.5 wt%
[l]DVF content, 90 mol%; CA content, 0.4 mol%

permeation side, 1.33 Pa. As can be seen in Table 1, both the normalized permeation rate and the Bz/H_2O selectivity of the CA/PDMSDMMA-DVB, CA/PDMSDMMA-DVS, and CA/PDMSDMMA-DVF membranes containing *tert*-butylcalix [4] arene (CA) were improved as compared to the PDMSDMMA-DVB, PDMSDMMA-DVS, and PDMSDMMA-DVF membranes. Although, the separation factors of the CA/PDMSDMMA-DVB and CA/PDMSDMMA-DVS membranes were lower than that of the PFA-g-PDMS/PMMA-g-PDMS membranes, the PSI of the former membranes was much greater than that of the latter one. In Table 1, it is found that the addition of CA into the cross-linked PDMSDMMA membranes cross-linked with a suitable cross-linker is significantly effective to obtain a higher permeation and separation characteristics. A CA/PDMSDMMA-DVF membrane with DVF of 90 mol% and CA of 0.4 wt% showed the best membrane performance, i.e., the normalized permeation rate, separation factor for Bz/H_2O

selectivity, and PSI were 1.86×10^{-5} mkg (m^{2}h)$^{-1}$, 5,027, and 9,350, respectively [7].

PV Selective Membranes for Separation of Organic Liquid/Organic Liquid Mixtures

Organic/organic selective membranes are effectively used for the purification and separation of industrial products and reuse of organic solvents based on separable recovery of organic mixtures.

Benzene/Cyclohexane Selective Membranes

The separation of benzene (Bz) and cyclohexane (Chx) by distillation is a very energy-intensive process, because the boiling points of the components are very similar. PV may be an alternative, more energy-efficient process for the separation of Bz/Chx mixtures. Therefore, many researchers have studied the PV properties of polymeric membranes for Bz/Chx separation.

In Table 2, the PV performance of various polymer membranes for the separation of Bz/Chx mixtures are listed [6]. When the PV performance is estimated by the pervaporation

Pervaporation Membranes, Table 2 PV performance of various polymer membranes for the separation of BZ/Chx mixtures [6]

Membrane[a]	Benzene in feed (wt%)	Temperature (°C)	NPR (kg μm/m^{2}h)	$\alpha_{Bz/Chx}$	PSI
PVA/PAAm	50	25	2.3	11.9	27.4
BP-3MPD/PD	50	70	2.7	14	37.8
BP-PEO	60	25–70	2.1	9.1	19.1
DSDA-DDBT	60	78	0.93	32	29.8
DSDA-DDBT	60	78	2.4	20	48
PU-TEOS	50	50	0.65	19	12.4
PGMA grafted	60	40–70	8.7	22	191.4
PS/PAA	50	20	48.4	9.6	464.6
PEMA-EGDM	10	40	8.7	6.7	58.3
PEMA-EGDM	10	40	55.1	3.9	214.9
n-LPC	50	10	13.1	2.0	26.2
s-LPC	50	10	7.5	1.9	14.3
BzChito	10	40	6.4	65	416.0
BzChito	50	40	1.5	13	19.5
BzCell	10	40	0.6	2.3	13.8
BzCell	50	40	33.6	9.1	305.7
TosCell	40	40	0.06	28.9	1.7

[a]*3MPD* 2,4,6-trimethyl-1,3-phenylenediamine, *BzChito* benzoyl chitosan, *BzCell* benzoyl cellulose, *BP* 3,3′,4,4′-biphenyltetracarboxylic dianhydride, *DDBT* dimethyl-3,7-diaminobenzothiophene-5,5′-dioxide, *DSDA* 3,3′,4,4′-diphenylsulfone tetracarboxylic dianhydride, *EGDM* ethylene glycol dimethacrylate, *n-LPC* nematic liquid crystalline polymer, *PAA* polyacrylic acid, *PAAm* polyallyl amine, *PAS* polyacrylonitrile-co-styrene, *PD* 1,3-phenylenediamine, *PEMA* polyethyl methacrylate, *PEO* polyethylene oxide, *PGMA* polyglycidyl methacrylate, *PMMA* polymethyl methacrylate, *PS* polystyrene, *PU* polyurethane, *TEOS* tetraethyl orthosilicate, *s-LPC* smectic liquid crystalline polymer, *TosCell* tosyl cellulose

separation index (PSI), which is the product of the permeation rate and the separation factor, PSI can be used as a measure of membrane performance during PV. It is found that poly(styrene)/poly(acrylic acid) (PS/PAA), benzoylchitosan (Bzchito) [9, 10], and benzoylcellulose (Bzcell) membranes showed higher performance for the separation of Bz/Chx mixtures during PV.

Organic/Organic Selective Membranes

PV separation of ternary and quaternary mixtures of ethyl acetate, water, ethanol, and acetic acid, which are present in the hydrolysis of ethyl acetate encountered in pharmaceutical industries was investigated. Water concentrations in the feed mixtures are in the range of 90–98 wt%, while the concentrations of ethyl acetate, ethanol, and acetic acid are much lower. PDMS was used as a membrane to separate organic compounds from aqueous streams. PV experiments showed that PDMS membrane was much more selective to ethyl acetate than other organic components.

An increase in the ethyl acetate concentration in feed mixture resulted in higher total permeation rates but lower selectivities of ethyl acetate. The blend membranes from a polymer blend of PAA and PVA were evaluated for the separation of methanol from methyl *tert*-butyl ether (MTBE) by PV. Methanol (MeOH) permeated preferentially through all blend membranes tested, and the MeOH/MTBE selectivity increased with increasing PVA content in the blends. However, a decrease in the permeation rate was observed with increasing PVA content. Upon increasing the feed temperature, the permeation rate increased and the MeOH/MTBE selectivity remained constant. In addition, the influence of cross-linking on the MeOH/MTBE selectivity was investigated. The PV permeation rate decreased with increasing cross-linking density; however, this was coupled with an increase in MEOH/MTBE selectivity. This was due to a more rapid decrease in the partial permeation rate of MTBE compared to that of methanol.

P

Sorption and PV experiments were carried out with cellulose triacetate membranes for the separation of MTBE and MeOH mixtures. In the PV experiments, the total and MeOH permeation rates increased with the increasing methanol concentration in the feed while the permeation rates of MTBE first increased and then decreased. The total permeation rates are significantly enhanced with increasing temperature. This temperature dependence was more pronounced at low methanol concentration, but the extent of increase of the total permeate rate was relatively constant when MeOH concentrations were greater than 10 %. The MeOH/MTBE selectivity decreased with increasing of methanol concentration and became more or less constant at high MeOH concentrations [14].

Selective Membranes for Isomers

Propanol and xylene isomer selective membranes are very important for the separation of industrial chemical products and energy saving for the separation of those mixtures.

PVA membranes containing β-CD (PVA/CD membrane) were prepared and the permeation and separation characteristics for propanol and xylene isomers through the PVA/CD membranes were investigated by PV [15]. The PVA/CD membrane preferentially permeated 1-propanol rather than 2-propanol from their mixtures. In particular, a mixture of 10 wt% 1-propanol concentration was concentrated to about 45 wt% through the PVA/CD membrane. The increase in CD content gave an increase in p-xylene/o-xylene selectivity through the PVA/CD membrane. This was attributed to the stronger affinity of CD for p-xylene compared with o-xylene. Especially, the PVA/CD membrane at a CD content of 40 wt% showed a higher separation factor for p-xylene/o-xylene selectivity. When the p-xylene concentration in the feed was lower, the p-xylene/o-xylene selectivity was improved. PAA membranes containing α-, β-, or γ-CD were prepared and used for the separation of o-/p-xylene mixture by PV. The native PAA membrane was almost impermeable for the xylene isomers, and the incorporation of CDs in the PAA membranes resulted in membranes having molecular recognition function, which selectively facilitated the transport of the xylene isomers. For all types of CDs, the facilitated transport occurred at CD concentrations higher than the threshold concentration. As the CD concentration increased, the permeation rates increased, while the o-xylene/p-xylene selectivities were almost constant. The selectivity for o-xylene/p-xylene selectivity of the membranes was strongly influenced by the types of CDs incorporated in the membranes [16]. The PV characteristics of xylene isomer mixtures through a fixed carrier membrane consisting of CA as a base polymer and dinitrophenyl (DNP) group as a selective fixed-carrier were studied. In the PV of xylene isomer mixtures, the DNP group selectively facilitated the transport of xylene isomers through the membrane. The order of the preferentially permeating component was p-xylene > m-xylene > o-xylene. Fractionation of o- and p-xylene isomeric mixtures was performed using PV with poly(urethane) (PU) membranes containing ZSM zeolite. The xylene vapor sorption isotherms exhibited a Henry's law relationship in this PU-zeolite blend. In binary solutions the individual xylene uptake was also proportional to the solvent composition. Although incorporating zeolite into the PU-zeolite membrane rendered a decrease in xylene solubility as compared with that sorbed in the PU film without zeolite addition, the increase of diffusion coefficient and diffusivity selectivity increases enhanced the separation efficiency using the PU-zeolite blend. Increasing the operating temperatures enhanced the xylene permeation rate of xylene. The permeation rates of xylene and selectivity increased with increasing zeolite content [17].

PV Selective Membranes for Facilitation of Chemical Reactions

Selective membranes for facilitation of chemical reactions are useful for reactors coupled with PV membrane separation technology. These systems can help to enhance the conversion of reactants for thermodynamically or kinetically limited reactions via selective removal of one or more product species from reaction mixtures.

PVA membranes cross-linked with sulfosuccinic acid (SSA) were used for the removal of water in the esterification with acetic acid by isoamylic alcohol. In order to study the effects of the cross-linking degree and, simultaneously, the amount of sulfonic groups, different membranes were prepared with SSA/PVA ratios in the range of 5–40 mol%. To eliminate the dependence between the amount of acid sites and the cross-linking degree, PVA membranes with the -SO_3H groups which were introduced by anchoring 5-sulfosalisilic acid (SA) on the PVA chains were also prepared. The consumed conversion of iso-amylic alcohol increased when the amount of sulfosuccinic acid used in the polymer cross-linking was increased from 5 % to 20 %. However, when cross-linking degree increased from 20 % to 40 %, its conversion increased only slightly, probably due to the increase of molecular mobility restriction in the PVA matrix. In the case of the PVA membranes introduced to the -SO_3H groups, the membrane activity for esterification increased with the polymer cross-linking [18]. Esterification of lactic acid and succinic acid with ethanol to generate ethyl lactate ($C_5H_{10}O_3$) and diethyl succinate, respectively, was studied in well-mixed reactors with solid catalysts (Amberlyst XN-1010 and Nation NR50) and two PV membranes (GFIF-1005 and T1-b). Experiments were carried out by a closed-loop system of a "batch" catalytic reactor and a PV unit employing GFIF-1005. The kinetics of PV is studied to obtain a working correlation for the permeation rate of water in terms of temperature and water concentration on the feed side of the pervaporator. The efficacy of PV-aided esterification was illustrated by attainment of near total utilization of the stoichiometrically limiting reactant within a reasonable time. Protocols for recovery of ethyl lactate and diethyl succinate from PV retentate were discussed and simultaneous esterification of lactic and succinic acids, which is an attractive and novel concept, is proposed [19]. Reaction-PV hybrid processes can be an alternative to classical chemical processes to enhance the conversion of equilibrium-limited reactions such as esterification and trans-esterification. The esterification of acetic acid with isopropanol coupled with PV was investigated. The synthesis and hydrolysis of isopropyl acetate have been studied using the commercial polymeric membrane PERVAP (R) 2201. The effect of temperature and feed composition on the permeation characteristics of the membrane was analyzed and preferential water permeation from the quaternary mixture involved in the esterification of acetic acid with isopropanol was discussed under the experimental conditions [20].

References

1. Binding RC, Lee RJ, Jennings JF, Mertin EC (1961) Separation of liquid mixtures by permeation. Ind Eng Chem 53:45–54. doi:10.1021/ie50613a030
2. Choo CY (1962) Membrane permeation in advances in petroleum chemistry and refining, chapter 2. In: Mcketta J (ed) Advances in petroleum chemistry and refining, vol IV. Interscience, New York
3. Yamada S (1981) Evaluation of pervaporation membrane for separation of liquid-liquid mixture. In: Japanes Membrane Society (ed) Evaluation of performance of artificial membranes. Kitami Shobo, Tokyo, pp 30–46
4. Uragami T (1998) Structures and properties of membranes from polysaccharide derivatives, polysaccharides. In: Dumitrium S (ed) Structural diversity and functional versatility. Marcel Dekker, New York/Basel/Hong Kong, pp 887–924
5. Uragami T (2005) Structures and functionalities of membranes from polysaccharide derivatives. In: Dumitrium S (ed) Polysaccharide, structural diversity and functional versatility, 2nd edn. Marcel Dekker, New York/Basel/Hong Kong, pp 1087–1122
6. Uragami T (2006) Polymer membranes for separation of organic liquid mixtures. In: Yanpoliski Y, Pinnau I, Freeman BD (eds) Materials science of gas and vapor separation. Wiley, London/New York, pp 355–372
7. Uragami T (2010) Selective membranes for purification and separation of organic liquid mixtures. In: Drioli E, Giorno L (eds) Comprehensive science and engineering, vol 2. Elsevier, Amsterdam/Boston/Heidelberg/London/New York/Oxford/Paris/San Diego/San Francisco/Singapore/Sydney/Tokyo, pp 273–324
8. Aptel P, Cuny J, Jozefonvicz J, Morel G, Neel J (1974) Liquid transport through membranes prepared by grafting of polar monomer onto poly (tetrafluoroethylene) films. III. Steady state distribution in membrane during pervaporation. J Appl Polym Sci 18:365–398. doi:10.1002/app.1974.070180205

P

9. Uragami T (2006) Separation materials derived from chitin and chitosan. In: Uragami T, Tokura S (eds) Material science of chitin and chitosan. Kodansha/Springer, Tokyo/Berlin/Heidelberg/New York, pp 113–163

10. Uragami T (2010) Separation membranes from chitin and chitosan derivatives. In: Kim SK (ed) Chitin, chitosan, oligosaccharides and their derivatives: biological activities and applications. CRC Press/Taylor & Francis Group, London/New York, pp 481–506

11. Uragami T, Wakita D, Miyata T (2010) Dehydration of an azeotrope of ethanol/water by sodium carboxymethylcellulose membranes cross-linked with organic or inorganic cross-linker. eXPRESS Polym Lett 11:681–691. doi:10.3144/expresspolymlet.2010.83

12. Al-Ghezawi N, Sanli O, Isiklan N (2006) Permeation and separation characteristics of acetic acid-water mixtures by pervaporation through acrylonitrile and hydroxy ethyl methacrylate rafted poly(vinyl alcohol) membrane. Sep Sci Technol 41:2913–2931. doi:10.1080/01496390600786010

13. Uragami T (2000) Pervaporation property of surface modified poly[1-(trimethylsilyl)-1-propyne] membranes. In: Pinnau I, Freeman BD (eds) Membrane formation and modification, vol 744, ACS symposium series. American Chemical Society, Washington, DC, pp 263–279

14. Niang M, Luo GS (2001) A triacetate cellulose membrane for the separation of methyl *tert*-butyl ether/methanol mixtures by pervaporation. Sep Purif Technol 24:427–435. doi:10.1016/j.bbr.2011.03.031

15. Miyata T, Iwamoto T, Uragami T (1994) Characteristics of permeation and separation for propanol isomers through poly(vinyl alcohol) membranes containing cycrodextrin. J Appl Polym Sci 51:2007–2014. doi:10.1002/app.1994.070511204

16. Kusumocahyo SP, Kanamori T, Sumaru T, Iwatsubo K, Shinbo T (2004) Pervaporation of xylene isomer mixture through cyclodextrins containing polyacrylic acid membranes. J Membr Sci 231:127–132. doi:10.1016/j.memsci.2003.11.011

17. Lue SJ, Liaw TH (2006) Separation of xylene mixtures using polyurethane – zeolite composite membranes. Desalination 193:137–143. doi:10.1016/j.desal.2005j.desal.2005.06/059

18. Castanherio JE, Ramos AM, Fonseca IM, Vita J (2006) Esterification of acetic acid by isoamylic alcohol over catalytic membranes of poly(vinyl alcohol) containing sulfonic acid groups. Appl Catal A Gen 311:17–23. doi:10.1016/j.apcata.2006.05.039

19. Benedict DJ, Parulekar SJ, Tsai SP (2006) Pervaporation-assisted esterification of lactic and succinic acids with downstream ester recovery. J Membr Sci 281:435–445. doi:10.1016/j.memsci.2006.04.012

20. Sanz MT, Gmehling J (2006) Esterification of acetic acid with isopropanol couplet with pervaporation: part I: kinetics and pervaporation studies. Chem Eng J 123:1–8. doi:10.1016/j.cej.2006.06.0006; Part II: study of a pervaporation reactor. Chem Eng J 123:9–14. doi:10.1016/j.cej.2006.06.0011

21. Ohshima T, Miyata T, Uragami T (2005) Selective removal of dilute benzene from water by various cross-linked poly(dimethylsiloxane) membranes containing *tert*-butylcalix[4]arene. Macromol Chem Phys 206:2521–2529. doi:10.1002/macp.20050337

PES (Poly(ether sulfone)), Polysulfone

Shohei Ida
Department of Materials Science, The University of Shiga Prefecture, Hikone, Shiga, Japan

Synonyms

Poly(aryl ether sulfone); Poly(arylene ether sulfone)

Definition

Poly(ether sulfone) and polysulfone are polymers respectively containing ether and sulfone group in repeating units. Conventionally, they stand for the specific commercialized aromatic amorphous thermoplastics carrying para-linked diphenylenesulfone and aromatic ether in their repeating units.

Introduction

In general, poly(ether sulfone) (PES) and polysulfone (PSF) specifically indicate the polymers carrying para-linked diphenylenesulfone and aromatic ether in the repeating units as shown in Fig. 1. These polymers are classified as amorphous thermoplastic polymers with clarity, high glass-transition temperature (T_g), and good mechanical strength. These polymers also possess outstanding stability and resistance to heat, oxidation, hydrolysis, and chemical

environments [1, 2]. By virtue of these good properties, they have been widely expanding their application field in, for example, automobile, electrical equipment, and household appliances, after the commercialization started in 1960s by Union Carbide Corporation, Inc. and Imperial Chemical Industries, Ltd. [3, 4].

A nomenclature "polysulfone" in a strict sense describes all polymers carrying sulfone groups in the repeating unit. Therefore, "polysulfone" contains both aliphatic and aromatic polymers. Among them, aliphatic polysulfones can be prepared by radical copolymerization of sulfur dioxide and vinyl monomers [5]. The polymer structures of aliphatic polysulfones are determined by the reactivity ratio of comonomers. For example, the combination of sulfur dioxide and alkene monomer often gives an alternating structure, while the combination with vinyl monomers carrying electron-withdrawing substituent like acrylate gives the polymer with low sulfone content. The obtained aliphatic polysulfones, however, are not applied to practical use because of unattractive properties and relatively low stability induced by β-hydrogen elimination.

Thus, most of commercialized polysulfones are aromatic with much better physical properties compared to aliphatic ones. Especially, aromatic polysulfones containing ether linkage (sometimes called "poly(aryl ether sulfone)s") are attracting much attention as good candidates for various application, and, in some cases, they are already in practical use. In this entry, the representatives of aromatic polysulfones, PES and PSF in Fig. 1, and their derivatives are discussed on their synthetic methods, chemical structures, physical properties, processing ways, and applications.

Synthesis

Nucleophilic Substitution Reaction Route. Commercial PES and PSF are synthesized by polycondensation via nucleophilic substitution mechanism, which was discovered in 1960s. As shown in Fig. 2, the polymerization is normally conducted by the reaction between dihalodiphenylsulfone and the salt of bisphenol compound, which is produced by the reaction of bisphenol compounds and bases like sodium hydroxide, potassium hydroxide, and potassium carbonate. The choice of bisphenol compound changes the structure of the obtained polymer. For example, PES and PSF are prepared from bisphenol-S (bis(4-hydroxyphenyl)sulfone) and bisphenol-A (4,4'-(propane-2,2-diyl)diphenol), respectively.

Because of the polycondensation mechanism, the purity of monomers and the stoichiometric balance of dihalide and bisphenol salt are important to obtain high molecular weight. A typical contaminant is meta-substituent of dihalide, which is inactive for the substitution reaction to behave as a terminator in the polymerization. For the stoichiometric balance, water produced by the reaction of bisphenol and base sometimes disturbs the polymerization because water hydrolyzes the dihalide to generate phenol compound. It changes the stoichiometric balance of the monomers and prevents to obtain polymers with high molecular weight. Hence, water should be thoroughly removed from the reaction system.

The electric condition of dihalide, the electronegativity of halogen atom, and the basicity of the base, which forms the salt with bisphenol compounds, also affect the substitution reaction. The fluoride compound is more reactive than chloride and bromide, but dichloride is often favored
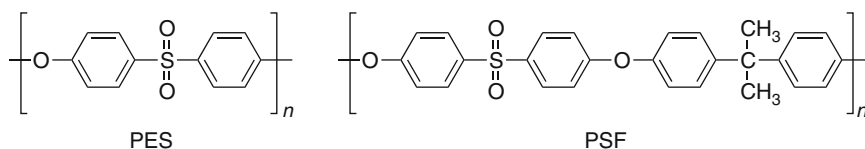
PES (Poly(ether sulfone)), Polysulfone, Fig. 1 The chemical structure of PES and PSF

PES (Poly(ether sulfone)), Polysulfone, Fig. 2 Synthesis of (**a**) PES and (**b**) PSF via nucleophilic substitution route
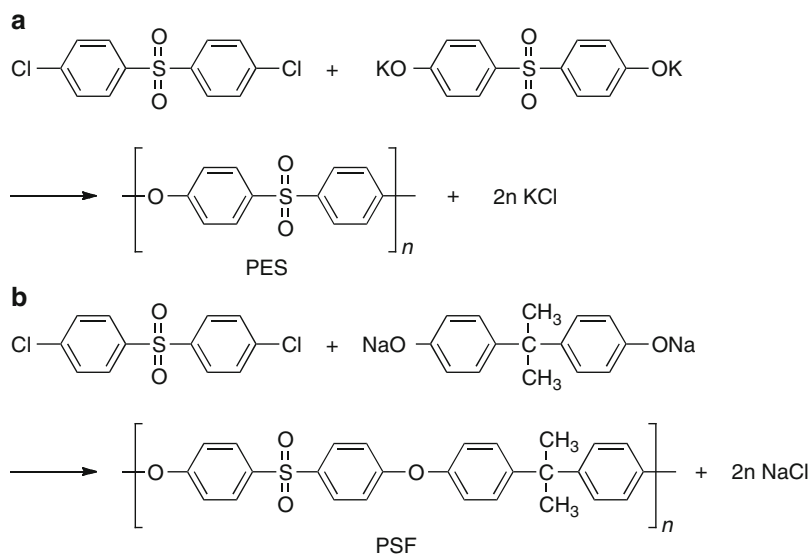
because of its cost. As for the base, strong base immediately forms the bisphenol salt and readily reacts with dihalides to produce high molecular weight polymers in a short period. But this way involves some problems in solubility of the salt and undesirable hydrolysis of dihalide. Hence, weak base such as potassium carbonate is favored especially in the synthesis of PES, which needs high reaction temperature.

The reaction is usually conducted in aprotic and polar solvent such as *N*-methylpyrrolidone (NMP), dimethylacetamide (DMAc), and dimethylsulfoxide (DMSO). Among them, DMSO is suitable for PSF synthesis, because it is a good solvent both for the polymer and the sodium salt of bisphenol-A. PSF synthesis is typically performed in DMSO at 130–160 °C, while PES synthesis requires higher reaction temperature. Therefore, the solvent with higher boiling point such as NMP is favored for PES synthesis.

Electrophilic Substitution Reaction Route. Another popular synthesis of PES and PSF is conducted by aromatic electrophilic substitution reaction. This Friedel-Crafts type polymerization is performed in the combination of sulfonyl chloride and aromatic ether in the presence of Lewis acid such as FeCl$_3$, AlCl$_3$, and BF$_3$ as shown in Fig. 3a. Single-monomer route with monomers containing both functional groups (Fig. 3b) is also applicable. In this Friedel-Crafts route, it is

difficult to obtain linear polymers because of accompanied branching reaction derived from substitution at the ortho position. It disturbs the industrial application, although single-monomer route is helpful to avoid this side reaction. In addition, the limited monomer versatility is also the reason.

Other Synthetic Routes. For the synthesis of other aromatic polysulfones especially containing phenyl-phenyl linkage, coupling reactions are also effective. As shown in Fig. 4, for example, polyphenylsulfone is prepared by nickel-catalyzed coupling reaction of dihalide compounds. In addition, other phenyl-phenyl coupling reactions such as Ullman coupling using copper catalyst and Scholl reaction with Lewis acid are also applicable.

Polymer Functionalization. By utilizing the abovementioned synthetic routes, various functionalized polysulfones can be prepared to improve thermal and mechanical properties. One strategy is the introduction of functional groups into the conventional monomers before polymerization. Another one is post-polymerization modification of polysulfones especially by incorporation of functional groups into aromatic rings. Besides, more complicated structures like telechelic polymers, block polymers, and graft polymers are also realized by recent advance in synthetic technique [6].

PES (Poly(ether sulfone)), Polysulfone, Fig. 3 Synthesis of PES via electrophilic substitution route
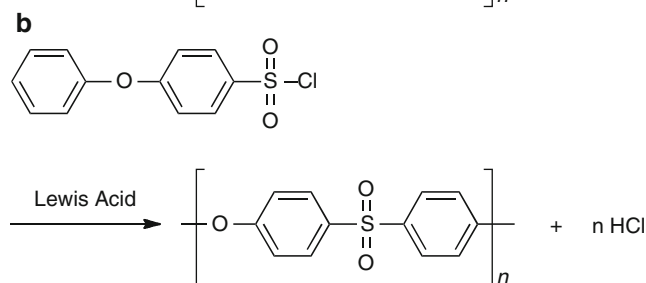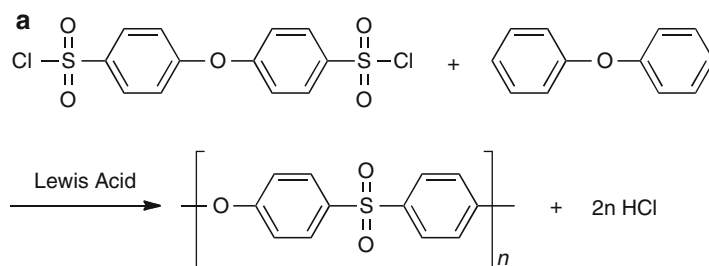
PES (Poly(ether sulfone)), Polysulfone, Fig. 4 Synthesis of polyphenylsulfone via Ni-catalyzed coupling reaction

Polyphenylsulfone
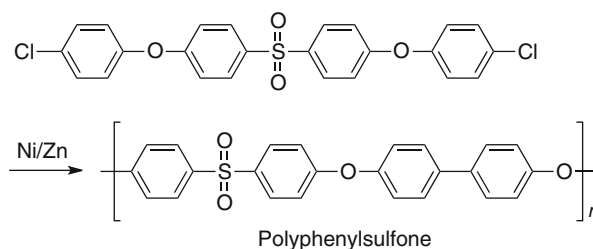
Chemical Structures

The properties of aromatic polysulfones are strongly affected by their chemical structures. Popular ways for control of polysulfone structure are changing bisphenol compound in polycondensation route, for example, bisphenol-S for PES and bisphenol-A for PSF synthesis. One additional example to improve the mechanical strength and thermal properties of polysulfone is utilizing 4,4'-biphenol for the synthesis of polyphenylsulfone.

Such aromatic polysulfones generally possess high stability against hydrolysis and acidic or basic condition because the polymer backbone is formed by chemically inert aromatic, ether, and sulfone groups. The rigid aromatic backbone and sulfone groups give high T_g to polysulfones. High oxidation state of the sulfur atoms and highly resonant structure through aromatic rings and the sulfone groups contribute to oxidation resistance. Therefore, polysulfones are not
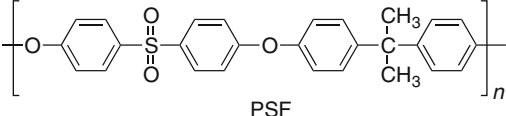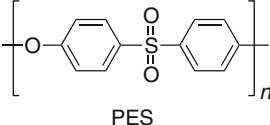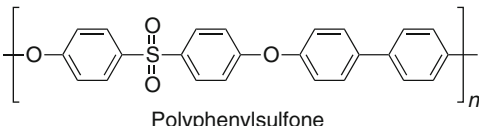
oxidized even by heat exposure in 150–190 °C. Due to the ether linkage, which gives chain flexibility to the backbone, polysulfones have good mechanical toughness. It also affects the rheological properties in the melting state. In concert with good rheological characteristics and high thermal stability, polysulfones can be fabricated at high temperature up to 400 °C for the melt processing.

The properties of polysulfones are also related to the backbone structure. In general, para-linked linear structure without any branching is important for favorable processability and high mechanical properties. Hence, precise synthesis is required to avoid the branching reaction.

Properties

Thermal Properties. Aromatic polysulfones like PES and PSF show outstanding thermal

PES (Poly(ether sulfone)), Polysulfone, Table 1 T_gs of commercially available polysulfones

Structure	T_g (°C)
PSF	185
PES	220
Polyphenylsulfone	220

properties. The characteristic thermal features of polysulfones are high T_g, good resistance to thermal oxidation, and structure stability under melt-processing condition at high temperature.

The T_gs of aromatic polysulfones typically ranges at 190–290 °C. Such high T_gs are attributed to the rigid backbone structures and sulfone groups. The T_gs of the commercially available polysulfones are shown in Table 1. As shown in Table 1, the T_g of polysulfones can be controlled by the chemical structure. PSF shows its T_g at 185 °C, which is lower than that of PES at 220 °C because of the presence of flexible isopropylidene groups. Chemical modification of polysulfone is also effective to obtain higher T_g. For example, methyl-substituted aromatic polysulfones show 60–70 °C higher T_g than non-substituted ones [7].

The thermal oxidative endurance is also the advantage of polysulfones. Thermogravimetrical analysis reveals that PES and PSF show no structural change up to about 500 °C. This high thermal stability is favorable for melt processing, and polysulfones can be easily fabricated at about 400 °C.

Optical Properties. The resins of PES and PSF are transparent because aromatic polysulfones are basically amorphous and non-crystallizable. This non-crystallizable nature leads to low shrinkage during processing into resin and high-dimensional stability during usage. Although the resins of PES and PSF are transparent, they show a slight yellow or amber color. These colors are produced at the process of melting fabrication at high temperature. The great effort to minimize this color has been made so far, and PSF currently exhibit the highest transparency with the lowest color among the aromatic polysulfone resins.

Mechanical Properties. Polysulfones like PES and PSF are tough and rigid polymers and exhibit the practical impact strength. They also show excellent strength and stiffness, which are much better than conventional aliphatic plastics. In addition, they can keep such high strength and stiffness even at high temperature. An elevated temperature normally decreases the strength and stiffness of polymer materials, but polysulfones maintain high level of their mechanical properties such as tensile modulus and creep resistance even at long-time exposure to high temperature. In the practical use, polysulfones are often reinforced by the addition of glass fiber to enhance their mechanical properties.

Flammability. Polysulfones exhibit a good flame retardation characteristic compared to

various engineering thermoplastics. Especially, PES is much resistant to burning than PSF probably due to its aromatic structure without aliphatic moieties. In addition, polysulfones have very-low-smoke-release characteristic.

Electrical Properties. Polysulfones are high insulation materials with high dielectric strength, low dielectric constant, and low dissipation factor over a wide range of temperature and frequency. Coupled with outstanding stability at high temperature and excellent low flammability, polysulfones are considered to be useful for electrical and electronic devices.

Solubility. Polysulfones have a limited solubility to common solvents because of their aromatic backbone and high polarity. As a rule, polysulfones are soluble in high polar solvents such as NMP, DMAc, and DMSO, which are often used as synthetic solvents. Pyridine and aniline are also good solvents for polysulfones. Among the representative polysulfones, PSF has relatively good solubility due to aliphatic isopropylidene group in the backbone. PSF can be soluble in less polar solvents including tetrahydrofuran, 1,4-dioxane, chloroform, dichloromethane, and chlorobenzene.

Polysulfones are basically insoluble in water, but they can absorb the moisture due to highly hygroscopic sulfone groups. Water uptake is sometimes problematic especially in engineering application. In that sense, PSF can significantly reduce the amount of water absorption compared to PES, which carries much sulfone groups in the backbone than PSF.

Resistance to Chemical Environments. Amorphous plastics are generally corroded to undergo cracking when the plastics are exposed to some chemical environments under stress. Polysulfones are not excluded from that and produce environmental stress cracking in certain condition. This environmental stress cracking is considered to relate with solubility of polymers. For example, ketones, esters, aromatic compounds, and chlorinated hydrocarbons easily induce stress cracking to polysulfones. On the other hand, they show good resistance to aliphatic hydrocarbons. Therefore, polysulfones can be good choices for the materials used where oils or greases frequently contact at high temperature.

Polysulfones also exhibit the excellent resistance to hydrolysis. They are not hydrolyzed even by exposure to boiling water, high-pressure steam, acids, bases, and salt solutions. Such good resistance to hydrolysis is the reason that polysulfones are selected as the practical materials prior to polycarbonates, polyesters, and polyamides. Basically, PES shows better resistance to chemical environments than PSF. Thus, PES is preferable for the usage in harsh condition. If PSF and PES are not enough to the target conditions, grass-fiber reinforcement is effective to further improve the chemical environmental resistance.

Radiation Resistance. Polysulfones have good resistance to electromagnetic radiation in the wide range of frequencies including microwave, infrared, and visible regions. Especially polysulfones exhibit excellent resistance to microwave radiation, which makes polysulfones suitable for the application in cookware. On the other hand, polysulfones absorb UV light to induce deterioration in mechanical properties derived from polymer degradation. Such UV-induced losses in mechanical properties are generally avoided by pigmentation and/or reinforcement of the resins.

Processing

As abovementioned, polysulfones show various advantages such as high T_g, transparency, excellent stiffness and strength, low flammability, insulation properties, hydrolysis resistance, and so on. As well as these features, the stability under fabrication process is also crucial for the commercialization of the products.

Polysulfones can be fabricated by various process including injection molding, extrusion, thermoforming, and blow molding. In the injection molding, for example, PSF is molded in the range of 325–400 °C, while PES is fabricated in the range of 360–400 °C. Here, the most important point is the high stability of polysulfones under high temperature. Polysulfones exhibit the excellent thermal oxidation endurance and structure stability under melt-processing condition at high temperature.

In addition, polysulfones produce no toxic and volatile by-products and remain odorless by heating during melt processing.

Applications

Because of the excellent properties and favorable characteristics for processing, polysulfones expand their area of practical applications. By virtue of chemical inertness, high stability in thermal and oxidative conditions, and low toxicity, polysulfones are permitted in various countries to be used in food processing applications with direct food contact such as carafes and service trays. The features required for the cookware are also crucial for the use in medical applications such as trays and devices. For the use in cookware and medical devices, the resistance to sterilization in boiling water, steam, and a variety of disinfectants is also important. For the medical uses, PSF membrane is especially utilized for the hemodiafiltration (artificial kidney).

High oxidation and hydrolysis endurance are suitable for the use in plumbing. Polysulfones are also highly resistant to chlorine and calcium deposits. Therefore, polysulfones are widely used in household plumbing. With chemically inert nature, polysulfone plumbing can be applied in chemical processing equipment.

High insulation properties of polysulfones coupled with low flammability and high-dimensional stability lead to the application in electric and electronic devices including packaging, printed circuit board, lighting sockets, and fuses. Design flexibility and high transparency are favored in the application in aircraft interiors. It also relates to the applications in transparent plastic components such as room dividers and window display case.

In general, both of PSF and PES can be applied to the abovementioned uses. Among them, PSF is often preferable in the view of cost, and PES is selected when higher thermal properties and chemical resistance are required. If both of PSF and PES are short of the requiring properties such as stability and strength, more functional polysulfones such as polyphenylsulfone are the candidates.

Related Entries

▶ Monomers, Oligomers, Polymers, and Macro-molecules (Overview)
▶ Polyphenylenes

References

1. El-Hibri MJ, Nazabal J, Eguiazabal JI, Arzak A (1997) Poly(aryl ether sulfone)s. In: Olabisi O (ed) Handbook of thermoplastics. Marcel Dekker, New York
2. El-Hibri MJ, Weinberg SA (2014) Polysulfones. In: Mark HF (ed) Encyclopedia of polymer science and technology, 4th edn. Wiley, New York
3. Göttgens S, Sanner W (2005) Polysulfones (PSU, PESU, PPSU). Kunstst Plast Eur 10:139–142
4. Clendinning RA, Dickinson BL (1999) Poly(aryl ether sulfone)s. In: Salamone JC (ed) Concise polymeric materials encyclopedia. CRC press LCC, Boca Raton
5. Tsonis CP (1999) Polysulfones. In: Salamone JC (ed) Concise polymeric materials encyclopedia. CRC press LCC, Boca Raton
6. Dizman C, Tasdelen MA, Yagci Y (2013) Recent advances in the preparation of functionalized polysulfones. Polym Int 62:991–1007. doi:10.1002/pi.4525
7. Imai Y (1999) Poly(ether sulfone)s and poly(ether ketone)s (methyl-substituted aromatic). In: Salamone JC (ed) Concise polymeric materials encyclopedia. CRC press LCC, Boca Raton

PET (Poly(ethylene terephthalate)) and PTT (Poly(trimethylene terephthalate))

Tomoyuki Ohishi and Hideyuki Otsuka
Department of Organic and Polymeric Materials, Tokyo Institute of Technology, Tokyo, Japan

Synonyms

Semi-aromatic polyester; Synthetic polyester

Definition

PET (poly(ethylene terephthalate)) is one of the synthetic semi-aromatic polyesters and has

terephthalic acid and ethylene glycol units in main chain. PTT (poly(trimethylene terephthalate)) is also a synthetic aromatic polyester with terephthalic acid and propylene glycol units. Both of PET and PTT are thermoplastics and they are used for various applications such as clothes and bottles. Although the term "polyester" is a category of polymers containing the ester linkages in their main chains, most commonly it refers to PET. PET and PTT are prepared by a polycondensation method from the corresponding monomers.

Introduction

Both of PET and PTT are known as thermoplastics with high mechanical strength, toughness, and fatigue resistance as well as good chemical, hydrolytic, and solvent resistance. They are used for bottles, clothes, packages, sports and recreation goods, household goods, and so on [1–4]. In this essay, preparation, properties, usages, and recycling of PET and PTT are described.

Poly(ethylene terephthalate), PET

PET is the most popular among synthetic polyesters and can be categorized into low-viscosity PET and high-viscosity PET. Low-viscosity PET typically has an intrinsic viscosity of less than 0.75 dL/g, while high-viscosity PET typically has an intrinsic viscosity of 0.9 dL/g or higher [5]. Low-viscosity PET is used in a wide variety of products, such as clothes and bottles. High-viscosity PET is tougher than the low-viscosity one and is used in tire cord, seat belts, etc.

General Synthetic Method of PET

PET is produced commercially from the corresponding monomers: ethylene glycol (EG) and either dimethyl terephthalate (DMT) or terephthalic acid (TA) (Fig. 1). Both of DMT and TA are solids at room temperature; a melting point of DMT is 140 °C and TA sublimes. At the early stage, DMT was available in the required purity but TA was not. Therefore, the DMT process was the first to be commercialized.
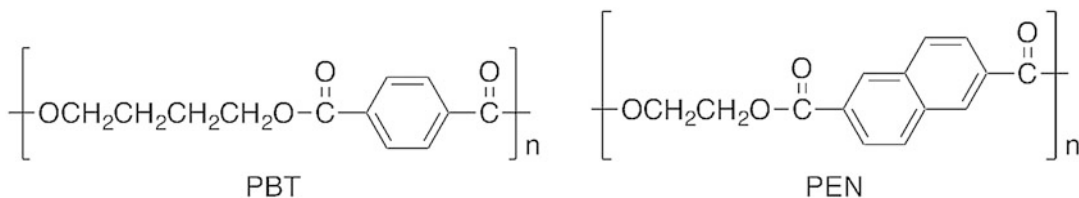
P
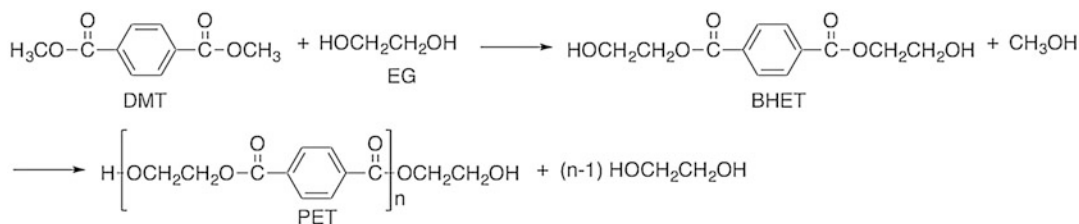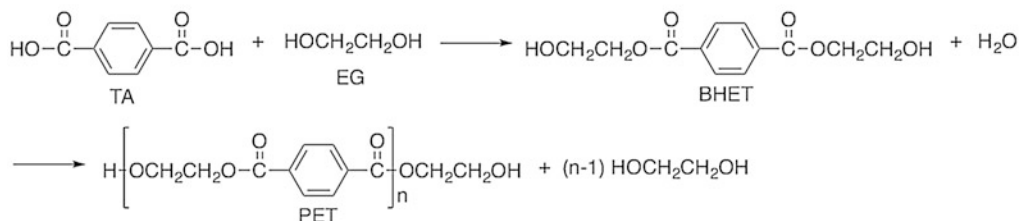
PET (Poly(ethylene terephthalate)) and PTT (Poly(trimethylene terephthalate)), Fig. 1 Synthesis of poly (ethylene terephthalate) (*PET*) by dimethyl terephthalate (*DMT*) and terephthalic acid (*TA*) processes

PET (Poly(ethylene terephthalate)) and PTT (Poly(trimethylene terephthalate)), Fig. 2 Chemical structures of poly(butylene terephthalate) (*PBT*) and poly(ethylene naphthalate) (*PEN*)

Nowadays, both of DMT and TA processes are used, because pure TA is available. In both processes, the intermediate bis(2-hydroxyethyl) terephthalate (BHET) monomer is first generated, accompanied by the elimination of either methanol (DMT process) or water (TA process).

The properties and usefulness of PET depend on the structure by appropriate control of process variables during polymerization and subsequent processing into products. Temperature control and the choice of polymerization catalysts are important to avoid unfavorable side reactions. The production of high-molecular-weight polymer requires the complete removal of the generated water or methanol in the polycondensation process.

Properties of PET

Crystallization Characteristics
Melting temperature of PET is 250–265 °C, and the glass transition temperature (T_g) is 67–81 °C [6]. PET can exist both as an amorphous polymer with high transparency and as a semicrystalline polymer, depending on its thermal and processing history. Furthermore, the thermal expansion coefficient and water absorption are small, and excellent dimensional stability is known. PET is not suited for injection molding because of its slower crystallization kinetics than polyamide and polyacetal.

The well-known method of increasing the rate of crystallization is increasing the number of crystal nuclei by the addition of nucleating agents. Highly crystallized PET by using nucleating agents does not deform even near the melting temperature. Such highly crystallized PET is used as heat-resistant food container. Also, there is a method of growing crystals in the crystallization temperature range or a method of growing crystal at low temperature by lowering the T_g by the addition of a plasticizer. Transparent containers for food products are produced by this method.

Poly(butylene terephthalate) (PBT) has high degree of crystallinity and melting temperature similar to PET (Fig. 2) [7]. PBT has lower temperature crystallization region than PET, and the crystallization kinetics is faster. Furthermore, fluidity in the mold is good because it has a low melt viscosity. PBT is excellent as an injection molding material.

Chemical Resistance and Gas Permeability
PET is not tolerant of various pharmaceuticals including alcohol. In particular, PET can be decomposed by transesterification in the presence of alcohol. On the other hand, PET dissolves or swells in trifluoroacetic acid, phenol, cresol, and chlorinated hydrocarbon [6]. Concentrated sulfuric acid or nitric acid can decompose PET. PET shows inferior stability to an aqueous heat treatment.

PET shows oxygen permeability; therefore, antioxidants such as vitamin C are added to the beverages inside PET bottles for long-term storage. Poly(ethylene naphthalate) (PEN) has rigid molecular chain because it has naphthalene 2,6-dicarboxylic acid units (Fig. 2). PEN has excellent hydrolysis resistance and ultraviolet light barrier resistance. Furthermore, oxygen permeability of PEN is much lower than that of PET.
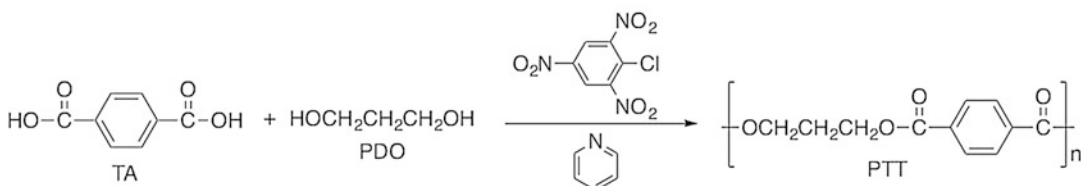
Recycling of PET

The chemical nature of PET permits easy recyclability by some recycling methods. Recycling
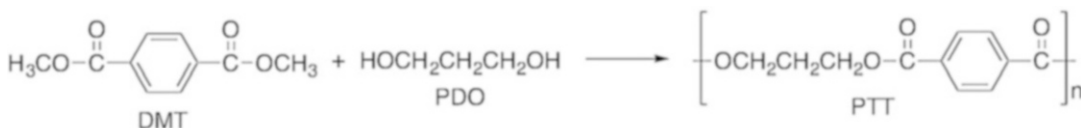
PET (Poly(ethylene terephthalate)) and PTT (Poly (trimethylene terephthalate)), Fig. 3 Synthesis of poly(trimethylene terephthalate) (*PTT*) by transesterification method from dimethyl terephthalate (*DMT*) and 1,3-propanediol (*PDO*)

PET (Poly(ethylene terephthalate)) and PTT (Poly (trimethylene terephthalate)), Fig. 4 Synthesis of poly(trimethylene terephthalate) (*PTT*) by direct polycondensation method in the presence of picryl chloride from terephthalic acid (*TA*) and 1,3-propanediol (*PDO*)

of PET has become an important process from the environmental viewpoint, and it has given commercial opportunity due to wide spread use and availability of PET bottles, packages, and fibers [8, 9]. While material recycling is well established, chemical recycling is highly dependent on the manner in which the depolymerization is carried out. The chemical recycling methods include processes such as alcoholysis, hydrolysis, aminolysis, and other processes [10]. For instance, controlled hydrolysis of polyethylene terephthalate using dilute HNO_3 as the catalyst is possible, and the acid hydrolysis is shown to be much more efficient compared to neutral and alkaline hydrolysis [11].

Poly(trimethylene terephthalate), PTT

Poly(trimethylene terephthalate) (PTT) is a recently commercialized aromatic polyester made by the melt polycondensation of 1,3-propanediol (PDO) and TA or DMT. Processes for spinning this polymer for use as carpet, textile, and nonwoven fibers and for special use as racket guts and musical bowstrings, umbrella fabric, artificial leather, and so on have been developed [12].

Synthesis of PTT by Direct Esterification and Polycondensation

PTT can be synthesized by polycondensation with purified TA or DMT and PDO (Fig. 3). The transesterification reaction can be catalyzed by ethylene glycol titanate, and antimony acetate catalyst can be used in the polycondensation reaction.

The direct polycondensation route is a generic polyester synthesis route, which is industrially carried out at high temperature above 200 °C under vacuum. In the laboratory scale, however, the synthesis of the PTT under mild conditions is also possible in the presence of picryl chloride, using pyridine as solvent (Fig. 4) [13]. In this case, purified TA and PDO react one another, giving PTT in good yield. This reaction generates trinitrophenyl ester of the active intermediate. This active ester reacts with alcohol to form a new ester linkage through an ester exchange reaction.

Bio-based PTT

PTT is a recently commercialized polyester as trade names Corterra® and bio-based Sorona® produced by Shell Chemicals and DuPont,

P

respectively [14, 15]. PTT is produced by the polycondensation reaction of PDO with TA or DMP. At the early stage, the main problem in commercialization of PTT was the high cost of PDO production, which was solved by Shell Chemicals. They developed the low-cost method of producing PDO from ethylene oxide. At present, the PDO used for the polymerization can be prepared either chemically or biologically. DuPont recently developed a biological process for the large-scale production of PDO using corn sugar as the raw material in place of petroleum [14–16]. DuPont's Sorona® is made from PDO derived from renewable corn sugar and terephthalic acid derived from fossil fuel. As a result, Sorona® production uses less energy and reduces greenhouse gas emissions [12].

References

1. Reese G (2003) Polyester fibers. In: Mark HF (ed) Encyclopedia of polymer science and technology, vol 3, 3rd edn. Wiley, New York, pp 652–678
2. Odian G (2004) Principles of polymerization, 4th edn. Wiley, Hoboken, New Jersey, pp 92–97
3. East AJ (2005) Polyester fibres. In: McIntyre JE (ed) Synthetic fibers, nylon, polyesters, acrylic, polyolefine. The Textile Institute, Wood Head Publishing Limited, Cambridge, pp 95–167
4. Venkatachalam S, Nayak SG, Labde JV, Gharal PR, Rao K, Kelkar AK. (2012) Degradation and recyclability of poly (ethylene terephthalate). In: Saleh HEDM (ed) Polyester, InTech, pp 75–98 http://www.intechopen.com/download/get/type/pdfs/id/39405
5. http://www.epa.gov/ttnchie1/ap42/ch06/final/c06s06-2.pdf
6. Rule M (1999) Physical constants of poly (oxyethylene-oxyterephthaloyl) (poly(ethylene terephthalate)). In: Brandrup J, Immergut EH, Grulke EA (eds) Polymer handbook, 4th edn. Wiley, New York, pp V113–V117
7. (a) Hobbs SY, Pratt CF (1975) Multiple melting in poly (butylene terephthalate). Polymer 16:462–464. (b) Pratt CF, Hobbs SY (1976) Comparative study of crystallization rates by d.s.c. and depolarization microscopy. Polymer 17:12–16
8. Cagiao ME, Calleja FJB, Vanderdonckt C, Zachmann HG (1993) Study of the morphology of semicrystalline poly (ethylene terephthalate) by hydrolysis etching. Polymer 34:2024–2029
9. Seo KS, Cloyd JD (1991) Kinetics of hydrolysis and thermal degradation of polyester melts. J Appl Polym Sci 42:845–850
10. Paszun D, Spychaj T (1997) Ind Eng Chem Res 36:1373–1383
11. Upasani PS, Jain AK, Save N, Agarwal US, Kelkar AK (2012) Chemical recycling of PET flakes into yarn. J Appl Polym Sci 123:520–525
12. http://www.dupont.com/products-and-services/fabrics-fibers-nonwovens/fibers/brands/dupont-sorona.html
13. Tanaka H, Iwanaga Y, Wu G, Sanui K, Ogata N (1982) Synthesis of polyesters by direct polycondensation with picryl. chloride Polym J 14:643–648
14. Kurian JV (2005) A new polymer platform for the future – Sorona® from corn derived 1,3-propanedio. J Polym Environ 13:159–167
15. Chuah HH (2004) Synthesis, properties and applications of poly (trimethylene terephthalate). In: Scheirs J, Long TE (eds) Modern polyesters: chemistry and technology of polyesters and copolyesters. Wiley, Chichester, pp 361–397
16. Wolfson W (2006) Spinning corncobs into socks farming plastics with "green" chemistry. Chem Biol 13:109–111

PET and Other Polyester Synthesis

Colin Wright and Coleen Pugh
Department of Polymer Science, Maurice Morton Institute of Polymer Science, The University of Akron, Akron, OH, USA

Definition

Polymers with ester (primarily $-CO_2-$) linkages in the polymer backbone result in the ability to undergo slow degradation; polyesters are typically biocompatible and biodegradable. (Polymers with an ester substituent pendant to the polymer backbone are not categorized as polyesters.)

Introduction and Historical Background

The first known natural polyester was shellac, which is secreted by the female *lac* insect. In ancient Egypt, it was used to embalm mummies, whereas it is now used in nail polish and as a primer coating on wood and other objects. Therefore, the first uses of polyesters were as adhesives

and coatings, applications that are now served by alkyd resins.

A more recently explored class of natural polyesters is the polyhydroxyalkanoates (PHAs), which are produced from carbon sources such as glucose by many microorganisms when under stress and accumulate as intracellular granules [1]. The PHAs are biocompatible and biodegradable and therefore applicable to biomaterials and eventually as sustainable replacements for conventional petroleum-derived plastics.

Synthetic polyesters [2] were first developed by Carothers and coworkers at DuPont in the late 1920s and 1930s. They first synthesized low molecular weight polyesters by polyesterification of aliphatic dicarboxylic acids with aliphatic diols and then established the ability to synthesize high molecular weight polyesters by removing water as it formed as the condensation by-product.

The synthetic polyester produced in highest volume is poly(ethylene terephthalate) (PET), which is produced by polyesterification of terephthalic acid with ethylene glycol.

Figure 1 presents the chemical structures of several common commercial polymers. Polyesters are used extensively as fibers and thermoplastics, although highly cross-linked thermosets are produced by curing alkyd resins, which are based on unsaturated polyesters.

Polyesters are not limited to simple linear structures; for example, introducing monomers with multiple functional groups causes branching in the polymer. Polyester dendrimers have been made by both convergent and divergent (Fig. 2) syntheses and are useful because of the large number of end groups in their well-controlled structures [3]. Star polyesters are of interest because the composition and number of arms can be tuned to control their physical properties [4].

There are many ways to modify the physical properties of polyesters [5]. Synthetically, the simplest approach is to control the polymer's molecular weight. Other approaches include by copolymerization of multiple monomers, adding functional monomers, varying the molecular architecture (linear, cycles, branched, stars, dendrimers), and cross-linking, including with
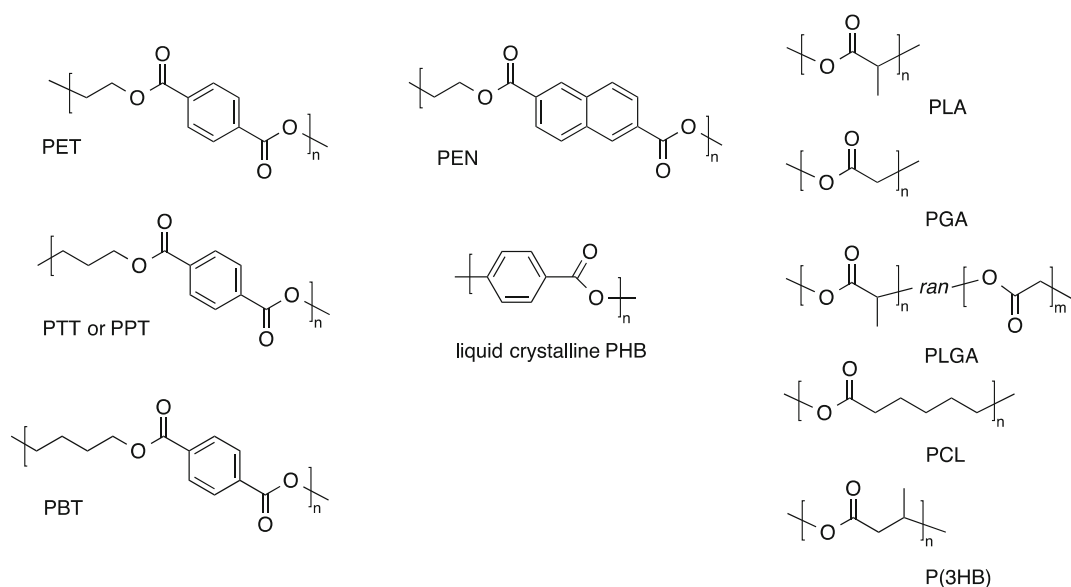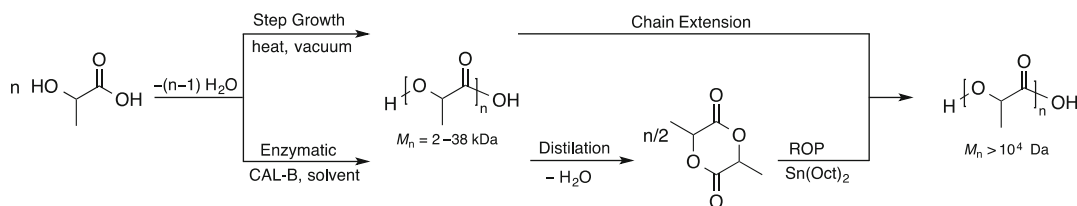

PET and Other Polyester Synthesis, Fig. 1 Chemical structures of common polyesters: *PET* poly(ethylene terephthalate), *PTT* poly(trimethylene terephthalate), *PPT* poly(propylene terephthalate), *PBT* poly(butylene terephthalate), *PEN* poly(ethylene naphthalate), *PHB*

poly(*p*-hydroxybenzoate), *PLA* poly(lactic acid), *PGA* poly(glycolic acid), *PLGA* poly(lactic acid–*co*–glycolic acid), *PCL* poly(ε-caprolactone), *P(3HB)* poly(3-hydroxybutyrate)
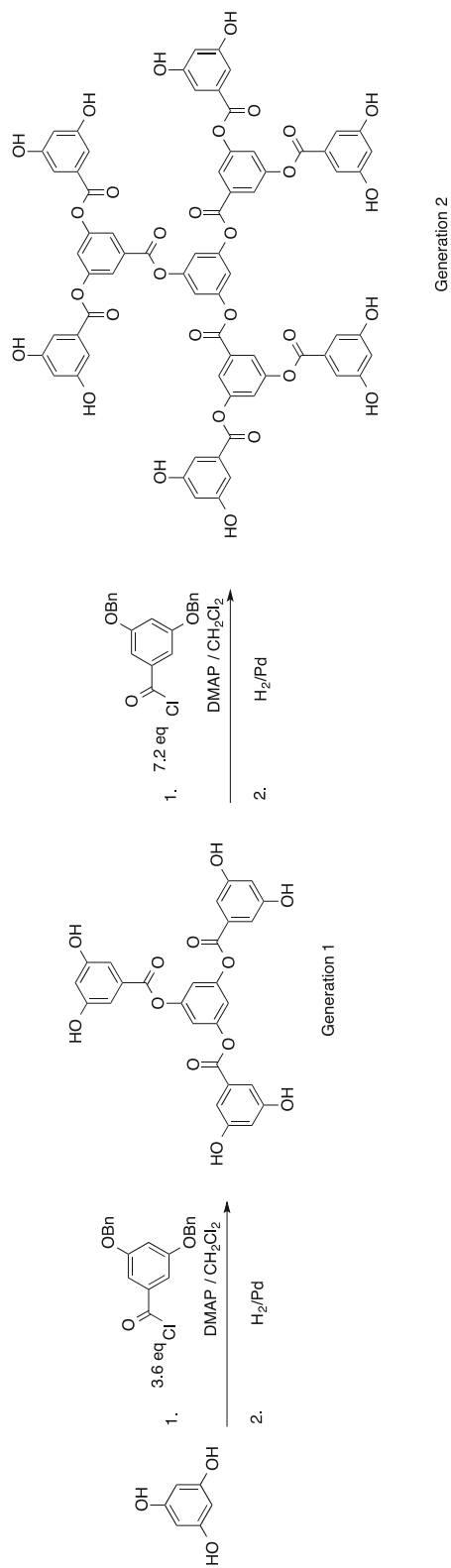
PET and Other Polyester Synthesis, Fig. 2   Example synthesis of a dendritic polyester

PET and Other Polyester Synthesis, Fig. 3 Three synthetic routes to polyesters using PLA as an example

variations in the cross-link density. The properties can also be manipulated physically by blending polymers, adding fillers, and annealing to increase crystallinity.

This chapter will focus on PET [5, 6], an important polymer for commodity applications, and poly(lactic acid) (PLA [7]), an important polymer for biological applications, although it is rapidly being developed for durable applications due to its sustainability and compostability.

Synthetic Routes

As outlined in Fig. 3 using PLA as an example, there are three main routes for synthesizing polyesters [2, 8]: step-growth polymerization, ring-opening polymerization (ROP), and enzymatic polymerization.

Simple condensation of lactic acid produces low molecular weight PLA with $M_n = 2,000–10,000$ g/mol, while more involved processes like azeotropic dehydrative condensation or chain extension can produce PLA with molecular weights above 10^4 g/mol. Similarly, PET is made in two steps to produce a final polymer with an M_n between 19,200 and 26,800 g/mol.

ROP is generally preferred over step-growth polymerization because it is better controlled, with polydispersity (Đ) often being less than 1.5. PLA can be polymerized by ROP using tin catalysts to produce polymers with molecular weights $>10^4$ g/mol. Poly(caprolactone) (PCL) with M_n ranging from 530 to 630,000 can also be synthesized by ROP [9]. Aromatic polyesters are also prepared from oligomeric macrocycles (rings with ≥ 14 atoms) to produce polymers with M_n 50,000–136,800 Da [10]. Ring-opening

polymerizations are covered in other sections of this encyclopedia.

The third main route for synthesizing polyesters is by enzymatic polymerization [11, 12] of hydroxyalkanoic acid and lactone monomers. The enzyme can be either free in solution or immobilized on a resin. CAL-B (or its immobilized equivalent, Novozym 435) is a popular enzyme for the synthesis of polyesters. L-Lactide has been polymerized using Novozym 435 in the presence of ionic liquids to produce PLLA with M_n around 37,800 Da. This is a growing area of research that strives to eliminate the need for toxic heavy metal catalysts while making the synthesis greener. Enzymatic polymerizations are covered in another entry in this section.

In addition to these three main routes, PHAs, especially poly(3-hydroxybutyrate) (P3HB), are currently produced metabolically [1] by Metabolix using microorganisms in fermenters.

## Synthesis of Polyesters by Polycondensations

As outlined in Fig. 4, polyesters are synthesized by step polymerizations by polycondensation of hydroxycarboxylic acids, or their esters or acid chlorides, with diols (AA + BB polymerization), as well as by polyesterification of the corresponding hydroxycarboxylic acids and derivatives (AB polymerization) [2, 8]. The esterification of carboxylic acids with an alcohol and transesterification of esters are both equilibrium reactions in which the small molecule by-products (water and alcohol, respectively) must be removed to achieve high molecular weight. In this case, the polymerization is usually performed in bulk in the melt state under vacuum to remove the
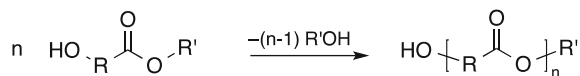
PET and Other Polyester Synthesis,
Fig. 4 Synthesis of polyesters by condensation reactions of dicarboxylic acids or their derivatives with diols or of hydroxycarboxylic acids or their derivatives

Reversible Reactions
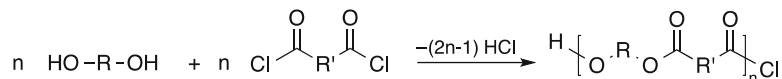
- carboxylic acid - alcohol esterification
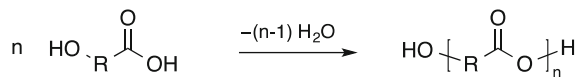
- transesterification

Irreversible Reactions

- carboxylic acid chloride - alcohol esterification

condensation by-product and in the presence of an acid catalyst to speed the reaction. Alternatively, the polymerization can be performed in solution in a solvent such as toluene that forms an azeotrope with the water or alcohol, and the azeotrope is removed by distillation throughout the polymerization to shift the equilibrium in the forward direction. Finally, the polymerization can be performed in a solvent at room temperature in the presence of a dehydrating agent such as a carbodiimide.

In contrast, the equilibrium of an esterification of a carboxylic acid chloride with an alcohol lies far to the side of the ester product and is therefore considered irreversible. In this case, the polymerization can be performed in solution without removing the small molecule by-product. However, it is advantageous to add an amine base to further activate the acid, as well as to consume the acid chloride generated.

Biological Uses of Polyesters

Polyesters play a large role in biological applications [13–15]. One of the most popular polyesters for biological use is PLA. Polyesters are part of the "2nd generation" of biological materials. They are designed to be resorbed by the body and to be bio-inert. Polyesters have found roles in almost all types of biomedical applications, including drug delivery, tissue engineering, dental work, bone regeneration, and as endodontic

sealers. The physical properties of biomaterials based on polyesters can be manipulated synthetically through variations in polymer molecular weight, and by copolymerization, such as copolymerization of LA and glycolic acid (GA) to produce PLGA, as well as physically through blending and even variations in device design.

Polyesters synthesized via step-growth polymerization tend to have lower molecular weight and a broader polydispersity. Although ROP produces high molecular weight polymers, purification is required to remove heavy metal catalysts for biological applications. Many researchers are therefore focusing on using enzymes to produce polyesters. This is an exciting and promising area of research.

PLA

PLA is prepared from lactic acid, which has two stereoisomers: polymerization of pure L-lactic acid (or L-lactide) produces PLLA and polymerization of pure D-lactic acid (or D-lactide) produces PDLA. PLA can be synthesized by all three of the main synthetic routes outlined in Fig. 3, with the most common route being ROP of lactides. PLA is popular in the biomedical field because of its biocompatibility and biodegradability and because the T_g of PLA and PLGA is higher than the body temperature (37 °C). PLA is a bulk-eroding polymer. In the form of a block
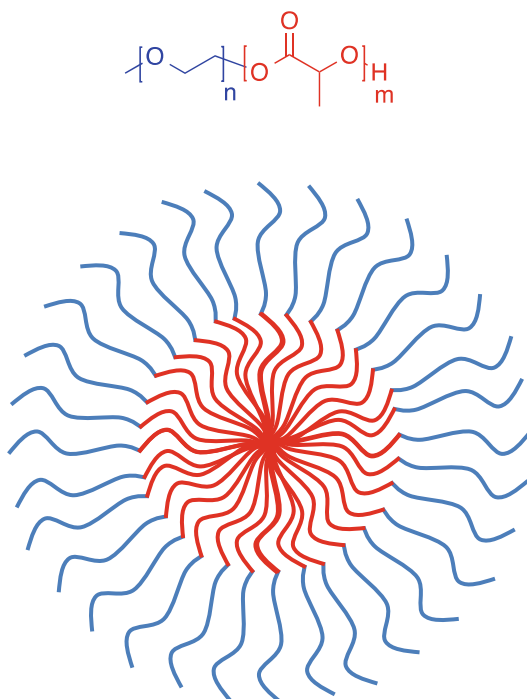
PET and Other Polyester Synthesis, Fig. 5 Micelle formation and drug encapsulation using block copolymers of a hydrophobic polyester block and a hydrophilic PEO block

copolymer with a hydrophilic block like poly (ethylene oxide) (PEO or PEG), PLA can encase hydrophobic drugs like paclitaxel and docetaxel in the core of micelles (Fig. 5), in which PLA is in the core and the hydrophilic PEO block is in the corona. These micelles help to solubilize the drug, protect the drug from being eliminated from the body, and deliver it where needed.

Commodity Uses of Polyesters

Linear aromatic polyesters are processed into films, fibers, injection, and blow molded parts and are therefore widely used as packaging materials, textile fibers, and bottles or containers. Liquid crystalline polyesters were developed to lower the processing temperature of aromatic polyesters and to increase their mechanical properties by extension and orientation during processing; however, the melting temperature of completely aromatic polyesters like

poly(p-hydroxybenzoate) (PHB) in Fig. 1 is too high to readily process and must be modified with comonomers to reduce the melting temperature. Polyesters are also used to produce block copolymer elastomers, in which the high-Tg polyester block acts as a physical cross-link for the soft block. Polyesters can be modified as described previously in order to become tougher, less brittle, and less thermally sensitive.

PET

The most important commercial polyester is PET [5, 6, 16]. It was discovered in 1946 and is produced all over the world; as of 2011, China is the largest producer of PET. PET has a white or cream color, is chemically and thermally stable, and is resistant to acids, bases, some solvents, and hydrocarbons. It is approved by the FDA for use in food packaging materials. PET is resistant to mildew, abrasions, and aging.

PET is made commercially by one of two routes (Fig. 6). The first route is direct esterification of terephthalic acid with ethylene glycol, followed by polycondensation with elimination of ethylene glycol as the condensation by-product. The second route involves transesterification of dimethyl terephthalate with ethylene glycol, followed by polycondensation with elimination of ethylene glycol. The dimethyl terephthalate was more common before highly pure terephthalic acid became readily available. PET is made in two steps by first synthesizing bis(hydroxyethyl terephthalate) (BHET) or a prepolymer (M_n between 4,800 and 6,700 g/moL). BHET or the prepolymer is then chain extended in the melt by heating under vacuum to produce a final polymer with M_n between 19,200 and 26,800 g/moL.

Degradation and Recycling of Polyesters

The polyesters that are traditionally used for commodity applications have long lifetimes before they degrade. The life-span is often decades longer than that of the products they are used for. Waste plastic has therefore accumulated

P
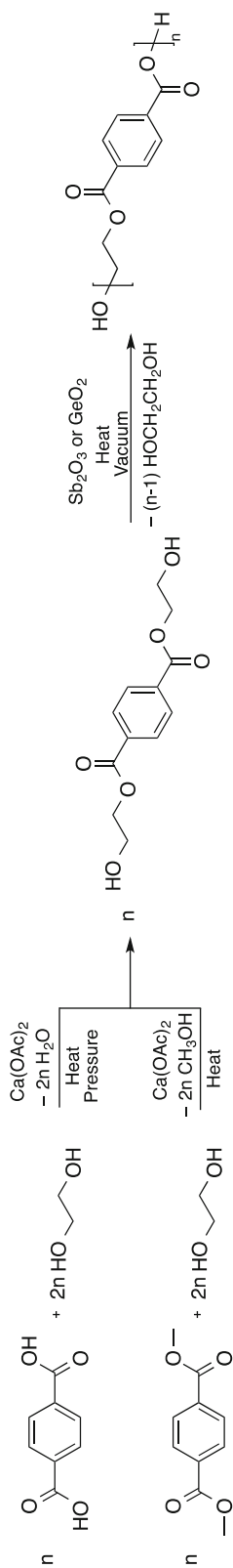
PET and Other Polyester Synthesis, Fig. 6 Industrial syntheses of PET

and will remain for long periods of time. Aliphatic polyesters are well situated to replace petroleum-based aromatic polyesters and polymers like polyethylene and polypropylene because they degrade relatively fast. Polyesters can be degraded by hydrolysis, solvolysis (in protic solvents such as methanol, ethanol, glycol, and water), and aminolysis and by naturally occurring enzymes, with the rate of hydrolysis being greatest for aliphatic polyesters, especially those that are amorphous.

Because of the large amount of PET in existence, considerable attention has been devoted to how to recycle the polymer [17]. Although it will slowly degrade as described above, the volume of PET waste accumulates each year. PET waste is also recycled using mechanical means such as flotation or solution washing. One disadvantage of mechanical recycling is the temperatures are not high enough to ensure sterilization of the recycled PET, and recycled PET therefore cannot be used for food applications. The waste products produced as part of the recycling process can also limit PET's recyclability.

Summary

Polyesters are a well established but growing class of polymers that will continue to play a major role in everyday life. Although PET will likely continue to be the most important polyester for commodity applications, the production and applications of green polyesters derived from green processes or renewable resources will also grow. Since these green polyesters are both sustainable and degradable in a relatively short time, their use as commodity polymers that replace nonbiodegradable petroleum-based polymers like PE and PP will grow if oil prices remain high, and they will continue to be major components of the "fourth-generation" biomaterials.

Related Entries

References

1. Suriyamongkol P, Weselake R, Narine S, Moloney M, Shah S (2007) Biotechnological approaches for the production of polyhydroxyalkanoates in microorganisms and plants – A review. Biotechnol Adv 25:148–175
2. Odian G (2004) Principles of polymerization, 4th edn. Wiley-Interscience, Hobken, pp 40–198
3. Twibanire JDK, Grindley TB (2012) Polyester Dendrimers. Polymers 4:794–879
4. Cameron DJA, Shaver MP (2011) Aliphatic polyester polymer stars: synthesis, properties and applications in biomedicine and nanotechnology. Chem Soc Rev 40:1761–1776
5. Deopura BL, Alagirusamy R, Joshi M, Gupta B (eds) (2008) Polyesters and polyamides, vol 71. Woodhead Publishing, Cambridge, UK
6. Aizenshtein EM (2013) Present and future polyethylene terephthalate fibres. Fibre Chem 45:125–132
7. Gupta B, Revagade N, Hilborn J (2007) Poly(lactic acid) fiber: An overview. Prog Polym Sci 32:455–482
8. Braun D, Cherdron H, Rehahn M, Ritter H, Voit B (2013) Polymer synthesis: theory and practice fundamentals, methods, experiments. Springer, Berlin
9. Labet M, Thielemans W (2009) Synthesis of polycaprolactone: a review. Chem Soc Rev 38:3484–3504
10. Hodge P (2014) Entropically Driven Ring-Opening Polymerization of Strainless Organic Macrocycles. Chem Rev 114:2278–2312
11. Kobayashi S, Makino A (2009) Enzymatic Polymer Synthesis: An Opportunity for Green Polymer Chemistry. Chem Rev 109:5288–5353
12. Idris A, Bukhari A (2012) Immobilized Candida antarctica lipase B: Hydration, stripping off and application in ring opening polyester synthesis. Biotechnol Adv 30:550–563

P

13. Hench LL, Polak JM (2002) Third generation bio-medical materials. Science 295:1014–1017
14. Battistella E, Varoni E, Cochis A, Palazzo B, Rimondini L (2011) Degradable polymers may improve dental practice. J Appl Biomater Biomech 9:223–231
15. Dinarvand R, Sepehri N, Manouchehri S, Rouhani H, Atyabi F (2011) Polylactide-co-glycolide nanoparticles for controlled delivery of anticancer agents. Int J Nanomedicine 2011:877–895
16. MacDonald WA (2002) New advances in poly(ethylene terephthalate) polymerization and degradation. Polym Int 51:923–930
17. Dutt K, Soni RK (2013) A Review on Synthesis of Value Added Products from Polyethylene Terephthalate (PET) Waste. Polym Sci Ser B 55:430–452

Petroleum Resin

Shinji Sugihara
Department of Applied Chemistry and Biotechnology, Graduate School of Engineering, University of Fukui, Bunkyo, Fukui, Japan

Synonyms

C_5/C_9 hydrocarbon resin

Definition

Thermoplastic hydrocarbon resins/polymers derived from monomers of cracked petroleum fractions such as C_5, C_9, and dicyclopentadiene feedstocks.

General Introduction

Petroleum resin is term in common use for low molecular weight, about M_w 500–5,000, thermoplastic hydrocarbon resins derived from cracked petroleum fractions. They are to be distinguished from high polymers such as polystyrene and polypropylene, which are pure-monomer-based resins essentially made from pure starting materials such as styrene and propylene, respectively. The petroleum resin generally has a tackifying effect and is suitable for use in paints and varnishes, coatings, printing ink, lithographic inks, paper, adhesives, rubber, concrete-curing compounds, and other areas where tackiness is required, literally in thousands of applications [1, 2].

Historically speaking, early petroleum resins were soft, unstable, and dark. However, they have been continuously improved to the point with the times. In the early 1940s, the United Gas Improvement Company (UGI) of Philadelphia, Pennsylvania, made an extensive study of conditions for cracking crude oil to obtain a high yield of resin formers and produced a pitch with low free-carbon content [3]. One index of the depth of cracking is the volume of gas produced per volume of crude oil fed to the unit.

Depending on the nature of the starting materials, which come from the deep cracking of petroleum distillates, three main petroleum resins are classified: aliphatic, aromatic, and dicyclopentadiene (DCPD) [4]. The petroleum distillates are called naphtha, and the feed streams to produce hydrocarbon resins are by-products of the naphtha cracking as shown in Fig. 1. Strictly speaking, naphtha is defined as the fraction of hydrocarbons in petroleum boiling between 30 °C and 200 °C. It consists of a complex mixture of hydrocarbon molecules generally having between 5 and 12 carbon atoms (C_{5-12}). It typically constitutes 15–30 % of crude oil, by weight. The naphtha can be divided into two groups: light naphtha (fraction boiling between 30 °C and 90 °C with 5–6 carbons) and heavy naphtha (fraction boiling between 90 °C and 200 °C with 6–12 carbons) [5].

Aliphatic Petroleum Resins

Aliphatic petroleum resins are mainly based on C_5 (including a small amount of C_4, and C_6) feedstock (C_5 resin oil) containing varying amounts of piperylene (1,3-pentadiene), isoprene, and various monoolefins in addition to nonpolymerizable paraffinic compounds. Figure 2 shows the polymerizable monomers (unsaturated compounds) in C_5 feedstock. The composition of the feedstock determines the
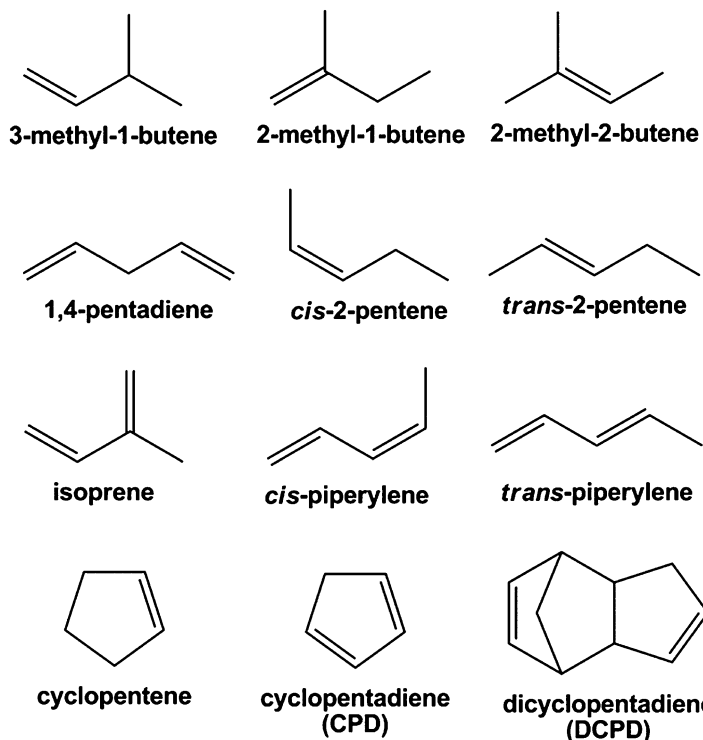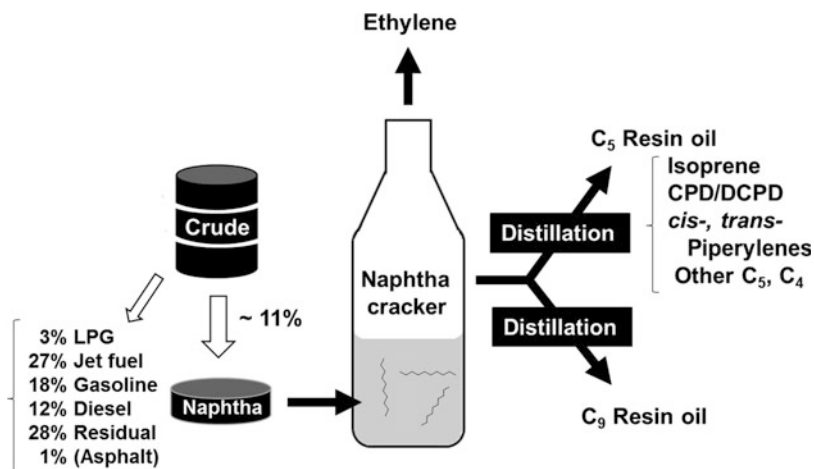
usefulness of C_5 resins [4]. As an example, the typical components (wt%) of C_5 feed identified by gas chromatography are shown in Table 1 [5]. The liquid C_5 feedstock can generally be polymerized to a hard resin using a Lewis acid catalyst and carefully selecting temperature and pressure to obtain the desired softening point and molecular weight. For Lewis acid catalysts,

$AlCl_3$ and BF_3 are the catalysts most often used for the polymerizations, i.e., cationic polymerization [6–8]. Other effective catalysts include $AlBr_3$, $TiCl_4$, $SnCl_4$, alkyl aluminum chlorides, and certain activated clays, such as attapulgite and montmorillonite. Brønsted acids such as H_2SO_4 and HCl/ether may be used as well [9]. In the presence of aluminum halides, resins

with higher molecular weight are formed than in the presence of BF$_3$ complexes. The structure of the polymerized resin is difficult to characterize since the various isomers of the feedstock will combine unpredictably. Otherwise, thermal polymerization is also applied to the preparation of the resins. The thermal polymerization is based on free radicals in the absence of catalyst, which is cheaper than cationic method, but it ends to produce darker resins. The thermally polymerized resin properties are not comparable with those of the cationically polymerizable resins due to limited controlling parameters of the polymerization.
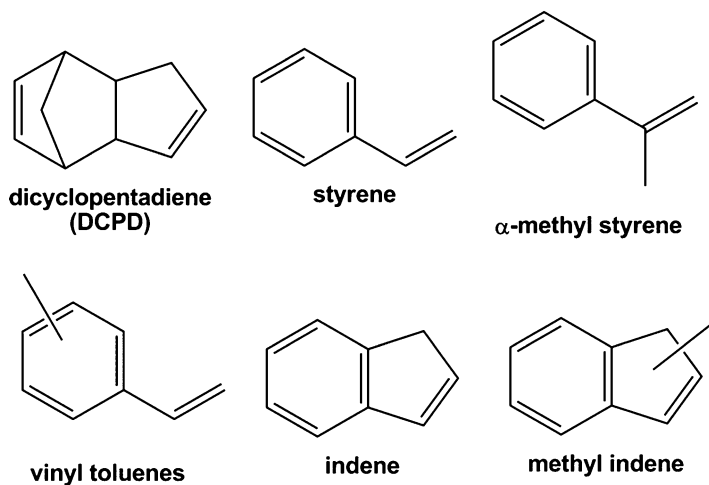
After polymerization, the catalysts are removed to give clear stable resin. These methods including thermal and cationic polymerization for aliphatic resin are the same as that for aromatic and dicyclopentadiene resins. These resin products are conditioned in flake, powder, granule, dispersion, or other forms and then widely used all over the world.
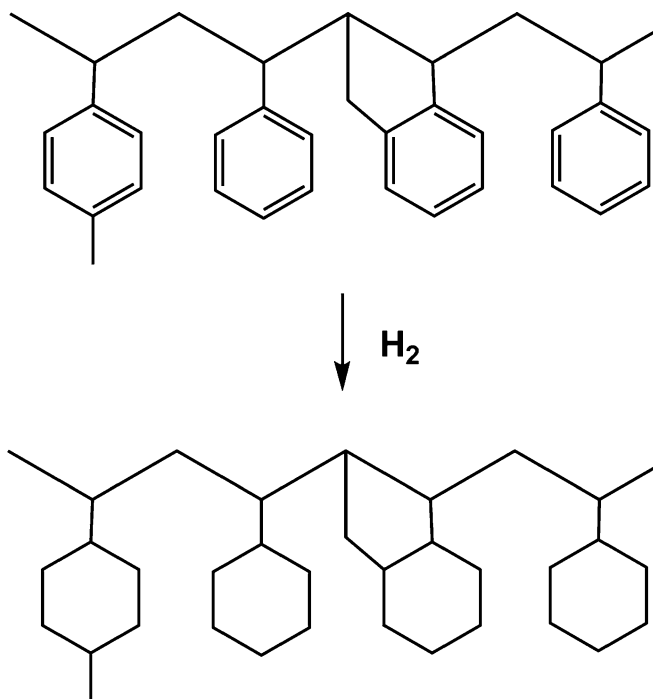
Aromatic Petroleum Resins and Their Hydrogenated Resins

Aromatic petroleum resin contains significant quantities of polyindenes, which are polymerized from indene being one of C$_9$ feedstock. The typical boiling range at atmospheric pressure is about 140–200 °C. Thus, lower boiling C$_5$ hydrocarbons are not present in this aromatic resin as shown in Table 1. Thus, such aromatic resins are produced from C$_9$ resin oil (including C$_8$, and C$_{10}$) that contains various monomers as illustrated in Fig. 3. Here, vinyl groups are basically reacted in order to produce aromatic resins as shown in Fig. 4. However, since C$_9$ resin oil is a relatively unrefined material, its polymerization

Petroleum Resin, Table 1 Composition of the resin oils

Petroleum resin	Components (wt%)
C$_5$ aliphatic	Isopentane (15.0), *n*-pentane (22.1), 3-methyl-1-butene (0.6), 2-methyl-1-butene (4.7), 2-methyl-2-butene (2.6), 1-pentene (3.4), 2,2-dimethyl butane (0.1), 1,4-pentadiene (1.6), *cis*-, *trans*-2-pentenes (5.4), 2,3-dimethyl butane (0.1), isoprene (15), 2-methyl pentane (0.6), 3-methyl pentane (0.3), cyclopentane (0.9), *n*-hexane (2.1), *cis*-, *trans*-piperylenes (8.7), cyclopentene (1.8), CPD/DCPD (14.5), other C$_4$ (0.5)
C$_9$ aromatic	Paraffins, benzene, toluene, styrene, α-methyl styrene, vinyl toluenes, indene, methyl indenes
Dicyclopentadiene (*DCPD*)	DCPD (70–95), codimers of DCPD with other dienes (e.g., methylcyclopentadiene, methylcyclopentadiene dimer, butadiene, isoprene, as well as styrene and/or indene)

Petroleum Resin, Fig. 3 C$_9$ petroleum resin oil composition (monomers for aromatic resins)

dicyclopentadiene (DCPD)

styrene

α-methyl styrene

vinyl toluenes

indene

methyl indene

Petroleum Resin, Fig. 4 Preparation of C_9 petroleum resins via cationic polymerization

styrene (St)
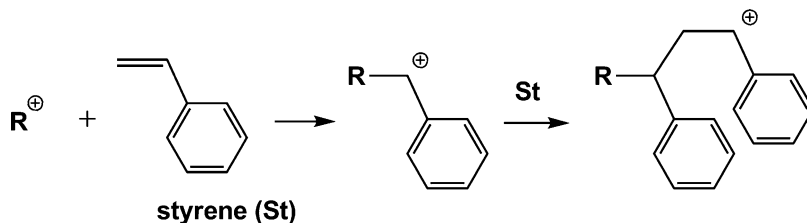
Petroleum Resin, Fig. 5 An example for hydrogenated C_9 petroleum resins

P

leads to much darker resins than other hydrocarbon resins.

C_9 resins are more compatible with polar elastomers than C_5 resins, due to their aromatic structure. However, the double bonds in their aromatic structure are relatively unstable. An effective way to stabilize these resins is to hydrogenate them. Thus, resins are often hydrogenated in solution. During hydrogenation, the aromatic ring structures gradually lose their aromatic nature and become cycloaliphatic as shown in Fig. 5. When the process is allowed to go to completion, the resultant product is fully hydrogenated hydrocarbon resin with full aliphatic character. The process can also be adjusted to prepare the partly hydrogenated resins, which is widely used in adhesive formulations. This is

because the resins still have some aromatic rings, and the aliphatic/aromatic balance gives these resins their unique properties. In theory, any degree of hydrogenation can be manufactured. Such hydrogenation process also can be applied to C_5 aliphatic resin and DCPD resin given later in order to change the residual C=C double bonds in the resin. As just described, this is a useful process to decrease its color and improve its stability toward heat, oxygen, and ultraviolet light after polymerization.

Dicyclopentadiene Resins

Dicyclopentadiene (DCPD) resin contains 70–95 % of DCPD feedstock with other dienes

Petroleum Resin, Table 2 Typical properties of petroleum resins

Resin	Softening point[a] (°C)	Color[b]	Bromine number[c]	Density (g/cm^3)
C_5 aliphatic	70–150	3–9	25–45	0.88–0.98
C_9 aromatic	95–140	7–11	3–22	1.04–1.09
DCPD	90–100	7–11	55–60	1.11
Hydrogenated C_9	70–140	>1	–	0.98–0.99
Hydrogenated DCPD	85–140	<1	2–3	1.10
C_5-C_9 mixed resins	Liquid-105	2–10	<25[d]	0.86–1.07
Styrene	Liquid-60–80	1–3	Nil	0.98–1.08
α-Methyl styrene	70–145	<1	2–8	1.06–1.08

[a]Measured by ring-and-ball method
[b]Gardner color scale in 50 % solution in toluene
[c]Bromine number (g Br_2/100 g) for degree of unsaturation
[d]Iodine number (g I_2/100 g)

as summarized in Table 1. They are usually manufactured by thermal polymerization in the absence of catalyst. In comparison with aliphatic and aromatic resins, DCPD resins are highly unsaturated. Thus, they can be chemically modified. To prepare the modified resins, either polymerization using special modified feedstock or modification after polymerization is conducted. For example, DCPD resins can react with maleic anhydride, drying oils, or rosin on heat treatment. Of course, catalytic hydrogenation of resins is also conducted to give high-quality water-white resins with a different solubility and compatibility profile than the original resin.

Mixed Resins

C_5 aliphatic and C_9 aromatic resins can be modified by mixing the two or three feed streams together at a carefully chosen ratio to produce hybrid polymers. This ratio determines the aliphatic/aromatic balance of the resin, which is an essential determinant of the resin's compatibility. For example, as the cloud points of the resins decrease, the compatibility with polar and aromatic polymers increases.

Table 2 summarizes typical properties of petroleum resins including their mixed resins and pure-monomer-based resins [4]. Mixed aliphatic/aromatic resins are manufactured with varying proportions of the above-described C_5 and C_9 feedstocks to produce resins with a range of softening points and molecular weights. These resins are chosen as usage. Thus, many resins are widely distributed

Related Entries

▶ Cationic Addition Polymerization (Fundamental)

References

1. Vredenburgh WA, Foley KF, Scarlatti AN (1986) Hydrocarbon resins. In: Mark HF, Bikales NM, Overberger CG, Menges G, Kroschwitz JI (eds) Encyclopedia of polymer science and engineering, vol 7, 2nd edn. Wiley, New York, pp 758–782
2. Hattori A (2005) Characteristics of petroleum resins for adhesives. TOSOH Res Technol Rev 49:69–72
3. McKetta JJ (ed) (1994) Encyclopedia of chemical processing and design. Marcel Dekker, New York
4. Zohuriaan-Mehr MJ, Omidian H (2000) Petroleum resins: an overview. J Macromol Sci Rev Macromol Chem Phys C40:23–49
5. Antos GJ, Aitani AM (eds) (2004) Catalytic naphtha reforming, second edition, revised and expanded. CRC Press, Boca Raton
6. Kennedy JP, Marechal E (1991) Carbocationic polymerization. Krieger, Malabar
7. Sawamoto M (1991) Modern cationic vinyl polymerization. Prog Polym Sci 16:111–172
8. Aoshima S, Kanaoka S (2009) A renaissance in living cationic polymerization. Chem Rev 109:5245–5287
9. Sugihara S, Tanabe Y, Kitagawa M, Ikeda I (2008) Facile metal-free living cationic polymerisation of various vinyl ethers by hydrogen chloride with ether. J Polym Sci Part A Polym Chem 46:1913–1918

Phase Behavior and Chemical Engineering Applications of Hyperbranched Polymers

Matthias Seiler[1] and Tim Zeiner[2]
[1]Heitkamp and Thumann group Düsseldorf, Evonik Degussa, Essen, North Rhine-Westphalia, Germany
[2]Department of Biochemical and Chemical Engineering, Laboratory of Fluid Separations, TU Dortmund, Dortmund, Germany

Synonyms

Chemical engineering applications or applications in separation science; Hyperbranched polymers or dendritic polymers; Phase behavior or solution behavior or thermodynamics

Definition

The phase behavior of hyperbranched polymers describes the phase separation of hyperbranched polymer blends/solutions in at least two phases in thermodynamic equilibrium. In the context of this entry, this could be two liquid phases or a liquid and a vapor phase.

The application of hyperbranched polymers in chemical engineering processes shown in this work refers to the use in process engineering applications as membrane processes or as extraction agent.

Introduction

A number of studies have been published focusing on dilute and semi-dilute properties of dendritic polymer solutions.

Dendritic polymers have a significantly lower intrinsic viscosity, Mark–Houwink exponent, hydrodynamic volume, and ratio of radius of gyration to hydrodynamic radius in comparison to their linear analogues of the same molar mass. Also the osmotic second virial coefficient was object of numerous research studies to characterize the effect of branching. As observed for many branched polymer solutions, branching decreases the second virial coefficient in "good" solvents ([1, 2] and references therein).

The large body of interdisciplinary research on dendritic polymers, i.e., dendrimers, dendrigrafts, and hyperbranched polymers, is a guarantee for emerging applications. For many potential applications of hyperbranched polymers in the field of chemical engineering, the phase behavior of hyperbranched polymer solutions is essential. Therefore, the following chapter gives an overview of the experimentally and theoretically investigated properties of hyperbranched polymer solutions.

The comprehension of the phase behavior is an essential prerequisite for contemporary polymer science and engineering. Phase separation and segregation often occur during the production and processing of polymers, either due to their necessity or owing to undesirable circumstances such as the incompatibility between polymers or an insufficient solvent power. This phase behavior originates in the properties of the polymer molecules in solution [3].

The impact of high-performance polymer blends on modern material science is significant and continuously growing. Especially improvements in performance characteristics such as rigidity, toughness, abrasion resistance, chemical and flame resistance, heat resistance, and ease of processing are of great importance ([1, 2, 4] and references therein). Even though in production and processing the equilibrium state is usually not reached, it is nevertheless of great importance to know what the equilibrium condition of the regarded system would be like, in order to understand the properties of a plastic, to operate a production process optimally, or to modify polymeric materials successfully [1].

In recent years the understanding of essential fundamentals such as the phase behavior of hyperbranched polymer solutions has grown [5–8]. But nevertheless the experimental investigation of the phase behavior of hyperbranched polymer systems is a crucial requirement for a successful introduction of new applications to

highly competitive markets. In this context, thermodynamic models, which accurately account for the impact of polymer branching on the phase behavior of polymer systems, play a very important role; they enable the optimization of new applications of hyperbranched polymers without requiring an unjustifiable amount of experimental phase equilibrium data [1, 6–8].

This chapter summarizes the most important studies on the phase equilibria of hyperbranched and other dendritic polymer systems. In the first section, properties of hyperbranched polymer solutions are described, followed by a second section focusing on the modeling of the phase behavior.

Properties of Hyperbranched Polymers in Solutions

Some groups reported the formation of micelles by the solvation of hyperbranched polymer in a solvent mixture. This micelle formation depends on the kind of hyperbranched polymer. In most cases the micelles are formed by copolymers ([1–3] and references therein). For this reason the effect of copolymer concentration on micelle formation was studied. In addition to copolymer concentration, also the impact generation number on the micelle formation were investigated ([1, 2] and references therein). In was shown that the generation number influences the micelle form. Recently Jin et al. [9] reviewed the application of biodegradable hyperbranched polymers to form micelles and showed that various molecular structures including micelles and vesicles have been prepared through the primary self-assembly processes. Hyperbranched polymer vesicles have a great potential to mimic cellular behaviors as model membranes.

Some groups demonstrated that the solubility of dendritic polymers can be tailored by introducing appropriate functionalities into the surface groups of the polymer. By means of hydrophilic functional end groups, hydrophobic dendritic polymers can become water soluble, and also water-soluble dendritic polymers can turn into hydrophobic molecules after functionalization

with hydrophobic groups ([1–3] and references therein). Some dissolved dendritic polymers exhibited considerable variable hydrodynamic radii which predominantly depend on solvent properties such as pH ([1–3] and references therein).

Regarding dendritic polymers, there are some reports in literature which discuss the influence of the macromolecular structure as well as the nature and number of chain end functionalities on the polymer solubility in selected solvents. It was found that dendritic polymers are highly soluble in solvents which are capable of solvating the numerous chain ends ([1–3] and references therein).

Also the influence of branching on phase behavior was analyzed. Recently, Cheng et al. [10] reported for the first time the influence of degree of branching (DB) on the thermoresponsive phase transition behaviors of hyperbranched multiarm copolymers. Two series of poly(ethyl-hydroxymethyl)-oxetane (PEHO)-star (polyethylenoxid) (PEO) (series I) and PEHO-star-poly(2-(dimethylamino)ethylmethacrylates (PDMAEMA) (series II) with the hydrophobic DB-variable PEHO core and different kinds of linear arms (PEO arms or PDMAEMA arms) were synthesized. It was found that these two series demonstrate thermoresponsive phase transitions with a lower critical solution temperature (LCST). The studies on the LCST transition mechanism indicate that series A belongs to the thermoresponsive polymer system with LCST transition based on a hydrophilic–hydrophobic balance, while series B belongs to the thermoresponsive polymer system with LCST transition based on coil-to-globule transition. For series A, the LCST phase transition is dependent on the DB of the PEHO core in copolymers, whereas for series B, the LCST phase transition is independent of the DB but it is pH sensitive.

In addition to the influence of degree of branching on phase behavior, also the formation of hydrogen bonding of hyperbranched polymers with polar functional groups was analyzed. Zagar and Zigon [11] used IR spectroscopy to obtain information about the extent and the type of hydrogen bonds. They determined that the

majority of the hydroxyl groups are hydrogen bonded and exist in four diverse assemblies which differ in terms of their strength.

Other researchers also used IR spectrometry to determine the accessibility of internal and terminal functional groups [1, 3]. The results show that in molecules of low generation number, the terminal groups are about as accessible (e.g., for solvent molecules) as those in linear polymers. However, these functional groups become less accessible as the generation number increases, presumably because the molecule folds back on itself to some degree resulting in a more compact, globular shape ([1, 3, 4] and references therein).

Infinite-dilution activity coefficients were also measured by several groups [1, 12]. Interesting results are reported by the Bertucco group [12], where the activity coefficients of polar and non-polar solvents in comb polymers and dendritic poly(propylene imine) of generation 2–5 were measured. Solvent activity coefficients at infinite dilution change with respect to the dendrimer generation number, reaching a minimum at generation 4 in the temperature range of 333–413 K [12]. Due to the exothermic formation of hydrogen bonding, alcohols form hydrogen bonds with the dendrimer more easily at low temperatures, and hence, the solubility decreases with increasing temperature [12]. Since they used dendrimers with a basic character, slightly acidic solvents showed better solvent qualities than others (THF, toluene, ethyl acetate).

Several groups [1, 6–8] studied the low- and high-pressure phase behavior of polymer solutions containing commercially available hyperbranched polymers. The studies investigate on the one hand the vapor–liquid phase equilibria (VLE) and on the other hand the liquid–liquid phase equilibria (LLE). At moderate pressures, the investigated VLE of differently branched hyperbranched polymers allowed for a discussion on how the degree of polymer branching, the nature and number of polymer functionalities, and the solvent polarity determine the slope of the bubble point curve and the solvent activity.

In Fig. 1a, bubble point lines of different dendritic polymer–solvent systems are shown at an equilibrium temperature of 393.15 K. In the case of ethanol as solvent, a steep rise of the isothermal partial pressure curves can be observed, whereas the lower solvent volatility of water results in a flatter curve shape. Although a variety of different polymers have been investigated (hyperbranched polyglycerol samples PG1 and PG3, linear polyglycerol (LPG), OH-terminated polyamidoamine dendrimer (PAMAM), hyperbranched polyester Boltorn H40, hyperbranched polyesteramide Hybrane H1500), it becomes obvious that the different VLE are more dominated by the solvent volatility and polarity than by the structures of the respective polymer. It is known that the degree of branching has a pronounced effect on the radius of gyration. However, when comparing polymers with a different degree of branching in the same solvent, only a small influence on the VLE was found such as observed for the hyperbranched polyglycerol PG1 (Mn = 1,400 g/mol) and its perfect linear polyglycerol analogue LPG in ethanol. The ethanol absorption by polyglycerol tends to increase with decreasing molar mass and increasing degree of polymer branching (Fig. 1a). This corresponds to a comparatively lower ethanol activity in the hyperbranched polyglycerol (Mn = 1,400 g/mol) solution (see Fig. 1b).

Apart from the latter system, Fig. 1b shows that there are only slight differences in the solvent activity for the investigated polymer solutions. This result underlines that the macromolecular topology, the chemical backbone structure, and, for a certain range, the molar mass of the polymer are of minor importance for the VLE. When comparing the results of Fig. 1a, b with the VLE investigations above, it can be concluded that the VLE of hyperbranched polymer solutions primarily depends on the interactions between the solvent molecules and the polymer functionalities and not on the degree of branching.

Furthermore, special attention was devoted to the influence of hyperbranched polymers on the VLE of azeotropic systems [1]. The extent of inter- and intramolecular hydrogen bond formation has a dominant impact on the solvent activity and therefore determines partition coefficients and relative volatilities ([1] and references therein).

P
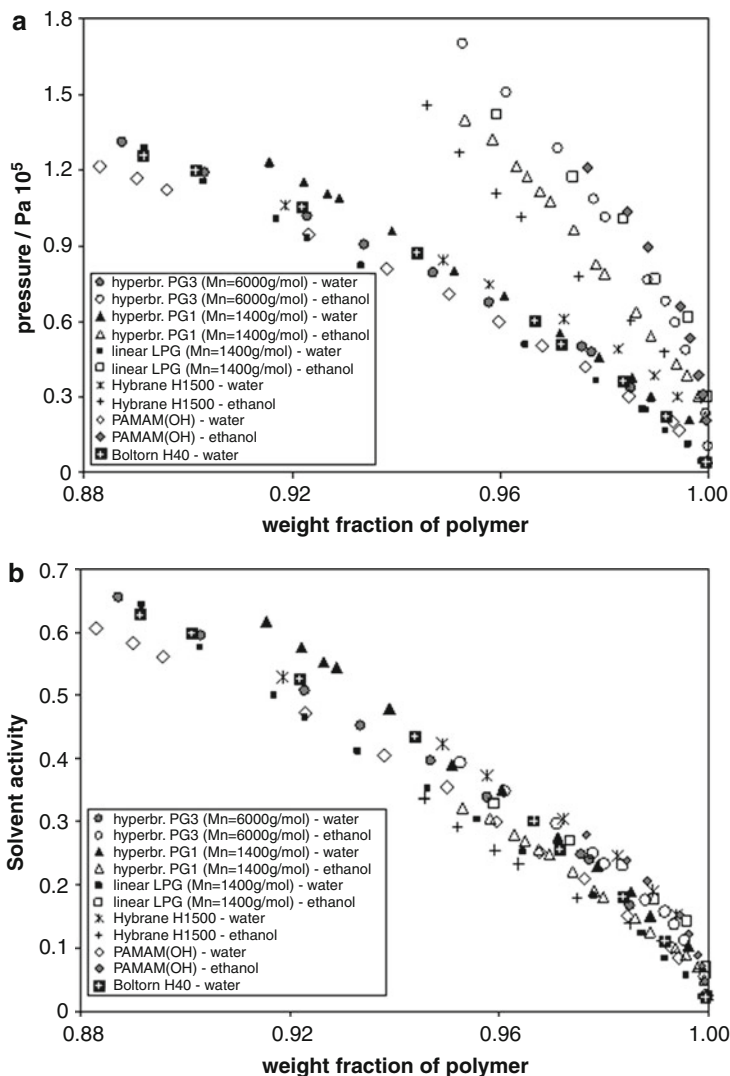
Phase Behavior and Chemical Engineering Applications of Hyperbranched Polymers, Fig. 1 Vapor–liquid equilibria of different polymer–solvent systems at T = 393.15 K. (**a**): Isothermal partial pressure curves of ethanol or water in different dendritic polymers. (**b**): Solvent activity versus polymer weight fraction. Polymer characteristics: PG3 = hyperbranched polyglycerol: Mn = 6,000 g/mol, Mw/Mn = 2.4, # of OH-groups = 80, DB = 0.62 (synthesized and characterized by Frey and Kautz). PG1 = hyperbranched polyglycerol: Mn = 1,400 g/mol, Mw/Mn = 1.5, # of OH-groups = 20, DB = 0.52 (synthesized and characterized by Frey and Kautz). LPG = linear polyglycerol (linear analogue of PG1): Mn = 1,400 g/mol, Mw/Mn = 1.3, # of OH-groups = 20, DB = 0 (synthesized and characterized by Frey and Kautz). Hybrane H1500 = hyperbranched polyglycerol: Mn = 1,500 g/mol, Mw/Mn = 5, # of OH-groups = 8, DB = 0.62 (synthesized and characterized by DSM). PAMAM(OH) = OH-terminated polyamidoamine dendrimer: Mw = 3,256 g/mol, Mw/Mn < 1.04, # of OH-groups = 16 (synthesized and characterized by Dendritech). Boltorn H40 = hyperbranched polyester: Mn = 2,833 g/mol, Mw/Mn = 1.5, # of OH-groups = 64 (synthesized and characterized by Perstorp). For further details see ISBN 3-18-382003-X

At large polymer concentrations, hydroxyl-functional hyperbranched polyesters tend to form agglomerates, limiting their polymer solubility and separation efficiency. On the other hand, highly soluble hyperbranched polymers break the azeotropic system behavior of a variety of aqueous azeotropic mixtures in a remarkable manner making them potential entrainer candidates for the extractive distillation.

Seiler et al. [1] and Koslowska et al. [6] investigated the high-pressure phase behavior of nonaqueous hyperbranched polymer solutions. In the system hyperbranched polyester Boltorn H20–ethanol–CO_2, the location of the upper critical solution temperature (UCST) curve proved to be dependent on the polymer molar mass and the solvent polarity and independent of the system pressure [1]. However, the LCST of the respective system strongly depends on the pressure. An increase in CO_2 concentration leads to a considerable shift of the LCST curve to lower system temperature. For the system hyperbranched polyester–ethanol–CO_2, the merging of the UCST and the LCST curve into the hourglass miscibility gap is observed at the CO_2 concentration of 50.5 wt% ([1] and references therein).

Koslowska et al. [6] measured the absorption of CO_2 in a liquid hyperbranched polymer and in hyperbranched polyglycerol solutions. Depending on pressure and temperature, they could measure a demixing of the polymer solution.

In addition to VLE, also LLE were experimentally investigated in literature. Several research groups investigated the solubility of hyperbranched polyethers and polyesters with different degree of branching in water ([1] and references therein). In the Enders group, the solubility of hyperbranched polyester in different solvent mixtures was analyzed [7].

The aforementioned properties were modeled using molecular dynamics or Monte Carlo simulations [13]. Molecular simulation can be used to study the dynamics of phase separation in hyperbranched polymer solution. It was found that the degree of polymer branching has

a pronounced effect on the radius of gyration and the center of mass diffusion of the polymer ([1] and references therein). Moreover Monte Carlo simulations are used to study the structural properties of an athermal hyperbranched polymer solution in diluted and high concentrated regimes [1]. Monte Carlo simulations were also used to study conformational structures formed by star and comb heteropolymers during kinetics of folding from the coil to the globule, as well as the corresponding equilibrium states ongoing from the good to the poor solution [1]. Boye et al. [13] could give the molecular understanding of phenomena that the shape of the hyperbranched polymers changes with the polarity of the solvent, which is also supported by experimental results.

The experimental results and simulations described above represent valuable information to test or develop thermodynamic models capable of describing the phase behavior of hyperbranched polymer systems. The most important modeling results are summarized in the following section.

Modeling the Phase Behavior of Hyperbranched Polymer Systems

In literature several models describing the phase behavior of hyperbranched polymer systems are suggested [1, 5–7]. In the framework of this review, the UNIFAC-FV model, the PC-SAFT (perturbed chain-statistical association fluid theory) EOS, and the lattice cluster theory (LCT) will be considered.

The UNIFAC-FV is a method to estimate solvent activities of polymer solutions. The approach is based on a group contribution method in combination with a free-volume correction.

In the framework of this approach, it is assumed that the complete theoretical equation for solvent activity of a polymer solution (a_i) contains combinatorial ($a_{com,i}$), residual ($a_{res,i}$), and free-volume terms ($a_{FV,i}$):

$$\ln(a_i) = \ln\left(a_{i,\,com}\right) + \ln\left(a_{i,\,res}\right) + \ln\left(a_{i,\,FV}\right) \quad (1)$$

The combinatorial part of the activity coefficient specifies the entropic part of an incompressible mixture. The interaction energy between different molecules of the mixture is described by the residual activity coefficient, and the difference between an incompressible and a compressible solution is calculated by the free-volume term. Seiler et al. [1] pointed out that with the help of the UNIFAC-FV model, the VLE of selected hyperbranched polymer solutions can be described in an adequate manner. However, the occurrence of LLE of hyperbranched polymer solutions cannot be predicted by the UNIFAC-FV model. Hyperbranched polymers are distinguished from linear polymers by their architecture, but this issue cannot be taken into account by the UNIFAC-FV. Unlike solvents, the activity coefficient of polymers depends strongly on the generation number. In LLE both activity coefficients are important, whereas in VLE only one of the solvent plays an important role. Therefore UNIFAC models successfully the VLE but not LLE.

For modeling hyperbranched polymers phase behavior, PC-SAFT can also be applied. To calculate high-pressure phase behavior including CO_2, it is extended with contributions for dipolar and quadrupolar interactions and a branching term describing the architecture of hyperbranched polymers [6]. The Helmholtz energy of polymer solution can be calculated as follows:

$$F = F^{id} + F^{hs} + F^{chain} + F^{multipole} + F^{branch} \quad (2)$$

where F^{id}, F^{hs}, F^{chain}, $F^{multipole}$, and F^{branch} are the ideal, hard-sphere, hard-chain, multipole, and branching contributions to Helmholtz energy F. The Helmholtz energy of a hard sphere is calculated by considering the individual molecules as hard spheres. These hard spheres can be connected to a chain and the contribution is calculated by the hard-chain Helmholtz energy. Dipolar and quadrupolar interactions are considered by the multipole term of the Helmholtz energy. The branching term accounts for the branching units that are given as rigid tetramer units within a hyperbranched macromolecule, and hence, only branching points with four bonds can be described. Here it has to be stated that the most branching points in a hyperbranched polymer are branching points of three; hence the description of polymer architecture by PC-SAFT is not accurate.

In the group of Freed a lattice theory for polymer solutions was derived, which is formally an exact mathematical solution of the Flory–Huggins lattice; however, most of this lattice theory fails to yield a dependence of solution properties on polymer architecture.

In 1991, Dudowicz and Freed [14] have developed a systematic expansion of the partition function of a lattice polymer using the LCT. This model takes into account the effect of branching on the thermodynamic properties of polymer blends [7].

Jang and Bae have used the LCT to model LLE of an aqueous hyperbranched polymer solution for the first time, but they did not use the LCT in a proper manner [7].

The Helmholtz free energy of the LCT can be calculated as follows:

$$F_{LCT} = F^{ath} + F^{int} + F^{as} \quad (3)$$

where the classical LCT consists of the athermal contribution F^{ath} and the interaction contribution F^{int}. The associative contribution F^{as} accounts for hydrogen-bonding effects.

The athermal part of the Helmholtz energy is developed by a series expansion of the partition function in the inverse coordination number $1/z$. This part depicts the entropic contribution of polymer's architecture. The interaction contributions are obtained from a series expansion of the partition function in the reduced interaction energy $\varepsilon_{ij}/k_B T$.

Using the LCT the critical concentration could successfully predict by just using one adjustable parameter and the knowledge of the chemical structure of the hyperbranched polymer. By using just one adjustable parameter, the low

Phase Behavior and Chemical Engineering Applications of Hyperbranched Polymers, Fig. 2 Influence of branching point on the polymer phase behavior. Model calculation was conducted with LCT by using the same interaction energy ($\frac{\Delta\varepsilon}{k_{\mathrm{B}}T} = 120$ K) and chain length (300 segments) but different architectures
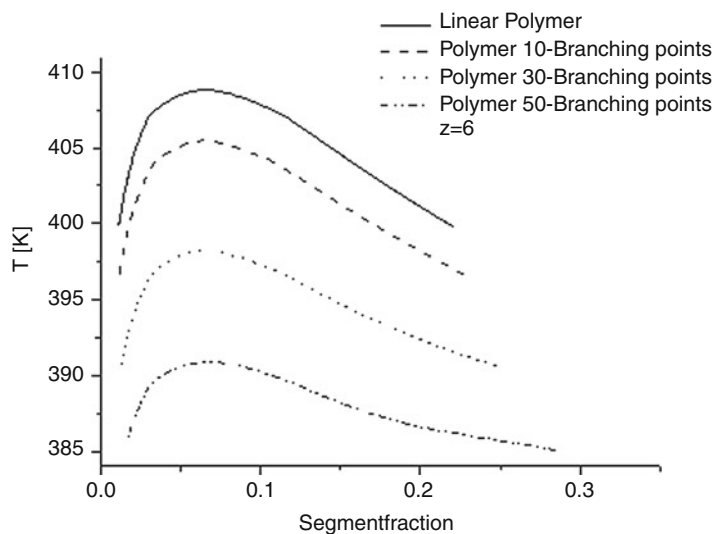
concentrated branch of the cloud point curve could be modeled in good accordance with experimental data, but there was a deviation between the calculated high concentrated branch and the experimental data. By the combination of the LCT with an association term, a good accordance between experimental data and calculations could be achieved. In addition to the calculation of the phase behavior of a polymer in a single solvent, the phase behavior of a hyperbranched polymer in mixed and demixed solvent was also modeled. In the case of the hyperbranched polymer solution in a mixed solvent, the ternary phase behavior could be calculated in good agreement with experimental data by adjusting the interaction parameters of the two solvents on the ternary phase behavior. Further the LCT in combination with Wertheim theory could predict the ternary phase behavior in good accordance with experimental data, based on all binary subsystems. In Fig. 2 model calculations can be seen using the LCT with the same interaction energy but different architecture. Following the calculations the critical temperature decreases with increasing number of branching points, but the critical composition remains the same. Moreover it is obvious that with increasing number of branching points of three, the cloud point curve gets broader and a shoulder in the curve appears.

Recently, the incompressible LCT has been further developed to the compressible LCT-EOS.

In the framework of the LCT-EOS, it is possible to calculate high-pressure phase equilibria as shown by Langenbach et al. [8].

Chemical Engineering Applications

Hyperbranched polymers might be used in a number of chemical engineering applications [1]. However, due to their relative high solution viscosity in comparison to other solvents used in the field of chemical engineering (i.e., entrainers for extractive distillation, extraction solvents or absorbents for extraction and absorption, respectively), most of these applications have substantial market entry barriers. This is why the following section focuses on one of the most promising application of hyperbranched polymers in this field, i.e., their use as membranes.

A wide variety of polymeric materials have been studied to evaluate their potential use as membrane materials for separation processes. However, most of the commercially available membrane materials developed so far are limited to linear polymers. During the last years, a number of research groups started focusing on hyperbranched polymer membranes ([1, 15–20] and references therein).

Wang et al. [15] reviewed the patent landscape for hyperbranched polymer membranes. They discussed patents on proton exchange membranes (PEM), bipolar membranes, gas separation membranes, and solid–liquid separation membranes.

PEM are used in fuel cells. These membranes are used to transport the protons and to separate the catalyst. For this reason this type of membranes requires both excellent proton conductivity and a sufficient mechanical strength. Hyperbranched polymers with the high density of functional end groups have the potential of being a good proton exchanger [15, 19]. Wang et al. [15] reported that most works use hyperbranched polymers as skeleton for the PEM. These PEM based on dendritic polymers show a higher proton conductivity, but lower fuel permeability. Moreover, some PEM based on dendritic polymers can control the pore size and therefore allow limiting of the water content in the pores [15]. Recently, Rakesh et al. [19] suggested new molecular simulation models for the identification and development of suitable hyperbranched PEM polymers offering a high proton conductivity. The newly developed material optimizes proton channel formation and water transport properties [19].

Wang et al. [15] discussed also the application of hyperbranched polymers in bipolar membranes. Bipolar membranes are composition membranes containing a cation exchange layer, an anion exchange layer, and an interfacial layer. By this bipolar membranes, water can be dissociated into hydrogen ions and hydroxyl ions under reverse potential bias. Former studies demonstrated that water dissociation reactions take place in the interfacial region of the bipolar membrane between the cation exchange and anion exchange layers. It is obvious that the composition of this region is important for the function of a bipolar membrane [15].

To improve the functionality of bipolar membranes, dendritic polymers were used as catalysts of the water dissociation process in the intermediate layer of the bipolar membrane [15]. Here two reverse effects were found: the

number of functional groups has a positive effect on water dissociation, but the steric hindrance has a negative effect. In other studies dendrimer–metal complexes were used. By the use of unbound metal ions, the catalytic effect in the intermediate layer increases, but they leach out. By the use of dendritic–metal complexes, this leaching can be minimized [15].

In addition to the aforementioned applications of hyperbranched polymers, also their use as high-performance gas separation membranes seems promising. Membrane-based gas separations have attracted much attention in the past decade since they offer many advantages over traditional separation processes such as low capital investment cost, low energy consumption, and simple operation [1, 15]. Hyperbranched polymers have many properties making them suitable for the use in gas separation membranes such as open nanoscaled structures and interior accessible cavities [15, 17, 20]. Recently Kanehashi et al. [18] reviewed the gas permeability and the synthesis of gas permeation of hyperbranched based gas permeation membranes. They demonstrated that – compared with other commercially available gas permeation membranes – the investigated membranes show a better permselectivity, higher stability, and compression resistance [18].

Suzuki et al. investigated the physical and gas transport properties of hyperbranched polyimide membranes prepared from a triamine, 1,3,5-tris(4-aminophenoxy)benzene (TAPOB), and a dianhydride, $4,4^L$ -(hexafluoroisopropylidene) diphthalic anhydride (6FDA) ([20] and references therein). These 6FDA–TAPOB hyperbranched polyimide membranes exhibited a remarkable thermal stability with a 5 % weight-loss temperature of 510 °C. The gas permeability and/or diffusivity of a polymer depends on the free volume. The fractional free-volume value of 6FDA–TAPOB was higher than those of the linear analogues, indicating looser packing of the molecular chains. The hyperbranched membrane exhibits a considerably high gas solubility and, as a result, shows high gas permeability [20]. Therefore, Suzuki et al. suggest that the low segmental mobility and the unique size

and distribution of free-volume holes arising from the characteristic hyperbranched structure of 6FDA–TAPOB provide an effective O2/N2 selectivity. Due to the high permeability and O2/N2 selectivity, Suzuki et al. conclude that the 6FDA–TAPOB hyperbranched polyimide meets the requirements of a high-performance gas separation membrane [20].

Wang et al. [15] also reported the use of dendritic polymers in solid–liquid separation membranes. Solid–liquid separation plays an important role in chemical, pharmaceutical, and biotechnological processes. Because of the high number of functional end groups, some components can be bound on these groups. These types of membranes were used, for instance, to separate metal ions from water [15].

Furthermore, hyperbranched polymers can be used in nanofiltration membranes [16]. Nanofiltration is a pressure-driven membrane process normally applicable for separating dissolved components having a molecular weight ranging from 200 to 1,000 Da. Most types of nanofiltration membranes consist of a selective layer and a microporous substrate. Chiang et al. [16] used hyperbranched polymers in nanofiltration membranes to obtain a membrane simultaneously owning high rejection to salt and high water permeation. They found out that the membrane has some special characteristics. So, the used membranes have a relative high molecular flux at the same molecular weight cutoff compared to membranes based on linear polymers. Moreover, the used membrane showed a relatively high salt rejection, but the salt rejection is relative selective. This selectivity can be explained by the functional groups of the used polymer [16].

In addition to the field of nanofiltration, dendritic polymers can also be used as ultrafiltration membranes [17]. For ultrafiltration, membranes are needed with a tunable pore size, chemical resistance, and good thermal properties. Because of the large number of functional end groups, hyperbranched polymers can be used to increase fouling resistance of ultrafiltration membranes. Moreover, due to the branched architecture of hyperbranched polymers, the inner porosity of ultrafiltration membranes can be controlled [17]. Zhao et al. [17] have shown that hyperbranched polymers are enriched on the membrane surfaces if the branch length is increased. So the surface character can be controlled. Therefore, with respect to field of chemical engineering, it can be concluded that hyperbranched polymers represent versatile and competitive materials especially in the area of membrane applications.

Related Entries

▶ Flory–Huggins Equation
▶ Hyperbranched Polyglycerols (Synthesis and Applications)

References

1. Seiler M (2006) Hyperbranched polymers: phase behavior and new applications in the field of chemical engineering. Fluid Phase Equilib 241:155–174. doi:10.1016/j.fluid.2005.12.042
2. Yan D, Gao C, Frey H (2011) Hyperbranched polymers: synthesis, properties, and applications, vol 8. Wiley, Weinheim
3. Furukawa T, Ishizu K (2012) Multibranched polymers in solution: stars, dendrimers, and hyperbranched polymers. In: Somasundaran P (ed) Encyclopedia of surface and colloid science, 2nd edn. Springer, New York, pp 4162–4179
4. Voit B, Komber H, Lederer A (2012) Hyperbranched polymers – synthesis and characterization aspects. In: Schlüter DA, Hawker C, Sakamoto J (eds) Synthesis of polymers: new structures & methods. Wiley-VCH, Weinheim
5. Wu Y (2013) Hyperbranched polymers in a supercritical fluid: recent progress on phase behavior and modeling. J Appl Solut Chem Model 2:33–46. doi:10.6000/1929-5030.2013.02.01.5
6. Kozłowska MK, Jürgens BF, Schacht CS, Gross J, de Loos TW (2009) Phase behavior of hyperbranched polymer systems: experiments and application of the perturbed-chain polar SAFT equation of state. J Phys Chem B 113:1022–1029. doi:10.1021/jp804459x
7. Enders S, Zeiner T (2011) Application of lattice cluster theory to the calculation of miscibility – and interfacial behavior of polymer containing systems. In: Ehlers TP, Wilhelm JK (eds) Polymer phase behavior. Nova Science Publishers, Hauppauge
8. Langenbach K, Enders S, Browarzik C, Browarzik D (2013) Calculation of the high pressure phase equilibrium in hyperbranched polymer systems with the

P

lattice-cluster theory. J Chem Thermodyn 59:107–113. doi:10.1016/j.jct.2012.12.002

9. Jin H, Huang W, Zhu X, Zhou Y, Yan D (2012) Biocompatible or biodegradable hyperbranched polymers: from self-assembly to cytomimetic applications. Chem Soc Rev 41:5986–5997. doi:10.1039/c2cs35130g

10. Cheng H, Xie S, Zhou Y, Huang W, Yan D, Yang J, Ji B (2010) Effect of degree of branching on the thermoresponsive phase transition behaviors of hyperbranched multiarm copolymers: comparison of systems with LCST transition based on coil-to-globule transition or hydrophilic-hydrophobic balance. J Phys Chem B 114:6291–6299. doi:10.1021/jp100714j

11. Žagar E, Žigon M (2011) Aliphatic hyperbranched polyesters based on 2, 2-bis (methylol) propionic acid – determination of structure, solution and bulk properties. Prog Polym Sci 36:53–88. doi:10.1016/j.progpolymsci.2010.08.004

12. Polese A, Mio C, Bertucco A (1999) Infinite-dilution activity coefficients of polar and nonpolar solvents in solutions of hyperbranched polymers. J Chem Eng Data 44:839–845. doi:10.1021/je9803025

13. Boye S, Komber H, Friedel P, Lederer A (2010) Solution properties of selectively modified hyperbranched polyesters. Polymer 51:4110–4120. doi:10.1016/j.polymer.2010.06.037

14. Dudowicz J, Freed KF (1991) Effect of monomer structure and compressibility on the properties of multicomponent polymer blends and solutions: 1. Lattice cluster theory of compressible systems. Macromolecules 24:5076–5095. doi:10.1021/ma00018a014

15. Wang J, Cheng Y, Xu T (2008) Current patents of dendrimers and hyperbranched polymers in membranes. Recent Pat Chem Eng 1:41–51. doi:10.2174/2211334710801010041

16. Chiang YC, Hsub YZ, Ruaan RC, Chuang CJ, Tung KL (2009) Nanofiltration membranes synthesized from hyperbranched polyethyleneimine. J Membr Sci 326:19–26. doi:10.1016/j.memsci.2008.09.021

17. Zhao YH, Qian YL, Pang DX, Zhu BK, Xu YY (2007) Porous membranes modified by hyperbranched polymers II: effect of the arm length of amphiphilic hyperbranched-star polymers on the hydrophilicity and protein resistance of poly (vinylidene fluoride) membranes. J Membr Sci 304:138–147. doi:10.1016/j.memsci.2007.07.029

18. Kanehashi S, Sato S, Nagai K (2010) Synthesis and gas permeability of hyperbranched and cross-linked polyimide membranes. Membr Gas Sep 1–27. doi:10.1002/9780470665626.ch1

19. Rakesh L, Mueller A, Chhetri P (2010) Development of a hyperbranched fuel cell membrane material for improved proton conductivity. Fluid Dyn Mater Process 6:179–202. doi:10.3970/fdmp.2010.006.179

20. Suzuki T, Yamada Y, Tsujita Y (2004) Gas transport properties of 6FDA-TAPOB hyperbranched polyimide membrane. Polymer 45:7167–7171

Phase Separation Kinetics in Polymer Blends

Mikihito Takenaka
Department of Polymer Chemistry, Graduate School of Engineering, Kyoto University, Kyoto, Japan

Synonyms

Coarsening processes of phase-separated structures in polymer blends

Definition

The self-assembling processes via spinodal decomposition (SD) of the A/B blend near the critical composition are classified, at least, into the following three regions: early stage, intermediate stage, and late stage. In the early stage, nonlinear effects on the growth of the concentration fluctuation are not significant so that the growth can be well approximated by the Cahn's linearized theory. In the intermediate stage, the nonlinear effects on the growth of the concentration fluctuation become increasingly important with time, and both the wavelength and the amplitude of the concentration fluctuation grow with time. In the late stage (c), the concentrations in the A- and B-rich domains reach those on the coexisting curve of the phase diagram, and only wavelength of the dominant mode of concentration fluctuation grows self-similarly.

Introduction

When a binary polymer A and B blend (A/B) is quenched from a single-phase state to a two-phase state inside its miscibility gap, the concentration fluctuation in the A/B blend grows with time in terms of both its spatial scale and amplitude (concentration contrast) toward a new equilibrium. This phase separation mechanism is

classically classified into two different types. One is for the A/B blend quenched into a metastable state between the coexisting curve and the spinodal curve. It has the instability only against the concentration fluctuation with its amplitude being close to a large concentration difference between the coexisting phases at a given quench depth. This phase separation mechanism is called nucleation and growth. The other case is found when the A/B blend is quenched inside the spinodal curve. It has the instability even against the concentration fluctuation with an infinitesimal amplitude. This second mechanism is called spinodal decomposition. This chapter focuses on the phase separation processes of binary A/B polymer blends via spinodal decomposition and gives a brief overview for the self-assembling via spinodal decomposition.
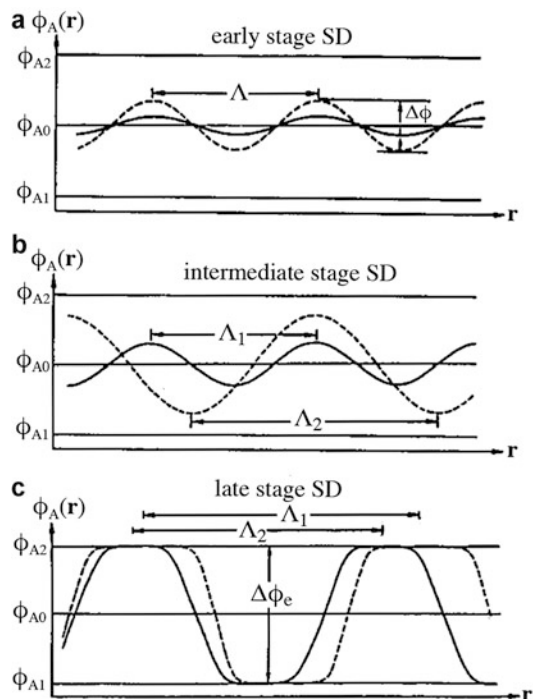
Spinodal Decomposition

Overview

The self-assembling processes via spinodal decomposition (SD) of the A/B blend near the critical composition are classified, at least, into the following three regions: (a) early stage, (b) intermediate stage, and (c) late stage as shown in Fig. 1 [1].

In the early stage (a), nonlinear effects on the growth of the concentration fluctuation are not significant so that the growth can be well approximated by the Cahn's linearized theory [2]. The magnitude of the scattering vector $q_m(t)$ (or the characteristic length $\Lambda_m(t) = 2\pi/q_m(t)$) of the dominant mode of concentration fluctuation is constant, independent of time t, and agrees with $q_m(0)$ at $t = 0$. Within the context of mean-field theory [3, 4], $q_m(0)$ at a temperature T is expressed as

$$q_m(0) = (3/2)^{1/2} R_g^{-1/2} \varepsilon_T^{1/2} \qquad (1)$$

for a symmetric polymer blend having the composition close to 50/50 and nearly the same size of the component chains A and B. Here, R_g is

Phase Separation Kinetics in Polymer Blends, Fig. 1 Time evolution of the concentration pattern in the (**a**) early, (**b**) intermediate, and (**c**) late stages of spinodal decomposition

a radius of gyration of the component polymer, and ε_T is defined by

$$\varepsilon_T = (\chi - \chi_S)/\chi_S = (T_S - T)/T_S \qquad (2)$$

where T_S indicates the spinodal temperature, and χ and χ_S are Flory-Huggins interaction parameter at T and T_S, respectively. The amplitude of the concentration fluctuations $\Delta\phi_q$ at the magnitude of the scattering vector q grows exponentially with t as

$$\Delta\phi_q(t) \sim \exp[R(q)t] \qquad (3)$$

The growth rate $R(q)$ appearing in Eq. 3 is given by

$$R(q) = D_{app}(T)q^2 \{1 - q^2/2q_m^2(0)\} \qquad (4)$$

where $D_{app}(T)$ is the interdiffusion coefficient between the components A and B. Thus, $\Delta\phi(t)$

for the dominant growth mode at $q = q_m(0)$ is given by

$$\Delta\phi(t) \sim \exp[R(q_m(0))t] \qquad (5)$$

In the intermediate stage (b), the nonlinear effects on the growth of the concentration fluctuation become increasingly important with time. Thus, the growth is affected by the nonlinear, mode-mode coupling described by the time-dependent Ginzburg-Landau (TDGL) equation [5]. This coupling leads to a decrease of $q_m(t)$ and a further increase of $\Delta\phi(t)$ with t. Specifically, $q_m(t)$ and $\Lambda_m(t)$ exhibit the power-law dependence on t:

$$2\pi/\Lambda_m(t) = q_m(t) \sim t^{-\alpha} \qquad (6)$$

In such power-law region, the growth of $\Delta\phi(t)$ with t becomes slower than that expected from Eq. 4.

In the late stage (c), the concentrations in the A- and B-rich domains, ϕ_{A1} and ϕ_{A2}, reach those on the coexisting curve of the phase diagram, and hence, the concentration fluctuation also reaches its equilibrium amplitude $\Delta\phi_e$. The interface between two coexisting domains has become narrow and well defined in the later part of the intermediate stage and/or the early part of the late stage. The time evolution of such domain structures having $\Delta\phi(t) = \Delta\phi_e$ can be characterized with three, time-dependent length parameters sketched in Fig. 2 [6]: The interdomain spacing is characterized by $\Lambda_m(t)$ that obeys Eq. (6) also in the late stage, and the waviness of interface (boundary) between the neighboring domains is specified by the mean radius of interface curvature, $R_m(t)$. The interface may be also diffuse, which can be characterized by the characteristic interfacial thickness t_1 defined by

$$t_1 \equiv \Delta\phi_e/[d\phi_A/dz]_{\phi_A=\phi_{A0}} \qquad (7)$$

where z is the local coordinate normal to the interface and ϕ_{A0} is the average concentration of the component A in the blend as depicted in Fig. 1c.
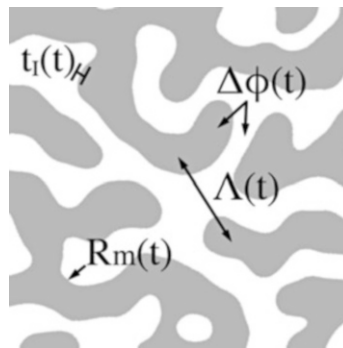
Phase Separation Kinetics in Polymer Blends, Fig. 2 Schematic picture of the phase-separated structures of binary polymer blends formed through spinodal decomposition

Dynamic Self-Similarity

Scattering techniques such as light scattering and small-angle neutron scattering provide the important and interesting information about the phase separation processes in polymer blends. For the phase separation occurring isotropically in the three-dimensional space, the scattering intensity $I(q, t)$ due to the incident radiation grows isotropically and thus depends only on the magnitude of the scattering vector q irrespective of the direction of scattering: q is defined in terms of the scattering angle θ and the wavelength of the incident radiation λ as

$$q = (4\pi/\lambda) \sin(\theta/2) \qquad (8)$$

Specifically, $I(q, t)$ in the intermediate and late stages of spinodal decomposition can be expressed as

$$I(q, t) \sim \left\langle \eta(t)^2 \right\rangle \Lambda_m^3(t) S(x) \text{ with } x = q/q_m(t) \qquad (9)$$

where $\Lambda_m(t)$ $(=2\pi/q_m(t))$ is the characteristic length representing the interdomain spacing, $\left\langle \eta(t)^2 \right\rangle$ is the mean-square deviation of the scattering contrast distributed in space, $S(x)$ is the scaling function that describes how the domains evolve with time, and $x(t)$ is the normalized magnitude of the scattering vector that determines the scaling function. $\left\langle \eta(t)^2 \right\rangle$ is determined by an order parameter defined as

$$\Delta\phi_A(\mathbf{r}, t) \equiv \phi_A(\mathbf{r}, t) - \phi_{A0} \qquad (10)$$

This $\Delta\phi_A(\mathbf{r}, t)$ represents the deviation of the concentration at a spatial position $\mathbf{r}$ and time t from its average ϕ_{A0} in the blend (and satisfies a relationship, $\int \Delta\phi_A(\mathbf{r}, t)\, d\mathbf{r} = 0$.) $\langle\eta(t)^2\rangle$ is essentially proportional to a spatial average of $\Delta\phi_A^2(\mathbf{r}, t)$ in the blend and thus describes the time evolution of the contrast of the phases.

A pattern of the phase growth is specified by the scaling function $S(x)$. If the statistical feature of the domains, e.g., the domain shape and connectivity, changes with time, $S(x)$ changes its x dependence with time. In contrast, if this statistical feature of the domains does not change and the domains enlarge *self-similarly*, the x dependence of $S(x)$ becomes independent of time. For this self-similar case, the domain structure is characterized by the single time-dependent length scale for the interdomain spacing, $\Lambda_m(t)$: The other length scale $R_m(t)$, the mean radius of interface curvature, grows with t in the same way as $\Lambda_m(t)$. Specifically, the dynamical scaling hypothesis [7, 8] holds in the case where these two length scales exhibit the same power-law type growth:

$$\Lambda_m(t) = R_m(t) \sim t^\alpha \qquad (11)$$

where α is an exponent characterizing the time evolution of $q_m (= 2\pi/\Lambda_m)$; cf. Eq. 6.

The maximum scattering intensity at respective time, $I_m(t) \equiv I(q_m, t)$, often exhibits a power-law type increase with time. From Eq. 9, this increase is related to $\langle\eta(t)^2\rangle$, $\Lambda_m(t)$, and $S(1)$ (the maximum S value at $x = q/q_m = 1$) as

$$I_m(t) \sim \left\langle \eta(t)^2 \right\rangle \Lambda_m^3(t) S(1) \sim t^\beta \qquad (12)$$

In the late stage of spinodal decomposition where the dynamic scaling hypothesis is valid, the factors $\langle\eta(t)^2\rangle$ and $S(1)$ have approached to their asymptotic values for full phase separation and become essentially independent of t. For this case, the time dependence of $I_m(t)$ described by Eq. 12 becomes $I_m(t) \sim \Lambda_m^3(t) \sim t^\beta$. Comparison of Eqs. 11 and 12 indicates

$$\beta = 3\alpha \qquad (13)$$

in the late stage of spinodal decomposition. In contrast, in the intermediate stage, $\langle\eta(t)^2\rangle$ significantly increases with t, and Eqs. 11 and 12 suggest

$$\beta > 3\alpha \qquad (14)$$

This difference between the intermediate and late stages can be conveniently examined for a scaled structure factor [7, 8] defined by

$$F(x, t) \equiv q_m^3(t) I(x, t) \qquad (15)$$

This $F(x, t)$ is experimentally evaluated, with no ambiguity, from the q_m and I data. From Eq. 12, $F(x, t)$ is expressed in terms of the contrast factor $\langle\eta(t)^2\rangle$ and the scaling function $S(x)$ as

$$F(x, t) \sim \left\langle \eta(t)^2 \right\rangle S(x) \qquad (16)$$

In the intermediate stage of spinodal decomposition, $\langle\eta(t)^2\rangle$ increases with t, and $S(x)$ changes its x dependence as well. Hence, $F(x, t)$ changes with t and exhibits no universal x dependence in the intermediate stage. In contrast, in the late stage where the dynamical scaling hypothesis is valid, $\langle\eta(t)^2\rangle$ and $S(x)$ become independent of t thereby allowing $F(x, t)$ to exhibit t-independent, universal x dependence. These features of $F(x, t)$ have been confirmed experimentally [6].

Related Entries

▶ Morphology in Blends of Rubbery Polymers

References

1. Hashimoto T (1988) Dynamics in spinodal decomposition of polymer mixtures. Phase Transit 12:47
2. Cahn JW (1965) Phase separation by spinodal decomposition in isotropic systems. J Chem Phys 42:93
3. de Gennes PG (1980) Dynamics of fluctuations and spinodal decomposition in polymer blends. J Chem Phys 72:4756

4. Binder K (1983) Collective diffusion, nucleation, and spinodal decomposition in polymer mixtures. J Chem Phys 79:6387

5. Kawasaki K, Ohta T (1983) Kinetics of fluctuations for systems undergoing phase transitions-interfacial approach. Physica A 118:175

6. Takenaka M, Hashimoto T (1992) Scattering studies of self-assembling processes of polymer blends in spinodal decomposition. II. Temperature dependence. J Chem Phys 96:6117

7. Binder K, Stauffer D (1974) Theory for the slowing down of the relaxation and spinodal decomposition of binary mixtures. Phys Rev Lett 33:1006

8. Binder K (1977) Theory for the dynamics of "clusters." II. Critical diffusion in binary systems and the kinetics of phase separation. Phys Rev B 15:4425

Photochromic Polymers

Masahiro Irie
Department of Chemistry and Research Center for Smart Molecules, Rikkyo University, Toshima-ku, Tokyo, Japan

Synonyms

Optical properties; Photochromism; Photomechanical effect; Polymer chain conformation

Definition

Polymers having chromophores, which undergo a reversible transformation between two isomers in one or both directions by photoirradiation, in the backbones or the side groups, are named photochromic polymers.

Introduction

Photochromism is defined as a reversible transformation of a chemical species between two isomers having different absorption spectra induced in one or both directions by photoirradiation [1, 2]. Table 1 shows typical photochromic chromophores, which exhibit (a) *trans-cis* isomerization, (b) zwitterion formation, (c) ionic

dissociation, and (d) ring formation and ring cleavage. These isomerizations not only change their colors but also induce certain changes in physical and chemical properties, such as geometrical structure, dipole moment, refractive index, fluorescence, and oxidation/reduction potential. When the chromophores are incorporated into polymer backbones or side groups, photoirradiation brings about changes in various properties of polymer solutions and solids, as shown in Table 2. These polymers having photochromic chromophores are named photochromic polymers. In this entry, a brief history of the research and recent progress are described.
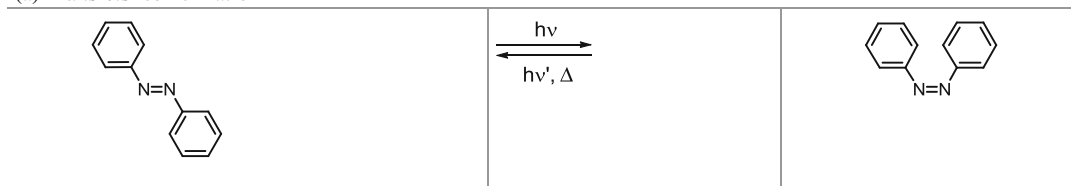
Polymer Chain Conformation

The conformation of polymer chains is a fundamental property of polymers in solution. The first attempt to control the polymer chain conformation by photoirradiation was carried out by Lovrien in 1967 [3]. A short chain photochromic azo dye (chrysophenine) was employed as a tool for the conformational change. The aqueous solution viscosity of poly(methacrylic acid) and the dyes was found to decrease upon photoirradiation (350 nm $< \lambda <$ 450 nm) and return to the initial value in the dark. The viscosity change was attributed to the change in the intermolecular interaction between the polymer chains and the photochromic dyes. If a polymer chain is normally coiled, it may be made extended by binding the dye in the all-*trans* form. Upon isomerization by light to the partially *cis* form, azo dyes become more water soluble and tend not to bind tightly as they do in the all-*trans* form. If they leave the polymer chains, the polymer chains are allowed to be relaxed into the natural compact coil conformation.

Azobenzene is a well-known photochromic molecule, which undergoes isomerization from the *trans* to the *cis* form upon irradiation with UV light and reverses upon heating or irradiation with visible light, as shown in Table 1 (a). During the isomerization, the molecule undergoes a large structure change. The distance between 4 and 4′ carbons decreases from 9.0 to 5.5 Å and the
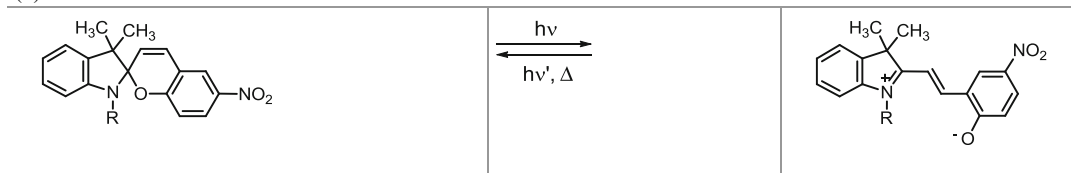
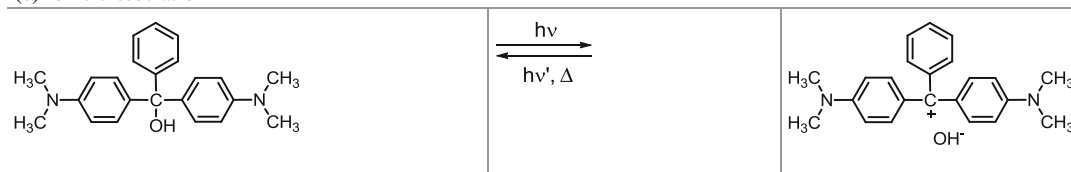**Photochromic Polymers, Table 1** Photochromic chromophores
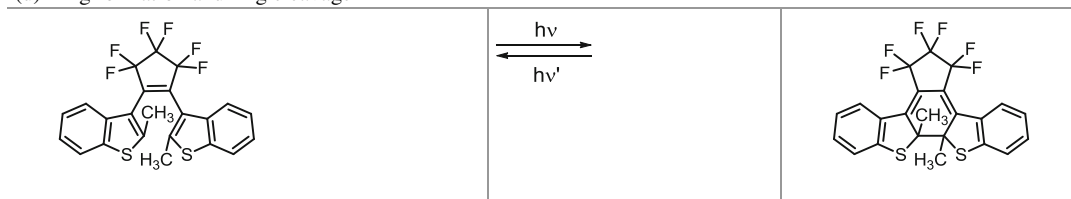
Types of reactions and examples		
(a) *Trans-cis* isomerization		
	$\xrightarrow{h\nu}$ $\xleftarrow{h\nu', \Delta}$	
(b) Zwitterion formation		
	$\xrightarrow{h\nu}$ $\xleftarrow{h\nu', \Delta}$	
(c) Ionic dissociation		
	$\xrightarrow{h\nu}$ $\xleftarrow{h\nu', \Delta}$	
(d) Ring formation and ring cleavage		
	$\xrightarrow{h\nu}$ $\xleftarrow{h\nu'}$	

P

dipole moment increases from 0.5 to 3.1 D. The property change can be used as a driving force to control the solution viscosity or the conformation of polymer chains by incorporating the residues into the polymer backbone. Various polyamides having the azobenzene residues in the backbone were synthesized, as shown in Fig. 1 [4].

Intrinsic viscosity, [η], of polymer (1) in *N, N*-dimethylacetamide was found to decrease from 1.22 to 0.50 dl/g upon UV irradiation and to return to the initial value in the dark. On alternate irradiation with UV and visible light, the viscosity reversibly changed as much as 60 %. Before irradiation the polymer has a rodlike extended conformation. The isomerization from the *trans* to the *cis* form kinks the polymer chain, resulting in a compact conformation and a decrease in the viscosity. The compact

conformation returns to the initial extended conformation either thermally or visible light irradiation, causing an increase in the viscosity. According to the above mechanism, rigidity of the polymer chains is expected to alter the amount of photodecrease of the solution viscosity. As expected, the amount of viscosity change was found to depend on the flexible methylene chains in the polymer backbone. The viscosity change of polymer (2) was 63 %, while it decreased to 41 % in polymer (3), 20 % in polymer (4), and 4 % in polymer (5). The absence of photodecrease of the viscosity in polymer (5) solution suggests that the flexible methylene chain acts as a strain absorber. The conformational change induced by the isomerization of azobenzene residues is relaxed in the connecting flexible methylene chains, resulting in no change

in the shape of polymer chains. A detailed study of photoinduced conformational changes using a time-resolved light scattering method revealed that the unfolding process of the polymer chains from the compact to the extended conformation takes place in the millisecond time range in solution [5, 6].

Another approach to regulate a polymer chain conformation is to control electrostatic repulsion among charges. As shown in Table 1 (c), triphenylmethane leucohydroxide dissociates into an ion pair upon UV irradiation with production of an intensely colored triphenylmethyl cation. The cation thermally recombines with the counter ion.
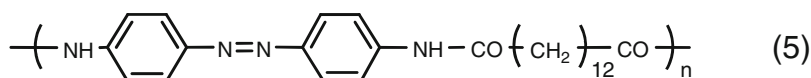
The leucohydroxide residues were introduced into the pendant groups by copolymerizing the vinyl derivative with *N,N*-dimethylacrylamide. Upon UV irradiation, the methanol solution became green and the viscosity, $\eta sp/C$, showed a remarkable increase from 0.55 to 1.6 dl/g. After the light was shut, the viscosity returned to the initial value with a half-life of 3.1 min. The close correlation between the viscosity and the absorption intensity at 620 nm implies that the electrostatic repulsion is responsible for the expansion of the polymer chain conformation.

Photomechanical Effect

Although it is, in principle, possible to amplify the photostimulated conformational changes of polymer chains in solution to a macroscopic change in the size of gels or solids, it is hard to link the molecular-scale events to the macroscopic shape change. The use of structural changes of photoisomerizable chromophores for the size change of polymer solid was proposed for the first time by Merian [7]. He studied a nylon filament fabric, 6 cm wide and 30 cm long, dyed with 15 mg/g azo dye. After exposure to a xenon lamp at a distance of 30 cm, the fabric was found to shrink as much as 0.33 mm (0.1 %).
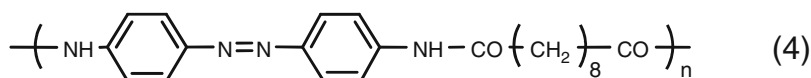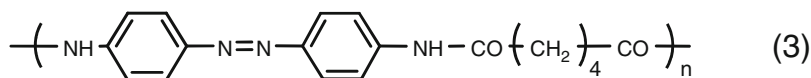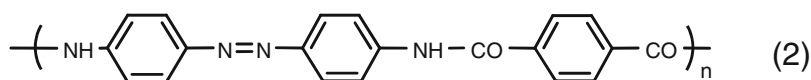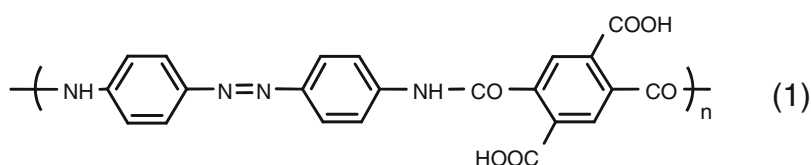
Photochromic Polymers, Table 2 Physical and chemical properties of photochromic polymers controlled by photoirradiation

Solution property	Solid property
Viscosity	Shape
pH	Surface wettability
Solubility	Sol-gel transition
Metal Ion capture capability	Miscibility of polymer blends
	T_g
	Membrane permeability
	Membrane potential
	Birefringence
	Surface relief grating

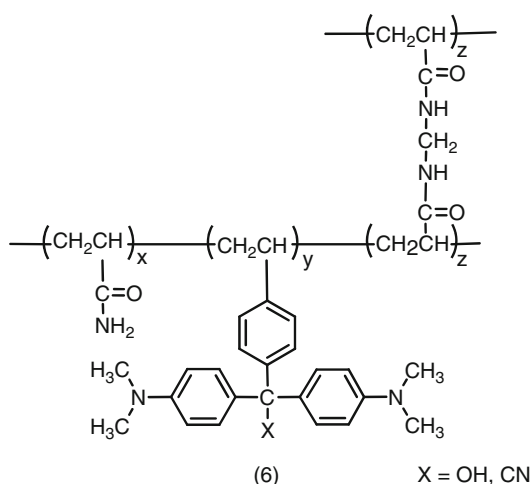**Photochromic Polymers, Fig. 1** Azobenzene polymers

Since this finding, many materials exhibiting photostimulated deformation have been reported. One example is a polyimide with azobenzene chromophores in the backbone studied by Agolini and Gay in 1970 [8]. They reported that 0.5 % contraction of the polymer film takes place at 200 °C under irradiation with UV irradiation. No correlation, however, was reported between the rate of isomerization and the film contraction. At such high temperature, the *cis* isomer content in the photostationary state would be very low. Thus, the isomerization is not the sole origin of the contraction of the system. Poly(ethyl acrylate) films cross-linked with spirobenzopyran groups or with 4,4′-dimethacryloyl-aminoazobenzene groups have been prepared and their photocontraction effects were examined. Although in both cases contraction upon UV irradiation and expansion in the dark were observed, the correlation between the isomerization of the photochromic chromophores and the contraction behavior was not evidenced. Local photo-heating effect could not be excluded as the main source of the photoinduced contraction.

In order to minimize the photo-heating effect, it was proposed to use solvent-swollen gels, in which rapid thermal conduction is supposed to suppress the photo-heating effect. Even when a solvent-swollen gel is used, there remains the question as to the relative contribution of the photo-heating to the observed photocontraction. Matéjka et al. [9] carefully examined the contribution of the photo-heating by measuring the temperature of a maleic anhydride-styrene copolymer gel with covalently bound pendant azobenzene groups in diethylphthalate. They inserted a thermocouple into the gel and measured the correlation between the temperature change and the film contraction. The response of force generation by photoirradiation correlates well with the change in the temperature of the gel. The result indicates that the decisive role played in the film contraction process be the local photo-heating due to light absorption. Many previous studies reporting to have observed photostimulated contraction have to be reexamined to check and evaluate the real photochemical effect. The most convenient way to judge whether the effect is
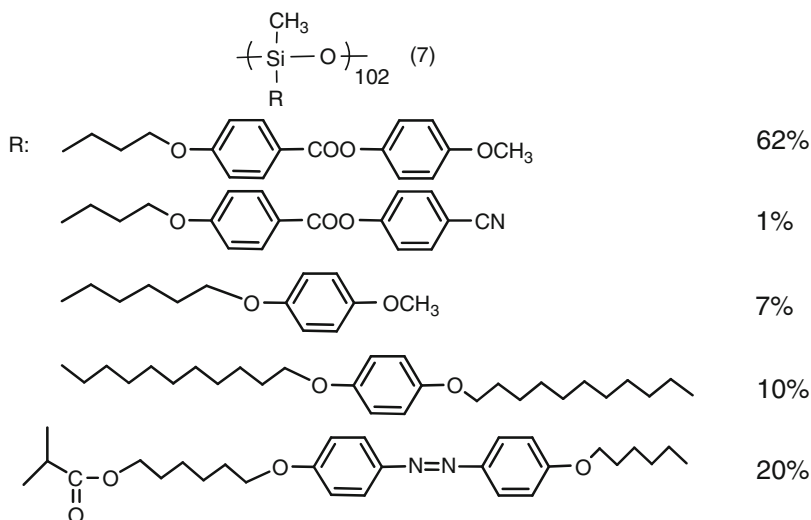
due to photochemistry or photo-heating is to measure the correlation between thermal isomerization rate of the photochromic chromophores and the recovery rate of the film length or the force after switching off the light. The recovery rate should always be slower than or almost equal to the rate of isomerization even when the recovery is induced by photoirradiation, if the process is associated with the photochemical reaction of the photochromic chromophores.

Although many systems showing photostimulated deformation have been reported, the deformation was limited to less than a few percent. If the deformation is larger than 10 %, it is safe to say that it is due to the photochemical effect. One photo-deformable material which shows a large deformation is polyacrylamide gel containing a small amount of triphenylmethane leucohydroxide or leucocyanide groups, as shown in Fig. 2 [5].

A disk-shaped gel (10 mm in diameter and 2 mm in thickness) having 3.7 mol% triphenyl-methane leucohydroxide residues showed photostimulated reversible dilation in water. Upon UV irradiation, the gel swells and the weight increases by as much as three times its original weight in 1 h. The dilated gel contracts in the dark to its original weight in 20 h. The cycles of dilation and contraction can be repeated several times. This gel is the first example showing

Photochromic Polymers, Fig. 2 Structure of the polyacrylamide gel

Photochromic Polymers,
Fig. 3 Structure of the
photochromic elastomer

$$\left(\begin{array}{c} CH_3 \\ | \\ Si - O \\ | \\ R \end{array} \right)_{102} \quad (7)$$

R: ⟶O⟶⟨⟩⟶COO⟶⟨⟩⟶OCH₃   62%

⟶O⟶⟨⟩⟶COO⟶⟨⟩⟶CN   1%

⟶O⟶⟨⟩⟶OCH₃   7%

⟶O⟶⟨⟩⟶O⟶   10%

⟶C–O⟶O⟶⟨⟩⟶N=N⟶⟨⟩⟶O⟶   20%

a reversible deformation of more than 100 %. The effect is purely photochemical and reversible.

The photo-dilation of the above gel is ascribed to an osmotic pressure change produced by photoionization of the leucohydroxides or leucocyanides. Therefore, the effect disappears in a dry system. In 2001 Finkelmann et al. [10] reported the first real photochemical contraction of liquid crystalline elastomers in the dry system. The elastomer is poly[oxy(methylsilylene)] having pendant mesogens as shown in Fig. 3.

The azobenzene pendant groups isomerize from the *trans* to the *cis* form upon irradiation with 365 nm light and revert to the initial *trans* form with a relaxation time of some 100 s in the dark. Upon irradiation with 365 nm light, the elastomer contracts as much as 22 % at 313 K, while it reverts to the initial length in 250 min after switching off the light. The shape change of the elastomer is ascribed to order-disorder phase transition from the nematic to the isotropic phase. The nematic elastomer is known to contract upon heating above the phase transition temperature from the nematic to the isotropic phase. When azobenzene chromophores are incorporated into the elastomer, the phase transition temperature shifts depending on the ratio of the *trans* and the *cis* form. The phase transition temperature change induced by photoirradiation causes the contraction isothermally. This is the mechanism

of the photoinduced shape change of the elastomer. Based on this mechanism, various photoresponsive liquid crystalline elastomers have also been prepared and their shape changes upon irradiation with polarized light were studied [11].

Surface Wettability

Surface wettability is an important property of polymer solids and plays an important role in printing, dyeing, and adhesion. The property depends on the surface free energy, which is expressed in terms of a sum of the dispersion energy and polar energy terms of the surface tension. When photoisomerizable chromophores, which change the polarity reversibly by photoirradiation, are incorporated into a polymer, the surface wettability is expected to become photo-controlled.

The surface wettability of a hydroxyethylmethacrylate–methacryloyl-2-hydroxyethyl-phenylazobenzene copolymer was measured by placing a water droplet on the film surface. The contact angle of the water droplet ($\cos\theta$) increases from 0.22 to 0.41 under UV irradiation, while it decreases to 0.22 upon irradiation with visible light. At the same time, the absorbance due to the *trans* form decreases upon

UV irradiation, while it increases upon visible irradiation. The close correlation between the contact angle and the absorbance indicates that the wettability change of the polymer surface is attributable to the structural change of the azobenzene chromophores. Similar wettability change was observed when triphenylmethane leucohydroxide residues were introduced to polystyrene. These wettability changes can be used for adsorption chromatography.

Sol-Gel Transition and Miscibility of Polymer Blends

The formation of three-dimensional infinite networks in a polymer by a chemical or physical process leads to a gel. Polymer gels are classified into two types, irreversible and reversible ones. The latter are formed by cross-linking due to physical interaction between certain points on different polymer chains, and the sol-gel phase transition is induced by a change in temperature. At temperature Tgel the polymer solution stops flowing, while above Tgel the gel melts to flow. CS_2 solution of polystyrene with pendant azobenzene groups was found to change Tgel upon photoisomerization of the azobenzene chromophores.

Miscibility of polymer blends is an attractive subject from both scientific and industrial view points. Several attempts have been carried out to make immiscible pairs of polymers miscible by incorporating a third component. Immiscible pair of polystyrene and poly(n-butyl methacrylate) becomes miscible when 1.8 % hydroxyl groups are introduced to polystyrene. The result demonstrates that small change in polymer properties alter miscibility markedly. This was confirmed for poly(methyl vinyl ether) blended with polystyrene having pendant stilbene groups. Stilbene isomerizes from the *trans* to the *cis* form upon irradiation with UV light ($300\,nm < \lambda < 400\,nm$) and reverts to the initial *trans* form upon irradiation with 254 nm light. When heated from room temperature, the blend containing *cis* stilbene groups turns optically opalescent at 78 °C, while the blend containing *trans* stilbene groups

still remains transparent at that temperature. The latter turns opalescent at 101 °C. The cloud point temperature of the blend containing 0.25 *cis* fraction is 23 °C lower than that of the blend having all-*trans* stilbene groups.

Solid properties, such as Tg, membrane permeability, and membrane potentials, can also be controlled by photoirradiation when photoisomerizable chromophores are incorporated into the polymers [5].

Surface Relief Grating

Photostimulated birefringence and dichroism upon irradiation with polarized light in polymers having azobenzene chromophores have been extensively studied [12, 13]. The polymers can be used for making volume holographic grating. In addition to such molecular-scale chromophore orientation, massive motion of materials on the surface at room temperature (well below Tg) was reported in 1995 under irradiation with interfering polarized light. Irradiation of polymer films having pendant azobenzene chromophores for a period longer than required for photoinduced orientation produces a modification of the film surface. Grating with depths of up to one micron was obtained. A variety of single beams creates different surface deformations. The surface relief gratings can find various applications, such as one-step holographic image storage, orientation layers in a liquid crystal cell, and so on.

Optical Properties

Photochromic chromophores so far described undergo thermally reversible photochromic reactions. The photogenerated isomers are unstable at room temperature and thermally return to the initial isomers. Therefore, photomodulated properties are unstable and disappeared even stored in the dark. In 1988 a new family of thermally irreversible photochromic chromophores, named diarylethenes, was developed [14]. The chromophores undergo an isomerization from the open- to the closed-ring form upon irradiation with UV
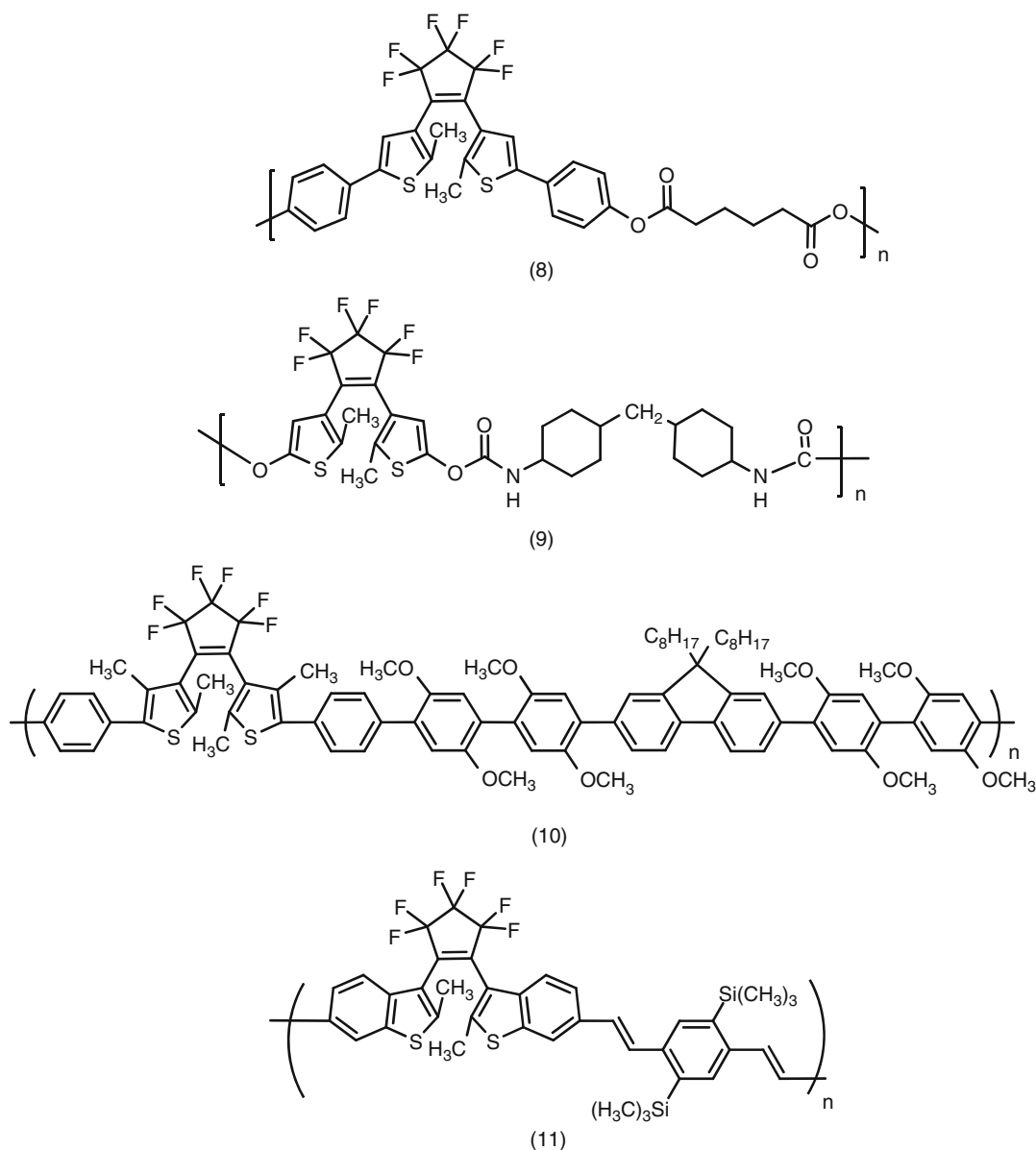
Photochromic Polymers, Fig. 4 Photochromic polymers having diarylethene units in the backbones

light, as shown in Table 1 (d), and the photogenerated isomers are stable at room temperature. The closed-ring form reverts to the initial open-ring form upon irradiation with visible light. When such thermally irreversible photochromic chromophores are incorporated into polymers, as shown in Fig. 4, the photochromic polymers reversibly switch the properties in two discrete states. Typical photoswitchable properties are shown in Table 3.

The change in the refractive index of materials is a key property for photonics applications [15]. The reversible modulation of the refractive index upon photoirradiation can be used for fabricating optical switches for waveguides, such as a Mach–Zehnder type switch or a Y-branch

Photochromic Polymers, Table 3 Photoswitchable properties and applications of diarylethene photochromic polymers

Property	Application
Refractive index	Mach–Zehnder type switch
	Y-branch switch
	Volume-phase holographic grating
Absorbance	Absorbance modulation optical lithography
	Multistate optical memory
Fluorescence	Bioimaging
Electrical conductivity	Molecular electronics

switch. For such application, the most important request is the concentration of photochromic chromophores. Although diarylethene chromophores exhibit a relatively large refractive index change in infrared region (800 nm $< \lambda <$ 1,700 nm) during the photoisomerization, a simple doping procedure to polymers is inadequate, because increasing the concentration induces the segregation of the dopants. To avoid this limit synthesis of photochromic polymers having diarylethenes in the backbones or the side groups has been explored. The polyether having diarylethenes (8) makes an amorphous film and exhibits the photostimulated refractive index change as large as 0.03 at 1,500 nm.

The modulation is also used for making phase holographic optical elements. If the modulation results from a photochromic process, these devices become rewritable. Volume-phase holographic gratings have interesting applications in optics and photonics, such as dispersing elements in astronomical instrumentation, in Raman spectroscopy, and as tunable filters. A polyurethane having diarylethenes in the backbone (9) has been used for such applications. The polymer was also used for absorbance modulation optical lithography. When the polyurethane has different kinds of diarylethene derivatives in the backbone, the polymer can be applied to multistate optical memory.

The change in electrical conductivity of a single diarylethene molecule upon photoirradiation has been studied both experimentally and theoretically. When the diarylethene switches are part of a conjugated main chain of a polymer, photoswitchable semiconducting polymers are obtained [16]. Diarylethene-oligophenylene-fluorene (10) and diarylethene-*p*-phenylene vinylene (11) polymers were prepared, and their reversible conductivity change was found to be as large as one order of magnitude.

The research of photochromic polymers was initially started from the fundamental study of polymer chain conformation in solution. Since the finding of photomechanical effect of polymer films, a lot of effort was paid to develop polymers which exhibit large photostimulated macroscopic change in the size. The photomechanical effect of polymers was finally realized in liquid crystalline elastomers. Now, the research is extended to develop various photonic devices. Although the present studies are limited to conceptual devices, they may find practical applications in the future.

Related Entries

▶ Electrochromic Polymers
▶ Optical Absorption of Polymers
▶ Optical Information Storage
▶ Refractive Index
▶ Stimuli-Responsive Polymers

References

1. Brown GH (1971) Photochromism. Wiley-Interscience, New York
2. Dürr H, Bouas Laurent H (2003) Photochromism: molecules and systems. Elsevier, Amsterdam
3. Lovrien R (1966) The photoviscosity effect. Proc Natl Acad Sci 57:236–242
4. Irie M, Hirano Y, Hashimoto S, Hayashi K (1981) Photoresponsive polymers. 2. Reversible solution viscosity change of polyamides having azobenzene residues in the main chain. Macromolecules 14:262–267
5. Irie M (1990) Photoresponsive polymers. Adv Polym Sci 94:27–67
6. Irie M (2008) Photochromism and molecular mechanical devices. Bull Chem Soc Jpn 81:917–926
7. Merian E (1966) Steric factors influencing the dyeing of hydrophobic fibers. Text Res J 36:612–618
8. Agolini F, Gay FP (1970) Synthesis and properties of azoaromatic polymers. Macromolecules 3:349–351

9. Matějka L, Ilavský M, Dušek K, Wichterle O (1981) Photomechanical effect in crosslinked photochromic polymers. Polymer 22:1511–1515

10. Finkelmann H, Nishikawa E, Pereira GG, Warner M (2001) A new opto-mechanical effect in solids. Phys Rev Lett 87:015501-1–015501-4

11. Ikeda T, Mamiya J, Yu Y (2007) Photomechanics of liquid-crystalline elastomers and other polymers. Angew Chem Int Ed 46:506–528

12. Delaire J, Nakatani K (2000) Linear and nonlinear optical properties of photochromic molecules and materials. Chem Rev 100:1817–1845

13. Natansohn A, Rochon P (2002) Photoinduced motions in azo-containing polymers. Chem Rev 102:4139–4175

14. Irie M (2000) Diarylethenes for memories and switches. Chem Rev 100:1685–1716

15. Bertarelli C, Bianco A, Castagna R, Pariani G (2011) Photochromism into optics: opportunities to develop light-triggered optical elements. J Photochem Photobiol C Photochem Rev 12:106–125

16. Tsujioka T, Irie M (2010) Electrical function of photochromic molecules. J Photochem Photobiol C Photochem Rev 11:1–14

Photochromism

Jiro Abe, Hiroaki Yamashita and Katsuya Mutoh
Department of Chemistry, School of Science and Engineering, Aoyama Gakuin University, Sagamihara, Kanagawa, Japan

Synonyms

Photochromy; Phototropy

Definition

Photochromism is simply defined as a light-induced reversible transformation of a chemical species between two forms that have different absorption spectra. Photochromic materials are a well-known class of molecules that change their color upon irradiation with light. The photogenerated species can be reversed to the initial species either thermally or by subsequent irradiation with a specific wavelength of light [1–3]. Photochromic systems can be classified into two categories depending on the thermal stability of the photogenerated species: T-type (thermally reversible type), when the photogenerated isomers revert thermally to their initial forms; P-type (photochemically reversible type), when they do not revert to the initial isomers even at elevated temperatures. Azobenzenes, spiropyrans, spirooxazines, benzopyrans, naphthopyrans, and hexaarylbiimidazoles are typical T-type photochromic compounds, while diarylethenes with heterocyclic rings and fulgides are stable P-type photochromic compounds. Switching of the physical and chemical properties of materials using photochromic compounds has been the subject of considerable research. There is an increasing interest in the use of organic photochromic compounds to modulate conductivity, fluorescence, magnetism, and shape at the bulk level [4]. One of their most common applications is their use in photochromic lenses that darken in sunlight. The ideal conditions for photochromic lenses are satisfied with molecules that can be stimulated by sunlight to rapidly develop an intense coloration in a wide range of visible light and can be returned to the initial state with fast fading kinetics in addition to fatigue resistivity for many coloring–decoloring cycles.

Azobenzene

Azobenzene and its derivatives have been well known as a dye, for example, they are used as food coloring, printer ink, optical recording material, and so on (Fig. 1). Azobenzene is composed of two aromatic rings where an azo linkage ($-N=N-$) joins the two phenyl rings. Azobenzene exhibits reversible photoisomerization around the $N=N$ double bond between the thermodynamically more stable *trans* isomer and the less stable *cis* isomer. The characteristic absorption band of the *trans* isomer at around 320 nm attributable to the $\pi-\pi^*$ transition decreases with the *trans–cis* isomerization upon UV light irradiation, and at the same time, the absorption band in the visible light region arising from the $n-\pi^*$ transition increases. In contrast,

Photochromism,
Fig. 1 Photochromism of
azobenzene
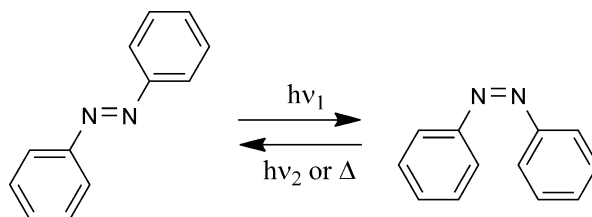
the *cis–trans* isomerization occurs following irradiation with visible light, which corresponds to the n–π^* transition of the *cis* isomer. This isomerization reaction also proceeds thermally. Since the photoinduced *trans–cis* isomerization of azobenzene causes a drastic structural change (the distance between 4 and 4' carbons decreases from 9 Å in the *trans* isomer to 5.5 Å in the *cis* isomer), the structural transformation has attracted interest for its potential applications for novel functional materials, such as molecular machines, photomechanical materials, light-driven actuator, and photoswitchable catalysts.

The first example of a molecular machine consisting of a photoresponsive azobenzene unit and a crown ether moiety as an ionophore was synthesized by Shinkai and co-workers, and its complexation and extraction properties were evaluated [5]. When the azobenzene-based molecular machine is irradiated by UV–vis light, the reversible conformation changes occur, leading to a change in the affinity toward alkali metal cations Li^+, Na^+, K^+, Rb^+, and Cs^+. Furthermore, Kinbara, Aida, and co-workers have reported a light-driven molecular scissors based on the reversible photo-transformation of azobenzene molecules [6]. The molecular scissors are composed of two phenyl groups as blade moieties, a ferrocene unit as a pivot part, and two phenylene groups as handle parts. Upon irradiation with UV–vis light, the molecular motion of azobenzene in the *cis–trans* isomerization process is translated into an open–close motion of the blade moieties through the pivot part. This light-driven motion was monitored by ^{1}H NMR and circular dichroism spectroscopy.

As mentioned above, while extensive studies have been carried out on the motion control of individual molecules in solution, the amplification of the molecular motion of azobenzene to macroscopic motion has also attracted great interest. Ichimura and co-workers have reported a light-driven motion of a liquid droplet on a photoresponsive surface [7]. In this study, a droplet such as olive oil is put on a silica plate modified with a calixarene derivative bearing azobenzene units at one of the rims of the cyclic skeleton. An asymmetric irradiation with UV–vis light causes a gradient in surface free energy due to the photoisomerization of azobenzene groups; as a result, the droplet can move one dimensionally on the silica plate. The direction and velocity of the droplet motion are tunable by varying the direction and steepness of the gradient in light intensity. Moreover, they also demonstrated that the fluid substance in a surface-modified glass tube can be moved by the asymmetrical irradiation. This result suggests potential applicability to microscale chemical process system.

Light-driven polymer actuators have attracted many researchers' interest due to their potential application as artificial muscles for robotic arms or motors. Ikeda and co-workers demonstrated that a single film of a cross-linked liquid–crystal network containing an azobenzene chromophore serves as a photomechanical actuator [8]. This photoresponsive actuator sheet can be repeatedly bent along any chosen direction by using linearly polarized UV–vis light. In the film, the azobenzene units in each liquid-crystalline domain are unidirectionally aligned. When the film is exposed to a linearly polarized light, the azobenzene units parallel to the polarized light are selectively excited to give the corresponding isomers, and therefore the macroscopic contraction is generated. Ikeda and co-workers have also successfully demonstrated that plastic motor can be driven by sophisticated motion of photoresponsive liquid-crystalline elastomer films laminated on polyethylene sheet over irradiation with UV and visible light.

P

Spiropyrans and Spirooxazines

Spiropyrans are the most amply studied family of the photochromic compounds (Fig. 2a). Particularly, from the 1980s to the 1990s, spiropyrans attracted attention due to their potential applicability in data recording and storage, optical switching displays, and nonlinear optics [9]. The photochromic reaction of spiropyran was discovered by Fischer and Hirshberg in 1952. Spiropyrans composed of two different heterocyclic moieties, a benzopyran and an indoline, linked orthogonally on a spiro carbon. Irradiation of spiropyrans with UV light brings about the C—O bond cleavage within several picoseconds and the subsequent *cis–trans* thermal isomerization of the C=C double bond in the microsecond range, leading to the formation of the merocyanines [10]. Most of the merocyanines are thermally unstable, leading to the back reaction to the initial spiro

form even in the dark. The thermal bleaching rates are generally low since the thermal bleaching processes of the merocyanines are attributable to the *cis–trans* thermal isomerization of the C=C double bond and the subsequent cyclization reaction. It is particularly worth noting that the merocyanines have zwitterionic characteristics. The isomerization processes of spiropyrans are, therefore, described by the reversible interconversion between the less polarized spiro form and highly polarized merocyanines, resulting in their unique photoswitching properties.

The photoswitching of nonlinear optical (NLO) properties of spiropyrans were extensively studied from the 1980s to the 1990s. Merocyanines have large molecular second-order nonlinear optical coefficients (β) due to their zwitterionic characteristics. In general, β is proportional to the difference in dipole moment ($\Delta\mu$) between the ground and exited states.
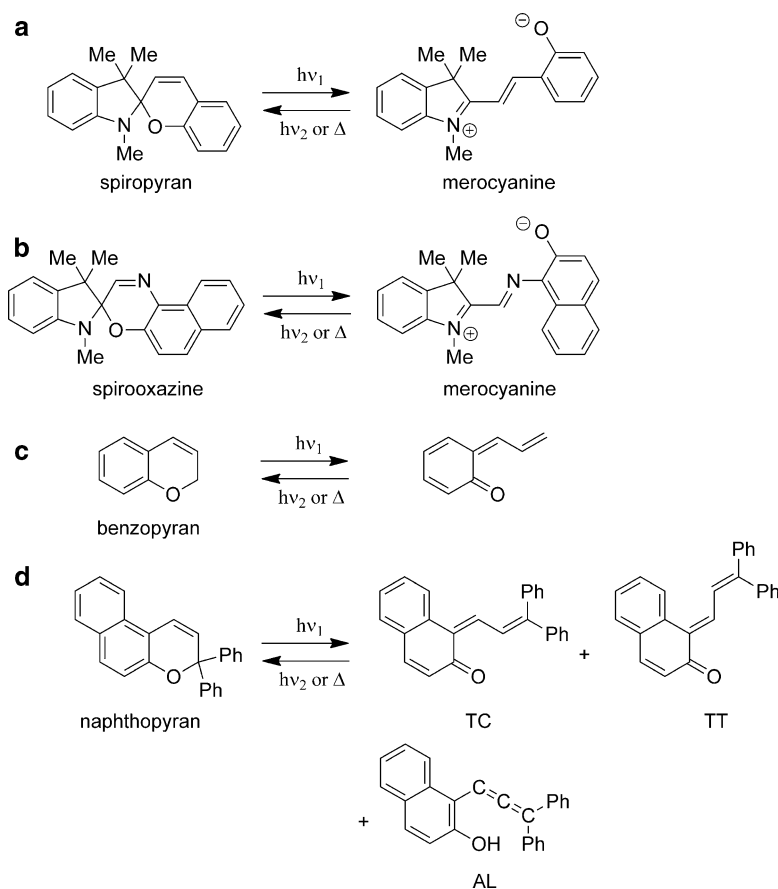
Photochromism,
Fig. 2 Photochromism of
(**a**) spiropyran,
(**b**) spirooxazine,
(**c**) benzopyran, and
(**d**) naphthopyran

The reversible interconversion between the spiro form (small β) and the merocyanine (large β) enables the photoswitching of the NLO properties. For example, the photoswitching of the second harmonic generation (SHG) intensity was reported for the spiropyran-doped poly(methyl methacrylate) (PMMA) and quasi-liquid crystal [9].

Recently, the photoswitching capabilities of spiropyrans have attracted much attention in the research field related to biology and biochemistry. The photoisomerization processes accompanied by significant change in affinity for solvents or ions, enabling the photoregulation of the fluorescence properties of small molecules, the mechanical and surface properties of the bulk materials, and the solubility and conformation of macromolecules. Particularly, photoresponsive polymer materials have been studied by many research groups. In an acidic aqueous solution at a certain temperature, a polymer material consisting of thermoresponsive polymer, poly(N-isopropylacrylamide) (NIPAM), as backbones and spiropyrans as side chains is known to exhibit dehydration and precipitation in response to the light irradiation, because protonated and positively charged merocyanines deprotonate and isomerize into hydrophobic spiro form.

Spirooxazines are the photochromic compounds closely related to spiropyrans and were synthesized at 1968 for the first time (Fig. 2b). Photochromic reaction of spirooxazines occurs in the same manner as that of spiropyran. Spirooxazines attracted attention because of the interest of its application to the ophthalmic lenses due to their relatively high fatigue resistance. Generally, the colored species of spirooxazines are blue color despite considerable research to control the photochromic properties of spirooxazines [1, 9].

In the process of studying the photochromic reaction of spiropyran, Becker et al. found that the benzopyran (2H-chromene) (Fig. 2c) undergoes photochromic reaction in 1966. The photochromic behavior of benzopyran is attributable to the C—O bond cleavage, resulting in the formation of the open-ring colored isomer, which revert back to the initial colorless isomer

thermally or photochemically with visible light [1]. It is known that the colored isomer of benzopyran is non-zwitterionic despite zwitterionic characteristics of merocyanines, which are the colored isomers of spiropyrans.

Naphthopyrans shows relatively fast thermal bleaching and have high fatigue resistance (Fig. 2d). And thus, naphthopyrans have been investigated extensively because of the interest of its application to the ophthalmic lenses. Irradiation of naphthopyrans with UV light brings about the C—O bond cleavage leading to colored isomers, the transoid-cis (TC), transoid-trans(TT), and allenyl-naphthol (AL) isomer. The AL isomer is less thermally stable than the others and observed only at low temperature. The TC isomer, which is the main product of the photochromic reaction, rapidly reverts back to the initial colorless isomer. On the other hand, the lifetime of the TT isomer is longer than that of the TC isomer. Generally, it takes a few minutes to several tens of minutes for the thermal bleaching of the TC isomer and several tens of minutes to a few hours for that of the TT isomer [1].

The photochromic lenses can control the optical transmittance in response to intensity of incident light, commonly UV light, by using the photochromic reactions. The preparation of commercially acceptable plastic photochromic lenses requires a variety of the photochromic properties such as color, optical density, thermal bleaching rare, fatigue resistance, etc. Since the mid-1980s, 3H-naphtho[2,1-b]pyran and 2H-naphtho[1,2-b] pyran (Fig. 3), which are main classes of naphthopyrans, have attracted attention as the

3H-naphtho[2,1-b]pyrans   2H-naphtho[1,2-b]pyrans
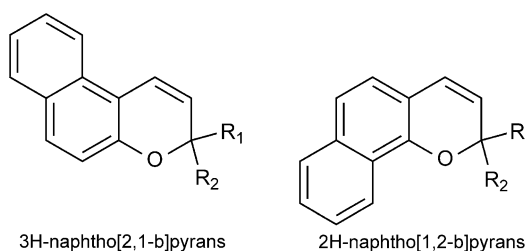
Photochromism, Fig. 3 Chemical structures of 3H-naphtho[2,1-b]pyrans and 2H-naphtho[1,2-b]pyrans
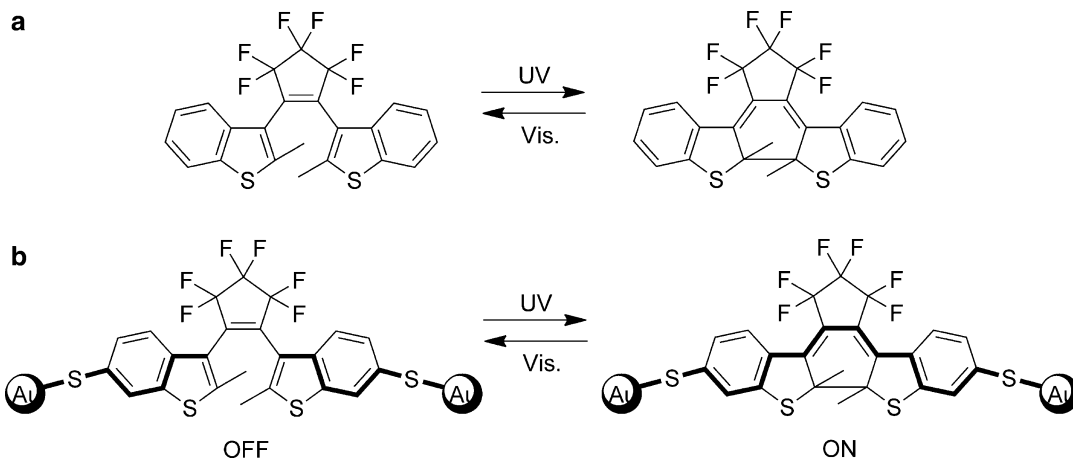
Photochromism, Fig. 4 (**a**) Photochromism of diarylethene and (**b**) photoelectrochemical switching of diarylethene

photochromic compounds suitable for practical ophthalmic lenses, and the substituent effect in the photochromic properties of these compounds have been closely examined [1]. Now, plastic lenses doped with 2H-naphtho[1,2-b]pyrans have already been in practical use.

Diarylethene

Diarylethene is one of the P-type photochromic molecules developed by Irie in 1980s. The colorless open-ring form of diarylethene undergoes a photocyclization reaction producing the colored closed-ring form upon exposure to UV light. The closed-ring form returns to the open-ring form by visible light irradiation (Fig. 4a). The remarkable feature of diarylethene is the fatigue resistance. Especially, diarylethenes having heterocyclic aryl groups are thermally irreversible and have high resistance to fatigue. According to the Woodward–Hoffmann rules, the thermal- and photocyclization reaction occur in disrotatory and conrotatory mode, respectively. The cyclization reaction of diphenylethene and difurylethene is demonstrated by the quantum chemical calculation to reveal the thermal stability of heterocyclic diarylethene. The aryl groups of the closed-ring form lose their aromaticity, whereas the aryl groups have the aromaticity in the open-ring form. Therefore, the aryl groups having large

aromaticity are destabilized in the closed-ring isomer. From this theoretical point, the thermally irreversible and fatigue-resistant diarylethene could be synthesized. The quantum yield of conversion to by-product in the coloration/decoloration cycle is less than 0.0001, and the cycle could be repeated more than 10,000 times. Such P-type photochromic molecules are expected to apply to the optical data storages and switches [3, 11].

The current optical data storages are based on the magneto-optic and the phase transition effect by the laser irradiation. However, in those systems, the light energy is changed into the thermal energy on the recording medium. The temperature of the medium is increased to Curie point or melting point, leading to the phase transition. The physical property changes resulting from the heating are used as records. On the other hand, the optical memories using photochromic compounds are based on a photon-mode recording. The photon-mode recording has several advantages such as high resolution and fast writing speed, compared with heat-mode recording. One of the important properties to apply the photochromic molecules to the optical memories is nondestructive readout because the light for readout also induces the photochromic reaction generating the initial isomer, resulting in the elimination of the recording. Therefore, several researchers focus on the fluorescence and IR

readout to avoid the destructive readout. The fluorescence readout is carried out at single-molecule level. Diarylethene possessing a fluorescent unit can modulate the fluorescence intensity by the photoconversion between the open-ring and closed-ring form. In addition, the isomerization by fluorescence excitation light can be restrained by controlling the S_1 energy level of the fluorescent unit. The infrared (IR) measurement is also efficient for the nondestructive readout because the energy of IR radiation does not cause any molecular change. The C=C stretching mode in the 1,400–1,650 cm^{-1} region is suitable to detect the difference of the two photo-isomers. In this spectral region, the open-ring isomer has three bands at 1,637, 1,592, and 1,544 cm^{-1}. On the other hand, the new three bands at 1,612, 1,574, and 1,503 cm^{-1} are appeared in the closed-ring isomer, which can be attributable to the new C=C bonds of photogenerated conjugated system. Therefore, the nondestructive reading is achieved by the detection of the remarkable molecular vibration spectra with switching the molecular structure upon UV and visible light irradiation [3].

The photochromic compounds change their physicochemical properties (e.g., refractive index, dielectric constants, electrochemical potentials, and geometrical structures) upon photoirradiation. These property changes with photochromism have the potential application to the photonic devices. Above all, the control of refractive indices is the most important for optical waveguide such as optical switches, variable frequency filters, attenuators, and phase shifters. For these applications, the thermal irreversibility is also a significant character. The reversible photocontrol of the electrochemical properties is of high interest for the application to the molecular electronic devices. Diarylethenes show large changes of their π-conjugation systems between the open-ring and closed-ring isomer. In the open-ring isomer ("OFF" state), the two thiophene groups are electronically separated and have no efficient interaction with each other. On the other hand, in the closed-ring isomer ("ON" state), the π electrons delocalize over the two thiophene groups. Therefore, the photoswitching

of the conductive properties between "ON" and "OFF" state can be achieved by connecting diarylethenes to metal nanoparticles or metal electrodes (Fig. 4b) [3].

One of the important features of diarylethene is crystalline photochromism [3]. Although there are many reports about photochromic molecules, the compounds which show photochromism in crystalline state are rare. The crystalline photochromism in which both isomers are thermally stable can be applied to the photonic devices and photomechanical materials. The open-ring form of diarylethene has two types of conformation in solution. One is the non-photochromic parallel conformation, and the other is the photochromic antiparallel conformation. Although only antiparallel open-ring form is existed in crystalline state, there are some crystals which cannot undergo a color change by UV light irradiation. The reactive character of diarylethene in crystalline state is explained as resulting from the difference in the distance between reactive carbon atoms. By investigating the reactivity–structure relationship, it was revealed that the photochromism of the diarylethene crystal in which the distance of the reactive sites is larger than 4.2 Å is suppressed. The reversible morphological change of the diarylethene crystal is observed, based on the structural changes with photoisomerization. On irradiation with UV light, the crystal shape is changed from square to lozenge reversibly. Moreover, the rodlike crystal bends with directionality when light is irradiated to the crystal inhomogeneously [12]. This rodlike crystal can lift the slug which weight is 200 times greater than that of the crystal. This light-driven actuator can be applied to the manipulators and photo-driven valves in the biochemical field.

Hexaarylbiimidazole

Hexaarylbiimidazole (HABI) was discovered in the early 1960s by Hayashi and Maeda, and it has since attracted significant interest because of its unusual physical properties (Fig. 5a) [13]. Various stimuli, such as heat, light, and pressure, readily cleave HABI into a pair of

Photochromism, Fig. 5 Photochromism of (**a**) hexaarylbiimidazole, (**b**) naphthalene-bridged imidazole dimer, and (**c**) [2.2]paracyclophane-bridged imidazole dimer
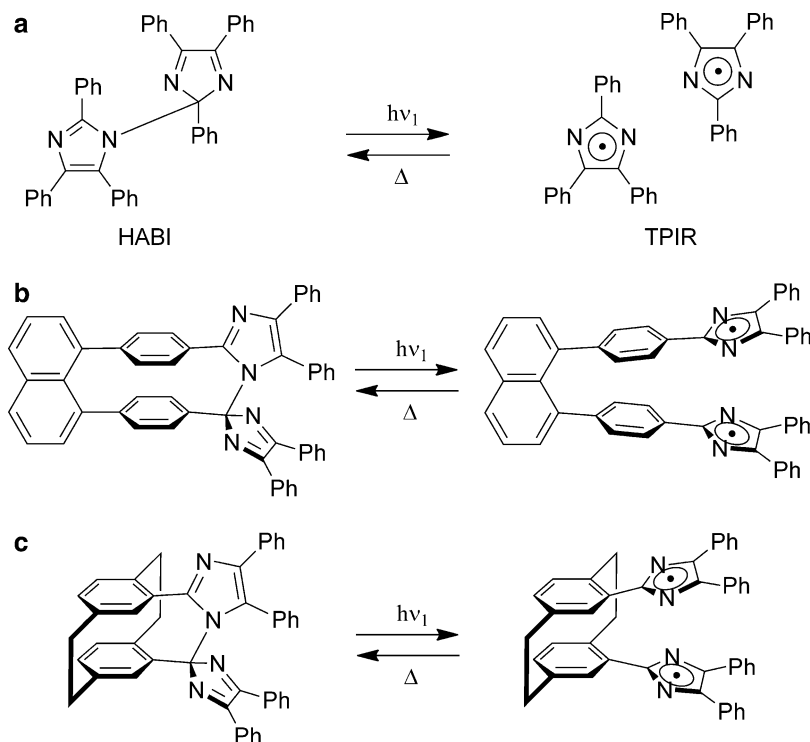
2,4,5-triphenylimidazolyl radicals (TPIRs), which thermally recombine to reproduce their original imidazole dimer. The solution of HABI changes from colorless to purple upon UV irradiation. This photochromic behavior is attributed to the photoinduced homolytic cleavage of the C—N bond between the imidazole rings. The photochromism of diarylethene is a closed-ring-/open-ring-type switching, while that of HABI is a closed-shell-/open-shell-type switching, which can be regarded as a diamagnetic/paramagnetic photoswitching. The dissociation of HABI into TPIRs occurs along the repulsive potential energy surface of the first excited singlet state with a time constant of 80 fs [3]. The high yield of TPIRs in solid matrices and their low sensitivity to the presence of oxygen have stimulated industrial interest in the use of HABIs as a photoinitiator for a variety of imaging materials.

There are a number of spectroscopic studies for the photochemical reaction of HABI and their derivatives [3]. The thermal transformation of TPIR into HABI in solution requires several

minutes at room temperature since the radical–radical reactions generally obey second-order kinetics. The recombination of the radical pairs (RPs) formed by photodissociation provides fundamental information on the solvent cage effect and the dynamic behavior of the encounter RPs in bimolecular chemistry. The nonreactive random encounter RP, which subsequently separates, is formed by diffusion, while the reactive random encounter RP is formed only when the RP approaches with their reactive sites facing each other. Thus, the diffusion process and spatial arrangement of the encounter RPs made it difficult to study of the reaction kinetics of the radical–radical reactions in solution. A number of investigations on the photodissociation processes yielding two of the same radicals via photoexcitation have been published for tetraphenylhydrazine and diphenyl disulfide derivatives. Ernsting et al. reported that bis(*p*-aminophenyl) disulfide undergoes the photodissociation in the time region of 40–100 fs in various solvents. Following excitation, Ernsting et al. observed that the geminate recombination

between the nascent radicals in viscous solutions occurs in the first 2 ps [14]. Similar results were confirmed for the other diphenyl disulfide derivative. Although the time constant of the dissociation in HABI is comparable to those for the diphenyl disulfide derivatives, the radical recombination process of TPIRs is very slow as described above. The recombination process in the time frame of seconds to hours required large activation entropy, indicating that the geometrical restriction for the recombination is severe. This restriction might contribute to the inhibition of the rapid geminate recombination in the nascent RP.

Recently, the bridged imidazole dimers (Fig. 5b, c) that show instant coloration upon exposure to UV light and rapid fading in the dark have been developed [3]. They also show photoinduced homolytic bond cleavage of the C—N bond between the imidazole rings and successive fast C—N bond formation. The diversity of the molecular design and the ease of synthesis make this class of photochromic compounds highly attractive for high-performance ophthalmic plastic lenses and revolutionary optical switching devices. In view of the thermal bleaching rate, the fast photochromism of the bridged imidazole dimers can be applied to real-time image processing at video frame rates. Thus, molecular design based on the photochromism of HABI can lead to the development of a new family of photochromic compounds with unprecedented switching speeds and remarkable stability. These could eventually evolve into solid-state photonic materials with unique photoresponsive characters.

Related Entries

▶ Optical Information Storage

References

1. Crano JC, Guglielmetti RJ (1999) Organic photochromic and thermochromic compounds. Plenum Press, New York
2. Dürr H, Bouas-Laurent H (2003) Photochromism: molecules and systems. Elsevier, Amsterdam
3. Irie M, Yokoyama Y, Seki T (2013) New frontiers in photochromism. Springer, Tokyo
4. Feringa BL, Browne WR (2011) Molecular switches, 2nd edn. Wiley-VCH, Weinheim
5. Shinkai S, Nakaji T, Nishida Y, Ogawa T, Manabe O (1980) Photoresponsive crown ethers. 1. Cis-trans isomerism of azobenzene as a tool to enforce conformational changes of crown ethers and polymers. J Am Chem Soc 102:5860–5865. doi:10.1021/ja00538a026
6. Kinbara K, Aida T (2005) Toward intelligent molecular machines: directed motions of biological and artificial molecules and assemblies. Chem Rev 105:1377–1400. doi:10.1021/cr030071r
7. Ichimura K (2000) Photoalignment of liquid-crystal systems. Chem Rev 100:1847–1873. doi:10.1021/cr980079e
8. Ikeda T, Mamiya J, Yu Y (2007) Photomechanics of liquid-crystalline elastomers and other polymers. Angew Chem Int Ed 46:506–528. doi:10.1002/anie.200602372
9. Berkoviz G, Krongauz V, Weiss V (2000) Spiropyrans and spirooxazines for memories and switches. Chem Rev 100:1741–1753. doi:10.1021/cr9800715
10. Tamai N, Miyasaka H (2000) Ultrafast dynamics of photochromic systems. Chem Rev 100:1875–1890. doi:10.1021/cr9800816
11. Irie M (2000) Diarylethenes for memories and switches. Chem Rev 100:1685–1716. doi:10.1021/cr980069d
12. Kobatake S, Takami S, Muto H, Ishikawa T, Irie M (2007) Rapid and reversible shape changes of molecular crystals on photoirradiation. Nature 446:778–781. doi:10.1038/nature05669
13. Hayashi T, Maeda K (1960) Preparation of a new phototropic substance. Bull Chem Soc Jpn 33:565–566. doi:10.1246/bcsj.33.565
14. Bultmann T, Ernsting NP (1996) Competition between geminate recombination and solvation of polar radicals following ultrafast photodissociation of bis(p-aminophenyl) disulfide. J Phys Chem 100:19417–19424. doi:10.1021/jp962151n

P

Photoinitiated Polymerization

Masamitsu Shirai
Department of Applied Chemistry, Osaka Prefecture University, Naka-ku, Sakai, Osaka, Japan

Synonyms

Photopolymerization

Definition

Polymerization is initiated by active species such as radicals, cations, or anions which are generated by the photoinduced chemical reactions of the initiators.

Introduction

Photoinitiated polymerization is one of the polymerization techniques of monomers, where the polymerization is initiated by reactive species such as radicals, cations, or anions that can be generated by photo-irradiation. Once initiated, the chain reaction will develop very much like in a conventional thermal polymerization, except for the much larger rates of initiation that can be reached by high irradiation dose. The photoinitiated polymerization is very important with regard to industrial applications. Highly cross-linked polymers are readily prepared by the photoinitiated polymerization of multifunctional monomers at room temperature. Liquid monomers can be turned to a solid by the polymerization. This technology is called UV curing.

The main advantage of the UV curing is the high polymerization rate and high conversion that can be achieved under intense irradiation. Another important feature of the photoinduced polymerization is that it takes place only at the irradiated areas, and thus, relief patterns can be obtained after irradiation using a mask and subsequent development with solvents. Furthermore, UV curing presents a number of other advantages such as room temperature operation, solvent-free formulations, and low energy consumption. Thus, the UV curing technology is now widely utilized in industries.

Most of the research efforts for photoinitiated polymerization are focused on the efficient photoinitiators, highly reactive monomers, functional monomers, and potential applications. A large variety of high-performance compounds (monofunctional and multifunctional monomers, photoinitiators, sensitizers) are now commercially available. Acrylate-based monomers, which are polymerized by a radical mechanism, have been thoroughly investigated. Photoinduced cationic polymerization of epoxides and vinyl ethers has also been studied because of their some properties such as insensitivity toward oxygen and living character providing a substantial dark polymerization. Since photoinitiators are essential for the photoinitiated polymerization, new photoinitiators which can generate radical, cation, or anion species have been developed. Those initiators are developed from the standpoint of high sensitivity at given wavelengths of irradiation light, environmental safety, and cost for industrial use.

## Basic Principle of Photoinitiated Polymerization

Photoinitiated polymerization is initiated by reactive species such as radicals and ions, which are generated by photo-irradiation [1–4]. Since most monomers do not form the initiating species when they are exposed to UV light, a photoinitiator must be added to the monomers. The over all process for the photoinitiated radical polymerization is shown in Fig. 1. Several types of lamps are used as light sources, e.g., medium-pressure Hg, low-pressure Hg, Xe, Hg–Xe, metal halide, and LED lamps as well as laser [1]. A wavelength region of the emitting light from the lamp must be consistent with the absorption region of the photoinitiator to obtain the effective generation of the reactive species from it. Recently the use of LED lamp is accelerated because it is an energy-saving light source compared to the conventional lamps. However, unfortunately, the LED lamp which can emit shorter wavelengths of light ($\lambda < 365$ nm) is not commercially available at present.

Initiator $\xrightarrow{h\upsilon}$ R· $\xrightarrow{M}$ R-M· $\xrightarrow{n\,M}$ Polymer
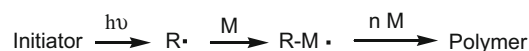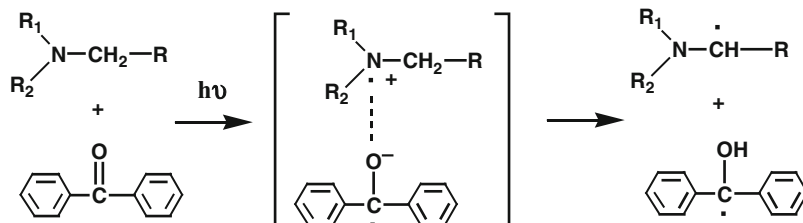
Photoinitiated Polymerization, Fig. 1 A process for photoinitiated radical polymerization

Photoinitiated Polymerization, Fig. 2 Photoinduced radial generation in type I system

DMPA
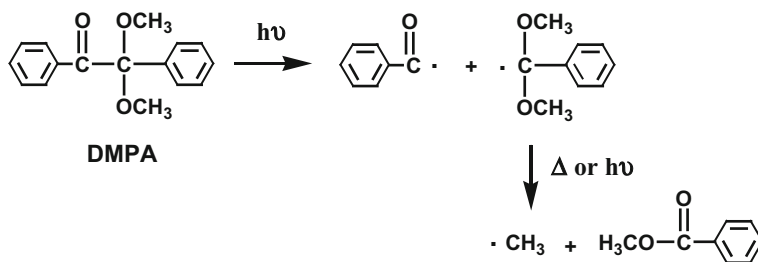
Photoinitiated Polymerization, Fig. 3 Photoinduced radial generation in type II system
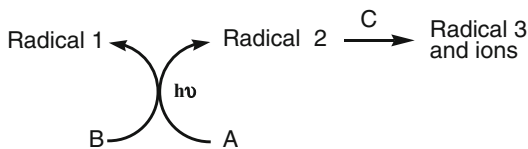

Photoinitiators

Photoinitiators can be divided into three types based on the reactive species (radical, cation, and anion) which can be generated by photo-irradiation.

Photoradical Initiators

Photoradical initiators are classified as one-component (type I system), two-component (type II system), and multicomponent photoinitiating systems [5]. The type I system is mostly based on the Norrish type I photoreaction of ketone compounds such as benzoin ethers, dialkoxyacetophenones, hydroxy alkyl phenyl ketones, benzoyl oxime esters, benzoyl phosphine oxides, morpholino ketones, and α-amino ketones. They are commercially available and generally sensitive to UV light (250–360 nm), while some of them are sensitive to longer wavelength light (~430 nm). Some organometallic compounds such as titanocene derivatives are sensitive to ~500 nm. A mechanism of the photoinduced radical generation from a benzoin ether derivative (2,2-dimethoxy-2-phenylacetophenone (DMPA)) is shown in Fig. 2. According to the Norrish type I photoreaction, DMPA generates radical species such as benzoyl, dimethoxy benzyl, and methyl radicals. The initiating species for the radical polymerization are

the benzoyl radical, the methyl radical, and, to a lesser extent, the dimethoxy benzyl radical that rather behaves as a chain-terminating agent. In the presence of solvents such as tetrahydrofuran in solution polymerization or of a substrate containing labile hydrogen atoms, the benzoyl radical can abstract a hydrogen atom to create benzaldehyde and a new initiating radical from the solvent or the substrate. Although both of the methyl and benzoyl radicals efficiently react with the monomer double bonds, in the case of the polymerization of methyl acrylate, the reactivity of the methyl radical is about 30 times higher than that of the benzoyl radical.

The type II system is based on electron transfer or hydrogen abstraction reactions of ketone compounds. A mixture of benzophenone and amine is a typical type II system which can generate radicals by the electron transfer from amine to ketone as shown in Fig. 3. There are photoinduced ketyl and aminoalkyl radicals. The reactivity of the aminoalkyl radical to methyl acrylate is 2–3 orders of magnitude higher than that of the ketyl radical. Thus, the ketyl radical is usually considered as a terminating agent for growing polymer chains. As a ketone component for the type II system, benzophenones, thioxanthones, camphorquinones, benzils, α-diketones, anthraquinones, and ketocumarines can be used. Many types of tertiary amines are employed as

P

Photoinitiated Polymerization, Fig. 4 Concept of multicomponent photoinitiation system

electron-donating components. Benzophenones and thioxanthones can also work through a direct hydrogen abstraction reaction in the presence of H donors such as alcohols and tetrahydrofuran. The hydrogen donor can also be a polymer chain having labile hydrogen atoms.

Many multicomponent photoinitiating systems have been proposed in order to improve the efficiency of the radical generation. An example of this concept is shown in Fig. 4. A mixture of **A** and **B** is irradiated to generate radicals 1 and 2. Here, concomitantly generated radical 2 acts as a scavenger of the growing polymer chain. The idea is to eliminate radical 2 by using appropriate quencher **C** to generate radical 3 and ions. Radical 3 initiates the polymerization similarly to radical 1.

There are so many kinds of mono- and multifunctional monomers which are radically polymerizable. Acrylate-based monomers are most widely used because the polymerization rate by the radical chain mechanism is very fast. Many types of acrylate-based multifunctional monomers including hyperbranched, dendritic, and telechelic types are developed and used in industrial applications. Methacrylate-based monomers are also widely used, though the polymerization rate is slow compared to acrylate-based monomers.

A mixture of multifunctional thiol and ene compounds with a photoradical initiator is radically polymerizable by a stepwise reaction mechanism [6]. Thiol-ene polymerization is based on a stoichiometric reaction of multifunctional olefins and thiols, e.g., thiol-vinyl ether, thiol-allyl ether, thiol-acrylate, and thiol-yne. The thiol-ene polymerization shows some interesting features: a very fast process, a low or no oxygen inhibition effect, formation of highly cross-linked networks

with good adhesion, reduced shrinkage and stress, and improved physical and mechanical properties.

Photoacid Generators

Compounds that can generate acids on irradiation of light are called photoacid generators (PAG) and significantly used as an initiator for photoinduced cationic polymerization of certain monomers [1, 7–9]. PAG can be divided into two groups according to their characteristics, i.e., ionic and nonionic types. The ionic PAG basically involves onium salts such as aryldiazonium, diaryliodonium, triarylsulfonium, and triarylphosphonium salts that contain anions (X^-) such as BF_4^-, SbF_6^-, AsF_6^-, PF_6^-, and $C_xF_ySO_3^-$. The mechanisms for their photolysis have been investigated in detail. When these onium salts are irradiated with ultraviolet (UV) light, they undergo photolysis to form Brønsted or Lewis acids. Diphenyliodonium and triphenylsulfonium salts are thermally very stable and commonly used as a photoinitiator for cationic polymerization. The chemical structures of diphenyliodonium and triphenylsulfonium salts can be modified by introducing alkyl groups onto the phenyl rings to change their spectral absorption characteristics and to enhance their solubility in organic solvents. Figure 5 shows mechanisms for the photoinduced generation of acids from iodonium- and sulfonium-salt PAG.

On the other hand, many types of nonionic PAG have been developed and used to generate carboxylic, sulfonic, and phosphoric acids upon irradiation. PAGs that can form sulfonic acids involve 2-nitrobenzyl esters of sulfonic acids, 2-diazo-1-oxo-1,2-dihydronaphthalene derivatives, imino sulfonates, N-hydroxyimide sulfonates, tris(methylsulfonyloxy)benzene, and so on. Nonionic PAG has a much wider range of solubility in organic solvents and in polymer films compared to onium salt PAGs. The nonionic PAGs are thermally less stable than the onium salt PAG.

The photoinduced cationic polymerization of epoxides, oxetanes, and vinyl ethers can be accomplished using diphenyliodonium and triarylsulfonium salts having SbF_6^-, AsF_6^-,

Photoinitiated Polymerization, Fig. 5 Mechanisms for photoinduced acid generation
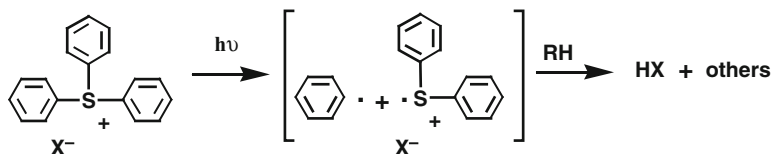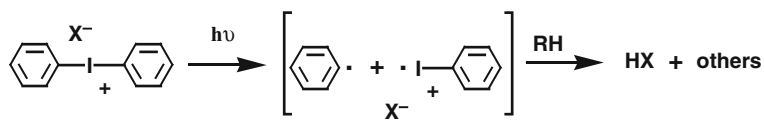
Photoinitiated Polymerization, Fig. 6 Photoinduced formation of epoxide-based networks using PBG
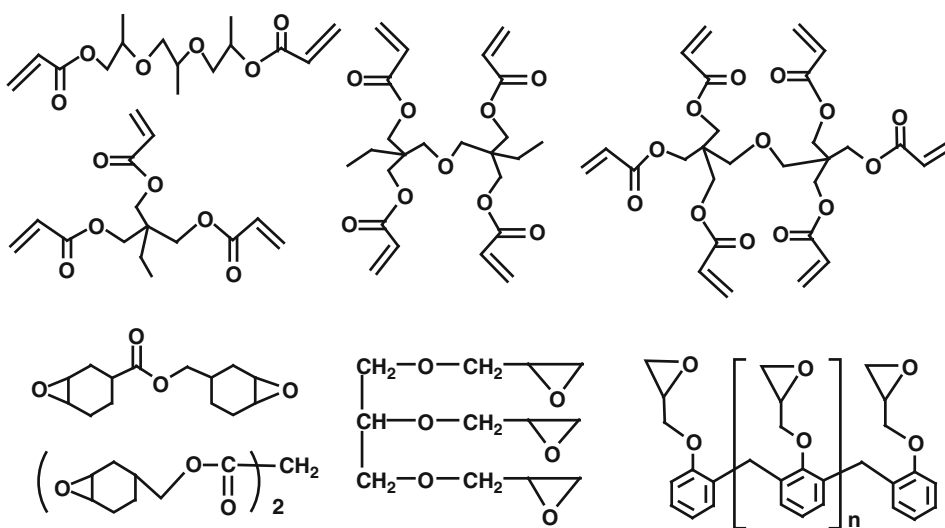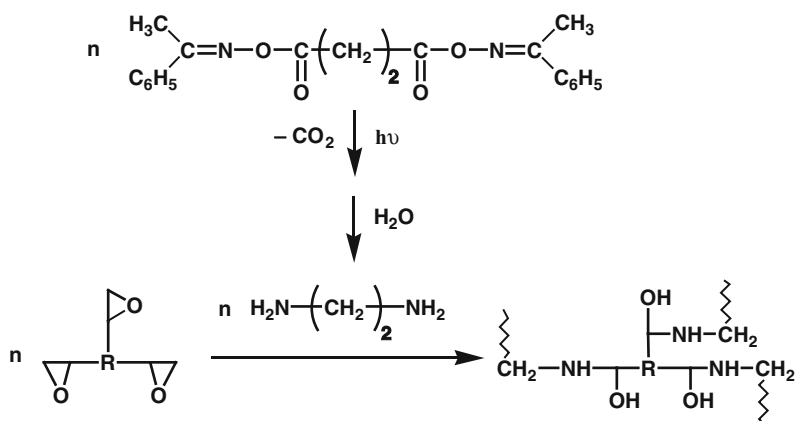
Photoinitiated Polymerization, Fig. 7 Commonly used multifunctional acrylates and epoxides

and PF_6^- as counter anions which have a non-nucleophilic nature. The photoinitiated polymerizations of multifunctional epoxides are especially significant in the industrial applications.

Photobase Generators

The compounds that can generate basic species including anion and amines on irradiation are called photobase generators (PBG) [1, 10]. PBG involves cobalt complexes, ammonium salts, O-acyloximes, carbamates, α-aminoketones, benzyloxycarbonyl derivatives, cinnamic acid derivatives, and so on. Many of them can generate alkylamines, but the example of the PBG that can generate anion or very strong base is quite limited. Thus, photochemically generated amine is mostly used as a cross-linker in the multifunctional epoxide system as shown in Fig. 6. PBGs are also used as catalysts for the base-catalyzed reactions to form polymer networks.

Applications

The photoinitiated polymerizations of multifunctional acrylate-based and epoxide-based monomers are very significant in relation to the industrial applications in wide areas [2, 4, 5, 9, 10]. Figure 7 shows examples of these monomers. UV curing is extensively used in various industrial areas, e.g., (i) coating applications on a variety of substrates such as wood, plastics, metal, papers, optical fibers, and so on; (ii) adhesive-related industries such as laminating and packaging; (iii) graphic art-related industries such as drying of inks, ink-jet, labels, and protective and decorative coatings; (iv) dentistry- and medicine-related industries such as restorative and preventative denture relining, wound dressing, ophthalmic lenses, artificial eye lens, and so on [11]; and (v) microelectronic-related industries such as solder resists and negative photoresists [12]. The applications of the photoinitiated polymerizations in high-tech areas are observed in the imaging technology industries dealing with photolithography for LSI production, 3D printing (three-dimensional photopolymerization or stereolithography), holographic recording, and UV imprint lithography [13].

Furthermore, from the scientific point of view, photoinitiated polymerization is a good tool to obtain polymers from thermally unstable monomers because the polymerization can be carried out at or even below room temperature.

Related Entries

► Anionic Addition Polymerization (Fundamental)
► Cationic Addition Polymerization (Fundamental)
► Free-Radical Addition Polymerization (Fundamental)
► Photolithography and Photoresist
► Polymerization Reactions (Overview)

References

1. Fourssier JP (2012) Photoinitiators for polymer synthesis. Wiley-VCH, Weinheim
2. Fouassier JP (2006) Photochemistry and UV curing: new trends 2006. Research Signpost, Kerala
3. Belfield KD, Crivello JV (2003) Photoinitiated polymerization. American Chemical Society, Washington, DC
4. Decker C (1996) Photoinitiated crosslinking polymerization. Prog Polym Sci 21:593–650. doi:10.1016/0079-6700(95)00027-5
5. Fouassier JP (2010) Photoinitiators for free radical polymerization reactions. In: Allen NS (ed) Photochemistry and photophysics of polymer materials. Wiely, Hoboken. doi:10.1002/9780470594179
6. Hoyle CE, Lee TY (2004) Thiol-enes: chemistry of the past with promise for the future. J Polym Sci Part A Polym Chem 42:5301–5338. doi:10.1002/pola.20366
7. Sangermano M (2012) Advances in cationic photopolymerization. Pure Appl Chem 84:2089–2101. doi:10.1351/PAC-CON-12-04-11
8. Kahveci MU, Yilmza AG, Yagci Y (2010) Photoinitiated cationic polymerization: reactivity and mechanistic aspects. In: Allen NS (ed) Photochemistry and photophysics of polymer materials. Wiely, Hoboken. doi:10.1002/9780470594179
9. Shirai M, Tsunooka M (1996) Photoacid and photobase generators: chemistry and applications to polymeric materials. Prog Polym Sci 21:1–45. doi:10.1016/0079-6700(95)00014-3

10. Suyama K, Shirai M (2009) Photobase generators: recent progress and application trend in polymers systems. Prog Polym Sci 34:194–209. doi:10.1016/j.propolymsci.2008.08.005
11. Jandt KD, Mills RW (2013) A brief history of LED photopolymerization. Dental Mater 29:605–617. doi:10.1016/j.dental.2013.02.003
12. Ito H (2005) Chemically amplified resists for microlithography. Adv Polym Sci 172:37–245. doi:10.1007/b97574
13. Lan H, Liu H (2013) UV-nanoimprint lithography: structure, materials and fabrication of flexible molds. J Nanosci Nanotechnol 13:3145–3172. doi:10.1166/jnn.2013.7437

Photolithography and Photoresist

Hiroto Kudo
Department of Chemistry and Materials Engineering, Faculty of Chemistry, Materials and Bioengineering, Kansai University, Suita, Osaka Prefecture, Japan

Synonyms

EB lithography; EUV lithography; Litho; Lithography; Resist; Resist material; UV lithography

Definition

Photolithography is a process to construct patterns using photoresist on a substrate by the exposure with a laser.

Introduction

Figure 1 depicts the process of photolithography system. The solution of photoresist is spin coating on the silicon wafer to form a thin film. The thin film was exposed by a laser and developed with a solvent to give two types of resist patterns: positive tone and negative tone. A positive tone can be obtained by that the exposed parts are soluble, and a negative tone can be done by that the exposed parts are insoluble in a developer.

Moore's law for the development of photolithographic technology predicts an exponential increase of microelectronic component densities as shown in Fig. 2 [1].

To achieve increased densities, new photolithography systems employ electron beams (EBs) and short-wavelength lasers, such as g-line ($\lambda = 436$ nm), i-line ($\lambda = 365$ nm), KrF ($\lambda = 248$ nm), ArF ($\lambda = 193$ nm), and extreme ultraviolet (EUV) ($\lambda = 13.5$ nm). At the same time, the appropriate photoresist materials have been developed according to the progress of photolithography systems. When designing photoresist materials for lithography systems, the requirements of their properties are as follows: (1) transparency in the laser, (2) good solubility and good film-forming ability to form thin film, (3) good photochemical reactivity, (4) sufficient mechanical integrity of the pattern, and (5) high etch resistance. The polymers based on phenol resins, polystyrenes, and polymethacrylates (polyacrylates) were modified with photoreactive groups and applied as photoresist in each photolithography systems [2, 3]. It was also reported that molecular photoresist materials based on low-molecular-weight phenol resins and cyclic oligomers were examined to offer higher-resolution resist patterns [4]. Furthermore, the chemical amplification resist system using a photoacid generator has offered enhanced photosensitivity by the exposure of a laser [5].

Chemical Amplification Photolithography System

Typical photoresist using chemical amplification photolithography system is shown in Fig. 3. This polymer contains t-butyloxycarbonyl (BOC) groups in the side chain. When the thin film prepared by the solution of photoresist material and photoacid generator (PAG) was irradiated by a laser, PAG decomposed to produce an acid H^+ at first. This H^+ attacks to a BOC group to give a new H^+ accompanying with carbon dioxide and isobutylene. The H^+ can be amplified one after another deprotection reaction. As a result, the

P

chemical reaction can occur under low exposure dose of a laser, i.e., the sensitivity of photoresist increases.

Molecular Photoresist

Molecular resist materials have been employed in EB and EUV lithography systems. Most of them have hydroxyl groups in the side chain, due to
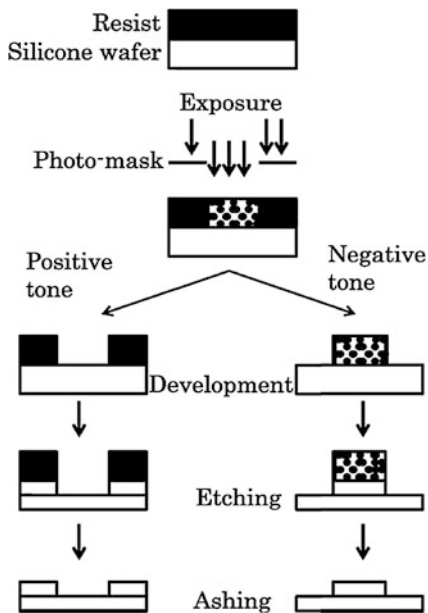
Photolithography and Photoresist, Fig. 1 Photolithography process

that they are expected to provide good film-forming ability and good adhesion to the substrate, owing to its hydrophilicity. At first, some calixarene derivatives showed high-resolution pattern using point beam EB irradiation [6, 7].

Ober et al. reported the synthesis of *p-t*-butylcalix [4] resorcinarene derivatives with pendant diazonaphthoquinone moieties, and a negative pattern with 60 nm resolution could be obtained by EB exposure system without chemical amplification (Fig. 4) [8].

Ueda et al. also reported a negative EB resist pattern using the mixture of calix [4] resorcinarene (CRA), 4,4′-methylenebis [2,6-bis(hydroxymethyl)phenol](MBHP) as a cross-linker and a photoacid generator. A clear pattern with 1.0 μm resolution could be obtained by i-line exposure system (Fig. 5) [9].

Hattori et al. reported the synthesis and EB resist pattern using a truxene derivative with pendant adamantyl ester groups (Fig. 6), and a clear 22 nm resolution pattern was obtained with an EB exposure system [10].

Oizumi et al. reported the synthesis of fullerene derivatives with pendant *t*-BOC and *t*-butyl ester groups and examined their patterning properties with an EUV lithography system (Fig. 7) [11]. A 45 nm-hp pattern as positive-type resist was obtained at EUV exposure dose of 12.5 mJ/cm^2, and resolution of up to 26 nm-hp could be obtained as positive tone.
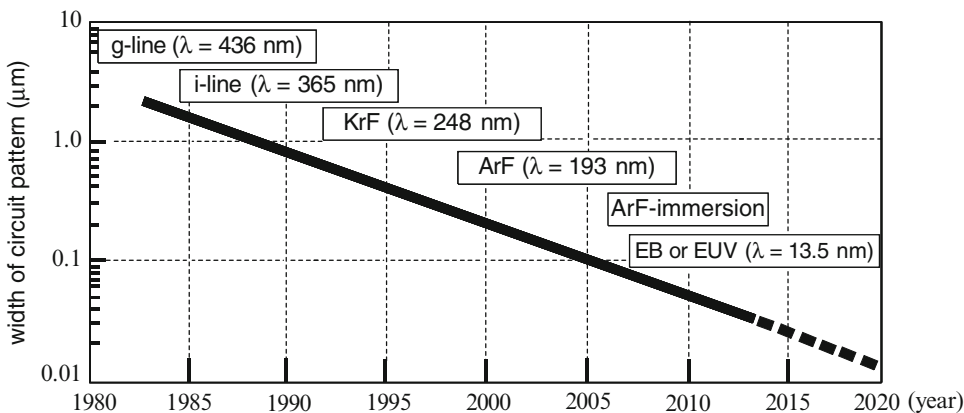
Photolithography and Photoresist, Fig. 2 Moore's law (development of IC chip)
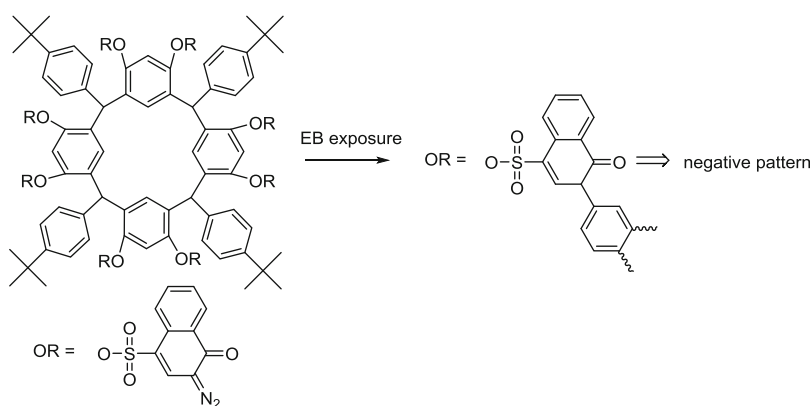
Photolithography and Photoresist,
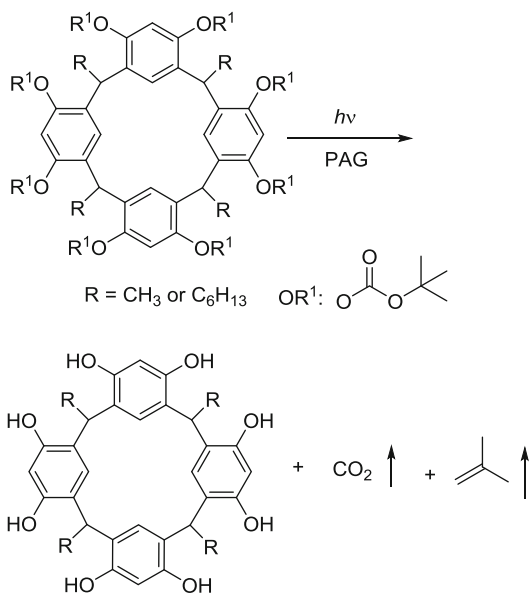**Fig. 3** Chemical amplification system using photoacid generator
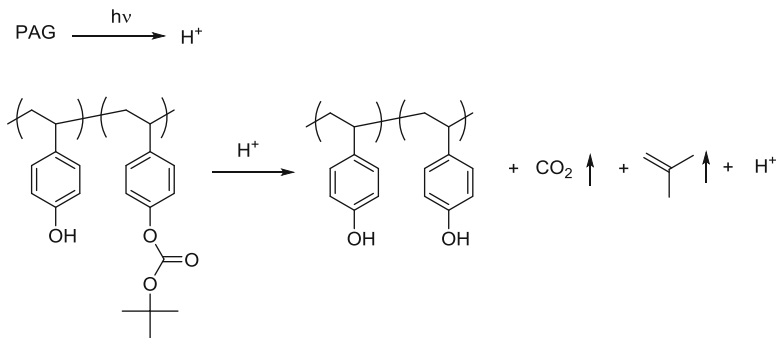
Photolithography and Photoresist,
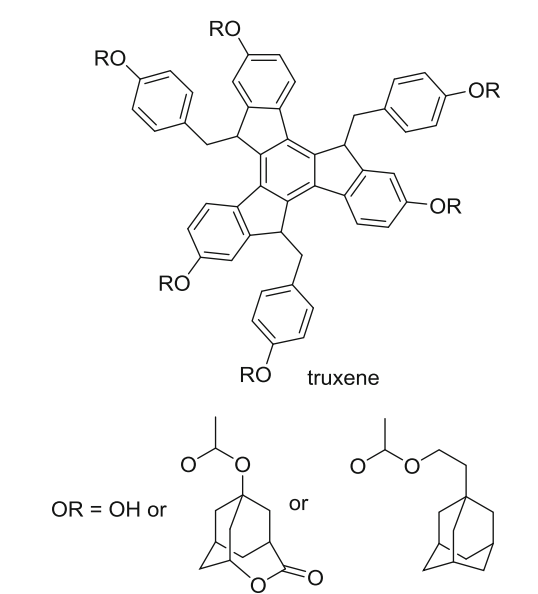**Fig. 4** Negative resist based on calixarene

Photolithography and Photoresist, Fig. 5 Positive resist based on calix[4]resorcinarene
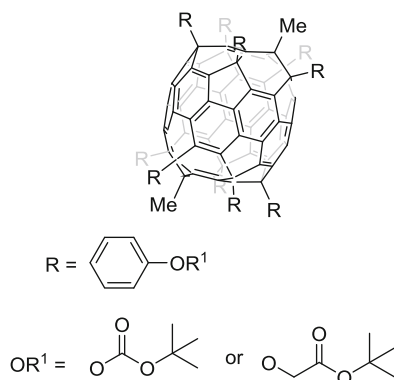
Photolithography and Photoresist, Fig. 6 Positive resist based on truxene

P

Kudo et al. reported the synthesis of noria (waterwheel-like ladder cyclic oligomer) derivatives with pendant photodegradable groups as EB and EUV resist materials (Fig. 8). Noria derivatives containing *t*-butoxycarbonyl groups [12] and *t*-butyl ester groups [13] showed clear line-and-space patterns with resolutions of $50 \sim 70$ nm in an EB resist system. The noria derivative containing adamantyl ester group (noria-AD) showed a clear line-and-space pattern with a resolution of 26 nm at an EUV exposure of 14.5 mJ/cm^2 [14].

Henderson et al. reported the synthesis of a photoacid-generator (PAG)-bonding molecular resist, tris[4-(*t*-butoxycarbonyloxy)-3.5-dimethylphenyl]sulfonium hexafluoroantimonate, and examined its patterning properties using EB and EUV exposure (Fig. 9) [15, 16]. The sensitivity and line-edge roughness (LER) were improved compared to those of non-PAG-bonding molecular resist, and a 50 nm resolution was obtained in the EB system.

Next-Generation Photolithography and Photoresist

In next-generation lithography systems, EB or EUV exposure systems are expected and a resolution of better than 15 nm is required. To obtain such high resolution, the photoresists must be very sensitive to exposure tool. However, high sensitivity is associated with increased roughness [line-edge roughness (LER) or line width roughness (LWR)], which is unfavorable for high resolution. That is, there is a trade-off of three factors: resolution of the resist pattern, LER value of the resist pattern, and sensitivity of the photoresist, as shown in Fig. 10. To overcome this trade-off, the development of new photoresist material has been required.

Photolithography and Photoresist, Fig. 7 Positive resist based on fullerene

Photolithography and Photoresist, Fig. 8 Positive resist based on noria
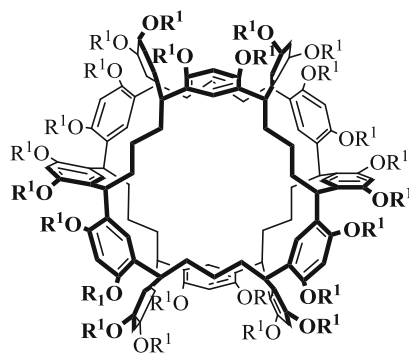
noria derivative	noria-BOC	noria-AD
OR^1		
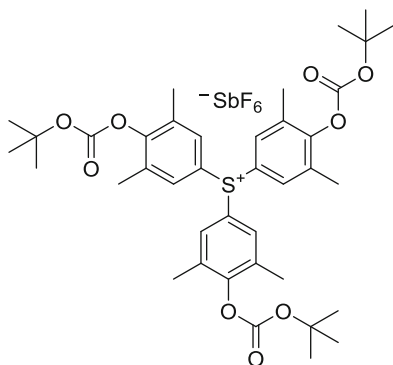
Photolithography and Photoresist, Fig. 9 PAG-bounding molecular resist

Photolithography and Photoresist, Fig. 10 Trade-off between sensitivity, line roughness, and resolution of resist pattern
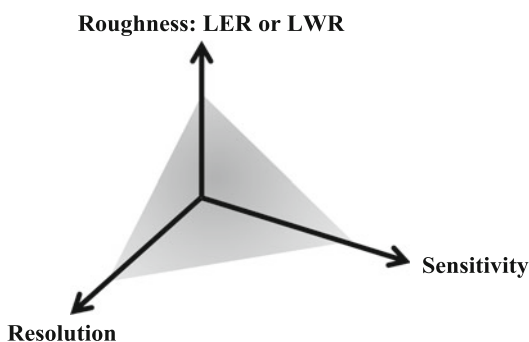
Summary

Various photoresists based on polymers and low-molecular-weight compounds have been investigated in attempts to obtain very high-resolution resist patterns in the next photolithography systems. However, there is a trade-off among characteristic properties such as resolution, line-edge roughness, and sensitivity of the photoresist. At such high resolution, the line-edge roughness of the resist pattern remains the most significant problem. Synthesis of new photoresist and improvement of exposure system must be investigated together to accomplish the problem.

Related Entries

▶ Photoinitiated Polymerization

▶ Photoresponsive Polymer

References

1. Goethals AM, Vandenberghe G, Pollentier M, Ercken P, Bisschop D, Maenhoudt M, Ronse K (2001) Recent progress in ArF lithography for the 100 nm node. J Photopolym Sci Technol 14:333–340. doi:10.2494/photopolymer.14.333

2. Ito H (2005) Chemical amplification resists for microlithography. Adv Polym Sci 172:37–245. doi:10.1007/b97574

3. Kinoshita H, Kurihara K, Ishii Y, Torii Y (1989) Soft x-ray reduction lithography using multilayer mirrors. J Vac Sci Technol B7:1648. doi:10.1116/1.584507

4. Nishikubo T, Kudo H (2011) Recent development in molecular resists for extreme ultraviolet lithography. J Photopolym Sci Technol 24:9–18. doi:10.2494/photopolymer.24.9

5. Willson CG, Ito H, Fréchet JMJ, Tessier TG, Houlihan FM (1986) Approaches to the design of radiation-sensitive polymeric imaging systems with improved sensitivity and resolution. J Electrochem Soc 133:181–187. doi:10.1149/1.2108519 R.L

6. Fujita J, Onishi Y, Ochiai Y, Matsui S (1996) Ultrahigh resolution of calixarene negative resist in electron beam lithography. Appl Phys Lett 68:1297–1299. doi:10.1063/1.115958

7. Ochiai Y, Manako S, Yamamoto H, Teshima T, Fujita J, Nomura EJ (2000) High -resolution, high-purity calix[n]arene electron beam resist. J Photopolym Sci Technol 13:413–417. doi:10.2494/photopolymer.13.413

8. Bratton D, Ayothi R, Deng H, Cao HB, Ober CK (2007) Diazonaphthoquinone molecular glass photo-resists: patterning without chemical amplification. Chem Mater 19:3780–3786. doi:10.1021/cm062967t

9. Ueda M, Takahashi D, Nakayama T, Haba O (1998) Three-component negative-type photoresist based on calix[4]resorcinarene, a cross-linker, and a photoacid generator. Chem Mater 10:2230–2234. doi:10.1021/cm980166n

10. Hattori S, Yamada A, Saito A, Asakawa K, Koshib T, Nakasugi T (2009) High resolution positive-working molecular resist derived from truxene. J Photopolym Sci Technol 22:609–614. doi:10.2494/photopolymer.22.609

11. Oizumi H, Tanaka K, Kawakami K, Itani T (2010) Development of new positive-tone molecular resists based on fullerene derivatives for extreme ultraviolet lithography. Jpn J Appl Phys 49:06GF04. doi:10.1143/JJAP.49.06GF04

12. André X, Lee JK, DeSilva A, Ober CK, Cao HB, Deng H, Kudo H, Watanabe D, Nishikubo T (2007)

P

Phenolic molecular glasses as resists for next-generation lithography. SPIE 6519:65194B. doi:10.1117/12.722919

13. Kudo H, Watanabe D, Nishikubo T, Maruyama K, Shimizu D, Kai T, Shimokawa T, Ober CK (2008) A novel noria (water-wheel-like cyclic oligomer) derivative as a chemically amplified electron-beam resist material. J Mater Chem 18:3588–3592. doi:10.1039/B805394D

14. Kudo H, Suyama Y, Nishikubo T, Oizumi H, Itani T (2010) Novel extreme ultraviolet (EUV)-resist material based on noria (water wheel-like cyclic oligomer). J Mater Chem 20:4445–4450. doi:10.1039/B925403J

15. Lawson RA, Lee CT, Yueh W, Tolbert L, Henderson CL (2008) Water-developable negative-tone single-molecule resists: high-sensitivity nonchemically amplified resists. SPIE 6923:69230Q. doi:10.1117/12.773188

16. Lawson RA, Lee CT, Whetsell R, Yueh W, Robert J, Tolbert L, Henderson CL (2007) Molecular glass photoresists containing photoacid generator functionality: a route to a single-molecule photoresist. SPIE 6519:65191N. doi:10.1117/12.712928

Photonic Crystal

Jae-Hwang Lee[1,2] and Edwin L. Thomas[1]
[1]Department of Materials Science and Nano Engineering, Rice University, Houston, TX, USA
[2]Department of Mechanical and Industrial Engineering, University of Massachusetts, Amherst, MA, USA

Synonyms

Periodic dielectric material; Photonic band gap material

Definition

Photonic crystals (PhCs) are inhomogeneous optical materials having periodically varying optical parameters (or dielectric constants) used to engineer and control the propagation and emission of photons. Light scattering arising from every inter-material interface of the periodic medium results in the coherent superposition of photons of specific energies (or frequencies) and depending on the phase relations can result in propagating and nonpropagating modes in various directions. This range of forbidden energies is called *photonic band gap* (PBG). If a PhC has PBG for all possible propagation directions and for all polarizations of light, the PBG is called a *complete* PBG and the other case is called a partial PBG or a *pseudo-gap*. Depending on the dimensionality of the spatial modulation of the optical parameters, 1D, 2D, and 3D PhCs are possible. The term, "photonic crystal" was originally coined by Yablonovitch for 3D PhCs [1].

The *photonic band diagram* is a useful tool and displays the photonic energy (or frequency) dispersion relation $\omega(\mathbf{k})$, as a function of wave vector, $\mathbf{k}$ (see Fig. 1). The photon speed is given by the group velocity, $v_g = \partial \omega / \partial k_z$. The dispersion relation for the photons in vacuum is entirely linear with a slope of c (dashed line) regardless of the size of the wave vector. The photonic band diagram of a 1D PhC for light incident along the layer normal (z-axis) is shown in Fig. 1a. In the 1D PhC, the slope (i.e., v_g) for small wave vectors (low frequencies) is also linear but scaled down by the effective refractive index (RI) of the PhC, n_{eff}, arising from the different RIs of the two constituent materials. In contrast, for wave vectors of magnitude near π/a where a is a periodicity (or a lattice constant) of the PhC, $\omega(k)$ is highly nonlinear. Because the electric field energy associated to a specific photonic mode is decreased as the electric field energy concentrates more in the high RI regions [2], the electric field, $E(z)$ with $k_z = \pi/a$ (Fig. 1c), has less energy $(-\Delta\omega)$ compared to that of the homogeneous medium of n_{eff}. On the other hand, the same electric field profile can exist by concentrating its high electric field in the low RI regions (Fig. 1d), which results in energy increase by $+\Delta\omega$. As there are no modes with an energy in the frequency region between ω_1 and ω_2, such photons entering from the exterior of a PhC from sufficiently low RI medium will be completely reflected regardless of polarizations. Although this 1D PBG opening occurs for wave vectors of multiples of π/a, the lowest PBG at $k_z = \pi/a$ is called as the *fundamental* PBG. The dispersion

Photonic Crystal, Fig. 1 The schematic illustration of the origin of a PBG (*red-orange* region) in one dimension. (**a**) Photonic energy dispersion relation in a 1D PhC. (**b**) The change of photonic energy at the band edge. (**c**) An electric field mode profile immediately below the gap. (**d**) An electric field mode profile immediately above the gap. Both modes are standing waves, $v_g = 0$
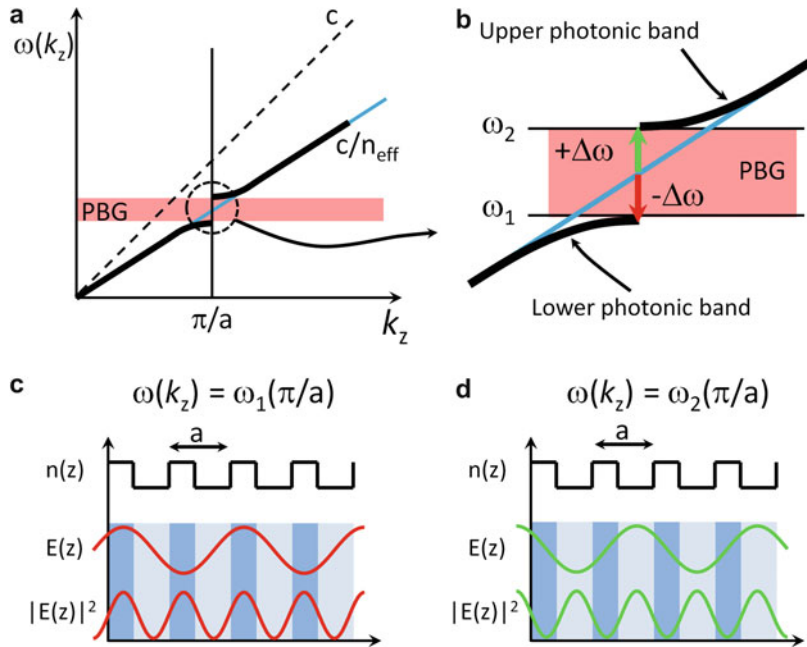

curve is discontinuous and the wave vector $k_z = \pi/a$ is referred as the *photonic band edge* (Fig. 1b). However, the propagation of photons in the xy-plane is still allowed for this 1D PhC. Due to the PBG opening, the photonic bands are flat near the photonic band edge, and this leads to an extremely slow group velocity. Although this physical origin of a PBG is still valid for 2D and 3D PhCs, achieving one or more frequency regions with a complete PBG is difficult and depends on the RI contrast, the symmetry, and topology of PhCs, as well as the volume fraction of the different dielectric components.

In almost all applications of PhCs, a higher contrast of RI is important as it generally leads to a stronger PBG effect due to the increased strength of interface scattering, allowing actual PhC devices to be smaller since fewer unit cells are required to control the propagation of photons.

History of 3D Photonic Crystals

Although a simple dielectric mirror (as commonly used in optical tables) can be considered as a 1D PhC, its generalized concept,

a 3D PhC, was first proposed by Yablonvitch [3] in 1987 as a hypothetical 3D periodic structure capable of inhibiting the spontaneous emission of a gain medium contained inside the structure to create a highly efficient laser. Since an excited atom in the hypothetical material cannot decay into a lower energy state via spontaneous emission if the emitting photon is not allowed to exist (no propagating mode) in the material, the excited state can have a long enough lifetime for stimulated emission which could lead to a very low threshold laser. Simultaneously John [4] also pointed out that one could potentially be able to locally confine photons within a small range ($\sim\lambda$) by locally disordered substructures within a globally periodic structure. As photons cannot exist within the PhC material except around the structural defects, the propagation path of photons can be tightly guided using designed defect networks in the material and thereby creating a type of integrated photonic circuit. Experimentalists were quick to try to make a 3D PhC and demonstrate the new effects. Due to the almost spherical Brillouin zone of the face-centered cubic (fcc) structure, the first 3D PhC was manually fabricated by creating a fcc lattice of air spheres in epoxy (a unit cell size of 12.7 mm).

P
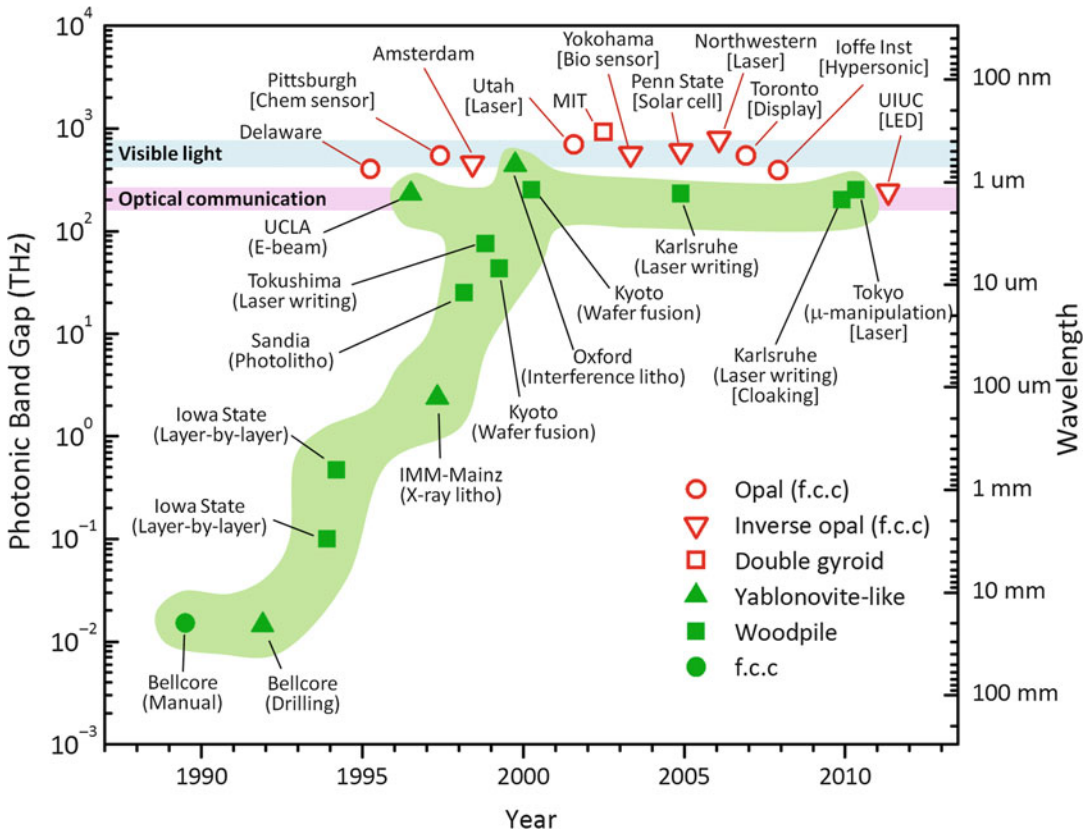
Photonic Crystal, Fig. 2 The experimental progress of 3D photonic crystals. The *green* symbols represent top-down approaches. Information in *parenthesis* and *brackets* are fabrication method and applications, respectively. The open/red symbols represent bottom-up self assembly approaches

A fundamental PBG of the 3D PhC was in the microwave regime (the green solid circle in Fig. 2). However, the PBG turned out to be only a pseudo gap rather than a complete gap (later on a complete gap of this fcc PhC was predicted at higher frequencies between the eighth and ninth photonic bands). Ho et al. were the first to theoretically predict a complete PBG as a fundamental PBG in a diamond structure [5], and various diamond-like 3D PhCs have been proposed, fabricated, and tested. During the first decade, fabrication was mainly top-down in the quest for the structure working in the optical telecomm regime (~1.5 μm). Interesting experimental demonstrations such as passive photonic circuits were demonstrated in the microwave regime with macro-scale PhCs. Since reaching the optical regime, the progress of 3D PhC research has been slow and has not yet achieved the original intention to commercially demonstrate integrated photonic circuits for on chip opto-electronics. Despite this slow progress, mainly due to the difficulties to build a precise 3D sub-micrometer structure using high RI materials, certain advances such as efficient lasing using a very high quality factor cavity in a 3D PhC with a complete PBG have been made recently [6].

Structures having a pseudo gap in the visible regime can be readily made by self-assembly. A synthetic opal structure with fcc symmetry was made by the colloidal self-assembly of polystyrene microspheres and exhibited a pseudo gap in the visible in 1995 [7], and its inverted structure or *inverse opal* structure by a sol-gel process (of titania), which is advantageous for a wider

Photonic Crystal,
Fig. 3 Schematic
illustration of several
important PhC structures.
Structures (**a**, **c**, **d**, **f**) can
exhibit a complete 3D PBG
in the optical regime for
sufficient RI contrast given
in parenthesis
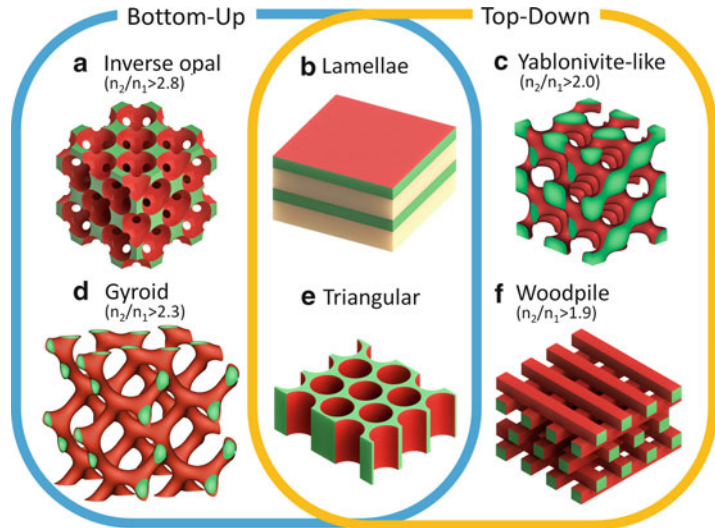
PBG, was produced and demonstrated a PBG along the [111] direction in 1998 [8]. Although the opal and inverse opal structures have basically same structure as the first macro-scale 3D PhC made in 1989, easy-to-make PhCs operating in the visible have been very attractive for other applications. A 3D PhC with the double gyroid morphology was formed by micro-phase separation of a high molecular weight di-block copolymer (BCP). A BCP comprised of covalently bonded immiscible polymer blocks undergoes micro-phase separation into various morphologies depending on the relative volume fractions and block molecular weights (see Fig. 3). In contrast to the PhCs fabricated by the top-down techniques, these bottom-up, mostly self-assembled PhCs were demonstrated in the visible regime from the beginning and are applicable to diverse applications including lasers, solar cells, sensors, and light-emitting diodes as shown in the visible spectrum region in Fig. 2.

Periodic Structures for Photonic Crystals

A variety of periodic dielectric structures have been introduced for PhCs, and some of them are illustrated in Fig. 3. Multilayer thin-film mirrors (1D PhC) with a quarter-wave thickness have been known for over a century [9] and are still the most widely used PhCs. For sufficiently high RI contrast ($n_2/n_1 > 1.5$), they can exhibit a complete PBG for light incident on the film surface. This very simple 1D PhC (Fig. 3b) can be created through a number of methods such as vapor-phase deposition (evaporation, chemical vapor deposition, sputtering), liquid-phase deposition (spin coating, dip coating, ionic layer-by-layer assembly, ink-jet printing), BCP self-assembly, and roll casting techniques. A triangular lattice consisting of air holes (Fig. 3e) is a simple 2D PhC having a 2D PBG for any in-plane propagation. In principle, a 3D PhC is also a 2D PhC; however, the 2D PhC can open a wider PBG than the 3D PhC at the same contrast of RIs due to optimizing its structure for in-plane wave vectors. Due to the compatibility with semiconductor processes, 2D PhCs have been applied to various photonic devices including photonic integrated circuitry, lasers, and LEDs, a decade earlier than 3D PhCs [10]. Another class of 2D PhCs is PhC fibers where a 2D PhC works as a periodic cladding layer in the radial direction for the light propagating along the axial direction [11].

To date, the fabrication of 3D PhCs exhibiting a complete PBG at optical frequencies is still challenging and mostly 3D PhCs having pseudo-gaps have been demonstrated. The first 3D PhC with a complete PBG (so-called

"yablonovite") was manually made at the macro scale by drilling three holes (aligned at $120°$ intervals around the azimuth and $35.26°$ off the normal) for each hexagonal mesh point on the top surface of a solid polymeric (epoxy) material. The optical version of yablonovite was also fabricated by e-beam lithography and X-ray lithography. More recently, a closely resembled structure (Fig. 3c) has been widely fabricated in the optical regime via multi-beam interference lithography. In this technique, a homogeneous photoresist exposed to a periodic optical standing wave created by the interference of mutually coherent laser beams and, for example, with a negative-tone photoresist, the high intensity region becomes an insoluble periodic solid/air structure after development. Interference lithography is quite advantageous to fabricate a wide variety of submicron polymer structures having various symmetries with a single (or small) number of exposures over a large area [12]. A number of advances toward 3D photonic devices have been made employing the *woodpile structure* (Fig. 3f) due to its robust complete PBG requiring a relatively low $n_2/n_1 > 1.9$ and a very simple geometry. Woodpile PhCs for optical frequencies have been fabricated by photolithography, interference lithography, direct laser writing using two-photon polymerization, and micro-transfer molding. Except for the photolithographic layer-by-layer approach consisting of repeated steps of deposition and photolithographic etching of high RI materials such as silicon ($n = 3.5$) and indium phosphide ($n = 3.2$), all other approaches for fabricating 3D polymeric-based PhCs require conversion or inversion processes to produce high-RI PhCs with a complete PBG. Because of low softening temperatures of polymers and difficulties of 3D deposition of high RI materials onto polymer scaffolds, the simple fabrication of high quality woodpile PhCs is still a processing challenge.

Self-assembled solid microspheres (opal structure) with the fcc and hexagonal closed-packed (hcp) lattice and their inverted structures (Fig. 3a) are the most frequently used 3D PhCs in the bottom-up approach (colloidal crystallization) because of many advantages such as low cost, wide area, high quality, and easy fabrication as well as their partial [111] PBG in the visible regime [13]. Since these PhCs only have a pseudo-gap for the opal structure and only a very fragile (i.e., a narrow PBG sensitive to fabrication imperfection) complete PBG between high-frequency photonic bands for the inverse opal structure with $n_2/n_1 > 2.8$, most of their applications such as sensors, lasers, and solar cells have been demonstrated, employing the low frequency [111] pseudo-gap. Despite this 1D-like use of these opal-based PhCs, their continuous 3D topology enables better mass and charge transport than the 1D PhCs and is an advantage for chemical and energy devices.

The 3D double gyroid bi-continuous morphology of a BCP can be converted to the single gyroid structure by selective etching of one polymer phase (Fig. 3d), and this structure can exhibit a complete PBG if a RI contrast between constituent polymer blocks is sufficient ($n_2/n_1 > 2.3$ with a volume solid fraction of 0.17). A major challenge in BCP photonic crystal applications is the need to synthesize very high molecular weight polymers (>100 kg/mol) in order to achieve the typical lattice periodicities ($10 \sim 50$ nm) necessary to create a PBG in the visible regime. Many BCP-based PhCs therefore employ domain swelling by addition of a solvent or homopolymer.

Polymer-Based Photonic Crystals and Applications

Polymer-based PhCs have been actively researched for more than a decade [14] and the current mature status of PhC research has lead to a pivotal role of polymers by virtue of several exclusive advantages including a wide range of optical functionalities (luminescence, optical nonlinearity), low cost, broad tunability, versatile hosting medium (for dyes, quantum dots, liquid crystals), flexibility (in mechanical and processing aspects), and production scalability despite their relatively low inherent RIs, typically ranging from $1.4 \sim 1.6$, resulting in narrow, partial PBGs [15, 16].

Photonic Crystal, Table 1 Examples of polymer-based PhCs for sensing various analytes/stimuli

Analytes/stimuli	PhC	Functional polymers
Humidity	Lamellae	Poly(2-hydroxyethyl methacrylate)
	Inverse opal	Polyacrylamide
pH	Opal	Hydrolyzed polyacrylamide
Ion	Lamellae	Poly(styrene)-b-poly(2-vinyl pyridine)
	Inverse opal	Poly(N-isopropylacrylamide)
Sugar	Opal	Polyacrylamide
	Lamellae	Polystyrene-b-poly(2-vinyl pyridine)
Strain	Lamellae	Poly(styrene)-b-poly(2-vinyl pyridine)
	Opal	Poly(styrene) sphere, poly(butadiene)
	Inverse opal	Poly(methyl methacrylate)
Blastwave	Yablonovite like	Photoresist epoxy
Temperature	Lamellae	Poly(styrene)-b-poly(isoprene)
	Inverse opal	Poly(N-isopropylacrylamide)

The application of PhCs for sensors spans a broad range of fields including energy, biomedical, and industrial fields [17]. For sensor applications, a PhC functions in two different roles: (i) a main sensing entity which changes its own optical properties in response to analytes, (ii) an assistant entity which enhances the light interaction with a desired analyte by its extraordinary optical dispersion (e.g., a flat photonic band). The latter role is potentially useful for photovoltaic applications as a slower v_g of photons arising from a flat photonic band can increase the photon-electron interaction for enhanced exciton generation. Considering the characteristics of polymers, the former approach, requiring a tunable PhC whose RIs and physical thickness are susceptible to target analytes, is quite attractive. 1D and 3D PhCs have been used in a thin-film form with responsive optical properties along the surface normal while 2D PhCs are used in a fiber style with the response in the radial direction.

Various polymer-based PhCs for humidity, pH, ionic, sugar, strain, blast wave, and temperature sensing have been demonstrated using 1D and 3D PhCs (Table 1). In chemical sensing, analyte-selective swelling/deswelling of polymeric PhCs is a main mechanism which results in changes of both lattice constant and RI depending on both relative selectivity and RI of a carrier solvent. These parameters can be optimized to achieve a high sensitivity and a highly responsive signal.

For example, with the changes induced by solvent swelling in RI (2 % increase or decrease depending on the RI of solvent) and thickness (5 % increase), a 1D PhC (for $n_2/n_1 = 1.60/1.45$) can exhibit a broad range of PBG shifts from 1.5 % to 7 % or PBG signal strength from 7 % enhancement to 38 % degradation depending on the selectivity and RI of solvent [15]. Since a 3D PhC can be a self-supporting structure with continuous air pores, a 3D PhC has benefits for a higher RI contrast (i.e., stronger signal) and rapid diffusion of analyte in the vapor phase enables a fast response time.

For biological/health applications of a polymeric PhC, binding molecular recognition groups (MRGs) to a polymer backbone are essential to allow analyte-driven selective swelling/deswelling behavior of a PhC. For example, a hydrogel combined with glucose oxidase or boronic acid can swell or can shrink dependent on the glucose concentration and a PhC made of functional polymers can be used for monitoring blood sugar. Moreover, heavy metal ions (e.g., Hg^{2+}, Pb^{2+}, Cu^{2+}) can also be detected as these ionic species cause a shrinkage of functionalized hydrogel opal PhC. Poly-acrylic acid hydrogel PhC can respond to pH; thus they can be utilized for food safety tags because pH correlates to CO_2 gas level, the prime indicator of bacterial activities. The intrinsic swelling behavior of hydrogel to humidity enables PhC-based sensors.

Physical stimuli (e.g., strain, temperature, pressure wave) are largely based on intrinsic physical

properties (modulus, thermal expansion coefficient) of constituent polymers rather than MRGs. Strain sensing PhCs are straightforward for easily deformable polymers, as the geometrical change (symmetry and lattice constant) affects the PBG [18]. In contrast, temperature broadly influences the behavior of polymers including volume, solubility, and polymer chain dynamics arising from the Flory-Huggins χ interaction parameter which is generally inversely proportional to temperature. For sensors based on these temperature-sensitive chi parameters, a PhC must be kept in contact with a solvent to enable solvent exchange limiting the versatility of the sensors. In contrast, a 1D PhC made of self-assembled liquid crystalline di-block copolymer demonstrated temperature-sensitive PBG change in a dry state by use of the order parameter of the liquid crystal. A PhC exposed to extreme stress such as blast and shock wave can be permanently deformed with a resultant PBG change acting as a blast injury dosimeter indicating the deposited shock energy.

Dynamically tunable reflective colors (or *structural color*) are attractive for display applications because of the full color capability of a single PhC pixel without need for a backlight. Electrochemically tunable 1D PhCs are possible using electrolytes to change the degree of swelling of self-assembled BCPs or opal-based PhCs. However such electrochemically driven pixels generally show an insufficient response time for video display, the faster capacitive actuation of an elastomeric opal PhC via application of high electric potential would be advantageous. To date, the experimentally demonstrated PBG shift (<50 nm) is insufficient to realize full colors even under a high applied voltage (~1 kV). But the inherent advantages of this approach such as a fast response time (~10 ms), low power consumption, and a stable device performance without electrochemical degradation are very attractive [15]. By taking the advantages of the approaches, electrostatic compression/relaxation of an opal PhC comprised of charged PS microspheres in a low viscosity liquid exhibits a full color performance with a reasonable response time (~100 ms) under low applied voltages (<5 V). Polymer-based PhC displays can be vulnerable to environmental perturbation especially temperature unless introducing a counter-temperature effect.

Photon engineering (e.g., improving photon coupling efficiency to a device, widening a solar acceptance angle of a device, enhancing internal quantum efficiency via increasing the photon interaction length) using polymeric PhCs is promising for lasing and photovoltaic applications. A self-assembled lamellar BCP was employed as external mirrors to construct a lasing cavity. Compared to conventional dielectric mirrors, low cost, solution processable, conformable, deformable, and tunable opportunities of the BCP PhC would be noteworthy for non-traditional laser applications. For example, a lasing device using the [111] feedback of an opal PhC comprised of polystyrene (PS) microspheres in a polydimethylsiloxane (PDMS) matrix was demonstrated on a flexible polymer substrate despite the small RI contrast between PS and PDMS. Using the exceptionally slow v_g appearing at the band edge (Fig. 1), band-edge lasing without an external cavity has also been demonstrated. Recent numerical simulations showed that fluorescence efficiency of phosphors embedded in a 1D PhC can be boosted up to seven times due to the slow v_g. Thereby, the enhanced photoluminescence efficiency of the phosphors can contribute not only to lasers but to high-efficiency white light-emitting-diodes (LEDs). Polymer photovoltaic (PV) cells have been intensively investigated. Engineering the interfacial morphology between the p- and n-type transport polymers to have features within a diffusion length of excitons has been considered as a key idea to improve PV efficiency of the polymer PV devices. In a PV cell, a PhC can serve not only for photon engineering but also for electrical transport engineering (exciton harvesting). In parallel with other approaches, the introduction of PhCs into PV devices is expected to create additional efficiency.

Summary

The field of PhC research has been vibrant for the last quarter century with a recent trend for

engineering-oriented research which is opening opportunities for polymer-based PhCs. New application areas in sensing and renewable energy and new photonic concepts such as periodic gain and loss materials, in which photon number is not conserved, are emerging with polymers and their ability to bind and host functional additives playing an increasing role. Conventional self-assembled colloidal and block polymer-based PhCs lead in many sensor and display applications. Top-down techniques including interference lithography, imprinting, and direct laser writing which all utilize polymers as primary materials to construct the photonic crystal are being combined to introduce aperiodic functional features in periodic structures and to improve fabrication characteristics. Fundamental investigations of the chemical and physical phenomena behind the dynamic responses of the polymer-based PhCs will bring important insight into polymer-solvent-analyte dynamics. Moreover, research efforts on the engineering aspects of PhCs such as production yield, fabrication time, response time, and packaging are necessary in order to attract more attention from the industrial sector. These efforts toward practical engineering of polymer-based PhC will also create greater opportunities to sustain basic polymer research.

Related Entries

▶ Chemical Sensor

▶ Nano-/Microfabrication

▶ Nonlinear Optical Properties

▶ Refractive Index

References

1. Yablonovitch E (2001) Photonic crystals: semiconductors of light. Sci Am 285:46–55
2. Joannopoulos JD, Johnson SG, Winn JN, Meade RD (2011) Photonic crystals: molding the flow of light. Princeton University Press, Princeton
3. Yablonovitch E (1987) Inhibited spontaneous emission in solid-state physics and electronics. Phys Rev Lett 58:2059–2062
4. John S (1987) Strong localization of photons in certain disordered dielectric superlattices. Phys Rev Lett 58:2486–2489
5. Ho KM, Chan CT, Soukoulis CM (1990) Existence of a photonic gap in periodic dielectric structures. Phys Rev Lett 65:3152–3155
6. Tandaechanurat A, Ishida S, Guimard D, Nomura M, Iwamoto S et al (2011) Lasing oscillation in a three-dimensional photonic crystal nanocavity with a complete bandgap. Nat Photon 5:91–94
7. Tarhan II, Watson GH (1996) Photonic band structure of fcc colloidal crystals. Phys Rev Lett 76:315–318
8. Wijnhoven JEGJ, Vos WL (1998) Preparation of photonic crystals made of air spheres in titania. Science 281:802–804
9. Prather DW, Shi S, Sharkawy A, Murakowski J, Schneider G (2009) Photonic crystals, theory, applications and fabrication. Wiley, Hoboken
10. Notomi M (2010) Manipulating light with strongly modulated photonic crystals. Rep Prog Phys 73:096501
11. Knight JC (2003) Photonic crystal fibres. Nature 424:847–851
12. Maldovan M, Thomas EL (2009) Periodic materials and interference lithography for photonics, phononics and mechanics. Wiley-VCH, Weinheim
13. von Freymann G, Kitaev V, Lotschzc BV, Ozin GA (2013) Bottom-up assembly of photonic crystals. Chem Soc Rev 42:2528
14. Edrington AC, Urbas AM, DeRege P, Chen CX, Swager TM et al (2001) Polymer-based photonic crystals. Adv Mater 13:421–425
15. Lee J-H, Koh H, Singer J, Jeon S-J, Stein O et al (2014) Ordered polymer structures for the engineering of photons and phonons. Adv Mater 26:532–569
16. Paquet C, Kumacheva E (2008) Nanostructured polymers for photonics. Mater Today 11:48–56
17. Nair RV, Vijaya R (2010) Photonic crystal sensors: an overview. Prog Quantum Electron 34:89–134
18. Chan EP, Walish JJ, Urbas AM, Thomas EL (2013) Mechanochromic photonic gels. Adv Mater 25:3934–3947

P

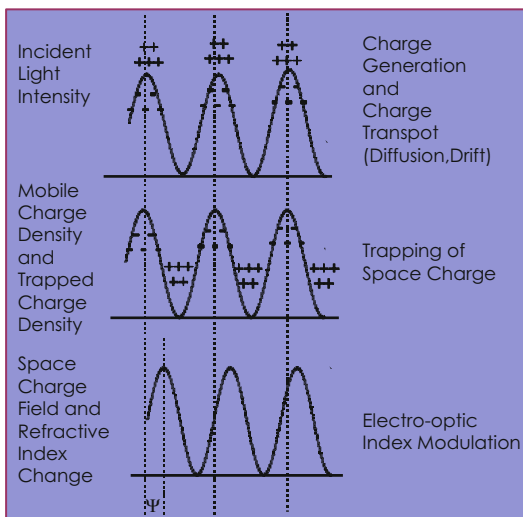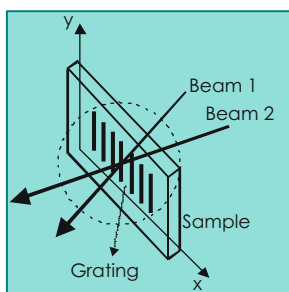# Photorefractive Polymer

Naoto Tsutsumi
Kyoto Institute of Technology, Matsugasaki, Sakyo, Kyoto, Japan

Synonyms

Holographic diffraction; Optical gain; Optical interference; Periodical variation of refractive index; Photoconductivity; Pockels effect; Polarizability anisotropy; Second-order optical nonlinearity

Definition

Photorefractivity is based on the holographic interference phenomena. Schematic description of photorefractive effect is shown in Fig. 1. Photorefractive effect is measured at the interference illumination of coherent two beams. At periodical bright region of interference pattern, hole and electron pairs are induced through photoexcitation of sensitizer and chromophore. Hole charge carriers are transported and trapped at dark region. The resultant charge carrier distribution induces space-charge field which causes the nonlinear refractive index modulation through Pockels effect in non-centrosymmetrically aligned nonlinear optical dyes. Important PR effect is that refractive index modulation is shifted to ψ from the illumination pattern. Shifted refractive index modulation leads to the optical

Photorefractive Polymer, Fig. 1 Schematic description of photorefractive effect in PR polymers

gain effect in addition to the holographic diffraction.

Although the photorefractive phenomena in inorganic PR crystals and organic PR polymer composites share the basic mechanism shown in Fig. 1, both have different transport mechanisms: In contrast to band-like transport in ordered inorganic crystals or semiconductors, in the case of organic PR polymer composite, hole or electron charge carriers transport through the energetically and spatially distributed disorder sites.

Historical Background

Photorefractive (PR) effect is based on a temporal spatial modulation of refractive index, upon illumination of coherent interfered beams, via the Pockels effect (linear electrooptic effect) which is induced by the space-charge field created by the photo-generated charge carriers. Thus, PR response requires the photoconductive properties including photocarrier generation and electrooptic nonlinearity. In the photorefractive medium, index grating due to purely diffusive or purely drift-induced charge motion is spatially shifted by $\pi/2$ relative to the intensity pattern, and thus, a unique phenomenon of two-beam coupling, where the propagation properties of one beam are reversibly controlled by another beam in the medium, is observed in addition to the holographic diffraction. Two-beam coupling optical gain can be employed for many applications, optical amplification, beam cleanup, self-pumped phase conjugators, etc. [1].

Since the first report of PR effect in inorganic crystal of lithium niobate ($LiNbO_3$) in 1966 [2], many inorganic nonlinear crystals exhibiting PR effect had been extensively investigated and theoretical approaches had been established [3]. Since the first demonstration of photorefractive effect in organic polymer was reported in 1991 [4], tremendous improvements of organic PR properties and performances have been achieved by peoples in the field of chemistry, physics, material science, and optical engineering. Large optical gain exceeding 200 cm^{-1} and almost full diffraction efficiency of 86 % (the rest 14 % is due to optical loss) had been reported in 1994 [5], although small
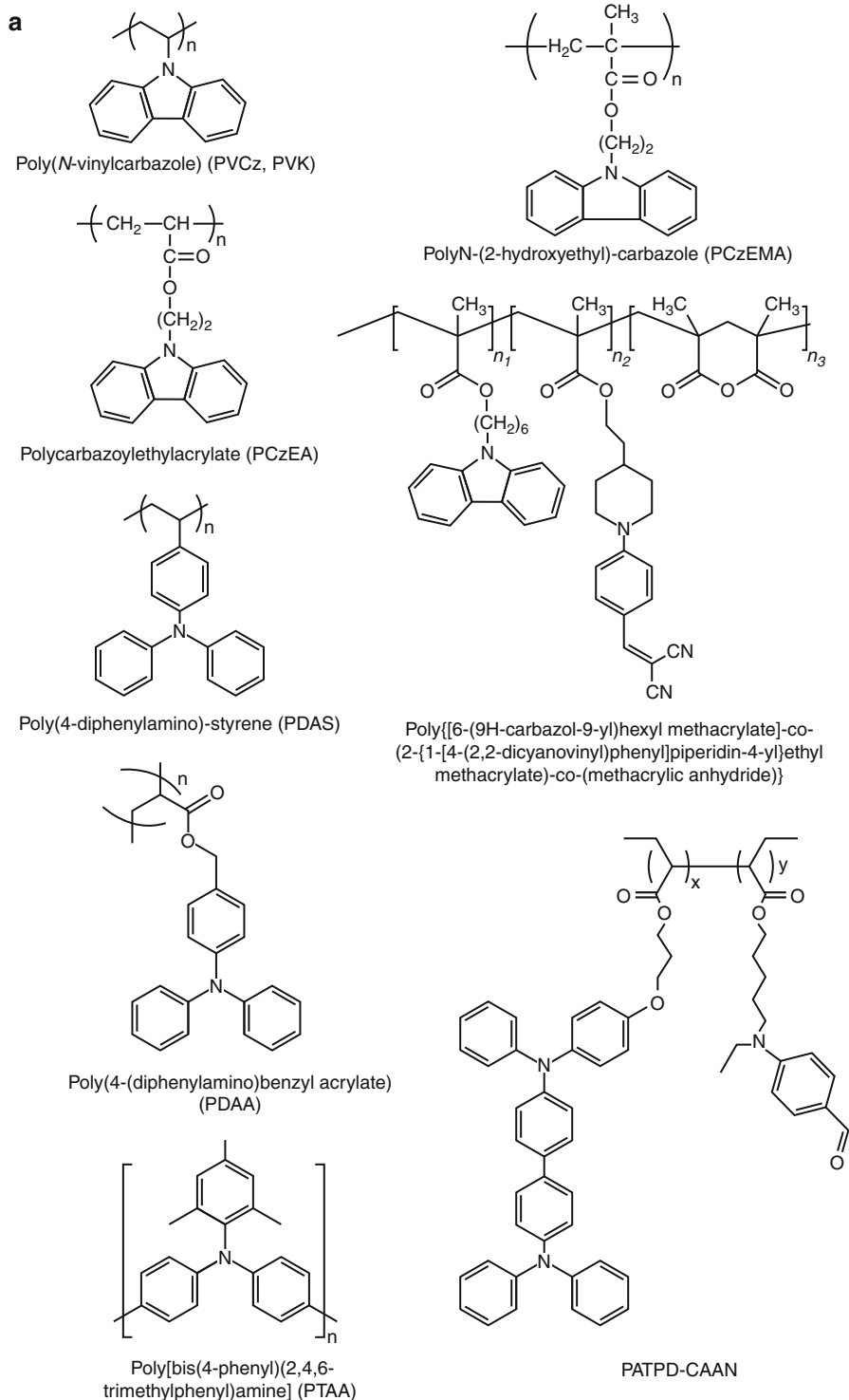
optical gain of 0.33 cm^{-1} and lower diffraction efficiency of 10^{-3} to 1 % were reported in the initial report in 1991. In almost two decades, several review articles including featured articles [6–15] and book chapters [16–21] highlight this dynamic optical field.
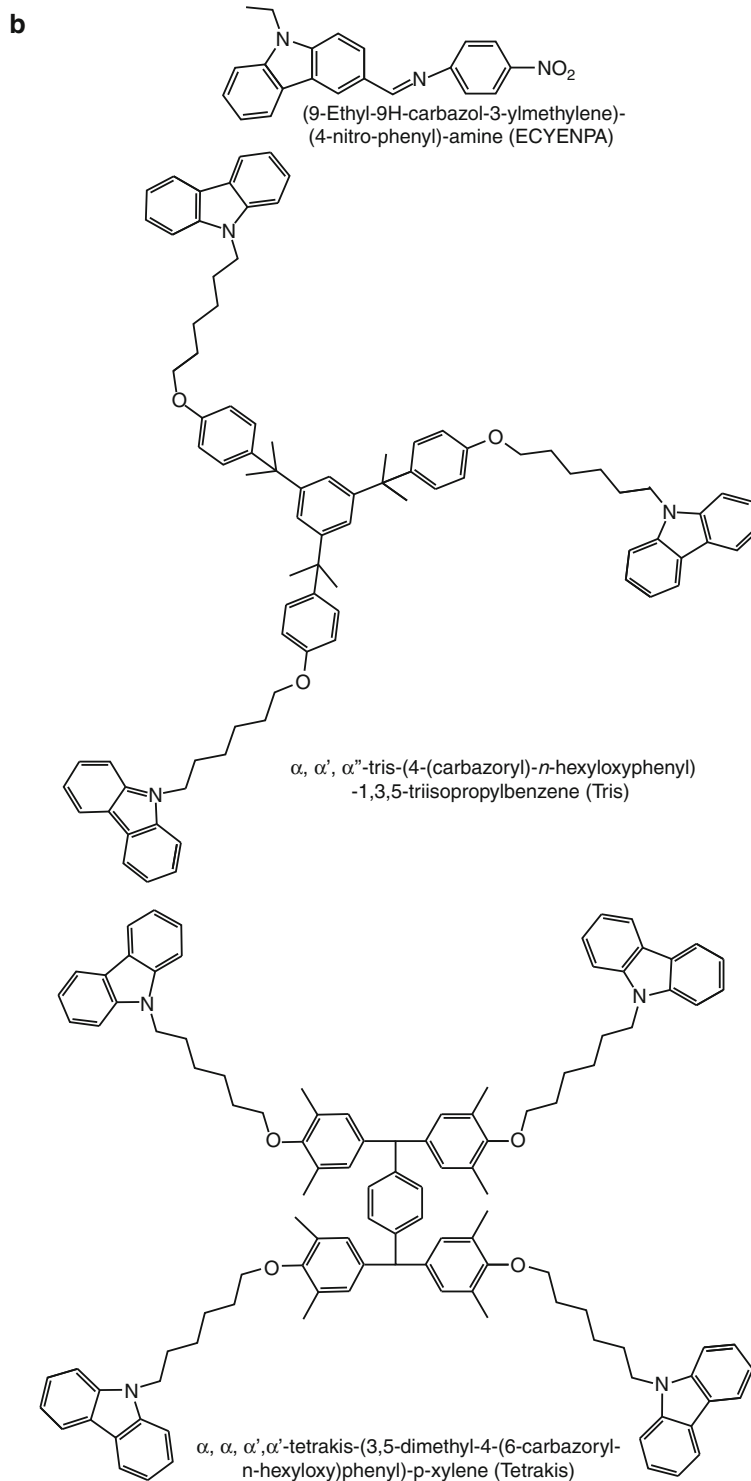
Chemical Requirements

Photorefractive polymers are consisted of photocarrier generator, carrier transporter, sensitizer, nonlinear optical dye, and plasticizer. Each component plays an important role for PR characteristics. Photoconductive polymer works as a photocarrier generator and carrier transporter. Sensitizer is usually used to enhance the photocarrier generation. Free hole carriers induced by photo excitation of sensitizer or photoconductive chromophore through ion pair formation of hole and electron. Generated hole carriers travel through the photoconductive hopping sites and are trapped in dark region. Nonlinear optical dye is responsible for the nonlinear refractive index modulation through Pockels effect. Plasticizer is added to control the glass transition temperature of polymer composite.
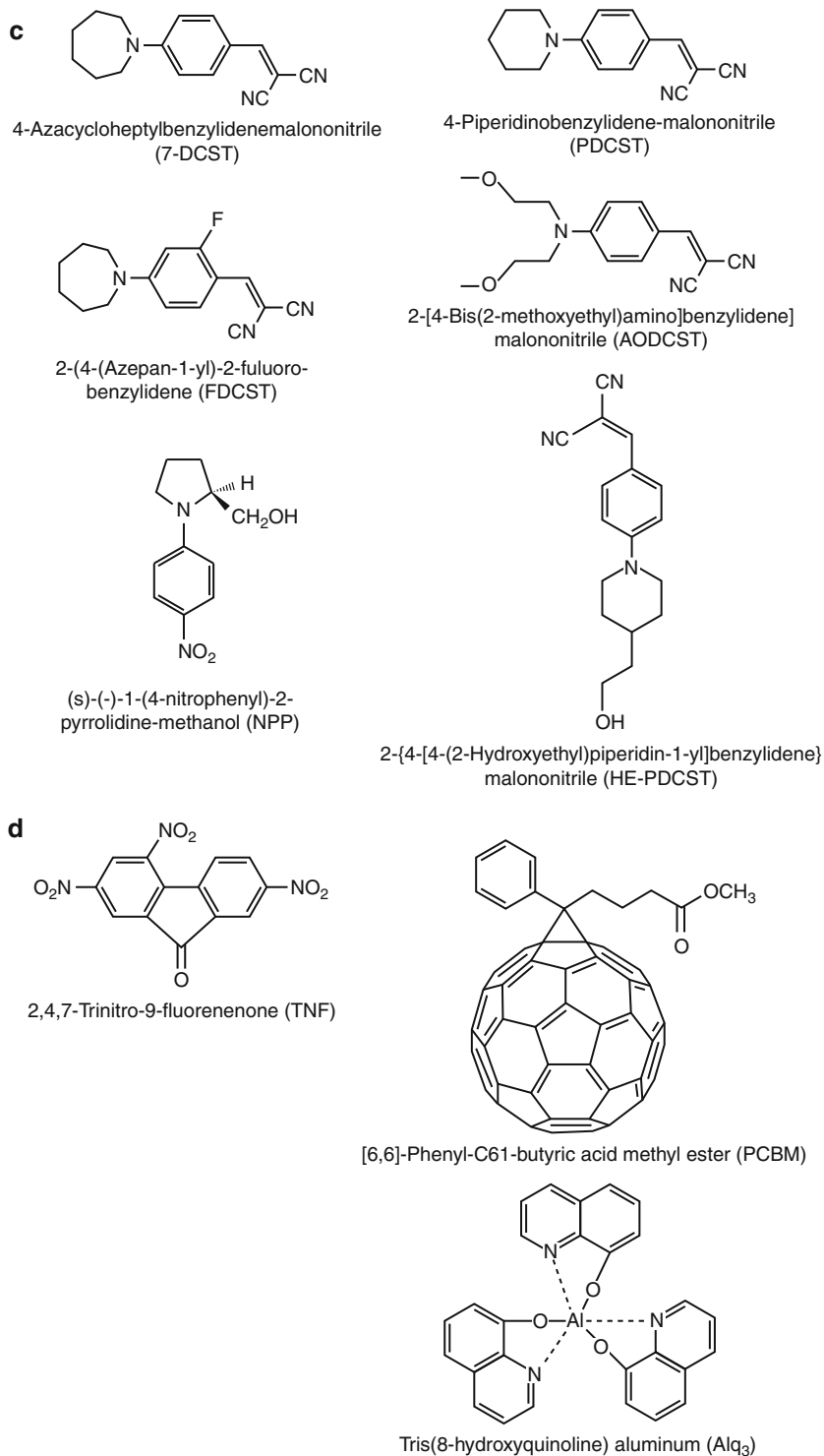
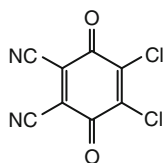Each chemical species are summarized in Fig. 2.

(a) **Photoconductive polymers**. The typical photoconductive polymers: carbazole (Cz)-based polymers – poly(N-vinylcarbazole) (PVCz, PVK), polycarbazoylethylacrylate (PCzEA), poly(2-(9-carbazoyl)ethyl methacrylate) (PCzEMA), poly[methyl-3-(9-carbazolyl)propylsiloxane] (PSX). Triphenyl-amine-based polymers – poly(acrylic tetraphenyldiaminobiphenol) (PATPD), poly (4-diphenylamino)styrene (PDAS), poly(4-(diphenylamino)benzyl acrylate) (PDAA), poly(4-((4-methoxyphenyl)(phenyl)amino) benzyl acrylate) (PMPAA), poly[bis(4-phenyl)(2,4,6-trimethylphenyl)amine] (PTAA), poly(N, N' -bis(4-hexylphenyl)-N'-(4-(9-phenyl-9H-fluoren-9-yl)phenyl)-4,4'-benzidine)(PF6-TPD).

(b) **Molecular glasses**. (9-Ethyl-9H-carbazol-3-ylmethylene)-(4-nitrophenyl)-amine (ECYENPA), α, α', α''-tris-(4-(carbazoryl)-n-hexyloxyphenyl)-1,3,5-triisopropylbenzene (tris), α, α, α', α'-tetrakis-(3,5-dimethyl-4-(6-carbazoryl-n-hexyloxy)phenyl)-p-xylene (tetrakis).

(c) **NLO dyes**. The typical nonlinear optical dyes for photorefractive composites: several aminostyrene types, 4-azacyclo-heptylbenzylidenemalononitrile (7-DCST), 4-di(2-methoxyethyl)aminobenzylidene malononitrile (AODCST), 4-piperidinobenzyl-idene-malononitrile (PDCST), 2-(4-(azepan-1-yl)-2-fluoro-benzylidene (FDCST), 2,5-dimethyl-4-(p-nitrophenylazo)anisole (DMNPAA), s-(−)-1-(4-nitrophenyl)-2-pyrolidene-methanol (NPP), (diethylamino)-nitrostyrene (DEANST), (p-diethylamino) benzaldehyde diphenylhydrazone (DEH), 2-dicyanomethylen-3-cyano-5,5-dimethyl-4-(4'-dihexylaminophenyl)-2,5-dihydrofuran (DCDHF-6), 2-{4-[4-(2-hydroxyethyl) piperidin-1-yl]benzylidene} malononitrile (HE-PDCST).

(d) **Sensitizers**. The typical sensitizers for photorefractive composites: 2,4,7-trinitro-fluorenone (TNF), 2,4,7-trinitro-9-fluorenylidene-malononitrile (TNFDM, TNFM), 2,4,5,7-tetranitro-9H-fluorine-9yilden malononitrile (TeNFM), tetracyanoethylene (TCNE), 7,7,8,8-tetracyanoquinnodimethane (TCNQ), [6, 6]-phenyl-C61-butyric acid methyl ester (PCBM), fullerene C$_{60}$, tetracyanobenzene (TCNB), tetracyanoqui-nodimethane (TCNQ), benzoquinone (BQ), 2,6-dimethyl-p-benzoquinone (MQ), 2,5-dichloro-benzoquinone (Cl$_2$Q), 2,3,5,6-tetrachloro-p-benzoquinone (chloranil), 2,3-dichloro-5,6-p-benzoquinone (DDQ).

(e) **Plasticizers**. The typical plasticizers for photorefractive composites: N-ethylcarbazole (ECZ), carbazoylethylpropyonate (CzEPA), triphenylamine (TPA), (2,4,6-trimethylphenyl)-diphenylamine (TAA), (4-(diphenylamino)phenyl)methanol (TPAOH), benzyl butyl phthalate (BBP), tricresyl phosphate (TCP), diphenylphthalate (DPP), dicyclohexyl phthalate (DCP).

P

a

Poly(*N*-vinylcarbazole) (PVCz, PVK)

PolyN-(2-hydroxyethyl)-carbazole (PCzEMA)

Polycarbazoylethylacrylate (PCzEA)

Poly(4-diphenylamino)-styrene (PDAS)

Poly{[6-(9H-carbazol-9-yl)hexyl methacrylate]-co-
(2-{1-[4-(2,2-dicyanovinyl)phenyl]piperidin-4-yl}ethyl
methacrylate)-co-(methacrylic anhydride)}

Poly(4-(diphenylamino)benzyl acrylate)
(PDAA)

PATPD-CAAN

Poly[bis(4-phenyl)(2,4,6-
trimethylphenyl)amine] (PTAA)

Photorefractive Polymer, Fig. 2 (continued)

b

(9-Ethyl-9H-carbazol-3-ylmethylene)-
(4-nitro-phenyl)-amine (ECYENPA)

α, α', α"-tris-(4-(carbazoryl)-*n*-hexyloxyphenyl)
-1,3,5-triisopropylbenzene (Tris)

α, α, α',α'-tetrakis-(3,5-dimethyl-4-(6-carbazoryl-
n-hexyloxy)phenyl)-p-xylene (Tetrakis)

Photorefractive Polymer, Fig. 2 (continued)

c

4-Azacycloheptylbenzylidenemalononitrile
(7-DCST)

4-Piperidinobenzylidene-malononitrile
(PDCST)

2-(4-(Azepan-1-yl)-2-fuluoro-
benzylidene (FDCST)

2-[4-Bis(2-methoxyethyl)amino]benzylidene]
malononitrile (AODCST)

(s)-(-)-1-(4-nitrophenyl)-2-
pyrrolidine-methanol (NPP)

2-{4-[4-(2-Hydroxyethyl)piperidin-1-yl]benzylidene}
malononitrile (HE-PDCST)

d

2,4,7-Trinitro-9-fluorenenone (TNF)

[6,6]-Phenyl-C61-butyric acid methyl ester (PCBM)

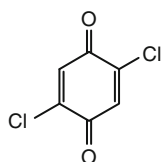Tris(8-hydroxyquinoline) aluminum (Alq₃)

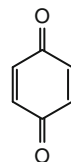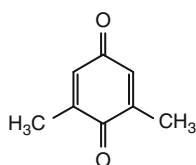**Photorefractive Polymer, Fig. 2** (continued)
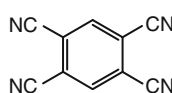
2,3-Dichloro-5,6-dicyano-p-benzoquinone
(DDQ)
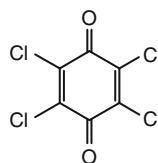
2,3,5,6-Tetrachloro-p-benzoquinone
(chloranil)

2,5-Dichloro-p-benzoquinone (Cl$_2$Q)

p-Benzo-quinone (BQ)

2,6-Dimethyl-p-benzoquinone (MQ)

1,2,4,5-Tetracyanobenzene (TCNB)

e
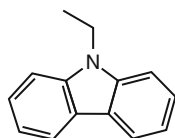
N-Ethylcarbazole (ECZ)

Carbazoylethylpropynate (CzEPA)

Benzyl n-Butyl phthalate (BBP)

Dicyclohexyl phthalate (DCP)

P

Diphenylphthalate (DPP)

Tricresyl Phosphate (TCP)

Photorefractive Polymer, Fig. 2 Structural formulae. (**a**) Photoconductors, (**b**) molecular glasses, (**c**) NLO chromophores, (**d**) sensitizers, (**e**) plasticizers

Molecular Design of Amorphous PR Materials

Three types of amorphous PR materials are designed.

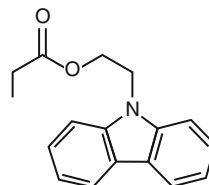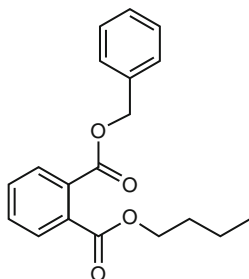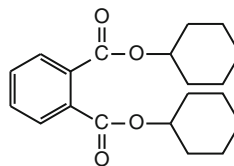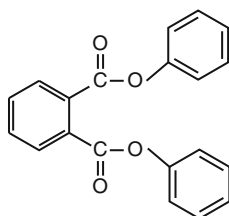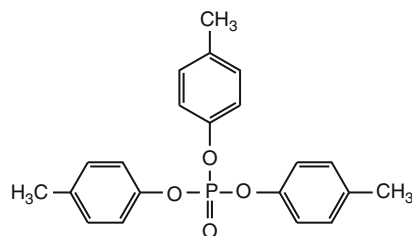### (a) **Photoconductive polymer-based PR composites** [6]

Photoconductive polymer-based PR composites are consisted of photoconductive polymer, nonlinear optical dye, plasticizer, and sensitizer. Almost PR polymeric composites studied in recent two decades are categorized in these type PR composites. Typical photoconductive polymer is poly(*N*-vinylcarbazole) which is a pioneer material in the field of photoconductive polymer. PR properties of poly(*N*-vinyl carbazole) (one of the pioneer photoconductive polymers)-based PR composites have extensively been investigated.

Approach of nonlinear optical polymer-based PR composites was first attempted but was abandoned in favor of the high performance of the photoconductive polymer-based PR composites.

(b) **Fully functionalized or monolithic PR polymers** [6]

Fully functionalized or monolithic PR polymers are categorized as PR polymer systems in which all components of photocarrier generation, carrier transport, and optical nonlinearity are embedded in one polymer backbone. In some cases, small amount of plasticizer and sensitizer is added. The merit of these systems is their phase stability in the long term and thus long shelf lifetimes. However, their carrier transport properties are inferior to those for the corresponding photoconductive polymer-based PR composites in (a).

(c) **Molecular glass-based PR materials**

Low molecular compounds of photoconductor (photocarrier generator, carrier transporter), nonlinear optical dye, sensitizer, and in some case plasticizer were mixed to form amorphous molecular glass PR composites. Monolithic compound is also used.

Toward High-Performance Photorefractivity in PR Polymer Composites

For almost all applications relying on reversible and updatable properties of PR materials, faster response time (higher response rate) and higher diffraction efficiency will be desired at the illumination as low as possible. Sensitivity is a measure for this performance. Several definitions of sensitivity have been found in the literature [20]. For absorbed PR materials, to account for absorption losses in the materials, usually external diffraction efficiency (η_{ext}) is taken for evaluation. External diffraction efficiency is related to internal diffraction efficiency (η_{int}) as

$$\eta_{ext} = \left(-\frac{\alpha d}{\cos\theta_1} \right) \eta_{int} \tag{1}$$

where α is absorption coefficient, d is thickness, and θ_1 is the internal angle.

Typical definition of sensitivity (S) is

$$S = \frac{\sqrt{\eta_{ext}}}{I\tau} \tag{2}$$

where I is light intensity and τ is response time.

Composition

Composition of PR material strongly affects the PR performances. Amorphous PR composites are fabricated with 30–50 wt% of photoconductive polymer, 20–40 wt% of NLO dye, 4–20 wt% of plasticizer, and 0.1 to a few wt % of sensitizer. Typical PR composition is photoconductive polymer/NLO dye/plasticizer/sensitizer = 44/35/20/1 (by wt.). Higher and lower content of NLO dye than 35 wt % will nominally cause lower diffraction efficiency and slower response time.

Molecular Weight of Polymers

The effects of molecular weight (Mw) of PVK on PR performances are investigated for PVK/liquid crystal/fullerene in the average Mn range between 10,000 and 66,000 g mol^{-1} [22] and for PVK/7-DCST/ECZ/TNF (44/35/20/1 by wt.)

in the average Mw range between 23,000 and 412,000 g mol^{-1} [23] and between 23,000 and 860,000 g mol^{-1} [24]. Optical gain increases with increasing average Mn [22]. Diffraction efficiency and response rate monotonically increase with average Mw in this range [23, 24]. This attributed to the dimer cation sites along longer polymer chain work as effective traps for hole charge carriers [23, 24].

Hole Mobility

Choice of photoconductive polymer is also important, because drift mobility of hole charge carriers in photoconductive polymer determines the response time of formation of space-charge field, thus holographic diffraction phenomena.

Despite the success achievement of PVK PR composites, PVK and related polymers with carbazole moiety have major drawback for PR performances. Typical PVK has low hole drift mobility in the order of 10^{-7}–10^{-6} cm^2 V^{-1} s^{-1} [25–28], which limits the response time of holographic diffraction. In contrast, triphenylamine (TPA)- and triphenylamine dimer (TPD)-based PR polymer composites show faster response of holographic diffraction than PVK PR composites. PDAS, one of the triphenylamine-based polymers, has the high hole mobility of 10^{-4}–10^{-3} cm^2 V^{-1} s^{-1} [29–31]. Time interval of diffracted hologram image is 1 s for PVK [32] and 50 ms for PDAS [33]. From these results, it is clearly shown that PDAS PR composites give clear diffracted hologram with faster response rate. Polymer with TPA and TPD moieties in the backbone gives faster drift mobility than the polymers with those moieties in the side chains such as PDAS. TPD-based PR polymer composite gives hole mobility in the range of 10^{-5}–10^{-4} cm^2 V^{-1} s^{-1} [34]. PTAA, in which TPA moiety in the backbone, shows faster drift mobility of 10^{-3}–10^{-2} cm^2 V^{-1} s^{-1} [35, 36]. Thus, it is expected that PTAA-based PR composites will give faster response with large diffraction efficiency.

Ionization Potentials of Molecules

The combination of photoconductive polymer, NLO dye, plasticizer, and sensitizer is also important. Ionization potentials of these compounds are an important measure for determining combination. Hole carrier transport is a key for determining holographic diffraction efficiency and response rate. Photoconductive polymer works as transport manifold for hole charge carriers. In this meaning, lower ionization potential of photoconductive polymer is preferred for faster drift mobility. Indeed, TPA- and TPD-based polymers are known to exhibit higher hole mobility with relatively lower ionization potentials. Ionization potentials for the additives of NLO dye, plasticizer, and sensitizer should be higher than that of photoconductive polymers, because additives with lower ionization potential will work as traps for hole transport. Ionization potentials (I_P) of photoconductive polymers, PVK and ECZ, 5.9 eV [37] and 5.57 eV [38]; PDAS, 5.56 eV [33]; TPA, 5.30 eV [39] and 5.55 eV; PTAA, 5.2 eV [40]; TAA, 5.88 eV; NLO dyes and PDCST, 5.82 eV; FDCST, 5.67 eV [33] and 6.06 eV; 7-DCST, 5.9 eV [41]; AODCST, 5.92 eV; and sensitizer and PCBM, 6.2 eV [42], are reported in the several literatures. The difference of I_P reported for the same molecule may be due to the difference of measurement condition. These values should be compared with the Fermi level (E_F), 4.8 eV, of indium tin oxide (ITO) electrode. When the difference between E_F of ITO and I_P of molecules is considerably small, within 0.4 eV, significant dark current flow disturbs the creation of space-charge field. This problem limits the use of photoconductive with higher hole mobility and lower ionization potential. In section "Hole Mobility," PTAA has the significant potentials for PR material, but lower ionization potential of PTAA limits the applying voltage because of significant large dark current flow. Tsutsumi's group in Kyoto Institute of Technology, Japan, has successfully solved this significant problem using the self-assembled monolayer (SAM)-coated ITO by the modification of ITO [43]. SAM of aminopropyltrimethoxysilane (APTMS) successfully changes the work function of ITO to be 4.3 eV for SAM-ITO [44]. PTAA-based PR polymer showed significant fast response time of 11.3 ms at 20 V μm^{-1} [43].

P

Monolithic PR Polymer

Mixing different molecules has risk for phase separation in long-time usage. To prevent this issue, molecular design based on the idea of fully functionalized or monolithic PR polymers is proposed. Monolithic methacrylate polymer attached carbazole and dicyano aminostyrene moieties to the backbone through spacer were prepared using a polymer analogous reaction [44]. In that system, however, since polymer analogous reaction is employed to prepare monolithic polymer, undesired side reaction to form anhydride group in the polymer backbone occurred. Nevertheless, the undesired side reaction, phase-separation free PR polymer, has been presented [44].

Sensitization

From the standpoint of chemical approach in PR polymer system, to seek more efficient molecules sensitizing photoconductor is most important because the selection of sensitizer controls the absorption of PR polymer composites at laser wavelength and dynamic PR performances. It is well known that sensitizer should absorb at the wavelength of laser used to effectively form the exciton at initial stage. Absorption, on the contrary, causes attenuating incident beams, which leads to the power loss of incident beams in PR polymer composites. Thus, the adequate concentration of sensitizer should be chosen to achieve the optimum PR performances. Usually the concentration range from 0.1 wt% to a few % of sensitizer is chosen as described in section "Composition." Usually because of hole photoconductors in PR polymer composites, sensitizer should serves as a trap of immobile electrons created upon photocarrier generation process.

TNF is one of the most useful sensitizers for PVK-based PR composite, because TNF and Cz moiety forms charge transfer (CT) complex whose spectra extends to the visible absorption region. Stronger sensitizer of THFDM extends CT absorption spectra from visible to near-infrared region. Fullerene and soluble derivative of PCBM is also commonly used as an effective sensitizer, because of their versatile and powerful class of organic sensitizers.

Several studies were devoted to examine the influence of the other sensitizers on PR performances. The effect of different sensitizers of a series of quinones, TNF, and TCNB on PR performances was investigated for PVK/7-DCST/DPP/sensitizer composites [45]. Faster response time of grating formation directly correlated to the larger density of charge carriers which significantly related to larger photocurrent resulting from stronger CT complex. Fastest response was measured for TNF- and DDQ-based composites. Quinone derivatives of BQ, MQ, and Cl_2Q with weaker electron affinity reduced PR performances and photocurrent.

Another approach for the effect of sensitizers on PR performances was investigated for PSX-based PR composites doped with five different sensitizers of TeNFM, TNF, TNFM, TCNE, and TCNQ with each electron affinity [46]. Higher photocurrent and faster holographic response time were measured going from TeNFM, over TNF to TNFM with increased absorption coefficient. However, the holographic response time was reduced for TCNE- and TCNQ-doped PR composites despite the fact that they had higher photocarrier generation. Hole mobility was reduced by the higher concentration of radical anion formed by illumination; thus, the grating buildup speed became hole mobility limited.

The other approach is the comparison of PR performances at NIR region for PT6-TPD PR composites sensitized by various PCBM derivatives with different accepting ability (reduction potential) [47]. Change of absorption coefficient with different sensitizers is negligible for PR performances at NIR region, and therefore the direct evaluation of electron affinity of sensitizers on PR performances was clearly measured. Holographic response rate, sensitivity, and charge carrier lifetime clearly follow the increase of first reduction potentials of PCBM derivatives.

Co-sensitization

Co-sensitization effect was demonstrated in PF6-TPD-based PR polymer sensitized by 5 wt% PCBM and additional sensitizer 1–5 wt% BQ [15, 48]. Because of higher electron affinity

of BQ than PCBM, the electron is effectively transferred to BQ after charge carrier generation on PCBM. With increase of BQ concentration, holographic characterization yielded an increase of refractive index modulation and steady-state gain coefficient, in conjunction with constant dynamic characteristics.

Another approach for co-sensitization is the use of Alq$_3$ as electron trap in a composite based on PATPD/7-DCST/C$_{60}$ [49], a liquid crystal containing composite of TPD/8-pertyloxy-4'-cyanobiphenyl (8OCB)/TNF [50] and a monolithic material of (9-Ethyl-9H-carbazol-3-ylmethylene)-(4-nitrophenyl)-amine (ECYENPA) [51]. 75 % increase of net optical gain, significant increase of diffraction efficiency from 15 % to 90 % at 532 nm at 42 V/μm, and drastic depression of photocurrent were measured by addition of 1 wt% Alq$_3$ into PTAPD composite [49]. Significant increase of optical gain from 232 to 424 cm^{-1} was measured for monolithic materials upon doping 2 wt% Alq$_3$ [50].

Molecular Aspects in NLO Molecules

NLO chromophores are incorporated into the PR materials to refractive index modulation due to space-charge field through Pockels effect, first-order electrooptics (EO) effect. Usually NLO chromophores consisted of the π-conjugated core end-capped with electro-donating and electro-accepting groups, respectively. Applying external electric field breaks centrosymmetry of initially randomly oriented molecules in the composites to allow the second-order optical nonlinearity. In low glass transition PR polymer composites, the orientation enhancement effect due to polarizability anisotropy by molecular orientation is added to EO effect [52]. For overall description, figure of merit (FOM) [53] is given by

$$\text{FOM} = \frac{9\mu_g\beta}{M} + \frac{2\mu_g{}^2\Delta\alpha}{kTM} \qquad (3)$$

where μ_g is the ground-state dipole moment, β is the first hyperpolarizability, M is the molar mass, k is Boltzmann's constant, T is the temperature, and $\Delta\alpha = \alpha_{\parallel} - \alpha_{\perp}$ is the polarizability anisotropy, i.e., the difference in optical polarizability parallel and perpendicular to the molecular axis.

Applications

Photorefractive Phase Conjugators

Phase conjugators are optical devices that can generate a phase conjugate wave of an incident electromagnetic wave [1]. In photorefractive media, phase conjugate wave can be produced. Phase conjugate wave of an incidence electromagnetic wave is referred to as a time-reversed wave, which propagates back to reversed direction in space. Thus, photorefractive media works as phase conjugator. Using a phase conjugator, distorted wave front can be restored. Figure 3 shows the schematic diagram of phase conjugator using degenerate four-wave mixing technique [54]. Original image (a) is distorted in a phase disorder medium. Distorted image (b) (object image) is then interfered with a reference beam in photorefractive medium. Using counter propagated probe beam, phase conjugated wave of distorted image is read out from photorefractive medium as a diffracted wave. Diffracted phase conjugated distorted image is propagated back through a phase disorder medium to restore the original wave front (restored image (c)). This technique can be applied to the wave restoring of wave distortion in long-distance optical fiber.

Holographic Optical Coherence Imaging (HOCI)

Holographic optical coherence imaging (HOCI) is a technique to capture the depth-resolved images from turbid and highly scattered medium using coherence gating [15, 55]. This technique is an invasive imaging tool for mapping the depth profile of biological tissues. Biological tissues are commonly absorptive in the visible region, but the absorption is reduced in the therapeutic window region, which spans from 600 to 1300 nm [56]. Transparency window of biological tissue is in the near-infrared (NIR) region, roughly 700–900 nm, which is used for

P
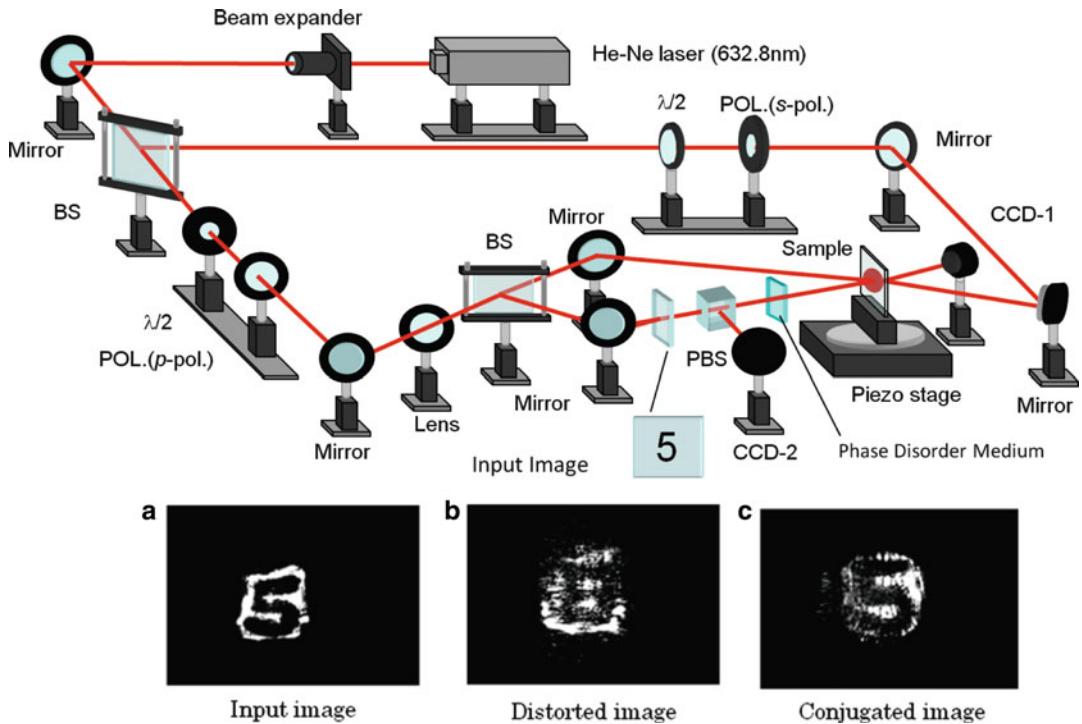
Photorefractive Polymer, Fig. 3 Image restoring of distorted image using photorefractive conjugator (conjugated mirror). (**a**) Original image, (**b**) distorted image, (**c**) restored image (Courtesy by Prof. Kawabe and Dr. Nishide, Chitose Institute of Science and Technology) (Reproduced from Miraizairyo 12,1, 36–41 (2012), Japan, with permission of NTS Inc, from Book of "Advanced Photonics Polymer: Materials and Applications", 2011, Japan, with permission of CMC Publishing and from CSJ Current Review 07, 2011, Japan (Kagakudojin))

biological mapping. Short-coherence light source of femtosecond NIR laser is commonly used. Using coherence-gated holographic imaging, image-bearing light captured in PR polymer medium can be read out as hologram images in real time without requiring any further computation steps. Therefore, the HOCI technique based on PR polymer devices is an image capturing method in a purely optical manner and in real time, which is in contrast to optical coherence tomography (OCT) technique, confocal scanning microscopy, and HOCI by digital holography.

Meerholz's group in the University of Cologne, Germany, has successfully demonstrated volumetric visualization of a 740 μm rat osteogenic sarcoma tumor spheroid using HOCI with femtosecond laser at 830 nm [55].

Updatable Holographic Display

Most striking feature of holography is to record and display full parallax 3-dimensional (3D) images. Holography reproduces true 3D images of objects, and people can see hologram of object in the medium just as it exists in front of them without wearing tired eye glasses. Recently, PR polymer composite opened a new door for updatable holographic 3D display based on dynamic holography. Polymer-based PR devices can be easily processed to large-scale size, and their response rates for recording and erasing are comparable or sometimes exceeding video rate. Thus, PR polymer-based holographic displays are highly desired for the realization of real-time 3D holographic display system without the need for any special eye glasses.

Peyghambarian's group in the University of Arizona, USA, has demonstrated updatable 3D holographic display using the combination of holographic stereographic method and PR polymer device [57–61]. Long persistence hologram is desired in viewing the same image and scene for minutes to hours. Controlling glass transition temperature of PR polymer device is one of way to achieve the criteria. Monochromatic horizontal parallax-only holographic stereogram was recorded into 4" × 4" display device consisted of PATPD-CAAN (50 wt%) as a photoconductive polymer, FDCST (30 wt%) as a NLO dye and ECZ (20 wt%) as a plasticizer for 2–4 min and stored for 3 h [57, 58]. Using pulse laser with 6 ns duration time delivering 200 mJ per pulse at a repetition rate of 50 Hz, each elemental hologram, hogel, was written with single pulse, and 100 hogels were recorded into a 4" × 4" display device consisting of PATPD-CAAN (49.5 wt%), FDCST (30 wt%), ECZ (20 wt%), and PCBM (0.5 %) for 2 s [60]. Multicolor reconstruction of hologram was also demonstrated [60]. Three-color holograms with brightness of 2500 cd/m^2 were also demonstrated in a 12" × 12" PR polymer display [61].

Tsutsumi's group in Kyoto Institute of Technology, Japan, recorded and simultaneously reconstructed 3D hologram of coin and 2-dimensional (2D) image using a spatial light modulator (SLM) display, an image in a PR polymer device consisting of PVK (44 wt%) as a photoconductive polymer, 7-DCST (35 wt%) as a NLO dye, CzEPA (20 wt%) as a plasticizer, and TNF (1 wt%) as a sensitizer [62]. Using the same PR composite, they also demonstrated dynamic 2D holographic image displayed by an SLM with refresh time of 1 s [32]. Furthermore, using PDAS whose drift mobility is 1,000 times faster than that in PVK, they demonstrated dynamic 2D holographic image displayed by an SLM with refresh time of only 50 ms in a PR polymer device consisting of PDAS (44 wt%), FDCST (35 wt%), ECZ (20 wt%), and PCBM (1 wt%) [33]. They also demonstrated 2D holographic image displayed by an SLM using a 4" × 4" PR display device consisting of PDAA (55 wt%), 7-DCST (40 wt%), BBP (4 wt%), and PCBM (1 wt%) [63].

Optical Computing and Image Amplification

PR materials can be applied to optical information processing such as real-time optical processing, image correlation detecting, optical interconnection, optical neural network, and optical computing [1]. Fig. 4 shows image correlation detecting: (a) Image data is interfered with reference mask 2 in PR device. (b) Reading beam with mask 2 can correctly read out image data, but reading beam with incorrect mask does not.

Photorefractive optical gain due to asymmetric energy transfer is a unique feature to amplify the original image. Image amplification can be achieved using the geometry of two-beam coupling [1]. Laser beam cleanup application is also achieved by two-wave mixing in photorefractive medium [1].

## Basic Measurements and Characterizations of PR Polymer Composites

Holographic diffraction efficiency and optical gain are main measurements for characterizing PR properties in PR polymer composites. Degenerate and nondegenerate four-wave mixing (DFWM, NFWM) is commonly used for measuring holographic diffraction efficiency. Two-beam coupling (2BC) method is used for measuring the optical gain due to asymmetric energy transfer.

Grating buildup time (inverse of rate or speed) is measured from the time profile of holographic diffraction efficiency or that of beam intensity change due to asymmetric energy transfer in 2BC measurement.

Holographic (internal) diffraction efficiency η_{int} is estimated using Eq. 4

$$\eta_{\text{int}}\% = \frac{I_{\text{d}}}{I_{\text{t}} + I_{\text{d}}} \times 100 \qquad (4)$$

where I_{d} is the intensity of diffracted beam and I_{t} is the intensity of transmitted beam. Optical gain due to asymmetric energy transfer is estimated using Eq. 5

P
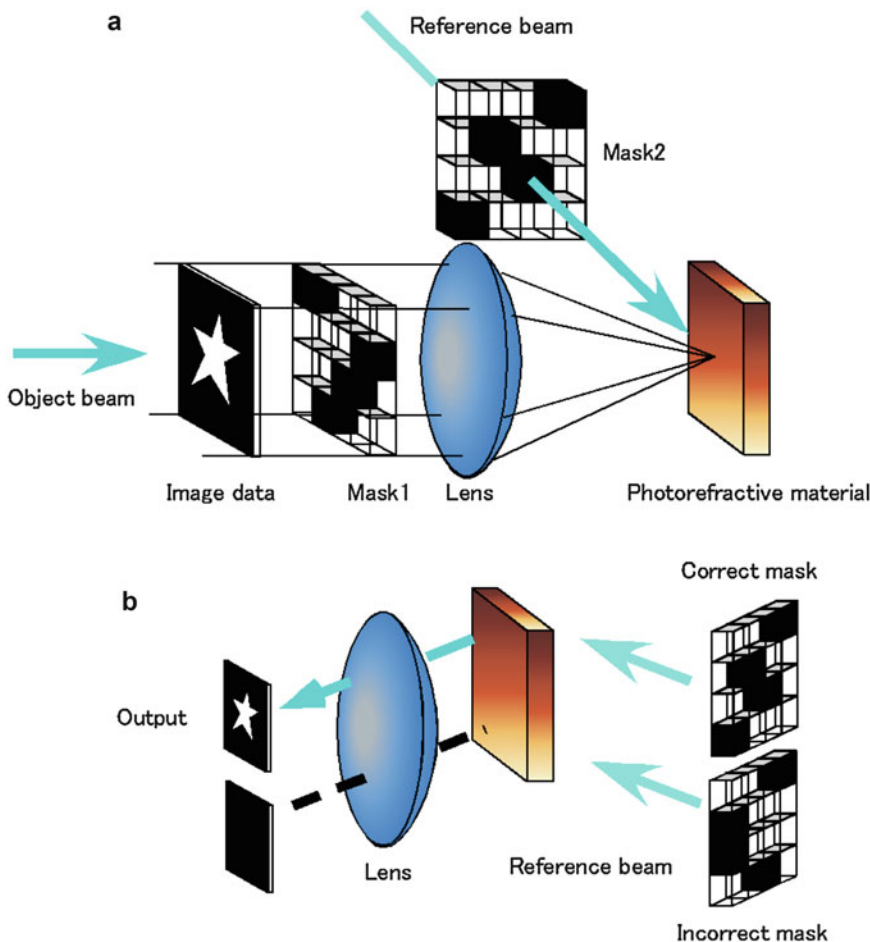
Photorefractive Polymer, Fig. 4 Image correlation method using photorefractive effect. (**a**) Interference pattern of image data with reference beam penetrated through mask 2 is recorded in PR medium. (**b**) Reading beam with a correct mask reproduces original data image (Courtesy by Prof. Sasaki, Tokyo University of Science) (Reproduced from Miraizairyo 12,1, 36–41 (2012), Japan, with permission of NTS Inc, from Book of "Advanced Photonics Polymer: Materials and Applications", 2011, Japan, with permission of CMC Publishing and from CSJ Current Review 07, 2011, Japan (Kagakudojin))

$$\Gamma = \frac{1}{d}\left[\cos\theta_1\frac{I_1(I_2 \neq 0)}{I_1(I_2 = 0)} - \cos\theta_2\frac{I_2(I_1 \neq 0)}{I_2(I_1 = 0)}\right] \tag{5}$$

where d is the sample thickness (optical length), θ_1 and θ_2 are the internal angles of two beams, and I_1 and I_2 are the transmitted intensities of writing beams 1 and 2.

Time profile of holographic diffraction efficiency is evaluated using a stretched exponential function of Kohlrausch-Williams-Watts (KWW) in Eq. 6,

$$\eta = \eta_0\left\{1 - \exp\left[-\frac{t}{\tau}\right]^\beta\right\} \tag{6}$$

where t is the time, η_0 is the steady-state diffraction efficiency, τ is the grating buildup time, and β is the parameter related to a deviation from the single exponential behavior $(0 \leq \beta < 1)$.

Alternative estimation method is using bi-exponential fitting of Eq. 7:

$$\eta = \eta_0 \left\{ p \left[1 - \exp\left(-\frac{t}{\tau_1}\right) \right] + (1-p) \left[1 - \exp\left(-\frac{t}{\tau_2}\right) \right] \right\}^2 \tag{7}$$

where τ_1 is the fast component of response time, τ_2 is the slow component of response time, and p is the contribution of fast component ($0 < p < 1$).

Theoretical Approaches

Coupled wave theory developed by Kogelnik [64] is commonly used to understand the holographic thick gratings.

In transmission grating, diffraction efficiency for p-polarized probe beam η_p is related to the refractive index modulation Δn using an equation of

$$\eta_p = \sin^2\left[K \Delta n_p \cos(\theta_B - \theta_A)\right] \tag{8}$$

where $K = \frac{\pi d}{\lambda (\cos \theta_A \cos \theta_B)^{1/2}}$, Δn_p is the refractive index modulation for p-polarized probe beam, d is the film thickness, λ is the wavelength of laser beam, and θ_A and θ_B are the diffraction angles of beam A and beam B in the film. Diffraction efficiency for s-polarized probe beam η_s is related to the refractive index modulation Δn_s using an equation of

$$\eta_s = \sin^2[K \Delta n_s \cos \theta_G] \tag{9}$$

Δn_s is the refractive index modulation for s-polarized probe beam, θ_G is the angle between the direction of grating vector and applied electric field [65]. The values of Δn_p and Δn_s can be individually estimated from Eqs. 8 and 9, respectively, but theoretically should be equivalent.

In reflection gratings, diffraction efficiency for s-polarized probe beam η_s is related to the refractive index modulation using an equation of

$$\eta_s = \tanh^2 \frac{\pi \Delta n d}{\lambda \cos \theta_0} \tag{10}$$

where θ_0 is the internal refraction angle ($\theta_0 = \theta_A$) [66].

Optical gain Γ is related to Δn with Eq. 11 [67],

$$\Gamma = \frac{4\pi}{\lambda} (\hat{e}_1 \cdot \hat{e}_2{}^*) \Delta n \sin \Phi \tag{11}$$

where $\hat{e}_1$ and $\hat{e}_2$ are the polarization unit vectors of the two writing beams and Φ is the phase shift between refractive index modulation and illumination pattern. Φ is calculated using Eq. 12 with Γ and Δn.

The Kukhtarev model [3] predicts

$$\tan \Phi = \left[\frac{E_D}{E_0} \left(1 + \frac{E_D}{E_q} + \frac{E_0^2}{E_D E_q} \right) \right] \tag{12}$$

where E_D is the diffusion field ($E_D = K_G kT/e$, where K_G is the grating wave vector, k is Boltzmann's constant, T is temperature, and e is the electronic charge), E_0 is the projection of the external electric field onto the grating wave vector, and E_q is the trap-limited space-charge field. E_q can be calculated by using Eq. 11 with the phase shift Φ, E_0, and the diffusion field of E_D.

The number density of traps was calculated from the trap-limited space-charge field E_q with the equation,

$$E_q = \frac{e N_T}{\varepsilon_0 \varepsilon_r K_G} \tag{13}$$

where N_T is the number density of the traps, ε_0 is the permittivity of vacuum, and ε_r is the relative dielectric constant of the composite.

The Kukhtarev model also predicts the space-charge field E_{SC}:

$$|E_{SC}| \approx E_q \left(\frac{E_D^2 + E_0^2}{E_0^2 + (E_q + E_D)^2} \right)^{1/2} \tag{14}$$

E_{SC} can be calculated using Eq. 14 with E_q.

Related Entries

▶ Birefringence of Polymer
▶ Holographic 3D Display
▶ Nonlinear Optical Properties
▶ Optical Information Storage
▶ Refractive Index

References

1. Yeh P (1993) Introduction to photorefractive nonlinear optics. Wiley Interscience, New York
2. Ashkin A, Boyd GD, Dziedzic JM, Smith RG, Ballman AA, Levinstein JJ, Nassau K (1966) Optically-induced refractive index inhomogeneities in $LiNbO_3$ and $LiTaO_3$. Appl Phys Lett 9:72
3. Kukhtarev NV, Markov VB, Odulov SG, Soskin MS, Vinetskii VL (1979) Holographic storage in electrooptic crystals I. Steady state. Ferroelectrics 22:949–960
4. Ducharme S, Scott JC, Twieg RJ, Moerner WE (1991) Observation of the photorefractive effect in a polymer. Phys Rev Lett 66:1846
5. Meerholtz K, Volodin BL, Sandalphon, Kippelen B, Peyghambarian N (1994) A photorefractive polymer with high optical gain and diffraction efficiency near 100 %. Nature 371:497
6. Moerner WE, Silence SM (1994) Polymeric photorefractive materials. Chem Rev 94:127–155
7. Zhang Y, Burzynski R, Ghosal S, Casstevens MK (1996) Photorefractive polymers and composites. Adv Mater 8:111–125
8. Moerner WE, Grunnet-Jepsen A, Thompson CL (1997) Photorefractive polymers. Ann Rev Mater Sci 27:585–623
9. Zilker SJ (2000) Materials design and physics of organic photorefractive systems. Chem Phys Chem 1:72–87
10. Wang Q, Wang L, Yu L (2000) Development of fully functionalized photorefractive polymers. Macromol Rapid Commun 21:723–745
11. Kippelen B, Peyghambarian N (2003) Photorefractive polymers and their applications. Adv Polym Sci 161:87–156
12. Ostroverkhova O, Moerner WE (2004) Organic photorefractives: Mechanisms, materials, and applications. Chem Rev 104:3267–3314
13. Sasaki T (2005) Photorefractive effect of liquid crystalline materials. Polym J 37:797–812
14. Thomas J, Norwood RA, Peyghambarian N, (2009) Non-linear optical polymers for photorefractive applications. J Mater Chem 19:7476–7489
15. Köber S, Salvador M, Meerholz K (2011) Organic photorefractive materials and applications. Adv Mater 23:4725–4763
16. Kippelen B, Meerholz K, Peyghambarian N (1997) An introduction to photorefractive polymers, In: Nalwa HS, Miyata S (eds) Nonlinear optics of organic molecules and polymers. CRC Press, Boca Raton
17. Meerholz K, Kippelen B, Peyghambarian N (1998) Noncrystalline organic photorefractive materials: chemistry, physics, and applications, In: Wise DL, Wnek GE, Trantolo DJ, Cooper TM, Gresser JD (eds) Photonic polymer systems. Marcel Dekker, New York
18. Bittner R, Meerholz K (2006) Photorefractive materials and their applications II: materials. In: Günter P, Huignard J-P (eds) Springer series in optical sciences, vol 114. Springer, Berlin, pp 419–486
19. Kippelen B (2006) Photorefractive materials and their applications II: materials. In: Günter P, Huignard JP (eds) Springer series in optical sciences, vol 114. Springer, Berlin, pp 487–534
20. Montemezzani G, Medrano C, Zgonik M, Günter P (2000) Nonlinear optical effects and materials. In: Günter P (ed) Springer series in optical sciences, vol 72. Springer, Berlin, pp 301–373
21. Simoni F, Lucchetti L (2006) Photorefractive effects in liquid crystals, In: Günter P, Huignard JP (eds) Photorefractive materials and their applications, vol 114, Springer series in optical sciences. Springer, Berlin, pp 571–603
22. Bai Y, Chen X, Wan X, Zhou Q, Liu H, Zhang B, Cong Q (2002) Influence of molecular weight on the photorefractivity of polymer/liquid crystal composites. Appl Phys Lett 80:10
23. Tsutsumi N, Kasaba H (2008) Effect of molecular weight of poly(N-vinyl carbazole) on photorefractive performances. J Appl Phys 104:073102
24. Kinashi K, Wang Y, Sakai W, Tsutsumi N (2013) Optimization of photorefractivity based on poly(N-vinylcarbazole) composites: an approach from the perspectives of chemistry and physics. Macromol Chem Phys 214(16):1789–1797
25. Tyutnev AP, Saenko VS, Kolesnikov VA, Pozhidaev ED (2007) Effect of hole scavenging and preirradiation on electron transport in polyvinyl-carbazole. Polym Sci Ser A 49:189
26. Khalifa MB, Vaufrey D, Bouazizi A, Tardy J, Maaref H (2002) Hole injection and transport in ITO/PEDOT/PVK/Al diodes. Mater Sci Eng C 21:277
27. Qian L, Yang SY, Jin ZS, Zhang ZJ, Zhang T, Teng F, Xu XR (2005) Enhanced performance of light-emitting diodes based on a nanocomposite of dehydrated nanotube titanic acid and poly(vinylcarbazole) (PVK). Phys Lett A 335:56
28. Khalifa MB, Vaufrey D, Tardy J (2004) Opposing influence of hole blocking layer and a doped transport layer on the performance of heterostructure OLEDs. Org Electron 5:187

29. Chen B, Lee CS, Lee ST, Webb P, Chan YC, Gambling W, Tian H, Zhu W (2000) Improved time-of-Flight technique for measuring carrier mobility in thin films of organic electroluminescent materials. Jpn J Appl Phys 39:1190

30. Kimoto A, Cho JS, Higuchi M, Yamamoto K (2004) Synthesis of asymmetrically arranged dendrimers with a carbazole dendron and a phenylazomethine Dendron. Macromolecules 37:5531

31. Bach U, De Cloedt K, Spreitzer H, Gratzel M (2000) Characterization of hole Transport in a new class of spiro-linked oligotriphenylamine compounds. Adv Mater 12:1060

32. Kinashi K, Wang Y, Nonomura A, Tsujimura S, Sakai W, Tsutsumi N (2013) Dynamic Holographic images using poly(*N*-vinylcarbazole)-based photorefractive composites. Polym J 45(6):665–670

33. Tsujimura S, Kinashi K, Sakai W, Tsutsumi N (2014) Recent advances in photorefractivity of poly(4-diphenylamino)styrene composites: Wavelength dependence and dynamic holographic images. Jpn J Appl Phys in press

34. Ogino K, Nomura T, Shichi T, Park SH, Sato H, Aoyama T, Wada T (1997) Synthesis of polymers having tetraphenyldiaminobiphenyl units for a host polymer of photorefractive composite. Chem Mater 9:2768–2775

35. Bobbert PA, Sharma A, Mathijssen SGJ, Kemerink M, de Leeuw DM (2012) Operational stability of organic field-effect transistors. Adv Mater 24:1146

36. Smith J, Zhang W, Sougrat R, Zhao K, Li R, Cha D, Amassian A, Heeney M, McCulloch I, Anthopoulos TD (2012) Solution-processed small molecule-polymer blend organic thin-film transistors with hole mobility greater than 5 cm^2/Vs. Adv Mater 24:2441

37. Thomas J, Fuentes-Hernandez C, Yamamoto M, Cammack K, Matsumoto K, Walker GA, Barlow S, Kippelen B, Meredith G, Marder SR, Peyghambarian N (2004) Bistriarylamine polymer-based composites for photorefractive applications. Adv Mater 16:2032

38. Jeon SO, Yook KS, Son HS, Lee JY (2010) An ethylcarbazole based phosphine oxide derivative as a host for deep blue phosphorescent organic light-emitting diode. J Lumin 130:2238

39. Ego C, Grimsdale AC, Uckert F, Yu G, Sranov G, Mullen K (2002) Triphenylamine-substituted polyfluorene-A stable blue-emitter with improved charge injection for light-emitting diodes. Adv Mater 14:809

40. Zhang W, Smith J, Hamilton R, Heeney M, Kirkpatrick J, Song K, Watkins SE, Anthopoulos T, McCulloch I (2009) Systematic improvement in charge carrier mobility of air stable triarylamine copolymers. J Am Chem Soc 131:10814

41. Thomas J, Christenson CW, Blanche P-A, Yamamoto M, Norwood RA, Peyghambarian N (2011) Photoconducting polymers for photorefractive 3D display applications. Chem Mater 23:416

42. Chu C-W, Shrotriya V, Li G, Yang Y (2006) Tuning acceptor energy level for efficient charge collection in copper-phthalocyanine-based organic solar cells. Appl Phys Lett 88:153504

43. Kinashi K, Shinkai H, Sakai W, Tsutsumi N (2013) Photorefractive device using self-assembled monolayer coated indium-tin-oxide electrodes. Org Electron 14:2987–2993

44. Giang HN, Kinashi K, Sakai W, Tsutsumi N (2012) Photorefractive composite based on monolithic polymer. Macromol Chem Phys 213:982–988

45. Tsutsumi N, Ito Y, Sakai W (2008) Effect of sensitizer on photorefractive nonlinear optics in poly(*N*-vinylcarbazole) based polymer composites. Chem Phys 344:189–194

46. Oh J-W, Moon IK, Kim N (2009) The influence of photosensitizers on the photorefractivity in poly[methyl-3-(9-carbazolyl)propylsiloxane]-based composites. J Photochem Photobiol A Chem 201:222–227

47. Köber S, Gallego-Gómez F, Salvador M, Kooistra FB, Hummelen JC, Aleman K, Mansurova S, Meerholz K (2010) Influence of the sensitizer reduction potential on the sensitivity of photorefractive polymer composites. J Mater Chem 20:6170–6175

48. Köber S, Prauzner J, Salvador M, Meerholz K (2009) In: Photorefractive materials, effects and devices: control of light and matter, PR09 topical meeting technical digest 2009. pp P1–46

49. Christenson CW, Thomas J, Blanche P-A, Voorakaranam R, Norwood RA, Yamamoto M, Peyghambarian N (2010) Grating dynamics in a photorefractive polymer with Alq3 electron traps. Opt Express 18:9358–9365

50. Wei Q, Liu Y, Chen Z, Huang M, Zhang J, Gong Q, Chen X, Zhou Q, Opt J (2004) Improvement in photorefractivity of a polymeric composite doped with the electron-injecting material Alq$_3$. A Pure Appl Opt 6:890–893

51. Zhang J, Chen Z, Liu Y, Huang M, Wei Q, Gong Q (2004) Improvement on the photorefractive performance of a monolithic molecular material by introducing electron traps. Appl Phys Lett 85:1323–1325

52. Moerner WE, Silence SM, Hache F, Bjorklund GC (1994) Orientationally enhanced photorefractive effect in polymers. J Opt Soc Am B 11:320–330

53. Wortmann R, Poga C, Twieg RJ, Geletneky C, Moylan CR, Lundquist PM, DeVoe RG, Cotts PM, Horn H, Rice JE, Burland DM (1996) Design of optimized photorefractive polymers: a novel class of chromophores. J Chem Phys 105:10637–10647

P

54. Tanaka A, Nishide J, Sasabe H (2009) Asymmetric energy transfer in photorefractive polymer composites under non-electric field. Mol Cryst Liq Cryst 504:44

55. Salvador M, Prauzner J, Köber S, Meerholz K, Turek JJ, Jeong K, Nolte DD (2009) Three-dimensional holographic imaging of living tissue using a highly sensitive photorefractive polymer device. Opt Express 17(14):11834–11849

56. Parrish JA (1981) New concepts in therapeutic photomedicine – photochemistry, optical targeting and the therapeutic window. J Invest Dermatol 77:45–50

57. Blanche PA, Tay S, Voorakaranam R, Saint-Hilaire P, Christenson C, Gu T, Lin W, Flores D, Wang P, Yamamoto M, Thomas J, Norwood RA, Peyghambarian N (2008) An updatable holographic display for 3D visualization. J Display Tech 4(4):424–430

58. Tay S, Blanche P-A, Voorakaranam R, Tunç AV, Lin W, Rokutanda S, Gu T, Flores D, Wang P, Li G, St Hilaire P, Thomas J, Norwood RA, Yamamoto M, Peyghambarian N (2008) An updatable holographic three-dimensional display. Nature 451:694–698

59. Christenson CW, Blanche P-A, Tay S, Voorakaranam R, Gu T, Lin W, Wang P, Yamamoto M, Thomas J, Norwood RA, Peyghambarian N (2010) Materials for an updatable holographic 3D display. J Display Tech 6(10):510–516

60. Blanche P-A, Bablumian A, Voorakaranam R, Christenson C, Lin W, Gu T, Flores D, Wang P, Hsieh W-Y, Kathaperumal M, Rachwal B, Siddiqui O, Thomas J, Norwood RA, Yamamoto M, Peyghambarian N (2010) Holographic three-dimensional telepresence using large-area photorefractive polymer. Nature 468:80–83

61. Lynn B, Blanche P-A, Bablumian A, Rankin R, Voorakaranam R, St Hilaire PS, LaComb L Jr, Yamamoto M, Peyghambarian N, Peyghambarian N (2013) Recent advancements in photorefractive holographic imaging. J Phys Conf Ser 415:012050

62. Tsutsumi N, Kinashi K, Nonomura A, Sakai W (2012) Quickly updatable hologram images using poly(N-vinyl Carbazole) (PVCz) photorefractive polymer composite. Materials 5:1477–1486

63. Giang HN, Kinashi K, Sakai W, Tsutsumi N (2014) Photorefractive response and real-time holographic application of a poly(4-(diphenylamino)benzyl acrylate)-based composite. Polym J 46:59–66

64. Kogelnik H (1969) Coupled wave theory for thick hologram gratings. Bell Sys Tech J 48:2909–2947

65. Tsutsumi N, Dohi A, Nonomura A, Sakai W (2011) Enhanced performance of photorefractive poly(N-vinyl carbazole) composites. J Polym Sci Part B Polym Phys 49:414–420

66. Tsutsumi N, Eguchi J, Sakai W (2005) High performance photorefractive molecular glass composites in reflection gratings. Chem Phys Lett 408:269–273

67. Günter P, Huignard JP (1988, 1989) Photorefractive materials and their applications, vols I and II. Springer, Berlin

Photoresponsive Polymer

Takahiro Seki
Department of Molecular Design and Engineering, Graduate School of Engineering, Nagoya University, Chikusa, Nagoya, Japan

Synonyms

Light-induced motions; Light-induced orientations; Light-responsive

Definition

When photoreactive units, in many cases photochromic ones, are introduced into polymers, photoresponsive polymers are prepared. Polymer micelles and solid films formed from such polymers can exhibit aggregation changes, molecular alignments, and deformations upon light irradiation.

Introduction

Smart polymeric materials are widely studied in areas of nanotechnology, materials chemistry, optics, electronics, and biomedical fields. Stimuli-responsive polymer systems provide smart switchable and tuning functions for many purposes. Light trigger is particularly fascinating because the polymer properties can be changed remotely without contact with sufficient spatial accuracy. In this section, several photoresponsive systems, including micelles, surfaces, thin films for photoalignment, and mechanical materials, are briefly overviewed. A comprehensive book has been published by Zhao and Ikeda [1], and readers can also refer to recent reviews [2–4] in this field. In recent research, block copolymers of controlled molecular mass are becoming more and more important for creating new photoresponsive functions. They self-assemble to form hierarchical nano- and mesoscopic regular

structures and morphologies, which will then lead to higher-level functions and expand applications. Photoresponsive polymers and block copolymers are mostly synthesized by controlled radical polymerizations encompassing atom transfer radical polymerization (ATRP), reversible addition fragmentation chain transfer (RAFT), and nitroxide-mediated polymerization [3].
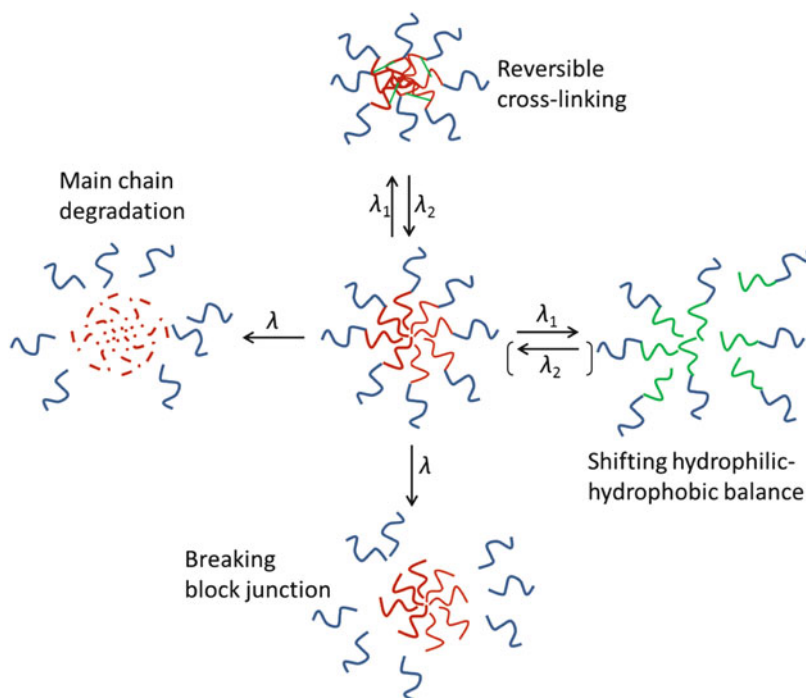
Polymer Micelles

In these systems, use of block copolymers is needed since the polymers require the amphiphilic nature to form defined aggregations in solutions. Light-responsive block copolymers can be grouped into four types based on their photoinduced structural changes. The aggregation state of polymeric micelles can be changed by (i) light-induced shifting in hydrophilic-hydrophobic balance, (ii) breaking block junction, (iii) main chain degradation, and (iv) reversible cross-linking (Fig. 1) [5, 6]. The most plausible application of photoresponsive block copolymer micelles are for controlled drug delivery applications. Since the

biocompatible and biodegradable characteristic features are required, poly(ethylene oxide) has been frequently used as the hydrophilic block. Photoresponsive moieties are introduced in the hydrophobic blocks. UV light is harmful to biological systems, and therefore photoresponsive micelles responding to near-infrared beam have recently been developed [5, 6].

Surface Functions

Wettability is a fundamental property of a solid surface and plays significant roles in biological systems and industries. Light-induced wettability changes and switching are realized on photoresponsive surfaces. The surface structures found in biological systems (both plants and creatures) have motivated many investigators to explore surfaces using artificial materials (bio-inspired approaches) [7, 8]. Some photochromic molecules exhibit considerable polarity changes during the photoisomerization. They are used for wettability switching surfaces. If the surface has a rough morphology, the change is


Photoresponsive Polymer, Fig. 1 Schematic illustration of various types of photoresponsive block copolymer micelles (Redrawn from Zhao et al. [5])

Photoresponsive Polymer, Fig. 2 Schematic drawings of irradiation with linearly polarized light (LPL) and oblique nonpolarized light (*upper*). The *lower* drawing shows a model of aligned monodomain formation of LCs by irradiation with linearly polarized light

Linearly polarized light

Oblique non-polarized light

E

Linearly polarized light
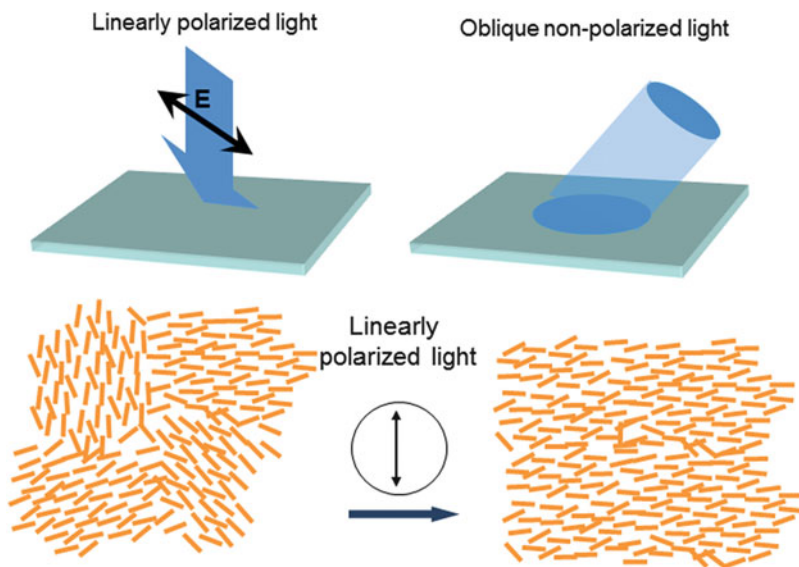
enlarged. A gradient light irradiation causes an asymmetrical wetting property on the surface, leading to macroscopic lateral motions of a liquid droplet.

Another important aspect regarding the polymer surface is the interaction with liquid crystal (LC) molecules. How to align nematic LCs on the substrate surface is a critical issue during the LC display panel productions. The rubbing technique on polymer films was always adopted for this purpose, but the photoalignment method is starting to be adopted instead of the rubbing because of its great advantages [9, 10]. The first demonstration of LC alignment control by surface photochemistry was provided by Ichimura et al. in 1988. They found that the E/Z (trans/cis) photoisomerization of an azobenzene monolayer on a substrate could switch the alignment of nematic LC molecules between the homeotropic and planar modes. This active functional surface is called a "command surface" or "command layer." Shortly after this finding, groups in the USA, Switzerland/Russia, and Ukraine reported almost at the same time a significant effect that angular selective excitation by linearly polarized light (LPL) onto photoreactive polymer surfaces causes uniaxial alignment of contacting LCs (Weigert effect, Fig. 2). Besides nematic LCs, the surface alignment process is now widely applied to various types of materials, including LCs of other features, polymeric materials, organic semiconductors, and inorganic materials [9].

Polymer Thin Films

Most polymer thin films are obtained by spin coating. To achieve precise structural controls, the Langmuir-Blodgett technique and layer-by-layer method have also been conducted. Surface-initiated (SI) polymerizations provide another class of polymer thin films. In these systems, one end of polymer chains is attached to a substrate surface. If the lateral polymer density is sufficiently high, surface brushes are formed, which provide unique molecular orientations and properties. With respect to photoresponsive polymer brushes, there are many examples of SI polymerizations for photochromic monomers such as spiropyran and azobenzene derivatives [11]. They exhibit fascinating smart responsive functions. When side chain LC polymers are employed, the brush LC chains adopt unique orientation in which the smectic lamellae are aligned vertically to the surface plane. In this orientation, the in-plane alignment of photoresponsive azobenzene mesogenic groups becomes

Photoresponsive Polymer, Fig. 3 Schematic illustrations of photoresponsive surface-grafted photoresponsive liquid crystalline polymers (*upper*) and in-plane photo-switching of microphase separation structure of photoresponsive LC polymer films (*lower*)
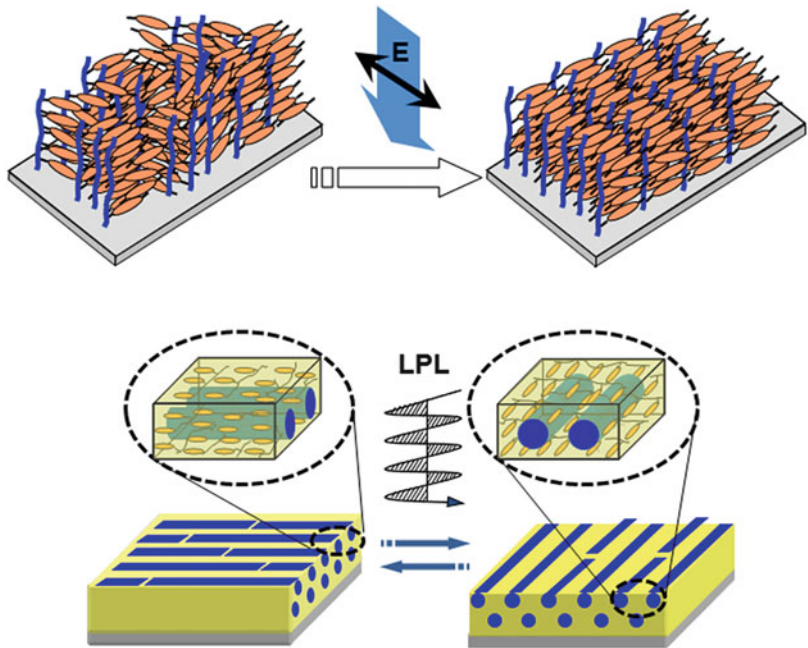
Photoresponsive Polymer, Fig. 4 Schematic illustrations of light-induced deformation of photoresponsive LC elastomer films (Redrawn from Ikeda et al. [13])

P
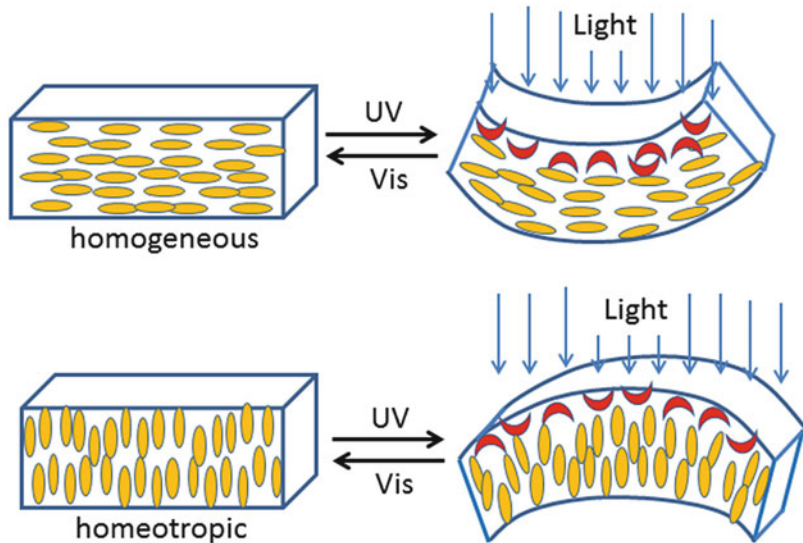
significantly effective (Fig. 3, upper). Introduction of a flexible chain between the substrate and the LC layer (diblock copolymer architecture) leads to even more efficient photoresponsive reorientation motions [11].

Microphase separation (MPS) of block copolymers provides arrays of periodic patterns with length scales of typically 10–50 nm via simple

and low-cost processes. Therefore, this phenomenon is extensively studied as the future material technologies beyond the photolithography technique. Great effort has been devoted to the photoalignment of MPS patterns of block copolymer films as well. The photoalignment at molecular levels can be converted to the mesoscopic MPS domain orientations of block copolymers

possessing azobenzene-containing side chains [9, 11, 12]. Many methods have been proposed so far to align MPS structure. Among them, the photoalignment strategy has a marked feature that the initial orientation can be overwritten to another direction by subsequent LPL irradiation. Such process can be repeated many times (Fig. 3, lower).

Macroscopic Mechanical Systems

In the last decade, epoch-making approaches in photoresponsive polymer materials have emerged, namely, the development of macroscopic photomechanical materials [12–16]. The photoisomerization or photo-cross-linking reaction of photoreactive units can directly change macroscopic material motions. The key to these processes is to assemble molecules and polymers in the ordered and oriented state. LC and crystalline states with retention of molecular motions within the assembly fulfill the conditions. Ikeda et al. initiated this research area, and many groups are currently making efforts to produce new photomobile systems. Typical photo-induced deformation behaviors of azobenzene-containing elastomer films are displayed in Fig. 4. Relating to this, investigations of self-healing and shape memory materials have also become areas of intensive research [16, 17].

Summary

Studies on photoresponsive polymers are forming active research areas, extending to various directions. Thanks to the great improvement of polymerization techniques, particularly in the controlled living radical polymerizations and controlled metathesis polymerizations, various monomer designs and polymer architectures possessing photoreactive groups have become available. The new polymer architectures lead to new photofunctions, which will then help designing new polymers. This synergetic effect leads to unending development of new ideas and new classes of applications. Detailed information on the photoresponsive polymers is available from books and reviews in the reference list.

Related Entries

▶ Photochromic Polymers
▶ Stimuli-responsive Polymers

References

1. Zhao Y, Ikeda T (2009) Smart light-responsive materials. Wiley, Hoboken
2. Ercole F, Davis TP, Evans RA (2010) Photo-responsive systems and biomaterials: photochromic polymers, light-triggered self-assembly, surface modification, fluorescence modulation and beyond. Polym Chem 1:37–54. doi:10.1039/b9py00300b
3. Schumers JM, Fustin CA, Gohy JF (2010) Light-responsive block copolymers. Macromol Rapid Commun 31:1588–1607. doi:10.1002/marc.201000108
4. Wang D, Wang X (2013) Amphiphilic azo polymers: molecular engineering, self-assembly and photo-responsive properties. Prog Polym Sci 38:271–301. doi: http://dx.doi.org/10.1016/j.progpolymsci.2012.07.003
5. Zhao Y (2012) Light-responsive block copolymer micelles. Macromolecules 45:3647–3657. doi:10.1021/ma300094t
6. Gohy JF, Zhao Y (2013) Photo-responsive block copolymer micelles: design and behavior. Chem Soc Rev 42:7117–7129. doi:10.1039/C3CS35469E
7. Ichimura K, Seki T (2011) Molecular switches. In: Feringa BL, Browne WR (eds) Photoinduced motion associated with monolayer, vol 2, 2nd edn. Wiley-VCH, Weinheim, pp 629–668
8. Wang S, Song Y, Jiang L (2007) Photoresponsive surfaces with controllable wettability. J Photochem Photobiol C Photochem Rev 8:18–29, http://dx.doi.org/10.1016/j.jphotochemrev.2007.03.001
9. Seki T, Nagano S, Hara M (2013) Versatility of photoalignment techniques: from nematics to a wide range of functional materials. Polymer 54:6053–6072, http://dx.doi.org/10.1016/j.polymer.2013.08.058
10. Yaroshchuk O, Reznikov Y (2012) Photoalignment of liquid crystals: basics and current trends. J Mater Chem 22:286–300. doi:10.1039/c1jm13485j
11. Seki T (2014) Meso- and microscopic motions in photoresponsive liquid crystalline polymer films. Macromol Rapid Commun 35:271–290, doi:10.1002/marc.201300763
12. Yu H (2014) Photoresponsive liquid crystalline block copolymers: from photonics to nanotechnology. Prog Polym Sci 39:781–815, doi:http://dx.doi.org/10.1016/j.progpolymsci.2013.08.005
13. Ikeda T, Mamiya J, Yu Y (2007) Photomechanics of liquid-crystalline elastomers and other polymers. Angew Chem Int Ed 46:506–528. doi:10.1002/anie.200602372
14. Yan Z, Ji X, Wu W, Wei J, Yu Y (2012) Light-switchable behavior of a microarray of azobenzene

liquid crystal polymer induced by photodeformation. Macromol Rapid Commun 33:1362–1367. doi:10.1002/marc.201200303

15. Palffy-Muhoray P (2012) In: Jeu WH (ed) Liquid crystal elastomers: materials and applications, vol 250, Advice polymer science. Springer, Berlin/Heidelberg, pp 95–118

16. Jiang HY, Kelch S, Lendlein A (2006) Polymers move in response to light. Adv Mater 18:1471–1475. doi:10.1002/adma.200502266

17. Habault D, Zhang H, Zhao Y (2013) Light-triggered self-healing and shape-memory polymers. Chem Soc Rev 42:7244–7256. doi:10.1039/C3CS35489J

pH-Responsive Polymer

Akifumi Kawamura and Takashi Miyata
Department of Chemistry and Materials
Engineering, Kansai University, Suita,
Osaka, Japan

Synonyms

pH-sensitive polymer; Polyelectrolytes

Definition

pH-responsive polymers are smart polymers that undergo changes in structures and properties such as conformation, hydrophilicity/hydrophobicity, solubility, volume, and so on in response to a change in pH. Polymers with acidic or basic groups like carboxy, sulfonyl, and amino groups are typically described as pH-responsive polymers because the ionization of the groups by pH changes results in changes in structures and properties of the polymer chains.

## Key Principles, Examples, and Synthesis of pH-responsive Polymers

pH-responsive polymers undergo changes in structures and properties such as conformation, hydrophilicity/hydrophobicity, solubility, and volume in response to external pH. For example,

poly(methacrylic acid) (PMAAc) shows reversible phase transition between soluble and insoluble state in response to pH changes. A change in pH induces the conformational changes in poly (L-lysine) between α-helix and random coil. Polymers with pH-cleavable groups such as polylactide and polyketal are also described as pH-responsive polymer. Whereas many types of pH-responsive polymers have been prepared, the term "pH-responsive polymers" is widely used to describe the polymers with ionizable groups whose ionization depends on pH. This entry focuses on the pH-responsive polymers with ionizable groups.

The key elements of pH-responsive polymers are the acidic or basic groups linked with the polymer backbone such as carboxy and amino groups. A change in pH influences the degree of ionization of acidic or basic groups, followed by generation of anions or cations. The generated anions or cations of a pH-responsive polymer cause a drastic extension of coiled chains by electrostatic repulsion and govern its conformation, hydrophilicity, or solubility in an aqueous solution.

A large number of pH-responsive polymers have been designed using various electrolyte groups. Representative pH-responsive polymers are summarized in Fig. 1. There are two major classes of pH-responsive polymers. One is polymers with acidic groups and the other is polymers with basic groups. Typical pH-responsive polymers with acidic groups are poly((meth)acrylic acid), poly(glutamic acid), and poly(aspartic acid) with carboxy groups, poly(styrenesulfonic acid) and poly(2-acryloylamino-2-methyl-propane-1-sulfonic acid) with sulfonic groups, and poly[2-(phosphonooxy)ethyl methacrylate] with phosphate groups. In contrast, the pH-responsive polymers with basic groups typically include poly(allylamine), poly(L-lysine), poly(ethyleneimine), poly(dimethylaminoethyl methacrylate), and polyamidoamine dendrimer, which have primary, secondary, or tertiary amino groups.

Typical pH-responsive polymers with ionizable groups are synthesized by conventional free radical polymerization, which can be employed

P
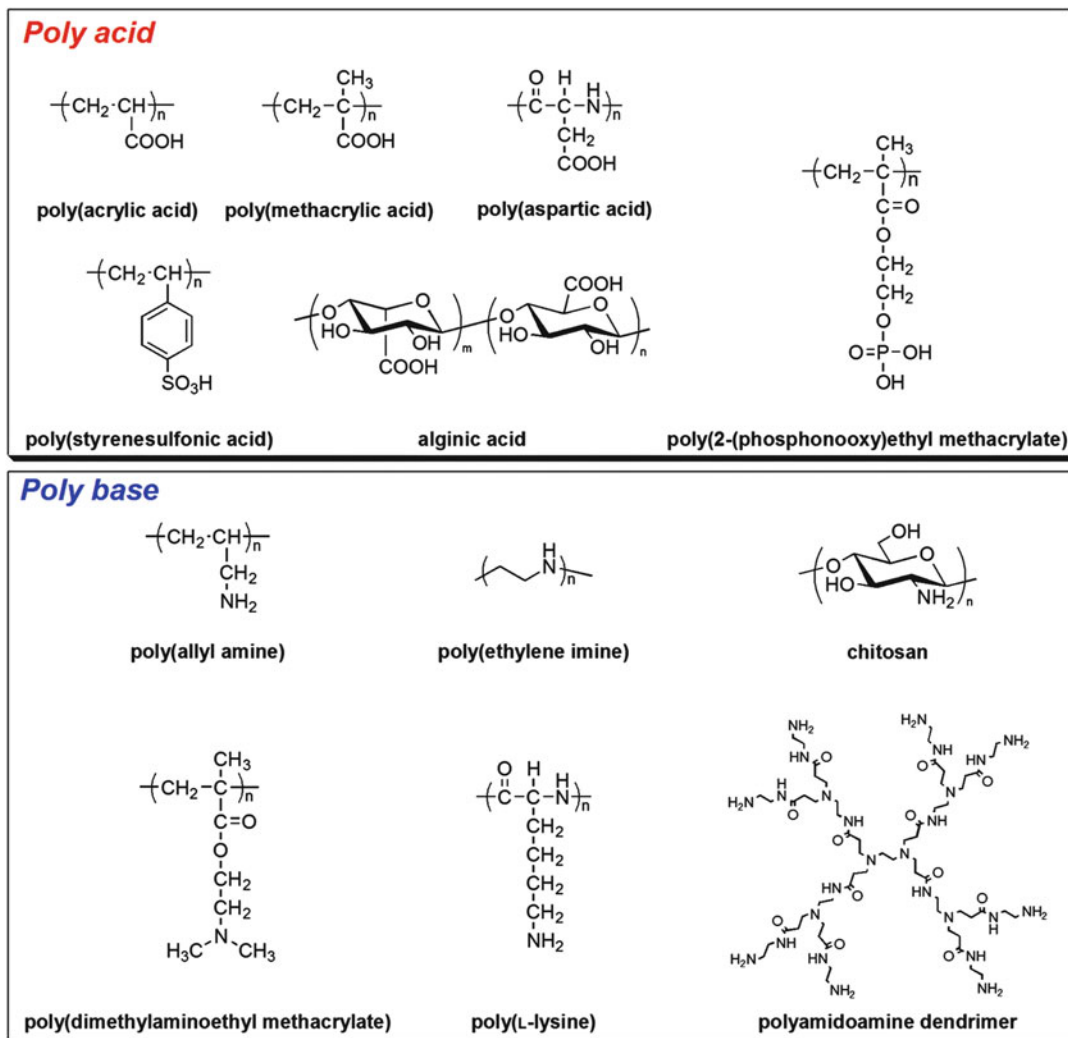
pH-Responsive Polymer, Fig. 1 Typical examples of pH-responsive polymers

for polymerization of a wide variety of vinyl monomers under mild reaction conditions. Typical applications of pH-responsive polymers are separation and purification. For example, pH-responsive linear polymers can realize easy separation of a protein through the electrostatic interaction [1]. The pH-responsive polymers interact with oppositely charged proteins, resulting in the precipitation of pH-responsive polymer-protein complexes. The precipitated proteins can be easily recovered and reused after the dissociation of the pH-responsive polymer-protein complexes by changing pH. Also, the pH-responsive

resin prepared by copolymerization of charged monomers with cross-linker is widely used as ion-exchange chromatographic support.

To prepare pH-responsive polymeric nanomaterials such as micelles and vesicles that change their structures in response to pH, well-defined pH-responsive polymers such as block, graft, and star polymers are strategically designed. However, the conventional free radical polymerization has limitations in control of the molecular weight, polydispersity, end functionality, structure, and composition of resultant polymers. Therefore, ionic living polymerizations

were employed to synthesize well-defined pH-responsive polymers with precisely designed structures. However, the ionic polymerizations were not widely utilized for the synthesis of well-defined pH-responsive polymers because it required stringent conditions and was limited to a relatively small number of monomers. In the 1990s, a novel controlled/living radical polymerization method was developed [2, 3]. By utilizing the controlled/living radical polymerization, well-defined block and graft copolymers and star and end-functional polymers with narrow molecular weight distributions can be synthesized under mild conditions. The key point of controlled/living radical polymerization is the establishment of a dynamic equilibrium between propagating radicals and dormant species. The dynamic equilibrium between propagating radicals and dormant species allows slow but simultaneous growth of polymer chains with minimum termination reaction. Recently, two types of controlled/living radical polymerizations were widely utilized for the synthesis of well-defined polymers: atom transfer radical polymerization (ATRP) and reversible addition-fragmentation chain transfer (RAFT) polymerization.

ATRP is based on the catalyzed, reversible cleavage of carbon-halogen bond in the dormant species by a redox process (Scheme 1a). In ATRP, alkyl halides are used as initiators, and a variety of transition metals and ligands are successfully employed as catalysts. Especially, the catalysts based on copper and N-containing ligands are often used. A wide variety of conjugated monomers such as (meth)acrylic esters, styrene, acrylamide, and acrylonitrile can be polymerized by ATRP. On the other hand, the drawback of ATRP is the use of a large amount of catalysts. However, the development of new ATRP techniques which are called "activators regenerated by electron transfer" (ARGET) and "initiators for continuous activator regeneration" (ICAR) allows decreasing the amount of catalyst.

RAFT polymerization involves conventional free radical polymerization in the presence of chain transfer agents (RAFT agents) which have the thiocarbonylthio groups ($S = C–S$) such as dithioesters, dithiocarbamates, trithiocarbonates, and xanthates. In RAFT polymerization, propagating radicals react with the $C = S$ double bond of RAFT agents to form the RAFT adduct radicals which act as dormant species (Scheme 1b). The equilibrium between active propagating species and dormant RAFT adduct radicals enables the production of well-defined polymers with narrow molecular weight distributions. RAFT polymerization is applicable to a variety of monomers such as (meth)acrylates, styrene, and acrylamides, whereas RAFT reagents are not tolerant to primary and secondary amines.
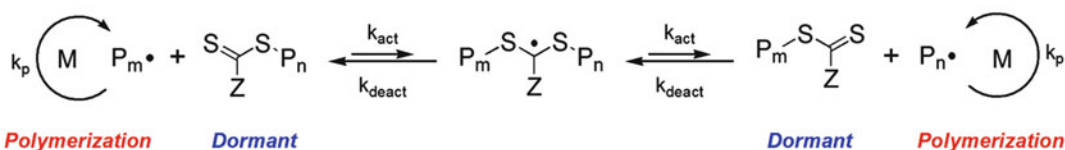
The ATRP and RAFT polymerization opened the door for the preparation of various types of polymeric nanomaterials such as micelles, vesicles, and brushes because they enabled the facile
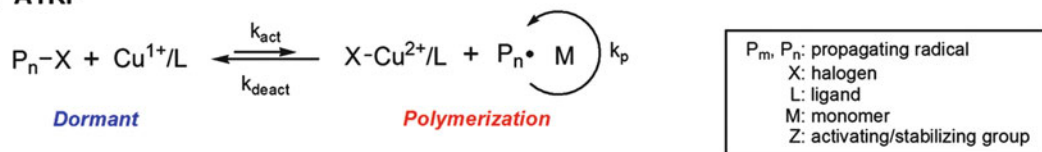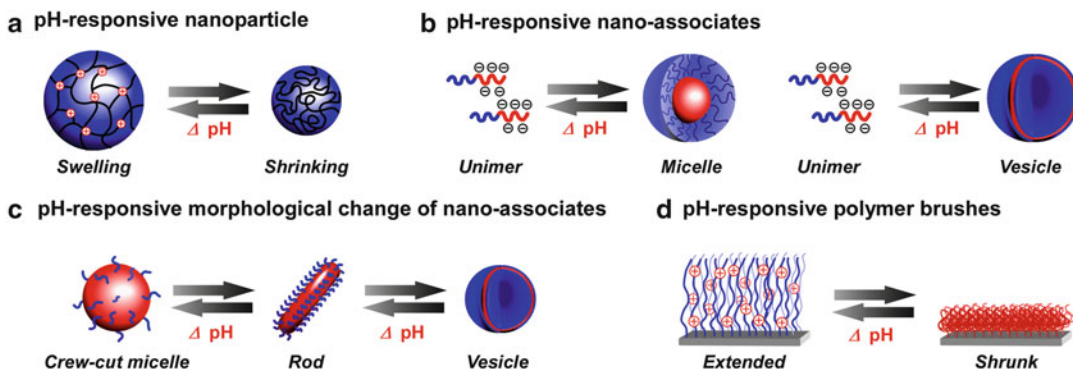

pH-Responsive Polymer, Scheme 1 Reaction mechanism for atom transfer radical polymerization (ATRP) (**a**) and reversible addition-fragmentation chain transfer (RAFT) polymerization (**b**)

pH-Responsive Polymer, Fig. 2 Typical pH-responsive nanomaterials. (**a**) pH-responsive nanoparticles; (**b**) pH-responsive nano-associates; (**c**) pH-responsive morphological change of nano-associates; and (**d**) pH-responsive polymer brushes

synthesis of well-defined block and graft copolymers under mild conditions. Using the ATRP and RAFT polymerization, furthermore, many researchers have developed a variety of stimuli-responsive nanomaterials that changed the structures and properties such as size, morphology, and wettability in response to external stimuli because a broad range of vinyl monomers can be strategically polymerized via ATRP and RAFT polymerization. For example, amphiphilic block copolymers with both pH-responsive block and hydrophobic block, which are easily synthesized by ATRP or RAFT polymerization, spontaneously form nano-associates such as micelles and vesicles. The polymeric micelles and vesicles with pH-responsive moieties undergo changes in the structures such as size and morphology in response to pH (Fig. 2). In addition, pH-responsive polymer brushes with accurately controlled molecular weight can be formed by *grafting from* polymerization from the ATRP initiator or RAFT agent that is attached onto a surface of substrate. The surface wettability of the substrate with pH-responsive polymer brushes changes by the external pH. These pH-responsive polymeric nanomaterials have attracted considerable attentions as smart materials for separation, adhesion, drug delivery system, and tissue engineering. The following sections focus on the typical studies on the applications of the pH-responsive polymers as nanomaterials such as nanoparticles, nano-associates, and brushes.

pH-Responsive Nanoparticles

Polymeric nanoparticles are generally defined as insoluble colloidal systems with sizes ranging approximately from 10 to 1,000 nm. Emulsion polymerization is the versatile technique for the preparation of polymeric nanoparticles. In conventional emulsion polymerization, surfactants composed of hydrophilic and hydrophobic groups are commonly used to stabilize and disperse monomer emulsions in a solvent. The polymerization proceeds within the monomer emulsions and produces nanoparticles with narrow size distributions. Stimuli-responsive nanoparticles that undergo changes in size in response to external stimuli such as pH and temperature are prepared by emulsion polymerization using monomers such as (meth)acrylic acid and *N*-isopropyl acrylamide. In the early 1990s, nano-sized poly(methyl methacrylate-*co*-acrylic acid) (P(MMA-*co*-AAc)) particles having pH-responsive carboxy groups were first prepared by emulsion polymerization [4]. The P(MMA-*co*-AAc) nanoparticles with a diameter of approximately 100 nm showed a drastic increase in diameter under basic conditions, whereas they shrank again under acidic conditions. The pH-responsive changes in the particle sizes are attributed to swelling/shrinking of the particles by changes in their internal osmotic pressure, which depend on the dissociation and association of their acidic or basic groups. The carboxy groups of the P(MMA-*co*-AAc) are

protonated under acidic conditions, whereas the carboxylate anions are generated by deprotonation of carboxy groups under basic conditions, which creates excess osmotic pressure inside the nanoparticles and results in swelling. The pH-responsive nanoparticles that swell under acidic conditions are also designed using monomers with an amino group such as *N, N*-dimethylaminoethyl methacrylate. These pH-responsive nanoparticles exhibited rapidly responsive swelling/shrinking changes because of their large surface area.

These pH-responsive nanoparticles have attracted considerable attention as smart drug carrier because pH changes in many specific or pathological compartments are important signals for drug targeting [5]. Drugs can be loaded into such pH-responsive nanoparticles through hydrophobic or electrostatic interactions. Nagasaki et al. developed pH-responsive nanogels that released drugs in the acidic environment of endosome [6]. The pH-responsive nanogels were prepared by surfactant-free emulsion polymerization of *N, N*-diethylaminoethyl methacrylate with poly(ethylene glycol) having a 4-vinylbenzyl group. The resultant pH-responsive nanogels with a diameter of approximately 90 nm swelled under acidic conditions below pH 7.5. Furthermore, doxorubicin (Dox), which is an anticancer drug, was successfully loaded within the pH-responsive nanogels. The Dox-loaded pH-responsive nanogels almost showed no initial burst release of Dox, whereas Dox was effectively released from pH-responsive nanogel at pH 5–6 that corresponds to the endosomal pH. Dox was released successfully from the Dox-loaded pH-responsive nanogel in response to endosomal pH and showed antitumor activity against the human hepatome cell line HuH-7, which is a natural drug-resistant tumor cell line.

Peppas et al. reported the pH-responsive nanospheres composed of poly(ethylene glycol) methacrylate (PEGMA) and poly(carboxylic acid) for oral drug delivery system [7]. Proton-accepting and proton-donating polymers typically interact with each other in an aqueous solution and organic solvents through hydrogen
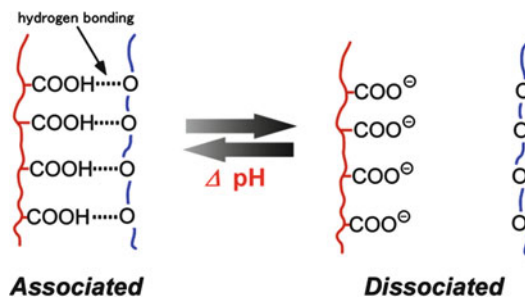
pH-Responsive Polymer, Fig. 3 Schematic of the pH-responsive complexation between poly(carboxylic acid) and poly(ethylene glycol) through hydrogen bonding

bonding. Poly(carboxylic acid) such as poly(methacrylic acid) (PMAAc) and poly(acrylic acid) (PAAc) with protonated carboxy groups interacts with PEG to form a stable complex through hydrogen bonding. However, an increase in pH induces the ionization of carboxy groups in poly(carboxylic acid), resulting in the dissociation of poly(carboxylic acid)/PEG complexes (Fig. 3) [8]. The pH-induced dissociation of poly(carboxylic acid)/PEG complexes was utilized to design pH-responsive nanospheres. The pH-responsive nanospheres shrank in an acidic pH owing to the hydrogen bonding between the carboxy groups and PEG chain, whereas they swelled upon increasing pH because of the ionization of carboxy groups. Insulin was successfully loaded into the pH-responsive nanospheres by simple diffusion method. Release of insulin from the pH-responsive nanospheres was depressed at low pH, but insulin was successfully released at high pH. At low pH, the formation of hydrogen bonding between poly(carboxylic acid) and PEG in the network of nanospheres inhibited the release of loaded insulin. On the other hand, insulin easily diffused from the nanosphere at high pH because the mesh size of nanospheres became large owing to the dissociation of poly(carboxylic acid)/PEG complexes. The insulin-loaded pH-responsive nanospheres have a potential application as oral insulin delivery devices. In addition to applications to DDS, pH-responsive nanoparticles were used as templates for the synthesis of metal nanoparticles and as substrates for the immobilization of enzymes.

P

pH-Responsive Nano-associates

As mentioned above, recent developments in controlled/living radical polymerization enabled us to synthesize well-defined polymers such as amphiphilic block and graft polymers consisting of hydrophilic and hydrophobic segments. The amphiphilic block and graft copolymers spontaneously form nano-associates such as micelle, vesicle, and lamellar by self-assembling in an aqueous solution. Because the water solubility of pH-responsive polymers can be manipulated by a pH change, pH-responsive nano-associates have been prepared from block and graft copolymers with pH-responsive moiety [9]. Eisenberg et al. reported detailed studies on the pH-responsive nano-associates prepared by polystyrene-*block*-poly(acrylic acid) (PS-*b*-PAAc) [10, 11]. PS-*b*-PAAc was less hydrophilic owing to the protonated carboxy groups of PAAc segments under acidic conditions. On the other hand, when the PAAc segments became hydrophilic by negative charges produced with increasing pH, PS-*b*-PAAc changed to an amphiphilic polymer. As a result, PS-*b*-PAAc spontaneously formed nano-associates in an aqueous solution with a basic pH. The morphologies of the PS-*b*-PAAc nano-associates depended on the composition, solvent, and preparation methodologies. For example, PS-*b*-PAAc with a long PS segment spontaneously associated to form spherical crew-cut aggregates with hydrophobic PS core and hydrophilic PAAc shell. The morphology of the PS-*b*-PAAc nano-associates was also controlled by pH. The addition of HCl induced the changes in morphology from spheres to rods and furthermore to vesicles because the protonation of the carboxy groups of the PAAc segment resulted in a decrease in the inter-shell repulsions. In contrast, ionization of the PAAc segment by the addition of NaOH caused a morphological change from vesicles to spheres by an increase in inter-shell repulsions.

A particular class of pH-responsive block copolymers present reversible self-assembly properties from unimer to nano-associate such as micelles and vesicles depending on pH. Arms et al. developed "schizophrenic" diblock copolymers which can self-assemble to form micelle in response to pH and temperature [12]. They synthesized a diblock copolymer based on poly(propylene oxide) and diethylaminoethyl methacrylate (PPO-*b*-PDEAEMA) via ATRP. In a dilute aqueous solution with pH 6.5 at 5 °C, PPO-*b*-PDEAEMAs were dissolved as a unimer because of the protonation of their amino groups. In a solution with pH 8.5 or higher, however, PPO-*b*-PDEAEMAs were spontaneously associated to form micelles. The micelles were composed of a hydrophilic PPO shell and a hydrophobic PDEAEMA core with deprotonated amino groups. On the other hand, PPO-*b*-PDEAEMA formed reverse micelles composed of PPO core and PDEAEMA shell in an aqueous solution at pH 6.5 with rising temperature because PPO block with M_n of around 2,000 became insoluble in an aqueous solution above 20 °C.

Schizophrenic vesicles were also prepared by Lecommandoux and coworkers [13]. They synthesized zwitterionic diblock copolymer, poly(L-glutamic acid)-*block*-poly(L-lysine) (PGA-*b*-PLL), by sequential anionic ring-opening polymerization of the corresponding α-amino acid *N*-carboxyanhydrides. The PGA-*b*-PLL was dissolved as a unimer in neutral pH (5 < pH < 9). At the acidic pH, PGA-*b*-PLL spontaneously formed vesicles with a diameter of 220 nm because the PGA block was neutralized and its secondary structure changed from random coil to a compact α-helical structure. Under the basic condition, the diameter of the PGA-*b*-PLL vesicles increased to 350 nm because the conformation of the protonated PLL block became a bulky random coil. Such pH-responsive nano-associates are expected to be promising candidates for drug delivery systems and smart catalysts.

pH-Responsive Polymer Brushes

Polymer brushes are ultrathin polymer layers that are tethered with one chain end to the surface of solid substrate. Polymer brushes are generally prepared by two methods: *grafting to* and

grafting from strategies. The *grafting to* method involves the introduction of pre-synthesized polymers through the physicochemical adsorption or chemical reactions. On the other hand, the development of controlled/living radical polymerization enables the facile preparation of well-defined polymer brushes based on the *grafting from* strategy, in which the polymerization is directly initiated from initiator-functionalized surfaces [14]. The surface-initiated controlled/living radical polymerization (SI-CRP) allows accurate control of brush thickness, composition, and architecture. An ATRP initiator and an RAFT agent can be easily introduced onto the surface of a substrate. For example, thiol derivatives linked with an ATRP initiator or an RAFT agent form self-assembled monolayer (SAM) on the gold surface. Also, chemisorption of organosilanes with an ATRP initiator or an RAFT agent enables the preparation of polymer brushes by ATRP or RAFT on the silicon oxide substrates including wafers, glass or quartz slides, and silica particles. A large number of reports on stimuli-responsive polymer brushes that undergo changes in surface properties in response to external stimuli such as pH and temperature have been published. Poly (dimethylaminoethyl methacrylate) (PDMAEMA) is one of the typical polymers used for the formation of pH-responsive polymer brushes. Based on the *grafting from* method, the PDMAEMA brushes were formed by the controlled polymerization from the ATRP initiator that was chemically linked on the gold substrate by the SAM fabrication method. PDMAEMA brushes were positively charged by the protonation of the amino groups under acidic conditions. As a result, the thickness of the PDMAEMA brushes increased with a decrease in pH. The neutron reflectivity measurements revealed that the PDMAEMA brushes adopted a less extended conformation under basic conditions. Furthermore, the pH responsiveness of the PDMAEMA brushes depended on the grafting density. The PDMAEMA brushes with more densely grafted chains swelled at a lower pH because their pK_a shifted as a function of grafting density. The pH-responsive protonation/deprotonation of surface-tethered polymer brushes also influenced the surface wettability. The PDMAEMA polymer brushes changed the wettability from almost complete wetting at pH < 3 to less hydrophilic at pH > 5. In contrast to the polybase brushes, the polyacid brushes such as PAAc became more hydrophilic at basic pHs than at acidic pHs. The thickness of the polyacid brushes increased with an increase in pH owing to the ionization of the polymer chains.

The oppositely charged block copolymer brushes with both positively and negatively charged groups were also prepared via SI-CRP. Under acidic and basic conditions, poly(acrylic acid)-*block*-poly(vinylpyridine) (PAAc-*b*-PVP) brush was well extended owing to the coulombic repulsion of the charged PAAc and PVP blocks. In contrast, the chains of PAA-*b*-PVP brushes shrank at a neutral pH because the net charge of PAA-*b*-PVP decreased at the neutral pH. These pH-responsive polymer brushes have many potential applications as smart nanomaterials for protein immobilization, cell adhesion, and chromatography because they can change the surface properties in response to pH.

Summary

pH-responsive polymers have been extensively studied from fundamentals to applications. The pH-responsive polymers have been synthesized by conventional radical and ionic polymerization. In addition, recent development of the controlled/living radical polymerization enables the facile synthesis of well-defined block and graft copolymers with acidic or basic groups, which are smart polymers for designing nanostructured particles or polymeric brushes as pH-responsive nanomaterials. The pH-responsive nanomaterials undergo drastic changes in their structures and properties such as size, morphology, and wettability in response to pH. Furthermore, dual stimuli-responsive nanomaterials such as temperature- and pH-responsive nanoparticles have been prepared by combining pH-responsive polymers with other stimuli-responsive polymers. Thus pH-responsive polymers are likely to become quite innovative and important smart materials in the future.

P

Related Entries

References

1. Xia J, Dubin PL (1994) Protein-polyelectrolyte complexes. In: Dubin PL, Bock J, Davies RM, Schulz DN, Thies C (eds) Macromolecular complexes in chemistry and biology. Springer, Heidelberg
2. Matyjaszewski K, Davis TP (2002) Handbook of radical polymerization. Wiley, Hoboken
3. Matyjaszewski K, Braunecker WA (2007) Controlled/living radical polymerization: features, developments, and perspectives. Prog Polym Sci 32:93–146. doi:10.1016/j.progpolymsci.2006.11.002
4. Sawai T, Yamazaki S, Ikariyama Y, Aizawa M (1991) pH-responsive swelling of the ultrafine microsphere. Macromolecules 24:2117–2118. doi:10.1021/ma00008a067
5. Beng HT, Kam CT (2008) Review on the dynamics and micro-structure of pH-responsive nano-colloidal systems. Adv Colloid Interface Sci 136:25–44. doi:10.1016/j.cic.2007.07.002
6. Oishi M, Nagasaki Y (2007) Synthesis, characterization, and biomedical applications of core-shell-type stimuli-responsive nanogels – nanogel composed of poly[2-(N, N-diethylamino)ethyl methacrylate] core and PEG tethered chains. React Funct Polym 67:1311–1329. doi:10.1016/j.reactfunctpolym.2007.07.009
7. Foss AC, Goto T, Morishita M, Peppas NA (2004) Development of acrylic-based copolymers for oral insulin delivery. Eur J Pharm Biopharm 57:163–169. doi:10.1016/S0939-6411(03)00145-0
8. Tsuchida A, Abe K (1982) Formation, structure and properties of intermacromolecular complexes. In: Interactions between macromolecules in solution and intermacromolecular complexes, vol 45, Advances in polymer science. Springer, Heidelberg, pp 1–119
9. Rodriguez-Hernandez J, Checot F, Gnanou Y, Lecommandoux S (2005) Toward 'Smart' nano-objects by self-assembly of block copolymers in solution. Prog Polym Sci 30:691–724. doi:10.1016/j.progpolymsci.2005.04.002
10. Mai Y, Eisenberg A (2012) Self-assembly of block copolymers. Chem Soc Rev 41:5969–5985. doi:10.1039/c2cs35115c
11. Moffitt M, Khogaz K, Eisenberg A (1996) Micellization of ionic block copolymers. Acc Chem Res 29:95–102. doi:10.1021/ar940080
12. Lin S, Billingham NC, Arms SP (2001) A schizophrenic water-soluble diblock copolymer. Angew Chem Int Ed 40:2328–2331. doi:10.1002/1521-3773(20010618)40:12<2328::AID-ANIE2328>3.0.CO;2-M
13. Rodriguez-Hernandez J, Lecommandoux S (2005) Reversible inside-out micellization of ph-responsive and water-soluble vesicles based on polypeptide diblock copolymers. J Am Chem Soc 127:2026–2027. doi:10.1021/ja043920g
14. Barbey R, Lavanant L, Paripovic D, Schuwer N, Sugnaux C, Tugulu S, Klok H (2009) Polymer brushes via surface-initiated controlled radical polymerization: synthesis, characterization, properties, and applications. Chem Rev 109:5437–5527. doi:10.1021/cr900045a

π-Conjugated Star-Shaped Oligomers in Organic Electronics and Photonics

Alexander L. Kanibolotsky[1,2] and
Peter J. Skabara[1]
[1]WestCHEM, Department of Pure an Applied Chemistry, University of Strathclyde, Glasgow, UK
[2]The National Academy of Sciences of Ukraine, L. M. Litvinenko Institute of Physical–Organic Chemistry and Coal Chemistry, Donetsk, Ukraine

Synonyms

Conjugated star-shaped systems; Star-burst molecules

Definition

Star-shaped conjugated oligomers are molecular systems consisting of a central unit (usually called the core), with radiating conjugated spokes (normally called the arms). The core unit often defines the geometry of a conjugated star-shaped

system, in some cases providing bulk dimensionality through intermolecular interactions in the solid phase of the material that lead to two-dimensional bulk order [1]. The arms bring in to the molecule precise electronic and optical properties of a well-defined conjugated system. The core unit might or might not provide the electronic communication between the arms leading to greatly varied photo-physical behavior between analogous materials sharing similar cores or arms. The combination of well-defined optical and electronic properties with a significant contribution from the conjugated system of the arms and the multidimensional architecture provided by the core marks star-shaped systems as popular objects of study in materials chemistry.

Introduction

A wide variety of π-functional systems are designed for applications in organic electronics and photonics. Among solution processable materials the most efficient are π-conjugated polymers. They are normally prepared by simple polymerization procedure. Polymers have exceptional film-forming properties and are amenable to cheap solution processing techniques. Careful design of the monomer allows the creation of a polymeric system with π-electronic interactions within the polymer backbone only (photonic applications) or providing an increase in dimensionality by involving interchain interactions (electronic applications). Branching of the conjugated backbone allows increasing dimensionality of interchain interactions. On the other hand, polymers suffer from their polydisperse character, end-group variation, and poor batch-to-batch reproducibility.

For several reasons, monodisperse π-functional systems with well-defined structures are excellent alternatives to conjugated polymers, particularly since they possess precise electronic characteristics with 100 % batch-to-batch reproducibility. Among them, low molecular weight systems and linear conjugated oligomers are the

most easily achievable, but their film-forming properties are significantly inferior compared to polymers. Intermolecular interactions in the solids often exhibit large intrinsic anisotropy due to the one-dimensional (1D) nature of the systems, which limits the electronic characteristics of the materials.

Star-shaped oligomers feature the best of both worlds. Being well-defined systems, they provide precise, completely reproducible electronic properties to the materials. With other factors being equal, the star oligomers are more soluble than their linear counterparts. Multidimensional architecture of the conjugated backbone, along with the propensity of the arms to be involved in π-π stacking, provides either multidimensional self-assembly or complete isolation of a conjugated molecular system in the solid. The advantages in materials properties brought by star-shaped molecular systems have to be sufficiently beneficial to compensate for other factors that are less desirable. For instance, the synthesis of star oligomers is much more complicated and usually includes numerous steps of repetitive coupling procedures. There are two main types of synthetic strategies that can be applied: divergent and convergent approaches. The divergent approach features repetitive coupling of monomeric units and benefits from the simplicity of the building block used in the synthesis, but the method suffers from difficulties in purification in the latter steps, especially if the coupling procedure on each arm is not high yielding. In the convergent strategy, the precursor arms are prepared separately and coupled to the core structure in the final step. The easy purification from partially coupled by-products and the possibility to create a library of arm precursor building blocks for the synthesis of various star-shaped systems makes the convergent approach the preferable route. A special type of convergent strategy involves the construction of the core structure in the final step of the synthesis, using a building block with arms attached to the core precursor. The various approaches in synthesis and the advantages in the properties of star oligomers have been reviewed thoroughly [2, 3].

Increasing Dimensionality of the Conjugated Backbone

The dimensionality of star oligomers can be related to the molecular architecture of the conjugated system (molecular dimensionality) or to the way the molecules interact with each other in the solid (bulk dimensionality) [1]. One of the reasons to synthesize the star oligomers is to investigate the molecular properties of a system with branched conjugated frameworks and increased molecular dimensionality. One of the most suitable objects for this task for photonics applications are oligo(9,9-dialkylfluorene) star-shaped systems since the alkyl substituents of the arms are directed orthogonally to the plane of the aromatic system and contribute to an amorphous morphology with suppressed aggregation in solutions and in the solid state. Therefore, the properties of the material depend mainly on the electronic properties of the molecular conjugated system. In contrast to simple trigonal 1 [4–6] and hexagonal 2 [7] benzene central units, the truxene core structure 3 creates additional steric hindrance towards aggregation and extends the conjugation of the arms by one fluorene unit, providing highly

efficient blue fluorescent oligofluorene-truxene star oligomers 4 (n = 1−4) [8] (Fig. 1).

The star oligomers 4 (n = 1–4) were studied by Raman spectroscopy and DFT calculations [9]. Electrogenerated chemiluminescence (ECL) by ion annihilation of the oligomers demonstrated blue ECL emissions at the same wavelengths as the fluorescence emissions [10]. The effect of the incorporation of 2,1,3-benzothiadiazole (BT) acceptor units into trigonal star oligofluorene-truxene systems has been studied, in which the BT molecule is positioned at every possible location within the oligofluorene arms [11]. These systems were found to be efficient green 5 (n = 4) and green/yellow 5 (n = 0-3) emitters. The optical properties of the oligofluorene-BT-truxene systems revealed pairwise correspondence of 5 (n = 0) to 5 (n = 3) and 5 (n = 1) to 5 (n = 2) with oligomer 5 (n = 4) being a unique member of the series. Star oligomer 2 (n = 1) with a hexagonal benzene core 2 showed an example of electronic communication between the arms in the oxidized state, by means of through-space toroidal hole delocalization due to sufficient π-π overlap between the proximal part of the adjacent arms.
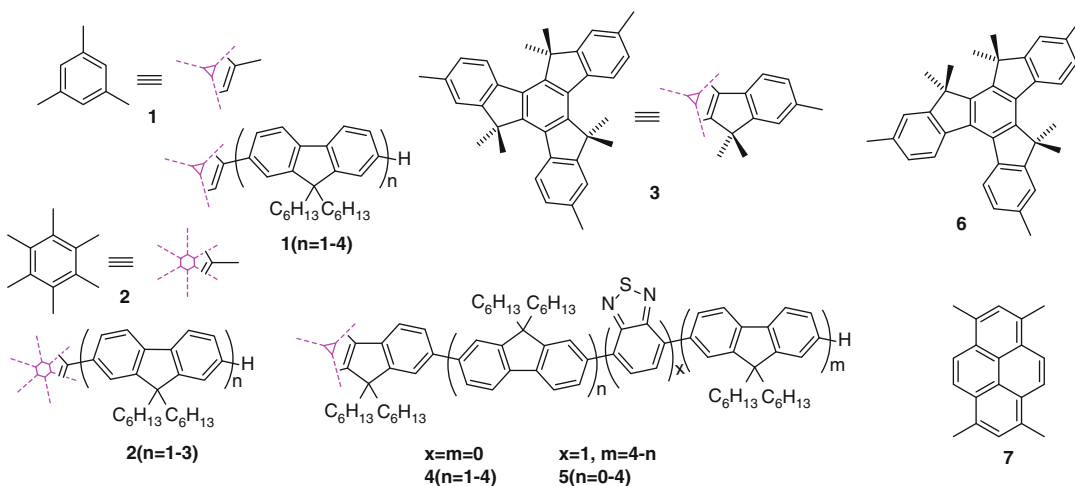
π-Conjugated Star-Shaped Oligomers in Organic Electronics and Photonics, Fig. 1 Examples of core structures and molecular architectures of selected star oligofluorenes. The three- and sixfold rotational axes are depicted by small equiangular *triangles* and *hexagons*,

respectively, with three and six *dashed lines* (*magenta symbol*), radiating from the core and representing the division of the molecules on the parts which are symmetry related (only one arm is shown for simplicity and conciseness)

Isotruxene **6** [12, 13] and pyrene **7** [14, 15] are examples of core units that provide electronic conjugation between the arms, which leads to more immediate saturation of optical properties as a function of an increase in the length of the arms. A meta-linkage between the arms in the trigonal benzene system **1** and star oligomers **4** (**n** = **1−4**) restricts electronic communication across the molecules in the ground state. However, it was shown by time-dependent density functional theory (TD-DFT) calculations [5] and fluorescence depolarization experiments [16] that the redistribution of excitation between the arms is possible in these systems due to a structural relaxation of the excited state. The exciton localization on one branch of the star oligomer is the consequence of Jahn-Teller splitting of an initially degenerate excited state, and the degeneracy provided by the threefold symmetry (C_3) of the conjugated system. This highlights the importance of the symmetry of star-shaped systems, which is defined by its core [2]. The symmetry also defines the leading multipole of a star oligomer with the charge transfer component. Molecular systems with a center of symmetry cannot have any multipole of order 2^{2n+1} (e.g., dipole or octupole), but normally possess a quadrupole as a leading multipole, whereas the leading term of multipole expansion for tetrahedral systems is an octupole [17]. The terms of multipole expansion are important features of star-shaped systems with push-pull

components. They control their nonlinear optical properties and two-photon absorption [18–20] and define electrostatic intermolecular interactions which might affect the bulk dimensionality of the material (*vide infra*).

From the Dimensionality of a Molecular Architecture to the Dimensionality of Intermolecular Interactions

The structure of the core defines the dimensionality of a star-shaped oligomer or the way the arms radiate from the core, which was shown to be removed to have an effect on the photophysics and electrochemical properties of the conjugated system. Molecular dimensionality on the other hand, along with the nature of the arm, defines the way the molecules interact with each other in the solid state. As was mentioned before, the oligofluorene arms usually prevent aggregation and intermolecular interactions in the condensed phase. Nevertheless, an extended core structure with a proper arrangement of electron-deficient and electron-rich aromatic units within the core might promote intermolecular interactions and increase bulk dimensionality. Thus, 1,4-dioxo-2,3,5,6-tetraphenyl-pyrrolo[3,4-c]pyrrole (DPP) has been used as a core structure for constructing a star-shaped system with four oligofluorene arms **8** [21] (Fig. 2), along with
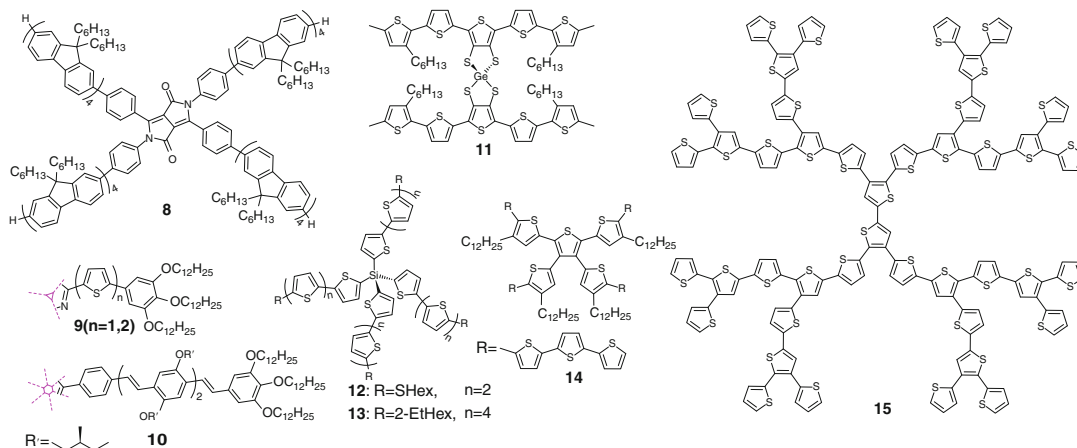
π-Conjugated Star-Shaped Oligomers in Organic Electronics and Photonics, Fig. 2 Examples of star-shaped molecular architectures that provide increased bulk dimensionality
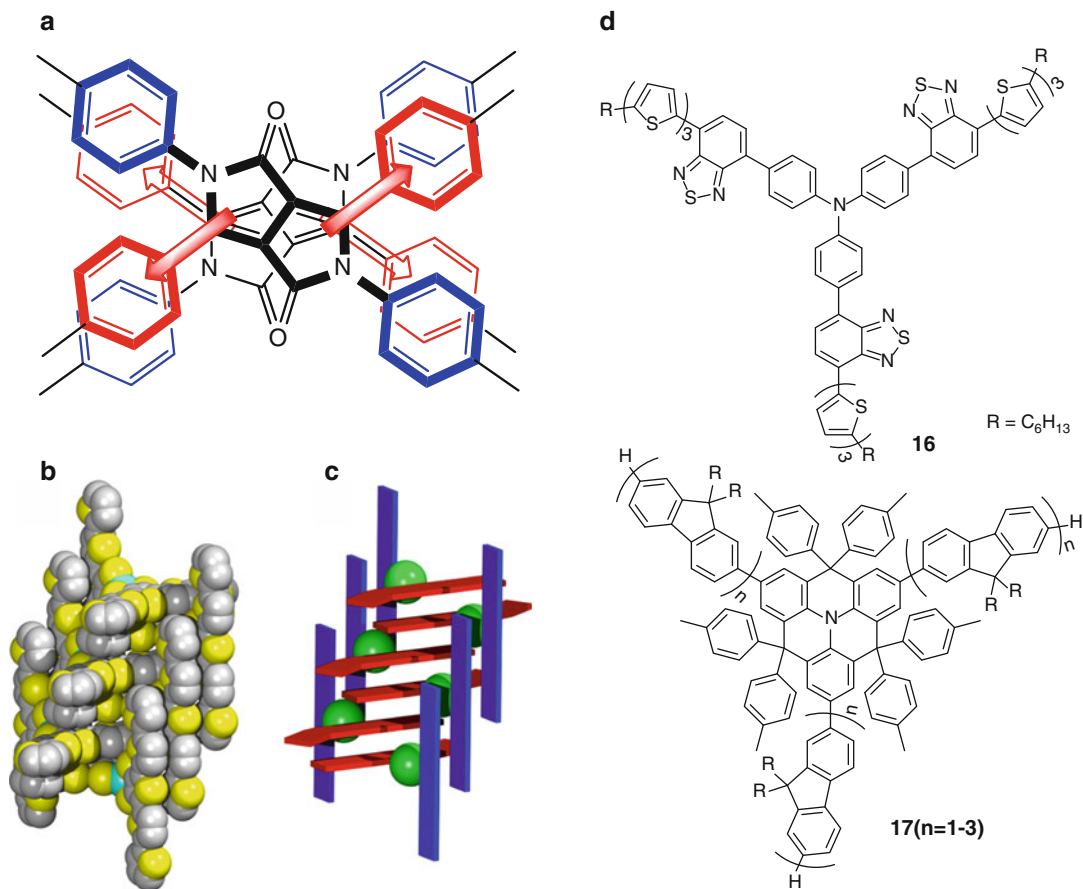
π-Conjugated Star-Shaped Oligomers in Organic Electronics and Photonics, Fig. 3 (**a**) Aggregation of star oligomer **8** due to its extended tetraphenyl DPP core; (**b**) self-assembly of oligomer **11** in the crystal (alkyl substituents omitted for clarity); (**c**) schematic representation of 2D-stacking interactions for oligomer 11; (**d**) selected structures (**16** and **17**) of star oligomers with amine cores for photovoltaic and OLED applications

two linear analogues with conjugated and nonconjugated connections between two oligofluorene arms through the core. Efficient energy transfer has been observed between the arms and the core in these systems. The quadrupolar star oligomer **8** was found to form aggregates not only in the solid but also in hexane solutions, due to the alternating positions of phenylene spacers and the 2D molecular architecture of the star oligomer (Fig. 3a). Another example of a 2D molecular system leading to 1D columnar intermolecular interactions was demonstrated recently. The octupolar trigonal D-A star oligomers **9** (**n** = **1**, **2**) based on 2,4,6-tris(thiophene-2-yl)-1,3,5-triazines were shown to self-assemble in a 1D columnar nanostructure [22]. Not only are the

quadrupolar and octupolar D-A star-shaped systems able to form 1D column aggregates but the self-assembly of the oligomers might be attributed solely to the 2D molecular architecture. A hexagonal star-shaped system with a hexaphenylbenzene core, oligophenylenevinylene (OPV) arms (**10**), and possessing chiral side chain alkyl substituents was found to form chiral columnar assemblies [23].

Cruciform star oligomers with a D_{2d} symmetric 9,9-spirobifluorene core structure were believed to restrict crystallization, forming an isomorphous glassy state, and were considered for application as highly emissive materials [24, 25]. However, the star oligothiophene **11** with the same symmetry core – 2,2'-spirobi[thieno[3,4-d][1, 3]dithiagermole] – was found

to self-assemble in the crystal structure to produce stacking interactions in two mutually orthogonal directions (Fig. 3b–c) [26]. In this case, the 3D molecular architecture of the cruciform oligothiophene yielded 2D bulk dimensionality in the bulk material.

A key goal in organic electronics for efficient charge transport is the realization of 3D intermolecular interactions in the condensed phase. It is especially important for donor materials in bulk heterojunction solar cells (BHJSC), where the bulk dimensionality of the donor phase should be matched with the nature of fullerene phases, which are popular acceptor materials in such devices. Intuitively, 3D molecular architecture might contribute to an increase in bulk dimensionality beyond two dimensions. The tetrahedral star oligomers **12–13** [27–29], the X-shaped system **14** [30], and the thiophene-based dendrimer **15** [31] are examples of such materials. Due to the branched nature of the latter conjugated system, **15** has much greater solubility compared to linear oligomers which require solubilizing alkyl chains.

Applications

The applications of star oligomers in electronics are defined by the electronic properties of the molecular conjugated system in combination with the propensity of the material to provide increased bulk dimensionality. A high bulk multidimensional character in star-shaped conjugated systems favors the fabrication of organic field effect transistors (OFET) without the need for molecular alignment and also increases the performance of BHJSCs. Thus, the wide bandgap 3D donor materials **12–15** would seem to be excellent candidates for photovoltaic applications from a structural perspective, but not for light harvesting. Dendrimer **15**, with an absorption onset at 600 nm, gave a power conversion efficiency (PCE) of 1.65 % in a BHJSC with $PC_{61}BM$ as an acceptor [31]. However, the 2D intermolecular interactions in the bulk of Ge-cruciform **11**, with an onset of absorption at

502 nm, appears to be more efficient providing a PCE of 2.26 % in a BHJSC with $PC_{71}BM$ as the acceptor [26]. The star oligomer **16** features benefits from both its star-shaped architecture and low bandgap of the donor material, providing an increase in PCE up to 4.3 % in a BHJSC containing $PC_{71}BM$ [32].

In contrast to the above, photonic applications featuring strong emitters require semiconductors with isolated molecules in the solid and overall zero bulk dimensionality. Among various photonic devices, organic lasers have found numerous applications in spectroscopy, data communication technology, and chemical sensing [33]. Star oligomers are ideal materials for optically pumped lasing media. Low optical losses of 2.3 cm^{-1} exhibited by a neat film of the star quaterfluorene **4** (**n = 4**) in amplified spontaneous emission experiments (ASE) point to an isotropic morphology in the film [34]. The related star oligomer **1** (**n = 4**) possessing a trigonal benzene core has shown a higher loss coefficient of 3.9 cm^{-1}, which is a strong indication of the contribution of the truxene core into an isotropic morphology of **4** (**n = 4**) in the solid state. The star terfluorene **4** (**n = 3**) demonstrated wavelength tunability in distributed feedback lasers, with a wide spectral range of 51 nm [35]. The compatibility of the oligofluorene-truxene series with a saturated polymer matrix allowed for oligomer **4** (**n = 3−4**) to be micro-patterned in a photocurable blend with the UV-transparent photoresist – 1,4-cyclohexanedimethanol divinyl ether (CHDV) – by direct laser writing [36], inkjet printing [37, 38], and dip pen nanolithography (DPN) [39]. The same polymer matrix and **4** (**n = 3**) were used to fabricate durable encapsulated flexible DFB lasers [40] (Fig. 4) and a free-standing emissive membrane [41].

For light-emitting diodes (LEDs), it is not only photoluminescence that is important but the mobility of the materials. The standard class of hole-conducting materials are triphenylamine-centered star oligomers. The star oligomer **17** (**n = 3**) possessing a planar triphenylamine core showed a current efficiency of 3.83 cd A^{-1} with a maximum luminance of 732 cd m^{-2} and turn on
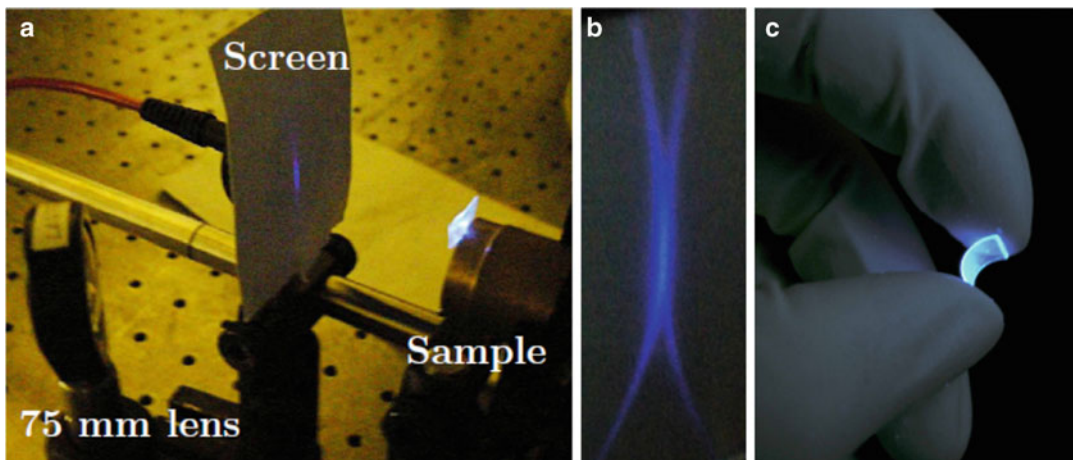
π-Conjugated Star-Shaped Oligomers in Organic Electronics and Photonics, Fig. 4 (**a**) A DFB flexible laser pumped with a focused pump spot; (**b**) image of the beam profile on a screen; (**c**) a laser demonstrating its flexibility and fluorescence under UV illumination (From ref [40])

voltage of 3.4 V [42]. The star oligofluorenes **2** (**n** = **2**−**4**) with a hexagonal benzene core exhibited good performance in LEDs, owing to their hole mobilities [7]. They demonstrated a current efficiency of 5.4 cd A^{-1} and maximum luminance of 1,962 cd m^{-2} for **2** (**n** = **4**), although the turn on voltage (6.9 V) was much higher than in the previous case.

Summary

Star-shaped oligomers feature some of the best attributes of polymeric materials, such as good solubility and film-forming properties. However, in contrast to polymers, they have well-defined structure and possess complete synthetic reproducibility and precise electronic characteristics. They are different from linear analogues through a series of features, including higher levels of molecular dimensionality, intramolecular electronic communication between arms, peculiarities of intramolecular charge and energy transfer, and symmetry-related effects on the electronic structure. The molecular dimensionality of star oligomers, along with the nature of the arms, affects their propensity to self-assemble and this defines the bulk dimensionality of the materials. The design of multidimensional architectures from conjugated systems often brings surprising results, such that the expansion of the molecular geometry in star oligomers might lead to completely different materials, even from structures that share the same symmetry of the core unit. A combination of the versatility of molecular design, which provides well-defined conjugated systems, with reproducible electronic properties, better solubility, and film-forming properties compared to linear systems, has made star oligomers an important family of organic materials in the quest for new properties and improved device performance.

Related Entries

▶ Conjugated Dendrimers
▶ Dendrimer-Like Star Branched Polymers
▶ Hyperbranched Conjugated Polymers
▶ Synthesis of Star Polymers

References

1. Skabara PJ, Arlin J-B, Geerts YH (2013) Close encounters of the 3D kind exploiting high dimensionality in molecular semiconductors. Adv Mater 25:1948–1954. doi:10.1002/adma.201200862
2. Kanibolotsky AL, Perepichka IF, Skabara PJ (2010) Star-shaped pi-conjugated oligomers and their

applications in organic electronics and photonics. Chem Soc Rev 39:2695–2728. doi:10.1039/b918154g

3. Roncali J, Leriche P, Cravino A (2007) From one- to three-dimensional organic semiconductors: in search of the organic silicon? Adv Mater 19:2045–2060. doi:10.1002/adma.200700135

4. Zhou XH, Yan JC, Pei J (2003) Synthesis and relationships between the structures and properties of monodisperse star-shaped oligofluorenes. Org Lett 5:3543–3546. doi:10.1021/ol035461e

5. Montgomery NA, Denis J-C, Schumacher S, Ruseckas A, Skabara PJ, Kanibolotsky A, Paterson MJ, Galbraith I, Turnbull GA, Samuel IDW (2011) Optical excitations in star-shaped fluorene molecules. J Phys Chem A 115:2913–2919. doi:10.1021/jp1109042

6. Tsiminis G, Montgomery NA, Kanibolotsky AL, Ruseckas A, Perepichka IF, Skabara PJ, Turnbull GA, Samuel IDW (2012) Laser characteristics of a family of benzene-cored star-shaped oligofluorenes. Semicond Sci Technol 27:094005. doi:10.1088/0268-1242/27/9/094005

7. Zou Y, Zou J, Ye T, Li H, Yang C, Wu H, Ma D, Qin J, Cao Y (2013) Unexpected propeller-like hexakis(fluoren-2-yl)benzene cores for Six-Arm star-shaped oligofluorenes: highly efficient deep-blue fluorescent emitters and good hole-transporting materials. Adv Funct Mater 23:1781–1788. doi:10.1002/adfm.201202286

8. Kanibolotsky AL, Berridge R, Skabara PJ, Perepichka IF, Bradley DDC, Koeberg M (2004) Synthesis and properties of monodisperse oligofluorene-functionalized truxenes: highly fluorescent star-shaped architectures. J Am Chem Soc 126:13695–13702. doi:10.1021/ja039228n

9. Moreno Oliva M, Casado J, Lopez Navarrete JT, Berridge R, Skabara PJ, Kanibolotsky AL, Perepichka IF (2007) Electronic and molecular structures of trigonal truxene-core systems conjugated to peripheral fluorene branches. Spectroscopic and theoretical study. J Phys Chem B 111:4026–4035. doi:10.1021/jp065271w

10. Omer KM, Kanibolotsky AL, Skabara PJ, Perepichka IF, Bard AJ (2007) Electrochemistry, spectroscopy, and electrogenerated chemiluminescence of some star-shaped truxene-oligofluorene compounds. J Phys Chem B 111:6612–6619. doi:10.1021/jp070765u

11. Belton CR, Kanibolotsky AL, Kirkpatrick J, Orofino C, Elmasly SET, Stavrinou PN, Skabara PJ, Bradley DDC (2013) Location, location, location - strategic positioning of 2,1,3-benzothiadiazole units within trigonal quaterfluorene-truxene star-shaped structures. Adv Funct Mater 23:2792–2804. doi:10.1002/adfm.201202644

12. Yang J-S, Lee Y-R, Yan J-L, Lu M-C (2006) Synthesis and properties of a fluorene-capped isotruxene: a new unsymmetrical star-shaped pi-system. Org Lett 8:5813–5816. doi:10.1021/ol062408s

13. Yang J-S, Huang H-H, Ho J-H (2008) Electronic properties of star-shaped oligofluorenes containing an isotruxene core: interplay of Para and Ortho conjugation effects in phenylene-based pi systems. J Phys Chem B 112:8871–8878. doi:10.1021/jp800448p

14. Liu F, Lai W-Y, Tang C, Wu H-B, Chen Q-Q, Peng B, Wei W, Huang W, Cao Y (2008) Synthesis and characterization of pyrene-centered starburst oligofluorenes. Macromol Rapid Commun 29:659–664. doi:10.1002/marc.200700847

15. Xia R, Lai W-Y, Levermore PA, Huang W, Bradley DDC (2009) Low-threshold distributed-feedback lasers based on pyrene-cored starburst molecules with 1,3,6,8-attached oligo(9,9-dialkylfluorene) arms. Adv Funct Mater 19:2844–2850. doi:10.1002/adfm.200900503

16. Montgomery NA, Hedley GJ, Ruseckas A, Denis J-C, Schumacher S, Kanibolotsky AL, Skabara PJ, Galbraith I, Turnbull GA, Samuel IDW (2012) Dynamics of fluorescence depolarisation in star-shaped oligofluorene-truxene molecules. Phys Chem Chem Phys 14:9176–9184. doi:10.1039/c2cp24141b

17. Buckingham AD (1959) Molecular quadrupole moments. Quart Rev Chem Soc 13:183–214. doi:10.1039/QR9591300183

18. Lee W-H, Lee H, Kim J-A, Choi J-H, Cho M, Jeon S-J, Cho BR (2001) Two-photon absorption and nonlinear optical properties of octupolar molecules. J Am Chem Soc 123:10658–10667. doi:10.1021/ja004226d

19. Katan C, Terenziani F, Mongin O, Werts MHV, Porrès L, Pons T, Mertz J, Tretiak S, Blanchard-Desce M (2005) Effects of (multi)branching of dipolar chromophores on photophysical properties and two-photon absorption. J Phys Chem A 109:3024–3037. doi:10.1021/jp044193e

20. Bhaskar A, Ramakrishna G, Lu Z, Twieg R, Hales JM, Hagan DJ, Van Stryland E, Goodson T (2006) Investigation of two-photon absorption properties in branched alkene and alkyne chromophores. J Am Chem Soc 128:11840–11849. doi:10.1021/ja060630m

21. Kanibolotsky AL, Vilela F, Forgie JC, Elmasly SET, Skabara PJ, Zhang K, Tieke B, McGurk J, Belton CR, Stavrinou PN, Bradley DDC (2011) Well-defined and monodisperse linear and star-shaped quaterfluorene-DPP molecules: the significance of conjugation and dimensionality. Adv Mater 23:2093–2097. doi:10.1002/adma.201100308

22. Yasuda T, Shimizu T, Liu F, Ungar G, Kato T (2011) Electro-functional octupolar pi-conjugated columnar liquid crystals. J Am Chem Soc 133:13437–13444. doi:10.1021/ja2035255

23. Tomović Ž, van Dongen J, George SJ, Xu H, Pisula W, Leclère P, Smulders MMJ, De Feyter S, Meijer EW, Schenning APHJ (2007) Star-shaped oligo(p-phenylenevinylene) substituted hexaarylbenzene: purity, stability, and chiral self-assembly. J Am Chem Soc 129:16190–16196. doi:10.1021/ja0765417

P

24. Pudzich R, Fuhrmann-Lieker T, Salbeck J (2006) Spiro compounds for organic electroluminescence and related applications. In: Emissive materials nanomaterials, vol 199. Springer, Berlin/Heidelberg, pp 83–142

25. Saragi TPI, Spehr T, Siebert A, Fuhrmann-Lieker T, Salbeck J (2007) Spiro compounds for organic opto-electronics. Chem Rev 107:1011–1065. doi:10.1021/cr0501341

26. Wright IA, Kanibolotsky AL, Cameron J, Tuttle T, Skabara PJ, Coles SJ, Howells CT, Thomson SAJ, Gambino S, Samuel IDW (2012) Oligothiophene cruciform with a germanium spiro center: a promising material for organic photovoltaics. Angew Chem Int Ed 51:4562–4567. doi:10.1002/anie.201109074

27. Roncali J, Frère P, Blanchard P, de Bettignies R, Turbiez M, Roquet S, Leriche P, Nicolas Y (2006) Molecular and supramolecular engineering of pi-conjugated systems for photovoltaic conversion. Thin Solid Films 511:567–575. doi:10.1016/j.tsf.2005.12.014

28. Roquet S, de Bettignies R, Leriche P, Cravino A, Roncali J (2006) Three-dimensional tetra(oligothienyl)silanes as donor material for organic solar cells. J Mater Chem 16:3040–3045. doi:10.1039/b604261a

29. Kleymyuk EA, Troshin PA, Khakina EA, Luponosov YN, Moskvin YL, Peregudova SM, Babenko SD, Meyer-Friedrichsen T, Ponomarenko SA (2010) 3D quater- and quinquethiophenesilanes as promising electron-donor materials for BHJ photovoltaic cells and photodetectors. Energy Environ Sci 3:1941–1948. doi:10.1039/c0ee00174k

30. Shang H, Fan H, Liu Y, Hu W, Li Y, Zhan X (2011) New X-shaped oligothiophenes for solution-processed solar cells. J Mater Chem 21:9667–9673. doi:10.1039/C1JM10814J

31. Ma C-Q, Fonrodona M, Schikora MC, Wienk MM, Janssen RAJ, Bäuerle P (2008) Solution-processed bulk-heterojunction solar cells based on monodisperse dendritic oligothiophenes. Adv Funct Mater 18:3323–3331. doi:10.1002/adfm.200800584

32. Shang H, Fan H, Liu Y, Hu W, Li Y, Zhan X (2011) A solution-processable star-shaped molecule for high-performance organic solar cells. Adv Mater 23:1554–1557. doi:10.1002/adma.201004445

33. Samuel IDW, Turnbull GA (2007) Organic semiconductor lasers. Chem Rev 107:1272–1295. doi:10.1021/cr050152i

34. Tsiminis G, Wang Y, Shaw PE, Kanibolotsky AL, Perepichka IF, Dawson MD, Skabara PJ, Turnbull GA, Samuel IDW (2009) Low-threshold organic laser based on an oligofluorene truxene with low optical losses. Appl Phys Lett 94:243–304. doi:10.1063/1.3152782

35. Wang Y, Tsiminis G, Yang Y, Ruseckas A, Kanibolotsky AL, Perepichka IF, Skabara PJ, Turnbull GA, Samuel IDW (2010) Broadly tunable deep blue laser based on a star-shaped oligofluorene truxene. Synth Met 160:1397–1400. doi:10.1016/j.synthmet.2010.04.016

36. Kuehne AJC, Elfstrom D, Mackintosh AR, Kanibolotsky AL, Guilhabert B, Gu E, Perepichka IF, Skabara PJ, Dawson MD, Pethrick RA (2009) Direct laser writing of nanosized oligofluorene truxenes in UV-transparent photoresist microstructures. Adv Mater 21:781–785. doi:10.1002/adma.200802656

37. Wu M, Gong Z, Kuehne AJC, Kanibolotsky AL, Chen YJ, Perepichka IF, Mackintosh AR, Gu E, Skabara PJ, Pethrick RA, Dawson MD (2009) Hybrid GaN/organic microstructured light-emitting devices via ink-jet printing. Opt Express 17:16436–16443

38. Wu M, Gu E, Zarowna A, Kanibolotsky AL, Kuehne AJC, Mackintosh AR, Edwards PR, Rolinski OJ, Perepichka IF, Skabara PJ, Martin RW, Pethrick RA, Birch DJS, Dawson MD (2009) Star-shaped oligofluorene nanostructured blend materials: controlled micro-patterning and physical characteristics. Appl Phys A: Mater Sci Process 97:119–123. doi:10.1007/s00339-009-5308-x

39. Hernandez-Santana A, Mackintosh AR, Guilhabert B, Kanibolotsky AL, Dawson MD, Skabara PJ, Graham D (2011) Dip-pen nanolithography of nanostructured oligofluorene truxenes in a photo-curable host matrix. J Mater Chem 21:14209–14212. doi:10.1039/C1JM11378J

40. Herrnsdorf J, Guilhabert B, Chen Y, Kanibolotsky AL, Mackintosh AR, Pethrick RA, Skabara PJ, Gu E, Laurand N, Dawson MD (2010) Flexible blue-emitting encapsulated organic semiconductor DFB laser. Opt Express 18:25535–25545. doi:10.1364/oe.18.025535

41. Guilhabert B, Laurand N, Herrnsdorf J, Chen Y, Mackintosh AR, Kanibolotsky AL, Gu E, Skabara PJ, Pethrick RA, Dawson MD (2010) Amplified spontaneous emission in free-standing membranes incorporating star-shaped monodisperse pi-conjugated truxene oligomers. J Optics 12:035503. doi:10.1088/2040-8978/12/3/035503

42. Liu C, Li Y, Zhang Y, Yang C, Wu H, Qin J, Cao Y (2012) Solution-processed, undoped, deep-blue organic light-emitting diodes based on starburst oligofluorenes with a planar triphenylamine core. Chemistry – A European Journal 18:6928–6934. doi:10.1002/chem.201200062

Pickering Emulsion Polymerization

Stefan A. F. Bon
Department of Chemistry, University of Warwick, Coventry, UK

Definition

A Pickering emulsion polymerization is an emulsion polymerization process whereby part of the

colloidal stability of the produced polymer dispersion is warranted by small solid particles that are adhered to the surface of the polymer latex particles. In essence, the nanoparticles serve as Pickering stabilizers, replacing and taking the role of traditional molecular surfactants throughout, and after, the emulsion polymerization process.

Note that Pickering emulsion polymerization is *not* the polymerization of emulsion droplets stabilized by particles. The polymerization of armored emulsion droplets most likely is either a Pickering suspension polymerization or a Pickering mini-emulsion polymerization. For an in-depth overview on Pickering polymerization techniques, the reader is referred to a review by Bon [1].

Historical Context

Pickering emulsion polymerization makes use of the phenomenon of Pickering stabilization, that is, the ability of solid particles to adhere to soft deformable interfaces. An example of a Pickering emulsion is oil droplets dispersed in water and armored with a layer of inorganic particles at their surface.

The Phenomenon of Pickering Stabilization

The use of Pickering stabilization can be traced back to patents on (froth) flotation in the eighteenth century, but was named after Spencer Umfreville Pickering for his seminal work on emulsions stabilized by solid particles used as insoluble emulsifiers [2]. The driving force for particles to adhere to the surface of emulsion droplets is the reduction in the overall interfacial free energy. When one compares the situation where the particles are dispersed in either the oil or water phase, leaving the liquid-liquid interface unperturbed with the scenario in which the particles have positioned themselves at the interface, hereby creating an effective area where direct contact between oil and water is avoided, often a deep well in the overall free energy profile is achieved which in essence irreversibly locks the particles at the interface.

A simple continuous model to describe Pickering stabilization for the scenario of a spherical particle adhered to an air-liquid interface was reported by Pieranski [3]. Particles that have the ability to adhere to the surface of emulsion droplets or droplets are also referred to as Pickering stabilizers.

Pickering Suspension Polymerization

The application of Pickering stabilizers in heterogeneous emulsion-based polymerization techniques finds its way back to the 1930s where, for example, Röhm and Trommsdorff used inorganic particles of talc, barium sulfate, aluminum oxide, kaolin clay, and others in the suspension polymerization of a variety of monomers [4]. The underlying reason why solid particles were explored as stabilizers in suspension polymerization was to suppress the tendency of the polymerizing emulsion droplets to stick to one another and thus to aggregate and fuse. This irreversible droplet collision and coalescence during the sticky phase in suspension polymerization needs to be avoided to warrant successful production of polymer beads. The role of the Pickering stabilizers at the surface of the polymerizing droplets/beads is to provide a protective barrier. However, the use of solid particles as emulsifiers led to the production of opaque beads. The Pickering stabilizers were therefore seen as contaminants, which were difficult to remove, which was a substantial disadvantage of the Pickering suspension polymerization process. The opportunity to fabricate composite polymer particles that were armored with a layer of solid, potentially functional, small particles was mostly overlooked. Reports on assembling particles onto emulsion droplets in which the resulting so-called supracolloidal structures themselves were seen as useful, for example, in the form of semipermeable capsules which were coined colloidosomes [5, 6], triggered renewed interest in using Pickering stabilizers in heterogeneous emulsion-based polymerization techniques [7].

Pickering Mini-emulsion Polymerization

The idea of miniaturizing Pickering suspension polymerization was first brought forward by

P

Landfester and coworkers in the mini-emulsion polymerization of styrene and 4-vinylpyridine in the presence of silica nanoparticles, which were added after the sonication step that generated the mini-emulsion monomer droplets [8]. This raises the question of whether or not the silica particles adhere to the emulsion droplets prior, or throughout, the polymerization reaction. Bon and coworkers were the first to generate mini-emulsion droplets in the presence of Laponite clay nano-disks, which were approximately 25 nm in diameter and 1 nm in height and served as Pickering stabilizers [9]. They reported the first detailed mechanistic investigation of the Pickering mini-emulsion polymerization process [10]. They discussed the packing and partitioning of the clay disks onto the surface of the polymer particles, hereby showing that for a certain window of ratios of Laponite to monomer the average particle size of the armored nanocomposite latex particles could be predicted. They also discussed the overall polymerization kinetics by monitoring monomer conversion versus time, clearly showing increased rates in Pickering mini-emulsion polymerizations with smaller droplets as a result of compartmentalization. One striking observation was a distinct retardation in the rate of polymerization up to intermediate monomer conversion, which became more pronounced for Pickering mini-emulsion polymerizations with smaller droplet size distributions. Clearly, the presence of clay disks at the surface of the droplets/latex particles influenced polymerization kinetics.

Since then, a wide range of nanoparticles have been explored in Pickering mini-emulsion polymerizations mainly to fabricate armored nanocomposite polymer latexes. The Pickering stabilizers used include clay disks, iron oxide, cellulose nano-whiskers, silica nanoparticles, and graphene oxide sheets.

The Emergence of Pickering Emulsion Polymerization

Adding nanoparticles to influence the emulsion polymerization process and to fabricate hybrid nanocomposite polymer colloids is a concept that dates back several decades and predates the development of Pickering mini-emulsion polymerization. The synthesis of nanocomposite latexes whereby inorganic nanoparticles were encapsulated and incorporated throughout the polymer matrix of the latex particles (raspberry morphology) was reported in a 1980 patent by Solc nee Hajna [11]. No referral to Pickering stabilization is made in these emulsion polymerizations, and the obtained morphologies of the nanocomposite latex particles are distinctly different, that is, raspberry morphologies instead of polymer latexes armored with a layer of nanoparticles. Long and coworkers described the emulsifier-free emulsion polymerization of methyl methacrylate in the presence of silica and alumina nanosols [12]. Whereas the successful encapsulation of the alumina nanosol was accomplished, the authors stated that the silica experiments did not lead to the desired raspberry morphology. However, in retrospect but not noticed and recognized by the authors, the emulsion polymerizations carried out in the presence of the silica sol could have been one of the first examples of a Pickering emulsion polymerization. Armes et al. and Wang and coworkers described that the emulsion copolymerization of styrene and 4-vinylpyridine in the presence of a waterborne nano-sized silica sol led to latex particles armored with a layer of silica nanoparticles [13, 14]. Wu and coworkers prepared poly (methyl methacrylate) latexes armored with silica particles by using a cationic auxiliary comonomer to promote attraction between the negatively charged silica particles and the polymer latex particles [15]. Amphiphilic Janus nanoparticles were used as stabilizers in emulsion polymerization by Walther and coworkers [16]. Results showed a clear dependence on the particle size distribution as a function of the amounts of Janus nanoparticles used. The above studies led to a better understanding on what the influence of nanoparticles on the mechanism of emulsion polymerization is, and from these and other earlier works, Pickering emulsion polymerization as heterogeneous polymerization technique emerged.
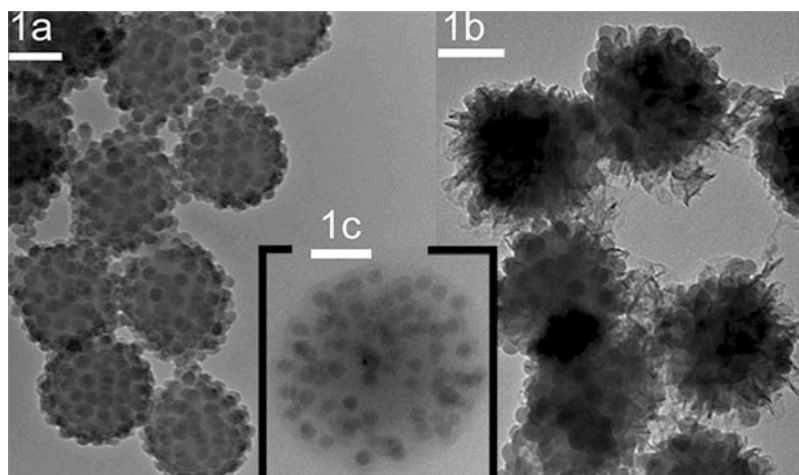
Pickering Emulsion Polymerization, Fig. 1 TEM images (scale bar = 100 nm) of (**a**) poly(methyl methacrylate) latex armored with silica nanoparticles obtained by Pickering emulsion polymerization. Multilayered nanocomposite polymer colloids with (**b**) a "hairy" outer layer of poly(acrylonitrile) and (**c**) a soft shell of poly(*n*-butyl acrylate). Reprinted with permission from Ref. [17]. ©2008 American Chemical Society
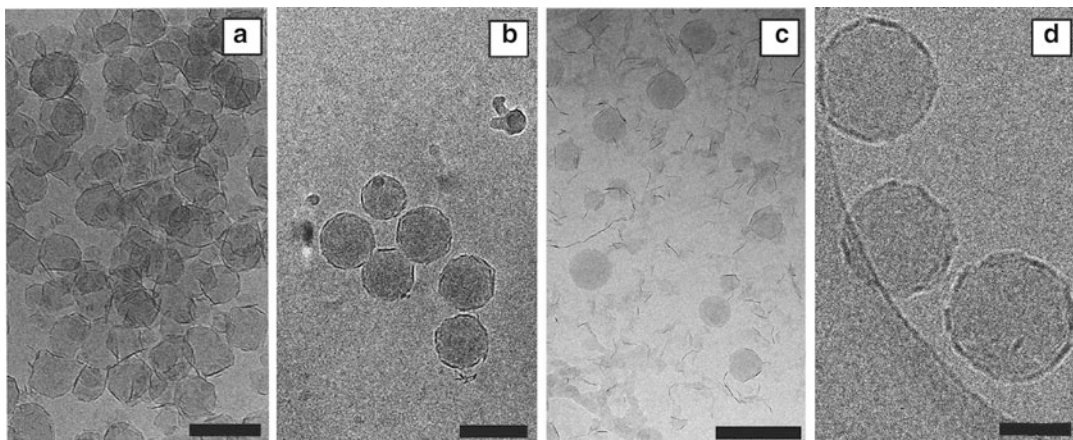
Pickering Emulsion Polymerization: A Mechanistic View

Bon and coworkers [17] and Armes et al. [18] reported independently in 2008 on Pickering emulsion polymerizations using silica sols as a Pickering stabilizer and established Pickering emulsion polymerization as a polymerization technique. Whereas in the work of Armes a special organically modified grade of silica sol was used, the work of Bon showed that this was not essential, hereby successfully demonstrating the Pickering emulsion polymerization of methyl and ethyl methacrylate up to 45 wt% overall solids under batch conditions (see Fig. 1), in the absence of auxiliary monomers, molecular surfactants, or cationic initiators.

Whereas more reports on Pickering emulsion polymerization start to emerge, a detailed mechanistic understanding on how Pickering emulsion polymerization works and how it differs from the conventional emulsion polymerization still has to be developed. A current understanding is as follows and will be described briefly in two stages, being (1) particle nucleation and (2) particle growth.

Particle Nucleation in Pickering Emulsion Polymerization

A good starting point is to compare particle formation in Pickering emulsion polymerization with nucleation in soap-free emulsion polymerization. In the latter particle formation occurs through homogeneous nucleation often with limited coagulation or assembly of primary particles. The mechanistic model for this is known as the Hansen-Ugelstad-Fitch-Tsai (HUFT) model. Initiation of polymerization in the water phase by reaction of a radical species, for example, a sulfate radical, with a monomer dissolved in the water phase followed by successive propagation steps leads to the formation of a polymer chain that becomes amphiphilic first and upon further growth will collapse on itself to form a primary latex particle. Swelling (with monomer) and further chain growth of these primary loci of polymerization in most cases lead to colloidal instability, meaning that a number of primary particles cluster together, eventually leading to a constant number of growing latex particles. This process is known as limited coagulation. A constant number of particles indicate the end of the particle formation stage.

Pickering Emulsion Polymerization, Fig. 2 Cryo-TEM images of polymer latex particles: (**a**) poly (MMA-*co-n*-(BA)/Laponite, (**b**) poly(Sty-*co*-BA)/ Laponite, (**c**) poly(Sty-*co*-2-EHA)/Laponite, and (**d**) poly(Sty-*co*-2-EHA)/Laponite with methacrylic acid. Scale bars of 100, 100, 200, and 50 nm, respectively. Reprinted with permission from Ref. [19]. ©2011 American Chemical Society

In a Pickering emulsion polymerization, not only the monomer droplets could potentially be covered with nanoparticles serving as stabilizer but also a considerable number of particles (if not all) will be present in the water phase. It is logical to see that the growing waterborne oligomers upon the start of the polymerization process will interact with and can thus physisorb onto the nanoparticles. Adhesion of a radical species leads to a hybrid primary particle. In essence the nucleation process is comparable with soap-free emulsion polymerization, with the addition that now heterocoagulation events between the nanoparticles and a growing oligomer or the nanoparticles with a growing primary of mature latex particle need to be taken into account. This is crucial for the success of Pickering emulsion polymerization. Otherwise, a blend between an ordinary soap-free latex and the nanoparticles dispersed in water will be the result. This interaction and thus wettability can be tuned by the use of small amounts of surfactant and auxiliary monomers or premodification of the surface characteristics of the nanoparticles (see Fig. 2).

Since the presence of nanoparticles has an effect on the particle formation stage, it is logical to see that they play a similar role as the molecular surfactants used in traditional emulsion polymerizations in that upon use of increased amounts, more latex particles and thus smaller average particle sizes of the armored latexes will be obtained. It is important to stress that too low amounts can lead to full coagulation and that the influence of increasing the concentration of Pickering stabilizers to large extents will lead to a fading out effect on reduction in size of the targeted armored latex particles. Indeed, this is observed by Bon and coworkers when the amounts of Laponite XLS clay are gradually increased in Pickering emulsion copolymerizations of styrene and *n*-butyl acrylate [19].

Particle Growth in Pickering Emulsion Polymerization

The growth of particles after their formation leads to an increase in volume of polymer (and monomer) and thus the surface area of the growing particles. This leads to exposed bare surface regions on the surface of the armored particle, which effectively are relatively hydrophobic. A high fraction of bare interface induces colloidal instability and triggers coagulation events. A main event will be heterocoagulation with a Pickering stabilizer (nanoparticle) in the water phase. In essence the nanoparticles are captured by the growing latex particles, leading to a gradual drop of the concentration of nanoparticles in the water phase. This has been monitored quantitatively and modeled with excellent agreement between experiments and theory [20]. The final

product will be polymer latex particles armored with a layer of nanoparticles.

Outlook

This short overview hopefully has shown that Pickering emulsion polymerization is an interesting form of emulsion polymerization that produces nanocomposite polymer latexes armored with nanoparticles. There is a need for a thorough mechanistic understanding of the process, and further developments in order to achieve this are required. For example, current technology does not allow for armored latexes with an overall solids content of over 50 wt%.

In addition, the use of armored latexes in design of materials and coatings has yet to lead to applications with a step change in performance and innovation. Whereas some interesting features have been found in their use in waterborne coatings and pressure-sensitive adhesives, further exploration is required to really establish if Pickering emulsion polymerization can lead to products of commercial value.

References

1. SAF Bon (2015) Pickering suspension, miniemulsion and emulsion polymerization, Chapter 4 In: Ngai T, Bon SAF (ed) Particle-stabilized emulsions and colloids: formation and applications. Royal Society of Chemistry, Cambridge, UK. doi: 10.1039/9781782620143 PDF eISBN:978-1-78262-014-3
2. Pickering SU (1907) Cxcvi. – emulsions. J Chem Soc Trans 91:2001–2021
3. Pieranski P (1980) Two-dimensional interfacial colloidal crystals. Phys Rev Lett 45:569–572. doi:10.1103/PhysRevLett.45.569
4. Röhm O, Trommsdorff E (1939) Process for the polymerization of methyl methacrylate. US Patent 2,171,765
5. Velev OD, Furusawa K, Nagayama K (1996) Assembly of latex particles by using emulsion droplets as templates. 1. Microstructured hollow spheres. Langmuir 12:2374–2384. doi:10.1021/la9506786
6. Dinsmore AD, Hsu MF, Nikolaides MG et al (2002) Colloidosomes: selectively permeable capsules composed of colloidal particles. Science 298:1006–1009. doi:10.1126/science.1074868
7. Bon SAF, Cauvin S, Colver PJ (2007) Colloidosomes as micron-sized polymerisation vessels to create supracolloidal interpenetrating polymer network reinforced capsules. Soft Matter 3:194–199. doi:10.1039/b612066k
8. Tiarks F, Landfester K, Antonietti M (2001) Silica nanoparticles as surfactants and fillers for latexes made by miniemulsion polymerization. Langmuir 17:5775–5780. doi:10.1021/la010445g
9. Cauvin S, Colver PJ, Bon SAF (2005) Pickering stabilized miniemulsion polymerization: preparation of clay armored latexes. Macromolecules 38:7887–7889. doi:10.1021/ma051070z
10. Bon SAF, Colver PJ (2007) Pickering miniemulsion polymerization using Laponite clay as a stabilizer. Langmuir 23:8316–8322. doi:10.1021/la701150q
11. Solc nee Hajna J (1983) Colloidal size hydrophobic polymers particulate having discrete particles of an inorganic material dispersed therein. US Patent 4,421,660A
12. Long F, Wang W, Xu Y, Cao T (1991) Study on encapsulation of organic polymers in the presence of inorganic sol particles. Tianjin Daxue Xuebao (J Tianjin Univ) 4:10–15
13. Barthet C, Hickey AJ, Cairns DB, Armes SP (1999) Synthesis of novel polymer-silica colloidal nanocomposites via free-radical polymerization of vinyl monomers. Adv Mater 11:408–410. doi:10.1002/(SICI)1521-4095(199903)11:5<408::AID-ADMA408>3.0.CO;2-Y
14. Wang Y, Feng L, Pan C (1999) Preparation and characterization of P(St-*co*-4VP) particles produced by using emulsifier-free emulsion polymerization. J Appl Polym Sci 74:1502–1507. doi:10.1002/(SICI)1097-4628(19991107)74:6<1502::AID-APP23>3.0.CO;2-E
15. Chen M, Zhou S, You B, Wu L (2005) A novel preparation method of raspberry-like PMMA/SiO$_2$ hybrid microspheres. Macromolecules 38:6411–6417. doi:10.1021/ma050132i
16. Walther A, Hoffmann M, Mueller AHE (2008) Emulsion polymerization using Janus particles as stabilizers. Angew Chem-Int Ed 47:711–714. doi:10.1002/anie.200703224
17. Colver PJ, Colard CAL, Bon SAF (2008) Multilayered nanocomposite polymer colloids using emulsion polymerization stabilized by solid particles. J Am Chem Soc 130:16850+. doi:10.1021/ja807242k
18. Schmid A, Tonnar J, Armes SP (2008) A new highly efficient route to polymer-silica colloidal nanocomposite particles. Adv Mater 20:3331–3336. doi:10.1002/adma.200800506
19. Teixeira RFA, McKenzie HS, Boyd AA, Bon SAF (2011) Pickering emulsion polymerization using laponite clay as stabilizer to prepare armored "Soft" polymer latexes. Macromolecules 44:7415–7422. doi:10.1021/ma201691u
20. Colard CAL, Teixeira RFA, Bon SAF (2010) Unraveling mechanistic events in solids-stabilized emulsion polymerization by monitoring the concentration of nanoparticles in the water phase. Langmuir 26:7915–7921. doi:10.1021/la904817f

P

Plastic Recycle

Haruo Nishida
Department of Biological Functions Engineering,
Graduate School of Life Science and Systems
Engineering, Kyushu Institute of Technology,
Wakamatsu-ku, Kitakyushu, Japan

Synonyms

Bio-based plastics; Biomass-based polymers;
Biomass-originated plastics; Biomass-originated
polymers; Bio-plastics; Biopolymers; Feedstock
recycling; Mechanical recycling; Physical
recycling; Primary recycling; Secondary
recycling; Tertiary recycling

Definition

Plastic recycling is the process of recovering used
or waste plastics and transforming them into use-
ful products by methods that include depolymer-
ization (chemical recycling) and/or reprocessing
(material recycling). Depolymerization entails
changing the recovered plastics into monomer
or low-molecular-weight materials (oligomers)
by means of heating, hydrolysis, acidolysis,
etc. in order to reproduce the original plastics.
Reprocessing involves melting down the recov-
ered plastics for molding into new products dif-
ferent in form from the melted-down originals.

Bio-based polymers are materials intention-
ally made from substances derived from renew-
able biological resources. The term refers to
modern materials that have undergone more
extensive processing than classical biomaterials.
Typically, such bio-based plastics are produced
by means of a mixed process of biological fer-
mentation and chemical reactions. Bio-based
polymers are often but not always biodegradable.

Introduction

Various bio-based polymers have been devel-
oped as shown in Fig. 1 [1]. Typical bio-based

polymers are poly(lactic acid) (PLA) [2] and poly
[(R)-3-hydroxybutyrate] (PHB) [3]. Even some
typical commodity plastics have also been syn-
thesized from biomass, for example, polyethyl-
ene, polypropylene, poly(methyl methacrylate),
polyamide-4, and polycarbonate.

Generally, the bio-based polymers, because of
reactive groups in their main chains, show excellent
degradabilities: biodegradability, hydrolysability,
photolysability, and thermal degradability
(pyrolysability). Typical bio-based polymers PLA
and PHB are well known not only as biodegradable
materials but also as chemically and mechanically
recyclable materials. They can be recycled to mono-
meric raw materials by thermal depolymerization or
hydrolysis. When purified, the monomeric materials
can be used in the manufacture of virgin polymers
with no loss of original properties. Much effort has
been expended in the recycling of PLA and PHB to
reach the present stage where they can be ideally
depolymerized to obtain pure monomeric materials.

If polymers synthesized from renewable
resources could be re-utilized in a cyclic manner
with precise control of their depolymerization, then
an ideal recycling system could be constructed for
polymeric products, in which the resources
expended and production energy could be mini-
mized. Hence, the significance of the development
of bio-based recyclable polymers is clear [4].

Besides chemical recycling, bio-based polymer
materials can also be reprocessed through mechan-
ical recycling. The mechanically recycled materials
are generally regarded as economical substitutes for
less-demanding or cost-sensitive applications; how-
ever, there are also some examples of upgrading
recycling and specific applications of the mechani-
cally reprocessed bio-based polymers.

Here, the depolymerization properties of some
typical bio-based polymers together with the pre-
sent state of material and chemical recycling will
be reviewed.

Material Recycling of Bio-Based Polymers

Polymers preserve their useful properties for a
finite time. However, the molecular weight
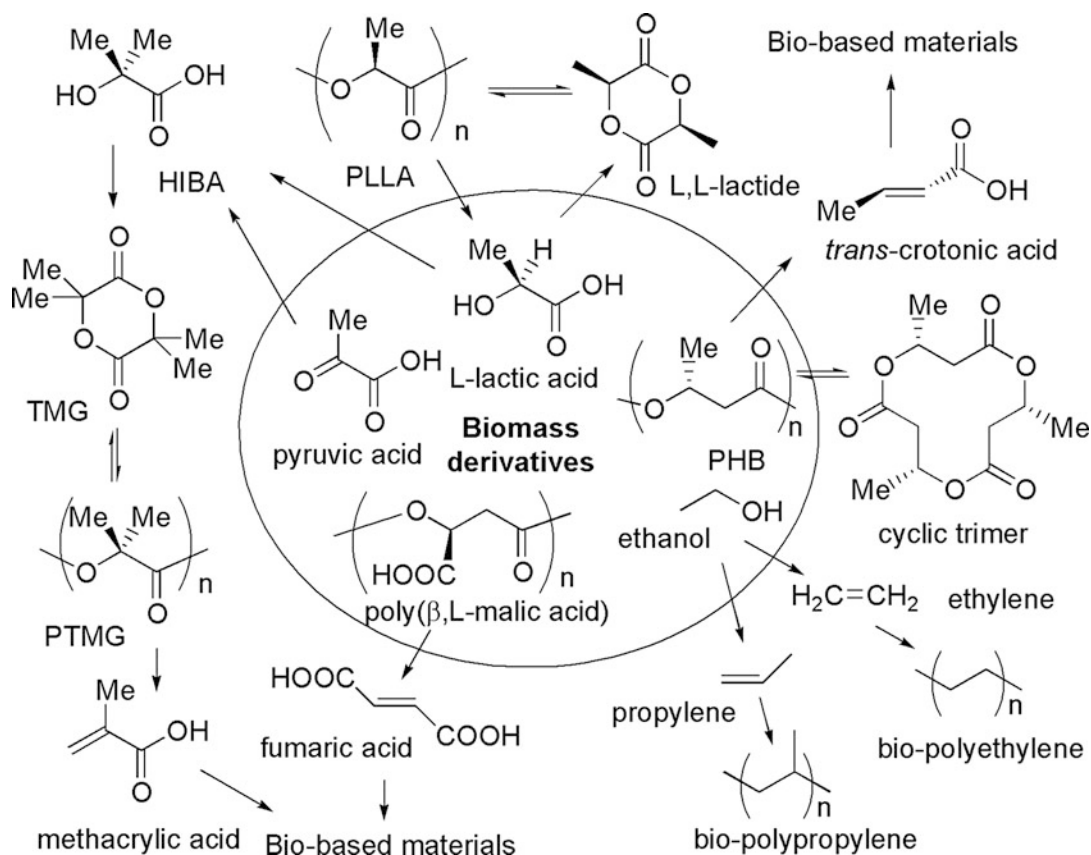
Plastic Recycle, Fig. 1 Bio-based polymers

gradually and inevitably decreases. For bio-based polymers, this degradation can be brought about by various environmental stimuli such as microorganisms, sunlight, rain, snow, wind, humidity, or seawater. The type of degradation mechanism of bio-based polymers depends on the kind of environmental stimulus received.

One issue that has been raised in relation to the recycling of bio-based polymers is contamination. It has been suggested that because bio-based polymers are of a different origin to regular plastics, they must be kept separate when recycled to avoid contaminating the recycling stream. However, since bio-based polymers have various specific properties based on their plant origins, they are capable of being reused in some applications requiring environmentally friendly materials. Here, some examples of material recycling of PLA are introduced.

Random Degradation Mechanism

Although PLA is synthesized from renewable resources such as starch, the production up to the polymeric form requires much energy and many steps (Fig. 2): i.e., fermentation and purification of lactic acid, condensation for oligomerization, thermal degradation into lactide, and polymerization [5]. If the depolymerization of PLA to intermediates can be achieved with high efficiency and selectivity, it will then be possible to reproduce PLA via the shortest and most energy-efficient route.

Generally, in the absence of other strong acids and bases, the polyesters undergo an autocatalytic random chain scission during hydrolysis as a result of acceleration by their carboxyl end groups [6]. For example, Pitt and Gu have observed a kinetic relationship described by $M_{nt}/M_{n0} = \exp(-kt)$ on the hydrolysis of PLLA

Plastic Recycle,
Fig. 2 Production process
of PLA from biomass
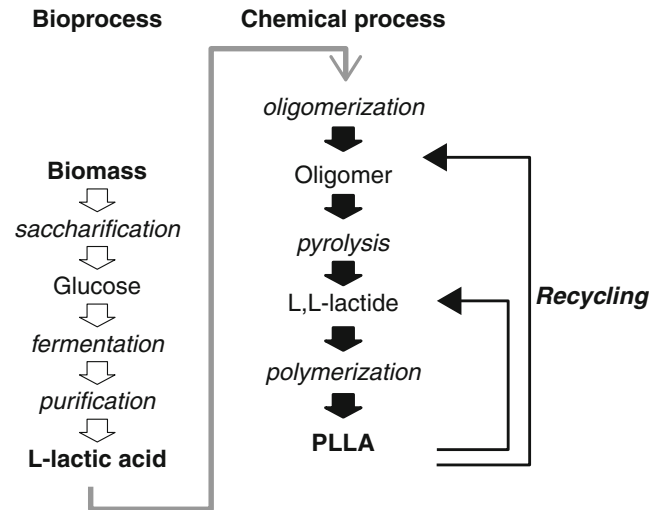
in a phosphate buffer solution (PBS) (pH 7.4), where M_{nt} and M_{n0} refer to the number-average molecular weight values at time t and t = 0, respectively. The relationship is derived from the autocatalytic random degradation kinetics.

In order to confirm the precise kinetics parameters, rate constant k and activation energy E_a values of PLLA hydrolysis, Mohd-Adnan et al. [7] investigated the hydrolysis using high-pressure steam in a temperature range of $100 \sim 130\,°C$. Exact molecular weights of hydrolysates were evaluated without the influence of weight loss. The changes in molecular weight could be successfully matched against simulation plots generated according to the autocatalytic hydrolysis mechanism, clearly indicating the critical point. Resulting k and E_a values were estimated as 8.4×10^{-5} ($100\,°C$) $\sim 7.2 \times 10^{-4}\,s^{-1}$ ($130\,°C$) and $87.2\,kJ\cdot mol^{-1}$, respectively.

Recycling of PLA into Materials for Ocean Businesses

Marine biological fouling, usually termed marine biofouling, is the undesirable accumulation of microorganisms, plants, and animals on immersed surfaces. Such accumulations can have dramatic economic and environmental costs, through increased fuel consumption to shipping, frequent dry-docking and painting for hull maintenance, the hindering of seaweed farming, etc. In preventing marine biofouling,

effective tributyltin (TBT) self-polishing copolymer paints have been the most successful. Following the banning of TBT as an antifoulant, several organic booster biocides have been used in conjunction with copper compounds in antifouling paints as alternative treatments.

Nowadays, environmentally friendly alternative methods of antifouling are being actively researched. These include treatments using natural products, fouling-release coatings, antifouling topographies, and electrical antifouling systems [8].

To prevent the development of marine biofouling, especially macrofouling, by the undesirable accumulation of organisms such as barnacles, mussels, algae, etc., many kinds of systems for slow-releasing antifoulants have been developed. These slow-release systems have been designed using surface-fragmenting/self-polishing matrices, in which the matrix polymers are hydrolyzed at ester groups of main and side chains. This allows antifoulants such as agricultural herbicide: diuron, cuprous oxide, and an antibacterial molecule: chlorhexidine to be gradually released during immersion time in seawater. Some biodegradable and bio-based polymers such as poly(3-hydroxyalkanoate)s (PHAs), poly(ε-caprolactone) copolymers, poly(ester-anhydride), PLA, graft copolymers containing poly(lactic acid) side chains, and poly(ε-caprolactone-co-lactide) have been

Plastic Recycle,
Fig. 3 Attachment ratios
of cypris larvae on PLLA
oligomers sheets
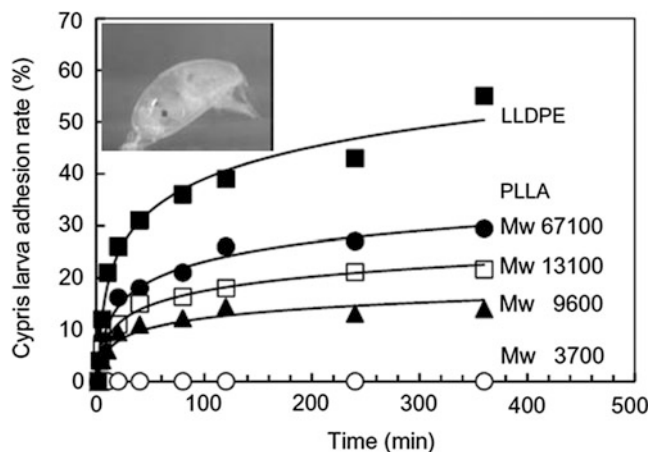
applied as environmentally benign surface-fragmenting/self-polishing matrices to controllably release the antifoulants. Langlois et al. indicated that the rate of biocide release was controlled by the amount of oligo(D,L-lactic acid) units in the graft copolymers. On the other hand, Faÿ et al. reported that the lower the molecular weight of poly(ε-caprolactone-co-lactide), the faster the release of biocide from antifouling paints, resulting in a decrease in the antifouling activity.

Recently, the ability of biodegradable polyester poly(L-lactic acid) (PLLA) to function as an anti-barnacle molecule was investigated [9]. Of particular interest was PLLA's slow release of lactic acid, which due to its acidity ($pKa = 3.86$) acts by inhibiting the network formation/cross-linking reactions of cement proteins at the surface layers of PLLA moldings. PLLA applied to immersed solid surfaces in seawater inhibited colonization by barnacles due to the slow-release property of lactic acid. The effect of the molecular weight of PLLA on anti-macrofouling activity was confirmed with the lowest-molecular-weight PLLA producing the lowest attaching ratio of *Balanus amphitrite* cypris larvae, which are the final larval stage of barnacles and are highly specialized to their role of locating and attaching to suitable surfaces for adult growth (Fig. 3). The anti-macrofouling function of low-molecular-weight PLLA was also confirmed in a natural sea environment.

Recycling of PLA for Agricultural Materials

Agricultural uses have been considered as promising applications of bio-based polymers. The soil burial test has been widely used for the determination of environmental degradation of PLA. The test simulates actual conditions found in agricultural uses. From the results, no degradation was observed in PLLA sheets buried in soil for 6 weeks, and only a small weight loss was observed in PLLA even after a 20-month soil burial test. These are typical results for PLLA indicating its poor biodegradability, because PLA-degrading microorganisms are not widely distributed in the natural environment, and thus, in this environment PLA is less susceptible to microbial attack [10].

To investigate the degradation behavior of agricultural mulching film, Copinet et al. prepared coextruded PLA/starch films, which were degraded under UV light treatment at 315 nm and mineralized in three kinds of media: a liquid medium containing no carbon source, an inert solid medium consisting of an aluminum-magnesium-iron silicate, and a compost medium. The UV irradiation showed a visual degradation of the starch part in films and had an enhancing effect on the degradation of the PLA part to give high biodegradation percentages of 92.4–93.4 % in the liquid medium, 80–83 % for the inert medium, and 79.1–80.3 % for the compost processing when compared with the results of biodegradation without the initial UV treatment.

P

Plastic Recycle,
Fig. 4 Raising seedling in a pot as material recycling of PLA
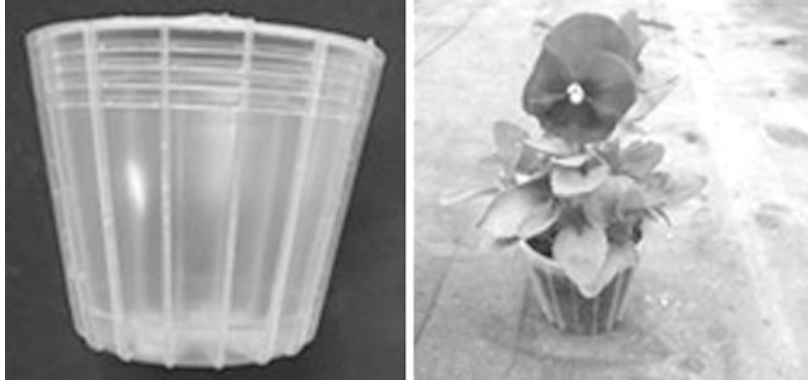
Plastic Recycle,
Fig. 5 Monitoring cap as a material recycling product of PLA
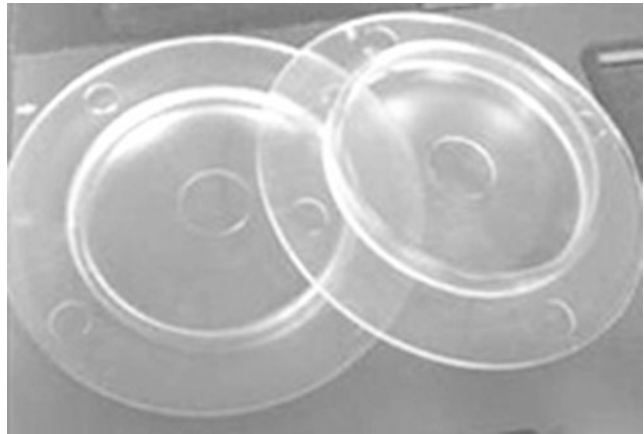
It is noteworthy that PLLA was shown to promote plant growth [11]. Hidebrandt et al., showed an increase in growth of marigold and sunflower when tissue cultures were treated with lactic acid. Tung et al. also reported significant increases in the biomass of young sugarcane plant treated with lactic acid. Moreover, Kinnersley et al. reported that dry weights of duckweed and corn were more than doubled when the plants were grown in media containing the dimer of L-lactic acid: L-lactoyl-lactic acid. Increases in chlorophyll accumulation and root growth may be due to the increased ability of plants to assimilate nutrients after treatment with L-lactoyl-lactic acid as a hydrolysis product of PLLA.

Nagasawa et al. investigated raising seedling pots as products of the material recycling of used tractor gear grips made of PLA by injection molding. The pots were used to raise the seedlings of pansies, resulting in consummate growth of pansy seedlings without any inhibitory activity when compared with conventional materials (Fig. 4). The pansy seedlings were transplanted into a field without taking the seedlings out of the pots.

Recycling of PLA into Construction Materials of Elevated Roads and Bridges

Recently, some of the floor slabs for elevated roads and bridges have been configured by using steel-concrete composite floor slabs. A steel-concrete composite floor system consisting of a bottom steel plate as the framework with channel steel reinforcements not only excels in terms of safety and construction capability but also helps shorten the construction period. Monitoring holes are used to check that the concrete has properly filled the steel framework and also for subsequent maintenance over the long term. Monitoring caps (Fig. 5),

which need to be transparent and mechanically durable during the filling and curing of concrete, are then required to spontaneously degrade and disappear within 2–3 years to expose the cured concrete surface. PLA having a low molecular weight (LMW-PLA) as a material recycling product has suitable properties for use as the monitoring cap.

The degradation behavior of the LMW-PLA monitoring cap was examined under environmental conditions designed to simulate that of the composite floor slab. Superheated steam treatment, UV-C irradiation, heating in the atmosphere, and a repeating cold and hot stimuli test were applied as acceleration tests of hydrolysis, photolysis, thermo-oxidation, and physical stressing, respectively. Although a decrease in the molecular weight of PLA was observed during all the acceleration tests, the degradation behavior in each test was different. The accelerated hydrolysis and thermo-oxidation proceeded in accordance with the autocatalytic random degradation kinetics. The accelerated photolysis was evaluated as proceeding according to a mixed process of autocatalytic and non-autocatalytic random degradation kinetics. From the comparison of racemization behavior among photolysis, hydrolysis, and thermal degradation, it was confirmed that the preferential racemization behavior of each of these three degradation processes is characteristic and distinct, being identified as chain-end racemization, poor racemization, or internal-unit racemization, respectively [12]. The cycle test under cold and hot stimuli at 10 °C and 50 °C for 10 min each induced not only a decrease in molecular weight in the manner of an autocatalytic random degradation but also a catastrophic decrease in mechanical properties at a critical point [13].

Obtained results were analyzed kinetically to estimate the reaction rate constant k values and thereby to predict the lifetime of a monitoring cap in an environment at the underside of an elevated road. The lifetime up to the point of disintegration can be controlled by selecting the initial molecular weight and thickness of the PLA monitoring cap.
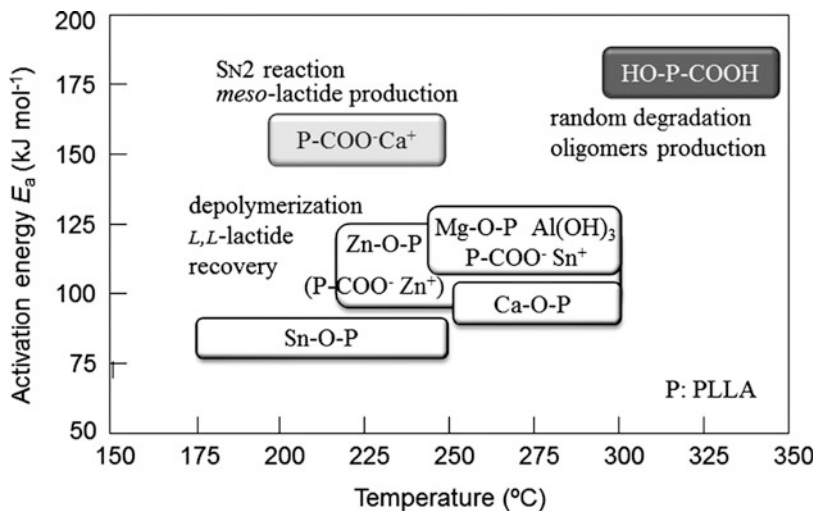
Chemical Recycling of Bio-Based Polymers

Chemical Recycling of PLA

PLA is prepared by the ring-opening polymerization of lactides, such as L,L-, D,D-, and *meso*-lactides, which are cyclic dimers of lactic acid. In particular, PLLA prepared from L,L-lactide is an especially well-known crystalline polymer. This ring-opening polymerization is an equilibrium reaction, in which the concentration of cyclic monomer is temperature dependent [14]. Therefore, the lactides are regenerated through the thermal depolymerization of PLA.

Thermal Degradation Catalysts

Some safe and effective catalysts for the thermal depolymerization of PLA have been developed [15]. In PLLA/alkali earth metal oxide systems, calcium oxide (CaO) and magnesium oxide (MgO) lowered the degradation temperature range of PLLA, as well as completely suppressing the production of oligomers other than lactides. CaO markedly lowered the degradation temperature but caused some racemization of lactide, especially in a temperature range lower than 250 °C. The racemization was avoided with MgO in the lower temperature range. This characteristic anti-racemization effect of MgO is due to the lower basicity of Mg compared to Ca. At temperatures lower than 270 °C, the pyrolysis of PLLA/MgO (5 wt%) composite occurred causing unzipping depolymerization and resulting in selective L.L-lactide production.

Aluminum compounds have been used not only as polymerization initiators but also as flame retardants for PLA. Degée et al. found that as-polymerized ω-alkoxyaluminium-PLA with Al(isopropoxide)$_3$ had a thermal stability comparable to purified PLA. On the other hand, a large amount (~50 wt%) of aluminum hydroxide (Al(OH)$_3$) is required to achieve adequate flame resistance for the PLA/Al(OH)$_3$ composite. Effects of Al(OH)$_3$ on the thermal degradation of PLLA composites have also been investigated. The thermal stabilization of the composite was improved at temperatures lower than 250 °C compared to as-polymerized PLLA. This

P

stabilization makes the melt processing of the composite easier. Nevertheless, at 250–300 °C the depolymerization of PLLA to lactides proceeded without any racemization reaction, selectively converting the polymer into L,L-lactide with $Al(OH)_3$ acting as a catalyst. This means that the $Al(OH)_3$ composite behaves as a multifunctional additive, which works not only as a flame retardant but also as a stabilizer during melt processing at temperatures lower than 250 °C and as a depolymerization catalyst in a temperature range of 250 ~ 300 °C.

Based on previously reported kinetic parameter values of PLLA thermal degradation, relationships among temperature ranges, activation energy values, and degradation mechanisms of the catalytic degradation of PLLA are summarized in Fig. 6 showing an activation energy map of PLLA thermal degradation.

Selective Depolymerization of PLA in Blends

Formation of a polymer alloy is a common way to improve the property of PLA. Many kinds of polymers such as polyethylene, polypropylene (PP), polystyrene (PS), poly(methyl methacrylate), bisphenol-A-polycarbonate, poly(ε-caprolactone), PHB, poly(butylene succinate) (PBS), poly(butylene succinate/adipate) (PBSA), and acrylonitrile butadiene styrene (ABS) have been used for preparing PLA alloys, some of which have been commercialized.

To achieve selective depolymerization of the PLA component, some polymer blends of PLA with linear low-density polyethylene (LLDPE), PS, PBS, and PBSA were prepared and thermally degraded with an MgO catalyst [16]. TGA curves of the blends clearly showed two-step weight-loss profiles, in which MgO promoted the PLA degradation selectively, shifting the temperature range of the PLA component. To clarify the influence of the coexisting polymer, the thermal degradation data were analyzed kinetically. From the analytical results, it was found that even in the presence of MgO, LLDPE, PS, and PBS, there was no effect on the depolymerization behavior of PLA and that PLA was effectively depolymerized into L,L-lactide with a low racemization ratio (Fig. 7). However, PBSA, which includes an adipate group as an easily degradable unit, influenced the depolymerization of PLA, resulting in the formation of *meso*-lactide. This formation occurs because some intermolecular reactions, including the SN_2 reaction at an asymmetrical methine carbon of PLA, may be caused by carboxyl anions of PBSA.

Chemical Recycling of Flame-Resisting Blends with Extruder

For the chemical recycling of PLA component in fire–resistant polymer alloys used for electric/electronic equipment, effects of $Al(OH)_3$ added as a flame retardant on the thermal
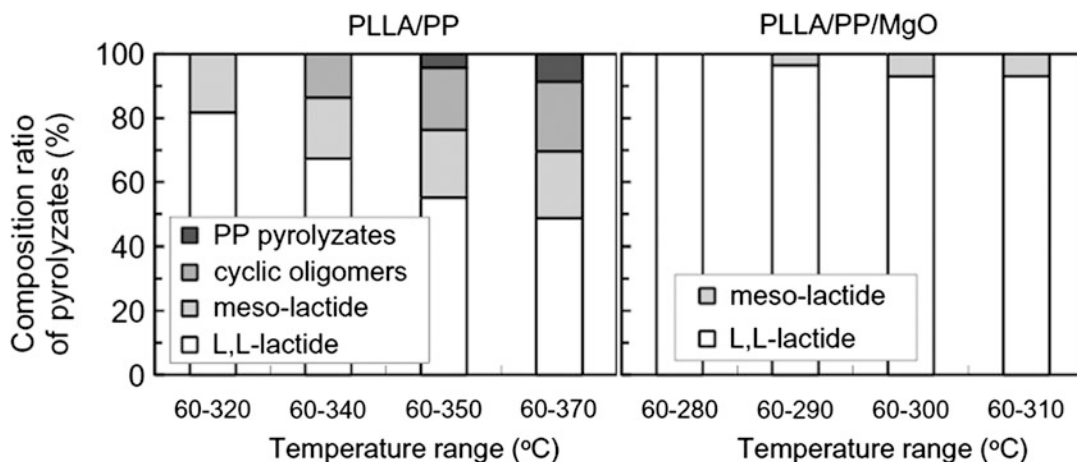
Plastic Recycle, Fig. 7 Composition ratios of pyrolyzates from PLLA/PP (80:20 wt/wt) and PLLA/PP/MgO (80:20:5 wt/wt/wt)

depolymerization of PLA component were evaluated with a practical twin screw extruder. As a result of examining the conversion from the PLA/PP/Al(OH)$_3$ [14:56:30 (wt/wt/wt)] compounds to lactide monomer, L,L-lactide purity of 90 % was achieved under a recovery ratio of about 90 %. Furthermore, the combination of Al(OH)$_3$ and MgO accelerated PLLA depolymerization as a synergetic catalyst to generate L,L-lactide.

Chemical Recycling of Poly (3-Hydroxybutyrate) (PHB)

Poly(3-hydroxybutyrate) (PHB) is a well-known microbial and biodegradable polymer, which is accumulated and stored by prokaryotic microorganisms at levels up to 90 % of their cellular dry weight. PHB has been attracting much interest from researchers not only as an environmentally compatible thermoplastic but also as a polymeric material obtainable from renewable resources and with a high melting temperature of around 180 °C.

A major problem with PHB when used as a thermoplastic is its thermal instability during melt processing. Therefore, intense interest has been shown in the thermal degradation of PHB and other related poly(hydroxyalkanoate)s (PHAs). It has been demonstrated that PHB is a chemically recyclable material with end products such as crotonic acid, linear oligomers having a crotonate end group [17], and a cyclic trimer as shown in Fig. 1. The main product is crotonic acid as a result of β-elimination.

Effects of Alkali Earth Compounds as Depolymerization Catalysts

In order to transform PHB into a specific monomer, precise control of the thermal degradation is crucial. In spite of the wealth of previous studies, there are few reports thus far which focus on the selective depolymerization of PHB into the monomer. In cases of PHB pyrolysis without a catalyst, the net yield of all butenoic acids (trans/cis-crotonyl acids (CAs) + 3-butenoic acid (BA)) as main pyrolysis products ranged from 39.5 wt% using thermal volatilization analysis to 87 total ion count % (TIC%) using Py-GC/MS analysis. In 2008, Ariffin et al. reported that ^{1}H NMR analysis of PHB pyrolyzates at 260 °C revealed the ratio *trans*-CA:*cis*-CA:oligomers = 67.7:3.1:29.2 (monomeric unit%). Kopinke et al. also reported on the production of a large amount of oligomers during the PHB pyrolysis, with the recovered monomer fraction being composed of *trans*-CA:*cis*-CA:BA = 100:10:2 (GC-area%).

When pyrolysis catalysts were used in PHB pyrolysis, Kim et al. reported the enhancement of PHB depolymerization by CaCl$_2$ or MgCl$_2$.

This enhancement was explained as being due to the Lewis acidity of Ca^{2+} and Mg^{2+} facilitating the formation of a double bond by the elimination of β-hydrogen. Kawalec et al. also reported on the enhancement of the thermal degradation of PHB by Na^+, K^+, and Bu_4N^+ counter cations at chain ends, proposing an E1cB mechanism.

Completely selective transformation of PHB into *trans*-crotonic acid was achieved by Ariffin et al. [18] during thermal degradation using Mg compounds: MgO and $Mg(OH)_2$ as catalysts. Through catalytic action, not only the temperature and E_a value of degradation lowered by 40–50 °C and 11–14 kJ·mol^{-1}, respectively, in comparison with 260–300 °C and around 300 kJ·mol^{-1} of PHB pyrolysis without any catalyst, but also significant changes in the selectivity of pyrolyzates were observed. Notably, $Mg(OH)_2$ and MgO showed nearly complete selectivity (~100 %) to *trans*-crotonic acid.

From the kinetic simulation analyses – random degradation and integral analyses – the pyrolysis of PHB/MgO was shown to start by a random degradation and gradually shift into an nth-order weight-loss behavior. PHB/$Mg(OH)_2$ also showed the same kinetics. These results showed the degradation process to be random β-elimination and/or E1cB mechanisms as the initial processes, followed by the unzipping β-elimination as the main degradation process, which was accelerated by chain-end crotonate groups.

Degradation Mechanisms

Under the pyrolysis conditions without any other reactant from the outside, autocatalytic or auto-accelerated random degradation may be induced by a large number of carboxyl compounds, which self-generate as the reaction progresses. The carboxyl compounds randomly attack ester groups on polymer chains to induce transesterification, resulting in the reproduction of carboxyl groups and a remarkable decrease in molecular weight.

In order to induce the auto-accelerated random degradation, carboxylic groups have to be self-proliferated in bulk. β-elimination as the initial process is just a self-proliferation reaction. The unzipping β-elimination occurring at the end of molecules, which, by precise kinetic analysis and theoretical calculation, was suggested to be the 0th-order reaction, is just a kinetically favored scission of polymer chains that repeatedly generate a large number of crotonic acids. These are the key factors in the auto-accelerated random degradation.

According to predictions based on the measured and analyzed results, an expected overall thermal degradation pathway of PHB is illustrated in Fig. 8.
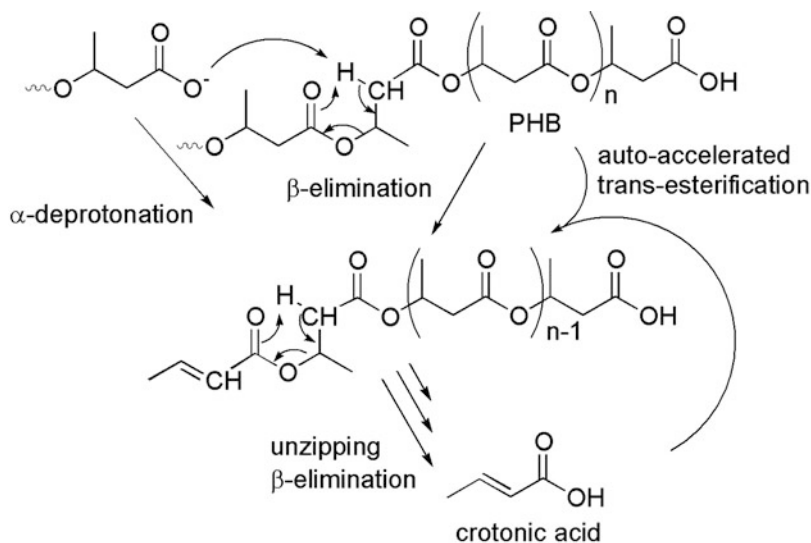
Plastic Recycle,
Fig. 8 Expected overall thermal degradation pathway of PHB

Chemical Recycling of Bio-Based Poly (Tetramethylglycolide) (PTMG)

PLLA has been attracting much interest from researchers as the plastic material of choice for sustainable systems. However, in practical applications, PLLA does have some drawbacks, such as slow crystallization, low impact resistance, hydrolyzability, and racemization. PLLA readily causes racemization from an L-unit to a D-unit in a chain under heating. Such racemization proceeds by the mechanism of ester-semiacetal tautomerization, causing a decrease in optical purity and crystallinity. This is a serious problem in the reproduction of practical materials via thermal depolymerization and re-polymerization. A fundamental and complete solution to this problem requires a modification of the chemical structure of lactic acid.

In order to overcome the problems associated with PLLA while preserving its superior properties, a bio-based and racemization-free polymer, poly(tetramethylglycolide) (PTMG) possessing superior depolymerizability for the reproduction, was developed. Previously, PTMG has been synthesized from petroleum by wholly chemical processes involving the ring-opening polymerization of tetramethylglycolide (TMG), which is a cyclic dimer of α-hydroxyisobutyric acid (HIBA). HIBA itself has also required preparation over many steps from petroleum using the cyanhydrin method for methyl methacrylate production. In 2010, a biosynthesis method of HIBA from renewable carbons was achieved. PTMG shows a high T_m at 185–190 °C and a characteristic thermal degradability into methacrylic acid, TMG, acetone, etc. However, the derivation of PTMG from biomass and its controlled depolymerization into monomers, which will be required for many commonly used polymers in the future, has been proposed by Nishida et al. [19].

Renewable resources: D/L-lactic acids and pyruvic acid derived from biomasses are employed as starting materials for the synthesis of HIBA, which is an acyclic monomer of PTMG. The bio-based HIBA is prepared by methylation of the acids and then converted into the cyclic dimer: TMG by a cyclic esterification.

The following synthesis of polymer PTMG is carried out by a ring-opening polymerization of TMG. The isolated PTMG showed T_m and T_g at 191 and 70 °C, respectively, about 15 °C higher than those of PLLA. The Tg transition signal was very weak, and the T_m peak shifted into higher temperatures of up to 206 °C with a corresponding increase in the heat treatment temperature. The weak T_g signal and high T_m value of PTMG suggest superior crystallization and heat resistance, respectively.

An interesting property of PTMG is the controllable depolymerization behavior into TMG and methacrylic acid (MA). In the thermal degradation of PTMG, it has been reported that TMG, MA, acetone, etc. are recovered as volatile products without any catalyst needed for the reaction control. By using appropriate catalysts, $Sn(Oct)_2$ or MgO for the selective depolymerization, the thermal degradation of PTMG was controlled successfully to generate TMG (80.8 %) or MA (80.6 %), respectively. Recovered TMG can be used to reproduce PTMG. Another selectable product MA was converted into a methacrylic ester: methyl methacrylate (MMA) after an esterification reaction. From the obtained MMA, a bio-based poly(methyl methacrylate) with high molecular weight (Mn 70,000 and Mw 238,000) was produced by free-radical polymerization in bulk. These results reveal PTMG as a superior recyclable material by the virtue of its controllable conversion into each monomer.

Chemical Recycling of Bio-Based Poly(β,L-Malic Acid)

Poly(β,L-malic acid) (PMLA) is a carboxylic-functionalized polyester produced by biological fermentation by *Myxomycetes* and certain filamentous fungi. PMLA is a perfectly biodegradable and biocompatible polymer with features ideally suited to function as a drug carrier to which tissue-specific tags can be covalently attached.

Portilla-Arias et al. [20] reported that poly(β, L-malic acid) was depolymerized above 200 °C by an unzipping mechanism from chain ends with the generation of fumaric acid (Fig. 1), which was secondarily converted into maleic acid and

anhydride. These aliphatic acids and anhydride are reused to be incorporated in many chemical products.

Summary

Many bio-based polymers are being developed one after another. In particular, recyclable bio-based polymers are proving to be of great interest as important materials from both a scientific and an environmental point of view. This is because they are capable of being used as environmentally friendly materials in some specific applications, such as anti-macrofouling materials, pots for raising seedlings, and monitoring caps in steel-concrete composite floor slabs. Moreover, the bio-based polymers have the further specific property of having excellent feedstock recyclability. Typically, PLLA and PHB are quantitatively converted into L,L-lactide and trans-crotonic acid, respectively, by using specific and environmentally friendly catalysts.

References

1. Chen GQ, Patel MK (2012) Plastics derived from biological sources: present and future: a technical and environmental review. Chem Rev 112:2082–2099. doi:10.1021/cr200162d

2. Auras R, Lim LT, Selke SEM, Tsuji H (eds) (2010) Poly(lactic acid):synthesis, structures, properties, processing, and applications. Wiley, Hoboken

3. Doi Y (1990) Microbial polyester. VCH Publishers, New York

4. Nishida H (2011) Development of materials and technologies for control of polymer recycling. Polym J 43:435–447. doi:10.1038/pj.2011.16

5. Vink ETH, Rabago KR, Glassner DA, Gruber PR (2003) Applications of life cycle assessment to nature Works^{TM} polylactide (PLA) production. Polym Degrad Stab 80:403–419. doi:10.1016/S0141-3910(02)00372-5

6. Gilbert RD, Stannett V, Pitt CG, Schindler A (1982) Chapter 8 the design of biodegradable polymers: two approaches. In: Grassie N (ed) Developments in polymer degradation -4. Applied Science Publishers, London

7. Mohd-Adnan AF, Nishida H, Shirai Y (2008) Evaluation of kinetics parameters for poly(L-lactic acid) hydrolysis under high-pressure steam. Polym Degrad

Stab 93:1053–1058. doi:10.1016/j.polymdegradstab.2008.03.022

8. Cao S, Wang JD, Chen HS, Chen DR (2011) Progress of marine biofouling and antifouling technologies. Chin Sci Bull 56:598–612. doi:10.1007/s11434-010-4158-4

9. Ishimaru N, Tsukegi T, Wakisaka M, Shirai Y, Nishida H (2012) Effects of poly(L-lactic acid) hydrolysis on attachment of barnacle cypris larvae. Polym Degrad Stab 97:2170–2176. doi:10.1016/j.polymdegradstab.2012.08.012

10. Tokiwa Y, Calabia BP (2006) Biodegradability and biodegradation of poly(lactide). Appl Microbiol Biotechnol 72:244–251. doi:10.1007/s00253-006-0488-1

11. Kinnersley AM, Scott TC, Yopp JH, Whitten GH (1990) Promotion of plant growth by polymers of lactic acid. Plant Growth Regul 9:137–146

12. Yasuda N, Tsukegi T, Shirai Y, Nishida H (2011) Characteristic chain-end racemization behavior during photolysis of poly(L-lactic acid). Biomacromolecules 12:3299–3304. doi:10.1021/bm200775r

13. Nishida H, Yamashita M, Nagashima M, Hattori N, Endo T, Tokiwa Y (2000) Theoretical prediction of molecular weight on auto-catalytic random hydrolysis of aliphatic polyesters. Macromolecules 33:6595–6601. doi:10.1021/ma992102j

14. Witzke DR, Narayan R, Kolstad JJ (1997) Reversible kinetics and thermodynamics of the homopolymerization of L-lactide with 2-ethylhexanoic acid Tin(II) salt. Macromolecules 30:7075–7085. doi:10.1021/ma970631m

15. Nishida H (2010) Part IV. Chapter 23: Thermal degradation. In: Rafael A, Lim LT, Selke SEM, Tsuji H (eds) Poly(lactic acid): synthesis, structures, properties, processing, and applications. Wiley, Hoboken

16. Omura M, Tsukegi T, Shirai Y, Nishida H, Endo T (2006) Thermal degradation behavior of poly(lactic acid) in a blend with polyethylene. Ind Eng Chem Res 45:2949–2953. doi:10.1021/ie051446x

17. Nishida H, Ariffin H, Shirai Y, Hassan MA (2010) Chapter 19: Precise depolymerization of poly (3-hydroxybutyrate) by pyrolysis. In: Elnashar MM (ed) Biopolymers. Sciyo, Rijeka

18. Ariffin H, Nishida H, Shirai Y, Hassan MA (2010) Highly selective transformation of poly[(R)-3-hydroxybutyric acid] into trans-crotonic acid by catalytic thermal degradation. Polym Degrad Stab 95:1375–1381. doi:10.1016/j.polymdegradstab.2010.01.018

19. Nishida H, Andou Y, Watanabe K, Arazoe Y, Ide S, Shirai Y (2011) Poly(tetramethylglycolide) from renewable carbon, a racemization-free and controlled depolymerizable polyester. Macromolecules 44:12–13. doi:10.1021/ma102289w

20. Portilla-Arias JA, Garcıa-Alvarez M, de Ilarduya AM, Holler E, Munoz-Guerra S (2006) Thermal decomposition of fungal poly(β, L-malic acid) and poly(β, L-malate)s. Biomacromolecules 7:3283–3290. doi:10.1021/bm060710i
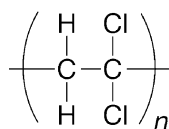
Poly(1,1-dichloroethylene)

Akihito Hashidzume
Department of Macromolecular Science,
Graduate School of Science, Osaka University,
Machikaneyama, Toyonaka, Osaka, Japan

Synonyms

Poly(vinylidene chloride); PVDC; Saran[®]

Definition

Poly(1,1-dichloroethylene) is polymer of 1,1-dichloroethylene and possesses the chemical shown in Fig. 1. It is generally called poly(vinylidene chloride) (PVDC).

Poly(1,1-dichloroethylene), Fig. 1 Chemical structure of poly(1,1-dichloroethylene) (*PVDC*)

Background

When SciFinder search for publications on "poly (vinylidene chloride)" is done, ca. 10,000 references are found as of December, 2013. Figure 2 demonstrates the numbers of references on PVDC published by year. The number of references by year commences to increase in the middle of 1950s, increases as the whole with repeating increase and decrease, and finally exceeds 400 in 2012. It is noteworthy that ca. 80 % of references on PVDC are patents, indicating that PVDC is an important polymer in industry. PVDC is homopolymer of vinylidene chloride (VDC). Because processing of PVDC is difficult due to its lack of thermal stability, copolymers rich in VDC have been widely utilized in industry. PVDC and VDC-rich copolymers are generally known as Saran[®].

PVDC was accidentally discovered by Wiley in 1933. In the early stage, PVDC was produced as a greasy, dark green film. It was utilized mainly in military uses, e.g., guard of fighter planes against salty sea spray, protection of bullets against moisture, and shoe insoles. After World War II, VDC copolymers have been widely utilized as packaging materials for foods and drugs in the forms of wrap films, multilayer films, and coated films because of the high barrier properties (see below).

This entry describes briefly production, properties, and applications of PVDC. This entry

P

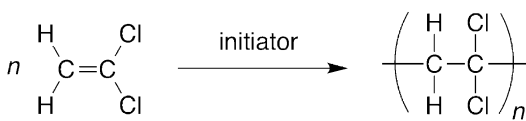**Poly(1,1-dichloroethylene), Fig. 2** The number of references published on PVDC by year
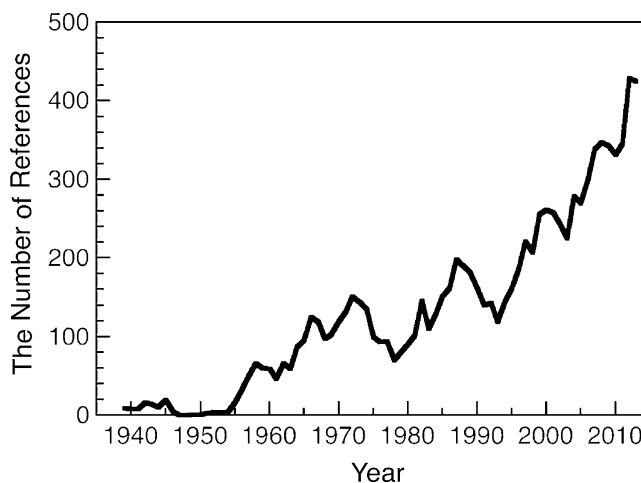
deals mainly with PVDC and partly with VDC copolymers. Readers who are interested in more details of VDC polymers can refer to an excellent comprehensive article by Wessling et al. [1].
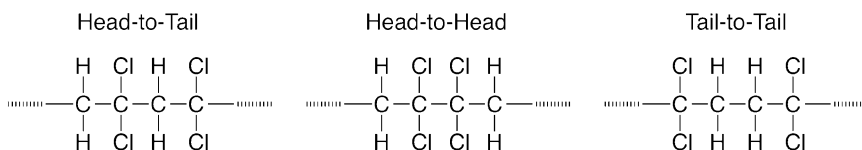
Production

PVDC is produced by polymerization of VDC (Fig. 3). VDC is polymerized by radical or anionic mechanism. Since anionic polymerization of VDC requires conditions free from moisture and oxygen and yields only PVDC of lower molecular weights, PVDC is usually prepared by radical polymerization. Because VDC possesses two chlorine atoms on a carbon atom, unlike vinyl chloride or other many vinyl monomers, PVDC does not contain any asymmetric carbons on the backbone, as can be seen in Fig. 1. Thus, the tacticity of PVDC cannot be mentioned. PVDC can be composed of head-to-tail, head-to-head, and tail-to-tail structures (Fig. 4). However, PVDC is obtained dominantly in head-to-tail fashion presumably because of the stability of propagating radical and the polarity of VDC based on the induction effect of two chlorine atoms.

VDC is copolymerized by radical mechanism with various vinyl monomers, including vinyl chloride (VC), acrylonitrile (AN), (meth)acrylates, styrene, and vinyl acetate, to form copolymers [2]. These VDC copolymers, especially with VC, AN, and (meth)acrylates, are of commercial importance.

In industry, VDC polymers are usually produced by emulsion polymerization and suspension polymerization. In emulsion polymerization, VDC and other vinyl monomers are solubilized in water using an anionic surfactant or a mixture of anionic and nonionic surfactants, and polymerization is initiated by a water soluble initiator, e.g., a redox initiating system. Emulsion polymerization of VDC yields polymers as latexes, which are sometimes used without purification. In suspension polymerization, a mixture of VDC and other vinyl monomers is dispersed in water using a stabilizer, e.g., modified cellulose, and the polymerization is initiated by a radical initiator soluble in the monomer mixture. Suspension polymerization of VDC gives polymers as small beads (150–600 μm in size).

Properties

PVDC is crystalline presumably because of the high symmetry of the chemical structure. Okuda [3] and Takahagi et al. [4] studied the crystal structure of PVDC by X-ray diffraction experiments. They reported almost the same crystal data of PVDC: the crystals are monoclinic P2$_1$ (P2$_1$ or P2$_1$/m) with lattice parameters a = 6.73 (6.71) Å, b = 12.54 (12.51) Å, c = 4.68 (4.68) Å (fiber axis), and γ = 123°35' (123 °). The number of monomer units in the unit cell is 4, and the density calculated for crystal is 1.957 (1.954) g cm^{-3}. (Here the data in parentheses were reported by Takahagi et al. [4].) The high crystallinity may be responsible for the properties of PVDC, e.g., the poor processability.

PVDC possesses high resistance to chemicals, i.e., PVDC is rather stable against acids, bases,

Poly(1,1-dichloroethylene), Fig. 3 Polymerization of VDC

Poly(1,1-dichloroethylene), Fig. 4 Head-to-tail, head-to-head, and tail-to-tail structures of diad in PVDC

Poly(1,1-dichloroethylene), Table 1 The K and a values in the Mark-Hawink-Sakurada equation determined for PVDC at 25 °C [7]

Solvent	$K/10^{-4}$ dL g^{-1}	a
NMP	1.31	0.69
TMSO	1.39	0.69
HMPA	2.58	0.65

Poly(1,1-dichloroethylene), Table 2 Permeabilities of representative permeants in PVDC [10]

Permeant	Temperature/ °C	Permeability^a/10^{-13}
He	34	0.233
N_2	30	0.000706
O_2	30	0.00383
CO_2	30	0.0218
H_2O	25	7.0

a. In cm^3 (273.15 K; 1.013×10^5 Pa) $\times$ cm/ ($cm^2 \times$ s $\times$ Pa)

and many types of chemicals. PVDC is soluble in relatively polar organic solvents, including hexamethylphosphoramide (HMPA), 1-methyl-2-pyrrolidone (NMP), tetramethylene sulfoxide (TMSO), benzonitrile, butyl acetate, 1,2-dichlorobenzene, *N*,*N*-dimethylacetamide, and *N*,*N*-dimethylformamide [5, 6]. On the other hand, PVDC is not soluble in water, alcohols, carbon disulfide, chloroform, ethyl bromide, and hydrocarbons [6]. The relationship between the molecular weight and the intrinsic viscosity of PVDC was determined for PVDC samples of a molecular weight range of $(0.8 - 12) \times 10^4$ at 25 °C using HMPA, NMP, and TMSO as a solvent [7]. The K and a values in the Mark-Hawink-Sakurada equation ($[\eta] = KM_v^a$, where $[\eta]$ and M_v denote the intrinsic viscosity and viscosity-average molecular weight, respectively) are listed in Table 1.

The mechanical properties of PVDC have been rather underexamined because it is difficult to prepare appropriate samples presumably because of the poor processability. On the basis of the high crystallinity, however, PVDC of extrusion grade shows relatively high density (1.7 g cm^{-3}), tensile strength (34.5 MPa), and tensile modulus (516.8 MPa) [8].

The glass transition temperature of PVDC of extrusion grade is -4 °C [8], and the melting point of crystal of PVDC is ca. 190–200 °C [9]. Since PVDC possesses a high content of chlorine, PVDC shows a higher flame resistance. However, when PVDC is heated above ca. 120 °C, PVDC undergoes degradable dehydrochlorination [1]. In addition, dehydrochlorination proceeds faster in polar solvents.

The most important feature of PVDC is its high barrier properties. In PVDC, the permeabilities of various gases, water, and odorous

materials are very low. These observations may indicate that PVDC possesses only pores of small free volumes presumably because of the high crystallinity and density. The permeabilities of representative permeants in PVDC are summarized in Table 2 [10].

Applications

Using the high barrier ability for gases, moisture, and odorous materials, VDC copolymers were widely applied to packaging materials, e.g., food wrapping materials, multilayer films, and coated films. VDC copolymers are also used as fibers, e.g., brushes, artificial grasses, filters for water treatment, fish nets, and doll hairs. VDC copolymers in latex form are also used as lacquer paints.

P

Related Entries

▶ Poly(Vinyl Chloride) (PVC)

References

1. Wessling RA, Gibbs DS, Obi BE, Beyer DE, DeLassus PT, Howell BA (2002) Vinylidene chloride polymers. In: Kirk RK, Othmer DF (eds) Encyclopedia of chemical technology. Wiley, New York. doi:10.1002/0471238961.2209142523051919.a01.pub2
2. Greenley RZ (1999) Free radical copolymerization reactivity ratios. In: Brandrup J, Immergut EH, Grulke EA (eds) Polymer handbook, vol 1, 4th edn. Wiley-Interscience, Hoboken, pp II/285–II/287
3. Okuda K (1964) Structures of vinylidene chloride–vinyl chloride copolymers. J Polym Sci A 2(4):1749–1764. doi:10.1002/pol.1964.100020418

4. Takahagi T, Chatani Y, Kusumoto T, Tadokoro H (1988) Molecular and crystal structure of poly (vinylidene chloride). Polym J 20(10):883–893. doi:10.1295/polymj.20.883
5. Wessling RA (1970) The solubility of poly(vinylidene chloride). J Appl Polym Sci 14(6):1531–1545. doi:10.1002/app.1970.070140611
6. Bloch DR (1999) Solvents and non solvents for polymers. In: Brandrup J, Immergut EH, Grulke EA (eds) Polymer handbook, vol 2, 4th edn. Wiley-Interscience, Hoboken, VII/505
7. Matsuo K, Stockmayer WH (1975) Solution viscosities and unperturbed dimensions of poly(vinylidene chloride). Macromolecules 8(5):660–663. doi:10.1021/ma60047a017
8. DeLassus PT, Whiteman NF (1999) Physical and mechanical properties of some important polymers. In: Brandrup J, Immergut EH, Grulke EA (eds) Polymer handbook, vol 1, 4th edn. Wiley-Interscience, Hoboken, V/165
9. Miller RL (1999) Crystallographic data and melting points for various polymers. In: Brandrup J, Immergut EH, Grulke EA (eds) Polymer handbook, vol 1, 4th edn. Wiley-Interscience, Hoboken, VI/14
10. Pauly S (1999) Permeability and diffusion data. In: Brandrup J, Immergut EH, Grulke EA (eds) Polymer handbook, vol 2, 4th edn. Wiley-Interscience, Hoboken, VI/551

Poly(acrylic acid) (PAA)

Ken Terao
Department of Macromolecular Science,
Graduate School of Science, Osaka University,
Toyonaka, Osaka, Japan

Synonyms

Poly(2-propenoic acid)

Definition

Poly(acrylic acid) (PAA) is a polymer of acrylic acid, which has a carboxylic group on each monomer unit. This polymer becomes a polyelectrolyte in water via dissociation of the acid groups.

## Chemical Structure and Synthesis

Poly(acrylic acid) (PAA) has a carboxyl group on every two carbon atoms of the main chain. It has high negative charge density when all carboxyl groups dissociate. This polymer and poly(sodium acrylate) (NaPAA) are thus one of the most abundantly used water-soluble anionic polyelectrolytes, e.g., dispersing agent, superabsorbent polymer, ion-exchange resin, etc. Furthermore, due to low toxicity, they are used as a food additive. They are synthesized industrially by radical polymerization of acrylic acid or sodium acrylic acid as shown in Fig. 1. Therefore, the molar mass distribution of the resultant polymer is broad.

PAA having narrower molar mass distribution can be synthesized by hydrolysis of a narrow-dispersed poly(*tert*-butyl acrylate) sample as shown in Fig. 2. The poly(*tert*-butyl acrylate) sample is synthesized by anionic [1] or controlled radical polymerization [2, 3]. This method makes it possible to synthesize many kinds of PAA containing block copolymers composed of polystyrene, poly(2-vinylpyridine), poly(methyl methacrylate), and poly(*n*-butyl methacrylate) [4] as well as regularly branched polymers, that is, star and comb polymers [5].

Recently, PAA samples in which dispersity index, that is, the ratio of weight-average to number-average molar mass, is ~1.1 can be purchased as research grade reagents. The abovementioned PAA and NaPAA samples are all atactic, but isotactic PAA is synthesized from isotactic poly(*tert*-butyl acrylate) [6].

Physical Properties

Both PAA and NaPAA are noncolored glass-like solid at room temperature, and the glass transition temperature of the former is 106 °C, and the latter cannot be determined directly because it is too high but can be estimated to be 230 °C from the extrapolation of copolymer data [6]. PAA is soluble in water, alkali water, alcohols, formamide, and dimethylformamide. 1,4-Dioxane and 0.2 M aqueous HCl were reported as theta solvents of
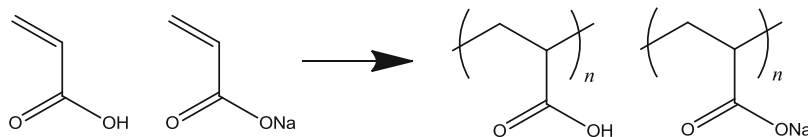
Poly(acrylic acid) (PAA), Fig. 1 Chemical structures of poly(acrylic acid) (PAA) and poly(sodium acrylate) (NaPAA)
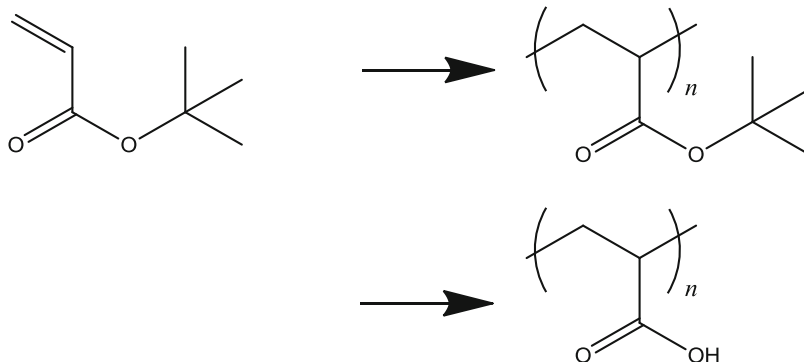
Poly(acrylic acid) (PAA), Fig. 2 Polymerization of tert-butyl acrylate and hydrolysis

PAA in which polymer chains behave as ideal chains. It should be noted that the theta solvents are classified as in between good and non-solvents. For NaPAA, 1.5 M aqueous NaBr at 15 °C and 1.12 M aqueous NaSCN at 30 °C are reported to be theta solvents [6].

Behavior in Aqueous Solution

Most of carboxyl groups of PAA do not dissociate to $-COO^- + H^+$ in water at neutral pH and in 1,4-dioxane because it is a typical weak acid as is the case with acetic acid (CH_3COOH). Since C–C bonds on the main chain are quite rotatable at room temperature, the chain structure in 1,4-dioxane is rather close to the random coil. Indeed, the characteristic ratio $C\infty$ (an indicator of polymer dimensions) is 6.7 in 1,4-dioxane at 30 °C. It should be noted that $C\infty$ is defined as $<r^2>/2n\ l^2$, where $<r^2>$ and l denote the unperturbed mean-square end-to-end distance of the polymer and the length of the C–C bond of the main chain, respectively. The degree of dissociation increases with neutralization by sodium hydroxide. Indeed, almost all the –COONa groups for NaPAA dissociate in water. NaPAA in aqueous solution behaves as a typical

polyelectrolyte, that is, one polymer chain has n negatively charged groups on each 0.25 nm of the polymer chain. Since long-range electrostatic repulsive force between two anionic groups substantially expands the polymer chains, solution viscosity is much higher than the random coil solution with the same concentration and polymer chain length. This indicates that NaPAA and/or partially neutralized PAA having high molar mass is useful as a thickening agent. In actuality, it is used in poultices to keep some medicine on the human skin.

Cross-Linked NaPAA (a Superabsorbent Gel)

If an appropriate cross-linking agent is added in the polymerization process of NaPAA or PAA, or an appropriate dose of γ-ray is irradiated to an aqueous PAA solution, the resultant polymer is no more dissolved in water, and thus, the hydrogel is obtained because the molar mass of each molecule thus prepared is extremely high; ideally, one gel particle consists of a few molecules. Even in this case, significant repulsion force arises between NaPAA part chains with adding water. This hydrogel may absorb water at most a
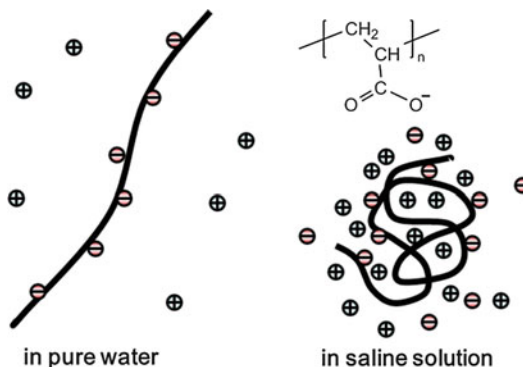
P

Poly(acrylic acid) (PAA), Fig. 3 Superabsorbent gel consisting of NaPAA with water

Poly(acrylic acid) (PAA), Fig. 4 Schematic representation of NaPAA in pure water and saline solution

thousand times of its weight (Fig. 3) depending on the degree of cross-linkage. This superabsorbent gel is used as disposable diapers, cold gels, water retention agents, and so on. Cross-linking of PAA is also used to prepare nanogels. For example, PAA nanogel can be obtained from γ-ray irradiation for PAA in water [7] or for poly(isoprene-*b*-acrylic acid) polymer micelles in water [8, 9]. In these processes using γ-ray irradiation, some PAA fragment chains abscise since hydroxyl radicals yielded by γ-ray irradiation both cross-link and disconnect the PAA chains.

Aqueous Solution with Monovalent Salt System

If the concentration of counterion (ionic strength) increases, the repulsion force and the chain dimension decrease with increasing the ionic strength as schematically shown in Fig. 4. Nagasawa et al. [10] reported ionic strength dependence of intrinsic viscosity of NaPAA in aqueous sodium chloride, where the intrinsic viscosity is an indicator of polymer dimensions. The resultant intrinsic viscosity steeply decreases with increasing ionic strength (or salt concentration). Indeed, the value for NaPAA with $M_w = 2 \times 10^6$ in 0.005 M NaCl is about 60 times larger than that in 4.17 M NaCl. In other words, solution viscosity of aqueous solution of NaPAA extremely decreases with adding salt having monovalent cation, such as Li^+, Na^+, K^+, and Cs^+. Viscosity index, the slope of double logarithmic plot of intrinsic viscosity vs. molecular weight, is 0.89 in 0.0025 M aqueous NaBr, and it decreases with increasing the concentration of NaBr and reaches 0.5 in 1.5 M solution [10]. The value of $C\infty$ was reported to be 11.1, which is a slightly larger value than that for PAA in 1,4-dioxane (6.7). This indicates that the repulsion force including electrostatic interactions between monomer units apparently disappears in 1.5 M aqueous NaBr (theta solvent); it should be noted that NaPAA solution with higher ionic strength becomes phase separated; visually the solution becomes turbid. In other words, the capacity of water in the abovementioned superabsorbent gel depends significantly on the ionic strength. Numerous theoretical works were done to explain this phenomenon, and the tendency was explained by using some approximation [11]. However, it is still difficult to explain the solution data quantitatively. One reason is that since NaPAA has very high electron density

Poly(acrylic acid) (PAA), Fig. 5 Schematic representation of stabilization of dispersion of particles. Parts of polymer chains (wavy curves) stick on the particles
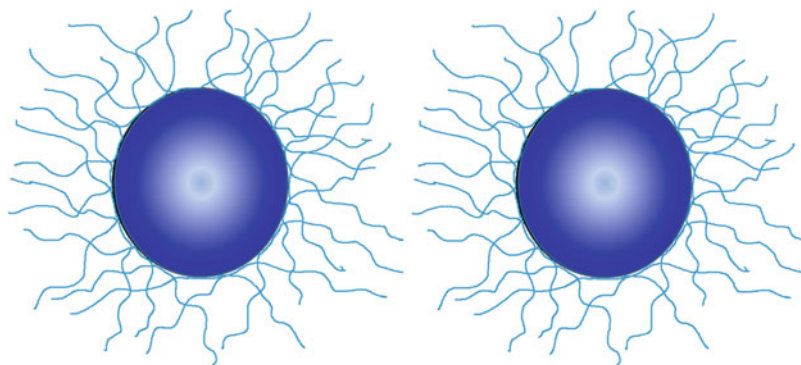
(4 nm^{-1} for NaPAA), counter ions should be located nearby the chain. This phenomenon is called the Manning condensation. For more details on this problem, see Refs. [11] and [12].

Aqueous Solution with Multivalent Salt System

Attractive interaction between anions and cations strongly depends on the valence of the salt. Thus, some multivalent cations strongly interact with anionic groups of NaPAA and stable complex may be yielded, that is, a chelation. This part usually strongly decreases the repulsion force between two NaPAA chains, and indeed with adding aqueous calcium chloride ($CaCl_2$) solution in aqueous NaPAA or PAA, hydrogel or precipitation is found even though the $CaCl_2$ solution is quite dilute, for example, molar concentration is 0.1 M. This chelating behavior is used as to remove multivalent cations such as Ca^{2+} and Mg^{2+} from aqueous systems. In actuality, NaPAA is used as detergent builder and remover of calcium carbonate scale. If the cation is a polymer, that is, polycation, such as polyvinylamine, permanent strong complex is obtained (polyion complex). Size of the complex strongly depends on the composition. Generally, precipitate of polyion complex can be obtained if the molar ratio of anionic and cationic groups is equivalent. Using this phenomenon layer-by-layer self-assembly of polyelectrolytes is well investigated. This self-assembly is applied on flat surfaces, colloidal particles, and cylindrical

systems to obtain high-performance membrane on the surface [13]. NaPAA and PAA are also adsorbed by the microparticles as shown in Fig. 5. If a sufficient number of the polymer chains are adsorbed, the particles are dispersed because of the strong repulsion force between NaPAA chains. Thus, PAA and NaPAA are used as dispersion agent.

Related Entries

▶ pH-Responsive Polymer

References

1. Ishizone T, Sugiyama K, Hirao A (2012) 3.18 – Anionic polymerization of protected functional monomers. In: Matyjaszewski K, Möller M (eds) Polymer science: a comprehensive reference. Elsevier, Amsterdam, pp 591–621
2. Satoh K, Kamigaito M, Sawamoto M (2012) 3.13 – Transition metal complexes for metal-catalyzed atom transfer controlled/living radical polymerization. In: Matyjaszewski K, Möller M (eds) Polymer science: a comprehensive reference. Elsevier, Amsterdam, pp 429–61
3. Matyjaszewski K, Spanswick J (2012) 3.12 – Copper-mediated atom transfer radical polymerization. In: Matyjaszewski K, Möller M (eds) Polymer science: a comprehensive reference. Elsevier, Amsterdam, pp 377–428
4. Kahveci MU, Yagci Y, Avgeropoulos A, Tsitsilianis C (2012) 6.13 – Well-defined block copolymers. In: Matyjaszewski K, Möller M (eds) Polymer science: a comprehensive reference. Elsevier, Amsterdam, pp 455–509
5. Yuan J, Müller AHE, Matyjaszewski K, Sheiko SS (2012) 6.06 – Molecular brushes. In: Matyjaszewski K, Möller M (eds) Polymer science:

P

a comprehensive reference. Elsevier, Amsterdam, pp 199–264

6. Brandrup J, Immergut EH, Grulke EA (1999) Polymer handbook. Wiley, New York

7. Kadlubowski S, Grobelny J, Olejniczak W, Cichomski M, Ulanski P (2003) Pulses of fast electrons as a tool to synthesize poly(acrylic acid) nanogels. Intramolecular cross-linking of linear polymer chains in additive-free aqueous solution. Macromolecules 36:2484–92

8. Pich A, Richtering W (2012) 6.09 – Polymer nanogels and microgels. In: Matyjaszewski K, Möller M (eds) Polymer science: a comprehensive reference. Elsevier, Amsterdam, pp 309–50

9. Narita T, Terao K, Dobashi T, Nagasawa N, Yoshii F (2004) Preparation and characterization of core-shell nanoparticles hardened by gamma-ray. Colloids and surfaces B. Biointerfaces 38:187–90

10. Takahashi A, Kato T, Nagasawa M (1967) The second virial coefficient of polyelectrolytes. J Phys Chem 71:2001–10

11. Nakamura Y, Norisuye T (2012) 2.02 – Polymer properties in solutions. In: Krzysztof M, Martin M (eds) Polymer science: a comprehensive reference. Elsevier, Amsterdam, pp 5–32

12. Dobrynin AV (2012) 1.05 – Solutions of charged polymers. In: Matyjaszewski K, Möller M (eds) Polymer science: a comprehensive reference. Elsevier, Amsterdam, pp 81–132

13. Seyrek E, Decher G (2012) 7.09 – Layer by layer assembly of multifunctional hybrid materials and nanoscale devices. In: Matyjaszewski K, Möller M (eds) Polymer science: a comprehensive reference. Elsevier, Amsterdam, pp 159–85

Poly(Arylene Ethynylene)s

Akshay Kokil
Center for Advanced Materials, University of Massachusetts Lowell, Lowell, MA, USA

Definition

Poly(arylene ethynylene)s are a class of conjugated polymers consisting of aromatic units connected by triple bonds.

Background

Conjugated semiconducting polymers are at the forefront in polymer science, since these materials combine the processability and mechanical properties of polymers with the readily tailored optoelectronic properties of organic molecules. The potential use of these "organic semiconductors" in light-emitting diodes (LEDs) [4, 5], field-effect transistors (FETs) [7], and photovoltaic cells [6, 17] have especially motivated the development of synthetic and processing protocols for conjugated macromolecular materials with unique field-responsive properties [11, 13, 15].

The distinctive electronic and physicochemical characteristics of conjugated polymers are governed by the nature of the polymer backbone and also by the intermolecular interactions. In the case for all classes of conjugated polymers, the field-responsive electronic as well as photophysical properties are a direct consequence of delocalized chemical bonding [14]. The overlap of p orbitals on successive carbon atoms enables the delocalization of π-electrons along the polymer backbones. The multiple atomic orbitals in the conjugated polymers translate into a large number of molecular orbitals, which form a band of energies. In a metal, this energy band is a continuum, due to a high density of electronic states with low binding energy electrons. These electrons can freely redistribute and under an applied electric field move easily from atom to atom. Hückel's theory predicts that in conjugated polymers, the π-electrons are delocalized over the entire chain. Hence, the electronic properties can also be well described by a continuous energy band. However, as a result of the Peierls instability, the density of π-electrons in conjugated organic molecules is not the same between all atoms; there is a distinct alternation between single- and multiple-bond character [14, 15]. Consequently, the electronic properties of conjugated polymers in their neutral oxidation state are usually better described by a filled conduction band (π-band, bonding) formed by the highest occupied molecular orbitals (HOMOs) and an empty valence band (π*-band, antibonding) formed by the lowest unoccupied molecular orbitals (LUMOs). Because the energy difference between the highest occupied and the lowest unoccupied
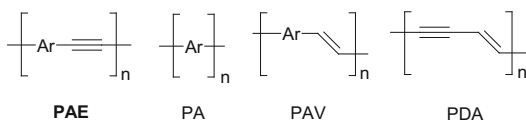
Poly(Arylene Ethynylene)s, Fig. 1 General schematic structures of poly(arylene ethynylene)s (*PAEs*), poly (arylene)s, poly(arylene vinylene)s (*PAVs*), and poly (diacetylene)s (*PDAs*)

band, referred to as band gap (E_g), is usually not near zero and because there are no partially filled bands, conjugated polymers are typically semiconductors in their undoped state. E_g depends on the molecular structure of the polymer's repeat unit and can be controlled via modification of the latter.

Among a plethora of materials platforms, poly (arylene ethynylene) (PAE) derivatives have attracted the attention of numerous research groups [1, 18]. PAEs consist of arene moieties separated by alkyne groups in the polymer backbone. The connection of these moieties results in an alternating sequence of single and multiple bonds and gives rise to π-conjugation along the macromolecules. PAEs are closely related to poly (arylene)s (PAs), poly(arylene vinylene)s (PAVs), and poly(diacetylene)s, which all represent important classes of conjugated polymers (Fig. 1) [18]. Although these materials utilize similar structural motifs, they display quite distinct electronic and photophysical properties. The chemical structure of PAEs can readily be tailored by altering the arene moiety, the connectivity (e.g., *meta* vs. *para* substitution), the introduction of heteroatoms or metals, the nature of solubilizing side chains, and the non-covalent interactions with metals. The possibility to integrate conjugated moieties other than arylenes and ethynylenes (e.g., vinylene groups, nonconjugated aliphatic spacers, etc.) represents another synthetic tool, which leads to PAE copolymers. These structural changes allow one to tailor the property matrix of these polymers over a wide range. Numerous PAEs and PAE copolymers have been reported in the last few decades, and this family of materials has established itself as an important class of conjugated polymers with interesting electronic and photophysical properties.

Synthetic Protocols

The most utilized protocol for synthesis of poly(arylene ethynylene)s employs the Heck–Cassar–Sonogashira–Hagihara palladium-catalyzed cross-coupling reaction – widely utilized for $C(sp^2) - C(sp)$ bond formation – between an aromatic diyne and an aromatic dihalide (Fig. 2) [1, 18]. This synthetic protocol is versatile and is compatible with a variety of functional moieties. The reactions yield good results when performed in an organic base such as diisopropylamine, triethylamine, or piperidine as cosolvent and $(PPh_3)_2PdCl_2$ or $(PPh_3)_4Pd$ as the catalyst. The use of CuI as cocatalyst accelerates the reaction, and lower reaction temperatures are made possible. Although the precise reaction mechanism is still unknown, the widely accepted mechanism involves two independent catalytic cycles, as shown in Fig. 2 [3]. The oxidized Pd catalyst is inactive, and formation of a Pd^0L_2 complex occurs in the reaction mixture. The reduction is facilitated either by the utilized ligands and solvents or by the copper acetylides (**A**).

In the first cycle, copper acetylides (**A**) are formed by abstraction of the acetylenic proton. Since the utilized amines are not basic enough for abstraction of the proton, the formation of a π-alkyne–Cu intermediate with a more acidic acetylenic proton is also possible. In the second cycle, rapid oxidative addition of the aryl halide to the Pd^0L_2 occurs. This is followed by the rate-determining transmetallation step to form the diorgano-Pd species (**B**). This species undergoes reductive elimination with the formation of $C(sp^2) - C(sp)$-coupled product and regeneration of the active Pd catalyst. The reactivity of the aryl halides for the reaction is aryl iodide > aryl triflates ≥ aryl bromides ≫ aryl chlorides. Iodoarenes are thus preferred candidates for the cross-coupling reactions. Since the active Pd catalyst is an electron-rich species, electron-withdrawing substituents on the aryl halide improve the reaction rate and yield. By performing the reaction in an emulsion, nanoparticles of PAEs can also be synthesized. PAEs containing organometallic complexes in
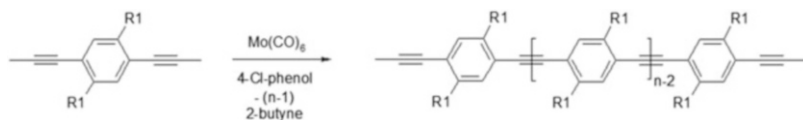
P

Poly(Arylene Ethynylene)s,
Fig. 2 Synthetic scheme for Heck–Cassar–Sonogashira–Hagihara Pd-catalyzed synthesis of PAEs (*top*) and the reaction mechanism (*bottom*)
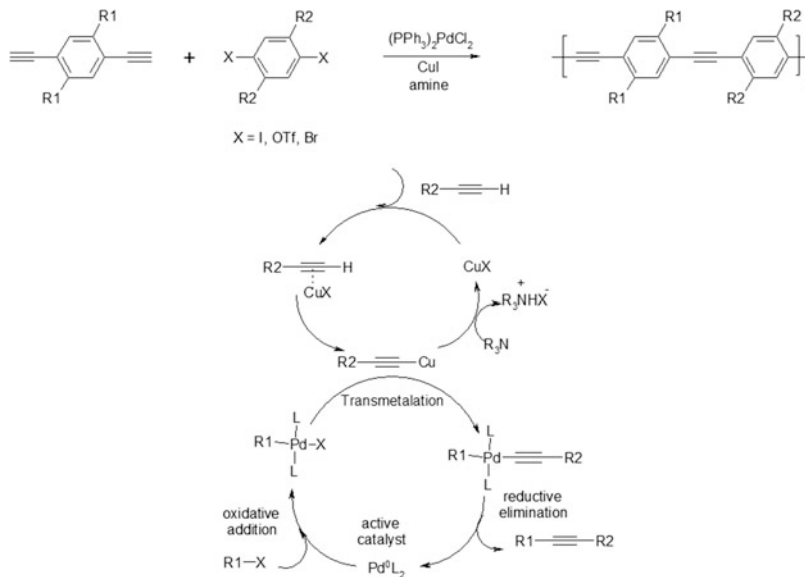
Poly(Arylene Ethynylene)s,
Fig. 3 ADIMET synthesis of PAEs

the backbone are synthesized using this protocol. The use of a trifunctional monomer in conjunction with the bifunctional monomers affords cross-linked and hyperbranched PAEs. Water-soluble PAE-conjugated polyelectrolytes (CPEs) can also be synthesized using this protocol. Typical ionic groups in the side are carboxylates (CO_2^-), sulfonates (SO_3^-), phosphonates (PO_3^{2-}), and quaternary ammonium (NR_3^+). Although this reaction protocol is suitable for a variety of functional moieties, exposure of the reaction mixture to oxidative agents or air leads to formation of butadiyne defects and side products through Glaser coupling of the terminal alkynes.

High-molecular-weight PAEs with well-defined end groups can also be synthesized using acyclic diyne metathesis polymerization (ADIMET, Fig. 3) [1,18,19]. A Mortreux-type catalyst system ($Mo(CO)_6$ and 4-chlorophenol or 2-fluorophenol) is typically utilized for the synthesis at elevated temperatures

(130–150 °C). In a typical ADIMET protocol, the polymerization of dipropynylarene under the reaction conditions occurs due to in situ formation of Schrock-type molybdenum carbyne intermediate as the active catalyst affording the PAE and a side product 2-butyne. Although this strategy affords high-molecular-weight and well-defined PAEs, it is highly sensitive to the nature of the utilized arene and works well for hydrocarbon moieties. However, sluggish reaction rates are observed for heteroatom-containing monomers systems. PAE macrocycles are also synthesized using this synthetic protocol.

Controlled catalyst transfer polycondensation can also be utilized for the synthesis of well-defined PPEs with relatively low dispersities [10]. Mechanistically, this type of polycondensation is similar to the Pd-catalyzed cross-coupling discussed above. However, in this case, the oxidative addition of the catalyst occurs intra-chain. This consequently gives rise to the "living" chain-growth-type characteristics of the obtained polymers.

Structure and Properties of PAEs

The oligomeric PPEs are rigid rods in solution, and their molecular weights determined by gel permeation chromatography (GPC) are overestimated by a factor of around 2. However, for higher molecular weight PPEs, the polymer chains in solution are not rigid rods. High-molecular-weight PPEs rather have conformations between a random coil and a rigid rod. A typical PPE displays a persistence length of around 15 nm [1, 18]. This means that short oligomeric segments in the PPE chain act as rigid rods, and the polymer chain is random coil comprised of these rigid segments. Upon complete reduction of the triple bonds in PPE, the number average molecular weight determined using GPC is reduced by a factor of around 1.4, which indicates a conformation change to that of a flexible coil.

PAEs are typically wide-band gap semiconductors and display absorption maxima in the 350–550 nm range in solution [1, 18]. Typically, it has been observed that electron-donating substituents induce a bathochromic (red) shift in the absorption spectra. On the other hand, electron-withdrawing substituents do not have a significant effect on the absorption spectra. The utilization of electron-poor monomers in conjunction with electron-rich comonomers affords donor–acceptor-type PAEs which display marked shift in the absorption maximum (>490 nm) [1, 18]. Due to a disruption in the conjugation, meta-linked PAEs display a hypsochromic (blue) shift in the absorption maximum as compared to their para-linked analogues. The optical properties of the meta-linked PAEs are dependent on the utilized solvent as the polymer conformation can significantly change from a random coil to a helix. In solution, the PAE repeat units can readily rotate around the alkyne moiety because of the low barrier of around 1 kcal/mol. In the solid state, a bathochromic shift in the absorption maximum is observed for the PAEs due to the coplanarization of the arene moieties. As an exception, for PAEs with bulky substituents, the red shift in the solid-state absorption maximum is relatively modest due to sterically induced coplanarized backbones in the solution.

The PAEs are known for their high fluorescence quantum yields, which make them a good candidate for a variety of applications. These polymers display quantum yields as high as 0.86 in solution and 0.36 in solid state [1, 18]. Typically, the PPEs with alkoxy or alkyl side chains display a yellowish-green fluorescence. However, for PAEs containing donor and acceptor moieties, the emission maximum can be significantly red shifted. The meta-linked PAEs display a blue-shifted photoluminescence owing to the loss in conjugation. Anionic and cationic CPEs with the same backbone display similar photophysical properties. The absorption and emission characteristics of the CPEs however are dependent on the nature of the solvent. Typically, the CPEs are soluble in polar organic solvents, however, start aggregating in water causing a bathochromic shift in the absorption maximum and quenching of fluorescence [8].

Although the optical properties of PAEs have been extensively investigated, the electronic properties of PAEs have received limited attention. PPEs display high ambipolar charge transport. PPEs with ethylhexyloxy and octyloxy side chains display hole and electron mobilities of the order of 10^{-3} cm^{2}V^{-1} s^{-1}. The charge transport in conjugated polymers occurs via intra-chain and inter-chain charge transport. The inter-chain charge transport is significantly lower that intra-chain charge transport for a typical disordered system. PPE–Pt^0 networks cross-linked by the coordination of the zerovalent Pt with two alkyne moieties display ambipolar charge carrier mobilities an order of magnitude higher (10^{-2} cm^{2}V^{-1} s^{-1}) than the linear polymers at low fields [9]. Electrical conductivity is one of the distinct properties of conjugated polymers. Chemical and electrochemical doping of the PPEs has resulted in electrical conductivities around 70 Scm^{-1} upon doping with SO$_3$ vapors [18].

The exciting photophysical properties of PAEs have enabled their applications as active materials in optoelectronic devices and sensors.

P

Organic Light-Emitting Diodes

The high fluorescence quantum yields in solution and solid state as well as their good photostability makes PAEs excellent candidates for application in LEDs. These devices consist of a thin film of the organic semiconductor sandwiched between a transparent anode (typically indium-doped tin oxide layer) and a metallic cathode having dissimilar work function. The built-in field (difference in the electrode work functions) gives rise to the diode device characteristics.

Upon application of an external field, holes and electrons are injected into the organic semiconductor. These can combine to give a singlet excited state, similar to the one created during photoluminescence. Emission of a photon can occur upon symmetry permitted relaxation to the ground state. This phenomenon of nonthermal emission of a photon is termed as electroluminescence (EL). PPEs containing alkoxy side chains display yellowish-green electroluminescence ($\lambda_{max} = 532$ nm, Fig. 4) with a high onset voltage (10 V) and brightness up to 80 cd/m^2 [18]. The low-lying HOMO of the PPEs hinders efficient hole injection into the active layer. The utilization of a hole transport layer as well as an electron transport layer improves the device performance with a significantly lower 4.5 V onset voltage and considerably higher brightness of 257 cd/m^2. The PPE–PPV copolymers also display similar EL characteristics as the PAE devices. The emission maximum from the LED can be tuned by altering the functional groups in the polymer backbone. A number of heteroaromatic
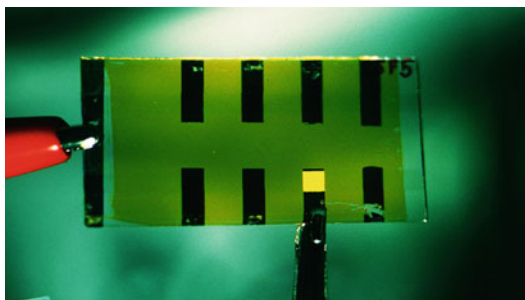
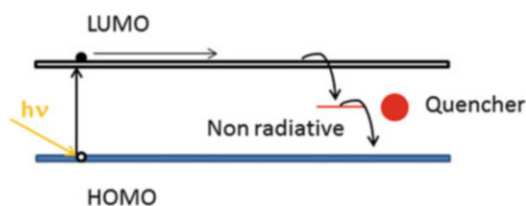**Poly(Arylene Ethynylene)s, Fig. 4** Photograph of a working ITO/ethylhexyloxy-octyloxy PPE/Al LED

comonomers have been incorporated in the PPE backbone, and each displays a distinct LED device performance which is closely related to the photoluminescence properties of the polymer. Electron-rich and electron-poor comonomers which form a donor–acceptor-type PPE typically display a bathochromic shift in the EL due to aggregation and excimer formation. Meta-linked PPEs display blue EL due to the reduced conjugation. Although the device performance is inferior to the LEDs fabricated with PPVs or polyfluorenes, PPE devices display superior stability. PPEs blended in a nonconjugated host polymer can be oriented in a specific direction by orientation of the matrix polymer. These oriented PPEs then display plane-polarized photoluminescence and can be utilized in twisted nematic liquid crystalline displays. Polarizing energy transfer from an unoriented dye to the oriented PPE doped in a host polymer can also be achieved for improving the emission characteristics of the system.
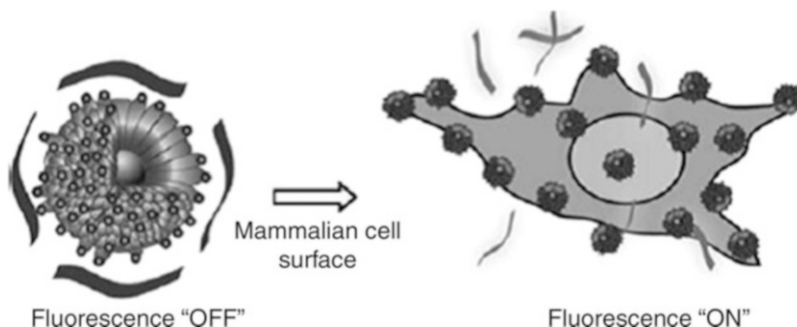
Chemosensing and Biosensing

The excellent photophysical properties coupled with ready tailorability of the polymer backbone and processability renders PAEs as ideal candidates for applications in a variety of sensors [16]. The exciton (electron hole-bound pair) generated upon absorption of a photon can relax back to the ground state through various radiative and non-radiative relaxation pathways. In the presence of a moiety with higher electron affinity, this electron can be transferred to it. This photoinduced electron transfer leads to a quenching of the photoluminescence and is employed in fluorescence "turn-off" sensors. On the other hand, the increase in photoluminescence upon interaction with a moiety is employed in fluorescence "turn-on" sensors. For a solution of luminescent organic dyes, multiple interactions with the analyte are necessary for effective fluorescence quenching of the solution. In conjugated polymer as the electrons are delocalized over the entire polymer chain, a single interaction with the analyte is capable of quenching the fluorescence of the whole

chain (Fig. 5) [12]. This significant amplification in fluorescence quenching was first exemplified using cyclophane containing PPEs as the sensing element and paraquat as the analyte. This concept was then applied for sensitive detection of explosive nitroaromatic compounds such as 2,4-dinitrotoluene (DNT) and 2,4,6-trinitrotoluene (TNT). PAEs containing three-dimensional bulky pentiptycene moieties display highly sensitive reversible detection of DNT and TNT. The bulky pentiptycene moieties reduce the π-stacking of PPEs in solid state and enhance the sensitivity. A number of PAE derivatives have been developed and utilized for chemosensing of various analytes [18]. The sensors based on conjugated polymers for detection of explosive vapors have matured into commercially available sensor modules that are deployed in field.

By incorporation of a variety of ligands in the side chains as well as the main chain of PAEs, sensing of metal ions is made possible. The coordination of the metal ions with the ligand introduces a trap state which leads to quenching of the fluorescence. The ability of metals for quenching the photoluminescence is employed in "turn-on" sensors for detection of a variety of biological analytes. This is achieved through indicator displacement assays (IDAs), where anionic PAEs electrostatically deposited on a metal nanoparticle display fluorescence quenching [2]. Upon introduction of a biological analyte to the assay, the PAEs are displaced by the biological moiety. The solubilized PAEs display a fluorescence signal for the subsequent detection (Fig. 6). This strategy is utilized for detection of proteins; distinguish between healthy, metastatic, cancerous, and murine mammalian cells; as well as differentiate between different species and strains of bacteria. CPEs are also utilized for turn-on detection of peptide sequences as well as turn-off enzyme assays [8].

Organic Photovoltaic Devices

Efficient photovoltaic performance requires materials with broadband absorption spanning the visible and near infrared region of the solar spectrum, high charge carrier mobilities, and optimal frontier molecular orbital energy levels along with other important morphological requirements. PAEs display high charge carrier mobilities, and the polymer backbone can be readily tailored. However, PAEs typically display wide-band gaps which have resulted only in modest efficiencies in bulk heterojunction solar cells. Recently, CPEs are

Poly(Arylene Ethynylene)s, Fig. 5 Band diagram depicting photoinduced electron transfer to the quencher molecule resulting in fluorescence quenching

Poly(Arylene Ethynylene)s, Fig. 6 Schematic depiction of fluorophore-displacement cell-detection array. Displacement of quenched fluorophore polymer (*dark strips*, fluorescence off; *light strips*, fluorescence on) by a cell with concomitant restoration of fluorescence

being utilized as sensitizers in dye-sensitized solar cells with iodide/triiodide as the redox couple [8]. For un-optimized devices, a 0.6 V open-circuit voltage, 2.7 mA/cm^2 short-circuit current density, and 0.9 % power conversion efficiency are obtained.

Summary

Over the past few decades, PAEs have matured into an important class of conjugated polymers. The ready tailorability of the polymer structure for obtaining diverse field-responsive characteristics makes this class of materials highly attractive. PAEs are at the forefront in research of display, chemosensor, and biosensor technologies. PAE-based conjugated polyelectrolytes are also interesting class of materials. With recent application in photovoltaic cells, the utilization of PAEs in optoelectronic devices other than LEDs has just begun. Further applications in organic electronics are still waiting to be realized. Using the facile synthetic protocols and a modular approach, many exciting possibilities for the synthesis of functional and application-specific unique structures of PAEs await.

References

1. Bunz UHF (2000) Poly(aryleneethynylene)s: syntheses, properties, structures, and applications. Chem Rev 100:1605–1644
2. Bunz UHF, Rotello VM (2010) Gold nanoparticle–fluorophore complexes: sensitive and discerning "Noses" for biosystems sensing. Angew Chem Int Ed 49:3268–3279
3. Chinchilla R, Nájera C (2007) The sonogashira reaction: a booming methodology in synthetic organic chemistry. Chem Rev 107:874–922
4. Greiner A, Weder C (2003) Light-emitting diodes. In: Kroschwitz JI (ed) Encyclopedia of polymer science and technology, 3rd edn. Wiley, New York
5. Grimsdale AC, Chan KL, Martin RE, Jokisz PG, Holmes AB (2009) Synthesis of light-emitting conjugated polymers for applications in electroluminescent devices. Chem Rev 109:897–1091
6. Hagfeldt A, Boschloo G, Sun L, Kloo L, Pettersson H (2010) Dye sensitized solar cells. Chem Rev 110:6595–6663
7. Horowitz G (1998) Organic field effect transistors. Adv Mater 10:365–377
8. Jiang H, Taranekar P, Reynolds JR, Schanze KS (2009) Conjugated polyelectrolytes: synthesis, photophysics, and applications. Angew Chem Int Ed 48:4300–4316
9. Kokil A, Shiyanovskaya I, Singer KD, Weder C (2002) High charge carrier mobility in conjugated organometallic polymer networks. J Am Chem Soc 124:9978–9979
10. Kang S, Ono RJ, Bielawski CW (2013) Controlled catalyst transfer polycondensation and surface-initiated polymerization of a pphenyleneethynylene-based monomer. J Am Chem Soc 135:4984–4987
11. Mark JA (ed) (1996) Physical properties of polymers handbook. American Institute of Physics, New York
12. McQuade DT, Pullen AE, Swager TM (2000) Conjugated polymer-based chemical sensors. Chem Rev 100:2537–2574
13. Nalwa HS (1996) Handbook of organic conductive molecules and polymers. Wiley, New York
14. Roth S, Caroll D (2004) One-dimensional metals, 2nd edn. Wiley, Weinheim
15. Skotheim TA, Reynolds JR (eds) (2007) Handbook of conducting polymers, 3rd edn. CRC Press, Boca Raton
16. Thomas SW, Joly GD, Swager TM (2007) Chemical sensors based on amplifying fluorescent conjugated polymers. Chem Rev 107:1339–1386
17. Thompson B, Fréchet JMJ (2008) Polymer-fullerene composite solar cells. Angew Chem Int Ed 47:58–77
18. Weder C (ed) (2005) Poly(arylene ethynylene)s – from synthesis to applications. Advances in polymer science series, vol 177. Springer, Heidelberg
19. Zhang W, Moore JS (2007) Alkyne metathesis: catalysts and synthetic applications. Adv Synth Catal 349:93–120

Poly(arylene-vinylene)s

Wallace W. H. Wong and James L. Banal
Bio21 Institute, School of Chemistry, University of Melbourne, Parkville, VIC, Australia

Synonyms

Light-emitting polymer; MDMO-PPV; MEH-PPV; Polymer light-emitting diode; PPV

Definition

Poly(arylene-vinylene)s are a class of luminescent polymers that has an aromatic ring (either

a simple benzene ring or heterocycles) and a vinylene unit attached as the repeat unit. They are the first class of polymers that demonstrated electroluminescence.

Introduction

Poly(arylene-vinylene)s (PAVs) are an interesting class of semiconducting polymer materials due to their luminescent properties. The first polymer light-emitting device constructed in 1990 was, in fact, derived from a PAV – poly (phenylene vinylene) (PPV) [1]. Since then, different polymers based on the arylene vinylene archetype have been developed for different purposes. Meticulous choice of a synthetic route is critical in achieving high-performance PAVs for specific applications.

Synthetic Routes for PAVs

The synthetic routes for PAVs can be classified into two widely used classes: precursor route and direct route. One of the general differences between the two routes is the solubility of the PAV that will be obtained, that is, both soluble and insoluble polymers can be obtained via the precursor route, while only soluble polymers can be obtained via the direct route. Soluble PAVs are commonly used in the fabrication of organic electronic devices due to its ease of processability. However, in multilayer devices, the use of

organic solvents for processing can cause dissolution of an already-deposited layer or polymer swelling if soluble PAVs are used. Insoluble PAVs are much preferred for such applications. Poly(phenylene vinylene) has been chosen as a prototypical PAV in all the synthetic routes that will be presented. While most of the methods that will be presented hereon can be generally used to access other PAVs, others are too harsh or substrate dependent, and, therefore, judicious choice of method is recommended.

Precursor Route

A common feature of all precursor routes is the formation of *p*-quinodimethane 2, the active propagating monomer. This intermediate is unstable but can be formed in situ from a base-catalyzed elimination of a leaving group. The nature of the leaving group depends on the type of precursor route. After the leaving group has been removed, another functional group called the polarizer is left on the monomer. This species will undergo polymerization to form the nonconjugated precursor polymer 4, with the polarizer still attached until the formation of the conjugated PAV polymer 5. While the formation of the *p*-quinodimethane intermediate was well known by spectroscopy, the polymerization mechanism was not well understood. The main dilemma was whether the polymerization proceeded via radical polymerization or anionic polymerization took a long time to be resolved (Fig. 1). It was soon realized that reaction conditions played a crucial role in determining the
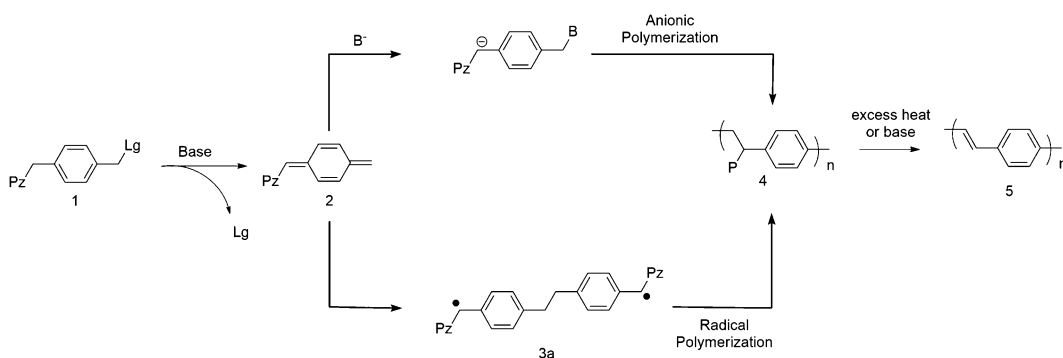
Poly(arylene-vinylene)s, Fig. 1 Simple mechanism for precursor route (*Lg* leaving group, *Pz* polarizer, *B⁻* base)
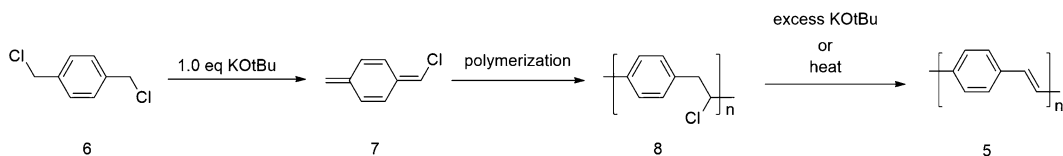
Poly(arylene-vinylene)s, Fig. 2 A general scheme for the Gilch route

polymerization pathway. The observation of a bimodal distribution of polymer molecular weights suggests that, under specific conditions, both radical and anionic polymerizations can simultaneously take place with the latter being responsible for the low molecular weight material. Appropriate control of reaction conditions can, however, let one mechanism dominate over the other.

The Gilch route (Fig. 2) proceeds by 1,6-dehydrohalogenation of a α,α'-dihalogenated p-xylene **6** with 1.0 equivalence of a strong base, such as KO^{t}Bu, to form the chlorinated p-quinodimethane **7**. Spontaneous dimerization of **7** leads to formation of biradicals, which initiates radical chain growth polymerization and gives the chloro precursor polymer **8**. Finally, excess base or high-temperature heating can form the conjugated polymer **5**. Alternatively, the addition of excess base to **6** can form the conjugated polymer without isolation of the precursor polymer, which is more attractive for industrial scale-up.

There are, however, several drawbacks using the Gilch method. Strong physical gelation commonly occurs, which can lead to insoluble polymer gels. Polymer chains can be disentangled by heating the gel at high temperatures (100 °C) for several hours. In addition, polymer backbone defects are prevalent using this method. During the polymerization propagation step of the precursor polymer, nonregioregular coupling of the monomer, i.e., tail-to-tail and head-to-head couplings (Fig. 3), forms defect sites, which can affect the optoelectronic properties of the polymer. Soluble derivatives of precursor **8**, by adding either solubilizing groups (typically long chain alkoxy or alkyl groups) on the vinylic bond or aromatic ring, are required as unsubstituted chlorine precursor polymers are generally insoluble in common organic solvents.

Since the original patent publication of the Wessling route in 1968, a number of different variations on leaving group based on the sulfonium substituent have emerged. The Wessling route uses a bisulfonium salt **7** as the pre-monomer material (Fig. 4). It can be easily accessed by substitution of tetrahydrothiophene from a α,α'-dichloro-p-xylene derivative. The polymerization mechanism for this route has been established as a radical polymerization.

There are several drawbacks in using this route. Due to the highly electrophilic character of the sulfonium group, a number of different undesirable reactions can happen, which includes premature elimination during polymerization that can lead to sp^3 defects on the polymer backbone. Electron-deficient conjugated precursors are generally not amenable for the Wessling route, which sets out restrictions to the nature of polymers that can be synthesized. The final conjugated polymer can be obtained after thermal treatment of the precursor polymer. Elimination products besides the conjugated polymer, such as hydrochloric acid, are undesirable to optoelectronic devices and, therefore, should be removed prior to device fabrication.

The sulfinyl route [2] was first developed by Vanderzande and co-workers to allow access to other PAV polymers (Fig. 5). Compared to the Gilch and Wessling routes, the pre-monomer in the sulfinyl route **9** is asymmetric and is inherently soluble in nonpolar solvents due to the presence of alkyl chains. The asymmetric nature of the sulfinyl pre-monomer allows sole formation of head-to-tail couplings during the propagation step of polymerization, and, hence, a polymer with high conjugated backbone fidelity can be obtained. The polymerization mechanism for the sulfinyl route is highly dependent on the reaction conditions and electronic nature of the
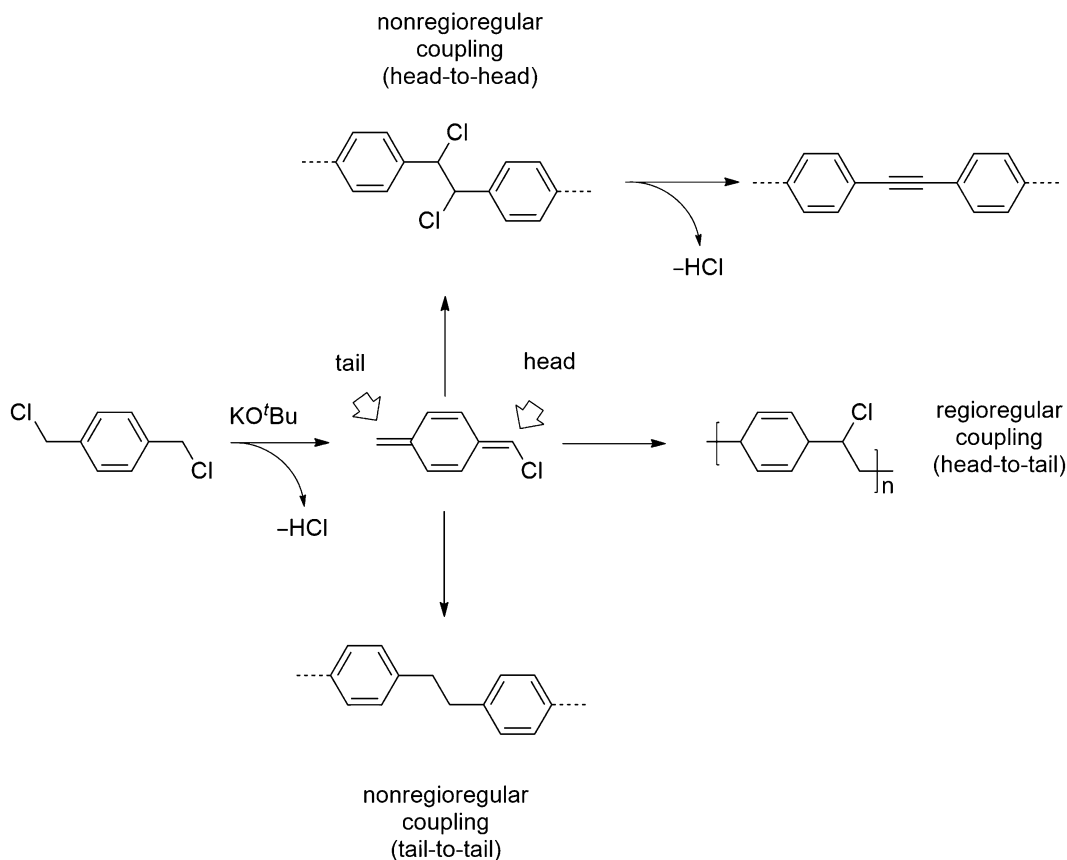
Poly(arylene-vinylene)s, **Fig. 3** Possible regiorandom couplings during Gilch synthesis
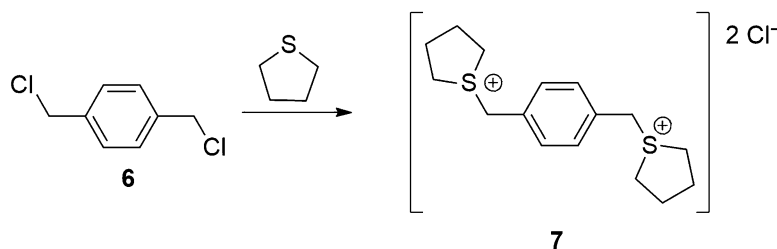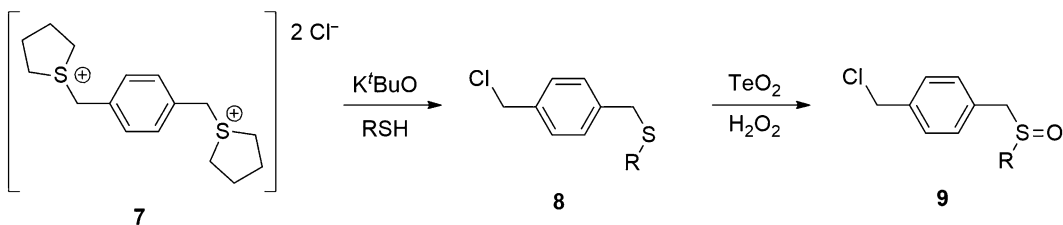

Poly(arylene-vinylene)s,
Fig. 4 The Wessling
route – towards synthesis of
bisulfonium salt

monomer. Typically, when electron-deficient or polar solvents are used, anionic polymerization becomes favored due to stabilization of the anionic intermediate in the initiation step.

A minor drawback of the sulfinyl route is the increased number of routes for the pre-monomer. The same group who developed the sulfinyl route reported a new pre-monomer that is more straightforward to synthesize than the sulfinyl route, the dithiocarbamate route **10** (Fig. 6) [3]. The earlier-mentioned drawbacks of the Gilch and Wessling routes are avoided using this method. However, it still lacks the polymer quality commonly observed when using the sulfinyl route. Another variation of the Wessling route – xanthate route **11** – was developed by Galvin and co-workers in 1995 (Fig. 6) [4]. Compared to the dithiocarbamate route, the

Poly(arylene-vinylene)s, Fig. 5 Sulfinyl derivative of the Wessling route
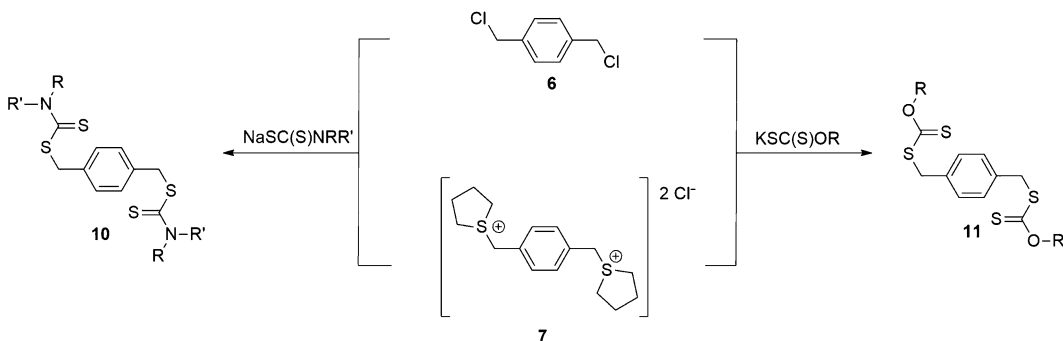
Poly(arylene-vinylene)s, Fig. 6 Dithiocarbamate and xanthate derivatives of the Wessling route

polydispersity of the polymer obtained via the xanthate route is usually broad with *cis* defects along the polymer chain, which reduces the overall effective conjugation length. While *cis* defects are usually undesirable for application where high electron mobility is of importance (e.g., transistors), it may be useful to other applications such as in LEDs where electron-hole migration should be short, which could lead to more efficient electron-hole radiative quenching and yield higher luminescence.

Direct Route

Compared to precursor routes, direct routes allow access to sp^3 and tolane defect-free polymers and alternating copolymers. Moreover, direct routes have milder conditions than precursor routes, and polymers derived from direct routes are often soluble in common organic solvents. However, molecular weights of polymers obtained by direct route are usually lower compared to precursor routes. Nevertheless, new polymers with various optoelectronic properties can be accessed using the direct route.

In principle, condensation methods involving alkenes with high preference towards the *trans* isomer should allow access to PAVs. One of the earliest condensation direct routes for poly (arylene-vinylene)s is the Wittig reaction. Symmetric dialdehydes are reacted with symmetric bis-benzylic phosphonium salts to form the required PAV. The initial PAV obtained via the Wittig route has low molecular weight with a number average molecular weight of 1,200 (~9 repeat units) and is insoluble. A known derivative of the Wittig reaction, Horner-Wadsworth-Emmons, utilizes a soluble dialkyl phosphonate as the phosphorus precursor, which allows the growing polymer to be soluble compared to the bisphosphonium precursor. Higher yields and molecular weights can then be obtained from the Horner modification. The Wittig and derivative routes are not sensitive to substituent effects, and, therefore, different derivatives with various optoelectronic properties and solubilities can be accessed with these routes. One of the drawbacks of using these routes is that only limited control can be achieved with regard to the *cis/trans*
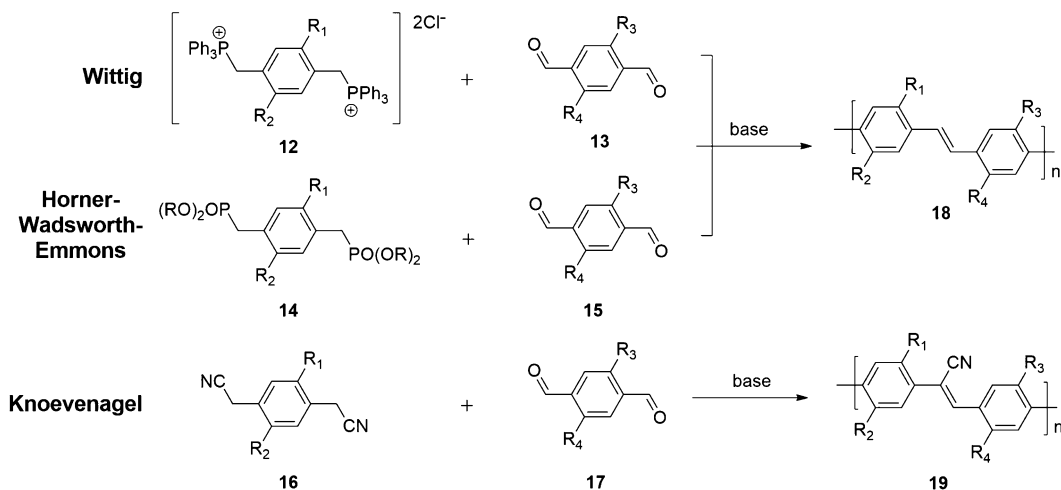
Poly(arylene-vinylene)s, Fig. 7 The Wittig, Horner-Wadsworth-Emmons, and Knoevenagel condensation routes
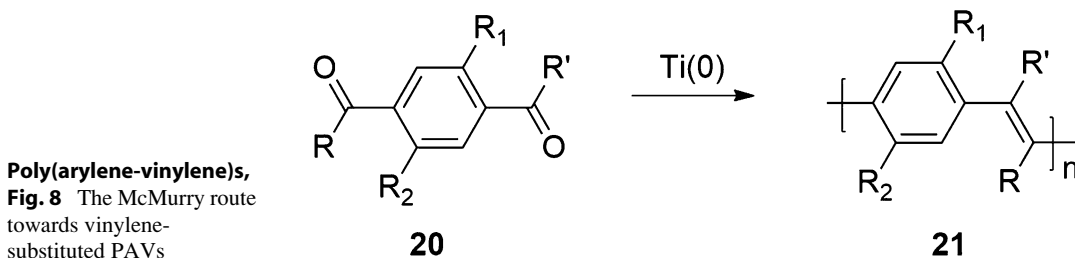

Poly(arylene-vinylene)s, Fig. 8 The McMurry route towards vinylene-substituted PAVs

content of the PAVs. The *cis* bonds can be isomerized into *trans* using iodine, but thorough dedoping of the polymer afterwards may be cumbersome. Another well-known condensation route involving alkene synthesis is the Knoevenagel condensation method (Fig. 7). However, as in the classical reaction, this route is limited to PAVs containing strong electron-withdrawing substituents, such as cyano groups on the vinylene unit.

The McMurry coupling of aldehydes and ketones under reducing conditions is a well-known methodology in alkene synthesis. Although PAVs have been successfully prepared by this route (Fig. 8), *cis* defects are unavoidable. The advantage of this methodology is that PAVs with substituents on the vinylene unit can be accessed. An obvious limitation of the McMurry methodology is that homopolymers or random copolymers of PAVs can only be achieved.

Palladium-catalyzed cross-coupling reactions have become an important toolbox for material synthesis. The Nobel Prize in Chemistry in 2010 awarded to Heck, Suzuki, and Negishi is a testament to its importance in the field of synthetic chemistry. A number of various polymers have been synthesized via Pd coupling reactions (Fig. 9). The Heck reaction was the first reported Pd-catalyzed polymerization method for PAVs. However, only a limited degree of polymerization was achieved due to poor solubility. Alkoxy substituents on the phenyl rings solubilize the growing polymer, which formed a PAV with a modest molecular weight.

While the *trans* isomer is mostly favored in the Heck reaction, *cis* and other isomers are unavoidable during the course of the reaction. Other Pd-catalyzed coupling reactions, such as Suzuki and Stille, can be utilized wherein the double bond isomerism can be perfectly controlled since the alkene precursor can be configured
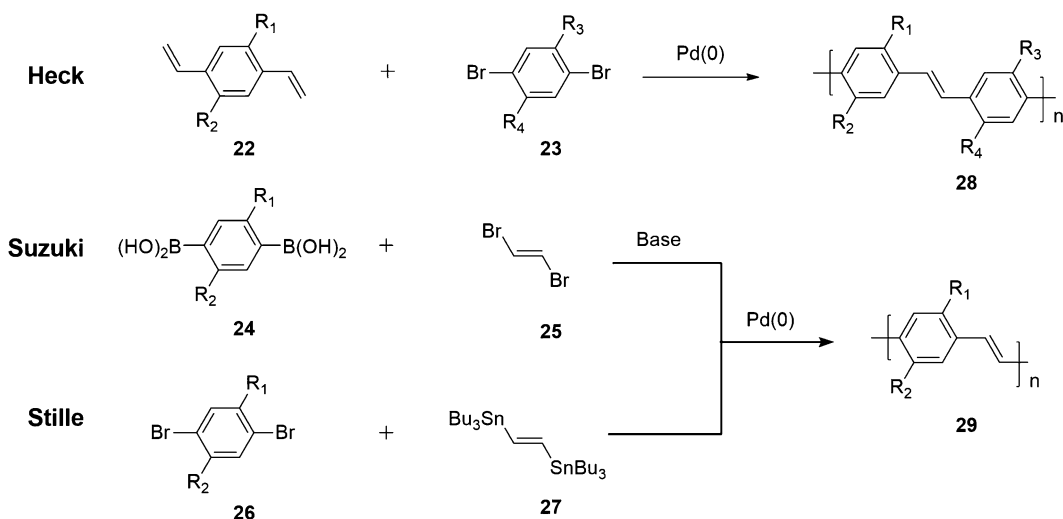
Poly(arylene-vinylene)s, Fig. 9 The Heck, Suzuki, and Stille polymerization reactions

Poly(arylene-vinylene)s, Fig. 10 Alkene metathesis reactions used in PAV synthesis
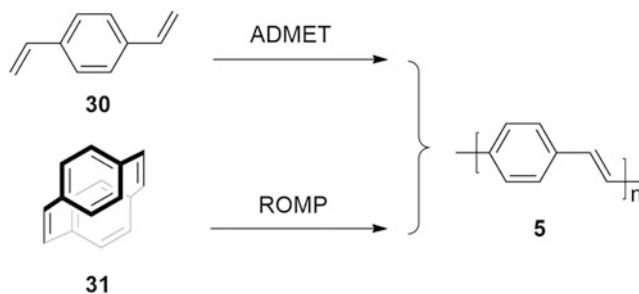
into the *trans* or *cis* isomer prior to polymerization. Cascade Suzuki-Heck reaction permits the use of easily acquired materials and decreases the amount of synthetic elaboration towards obtaining the precursors as compared to divinyl arenes. Polymerization methods involving Pd catalysts typically have two strategies – AA-/BB-type or AB-type monomer approaches. In the AB-type monomer approach, there is an inherent stoichiometric balance; therefore, polymers derived from this strategy have low polydispersity and high molecular weight. The caveat of the AB-type monomer approach is that the monomers are usually difficult to synthesize and purify. The AA-/BB-type monomer approach is commonly used due to its synthetic accessibility, but careful control of stoichiometric balance is required to obtain high molecular weight polymers with reasonable polydispersity.

Other important transition metal-catalyzed polymerization reactions are alkene metathesis reactions. Similar to palladium cross-coupling reactions, a Nobel Prize in Chemistry was awarded to Grubbs, Schrock, and Chauvin in 2005. Ring-opening metathesis polymerization (ROMP) and acyclic diene metathesis (ADMET) have both been used towards the synthesis of PAVs (Fig. 10).

The preparation of PPV via ADMET polymerization was first demonstrated by Kumar and Eichinger [5]. ADMET polymerization allows the synthesis of PAV with reasonable molecular weights as long as there is a right combination between catalyst and reaction conditions. The choice of which is not a trivial matter as different ADMET catalysts have different *trans-cis* preference ratios. Another useful alkene metathesis polymerization for PAV synthesis is ROMP.

Grubbs and co-workers [6] first reported the successful synthesis of PAV with high molecular weight and narrow polydispersity using ROMP. Since then, a number of different monomer precursors have been synthesized to adjust the molecular weight and polydispersity of the resulting PAV. However, one of the major drawbacks of this method is that the synthesis of the monomer units is tedious and requires multistep approaches; thus, it is not often used compared to other methods.

Properties of Poly(arylene-vinylene)s

PAVs have interesting optoelectronic properties that are useful for organic electronics. Fine-tuning the properties of PAVs is crucial towards developing high-performance organic electronic devices. There are several common strategies to modify the properties of PAVs. Side chains on the phenylene moiety can influence a multitude of effects including solubility, bulk morphology, and optical properties of PAVs. The prototypical poly(*p*-phenylene vinylene) (PPV; **5**) has a yellow-green fluorescence with two emission peaks at 520 and 551 nm. Appending electron-donating alkoxy groups bathochromically shifts the luminescence wavelength of PPVs (Fig. 11). The monomethoxy derivative of PPV **32** has a single maximum peak emission wavelength at 550 nm, while the dimethoxy derivative of PPV **33** emits at 603 and 650 nm. Increasing the chain length of the alkoxy group also lowers the glass transition temperature of the polymer and solubility of the polymer. Branched alkoxy chains increase the solubility of PPVs further, such as in poly[2-methoxy-5-(2-ethylhexyl)-1,4-phenylene vinylene] or MEH-PPV **34**. The position of the alkoxy substituents also affects the optical properties of substituted PPVs as in **35** and **36**. The 2,5-disubstituted PPV **35** is a red-orange emitter ($\lambda_{em} = 626$ nm) [7], while the 2,3-disubstituted PPV **36** is a green emitter ($\lambda_{em} = 513$ nm). Steric repulsions between the 2-ethylhexyl and vinylic protons in **36** force the polymer backbone to twist out of planarity, which reduces the effective conjugation length and

blueshifts the emission. The length of the alkoxy chain **37a–d** can also affect the luminescence efficiency. While photoluminescence intensity of long *n*-alkoxy chains increases linearly, the electrogenerated luminescence (EL) efficiency, however, goes through a maximum and then decreases again with longer side chains, which is due to the change in solubility and thus film homogeneity.

Similarly, aryloxy substitution can also be used to fine-tune the physical and optical properties of PPVs (Fig. 11). Aryloxy-substituted PPVs **38** and **39** redshift the emission of PPVs but not as much compared to alkoxy-substituted PPVs. Interestingly, the redshift of emission in the solid state is more pronounced in **38** than in **39**. The position of substituents for further substitution on the aryloxy side chain also affects the emission properties of aryloxy-substituted PPVs. The *ortho* **40**, *meta* **41**, and *para* **42** positional isomers of aryloxy-substituted PPVs have emission peaks at 549, 560, and 585 nm, respectively. This chromic behavior has been attributed to severe steric hindrance between the alkoxy chain attached to the aryloxy substituent and vinyl protons, which reduces coplanarity of the polymer backbone. The steric effect is pronounced in the *ortho* **36** derivative.

Thioalkyl substituents can act as a donor or acceptor depending on the oxidation state of sulfur (Fig. 12). The emission of the thiol analog of MEH-PPV **43** is blueshifted ($\lambda_{em} = 556$ nm), which suggests that thioalkyl substituents are weaker electron donors compared to alkoxy substituents. Changing the oxidation state of the sulfur like in the hexylsulfinyl-substituted PPV **44b** bathochromically shifts the emission to yellow ($\lambda_{em} = 550$ nm), which is mainly due to the intramolecular donor-acceptor interaction between the sulfinyl and alkoxy substituents, compared to the thiohexyl-substituted PPV **44a** ($\lambda_{em} = 550$ nm).

Other substituents such alkyl **45** and silyl **46** substituents do not shift the emission wavelength of PPV. They do, however, have remarkable solid-state photoluminescence ($\eta_{PL,46} = 62$ %; $\eta_{PL,47} = 60$ %) compared to unsubstituted PPV. Considering their processability as

P
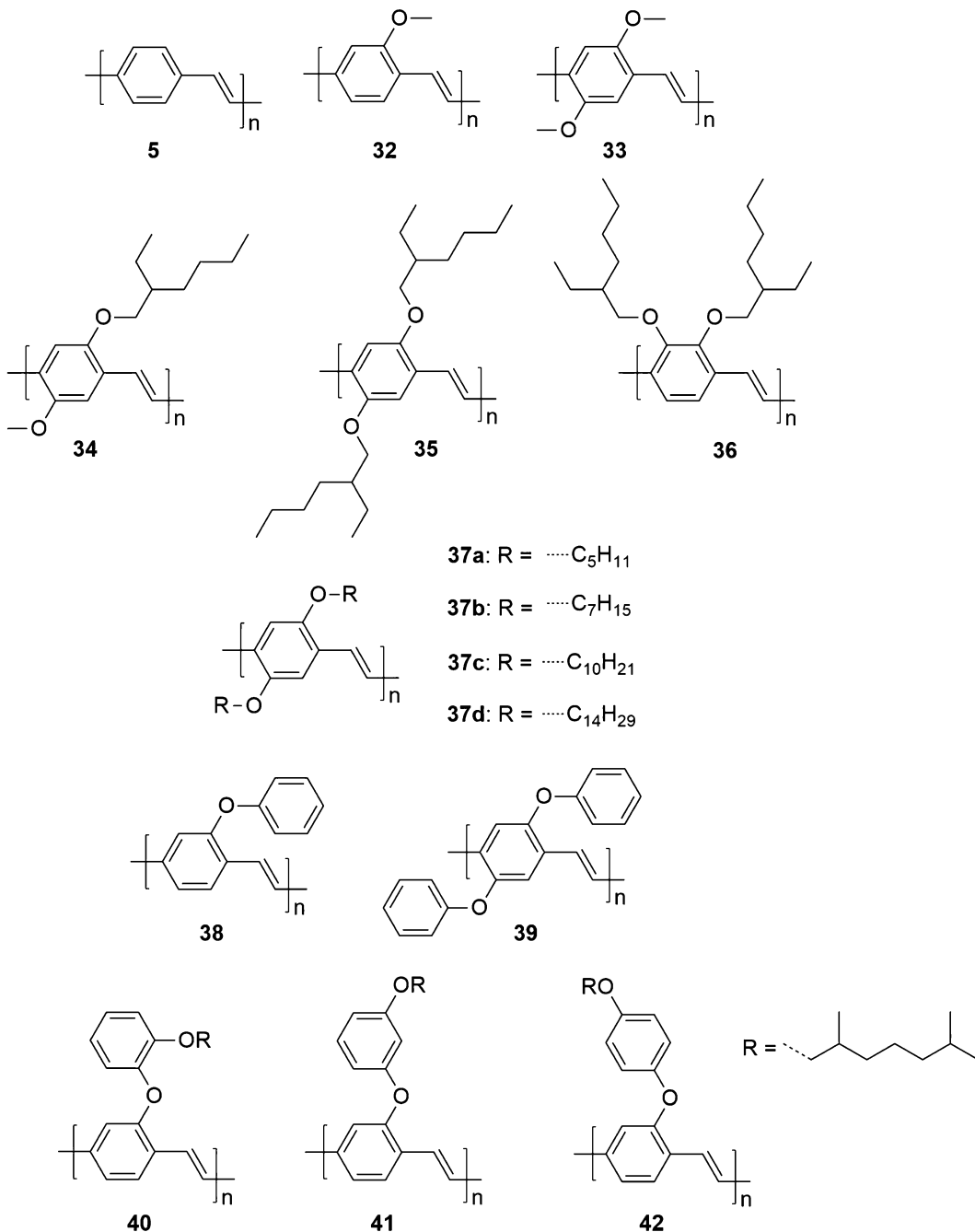
Poly(arylene-vinylene)s, Fig. 11 PAVs with various substitution patterns

compared to insoluble, intractable, and infusible unsubstituted PPV, they are more attractive materials for green-emitting light-emitting diodes. Alkylamino-substituted PPV **47** shows pH-dependent behavior, which can tune the

emission wavelength of dilute polymer solutions (Fig. 12).

Extending the π-conjugation of the phenylene ring by expanding the aromatic system is also a viable way to fine-tune the properties of PAVs (Fig. 13).

Poly(arylene-vinylene)s,
Fig. 12 2,5-substituted
PAVs with varying side
chains

44a: R = S
44b: R = SO
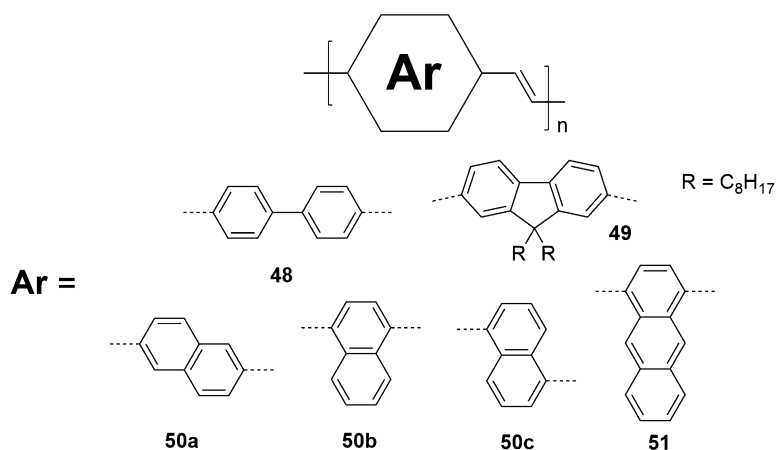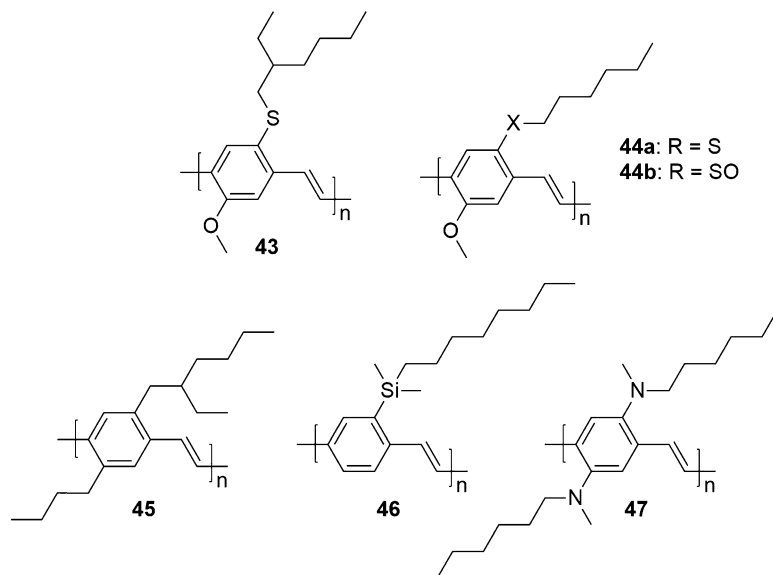
Poly(arylene-vinylene)s,
Fig. 13 PAVs with
polyaromatic hydrocarbons

Ar =

48

49

R = C_8H_{17}

50a   50b   50c   51

Polyphenylenes are known blue emitters. Thus, increasing the phenylene content in PAVs, like in poly(4,4′-biphenylene vinylene) **48** (λ_{em} = 467, 497), shifts the emission to blue-green [8]. Fastening the biphenyl rings like in poly (fluorenylene vinylene) **49** shifts the emission a little ($\lambda_{em,max}$ = 507 nm) [9]. Polyaromatic hydrocarbons like naphthalene (**50a**, **50b**, **50c**) and anthracene **51** can be used instead of phenyl. Similar to PPVs, poly(naphthylene vinylene)s have substitution-dependent chromic behavior. Poly(2,6-naphthylene vinylene) **50a** has an emission maximum at 518 nm and has a green color; poly(1,4-naphthylene vinylene) **50b** has an

emission at 605 nm and has a yellow-orange color; and poly(1,5-naphthylene vinylene) **50c** has an emission at 480 nm. Interestingly, for the anthracene derivative, poly(9,10-anthracene vinylene) cannot be synthesized via the Wessling route due to extra stabilization of the p-quinodimethane in the 9,10-position. However, the p-quinodimethane at the 1,4-position is less stable, and poly(1,4-anthracene vinylene) **51**can be synthesized. The polymer **51** has a thin film emission at 590 nm.

Poly(heteroarylene vinylene)s (Fig. 14) can help bathochromically shift the emission and fine-tune the energy levels of PAVs. More

Poly(arylene-vinylene)s,
Fig. 14 PAVs with
heterocyclic cores
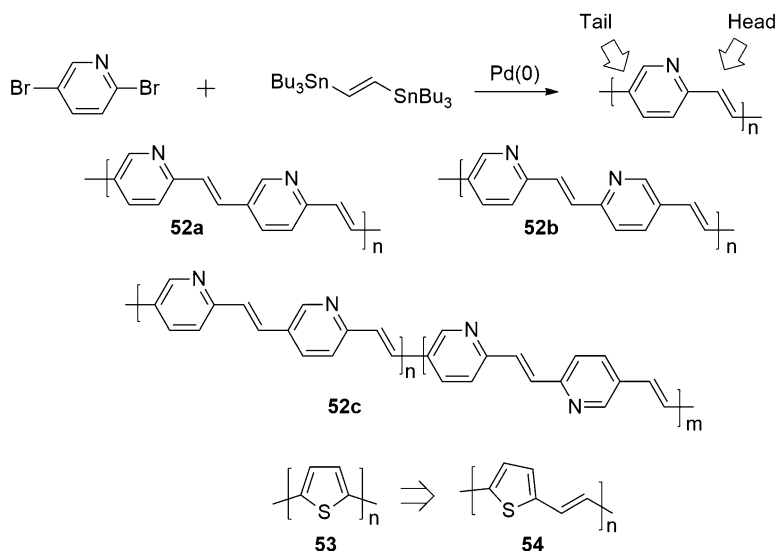
electronegative atoms such as nitrogen and sulfur can be incorporated into the PAV backbone and adjust the electron affinity of the polymer. Poly (2,5-pyridinylene vinylene)-type polymers are the well-studied class of poly(heteroarylene vinylene)s. Due to the lower symmetric nature of pyridine than phenylene, regioisomers and/or random copolymers can exist from the Stille coupling of dibromopyridine and *trans*-1,2-bis(tributylstannyl)ethene – head-to-tail **52a**, head-to-head **52b**, or random **52c**. The electrogenerated luminescence wavelength of each polymer varies – 584, 605, and 575 nm. The bathochromic shift of electrogenerated luminescence suggests that regioregular isomers have longer effective conjugated lengths compared to the random polymeric material.

Another class of poly(heteroarylene vinylene)s are poly(thienyl vinylene)s (Fig. 14). Typically, these polymers have very low electroluminescence. Poly(thienyl vinylene) **54** has a very low luminescence (even lower than its analog poly(thiophene) **53**), which is probably due to its small singlet–triplet gap, but has broad absorption which is useful for organic solar cells. Other known strategies involved in tuning PAVs include use of copolymer with different aromatic moieties and attaching conjugated chromophores as side chains. Considering the number of permutations possible, the number of polymers then

becomes too large that it is impossible to discuss all of them. Thus, a highlight of the best-performing polymers in their respective applications will be discussed from here on.

Applications of Poly(arylene-vinylene)s

One of the most prominent applications of PAVs is in polymer light-emitting diodes (PLED) (Fig. 15). Optimizing the electronic properties of the PAVs for PLED cannot be overemphasized. As mentioned previously, one well-known strategy is to use copolymers to fine-tune the electronic properties of PAVs. Using Gilch polymerization, controlling the concentration ratio of different monomers can, in principle, produce statistical copolymers. Record efficiencies have been achieved using copolymers **55a** and **55b**, which showed very high luminescence efficiencies (10.5 cd/A and 11.5 cd/A, respectively) [10].

Light-emitting diodes derived from PPVs suffer from charge injection imbalance from both the cathode and anode. The electron-accepting ability of PPVs is less efficient than their hole-accepting ability; thus, much of the synthetic efforts has been to adjust the electron affinity of PPV polymers. Electron and hole charge injection must be balanced to achieve high-efficiency
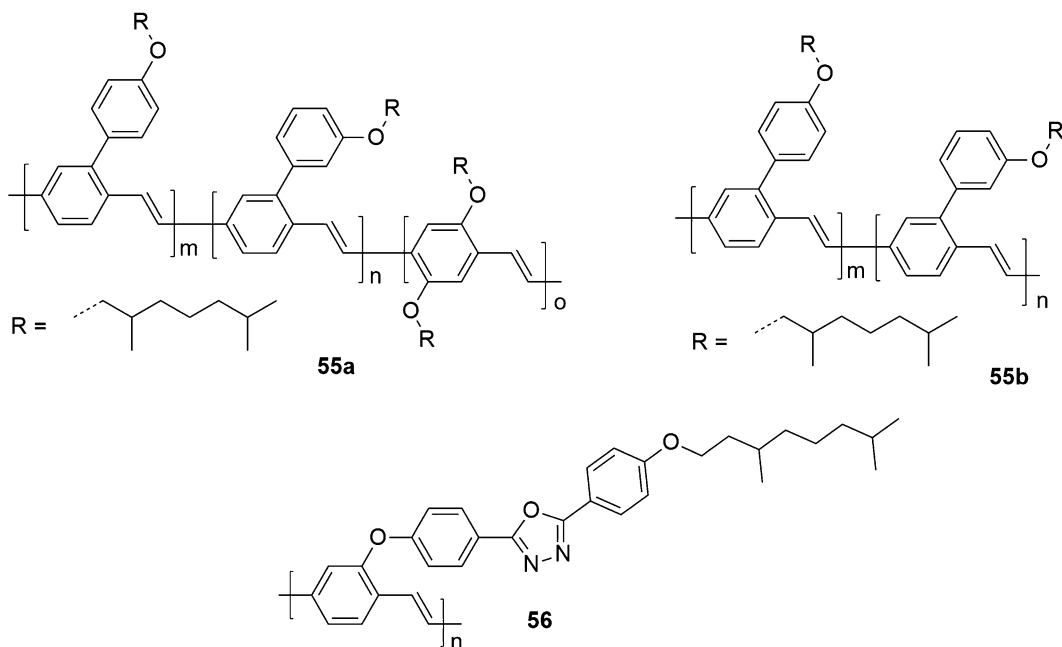
Poly(arylene-vinylene)s, Fig. 15 Structures of polymer high-performance materials for polymer light-emitting diodes

polymer light-emitting diodes. Oxadiazole pendant-bearing PPV**56** has the highest PLED efficiency reported with a luminescence efficiency of 21.1 cd/A and a turn-on voltage of 5 V. The high efficiency observed has been ascribed to a double-channel charge transport – holes along the PPV unit while electrons along the oxadiazole pendant. Thus, injected electrons easily recombine with holes [11].

Other applications for PAVs as light-emitting materials are solid-state lasers. Solid-state lasing from semiconducting polymers is an interesting application for PPVs. First reported in 1992 using MEH-PPV solution as lasing medium [12], a number of different PPV derivatives have been tested for lasing applications. Polymer **45** is promising for solid-state organic lasers due to its low energy threshold (0.2 ± 0.1 μJ/pulse) [13]. Current research impetus is towards lowering of the energy threshold for lasing, extending the wavelength coverage, improving the conversion efficiency, enhancing device lifetime, and improving beam quality and wavelength tunability [14].

Bioimaging using multiphoton fluorescence imaging incorporates polymer aggregates or "polymer dots" using MEH-PPV **34**, CN-PPV **57**, and PF-PV **58** polymers (Fig. 16). Polymer dots typically have sizes smaller than 20–30 nm, and they typically do not suffer from photoblinking and toxicity commonly observed in quantum dots. Controlling the surface functionalization in polymer dots is still a challenge [15].

Organic photovoltaic (OPV) is one of the most active research areas for organic electronics. Several PAV molecules have been used for such application (Fig. 17). MEH-PPV **34** was the first PPV-based solar cell reported using bulk heterojunction geometry using C_{60} as electron acceptor [16]. Regioregular MDMO-PPV **59** blended with phenyl-C_{61}-butyric acid methyl ester (PCBM) is the highest reported PPV-based organic solar cell with an efficiency of 3.1 %, while regiorandom MDMO-PPV **60** has only achieved 1.7 % [17]. The crystallinity of the regioregular MDMO-PPV provides a pathway for efficient hole transport

Poly(arylene-vinylene)s,
Fig. 16 Structures of PAV
polymers aggregated to
form polymer dots (Pdots)
used for bioimaging
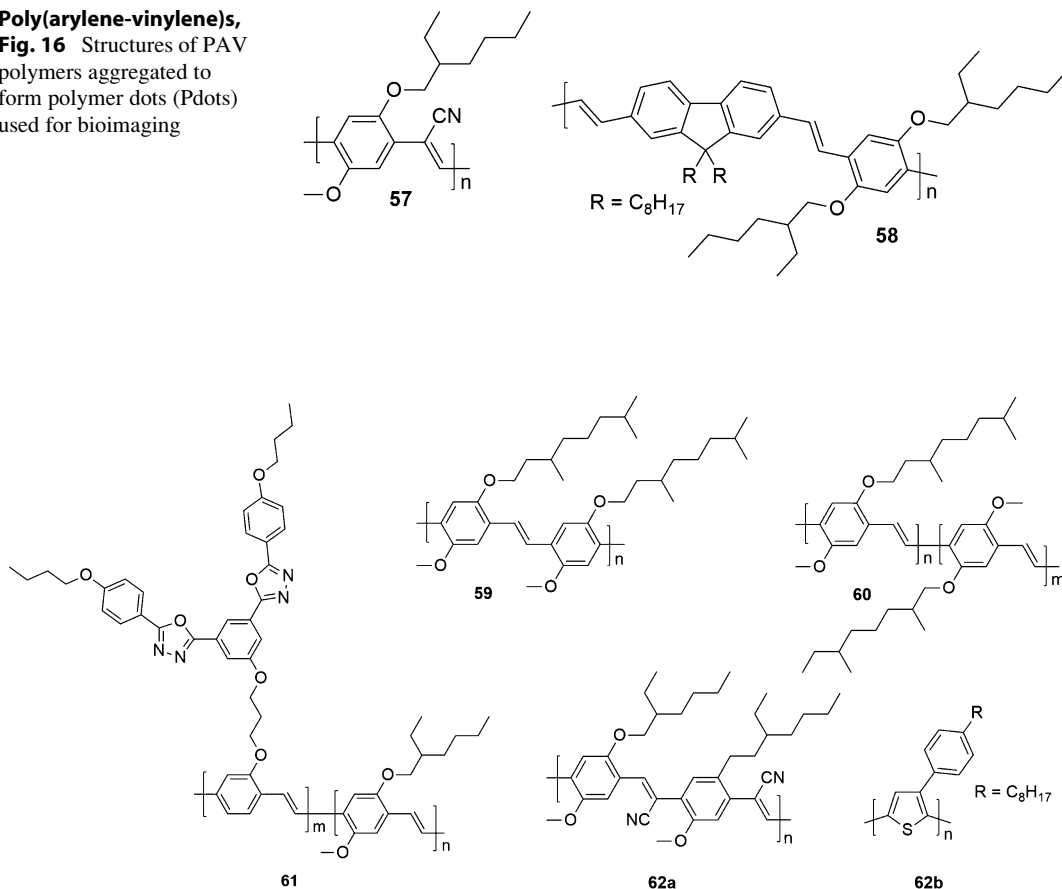
Poly(arylene-vinylene)s, Fig. 17 PAV polymers used for OPV application

towards the cathode and better mixing between
PCBM and MDMO-PPV. Balanced charge trans-
port is also crucial towards OPV devices with
high efficiencies. Conjugated side chains have
also been attached on PPVs to allow efficient
charge separation and transport through the poly-
mer:PCBM blends. Oxadiazole pendants on PPV
backbone **61** have been synthesized and gave an
efficiency of 1.6 % [18]. Attaching cyano
substituents on the PPV backbone can increase
the electron affinity of the PPVs. As a result of the
electron-withdrawing effect of cyano groups, the
resulting PPV **62a** can be a suitable
electron acceptor in lieu of PCBM. One of the
earliest demonstrated polymer:polymer solar
cells was developed using **62a** as electron accep-
tor and **62b** as electron donor in a bilayer
device [19].

Related Entries

▶ Polymers for Solar Cells
▶ Polymer Lasers and Optical Amplifiers

References

1. Burroughes JH, Bradley DD, Brown AR, Marks RN,
   Mackay K, Friend RH, Burns PL, Holmes AB
   (1990) Light-emitting diodes based on conjugated poly-
   mers. Nature 347:539–541. doi:10.1038/347539a0
2. Louwet F, Vanderzande D, Adriaensens P, Gelan
   J (1992) The synthesis of poly(1,4-phenylene-1,2-
   ethanediyl) derivatives: an adaptation of the wessling
   route. Synth Met 52:125–130. doi:10.1016/0379-
   6779(92)90025-E
3. Henckens A, Colladet K, Fourier S, Cleij TJ,
   Lutsen L, Gelan J, Vanderzande D (2005) Synthesis
   of   3,4-diphenyl-substituted   poly(thienylene
   vinylene),   low-band-gap   polymers   via   the

dithiocarbamate Route. Macromolecules 2005: 19–26. doi:10.1021/ma047940e

4. Son S, Dodabalapur A, Lovinger AJ, Galvin ME (1995) Luminescence enhancement by the introduction of disorder into poly(p-phenylene vinylene). Science 269:376–378. doi:10.1126/science.269.5222.376

5. Kumar A, Eichinger BE (1992) Synthesis of poly (1,4-phenylenevinylene) by metathesis of p-divinylbenzene. Makromol Commun Rapid Commun 13:311–314. doi:10.1002/marc.1992.030130603

6. Conticello VP, Gin DL, Grubbs RH (1992) Ring-opening metathesis polymerization of substituted bicyclo[2.2.2]octadienes: a new precursor route to poly(1,4-phenylenevinylene). J Am Chem Soc 114:9708–9710. doi:10.1021/ja00050a088

7. Andersson MR, Yu G, Heeger AJ (1997) Photoluminescence and electroluminescence of films from soluble PPV-polymers. Synth Met 85:1275–1276. doi:10.1016/S0379-6779(97)80238-X

8. Van Der Borght M, Vanderzande D, Gelan J (1998) Synthesis of high molecular weight poly(4,4′-bisphenylene vinylene) and poly (2,6-naphthalene vinylene) via a non-ionic precursor route. Polymer 39:4171–4174. doi:10.1016/S0032-3861(97)10129-X

9. Jin S-H, Kang S-Y, Kim M-Y, Chan YU, Kim JY, Lee K, Gal Y-S (2003) Synthesis and electroluminescence properties of poly(9,9-di-n-octylfluorenyl-2,7-vinylene) derivatives for light-emitting display. Macromolecules 36:3841–3847. doi:10.1021/ma0300490

10. Becker H, Spreitzer H, Kreuder W, Kluge E, Schenk H, Parker I, Cao Y (2000) Soluble PPVs with enhanced performance – a mechanistic approach. Adv Mater 12:42–48. doi:10.1002/(SICI)1521-4095(200001) 12:1<42::AID-ADMA42>3.0.CO;2-F

11. Jin S-H, Kim M-Y, Kim JY, Lee K, Gal Y-S (2004) High-efficiency poly(p-phenylenevinylene)-based copolymers containing an oxadiazole pendant group for light-emitting diodes. J Am Chem Soc 126:2474–2480. doi:10.1021/ja036955+

12. Moses D (1992) High quantum efficiency luminescence from a conducting polymer in solution: a novel polymer laser dye. Appl Phys Lett 60:3215–3216. doi:10.1063/1.106743

13. Hide F, Díaz-García MA, Schwartz BJ, Andersson MR, Pei Q, Heeger AJ (1996) Semiconducting polymers: a new class of solid-state laser materials. Science 273:1833–1836. doi:10.1126/science.273.5283.1833

14. Chénais S, Forget S (2012) Recent advances in solid-state organic lasers. Polym Int 61:390–406. doi:10.1002/pi.3173

15. Wu C, Chiu DT (2013) Highly fluorescent semiconducting polymer dots for biology and medicine. Angew Chem Int Ed 52:3086–3109. doi:10.1002/anie.201205133

16. Yu G, Gao J, Hummelen JC, Wudl F, Heeger AJ (1995) Polymer photovoltaic cells: enhanced efficiencies via a network of internal donor-acceptor heterojunctions. Science 270:1789–1791. doi:10.1126/science.270.5243.1789

17. Tajima K, Suzuki Y, Hashimoto K (2008) Polymer photovoltaic devices using fully regioregular poly[(2-methoxy-5-(3′,7′-dimethyloctyloxy))-1,4-phenylenevinylene]. J Phys Chem C 112:8507–8510. doi:10.1021/jp802688s

18. Wen S, Pei J, Zhou Y, Xue L, Xu B, Li Y, Tian W (2009) Synthesis and photovoltaic properties of poly(p-phenylenevinylene) derivatives containing oxadiazole. J Polym Sci A Polym Chem 47:1003–1012. doi:10.1002/pola.23158

19. Granström M, Petritsch K, Arias AC, Lux A, Andersson MR, Friend RH (1998) Laminated fabrication of polymeric photovoltaic diodes. Nature 395:257–260. doi:10.1038/26183

Poly(cyclic olefin)s

Takuya Isono[1] and Toshifumi Satoh[2]
[1]Division of Biotechnology and Macromolecular Chemistry, Faculty of Engineering, Hokkaido University, Polymer Chemistry Laboratory, Sapporo, Japan
[2]Faculty of Engineering, Division of Biotechnology and Macromolecular Chemistry, Laboratory of Molecular Materials Chemistry, Hokkaido University, Sapporo, Japan

Synonyms

Cyclic olefin copolymer; Cyclic olefin polymer; Cycloolefin copolymer; Cycloolefin polymer; Polycyclic olefin; Polycycloolefin

Definition

Poly(cyclic olefin), i.e., cyclic olefin polymer, is a polymer prepared from a strained cyclic olefin, such as cyclobutene, cyclopentene, cycloheptene, cyclooctene, cyclooctadiene, cyclooctatetraene, dicyclopentadiene, or norbornene, by ring-opening metathesis polymerization or vinyl addition polymerization. In order to obtain a functional olefin polymer, the copolymerizations of the cyclic olefin with ethylene, propylene, a higher 1-alkene, and polar monomer have also been studied. The cyclic olefin polymers and their

copolymers are very important industrial materials with a glass-like optical clarity, low water absorption, and good mechanical properties.

Introduction

Poly(cyclic olefin)s, such as polycycloalkene, polynorbornene (polyNB), and polydicyclopentadiene (polyDCPD), were mainly obtained by the ring-opening metathesis polymerization (ROMP) [1–5] or vinyl addition polymerization [6, 7] of a strained cyclic olefin using metal-based catalysts, as shown in Fig. 1. For example, the polymerization of norbornene (NB) using tungsten, molybdenum, ruthenium, tantalum, or vanadium catalytic system produces *cis*- and/or *trans*-polyNB through the ROMP in a living fashion, whereas the polymerization of NB using

zirconium, palladium, nickel, or chromium catalytic system produces polyNB through the vinyl addition polymerization without ring opening. The titanium and cobalt catalyst systems are interesting cases where both reactions possibly depend on the cocatalyst ratio or the type of cocatalyst [8–11]. In this entry, the results of the cyclic olefin polymerization through the ROMP and vinyl addition polymerization are summarized.

Poly(cyclic olefin)s by Ring-Opening Metathesis Polymerization

The ROMP of strained cyclic olefins has been extensively studied and some have led to commercial development, as shown in Fig. 2. One of the propagation steps in the ROMP of a cyclic olefin is shown in Fig. 3. The bond redistribution
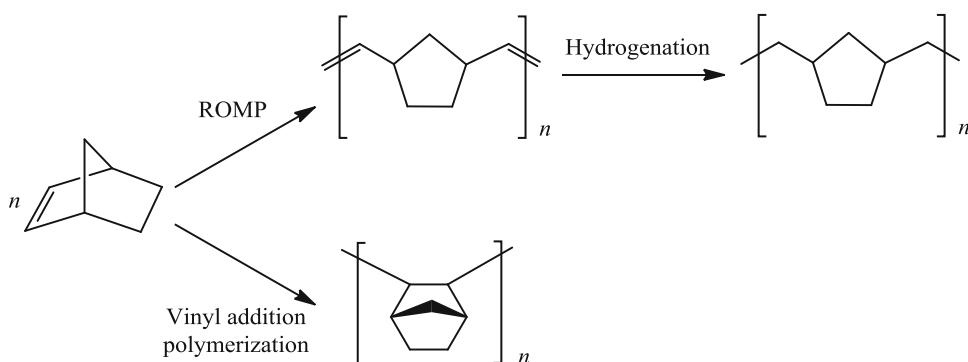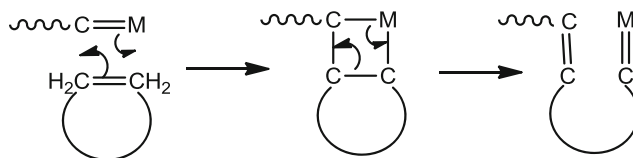

Poly(cyclic olefin)s, Fig. 1 Ring-opening metathesis polymerization or vinyl addition polymerization of norbornene
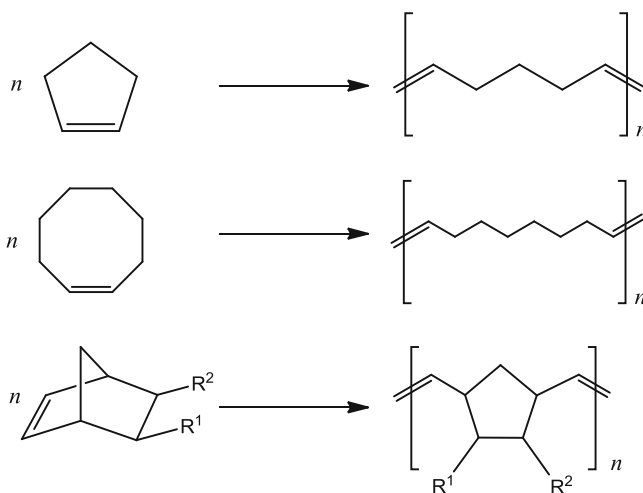
Poly(cyclic olefin)s, Fig. 2 Ring-opening metathesis polymerization of cyclopentene, cyclooctene, and norbornene

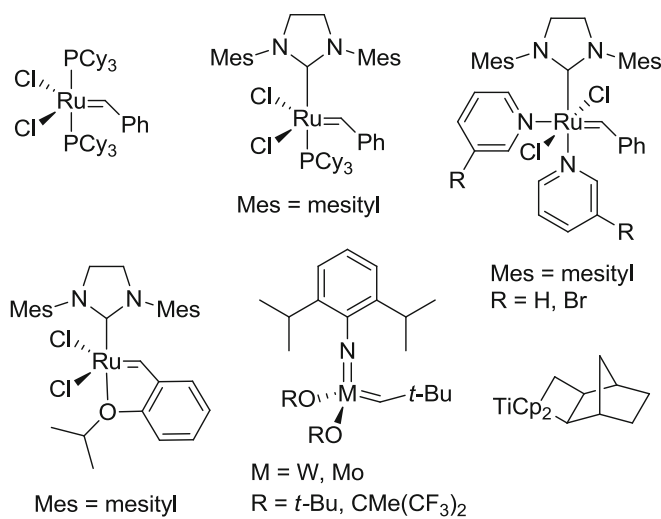**Poly(cyclic olefin)s, Fig. 3** Propagation steps in ring-opening metathesis polymerization of a cyclic olefin (*M* metal)

TiCl$_4$, VCl$_4$, VOCl$_2$, MoCl$_5$, WCl$_6$, WOCl$_4$ / Et$_3$Al, BuLi, Me$_4$Sn

Mes = mesityl

Mes = mesityl
R = H, Br

M = W, Mo
R = *t*-Bu, CMe(CF$_3$)$_2$

Mes = mesityl

**Poly(cyclic olefin)s, Fig. 4** Representative catalysts for ring-opening metathesis polymerization

during the polymerization is due to an intermediate metal carbene species that reacts with a double bond to form a transient metallacyclobutane leading to a polymer with a *cis-* or *trans*-double bond. The ROMP processes generally employ tungsten, molybdenum, ruthenium, tantalum, vanadium, or titanium catalysts, as shown in Fig. 4. The polymerization rate appears to be a function of the reactivity of the metal carbene rather than of the ring strain in the cyclic olefin. Even a relatively unstrained monomer, such as cyclohexene, will undergo the ROMP under appropriate conditions [12].

The control of the stereochemistry in the obtained polymer is possible through the choice of the reaction conditions, such as the catalyst, cocatalyst, activator, solvent, and temperature. For example, a highly *cis*-polyNB was prepared using the ReCl$_5$/EtAlCl$_2$/ethyl acrylate catalyst system, whereas the IrCl$_3$·xH$_2$O/EtAlCl$_2$ catalyst system led to *trans*-polyNB [6]. The increasing stereoregularity in the poly(cyclic olefin) can

vary thermal properties, such as the glass transition temperature (T_g) and melting temperature (T_m). For example, a polyNB lacking stereoregularity is a noncrystalline material with T_g of 35 °C, whereas a high *trans*-polyNB appears to be crystalline with T_m of 202 °C [13].

The unsaturated nature of polyNB caused the low thermal stability as a consequence of oxidative degradation, which makes polyNB difficult to be used for molding process. This problem can be overcome by saturating the polyNB through either catalytic hydrogenation or non-catalytic diimide method leading to a hydrogenated polyNB consisted of alternating ethyl and cyclopentyl repeating units. The physical properties of the hydrogenated polyNB are quite different from those of polyNB. For example, polyNB is an amorphous material with T_g of 35 °C, while hydrogenated polyNB is a crystalline with an equilibrium T_m of 156 °C [14]. The hydrogenated polyNBs prepared from NB derivatives having substituents at 2- and/or 3-positions (R^1 and R^2,

P

Poly(cyclic olefin)s,
Fig. 5 Ring-opening
metathesis polymerization
of dicyclopentadiene
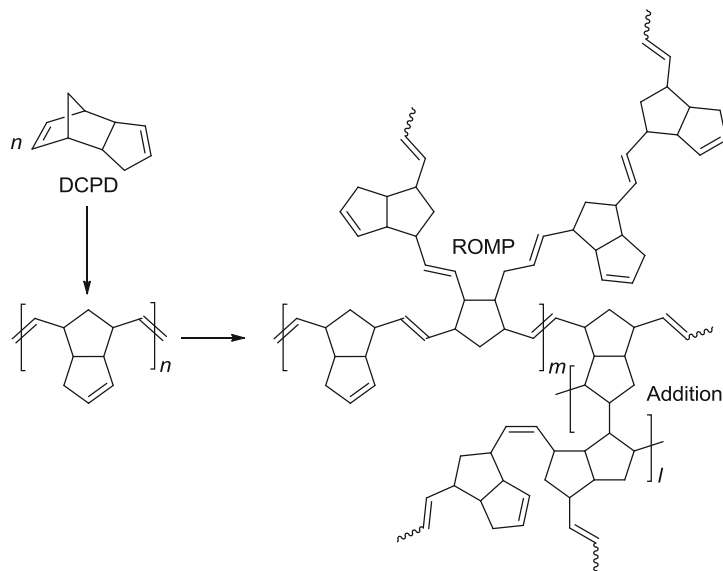
see Fig. 2) possess amorphous and transparent characters [15].

As another commercial product, polydicyclopentadiene (polyDCPD) was also prepared by the ROMP of dicyclopentadiene (DCPD) as the strained tricyclic monomer [16–19]. The polymerization involved two steps: an initial ROMP of the more strained bicyclic system and a ROMP and/or vinyl addition of the remaining double bond with subsequent crosslinking, as shown in Fig. 5 [17]. The high reactivity of DCPD is adaptable to a reaction injection molding (RIM) system for preparing polyDCPD, which has a combination of important properties, such as a high impact resistance, high chemical corrosion resistance, high heat deflection temperature, etc.

The ROMP of 1,3,5,7-cyclooctatetraene (COT) yields the conductive polymer, polyacetylene (Fig. 6) [20–23]. No solvent is required for this polymerization and a silver film including *cis* and *trans* conjugated double bonds was obtained. The random copolymerization of COT with other cyclic olefins, such as cyclooctadiene (COD), produced linear copolymers with various conjugation lengths [22]. The polyacetylene diblock copolymers synthesized by the ROMP of COT and norbornene derivatives formed unique nanocaterpillar supramolecules [23]. Even though pristine polyacetylene is
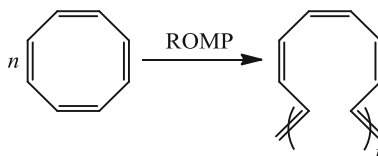
Poly(cyclic olefin)s, Fig. 6 Ring-opening metathesis polymerization of 1,3,5,7-cyclooctatetraene

unstable in air, the polyacetylene segments in the nanocaterpillar supramolecule are very stable because of the protection of the shell segments in the supramolecule.

Poly(cyclic olefin)s Through Vinyl Addition Polymerization

As described in the Introduction, poly(cyclic olefin)s can also be obtained by the vinyl addition polymerization of a strained cyclic olefin without ring opening. In general, catalysts containing titanium, zirconium, nickel, palladium, cobalt, chromium, and vanadium have been used for the vinyl addition polymerization [6, 7]. The neutral metal complexes require a cocatalyst, such as methylaluminoxane (MAO) or tris(pentafluorophenyl)borane (see Fig. 7), for their activation, while the cationic palladium complexes are active without a cocatalyst.
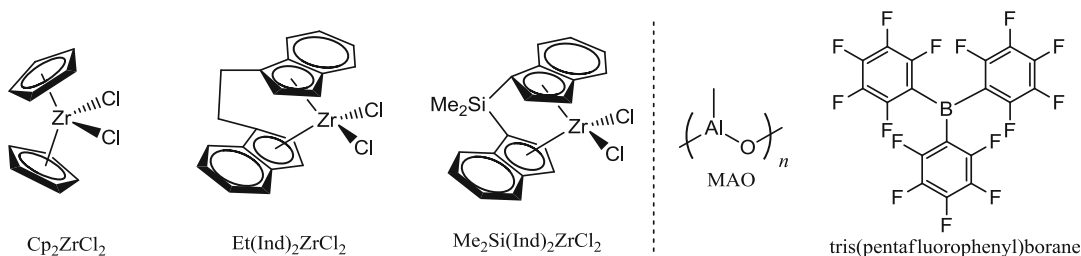
Poly(cyclic olefin)s, Fig. 7 Zirconocene catalyst and cocatalysts for vinyl addition polymerization of norbornene
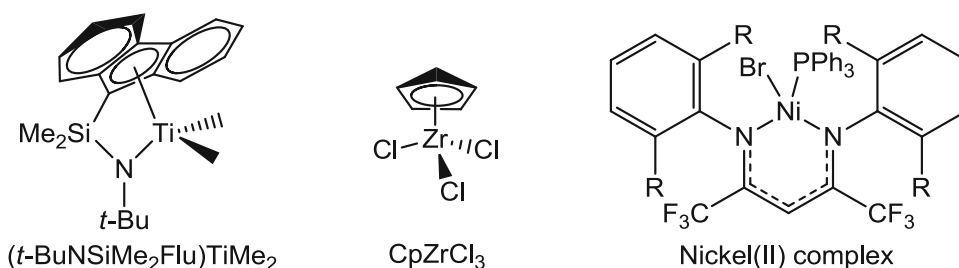
Poly(cyclic olefin)s, Fig. 8 Catalysts for the vinyl addition polymerization that produced the soluble polynorbornene

Poly(cyclic olefin)s via the vinyl addition polymerization have been widely used as high performance materials in the industry because of their special optical and mechanical properties. For example, the polyNB obtained 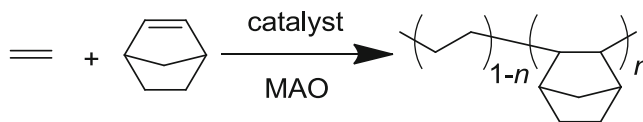via the vinyl addition polymerization possesses specific properties, such as a high transparency, high thermal stability, high glass transition temperature, low birefringence, low water absorption, and excellent dielectric properties, because its chemical structure contains a saturated carbon skeleton. Thus, the polyNB via the vinyl addition polymerization has been the focus of much attention from the viewpoint of a high performance polymer.

The vinyl addition polymerization of NB was first studied using a conventional Ziegler-Natta $TiCl_4/R_3Al$ catalyst system in the early 1960s [10], but the system showed a very low activity. Metallocene catalysts consisting of a metallocene of group IV (mostly zirconium) and MAO allowed the polymerization of cyclobutene, cyclopentene, and NB. The metallocene, $Et(Ind)_2ZrCl_2$ and $Me_2Si(Ind)_2ZrCl_2$ (Fig. 7), in combination with MAO showed a significantly high polymerization activity toward cyclic

olefins [24]; these catalyst systems were 100 times more active than the Cp_2ZrCl_2/MAO catalyst system. However, the obtained polyNBs showed a low solubility in common organic solvents and decomposed before they melted.

Recently, the catalyst systems, such as the group IV single-site catalyst system and late transition metal catalyst system, were reported to be highly active for the vinyl addition polymerization that produced the soluble polyNB [25–28]. The half sandwich titanocene (t-BuNSiMe$_2$Flu)TiMe$_2$-Ph$_3$CB(C$_6$F$_5$)$_4$/Oct$_3$Al catalyst system showed good activities to produce a high molecular weight polyNB with a narrow polydispersity (Fig. 8) [25, 28]. The commercially available half-zirconocene CpZrCl$_3$ activated by the isobutyl-modified MAO effectively catalyzed the vinyl addition polymerization to produce the soluble polyNB [27]. Nickel(II) complexes bearing fluorinated β-diketiminate ligands also exhibited a high catalytic activity for the vinyl addition polymerization of NB [28].

In order to modify the poor solubility and processability of the cyclic olefin homopolymer

Poly(cyclic olefin)s, Fig. 9 Vinyl addition copolymerization of norbornene with ethylene

and obtain a functionalized poly(cyclic olefin), the vinyl addition copolymerization of cyclic olefin with ethylene, propylene, higher 1-alkene, polar monomer, and NB derivative has also been studied [29–33]. Cyclic olefin copolymers are some of the most important thermoplastic materials with specific properties, such as transparency, low water absorption, heat resistance, chemical stability, and easy moldability. There versatile properties enable their industrial use in packing, electronic data storage, optical applications, etc. The properties of the cyclic olefin copolymers are controlled by the monomer structure, monomer composition, sequence distribution, and the stereoregularity of the cyclic olefin units in the copolymer. In particular, the copolymerization of NB with ethylene has been the focus of much attention from the viewpoint of industrial applications, because ethylene-NB copolymers are soluble, transparent, and amorphous materials (Fig. 9). Depending on the NB content in the ethylene-NB copolymer, the T_g value can be varied in the range of ca. 0–220 °C. It is interesting to note that the T_g value of 226 °C for a copolymer with 79 % norbornene content is slightly higher than the reported T_g value of 220 °C for pure polyNB [34].

Summary

In this entry, the ring-opening metathesis polymerization and vinyl addition polymerization of the strained cyclic olefins to produce poly(cyclic olefin)s were introduced. The poly(cyclic olefin)s are very important industrial materials with a high transparency and high thermal stability. Research of the homo- and copolymerizations of cyclic olefins is still in progress for the development of a functional olefin polymer.

Related Entries

▶ Ring-Opening Metathesis Polymerization

References

1. Bielawski CW, Grubbs RH (2007) Living ring-opening metathesis polymerization. Prog Polym Sci 32(1):1–29
2. Kress J, Wesolek M, Osborn JA (1982) Tungsten (IV) carbenes for the metathesis of olefins. Direct observation and identification of the chain carrying carbene complexes in a highly active catalyst system. J Chem Soc Chem Commun :514–516
3. Murdzek JS, Schrock RR (1987) Well-characterized olefin metathesis catalysts that contain molybdenum. Organometallics 6:373–1373
4. Schwab P, France MB, Ziller JW, Grubbs RH (1995) A series of well-defined metathesis catalysts-synthesis of [RuCl2(=CHR)(PR3)2] and Its reaction. Angew Chem Int Ed Engl 34:2039–2041
5. Nomura K, Zhang S (2011) Design of vanadium complex catalysts for precise olefin polymerization. Chem Rev 111:2342–2362
6. Janiak C, Lassahn PG (2001) Metal catalysts for the vinyl polymerization of norbornene. J Mol Catal A Chem 166:193–209
7. Tritto I, Boggioni L, Sacchi MC, Locatelli P (1998) Cyclic olefin polymerization and relationships between addition and ring opening metathesis polymerization. J Mol Catal A Chem 133:139–150
8. Goodall L, McIntosh LH III, Rhodes LF (1995) New catalysts for the polymerization of cyclic olefins. Makromol Chem Macromol Symp 89:421–432
9. Seehof N, Mehler C, Breunig S, Risse W (1992) Pd2+ catalyzed addition polymerizations of norbornene and norbornene derivatives. J Mol Catal 76:219–228
10. Sartori G, Ciampelli FC, Cameli N (1963) Polymerization of norbornene. Chim Ind (Milan) 45:1478–1482
11. Tsujino T, Saegusa T, Furukawa J (1965) Polymerization of norbornene by modified Ziegler-catalysts. Makromol Chem 85:71–79
12. Patton PA, Lillya CP, McCarthy TJ (1986) Olefin metathesis of cyclohexene. Macromolecules 19:1266–1268
13. Truett WL, Johnson DR, Robinson IM, Montague BA (1960) Polynorbornene by coördination polymerization. J Am Chem Soc 82:2337–2340

14. Lee L-BW, Register RA (2005) Hydrogenated ring-opened polynorbornene: A highly crystalline atactic polymer. Macromolecules 38:1216–1222

15. Yamazaki M (2004) Industrialization and application development of cyclo-olefin polymer. J Mol Catal A Chem 213:81–87

16. Constable GS, Lesser AJ, Coughlin EB (2004) Morphological and Mechanical Evaluation of Hybrid Organic–Inorganic Thermoset Copolymers of Dicyclopentadiene and Mono- or Tris(norbornenyl)-Substituted Polyhedral Oligomeric Silsesquioxanes. Macromolecules 37:1276–1282

17. Schaubroeck D, Brughmans S, Vercaemst C, Schaubroeck J, Verpoort F (2006) Qualitative FT-Raman investigation of the ring opening metathesis polymerization of dicyclopentadiene. J Mol Catal A Chem 254:180–185

18. Mol JC (2004) Industrial applications of olefin metathesis. J Mol Catal A Chem 213:39–45

19. Hensle EM, Blum SA (2013) Phase separation polymerization of dicyclopentadiene characterized by in operando fluorescence microscopy. J Am Chem Soc 135(33):12324–12328

20. Korshak YV, Korshark VV, Kanischka G, Höcker H (1985) A new route to polyacetylene. Ring-opening polymerization of 1,3,5,7-cyclooctatetraene with metathesis catalysts. Makromol Chem Rapid Commun 6:685–692

21. Klavetter FL, Grubbs RH (1988) Polycyclooctatetraene (polyacetylene): synthesis and properties. J Am Chem Soc 110:7807–7813

22. Scherman OA, Grubbs RH (2001) Polycyclopctatetraene (polyacetylene) produced with a ruthenium olefin metathesis catalyst. Synth Met 124:431–434

23. Yoon KY, Lee IH, Kim KO, Jang J, Lee E, Choi TL (2012) One-Pot in Situ Fabrication of Stable Nanocaterpillars Directly from Polyacetylene Diblock Copolymers Synthesized by Mild Ring-Opening Metathesis Polymerization. J Am Chem Soc 134:14291–14294

24. Kaminsky W, Bark A, Arndt M (1991) New polymers by homogenous zirconocene/aluminoxane catalysts. Makromol Chem Macromol Symp 47:83–93

25. Hasan T, Nishii K, Shiono T, Ikeda T (2002) Living Polymerization of norbornene via vinyl Addition with ansa-fluorenylamidodimethyltitanium complex. Macromolecules 35:8933–8935

26. Hasan T, Ikeda T, Shiono T (2004) Highly efficient ti-based catalyst systems for vinyl addition polymerization of norbornene. Macromolecules 37:7432–7436

27. Nishizawa O, Misaka H, Kakuchi T, Satoh T (2008) Vinyl addition polymerization of norbornene using cyclopentadienylzirconium trichloride activated by isobutyl-modified methylaluminoxane. J Polym Sci Part A Polym Chem 46:1185–1191

28. Li Y, Wang L, Gao H, Zhu F, Wu Q (2006) Novel nickel (II) complexes chelating β-diketiminate ligands: synthesis and simultaneous polymerization

and oligomerization of ethylene. Appl Organomet Chem 20:436–442

29. Nishizawa O, Misaka H, Sakai R, Kakuchi T, Satoh T (2008) Copolymerization of ethylene and norbornene using cyclopentadienylzirconium trichloride activated by isobutyl-modified methylaluminoxane. J Polym Sci Part A Polym Chem 46:7411–7418

30. Apisuk W, Trambitas AG, Kitiyanan B, Tamm M, Nomura K (2013) Efficient ethylene/norbornene copolymerization by half-titanocenes containing imidazolin-2-iminato ligands and MAO catalyst systems. J Polym Sci Part A Polym Chem 51:2575–2580

31. Sudo A, Morishita H, Endo T (2010) Synthesis of a norbornene monomer having cyclic carbonate moiety based on CO_2 fixation and its transition metal-catalyzed polymerizations. J Polym Sci Part A Polym Chem 48:3896–3902

32. Rodriguez B, Delferro M, Marks TJ (2008) Neutral Bimetallic Nickel(II) phenoxyiminato catalysts for highly branched polyethylenes and ethylene-norbornene copolymerization. Organometallics 27:2166–2168

33. Chen L, Zhong Z, Chen C, He X, Chen Y (2014) N,O-chelating bidentate Ni (II) and Pd (II) complexes for copolymerization of norbornene and norbornene ester. J Organomet Chem 752:100–108

34. Rische T, Waddon AJ, Dickinson LC, MacKnight WJ (1998) Microstructure and morphology of cycloolefin copolymers. Macromolecules 31:1871–1874

Poly(Diene)s: Polybutadiene and Polyisoprene

Ikuyoshi Tomita
Department of Electronic Chemistry, Interdisciplinary Graduate School of Science and Engineering, Tokyo Institute of Technology, Yokohama, Japan

Synonyms

Diene polymerization; Polymerization of 1,3-conjugated dienes

Definition

Poly(diene)s are products obtainable by the polymerization of diene monomers carrying two olefin units. In the case of poly(diene)s from conjugated

1,3-diene monomers, in which two olefin units are conjugated to each other, the resulting polymers are often applied to important industrial products such as synthetic elastomers. Poly(1,3-diene)s contain double bonds in the main chain and/or in the pendant group as a result of 1,4- and/or 1,2-polymerizations, respectively. Not only the selectivity of 1,4- and 1,2-polymerizations but also that between *cis* and *trans* for the 1,4-polymerizations and the stereoselectivity in the 1,2-polymerization also affect largely the properties of the polymers. Wide varieties of polymerization techniques including the radical, ionic, and coordination polymerizations have been investigated in detail to obtain excellent materials from diene monomers.
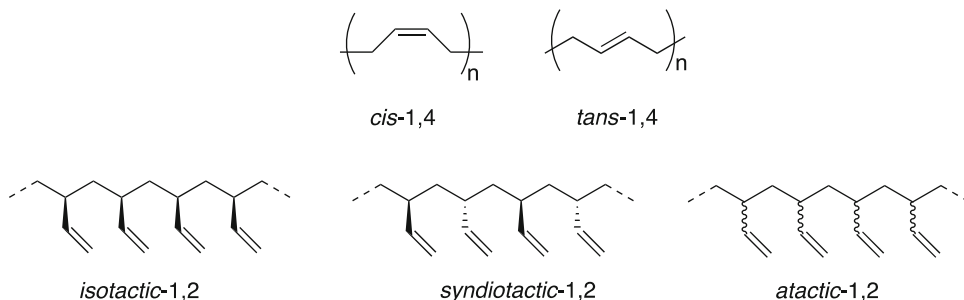
Introduction

Dienes are important monomers for a variety of polymerization techniques including the radical, ionic, and coordination polymerizations [1]. The polymerizations of both nonconjugated and conjugated dienes have been widely studied. In cases of the nonconjugated dienes in which two olefin units are connected with spacers, both the structure of the monomers and the polymerization conditions are important factors to obtain linear polymers through the selective intramolecular annulation process, otherwise the cross-linking reaction takes place to provide network materials [2]. Allene and its derivatives are also unique nonconjugated dienes whose polymerization can provide linear polymers consisting of 1,2- and/or 2,3-polymerized units under the appropriate

polymerization conditions [3]. They are suitable to carry out living polymerizations that are tolerant to the functional groups in both the substituents and the polymerization media.

The polymerizations of conjugated dienes such as 1,3-butadiene ($CH_2 = CH–CH = CH_2$), isoprene ($CH_2 = C(CH_3)–CH = CH_2$), and chloroprene ($CH_2 = CCl–CH = CH_2$) have widely been studied, and both homopolymers and copolymers derived from the diene monomers are important industrial products for many applications. For example, poly(1,3-butadiene) and its derivatives are widely used as synthetic rubber possessing excellent elastic properties, wear- and abrasion-resistant properties, and thermal stability suitable for tires, damper materials, hoses, sealants, adhesives, etc. The possible microstructures produced from the 1,3-dienes are *trans*-1,4-, *cis*-1,4-, and 1,2-polymerized units. In the case of the 1,2-polymerization, the stereoselectivity in the polymerization also gives isotactic, syndiotactic, and atactic 1,2-units (as typical examples of microstructures from 1,3-butadiene, see Fig. 1).

The composition of these microstructural isomers is dependent upon the structure of the diene monomers and the polymerization conditions, and the microstructure affects largely the properties of the resulting poly(diene)s. In the case of poly(1,3-butadiene), for example, the polymers consisting of *cis*-1,4-rich structures are elastomeric materials, while *trans*-1,4-rich and some of the stereospecific 1,2-polymers are crystalline products. In addition, the reactivity of the double bonds in the poly(diene)s is dependent upon the structure of the olefinic units (i.e., the
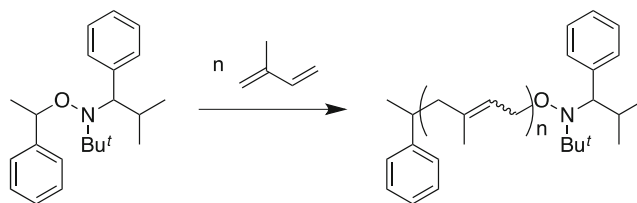

Poly(Diene)s: Polybutadiene and Polyisoprene, Fig. 1 Microstructures of poly(1,3-butadiene)
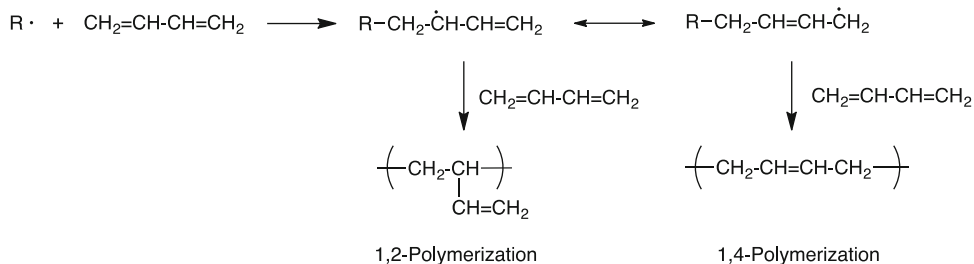
Poly(Diene)s: Polybutadiene and Polyisoprene, Fig. 2 Production of 1,2- and 1,4-polymerized units in the radical polymerization of 1,3-butadiene

Poly(Diene)s: Polybutadiene and Polyisoprene, Fig. 3 Nitroxide-mediated polymerization (NMP) of isoprene

microstructure of the polymers). Accordingly, the control of the microstructure of the poly (diene)s is important for their chemical functionalization through polymer reactions using addition reactions such as hydrometallations [4].

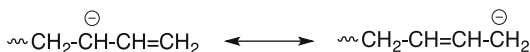## Radical Polymerization of 1,3-Dienes

Under the radical polymerization conditions, polymers consisting of both 1,2- and 1,4-polymerized units are produced from 1,3-butadiene through the delocalized allyl radical intermediates. The Q-e parameters are 1.70 and -0.50 for 1,3-butadiene and 1.99 and -0.55 for isoprene, respectively. The large Q values indicate that 1,3-dienes can be classified to the conjugated monomers. Due to the steric factor of the growing radical species and the thermodynamic stability of the produced olefinic structures, the 1,4-polymerized units are predominant over the 1,2-units, and the *trans*-1,4-units are more favorable than the *cis*-1,4-units especially under milder polymerization conditions (Fig. 2). In the polymerizations of isoprene and chloroprene, the higher 1,4-polymerization selectivity is observed compared to that of 1,3-butadiene. The radical emulsion polymerization of

1,3-dienes can also be performed, and industrially important products such as poly(chloroprene) and copolymers of 1,3-butadiene and vinyl monomers such as styrene are often prepared by this technique.

Some well-defined poly(diene)s and their copolymers have been prepared under the controlled radical polymerization conditions. For example, on the basis of the nitroxide-mediated polymerization (NMP) technique, the homopolymerization of isoprene and both the random and block copolymerizations of isoprene with some vinyl monomers such as acrylates and styrene successfully provide (co)polymers with controlled molecular weights and narrowly dispersed molecular weight distributions (Fig. 3) [5]. Also, the random copolymerization of acrylonitrile (AN) and 1,3-butadiene (BD) takes place to give copolymers having relatively narrowly dispersed molecular weight distributions by means of the reversible addition fragmentation chain transfer (RAFT) polymerization technique.

Ionic Polymerization of 1,3-Dienes

In the anionic polymerization of 1,3-butadiene, the growing anions have chances to be delocalized to the 2 and 4 carbons, and the anions

$$\text{\textasciitilde\textasciitilde}CH_2\text{-}\overset{\ominus}{CH}\text{-}CH=CH_2 \quad \longleftrightarrow \quad \text{\textasciitilde\textasciitilde}CH_2\text{-}CH=CH\text{-}\overset{\ominus}{CH_2}$$

**Poly(Diene)s: Polybutadiene and Polyisoprene,
Fig. 4** Growing anions in the anionic polymerization of
1,3-butadiene

can form tight and loose ion pairs, depending on
the nature of counter cations and the polymeriza-
tion solvents (Fig. 4) [6]. These features have
been proposed to affect the microstructure of
the polymers.

The soft cations and the polar polymerization
media tend to form free anionic growing species
or loose ion pairs (i.e., solvent-separated ions)
that bring about the preferential production of
the 1,2-polymerized units. In the case of isoprene,
the polymerization of the vinyl unit
($CH_2 = CH–$), the 3,4-polymerization, takes
place under the analogous conditions due to
both the steric and electronic factors of the two
kinds of double bonds.

In the case of the polymerization with hard
cations such as lithium and/or the polymerization
in less polar solvents, the content of the
1,4-polymerization in the produced polymer
increased which can be explained by the prefer-
ential formation of the covalent species
($\text{\textasciitilde}CH_2–CH = CH–CH_2–Li$). The formation of
cis-1,4 is favorable than trans-1,4, which was
proposed to be due to the higher reactivity of
the corresponding anionic growing species and
the relatively slow isomerization from initially
produced cis- to trans-anions.

The anionic polymerization has the longest his-
tory in the living (co)polymerization of 1,3-dienes
(and also all the monomers). Block copolymers
from 1,3-butadiene and some vinyl monomers can
be produced by the sequential copolymerization of
the two monomers. For example, the block copol-
ymer of 1,3-butadiene and styrene are well-known
commercially important thermoplastic elastomers
obtainable by this technique.

The anionic polymerization of some
substituted dienes has also been studied. For
example, 1,3-cyclohexadiene can be (co)poly-
merized anionically that provides well-defined
(co)polymers whose oxidation provides poly(p-
phenylene) and its block copolymers [7].

To the contrary, the cationic polymerization
is generally not suitable for the production of
polymers from 1,3-butadiene or isoprene due to
the presence of cyclization and intermolecular
cross-linking processes [8]. However, it has
been reported that some substituted 1,3-dienes
such as 1-alkoxy-1,3-butadienes and 1-phenyl-
1,3-butadiene provide polymers with 1,4-
polymerized structures through the cationic
growing species stabilized by these substituents.

Coordination Polymerization of 1,3-Dienes

As is the case for the polymerization of olefins,
the coordination technique is the promising
method to control the microstructure of the poly-
mers of 1,3-dienes. Many studies have been car-
ried out to obtain poly(1,3-diene)s possessing
well-defined microstructure as well as stereoreg-
ularity [9, 10]. The Ziegler–Natta, metallocene,
and nonmetallocene catalysts have been
employed as catalysts for the polymerization of
conjugated dienes such as 1,3-butadiene and iso-
prene. For example, elastomeric polymers with
high cis-1,4-contents have successfully been pre-
pared from 1,3-butadiene and isoprene by the use
of catalysts containing early transition metals
such as Ti and Zr, late transition metals such as
Ni, and lanthanide metals such as Sm and Gd.

The selective synthesis of crystalline
trans-1,4-polymers from 1,3-butadiene and
those from isoprene has also been achieved
based on a wide variety of metal catalysts. Like-
wise, the 1,2-polymers of 1,3-butadiene and the
3,4-polymers from isoprene have been prepared
using some transition metal-based catalysts.
Some of these systems accompany the
stereocontrol of the vinyl polymerization units
to give both syndiotactic and isotactic polymers.
It was reported that the 1,2-polymers with high
syndiotactic contents are crystalline materials
with rather high melting temperature (~200 °C).

Some of the catalysts mentioned above also
serve as excellent living polymerization catalysts
for conjugated dienes. Especially, the progress of
the lanthanide-based catalysts gives us the chance

to obtain well-defined block and random copolymers from conjugated dienes and vinyl monomers such as styrene.

Related Entries

References

1. Odian G (1991) Principles of polymerization. Wiley-Interscience, New York
2. Coates GW (2000) Precise control of polyolefin stereochemistry using single-site metal catalysts. Chem Rev. doi:10.1021/cr990286u
3. Endo T, Tomita I (1997) Novel polymerization methods for allene derivatives. Prog Polym Sci. doi:10.1016/S0079-6700(96)00022-6
4. McGrath MP, Sall ED, Tremont SJ (1995) Functionalization of polymers by metal-mediated processes. Chem Rev. doi:10.1021/cr00034a004
5. Nicolas J, Guillaneuf Y, Lefay C, Bertin D, Gigmes D, Charleux B (2013) Nitroxide-mediated polymerization. Prog Polym Sci. 137 doi:10.1016/j.progpolymsci.2012.06.002
6. Van Beylen M, Bywater S, Smets G, Szwarc M, Worsfold DJ (1988) Developments in anionic polymerization – A critical review. Adv Polym Sci. doi:10.1007/BFb0025275.
7. Hadjichristidis N, Pitsikalis M, Iatrou H (2005) Synthesis of block copolymers. Adv Polym Sci. doi:10.1007/12_005
8. Kennedy JP (1975) Cationic polymerization of olefins: a critical inventory. Wiley, New York
9. Porri L, Giarrusso A (1989) Conjugated diene polymerization. In: Allen SG (ed) Comprehensive polymer science. Pergamon, Oxford
10. Takeuchi D (2013) Stereoselective polymerization of conjugated dienes. In: Encyclopedia of polymer science and technology. Wiley, Hoboken

Poly(ether ketone) and Poly(ether sulfone) Synthesis

Kaylie J. Smith
Leafield Technical Centre, Ketonex Ltd, Langley, Witney, Oxfordshire, UK
Department of Chemistry, Chemistry Research Laboratory, The University of Oxford, Oxford, UK

Synonyms

Engineering thermoplastic; High-performance thermoplastic; Polyaryletherketone; Polyarylethersulfone

Definition

Poly(ether ketone)s and poly(ether sulfone)s may be synthesized by a range of methods, broadly divided into nucleophilic and electrophilic routes.

Introduction

Poly(ether ketone)s (PEKs) and poly(ether sulfone)s (PESs) are related classes of high-performance polymers, often used in engineering applications. They exhibit a range of attractive properties such as thermal resistance, chemical resistance, and mechanical strength and are therefore suitable for advanced applications in extreme environments such as medical devices, aerospace engineering, and industrial manufacturing [1]. The development of these

P

materials has occurred over the past 50 years as more advanced applications have become apparent and more common materials such as polycarbonate became unsuitable. Poly(ether ether ketone) (PEEK) is the most well-known material in this family and is commercially available at high volumes. A variety of other materials in these families are also commercially available from a range of suppliers.

General Structure and Nomenclature

PEKs and PESs are formed of aromatic subunits linked by ether and ketone groups or ether and sulfone groups, respectively. Most commonly, the aromatic portions are phenylene groups, but other substituted or unsubstituted aromatic moieties may be incorporated. The aromatic units in one chain may be all the same or different, e.g., phenylene or phenylene and biphenylene. The typical nomenclature for PESs and PEKs is to refer to a phenylene-ether unit as "E," a phenylene-ketone unit as "K," and a phenylene-sulfone unit as "S." In this way, the polymer is represented by the constituents of the repeat unit. For example, poly(*e*ther *e*ther *k*etone) or "PEEK" has a repeat unit of –[Ph – *e*ther – Ph – *e*ther – Ph – *k*etone] –, where Ph represents phenylene.

General Properties of Poly(ether sulfone)s and Poly(ether ketone)s

PESs are aromatic polymers with high glass transition temperatures (T_g). Electronegativity of the sulfone promotes delocalization across the sulfone group [2]. The associated resonance structures increase S-C chain rigidity, increasing T_g. Ether linkages are required to competitively decrease the chain rigidity and maintain processability. This is in contrast to poly(phenylene sulfone) which does not exhibit a T_g before its decomposition temperature [3]. The steric arrangement of the tetrahedral sulfone group restricts the packing ability of the polymer chain, reducing the degree of crystallinity and

therefore decreasing the melting temperature (T_m). Due to this effect, PES is often amorphous, although semicrystalline PES is induced by some solvents, e.g., dichloromethane, and with copolymerization with other crystallizing monomers. Unlike PEKs which may be semicrystalline, this amorphous character excludes PES from applications requiring solvent resistance. PES can be produced by both nucleophilic and electrophilic routes.

PEKs are similar in structure to PESs but instead have ether and ketone functionality between the aromatic subunits. Like PESs, the attraction of the PEK family is the combination of high glass transition temperatures (T_g) with comparatively low melting temperatures (T_m). This allows the polymers to be easily processed while maintaining high use temperatures. Altering the order and ratio of ether to ketone groups in the repeat unit affects the thermal properties of the polymers, namely, the T_g and T_m. As Fig. 1 shows, increasing the ratio of ketone groups compared to ether groups acts to increase both the T_g and T_m values [1, 4]. The incorporation of ketones increases the rigidity of the polymer chain due to the possible resonance structures along the chain. However, unlike PESs, the geometry of the ketone allows the formation of crystalline domains. The greater percentage crystallinity (of a maximum of 30–35 % for PEKs [4]) increases the T_m and imparts solvent resistance, widening the market for potential applications. As with PESs, PEKs can also be produced by both nucleophilic and electrophilic routes.

Synthetic Routes to Poly(ether ketone)s and Poly(ether sulfone)s

There is a wide variety of accepted methods for the synthesis of PESs and PEKs. Generally, they may be split into nucleophilic and electrophilic routes, each having their own advantages.

Nucleophilic Synthetic Routes
The nucleophilic synthetic route to PESs and PEKs is ether forming. For the formation of

Polymer	Structure	T_g/°C	T_m/°C
PEEK		143	334
PEK		154	367
PEEKK		158	363
PEKEKK		161	377
PEKK		165	386
PES		224	–

Poly(ether ketone) and Poly(ether sulfone) Synthesis, Fig. 1 Crystalline glass transition temperatures (T_g) and melting temperatures (T_m) for common poly(ether ketone)s and poly(ether sulfone) with all *1,4-* conformation (Data from Refs. [1, 4], Figure adapted from Ref. [4])

P
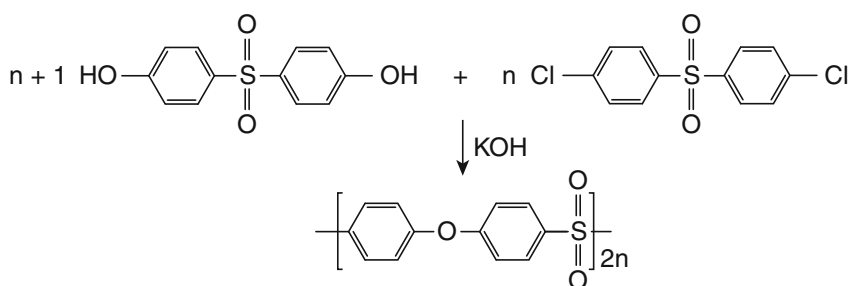
Poly(ether ketone) and Poly(ether sulfone) Synthesis, Fig. 2 The nucleophilic synthesis of poly(ether sulfone)

PESs, this requires the use of dihydroxy- and di-halogenated sulfone-containing monomers [5], exemplified in Fig. 2. The dihydroxy monomer is converted to the bis-phenate in the presence of alkali metal salts such as potassium hydroxide prior to polymerization. Due to the electronegativity of the sulfone, the chloride is easily displaced. Based on this system, a range of other monomers may be used to produce polymers with altered properties [2]. For example, the incorporation of a diphenyl moiety increases the T_g substantially. A self-polymerization route is achieved using the difunctional monomer 4-hydroxy-4′-chlorophenyl sulfone.

Poly(ether ketone) and Poly(ether sulfone) Synthesis, Fig. 3 The nucleophilic synthesis of poly(ether ketone)

The PES nucleophilic synthetic technology is partially transferable to PEKs. However, under the same reaction conditions, high molecular weight PEKs are unachievable. Reactions using the 4,4′-dichlorobenzophenone monomer are unsuccessful [2], therefore requiring the use of fluorine-containing monomers which have greater reactivity on the adjacent carbon due to the electronegativity of the fluorine. 4,4′-Difluorobenzophenone is the alternative monomer [6], exemplified in Fig. 3.
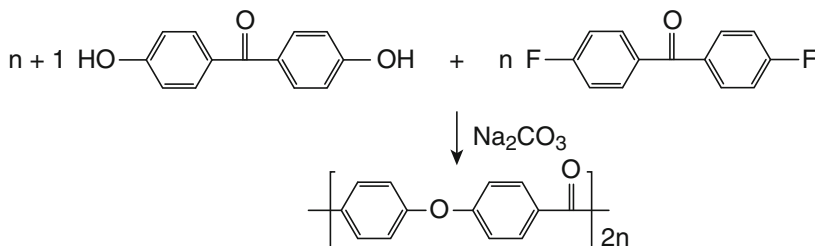
Electrophilic Synthetic Routes

The electrophilic route to PESs and PEKs is via the aromatic sulfone-forming or ketone-forming Friedel-Crafts sulfonylation and acylation reactions [7]. This is an electrophilic aromatic substitution reaction between a sulfonyl chloride or a carboxylic acid chloride and an arene, resulting in the formation of an aromatic sulfone or an aromatic ketone, catalyzed by a Lewis acid, commonly $AlCl_3$ or $FeCl_3$ for PESs.

The $AlCl_3$ catalyst complexes with the chlorine atom on the sulfonyl chloride or the acid chloride, resulting in the formation of a stable sulfonylium or acylium ion. This ion then attacks the benzene ring in the second monomer to produce an aromatic sulfone or an aromatic ketone, eliminating a molecule of HCl. The benzene ring of the second monomer must be activated to electrophilic attack. Although the $AlCl_3$ is regenerated, a proportion of it is consumed by complexation with the newly formed sulfone or ketone which acts as a Lewis base. The $AlCl_3$ also complexes to any carbonyl oxygen atoms present in the reactant or product molecules. Therefore, a molar equivalent to the carbonyl groups must be added in addition to the catalytic quantity to achieve a successful reaction. Multiple

substitutions do not occur since monosubstitution deactivates the aromatic ring to further substitutions due to the electron-withdrawing capabilities of the acyl group.

The standard Friedel-Crafts sulfonylation or acylation reaction may be adapted to a Friedel-Crafts condensation polymerization [8, 9]. In this case, difunctional monomers are required, namely, aromatic diacylchlorides and monomers capable of electrophilic aromatic substitution.

The electrophilic synthesis of PESs offers a route using cheaper monomers and lower reaction temperatures than the nucleophilic route. The polymerization requires the use of phenoxyaroyl and phenoxyarenesulfonyl halide monomers, together with a Friedel-Crafts catalyst such as $FeCl_3$, exemplified in Fig. 4.

Initial attempts to produce PEKs by an electrophilic Friedel-Crafts acylation reaction employed diphenyl ether as the aromatic monomer [10], Fig. 5. Diphenyl ether is highly activated to substitution at the *para*-position and moderately activated at the *ortho*-position, with little selectivity. During polymerization, *ortho*-substitution increases the likelihood of cyclization and gelation reactions which even in small quantities substantially decrease the melt stability of the polymer.

A room temperature modified Friedel-Crafts method avoids this issue [11]. Suitable monomers include the combination of a diacid dihalide with a polynuclear aromatic compound with two active carbon atoms, catalyzed by $AlCl_3$, Fig. 6. The use of a dimethyl sulfone controlling agent produces a tractable gel.

Replacing the diphenyl ether with a ketone-containing monomer such as 1,4′-diphenoxybenzophenone "EKE" or 1,4′-bis(4-phenoxybenzoyl)benzene "EKKE" [11]

Poly(ether ketone) and Poly(ether sulfone) Synthesis, Fig. 4 The electrophilic synthesis of poly(ether sulfone)
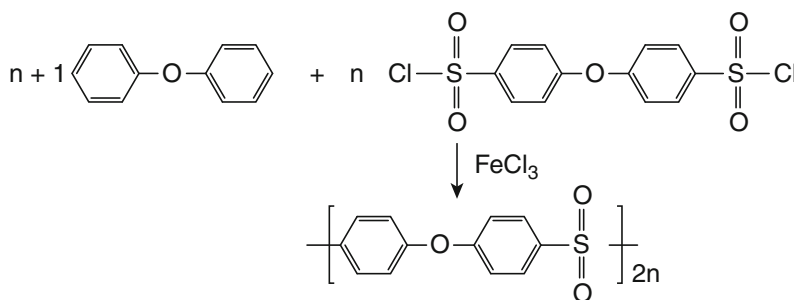
Poly(ether ketone) and Poly(ether sulfone) Synthesis, Fig. 5 The electrophilic synthesis of poly(ether ketone ketone)
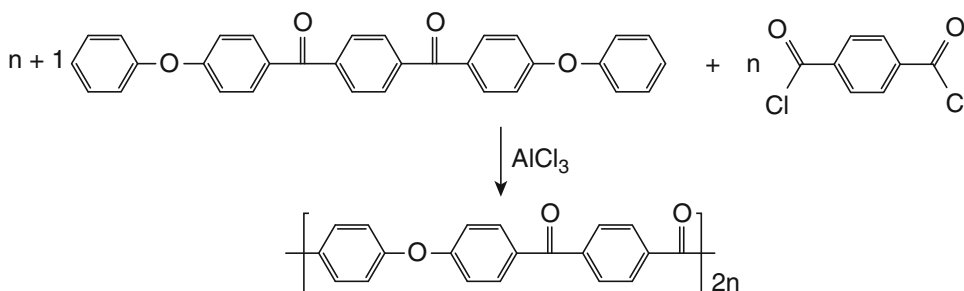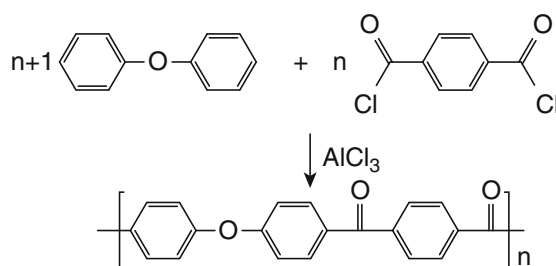
Poly(ether ketone) and Poly(ether sulfone) Synthesis, Fig. 6 The modified Friedel-Crafts synthesis of poly(ether ketone ketone)

decreases the overall reactivity of the monomer and increases the selectivity of substitution. The ketones deactivate both the *ortho-* and *para*-positions of the terminal aromatic rings to electrophilic attack, but do not entirely inhibit the reaction. The *ortho*-deactivation virtually eliminates substitution, but *para*-activation is maintained.

A modification of this process allows the production of PESs and PEKs as a fine dispersion with high reactor loading [12].

Since the PEK produced is semicrystalline unlike PES, it can be problematic to maintain

the oligomers in solution long enough to produce a high molecular weight polymer. A wide variety of methods are known to combat this issue, including the use of high temperature reactions and the use of a mixed boron trifluoride/hydrogen fluoride system [2, 3].

Modifications to Poly(ether sulfone) and Poly (ether ketone) Structures

Other than the bulk materials, PESs and PEKs have been modified to address a range of applications. This includes in-chain and pendant modification. A wide range of functional groups may be built

into the main chain by the incorporation of a range of monomers. Other than ether, ketone, and sulfone groups, possible functionality includes imide, amide, naphthalene, ester azo, phenylquinoxaline, benzimidazole, benzoxazole, benzothiazole, and aliphatic groups [13, 14]. These monomers alter the T_g and T_m due to chain rigidity and crystallinity. A range of methods exists for the sulfonation of PEEK and other materials for use in fuel cell membranes [15].

Related Entries

▶ PES (Poly(ether sulfone)), Polysulfone
▶ Polyaryletherketone
▶ Polyetherimide

References

1. McKeen LW (2008) Effect of temperature and other factors on plastics and elastomers. William Andrew Publishing, Norwich
2. McGrail PT (1996) Polyaromatics. Polym Int 41:103–121
3. Brydson JA (1999) Plastics materials. Butterworth-Heinemann, Oxford
4. Kemmish D (2010) Update on the technology and applications of polyaryletherketones. Smithers Rapra, Shawbury
5. Jones MEB (1966) Manufacture of polysulphones. Br Patent 1016245
6. Attwood TE, Dawson PC, Freeman JL, Hoy LRJ, Rose JB, Staniland PA (1981) Synthesis and properties of polyaryletherketones. Polymer 22:1096–1103
7. Clayden J, Greeves N, Warren S, Wothers P (2001) Organic chemistry. Oxford University Press, Oxford
8. Cowie JMG, Arrighi V (2007) Polymers: chemistry and physics of modern materials. CRC Press, Boca Raton
9. Flory PJ (1953) Principles of polymer chemistry. Cornell University Press, Ithaca
10. Bonner WH (1962) Aromatic polyketones and preparation thereof. US Patent 3,065,205
11. Jansons V, Gors C (1987) Preparation of aromatic polymers. US Patent 4,709,007
12. Towle IDH (2011) Method for preparing poly(ether ketone ketones). Br Patent Application 2011/004164 A2
13. Rao VL (1995) Polyether ketones. J Macromol Sci Rev Macromol Chem Phys 35(4):661–712
14. Horner PJ, Whiteley RH (1991) Aromatic ether-ketone-"X" polymers Part 1. Synthesis and properties. J Mater Chem 1(2):271–280
15. Zaidi J, Matsuura T (2010) Polymer membranes for fuel cells. Springer, New York

Poly(L-Lactide)

Hideto Tsuji
Department of Environmental and Life Sciences, Graduate School of Engineering, Toyohashi University of Technology, Toyohashi, Aichi, Japan

Synonyms

PLLA; Poly(L-Lactic acid).

Definition

Poly(L-lactide) is a polymer synthesized by the ring-opening polymerization of L-lactide or polycondensation of L-lactic acid.

Historical Background

Historical outlines of poly(lactide), i.e., poly(lactic acid) (PLA), can be summarized as follows [1]. Synthetic routes to the linear dimer of lactic acid, i.e., lactoyllactic acid, and lactic acid oligomers from trimers to heptamers by the condensation (or esterification) of lactic acid by the removal of water at elevated temperatures such as 130 °C were reported in 1845 and 1914, respectively. Ring-opening polymerization of lactide, i.e., the cyclic dimer of lactic acid, was suggested in 1932 and developed in 1954, for the synthesis of high-molecular-weight (HMW) poly(lactic acid) (PLA). PLA can be hydrolyzed in the human body, and the formed lactic acid and oligomers are metabolized safely with very low harmful effects to the human body; consequently, PLA and its copolymers have been investigated widely for their biomedical applications since the breakthrough work by Kulkarni et al. in the late 1960s. In addition, PLA and its copolymers have been studied for pharmaceutical applications such as matrices for drug delivery systems (DDSs) since the late 1970s.

Through the 1980s and 1990s, basic information concerning the synthesis, physical properties, crystallization behavior, and biomedical and pharmaceutical applications of PLA and its copolymers was obtained. A large amount of research has been targeted toward the synthesis and molecular characterization of PLA and its copolymers, and the crystallization, spinning, and physical properties of PLA-based materials have been investigated intensively. In addition, studies have focused on a wide variety of biomedical and pharmaceutical applications and the in vitro and in vivo degradation of PLAs and their copolymers. Moreover, the stereocomplex formation of poly(L-lactide), i.e., poly(L-lactic acid) (PLLA), with poly(D-lactide), i.e., poly(D-lactic acid) (PDLA), was reported in 1987. Stereocomplexed materials have high mechanical performances, good resistance to hydrolytic/thermal degradation, and gas barrier properties. Since the latter half of the 1990s,

PLA and its copolymers have attracted significant attention in terms of commodity and industrial applications and have been recognized as substitutes for commercial petro-based polymers because of their cost-effective production from renewable plant resources. Figure 1 shows the synthesis, recycling, and degradation of PLLA [2].

Synthesis

Monomer

L-Lactic acid (Fig. 2) is the monomer of PLLA and is synthesized through bacterial fermentation with carbohydrates such as glucose [1]. L-Lactic acid [melting temperature (T_m) = 16.8 °C] is a 2-(or α-)hydroxycarboxylic acid, well known as a compound having an asymmetric carbon atom. Of the sources of carbohydrates, starch from corn is most frequently utilized for glucose production because of the high yield of glucose from corn
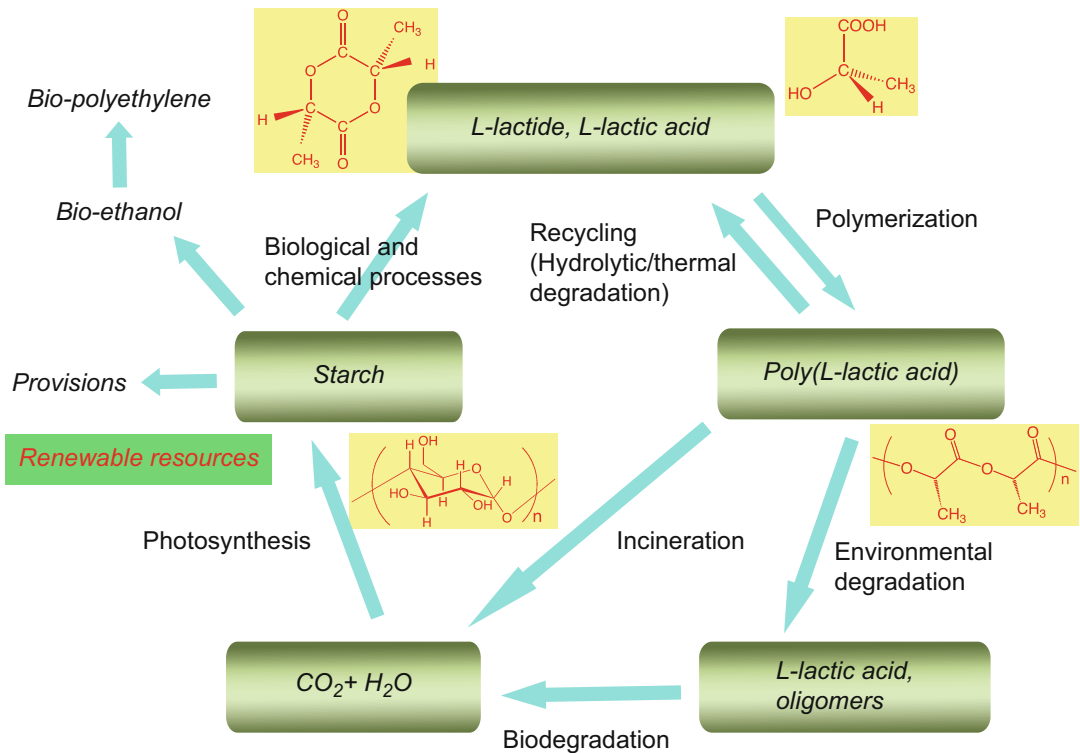
Poly(L-Lactide), Fig. 1 Synthesis, recycling, and degradation of PLLA (Reproduced from Tsuji [2]. Copyright (2008), with permission from Yoneda Shuppan)
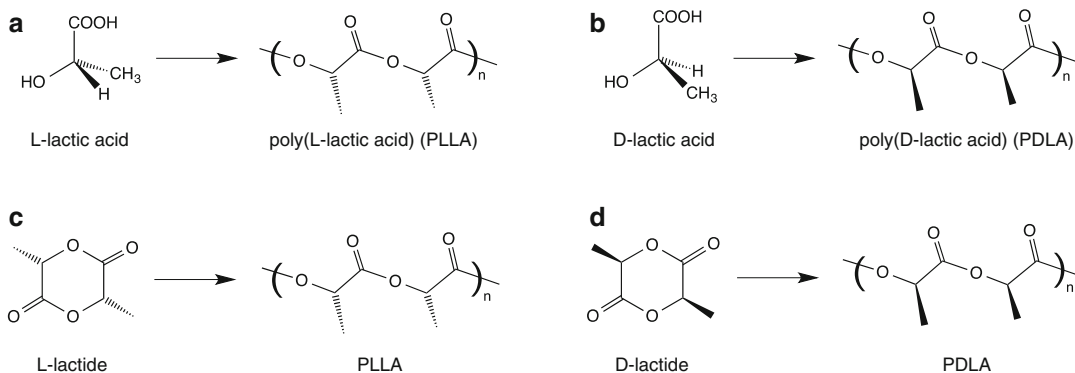
Poly(L-Lactide), Fig. 2 Synthesis of PLLA and PDLA

compared with those from potato, sugar beet, and so on. However, the use of corn as the raw material for PLLA reduces the amount of corn available for food provision. Moreover, the potential production of corn is limited, and its yield is affected by the weather conditions. Lactic acids include optically active compounds with L- and D-forms [(S)- and (R)-forms, respectively]. In a normal atmosphere, L-lactic acid deliquesces rapidly to L-lactic acid aqueous solution, and therefore, L-lactic acid is normally supplied as an aqueous solution. The yield, dominant enantiomeric form, and optical purity of lactic acid are determined by the type of lactobacillus used and the fermentation conditions [1]. From industrial and material points of view, a high yield and optical purity and a low concentration of impurities are crucial in the production of lactic acid.

Lactides (Fig. 2) are the cyclic dimers of lactic acids and have three different forms: (1) L-lactide [melting temperature (T_m) = 95–99 °C], which comprises two L-lactic acids, (2) D-lactide (T_m = 95–99 °C), which comprises two D-lactic acids, and (3) meso-lactide (MLA), which comprises one L-lactic acid and one D-lactic acid. Racemic lactide or DL-lactide (T_m = 124 °C) is a 1:1 physical mixture or a 1:1 racemic compound (stereocomplex) of L- and D-lactides. The industrial and laboratory method used for lactide synthesis is the thermal depolymerization of low-molecular-weight PLAs obtained by the polycondensation of lactic acids. The obtained crude lactides should be purified for the synthesis

of HMW PLA and PLA with a strictly controlled molecular weight.

PLLA

As shown in Fig. 2, relatively low-molecular-weight PLLA can be synthesized by condensation polymerization of L-lactic acid at an elevated temperature under reduced pressure, whereas the ring-opening polymerization of L-lactide is used for the synthesis of HMW PLLA and PLLA with a strictly controlled molecular weight [1–4]. By the use of a comonomer (including enantiomeric comonomer D-lactic acid or D-lactide) and coinitiator (alcohols) and chain-extending reagents, PLAs with various architectures including stereocopolymers can by synthesized [1–4]. Also, the combination of PLA with both hydroxyl-terminated and branched chain extenders such as isocyanates having three or more –N = C = O groups, or star-shaped hydroxyl-terminated PLA with linear or branched chain extenders, will yield cross-linked PLAs [1–4].

Crystallization

The higher-order structures related to crystallization, such as crystallinity and degree of orientation, greatly affect the physical properties and degradation behavior of PLLA and its copolymer-based materials. Crystallization of PLLA proceeds in the form of spherulites

(spherical assemblies of crystalline and amorphous regions) in bulk from the melt and of single crystals in a dilute solution [1–4]. In the case of spherulites, the induction period, spherulitic number per unit volume, and radial growth rate determine the total crystallization rate.

Homocrystallization

Crystallization (homocrystallization) of HMW PLLA and its copolymers occurs in bulk in the temperature range between the glass transition temperature ($T_g = 60$ °C) and T_m (170–180 °C). Various types of crystals of α- [1–4], α″- [5], β- [1–4], γ- [1–4], δ-(or α′-) [1–4], and ε- [6] forms (or modifications) are reported to be formed. α- and δ-(or α′-) forms are the most general ones for PLLA crystallized in bulk and in solution. The former and latter forms are produced at relatively high and low crystallization temperature (T_c) ranges, above and below 110−120 °C, respectively. The formation of the α″-form occurs under highly pressurized carbon dioxide. The β-form is created by thermal drawing, whereas the γ-form is produced by epitaxial crystallization on hexamethylbenzene. Also, the formation of the ε-form occurs in the presence of solvents such as N,N-dimethylformamide and tetrahydrofuran. PLLA can crystallize into eutectic crystals with pentaerythrityl tetrabromide, hexamethylbenzene, and urea [4].

The crystallization of PLLA and its copolymers in bulk proceeds via regime I, II, and III kinetics depending on T_c. The regime transitions from III to II and from II to I take place in the T_c range 110–120 °C and around 160 °C, respectively [1]. The radial growth of spherulites (G) reaches a maximum at around 130 °C for HMW PLLA, whereas the overall crystallization rate, which is determined by the induction period, number of spherulite nuclei per unit mass, and G, is maximized at around 110 °C [1]. The crystallizability of PLLA copolymers decreases with the fraction of comonomer units.

Stereocomplex Crystallization

Stereocomplex (homo-stereocomplex) formation of PLLA with PDLA, which is the enantiomeric polymer of PLLA, was reported in 1987 [7, 8].

In stereocomplex crystalline regions, PLLA and PDLA are packed side by side, that is, one PLLA chain is surrounded by three PDLA chains and vice versa. Stereocomplex crystallization can occur not only in PLLA/PDLA polymer blends but also in stereoblock PLA, as far as crystallizable PLLA and PDLA segments coexist [7, 8]. Because of the improved high mechanical performance, resistance to hydrolytic/thermal degradation, and gas barrier properties compared with the constituent polymer, numerous studies have been performed in this area [7, 8]. The most typical change in physical properties is the increase in T_m of about 50 °C. The T_m value of the PLLA/PDLA stereocomplex is 220–230 °C. Furthermore, hetero-stereocomplex formation was reported for PLLA with poly(D-2-hydroxybutayrate), i.e., poly(D-2-hydroxybutanoic acid) [P(D-2HB)], which has the opposite configuration to that of PLLA and a different side chain (ethyl group) from that of PLLA (methyl group) [1]. Owing to the phase-separated structure, interaction between PLLA and P(D-2HB) occurs only at their interface, and therefore, the effects of blending on the properties are not as strong as those for PLLA and PDLA. Also, PLLA or PDLA can be incorporated into poly(L-2-hydroxybutayrate), i.e., the poly(L-2-hydroxybutanoic acid)/ P(D-2HB) stereocomplex, to form a ternary stereocomplex [9, 10].

Physical Properties

The physical properties (including the mechanical properties) of PLLA and its copolymers depend on their molecular structures, higher-ordered structures, fillers, and material morphology.

Mechanical Properties

PLLA normally has the following mechanical properties: tensile strength $= 50$–70 MPa, tensile modulus $= 3$–4 GPa, elongation at break $= 2$–10 %, flexural strength $= 100$ MPa, flexural modulus $= 4$–5 GPa, notched Izod impact resistance $= 2.0$–7.0 kJ m^{-2}, unnotched

P

Izod impact strength $= 13$–$35 \, \text{kJ m}^{-2}$, and Rockwell hardness $= 82$–88 H [3]. The calculated crystallite moduli or ultimate Young's moduli along the chain axis in the crystal lattice of PLLA were reported to be 14.7 (α-form), 12.9 (δ-form or disordered α-form), and 6.7 GPa (mesophase), which are in good agreement with the values obtained by the X-ray diffraction method (13.76 ± 0.17, 12.58 ± 0.15, and 7.47 ± 0.20 GPa, respectively) [11].

Thermal Properties

As stated above, HMW PLLA with a molecular weight over 10^5 and optical purity near 100 % has a T_g of around 60 °C and a T_m of 170–190 °C, depending on the preparation procedure and conditions, and the equilibrium T_m ($T_m{}^0$) values are reported to be in the range 205–215 °C [1–4]. Several values (93, 135, 142, and 203 J g^{-1}) have been reported for the melting enthalpy of a crystal with infinite thickness ($\Delta H_m{}^0$, melting enthalpy (ΔH_m) at crystallinity = 100 %) [4]. PLLA with a molecular weight over 10^5 and optical purity near 100 % is thermally degraded to form mostly L-lactide at around 250 °C [1].

Permeability

The permeabilities of PLA-based materials have been investigated in terms of their drug-release profiles, whereas recently, the permeabilities of various gases through PLA-based materials have been studied because the permeability of PLLA toward carbon dioxide, oxygen, and water vapor is important for packing applications [1]. The CO_2, O_2, and water vapor permeability coefficients are reported to be in the range 1.99–4.18 $\times 10^{-17}$ (25–45 °C and 0 % RH), 3.5–11 $\times 10^{-18}$ (5–40 °C and 0 % RH), and 1.48–2.20 $\times 10^{-14}$ kg m/(m^2 s Pa) (10–37.8 °C and 40–90 % RH), respectively [3].

Surface Properties

The surface hydrophilicity of the materials is important if they are utilized for biomedical and pharmaceutical applications. Surface treatment effectively alters the surface hydrophilicity without affecting the bulk material properties.

General methods for changing the surface hydrophilicity of polymers include plasma treatment, surface grafting, coating, and alkaline treatment [1]. Polymer surfaces with contact angles of around 70° exhibit the highest cell adhesion [1]. Therefore, adjustment of the hydrophilicity of PLA-based materials by surface treatment leads to higher cell affinities for the material and better adhesion.

Optical Properties

PLA does not transmit UV-C light, and it is transparent to almost all UV-B and UV-A light; therefore, the application of transparent PLA films may require additives to block UV light transmission [12]. PLLA is optically active and has specific optical rotation values from -155 to $-160°$ dm^{-1} g^{-1} cm^3 [1–4]. The specific optical rotation values can be used to check the optical purities of PLA polymers.

Miscellaneous Properties

The density of PLLA is in the range 1.25–1.29 g cm^{-3} [4]. Oriented PLLA materials have a piezoelectric property, which increases with increasing draw ratio or chain orientation [1–4]. Oriented PLLA materials can be utilized to accelerate the regeneration of fractured bones in biomedical applications [1–4]. On the other hand, the conductivity of PLLA has been reported to be improved remarkably upon the incorporation of nanostructured carbon (such as multiwalled and single-walled carbon nanotubes) owing to the facile formation of a network structure because of its high aspect ratio [1].

High-Performance PLLA

Effective methods to improve the mechanical properties and thermal/hydrolytic degradation resistance of PLA-based materials can be summarized as follows: elevation of the crystallinity by using nucleating or crystallization-accelerating agents, formation of (nano)composites or fiber-reinforced plastics (FRPs), and stereocomplexation. In a book chapter [1], these methods of PLA-based materials are discussed in detail. The additives or fillers can be classified into subgroups according to their origin

(biobased or non-biobased) and biodegradability (biodegradable or nonbiodegradable).

Degradation

Hydrolytic Degradation

PLLA and its copolymers are aliphatic polyesters, and their ester groups are susceptible to hydrolytic degradation in the presence of water according to the following reaction:

$$-COO- + H_2O \rightarrow -COOH + HO-.$$
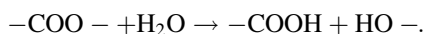
The hydrolytic degradation mechanism, behavior, and rate of PLLA and its copolymer are affected greatly by material- and media-related factors and the methods utilized to monitor the degradation. Of the material-related factors, molecular weight and crystallinity are crucial in determining the hydrolytic degradation rate of PLLA and its copolymers [1–4, 13, 14]. As in other hydrolyzable biodegradable polymers, the chains in the crystalline regions are more resistant to hydrolytic degradation than those in the amorphous region. Therefore, the hydrolytic degradation proceeds first in the amorphous regions and then in the crystalline regions. The hydrolytic degradation of water-insoluble HMW PLLA and its copolymer-based materials proceeds via bulk and surface erosion mechanisms when degraded in neutral aqueous media and catalytic aqueous media (alkaline aqueous media or media with enzymes such as proteinase K), respectively. The hydrolytic degradation mechanism of oligomeric water-soluble PLA on the molecular level depends on the pH of the medium (Fig. 3) [15]. In acidic media, hydrolytic degradation proceeds via chain-end scission of a lactyl monomer unit to form lactic acid, whereas in alkaline media, hydrolytic degradation occurs via backbiting to form a lactide (dimer of lactic acid), which is further hydrolyzed to give lactoyllactic acid and then lactic acid. Hydrolytic degradation is the most important feature of PLLA and its copolymers and is frequently applied in biomedical, pharmaceutical, and environmental applications.

Under physiological conditions (pH = 7.4, temperature = 37 °C), the hydrolytic degradation occurs via a bulk erosion mechanism. Under such conditions, the molecular weight decreases first, and then weight loss occurs. In other words, the induction period for the decrease in molecular weight is much shorter than that for weight loss. In the case of bulk erosion, the molecular weight decrease is sensitive to hydrolytic degradation, and its rate can be used as an indicator of the hydrolytic degradation rate. The hydrolytic degradation rate (k) values can be estimated from the change in number-average molecular weight (M_n) by using the following equation:

$$\ln M_n(t) = \ln M_n(t_0) - kt, \qquad (1)$$

where $M_n(t)$ and $M_n(t_0)$ are the M_n values at hydrolytic degradation times t and t_0, respectively; the k values obtained are in the range $2–7 \times 10^{-3}$ day^{-1} [1–4, 13, 14]. There are numerous articles regarding the hydrolytic degradation of PLA-based materials. Detailed and summarized information on the hydrolytic degradation of PLLA and its copolymers can be found in the review articles [1–4, 13, 14].

Biodegradation

Biodegradation can be defined as the enzyme-catalyzed hydrolytic degradation of HMW PLLA and its copolymers to form water-soluble low-molecular-weight lactic acid oligomers and monomer (1st stage) and the subsequent bio-assimilation of such degradation products to carbon dioxide and water (2nd stage). Here, the enzymes are derived from environmental microbes. Since the density of the microbes that release the enzymes to catalyze the hydrolytic degradation of PLLA and its copolymers is very low, the biodegradation rates of PLLA and its copolymers in environments such as sea water and soil are low compared with those of other biodegradable polyesters such as poly (ε-caprolactone) (PCL) and poly[(R)-3-hydroxybutyrate] [P(R-3HB)] [1–3, 13]. In most cases, the hydrolytic degradation of PLLA and its copolymers in the environment proceeds via

P
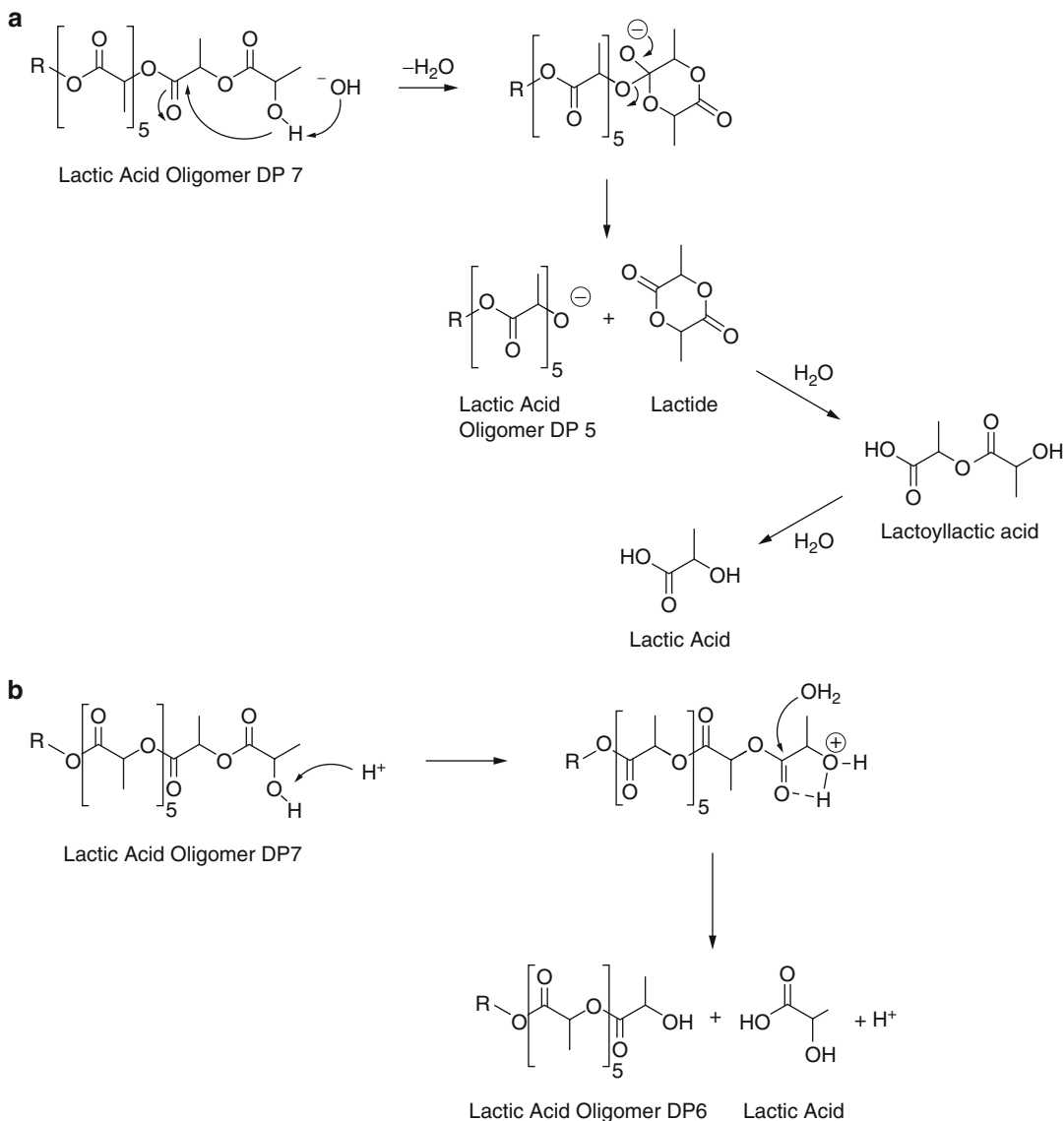
Poly(L-Lactide), Fig. 3 Hydrolytic chain cleavage mechanism of PLLA in acidic and alkaline solutions (Reproduced from de Jong et al. [15]. Copyright (2001), with permission from Elsevier)

abiotic (or nonenzymatic) hydrolytic degradation followed by the bio-assimilation of water-soluble degradation products [1–3, 13]. The carbon in PLLA and its copolymers is originally derived from carbon dioxide in the atmosphere and therefore will not alter the total amount of carbon dioxide upon bio-assimilation. The very low bio-degradation rates of PLLA and its copolymers mean that carbon dioxide is retained in the polymers for a long time.

Thermal Degradation

Upon heating PLLA over 250 °C, weight loss occurs by thermal degradation, and as a result, the volatile components are released [1–3, 13]. Therefore, a high processing temperature (250 °C or higher) should be avoided for the preparation of products made from PLLA and its copolymers. Volatile components formed by thermal degradation include lactides, cyclic oligomers ranging from trimers to hexamers, CO, CO_2,
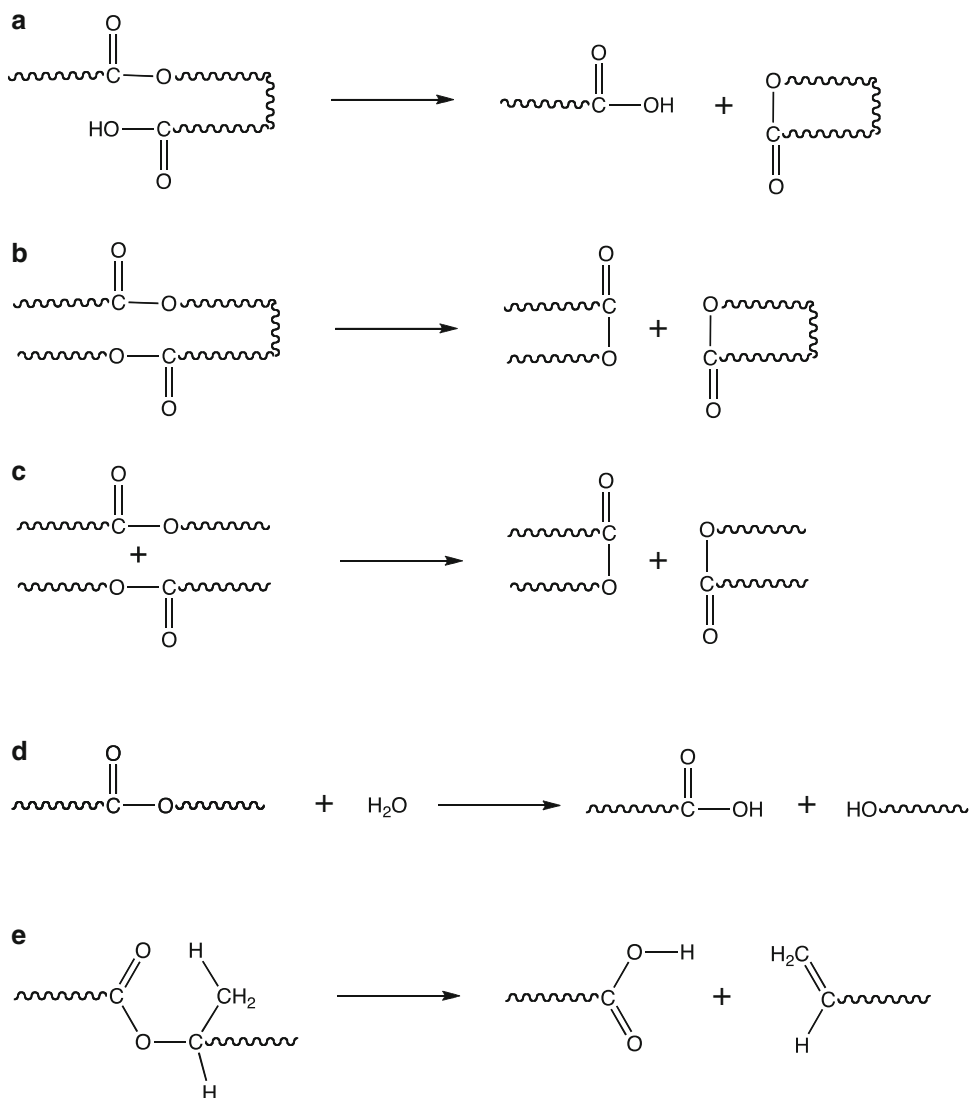
Poly(ʟ-Lactide), Fig. 4 Nonradical thermal degradation of PLA (Reproduced from Wachsen et al. [17]. Copyright (1997), with permission from Elsevier)

acetaldehyde, and methylketene [1–3, 13]. The thermal degradation of PLLA below 250–300 °C gives lactides, which can be utilized for the synthesis of HMW PLLA. With increasing degradation temperature and time, the probability of racemization increases, resulting in a low optical purity of the lactide even if the starting PLLA has a high optical purity [1–3, 13, 16]. Figure 4 shows the probable nonradical reactions that occur during PLA thermal degradation [17]. Lactides and cyclic oligomers are formed via intramolecular

transesterification reactions (a) and (b), resulting in a small decrease in molecular weight. The process (a) is called "backbiting," which forms lactides and can be suppressed by the acetylation reaction of terminal hydroxyl groups [1–3, 13]. Basically, intermolecular transesterification reaction (c) will not change the overall molecular weight distribution of PLLA. However, chain cleavage via hydrolytic degradation reaction (d) and *cis*-elimination reaction (e), which is similar to the Norrish type II photodegradation
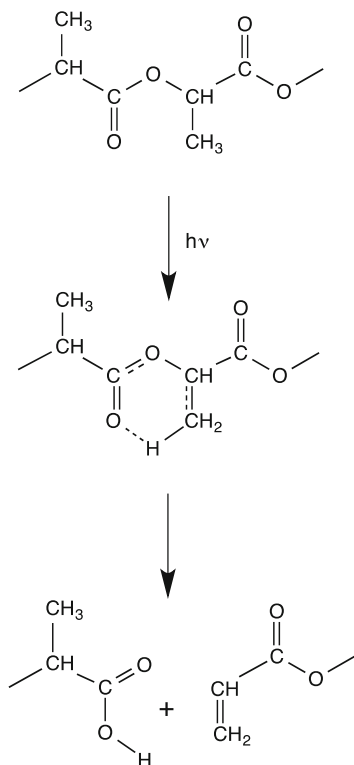
Poly(ʟ-Lactide), Fig. 5 Photodegradation of PLA (Reproduced from Tsuji et al. [18]. Copyright (2006), with permission from Elsevier)

reaction, both reduce the molecular weight significantly, and the latter reaction alters the terminal group structure.

Photodegradation

When released in the environment, PLLA is subject to biodegradation, hydrolytic degradation, and photodegradation by ultraviolet (UV) light. UV light-induced chain cleavage at the ester groups of PLA is reported to occur via the Norrish type II mechanism [1–3, 13] shown in Fig. 5 [18]. It has been reported that increased crystallinity decreases the photodegradation rate of PLLA [18]. The photodegradation of PLLA occurs simultaneously in the amorphous and crystalline regions, in marked contrast with hydrolytic degradation, although the chains in the crystalline regions are more resistant to photodegradation than those in the amorphous region [13]. UV treatment accelerates the hydrolytic degradation

of PLLA [19]. Therefore, the synergistic effects of photodegradation and hydrolytic degradation are thought to accelerate the degradation of PLLA and its copolymers in the environment.

Recycling

Recycling of PLLA to its monomer ʟ-lactic acid or ʟ-lactide can be attained by hydrolytic or thermal degradation, respectively. Hydrolytic degradation during the use of PLA-based materials causes a significant decrease in molecular weight, and the thermal stability of PLA-based materials during melt processing is relatively low compared with that of petro-derived polymers. Consequently, the recycling of PLA to lactic acid or lactide monomers is preferable compared with the material recycling, as in the case of PET. The recycling of PLA to lactic acid or lactide monomers prolongs the period that the carbon in PLA (originally from carbon dioxide in the atmosphere) is held in the materials. The highest yield values of lactic acid and lactide recovery are about 90 % if the conditions for recovery are selected carefully [1–4, 13, 14, 16]. A reaction temperature that is too high will cause a low yield and racemization-induced low optical purity of the monomer [1–4, 13, 14, 16], the latter of which will, in turn, lower the mechanical performance of resynthesized PLA.

Applications

PLLA can be utilized as an effective alternative to petro-based polymers in a variety of applications such as for packing materials, automotive materials including floor mats and spare tire covers, and the chassis of electrical appliances of computers, mobile phones, and remote controls [3]. Environmental applications of PLLA and its copolymers include materials for composting [20] and for absorbing harmful and persistent contaminants, denitrification-assisting materials, and bioremediation-assisting materials [3]. As mentioned above, biodegradable polyesters including PLLA and its copolymers can be

Poly(L-**Lactide**), **Table 1** Medical applications of bioabsorbable polymers (Reprinted from Ikada and Tsuji [20]. Copyright (2000), with permission from Wiley-VCH)

Function	Purpose	Examples
Bonding	Suturing	Vascular and intestinal anastomosis
	Fixation	Fractured bone fixation
	Adhesion	Surgical adhesion
Closure	Covering	Wound cover, local hemostasis
	Occlusion	Vascular embolization
Separation	Isolation	Organ protection
	Contact inhibition	Adhesion prevention
Scaffold	Cellular proliferation	Skin reconstruction, blood vessel reconstruction
	Tissue guide	Nerve reunion
Capsulation	Controlled drug delivery	Sustained drug release

applied as biomedical and pharmaceutical materials [1–4, 13, 14, 20]. The functions and purposes of bioabsorbable polymers including PLLA and its copolymers are summarized in Table 1 [20]. Bioabsorbable biomedical materials should be nontoxic, effective, sterilizable, and biocompatible. In addition, bioabsorbable biomedical materials should have the appropriate degradation rate required for each application.

Summary

In this chapter, an overview of the basic aspects of PLLA and its copolymers has been presented. The crucial issues for the utilization of PLLA-based materials as alternatives to petro-based polymeric materials are the reduction of the production cost and environmental impact and the enhancement of the mechanical performance and resistance to hydrolytic/thermal degradation. Another important goal is to produce PLLA from nonedible raw materials rather than from edible materials such as corn, as utilized today.

(Nano)composites and FRP formation are effective for the production of high-performance PLLA-based materials. However, the balance between high performance and environmental impact (and production cost) has to be considered. Too high an environmental impact of greatly modified PLLA-based materials should be avoided, and in such a case, the high intrinsic performances of polymeric materials such as aromatic polyamide- or polyimide-based materials must be used instead. PLA should be used more frequently when the functionality of hydrolizability is required, as in the cases of biomedical, pharmaceutical, and environmental applications.

Related Entries

▶ Biobased Polymers
▶ Biodegradable Materials
▶ Biodegradable Polymers
▶ Controlled Release
▶ Stereocomplexed Polylactides

References

1. Tsuji H (2014) Poly(lactic acid). In: Kabasci S (ed) Bio-based plastics: materials and application, Wiley series in renewable resources. Wiley, West Sussex, pp 171–239
2. Tsuji H (2008) Poly(lactic acid): fundamentals and applications of plant-derived plastics (in Japanese). Yoneda Shuppan, Tokyo
3. Auras R, Lim L-T, Selke SEM, Tsuji H (eds) (2010) Poly(lactic acid): synthesis, structures, properties, processing, and applications, Wiley series on polymer engineering and technology. Wiley, Hoboken
4. Tsuji H (2002) Polylactide. In: Doi Y, Steinbüchel A (eds) Polyesters 3. Biopolymers, vol 4. Wiley-VCH, Weinheim, pp 129–177
5. Marubayashi H, Akaishi S, Akasaka S, Asai S, Sumita M (2008) Crystalline structure and morphology of poly(L-lactide) Formed under high-pressure CO_2. Macromolecules 41:9192–9203
6. Marubayashi H, Asai S, Sumita M (2012) Complex crystal formation of poly(L-lactide) with solvent molecules. Macromolecules 45:1384–1397
7. Tsuji H (2005) Poly(lactide) stereocomplexes: Formation, structure, properties, degradation, and applications. Macromol Biosci 5:569–597

P

8. Fukushima K, Kimura Y (2006) Stereocomplexed polylactides (Neo-PLA) as high-performance bio-based polymers: their formation, properties, and application. Polym Int 55:626–642

9. Tsuji H, Hosokawa M, Sakamoto Y (2012) Ternary stereocomplex formation of one L-configured and two dconfigured optically active polyesters, poly(L-2-hydroxybutanoic acid), Poly(D-2-hydroxybutanoic acid), and Poly(D-lactic acid). ACS Macro Lett 1:687–691

10. Tsuji H, Hosokawa M, Sakamoto Y (2013) Ternary stereocomplex crystallization of poly(L-2-hydroxybutanoic acid), poly(D-2-hydroxybutanoic acid), and poly(D-lactic acid) from the melt. Polymer 54:2190–2198

11. Wasanasuk K, Tashiro K (2012) Theoretical and experimental evaluation of crystallite moduli of various crystalline forms of poly(L-lactic acid). Macromolecules 45:7019–7026

12. Auras R, Harte B, Selke S (2004) An overview of polylactides as packaging materials. Macromol Biosci 4:835–864

13. Tsuji H (2007) Degradation of poly(lactide)-based biodegradable materials. Nova, New York

14. Tsuji H (2010) Hydrolytic degradation. In: Auras R, Lim L-T, Selke SEM, Tsuji H (eds) Poly(lactic acid): synthesis, structures, properties, processing, and applications, Wiley series on polymer engineering and technology. Wiley, Hoboken, pp 345–381

15. de Jong SJ, Arias ER, Rijkers DTS, van Nostrum CF, Kettenes-van den Bosch JJ (2001) New insights into the hydrolytic degradation of poly(lactic acid): participation of the alcohol terminus. Polymer 42:2795–2802

16. Tsuji H, Fukui I, Daimon H, Fujie K (2003) Poly(L-lactide) XI. Lactide formation by thermal depolymerisation of poly(L-lactide) in a closed system. Polym Degrad Stab 81:501–509

17. Wachsen O, Reichert KH, Krüger RP, Much H, Schulz G (1997) Thermal decomposition of biodegradable polyesters-III. Studies on the mechanisms of thermal degradation of oligo-L-lactide using SEC, LACCC and MALDI-TOF-MS. Polym Degrad Stab 55:225–231

18. Tsuji H, Echizen Y, Nishimura Y (2006) Photodegradation of biodegradable polyesters: a comprehensive study on poly(L-lactide) and poly(ε-caprolactone). Polym Degrad Stab 91:1128–1137

19. Tsuji H, Shimizu K, Sato Y (2012) Hydrolytic Degradation of Poly(L-lactic acid): Combined Effects of UV Treatment and Crystallization. J Appl Polym Sci 125:2394–2406

20. Ikada Y, Tsuji H (2000) Biodegradable polyesters for medical and ecological applications. Macromol Rapid Commun 21:117–132

Poly(methyl methacrylate) (PMMA)

Raita Goseki and Takashi Ishizone
Department of Organic and Polymeric Materials, Tokyo Institute of Technology, Meguro-ku, Tokyo, Japan

Synonyms

Acrylic glass; Methacrylic resin; PMMA; Polymethacrylate

Definition

Poly(methyl methacrylate) (PMMA) is a polymer of methyl methacrylate (MMA) and an ester of poly(methacrylic acid) chemically. PMMA is usually synthesized by the radical polymerization of MMA, and the anionic and coordination polymerizations are also available. PMMA is one of the methacrylic resins, generally called as acrylic resin. PMMA is a transparent thermoplastic showing impact-resistant, weather-resistant, and chemical-resistant properties and is known as a substitute for inorganic glass. Since PMMA is rigid and light in weight and has color versatility, it is used in various applications across optical materials, automobiles, electronics, displays, and other industries.

Manufacturing Method

Poly(methyl methacrylate) (PMMA) is usually obtained by the addition polymerization of methyl methacrylate (MMA) (Fig. 1). In the middle of the 1930s, ICI Acrylics (now Lucite International) invented the first commercial process, so-called acetone cyanohydrin (ACH) route, for producing MMA monomer. In the ACH process, acetone and hydrogen cyanide are first reacted to produce acetone cyanohydrin. Then, the resulting cyanohydrin is converted into methacrylamide

Poly(methyl methacrylate) (PMMA), Fig. 1 Synthesis of PMMA by addition polymerization of MMA
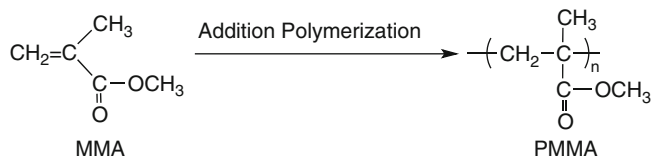
sulfate with sulfuric acid, and the product is finally treated with a methanol/water mixture under heating to form MMA and ammonium (bi)sulfate. Up to now, many companies tried to develop new synthetic processes for MMA to reduce the byproducts and the total cost and to find milder reaction conditions without toxic or corrosive chemicals. In those processes including oxidation of alkenes, ethylene, propylene, or isobutylene is a key starting material for the production of MMA.

In industry, most of PMMA is produced by the radical polymerization of MMA including emulsion polymerization, solution polymerization, and bulk polymerization. Methacrylic plastics are generally available in three forms: flat sheets, elongated shapes (rods and tubes), and powder depending on the polymerization method. Mitsubishi Rayon, Lucite International, Arkema, Chi Mei, Evonik, Kuraray, LG MMA, and Sumitomo Chemical are present major suppliers of PMMA.

Polymerization

As mentioned above, PMMA is mainly produced by the radical polymerization of MMA in industry, while anionic and coordination polymerization of MMA can be also performed to give PMMA. The thermal property of PMMA strongly depends on the stereoregularity (or tacticity) similar to other vinyl polymers, such as polypropylene and polystyrene. It is known that the stereoregularity of polymers is largely affected by the polymerization mechanism. The stereoregularity of PMMA has been well established and can be measured by ^{1}H and ^{13}C NMR spectroscopies to determine the triad (*rr*, *mr*, and *mm*
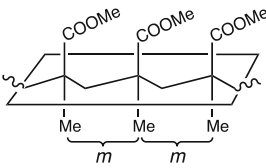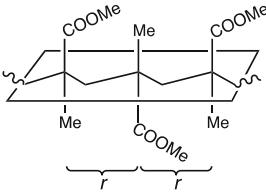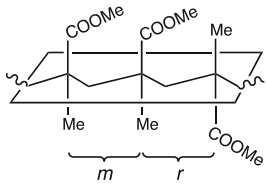
values) and even pentad contents [1]. The commercially available PMMA, produced by radical polymerization, serves as an amorphous polymer possessing slightly syndiotactic-rich configuration (*rr* = 60 $\sim$ 70 %). On the other hand, PMMAs possessing highly controlled stereoregularities, such as *mm*-rich (isotactic), *rr*-rich (syndiotactic), and *mr*-rich (heterotactic) PMMAs, show crystalline properties [2] (Table 1). It is noted that the glass transition temperature (T_g) of PMMA tends to increase with the *rr* triad content.

In addition to a variety of thermal properties, the stereoregularity of PMMA also plays an important role in the formation of stereocomplex, which is a crystalline-like structure consisting of isotactic and syndiotactic PMMA segments [2]. Since the discovery of the PMMA stereocomplex, several novel materials, such as silica hybrids [3], fullerene assemblies [4], and hollow capsules by layer-by-layer assembly [5], have been invented by skillfully exploiting this complex formation. Since the highly isotactic and syndiotactic stereoregularities of PMMA segments are necessary to form the stereocomplex, continuous and numerous attempts in the polymerization system of MMA have been carried out to achieve the high order regulation of tacticity.

Radical Polymerization of MMA
As mentioned above, radical polymerization is the most popular synthetic method of PMMA. PMMA powder is commonly produced by suspension polymerization, in which the reaction takes place between tiny droplets of MMA suspended in water and radical initiator. This results in grains of powder suitable for the molding or the extrusion. PMMA flat sheets are manufactured by bulk polymerization of liquid

Poly(methyl methacrylate) (PMMA), Table 1 Relationship between stereoregularity and thermal property of PMMA

	Chemical structure	T_g	T_m
Isotactic PMMA		≈ 50	159
Syndiotactic PMMA		≈ 130	150
Heterotactic PMMA		≈ 90	166
Commercially available PMMA		≈ 70	Amorphous
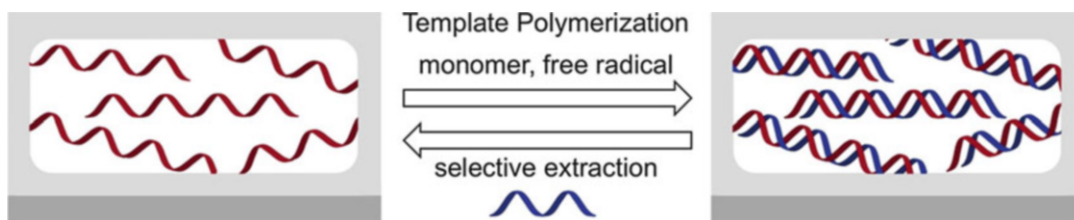
Poly(methyl methacrylate) (PMMA), Fig. 2 Template polymerization on the thin porous film with regular nanospace

MMA monomer between two plates of glass. The bulk polymerization can be carried out in a water bath or a hot oven. PMMA block (or thick plate) can be assembled by the adhesion of PMMA plates with the viscous syrup containing MMA, PMMA, and radical initiator and then followed by heating and/or irradiation for a complete consumption of MMA.

Although the stereo controls of polymers in the radical polymerization are usually difficult, the stereoregulated PMMA has been synthesized by the template polymerization using other stereoregulated polymers. As a most valuable

example, the stereocomplex thin film consisting of a 1:1 mixture of PMMA and poly(methacrylic acid) (PMAA) is used for the precursor of the template [6] (Fig. 2). From the stereocomplex, the alternative extraction of PMMA or PMAA is possible by the suitable solvent to form the thin porous film consisted of one component as an effective template. For example, when the template polymerization of MMA is carried out on a porous thin film of syndiotactic PMAA ($rr > 92$ %), the stereoregulated PMMA with highly isotactic configurations ($mm > 92$ %) can be obtained. On the other hand, syndiotactic

Poly(methyl methacrylate) (PMMA),
Fig. 3 Initiators for living anionic polymerization of MMA
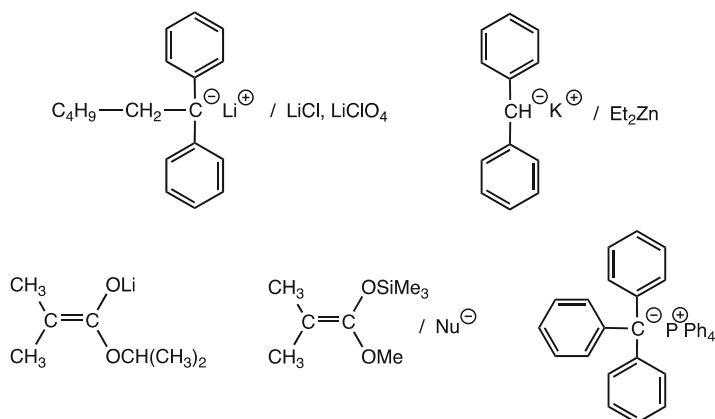
PMAA ($rr > 94$ %) is produced by the template polymerization of methacrylic acid (MA) using a porous thin film of isotactic PMMA ($mm > 96$ %) as a template.

Anionic Polymerization of MMA

MMA is a typical α,β-unsaturated carbonyl compound showing high anionic polymerizability, since the electron density of C=C bond is remarkably reduced by the electron-withdrawing COOMe group. On the other hand, MMA is difficult to polymerize with the cationic initiators. The anionic polymerization of MMA can be readily initiated with various anionic initiators, such as organolithiums, Grignard reagents, and even alkoxides. The organolithiums showing high nucleophilicities are usually necessary for the high initiation efficiencies to regulate the molecular weights of the produced PMMA. In the anionic polymerization of MMA, the nature of the solvent and the reaction temperature deeply affect the yield and the tacticity of the resulting PMMA. In general, organolithium-mediated polymerization of MMA in a nonpolar solvent, such as toluene, affords *mm*-rich PMMA, while *rr*-rich PMMA forms in a polar solvent, such as THF [7]. On the other hand, a PMMA with 52 % *mr* content is obtained, when the polymerization is performed with organopotassium initiators, such as diphenylmethylpotassium (Ph$_2$CHK), in THF [8]. Thus, remarkable effects of solvent and counter cation on the stereoregularity are observed in the anionic polymerization of MMA. From the viewpoints of molecular weight

control, a number of effective initiator systems have been intensely developed, as shown in Fig. 3. These initiator systems effectively induce the living anionic polymerization of MMA to give the PMMA predicted molecular weight and narrow molecular weight distributions (M_w/$M_n < 1.1$). The systems include the bulky and π-conjugated carbanions in the presence of common salts or Lewis acidic additives [9–11], lithium enolate [12], silyl ketene acetal in conjunction with nucleophilic activator [13], and metal-free anion [14].

In addition to the controls on molecular weights, a series of well-defined PMMAs with highly isotactic, syndiotactic, and heterotactic configurations have been synthesized by selecting the suitable initiator systems and solvents [7] (Fig. 4). Organolithium (RLi) or Grignard reagent (RMgX) in the presence of Lewis acidic additives, such as R$_3$Al [15], R$_{3-n}$(R'O)$_n$Al [16], and MgX$_2$ [17], effectively induces the stereospecific living anionic polymerization of MMA in toluene along with the precise control of molecular weights and molecular weight distributions.

Coordination Polymerization of MMA

In the coordination polymerization of MMA, a number of transition metal catalysts have been developed and employed to control the polymerization [18, 19] (Fig. 5). In particular, various single-site polymerization catalysts called "metallocenes" are effective to narrow the molecular weight distribution of PMMA. The

Poly(methyl methacrylate) (PMMA), Fig. 4 Stereospecific living anionic polymerization of MMA
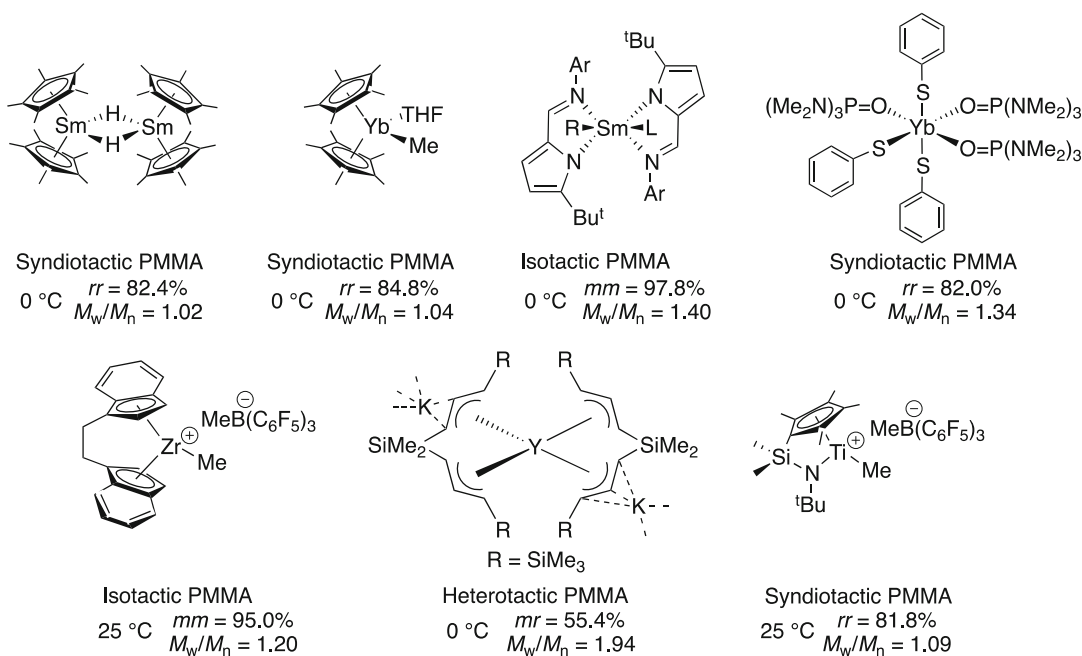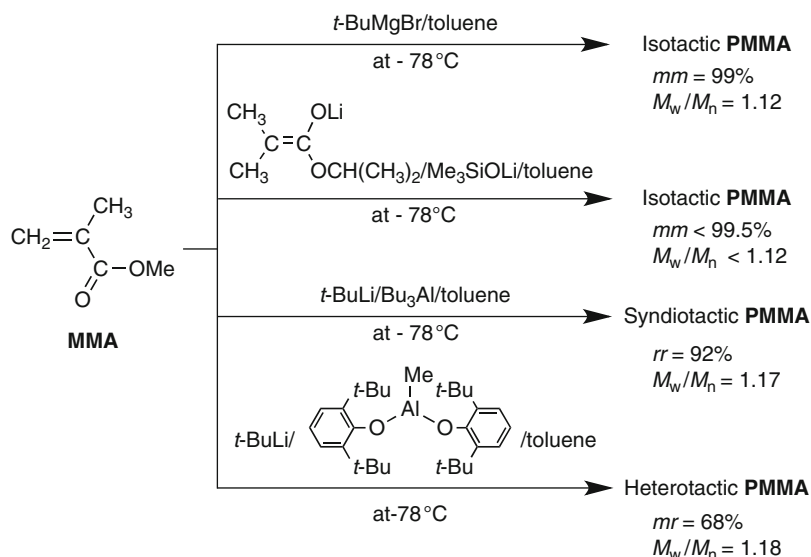
Poly(methyl methacrylate) (PMMA), Fig. 5 Catalysts for stereospecific coordination polymerization of MMA

relationship between the catalyst symmetry and the stereospecificity of the polymerization has been investigated to synthesize a series of highly stereoregulated PMMAs. By the catalysts shown in Fig. 5, stereoregulated PMMAs have been produced by the initiation with transition metal catalysts possessing appropriate ligands above 0 °C.

Esterification of PMAA

PMMA can be prepared not only by the polymerization of MMA but also by the esterification of PMAA. In fact, various esterification methods for carboxylic acids are available for the synthesis of PMMA. Among them, diazomethane is a conventional reagent effective for the

complete methylation of PMAA. It is known that the stereoregularities of the polymethacrylates strongly depend on the monomer structures, particularly on the ester substituents, as well as the polymerization method. The methylation, or conversion of PMAA to PMMA, is often performed in order to determine the stereoregularities of PMAA and other polymethacrylates, since the characterization of stereoregularity for PMMA is well established. For example, a poly (trimethylsilyl methacrylate) is first obtained by the anionic polymerization of trimethylsilyl methacrylate [20]. Then, the resulting polymer is converted into PMMA via the hydrolysis of the trimethylsilyl ester and the subsequent methylation of the PMAA. The NMR measurement of the PMMA obtained by the two-step polymer reactions is finally performed to determine the stereoregularity of the initial poly(trimethylsilyl methacrylate).

Property

Most importantly, PMMA transmits up to 92.6 % of visible light and shows a very low birefringence ($\Delta n = -0.0043$, refractive index; $n = 1.49$). Therefore, PMMA is widely used as a representative transparent thermoplastic material for various optical media. PMMA dissolves in many organic solvents, such as benzene, chloroform, acetone, and tetrahydrofuran, but is insoluble in hexane, methanol, and water. However, PMMA is rather hygroscopic and can absorb about 2 wt% of water despite of its insolubility in water. This hygroscopic property often causes the serious dimensional change of PMMA materials. PMMA is a strong and lightweight material having a density of 1.17–1.20 g/cm^3, which is less than half of inorganic glass (2.5 g/cm^3). The glass transition temperature (T_g) of PMMA is observed in the range from 50 °C to 130 °C depending on their stereoregularity as shown in Table 1. Heat molding of PMMA is possible and usually performed over 190 °C. On the other hand, thermal zipper-like depolymerization of PMMA is often observed to result in a decline of mechanical property due to the decrease of molecular weight under the thermal treatment process. Therefore, the copolymerization of MMA with small amount of acrylate monomers has been used to prevent such main chain degradation and to keep properties of PMMA.

Although the methyl ester function of PMMA can be hydrolyzed under acidic or basic conditions to form the repeating unit of PMAA, PMMA is rather stable and highly weather resistant. In fact, since the environmental stability of PMMA is superior to other plastics such as polystyrene and polyethylene, it is often used as the materials for outdoor uses. Moreover, the property of PMMA can be easily modified by copolymerizing MMA with other vinyl monomers including acrylates, and various modified polymeric materials based on PMMA have been invented.

Uses

As described above, the homopolymer of MMA and its copolymers are prepared and used as PMMA-based materials. In this section, such modified PMMA materials are also introduced as PMMA. It is known that PMMA shows high transparency, durability, and shock resistance, and the coloring is rather easy due to the adequate polarity. Since PMMA has above excellent performances, it is used in various fields and applications, such as window material for a construction (Fig. 6), lenses of glasses, cover of a light, road sign and displays, stationery, and
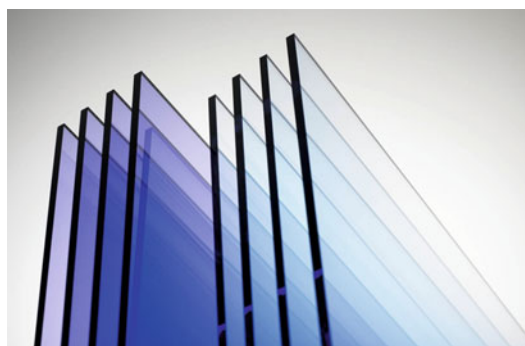
Poly(methyl methacrylate) (PMMA), Fig. 6 Colored PMMA plate (Mitsubishi Rayon Co., Ltd.)

Poly(methyl methacrylate) (PMMA), Fig. 7 Automobile taillight lenses (Sumitomo Chemical Co., Ltd.)

Poly(methyl methacrylate) (PMMA), Fig. 8 Automobile visors (Sumitomo Chemical Co., Ltd.)

handicraft, as a typical substitute of inorganic glass.

Historically, "acrylic glass" made of PMMA was first used for military purposes, such as canopies for airplanes, windshield, and submarine periscopes, during World War II. Recently, it is widely applied for lenses and visors of vehicles due to its transparency, lightness, and durability (Figs. 7 and 8). Compared with inorganic glass, PMMA panel, organic glass, is very tough, pressure resistant, and shatter resistant. It can be formed in a wide variety thickness by the development of the molding technology of PMMA plate. In fact, manufacture of the extremely large-sized water tank, which has 600 mm of thickness of PMMA plate, in the aquarium is possible using the special assembling method (Figs. 9 and 10).

Optical fiber is usually made from inorganic silica and used for the long-distance communication, such as a submarine cable. On the other hand, organic optical fibers are mainly made from PMMA and widely used for short-distance communication because of the flexibility, the ease of installation, and the reasonable costs (Fig. 11), although they have disadvantages, such as the poor heat tolerance and the attenuation higher than inorganic glass fiber.

Poly(methyl methacrylate) (PMMA), Fig. 9 Large PMMA panel with 8.2 m height, 22.5 m width, and 600 mm thickness at Okinawa Churaumi Aquarium in Japan (Sumitomo Chemical Co., Ltd. and Nippura Co., Ltd.)

Poly(methyl methacrylate) (PMMA), Fig. 10 Manufacturing of large PMMA panel at Okinawa Churaumi Aquarium in Japan (Sumitomo Chemical Co., Ltd. and Nippura Co., Ltd.)
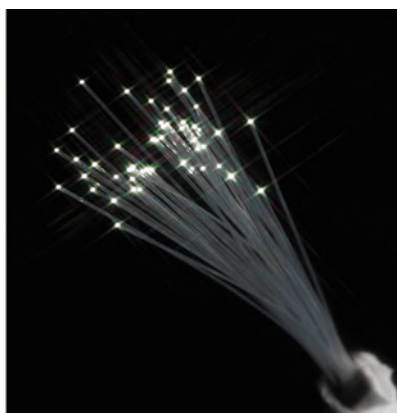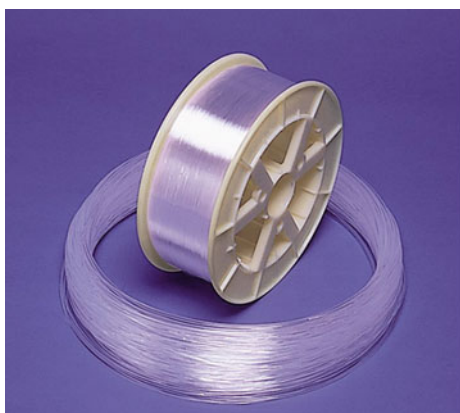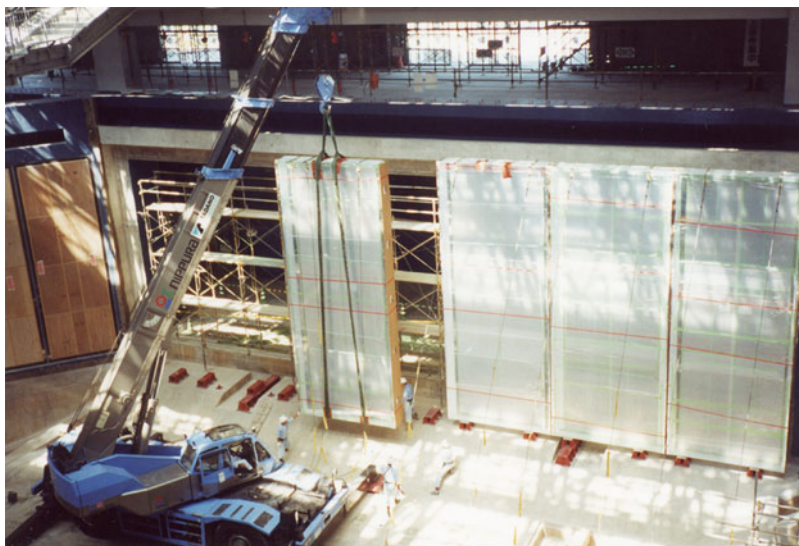
Poly(methyl methacrylate) (PMMA), Fig. 11 PMMA optical fibers (Mitsubishi Rayon Co., Ltd.)

Specially designed PMMA panel can be used as a light guide plate, when a dot matrix or a line matrix is properly patterned on its bottom face (Fig. 12). In the light guide plate, the light source is usually installed on its edge to make the device slim. The light guide plate can evenly distribute the light from the source over the upper face of the panel, and it acts as a backlight to maximize the uniformity of light for liquid crystalline display and LED.

PMMAs are also extensively used in medical and dental applications because of the good compatibility with human tissue. The emulsion of PMMA in water is used as aqueous acrylic paints and adhesives.

Poly(methyl methacrylate) (PMMA), Fig. 12 Light guide plate with dotted pattern on the back surface for reflection purposes (Sumitomo Chemical Co., Ltd.)

Related Entries

References

1. Hatada K, Kitayama T, Ute K (1988) Stereoregular polymerization of α-substituted acrylates. Prog Polym Sci 13:189–276. doi:10.1016/0079-6700(88)900004-4

2. Hatada K (1999) Stereoregular uniform polymers. J Polym Sci A Polym Chem 37:245–260. doi:10.1002/(SICI)1099-0518(19990201)37:3<245::AID-POLA1>3.0.CO;2-9

3. Kumar AA, Adachi K, Chujo Y (2004) Synthesis and characterization of stereoregular poly(methyl methacrylate)-silica hybrid utilizing stereocomplex formation. J Polym Sci A Polym Chem 42:785–794. doi:10.1002/pola.10880

4. Kawauchi T, Kumaki J, Yashima E (2006) Nanosphere and nanonetwork formations of [60] fullerene-end-capped stereoregular poly(methyl methacrylate)s through stereocomplex formation combined with self-assembly of the fullerenes. J Am Chem Soc 128:10560–10567. doi:10.1021/ja063252u

5. Kida T, Mouri M, Akashi M (2006) Fabrication of hollow capsules composed of poly(methyl methacrylate) stereocomplex films. Angew Chem Int Ed 45:7534–7536. doi:10.1002/anie.200602116

6. Serizawa T, Hamada K, Akashi M (2004) Polymerization within a molecular-scale stereoregular template. Nature 429:52–55. doi:10.1038/nature02525

7. Hatada K, Kitayama T (2000) Structurally controlled polymerizations of methacrylates and acrylates. Polym Int 49:11–47. doi:10.1002/(SICI)1097-0126(200001)49:1<11::AID-PI346>3.0.CO;2-6

8. Ozaki H, Hirao A, Nakahama S (1995) Anionic polymerization of alkyl methacrylates in the presence of diethylzinc. Macromol Chem Phys 196:2099–2111. doi:10.1002/macp.1995.0219600702

9. Baskaran D (2003) Strategic developments in living anionic polymerization of alkyl (meth)acrylates. Prog Polym Sci 28:521–581. doi:10.1016/S0079-6700(02)00083-7

10. Varshney SK, Hauteker JP, Fayt R, Jerome R, Teyssie P (1990) Anionic polymerization of (Meth)acrylic monomers. 4. Effect of lithium salts as ligands on the "Living" polymerization of methyl methacrylate using monofunctional initiators. Macromolecules 23:2618–2622. doi:10.1021/ma00212a004

11. Baskaran D, Sivaram S (1997) Specific salt effect of lithium perchlorate in living anionic polymerization of methyl methacrylate and tert-butyl acrylate. Macromolecules 30:1550–1555. doi:10.1021/ma961118w

12. Kitaura T, Kitayama T (2007) Anionic polymerization of methyl methacrylate with the aid of lithium trimethylsilanolate (Me_3SiOLi) – superior control of isotacticity and molecular weight. Macromol Rapid Commun 28:1889–1893. doi:10.1002/marc.200700409

13. Webster OW, Hertler WR, Sogah DY, Farnham WB, RajanBabu TV (1983) Group-transfer polymerization. 1. A new concept for addition polymerization with organosilicon initiators. J Am Chem Soc 105:5706–5708. doi:10.1021/ja00355a039

14. Zagala AP, Hogen-Esch TE (1996) Anionic synthesis of narrow MWD PMMA at ambient temperature in the presence of tetraphenylphosphonium cation. Macromolecules 29:3038–3039. doi:10.1021/ma951405k

15. Kitayama T, Shinozaki T, Masuda E, Yamamoto M, Hatada K (1988) Highly syndiotactic poly(methyl methacrylate) with narrow molecular weight distribution formed by tert-butyllithium-trialkylaluminium in toluene. Polym Bull 20:505–510. doi:10.1007/BF00263663

16. Tabuchi M, Kawauchi T, Kitayama T, Hatada K (2002) Living polymerization of primary alkyl acrylates with t-butyllithium/bulky ammonium Lewis acids. Polymer 43:7185–7190. doi:10.1016/S0032-3861(02)00461-5

17. Hatada K, Ute K, Tanaka K, Kitayama T, Okamoto Y (1985) Preparation of highly isotactic poly(methyl methacrylate) of low polydispersity. Polym J 17:977–980. doi:10.1295/polymj.17.977

18. Chen EY-X (2009) Coordination polymerization of polar vinyl monomers by single-site metal catalysts. Chem Rev 109:5157–5214. doi:10.1021/cr9000258

19. Rodriguez-Delgado A, Mariott WR, Chen EY-X (2004) Living and syndioselective polymerization of methacrylates by constrained geometry titanium alkyl and enolate complexes. Macromolecules 37:3092–3100. doi:10.1021/ma04977g

20. Kitayama T, He S, Hironaka Y, Iijima T, Hatada K (1995) Preparation of highly stereoregular poly(methacrylic acid) by stereospecific anionic polymerization of trimethylsilyl methacrylate. Polym J 27:314–318. doi:10.1295/polymj.27.314

Poly(phenylene oxide) and Poly(phenylene sulfide) Syntheses

Shiro Kobayashi
Center for Fiber and Textile Science, Kyoto
Institute of Technology, Matsugasaki, Sakyo-ku,
Kyoto, Japan

Synonyms

Composite materials; Condensation polymerization; Engineering plastics; Enzymatic catalyst; Enzyme model complex; High performance plastics; Oxidative polymerization

Definition

Synthesis of poly(phenylene oxide) and poly (phenylene sulfide) and their polymer properties.

Background

Poly(phenylene oxide) (PPO), which is sometimes called poly(phenylene ether) (PPE), and poly(phenylene sulfide) (PPS) are practically important and widely used as high performance engineering plastics. The synthetic reactions of both belong to a typical type of condensation polymerization via step-growth pathways. The polymerization reaction of the former is unique, known as an oxidative coupling polymerization. Proceedings of these synthesis reactions are briefly described. Important property data and applications of these polymers are also given.

Synthesis Reaction of Poly(phenylene oxide) (PPO) or poly(phenylene ether) (PPE) and Polymer Properties

With the pioneering work by Hay et al. (General Electric Co. or GE), PPO was first synthesized via oxidative polymerization in 1959 [1, 2]. They reported a new catalyst of copper/amine using oxygen gas as an oxidant for the oxidative coupling of 2,6-disubstituted phenols (Fig. 1). When R = methyl, the reaction in nitrobenzene/ pyridine at room temperature absorbed a stoichiometric amount of oxygen for 26 min, and C-O coupling occurred to produce PPO with high molecular weight, M_n = 28,000 in 84 % yield. The IUPAC name of PPO is poly(oxy-2,6-dimethyl-1,4-phenylene). When R is bulky like a *t*-butyl group, the C-C coupling product of a dimer (3,3′,5,5′-tetra-*t*-butyldiphenoquinone, DPQ) was the sole product.

The mechanism of the oxidative coupling to selectively form C-O coupling to polymer PPO has been studied by many chemists, and three possible pathways have been proposed, for the case of the polymerization of 2,6-dimethylphenol (DMeP) shown in Fig. 2 [3, 4], (i) coupling of free phenoxy radicals resulting from one-electron oxidation of DMeP, (ii) coupling of phenoxy radicals coordinated to catalyst complex, and (iii) coupling of phenoxonium cation formed by two-electron oxidation of DMeP. Although it

Poly(phenylene oxide) and Poly(phenylene sulfide) Syntheses, Fig. 1 Reaction pathways of a 2,6-disubstituted phenol via oxidative coupling
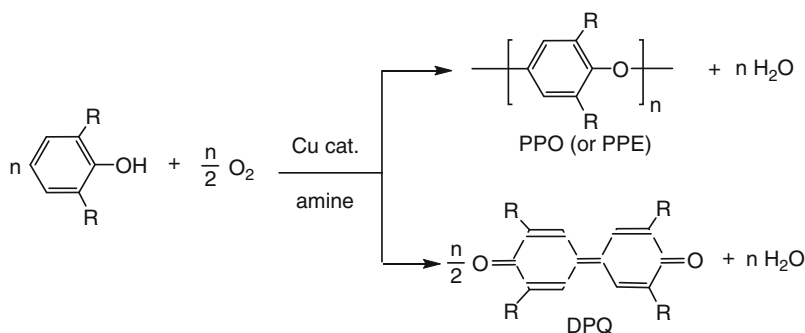
(i) coupling of free phenoxy radicals
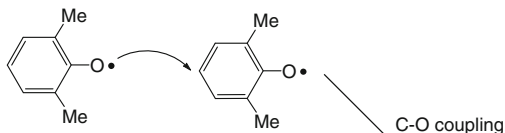
(ii) coupling of phenoxy radicals coordinated to catalyst
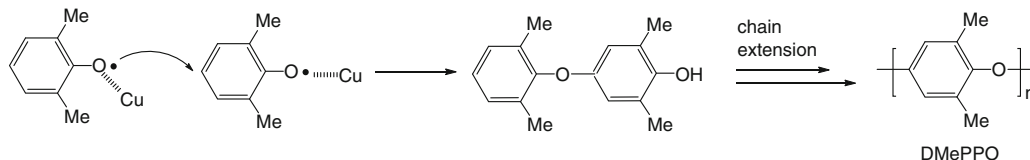
(iii) coupling of phenoxonium cation with phenol
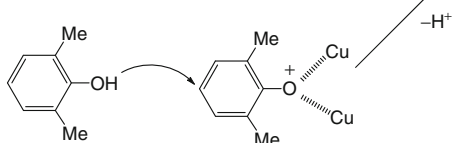
Poly(phenylene oxide) and Poly(phenylene sulfide) Syntheses, Fig. 2 Conceivable mechanisms of oxidative coupling polymerization of 2,6-dimethylphenol (DMeP)

was reported that reaction mechanism (iii) would be most probable [5], the mechanism for the C-O coupling has not been fully clarified yet.

In contrast to the copper-catalyzed oxidative PPO synthesis, the oxidative reaction of DMeP using an oxidant like benzoyl peroxide or alkaline ferricyanide did not yield PPO, but yielded a dimer DPQ as the main product. Therefore, the reaction shown in Fig. 1 seems specific for affording PPO [6].

So far, a variety of PPO derivatives with different substituents have been prepared; DMePPO from DMeP is the most important and most widely used practically. DMePPO is a hard, tough, ductile, and white material showing values of T_g (glass transition temp.) of 205 °C, T_m (crystal melting temp.) of 267 °C, density 1.06 g/cm^3 at 23 °C, tensile strength 80 MPa at 23 °C, and elongation at break of 20–40 % at 23 °C. DMePPO is soluble in many organic solvents such as toluene, benzene, and halogenated hydrocarbons. DMePPO is not used as a single component polymer due to its melt viscosity being too high for injection molding; however, it is freely miscible with many kinds of polymers.

It is normally blended with polystyrene and the blend has been commercially produced as an engineering thermoplastics by GE company from 1960 with the trade name of "Noryl" [7]. The amount of DMePPO production is over 10^5 t/year [3, 4].

Physical properties of the blend can be controlled by the blend ratio of both polymers. DMePPO can also be blended with nylons or other polymers when employing compatibilizers. The blends are widely used as structural component materials for housing construction, electronics parts, household appliances, automobile parts, etc. The blends are often replacements for with metal parts to reduce the weight in various applications.

Preparation of PPO from unsubstituted phenol needs drastic conditions, e.g., typically using the Ullmann ether synthesis as shown in Fig. 3. A CuCl/pyridine complex in 1,4-dimethoxybenzene induced the polymerization at a high temperature of 200 °C [6].

A recent review paper covered comprehensive studies on polymer synthesis using enzymes and enzyme model compounds as catalyst [8].
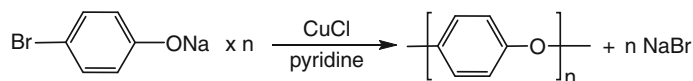
Poly(phenylene oxide) and Poly(phenylene sulfide) Syntheses, Fig. 3 Ullmann reaction for PPO synthesis
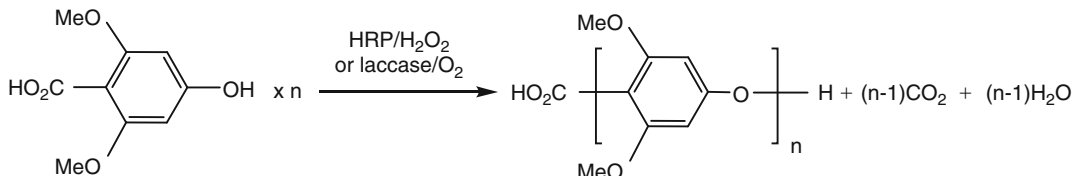
Poly(phenylene oxide) and Poly(phenylene sulfide) Syntheses, Fig. 4 Syringic acid produced a PPO via oxidative coupling polymerization

One such study revealed new polymerization reactions to afford PPO polymers. Horse radish peroxidase (HRP) or laccase enzyme was employed for the polymerization of syringic acid, a natural product, yielding poly(2,6-dimethoxy-1,4-phenylene oxide) while liberating carbon dioxide (Fig. 4) [9]. This type of polymerization is not possible by a metal complex catalyst. Note that laccase has a Cu-containing active site and HRP is a heme-containing Fe-active site [3, 4].

In the oxidative coupling polymerization of ortho-unsubstituted phenols, it was extremely difficult to control the coupling regioselectivity by conventional catalysts or even enzyme catalysts. These reactions generate free phenoxy radicals, in which ortho-positions readily take part in the further reactions. Tyrosinase is a Cu-containing enzyme for oxidation reactions like laccase. A tyrosinase model complex (Fig. 5a) catalyzed oxidative coupling polymerizations while suppressing the reaction at ortho-positions and produced unsubstituted PPO from unsubstituted 4-phenoxyphenol (Fig. 6a) [10] and 2,5-DMePPO from 2,5-dimethylphenol (Fig. 6b) [11]. In these reactions, an intermediate phenoxy radical is considered not free, but complexed with Cu, and thus, "controlled radical" species is involved in the coupling reaction, where the ortho-position is blocked from attacking by another radical species.

As a typical example of the polymerization of 2,5-dimethylphenol, the reaction was carried out at 40 °C in toluene under oxygen gas (1 atm) for
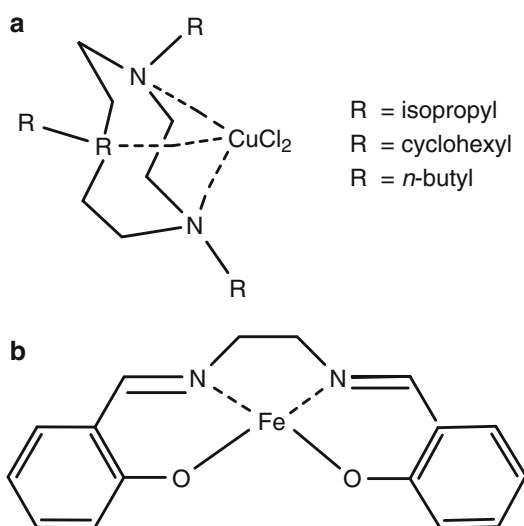
Poly(phenylene oxide) and Poly(phenylene sulfide) Syntheses, Fig. 5 (**a**) Tyrosinase model complexes, and (**b**) HRP model complex: Fe(salen) complex [3, 4]

24 h with 5 mol % of Cu-containing tyrosinase model complex to give a white polymer of 2,5-DMePPO in 78 % isolated yield [11]. The polymer had values of $M_n = 3,900$ and $M_w = 19,300$. It is the first example showing heat-reversible crystallinity (T_{m1} and $T_{m2} = 308$ and 303 °C, respectively), in contrast to noncrystalline polymer of DMePPO.

An HRP model complex, Fe(salen) complex (Fig. 5b), catalyzed the oxidative polymerization of 2,6-difluorophenol to poly(2,6-difluoro-1,4-phenylene oxide) (2,6-DFPPO) (Fig. 6c) [12].
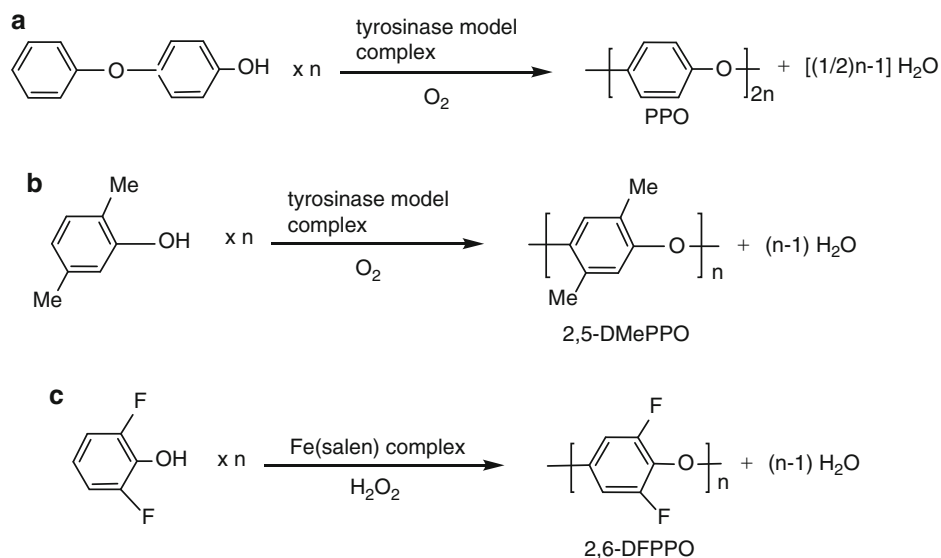
Poly(phenylene oxide) and Poly(phenylene sulfide) Syntheses, Fig. 6 Radical-controlled oxidative polymerizations by a tyrosinase model complex catalyst: (**a**) from 6-phenoxyphenol to PPO and (**b**) from 2,5-dimethylphenol to 2,5-DMePPO, and (**c**) Fe(salen)-catalyzed oxidative polymerization of 2,6-difluorophenol

a $2\ p\text{-}C_6H_4Cl_2 + 3\ Na_2CO_3 + 4\ S = \text{-}(C_6H_4SC_6H_4S)\text{-} + Na_2S_2O_3 + 4\ NaCl + 3\ CO_2$
       PPS

b $3\ p\text{-}C_6H_4Cl_2 + 4\ Na_2CO_3 + 4\ S = \text{-}(C_6H_4SC_6H_4SC_6H_4S)\text{-} + Na_2SO_4 + 6\ NaCl + 4\ CO_2$
       PPS
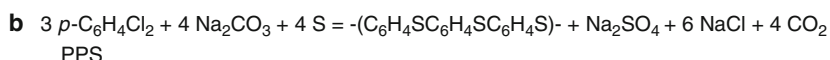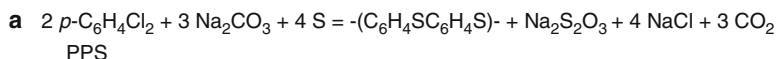
Poly(phenylene oxide) and Poly(phenylene sulfide) Syntheses, Fig. 7 Postulated mechanism of PPS formation from a mixture of *p*-dichlorobenzene, sodium carbonate, and sulfur

Further, Fe(salen) complex catalyzed oxidative polymerization of 2,6-disubstituted phenols in 1,4-dioxane to produce 2,6-disubstituted PPO [13].

Synthesis Reaction of Poly(phenylene sulfide) (PPS) and Polymer Properties

Poly(phenylene sulfide) or PPS is a PPO analogue, in which the oxygen is replaced with sulfur.

PPS is also one of the well-known high performance engineering plastics.

In the early stage of research, one of the good reactions leading to PPS was reported: a mixture of *p*-dichlorobenzene, sodium carbonate, and sulfur was heated at 300–340 °C and the formation of PPS was noticed [14, 15]. Reactions (a) and

(b) in Fig. 7 were considered about what happened in the mixture during the reaction, since the formation of thiosulfate and sulfate was actually observed.

Then, a self-condensation reaction of alkali metal salts of *p*-halothiophenol was developed. The reaction was carried out below the melting point of the salts and appeared to involve a solid-state reaction (Fig. 8) [16]. The order of polymerization reactivity of the sodium salts was I > Br > Cl ~ F, and the order of the reaction of the alkali metal salts of *p*-bromothiophenol was Li > Na > K. Linear PPS is stable up to 400 °C in air and nitrogen.

An improved process was explored by Phillips Petroleum Co. in 1967. The reaction of *p*-dichlorobenzene with sodium sulfide was carried in a polar organic solvent like *N*-methylmorpholine, and the product PPS was
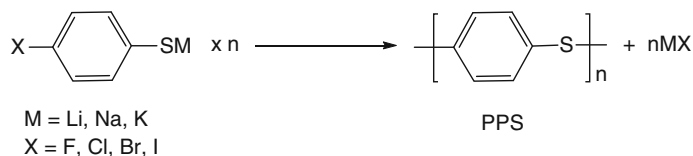
Poly(phenylene oxide) and Poly(phenylene sulfide) Syntheses, Fig. 8 Self-condensation reaction to poly(phenylene sulfide) (PPS)
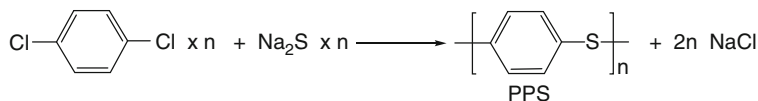
Poly(phenylene oxide) and Poly(phenylene sulfide) Syntheses, Fig. 9 Synthesis of poly(phenylene sulfide) (PPS)

first commercialized by the same company as the trade name of "Ryton" PPS in 1973 (Fig. 9) [17]. The IUPAC name of PPS is poly(thio-1,4-phenylene).

The reaction (Fig. 9) is of an A-A + B-B classical type step-growth polycondensation. A mechanistic study of the polycondensation showed to be a consequence of unequal rate constant depending on the propagating chain length, the behaviors of which are deviated from those of the classical type reaction. During the reaction, cyclic oligomer formation was observed as a side reaction [18]. The impact strength properties of PPS blended with various polymers and/or inorganic fillers were studied in relation to the crystallinity of the PPS blends [19]. The impact strength of 17 sample blends increased with decrease in the crystallinity, regardless of the method of preparing the blends.

PPS is a semicrystalline, high performance engineering thermoplastic [17]. The molecular weight of PPS determined by gel permeation chromatography or light scattering method was estimated as ~18,000. Differential thermal analysis showed that PPS is amorphous, having a broad melting point (T_m) at 285 °C and a glass transition (T_g) at 85 °C. Its density is 1.35 g/cm³, tensile strength 65.5 MPa, and elongation 1.6 %. When it is heated at around 315 ~ 360 °C, its cross-linkings and its molecular weight increase,

leading to infusible resins. PPS shows properties of excellent thermal stability, good mechanical behavior, antichemical stability, inflammable nature, etc.

PPS is insoluble in almost all organic solvents below 200 °C and is miscible with some organic polymers. It shows, however, a good compatibility with inorganic substances and thus, reinforced PPS and/or PPS resins can be obtained as a variety of composite materials with many inorganic fillers like glass fiber, carbon fiber, and others. The properties of PPS resins can be controlled by changing the nature and amount of the filler. They are widely used in areas of electronic product parts, automobile parts, precision machinery parts, chemical industry parts, etc. PPS is also used as coating materials. In 1985, the Phillips Petroleum Co. had a plant capacity of 5.4 × 10³ t/year for the PPS production.

Related Entries

- ▶ PES (Poly(ether sulfone)), Polysulfone
- ▶ PET (Poly(ethylene terephthalate)) and PTT (Poly(trimethylene terephthalate))
- ▶ PET and Other Polyester Synthesis
- ▶ Poly(ether ketone) and poly(ether sulfone) Synthesis
- ▶ Polyimide Synthesis

References

1. Hay AS, Blanchard HS, Endres GF, Eustance JW (1959) Polymerization by oxidative coupling. J Am Chem Soc 81:6335–6336
2. Hay AS (1962) Polymerization by oxidative coupling. II. Oxidation of 2,6-disubstituted phenols. J Polym Sci 58:581–591
3. Kobayashi S, Higashimura H (2003) Oxidative polymerization of phenol revisited. Prog Polym Sci 28:1015–1048
4. Higashimura H (2012) Oxidative coupling polymerization. In: Matyjaszewski K, Moeller M (ed) Polymer science: a comprehensive reference, vol 5. Elsevier, Amsterdam, pp 141–173
5. Beasjou PJ, Driessen WL, Challa G, Reedijk J (1997) AB initio calculation on 2,6dimethylphenol. Evidence of an important role for the phenoxonium cation in the copper-catalyzed oxidative phenol coupling reaction. J Am Chem Soc 119:12590–12594
6. Haynes CG, Turner AH, Waters WA (1956) The oxidation of monohydric phenols by alkaline ferricyanide. J Chem Soc 2823–2826
7. Aycock D, Abolins V, White DM (1988) Poly (phenylene ether). In: Mark HF (ed) Encyclopedia of polymer science and engineering, vol 13, 2nd edn. Wiley-Interscience, New York, pp 1–30
8. Kobayashi S, Makino A (2009) Enzymatic polymer synthesis: an opportunity for green polymer chemistry. Chem Rev 109:5288–5353
9. Ikeda R, Uyama H, Kobayashi S (1996) Novel synthetic pathway to a poly(phenylene oxide). Laccase-catalyzed oxidative polymerization of syringic acid. Macromolecules 29:3053–3054
10. Higashimura H, Kubota M, Shiga A, Fujisawa K, Koro-oka Y, Uyama H, Kobayashi S (2000) 'Radical-controlled' oxidative polymerization of 4-phenoxyphenol by a tyrosinase model complex catalyst to poly(1,4-phenylene oxide). Macromolecules 33:1986–1995
11. Higashimura H, Fujisawa K, Moro-oka Y, Naamekawa S, Kubota M, Shiga A, Uyama H, Kobayashi S (2000) New crystalline polymers: poly (2,5-dialkyl-1,4-phenylene oxide). Macromol Rapid Commun 21:1121–1124
12. Ikeda R, Tanaka H, Uyama H, Kobayashi S (2000) Oxidative polymerization of 2,6-difluorophenol to crystalline poly(2,6-difluoro-1,4-phenylene oxide). Macromolecules 33:6648–6652
13. Tonami H, Uyama H, Kobayashi S, Higashimura H, Oguchi T (1999) Oxidative polymerization of 2,6-disubstituted phenols by iron-salen complex. J Macromol Sci Pure Appl Chem A36:719–730
14. Macallum D (1948) A dry synthesis of aromatic sulfides: phenylene sulfide resins. J Org Chem 13:154–159
15. Lenz RW, Carrington WK (1959) Phenylene sulfide polymers. I. Mechanism of the macallum polymerization. J Polym Sci 41:333–358
16. Lenz RW, Handlovits CE, Smith HA (1962) Phenylene sulfide polymers. III. The synthesis of linear polyphenylene sulfide. J Polym Sci 58:351–367
17. Hill HW Jr, Brady DG (1988) Poly(arylene sulfide)s. In: Mark HF (ed) Encyclopedia of polymer science and engineering, vol 11, 2nd edn. Wiley-Interscience, New York, pp 531–557
18. Fahey DR, Hensley HD, Ash CE, Senn DR (1997) Poly(p-phenylene sulfide) synthesis: a step-growth polymerization with unequal step reactivity. Macromolecules 30:387–393
19. Lu D, Yang Y, Zhuang G, Zhang Y, Li B (2001) A study of high-impact poly(phenylene sulfide). I. The effect of its crystallinity on its impact properties. Macromol Chem Phys 202:734–738

Poly(tetrafluoroethylene) and Other Fluorine-Containing Polymers

Hiroaki Shimomoto
Department of Material Science and Biotechnology, Graduate School of Science and Engineering, Ehime University, Matsuyama, Ehime Prefecture, Japan

Synonyms

Fluorinated polymer; Fluoropolymer; Perfluorinated polymer; PTFE

Definition

Poly(tetrafluoroethylene) is a synthetic polymer bearing repeating $-CF_2-CF_2-$ units, which is produced by polymerization of tetrafluoroethylene, $CF_2 = CF_2$. Fluorine-containing polymers can be defined as polymers which contain one or more fluorine atoms in their chemical structures in a broad sense. They are divided into two groups: perfluorinated (fully fluorinated) polymers, which are composed of $C-C$ and $C-F$ bonds and in some cases heteroatoms including oxygen atom [no $C-H$ or $C-X$ (X = halogens other than fluorine atom) bond in their repeating units]; and partially fluorinated polymers containing $C-H$ and/or $C-X$ bonds in their repeating units.

Background

Fluorine-containing polymers have unique characteristics, such as chemical and thermal stability, low surface energy, and a low dielectric constant. These are imparted by the specific properties of a fluorine atom, i.e., high electronegativity, small size, and high bond strength to carbon atom. In a broad sense, every polymer can be transformed into a fluorine-containing polymer by introducing a fluorinated group in the chemical structure. The incorporation of fluorine into polymers can be achieved by post-polymerization or polymerization of the corresponding fluorinated monomers. In fact, a number of perfluorinated (fully fluorinated) and partially fluorinated polymers have been developed for a broad range of applications, including plastics, elastomers, electronics, agriculture, pharmaceuticals, and medicine. This entry briefly describes typical examples from fluoroolefin-based polymers and other fluorine-containing polymers to illustrate the impact of fluorination on their properties.

Poly(tetrafluoroethylene)

Poly(tetrafluoroethylene) (PTFE) is a perfluorinated linear $C-C$ main chain polymer with the formula $-(CF_2-CF_2)_n-$ and an analog of polyethylene (PE) in which all the hydrogen atoms are replaced by fluorine atoms. However, the PTFE and PE have markedly different properties and are prepared in totally different processes [1–5].

PTFE is essentially produced by free radical polymerization of gaseous tetrafluoroethylene (TFE; $CF_2 = CF_2$) in an aqueous medium in the presence of an initiator and other additives, with or without a surfactant. There are two distinct methods for the commercial TFE polymerization, i.e., suspension polymerization and emulsion or dispersion polymerization. In the former case, TFE is polymerized with a small amount of or no dispersing agent with vigorous agitation to obtain precipitated resins (granular resins), which are mainly used for molding and ram

extrusion. The latter polymerization with a fluorinated surfactant allows submicron particles to be dispersed in water. The dispersion products are used for coating and converted to fine powder for paste extrusion.

In the crystalline state, PTFE has a helical conformation due to the larger volume of fluorine atom than that of hydrogen along the $C-C$ backbone, while PE has a planar zigzag molecular conformation. The rigid helical chains of PTFE can crystallize easier and result in a high crystallinity of over 90 %. The melting point is about 330 °C, which is much higher than that of PE. Also, PTFE undergoes several crystalline-to-crystalline transitions in the range of sub-ambient temperature to the melting point. At approximately 20 °C, the triclinic pattern changes to a hexagonal unit cell with a slight untwisting in the helical conformation, resulting in a large expansion in the specific volume of the whole polymer (1.0–1.8 %). There is an additional smaller transition at 30 °C. Because of the compact crystalline structure and the dense packing of fluorine atoms, PTFE is the heaviest polymer materials with a density of 2.1 g/cm^3.

One of the most distinguished properties of PTFE is its outstanding chemical and thermal stability. It is chemically inert except to a very few chemicals such as molten alkali metals and turbulent liquid or gaseous fluorine. PTFE can be continuously used below 260 °C and shows no obvious degradation below around 440 °C. The remarkable stability is due to the fact that PTFE is formed solely from strong $C-C$ and superstrong $C-F$ bonds, and the fluorine atoms form a protective sheath around the $C-C$ backbone. This chemical structure gives other special properties including low surface energy, a dielectric constant, a low friction coefficient, nonadhesiveness, and insolubility in any common solvents.

Representative Examples of Fluoroolefin-Based Polymers Other Than PTFE

PTFE has some limitations in its physical properties for its application, such as lower tensile

P

Semicrystalline

(Perfluorinated)
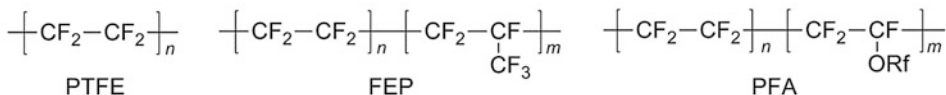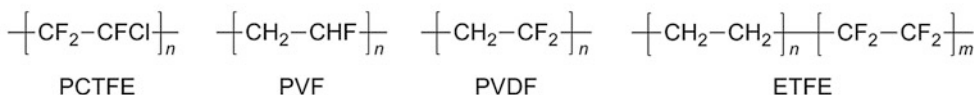
$$\left[CF_2-CF_2\right]_n \qquad \left[CF_2-CF_2\right]_n\left[CF_2-CF\atop CF_3\right]_m \qquad \left[CF_2-CF_2\right]_n\left[CF_2-CF\atop ORf\right]_m$$

PTFE   FEP   PFA

(Partially fluorinated)

$$\left[CF_2-CFCl\right]_n \qquad \left[CH_2-CHF\right]_n \qquad \left[CH_2-CF_2\right]_n \qquad \left[CH_2-CH_2\right]_n\left[CF_2-CF_2\right]_m$$

PCTFE   PVF   PVDF   ETFE

Amorphous

$$\left[CF_2-CF_2\right]_n\left[CF-CF\atop O\quad O\atop F_3C\;\;CF_3\right]_m \qquad \left(CF_2-CF-CF-CF_2\atop O\quad CF_2\atop CF_2\right)_n \qquad \left[CF_2-CF\atop X\right]_n\left[CH_2-CH\atop OR\right]_m$$

TFE/PDD   PPBVE   FEVE

Ionomer

$$\left[CF_2-CF_2\right]_n\left[CF_2-CF\atop O\atop Rf\atop SO_3H\right]_m$$

TFE/PFSA
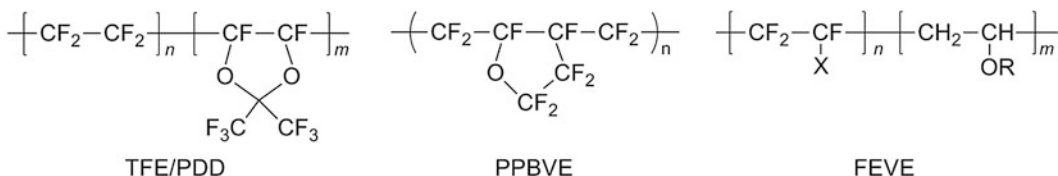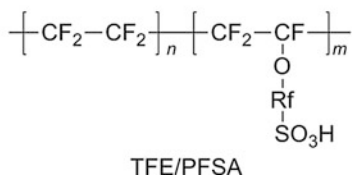
Poly(tetrafluoroethylene) and Other Fluorine-Containing Polymers, Fig. 1 Representative examples of fluoroolefin-based polymers

strength and creep resistance compared to other engineering polymers. Thus, various fluoropolymers have been developed to overcome the drawbacks of PTFE materials [1, 3–5], although PTFE is still the dominant commercial fluoropolymer due to its excellent properties. Representative examples of fluoroolefin-based polymers are listed in Fig. 1.

FEP (*f*luorinated *e*thylene *p*ropylene) and PFA (*per*fluoro*a*lkoxy) resins are random copolymers of TFE with hexafluoropropylene and perfluoroalkyl (Rf) vinyl ethers (e.g., perfluoropropyl vinyl ether), respectively. The introduction of the comonomers reduces the crystallinity of PTFE. Thus, these perfluorinated

copolymers combine most of the desirable properties of PTFE with melt processability.

Partially fluorinated polymers have different properties and processing characteristics from perfluorinated polymers. Poly(chlorotrifluoroethylene) (PCTFE) is a semicrystalline polymer made by the polymerization of chlorotrifluoroethylene. In comparison with PTFE, it has improved mechanical properties, better optical clarity, and lower gas permeability but inferior thermal stability, chemical resistance, and electrical properties. It also has a somewhat higher critical surface tension and coefficient of friction. Poly(vinyl fluoride) (PVF) is the least fluorinated of the commercial fluoroplastics, but the presence

of fluorine still has a significant effect on its properties. Poly(vinylidene fluoride) (PVDF), which is produced by polymerization of vinylidene fluoride ($CH_2 = CF_2$), has several different properties from other fluoropolymers. The alternating CH_2 and CF_2 units produce a net dipole moment nearly perpendicular to the polymer main chain, imparting solubility toward some polar solvents, high dielectric constant, high dielectric loss factor, and under certain conditions, piezoelectric behavior. Some block copolymers of vinylidene fluoride and other fluoroolefins have been prepared by iodine transfer polymerization [6, 7] and other methods [8–10]. The products consisting of soft and hard segments are used for commercially important fluorinated thermoplastic elastomers [8–10]. Poly(ethylene-*co*-TFE) (ETFE) is a nearly alternating copolymer of ethylene and TFE because the monomers have a strong tendency to alternate during polymerization. Although ETFE is isomeric with PVDF, its properties, especially electrical properties, are quite different.

The aforementioned semicrystalline fluoropolymers are industrially important, but have certain drawbacks such as low optical clarity and poor solubility. TFE/PDD (copolymer of TFE with perfluoro-2,2-dimethyl-1,3-dioxole; Teflon® AF) and PPBVE (product of cyclopolymerization of perfluoro-3-butenyl-vinyl ether; Cytop®) are examples of commercial amorphous fluoropolymers, which combine high optical clarity and solubility with outstanding chemical, thermal, and electrical properties [1, 11, 12]. FEVE (*f*luoro*e*thylene *v*inyl *e*ther) comprises alternating sequences of fluoroolefin (mainly TFE or chlorotrifluoroethylene) and several specific vinyl ethers. The combination of several kinds of nonfluorinated vinyl ether monomers provides the polymer with various properties necessary for coatings and paints, such as solubility, cross-linking reactivity and good adhesion, compatibility toward pigments, and flexibility of the final finish [13]. In addition, the alternating sequence provides the high weather resistance of the resultant paint finish.

TFE/PFSA (copolymer of TFE with a perfluorosulfonic acid; Nafion®), a perfluorinated polymer that contains sulfonic acid groups onto a TFE backbone, is also an important fluoropolymer material. It is the first of a class of synthetic polymers with ionic properties which are called ionomers. The combination of the outstanding stability of TFE backbone with the sulfonic groups allows broad application including proton exchange membrane for fuel cells [14, 15].

Other Fluorine-Containing Polymers

There are many other types of fluorine-containing polymers, since any C−H bonds in nonfluorinated polymers can theoretically be replaced with C−F bonds. An effective fluorination imparts more excellent characteristics without reducing the inherent characteristics of original good nature of nonfluorinated polymers. To illustrate the impact of fluorination on the properties, several examples are described below (Fig. 2).

Perfluoropolyethers are composed of repeating units of small perfluorinated aliphatic oxides such as perfluoroethylene oxide or perfluoropropylene oxide. They exhibit several important features such as uniform viscosity over a wide range of temperatures, low surface tension, oxidative resistance, high chemical and thermal stability, and low vapor pressure [16, 17]. Thus, they are the lubricants of choice for most magnetic media applications, and they have important uses in spacecraft and other demanding applications such as high-vacuum pump oil.

Polymers with perfluoroalkyl (Rf) groups in the side chain exhibit excellent surface properties [1, 18, 19]. Typical examples of these polymers are poly[(meth)acrylate]s with long Rf groups. These polymers have a critical surface tension that is much lower than that of PTFE and can be utilized as water and oil repellents. This is attributed to the presence of many CF_3 groups as well as the formation of liquid crystalline ordered structures composed of fluoroalkyl chains on the surfaces. In addition, poly[fluoroalkyl (meth) acrylate]s have many other properties that differ from those of hydrogenated polymer counterparts (e.g., good transparency, low refractive index,

P
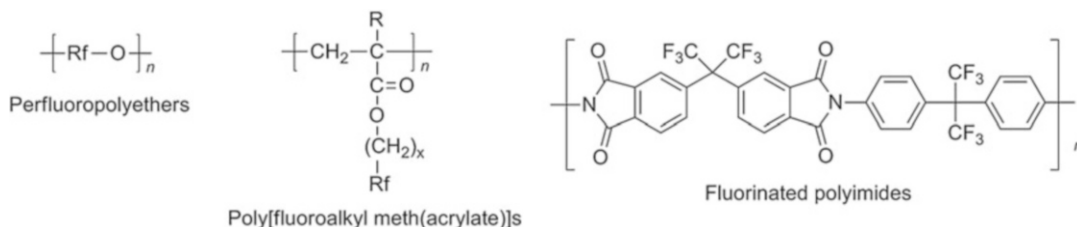
Poly(tetrafluoroethylene) and Other Fluorine-Containing Polymers, Fig. 2 Examples of fluorine-containing polymers other than fluoroolefin-based polymers

low moisture absorption), with readily synthesized and crafts-friendly properties. Also, it should be noted that controlled/living polymerization methods developed in the past few decades have allowed the synthesis of well-defined fluorinated polymers with various architectures including block, graft, end-functionalized, branched, and star-shaped polymers [7, 18, 19].

Fluorinated groups have also been introduced into a variety of condensation polymers. For example, fluorinated polyimides are of particular interest for applications in electronics. In general, fluorination provides unique properties to polyimides, such as improvement of the transparency, reduced dielectric constants and refractive indices, lower moisture absorption, and improved process performance [20].

References

1. Feiring AE (1994) Fluoroplastics. In: Banks RE, Smart BE, Tatlow JC (eds) Organofluorine chemistry: principles and commercial applications. Plenum Press, New York/London
2. Gangal SV (2003) Perfluorinated polymers, polytetrafluoroethylene. In: Mark HF (ed) Encyclopedia of polymer science and technology, vol 3, 3rd edn. John Wiley & Sons, Hoboken, pp 378–402
3. Drobny JG (2008) Basic chemistry of fluoropolymers. In: Technology of fluoropolymers, 2nd edn. CRC Press, Boca Raton
4. Drobny JG (2008) Properties of commercial fluoropolymers. In: Technology of fluoropolymers, 2nd edn. CRC Press, Boca Raton
5. Ednesajjad S (2013) Introduction to fluoropolymers. In: Ednesajjad S (ed) Introduction to fluoropolymers: materials, technology and applications. William Andrews/Elsevier, Waltham
6. Tatemoto M (1985) Iodine transfer polymerization of fluoroalkenes. Int Polym Sci Technol 12:85–97
7. Ameduri B, Boutevin B (2004) Well-Architectured fluoropolymers: synthesis, properties and applications. Elsevier, Oxford
8. Logothetis AL (1994) Fluoroelastomers. In: Banks RE, Smart BE, Tatlow JC (eds) Organofluorine chemistry: principles and commercial applications. Plenum Press, New York/London
9. Drobny JG (2008) Properties, processing, and applications of fluoroelastomers. In: Technology of fluoropolymers, 2nd edn. CRC Press, Boca Raton
10. Drobny JG (2013) Fluoroelastomers. In: Ednesajjad S (ed) Introduction to fluoropolymers: materials, technology and applications. William Andrews/Elsevier, Waltham
11. Resnick PR, Buck WH (1999) Teflon® AF: a family of amorphous fluoropolymers with extraordinary properties. In: Hougham G, Cassidy PE, Johns K, Davidson T (eds) Fluoropolymers 2: properties. Kluwer Academic/Plenum Publishers, New York
12. Drobny JG (2008) Other fluoropolymers. In: Technology of fluoropolymers, 2nd edn. CRC Press, Boca Raton
13. Yamabe M (1994) Fluoropolymer coatings. In: Banks RE, Smart BE, Tatlow JC (eds) Organofluorine chemistry: principles and commercial applications. Plenum Press, New York/London
14. Yamabe M, Miyake H (1994) Fluorinated membranes. In: Banks RE, Smart BE, Tatlow JC (eds) Organofluorine chemistry: principles and commercial applications. Plenum Press, New York/London
15. Mauritz KA, Moore RB (2004) State of understanding of Nafion. Chem Rev 104:4535–4585
16. Sianesi D, Marchionni G, Pasquale RJD (1994) Perfluoropolyethers (PFPEs) from perfluoroolefin photooxidation: Fomblin® and Galden® fluids. In: Banks RE, Smart BE, Tatlow JC (eds) Organofluorine chemistry: principles and commercial applications. Plenum Press, New York/London
17. Ohsaka Y (1994) Perfluoropolyethers fluids (Demnum®) based on oxetanes. In: Banks RE, Smart BE, Tatlow JC (eds) Organofluorine chemistry: principles and commercial applications. Plenum Press, New York/London
18. Hansen NML, Jankova K, Hvilsted S (2007) Fluoropolymer materials and architectures prepared

by controlled radical polymerizations. Eur Polym J 43:255–293

19. Hirao A, Sugiyama K, Yokoyama H (2007) Precise synthesis and surface structures of architectural per- and semifluorinated polymers with well-defined structures. Prog Polym Sci 32:1393–1438

20. Ando S, Matsuura T, Sasaki S (1999) Fluorine-containing polyimides. In: Hougham G, Cassidy PE, Johns K, Davidson T (eds) Fluoropolymers 2: properties. Kluwer Academic/Plenum Publishers, New York

Poly(thiophene)s

George Barnes, Chin Pang Yau and Martin Heeney
Department of Chemistry, Imperial College London, London, UK

Synonyms

P3AT; P3HT; PT

Definition

Poly(thiophene)s are a class of conjugated polymer that are comprised of repeating units of thiophene or fused aromatic thiophene along the backbone. Often the thiophene rings contain alkyl side chains as solubilizing units to enable good processability of the polymer. They have promising performance in a range of applications.

Introduction

Within the realms of conjugated polymer research, thiophene-containing materials have been one of the most widely investigated materials. Thiophene-containing polymers have been investigated in almost every reported application of conjugated polymers, ranging from organic solar cells and organic field effects transistors to sensors, electrochromics, thermoelectric devices, and more [1]. The prevalence of thiophene as

a comonomer in conjugated polymers is likely due to a combination of factors. It is readily available, and the chemistry of thiophene is well developed and understood, enabling the functionalization of the core skeleton with a range of substituents as well as the ready incorporation into polymer backbones. This in turn allows the optical, electronic, and morphological properties of the resulting polymers to be readily tuned by the introduction of different substituents, as well as the incorporation of different comonomers. In addition the relatively high polarizability of the sulfur atoms in the thiophene backbone has also been suggested to play a beneficial role in charge transport.

Much of the research into poly(thiophene)s has been focused upon tuning the optoelectronic properties of the conjugated backbone for particular device applications. Since many device properties are particularly sensitive to the solid-state microstructure of the polymer, particular effort has also been dedicated to controlling the organization of these polymers in the solid state. Thus, for example, the choice of comonomer units can affect the backbone planarity and therefore the ability of the polymers to aggregate and order in the solid state, while the choice of solubilizing alkyl chain can help promote self-organization in the solid state and allow close packing of the conjugated backbones. In addition to the chemical design of the polymer backbone, the molecular weight and polydispersity also have a critical role to play in device performance. Another critical factor is the choice of synthetic route to the chosen polymer, since chemical defects introduced by synthesis can have a deleterious influence on device performance. Contaminants resulting from the synthesis, such as catalyst residue, can also have a negative impact on device performance, and purification procedures are therefore important [2].

Classes of Polythiophene

Polythiophene
The simplest polythiophene polymer is that resulting from the homopolymerization of

P
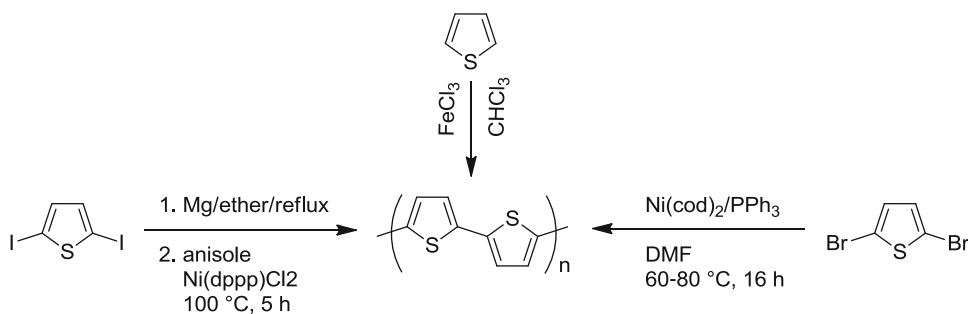
Poly(thiophene)s, Fig. 1 Various synthetic methods for the synthesis of polythiophene
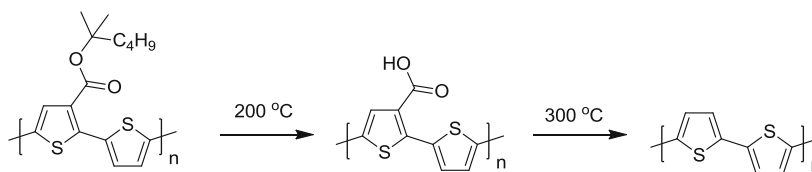
Poly(thiophene)s, Fig. 2 Thermal conversion of a soluble ester-functionalized polythiophene into an insoluble carboxylic acid-functionalized polythiophene and further decarboxylation to polythiophene

unsubstituted thiophene. In the early 1980s, the first synthetic routes to non-alkylated polythiophenes were reported (Fig. 1) by a variety of routes [3]. In all cases, low molecular weight polymer was isolated which was very poorly soluble in common organic solvents. Despite the poor processability of the material, the high temperature stability and promising electrical conductivity of the polymer stimulated much interest in this class of polymer.

Much of this interest has been focused upon improving the processability of polythiophene to facilitate its use in practical applications. Two basic approaches have been developed to overcome the poor solubility. The first is to utilize a soluble precursor polymer, which following processing can then be converted in situ, usually by thermal or photochemical means, into the intractable polymer. In the case of polythiophene, thermally cleavable ester groups have been reported as a promising approach (Fig. 2) [4]. The inclusion of the long alkyl chain ester groups on the polymer backbones renders it soluble in a range of common solvents, enabling the printing of thin film. Subsequent heating of the polymer to 200 °C results in a Chugaev-type

elimination of an alkene to afford a carboxylic acid substituted polythiophene which is insoluble in most organic solvents. Further heating to 300 °C results in decarboxylation to afford the native polythiophene. One drawback with this route is the relatively high temperatures required, which are not compatible with many of the plastic substrates which are desirable for device applications. Thus lower temperature cleavable side chains, such as dimethyloctylsilyl, have been developed which can cleave at room temperature in the presence of acid [5]. However poor film quality can still be a problem with such approaches, due to the formation of small molecule side products during the cleavage process.

A common alternative approach has been to attach solubilizing side chains to the polymer backbone, such that they become soluble in organic solvents and can be formulated and processed. As the polymer growth take place in solution, the improved solubility allows for higher molecular weights and thus higher degrees of polymerization to be synthesized. This is a fundamentally different approach to the chemical conversion route, since the inclusion of functional groups onto the backbone of the
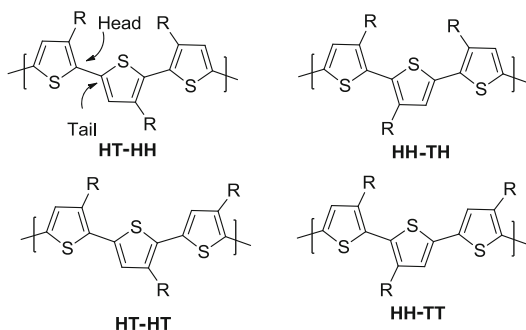
Poly(thiophene)s, Fig. 3 Regiochemistries and possible isomers for coupled thiophenes (head-to-tail (**HT**), head-to-head (**HH**), tail-to-tail (**TT**))

polythiophene has a significant effect on its optoelectronic and morphological properties. Such groups have both a direct electronic influence, through inductive or mesomeric effects, and more subtle steric effects which influence how the polymer backbone can planarize and order in the solid state.

Poly(3-alkyl)thiophenes

One particularly important and well-investigated class of thiophene polymer is poly(3-alkyl)thiophene (P3AT), in which an alkyl group is introduced into the three-position of the thiophene ring as a solubilizing substituent. The hexyl-substituted polymer poly(3-hexyl)thiophene (P3HT) is one of the most widely investigated of all conjugated polymers. Hexyl offers a good balance between being sufficiently long to confer good solubility to the polymer without diluting the conjugated backbone with too much insulating alkyl chain.

The introduction of an alkyl chain however causes an increased synthetic complication since the resulting monomer has reduced C_S symmetry compared to thiophene itself. Coupling of 3-alkylthiophene monomer units can therefore result in several possible regiochemistries in the polymer backbone. These are known as head-to-head (HH), head-to-tail (HT), or tail-to-tail (TT) couplings (Fig. 3). The percentage of head-to-tail couplings in the polymer backbone is referred to as the regioregularity (RR) of the polymer and can be readily assigned by NMR

integration of the aromatic and methylene protons. Polymers with a random orientation of the alkyl side chains are known as regiorandom (RRa) [3].

The regioregularity of P3ATs has a significant influence on the properties of the polymer backbone, and as such it should always be reported in any study. When R is alkyl, head-to-head linkages result in a significant steric interaction between the adjacent thiophene monomers and cause a twisting of the monomers away from fully coplanar. This results in a reduced conjugation length and can also reduce the ability of the polymer to order in the solid state. This can be clearly observed in the optical spectra of P3ATs of varying regularity. For polymers with RR around 70 %, the maximum absorption of thin films appears around 480 nm, corresponding to a $\pi - \pi^*$ transition, whereas fully regioregular P3ATs have a red shifted absorption of approximately 560 nm in the solid state, with marked vibronic shoulders to higher wavelengths [6]. The polymer regioregularity is also a key factor that can influence the degree of polymer crystallinity. Hence P3ATs tend to crystallize in a lamellar-like structure, in which adjacent polymer backbones stack together face to face (π stacked) to form sheet like structures with extended interchain π stacking. These sheets are vertically separated by the alkyl chains that extend from the backbone. Many studies have demonstrated that conductivity, absorption length, and photovoltaic and transistor device performance are affected by the regioregularity [7]. For example, the charge carrier mobility of P3HT in field-effect transistor (FET) devices has been shown to vary over three orders of magnitude as the regioregularity is reduced from 98 % to 70 %. In this case, it was demonstrated that the RR affected the orientation of spun cast films on the transistor substrate, with low RR polymer orientating with their conjugated backbones more face-on to the substrate and high RR film orientating with the conjugated backbones perpendicular to the substrate, thereby facilitating charge transport in the transistor channel [8]. However the processing conditions were noted to influence this orientational preference, with drop cast low RR films exhibiting perpendicular orientation and significantly high

Poly(thiophene)s,
Fig. 4 Structure of some
thiophene copolymers

P1a R = H
P1b R = −C₁₂H₂₅
P1c R = −OC₁₂H25
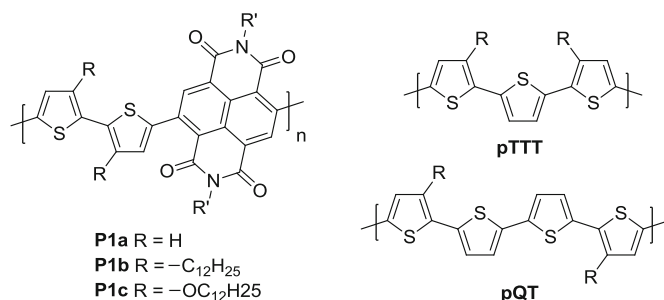
mobility than spun cast. This highlights the
importance of processing as well as molecular
structure on device performance.

The nature of the side chain has a significant
influence on the polymer properties. The inclu-
sion of longer alkyl chains like octyl or decyl
leads to a reduced melting point of the polymer
and therefore improved solubility. The device
performance of these longer chain analogues in
photovoltaic devices tends to be reduced,
although transistor performance is similar for
devices with well-optimized film fabrication.
The inclusion of branched alkyl chains like
2-ethylhexyl significantly lowers the melting
point and suppresses the crystallization kinetics,
leading to the initially erroneous observation that
amorphous polymers were produced. Subsequent
investigations revealed that regioregular poly
(3-(2'-ethylhexyl))thiophene did form semicrys-
talline thin films, with a structure remarkably
similar to P3HT but with slightly increased
backbone spacings [9].

Alkoxy- and alkylthio-substituted
polythiophenes have also been reported. As
expected the electron-donating effect of the alk-
oxy group leads to a reduction in ionization
potential for the polymer, relative to P3ATs,
resulting in the formation of polymers which are
stable in the oxidized state. Importantly the incor-
poration of alkoxy groups has been shown to
planarize the head-to-head linkage in comparison
to the alkyl analogue. This is due to the smaller
van der Waals radius (1.5 Å) of oxygen compared
to the methylene group (2.0 Å) and the favorable
electrostatic attraction between oxygen and
neighboring thienyl sulfur atoms. Hence the
incorporation of head-to-head linked bithiophene

monomers can be a useful design tool, facilitating
solubility of the polymer in solution while
enabling favorable planarization in the solid
state. An example of this can be seen in Fig. 4,
in which bithiophene with various substituents
has been copolymerized with naphthalene
diimide [10]. Here the unsubstituted bithiophene
copolymer **P1a** has an optical band gap of
1.48 eV in thin film. The inclusion of a head-to-
head alkyl bithiophene linker in **P1b** results in an
increase in the band gap to 1.56 eV due to the
increase in torsional disorder reducing the effec-
tive conjugation length. In contrast the head-to-
head alkoxy bithiophene polymer **P1c** has the
lowest band gap of all three polymers at
1.08 eV, due to the combination of a planar back-
bone and the increased electron donation of the
alkoxy chains.

An interesting subclass of poly(alkyl)thio-
phene are copolymers in which some of the
alkyl side chains have been removed, such as
poly(3,3″-dialkylterthiophene) (**PTT**) or poly
(3,3″-dialkyl-quaterthiophene) (**PQT**) [11].
Here the reduction in alkyl chain density removes
any possibility for HH couplings allowing for
planarization of the polymer backbone. The
change in side-chain density also facilitates syn-
thesis, since centrosymmetric monomers can now
be utilized. However the reduction in side-chain
density also results in a reduction in polymer
solubility, so longer side chains are usually used
to maintain solubility. In both cases the reduction
in the number of electron-donating alkyl chains
compared to P3ATs manifests itself as a slight
increase in the oxidation potential of the polymer
backbone. In the case of **PQT**, this was shown to
be beneficial to the ambient stability of field-

effect transistor devices. The reduction in alkyl side-chain density also results in changes to the thermal behavior of the polymers and the solid-state packing. Thus **PQT** with dodecyl side chains exhibit a relatively low-temperature transistor to a liquid crystal phase around 120 °C. Annealing films within this mesophase was found to result in an improvement in thin film order and therefore transistor performance. **PQT** was found to pack in lamellar-like films, in which the alkyl side chains from adjacent polymer backbone interdigitate [11].

Polythiophene with Fused Aromatic Rings

The synthesis of polythiophene with fused aromatic units in the backbone has been a popular research theme. The incorporation of fused aromatic influences a multitude of properties including optical properties, solubility, oxidation potential, and morphology. A huge range of fused aromatics have been investigated as comonomers, which are too numerous to summarize in this entry [1]. Instead we highlight a few classes of well-investigated polymers. As shown in Fig. 5, there have been many polymers incorporating fused thienoacenes in the backbone. Polymer **P2**, also known as poly[2,5-bis(3-alkylthiophen-2-yl) thieno(3,2-b)thiophene] (PBTTT), has been widely investigated as a polymer for FETs. It is structurally similar to **PQT**, but the inclusion of

the rigid thieno[3,2-b]thiophene comonomer reduces the torsional freedom compared to the 2,2'-bithiophene unit in **PQT**, resulting in a more rigid backbone. **PBTTT** also exhibits liquid crystalline behavior, and annealing in the mesophase results in the formation of well-ordered crystalline domains in which the side chains are interdigitated [12]. Although the lamellar is surprisingly well ordered for a polymeric material, it has been shown that there is still appreciable paracrystalline disorder in the π stacking direction [13]. Nevertheless promising field-effect mobilities around 1 cm^2/Vs have been reported. Interestingly **PBTTT** is also shown to form bimolecular co-crystals upon blending with fullerene derivatives for solar cell applications. The fullerenes intercalate into the interdigitated side chains resulting in an increase in lamellar spacing [12].

Polymer **P3** is a structural isomer of **PBTTT** in which the solubilizing alkyl chains are incorporated on the rigid thienothiophene, rather than the bithiophene which has some rotational freedom. This was found to result in an increase in the polymer band gap, as well as increases in the polymer melting point and π-π packing distances. These changes are thought to stem from increased disorder in the polymer backbone, possibly as a result of the greater conformational disorder of the unsubstituted bithiophene versus the dialkylated bithiophene. Similar differences are
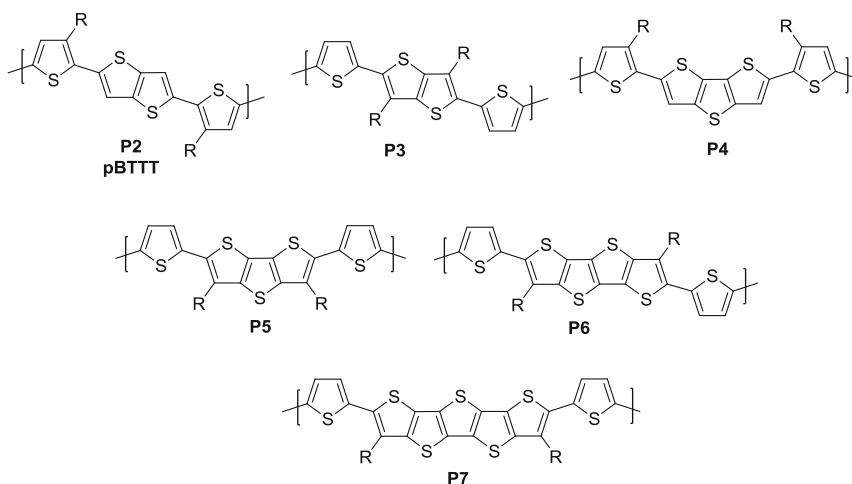
Poly(thiophene)s, Fig. 5 Structures of some fused thiophene copolymers

Poly(thiophene)s,
Fig. 6 Isomers of
benzodithiophene
incorporated into
polythiophenes
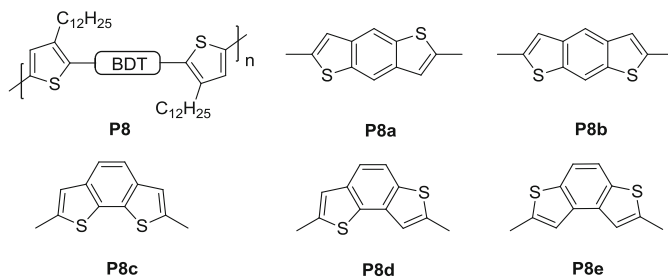
observed for **P4** versus **P5**, in which the alkyl chains are again moved from the bithiophene to the rigid fused aromatic. Comparing polymers **P5**, **P6**, and **P7** resulted in a noticeable odd-even effect on their properties depending on the number of fused aromatic rings. Thus polymer **P6** was found to have a smaller band gap and form more ordered thin films, compared to **P5** and **P7**, which manifested as improved FET mobility. A common design feature for many of the most well-ordered polymers which demonstrate the highest FET mobility is the utilization of a monomer repeat unit that has an axis of C_2 rotational symmetry perpendicular to the backbone (such as **P2**, **P3**, and **P6**) [14].

There is also a large class of polythiophenes incorporating thiophene fused to other aromatic rings such as benzene, naphthalene, pyridine and anthracene, and many others [15]. In many of these examples, various isomers of the thiophene-containing aromatic are possible. For example, in Fig. 6, the structures of dialkylated bithiophene copolymers of various isomers of benzodithiophene (BDT) are shown (**P8**). Because of the different bonding geometry of the various BDTs synthesized, each polymer was shown to induce a different backbone curvature into the resulting polymer, ranging from linear for **P8a** to slightly nonlinear for **P8b** to increasingly curved for polymers **P8c** through **P8e** [16]. The backbone curvature could be quantified based on force-field modeling of the backbone geometry. Interestingly many polymeric properties were shown to be dependent on the amount of backbone curvature, including solubility with the most linear polymer exhibiting the lowest solubility. Perhaps unsurprisingly the

polymers with the highest curvature (**P8d** and **e**) also resulted in the least ordered polymer thin films and the lowest FET mobilities. Optimal performance was found for **P8c** which offered the best balance between curvature and solubility. Polymers **P8b** and **P8d** also had the widest optical band gaps, due to the meta-substituted isomeric patterns, which prevented full delocalization along the polymer backbone. Subsequent studies have found that backbone curvature is an important design parameter to be optimized, since it influences the ability of the conjugated backbones to overlap closely in the solid state. BDT polymers based upon alkylated analogues of **P8a** in which is central phenyl ring is alkylated are also an important class of photovoltaic donor polymer. Polymerization with a range of electronic-deficient monomers has afforded some of the highest-efficiency solar cell donor materials [15].

The final important class of polythiophene materials is that featuring bridged bithiophenes (Fig. 7), in which the bithiophene unit is held rigid and coplanar by a bridging atom ensuring good delocalization. A variety of different bridging atoms have been investigated such as C, Si, Ge, or N. Unlike the bridging S in the examples seen in Fig. 5, each of these bridging atoms is able to incorporate two or one alkyl chains to act as solubilizing substituents [1, 17]. In these cases the point of attachment of the solubilizing chains at the bridging position does not typically cause steric interference with adjacent monomer groups, facilitating backbone delocalization and planarization. The nature of the heteroatom also has significant impact on the electronic properties and morphological properties of the backbone. Thus, for

Poly(thiophene)s,
Fig. 7 Structure of bridged
bithiophene monomers and
polymers

X = CR$_2$, SiR$_2$, GeR$_2$, C=O, N-R, P-R

P9a X = C(C$_2$C$_6$)$_2$
P9b X = Si(C$_2$C$_6$)$_2$
P9c X = Ge(C$_2$C$_6$)$_2$
P9d X = C(C$_{16}$)$_2$
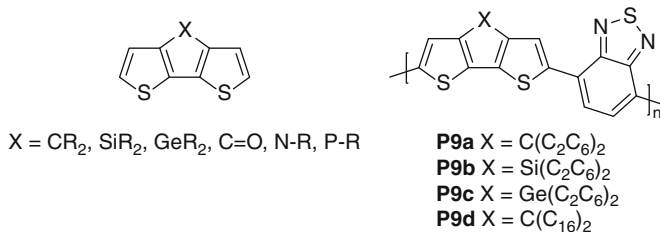
example, in comparing low band gap polymer with benzothiadiazole (structures **P9a–c**), it was found that the C-bridged polymer was amorphous, whereas the Si- and Ge-bridged polymers exhibited semicrystalline ordering. This was rationalized on the basis of the longer C–Si/Ge bond compared to the C–C bond, which reduced steric strain between the solubilizing 2-ethylhexyl groups and the adjacent backbone monomers facilitating π-stacking. The change in polymer crystallinity manifested itself as improved photovoltaic properties in blends with fullerene derivatives. The change in heteroatom also influences the band gap of the polymer, partly as a result of the changed geometry of the monomer due to the changing bond lengths and partly due to electronic interactions between the LUMO of the carbon framework and the σ* orbitals of the Si/Ge heteroatoms.

The important role of the side chains and molecular weight can also be seen in comparing the properties of **P9a** with branched 2-ethylhexyl groups to **P9d** with linear hexadecyl groups. Initial reports of both polymers found that there was little evidence of molecular order by XRD in either case, although the **P9d** exhibited FET mobility one order of magnitude higher than **P9a**. However care must be taken in comparing measurements in different transistor geometries due to the pronounced role this has in device performance. More interesting was the fact by improving the molecular weight of **P9d**, clear evidence was found of molecular ordering by XRD, and this correlated with further improvements in FET mobility, up to 3.3 cm^2/Vs for films orientated by dip coating and up to 5.5 cm^2/Vs for single fiber devices [1]. The above study clearly highlights the importance of optimizing side chains, molecular weight, and processing conditions on device performance.

Synthetic Methods

The synthesis of polythiophenes has been reported by a wide variety of methods. In particular the synthesis of P3AT has probably been investigated more than any other conjugated polymer, with a variety of routes reported. Part of this reason is the interest in P3HT itself as a versatile organic semiconductor, and partly this is due to the fact that P3HT is a well-soluble polymer that is easy to characterize by NMR and mass spectroscopy. This gives information on the regioregularity of the side chains, which can be utilized as an excellent probe for the versatility and robustness of any polymerization chemistries, since head-to-head or tail-to-tail defects are readily identified. In this respect, P3HT is unlike many other conjugated polymers, particularly low band gap materials, in which the NMR spectra are typically broad and featureless and is it therefore difficult to probe possible miscouplings in the backbone.

Kumada and Negishi Coupling
The nickel-catalyzed Kumada cross-coupling of 2-bromo-5-thienyl magnesium bromide, prepared by insertion of magnesium metal into 2,5-dibromothiophene, was first reported for the preparation of unsubstituted polythiophene in the early 1980s. A similar approach was initially utilized to P3ATs by the reaction of 2,5-diiodo-3-alkylthiophene with magnesium metal, followed by polymerization of the resulting Grignard with Ni(dppp)Cl$_2$. However the Mg insertion reaction results in a mixture of unreacted starting material, mono- and di-Grignard reagents, and thus relatively poor molecule weights were observed, with high polydispersity and low regioregularity [3]. An improvement was

P

Fig. 8 Three methods of
preparation of regioregular
poly(3-alkyl)thiophene by
Kumada or Negishi cross-
coupling
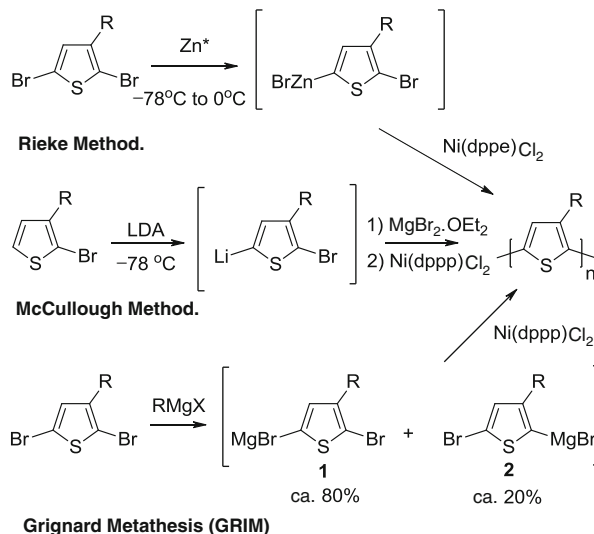
developed by McCullough, who developed a regiospecific route to the formation of 2-bromo-3-alkyl-5-thienyl magnesium bromide (**1**) in situ, commonly referred to as the McCullough method (Fig. 8). Addition of a bidentate nickel catalyst afforded regioregular P3AT in good molecular weight and yield. Although a breakthrough at the time, the necessity to carefully control the cryogenic temperature to prevent unwanted rearrangements of the thienyllithium intermediate was a disadvantage, and the route has largely been superseded.

Around the same time, an alternative route to RR P3ATs was reported by Rieke, in which 2-bromo-3-alkyl-5-thienyl zinc bromide was used as the monomer [3]. This was formed by direct insertion of highly active Rieke zinc (Zn*) into 2,5-dibromo-3-alkylthiophene. This was found to occur regioselectively at the five-position, if low (-78 °C) temperatures were used for the initial addition. Upon warming to room temperature and addition of a catalyst, P3AT was produced. Rieke also reported that the nature of the catalyst had a strong influence on the regioregularity of the polymer produced, with bidentate Ni(dppe)Cl$_2$ catalyst affording high RR, while Ni(PPh$_3$)$_4$ with more labile ligands resulted in lower RR. The analogous Pd catalysts both afforded lower RR still. The main

advantage of the Rieke route is the use of organozinc reagents, which, unlike Grignard reagents, are tolerant to a wide range of functional groups. More recent research has shown it is possible to generate the required organozinc regents by alternative routes, such as lithiation and transmetallation with ZnCl$_2$ or direct insertion of zinc dust into 5-iodo-2-bromo-3-alkylthiophene [18].

An improved synthesis not requiring cryogenic temperature was subsequently reported by McCullough and co-workers, known as the Grignard metathesis or GRIM method (Fig. 3) [7]. Treatment of a solution of 2,5-dibromo-3-alkylthiophene with one equivalent of any alkyl or vinyl Grignard reagent resulted in a metathesis reaction to afford an alkyl bromide and a mixture of 2-bromo-3-alkyl-5-thienyl magnesium bromide (**1**) and 5-bromo-3-alkyl-2-thienyl magnesium bromide (**2**) in an approximate 4:1 ratio, independent of the reaction temperature and nature of the Grignard reagent used. Surprisingly addition of Ni(dppp)Cl$_2$ to the mixture resulted in the formation of P3AT of high RR and molecular weight, with yields around 80 %. The high regularity from a mixed starting monomer was shown to result from the slow rate of coupling to form HH defects, in comparison to TT or HT. Thus any TT defect that is formed will subsequently show a preference for HT coupling.
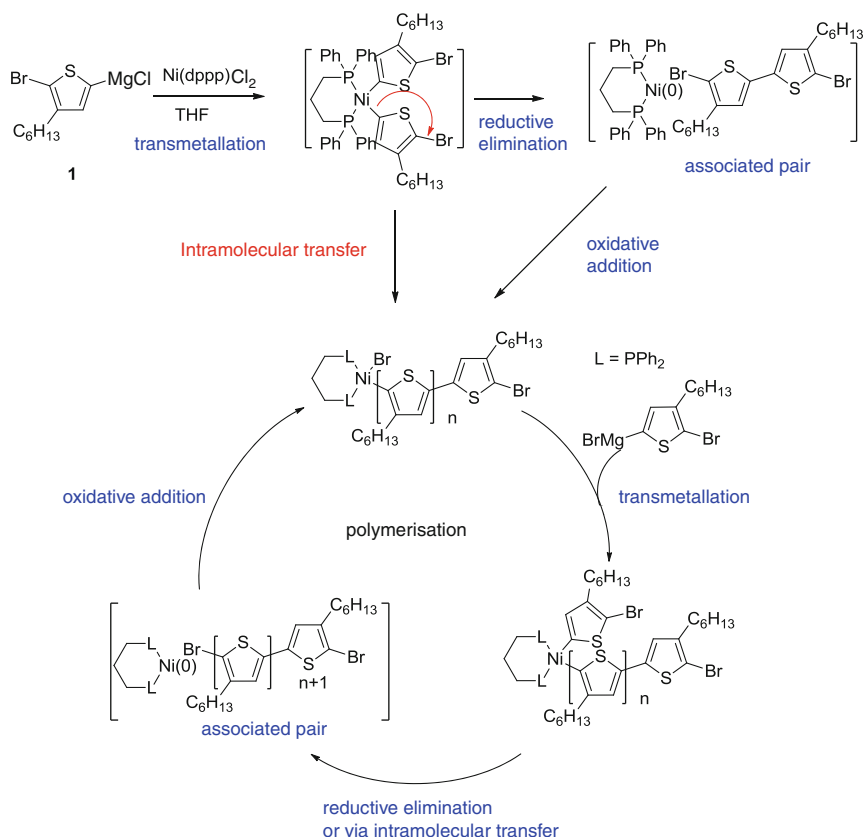
Poly(thiophene)s, Fig. 9 Proposed mechanism of nickel-initiated chain growth P3HT

It was later discovered that the GRIM polymerization exhibited characteristics typically associated with a chain growth mechanism with some "living" character [19]. Thus molecular weight was found to increase linearly with conversion and the molecular mass found to depend on the ratio between Grignard monomer and catalyst. This was an exciting result since the Kumada cross-coupling reaction is formally a condensation reaction and these are typically associated with a step-growth mechanisms. The mechanism shown in Fig. 9 and proposed simultaneously by the groups of Yokozawa and McCullough is generally accepted, although some of the details are still unclear. The first step of the reaction is reduction of the Ni(II) precatalyst by dimerization of two equivalents of thienyl Grignard monomer **1** to afford a TT dimer. It is then suggested that the resulting Ni(0) formed stays associated with the resulting

dimer, possibly by the formation of a π-complex. This associated complex then undergoes rapid oxidative insertion of the Ni(0) into one of the C–Br bonds. Alternatively it is suggested that the catalyst undergoes an intramolecular transfer from the Ni(II) complex into one of the C–Br bonds (a process known as catalyst transfer). The net result of either mechanism is similar, in that the resulting Ni(II) complex with the tail-to-tail dimer now initiates the catalytic cycle. Propagation then occurs via transmetallation with 2-bromo-3-hexyl-5-thienyl magnesium chloride, followed by reductive elimination to form the "associated pair" or intramolecular transfer of the catalyst to the C-Br chain end. In the case of the "associate pair" mechanism, it is believed that the Ni(0) forms a complex with the growing polymer chain directly after reductive elimination, and then this diffuses to the chain end and inserts oxidatively into the carbon halogen
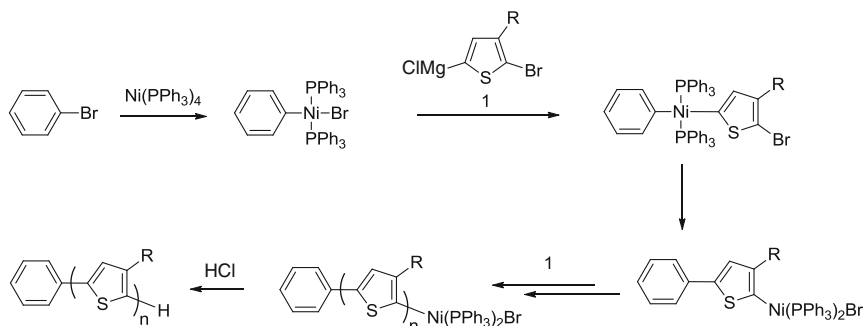
Poly(thiophene)s, Fig. 10 Preparation of an external initiator and subsequent polymerization of P3HT

bond [18]. The resting state of the polymerization has been observed by NMR techniques to be either of the two Ni(II) complexes before or after transmetallation depending on the exact bidentate ligand used, but the proposed Ni(0) associate pair has never been directly observed experimentally [20]. In either explanation the important factor is that the Ni catalyst stays associated with the growing polymer chain. This polymerization has been termed Kumada catalyst-transfer polycondensation (KCTP) by Yokozawa [19].

A key highlight of this proposed mechanism is that the polymer chain grows directly from a Ni(II) initiator (in the case of the GRIM polymer, this is formed in situ by the dimerization of monomer **1**) and stays associated with one growing polymer chains. This rapidly led to the realization that an external initiator could be added to the monomer mixture to grow P3AT under well-controlled conditions. Thus, for example, the addition of PhNi(PPh$_3$)$_2$Br, itself prepared from the reaction of phenyl bromide with Ni(PPh$_3$)$_4$, was shown by Kiriy to initiate the polymerization of a solution of 2-bromo-3-hexyl-5-thienyl magnesium chloride (**1**) (Fig. 10). The resulting polymer had almost complete inclusion of the phenyl end group if the polymerization was performed at 0 °C, although at these temperatures rather low molecular weights are produced due to the low solubility of the growing polymer [21].

Subsequent work into a range of initiators demonstrated that P3HT could be grown off a number of suitably functionalized surfaces [22]. For example, by the treatment of cross-linked poly(4-bromostyrene) with Ni(PPh$_3$)$_4$ followed by monomer **1**, it was possible to grow P3HT directly on the surface of the polystyrene film. Similar work allowed the functionalization of silica nanoparticles. Further work has also investigated the role of the initiator structure on the polymerization process. Improved polymerization control has been reported using initiators which contain an ortho-substituent group, due to a stabilization of the Ni complex. Bidentate phosphine ligands like dppp or dppe also promote improved regioregularity and a reduction in chain transfer reactions. More complex trifunctional initiators have also been used to prepare star-shaped polythiophenes with three arms in narrow polydispersity [20].

The GRIM polymerization has been used to polymerize a variety of thiophene-based polymers, with the only limitation being that the thienyl Grignard reagent must be compatible with the side-chain functionality. Thus polymers with alkoxy or alkylsulfanyl side chains have been synthesized, as well as those with more complex side chains such as alkyne groups for subsequent functionalization by click methodology. The GRIM polymerization has also been particularly successful to prepare all conjugated block copolymers. Since the reaction still has a reactive chain end when all monomer has been consumed, block copolymers can be prepared simply by the addition of a second thienyl Grignard monomer. For example, block copolymers containing straight chain hexyl groups and branched 2-ethylhexyl groups have been prepared which demonstrate interesting phase

segregation in thin films [20]. The polymer chain can also be endcapped at the end of the polymerization by the addition of additional Grignard reagent. The use of vinyl Grignard allows the formation of monofunctionalized polymers due to trapping of the Ni catalyst on the newly formed vinyl terminal group [7]. Such polymers have been subsequently transformed, via standard transformation involving hydroboration, oxidation, and esterification into macroinitiators suitable for living radical-type polymerizations [23].

Although the GRIM route and the closely associated Negishi coupling have shown great promise in the synthesis of most analogues of P3ATs, they are not extensively used in the synthesis of alternating copolymers involving thiophene-based monomers (e.g., structures **P2** to **P9**). This is due to the difficulty in forming suitably functionalized mono-Grignard for polymerization. The alternative route of forming a di-organozinc or magnesium reagent and coupling this with a dihalide is also problematic, because of the difficulty in forming the required organometallics in the high purity required for polymerization. For these reasons, alternating polythiophenes have mainly been synthesized by other routes.

Suzuki, Stille, and Direct Arylation Polymerizations

The Suzuki cross-coupling of an aryl halide with an organoboron reagent has been extensively used for the preparation of many conjugated polymers. It is particularly useful for the synthesis of polyfluorene- or polyphenyl-based materials but has been less utilized in the preparation of thiophene-rich polymers [24]. One of the issues is that the use of electron-rich thienyl boronic acids or esters can lead to deboronation during the polymerization, limiting molecular weight. Thus the organoboron containing monomer should preferentially be non-thiophene if possible, i.e., in the synthesis of polymer **P9a** by Suzuki polycondensation, the bisboronic ester is preferentially placed on the 2,1,3-benzothiadiazole monomer rather than the bridged bithiophene. A second issue with the polymerization is the requirement for a base to activate the boronic ester/acid for cross-coupling. Since many of the commonly used bases are aqueous, this can lead to two-phase reaction media and the requirement for phase-transfer catalysts to facilitate mixing. Solubility of the growing polymer can be an issue in such two-phase mixtures.

An early reported issue with Suzuki polymerization was the endcapping of the growing polymer chain by the transfer of aryl groups from the phosphine ligands used in the polymerization. This can be suppressed by the use of more bulky ligands like tri(o-tolyl)phosphine or by the use of ligand-free catalysts [24]. The polymerization of P3HT itself has been investigated in some detail as shown in Fig. 11. In this case bulky, electron-
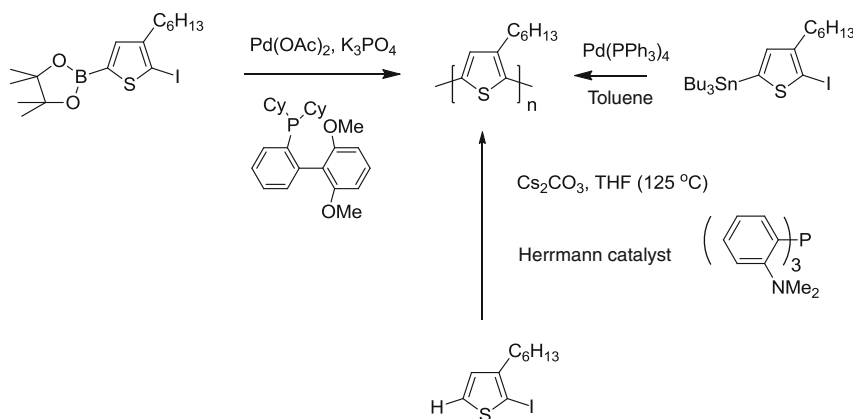
Poly(thiophene)s, Fig. 11 Suzuki, Stille, and direct arylation routes to P3HT

rich ligands afforded the best results, and high RR polymers with reasonable molecular weights were formed. Interestingly, the boronic ester in this case was formed directly from 2-bromo-3-hexylthiophene by an iridium catalyzed borylation reaction. This route does not involve the use of strong bases or nucleophilic organometallics and may be useful for the synthesis of materials where sensitive functionality is included in the polymer backbone [18]. More recent results also suggest the use of very electron-rich ligands can increase the polymerization speed considerably, reducing the time for the thiophene boronates to undergo undesired cleavage reactions [25].

The Stille cross-coupling of an organostannane with an aryl halide has been widely used in the preparation of thiophene-containing polymers. Unlike thienyl boronates, thienyl stannanes show good stability under the conditions of polymerization. No added base is required for activation in the case of a Stille polymerization (unlike Suzuki coupling), so it is ideal for the introduction of sensitive functionality. The major drawback with the Stille polymerization is both the high toxicity of organotin reagents and the difficulty in obtaining monomer with sufficient purity to form high molecular weight polymers. For low molecular weight monomers, this can be partly solved by using trimethylstannyl-based monomers rather than tributylstannyl, since the former tend to be crystalline rather than oils in the case of the latter, facilitating purification. The trimethyltin chloride or bromide by-products are also water soluble, which facilitates removal after polymerization. However the significantly higher toxicity of the trimethyltin derivatives should be noted. In the case of more complex monomers, purification can be difficult due to the fact that many organotin groups destannylate during attempted chromatographic purification upon silica or alumina. This can be solved by using reverse phase silica or cross-linked polystyrene as the stationary phase. Often however monomers are used crude, which can reduce molecular weight.

In the case of P3AT itself, the polymerization of 2-iodo-3-hexyl-5-tributylstannylthiophene with Pd(PPh$_3$)$_4$ affords highly regioregular polymer with molecular weights greater than 20 kDa. Interestingly the polymer could be isolated after the reaction with the tributylstannyl group still intact, which allowed for further functionalization. In terms of catalysts for the reaction, it is worthwhile highlighting that Pd(0) catalysts such as Pd$_2$(dba)$_3$ in combination with a phosphine ligand are preferred over Pd(II) pre-catalysts like Pd(PPh$_3$)$_2$Cl$_2$. This is due to the fact that reduction of the Pd(II) catalyst in situ often occurs by dimerization of the organostannane, which potentially interferes with the stoichiometry of the reaction. A great many examples of alternating or random thiophene-containing polymers have been synthesized by the Stille polycondensation. These have recently been reviewed in depth, but the popularity of the Stille polycondensation stems from its tolerance to a range of functional group and the reliability of the reaction [26].

A comparatively recent development in the plethora of cross-coupling reactions has been the palladium-catalyzed coupling between the C–H bond of various aromatic rings and aryl halides (or pseudo halides) in the presence of base, a process now commonly termed direct arylation. The main advantage to this approach is it obviates the need for an organometallic group to direct the coupling and therefore offers significant simplification in terms of cost and number of synthetic steps. The potential of such approaches has been recognized in the synthesis of polythiophenes, and a number of reports have investigated the use of direct arylation polymerization or DARP. As always P3HT has been a popular synthetic target.

The first reports of direct arylation polymerization of 2-bromo-3-hexylthiophene by Pd(OAc)$_2$ in the presence of base to give P3HT were in the late 1990s, although relatively low molecular weights were observed at that time. There was subsequently little improvement for over a decade until Ozawa reported that much high yield, molecular weights and RR could be obtained by the use of a more electron-rich ligand (Fig. 11) in the presence of Herrmann's catalyst and Cs$_2$CO$_3$. The reaction was performed in

pressurized THF to ensure good solubility of the growing polymer chain. One issue with direct arylation is the possibility of multiple sites of cross-coupling, since there is no organometallic group to direct the coupling. In P3HT there is the possibility of coupling to both the α (5-)position and the β (4-)position on the thiophene. Although the α position shows a higher reactivity than the β, as the polymer chain grows, the number of β position available for miscouplings grows versus the α, which is only available at the chain end. Thus chain branching might be expected and is indeed observed under certain conditions. The degree of branching is sensitive to the exact reaction conditions (catalyst, base, solvent). Although undesirable in many cases, this side reaction has been exploited to prepare hyperbranched polymers with variable degrees of branching [27].

The simplest way to avoid the issue of branching is to use 3,4-disubstituted thiophene monomers, in which coupling at the β position is not possible. Thus several examples of 3,4-disubstituted thiophene-based copolymers have now been reported in good yield and molecular weight. The method is particularly amenable to alternating copolymer with a variety of aryl dihalides as comonomers [27].

Conclusions

Thiophene or fused thiophene aromatics are very common structural building blocks in conjugated polymers for a range of applications. Many of the best performing materials for the numerous applications of conjugated polymers incorporate thiophene, from poly(3,4-ethylenedioxythiophene) (PEDOT) for use as hole injection layers in OLED devices to complex low band gap copolymers for photovoltaic applications. In fact, it is difficult to find an application of organic electronics in which thiophene-based polymers do not excel. The promising performance of such polymers is due to a combination of factors, but the synthetic developments in the control and understanding of polymerization techniques over the last few years have been particularly

significant. This is turn has led to better characterized materials with fewer defects and therefore an increased understanding of the critical factors which ultimately control the polymeric properties. Further improvements in the control of polymerization for an expanding series of monomers are expected to increase the number of applications for conjugated materials still further.

References

1. Guo X, Baumgarten M, Müllen K (2013) Designing π-conjugated polymers for organic electronics. Prog Poly Sci 38:1832–1908
2. Krebs FC, Nyberg RB, Jorgensen M (2004) Influence of residual catalyst on the properties of conjugated polyphenylenevinylene materials: palladium nonaparticles and poor electrical performance. Chem Mater 16:1313–1318
3. McCullough R (1998) The chemistry of conducting polythiophenes. Adv Mater 10:93–116
4. Liu J, Kadnikova EN, Liu Y, McGehee MD, Fréchet JMJ (2004) Polythiophene containing thermally removable solubilizing groups enhances the interface and the performance of polymer–titania hybrid solar cells. J Am Chem Soc 126:9486–9487
5. Bundgaard E et al (2012) Removal of solubilizing side chains at low temperature: a new route to native poly(thiophene). Macromolecules 45:3644–3646
6. Brabec CJ, Heeney M, McCulloch I, Nelson J (2011) Influence of blend microstructure on bulk heterojunction organic photovoltaic performance. Chem Soc Rev 40:1185–1199
7. Osaka I, McCullough RD (2008) Advances in molecular design and synthesis of regioregular polythiophenes. Acc Chem Res 41:1202–1214
8. Sirringhaus H et al (1999) Two-dimensional charge transport in self-organized, high-mobility conjugated polymers. Nature 401:685–688
9. Rivnay J, Mannsfeld SCB, Miller CE, Salleo A, Toney MF (2012) Quantitative determination of organic semiconductor microstructure from the molecular to device scale. Chem Rev 112:5488–5519
10. Guo XG, Watson MD (2008) Conjugated polymers from naphthalene bisimide. Org Lett 10:5333–5336
11. Ong BS, Wu Y, Li Y, Liu P, Pan H (2008) Thiophene polymer semiconductors for organic thin-film transistors. Chem Eur J 14:4766–4778
12. McCulloch I et al (2009) Semiconducting thienothiophene copolymers: design, synthesis, morphology, and performance in thin-film organic transistors. Adv Mater 21:1091–1109

P

13. Noriega R et al (2013) A general relationship between disorder, aggregation and charge transport in conjugated polymers. Nat Mater 12:1038–1044

14. He M et al (2010) Importance of C2 symmetry for the device performance of a newly synthesized family of fused-ring thiophenes. Chem Mater 22:2770–2779

15. Chochos CL, Choulis SA (2011) How the structural deviations on the backbone of conjugated polymers influence their optoelectronic properties and photovoltaic performance. Prog Polym Sci 36:1326–1414

16. Rieger R, Beckmann D, Mavrinskiy A, Kastler M, Müllen K (2010) Backbone curvature in polythiophenes. Chem Mater 22:5314–5318

17. Wang C, Dong H, Hu W, Liu Y, Zhu D (2011) Semiconducting π-conjugated systems in field-effect transistors: a material odyssey of organic electronics. Chem Rev 112:2208–2267

18. Marrocchi A, Lanari D, Facchetti A, Vaccaro L (2012) Poly(3-hexylthiophene): synthetic methodologies and properties in bulk heterojunction solar cells. Energy Environ Sci 5:8457–8474

19. Yokozawa T, Yokoyama A (2009) Chain-growth condensation polymerization for the synthesis of well-defined condensation polymers and pi-conjugated polymers. Chem Rev 109:5595–5619

20. Bryan ZJ, McNeil AJ (2013) Conjugated polymer synthesis via catalyst-transfer polycondensation (CTP): mechanism, scope, and applications. Macromolecules 46:8395–8405

21. Okamoto K, Luscombe CK (2011) Controlled polymerizations for the synthesis of semiconducting conjugated polymers. Polym Chem 2:2424–2434

22. Marshall N, Sontag SK, Locklin J (2011) Surface-initiated polymerization of conjugated polymers. Chem Comm 47:5681–5689

23. Scherf U, Gutacker A, Koenen N (2008) All-conjugated block copolymers. Acc Chem Res 41:1086–1097

24. Sakamoto J, Rehahn M, Wegner G, Schluter AD (2009) Suzuki polycondensation: polyarylenes à la carte. Macromol Rapid Commun 30:653–687

25. Liu M et al (2013) Synthesis of thiophene-containing conjugated polymers from 2,5-thiophenebis(boronic ester)s by Suzuki polycondensation. Polym Chem 4:895–899

26. Carsten B, He F, Son HJ, Xu T, Yu L (2011) Stille polycondensation for synthesis of functional materials. Chem Rev 111:1493–1528

27. Okamoto K, Zhang J, Housekeeper JB, Marder SR, Luscombe CK (2013) C–H arylation reaction: atom efficient and greener syntheses of π-conjugated small molecules and macromolecules for organic electronic materials. Macromolecules 46:8059–8078

Poly(vinyl alcohol) (PVA)

Kotaro Satoh
Department of Applied Chemistry, Graduate School of Engineering, Nagoya University, Nagoya, Japan

Synonyms

Poly(ethenol); Poval; PVOH; Vinyl alcohol homopolymer

Definition

Poly(vinyl alcohol) is a synthetic polymer bearing repeating $-CH_2-CH(OH)-$ units, which is generally prepared from post-polymerization reaction of a homopolymer obtained from a protected monomer, such as vinyl acetate.

Introduction

Although poly(vinyl alcohol) (PVA) is one of the synthetic polymers composed of vinyl monomer units similarly to polystyrene or polypropylene, PVA cannot usually be prepared directly from vinyl alcohol as the monomer because vinyl alcohol itself is unstable and readily tautomerized into acetaldehyde. Therefore, it is usually prepared by the polymerization of a protected monomer, such as vinyl ester, followed by deprotection.

From the first breakthrough patent of the vinyl acetate (VAc) preparation and polymerization into PVA by W.O. Herrmann et al. in 1924, the production of PVA has progressed to a process of common polymeric materials [1, 2]. Nowadays, PVA in industrial applications is generally obtained from the saponification or hydrolysis of homopolymer of VAc (Fig. 1). Although PVA is one of the oldest synthetic polymers, it still has been attracting much attention in the
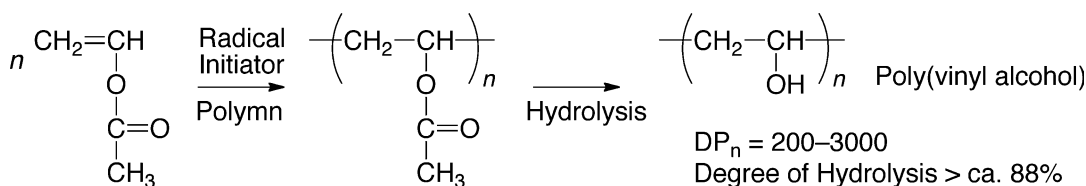
Poly(vinyl alcohol) (PVA), Fig. 1 Preparation of poly(vinyl alcohol) by radical polymerization of vinyl acetate

Poly(vinyl alcohol) (PVA), Fig. 2 Preparation of poly(vinyl alcohol-co-ethylene)
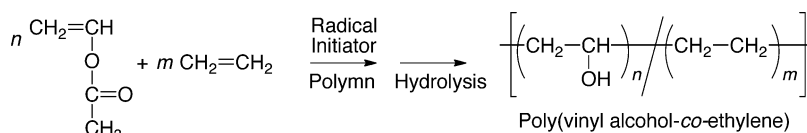
Poly(vinyl alcohol) (PVA), Fig. 3 Poly(vinyl alcohol) as a precursor for poly(vinyl acetal)
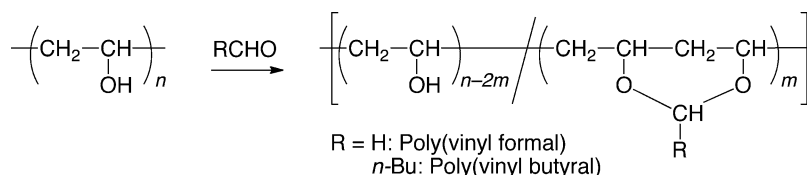
chemical, material, and medical fields because of a unique combination of its properties including solubility in water, film orientation characteristics for the polarizer of a liquid crystal display, adhesive ability to a number of substrates, low toxicity, biodegradability, and biocompatibility [3–9]. These properties depend on degree of the hydrolysis as well as the primary structures of the original precursor of poly(vinyl acetate) (PVAc), such as head-to-tail regioselectivity, molecular weight, and tacticity. Therefore, from the viewpoint of synthetic chemistry, the control of the VAc polymerization is still a challenging topic to improve the properties of PVA and further contributes to the development of the PVA-based materials as well as the new polymerization systems for other protecting monomers.

Not only PVA homopolymers but also a number of PVA-related materials are industrially produced and commercially available in many grades [3]. Copolymerization is a useful method for developing another polymeric material with different properties. Typically, the copolymerization of VAc with ethylene followed by hydrolysis results in ethylene-vinyl alcohol

copolymer, which has excellent gas barrier properties with low permeability (Fig. 2). Since PVA has many functional hydroxyl groups in the side chain, chemical modification of PVA is also efficient to obtain a polymer with other properties. For example, the reaction with aldehyde compounds, such as formaldehyde and butanal, leads to intramolecular cyclization of adjacent two hydroxyl groups to form acetal ring, which are called poly(vinyl formal) and poly(vinyl butyral) resins, respectively (Fig. 3).

Polymerization of Vinyl Acetate for PVA Production

VAc can be homopolymerized only via a neutral radical intermediate, as shown in Fig. 1 [10]. In industry, the VAc polymerization for PVA production is usually conducted with solution polymerization technique using methanol as the solvent. The homogeneous solution of PVAc in methanol is diverted to the subsequent saponification/hydrolysis process, in which the polymer turns into PVA and becomes insoluble and

solidified in methanol. During radical polymerization of VAc, the highly reactive growing species renders the primary structure of the resultant PVAc difficult to be controlled: the VAc radical polymerization has great tendency to undergo a chain transfer to methyl group of the acetyl substituents both on the polymer and monomer as well as a termination by hydrogen atom abstraction rather than radical-radical recombination [11]. Therefore, the degree of polymerization during VAc free radical polymerization generally obeys the traditional Lewis-Mayo equation. Another structural defect inherent to PVAc is the head-to-head linkage caused by the misdirected insertion of the monomer, in which the two carbons of the vinyl group are not distinguished well enough in terms of the electric polarization due to the nonconjugated nature of the VAc monomer. In addition, the stereochemistry during radical polymerization has also been very hard to control due to the lack of efficient methods that can induce the directed insertion or addition of the monomer to the free radical growing end.

State of the Art in Vinyl Acetate Polymerization

Controlled or living polymerization is one of the most promising methods for the production of polymers with controlled molecular weights and their distributions. There have been a tremendous number of reports on the living or controlled radical polymerization systems in the past two decades [12]. There also appear effective systems for the polymerization of VAc to afford the polymers with precisely controlled molecular weights and narrow molecular weight distributions. They include the macromolecular designs via the interchange of xanthate (MADIX)/reversible addition-fragmentation chain transfer (RAFT), iron-catalyzed, degenerative iodine transfer, cobalt-mediated, and organotellurium- and organostibine-mediated processes. Most of them are based on the degenerative chain transfer process, which accomplishes the molecular weight control via a reversible interconversion between

the growing radical and the covalent dormant species in the presence of radical reservoir. These techniques allow novel macromolecular architectures, such as block copolymers and star-shaped polymers composed of a PVA segment.

To control tacticity, i.e., stereochemistry, during radical polymerization, is another challenging topic [13]. As for the tacticity control during radical polymerizations, acidic compounds as additives, such as protic solvents like fluoroalcohols and Lewis acids (like lanthanide triflates), have proved effective for monomers with pendent polar groups. The syndiospecific radical polymerization of VAc proceeds in a bulky fluoroalcohol like $(CF_3)_3COH$, which most probably interacts with the carbonyl group of the monomer and/or the growing chain end via hydrogen bonding to induce steric repulsion around the growing terminal. The following saponification of the syndiotactic PVAc yields the syndiotactic PVA with higher melting temperature than that of the atactic PVA prepared from bulk or methanol solution polymerization of VAc. The use of fluoroalcohol solvent is also effective for increasing regioselectivity to significantly suppress the head-to-head propagation. Thus, the control of the chemospecificity, stereospecificity, and regiospecificity during the radical polymerization of VAc would lead to an innovative PVA [14].

Preparation of PVA from Other Monomers

There are more ways to prepare PVA than using VAc in the literature. A wide variety of vinyl esters ($CH_2=CH-OCOR$) can be polymerized via free radical polymerization to produce the PVA precursor similarly to VAc [11]. Vinyl ethers ($CH_2=CH-OR$) can be homopolymerized via cationic polymerization using a Lewis acid catalyst. The homopolymer of vinyl ether with a bulky substituent, such as *tert*-butyl vinyl ether, can be easily hydrolyzed under acidic condition, subsequently to form PVA (Fig. 4) [15, 16]. Specifically, cationic polymerization of vinyl ether
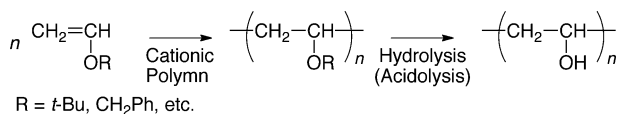
Poly(vinyl alcohol) (PVA), Fig. 4 Preparation of poly(vinyl alcohol) by cationic polymerization of vinyl ether

Poly(vinyl alcohol) (PVA), Fig. 5 Preparation of poly(vinyl alcohol) by aldol group transfer polymerization of silyl enol ether
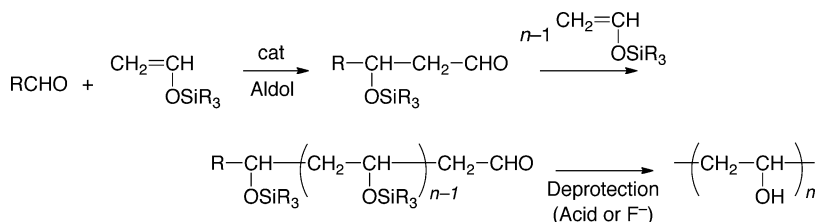
often gives relatively isotactic polymers, which consequently lead to isotactic PVA.

Aldehydes are known to undergo cross-aldol reaction with a silyl enol ether (silyl vinyl ether, $CH_2=CH-OSiR_3$) to form a compound with silylated alcohol and newly formed aldehyde. Repeating the cross-aldol reaction of acetaldehyde at the growing chain end, which is a tautomer of unstable vinyl alcohol, one can obtain a silylated vinyl alcohol polymer with a terminal aldehyde group (Fig. 5) [17]. This polymerization is called aldol group transfer polymerization (aldol-GTP). Under judicious conditions, the aldol-GTP of silyl enol ether proceeds in a living fashion, in which the molecular weight of resultant polymer increases with monomer conversion and agrees with the calculated values assuming that one aldehyde molecule generates one polymer chain. Although several attempts have been done for the direct isomerization polymerization of acetaldehyde, only oligomers of PVA have so far been obtained directly from acetaldehyde as the monomer.

Properties of PVA

The most characteristic property of PVA (typically originated from PVAc) is its solubility toward water, which depends both on the degree of polymerization and hydrolysis of PVAc [3]. Especially, the degree of hydrolysis significantly affects the water solubility, in which the original hydrophobic PVAc generally turns hydrophilic as the hydrolysis reaction proceeds due to the increasing affinity toward water with the hydroxyl groups. PVAc generally becomes water soluble over the range of 80 % hydrolysis degree, in which the water solubility slightly decreases as the polymerization degree increases. The solubility in water also depends on the temperature. PVA with low degree of hydrolysis (80–85 %) shows lower critical solution temperature (LCST)-type phase diagram, in which the solubility becomes lower at a higher temperature [18].

Meanwhile, too many adjacent hydroxyl groups in the consecutive side chain conclusively in turn result in water-insoluble polymers, because of the inter- and intramolecular hydrogen bondings to cause high crystallinity like cellulose, a kind of natural polymer with many hydroxyl groups. More specifically, over 90 % hydrolysis degree, its water solubility gradually decreases after drying, and when the hydrolysis degree becomes over 98 %, the polymer does not show water solubility at ambient temperature anymore. In addition, thermal annealing or stretching for crystallization dramatically decreases the water solubility of PVA with high hydrolysis degree [3]. Consequently, a molded specimen or thread of pure PVA with quantitative hydrolysis degree and high crystallinity is hard to dissolve or sometimes insoluble in water after drying similarly to cellulose. Therefore, one has

P

to tune the degree of hydrolysis depending on the water-soluble applications. In other words, only PVA with an adequate number of acetyl groups in the side chain (partially hydrolyzed PVAc) is accessible to many water-soluble applications.

Thus, many kinds of PVA with different degrees of hydrolysis and polymerization are now commercially available depending on their application. Typically, the commercially available water-soluble PVA has around 88 % hydrolysis degree and that of "fully hydrolyzed" grade PVA is around 98–99 %, whereas the degree of polymerization is in the range of 200–3,000.

Application of PVA and Related Polymers

Owing to its several characteristic properties, such as solubility in water, orientation characteristics, adhesive ability to a number of substrates, low toxicity, biodegradability, and biocompatibility, over one million metric tons of PVA is now produced in industry and consumed for wide variety of applications every year [3]. For example, the water-soluble PVA is used in paper manufacture, especially specialty papers, as a binder or primer; in textile warp sizing; in adhesives as an aqueous adhesive solution; and in other polymer production like poly(vinyl chloride) as a surfactant for emulsion or suspension polymerization.

PVA fiber is one of the most traditional applications of PVA, of which the first example is poly (vinyl formal) from PVA and formaldehyde developed in Japan by Sakurada et al. in 1939 and then Kurashiki Rayon Co., Ltd. (now Kuraray Co., Ltd.), started commercial production in 1950, which is often called as vinylon [19]. PVA fiber is not suited for clothing application. However, superiorly strong mechanical properties can be gained by orientation of polymer chains during drawing or stretching owing to high crystallinity by pendent hydroxyl groups, which leads to high resistance to water and chemicals including alkali and natural conditions. Therefore, PVA fiber is now composed of PVA homopolymer and the name of vinylon often indicates the PVA fiber. The excellent mechanical properties have widened the PVA fiber application, of which the example is that the PVA fiber is now also used as reinforcement in cement sheets as an alternative for asbestos in construction industry.

PVA film is widely used for packaging including a food packaging as barrier films and a water-soluble and biodegradable film for packaging of detergents, water-soluble chemicals, agrochemicals, fishing, and dyes [3]. For food packaging film, the copolymer of vinyl alcohol and ethylene is also used rather than PVA homopolymer in terms of water resistance, although its original gas permeability at dry condition is higher than that of PVA. As for the water-insoluble application, the water resistance of a dried PVA film increases with increasing molecular weights and degree of hydrolysis of the raw material polymers, which can be further improved by heat treating or annealing of the dried film at a higher temperature over 100 °C. Polyols, such as glycerol, ethylene glycol, di- and triethylene glycol, and oligomer of ethylene glycol, can be used as plasticizers for PVA up to 30 wt%. PVA film as a water-soluble film is also used for laundry bags, water transfer printing, and embroidery applications. Nowadays, polarizer in liquid crystal display (LCD) is another major application of PVA films, which is the most essential component in the LCD panel, and LCD holds 95 % consumption share of global polarizer production [20]. The polarizer film is prepared by stretching the PVA film, which is followed by doping of iodine molecule and tucking with triacetyl cellulose (TAC) films. The market of PVA film for polarizer is oligopolized by Japanese two manufacturers, Kuraray Co., Ltd., and Nippon Synthetic Chemical Industry Co., Ltd., most of which are consumed by the polarizer manufacturers in Asia. The worldwide demand of PVA film for polarizer is now estimated to be over 200 million square meters.

PVA is also used as the raw material in the manufacture of poly(vinyl butyral) resin, which is mainly used in automotive and architectural fields as a protective interlayer bonded between two panels of laminated glass.

References

1. Baum E, Deutsch H, Herrmann WO (1924) Esters of vinyl alcohol. DE Patents 483,780
2. Hachnel W, Herrmann WO (1924) Vinyl alcohol. DE Patents 480,866
3. Finch CA (ed) (1992) Polyvinyl alcohols developments. Wiley, Chichester
4. Miyasaka K (1993) PVA-iodine complexes: formation, structure, and properties. In: Zachmann HG (ed) Structure in polymers with special properties, vol 108, Advances in polymer science. Springer, Heidelberg, pp 91–129
5. Chiellini E, Corti A, D'Antone S, Solaro R (2003) Biodegradation of poly (vinyl alcohol) based materials. Prog Polym Sci 28:963–1014. doi:10.1016/S0079-6700(02)00149-1
6. Jayasekara R, Harding I, Bowater I, Lonergan G (2005) Biodegradability of a selected range of polymers and polymer blends and standard methods for assessment of biodegradation. J Polym Environ 13:231–251. doi:10.1007/s10924-005-4758-2
7. Drury JL, Mooney DJ (2003) Hydrogels for tissue engineering: scaffold design variables and applications. Biomaterials 24:4337–4351. doi:10.1016/S0142-9612(03)00340-5
8. Miyata T, Uragami T, Nakamae K (2002) Biomolecule-sensitive hydrogels. Adv Drug Deliv Rev 54:79–98. doi:10.1016/S0169-409X(01)00241-1
9. Lee KY, Mooney DJ (2001) Hydrogels for tissue engineering. Chem Rev 101:1869–1879. doi:10.1021/cr000108x
10. Odian G (2004) Principles of polymerization, 4th edn. Wiley, Hoboken
11. Moad G, Solomon DH (2006) The chemistry of radical polymerization, 2nd edn. Elsevier, Oxford
12. Matyjaszewski K, Davis TP (eds) (2002) Handbook of radical polymerization. Wiley, Hoboken
13. Yamada K, Nakano T, Okamoto Y (1998) Stereospecific free radical polymerization of vinyl esters using fluoroalcohols as solvents. Macromolecules 31:7598–7605. doi:10.1021/ma980889s
14. Satoh K, Kamigaito M (2009) Stereospecific living radical polymerization: dual control of chain length and tacticity for precision polymer synthesis. Chem Rev 109:5120–5156. doi:10.1021/cr900115u
15. Murahashi S, Yuki H, Sano T, Tadokoro H, Yonemura U, Chatani Y (1962) Isotactic polyvinyl alcohol. J Polym Sci 62(174):S77–S81. doi:10.1002/pol.1962.1206217430
16. Okamura S, Kodama T, Higashimura T (1962) The cationic polymerization of t-butyl vinyl ether at low temperature and the conversion into polyvinyl alcohol of poly-t-butyl vinyl ether. Makromol Chem 53:180–191. doi:10.1002/macp.1962.020530118
17. Sogah DY, Webster OW (1986) Sequential silyl aldol condensation in controlled synthesis of living poly (vinyl alcohol) precursors. Macromolecules 19:1775–1777. doi:10.1021/ma00160a052
18. Nord FF, Bier M, Timasheff SN (1951) Investigations on proteins and polymers. IV. Critical phenomena in polyvinyl alcohol acetate copolymer solutions. J Am Chem Soc 73:289–293. doi:10.1021/ja01145a095
19. Sakurada I (1985) Polyvinyl alcohol fibers. Marcel Dekker, New York
20. Land EH (1951) Some aspects of the development of sheet polarizers. J Opt Soc Am 41:957–963. doi:10.1364/JOSA.41.000957

Poly(vinyl chloride) (PVC)

Yukikazu Takeoka
Graduate School of Engineering, Nagoya University, Nagoya, Japan

Synonyms

Poly(1-chloroethylene); Polychloroethylene; PVC

Definition

Poly(vinyl chloride) (PVC) (CAS number 9002-86-2) is a synthetic resin made from vinyl chloride and is a member of a large family of polymers broadly referred to as "vinyls." The chemical formula for vinyl chloride is $H_2C=CHCl$, and the formula for PVC is $(H_2C–CHCl)_n$, where n is the degree of polymerization. This polymer is one of the most widely used commercial thermoplastic materials. PVC is one of the earliest produced polymers and now one of the three most abundantly produced synthetic polymers [1, 2].

History

Vinyl chloride is a colorless, highly flammable gas with a faint sweet odor that was first reported by Justus von Liebig and his research student, Henri Victor Regnault, in 1835; Regnault also reported the polymerization of this compound in 1838 [3]. Regnault observed that vinyl chloride

polymerized to form a white powder upon exposure to sunlight. Some later works revealed that the polymerized object was PVC, but, according to some other papers, the polymerized object was poly(vinylidene chloride). Thus, it is commonly believed that PVC was first prepared by a German chemist named Eugen Baumann in 1872, and Baumann is often credited as the inventor of PVC. The industrial development of PVC resins began approximately 50 years later. Full-scale commercial production began in Germany in 1931, while PVC was produced commercially in the USA in 1933. During World War II, PVC became the material of choice to protect electrical wires for military [4].

Process of Manufacture

Unlike other thermoplastics that are entirely derived from oil, PVC is manufactured from two starting materials: ethylene and sodium chloride. Ethylene is derived from a cracking process involving a feedstock based on oil. Chlorine is produced via the electrolysis of sodium chloride in salt water and is then combined with the ethylene obtained from oil. The resulting chemical is ethylene dichloride, which can be converted to vinyl chloride at high temperatures. Alternatively, vinyl chloride is obtained by reacting ethylene with oxygen and hydrogen chloride over a copper catalyst. Consequently, vinyl chloride and PVC consist of 57 % chlorine and 43 % hydrocarbon. Vinyl chloride boils at $-13.4\ ^\circ\mathrm{C}$ and is normally stored and shipped as a liquid under pressure. Generally, PVC is produced via the free radical polymerization of vinyl chloride (Fig. 1) with initiators, such as organic peroxides, in thick-walled, high-pressure-rated steel vessels. Currently, PVC is produced using various processes to generate increasingly specialized PVC
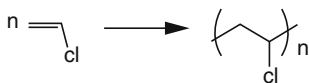
Poly(vinyl chloride) (PVC), Fig. 1 Polymerization of vinyl chloride

varieties that are tailored for specific end markets and new processing technologies. Commercially, PVC is mainly produced by solution, bulk, suspension, and emulsion polymerizations. Tacticity of PVC changes according to the reaction conditions. Most of the products are usually atactic [5].

Properties

Pure PVC is a white, brittle solid. The glass-transition temperature of PVC homopolymers is near 80 °C. The reported amount of crystallinity is in the range of between 5 % and 10 %. The presence of chlorine gives excellent fire resistance to PVC. Moreover, PVC exhibits excellent electrical insulation characteristics. These properties make PVC an ideal material for wire coating and architectural materials. Pure PVC is rigid, difficult to burn, and highly resistant to strong acids and bases, most other chemicals, and many organic solvents. The Flory-Huggins parameter (polymer-solvent interaction parameter) of PVC ranges from 19.2 to 22.1 $(\mathrm{MPa})^{1/2}$ [2]. In addition, PVC is not biodegradable. Due to its durability, PVC can be used in a variety of applications. Usually, thermoplastics are supplied as pellets. However, PVC resin is often supplied as a powder, and long periods of storage are possible because PVC resists oxidation and degradation. Because PVC is one of the least expensive plastics, easy to mold, and lightweight, it is predominant in the construction industry.

Applications

The major factors that favor the use of PVC for various applications are its range of flexibility, low toxicity, chemical stability, cost-effectiveness, ease of fabrication, biocompatibility, etc. More than 30 million tons of PVC were used worldwide in recent years. PVC is used in numerous applications that require a longevity ranging from short to extended periods of time. Approximately 60 % of the PVC that is used in various applications is expected to have a lifetime exceeding 40 years. The applications for PVC fall

into two broad categories depending on its formulation.

Pure PVC is a glassy polymer at room temperature and is used for molding and profile extrusions with few additives. The typical products produced from glassy PVC include window frames, water pipes, credit cards, bottles, house siding, and containers. However, pure PVC is unstable when exposed to visible and UV light. To address these disadvantages and make PVC suitable for different applications, antioxidants and stabilizers are added.

To use PVC in flexible or elastomeric applications, plasticizers such as phthalates must be mixed with the PVC to lower the glass-transition temperature. This type of PVC typically contains 30–40 wt% plasticizers. To a large extent, the type and amount of plasticizer determines the properties of the plasticized composition. In this soft and flexible form, PVC is used in electrical cable insulation and many other applications where PVC replaces rubber. In the healthcare industry, flexible PVC, produced by the addition of phthalates, is used to make blood bags, feeding tubes, and many other items [6]. Many other applications include hoses, imitation leathers, cables, packaging films, vinyl flooring, and car interiors.

Environmental Impact, Sustainability, and Recycling

PVC degradation during processing and use has been one of the most essential elements of PVC science and technology. Moreover, although PVC use has grown tremendously over the last 70 years, health and environmental problems have been associated with its use, including the effects of the vinyl chloride, phthalate plasticizers, and other contaminants, such as dioxins and heavy metals. For example, vinyl chloride has been identified as a carcinogen. Recycling PVC materials is more difficult than other widely used plastics due to the thermal stability of PVC and the diverse additives used for various products. However, recently, the recycling efficiency of PVC has been improved. Recycled PVC is

Poly(vinyl chloride) (PVC), Fig. 2 The Society of Plastics Industry recycling codes of PVC

break to small chips, impurities removed, and the product refined to make pure white PVC. The Society of Plastics Industry recycling codes of PVC is 3 shown in Fig. 2.

References

1. Sarvetnick HA (1969) Polyvinyl chloride. Van Nostrand Reinhold Co., New York
2. Brandrup J, Immergut EH, Grulke EA (1999) Polymer handbook. Wiley, New York
3. Carraher CE Jr (2012) Introduction to polymer chemistry. CRC Press, Boca Raton
4. Patrick SG (2005) Practical guide to polyvinyl chloride. Rapra Technology Limited, Shrewsbury
5. Endo K (2002) Synthesis and structure of poly(vinyl chloride). Prog Polym Sci 27:2021–2054
6. Blass CR (2001) The role of poly(vinyl chloride) in healthcare. Rapra Technology Limited, Shrewsbury

Polyacetylenes

Fumio Sanda
Faculty of Chemistry, Materials and Bioengineering, Department of Chemistry and Materials Engineering, Kansai University, Suita, Osaka, Japan

Synonyms
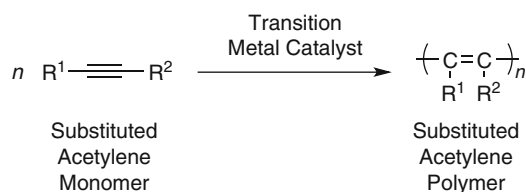
Acetylene polymer; Substituted polyacetylene

Definition

Polyacetylenes are polymers of non-, mono- and disubstituted acetylene monomers.

Introduction

The polymerization of substituted acetylene monomers using transition metal catalysts

Polyacetylenes, Fig. 1 Polymerization of substituted acetylene

provides substituted acetylene polymers (Fig. 1) [1–6]. The group 6 transition metal chlorides such as $MoCl_6$ and WCl_5 catalyze the polymerization of mono- and disubstituted acetylenes. Mo and W catalysts polymerize acetylenes via the metathesis mechanism, wherein the active species are metal carbenes. The stereoregularity (*cis/trans*) of the double bonds in the main chain is not controlled. On the other hand, Rh and Pd complexes polymerize monosubstituted acetylenes via the coordination–insertion mechanism to give *cis*-stereoregular polymers. Development of these transition metal catalysts has enabled us to synthesize a variety of substituted acetylene polymers. The formed polymers possess carbon–carbon alternating double bonds along the main chain with various side groups. Consequently, they exhibit unique and interesting properties based on the particular conjugated structure. This chapter deals with the polymerization of substituted acetylenes and characterization of the formed polymers.

Polymerization of Monosubstituted Acetylenes

Aromatic monosubstituted acetylenes including phenylacetylene and its derivatives efficiently undergo polymerization with transition metal catalysts to give high molecular weight polymers showing air stability, solubility, and processability. These features are advantageous compared with non-substituted polyacetylene. Mo, W, and Rh catalysts in combination with suitable cocatalysts are effective for the polymerization of aromatic monosubstituted acetylenes. Aliphatic monosubstituted acetylenes also undergo polymerization with transition metal catalysts. When Rh-based *cis*-stereoregular polymers are substituted with optically active groups, they possibly form helical structures with predominantly one-handed screw sense. The secondary structures (helix or random, helical sense, degree of twisting, aggregation, etc.) are controllable by external stimuli such as heat, solvent, pH, and photo-irradiation.

Polymerization of Disubstituted Acetylenes

Aromatic disubstituted acetylenes undergo polymerization with metathesis catalysts including Nb, Mo, Ta, and W, while they do not polymerize with non-metathesis Rh catalysts. Poly(diphenylacetylene) is a typical example of aromatic disubstituted acetylene polymers. It is thermally very stable, but the drawback is insolubility in any solvents, resulting in difficult fabrication. Introduction of alkyl groups on the phenyl rings enhances the solubility. As a result, the polymers become processable and applicable to oxygen-enriching membranes and photoelectrically functional materials. Aliphatic disubstituted acetylene monomers such as 2-alkynes undergo polymerization with Mo catalysts to give polymers with molecular weights over one million. Nb, Ta, and W catalysts are less active for these monomers.

Functions of Substituted Acetylene Polymers

Photoelectric Function
Poly(phenylacetylene) and its ring-substituted derivatives exhibit photoelectric functions. For example, a membrane fabricated from a poly(phenylacetylene)/CdS hybrid shows excellent photoconductivity [7]. Poly(phenylacetylene)s bearing TEMPO radicals serve as positive electrode materials for organic radical batteries [8]. Aromatic disubstituted acetylene polymers commonly show more excellent photoelectric properties than aromatic monosubstituted

acetylene polymers because of the more largely spread π-conjugation. Poly(diphenylacetylene)s show strong blue–green emission. An LED composed of ITO/PEDOT/diphenylacetylene copolymer/Ca/Al showed very high device performance [9].

Gas Permeability

Disubstituted acetylene polymers show extremely high gas permeability. Poly (1-trimethylsilyl-1-propyne) (PTMSP) is the most gas-permeable polymer ever reported (Fig. 2) [10]. The oxygen permeability coefficient
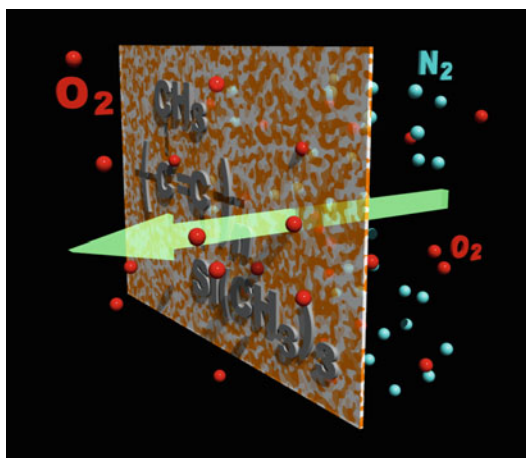
Polyacetylenes, Fig. 2 Image of oxygen-enrichment membrane of PTMSP

(P_{O_2}) of PTMSP ranges from 4,000 to 9,000 barriers, ca. ten times larger than that of poly (dimethylsiloxane), a commercially available oxygen-permeable material. Substituted acetylene polymers with large P_{O_2} values contain spherical substituents such as t-Bu and Me_3Si groups. In contrast, a majority of less permeable substituted acetylene polymers possess long n-alkyl groups. Poly(diphenylacetylene) is solvent insoluble as mentioned above, while its derivatives with bulky ring substituents are soluble in common organic solvents such as toluene, and therefore they can be fabricated into membranes by solution casting. A poly (diphenylacetylene) membrane can be prepared by the desilylation of a poly[1-phenyl-2-p-(trimethylsilyl)phenylacetylene] membrane catalyzed by trifluoroacetic acid [11]. The prepared polymer membrane shows excellent thermal stability, solvent resistance, and gas permeability.

Chiroptical Property

Rh-based polymers of N-propargylamides bearing optically active side chains adopt helical conformations with predominantly one-handed screw sense stabilized by the steric repulsion between the side chains and intramolecular C=O•••H–N hydrogen bonding (Fig. 3) [12]. The addition of polar solvent such as methanol leads to collapse of the helical structure, because the formation of intramolecular hydrogen bonding is disturbed by

Polyacetylenes, Fig. 3 Possible helical conformations of poly(N-propargylamide). *Top*: tightly twisted helix forming $i + 3 \rightarrow i$ C=O•••H–N intramolecular hydrogen bonding. *Bottom*: loosely twisted helix forming $i + 2 \rightarrow i$ C=O•••H–N intramolecular hydrogen bonding
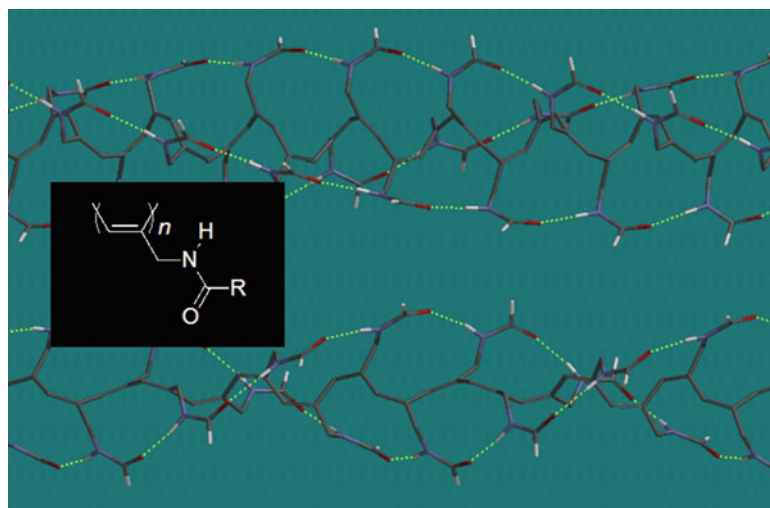
methanol. Polymer gels consisting of helically twisted poly(*N*-propargylamide)s recognize chirality more prominently than the analogous non-helical polymer gels.

Propargyl alcohol is the most simple acetylene monomer that has a hydroxy group; it undergoes polymerization with Ni, Rh, and Pd catalysts. 1-Methylpropargyl alcohol is a chiral derivative of propargyl alcohol and has various applications in the field of organic chemistry. The polymerization of 1-methylpropargyl alcohol and its ester derivatives using Rh catalysts give the corresponding polymers that form helices [13]. It is likely that the remarkable ability of such a small chiral moiety to induce helicity is due to the location of the chiral group adjacent to the main chain. In other words, the presence of a stereogenic center in close proximity to the main chain is effective to induce a helix stabilized by steric repulsion between the side chains. The helicity can be tunable by temperature, solvent, pH, and photo-irradiation. Since the color of helically twisted polymers of substituted acetylenes is changed according to the degree of twisting, i.e., conjugation length, they are expected to be useful as sensing materials [14].

Summary

In this chapter, the catalysts for the polymerization of substituted acetylene monomers and the basic properties of the formed polymers have been reviewed. The conjugation in substituted acetylene polymers plays an important role in their photoelectric properties. It is noteworthy that the properties of the polymers largely vary depending on the side chains. Further study on catalysts and molecular design of substituted acetylene polymers may lead to progress in precisely controlled polymerization using transition metal catalysts and development of functional materials showing useful photoelectric, gas-permeable, and sensing properties.

Related Entries

▶ Polymerization of Substituted Acetylenes

References

1. Aoki T, Kaneko T, Teraguchi M (2006) Synthesis of functional π-conjugated polymers from aromatic acetylenes. Polymer 47:4867–4892
2. Masuda T (2007) Substituted polyacetylenes. J Polym Sci Part A Polym Chem 45:165–180
3. Yashima E, Maeda K, Iida H, Furusho Y, Nagai K (2009) Helical polymers: synthesis, structures, and functions. Chem Rev 109:6102–6211
4. Akagi K (2009) Helical polyacetylene: asymmetric polymerization in a chiral liquid-crystal field. Chem Rev 109:5354–5401
5. Liu J, Lam JWY, Tang BZ (2009) Acetylenic polymers: syntheses, structures, and functions. Chem Rev 109:5799–5867
6. Shiotsuki M, Sanda F, Masuda T (2011) Polymerization of substituted acetylenes and features of the formed polymers. Polym Chem 2:1044–1058
7. Xu HP, Xie BY, Yuan WZ, Sun JZ, Yang F, Dong YQ, Qin A, Zhang S, Wang M, Tang BZ (2007) Hybridization of thiol-functionalized poly(phenylacetylene) with cadmium sulfide nanorods: improved miscibility and enhanced photoconductivity. Chem Commun 1322–1324
8. Qu J, Katsumata T, Satoh M, Wada J, Igarashi J, Mizoguchi K, Masuda T (2007) Synthesis and charge/discharge properties of polyacetylenes carrying 2,2,6,6-tetramethyl-1-piperidinoxy radicals. Chem Eur J 13:7965–7973
9. Yang SH, Huang CH, Chen CH, Hsu CS (2009) Synthesis and electroluminescent properties of disubstituted polyacetylene derivatives containing multi-fluorophenyl and cyclohexylphenyl side groups. Macromol Chem Phys 210:37–47
10. Masuda T, Isobe E, Higashimura T, Takada K (1983) Poly[1-(trimethylsilyl)-1-propyne]: a new high polymer synthesized with transition-metal catalysts and characterized by extremely high gas permeability. J Am Chem Soc 105:7473–7474
11. Teraguchi M, Masuda T (2002) Poly(diphenylacetylene) membranes with high gas permeability and remarkable chiral memory. Macromolecules 35:1149–1151
12. Nomura R, Tabei J, Masuda T (2001) Biomimetic stabilization of helical structure in a synthetic polymer by means of intramolecular hydrogen bonds. J Am Chem Soc 123:8430–8431
13. Suzuki Y, Shiotsuki M, Sanda F, Masuda T (2007) Chiral 1-methylpropargyl alcohol: a simple and powerful helical source for substituted polyacetylenes. Macromolecules 40:1864–1867
14. Suzuki Y, Shiotsuki M, Sanda F, Masuda T (2008) Synthesis and helical structure of poly(1-methylpropargyl ester)s with various side chains. Chem Asian J 3:2075–2081

Polyacrylonitrile (PAN)

Kazuki Sada, Kenta Kokado and Yuki Furukawa
Department of Chemistry, Faculty of Science,
and Graduate School of Chemical Sciences and
Engineering, Hokkaido University, Sapporo,
Japan

Synonyms

PAN; Poly(1-acrylonitrile); Polyacrylonitrile

Definition

Polyacrylonitrile (PAN) is a derivative of poly-ethylene that has a nitrile (CN) group in the unit structure, named as poly(1-acrylonitrile) according to IUPAC nomenclature.

Basics

Polyacrylonitrile (PAN) is a semicrystalline organic polymer with the formula $(C_3H_3N)_n$ and has a nitrile (CN) functional group attached on polyethylene backbone as the unit structure, as shown in Fig. 1. The nitrile group acts as a hydro-gen bonding acceptor due to a lone pair on nitro-gen atom and has a large dipole moment between electron-deficient carbon atom and electron-rich nitrogen atom, which enables us to use them for relatively strong attractive interactions. Indeed, the strong intermolecular interaction induces the high strength and high resistance for various organic solvents.

PAN is predominantly white powder up to 250 °C and shows thermoplastic, but it does not melt under normal conditions; instead it becomes darker due to degradation before melting above

this temperature. Having a relatively high glass transition temperature, around 100 °C [1, 2], PAN has low thermal plasticity and cannot be used as a plastic material due to the high melting point (317 °C [1]) of crystallized PAN. Its limited solubility in common organic solvents coupled with superior mechanical properties of its fibers is due to intermolecular forces between the polymer chains. PAN is not stable under drying process and becomes brittle during the drying process. For chemical stability against chemical reagents, the nitrile group has relatively low reactivity, and thermal oxidation induces degradation of PAN to carbon fibers.

Synthesis

PAN is synthesized from acrylonitrile (AN), i.e., 2-propenenitrile in IUPAC nomenclature. The vinyl group of AN is stabilized by resonance with the nitrile group, and it behaves as an electron-deficient monomer due to strong electron-withdrawing ability of the nitrile group. As the evaluation of reactivity of AN for poly-merization, the Alfrey-Price Q and e values of AN were determined as 0.48 and 1.23 [1], respec-tively, and thus synthesis of PAN via cationic polymerization is difficult.

Commercially, PAN is synthesized via free radical polymerization without control over molecular structure. Simple copolymerizations with various vinyl compounds and covalently linked composite materials with other polymers and nanomaterials have been prepared in the sim-ilar radical polymerization. For an example, the mixture of starch and ceric ion (redox initiator) can initiate polymerization of AN, i.e., starch grafting, and following hydrolysis of cyano group produces a superabsorbent hydrogel with water absorption larger than 400 times its weight [3].

For challenge toward precise polymerization of AN for controlled polymer structure, tacticity of PAN can be controlled by applying restriction of movement of AN in urea canal complex initi-ated by γ-ray irradiation [4]. Controlled radical polymerization of acrylonitrile with narrow

Polyacrylonitrile (PAN),
Fig. 1 Molecular structure of PAN
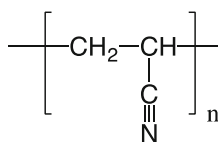
distribution can be accomplished by using atom-transfer radical polymerization (ATRP) catalyzed by copper complex [5]. Dithioesters [6], alkoxyamines [7], and nitroxides [8] are also usable for controlled radical polymerization of AN.

PAN can also be prepared by anionic polymerization, which shows better control than free radical polymerization. AN is determined as C group monomer in Tsuruta's classification, indicating sodium alkoxide, alkyl zinc, and alkyl aluminum can initiate its polymerization. However, the living character of anionic polymerization is lost because of side reactions such as attack on α-protons activated by the cyano groups or direct attack of the propagating anion on the cyano groups, causing lower molecular weight compared to radical polymerization [9]. The side reactions cause branched structures or deactivation of active sites. Coordination polymerization is also applicable to the synthesis of PAN by employing alkyl iron, alkyl copper, or rare earth complex. Current researches have disclosed that, in some coordination polymerization system of AN, the polymerization proceeds according to anionic polymerization mechanism [10].

Utility of PAN

With respect to utilization of PAN as materials, PAN has the following unique and well-known characteristics: low density, thermal stability, high strength, and modulus of elasticity, resistance and chemical stability against most chemicals and solvents, sunlight, heat, and microorganisms, slow burning and charring, reactivity toward nitrile reagents for modification of PAN, compatibility with certain aprotic polar solvents such as DMF and DMSO, ability to orient, and low permeability toward various gaseous materials. These properties have established PAN as essential polymer materials in chemical industry, and PAN plays a key role in high-tech industry these days. For an example, because of transparent, higher barrier ability for gas and low swellability for chemicals, PAN is used for wrapping materials for foods such as tea, coffee, rice, fish, and eggs, and chemicals, drugs, electronics, and cosmetics. Due to the chemical stability and hydrophilicity of PAN, PAN is used as nonwoven meshes for ultrafiltration, inner support of hollow fibers for reverse osmosis membranes, and membrane support, especially in biotechnology and environmental engineering applications. Other applications of PAN are due to high-strength fibers for outdoor awnings like tents, sails for yachts, knitted clothing like socks and sweaters, and fillers for high-strength materials for military and commercial aircrafts.

PAN for Polymer Electrolyte

PAN is used as host polymer electrolytes defined as a membrane that possesses transport ability of electron, hole, or ions for electrochemical systems such as fuel cells, lithium batteries, supercapacitors, and electrochromic devices [11, 12]. The advantages of the polymer electrolytes include no internal shorting, leakage of electrolytes, and noncombustible reaction products at the electrode surface existing in the electrolyte solution. Among the polymer hosts, PAN can provide homogenous and hybrid electrolyte membranes consisting of electrolyte salts such as $LiClO_4$ and $LiN(CF_3SO_2)_2$ and the plasticizer such as ethylene carbonate (EC) and propylene carbonate (PC) [13]. The conductivity of PAN-based polymer electrolytes reaches to the order of 10^{-3} S cm^{-1} at ambient temperature [14]. Encapsulating Li salt solutions of $LiN(CF_3SO_2)_2$, $LiAsF_6$, $LiCF_3SO_3$, and $LiPF_6$ in a plasticizer mixture of EC and PC with PAN also provides PAN-based polymer electrolyte with the similar Li conductivity. Cyclic voltammetry studies revealed that the electrolytes have an inherent oxidation stability window exceeding 5 V versus Li$^+$/Li [15]. The relatively high conductivity is a favorable characteristic of PAN-based polymer electrolytes, although PAN is inactive in the ionic transport mechanism. PAN acts as a matrix for structural stability due to its good compatibility to both the plasticizers and these Li salts.

PAN as a Precursor for Carbon Fiber

One of the most important utilities of PAN as raw materials is a precursor for production of carbon fiber [16–18]. Today, more than 90 % of commercial carbon fibers are prepared from PAN. PAN produces carbon fibers with high performance such as remarkable high tensile properties, low densities (less than 2.0 gcm^{-3}), high thermal stability, chemical resistibility, electrical and thermal conductivities, and creep resistance. It has high tensile strength (2.5–3.8 GPa) and high tensile modulus (227–405 GPa) with small strain (0.8–1.76 %) and attracts considerable interest in diverse fields of material sciences. Methods for preparation of PAN-based carbon fiber include four steps of preparation of fibers and thermal conversion processes under controlled conditions as shown in Fig. 2: (1) fiber formation by electrospinning or other methods in some polar solvents; (2) stabilization by heating in the temperature range of 180 ~ 300 °C under oxidative atmosphere for hours to improve thermal stability, to prevent fiber melting, and to increase carbon yield; (3) carbonization in an inert atmosphere in the temperature range of 350 ~ 1,700 °C to remove most of the non-carbon atoms; and (4) optional graphitization at the temperature higher than 2,000 °C for a formation of graphitic structure and improvement of the ordering and orientation of the crystallites in the direction of the fiber axis. PAN-based carbon fibers generally have been used as both high-tech and common daily manufacturing materials in civil and military aircrafts, automobiles, missiles, solid propellant rocket motors, turbine rotors, and high-grade sporting goods such as pressure vessels for diving, fishing rods, tennis rackets, badminton rackets, carbon shafts for golf clubs, and high-tech bicycles.

Electrospinning of PAN for Nanofiber Production

Fiber-forming processes for PAN play a key role for production of functional materials based on PAN [19]. In early times, because of difficulties in solubilization, no progress was made in converting into a usable fiber until 1925. The discovery of the aprotic polar solvents suitable for spinning of PAN such as *N,N*-dimethylformamide (DMF), dimethyl sulfoxide (DMSO), *N,N*-dimethylacetamide (DMAc), and dimethylsulfone developed for manufacturing of PAN fibers, which soon expanded applicability for electrospinning technique invented in 1934 to produce nanofibers of polymer materials by applying high voltage to a polymer solution until a small jet of polymer solution ejects. The electrospinning parameters such as applied electric field, solution conductivity, jet length, solution viscosity, surrounding gas and its flow rate, and the geometry of the collector assembly control the fiber diameter and its morphology [20]. Compared to other methods for production of PAN nanofibers, such as vapor growth, arc discharge, laser ablation, and chemical vapor deposition, the electrospinning can easily generate nanofibers with diameters from 10 nm to several μm under the application of an electrostatic force. Appreciable electrostatic forces occur between the dipoles of adjacent nitrile groups and this intramolecular interaction restricts the bond rotation, leading to a stiffer chain.

Composite Materials of PAN and PAN-Based Carbon Fibers

Significant progress has been accomplished preparation of composite nanofibers of PAN and PAN-based carbon fiber for exploring new functional materials [16, 17, 19, 20, 22]. Mostly, the first step involves electrospinning of PAN in the presence of the target components or precursors to be included in the composite nanofibers in solution or in bulk solid. Then, the composite fibers of PAN are converted to carbon nanofiber composites by standard thermal conversion processes. For example, the composites of metal nanoparticles in the carbon nanofibers are prepared in the presence of noble metal salts or metal complexes such as iron(III)

P

Fig. 2 Schematic drawing
of the formation of
carbonized structure
from PAN
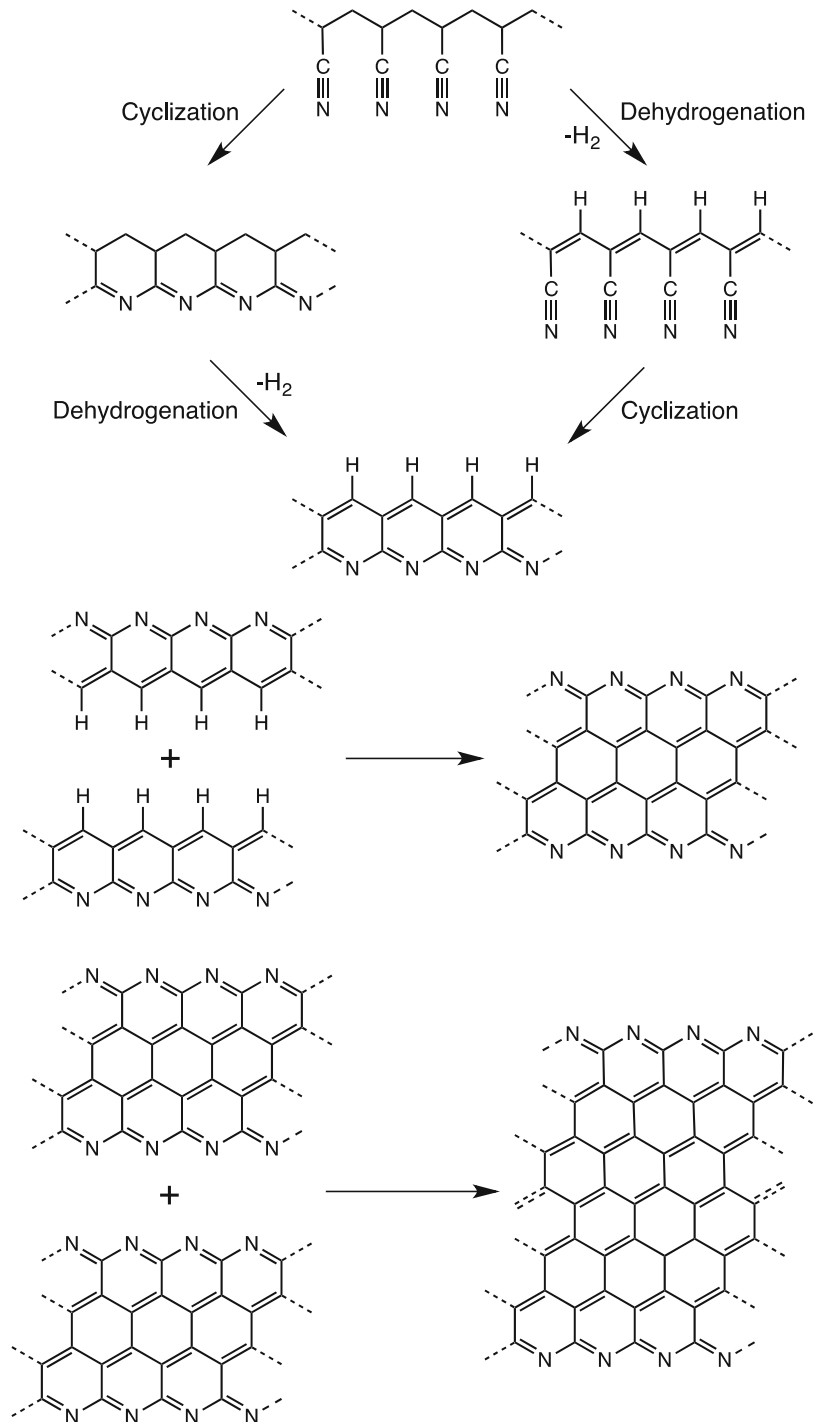
acetylacetonate [21] and Ag(NO)$_3$ [23] for surface-enhanced Raman scattering (SERS) active material as additives during electrospinning. Metal oxides such as TiO$_2$, MnO$_2$, and ZnO [24] are used for the composites with semiconductors for potential applications as sensors, catalyst supports in fuel cells, and energy storage devices. Metal salts such as LiCl, NaNO$_3$,

NaCl, and $CaCl_2$ are used as electrolytes or templates for their large interfacial area with porous structure after removal of them by thermal treatment [25]. Incorporation of carbon nanotubes (CNTs) such as single-walled carbon nanotubes (SWNT) and multi-walled carbon nanotubes (MWCNT) is described as an ultrahigh-strength material, superior to both ordinary carbon fibers and other high-strength materials [26–28]. The molecular orientation and microstructure of PAN composites are strongly affected by incorporation of CNTs as fillers. The other important aspects of the nanocarbon composites are improvement of thermal conductivity, electrical property, and thermal and dimensional stabilities, due to the highly anisotropic orientation and formation of complexes of CNTs. These composites are promising due to these enhanced property compared to the nascent PAN. They provide a new class of functional materials in a wide range of applications such as filtration, structural materials, garments, insulators, medical, and energy storage devices. The accelerating technologies will soon overcome the drawback of small production in laboratory scale to large industrial scale production, which will decrease the cost of the production of these materials.

Related Entries

▶ Application of CL/P Nanocomposites
▶ Nanofibers and Electrospinning

References

1. Beevers B (1964) Dependence of the glass transition temperature of polyacrylonitrile on molecular weight. J Polym Sci A 2:5257
2. Brandrup J, Immergut ET (1989) Polymer handbook, vol 57, 3rd edn. Wiley-Interscience, New York
3. Reyes Z, Rist CE, Russell CR (1966) Grafting vinyl monomers to starch by ceric ion. I. Acrylonitrile and acrylamide. J Polym Sci A-1 4:1031
4. Matsuzaki K, Uryu T, Okada M, Shiroki H (1968) The stereoregularity of polyacrylonitrile and its dependence on polymerization temperature. J Polym Sci A-1 6:1475
5. Matyjaszewski K, Jo SM, Paik H-J, Gaynor SG (1997) Synthesis of well-defined polyacrylonitrile by atom transfer radical polymerization. Macromolecules 30:6398
6. Tang C, Kowalewski T, Matyjaszewski K (2003) RAFT polymerization of acrylonitrile and preparation of block copolymers using 2-cyanoethyl dithiobenzoate as the transfer agent. Macromolecules 36:8587
7. Benoit D, Chaplinski V, Braslau R, Hawker CJ (1999) Development of a universal alkoxyamine for "Living" free radical polymerizations. J Am Chem Soc 121:3904
8. Li D, Brittain WJ (1998) Synthesis of poly(N, N-dimethylacrylamide) via nitroxide-mediated radical polymerization. Macromolecules 31:3852
9. Ono H, Hisatani K, Kamide K (1993) NMR spectroscopic study of side reactions in anionic polymerization of acrylonitrile. Polym J 25:245
10. Schaper F, Foley SR, Jordan RF (2004) Acrylonitrile polymerization by Cy_3PCuMe and $(Bipy)_2FeEt_2$. J Am Chem Soc 126:2114
11. Stephan AM (2006) Review on gel polymer electrolytes for lithium batteries. Eur Polym J 42:21
12. Song JY, Wang YY, Wan CC (1999) Review on gel-type polymer electrolytes for lithium batteries. J Power Sources 77:183
13. Watanabe M, Kanba M, Nagaoka K, Shinohara I (1983) Ionic conductivity of hybrid films composed of polyacrylonitrile, ethylene carbonate and $LiClO_4$. J Polym Sci Polym Phys Ed 21:939
14. Abraham KM, Alamgir M (1990) Li^+-conductive solid polymer electrolyte with liquid-like conductivity. J Electrochem Soc 137:1657
15. Appetecchi GB, Croce F, Ramagnoli P, Scrosati B, Heider U, Osten R (1999) High performance of gel-type lithium electrolyte membranes. Electrochem Commun 1:83
16. Huang X (2009) Fabrication and properties of carbon fibers. Materials 2:2369
17. Liu Y, Kumar S (2012) Recent progress in fabrication, structure, and properties of carbon fibers. Polym Rev 52:234
18. Rahaman MSA, Ismail AF, Mustafa A (2007) A review of heat treatment on polyacrylonitrile fiber. Polym Degrad Stab 92:1421
19. Nataraj SK, Yang KS, Aminabhavi TM (2014) Polyacrylonitrile-based nanofibers A state-of-the-art review. Prog Polym Sci 39:1473
20. Wang T, Kumar S (2006) Electrospinning of polyacrylonitrile nanofibers. J Appl Polym Sci 102:1023
21. Park SH, Jo SM, Kim DY, Lee WS, Kim BC (2005) Effects of iron catalyst on the formation of crystalline domain during carbonization of electrospun acrylic nanofiber. Synth Met 150:265
22. Zhang L, Aboagye A, Kelkar A, Lai C, Fong H (2014) A review: carbon nanofibers from electrospun polyacrylonitrile and their applications. J Mater Sci 49:463
23. Wang Y, Yang Q, Shan G, Wang C, Du J, Wang S, Li Y, Chen X, Jing X, Wei Y (2005) Preparation of

P

silver nanoparticles dispersed in polyacrylonitrile nanofiber film spun by electrospinning. Mater Lett 59:3046

24. Drew C, Liu X, Ziegler D, Wang X, Bruno FF, Whitten J, Samuelson LA, Kumar J (2003) Metal oxide-coated polymer nanofibers. Nano Lett 3:143

25. Qin XH, Yang EL, Li N, Wang SY (2007) Effect of different salts on electrospinning of polyacrylonitrile (PAN) polymer solution. J Appl Polym Sci 103:3865

26. Song K, Zhang Y, Meng J, Green EC, Tajaddod N, Li H, Minus ML (2013) Structural polymer-based carbon nanotube composite fibers: understanding the processing–structure–performance relationship. Materials 6:2543

27. Chae HG, Minus ML, Rasheed A, Kumar S (2007) Stabilization and carbonization of gel spun polyacrylonitrile/single wall carbon nanotube composite fibers. Polymer 48:3781

28. Sreekumar TV, Liu T, Min BG, Guo H, Kumar S, Hauge RH, Smalley RE (2004) Polyacrylonitrile single-walled carbon nanotube composite fibers. Adv Mater 16:58

Polyamide Syntheses

Mohammad Asif Ali and Tatsuo Kaneko
School of Materials Science, Japan Advanced Institute of Science and Technology (JAIST), Nomi, Ishikawa, Japan

Synonyms

Nylon; Polyamide; Polycondensation; Salt monomer

Definition

A polyamide is a polymer whose backbone contains the amide linkage {−CONH- or −CONR- (R, substitute group)} and that generally exhibits high thermomechanical performances such as high softening temperature, high thermal degradation temperature, high mechanical modulus, high strength, and low creep, which allow widespread uses as engineering thermoplastics, films, and fibers. Nylon-6,6^{TM}, comprised of a hexamethylene group and amide linkages, is one of the most commercialized polyamides. Numerals 6,6 are the carbon numbers of the diamine and dicarboxylate used as alkylene monomers, respectively. Aromatic polyamides are also available; for example, Kevlar^{TM} poly(p-phenyleneterephthalamide) is applied as a fiber with ultrahigh strength for bullet-proof jackets. A polypeptide is a kind of polyamide derived from an amino acid monomer. Cyclic amide such as pyrrolidone ring may also comprise the polyamide backbone.

Introduction

Nylon^{TM} is a basic term that represents an important class of polyamides. Nylon^{TM} is an important semicrystalline thermoplastic known as aliphatic polyamides [1]. The ability to form strong hydrogen bonds between NH and CO groups is a major driving force for the crystallization of Nylon^{TM} [1, 2]. Nylon^{TM} generally exhibits relatively high mechanical properties, such as Young's modulus, toughness, strength, low creep, and good thermal resistances, which allow widespread use [2, 3]. The basic types of Nylon-X,Y refer to the number of carbon atoms in the monomers; the most commercialized Nylon^{TM} is Nylon-6,6 and Nylon-6 [1, 2].

The pioneering work of Carothers and his colleagues at DuPont led to the discovery of Nylon-6,6 in 1930 [1, 2]. In 1935, DuPont patented Nylon^{TM} fibers with outstanding properties [4], which are a kind of synthetic protein [4]. In 1939, Nylon^{TM} was first displayed during the world exhibition in New York, NY, which provided the initial two letters of Nylon^{TM} [4]. During World War II, Nylon^{TM} was used for military materials in airspace tire, lightweight parachutes, and waterproof tents since the synthetic polyamides easily replaced silk, which was very difficult to mass-produce [4]. At the end of the nineteenth century, it was more commercialized, and after the war the demand of Nylon^{TM} abruptly increased [1, 2]. After Carother's patent, a new polyamide from caprolactam was simultaneously being developed [3, 4] by Schlack in Germany; this was later commercialized in 1938 as Perlom^{TM}. The thermoplasticity of polyamides, including their good rheological behavior in the molten

state and the excellent deformability of processed fibers, has ensured their continuous development in Europe, the USA, and Japan [2, 5].

There are two pillars for the synthesis of polyamides by step polymerizations: (1) thermal polycondensation and (2) lactam polymerization were latter joined third: low-temperature interfacial and solution polymerizations to produce aliphatic polyamides as established by Morgen et al. in 1957 [6]. DuPont researchers later overcame the problems inherent to melt polycondensations [6] by using interfacial or solution polymerization for the preparation of Nomex[TM] and Kevlar[TM] [1, 2]. Yamazaki et al. [7] later developed a direct polymerization method in solution by utilizing a condensing agent, which is a highly promising technique for polyamide synthesis [8]. Many polycondensation synthetic routes have continued to be developed that have improved the quality of polyamides [5, 8].

Polymers with nitrogen heteroatoms in the main chains have different properties than hydrocarbon polymers and those with oxygen heteroatoms [9]. Among them, polyamides are special because their amide linkage induces a strong hydrogen bonding [9]. However, incorporation of the nitrogen atom increases the cost relative to polyesters [2]. Nylon-6,6 and Nylon 6 have overcome the cost-performance problems and have excellent applications [3]. In addition to these conventional Nylons, new polyamides with a variety of molecular designs have been developed, including the conceptually new bio-derived polyamides: Nylon-11, Nylon-12, Nylon-6,6, Nylon-6,10, etc. [6]. The demand for more environmentally friendly plastics has prompted the development of sustainable polymers, thereby possibly contributing to a low-carbon footprint and to the solution of the plastic waste problem by adding recyclability functions. Much work on postindustrial environmental degradability, reuse, and recycling [2, 3] has made it possible to recycle Nylon-6. Recently, itaconic acid has been introduced as a bio-derived monomer for the preparation of polyamides with environmental degradability and recyclability [10].

This entry describes the synthesis and properties of conventional polyamides and newly developed polyamides derived from itaconic acid via a salt monomer method [10].

Polymerization Methods

Polymerization methods are classified below by the reaction conditions:

1. Bulk polycondensation
   Direct polymerization of diamine with dicarboxylic acid
   Salt monomer method
   Solid-state polymerization
2. Solution polymerization
   Homogeneous system
   Interfacial system
      and by the monomer structures:
3. Polycondensation of dicarboxylic acid or diamine derivatives
   Polycondensation of N-silylated diamine and diacid chloride
   Polycondensation of diisocyanates and dicarboxylic acids

Bulk Polycondensation

Bulk polymerization is a melt polymerization of a mixture of diamine and diacid monomers or a 1:1 salt of these monomers.

Direct polycondensation of diamine and dicarboxylic acid: Commercial aliphatic polyamides are generally produced by a simple direct polycondensation of a diacid and a diamine. Direct polycondensation of an equimolar amount of the two monomers can produce a high molecular weight polymer. A good example (Fig. 1) is Nylon-6,6 produced by the polycondensation of adipic acid and hexamethylenediamine [2, 11].

Condensed water should be removed using a vacuum, and impurities and catalyst are removed by purification. The resulting polyamide has high thermomechanical properties [3]. Acid catalysts such as sulfuric acid or sulfonic acid are sometimes required to promote the polycondensation, such as in the synthesis of high molecular weight aromatic polyamides [1, 3]. However, the

P

Polyamide Syntheses,
Fig. 1 Synthesis of
polyamide from
hexamethylenediamine and
adipic acid
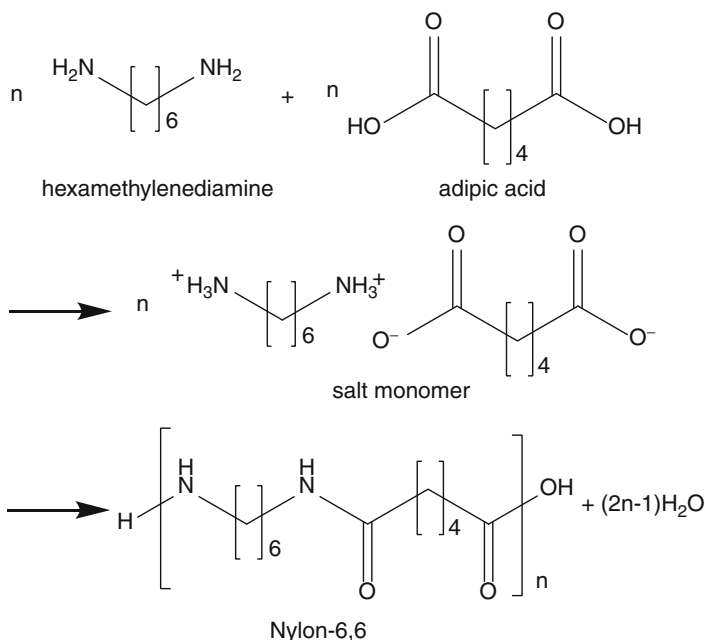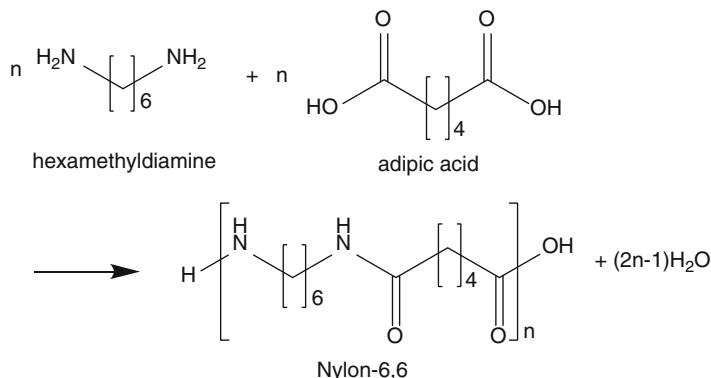
Polyamide Syntheses,
Fig. 2 Synthesis of Nylon-
6,6 derived from a salt of
hexamethylenediamine and
adipic acid

polymerization of these simple mixtures is not always efficient due to oxidation, vaporization, or side reactions, which change the 1:1 stoichiometric ratio of diamine and diacid required to produce a high molecular weight polyamide. The direct polymerization can also be performed in solution.

Melt polymerization of salt monomers: The use of nylon salts overcomes the stoichiometry problems of the direct methods for preparing polyamides. The salt state of the monomers precludes their vaporization at the high temperature of the polycondensation in order to maintain their 1:1 stoichiometry [2, 10]. The salt is formed as a white powder immediately after mixing equimolar amounts of the diacid and diamine in an alcoholic solution [2, 3, 9]. After filtration of the white powder, salt monomer is obtained in very high yields of >90 wt%. If the salt monomer is dried, it can be used directly for polymerization in a sealed reaction tube at a temperature slightly higher than the salt's melting point. In the melt state of the salt, water is produced as steam [2, 10]. This water should be removed under vacuum to reach high degrees of polymerization (Fig. 2) [1, 12]. Salt-state polymerization is generally a kind of melt polymerization, but solid-state polymerization is also possible when the
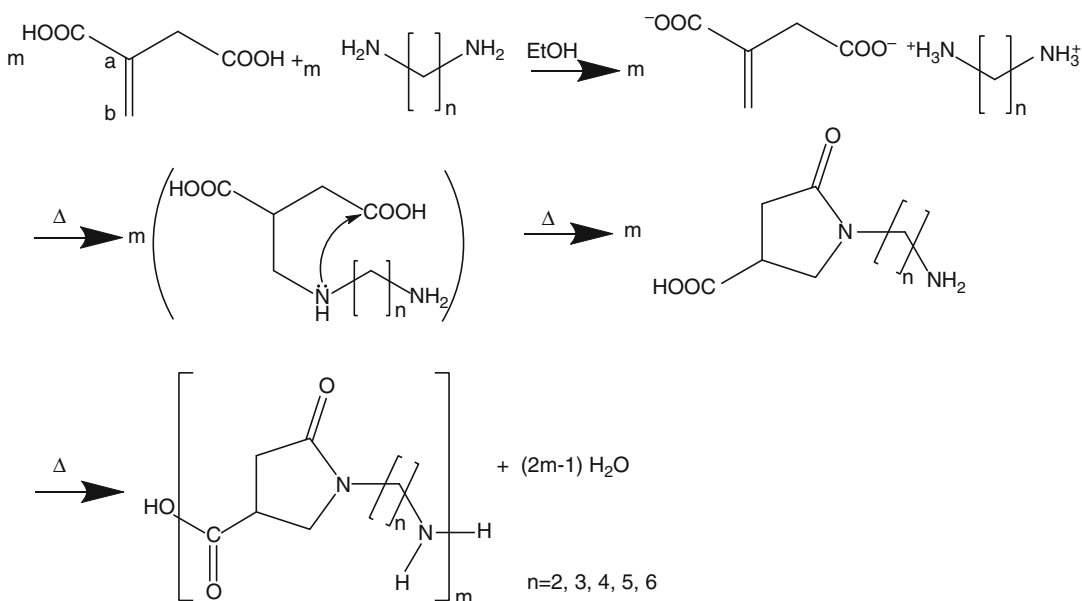
Polyamide Syntheses, Fig. 3 Synthesis of bio-based aromatic polyamides containing pyrrolidone ring derived from itaconic acid salts with aliphatic diamines

melting points of the produced polymers are higher than the reaction temperature. Salts of hexamethylenediamine and sebacic acid or adipic acid can be melt-polymerized to form Nylon-6,10 and Nylon-6,6, respectively [5, 12].

Itaconic acid-based polyamide must be synthesized from organic salts of itaconic acid with diamine (Fig. 3) because the direct polymerization involves the side reaction of a Michael-like addition of the amine to the double bond and nearest carbonyl to form imine in addition to the regular amidation, resulting in three-way branching. The side reaction changes the 1:1 monomer stoichiometry and thereby prohibits the formation of high molecular weight polyamides, even when the amount of the side reaction ratio is very small. Itaconic acid-based copolymers produced by the organic salt of itaconic acid with aliphatic diamines have a cyclic amide ring, pyrrolidone, in the polyamide backbone [10, 13]. The pyrrolidone ring forms by the reaction of the abovementioned imine with the aliphatic carboxylic acid as shown in Fig. 3. The pyrrolidone ring is opened by UV-light irradiation and by composting in a landfill for extensive periods of time, thereby reducing the molecular weight of the polymer. The T_g ranges

between 80 °C and 97 °C, which is higher than those of Nylon-6 and Nylon-6,6. The higher T_g is attributed to the rigid pyrrolidone ring in the polymer backbone, in addition to the hydrogen-bonding amide groups [10, 13].

Solid-state polymerization: Solid-state polycondensation is generally used to increase the molecular weight of solid prepolymers (or monomers) derived from diamine-diacid mixture or salt monomer. Solid-state polymerization is a thermal polycondensation process, with or without an added catalyst, at an appropriate pressure and temperature [12]. The prepolymer powder is in a gel-like solid to melt state quasi-solid or equally "quasi-melt stage" (QSMS) [12, 14]. Reaction temperatures have to adjust 10–15 °C below the melting point but over the glass transition temperature of the prepolymers [12]. The solid-state polymerization proceeds through the end-group mobility, which is high enough to react [14]. The solid-state reaction can actually start at much lower temperatures than molten-state temperature. However, the reaction time needed to reach a particular molecular weight is much longer than those prepared in melt or solution [11, 12].

The solid-phase polycondensation of salt monomer in vacuum produced a slightly higher molecular weight polymer compared to polymerization under an inert gas or nitrogen gas [11, 12]. The removal of the water by-product determines the molecular weight of the polymer. Many industries prefer the solid-state polymerization because bulk polymerization is very useful for isolation and purification and produces high molecular weight polyamides [2, 12, 15]. By-products are removed by heating the dry starting materials or prepolymer in an oxygen-free atmosphere (i.e., under flowing gas or high pressure or in vacuo) [1–3]. The condensed process is carried out in three ways: (1) under vacuum, (2) in side steam of inert atmosphere, and (3) in a fluidized bed. Adding a drying agent to the prepolymers can improve their processability and operational properties by acting as a plasticizer [12]. A variety of polyamides have been synthesized through solid-state polymerization, including Nylon-6, Nylon-6,6, Nylon-4,6, Nylon-4,T (terephthalic acid), and Nylon-4,I (isophthalic acid) [12, 16]. The overall rate of SSP depends on the following three chemical or physical steps: (1) reaction kinetics of the chain extension reaction through collision of functional end groups, (2) internal diffusion of the reaction by-products within the polymer particle, and (3) external transport of the by-products from the polymer particle to the sweep-gas phase [12, 17].

Solution Polycondensation

Homogeneous system. Solution polycondensation is applied when melt polycondensation is difficult or impossible. In the solution polycondensation, the monomers must dissolve in a solvent in the presence or absence of a condensing agent. The solvent should be unreactive toward the condensing agent, catalyst, and reaction mixture. After the polymerization, solvent, oligomers, and/or catalyst must be removed by (re)precipitation from a poor solvent for the polymer and by washing and drying of the polymers [3, 4].

Solution polymerizations have some limitations: (1) the temperature is limited by the solvent boiling point, (2) it may be difficult to remove a high boiling point solvent from polymers, and (3) the solvents must be totally anhydrous [1]. As an example, 1,3-phenylenediamine is reacted with 1,3-phthaloyl chloride in chloroform in the presence of triethylamine.

Interfacial system. An interfacial polymerization was developed by Morgen et al. [7]. In interfacial polycondensation, the reaction occurs at the interface between an aqueous solution of the diamine monomer and a water-immiscible organic solvent containing the diacid chloride in a nonequilibrium reaction [7]. The interfacial polymerization produces a high molecular weight polyamide in high yield in a short period of time under ambient conditions of temperature and pressure [1, 2]. In interfacial polymerization the reaction between the acid chloride with diamine forms HCl as byproduct, it is difficult to remove HCl condensed as a result of reaction, which affects the polymerization in a long time polymerization to require inorganic bases in the aqueous phase to neutralize the by-product HCl.

In the interfacial polymerization, large volume reactions are possible to produce high molecular weight polymers with high glass transition temperatures and high mechanical properties. Nylon-6,6 and Nylon-6,10 are readily prepared by interfacial polymerization (Fig. 4) [1, 2]. A few polyamides like Nylon-2,10, Nylon-4,10, and their copolymers are also prepared from the interfacial method [1]. Some of the aromatic polyamides are also synthesized by the interfacial polycondensation of the corresponding diamines and acid chloride.

Other systems: Some aliphatic and aromatic polyamides are not readily prepared at a low temperature due to the low reactivity of the monomers or at a high temperature because of side reactions [1, 10]. This reduces the molecular weight and therefore the performance of the polymer [4]. However, addition of a condensation agent may enhance the rate of reaction as well as the performance of the resulting materials. Polar solvents such as DMF, NMP, and DMAc in which the monomer and resulting polyamide are partially or wholly soluble are also commonly used [1, 2, 12]. For instance, phosphate derivatives with some organic bases can accelerate the
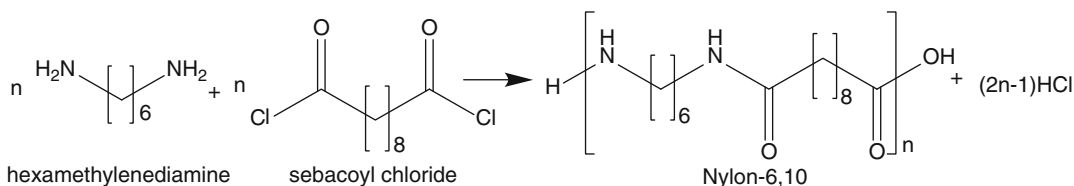
Polyamide Syntheses, Fig. 4 Synthesis of Nylon-6,10 from hexamethylenediamine and sebacoyl chloride through interfacial polymerization

Polyamide Syntheses, Fig. 5 Intermediates activating the polyamide synthesis through the reaction of acid with a salt of triphenyl phosphite/ pyridine
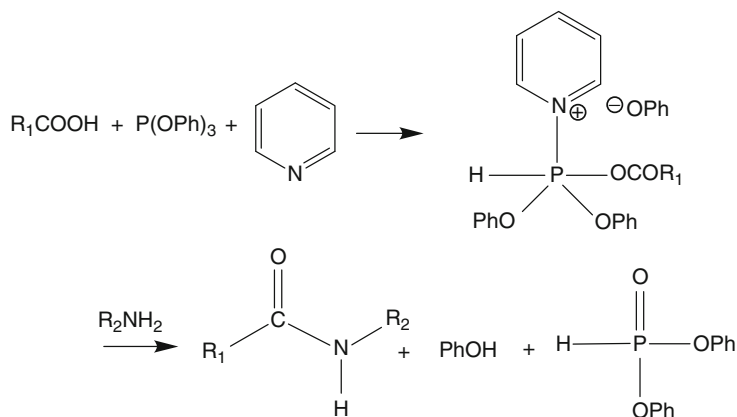
Polyamide Syntheses, Fig. 6 Synthesis of polyamide *N*-trimethylsilyl-substituted amines with acid chloride
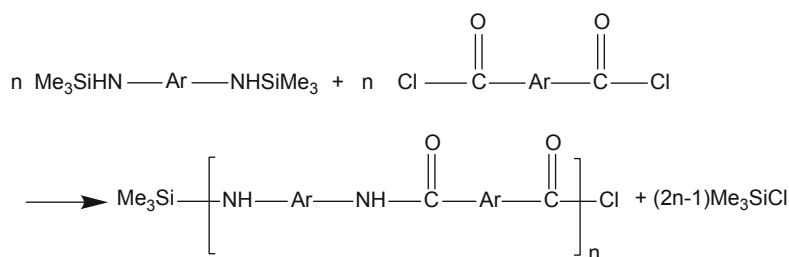
rate of reaction and increase the molecular weight of the resulting polymer. The diacid monomer forms an ester with triphenyl phosphite/pyridine in NMP solvent to produce activated acid esters, and then the esters react with diamines to form the polyamide (Fig. 5).

Polycondensation of Acid or Amine Derivatives

Polycondensation of *N*-silylated diamine and diacid chloride. Aromatic diamines have low reactivity due to their lower basicity and therefore require high temperature to condense with diacid chlorides. Silylation of the diamine increases its reactivity and improves its solubility; *N*-trimethylsilyl-substituted amines react with acid chloride to produce a high molecular weight polymer with elimination of trimethylsilyl chloride (Fig. 6) [16]. The high molecular weight aromatic polyamide can be prepared at a low temperature in solution by polycondensation of *N,N*-bis(trimethylsilyl)-substituted aromatic diamines and aromatic diacid chlorides in NMP solvent [1, 2, 16]. Additional advantages of the *N*-silylated diamine route are easy separation and product purification due to high solubility in NMP, as well as reduced boiling point and less oxidation. The other benefit is that the

Polyamide Syntheses,
Fig. 7 Mechanism of
amide formation via
N-carboxyanhydride from
isocyanate reaction with
carboxylate. Cyclic
N-carboxyanhydride is
formed in α-amino acid
where R = R′
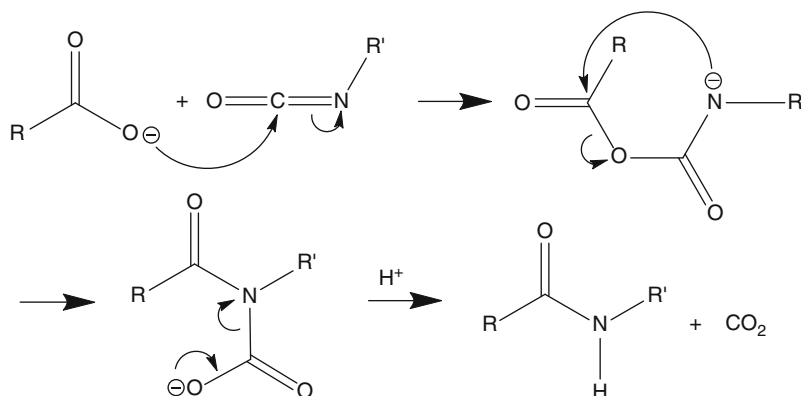
trimethylsilyl chloride by-product can be recycled and reused.

Polycondensation of diisocyanates and dicarboxylic acids: Diisocyanates react with carboxylic acids to form an amide group (Fig. 7). Isophthalic acid reacts with 1,3-phenylene diisocyanate to produce aromatic polyamides. Other acid and amine derivatives such as dinitriles can be used in place of dicarboxylic acids and esters to prepare polyamides in the presence of water [2, 3].

Properties

The most distinguishing structural characteristic of polyamides is the ability of the amide groups to form hydrogen bonds between adjacent polymer chains [1–3]. Polyamides are therefore strong, tough, and stable at elevated temperature, have low friction, and are processable with good appearance [3]. The melting point is dominated by the ratio of CONH groups to CH_2 groups, which also affects the glass transition temperature [4, 5]. Although the ratio of -CH_2/-CONH- in Nylon-6 and Nylon-6,6 are identical, Nylon-6,6 forms more H-bonds than Nylon-6 in either parallel or antiparallel arrays and therefore crystallizes more efficiently and has a higher melting point [5]. The chain length affects the melting point of polyamides, although the melting point of aliphatic polyamides decreases as the length of the aliphatic segment increases: Nylon-4,6 (300 °C), Nylon-6,6 (260 °C), Nylon-6,10 (225 °C), and Nylon-6,12 (210 °C). The melting

temperature of aliphatic polyamides also exhibits odd/even alternation, with polyamides containing an odd number of methylene groups having higher melting temperatures than those with an even number of methylene groups [1, 3]. In polyamides and copolyamides with different degrees of crystallinity, the chain length affects the melting points. For example, the melting temperature of Nylon-11 (190 °C) is higher than that of Nylon-12 (180 °C) [1, 16].

On the other hand, the glass transition temperature originates from the molecular motion of amorphous regions, like translation motion, length of the alkyl chain, vibration of atoms, movement of crystal lattice, and chain uncoiling [6]. The glass transition is also affected by the polymer chain length and amide content, which hydrogen bonds to increase crystallization [3]. The glass transition temperature (T_g) of nylon increases with increasing crystallization. Due to the amide linkage, nylons are hygroscopic and absorb moisture, which has a plasticizing effect and reduces the mechanical properties of tensile strength and Young's modulus, although the impact strength increases [2]. Nylons with lower contents of amide linkages show lower water absorption, inducing the decrease of T_g. The water absorption of nylons range from 2 % to 10 %, which affects their T_m, T_g and chain stiffness [4, 2].

While the higher crystallinity impacts all of the major properties of polyamides, the high moisture absorption reduces the crystallinity of polyamides. In particular, a high degree of
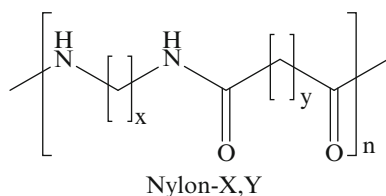
crystallinity provides abrasion resistance, high stiffness, high density, high Young's modulus, high chemical resistance, and better dimensional stability, but decreases elongation, impact resistance, thermal expansion, and gas permeability [2, 3, 17]. Although the stiffness, tensile strength, and yield point of polyamides increase with increasing crystallinity, these properties are independent of molecular weight [2]. Nucleating agents such as inert mineral fillers like clay, talc, and chalk are added to a polymer to increase its crystallinity and thereby enhance its abrasion resistance. Nylons that are transparent have an amorphous structure, which is controlled by (co)polymerization of the appropriate monomers, such as partially aromatic or cycloaliphatic AB, AA, or BB monomers, in order to have acceptable stiffness [1, 2].

Amides are generally hydrolyzed under acidic and alkaline conditions. Some polyamides are stable in alkaline solution but easily hydrolyzed in acidic media [2]. With the exception of aramid Kevlar™, almost all of the polyamides are slowly hydrolyzed in water. However, due to their poor solubility in common organic solvents, aramids are difficult to process, which limits their applications [12].

Aliphatic Polyamides

Aliphatic polyamides, Nylon-X,Y (Fig. 8), are produced commercially by polycondensation of diamines with diacids or diacid chlorides, self-condensation of amino acids, and ring-opening polymerization of lactams [1, 7]. A high molecular weight polymer is prepared from pure monomer, and the stoichiometric ratio of comonomers affects the polyamide properties; an equimolar mixture forms a salt referred to as a salt monomer or nylon salt [10].
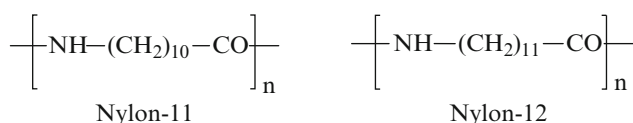
The melting temperature of Nylon-6,6 is higher than that of Nylon-6. Their major difference is the number of components: Nylon-6 has six carbons in the alkyl segment, while Nylon-6,6 is made from two components, a six-carbon diacid and a six-carbon diamine [4, 12]. Nylon-6,6 is therefore more crystalline and has a higher melting point than Nylon-6, and Nylon-6 is more mobile than Nylon-6,6. Nylon-6 and Nylon-6,6 have similar properties, but Nylon-6 is slightly more tough [12]. Nylon-6,6 has a better balance of strength, stiffness, and thermomechanical properties than Nylon-6 [4]. Nylon-6 and Nylon-6,6 are in great demand today because of their excellent properties and good ductility, which are suitable for glass-reinforced products, used as long-term thermomechanical materials that are resistant to hydrolysis and moisture [4, 17]. Reinforced polyamides are used in the automobile industry to prepare electrical systems, pedals, and the cooling systems, rims, and vehicle pedal assemblies [12]. Nylon-6 and Nylon-6,6 can be blended with aromatic polyamides, and small proportions of Nylon-6 can be blended with Nylon-6,6 for newer industrial applications. The Nylon-6/6,6 blends produce good films [3, 17].

Nylon-11 and Nylon-12 (Fig. 9), including their fibers, have properties similar to those of their Nylon-6 "sister materials" [1, 3, 12]. Both Nylon-11 and Nylon-12 have high chemical resistance to oil products, petrol, fatty substances, lubricants, and some organic solvents. They swell easily but do not dissolve in phenol and acetic acid and are stable in 33 % HCl solution. In contrast, Nylon-6 and Nylon-6,6 decompose easily in acidic solutions [3].

Polyamide Syntheses, Fig. 8 Structures of Nylon-X,Y

Polyamide Syntheses, Fig. 9 Structures of Nylon-11 and Nylon-12

Nylon-11 (Fig. 9) is called Rilsan^TM and is produced by polycondensation of 11-aminoundecanoic acid, which is derived from renewable castor oil, at 220 °C with removal of water [16]. Nylon-11 has a relatively low moisture absorption due to the long alky segment and high chemical resistance due to intermolecular hydrogen bonding. It is also able to accept a high loading of fillers. However, the cost of Nylon-11 is high and it is less heat resistant than the other types of polyamides [1, 3].

Nylon-12 (Fig. 9) is produced by the ring-opening polymerization of laurolactam (dodecalactam) at around 290 °C in the presence of phosphoric acid. The dodecalactam is prepared from cyclododecatriene, similar to the conversion of benzene to caprolactam [15]. Nylon-12 has extremely good mechanical properties over a wide temperature range. The melting temperature of Nylon-12 is lower than that of Nylon-11 due to its lower amide content [3, 15].

Due to the flexible alkyl segment of Nylon-11 and Nylon-12, they are more suitable for automobile industries as well as electrical cables and pipes for natural gas transportation, sports article, and medical to pneumatics [3]. Nylon-11 is used for packaging materials, UV and weather resistance, and flame resistance properties [8, 16]

Nylon-4,6 is prepared from the salt of 1,4-diaminobutane and adipic acid. Its melting temperature is 290 °C [4]. It has excellent mechanical properties at room temperature and at high temperature. Nylon-4,6 has the highest grades of impact due to its excellent resistance, wearing ability, processability, chemical resistance, and high stiffness. Polyamides are used for making mechanical rubber good, sewing thread and filters, and some fiber applications [1, 4]. The melting temperature and mechanical properties of Nylon-4,6 are higher than those of Nylon-6 and Nylon-6,6 due to the higher amide content; however, it absorbs more moisture [2, 15].

There are some bio-derived aliphatic polyamides, which minimize their carbon footprint. Nylon-11, Nylon-6,12, Nylon-6,10, Nylon-6, Nylon-6,6, Nylon-10,12, and Nylon-4,10 can be derived from castor oil [15]. Nylon-6,12 is

suitable for weather-resistant jackets. Nylon-6,10 is prepared by interfacial polymerization of sebacoyl chloride and hexamethylenediamine [2, 15, 17]. Nylon-10,10 is prepared by the reaction of decanediamine with sebacic acid derived from castor oil. Its properties are similar to those of Nylon-12, but it is less chemically resistant, absorbs less moisture, and is more adhesive due to its flexible structure. Nylon-10,10 can be easily injection molded and is used for electronic devices in housing, flexible tubes, and pneumatic tubes [1, 15]. Nylon-4,10 is produced from 1,4-diaminobutane and sebacic acid derived from castor oil. Nylon-10,12 is produced from 1,10-decamethylene diamine and sebacic acid (derived from castor oil). Bio-based polyamides are needed to minimize their carbon footprint and reduce global warming [1, 2].

Aromatic Polyamides

Due to their rigid backbones, especially the entirely *p*-substituted derivative [18], aromatic polyamides have high thermomechanical properties (tensile and impact resistance), are chemically resistant to alkali, and are hydrolytically stable [8, 6]. They are useful for high-performance technologies and can therefore fulfill the future demand for rigid thermomechanical materials [18], including rubber replacements; commodity articles like parachutes, boats, electrical motors, thermoplastic pipes, and fan blades; and cutting edge technologies like optically active polyamides, gas separation membranes, ion exchange membranes, and thermoresistant jackets [2]. Aramid-based membranes are superior to cellulose acetate in reverse osmosis applications [15] and, due to their pH and chemical resistance, can be cleaned with acid and caustic solutions [18]. However, aromatic polyamides have poor solubility and are difficult to process, which restricts their applications [4].

The two most popular commercial aramids are Nomex^TM (Fig. 10) and Kevlar^TM (Fig. 11). Morgan (DuPont) discovered Nomex^TM in 1958 and it was later commercialized in 1961. Kevlar^TM was discovered by Kwolek (Du Pont) in 1965 and was later commercialized in 1971. Nomex^TM is synthesized by polymerization of

Polyamide Syntheses,
Fig. 11 Synthesis of
Kevlar[TM] from
p-phenylenediamine and
terephthaloyl chloride
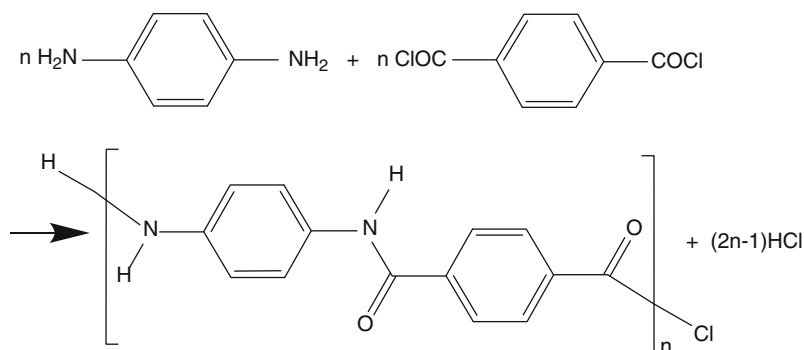
m-phenylenediamine and isophthaloyl chloride
[18]. Nomex[TM] has a high melting point
(400 °C) and high thermal stability. Its fiber is
drawn from a highly polar solution of DMF
containing lithium chloride [15].

Kevlar[TM] is synthesized by polymerization of
different isomers, terephthaloyl chloride and
p-phenylenediamine (Fig. 11) [1, 2, 15]. The
melting point (500 °C) of this entirely
p-substituted polyamide is 100 °C higher than
that of Nomex[TM], and its T_g is 300 °C. Kevlar[TM]
is insoluble in polar solvents like NMP, DMAc,
and DMF because of its rigid-rod backbone and
intermolecular hydrogen bonds (Fig. 12),
although it dissolves in concentrated sulfuric
acid, which can be used for fiber formation [18].
The properties of Kevlar[TM] fiber are superior to
those of Nomex[TM] fiber. With a strength compa-
rable to steel, Kevlar[TM] forms the strongest
man-made fiber and is used as a tire cord, in
ballistic vests, boats, and brake pads

[18]. Flexible segments can be introduced to sol-
ubilize Kevlar[TM] and improve its processability
by disrupting the chain symmetry and regularity
and by destroying the hydrogen bonding [1, 2, 15,
18]. These structural modifications also lower the
glass transition temperature [1, 2, 18]. In both
aramids, 85 % of the amide linkages are directly
attached to the two aromatic rings.

Aromatic polyamides with glass transition
temperatures of 156–242 °C have also been
made from bio-based monomers that introduce a
heterocyclic ring [19]. Figure 13 shows itaconic
acid-derived polyamides prepared with diamines
such as 4,4′-diaminodiphenyl ether (PA-1),
p-phenylenediamine (PA-II), *m*-xylenediamine
(PA-III), and *p*-xylenediamine (IV).

The glass transition temperatures were 199 °C
(PA-I), 242 °C (PA-II), 156 °C (PA-III), and
173 °C (PA IV). PA-II has the highest thermal
stability because of *para*-substitution without
an ether linkage and no methylene groups [19].
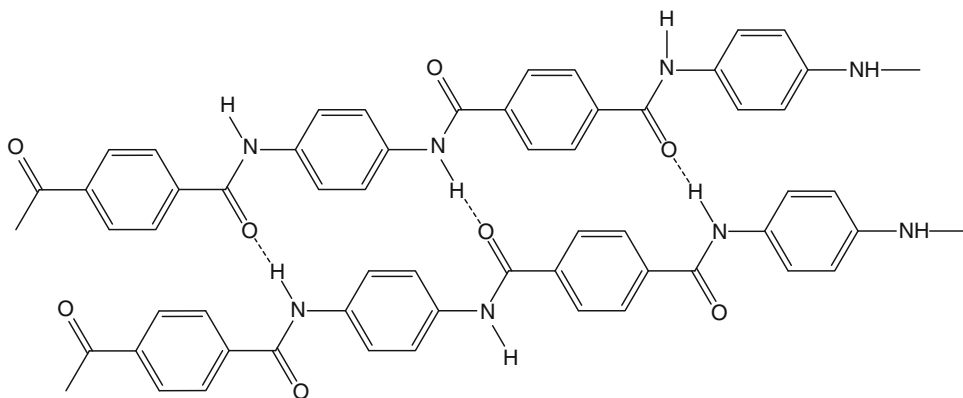
Polyamide Syntheses, Fig. 12 Molecular structure of Kevlar^{TM} forming intermolecular hydrogen bonds
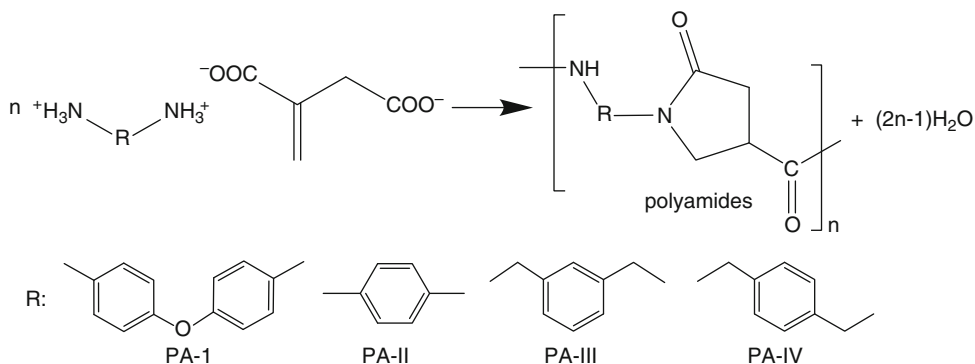
Polyamide Syntheses, Fig. 13 Synthesis of bio-based aromatic polymer derived from itaconic acid salts with aromatic diamines

The heterocyclic ring enhances the fatigue resistance and wearing durability and promotes strong intermolecular hydrogen bonding [19].

Other Polyamides

Aliphatic polyamide finds many industrial and textile applications due to their high mechanical strength and durability [3, 6, 15]. Aromatic polyamides have outstanding properties but poor solubility, whereas aliphatic-aromatic polyamides that incorporate a diacid or diamine with a flexible aliphatic segment have excellent properties and good solubility [3, 15]. Aromatic-aliphatic polyamides have higher melting temperatures, glass transition temperatures, and mechanical properties than Nylon-6 and Nylon-6,6 [15]. The solubility of aromatic polyamides is

also increased by incorporating ether linkages, trifluoromethyl groups, amide-imide linkages, sulfur-containing groups, or alicyclic groups that are less rigid than aromatic rings [20].

Mitsubishi prepared poly(*m*-xylylene adipamide) (MXD-6), by polycondensation of *m*-xylylene diamine with adipic acid (Fig. 14). MXD-6 exhibits a glass transition in the range of 85–100 °C and a melting point in the range of 235–240 °C [9, 15, 18].

Qiana^{TM} developed by DuPont is an aliphatic-aromatic nylon fiber [20] with a melting point of 275 °C. It is prepared by a polycondensation of bis(4-aminocyclohexyl)methane and dodecanedioic acid (Fig. 15), generally for shirt, military clothes, ropes, and ladies gowns.

Polyamide Syntheses, Fig. 14 Synthesis of poly(*m*-xylylene adipamide) from *m*-xylylene diamine with adipic acid
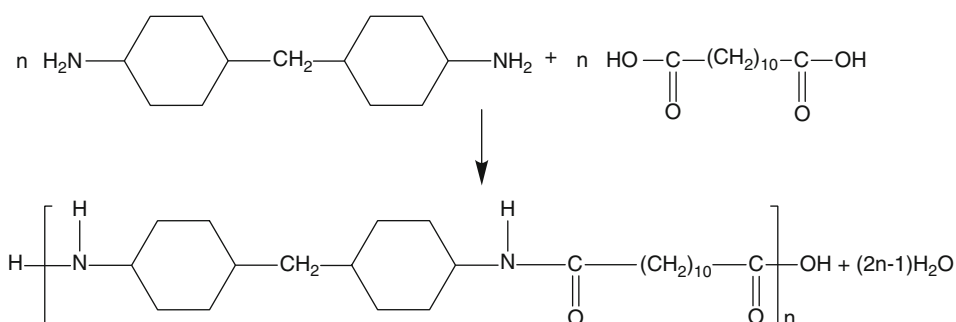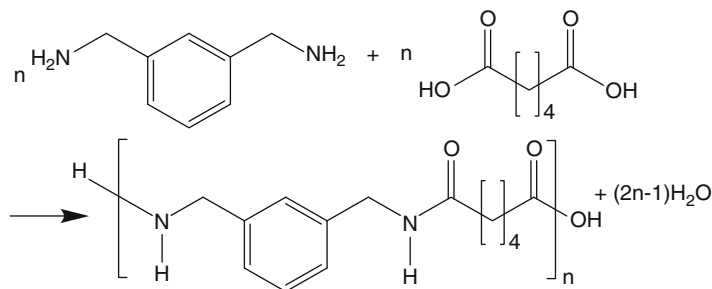
Polyamide Syntheses, Fig. 15 Synthesis of Qiana[TM] polymer from bis(4-aminocyclohexyl)methane and dodecanedioic acid

Summary and Future Development

The demand for polyamides increased in various areas such as the automobile industry, which is further developing these polymers due to the demand for reduced weight and increased fuel efficiency. The increased demands of polyamides and their unimaginable ability to replace conventional polymers encourage researchers to develop polymers directly from biomass. To develop such bio-based polymers (e.g., polyamide, copolyamide, and aromatic polyamide), sustainable synthetic pathways are required with remarkable improvement in thermomechanical, electrical, and optical properties. In addition to various methods for preparing polymers, facile techniques are still required to improve the performance of such materials. Therefore, much more work is needed to develop a synthetic route for the prediction of a variety of polyamides with greatly improved polymer properties.

Itaconic acid-based polyamide and its copolyamides are bio-derived and can therefore minimize the carbon footprint. They also reduce the demand on the endangered supply of petroleum materials. New synthetic routes are still being developed for new polyamides as well as new bio-based and chemical pathways. The goals have been only partially achieved. Some innovative techniques for improving material properties through hybrid methods can fulfill the future goals of materials. Increasing demand and development of bio-based polyamides, researchers try to focus on innovation for polyamide material to find the answer for health and nutrition problems and global warming as well as reduce the price of such materials.

Related Entries

▶ Biobased Polymers

References

1. Kricheldorf HR (1991) Handbook of polymer synthesis. CRC Press, New York
2. Olabisi O (1997) Handbook of thermoplastics. CRC Press, New York
3. Gupta A (2006) The complete technology book on industrial polymers, additives, colourants and fillers. Asia Pacific Business Press, New Delhi
4. Sindair R (2014) Textiles and fashion: materials, design and technology. Woodhead, Cambridge, UK
5. Lewin M (2006) Handbook of fiber chemistry, 3rd edn. CRC Press, New York
6. Morawetz H (1995) Polymers: the origins and growth of a science. Dover Publications, New York
7. Fakirov S (2005) Handbook of condensation thermoplastic elastomers. Wiley, Hoboken
8. Thomas S, Visakh PM (2010) Handbook of engineering and specialty thermoplastics, vol 4. Wiley, Hoboken
9. Balsaraf VM, Pawar AV, Mane PA (2010) Applied chemistry, vol I, 2nd edn. I.K. International, New Delhi
10. Ali MA, Tateyama S, Oka Y, Okajima M, Kaneko D, Kaneko T (2013) High-performance biopolyamides derived from itaconic acid and their environmental corrosion. Macromolecules 46:3719–3725
11. Braun D, Cherdron H, Rehahn M, Ritter H, Voit B (2013) Polymer synthesis: theory and practice fundamentals, methods, experiments. Springer, Berlin
12. Papaspyrides CD, Vouyiouka SN (2009) Solid state polymerization. Wiley, Hoboken
13. Wang Z, Wei T et al (2014) Synthesis of fully bio-based polyamides with tunable properties by employing itaconic acid. Polymer 55:4846–4856
14. Vouyiouka SN, Karakatsani EK, Papaspyrides CD (2005) Solid state polymerization. Prog Polym Sci 30:10–37
15. Mishra SP (2010) A text book of fiber science and technology. New Age International Publishers, New Delhi
16. Salamone JC (1998) Concise polymeric materials encyclopedia. CRC Press, Boca Raton
17. Lewin M (2006) Handbook of fiber chemistry, 3rd edn. CRC Press, New York
18. Garcia JM, Garcia FC, Serna F, de.la Pena J (2010) High-performance aromatic polyamides. Prog Polym Sci 35:623–686
19. Ali MA, Tateyama S, Kaneko T (2014) Synthesis of rigid-rod but degradable biopolyamides from itaconic acid with aromatic diamines. Polym Degrad Stab 109:367–372
20. Board N (2003) The complete technology book on textile spinning, weaving, finishing and printing. Asia Pacific Business Press, New Delhi

Polyamines

Yasuhiro Morisaki
Department of Polymer Chemistry, Graduate School of Engineering, Kyoto University, Nishikyo-ku/Kyoto, Japan

Synonyms

Imino-group-containing polymer; Poly(ethylene imine)s

Definition

Organic compounds containing two or more amino $(-NH_2)$ groups and/or imino $(-NR-)$ groups.

Polyamines, i.e., aliphatic hydrocarbons containing two or more amino $(-NH_2)$ and/or imino $(-NH-)$ groups, are ubiquitous in living systems. Polyamines play essential roles in biological processes as they contribute to cell division, nucleic acid synthesis, etc. Naturally occurring polyamines are acyclic with terminal amino groups. Figure 1 shows the structures of representative polyamines in the human body. On the other hand, synthetic polyamines are linear and branched polymers consisting of imino groups $(-NR-:$ R = H, alkyl, aryl, etc.) in the main chain. Of note, polymers containing amino groups only in the side chain are not classified as polyamines.

Polyamines have various desirable characteristics such as high water solubility, adsorptivity, high cationic charge density, and high reactivity. Hence, they find numerous applications as adhesives, paints, chelating agents for heavy metals, additives for metal plating, coagulating agents for water treatment, dispersing agents, resin-curing agents, aldehyde adsorbents, CO_2 adsorbents, transfection reagents, etc.

One of the most investigated synthetic polyamines is poly(ethylene imine) (Fig. 2) [1, 2]. Because of the presence of secondary and tertiary amine moieties in the poly(ethylene imine) main
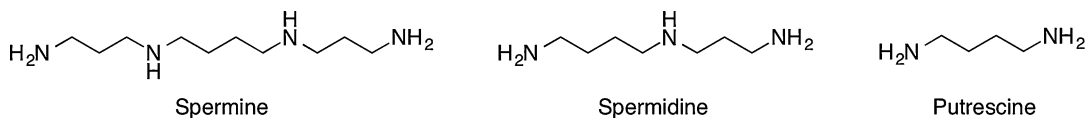
Polyamines, Fig. 1 Representative polyamines in a human body

Polyamines, Fig. 2 Structure of poly (ethylene imine)
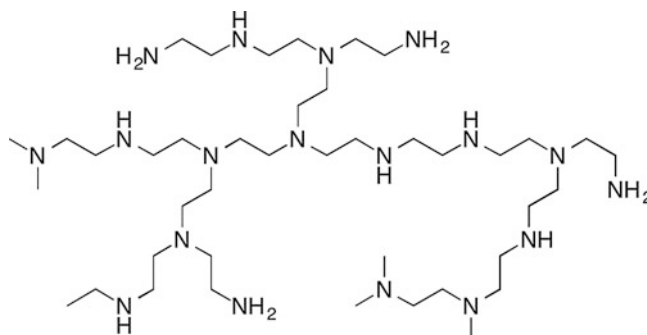
chain, *N*-functionalization can be readily carried out by nucleophilic substitution and Michael reaction using various electrophiles. The representative synthetic routes to poly(ethylene imine)s as well as to polyamine derivatives are as follows.

Ring-Opening Polymerization of Ethylene Imine (Aziridine)

Poly(ethylene imine) is synthesized by the ring-opening polymerization of ethylene imine (aziridine) in the presence of a Lewis acid or proton [3]. As shown in Fig. 3, the reaction is initiated by coordination of the Lewis acid to ethylene imine or by protonation of ethylene imine, to afford the reactive species, which then attacks a second ethylene imine monomer. Ring-opening reaction and successive nucleophilic attack proceed repeatedly to afford the corresponding polymer. Nucleophilic attack of the secondary amine in the main chain forms a quaternary ammonium species, resulting in the formation of branched structures. Such branched poly(ethylene imine)s are liquid at room temperature. They are well soluble in water, methanol, ethanol, and acetone, whereas they are not soluble in benzene, tetrahydrofuran, acetone, and hexane.

This ring-opening approach can also be extended to *N*-substituted ethylene imines (Figs. 4 and 5). Bulky *N*-substituents suppress the nucleophilic attack of amines in the polymer main chain, affording linear *N*-substituted poly (ethylene imine). Figure 4 shows ring-opening polymerization of *tert*-butylaziridine; this polymerization is controlled to give the target polymer with narrow polydispersity [4]. Benzyl- [5], perfluoroacyl- [6], and pyranyl-substituted [7] aziridine are also polymerized, and the substituents are readily removed after polymerization to afford linear poly(ethylene imine)s. Linear poly (ethylene imine)s are generally crystalline ($T_m = 58.5\ °C$) [8]. They are soluble in chloroform and methanol, whereas they are not soluble in benzene, diethylether, and acetone.

Ring-Opening Polymerization of Oxazolines

An alternate synthetic route to poly(ethylene imine) is the cationic ring-opening polymerization of oxazolines [1], which affords the corresponding poly(*N*-acyl ethylene imine)s, as shown in Fig. 6. Thermodynamically favored amide structures are formed by the ring opening, leading to the smooth polymerization. Acid or alkaline hydrolysis can be carried out to obtain
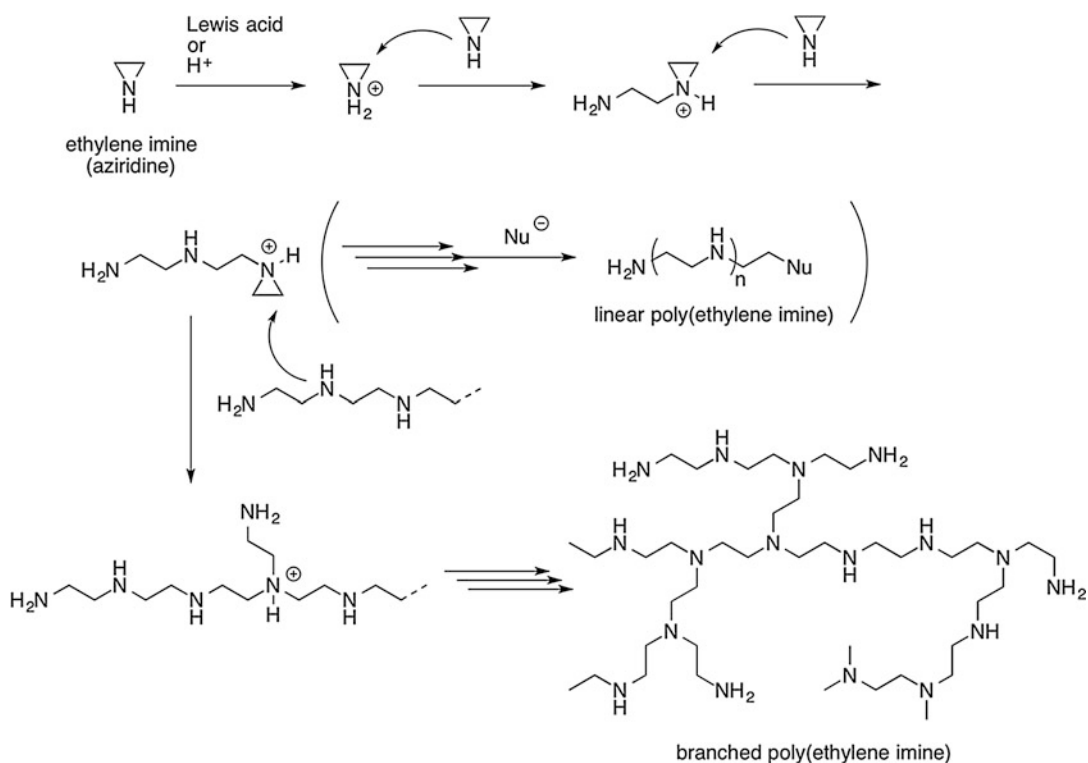
Polyamines, Fig. 3 Ring-opening polymerization of ethylene imine
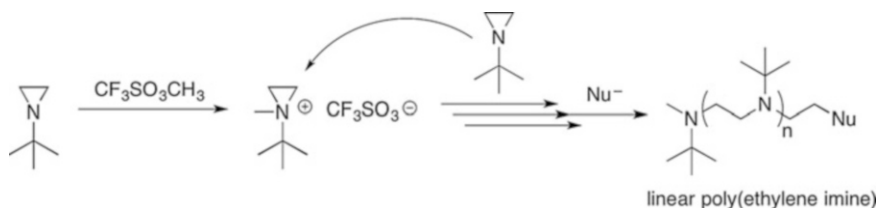
Polyamines, Fig. 4 Ring-opening polymerization of *N-tert*-butylaziridine

non-substituted linear poly(ethylene imine)s. The reaction proceeds in a living manner; therefore, polydispersity of the obtained polymer is narrow, and the polymer chain end can be functionalized with termination with various nucleophiles such as amines. Figure 7 shows the representative example of the ring-opening polymerization of oxazolines and the synthesis of poly(2-oxazoline) macromonomer [9].

Synthesis of Polyamines by Polyaddition

Michael Addition
Bifunctionalized acrylamides are readily polymerized with diamines; in other words, Michael addition polymerization proceeds to afford polyamines. The reaction of aliphatic primary amines provides polymers with secondary amine
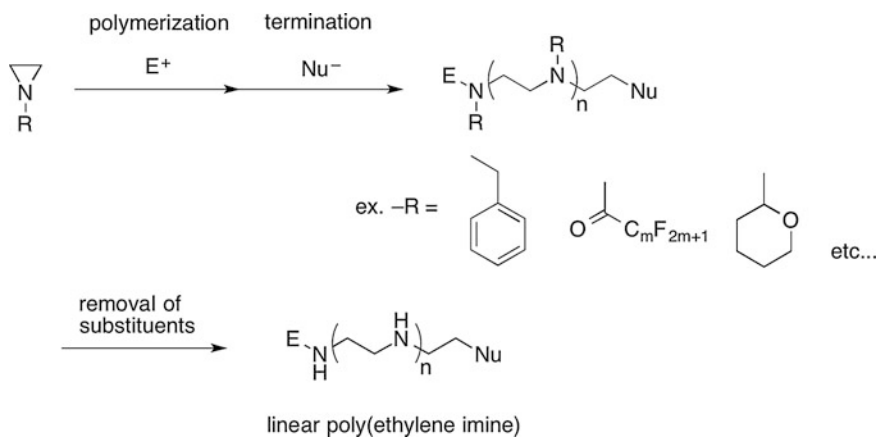
Polyamines, Fig. 5 Ring-opening polymerization of *N*-substituted aziridines and removal of the *N*-substituents
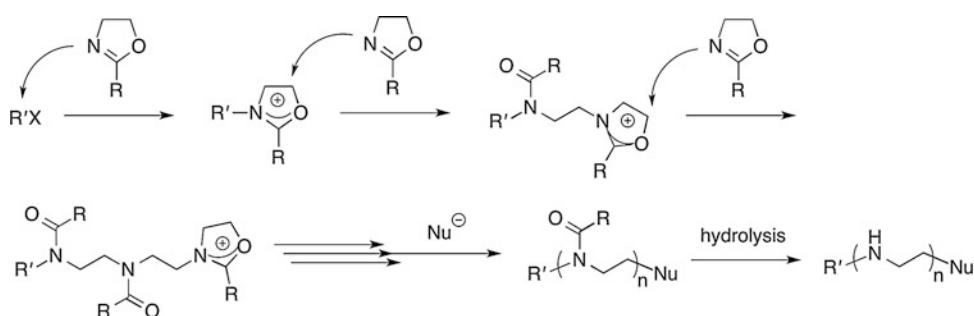
Polyamines, Fig. 6 Ring-opening polymerization of oxazoline derivative
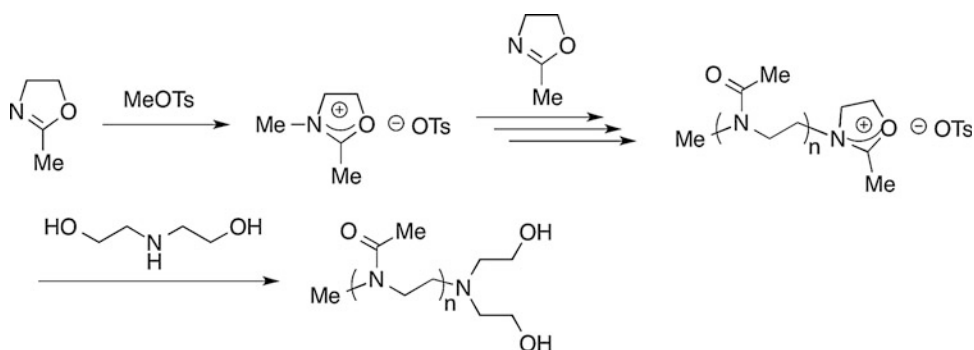
Polyamines, Fig. 7 Synthesis of poly(2-oxazoline) macromonomer

moieties, resulting in the formation of network polymers. Bulky primary amines suppress the cross-linking reactions to afford linear polyamines. For example, as shown in Fig. 8, the polymerization of methylene bisacrylamide with Jeffamine® yields the corresponding polyamine,

which is an alcohol-soluble crystalline polyamine [10].

Polyaddition with Bisepoxides

Ring-opening reaction of epoxide with nucleophile can be applied in synthesis of
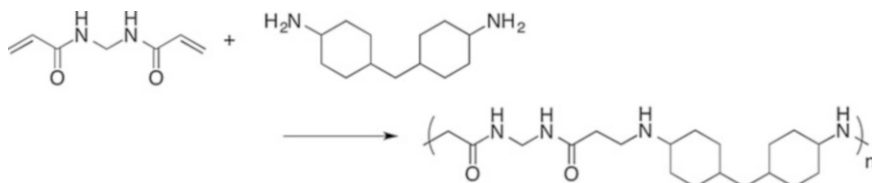
Polyamines, Fig. 8 Synthesis of polyamine by Michael addition
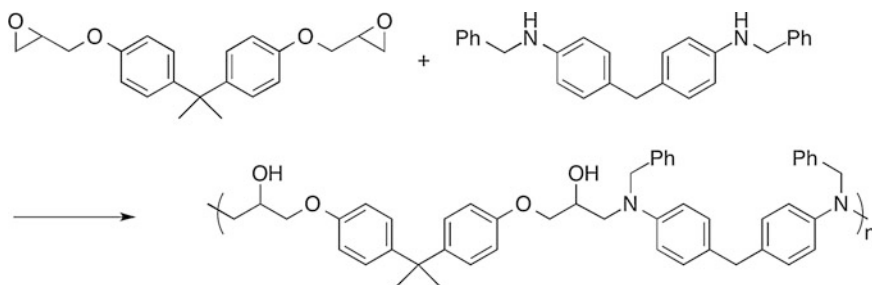
Polyamines, Fig. 9 Synthesis of polyamine from bisepoxide
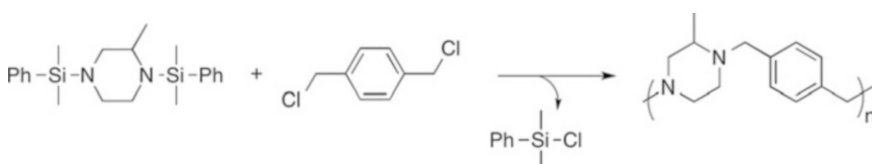
Polyamines, Fig. 10 Synthesis of polyamine by polycondensation
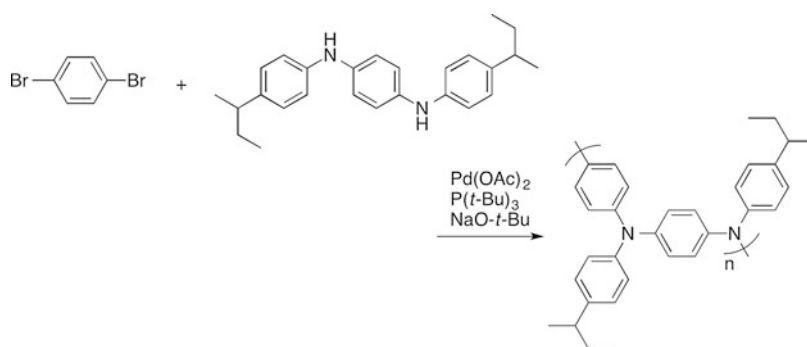
Polyamines, Fig. 11 Synthesis of poly (triarylamine) by palladium-catalyzed amination

polyamines together with the formation of a hydroxyl group. The hydroxyl group attacks other epoxide, when the nucleophilicity of the nucleophile is weak; thus, during polymerization, cross-linking occurs to afford network polymer. In order to obtain linear polymer, stronger nucleophiles such as amines are required. In Fig. 9, the representative example of the polyaddition of bisepoxide with amine is shown. The reaction of bisphenol-A-glycidylether with secondary diamine affords the corresponding polyamine in good isolated yield [11]. The polymer is well soluble in common organic solvents.

Synthesis of Polyamines by Polycondensation

Nucleophilic Substitution

Aliphatic polyamines are generally obtained by nucleophilic substitutions of diamines with dihalides; however, elimination of HX in dihalides by base occurs to terminate the polycondensation. To overcome this difficulty, polymerization of *N*-silyldiamine with dichloroxylene was reported, as shown in Fig. 10 [12]. The reaction provides a neutral by-product (PhMe$_2$SiCl) instead of acidic by-products, and elimination does not occur by using a benzylic compound.

Amination of Aryl Halides

Palladium-catalyzed amination of aryl halides is a powerful tool for syntheses of poly(triarylamine)s; this reaction was independently developed by Hartwig [13] and Buchwald [14]. Polymerization of dibromobenzene with bisamine in the presence of Pd(OAc)$_2$ with P(*t*-Bu)$_3$ affords the corresponding poly(triarylamine), as shown in Fig. 11 [15]. Triarylamine polymers are promising candidates for a hole-transporting layer of electronic devices [16].

References

1. Kobayashi S (1990) Ethylenimine polymers. Prog Polym Sci 15:751
2. Jäger M, Schubert S, Ochrimenko S, Fischer D, Schubert US (2012) Branched and linear poly(ethylene imine)-based conjugates: synthetic modification, characterization, and application. Chem Soc Rev 41:4755
3. Jones GD, Langsjoen A, Neumann SMMC, Zomlefer J (1944) The polymerization of ethylenimine. J Org Chem 9:125
4. Munir A, Goethals EJ (1981) Reactions of cationic living poly(tert-butyl aziridine). J Polym Sci Polym Chem Ed 19:1985
5. Goethals EJ, Bossaer P, Deveux R (1981) The polymerization behavior of 1-benzyl-2,2-dimethyla-ziridine. Polym Bull 6:121
6. Demember JR, Taylor LD (1979) Reinvestigation of the chemical-reactivity of n-perfluoroacylaziridines. J Polym Sci Polym Chem Ed 17:1089
7. Weyts KF, Goethals EJ (1988) New synthesis of linear polyethyleneimine. Polym Bull 19:13
8. Saegusa T, Ikeda H, Fujii H (1972) Crystalline polyethylenimine. Macrmolecules 5:108
9. Kobayashi S, Uyama H, Shirasaka H (1990) Synthesis and polymerization of poly(2-oxazoline) macromonomers having a glycol group. Makromol Chem Rapid Commun 11:11
10. Shchori E (1983) Poly (secondary amine)s from diacrylates and diamines. J polym Sci Polym Lett Ed 21:413
11. Hörhold HH, Grützner RE (1987) Cyclodimer aus bisphenol-A-diglycidylether und N,N'-disubstituiertem 4,4'-diaminodiphenylmethan. Acta Polym 38:247
12. Kleve JF (1964) Poly (xylylenylpiperazine) novel polyamine. J Polym Sci Part A 2:2673
13. Louie J, Hartwig JF (1995) Palladium-catalyzed synthesis of arylamines from aryl halides - mechanistic studies lead to coupling in the absence of tin reagents. Tetrahedron Lett 36:3609
14. Guram AS, Tennels RA, Buchwald SL (1995) A simple catalytic method for the conversion of aryl bromides to arylamines. Angew Chem Int Ed 34:1348
15. Goodson FE, Hauck SI, Hartwig JF (1999) Palladium-catalyzed synthesis of pure, regiodefined polymeric triarylamines. J Am Chem Soc 121:7527
16. Thelakkat M (2002) Star-shaped, dendrimeric and polymeric triarylamines as photoconductors and hole transport materials for electro-optical applications. Macromol Mater Eng 287:442

Polyanhydride Synthesis

Stéphan Bien-Aimé and Kathryn Uhrich
Department of Chemistry and Chemical Biology, Rutgers University, Piscataway, NJ, USA

P

Synonyms

Condensation polymers; Ring-opening polymerization

Definition

Polyanhydrides are a class of polymers where the linkages between repeat units are anhydride bonds (Fig. 1).

Introduction

Polyanhydrides are surface-eroding polymers; they exhibit rates of hydrolysis faster than rates

of diffusion. As a result, erosion is limited to the outer surface of the polymer, which allows the polymer backbone's structural integrity to be maintained throughout the degradation process (Fig. 2) [1]. Surface erosion is an important property of polyanhydrides because it permits degradation to be well controlled. The hydrophobicity of the polymer composition, coupled with hydrolytically labile anhydride linkages, can lead to a constant and controlled release profile of bioactives from polyanhydride-based systems [2]. Typically, the hydrolytic degradation lasts days or months depending on the polymer chemistry. Biocompatibility studies, both in vitro and in vivo, revealed that polyanhydrides generally degrade to their acid counterparts as noncytotoxic products [3]. Hence, they are useful for various biomedical applications such as in drug delivery and implantable biomaterial.

Although the advantages of polyanhydrides are numerous, several drawbacks exist with this class of polymers. Polyanhydrides manifest low mechanical strength and, as anticipated from their anhydride linkages, are highly susceptible to degradation upon exposure to moisture [4]. Moreover, upon storage at room temperature, these polymers are subject to spontaneous depolymerization into oligomers as a result of water exposure. Consequently, polyanhydrides need to be stored under moisture-free, low temperature conditions which will help in slowing or preventing degradation.

Synthesis

Many polymerization techniques are employed for the synthesis of polyanhydrides; four of which deserve considerable attention based on common use. One method employed for the synthesis of polyanhydrides is ring-opening polymerization (ROP). During ROP, a cyclic anhydride, in the presence of an anionic or cationic initiator, undergoes ring cleavage, thus allowing subsequent polymerization to take place where further cyclic anhydride monomers can join to form a larger polymer chain [4]. For instance, poly(adipic anhydride) can be prepared from cyclic adipic anhydride using aluminum trichloride (cationic) or sodium hydride (anionic) initiators (Fig. 3) [4]. In another technique, polyanhydrides are prepared by condensation of diacids and acyl dichlorides (Fig. 4) [4]. The reactants are dissolved in a single solvent such as dichloromethane, in the presence of a base (i.e., triethylamine) and cooled in an ice bath [4]. The rapid reaction of carboxylates with acyl chlorides typically results in complete polymerization within an hour.

Melt-condensation polymerization and solution polymerization are also two common condensation methods used to synthesize polyanhydrides. Melt-condensation polymerizations are carried out above the melting temperature and below the decomposition temperature of the monomers [4, 5]. Because those temperatures range from 150 °C to 200 °C, heating must be closely monitored to prevent decomposition of the resulting polymer. Consequently, this polymerization technique is not suitable for
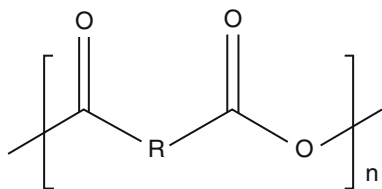
Polyanhydride Synthesis, Fig. 1 Chemical structure of polyanhydride repeat unit

Polyanhydride Synthesis, Fig. 2 Surface-eroding mechanism of polyanhydrides

H₂O uptake (hydrates surface)   Degradation (bond hydrolysis)   Erosion (solubilization of degradation products)
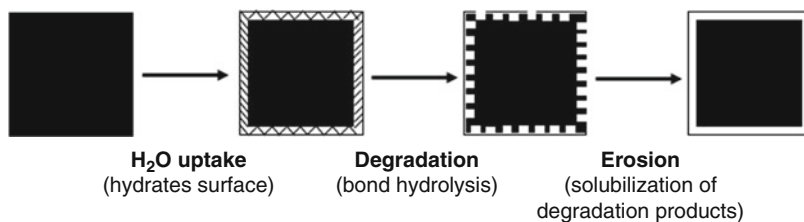
**Polyanhydride
Synthesis,
Fig. 3** Synthesis of poly
(adipic anhydride) from
cyclic adipic anhydride
monomer by ROP
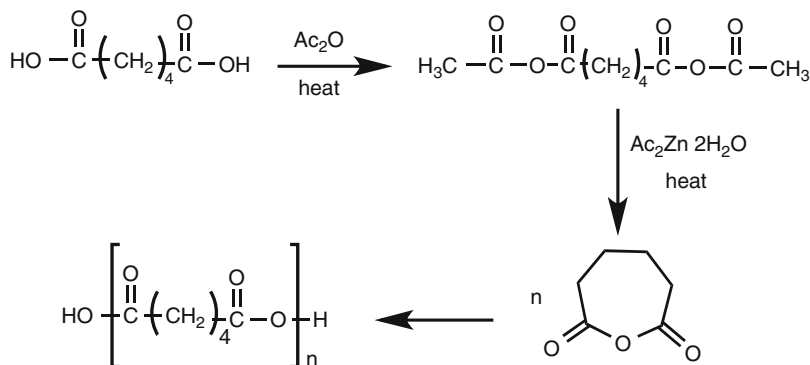
**Polyanhydride
Synthesis,
Fig. 4** Condensation of
diacids and diacyl chlorides
to form polyanhydride
copolymers
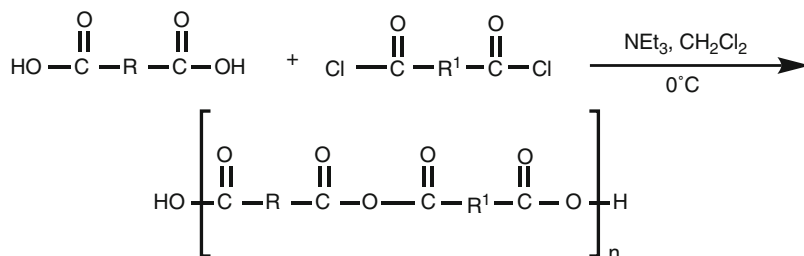
heat-sensitive monomers, which require milder reaction conditions [4, 5]. However, melt-condensation is reproducible and amenable to scale-up, from milligrams to tens of grams [5]. As an alternative to melt-condensation polymerization, solution polymerization can be used for thermally sensitive monomers; yet this method requires exact stoichiometry and often yields lower molecular weight polymers when compared to melt-condensation polymerization [4, 5].

In synthesizing polyanhydrides, other functional groups, such as esters, can also be chemically incorporated into the backbone. For instance, Schmeltzer and Uhrich have synthesized salicylate-based poly(anhydride-esters) (PAEs) by melt-condensation and solution polymerizations [5]. Salicylate-based polymers are unique because non-steroidal anti-inflammatory drugs (NSAIDs) are chemically incorporated into the polymer backbone, instead of being physically admixed or attached as a pendant group [2]. The process of formation of salicylate-based PAE via melt-condensation involves three steps. Initially, the free salicylate (**1**) is coupled with a diacyl chloride (**2**) or linker

molecule in the presence of pyridine to yield diacid (**3**) (Fig. 5) [5]. The salicylate-based diacid (**3**) is then reacted with excess acetic anhydride to form acetyl-terminated monomer (**4**) [5]. Finally, the polymer precursor (**4**) is heated to 180 °C under vacuum (<2 mmHg) to yield the salicylate-based PAE (**5**) [5]. For comparison, Schmeltzer and Uhrich have also prepared salicylate-based PAEs via solution polymerization in which the salicylate-based diacid (**3**) is suspended in anhydrous dichloromethane and cooled to 0 °C in the presence of triethylamine as a base and triphosgene as the coupling agent (Fig. 6) [5]. The salicylate-based PAE obtained from both polymerization techniques exhibits controlled bioactive release upon hydrolysis [5].

Characterization

After synthesis, polyanhydrides' structures are verified by using different analytical instruments. Proton nuclear magnetic resonance (^{1}H-NMR) spectroscopy is used to confirm the polymer's chemical composition. Broadened peaks generally

Fig. 5 Preparation of salicylate-based poly (anhydride-esters) **5** via melt-condensation
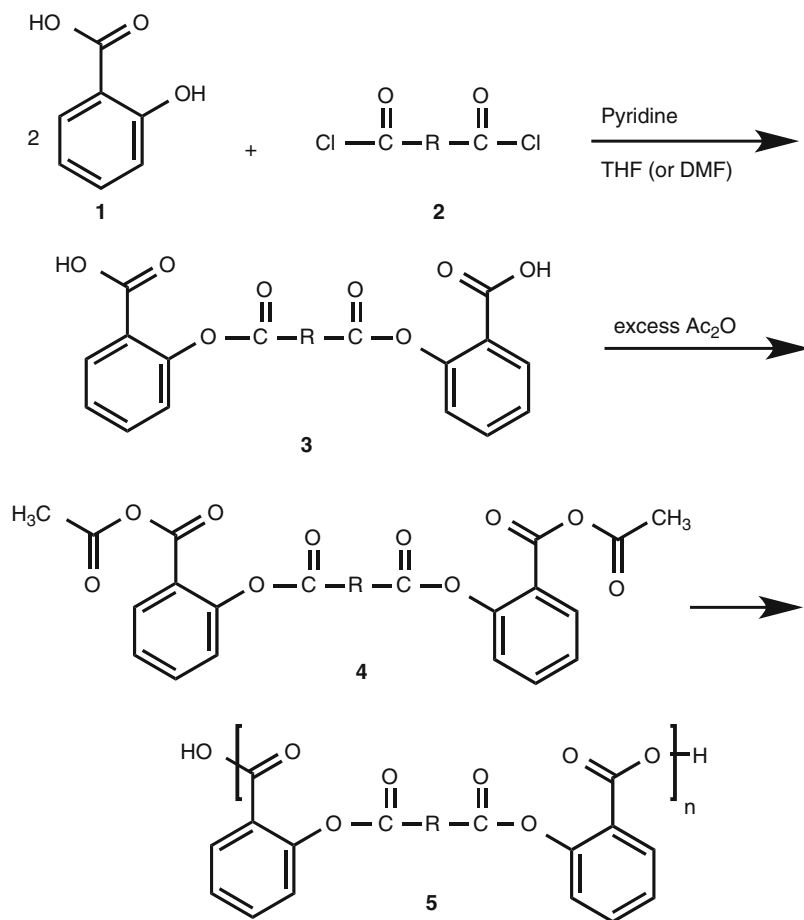
suggest that polymerization has occurred [4]. Infrared (IR) spectroscopy is used to identify the functional groups present in the polymers and to verify the appearance of anhydride peaks. The IR spectra of salicylate-based PAEs synthesized via solution polymerization by Schmeltzer and Uhrich exhibit sharp and narrow bands, indicating a well-defined polymer structure [5]. In contrast, the IR spectra of salicylate-based PAEs synthesized via melt polymerization are broader, suggesting that the anhydride bonds may undergo thermal rearrangement, yielding aromatic esters as illustrated in Fig. 7 [5]. Nonetheless, both polymers exhibit controlled release of salicylic acid.

Polymer molecular weights and polydispersity indices (PDIs) are determined by gel permeation chromatography (GPC). In the case of poly (anhydride-esters), Uhrich's laboratory obtains molecular weight between 15,000 and 45,000 Da with lower PDIs (1.1–2.0) than polyanhydrides discussed in the literature (2.0–15.0) [6]. To further characterize polyanhydrides, differential scanning calorimetry (DSC) and thermogravimetric analysis (TGA) are used to ascertain polymers' thermal properties and purity. DSC is used to determine polymers' glass transition (T_g), melting (T_m), and crystallization (T_c) temperatures [7]. In the case of PAEs, Uhrich et al. reported T_gs between 40 °C and 55 °C. Such a range is beneficial for in vivo applications because the PAEs will not deform once implanted in the body, which has an internal temperature of 37 °C. TGA, which measures heat lost as a function of temperature, is performed to obtain polyanhydride decomposition (T_d) temperatures [8].

Polyanhydride Synthesis,
Fig. 6 Preparation of salicylate-based poly (anhydride-esters) **5** via solution polymerization
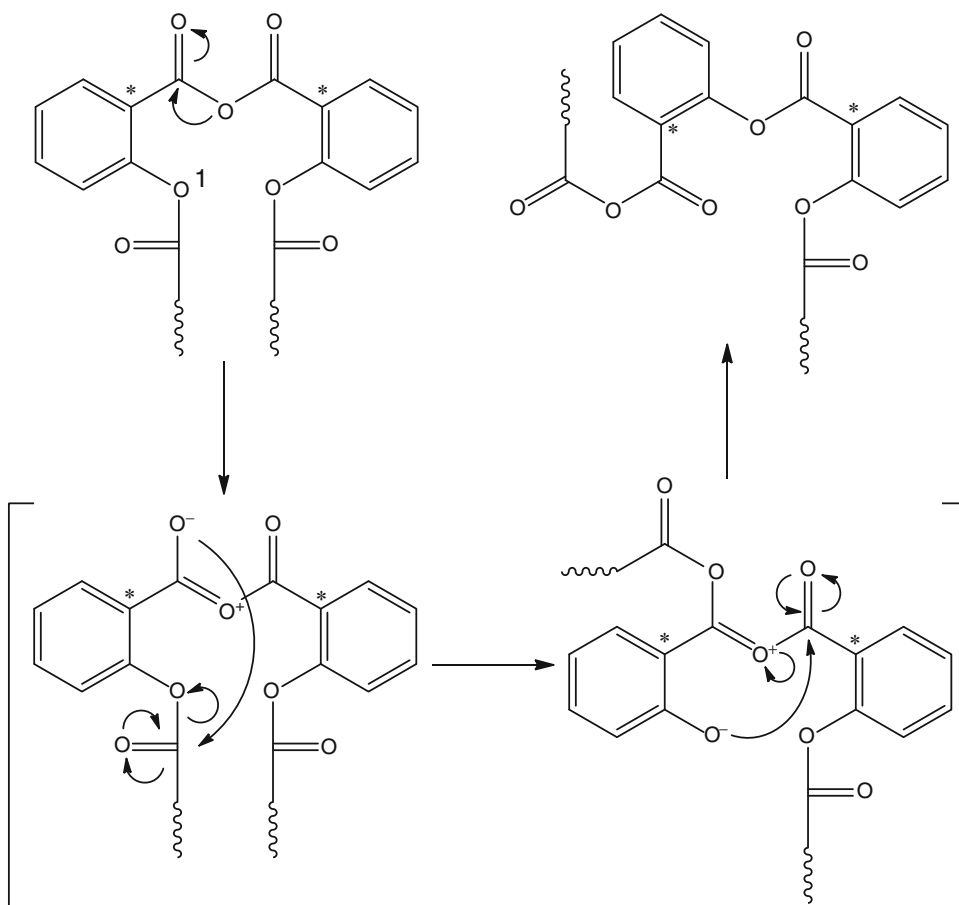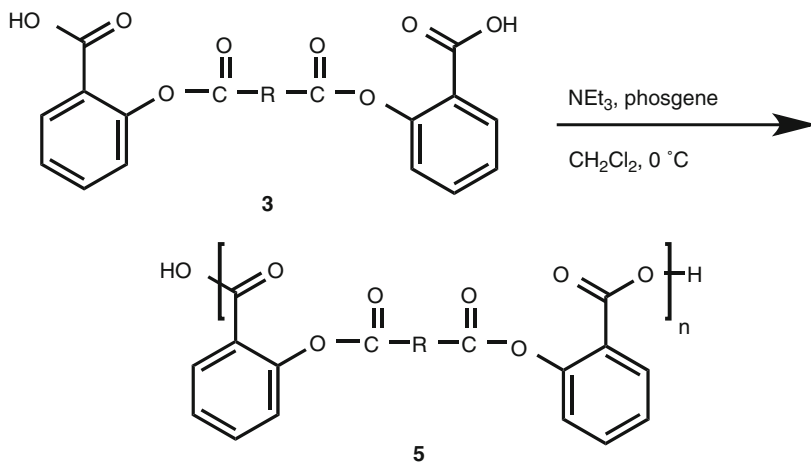
Polyanhydride Synthesis, Fig. 7 Proposed mechanism of the salicylate–anhydride thermal rearrangement

P

Application

Polyanhydrides have been employed in the biomedical field as controlled release devices. The most recognized example and FDA-approved drug delivery system comprised of polyanhydrides is the GLIADEL® Wafer for the treatment of glioblastoma, a type of brain tumor. This implant is composed of polifeprosan 20, a polyanhydride copolymer consisting of poly [bis (p-carboxyphenoxy)] propane and sebacic acid in a 20:80 M ratio [9]. An anticancer drug, carmustine, is physically admixed within the copolymer matrix. GLIADEL® Wafer is placed into the surgical cavity following removal of glioblastoma to locally release carmustine, thus destroying any remaining tumor cells [9].

Similarly, as mentioned above, the Uhrich lab has synthesized and developed salicylate-based PAEs for controlled drug delivery. The polymer, by undergoing surface erosion, degrades and releases the bioactive [1]. An advantage of these PAEs is the fact that they are capable of achieving high drug loading (50–80 %) in a reproducible manner. In addition, these PAEs can be formulated into different geometries such as tablets, coatings, hydrogels, and microspheres [10]. Depending on the chemistry of the polymer backbone, the rate of release can be monitored to satisfy the requirements of the intended medical applications.

Related Entries

▶ Biodegradable Materials
▶ Chain-Growth Condensation Polymerization
▶ Controlled Release
▶ Free-Radical Ring-Opening Polymerization
▶ Monomers, Oligomers, Polymers, and Macromolecules (Overview)
▶ Polymeric Drugs

References

1. Whitaker-Brothers K, Uhrich KE (2006) Investigation into the erosion mechanism of salicylate-based poly (anhydride-esters). J Biomed Mater Res: Part A 76:470–473
2. Schmeltzer RC, Uhrich KE (2006) Synthesis and characterization of antiseptic-based poly(anhydride-esters). Polym Bull 57:281–291
3. Langer R (1986) Biopolymers in controlled release systems. In: Piskin E, Hoffmann A, Nijhoft M (ed) Polymer biomaterials. Springer, Netherlands
4. Kumar N, Langer R, Domb AJ (2002) Polyanhydrides: an overview. Adv Drug Deliv Rev 54:889–910
5. Schmeltzer RC, Jonhson M, Griffin J, Uhrich KE (2008) Comparison of salicylate-based poly(anhydride esters) formed *via* melt-condensation *versus* solution polymerization. J Biomater Sci Polymer Edn 19:1295–1306
6. Schmeltzer RC, Anastasiou TJ, Uhrich KE (2003) Optimized synthesis of salicylate-based poly (anhydride-esters). Polymer Bull 49:44–448
7. Gooch JW (2011) Differential scanning calorimeter. In: Goocj J (ed) Encyclopedia dictionary of polymers. Springer, Berlin/Heidelberg
8. Gooch JW (2011) Thermogravimetric analysis. In: Goocj J (ed) Encyclopedia dictionary of polymers. Springer, Berlin/Heidelberg
9. Kleinberg L (2012) Polifeprosan 20, 3.85 % carmustine slow-release wafer in malignant glioma: evidence for role in era of standard adjuvant temozolomide. Core Evid 7:115–130
10. Rosario-Meléndez R, Harris CL, Delgado-Rivera R, Yu L, Uhrich KE (2012) PolyMorphine, an innovative biodegradable polymer for extended pain relief. J Control Release 162:538–544

Polyaniline

Thomas P. Farrell[1] and Richard B. Kaner[2]
[1]Department of Chemistry and Biochemistry, California NanoSystems Institute, University of California, Los Angeles, CA, USA
[2]Department of Chemistry and Biochemistry, Materials Science and Engineering, California NanoSystems Institute, University of California, Los Angeles, CA, USA

Synonyms

Poly(*para*-phenyleneamineimine)

Definition

Polyaniline is the head-to-tail coupled polymer of aniline.

Introduction

The birth of the field of conducting polymers is normally associated with the discovery of high conductivity in doped polyacetylene in the 1970s, but the polymer of aniline (aminobenzene) has appeared in the scientific literature as far back as the 1860s [1]. These highly colored oligomers and polymers of anilines were originally used as the blue dyes for denim and other types of clothing. Their structures were unknown and the concept of electron delocalization in organic molecules had yet to be understood. When organic metals became a target for synthesis in the 1980s, the chemistry of polyaniline became relevant again, and materials' chemists pursued many avenues in attempting to produce an air-stable version of polyacetylene that might 1 day replace expensive metals and semiconductors in electronic devices. The advent of nanoscience in recent years has expanded the potential use of these conducting plastics, and polyaniline's proclivity to form nanostructures has made it one of the most widely studied nanostructured conducting polymers. The structure of polyaniline is shown below in Fig. 1.

A major limitation to the use of metallic materials is the difficulty in manipulating them under ambient conditions. Usually high heat, large electrical potentials, or large amounts of force are required to deposit traditional conductors into a desired shape or location. As polymers are readily processed by solution or in melts, this appeared as an obvious advantage for polymeric conductors. Unfortunately, the initial results with polyacetylene and early studies of the other major conducting polymer families including polyanilines, polythiophenes, and polypyrroles

indicated that these materials were essentially infusible and insoluble. Systematic studies, however, demonstrated that with careful control over the polymer chemistry and creative use of solvents and surfactants, some of these conducting materials could be deposited like conventional polymers from solution. Nanostructured conducting polymers further expanded the processing options of conducting polymers through the formation of charge-stabilized colloids, where the high surface area of nanomaterials and their tunable surface functionalities allowed scientists to form thin films of conducting materials from highly colored aqueous "inks." The leading conducting polymer from a commercial perspective is poly(3,4-ethylenedioxythiophene)-poly(styrenesulfonate) known as PEDOT:PSS. Essentially, the PSS dopant for this polythiophene derivative both imparts conductivity and enables this nanostructured conducting polymer to disperse in water. Polyaniline is also commercially available, and its nanostructured forms are dispersible in water.

Polyaniline is synthesized from the inexpensive aniline monomer through a simple oxidative process in aqueous media, meaning the overall process is scalable and relatively inexpensive. The impurities produced are easily washed away with water and alcohols, and the resulting material takes on a brilliant green color, making it a visually appealing material to investigate. One of the most interesting properties of polyaniline is the dependence of its resistivity on the local pH environment, where a small amount of acid or base can produce a resistivity change of 10 orders of magnitude or greater. While polyaniline in its undoped state displays resistivity in the insulating regime, doping with different acids has led to
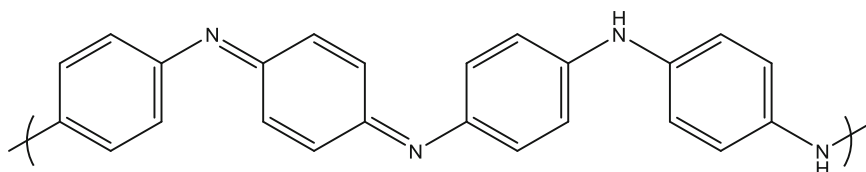
Polyaniline, Fig. 1 The repeat unit of polyaniline. Aromatic rings are linked in the para-positions by either amine or imine functional groups. The oxidation state shown above, with two imine nitrogens and two amine nitrogens per tetrameric repeat unit, is known as the emeraldine oxidation state

highly conductive materials with recent reports of essentially metallic polyaniline [2]. The combination of highly tunable electronic properties with a facility for nanostructure formation through relatively simple synthetic methods ensures that polyaniline will continue to be of great interest to the materials science community.

Synthesis of Polyanilines

Whereas many organic syntheses involve multiple steps and difficult purifications, the synthesis of all-organic polyaniline is a one-pot reaction that occurs rapidly, with purification steps that are straightforward and require minimal effort.

The reaction is initiated when aniline is exposed to an oxidizing agent and an electron is stripped from the aniline monomer, generating a radical cation that is very reactive. This aniline radical searches until it finds an equivalent molecule and the two link together. After losing two protons, the dimer re-aromatizes and the coupling process continues until a long-chain polymer is produced [3]. The oxidant that initiates this reaction can be either a chemical oxidant or the working electrode of an electrochemical cell. The scheme shown in Fig. 2 depicts aniline being oxidized by ammonium peroxysulfate in the presence of a strong acid (HA) which could be something as simple as hydrochloric acid. The resultant material is a chain of aromatic rings connected through the para-positions, via amine functional groups. The most appropriate way to depict the repeat unit in polyaniline is by showing the tetrameric unit, where three of the aromatic rings are benzenoid and the fourth is quinoid

(on the far right). This is indicative of the so-called emeraldine oxidation state, which is naturally occurring in wet-air conditions and appears either blue or green. As radical processes are known to be rapid and hard to control, initially there was uncertainty about the true structure of polyaniline and whether the oxidative process really produced such a homogeneous backbone structure. Confirmation of the structure was made through a very clever synthetic strategy (depicted in Fig. 3) where a condensation reaction was used to synthesize the ideal head-to-tail polymer poly(1,4-phenyleneamineimine) and characterization of the material produced a nearly identical spectroscopic signature to polyaniline [4].

As mentioned earlier, purification of polyaniline is straightforward since the product is insoluble in the polymerization media as well as in most common solvents. This allows for simple washing steps using various solvents to remove salts or short-chain oligomers that arise from chain termination steps, e.g., when two short chains link together and precipitate. Further purification and isolation of the material may involve a drying step so that the polymer can be further manipulated as a solid. Note that due to the hydrophilic nature of the basic functional groups on polyaniline's backbone, polyaniline is extremely hygroscopic, picking up over 5 wt% water from the air even in low humidity. Additionally, subtle modifications in the synthetic parameters can have a drastic effect on the resulting structure and properties of the material produced.

The traditional chemical method for making polyaniline consists of dropwise addition of an
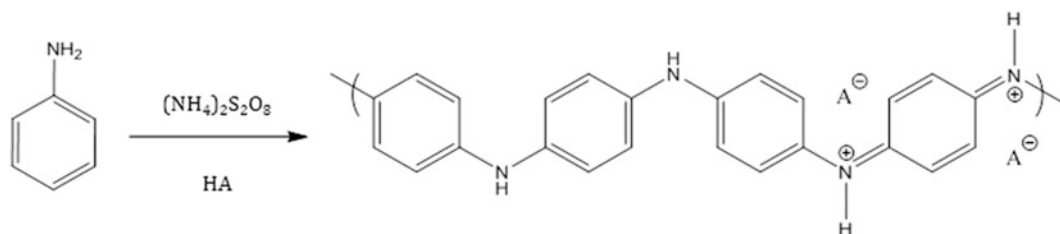
Polyaniline, Fig. 2 The chemical (or electrochemical) oxidation of aniline at low pH produces the doped, conductive form of polyaniline, depicted in the green emeraldine salt form
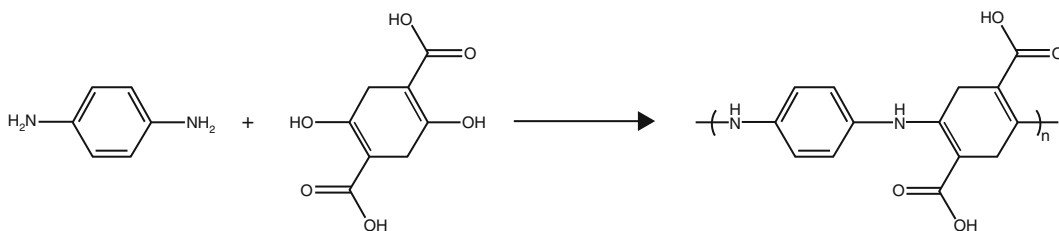
Polyaniline, Fig. 3 The Wudl-Honzl approach to make poly(*para*-phenyleneamineimine). Condensation polymerization at 60 °C produces the carboxylated polyaniline, which can be thermally de-protected to produce the leucoemeraldine analog of polyaniline. Exposure of this material to atmospheric oxygen converts the light gray product to a deep blue/black material via reflected light, similar in spectroscopic signature to conventionally synthesized polyaniline

oxidizing agent to an acidic solution of aniline at low temperature (1–5 °C) [5]. This low temperature and slow oxidant addition is meant to slow down the rapid oxidative polymerization in order to produce a more well-controlled, regular structure. A variation on this method involves performing the reaction at extremely low temperatures by suppressing the freezing point of the aqueous solution by adding a large quantity of salt (sometimes over 5 M) [6]. This method is generally accepted to produce a relatively high molecular weight polymer, approaching 160 kDa. Conversely, performing the reaction at room temperature causes the reaction to proceed rapidly, resulting in a lower molecular weight polymer, often less than 20 kDa [7]. Further modification of the polymerization conditions by including immiscible solvents or other additives as well as controlling mass transfer in the solution provides additional tools for tuning the structure, morphology, and resulting properties of the polymer.

Nanoparticle Formation

Many conducting polymers, including the original polyacetylene produced via Ziegler-Natta catalysis, possess interesting morphologies on the nanoscale. The emerging applications of nanomaterials make understanding the mechanisms and methods that produce these materials of great importance.

Most nanoparticle formation strategies are categorized primarily into two methods:

top-down and bottom-up. Since the individual polymers comprising conducting polymer nanomaterials are at most a few nanometers, all of the techniques for nanoparticle formation in polyaniline can be described as bottom-up. A better way to distinguish between these methods relies on the presence or absence of an external template to confer nanostructure. Templated synthesis requires a sacrificial nanomaterial such as a porous aluminum oxide, so that when polyaniline is synthesized, it occupies all of the pore space within the template. Removal of the template then affords polyaniline in the inverse morphology, nanowires in the case of aluminum oxide [8]. A clever technique using vanadium oxide nanowires as oxidant and hard template produces a coating of polyaniline around the inorganic nanowires. Dissolution of the oxide then produces nanotubes of polyaniline [9]. Organic materials can also be used as templates and removed in similar fashion. Molecular surfactants, capable of producing micelles of aniline within an aqueous phase, can confer their morphology upon the resulting polyaniline and are easily washed away [10]. Additionally, amphiphilic block copolymers or terpolymers can be used to produce various microporous morphologies where polyaniline nanostructures can deposit within the void space [11].

While templated methods of nanoparticle formation are attractive in that the homogeneity of the resulting polyaniline nanomaterials is as regular as the sacrificial template, the additional steps required in template removal can make the

P
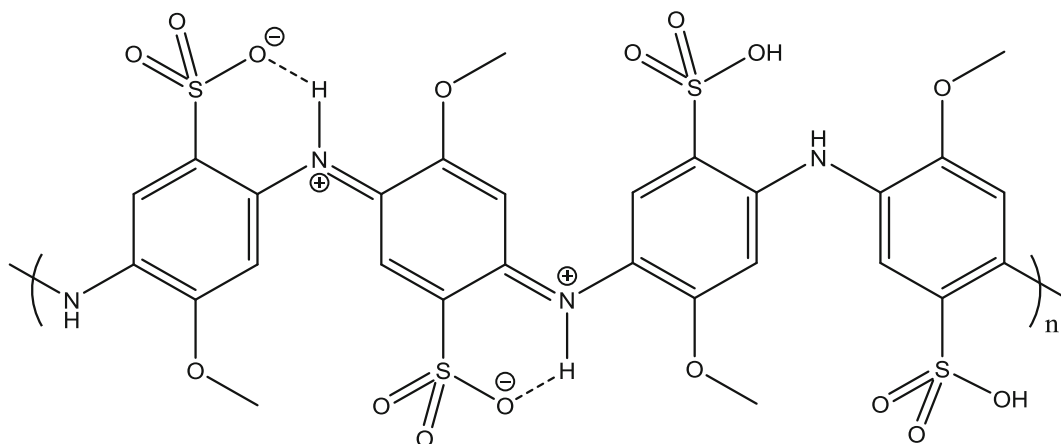
Polyaniline, Fig. 4 The repeat unit of poly (methoxyaniline sulfonate) (PMAS) shown in the emeraldine oxidation state. The sulfonic acid groups along the polymer backbone protonate the imine nitrogens to produce the conducting emeraldine salt form of polyaniline. The methoxy groups are required to increase electron density in the four-position on the ring during synthesis, as the sulfonic group is highly electron withdrawing

synthetic process cumbersome. One of the most versatile techniques for producing long nanowires for most polymers is electrospinning [3]. In this technique, a concentrated polymer solution is extruded through a small nozzle by the application of a high electric field strength. This technique relies on the ability to form concentrated solutions of polyaniline, which is not a trivial endeavor. The strong pi stacking and hydrogen bonding interactions present in polyanilines make them notoriously insoluble in common organic solvents. The insulating emeraldine base form of polyaniline can be processed from *N*-methylpyrrolidone at high concentrations, but is only metastable in solution unless secondary or tertiary amine cosolvents are used [12]. In order to process the conducting emeraldine salt form of polyaniline, the emeraldine base form must be combined with a Brönsted acid that confers solubility unto the polymer by behaving both as a dopant and as a surfactant. Acids such as camphorsulfonic acid and dodecylbenzenesulfonic acid are known for their ability to solubilize polyaniline in solvents such as *m*-cresol, chloroform, toluene, xylenes, and some concentrated organic acids [2].

The alternative strategy in solubilizing polyaniline is chemical derivation, where different functional groups are attached to the polymer backbone. These functional groups have the dual purpose of preventing strong interchain interactions and improving interactions with solvent molecules. Alkylated polyanilines can be processed from low-polarity organic solvents, and sulfonated polyaniline can be processed from aqueous systems. The structure of the water-soluble polymer, poly(methoxyaniline sulfonate), is shown in Fig. 4.

The other primary template-free method is in situ nanostructure formation during the polymerization process. This method takes advantage of the intrinsic morphology of these semirigid rod polymers and their propensity to form nanostructures. First, the electrochemical oxidation of aniline in hydrochloric acid has been shown to produce "spaghetti-like" materials on the electrode surface when the potential and current density at the working electrode is sufficient [2]. This straightforward process makes an excellent utilization of materials and deposits the polymer directly onto the substrate, eliminating the requirement for post-synthetic processing. Limitations of this technique include the requirement of the substrate to be electrically conducting as well as prospective complications in large-scale nanomaterial production.

Careful control over the chemical synthesis of polyaniline can also produce nanostructures. Analogous with electrochemical synthesis, the deposition parameters during synthesis are the determining factor as to whether a nanostructure will be produced. Although the monomer, aniline, is soluble in the polymerization media, as the reaction proceeds the oligomeric species reach a critical size and concentration, causing oligomers to stack together and form insoluble materials within the aqueous phase. The process of forming a new phase in an otherwise homogeneous system is referred to as nucleation. If the nucleation process occurs in a consistent manner for all nuclei, nanoparticle formation predominates [11]. The goal then is to select parameters that favor homogeneous nucleation. One of the first techniques developed in this light was the interfacial synthesis of polyaniline in an aqueous/organic system, where the oxidant is dissolved in the acidic aqueous medium and the monomer is in the organic phase. Oxidation and chain growth occur at the interface of the two liquids where monomer and oxidant interact. Presuming the right solvents are chosen, doped polyaniline nanofibers are produced, dispersing into the aqueous phase as a charge-stabilized colloid. Performing the synthesis in the presence of different acidic dopants produces nanofibers with controllable diameters [13]. Another technique for producing a homogeneous nucleation condition is by rapidly mixing two aqueous phases, one containing the monomer and the other the oxidant [14]. If the two solutions are rapidly combined and then allowed to sit under diffusion-limited conditions, all of the oxidant is consumed at the same time and a homogeneous dispersion of nanofibers result. It is worth noting that external forces such as shearing and agitation disrupt the nucleation conditions and nuclei form sequentially and eventually result in agglomerated structures [15].

Aniline Oligomers

Although not technically "polymeric materials," oligomeric anilines are proving to be very useful model materials for determining the relationship between the packing arrangement within nanostructured polyaniline and the resultant electronic properties [16]. In analogy with oligoacenes commonly used in small-molecule semiconductor applications, oligoanilines offer another method to process semiconductors from solution where the related polymeric material is difficult to process. Additionally, the fact that these oligomers can be produced as pure materials as opposed to polymers with varying polydispersity means less variability in batch-to-batch syntheses. There now exist many strategies for producing oligomers of aniline, ranging from oxidative coupling [17] to organometallic-catalyzed coupling [18] to the Moore-Honzl approach described earlier for the synthesis of poly(*para*-phenyleneamineimine) [4].

These well-defined oligomeric materials were previously found to be electrically insulating, lacking the long conjugation lengths that are generally associated with the long chains in conducting polymers. This was surprising, because when aniline oligomers reach a degree of polymerization of 8 (i.e., an octamer), the spectroscopic signatures are nearly identical to polyaniline and show the same reduction-oxidation peaks under cyclic voltammetry studies [19]. The limiting factor in conductivity in these materials turns out to be charge carrier hopping between conjugated segments [16]. Polyanilines have poorly defined structures/conformations in the solid state as they rapidly and irreversible precipitate during synthesis. If the stacking of these materials in the solid state can be improved, so then will the mobility of charge carriers. Recently it has been shown that the tetramer of aniline can be crystallized into well-defined nanowires, nanobelts, and nanoflowers that have unprecedentedly high conductivities. Whereas the mobility in these oligomers in the direction of the polymer chain is limited by the oligomer length, the mobility in two dimensions (charge hopping) is drastically improved due to the long-range ordering of these crystalline materials [16].

P

Applications of Polyaniline Nanomaterials

Charge-Stabilized Colloids

When polyaniline is placed in an acidic environment, the basic functional groups along the polymer backbone become protonated and positively charged quaternary nitrogen groups are produced (see Fig. 5 below). These positive charges are accompanied by the counter-anion of the protonic acid. Nanostructured polyaniline, a high surface area material, carries this charge on its surface producing a high charge to mass ratio. The electrostatic repulsive effect of these like charges between nanofibers allows the nanofibers to stay dispersed in solution despite their density being higher than the aqueous system they are dispersed in. This charge-stabilized colloid enables the processing of conducting polyaniline in aqueous systems where polyaniline is normally completely insoluble [20]. This innovation has opened the possibility of using aqueous-based coatings for a large range of applications where high surface area semiconductors offer operational advantage over more dense organic solvent-based analogs.

Immediate applications that arise from the water processability of these materials include coatings that previously could only be done using the organic solvents required for dissolving counterion-solubilized polyaniline. As mentioned earlier, the common organic solvents for processing the conducting form of polyaniline are toluene, chloroform, *m*-cresol, xylenes, and some halogenated organic sulfonic acids. All of these solvents will swell or dissolve most plastics. Therefore, an aqueous dispersion can be used to produce conductive coatings for antistatic applications where the insulating nature of plastics makes them vulnerable to charge buildup followed by short-circuiting or dielectric breakdown. Moderate levels of conductivity also can be used for electromagnetic interference shielding. With an increasing trend toward environmentally friendly water-based polymer coating systems, this aqueous dispersibility also opens the door to conducting polymer composites that leverage the conductivity of polyaniline and the bulk mechanical properties of conventional polymers.
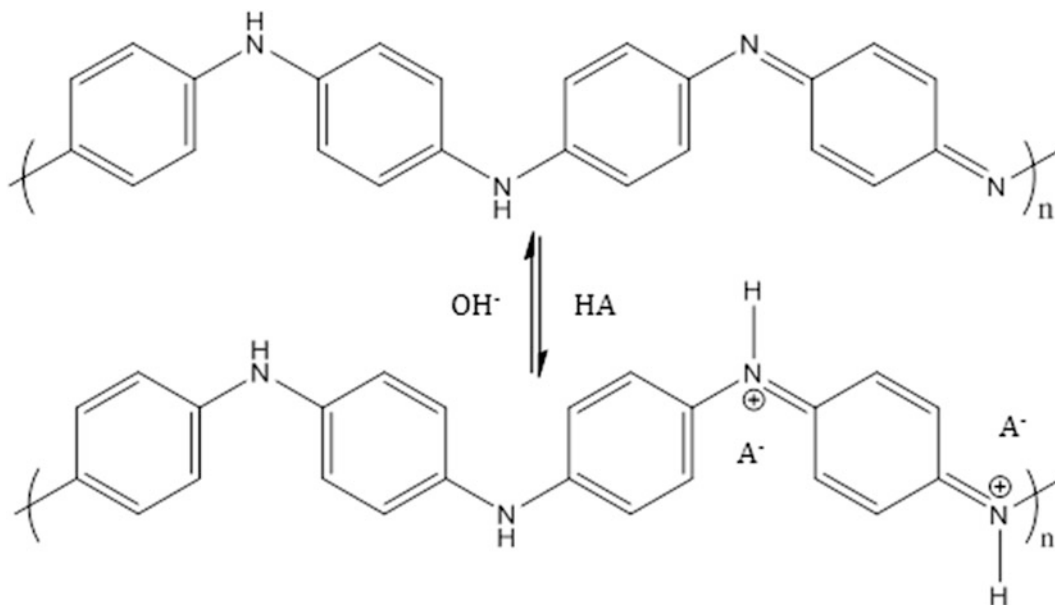
Polyaniline, Fig. 5 The imine nitrogens on the polyaniline backbone become protonated upon exposure to strong acids. This produces the emeraldine salt form of polyaniline that is conducting

Nanotechnology-Enabled Sensors

Since the doping process in polyaniline produces a change in resistivity over many orders of magnitude, polyaniline nanofibers may be an ideal active material for resistive-type sensors, known as chemiresistors. Although the most obvious method of detection in polyaniline resistive-type sensors is the doping/dedoping reaction, other processes such as reduction or oxidation, swelling by certain organic compounds, or polymer chain decoiling have been shown to affect the resistivity of polyaniline to a discernible degree [21]. In addition to being easily deposited upon an electrode array from an aqueous dispersion, these organic nanomaterial sensors can be operated at room temperature, whereas many inorganic semiconductors require elevated temperatures for efficient analyte detection [22].

The main physical advantage to using nanostructured polyaniline as opposed to conventional bulk polyaniline for sensing is that the nanostructured polyaniline has a high porosity that is easily accessible to gas molecules. When polyaniline is cast into a dense film from an organic solvent to be used as a sensor, the target analyte is required to dissolve and diffuse into the dense polyaniline active material before any sensor response is observed. For nanostructured polyaniline, the highly accessible pore space allows for much better mass transfer and access to the polymer/electrode interface that in turn produces a much faster response time. A typical nanostructured polyaniline with a diameter of 50 nm will have a surface area of around 50 m^2g^{-1}, whereas its dense film counterpart is limited to just the area of the film surface [14]. The effect of this surface area and porosity is dramatic. Upon exposure to acidic or basic vapors, a nanofiber chemiresistor has a response time over ten times faster than a conventional dense film chemiresistor. In addition to detecting strong acids and bases, chemical reactions can be used to generate strong acid by-products such as converting hydrogen sulfide to HCl using $CuCl_2$ that can dope polyaniline and register a significant response [21].

High Surface Area Electrodes

The same high surface area that makes polyaniline nanofibers useful for sensors can also make it useful in energy storage and conversion devices. While batteries do not require high surface area to achieve high energy storage density, supercapacitor energy storage density is largely influenced by the surface area of the electrode materials. Likewise, pseudo-capacitors benefit from high surface area, but now can take advantage of the reversible oxidation-reduction reactions present in the underlying chemical structure of polyaniline. Unlike other conducting polymers, polyanilines possess two reversible oxidative transformations as shown in Fig. 6.

This can be seen in the cyclic voltammogram of polyanilines, where instead of a single oxidation-reduction peak, two will be observed. A "pseudo-capacitive" device, using polyaniline nanomaterial electrodes, will therefore store charge both through the electrical double layer on the electrode surface and in redox reactions within the bulk of the electrode material itself.

Inorganic-Organic Nanocomposites

Another application of these high surface area materials is to act as functional scaffolds for inorganic nanoparticles. The facile and reversible oxidation and reduction of polyaniline allows the polymer to behave as either an oxidizing agent or a reducing agent when combined with different materials. Treatment of polyaniline nanofibers with metal salts allows polyaniline to act as a reducing agent that donates electrons to the oxidized metal ion, causing deposition of metallic particles on top and within the polyaniline nanofiber network [21]. The resulting inorganic-organic nanocomposite materials maintain the high surface area and dispersibility of the original polyaniline nanofibers and thus can be deposited and used as sensor materials or other electronically active materials. Gold-decorated polyaniline nanofibers have been explored for use in bistable memory devices [23].

Polyaniline nanofiber composites with metal nanoparticles can also be used in heterogeneous catalysis. Reduction of palladium(II) salts by polyaniline produces very small particles of

P
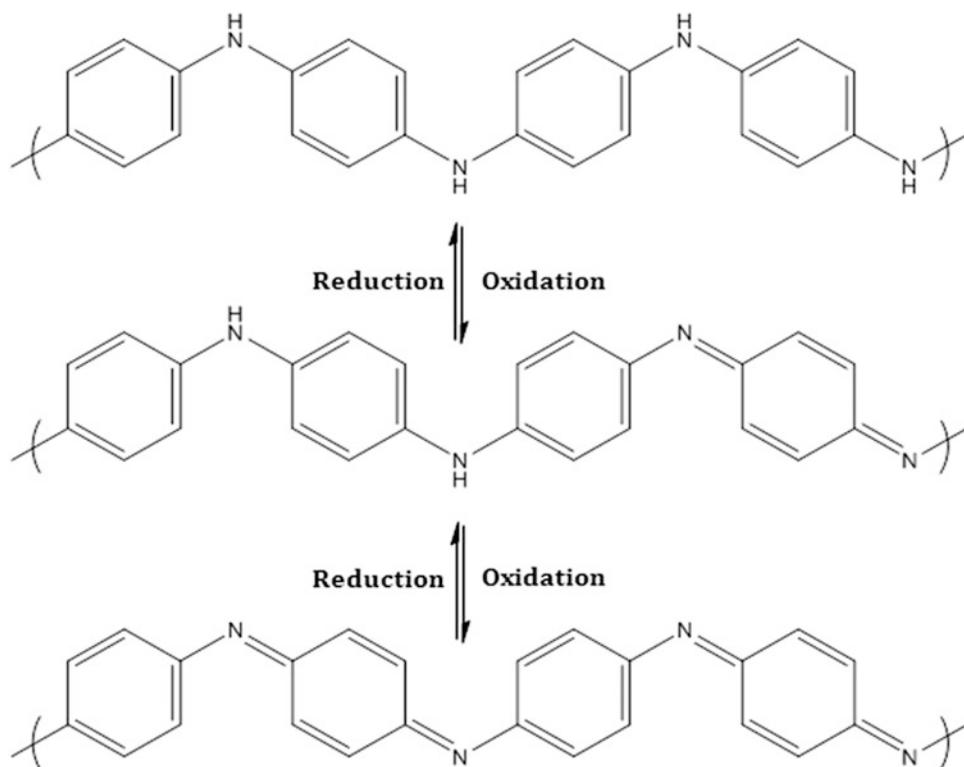
Polyaniline, Fig. 6 The repeat unit of the three major oxidation states of polyaniline. *Top* to *bottom*: leucoemeraldine (fully reduced), emeraldine (half oxidized, water stable and air stable), and pernigraniline (fully oxidized). The chemical structures each depict a deprotonated base form of polyaniline
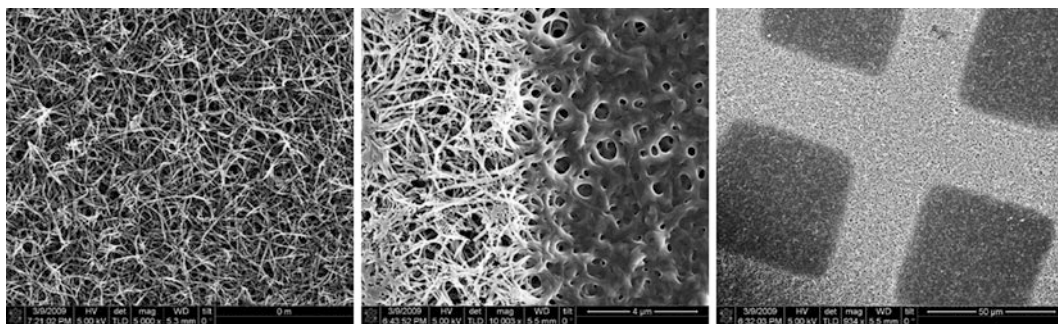
Polyaniline, Fig. 7 Scanning electron micrographs showing the morphology of polyaniline nanofibers synthesized by the rapid mixing synthesis in the presence of the aniline dimer (*left*). If exposed to an intense flash of light, polyaniline nanofibers weld together and lose their high surface area and nanofibrillar morphology (*center*). Opaque materials can be used to form a patterned photomask. Upon exposure to high-intensity light such as a camera flash or laser, exposed areas form a dark, welded, insulating material, and shaded areas remain conductive and nanofibrillar (*right*)

palladium(0), the catalyst used for carbon-carbon bond formation between aromatic molecules in Suzuki coupling reactions [24]. Since polyaniline nanofibers form a dispersion and not a solution, centrifugation can be used to pull the dense fibers out of the dispersion in order to recover the product of coupling reactions without time-consuming extraction steps.

Flash Welding

Polyaniline nanofibers are known to undergo a morphological transformation upon exposure to an intense pulse of light such as a camera flash. Examination of the polymeric nanostructure prior to and after exposure to a camera flash shows the disappearance of nanofibers due to a photothermal phenomenon. The process is believed to be a result of the low fluorescence efficiency of polyaniline and its propensity to cross-link. Figure 7 shows how the morphology of polyaniline nanofibers is altered by flash welding. This technique can be used to create patterns and to form simple actuators [25]. While melt-induced flash welding appears to be unique to conducting polymers, understanding this technique may allow its application to other nanostructured organic materials.

Conclusions

Strategies for producing and implementing nanostructured polyaniline continue to be investigated within the materials community. Properties such as high surface area and processability from aqueous systems allow these materials to be implemented successfully into a wide range of applications. Further innovation and fine-tuning of chemical structure and morphology may see polyaniline replacing traditional materials in certain places or even opening the door to new, yet to be discovered, applications.

Related Entries

▶ Conducting Polymers

References

1. Letheby H (1862) On the production of a blue substance by the electrolysis of sulphate of aniline. J Chem Soc 15:161–163
2. Lee K, Cho S, Park HS, Heeger AJ, Lee CW, Lee HS (2006) Metallic transport in polyaniline. Nature 441:65
3. Wallace GG, Spinks GM, Kane-Maguire LAP, Teasdale PR (2009) Conductive electroactive polymers: intelligent polymer systems, 3rd edn. CRC Press, Boca Raton
4. Vachon D, Angus RO Jr, Lu FL, Nowak M, Liu ZX, Schaffer H, Wudl F, Heeger AJ (1987) Polyaniline is poly-para-phenyleneamineimine- Proof of structure by synthesis. Synth Met 18:297
5. MacDiarmid AG, Chiang JC, Richter AF, Somarisi NLD (1987) In: Alcacer L (ed) Conducting polymers, special applications. Reidel, Dordrecht, p 105
6. Min G (2001) Inorganic salts effect on the properties of polyaniline. Synth Met 119:273
7. Adams PN, Laughlin PJ, Monkman AP, Kenwright AM (1996) Low-temperature synthesis of high molecular weight polyaniline. Polymer 37:3411
8. Martin CR (1995) Template synthesis of electronically conductive polymer nanostructures. Acc Chem Res 28:61
9. Zhang XY, Goux WJ, Manohar SK (2004) Synthesis of polyaniline nanofibers by "nanofiber seeding". J Am Chem Soc 126:4502
10. Li GC, Zhang ZK (2004) Synthesis of dendritic polyaniline nanofibers in a surfactant gel. Macromolecules 37:2683
11. Tran HD, Li D, Kaner RB (2009) One-dimensional conducting polymer nanostructures: Bulk synthesis and applications. Adv Mater 21:1487–1499
12. Norris ID, Mattes BR (2007) Conducting polymer fiber production and applications. In: Skotheim T, Reynolds J (eds) Handbook of conducting polymers, vol 2, 3rd edn. Marcel Dekker, New York
13. Huang J, Kaner RB (2004) A general chemical route to polyaniline nanofibers. J Am Chem Soc 126:851
14. Huang J, Kaner RB (2004) Nanofiber formation in the chemical polymerization of aniline: A mechanistic study. Angew Chem Int Ed 43:5817
15. Huang J, Virji S, Weiller BH, Kaner RB (2003) Polyaniline nanofibers: Facile synthesis and chemical sensors. J Am Chem Soc 125:314
16. Wang Y, Tran HD, Liao L, Duan X, Kaner RB (2010) Nanoscale morphology, dimensional control, and electrical properties of oligoanilines. J Am Chem Soc 132(30):10365–10373
17. Zhang WJ, Feng J, MacDiarmid AG, Epstein AJ (1997) Synthesis of oligomeric anilines. Synth Met 84:119–120
18. Sadighi JP, Singer RA, Buchwald SL (1998) Palladium-catalyzed synthesis of monodisperse, controlled-length, and functionalized oligoanilines. J Am Chem Soc 120:4960
19. Lu FL, Wudl F, Nowak M, Heeger AJ (1986) Phenyl-capped octaaniline (COA)- An excellent model for polyaniline. J Am Chem Soc 108:8311
20. Li D, Kaner RB (2005) Processable stabilized-free polyaniline nanofiber aqueous colloids. Chem Commun 26:3286
21. Virji S, Fowler JD, Baker CO, Huang J, Kaner RB, Weiller BH (2005) Polyaniline nanofiber composites with metal salts: Chemical sensors for hydrogen sulfide. Small 1:624

P

22. Huang J, Kaner RB (2007) Polyaniline nanofibers: synthesis, properties, and applications. In: Reynolds J, Skotheim T, Elsenbaumer R (eds) Handbook of conducting polymers, vol 1, 3rd edn. Marcel Dekker, New York
23. Tseng RJ, Huang J, Ouyang J, Kaner RB, Yang Y (2005) Polyaniline nanofiber/gold nanoparticle nonvolatile memory. Nano Lett 5:1077
24. Gallon BJ, Kojima RW, Kaner RB, Diaconescu PL (2007) Palladium nanoparticles supported on polyaniline nanofibers as a semi-heterogeneous catalyst in water. Angew Chem Int Ed 46:7251
25. Baker CO, Shedd B, Innis PC, Whitten PG, Spinks GM, Wallace GG, Kaner RB (2008) Monolitic actuators from flash-welded polyaniline nanofibers. Adv Mater 20:155

Polyaryletherketone

Osamu Urakawa
Department of Macromolecular Science,
Graduate School of Science, Osaka University,
Toyonaka, Osaka, Japan

Synonyms

Aromatic polyetherketone; PAEK

Definition

Polymers in which phenyl rings, ethers, and ketones are linearly connected by covalent bonds.

Introduction

Polyaryletherketones (PAEKs) are generally named in terms of "E" and "K" which represents the sequence of ether and ketone groups, respectively, in the repeating units of polymers. The most common ones are polyetherketone (PEK), polyetheretherketone (PEEK), polyetherketoneketone (PEKK), polyetheretherketoneketone (PEEKK), and polyetherketoneetherketoneketone (PEKEKK), all of which are produced commercially. Their structures are shown in Fig. 1.

Manufacturing of Polyaryletherketones

PAEKs can be made by two general routes: nucleophilic reaction and electrophilic reaction [1–4]. In both cases the important point for the homogeneous reaction is to avoid the crystallization and precipitation of polymers in solution during the reaction.

Formation of the ether link is achieved through the nucleophilic reaction. As an example, Fig. 2 shows the synthetic scheme of PEEK from 4,4′-difluorobenzophenone (DFB) and hydroquinone (HQ). The alkali metal (sodium carbonate) deprotonates the HQ to give an HQ salt. The HQ anion then attacks the DFB in a nucleophilic manner resulting in the formation of an ether bond. This reaction is conducted typically at around 320 °C in polar aprotic solvents such as diphenyl sulfone to avoid the precipitation of the produced polymers due to crystallization. Polymerized product is then isolated by removal of alkali metal fluoride and the solvent.

PEKs are synthesized from 4,4′-dihydroxybenzophenone (DHB) and DFB (two-monomer route) in the same way shown in Fig. 2. Alternatively, single-monomer route using 4-fluoro-4′-hydroxybenzophenone as a starting material is possible [4]. However, in this reaction, a branching structure is involved since a carbanion is formed by losing a proton bonded to the ortho-position of the fluoro group. Therefore, two-monomer route is usually preferred.

PEEKK and PEKEKK are produced by a nucleophilic way from 1,4-bis(4-fluorobenzoyl) benzene (FBB) and HQ and from FBB and DHB, respectively. PEKK is synthesized from 1,4-bis (4-hydroxybenzoyl)benzene and FBB.

Formation of the carbonyl link by electrophilic acylation is shown in Fig. 3. This synthesis is conducted by the Friedel-Crafts polycondensation.

For example, PEK is prepared from 4-phenoxybenzoyl chloride, and PEKK is from diphenyl ether and terephthaloyl chloride and AlCl$_3$ as a catalyst.

Polyaryletherketone, Fig. 1 Structures of PAEKs
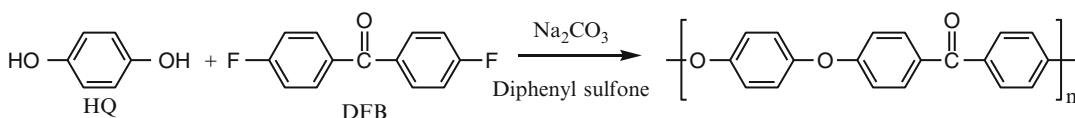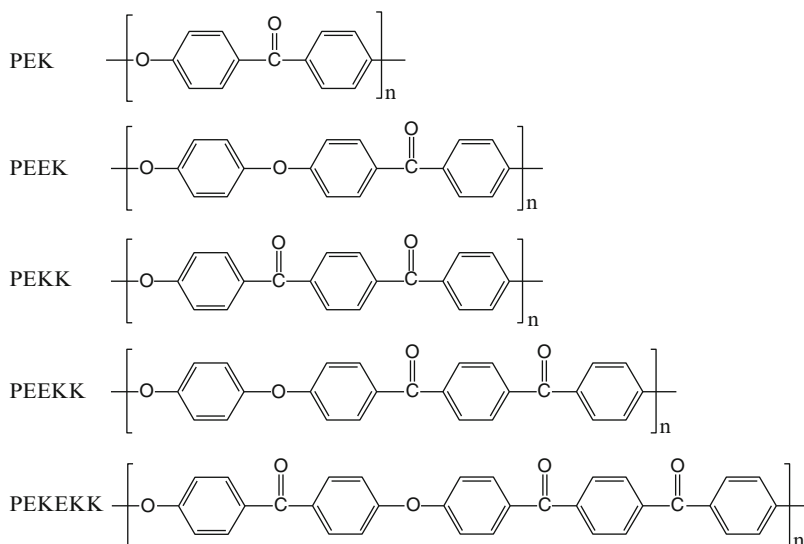
Polyaryletherketone, Fig. 2 Synthetic route of PEEK
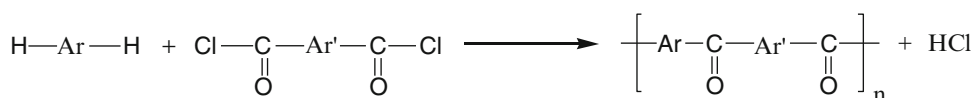
Polyaryletherketone, Fig. 3 Friedel-Crafts polycondensation

Thermal Properties

Most PAEKs are semicrystalline, melted process-able materials which combine very high temperature performance with chemical resistance, low flamma-bility, rigidity, toughness, excellent wear, and fatigue resistance. Table 1 shows the glass transition and melting temperatures of PAEKS [2, 4, 5].

Chain polarity and rigidity increase with the presence of ketone units and thus glass transition temperature (T_g) increases with increasing ketone to ether (K/E) ratio as can be seen in Table 1. For linear, all para-substituted chains melting tem-perature also increases with K/E ratio, and the

Polyaryletherketone, Table 1 Glass transition and melting temperatures

PAEKs (all para substituted)	T_g/°C	T_m/°C
PEEK [5]	143	334
PEK [4]	154	367
PEEKK [5]	158	363
PEKEKK [5]	161	377
PEKEKK [4]	–	383
PEKK [5]	165	386

T_g/T_m ratio is ∼2/3. By incorporating non-para or non-crystallizable units in the polymer backbone, the melting point is purposely reduced without a large effect on T_g. This method is used to increase

the easiness of material processing. For instance, PEKK products are synthesized from diphenyl ether and the mixture of terephthaloyl chloride and isophthaloyl chloride with $AlCl_3$ to improve the processability through the reduction of the crystallinity.

Further increase of T_g can be achieved by the incorporation of sulfone groups into the backbone of the PAEK polymer chain [2, 6]. For example, by adding the monomer shown in Fig. 4 to a standard PEK polymerization, T_g increases in excess of 175 °C.

Mechanical Properties

Table 2 lists the typical mechanical properties measured at room temperature for PAEKs [2]. Three PEEKs produced by Victrex Ltd. are included here to illustrate the effect of molecular weight [7]. The number in the code name is roughly proportional to the viscosity so that the larger number corresponds to the higher molecular weight. Increase of the molecular weight results in the higher values of elongation to break and notched Izod impact strength. Contrary, tensile strength and flexural modulus are insensitive to the molecular weight. These properties of PAEKs decrease substantially above the T_g but useful residual values are maintained close to T_m. For example, tensile strength and flexural modulus of PEEK (450G) at 250 °C become

12 MPa and 0.3 GPa, respectively, but are still high. From the large difference of unnotched and notched Izod impacts, it can be said that PAEKs are notch sensitive.

The processing conditions used to mold PAEKs is also important, because it can influence the crystallinity, and hence the mechanical properties. For example, annealing of PEEK at 220 °C results in the maximum growth rate of crystallization. In PEEKs the degree of crystallinity is typically in the range of 30–35 %.

Other Properties

Crystallites in PAEKs impart excellent solvent resistance. For example, PEEK is insoluble in all common solvents. It dissolves only in strong acids, such as concentrated sulfuric acid and hydrofluoric acid at room temperature. This is due to protonation of carbonyl groups, but in other cases, there is actual reaction: sulfonation of aromatic rings. Another reagent to attack PAEKs is halogen (bromine, chlorine, and fluorine) which halogenates aromatic rings.

PAEKs have a high volume resistivity and a low dielectric dissipation factor. These properties are retained over a wide range of temperature up to the T_g. Electrical properties of PAEKs are listed in Table 3 [7, 8]. High level of dielectric strength and low loss tangent make PAEKs excellent insulating materials.

Applications

Because of its robustness and excellent wear performance, PAEKs are used in demanding applications, including bearings, piston parts,

Polyaryletherketone, Fig. 4 Monomer used to increase T_g

Polyaryletherketone, Table 2 Mechanical properties of PAEKs [2]

	PEEK 90G	PEEK 150G	PEEK 450G	PEK	PEKEKK	PEKK
Tensile strength/MPa	110	110	100	110	115	110
Tensile elongation/%	15	25	45	20	20	12
Flexural modulus/GPa	4.3	4.3	4.1	4.1	4.1	4.5
Unnotched Izod impact/kJm^{-2}	No break	No break	No break		No break	
Notched Izod impact/kJm^{-2}	4.5	5.0	7.5	6.0	6.0	7 [8]

Polyaryletherketone, Table 3 Electric properties of PAEKs

	PEEK [7]	PEK [7]	PEKEKK [7]	PEKK [8]
	VICTREX PEEK 450G	VICTREX HT G45	VICTREX ST G45	Infinite polymer system II PPL-C4050
Dielectric strength/kV mm^{-1} (IEC 60243-1)	23	23	23	23.6 (ASTM D149)
Dielectric constant (1 kHz at 23 °C) (IEC 60250)	3.1		3.0	3.3 (ASTM D150)
Loss tangent (1 MHz at 23 °C) (IEC 60250)	0.004		0.004	0.004 (1 kHz) (ASTM D150)
Volume resistivity/Ω cm (IEC 60093)	10^{16}	10^{16}	10^{16}	10^{16} (ASTM D257)

compressor plates, pump impellers, and valve linings. For aerospace applications, PAEK has been replacing metals and traditional composites because of its lightweight, resistance to the harsh environments, reduced manufacturing costs, and excellent processing flexibility. Electrical applications range from wire coating to semiconductor wafer carriers which need abrasion resistance, chemical resistance, and good load bearing properties at high temperature. Low level of loss tangent is of particular importance for silicon chip manufacture. PAEKs are also used as medical implants such as spinal fusion devices and reinforcing rods.

References

1. Parker D, Vussink J, Grampel HT, Wheatley GW, Dorf EU, Ostlinning E, Reinking K, Schubert F, Junger O (2012) Polymers, high-temperature. In: Ullmann's encyclopedia of industrial chemistry (online version). Wiley-VCH, Weinheim
2. Kemmish D (2010) Update on the technology and applications of polyaryletherketones. iSmithers, Shropshire
3. Kemmish D (1995) High performance engineering plastics (Rapra review reports). Para Technology, Shropshire
4. Attwood TE, Dawson PC, Freeman JL, Hoy LRJ, Rose JB, Staniland PA (1981) Synthesis and properties of polyaryletherketones. Polymer 22:1096–1103. doi:10.1016/0032-3861(851)90299-8
5. Shibata M, Yosomiya R, Wang J, Zheng Y, Zhang W, Wu Z (1997) Relationship between molecular structure and thermal properties of poly(aryl ether ketone)s. Macromol Rapid Commun 18:99–105. doi:10.1002/marc.1997.030180205
6. Kemmish DJ, Newton AB, Staniland PA (1990) VICTREX MFG LTD EP0397356 B1
7. Victrex plc, Datasheets (2014) http://www.victrex.com/en/datasheets/. Accessed 22 Jan 2014
8. Merle Bell, Daniel Bagley (2003) Greene, Tweed Of Delaware, Inc. US20030032339 A1

Polycarbazoles

Sung Ju Cho
Department of Chemistry, Western University, London, ON, Canada

Synonyms

Conjugated polymers; Light-emitting diodes (LED); Organic solar cells; Synthesis

Definition

Carbazole is a tricyclic fused aromatic hydrocarbon consisting of two benzene rings fused to a pyrrole ring. Polycarbazoles are carbazole-based polymeric materials which have potential applications in organic electronic devices such as light-emitting diodes (LEDs) and organic solar cells.

Introduction

Carbazole **1** may be considered either as a tricyclic fused aromatic hydrocarbon consisting

P

of two benzene rings fused to a pyrrole ring or as a bridged biphenylene system similar to fluorene but with a nitrogen bridge as compared to a carbon bridge (Fig. 1). The standard numbering of the positions is the same in the two systems as shown with the carbazole nitrogen being sometimes referred to as the 9-position. While carbazole is isoelectronic with fluorine, the presence of the electron rich nitrogen gives it a higher HOMO energy which makes it more readily oxidizable and a better hole acceptor than fluorine. Carbazole derivatives including polycarbazoles have been used like their fluorene analogues in electronic devices such as light-emitting diodes (LEDs) and solar cells [1–5]. The main differences between the properties of carbazole- and fluorene-based materials arise from the higher HOMO energies and better hole-accepting abilities of the carbazoles and in the stability of the nitrogen toward oxidation; the 9-position of fluorene is readily oxidized, which affects the emission color of fluorene-based materials in LEDs.

The presence of the *ortho-/para*-directing activating nitrogen also makes the chemistry of

carbazole significantly different from that of fluorene. Whereas fluorene undergoes electrophilic substitution at the 2,7-positions, carbazole reacts preferentially at the 3- and 6-positions or if those are blocked then at the 1- and 8-positions. In addition to substitution of the benzene rings, attachment of aryl groups at the nitrogen is generally straightforward using aryl amination chemistry. As a result, four types of conjugated polycarbazoles are possible (Fig. 2) with respectively 3,6- 1,8-, 2,7-, and 3,9-substituted carbazoles of which only the 2,7-substituted carbazoles are inaccessible from carbazole and must be made by total synthesis. The poly (2,7-carbazole)s retain all-carbon conjugation, with conjugation in the others going through the nitrogen bridgehead atom. Because of the electron-rich nature of the 3- and 6-positions in 2,7-carbazole derivatives including polymers, they are susceptible to degradation arising from oxidation at these positions during passage of charge through them as occurs in devices such as LEDs. This can be overcome using ladder-type polymers in which the carbazoles are doubly linked through both the 3,6- and the 2,7-positions. These materials retain the through-carbon conjugation seen in the 2,7-carbazole-based polymers, but the substituted 3- and 6-positions resist oxidation there. These structures are attractive candidates for optoelectronic device materials since the rigid structure of ladder-type conjugated polymers usually results in small Stokes' shifts and sharply resolved

Polycarbazoles, Fig. 1 Structure of carbazole and fluorene
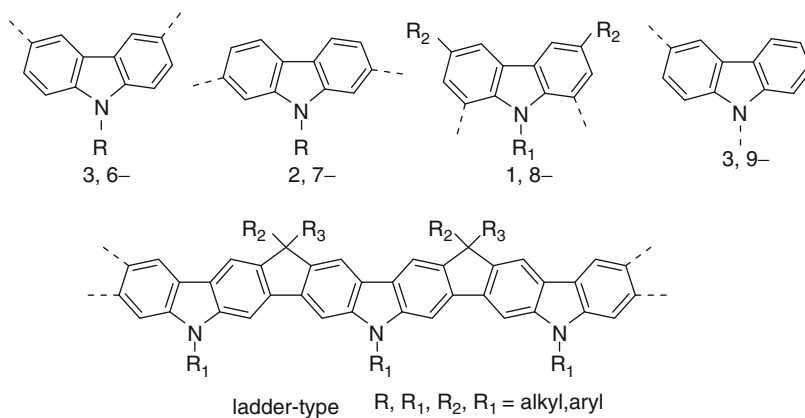
Polycarbazoles, Fig. 2 Structure of polycarbazoles

**Polycarbazoles,
Fig. 3** Synthesis of poly
(3,6-carbazole)s via
oxidative polymerization
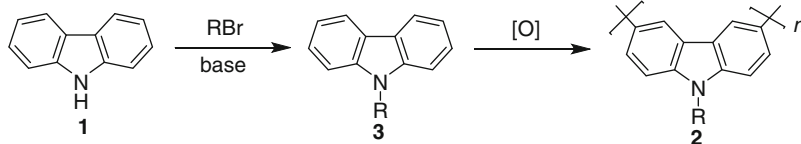
**Polycarbazoles,
Fig. 4** Synthesis of poly
(3,6-carbazole)s via
Yamamoto polymerization
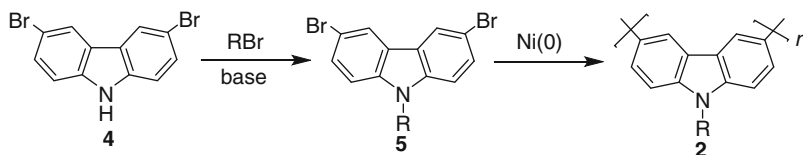
vibronic features as well as high luminescence efficiencies.

Synthesis

Polymers, including copolymers, containing carbazole units in the main chain have been prepared by a variety of methods of which transition metal-mediated cross-coupling reactions have been the most successful. The properties of these materials and thus their potential as active materials in a variety of optoelectronic devices depend crucially upon whether the carbazole units are linked through the 3,6-, 1,8-, 2,7-, or 3,9- positions. As mentioned above, the 2,7-carbazole units are not accessible from carbazole and are made in a short high-yielding total synthesis from a commercially available material, while the other units can be made in a few high-yielding steps from the readily available carbazole. Ladder-type polycarbazoles have been prepared in which the units are linked simultaneously through both the 2,7- and 3,6-positions and are made by routes involving precursor poly(2,7-carbazole)s.

Poly(3,6-carbazole)s

Poly(3,6-carbazole)s are readily synthesized starting from carbazole. In order to obtain solubility, an alkyl group must be attached at the nitrogen. The synthesis of poly(N-alkyl-3,6-carbazole)s **2** appears possible in two steps starting from the alkylation of carbazole **1** (Fig. 3) with an alkyl halide and base (potassium carbonate, sodium hydride, and sodium hydroxide have all

been used for this reaction) followed by oxidative polymerization of the resulting N-alkylcarbazole **3**. However, to date oxidation of **3** is reported to produce only a mixture of oligomers consisting mainly of the dimer with small amounts of higher oligomers [6].

As a result, polymers are made starting from the commercially available 3,6-dibromocarbazole **4** (Fig. 4). Alkylation of this gives the monomers **5** [7], which can then be reductively polymerized to the desired polymers **2**, either by electrochemical reduction using catalytic nickel(II) [8] or by a Yamamoto-type polycondensation using stoichiometric amounts of a commercially available nickel(0) reagent [7]. The former produces polymers of low molar mass (ca. 3 kDa) corresponding to only 15–20 units. Using standard Yamamoto reaction conditions in which the monomer is added to the nickel(0) complex also produces relatively low molar masses (<10 kDa), but by reversing the order of addition of reagents, polymers with number-average molar masses of >50 kDa can be obtained. Using branched alkyl chains increases the solubility of the polymers and thus gives higher molar mass polymers. Suzuki or other cross-coupling reactions of **5** can also be performed to make either the homopolymers **2** or a wide range of alternating copolymers [3]. The polymers **2** obtained by Suzuki condensation of **5** with a carbazole-3,6-bisboronate are of only moderate molar mass (<10 kDa) [9], so the Yamamoto procedure is to be preferred, despite the cost of the reagent, as it involves fewer steps and can produce higher mass polymers.

P

Polycarbazoles,
Fig. 5 Synthesis of poly
(1,8-carbazole)s via
Yamamoto polymerization
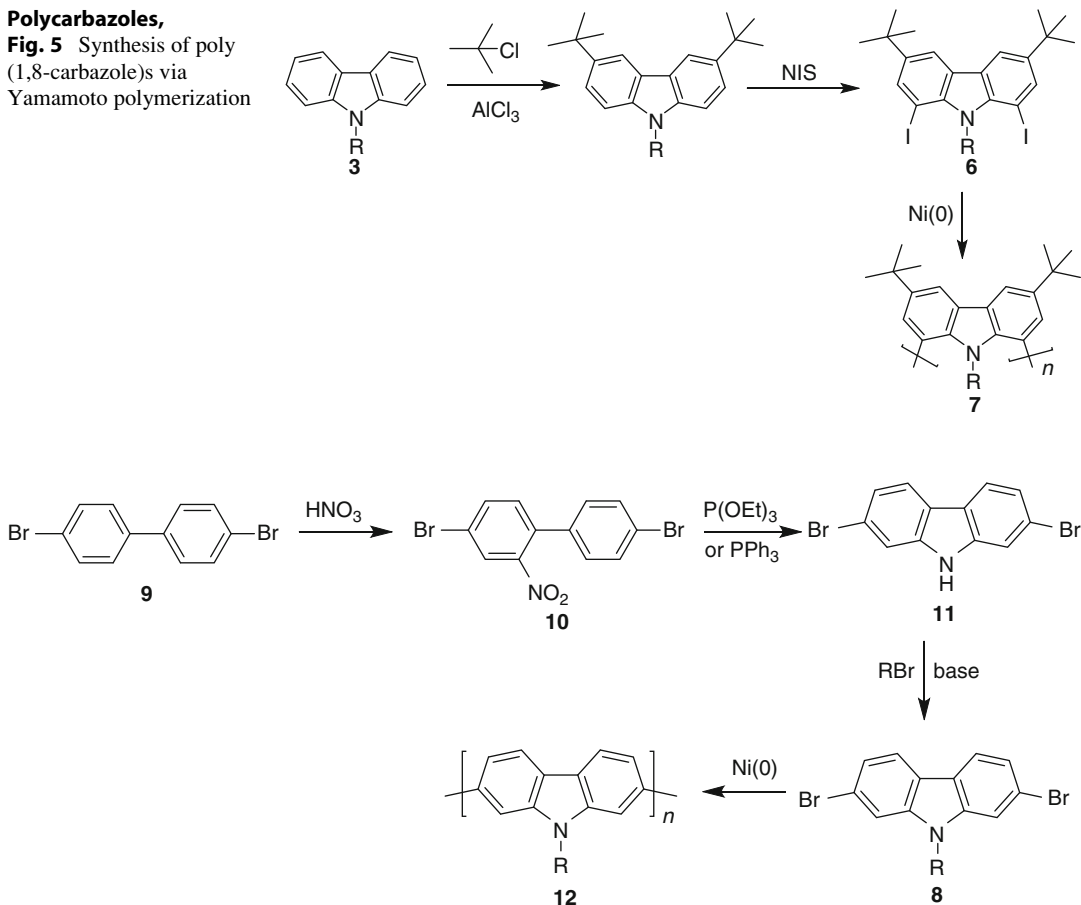
Polycarbazoles, Fig. 6 Synthesis of poly(2,7-carbazole)s from dibromobiphenyl **9**

Poly(1,8-carbazole)s

To make 1,8-substituted carbazoles, one must first substitute the more sterically accessible 3- and 6-positions, as shown in Fig. 5 for the synthesis of the 1,8-diiodide **6** in good yield from *N*-alkyl carbazole **3** [10]. Reductive coupling of this monomer under standard Yamamoto conditions then produces a homopolymer **7**, whose low molar mass ($M_w = 1.4$ kDa) indicates that it is an oligomer [11]. This is presumably because of the steric congestion at the 1,8-positions due to the presence of the nearby alkyl chain. Higher molar mass copolymers are obtainable by coupling **6** with other units by Suzuki, Sonogashira, or other cross-coupling reactions, but here also the molar masses are only moderate (<10 kDa). The steric repulsion at the 1- and 8-positions also leads to torsion

along the polymer chain so these materials show absorption edges in the blue region of the spectrum while their emission is blue-green as they emit in both the blue and green regions of the spectra.

Poly(2,7-carbazole)s

Unlike the previous two classes of polymers, the monomers for poly(2,7-carbazole)s 2,7-dihalocarbazoles, such as the dibromide **8**, have to be made by total synthesis. The most efficient synthesis of **8** shown in Fig. 6 requires only three high-yielding steps from commercially available dibromobiphenyl **9** [12]. The key step is the reductive ring closure of the nitrobiphenyl **10** to form the dihalocarbazole **11**. This was performed by the Cadogan method using triethylphosphite [13] until a new procedure using
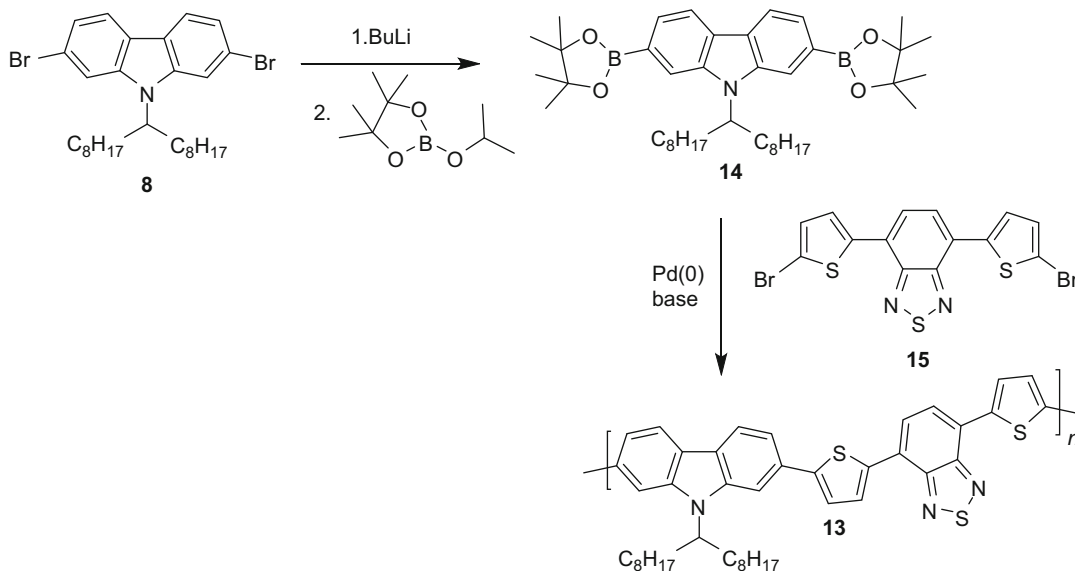
Polycarbazoles, Fig. 7 Synthesis of benzodithiazole copolymer **13** from 1,7-dibromocarbazole **8**

triphenylphosphine was introduced [14]. This method is more convenient as the phosphine reagent is less toxic and it is frequently higher yielding than the Cadogan method. Also, the phosphine oxide byproduct is more easily removed from the reaction mixture. Alkylation of **11** using an alkyl halide or tosylate and base (sodium hydride or potassium carbonate have both been used) then gives the desired monomer **8** [12, 15]. The polymers **12** are then readily accessible by Yamamoto polycondensation [16, 17]. To obtain high molar masses, it has been found necessary to use long preferably branched alkyl chains, which make the polymers readily soluble.

The carbazole-based polymer which has to date demonstrated the highest efficiency (>6 %) in solar cells is the benzodithiazole copolymer **13** whose synthesis is shown in Fig. 7 as an illustration of the synthesis of such copolymers in general [15]. The *N*-alkylcarbazole **8** is converted into the bisboronate **14** by lithiation followed by addition of a boron-pinacol ester. This is then reacted with one equivalent of the dihalide **15** to produce the alternating copolymer **13**. By maintaining strict control of the relative stoichiometry of the two reagents, number (M_n) and weight-averaged (M_w) molecular masses of

37 and 73 kDa respectively were obtained. By further optimization, the molar masses might be improved and/or the polydispersity lowered, which is favorable for controlling polymer properties and optimizing device performance.

The electrochemical stability of poly(2,7-carbazole)s is questionable as the high electron density at the free 3- and 6-positions makes oxidation at these sites facile, leading to possible cross-linking or other reactions through the resulting cations. The stability of the *N*-alkyl groups is also suspect, and it is thought that *N*-aryl carbazoles might be more stable. Arylation of the nitrogen is possible through either copper-mediated Ullmann coupling or palladium-catalyzed Buchwald-Hartwig aryl amination methods. An aryl iodide is needed to arylate 2,7-dibromocarbazole as the more reactive iodide can be reacted under mild conditions without risk of self-condensation of the carbazole. The synthesis of an arylcarbazole-based copolymer **16** is shown in Fig. 8 as illustrative of the methods used. Coupling of dibromocarbazole **11** with 3,5-dimethoxyiodobenzene **17** catalyzed by copper(I) produces the *N*-arylcarbazole in good (73 %) yield [18]. Longer alkyl chains were introduced to improve the solubility of the final product.
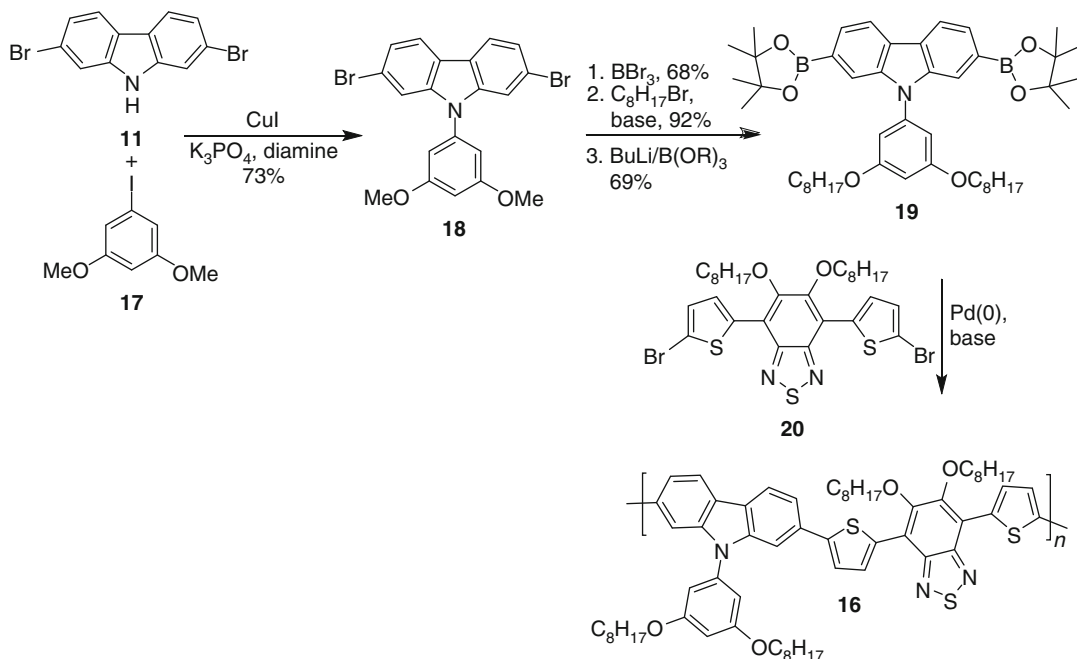
Polycarbazoles, Fig. 8 Synthesis of copolymer of 9-arylcarbazole
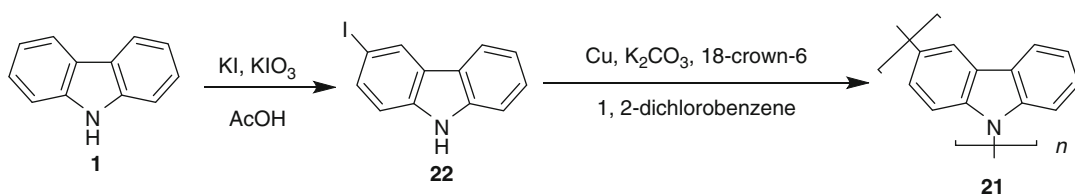
Polycarbazoles, Fig. 9 Synthesis of poly(3,9-carbazole)

The synthesis of the diboronate **19** and the condensation with the acceptor unit **20** then follow the same procedure as for the *N*-alkylcarbazole polymer **13** above.

Poly(3,9-carbazole)s

The problem of self-condensation in synthesis of *N*-aryl-dihalocarbazoles alluded to above can be exploited to produce 3,9-carbazole-based polymers as shown in Fig. 9. The polymer **21** is obtained directly by reaction of 3-iodocarbazole **22** with copper(I) [19]. Due to the lack of solubilizing groups, the material has low solubility and thus low molar mass (M_n = 2.36 kDa, M_w = 5.07 kDa), but it should be possible to make soluble polymers by applying this

methodology to 6-alkyl-3-iodocarbazoles. As **21** has an ionization potential of 5.45 eV, these might be suitable for use as hole-transport materials, but poor film quality prevents use of **21** as such. Also using 3,6-diiodocarbazole this type of reaction might be used to make hyperbranched or dendritic macromolecules with possible application as hole transporters or matrices for emitters.

Ladder-Type Polycarbazoles

One obvious way to get around the problem of oxidation at the 3- and 6-positions in poly (2,7-carbazole)s is to substitute these sites by making double stranded ladder-type polymers **23** as shown in Fig. 10 [20]. Acylation of the 2,7-dihalocarbazole **8** using an aryl acid halide
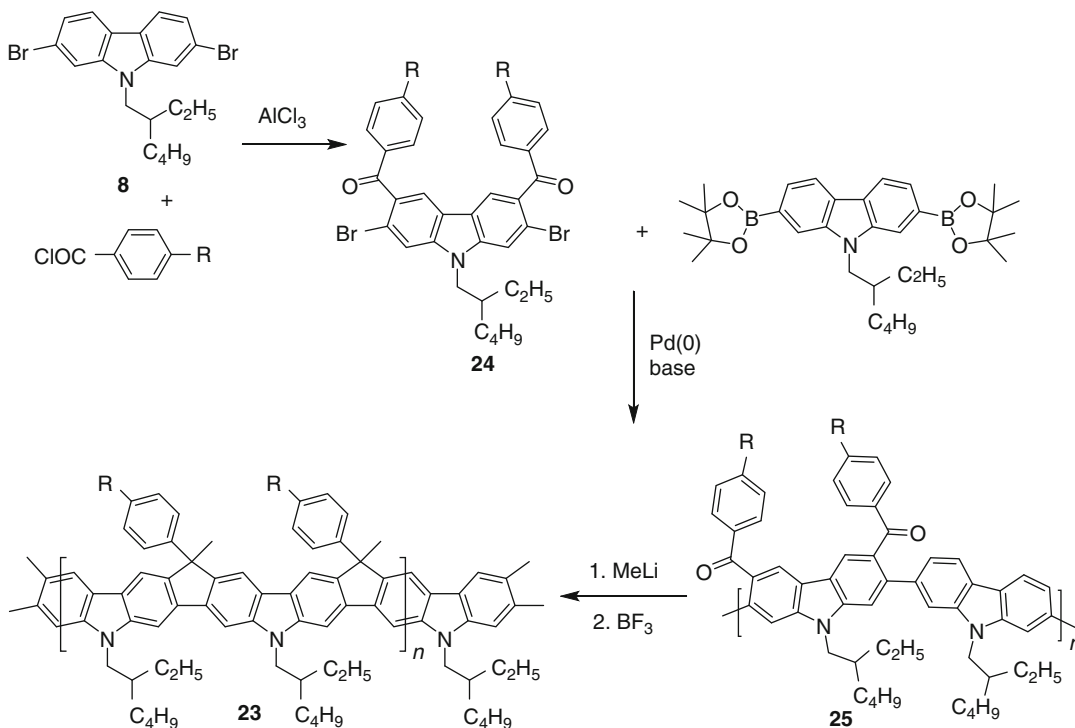
Polycarbazoles, Fig. 10 Synthesis of ladder-type polycarbazole

or anhydride occurs at the 3,6-positions to give a diacyl adduct **24**. The use of a substituted benzoic acid derivative enhances the solubility of the resulting monomer and polymers derived from it. Suzuki coupling of **24** with a diboronate then produces the alternating copolymer **25**. This had a molar mass (M_n) by GPC of 17 kDa corresponding to a degree of polymerization of ca. 33 units. Treatment of **25** with methyl lithium converted all the ketone units to carbinols, and boron trifluoride then induced ring closure to form the desired ladder-type polymers **23**. These were found to undergo aggregation in solution producing broad peaks in the ^{1}H NMR spectra, which complicated structural analysis. However, by diluting the solutions sufficiently, it was possible to obtain absorption and emission spectra with small Stokes' shifts and the sharp, well-resolved features characteristic of ladder-type materials, confirming the structures. These polymers displayed blue-green emission with emission maxima between 470 and 480 nm and ionization potentials of 5.2–5.3 eV making them

suitable for use as hole-transporting emissive materials in OLEDs. They have been tested as donor materials for BHJ solar cells, but the device results were very poor, probably due to poor charge transport [5].

Properties and Applications

Conjugated polymers have been widely used for organic electronics because of their superior optical and electrical properties. As mentioned above, carbazoles are isoelectronic with the corresponding fluorenes, but the electron-rich nitrogen atom on the bridge makes them better hole-acceptor or hole-transfer materials. Poly(3,6-carbazole)s because of their limited conjugation have large bandgaps and produce blue emission. In addition, their good solubility makes it easy to make a good film by spin coating so that they have been developed as blue-light emitters in LEDs [3]. Because of their large bandgaps and high-lying triplet energy levels, the homopolymers **2** (and some copolymers) have also

been investigated as host materials for blue-emitting phosphors in LEDs [3]. It has been reported that the intra- and intermolecular charge carrier mobility in poly(3,6-carbazole)s **2** is higher than in their 2,7-carbazole analogues [9]. Poly (2,7-carbazole)s are large bandgap blue-emitting materials whose emission spectra closely match those of polyfluorenes but which do not display the long wavelength emission seen from the latter due to the formation of defects [3]. They have also been used as electron-donating materials in bulk heterojunction (BHJ) solar cells [5]. Due to their absorption lying only in the higher energy part of the spectrum, the resulting devices display modest efficiencies (<1 %) [16]. By copolymerizing 2,7-carbazoles with other units, it is possible to tune their bandgap so as to produce materials with emission colors other than blue [3] or which act as much more efficient donor materials in solar cells [5], due to their having absorption over a much wider range of the visible spectrum. The copolymerization of a carbazole as an electron-rich donor unit with an electron-accepting unit in particular has been used to make medium- or low-bandgap materials for such applications with efficiencies of over 6 % reported from best devices [5]. In summary, relatively easy solution process and predominant blue emission made polycarbazoles potential candidate for highly efficient blue-emitting diodes and organic phosphorescent EL devices, while copolymers with suitable electron-accepting units have much promise as active components in solar cells.

Related Entries

▶ Ladder-Type Polymers
▶ Polyfluorenes
▶ Polymers for Solar Cells
▶ Polyphenylenes

References

1. Grazulevicius JV, Strohriegl P, Pielichowski J, Pielichowski K (2003) Carbazole-containing polymers: synthesis, properties and applications. Prog Polym Sci 28:1297
2. Morin J-F, Leclerc M, Ades D, Siove A (2005) Polycarbazoles: 25 years of progress. Macromol Rapid Commun 26:761
3. Grimsdale AC, Chan KL, Martin RE, Jokisz PG, Holmes AB (2009) Synthesis of light-emitting conjugated polymers for applications in electroluminescent devices. Chem Rev 109:987
4. Cheng Y-J, Yang S-H, Hsu C-S (2009) Synthesis of conjugated polymers for organic solar cell applications. Chem Rev 109:5868
5. Li J, Grimsdale AC (2010) Carbazole-based polymers for organic photovoltaic devices. Chem Soc Rev 39:2399
6. Romero DB, Schaer M, Leclerc M, Adès D, Siove A, Zuppiroli L (1996) The role of carbazole in organic light-emitting devices. Synth Met 80:271
7. Zhang Z-B, Fujiki M, Tang H-Z, Motonaga M, Torimitsu K (2002) The first high molecular weight poly(N-alkyl-3,6-carbazole)s. Macromolecules 35:1988
8. Ngblio E, Ades D, Chevrot C, Siove A (1990) Synthesis and characterization of poly (N-butyl-3,6-carbazolediyl). Polym Bull 24:17
9. Yasutani Y, Honsho Y, Saeki A, Seki S (2012) Polycarbazoles: relationship between intra- and intermolecular charge carrier transports. Synth Met 162:1713
10. Michinobu T, Osako H, Shigehara K (2008) Alkyne-linked poly(1,8-carbazole)s: a novel class of conjugated carbazole polymers. Macromol Rapid Commun 29:111
11. Michinobu T, Osako H, Shigehara K (2009) Synthesis and properties of conjugated poly(1,8-carbazole)s. Macromolecules 42:8172
12. Dierschke F, Grimsdale AC, Müllen K (2003) Efficient synthesis of 2,7-dibromocarbazoles as components for electroactive materials. Synthesis 16:2470
13. Cadogan JIG, Cameron-Wood M, Mackie RK, Searle RJG (1965) The reactivity of organophosphorus compounds. Part xix. Reduction of nitro-compounds by triethyl phosphite: a convenient new route to carbazoles, indoles, indazoles, triazoles, and related compounds. J Chem Soc 4831
14. Freeman AW, Urvoy M, Criswell ME (2005) Triphenylphosphine-mediated reductive cyclization of 2-nitrobiphenyls: a practical and convenient synthesis of carbazoles. J Org Chem 70:5014
15. Blouin N, Michaud A, Leclerc M (2007) A low-bandgap poly(2,7-carbazole) derivative for use in high-performance solar cells. Adv Mater 19:2295
16. Li J, Dierschke F, Wu J, Grimsdale AC, Müllen K (2006) Poly(2,7-carbazole) and perylene tetracarboxydiimide: a promising donor/acceptor pair for polymer solar cells. J Mater Chem 16:96
17. Iraqi A, Wataru I (2004) Preparation and properties of 2,7-linked N-alkyl-9h-carbazole main-chain polymers. Chem Mater 16:442

18. Liu X, Wen W, Bazan GC (2012) Post-deposition treatment of an arylated-carbazole conjugated polymer for solar cell fabrication. Adv Mater 24:4505
19. Grigalevicius S, Grazulevicius JV, Gaidelis V, Jankauskas V (2002) Synthesis and properties of poly(3,9-carbazole) and low-molar-mass glass-forming carbazole compounds. Polymer 43:2603
20. Dierschke F, Grimsdale AC, Müllen K (2004) Novel carbazole-based ladder-type polymers for electronic applications. Macromol Chem Phys 205:1147

Polycarbonate Synthesis

Anirudha Singh
Translational Tissue Engineering Center, Departments of Urology and Biomedical Engineering, Wilmer Eye Institute, Johns Hopkins University, Baltimore, MD, USA

Synonyms

Condensation polymerization; Interfacial polymerization; Melt polymerization

Definition

Polycarbonates (PCs) are one of the most versatile thermoplastic polymers with applications ranging from high-end engineering applications to biomaterials. The main chains of PCs contain a repeating carbonate $[-O-C(=O)-O-]$ linkage and a major moiety consists of aromatic and/or aliphatic units (Fig. 1).

Introduction

The history of PCs goes back to the late nineteenth and early twentieth centuries; however, in a major breakthrough, Bayer and GE in 1953 independently produced a high molecular weight PC based on bisphenol-A (BPA) with unparalleled engineering properties, which changed the landscape of industrial manufacturing of PC [1]. Traditionally, aromatic polycarbonates have dominated polycarbonate engineering business with applications ranging from NASA astronaut's helmet and visor, to mobile phones, to the Segway human transporter due to their high-heat resistance, clarity, impact resistance, chemical resistance, excellent moldability, and dimensional stability [2]. In recent years, aliphatic polycarbonates are also increasingly becoming popular in biomedical engineering applications due to their biocompatibility, low cytotoxicity, and biodegradability [3].

Synthesis

PCs are mainly synthesized by the following methods: (1) **interfacial (solvent based)** and (2) **melt condensation** polymerizations. In the interfacial method (Fig. 2), BPA–PC is synthesized by adding phosgene to a stirred slurry of aqueous sodium hydroxide, catalytic amine (e.g., triethylamine or pyridine), and BPA in a solvent, such as dichloromethane. To control the molecular weight of the polymer, a monofunctional phenol, such as phenol, *p-t*-butylphenol, or *p*-cumylphenol, is often added to the slurry to end the chain extension [1]. The pH of the reaction is carefully controlled throughout the reaction, which has a tremendous effect on the catalytic effect of amines, hydrolysis of phosgene, and reaction rates and formation of oligomers, chloroformates, and other side products [1]. The synthesized solvent-dissolved PC is purified and further isolated by separating the aqueous salt solution, washing the organic phase with an aqueous hydrochloride solution and water, and finally removing the solvent by either steam crumbing or devolatilization [1].

A wide range of techniques for interfacial synthesis has made it possible to prepare a large range of polycarbonate materials in a large-scale use. However, the toxicity of phosgene and chlorinated solvents remains a challenge toward the environmental friendly production of PC [4]. As shown in Fig. 3, **melt polymerization** of PC is an alternative synthetic method that utilizes diphenyl carbonate (DPC), which can also be prepared by a variety of non-phosgene methods,

P

in a melt phase polycondensation reaction [1, 5]. In this process, BPA is reacted with a high-quality DPC in the presence of a minimal amount of basic catalyst (e.g., NaOH/LiOH) at a high temperature [1, 5]. This leads to transesterification with loss of phenol, which is removed via distillation [5]. The polymerization can be stopped by either bringing the reactor to ambient pressure or end capping the polymer chain by the addition of phenyl moieties [1, 5]. The polymer can be further compounded directly following the last reaction stage. Diphenyl carbonate is synthesized either directly, from phosgene and phenol, or by a multistep transesterification process from dimethyl carbonate, which is synthesized directly by carbonylation of CO or CO_2 [4, 5]. As the polymerization proceeds, the molecular weight and, henceforth, the melt viscosity also increase, making phenol removal and driving of the reaction forward difficult [1, 4]. Although, this is partially

overcome by applying vacuum and increasing the temperature, prolonged heating can lead to side reactions that give a slightly yellowish color to the product, which remain a major challenge to synthesize higher molecular weight polycarbonates [1, 4]. The melt process is employed to manufacture excellent quality, low to medium molecular weight resins, especially optical grade PCs, as these have low residuals [1]. As an extension to melt polymerization, **solid-state polymerization** (SSP) can be employed post-PC synthesis to increase the molecular weight. In SSP of PCs, prepolymers/oligomers can be further heated above their glass transition temperature (T_g) but below their melting temperature (T_m) under vacuum or in a stream of an inert gas (N_2 or dense CO_2) or solvent (e.g., acetone) [1, 4, 6]. Polymerization temperatures above T_g but below T_m facilitate higher chain mobility and prevent PC to melt and coalesce, driving forward the thermodynamic

Polycarbonate Synthesis, Fig. 1 Examples of polycarbonates: (**a**) aromatic-bisphenol-A carbonate and (**b**) aliphatic-trimethylene carbonate
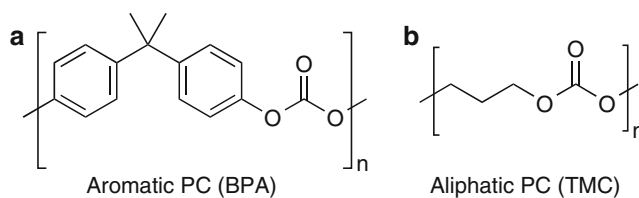
Polycarbonate Synthesis, Fig. 2 Interfacial polymerization via phosgene and bisphenol-A
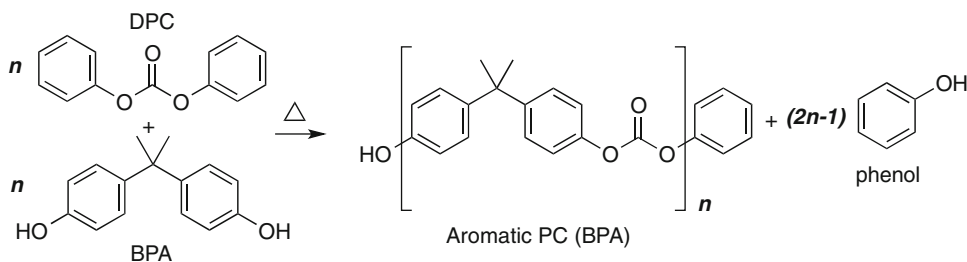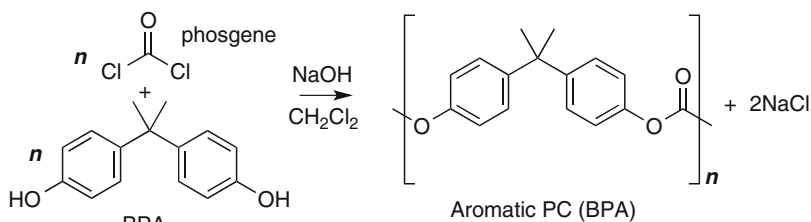
Polycarbonate Synthesis, Fig. 3 Melt polymerization via phosgene and bisphenol-A
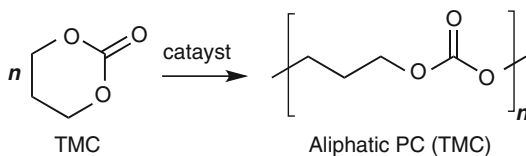
Polycarbonate Synthesis, Fig. 4 Ring-opening polymerization of TMC

equilibrium of polymerization, which increases the overall molecular weight of the polymer by chain extension on the removal of the by-product (e.g., phenol) [1, 4, 6].

Ring-opening polymerization (ROP), another method, especially employed to synthesize aliphatic polycarbonates, can yield a wide range of aliphatic PCs with small to high molecular weights, without formation and removal of any by-products as in step polymerizations [3, 7]. In addition to aliphatic cyclic rings, cyclic tetramer of BPA and a mixture of oligomeric–cyclics have also been investigated, although with relatively lower yields and multiple purification steps [1]. The most commonly used cyclic carbonates for ROPs are the five- and six-membered ring monomers [7]. For example, Fig. 4 presents the ROP of trimethylene carbonate in appropriate conditions to synthesize trimethylene carbonate, which finds applications in biodegradable materials [7]. ROP can be conducted in melt or in solution by the variation of the mechanisms, including cationic, anionic, coordination–insertion, monomer activation, monomer and initiator dual activation, and enzymatic activation mechanisms [7]. There are a number of catalysts available for the ROP of cyclic carbonates, including transition metal catalysts, alkyl halides, basic and acidic, and metal-free organocatalysts (e.g., *N*-heterocyclic carbine, phosphazenes, triflic acid, amines, and enzymes) [7, 8]. Recent advances in CO_2-based copolymerization techniques have made it possible to prepare aliphatic PCs at a relatively low cost on an industrial scale [3, 7, 8], with applications ranging from thermoplastics to tissue engineering applications as electrospun fibers, biodegradable elastomers, hydrogels, and drug delivery carriers [3, 7, 8]. Aliphatic PCs have also been synthesized by copolymerization of CO_2 with epoxide using a zinc catalyst or a strong base with crown ether [9].

New PCs and their synthetic methods have been continuously explored and developed to overcome the challenges associated with the conventional melt and interfacial polymerization techniques and the manufacturing processes of starting monomers and solvents. For example, in a major breakthrough, Asahi Kasei recently developed a green process that manufactures two important products, high-quality polycarbonate (PC) and high-purity monoethylene glycol (MEG), in high yields, from three starting materials, ethylene oxide (EO), CO_2, and bisphenol-A, without the need of phosgene or chlorinated solvent [4]. Copolymers of aromatic–aliphatic PCs, including natural phenol-derived PCs (e.g., tyrosol, homovanillyl alcohol, tyrosine), are also getting much attention in various engineering applications due to their unique combination of properties [10].

Perspective

Bisphenol-based polycarbonates and copolymers have dominated the applications of engineering polymers since the 1950s. Many innovations in synthetic schemes and processes to manufacture polycarbonates and adjust their final properties according to the desired applications have led to many versions of polycarbonates, including superior flow, high-heat, flame-retardant, and high-impact polycarbonates. However, in recent decades, a range of aliphatic polycarbonates and their copolymers has been explored for their nonconventional applications in new emerging markets, such as in biodegradable elastic scaffolds and drug delivery carriers. Similarly, green and environmental friendly synthetic processes are getting much attention in both laboratories and in industries due to the lower cost and less toxicity associated with the starting materials. Sustainable technologies with lower carbon footprints by using nonfossil-based starting monomers and efficient catalysts for CO_2-based polycarbonate manufacturing technologies will continue to be the future directions and endeavors in the polycarbonate synthesis and manufacturing area.

P

References

1. Brunelle DJ, Smigelski PM, Boden EP (2005) Evolution of polycarbonate process technologies. ACS Symp Ser 898:8–21, Oxford University Press
2. http://www.sabic-ip.com/gep/Plastics/en/ProductsAndServices/InnovationTimeline/lexan.html
3. Rokicki G (2000) Aliphatic cyclic carbonates and spiroorthocarbonates as monomers. Prog Polym Sci 25:259–342
4. Fukuoka S, Tojo M, Hachiya H, Aminaka M, Hasegawa K (2007) Green and sustainable chemistry in practice: development and industrialization of a novel process for polycarbonate production from CO_2 without using phosgene. Polym J 39:91–114
5. Pressman EJ, Johnson BF, Shafer SJ (2005) Monomers for polycarbonate manufacture: synthesis of BPA and DPC. ACS Symp Ser 898:22–38, Oxford University Press
6. Gross SM, Roberts GW, Kiserow DJ, DeSimone JM (2001) Synthesis of high molecular weight polycarbonate by solid-state polymerization. Macromolecules 34:3916–3920
7. Mespouille L, Coulembier O, Kawalec M, Dove AP, Dubois P (2014) Implementation of metal-free ring-opening polymerization in the preparation of aliphatic polycarbonate materials. Prog Polym Sci 39:1144–1164
8. Xu J, Ellva F, Jie S (2014) Renaissance of aliphatic polycarbonates: new techniques and biomedical applications. J Appl Polym Sci 131:39822
9. Miao CX, Wang JQ, He LN (2008) Catalytic processes for chemical conversion of carbon dioxide into cyclic carbonates and polycarbonates. Open Organic Chem J 2:68–82
10. Sommerfield SD, Zhang Z, Costache MC, Vega SL, Kohn J (2014) Enzymatic surface erosion of high tensile strength polycarbonates based on natural phenols. Biomacromolecules 15:830–836

Polycatenanes

Hiroyasu Yamaguchi and Akira Harada
Department of Macromolecular Science,
Graduate School of Science, Osaka University,
Machikaneyama, Toyonaka, Osaka, Japan

Synonyms

Mechanically interlocked cyclic molecules

Definition

Polycatenanes are defined as polymers containing a number of monomers linked in the fashion of a catenane, a mechanically interlocked molecular architecture consisting of two or more interlocked macrocycles. The interlocked rings cannot be separated without breaking the covalent bonds of the macrocycles.

Introduction

Compounds consisting of two or more mechanically interlocked macrocycles [1–3] – catenanes have high degrees of freedom and mobility of the whole molecule or its components, compared with other conventional covalently connected molecules. The interlocked macrocycles of catenanes can rotate and move within each other. They cannot be destroyed without breaking at least one of the covalent bonds of the macrocycles. Polycatenanes, polymers containing a number of macrocycles linked in the fashion of a catenane, have received considerable attention because of their unique rheological, dynamic, mechanical, and thermal properties [4–14]. Many polycatenane-like structures in the crystalline state based on assembly of metal-organic frameworks have been also studied [15–23].

Classification of Polycatenanes

According to the catenane structures in the polymer chain, the polycatenanes can be divided into classes (Fig. 1); main-chain polycatenanes ([n] catenanes (A) and bridged poly[2]catenanes (B)), side-chain polycatenanes (C and D), polyrotaxanes based on cyclic polymers (E), and catenane structures in the polymer networks (F and G).

Class A, [n]catenane (n is a large number), represents a series of linear polymers consisting of only mechanically interlocked macrocycles. Class B is derived from [x]catenanes by incorporating the bifunctional [x]catenane subunits, in which both rings are functionalized, into linear
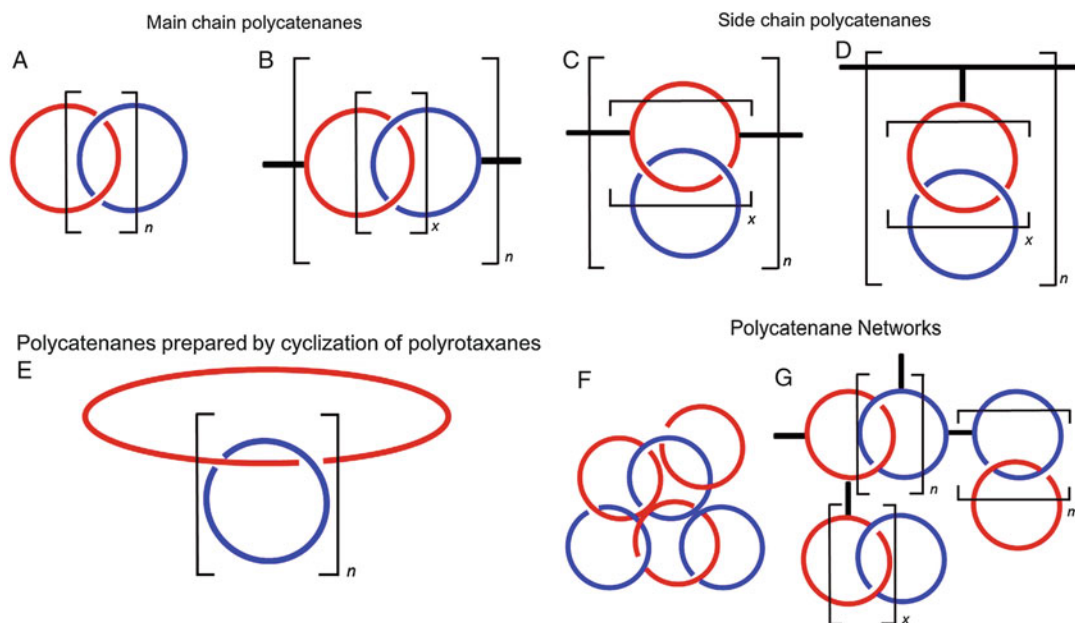
Polycatenanes, Fig. 1 Classification of polycatenanes

polymer main chains. The cleavage of the physical linkages of the catenane subunits will lead to degradation of the polymer chains. A polycatenane in class C is an isomer of that in class B. They are formed by incorporating [x]catenanes bearing two functional groups or a single bifunctional moiety on the same ring into polymer chains. Class D is the [x]catenane whose subunits exist as pendant groups. Polycatenanes in class E can be synthesized as the products of the end-to-end cyclization reaction of polypseudorotaxanes or polyrotaxanes. Pseudorotaxanes are generally precursors to catenanes. A pseudorotaxane is a supramolecular species consisting of a linear molecule (guest) threaded through a macrocyclic molecule (host). Polycatenanes of class F have networks which are solely formed by catenane subunits. Class G represents a series of universal networks. The catenane subunits exist as branches, cross-link points, or repeating units in the polymer networks.

Main-Chain Polycatenanes

Poly[2]catenanes can be prepared by the polymerization of bifunctional [2]catenanes or bis[2] catenanes. Reductive coupling, Sonogashira

reaction, Suzuki–Miyaura reaction, and Stille coupling have been examined to prepare poly[2] catenanes. The efficient preparation of polycatenane A requires the macrocycle precursors to be preorganized in favor of the cyclization reactions. The preorganization can be achieved by utilizing template effects, such as $\pi - \pi$ stacking, metal coordination, hydrogen bonding, and hydrophobic interactions. There are some ways for preparation of polycatenanes of class A (Fig. 2). The strategy for route A (i) is based on the polymerization between template-preorganized bifunctional monomers [24]. Shaffer and Tsay [25] applied a template-directed stepwise polymerization method (route A (ii)). In this route, high dilution techniques were used to favor the cyclization reactions. Route A (iii) could afford linear polycatenanes by stepwise threading and cyclization, but the separation after each step was difficult and the yield was low. A catenane having 1,3-diene-functionalized ring moiety underwent the Diels–Alder reaction followed by ozonolysis to give the corresponding ring-expanded catenane in good yield. Takata et al. used a Diels–Alder reaction and ozonolysis to enlarge one ring of

Polycatenanes,
Fig. 2 Synthesis of poly
[2]catenanes of class A
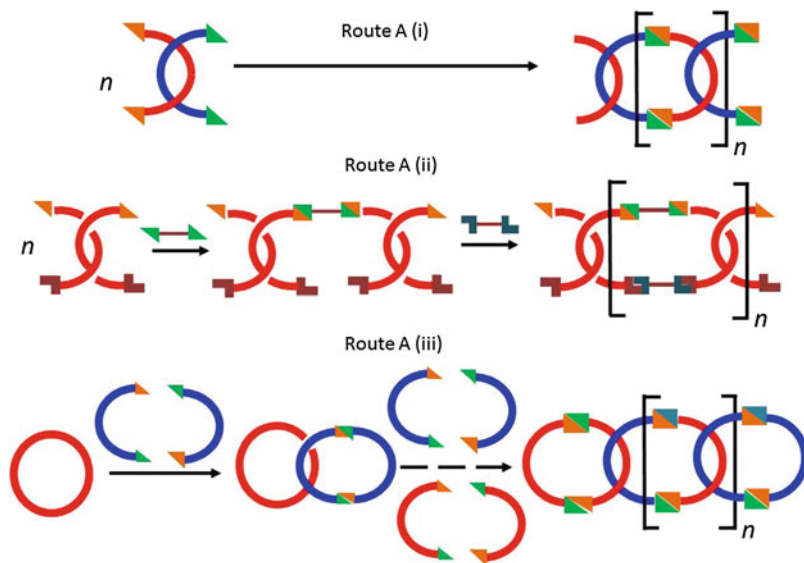
a [2]catenane for the preparation of poly[n] catenane [26]. Stoddart et al. synthesized [5]-, [6]-, and [7]catenanes by employing a stepwise synthetic approach [27]. [5]catenane has been called olympiadane because its structure resembles the well-known symbol of the Olympics.

Functional [2]catenane monomers are prepared first and then polymerized in order to prepare poly[2]catenanes (Fig. 3). In route B (i), bifunctional [2]catenanes are formed directly by the cyclization reactions of preorganized precursors. In route B (ii), bifunctional [2]catenanes are prepared by the template-directed coupling reactions of two different kinds of hemicycle precursors with or without functional groups. Route B (iii) involves stepwise cyclization of the two kinds of hemicycle precursors with and without functional groups. After the first cyclization reaction, one of the hemicycle precursors threads through the macrocycle formed during the first cyclization step. During the second cyclization step, noncovalent bonds are used as templating units. Route B (iv) is similar to route B (iii), but the macrocycle precursors involved before the second cyclization step are replaced by linked- or bis(macrocycle)s. Amide- and phenanthroline-based poly[2]catenanes were synthesized by using a rigid [2]catenane linkage [28] or employing three-dimensional template effect of

transition metals [29]. Stoddart et al. constructed poly[2]catenane system bearing tetracationic cyclophane-aromatic crown ether [30]. They utilized the charged π-donor/π-acceptor template methodology, which took advantage of strong binding affinities between a bipyridinium-based cyclophane and a crown ether ring. The driving forces include several noncovalent interactions, such as π-π stacking, edge-to-face interactions between aromatic rings, and hydrogen bonding.

Side-Chain Polycatenanes

Side-chain polycatenanes are polymers in which the catenane subunits are part of the pendant groups. The bifunctional [2]catenane monomers bearing both functional groups on the same ring are synthesized first and then incorporated into the polymer to produce side-chain poly[2] catenanes (route C (i) in Fig. 4), or the macrocycles are incorporated into the polymer backbone first and then cyclization reactions of the other macrocycle's precursors via pseudorotaxane formation afford side-chain poly[2]catenanes (route C (ii)). The monofunctionalized [2]catenane is directly incorporated via grafting reactions (route D (i)). The macrocycles are grafted onto the polymer first, and this process is followed by the cyclization reaction between the second macrocycle's
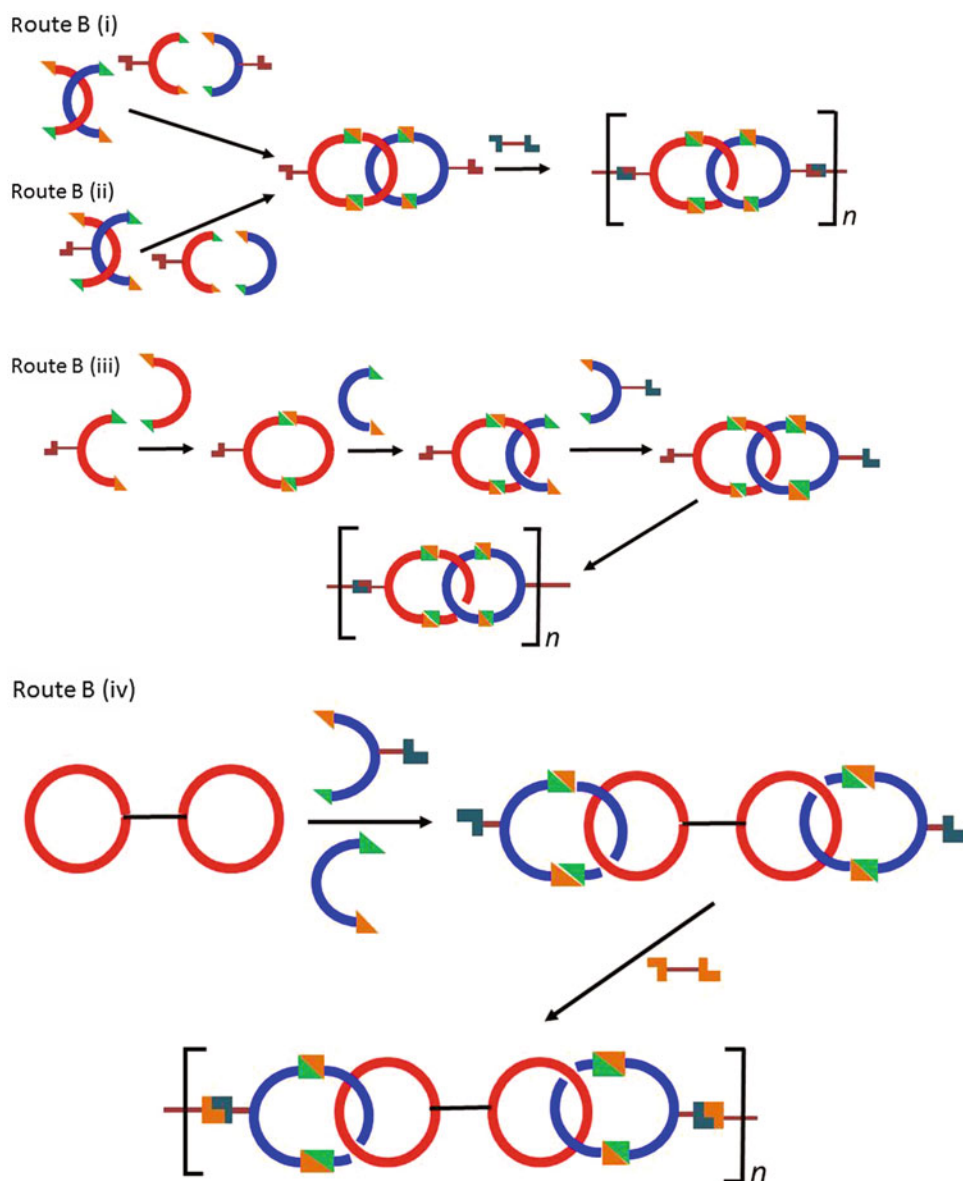
Polycatenanes, Fig. 3 Synthesis of linear main-chain poly[2]catenanes of class B

precursors via a pseudorotaxane intermediate (route D (ii)) [31]. A side-chain poly[2]rotaxane can be also synthesized by click chemistry [32].

Polycatenanes Prepared by Cyclization of Polyrotaxanes

Harada et al. reported a synthesis of polymeric catenanes based on cyclodextrins. First, the poly (ethylene glycol) (PEG) with a 9-anthryl group at one end of the polymer chain was prepared; the 9-anthryl group prevents dethreading and forms dimers upon photoirradiation. Then the PEG was treated with α-CD and polypseudorotaxane was obtained. The polypseudorotaxane was capped with another 9-substituted anthracene to afford polyrotaxanes. The exposure of polyrotaxane to visible light in dilute solution gave a polycatenane (Fig. 5) [33].
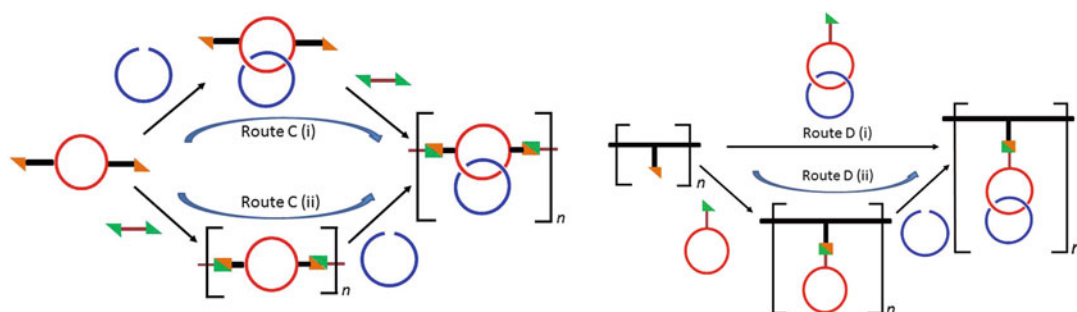
Polycatenanes, Fig. 4 Synthetic routes for side-chain polycatenanes (class C and class D)
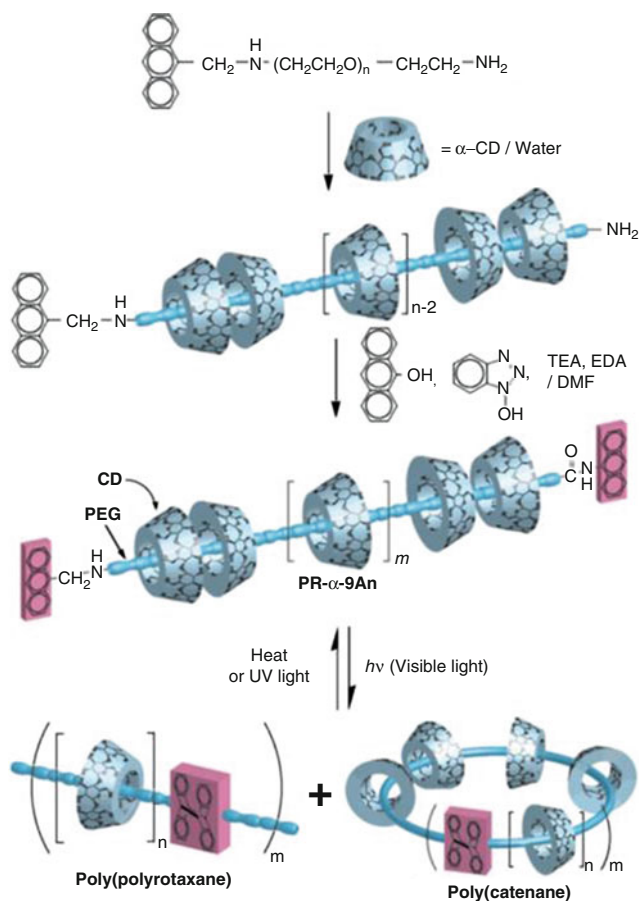
Polycatenanes, Fig. 5 A polycatenane prepared by cyclization of polyrotaxanes (class E) (Reprinted with permission from Ref. [33]. Copyright 2003 American Chemical Society)

Polycatenane Network

In polycatenane networks, some rings are interlocked with more than two other rings and act as cross-link points. The catenane subunits exist as branches, cross-link points, or repeating units in the polymer networks. Kim reported the self-assembly and X-ray crystal structure of a polycatenated two-dimensional polyrotaxane net in which cyclic cucurbituril beads are threaded onto two-dimensional coordination polymer networks [34]. Gibson et al. reported preparation of polyamide-based polypseudorotaxanes containing polycatenane structures [35].

Related Entries

▶ Calixarenes-Based Supramolecular Polymers
▶ Crown Ethers-Based Supramolecular Polymers
▶ Cucurbiturils-Based Supramolecular Polymers
▶ Cyclodextrins-Based Supramolecular Polymers
▶ Dynamic Mechanical Properties
▶ Molecular Self-Organization
▶ Polyrotaxanes (Conjugated)
▶ Polyrotaxanes: Synthesis, Structure, and Chemical Properties
▶ Supramolecular Network Polymers
▶ Supramolecular Polymers (Coordination Bonds)
▶ Supramolecular Polymers (Host-Guest Interactions)

References

1. Hudson B, Vinograd J (1967) Catenated circular DNA molecules in HeLa cell mitochondria. Nature 216:647–652
2. Wikoff WR, Liljas L, Duda RL, Tsuruta H, Hendrix RW, Johnson JE (2000) Topologically linked protein rings in the bacteriophage HK97 capsid. Science 289:2129–2133
3. Fang L, Olson MA, Benitez D, Tkatchouk E, Goddard WA III, Stoddart JF (2010) Mechanically bounded macromolecules. Chem Soc Rev 39:17–29
4. Amabilino DB, Stoddart JF (1993) Self-assembly and macromolecular design. Pure Appl Chem 65:2351–2359
5. Gibson HW, Bheda MC, Engen PT (1994) Rotaxanes, catenanes, polyrotaxanes, polycatenanes and related materials. Prog Polym Sci 19:843–945
6. Semlyen JA, Wood BR, Hodge P (1994) Cyclic polymers: past, present and future. Polym Adv Technol 5:473–478
7. Gong C, Gibson HW (1997) Polyrotaxanes and related structures: synthesis and properties. Curr Opin Solid State Mater Sci 2:647–652
8. Clarkson GJ, Leigh DA, Smith RA (1998) From catenanes to mechanically-linked polymers. Curr Opin Solid State Mater Sci 3:579–584
9. Brunsveld L, Folmer BJB, Meijer EW, Sijbesma RP (2001) Supramolecular polymers. Chem Rev 101:4071–4097
10. Harada A (2001) Cyclodextrin-based molecular machines. Acc Chem Res 34:456–464
11. Carlucci L, Ciani G, Proserpio DM (2003) Polycatenation, polythreading and polyknotting in coordination network chemistry. Coord Chem Rev 246:247–289
12. Takata T, Kihara N, Furusho Y (2004) Polyrotaxanes and polycatenanes: recent advances in syntheses and applications of polymers comprising of interlocked structures. Adv Polym Sci 171:1–75
13. Arico F, Badjic JD, Cantrill SJ, Flood AH, Leung KC-F, Liu Y, Stoddart JF (2005) Templated synthesis of interlocked molecules. Top Curr Chem 249:203–259
14. Niu Z, Gibson HW (2009) Polycatenanes. Chem Rev 109:6024–6046
15. Zhu H-F, Zhao W, Okamura T-A, Fan J, Sun W-Y, Ueyama N (2004) Syntheses and crystal structures of 1D tubular chains and 2D polycatenanes built from the asymmetric 1-(1-imidazolyl)-4-(imidazol-1-ylmethyl)benzene ligand with metal salts. New J Chem 28:1010–1018
16. Sague JL, Fromm KM (2006) The first two-dimensional polycatenane: a new type of robust network obtained by Ag-connected one-dimensional polycatenanes. Cryst Growth Des 6:1566–1568
17. Qin C, Wang X-L, Wang E-B, Su Z-M (2008) Catenation of loop-containing 2D layers with a 3D pcu skeleton into a new type of entangled framework having polyrotaxane and polycatenane character. Inorg Chem 47:5555–5557
18. Lan Y-Q, Li S-L, Qin J-S, Du D-Y, Wang X-L, Su Z-M, Fu Q (2008) Self-assembly of 2D → 2D interpenetrating coordination polymers showing polyrotaxane- and polycatenane-like motifs: influence of various ligands on topological structural diversity. Inorg Chem 47:10600–10610
19. Kuang X, Wu X, Yu R, Donahue JP, Huang J, Lu C-Z (2010) Assembly of a metal-organic framework by sextuple intercatenation of discrete adamantine-like cages. Nat Chem 2:461–465
20. Yang G-S, Zang H-Y, Lan Y-Q, Wang X-L, Jiang C-J, Su Z-M, Zhu L-D (2011) Synthesis and characterization of two {Mo6}-based/template metal-organic frameworks. Cryst Eng Commun 13:1461–1466
21. Jiang L, Meng X-R, Kuang X-J, Lu T-B (2012) Constructions of two polycatenanes and one polypseudorotaxane by discrete tetrahedral cages and stool-like building units. Sci Rep 2:668
22. Black SP, Stefankiewicz AR, Smulders MMJ, Sattler D, Schally CA, Nitschke JR, Sanders JKM (2013) Generation of a dynamic system of three-dimensional tetrahedral polycatenanes. Angew Chem Int Ed 52:5749–5752
23. Chen Q, Jiang F, Yuan D, Chen L, Lyu G, Hong M (2013) Anion-driven self-assembly: from discrete cages to infinite polycatenanes step by step. Chem Commun 49:719–721
24. Amabilino DB, Stoddart JF (1995) Interlocked and intertwined structures and superstructures. Chem Rev 95:2725–2829
25. Shaffer TD, Tsay L-M (1991) Pre-rotaxane polymers. J Polym Sci Part A Polym Chem 29:1213–1215
26. Watanabe N, Kihara N, Takata T (2001) Change of connectivity on catenane ring: ring expansion by annulation-ring scission sequence. Org Lett 3:3519–3522

P

27. Amabilino DB, Ashton PR, Reder AS, Spencer N, Stoddart JF (1994) Olympiadane. Angew Chem Int Ed Engl 33:1286

28. Muscat D, Koehler W, Raeder HJ, Martin K, Mullins S, Mueller B, Muellen K, Geerts Y (1999) Synthesis and characterization of poly[2]catenanes containing rigid catenane segments. Macromolecules 32:1737–1745

29. Weidmann J-L, Kern J-M, Sauvage J-P, Geerts Y, Muscat D, Muellen K (1996) Poly[2]-catenanes containing alternating topological and covalent bonds. Chem Commun 32:1243–1244

30. Odell B, Reddington MV, Slawin AMZ, Spencer N, Stoddart JF, Williams DJ (1998) Cyclobis (paraquat-p-phenylene). A tetracationic multipurpose receptor. Angew Chem Int Ed Engl 27:1547–1550

31. Hamers C, Raymo FM, Stoddart JF (1998) Molecular meccano. Part 42. Main-chain and pendant poly([2] catenane)s incorporating complementary π-electron-rich and -deficient components. Eur J Org Chem 1998:2109–2117

32. Bria M, Bigot J, Cooke G, Lyskawa J, Rabani G, Rotello VM, Woisel P (2008) Synthesis of a polypseudorotaxane, polyrotaxane, and polycatenane using click chemistry. Tetrahedron 65:400–407

33. Okada M, Harada A (2003) Poly(polyrotaxane): photoreactions of 9-anthracene-capped polyrotaxane. Macromolecules 36:9701–9703

34. Whang D, Kim K (1997) Polycatenated two-dimensional polyrotaxane net. J Am Chem Soc 119:451–452

35. Delaviz Y, Gibson HW (1992) Macrocyclic polymers. 2. Synthesis of poly(amide crown ethers) based on bis(5-carboxy-1,3-phenylene)-32-crown-10. Network formation through threading. Macromolecules 25:4859–4862

Polyelectrolytes for Batteries

Eliana Quartarone and Piercarlo Mustarelli
Department of Chemistry and INSTM,
University of Pavia, Pavia, Italy

Synonyms

Lithium batteries; Polymer electrolytes

Definition

The polyelectrolytes are polymeric single-ion conductors including charged groups along the backbone.

Solid Polymer Electrolytes: The Current State of Understanding

The concept of solid polymer electrolyte (SPE) dates back to the 1970s when Armand first proposed a new ion conductor based on a lithium salt properly complexed by a polar and aprotic polymer matrix without the use of organic solvents [1]. Ever since, a number of polymer/salt systems have been presented and deeply investigated, such as those based on PMMA, PAN, or PVDF [2–5]. In spite of the wide spectrum of SPEs available in the literature, the preferred combinations are still those based on polyethylene oxide (PEO), which allows a better Li solvation due to its structural similarity to the crown ethers and to the presence of ether oxygen in the structure. In case of PEO-LITFSI complexes, ionic conductivity of the order of 10^{-4} S cm^{-1} has been reached at room temperature in the presence of proper nanofiller dispersions [6]. In these solid electrolytes, Li transport takes place in the amorphous polymer domains (above the glass transition temperature, T_g), where the chains are more flexible, via ion hopping promoted by the segmental motion along the polymer backbone. The ionic conductivity of the PEO electrolytes, therefore, strictly depends on both crystallinity degree and T_g of the amorphous phase [7]. For these reasons, the research on SPEs has been ever focused on the enlargement of the amorphous fraction by means of several approaches, as, for instance, the choice of proper Li salt concentration, the incorporation of liquid plasticizers, and the dispersion of inorganic particles [6, 8].

Due to the promising conductivity values obtained in some polymer/salt complexes, SPEs are considered as a possible alternative to the liquid electrolytes in Li- or Na-based batteries. Basically, the use of "dry" systems as SPEs, in fact, may limit some important drawbacks related to the solvent leakage, the high Li reactivity, and the consequent formation of dendrites [9]. They behave both as the separator and the electrolyte, also leading to more stable solid-state interfaces. Further, in terms of battery safety, the presence of a polymer in the cell may guarantee higher thermal stability and thermal excursion up to 200 °C.

The solid polymer electrolytes are bi-ionic systems. This means that both anions and cations are mobile; unfortunately the bulk conductivity is primarily due to the anion mobility. In fact, lithium transference numbers, t_{Li+}, as low as 0.1–0.3 are generally obtained in case of PEO-based electrolytes [9]. The higher mobility causes an accumulation of anions around the electrode because it exchanges with Li$^+$ only. The resulting gradients in the salt concentration are responsible for the electrode polarization and do lead to worsening of performances. Some attempts to overcome this drawback have been carried out during these last decades, as for instance the use of large and heavy anions (e.g., TFSI$^-$) or of anion receptors, like boron, linear and cyclic azo-ether compounds, or calix-arene derivatives [10], which behave similarly to the crown ethers in case of cations. However, these strategies failed for different reasons: in some cases no substantial enhancement of t_{Li+} was observed, in other ones the complexation of the anion caused a conductivity decrease.

Polyelectrolytes

The more realistic strategy to forbid counterion diffusion is the anion anchoring to the polymer chains via chemical bonding to form single-ion conductors. The systems including charged groups along the backbone are known as polyelectrolytes [9]. In the particular case of batteries, this approach results in free cations with higher large-range mobility and consequently t_{Li+} values very close to unit.

Several classes of polymers were investigated as matrices for single-ion conduction, ranging from organic and/or inorganic polyanions to polymeric ionic liquids and charged di- or triblock copolymers (see Fig. 1). The most relevant of them will be explored in more details in the following sections.

Charged Polymers

The firstly investigated polyelectrolytes were based on polymers with strong solvation, generally including oxygen atoms along the backbone.
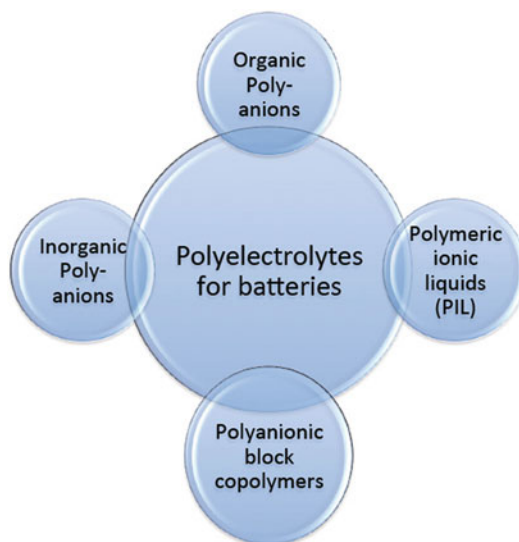
Polyelectrolytes for Batteries, Fig. 1 Polymer systems as single-ion conductors for batteries
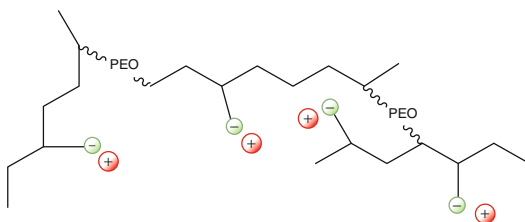
Polyelectrolytes for Batteries, Fig. 2 Typical structure of polyelectrolytes with anionic pendant group. The anions may be, for instance, carboxylate, phenolate, sulfonate, whereas the cation may be Li or Na

Two main systems were explored: (i) polymers with the anion attached as a pendant group, in particular carboxylates (–COO$^-$), sulfonates (SO$_3^-$), and phenolates (PhO$^-$) (see Fig. 2), and (ii) polymers where the anion is included along the main chain such as, for instances, borates (BO$_4^-$), aluminates (AlO$_4^-$, AlS$_4^-$), and siloxyaluminates [(SiO$_4$)Al$^-$] (Fig. 3).

In the former case, alkali metal salts of poly (methacrylic acid) and polysulfonic acid were explored, containing (or sometimes even blending with) units of polyethylene oxide with different molecular weights [11].

Ohno and coworkers proposed poly(oligo-oxyethylene)methacrylate- and PEO-methacrylic

Polyelectrolytes for Batteries,
Fig. 3 Examples of polyelectrolytes with the anion incorporated along the polymer backbone
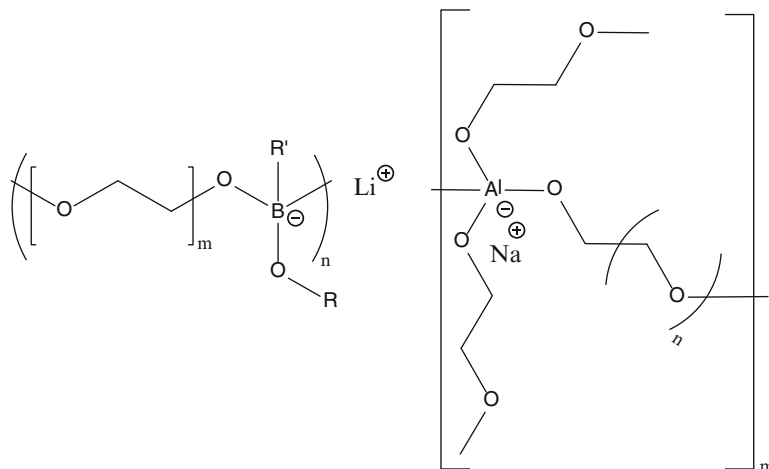
acid-based systems as polyelectrolytes for lithium batteries. Ionic conductivity ranging from 10^{-6} to 10^{-4} S cm^{-1} at temperature higher than 50 °C was measured, depending on the polymer structure [12]. Similar performances were observed for comb-like systems constituted by polystyrene-sulfonates, PEO with perfluoroalkyl-sulfonated end groups, and also polysiloxanes with ethylene oxide (EO) oligomers and sulfonate anions as the pendant moieties. In this case, the ionic transport sensibly depends on factors like the EO chain length or the Li/EO molar ratio. However, in spite of the high transference number, too low conductivity values ($<10^{-6}$ S cm^{-1}) were generally obtained at room temperature [13].

As already reported above, alternative polyelectrolytes with t^+ close to unity may be based on inorganic polymers including anionic repeating units with larger radius in the main chains, such as aluminates or borates. Stable inorganic systems were proposed, as, for instance, alkoxyaluminate [Al(OR)$_4^-$] or thioaluminate [Al(SR)$_4^-$]. Single-ion conductivity at room temperature of about 10^{-7} S cm^{-1} was first observed for aluminate complexes, which was successively improved by about one magnitude order by increasing the anion dimensions, as in the case of thioaluminate or aluminosilicate [14]. However, due to the limited aluminum chemistry, only a few systems were explored as Li$^+$ conductors.

Polymers incorporating other types of fragments (e.g., borates) were deeply investigated in order to enhance the single-ion conductivity. Taking into account the good reactivity of organoboron compounds, several alkyl- and/or aromatic borates matrices were synthesized, generally including oligoethylene oxide side chains. Particularly stable polymers were also obtained by introducing boroxine rings, characterized by strong π-π interactions between the O-atom and the adjacent boron one. However, these strategies to enhance the single-ion conductivity were also not particularly successful. Values generally lower than 10^{-6} S cm^{-1} were, in fact, obtained below 50 °C, without the addition of proper plasticizers [15, 16].

In spite of the high transference number, the ionic transport of this class of polyelectrolytes is absolutely not competitive with respect to the bi-ionic SPEs. Two factors reduce the ionic mobility of polyelectrolytes, both of them being strictly related to the ionomer chemical structure. One of these is the presence of strongly coordinating O-units along the backbone, which results in an extended localization of the cation around the blocked anion sites, which causes tight ion pairing, aggregation, and a consequent decrease of the free ions effectively available for the transport. Another aspect is the higher rigidity of such polymers, which is induced by the ionizable groups attached to the chain and by the related interchain cross-linking interactions between polyanion and cations [17, 18].

For these reasons, the more recent strategies to enhance the ionic conductivity of polyelectrolytes pointed to the increase of the polymer dynamics and/or the density of the free conducting ions. Following the first approach, polymers with low glass transition temperatures were synthesized in order to improve the chain segmental motion, which assists the ionic mobility. The number of actually available conducting ions is, in contrast, increased by synthesizing ionomers with larger-bonded anions, whose negative charge is strongly delocalized in order to reduce the possibility of ion pairing and aggregation. To this end, one of the best performing anions is bis(trifluoromethanesulfonyl)imide (TFSI$^-$) whose weak coordinating action favors a high charge carrier concentration.

Several systems, ranging from polyphosphazenes to polysiloxanes and polyepoxide ethers with glass transition temperature lower than $-60\ °C$, were then proposed in the literature. Polysiloxane-based ionomers, for instance, displayed very flexible architectures characterized by low viscosity, in particular if condensed with PEO oligomers (generally in the range 2–7) [19]. When doped with lithium salts, they can reach high enough ionic conductivity (0.1–1 mS cm^{-1}), depending on the amount of ethylene oxide oligomers and on the LiX nature, without serious increases in the T$_g$ values. Many systems were consequently explored, containing short oligoether side chains and several anions, namely, TFSI$^-$, phenolates, naphtholates, and perfluorosulfonates [13, 19]. Recently, polysiloxane-based single-ion conductors containing cyclic carbonates and different lithium tetraphenylborates as side chains were synthesized with a relatively high content of conducting ion (about 5 %) and low activation energy. The maximum allowed ionic conductivity at 20 °C was found to be still low (around 10^{-7} S cm^{-1}), likely due to the high T$_g$s (roughly in the range between $-20\ °C$ and $-6\ °C$), but further improvements were observed by introducing proper amounts of PEG-based plasticizers [19].

Similarly to poly(organosiloxanes), polyphosphazenes are hybrid organic-inorganic polymers constituted by a backbone of alternating P- and N-atoms with two organic side groups bonded to each phosphorus. A lot of architectures are known, depending on the nature of the side groups. Polyphosphazenes with linear or branched EO lateral chains are particularly suitable to dissolve lithium salts due to the ability of oxygen units to coordinate Li$^+$ cations. For this reason they are potential electrolytes for lithium batteries [20, 21]. The transport mechanism has not been completely addressed yet. However, it seems strictly correlated to the polymer glass transition temperature. In particular, the ionic migration is greatly affected by T_g increases due to the reversible cross-linking interactions resulting from the cation coordination by the O-units distributed on different side chains. Several polyphosphazene single-ion conductors were investigated [20, 21]. In 2006, Allcock and co. proposed immobilized sulfonimide lithium sources linked to the polyphosphazene backbone, containing methoxy(ethoxy)ethoxy moieties as cation-solvating co-substituents. A maximum ionic conductivity of about 2.5×10^{-6} S cm^{-1} was obtained at room temperature, which increased up to 1 mS cm^{-1} in case of the system gelled by proper amounts of methyl-pyrrolidone as the plasticizer [20, 21].

Charged Block Copolymers

Another alternative strategy to promote charge dissociation and to enhance Li$^+$ mobility in a single-ion conductor was to spatially isolate the anions in a secondary phase of the polymer electrolyte. This was recently carried out through the design of proper architectures based on graft block copolymers [22–24]. The most common structures are the AB diblock or BAB triblock copolymers, where A is the ion-conducting block and B the unit conferring mechanical strength. Such blocks are chemically different and end-to-end bonded. Under specific conditions, it is possible to induce a net repulsion between the polymer blocks, leading to a microphase separation into periodically spaced nanodomains [22–24]. The main concept, here, is to order the polyelectrolytes into two parts: (i) a secondary domain in which

P

the attached anion is immobilized and (ii) ionically conducting block nanodomains where Li^+ cations are localized and where a continuous ion-conducting pathway is created. In principle, by this way it should be possible to increase t^+ up to the unit, without seriously sacrificing ionic mobility. Such nanoscaled morphology provides good mechanical performances at a macroscopic level. In particular, by choosing two non-crystallizing blocks with low glass transition temperatures, T_gs, films with mechanical strength comparable to that one of cross-linked systems can be obtained, preserving the high local chain mobility necessary for good Li^+ transport.

Single-ion conductors based on block copolymers were firstly investigated by Sadoway and coworkers, who proposed self-doped block copolymer electrolytes (SDBCEs), whose Li^+ transference number approached 0.9. Such systems were composed by the block components polylauryl methacrylate (PLMA) and poly [(oxyethylene)$_9$ methacrylate] (POEM) as the anionic part. The Li^+ carriers were provided through the addition of lithium methacrylate into the backbone following three distinct architectures: (i) random, within the hydrophilic block

P(LiMA-r-POEM); (ii) random, within the hydrophobic one P(LMA-r-LiMA); or (iii) as a separated block PLMA-b-PLiMA-b-POEM. However, the ionic conductivity never exceeded 10^{-5} S cm^{-1} at 70 °C, and this limitation was interpreted in terms of a still low-level ionic dissociation [22–24].

A similar approach was recently tried by Armand and coworkers [25]. They designed a single-ion conductor based on a polyanionic block copolymer BAB and on TFSI$^-$ as the anion. Due to the well-known charge delocalization of the imide, Li^+ weakly interacts with the anionic counterpart; consequently, a higher dissociation degree may be reached. In this case, the B block is a polyelectrolyte based on poly(styrene trifluoroethanesulfonimide of lithium) P (STFSILi), bonded to a central linear PEO unit (see Fig. 4).

The maximum ionic conductivity found at 60 °C was 1.3×10^{-5} S cm^{-1} which is half an order of magnitude higher than that previously reported in the literature [22–24]. The Li^+ transport number determined for this electrolyte was larger than 0.85, and a promising electrochemical stability window up to 5 V vs. Li was also reported.

Polymeric Ionic Liquids (PIL)

More recently, attention has been devoted to novel single-ion conductors based on polymeric ionic liquids as advanced electrolytes, which combine the beneficial properties of ionic liquids with those of the more traditional polyelectrolytes. As it is well known, ionic liquids are room temperature molten salts, which remain liquid in wide temperature range. They show unique properties, such as non-flammability, low volatility, and good thermal and electrochemical stability. ILs also have good ionic conductivity due to the high ion concentration and mobility. When doped with lithium salts, they are potential and safer electrolytes, alternative to the conventional solutions based on the organic carbonates [26]. During this last decade, the introduction of groups associated to the ionic liquids (for instance organic cations such as pyrrolidinium, imidazolinium, pyperidinium) and of hydrophobic counteranions (like BF_4^-, PF_6^-, triflate, sulfonimide, etc.) into functional polymers generated a new family of polyelectrolytes for different applications, including lithium batteries.

Polymeric ionic liquids, also called poly(ionic liquids), PILs, are polymers whose repeat unit contains a cation (polycations) or an anion (polyanions) or both (poly-zwitterions). Furthermore, different types of copolymers and macromolecular architectures (e.g., random, block, grafted, branched) may be possible due to the good reactivity of the starting monomers.

The general synthetic approach of PILs consists of the radical polymerization of the vinyl functional groups covalently introduced on the ionic liquid monomer. By this strategy, Ohno et al. firstly obtained several polymeric ionic liquids through anion exchange reaction of vinyl-alkyl imidazolium halide with different counteranions [27–29].

By properly combining different cations, anions, and polymer backbones, it is possible to tailor the structure of these novel polyelectrolytes for specific technological applications. In the particular case of electrolytes for lithium batteries,

PILs show the potential advantage to combine the abovementioned benefits of ionic liquids with those ones of polymers, namely, mechanical stability, freestanding properties, safety, easier processing, packaging, etc. However, as in the case of other polyelectrolytes, the ionic conductivity is often too low for practical applications. Typical conductivity values obtained with the ionic liquids are around 10^{-3} S cm^{-1} at room temperature. After the polymerization process, the conductivity dramatically falls, sometimes even to two to four orders of magnitude. Ohno, for instance, found values 10^4 times lower for the system based on ethylvinylimidazolium-TFSI after the polymerization [27–29]. This phenomenon has been rationalized in terms of a remarkable increase of T_g and a reduction of the free mobile ions because of the covalent bonding of the monomer components.

The decrease of the ionic mobility in PILs is more evident in the case of polycation-type ionic liquids. For what concerns the poly(anions) ILs, in fact, the ionic conductivity is higher, probably because the cation mobility counts more than the anion one in lowering the polymer glass transition temperature. Since in the case of batteries, the charge carrier is the cation, in particular Li$^+$ or Na$^+$, polyanion-based configuration is preferred, with two important requirements: (i) counteranions with weak basicity and diffused charge (for instance, TFSI$^-$, RSO$_3^-$, PF$_6^-$) in order to further improve the ion transport and dissociation and (ii) chemically and electrochemically stable cations, such as alkylammonium, imidazolium, and mostly pyrrolidinium, with proper alkyl-based side chains.

The ion mobility in PILs may be made more efficient by copolymerization of oppositely charged monomers, namely, IL monomers (the anion) with functional Li salt monomers (the cation), which generally include ethylene oxide oligomers in order to enhance the backbone flexibility. In these architectures both transference number and ionic conductivity strictly depend on the monomers composition, and a good balance between t^+ and σ is sometimes difficult

P

to obtain. Ohno and co. prepared a copolymer polyelectrolyte based on methacryloyl octa(ethylene oxide)-2-sulfobenzoate lithium salt and the more conductive 1-[6-(acryloyloxy)hexyl]-3-ethylimidazolium bis(trifluoromethylsulfonyl) imide. They showed that the conductivity decreases by increasing the Li fraction, contrary to what happens for t^+. A compromise composition was identified at 50 mol% of Li salt, whose conductivity and transference number at 30 °C exceed 10^{-5} S cm^{-1} and 0.4, respectively. Again, this was explained with a poor dissociation degree of the matrix [27–29].

In spite of the great number of proposed structures, the transport properties of the PILs are still poor. Conductivity values in the range 10^{-8} to 10^{-5} S cm^{-1} have been generally found at room temperature, too far from the requirement for a practical application as active separators in lithium batteries. A sensible improvement may be reached by incorporating poly(ionic liquids) onto inorganic particles to form core-shell structures, which also show additional functional properties, such as structural stability and transport tenability, depending on the ionic materials. Very recently, a novel organic-inorganic core-shell architecture based of SiO$_2$-poly (vinylbenzyl-trimethylammonium) BF$_4$ was synthesized, reaching room temperature conductivity significantly higher than that one found for the similar pure PIL (10^{-4} vs. 10^{-5} S cm^{-1}) [30].

A more efficient approach to enhance the PIL ion mobility is the tailoring of polyelectrolytes based on the mixture of IL and PILs. In this case, the single ionic liquid acts as both additional charge carrier and nonvolatile plasticizer.

The resulting materials show good conductivity, ranging between 10^{-3} and 10^{-2} S cm^{-1}, which may be further increased by increasing the IL content in the ion gel. However, the ionic liquid fraction must be limited in order to preserve the polymer mechanical properties.

The McFarlane group tested different Li polyelectrolyte-in-ionic liquid systems, based on novel alkali metal ionic liquids (AMILs), mostly containing Li ions, and on poly(lithium acrylamide propanesulfonate)- or lithium poly(sulfopropylacrylate)-based polymers and copolymers [31–33]. The IL behaves as a good solvating medium for the copolymer polyelectrolyte. The resulting conductivity is of the order of 10^{-2} S cm^{-1}, which means to two to three times higher than that of the corresponding homopolymer, depending on both the IL/polyelectrolytes ratio and the Li content. A good dissociation of Li cations is also observed due to the presence of anions bonded to the polymer chains.

Other very promising systems as "Li ion dissociation enhancers" are the zwitterions, namely, ionic liquids where both the anion and cation are immobilized on the same structure. The zwitterionic compounds may enhance the ionic conductivity up to about seven times with respect to the pure polyelectrolyte [34]. In case of addition of 1-butylimidazolium-3-(n-butanesulfonate) dissociator to lithium methylacrylate copolymers (Fig. 5), the ionic conductivity achieves a maximum close to 0.6 mS cm^{-1} at 30 °C, in the presence of a Li$^+$ mole fraction in the copolymer of about 0.050.

NMR analyses confirmed that this improvement is effectively related to an increase of lithium
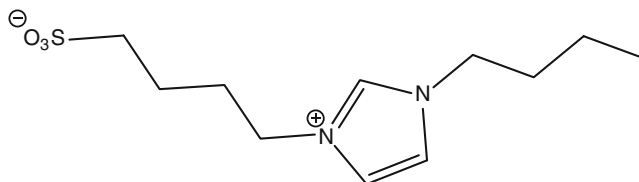
Polyelectrolytes for Batteries, Fig. 5 1-butylimidazolium-3-(*n*-butanesulfonate), zwitterionic compound used as a Li ion dissociation enhancer in polyelectrolytes for lithium batteries [34]

ion mobility within the zwitterion-polyelectrolyte system. However, the actual effect of the zwitterion on the Li dissociation is not totally understood. One reasonable hypothesis could be that the zwitterion screens the anion bonded to the polymer chain by means of coulombic interactions, so impeding the Li^+ coordination. Another maybe even more probable reason is that the charge carrier preferably interacts with the sulfonate group of the zwitterion rather than with that one on polymer. This likely improves the Li dissociation in the polyelectrolyte backbone.

Conclusions

Polyelectrolytes have been extensively studied in recent years. However, the attempt to combine high ionic conductivity and high lithium transport number to date has not yet given good results, likely because of the strong anion-cation interactions, which make the structure stiffer and decrease the cation mobility. Likely, the best choice for the future will be given by polymeric ionic liquids, which combine the ILs advantages (conductivity, safety) with those of polymers (mechanical stability and processability). Lithium dissociation enhancers will be likely needed to obtain commercially interesting electrolytes.

Related Entries

▶ Block Copolymer Synthesis
▶ Conducting Polymers
▶ Ion-Containing Polymer Synthesis

References

1. Armand M, Chabagno JM, Duclot MJ (1979) Polyethers as solid electrolytes. In: Vashishta P (ed) Fast ion transport in solids. North Holland, New York, p. 131
2. Gray FM (1997) Polymer electrolytes. Royal Society of Chemistry, London
3. Arora P, Zhang Z (2004) Battery separators. Chem Rev 104:4419–4462
4. Armand MB, Bruce PG, Forsyth M, Scrosati B, Wieczorek W (2011) Polymer electrolytes. In: Bruce DW, O'Hare D, Walton RI (eds) Energy materials. Wiley, Chichester. doi:10.1002/9780470977798.ch1
5. Hollinan DT, Balsara NP (2013) Polymer electrolytes. Annu Rev Mater Res 43:503–525
6. Quartarone E, Mustarelli P (2011) Electrolytes for solid-state lithium rechargeable batteries: recent advances and perspectives. Chem Soc Rev 40:2525–2540
7. Ratner MA, Shriver DF (1988) Ion transport in solvent-free polymers. Chem Rev 88:109–124
8. Quartarone E, Mustarelli P, Magistris A (1988) PEO-based composite electrolytes. Solid State Ionics 110:1–14
9. Maranas JK (2012) Polyelectrolytes for batteries: current state of understanding. In: Page K (ed) Polymers for energy storage and delivery: polyelectrolytes and fuel cells. ACS Symposium Series. American Chemical Society, Washington, DC
10. Mazor H, Golodnitsky D, Peled E, Wieczorek W, Scrosati B (2008) A search for single-ion conducting polymer electrolyte: combined effect of anion trap and inorganic filler. J Power Sources 178:736–743
11. Dias FB, Plomp L, Veldhuis JBJ (2000) Trends in polymer electrolytes for secondary lithium batteries. J Power Sources 88:169–191
12. Ohno H, Ito K (1995) Poly(ehtylene oxide)s having carboxylate groups on the chain end. Polymer 36:891–893
13. Snyder JF, Ratner MA, Shriver DF (2003) Ion conductivity of comb polysiloxane polyelectrolytes containing oligoether and perfluoroether sidechains. J Electrochem Soc 150:A1090–A1094
14. Onishi K, Matsumoto M, Shigehara K (1998) Thioaluminate polymer complexes as single-ionic solid electrolytes. Chem Mater 10:927–931
15. Cakmak G, Verhoeven A, Jansen M (2009) Synthesis and characterization of solid single ion conductors based on poly[lithium tetrakis(ethyleneboryl)borate]. J Mater Chem 19:4310–4318
16. Nishihara Y, Miyazaki M, Tomita Y, Kadono Y, Takagi K (2008) Synthesis and ion-conducting characteristics of inorganic-organic hybrid polymers bearing a tetraarylpentaborate unit. J Polym Sci Polym Chem 46:7913–7918
17. Wang JHH, Colby RH (2013) Exploring the role of ion solvation in ethylene oxide based single-ion conducting polyanions and polycations. Soft Matter 9:10275–10286
18. Wang W, Tudryn GJ, Colby RH, Winey KI (2011) Thermally driven ionic aggregation in poly(ethylene oxide)-based sulfonate ionomers. J Am Chem Soc 133:10826–10831

P

19. Liang S, Choi UH, Liu W, Runt J, Colby RH (2012) Synthesis and lithium ion conduction of polysiloxane single-ion conductors containing novel weak-binding borates. Chem Mater 24:2316–2323

20. Allcock HR (2012) Polyphosphazene elastomers, gels, and other soft materials. Soft Matter 8:7521–7532

21. Allcock HR, Welna DT, Maher AE (2006) Single-ion conductors-polyphosphazenes with sulfonimide functional groups. Solid State Ionics 177:741–747

22. Sadoway DR (2004) Block and graft copolymer electrolytes for high-performance, solid-state, lithium batteries. J Power Sources 129:1–3

23. Niitani T et al (2005) Synthesis of Li$^+$ ion conductive PEO-PSt block copolymer electrolyte with microphase separation structure. Electrochem Solids State Lett 8:A385–A388

24. Sadoway D, Huang B, Trapa PE et al (2001) (2001) Self-doped block copolymer electrolytes for solid-state rechargeable lithium batteries. J Power Sources 97–98:621–623

25. Bouchet R, Maria S, Meziane R, Aboulaich A, Lienafa L et al (2013) Single-ion ABA triblock copolymers as highly efficient electrolytes for lithium-metal batteries. Nat Mater 12:452–457

26. Armand M, Endres F, MacFarlane DR, Ohno H, Scrosati B (2009) Ionic-liquid materials for the electrochemical challenges of the future. Nat Mater 8:621–629

27. Ohno H (2007) Design of ion conductive polymers based on ionic liquids. Macromol Symp 249–250:551–556

28. Mecerreyes D (2011) Polymeric ionic liquids: broadening the properties and applications of polyelectrolytes. Prog Polym Sci 36:1629–1648

29. Shapov AS et al (2011) Polymeric ionic liquids: comparison of polycations and polyanions. Macromolecules 44:9792–9803

30. Wang P, Zhou Y-N, Luo J-S, Luo Z-H (2014) Poly (ionic liquid)s-based nanocomposite polyelectrolytes with tunable ionic conductivity prepared via SI-ATRP. Polym Chem 5:882–891

31. Sun J, MacFarlane DR, Forsyth M (2002) Lithium polyelectrolyte-ionic liquid systems. Solid State Ionics 147:333–339

32. Ogihara W et al (2004) Ionic conductivity of polymer gels deriving from alkaly metal ionic liquids and negatively charged polyelectrolytes. Electrochim Acta 49:1797–1801

33. Tiyapiboonchaiya C et al (2003) Polyelectrolytes-in-ionic-liquids electrolytes. Macromol Chem Phys 204:2147–2154

34. Tiyapiboonchaiya C, Pringle JM, Sun J et al (2004) The zwitterion effect in high-conductivity polyelectrolytes materials. Nat Mater 3:29–32

Polyetherimide

Osamu Urakawa
Department of Macromolecular Science,
Graduate School of Science, Osaka University,
Toyonaka, Osaka, Japan

Synonyms

PEI

Definition

Polyetherimide (PEI) is a polymer containing cyclic imide especially of five-membered ring and ether units in the backbone. PEI is categorized as a special class of polyimide (PI) which is a condensation polymer derived from bifunctional carboxylic anhydrides and primary diamines. Polymers classified as PEI generally have a structure shown in Fig. 1 [1]. Ultem, whose chemical structure is shown in Fig. 2, is a typical example of PEI. Other polymers involving imide and ether units are usually called polyimide [2]. In this entry, however, PEI is broadly defined from the structural viewpoint and to include all polyimides containing ether units.

Introduction

Polyimides are high-performance super-engineering plastics exhibiting high heat resistance, excellent mechanical property, inherent flame resistance, and solvent resistance. Structures of polyimide containing ether units are shown in Fig. 2.

All these specific PIs were industrially developed (the manufacturer's name is described in the figure). Among them, Ultem [1, 3, 4] and Aurum [5] are thermoplastic, and Kapton [6] and Upilex [7] are non-thermoplastic polymers.

Polyetherimide,
Fig. 1 General structure of
polyetherimide
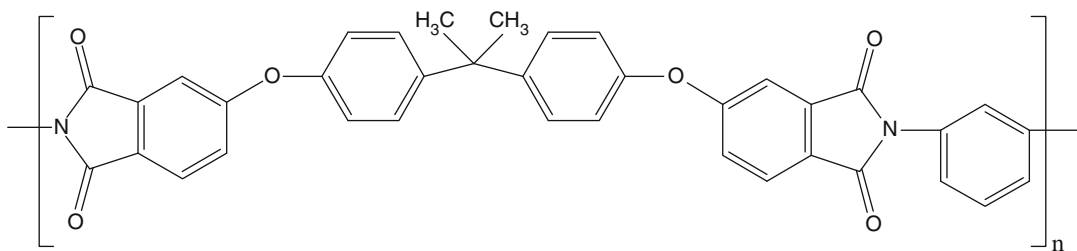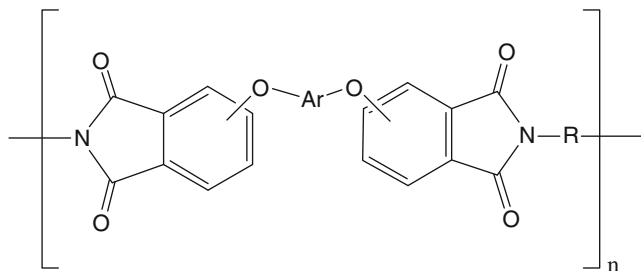
Ultem (General Electric)
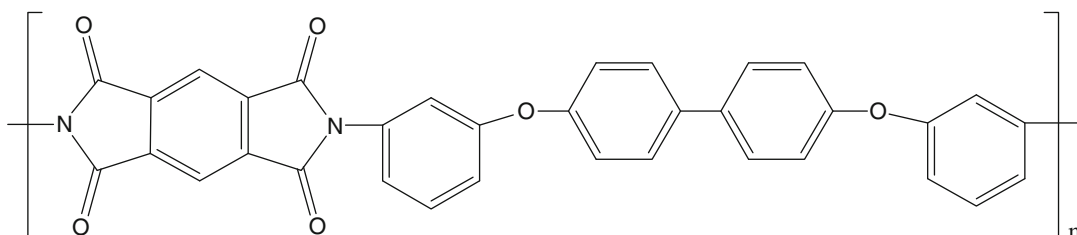
Aurum (Mitsui Chemicals)
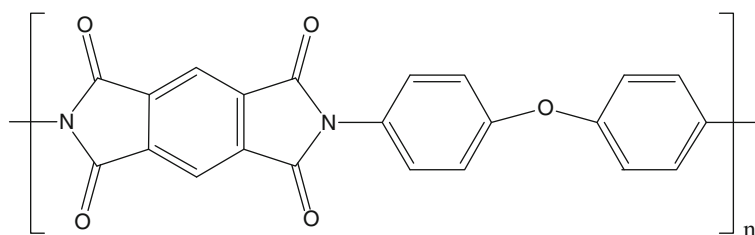
Kapton (Du Pont)
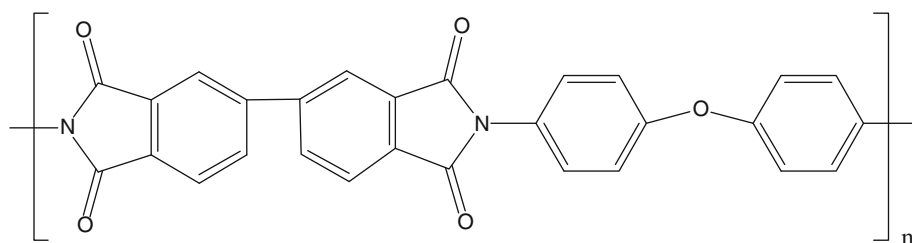
Upilex-RN (Ube Industries)

Polyetherimide, Fig. 2 Structures of polyimides containing ether units and their manufacturer's name

Upilex-S (Ube Industries)

LaRC-TPI (NASA)
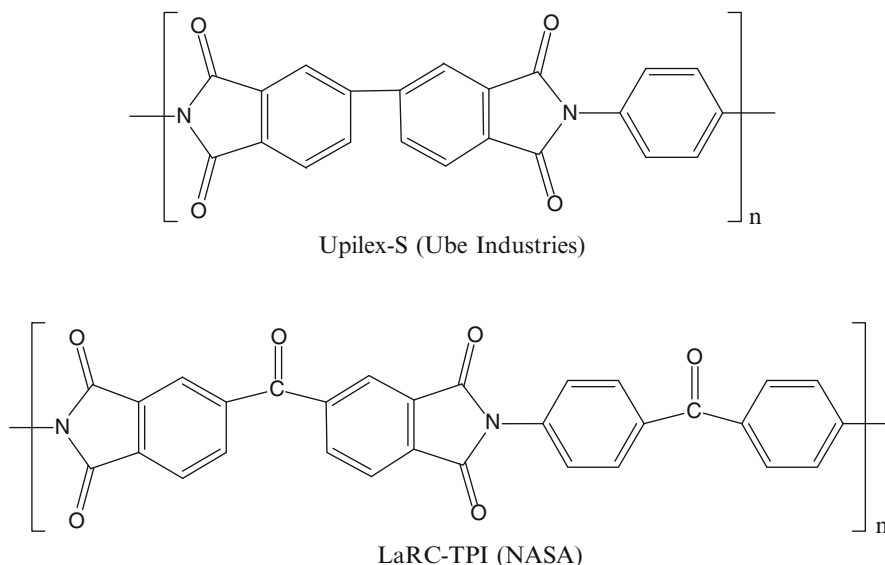
Polyetherimide, Fig. 3 Structures of polyimides having no ether unit

Polyimides which do not have ether group but have similar properties like heat resistance, solvent resistance, flame resistance, etc., are shown in Fig. 3. The inclusion of ether group in PI's aromatic dianhydride and/or aromatic diamine building blocks adds the flexibility to the rigid backbone structure resulting in the improvement of the melt processability without spoiling melt stability. Upilex-S [7] is non-thermoplastic resin, but LaRC-TPI [8] is thermoplastic because of the inclusion of carbonyl group which also adds the flexibility.

Production

Poly(4,4′-oxydiphenylene-pyromellitimide), produced by DuPont under the trade name of Kapton, is the first product of polyimides [9]. This polymer is insoluble in any organic solvents and also infusible. Therefore, it is synthesized by way of poly (amidic acid) which is soluble in polar solvent, such as N-methyl-2-pyrrolidone (NMP) and N, N-dimethylacetamide (DMAc). Polycondensation

of pyromelitic dianhydride and 4,4′-oxydiphenylamine in NMP gives the poly(amic acid) as shown in Fig. 4. The ring closure is carried out at high temperatures (>200 °C) or by using amine catalysts. For making Kapton film, poly(amic acid) solutions are firstly casted and after that imidization is induced.

Thermoplastic PEI, Ultem, is synthesized by melt polycondensation of bisphenol A dianhydride with a diamine, usually m-phenylenediamine as shown in Fig. 5a. For the synthesis of dianhydride compound, 2 mol of phthalic anhydride react with one mole of bisphenol A. For the poly(amic acid) produced through the polycondensation with diamine, the ring closure reaction is induced by heat.

The reverse order of reaction route is also possible, that is, starting with the imide forming sequence and using aromatic nucleophilic substitution to produce polymer as shown in Fig. 5b.

However, the first synthetic route often gives better yields, because of the stability of tetracarboxylic dianhydrides. The route (a) is actually utilized to produce Ultem resin in industry.
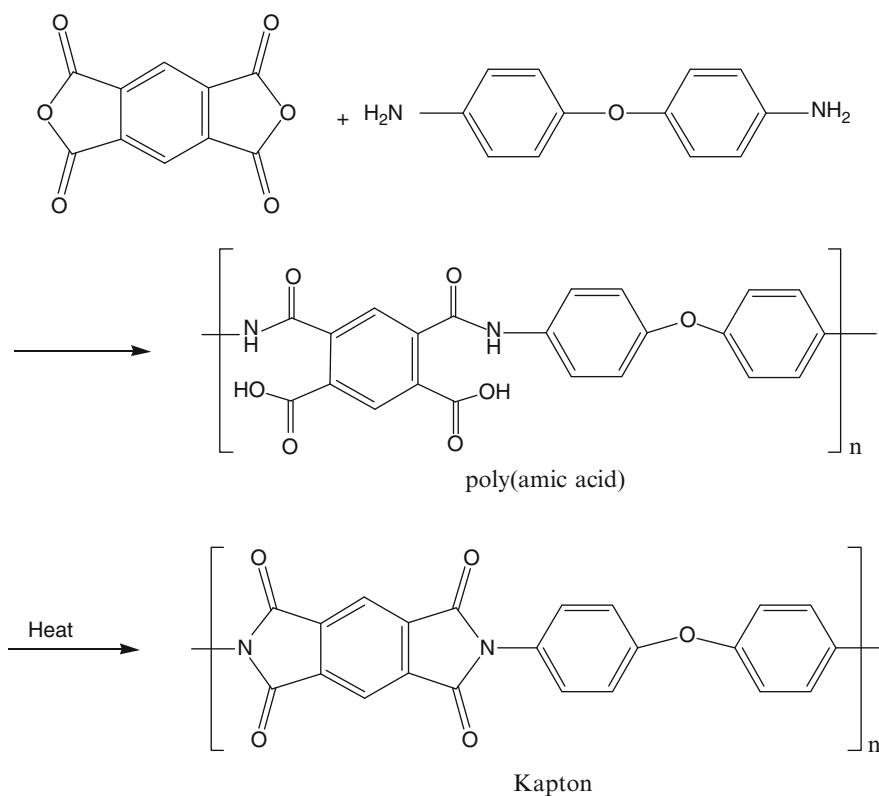
Polyetherimide, Fig. 4 Synthetic route of Kapton

Properties

Thermal Properties

Since most of PIs are infusible, molded items of PI resins are very limited and expensive. Accordingly, PIs with enhanced melt processability without sacrificing heat-resistant properties so much have been developed. The methodology is to decrease the glass transition temperature T_g by adding the flexibility to polymer chain backbone and/or by reducing the interchain interaction. The following are the practical methods to lower the T_g: (1) introducing chemical groups with higher rotational degree of freedom (e.g., –O–, –S–, –SO$_2$–, –CO–, –C(CH$_3$)$_2$–) in the chain backbones, (2) introducing asymmetric structure in the backbone by using *m*- or *o*-linkage in aromatic groups, and (3) introducing bulky groups such as –C$_6$H$_5$, –CH$_3$, and –CF$_3$ into the

backbone aromatic rings resulting in the decrease of intermolecular packing. Ultem and Aurum shown in Fig. 1 and LaRC-TPI shown in Fig. 2 are the examples of the thermoplastic resins developed by using the strategy described above. The T_gs of typical PIs along with melting temperature T_m are summarized in Table 1. LaRC-TPI and Aurum exhibit melting temperatures but others do not. Ordered aggregate structure which is distinguished from crystalline phase, sometimes called smectic phase, is known to exist in Kapton and Upilex resins [11]. Such aggregated structure makes these materials non-thermoplastic. In contrast, Ultem is amorphous and has the highest melt processability among these PI resins.

Structures of some stereoisomers of PI obtained by condensation polymerization of three BPDA (biphthalic anhydrid) isomers and
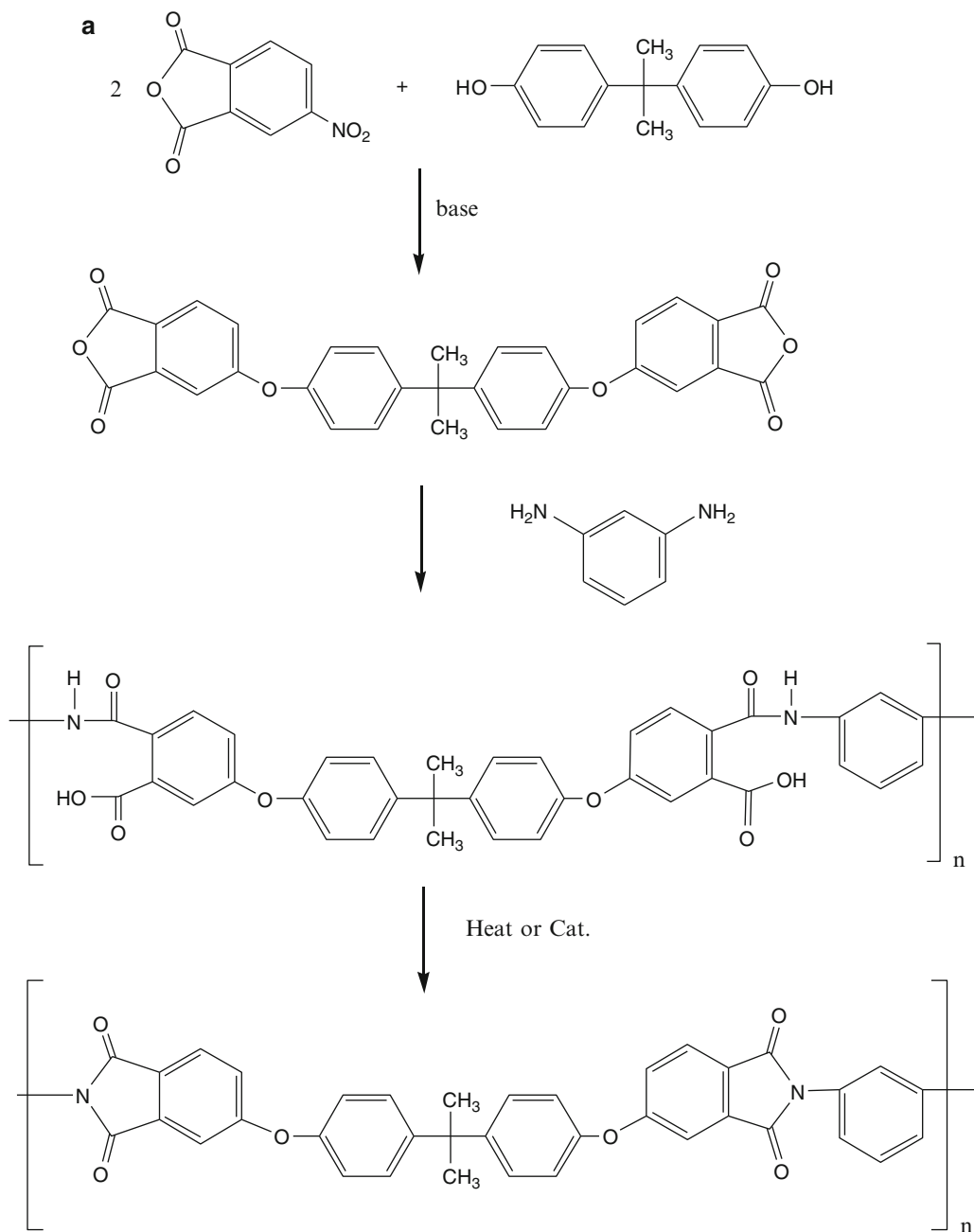
Polyetherimide, Fig. 5 (continued)

ODA (4,4′-diamino diphenyl ether) are shown in Fig. 6. T_g, and the solubility in NMP is summarized in Table 2 [12]. T_g increases in the order of structural asymmetry, s-BPDA/ODA < a-BPDA/ODA < i-BPDA/ODA. This will be because the local rotation of the rigid imide ring and the

Polyetherimide, Fig. 5 Two synthetic routes of Ultem

adjacent phenyl groups is more hindered for the asymmetric BPDA due to larger steric hindrance and the size of segmental motion becomes larger. On the other hand, the solubility in NMP increases in the reverse order of T_g. This is attributable to the decrease of the polymer-polymer aggregation for asymmetric BPDA structures.

P

Mechanical Properties

Several mechanical properties of unreinforced PIs (Kapton, Upilex-RN, Ultem, and AURUM) are summarized in Table 3. Vespel [13] and

Polyetherimide, Table 1 Glass transition temperatures

Name	$T_g/°C$	$T_m/°C$
Upilex-S [10]	>500[a]	–
Kapton [6, 10]	360–410	–
Upilex-RN [10]	285	–
LaRC-TPI [8]	250–260	330–350
Aurum [5]	250	388
Ultem [2, 3]	217	–

[a]Higher than the thermal degradation temperature

Upimol [14] are the polyimide shapes produced by sinter molding method of Kapton and Upilex-RN powders, respectively.

All PIs have higher mechanical strength than general engineering plastics such as polyacetal, polyamide, polycarbonate, etc. Because of the high T_g, such mechanical properties are preserved at high temperatures. PI has small degree of creep deformation under a long-term load and practically an excellent dimension stability. Impact strength is also high due to the flexible structure of ether part making these resins ductile. Note that this property is notch sensitive, however, which can be overcome

s-BPDA/ODA

a-BPDA/ODA

i-BPDA/ODA

Polyetherimide, Fig. 6 Structures of three stereoisomers of BPDA/ODA

Polyetherimide, Table 2 T_g and solubility of stereoisomers of BPDA/ODA [12]

	$T_g/°C$	Solubility in NMP
s-BPDA/ODA	262	×
a-BPDA/ODA	319	△
i-BPDA/ODA	330	○

×, insoluble; △, partly soluble; ○, soluble

by making sure that parts made of PI have well-rounded edges. Fatigue properties of PIs are also good.

Electrical Property

Electrical properties along with other properties are summarized in Table 4. PIs have high

Polyetherimide, Table 3 Mechanical properties of unreinforced PIs

		Temp.	Test method (ASTM[a])	Vespel SP-1 [13]	Upimol-R [14]	Ultem 1000 [3]	Aurum PL450C[5]
Tensile strength/MPa		23 °C	D638 or D1708 (Vespel)	86.2	116	105	92
		260 °C		41.4	41		
Flexural strength/MPa		23 °C	D790	110.3	161	152	137
		260 °C		62.1	59		
Flexural modulus/GPa		23 °C	D790	3.10	4.165	3.43	2.940
		260 °C		1.72	2.087		
Izod impact strength/J m^{-1}	Notched		D256	79	74.5	49	90
	Unnotched			1,600	919	1,274	
Tensile elongation/%		23 °C	D638 or D1708 (Vespel)	7.5	5.0	60	90
		260 °C		7.0	6.0		

[a]www.astm.com

P

Polyetherimide, Table 4 Properties of PI films

	Test method (ASTM[a])	Kapton-100NH [6]	Upilex-RN [15]	Ultem 1000 [3]	Aurum PL450C [5]
Density/g cm^{-3}	D-1505	1.42	1.39	1.27	1.33
Thermal expansion coefficient/10^{-5} K^{-1}	D696	2	4.3	5.6	5.5
Thermal conductivity/ W m^{-1} K^{-1}	C-177	0.12	0.24	0.22	0.17
Limiting oxygen index/%	D-2863	37	55 (JIS K7201)	47	47
Flammability	UL-94	V-0	V-0	V-0	V-0
Dielectric constant @ 1 kHz	D-150	3.9	3.2	3.15	3.2
Dielectric loss @ 1 kHz	D-150	0.0036	0.0018	0.0013	0.0009
Dielectric strength/kV cm^{-1}	D-149	303 (25 μm)	260 (25 μm)	37 (320 μm)	157 (100 μm)
Volume resistivity/Ω m	D-257	1.5×10^{15}	4.3×10^{14}	1.0×10^{15}	10^{14}–10^{16}
Water absorption 24 h@23 °C/%	D-570	4	1.4	0.25	0.34

[a]www.astm.com

dielectric strength, nearly constant dielectric constant, and low dielectric loss $<10^{-3}$ over a wide range of temperature. Due to these excellent electrical properties together with the chemical stabilities over a wide range of environmental conditions, PIs can be used in a variety of electrical and electronic insulation applications, especially in the case of high temperature use.

Flammability

PIs shown in Table 4 have the highest UL-94 flammability resistance rating V-0 as characterized by high limiting oxygen indices resulting from the highly aromatic structures (high hydrogen to carbon molar ratio). Therefore, PI resins satisfy the most severe flammability requirements for several industrial usages, such as electrical and electronics industry, building and construction industry, and automotive and aircraft industry.

Chemical Resistance

PI materials are not affected by commonly used solvents and oils, including hydrocarbons, esters, alcohols, weak acid, and alkali. The amorphous PEI (Ultem) dissolves in a few polar solvents, e.g., chlorinated aliphatics, chlorinated aromatics, NMP, etc.

Radiation Resistance

PIs have excellent radiation resistance and are frequently used in high radiation environments where a flexible insulating material is required. Especially in outer space, Kapton and Upilex are used for applications that require high radiation resistance, thermal, and electrical insulation.

Uses

PIs are used in several industrial segments: metal alternative, precision machinery, industrial machinery parts, electrical and electronic parts

(substrate for flexible circuit films, circuit boards, connectors, switches), and automotive and transport equipment parts.

References

1. Johnson RO, Burlhis HS (1983) Polyetherimide: a new high-performance thermoplastic resin. J Polym Sci Polym Symp 70:129–143
2. Parker D, Vussink J, Grampel HT, Wheatley GW, Dorf EU, Ostlinning E, Reinking K, Schubert F, Junger O (2012) Polymers, high-temperature. In: Ullmann's encyclopedia of industrial chemistry. Wiley, Weinheim (online version)
3. Saudi Basic Industries Corporation. http://www.sabic-ip.com/gep/Plastics/en/ProductsAndServices/ProductLine/ultem.html, http://www.sabic-ip.com/gepapp/eng/weather/weatherhtml?sltRegionList=1002002000%26sltPrd=1002003018%26sltGrd=1002011252%26sltUnit=0%26sltModule=DATASHEETS%26sltVersion=Internet%26sltType=Online
4. Wirth JG, Heath DR (1973) US Patent 3,730,946
5. Mitsui Chemicals. http://www.mitsuichem.com/service/functional_polymeric/compound/aurum/, DuPont. http://www2.dupont.com/Vespel/en_US/assets/downloads/aurum/pl450c.pdf
6. DuPont. http://www2.dupont.com/Kapton/en_US/, http://www2.dupont.com/Kapton/en_US/assets/downloads/pdf/HN_datasheet.pdf
7. Ube Industries. http://www.upilex.jp/e_index.html
8. Hou TH, Bai JM (1990) LaRC-TPI 1500 series polymers. NASA contractor report 181899
9. Takekoshi T Chapter 2: Synthesis of polyimides. In: Ghosh MK, Mittal KL (eds) Polyimides: fundamentals and applications, plastic engineering. Marcel Dekker, Inc., New York, 1996, pp 7–48
10. Salamone JC (1996) Polymeric materials encyclopedia, vol 8. CRC Press, Boca Raton
11. Isoda S, Shimada H, Kochi M, Kambe H (1981) Molecular aggregation of solid aromatic polymers. I. Small-angle X-ray scattering from aromatic polyimide film. J Polym Sci Polym Phys Ed 19:1293–1312
12. Chen C, Yokota R, Hasegawa M, Kochi M, Horie K, Hergenrather P (2005) Isomeric biphenyl polyimides. (I) Chemical structure-property relationships. High Performance Polymers 17:317–333
13. DuPont. http://www2.dupont.com/Vespel/en_US/assets/downloads/vespel_s/Vespel_SP-1_DF.pdf
14. Ube Industries. http://www.ube.es/archivos/pdfs/UPIMOL-R,S-569.pdf
15. Ube Industries. http://www.ube.es/archivos/pdfs/UpilexRN-566.pdf

Polyethers

Arihiro Kanazawa
Department of Macromolecular Science,
Graduate School of Science, Osaka University,
Toyonaka, Osaka, Japan

Synonyms

Polyol

Definition

Polyethers are polymers with ether bonds (C–O–C) in their main chain. Polymers categorized as polyethers include polyoxyalkylenes (Fig. 1), polyoxyarylenes, epoxy resins, polyaryletherketone (PAEK), polyetherimide (PEI), and polyethersulfone (PESU) [1]. The simplest polyoxyalkylenes are polymers with a -[O(CH$_2$)$_x$]- unit structure, such as polyoxymethylene (POM), poly(ethylene oxide) (PEO), poly(trimethylene oxide) (or polyoxetane), and poly(tetramethylene oxide) [or polytetrahydrofuran (poly(THF))]. Polyoxyalkylenes also include polymerization products from substituted cyclic ethers, such as poly(propylene oxide) (PPOX), polyepichlorohydrin, poly(glycidyl ether)s, and poly[3,3-bis(chloromethyl)oxetane (BCMO)]. Polyacetal, a polymer containing acetals in its main chain, is also a polyoxyalkylene. Polyoxyarylenes are polymers that contain aryl ether bonds in their main chain, for example, poly (phenylene oxide) (PPO).

This entry details the syntheses, properties, and applications of polyoxyalkylenes and epoxy resins. Other polyethers – POM, polyacetals, PPO, PAEK, PEI, and PESU – are discussed in other entries.

Synthesis of Polyoxyalkylenes

Polymerization and History of Cyclic Ethers
Polyoxyalkylenes are typically synthesized via the ring-opening polymerization of cyclic ethers.

The ring strain in cyclic ethers drives their polymerization; hence, their polymerizability is highly dependent on the number of atoms in the rings [2]. Three-, four-, five-, and seven-membered cyclic ethers have been reported to yield polymers via ring-opening mechanisms. Ring strain is divided into strain from the bond angles and from the repulsion of hydrogen atoms attached to the rings. The former strain drives the polymerizations of three- and four-membered cyclic ethers, whereas the latter strain drives the polymerization of five- and seven-membered rings. Cyclic ethers with six-membered rings have not undergone ring-opening polymerization because of the very small bond-angle and hydrogen-repulsion strains.

The first reported ring-opening polymerization of a cyclic ether was the generation of ethylene oxide (EO) oligomers by Wurts in 1863. He obtained these oligomers by heating the mixture of EO and water in a sealed tube. In 1929, Staudinger et al. examined the polymerization of EO using various basic compounds. They found that several compounds, including SrO and CaO, effectively yielded high-molecular-weight polymers. The polymerizations of other cyclic ethers have also been reported: propylene oxide (PO) by Levene et al. in 1927, THF by Meerwein et al. in 1937, and BCMO by Farthing in 1951. Since these pioneering reports [2], researchers have developed a wide variety of polymerization systems that involve anionic, cationic, and coordination mechanisms and the use of various initiators, metal catalysts, and organocatalysts. These polymerizations will be described in detail below.

The polycondensation of diols is theoretically another route to produce polyoxyalkylenes. The intermolecular dehydration of two hydroxy groups generates an ether bond. However, only oligomeric products are obtained via the acid-catalyzed condensation of ethylene glycol because of the frequent occurrence of intramolecular dehydration reactions. Therefore, the ring-opening polymerization of cyclic ethers is practical for the synthesis of polyoxyalkylenes.

P

Polyethers,
Fig. 1 Polyoxyalkylenes

Poly(ethylene oxide)   Polyoxetane   Polytetrahydrofuran

Poly(propylene oxide)   Polyepichlorohydrin   Poly(glycidyl ether)
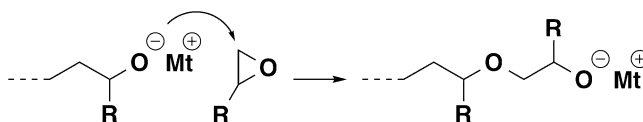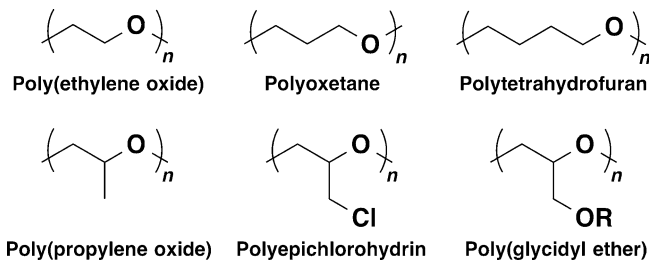
Polyethers, Fig. 2 Propagation reaction for anionic ring-opening polymerization of oxiranes

Oxirane Polymerization

Three-membered cyclic ethers, or oxiranes (oxacyclopropane), polymerize via anionic, cationic, and coordination mechanisms [2, 3].

The anionic ring-opening polymerization of oxiranes [4] is initiated by nucleophilic compounds such as alkali-metal alkoxides, hydrides, and Na-naphthalene. Organic compounds such as tertiary amines, *N*-heterocyclic carbenes, and ammonium or phosphonium salts are also used as anionic initiators. Either the compounds themselves or an anionic species derived from them attacks the α- or β-carbon of an oxirane to induce the ring-opening reaction, which generates a propagating anionic alkoxy species. This anionic species also attacks an oxirane molecule to yield a similar anionic species. Successive reactions with oxirane molecules generate the polyoxyalkylenes (Fig. 2). EO polymerization continues in this manner, i.e., a "living" reaction, without side reactions and produces high-molecular-weight polymers. In contrast, the polymerizations of oxiranes having substituents often accompany side reactions. For example, a propagating anionic species attacks and abstracts a proton from a PO methyl group to generate a "dead" chain, i.e., a polymer chain that no longer polymerizes, and an anionic alkoxy species containing a vinyl group. Therefore, this reaction acts as a chain-transfer reaction and limits the achievable molecular weights of the products.

The above drawbacks for anionic ring-opening polymerizations have been overcome via coordination polymerization [4]. This process is catalyzed using a metal compound, which coordinates both an oxirane monomer and the propagating chain end, in conjunction with a nucleophilic initiating species. Metal catalysts that have been used for this process include iron (III) chloride; alkyl aluminum; alkyl zinc; aluminum or zinc porphyrins; aluminum phenoxides; salen complexes of aluminum, chromium, and cobalt; and double-metal cyanide complexes. The polymerization proceeds via a nucleophilic attack on the coordinated monomer, which has a weakened carbon–oxygen bond because of its coordination to the metal center (Fig. 3). Because the nucleophilic species that propagate during the coordination ring-opening polymerization are similar to those that propagate during the anionic polymerization, this polymerization technique is often called "coordination anionic polymerization."

During anionic and coordination polymerizations, the propagating anionic/nucleophilic species attack the less sterically hindered carbon in the oxirane monomer. For example, PO, a methyl-substituted oxirane, almost exclusively undergoes β-scission, i.e., cleavage of the bond between the oxygen and non-substituted carbon, to form highly regioregular polymers (polymers with head-to-tail sequencing). In addition, the configuration at the substituted carbon is retained during ring opening,

Polyethers,
Fig. 3 Propagation
reaction for coordination
ring-opening
polymerization of oxiranes
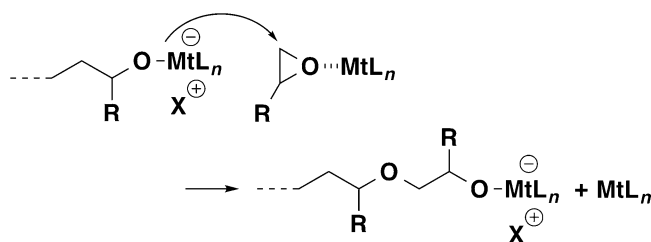
Active chain end mechanism
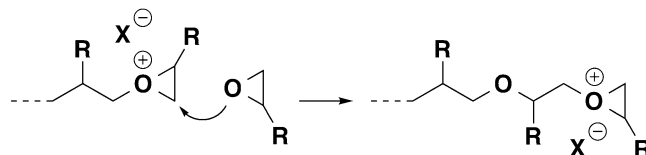
Activated monomer mechanism
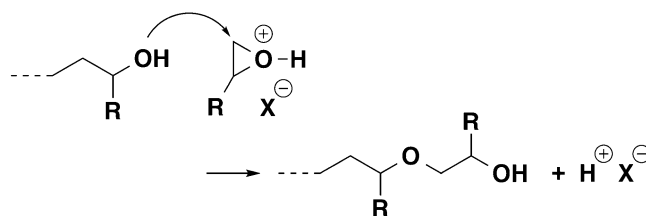
Polyethers,
Fig. 4 Propagation
reactions for cationic ring-
opening polymerization of
oxiranes

which means stereoregular polymers can be obtained from enantiomerically pure monomers. In fact, the anionic polymerization of $d(+)$-PO using KOH yields a crystalline, stereoregular PPOX, whereas the polymerization of racemic PO yields amorphous products. Furthermore, this stereoselective polymerization proceeds via a coordination mechanism that involves metal complex catalysts. The first example is PO polymerization using iron(III) chloride. This polymerization produces both crystalline, stereoregular polymers and amorphous, stereoirregular products from racemic monomers. Iron complexes that contain alkoxide groups, which are generated in situ via the reaction of iron(III) chloride with PO, or species produced by the partial hydrolysis of iron (III) chloride by adventitious water are considered to be the actual catalytic species during this stereoselective polymerization. The preferential coordination of either enantiomer to an enantiomorphic site on the metal complexes appears to be responsible for the selectivity.

Another system that polymerizes oxiranes is cationic ring-opening polymerization [5].

Potential initiators include strong protic acids and metal-halide Lewis acids. Two mechanisms for cationic ring-opening polymerization have been developed: the active chain-end mechanism and the activated monomer mechanism (Fig. 4). The active chain-end mechanism is a conventional polymerization that proceeds via the attack of a monomer molecule on the carbon adjacent to the chain-end oxonium cation. However, this mechanism often involves side reactions, such as back biting, that yield large quantities of cyclic oligomeric products, which makes the production of high-molecular-weight polymers difficult. Proton elimination at the chain ends and intermolecular chain transfers also occur via the chain-end mechanism. In contrast, the polymerizations by the activated monomer mechanism proceed with fewer side reactions and lower oligomer yields. This technique employs hydroxy compounds combined with strong protic acids. A monomer molecule is activated by the addition of an acidic proton, followed by the attack of a hydroxy group at the activated monomer. This reaction generates
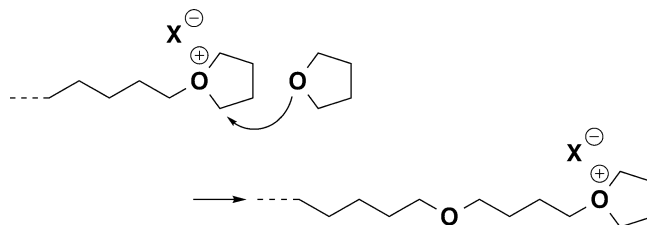
a ring-opened product that contains a hydroxy group and liberates a proton, which activates successive monomers that react with this hydroxy group. Because the oxonium cations are not generated at the chain ends, back-biting reactions do not occur and the polymerization proceeds in a living-like manner.

Oxetane, Oxolane, and Oxepane Polymerizations

Four-, five-, and seven-membered cyclic ethers – oxetane, oxolane, and oxepane, respectively – yield polymers via cationic ring-opening polymerization [2].

Oxetane is highly polymerizable due to its large strain. Various oxetanes with substituents in the 3-position, such as BCMO, also yield polymers. Lewis acids such as BF$_3$ polymerize oxetane but require a small amount of water. The proton generated via the reaction of a Lewis acid with water possibly initiates the polymerization. The reaction propagates via the active chain-end mechanism, i.e., the S$_N$2-type attack of a monomer at the oxonium cation at the chain end, as was the case for the cationic polymerization of oxiranes. Intramolecular transfer generates primarily a cyclic tetramer with a 16-membered ring and a cyclization ratio that is dependent on the oxetane substituents. Oxetane polymerization also likely proceeds via the activated monomer mechanism in the presence of hydroxy compounds.

A non-substituted oxolane, THF, also polymerizes via a cationic ring-opening mechanism. However, the polymerizability of THF is low relative to that of oxiranes and oxetanes because of its low ring strain. In fact, an equilibrium exists between the monomer and polymer during THF polymerization at not so high temperatures; i.e., the ceiling temperature of THF polymerization is relatively low (~85 °C) [2]. In addition,

substituents strongly reduce the oxolane polymerizability because they alter the balance between the strain in the ring and the strain in the generated polymer chain.

THF, similar to oxirane and oxetane, polymerizes via an active chain-end mechanism (Fig. 5). A THF molecule attacks the carbon atom adjacent to the cationic oxonium on the propagating chain end. It should be noted that the THF polymerization proceeds in a living fashion when suitable initiators are employed. Initiators such as trifluoromethanesulfonic acid form a dormant species with a covalent carbon–oxygen bond at the chain end, and the bond reversibly dissociate to generate a propagating oxonium ion. However, conditions for the activated monomer mechanism, i.e., protic acids and hydroxy compounds, do not initiate the THF polymerization, most likely because the secondary oxonium ion formed by THF and a proton exhibits extremely low reactivity toward nucleophilic attack by a hydroxy group.

Small concentrations of oxiranes have been reported to enhance the polymerizations of oxetane and THF. During the cationic polymerization of these monomers, oxiranes such as epichlorohydrin and PO preferentially undergo ring opening to generate tertiary oxonium ions during the initiation step. This process is followed by the reaction of the generated oxonium ions with oxetane or THF and smooth propagation. These compounds, called "promoters," facilitate the polymerization not by increasing the kinetic constants of the propagation reactions but rather by increasing the concentrations of the propagating species.

A seven-membered cyclic ether, oxepane, also polymerizes via the cationic mechanism; however, its reactivity is lower than that of THF. The strain in oxepane is derived from the repulsion of quasi-axial hydrogen atoms.

Properties and Applications of Polyoxyalkylenes

Polyoxyalkylenes contain carbon and oxygen atoms in their backbone and thus have properties that depend on the ratios of these atoms. For example, PEO is amphiphilic, i.e., PEO dissolves in both water and various organic solvents. In contrast, polyoxyalkylenes that contain higher ratios of carbon, such as poly(oxetane), poly (THF), and PPOX, do not dissolve in water because of their increased hydrophobicity. The thermal properties of polymers also differ; simple polyoxyalkylenes – PEO, PPOX, poly(oxetane), and poly(THF) – commonly have lower glass-transition temperatures (–100 °C to –40 °C) [6] and higher melting points (30–80 °C) [7] compared to room temperature.

The properties of polyoxyalkylenes are also affected by their side-chain substituents. Various functional groups can be introduced into the side chains of poly(glycidyl ether)s. Their syntheses and applications are actively investigated. In addition, polyepichlorohydrin, a polyoxyalkylene that contains chlorine in its side chains, is used industrially because of its unique properties.

Poly(Ethylene Oxide) (PEO)

PEO (Fig. 1) is probably the most widely studied and used polyoxyalkylene because its amphiphilicity, neutrality, and nontoxicity suit many purposes across various fields, including the biomedical field [8, 9]. Two names, poly(ethylene oxide) (PEO) and poly(ethylene glycol) (PEG), are commonly used, although both describe polymers with the same -(OCH$_2$CH$_2$)- structure. The names PEO and PEG are used to describe relatively high- and low-molecular-weight products, respectively. The former name is used for all the polymers in this essay.

The most attractive features of PEO are its hydrophilicity and nontoxicity. PEOs attached to hydrophobic moieties are widely used as nonionic surfactants (Fig. 6) for commodities such as cosmetics and detergents. PEOs containing a hydroxy group at one chain end and a long alkyl group (C$_{12}$ to C$_{18}$), aromatic group, or PPOX segment at the other chain end are

Polyethers, Fig. 6 Nonionic surfactant having a PEO chain and a hydrophobic moiety

commercially available from numerous companies. These PEO-based nonionic surfactants form micelles in water that can contain hydrophobic compounds.

The hydrophilicity and nontoxicity of PEOs have also enabled their use in biomedical applications. Some proteins exhibit therapeutic activity but insufficient efficiencies from a quantitative viewpoint because of drawbacks such as short blood circulation times, low stability, or poor solubility. Attaching a PEG chain, or "PEGylation," can overcome these drawbacks. PEG chains covalently attached to proteins exhibit a stealth effect, which weakens their immunogenicity and protects them from enzymatic degradation. The blood circulation time is also improved due to the increased hydrodynamic size. In addition, the hydrophilicity of PEO improves the water solubility of hydrophobic proteins. Numerous PEGylated pharmaceutical products have been approved by the US Food and Drug Administration (FDA).

The PEGylation of proteins often involves the use of N-terminus amines or lysine residues [10]. The amino groups are alkylated or acylated using PEOs that contain end-functional groups such as dichlorotriazine, tresylate, carbonate, aldehyde, or ester groups (Fig. 7). The thiol in cysteine residues is also available for PEGylation. PEOs that contain alkenyl groups, such as maleimide, at one chain end react with thiols.

PEGylation is also used for drugs other than proteins. However, significantly fewer examples have been reported relative to the PEGylation of proteins, because PEGylated small molecules do not usually exhibit activity superior to that of the original drugs. The shielding effect, i.e., the PEO-induced hindrance of the interaction between the drug molecules and the active sites in living organisms, is responsible for such cases. In contrast, PEGylated dendrimers are used as

Polyethers, Fig. 7 PEGylation of proteins through the reaction with an amino group

carriers for small-molecule drugs. Because the drugs are not covalently bonded to the PEGylated dendrimers, the shielding effect does not occur and the drugs retain their activity. The small-molecule drugs encapsulated in dendrimer cores are gradually released into the body. The drug loading and releasing depends on the interactions between the dendrimer core and the drug.

Their flexibility is another valuable feature of PEOs. A telechelic PEO containing hydroxy groups at both chain ends is used during the industrial synthesis of polyurethanes. PEO-based polyurethanes exhibit elastomeric properties due to the flexibility of the PEO segments. Polyoxyalkylenes used as polyols for polyurethane synthesis are described below.

PEO has been used as an electrolyte for lithium-ion batteries. Because ether oxygen atoms act as Lewis bases, positive lithium ions interact with them and move through the PEO chains. PEOs are very attractive solid battery electrolytes because of their safety, which stems from the PEO electrolyte having no risk of leaking. Another advantage of this flexibility is that it allows batteries to be manufactured in any shape. However, a practical battery with a PEO electrolyte has not yet been manufactured because of the low conductivity of PEO at room

temperature that stems from its tendency to crystallize. Numerous companies are currently investigating approaches to improve the conductivity of PEO. In addition, because PEO is highly conductive at high temperatures, its possible use in car batteries is also being investigated.

Poly(Propylene Oxide) (PPOX) and Polytetrahydrofuran [Poly(THF)]

PPOX has a PEO backbone with a methyl substituent on each repeating unit (Fig. 1). Because of their similarity, PPOX exhibits many properties similar to those of PEO; however, unlike PEO, PPOX is not hydrophilic and does not dissolve in water. The structure of poly(THF) contains two more methylene groups per PEO repeating unit (Fig. 1) and is also hydrophobic. Both PPOX and poly(THF) are industrially produced in very large scales.

PPOX and poly(THF) are primarily used as polyols in the synthesis of polyurethanes. These polyethers make the polyurethanes flexible. In addition, PPOX is used as the hydrophobic segment in nonionic surfactants. Block copolymers with PEO are available from many companies. In particular, micelles of PEO–PPOX block copolymers in water are the most broadly studied amphiphilic polymers for drug delivery system

carriers among the various amphiphilic polymers. Hydrophobic drugs are encapsulated within the micellar core, and the micelles are transported via the bloodstream [11].

Polyepichlorohydrin

Polyepichlorohydrin contains chloromethyl substituents (Fig. 1), from which it derives unique properties [12]. Because of the relatively high polarity of its carbon–chlorine bonds, this polymer exhibits good oil resistance. Its high rate of agglomeration results in low gas permeability. The polymer also exhibits resistance to heat and cold. Furthermore, epichlorohydrin copolymers with ethylene oxide and/or allyl glycidyl ether exhibit improved properties. Ethylene oxide provides flexibility at low temperatures without loss of the oil resistance. The allyl group in allyl glycidyl ether prevents the degradation of the copolymer main chains by oxygen and ozone.

These properties for epichlorohydrin (co)polymers allow their use in oil and air hoses. Their properties render them particularly well suited for use in a variety of automobile hoses. Furthermore, epichlorohydrin copolymers have been recently used in office automation equipment. Their unique semiconductivity makes them appropriate for use in electrification, transfer, and image development rollers in printers and copiers.

Poly(Glycidyl Ether)s

Glycidyl ethers are oxiranes that contain a -CH_2OR substituent. Because glycidyl ethers are synthesized from an alcohol and epichlorohydrin, a variety of functional groups, such as allyl, ester, epoxide, alkynyl, tosylate, phenyl, benzyl, azide, carbonate, and sulfhydryl groups, can be introduced as moiety R. Poly(glycidyl ether)s (Fig. 1) exhibit various properties due to their functional groups. Many glycidyl ether monomers are commercially manufactured on an industrial

scale. In addition, various monofunctional glycidyl ethers are used as reactive diluents in the synthesis of epoxy resins.

Glycidyl ether copolymers with other oxiranes, especially ethylene oxide, have attracted increasing attention as functional materials [13]. Various glycidyl ethers can be randomly copolymerized with ethylene oxide to yield polyethers with side-chain functional groups. These polymers possess both the characteristics of PEO and the functionalities derived from the introduced groups; however, their properties depend on the composition ratio. The post-modification of side chains such as hydroxy, vinyl, and azide groups allows a wide variety of functional groups to be incorporated. The applications of glycidyl ether copolymers are widely studied, particularly in the biomedical field.

Epoxy Resins

Epoxy resins are polymers that contain multiple epoxy groups in a polymer chain [14]. These polymers react with curing agents, such as diamines and anhydrides, to yield cross-linked polymers. The cured polymers generally exhibit good heat, solvent, acid, and alkaline resistances, good mechanical and adhesive properties, and good dimensional stability, and these properties depend on the chemical structure of the resin. Thus, epoxy resins are used in adhesives, electrical materials, and paint. Both the prepolymers and the cured polymers are referred to as epoxy resins.

The most widely used prepolymer is synthesized from bisphenol A and epichlorohydrin (Fig. 8). This polymer contains ether bonds and phenyl groups in the main chain and epoxy groups at each chain end. Other prepolymers that contain plural epoxy groups at the chain ends are synthesized from polyols, such as telechelic PEO and PPOX. A variety of prepolymers are available on industrial scales. The reaction of these epoxy

Polyethers, Fig. 8 A prepolymer synthesized from bisphenol A and epichlorohydrin
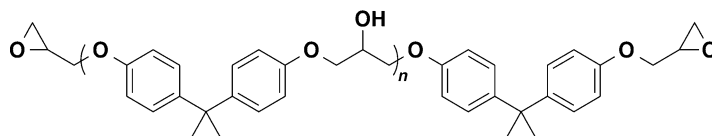
groups with multifunctional amines yields a cured polymer. For example, a diamine functions as a four-function compound that yields densely cross-linked products.

References

1. Metanomski WV (1999) Nomenclature. In: Brandrup J, Immergut EH, Grulke EA (eds) Polymer handbook, 4th edn. Wiley, New York
2. Saegusa T (1971) Kaikan Jugo. Kagakudojin, Kyoto
3. Penczek S, Cypryk M, Duda A, Kubisa P, Slomkowski S (2007) Living ring-opening polymerizations of heterocyclic monomers. Prog Polym Sci 32:247–282
4. Brocas AL, Mantzaridis C, Tunc D, Carlotti S (2013) Polyether synthesis: from activated or metal-free anionic ring-opening polymerization of epoxides to functionalization. Prog Polym Sci 38:845–873
5. Kubisa P, Penczek S (1999) Cationic activated monomer polymerization of heterocyclic monomers. Prog Polym Sci 24:1409–1437
6. Andrews RJ, Grulke EA (1999) Glass transition temperatures of polymers. In: Brandrup J, Immergut EH, Grulke EA (eds) Polymer handbook, 4th edn. Wiley, New York
7. Miller RL (1999) Crystallographic data and melting points for various polymers. In: Brandrup J, Immergut EH, Grulke EA (eds) Polymer handbook, 4th edn. Wiley, New York
8. Dimitrov I, Tsvetanov CB (2012) High-molecular-weight poly(ethylene oxide). In: Matyjaszewski K, Möller M (eds) Polymer science: a comprehensive reference. Elsevier, Amsterdam
9. Dimitrov I, Tsvetanov CB (2012) Oligomeric poly (ethylene oxide)s. Functionalized poly(ethylene glycol)s. PEGylation. In: Matyjaszewski K, Möller M (eds) Polymer science: a comprehensive reference. Elsevier, Amsterdam
10. Roberts MJ, Bentley MD, Harris JM (2002) Chemistry for peptide and protein PEGylation. Adv Drug Deliv Rev 54:459–476
11. Chiappetta DA, Sosnik A (2007) Poly(ethylene oxide)–poly(propylene oxide) block copolymer micelles as drug delivery agents: improved hydrosolubility, stability and bioavailability of drugs. Eur J Pharm Biopharm 66:303–317
12. Otaka T (2005) The recent trend of epichlorohydrin rubber. Nippon Gomu Kyokaishi 78:73–77
13. Obermeier B, Wurm F, Mangold C, Frey H (2011) Multifunctional Poly(ethylene glycol)s. Angew Chem Int Ed 50:7988–7997
14. Ise N, Imanishi Y, Kawabata S, Sunamoto J, Higashimura T, Yamakawa H, Yamamoto M (1995) Shin Kobunshikagaku Joron. Kagakudojin, Kyoto

Polyethylene (PE; Low Density and High Density)

Taka-aki Okamura
Department of Macromolecular Science, Graduate School of Science, Osaka University, Toyonaka, Osaka, Japan

Synonyms

Polymethylene

Definition

The polymer with repeated ethylene ($-CH_2CH_2-$) unit produced by the polymerization of gaseous ethylene. Generally, copolymers of ethylene with α-olefines, showing similar structures, are included in this category.

Classification

Polyethylene is classified into several categories based on the density that deeply depends on branching: almost linear high-density polyethylene (HDPE, 0.94–0.96 g cm^{-3}), branched low-density polyethylene (LDPE, 0.915–0.925 g cm^{-3}), and medium-density polyethylene (MDPE, 0.925–0.94 g cm^{-3}) with intermediate density [1]. Linear low-density polyethylene (LLDPE), made by copolymerization of ethylene with α-olefines, is known. Very low-density polyethylene (VLDPE) is also commercially available (Fig. 1).

History

In 1898, von Pechmann accidentally synthesized a white flocculent substance from an ethereal solution diazomethane on standing, which was characterized by Bamberger and Tschirner after 2 years and termed "polymethylene" with repeated methylene ($-CH_2-$) unit. The polymer was produced by the following decomposition reaction:
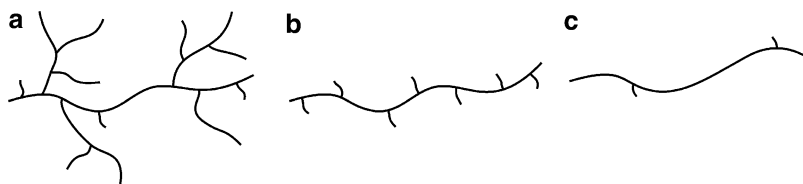
Polyethylene (PE; Low Density and High Density), Fig. 1 Schematic molecular structures of (**a**) LDPE, (**b**) LLDPE, and (**c**) HDPE

$$n(CH_2N_2) \rightarrow (CH_2)_n + nN_2$$
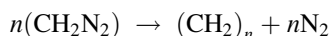
Direct polymerization of ethylene to polyethylene was also accidentally achieved by two researchers of Imperial Chemical Industries, Ltd (ICI), Fawcett and Gibson, in 1933 during a systematic study about influence of high-pressure on organic reactions under 3,000 atm. At first, the polymer was obtained as a trace amount of white powder in a reaction vessel, but a commercial-scale plant was constructed by ICI and industrial production was started in 1939. The obtained polyethylene by this process was highly branched LDPE.

After that, relatively low-pressure polymerization was developed by several companies and researchers. One of them is chromium oxide supported on silica developed by Phillips Petroleum (referred to Philips catalyst). Numerous patents on such catalysts, e.g., reduced molybdenum oxide on activated alumina, were announced by Standard Oil. In 1953, Ziegler found that TiCl$_4$-AlEt$_3$ catalyst induced the polymerization of ethylene under ordinary pressure to give HDPE during the searing possible combinations of alkyl aluminum and various transition metals after the discovery of nickel effect by accident [2]. In the 1960s, Mitsui Petrochemicals and Montecatini independently found that anhydrous MgCl$_2$-supported TiCl$_4$ with AlEt$_3$ significantly enhanced catalytic activity and resulted in the omission of de-ashing process in manufacturing plants [3, 4].

Soluble conventional Ziegler-Natta catalysts, Cp$_2$TiCl$_2$–AlEt$_3$ (or AlBu$_3$, Et$_2$AlCl; Cp = cyclopentadienyl), polymerize ethylene but are not very active. In 1976, Kaminsky and coworker reported that Cp$_2$TiCl$_2$ showed fairly high

activity for the polymerization of ethylene when methylalumoxane (MAO) that was prepared by addition of equimolar water to Me$_3$Al was used. Metallocenes of the Group 4 elements (Ti, Zr, Hf) show similar catalytic activity with MAO, which are called Kaminsky catalysts. Cationic metallocene complexes of the Group 4 elements with bulky counter anion, BPh$_4^-$ or B(C$_6$F$_5$)$_4^-$, show catalytic activity for the polymerization without MAO [3].

Catalysts

In the polymerization process of ICI under high pressure, a small amount of oxygen may be used as a catalyst [2]. Ziegler catalysts contain TiCl$_4$ and alkylaluminums, typically AlEt$_3$. Although both TiCl$_4$ and AlEt$_3$ are liquid, mixing these materials in hydrocarbon give brown slurry owing to the formation of β-TiCl$_3$ and so forth, which act as heterogeneous catalysts. The exact active species is unclear, but the most active species is considered to be Ti(III). A combination of TiCl$_3$ and Et$_2$AlCl (or AlEt$_3$) was developed by Natta for the catalyst to polymerize propylene, which is called Natta catalyst. These catalysts are categorized to Ziegler-Natta catalysts including widely the related binary combination of the Group 4–8 transition metal compounds and Group 1–3 alkylmetals. Because typical heterogeneous Ziegler-Natta catalysts have plural active sites, they are called multi-site catalysts. On the other hand, Kaminsky-type catalysts are called single-site catalysts, which contain metallocenes of the Group 4 elements. It had been difficult to obtain high molecular weight polyethylene by late transition metal elements because of easy β-elimination

P

reaction [3]. In 1995, Brookhart reported Ni and Pd diimine compound without cyclopentadienyl (Cp) ligand as a highly active ethylene polymerization catalysts. Such post-metallocene catalysts have non-organometallic coordination, such as N and O, and enable the use of the other cheap late transition metals (Fe, Co) keeping the catalytic activity [5].

Low-Density Polyethylene (LDPE)

LDPE is produced by the free radical polymerization of ethylene under very high pressure and high temperatures, resulting in highly branched structure, containing both ethyl and butyl branches formed by backbiting, giving 30–40 methyl group per 1,000 carbon atoms determined by infrared (IR) spectra or nuclear magnetic resonances (NMR) and containing a few long branches per 1,000 carbon atoms formed by transfer to polymer. Backbiting is internal chain transfer that is the terminal of a growing polymer chain abstracts H atom from an internal $-CH_2-$ group to give a side chain. The branching forms irregular structures, which disturb the packing of the polymers and lower the crystallinity (below about 50 %), hence reduces the density of the solid polymer. The low crystallinity lowers the melting point (about 80–110 °C) and gave soft, flexible, and transparent character to the solid polymer. Typically LDPE exhibits a tensile modulus of 0.2 GPa, a tensile strength of 10 MPa, an elongation at break of 800 %, and an Izod impact strength of >15 J (12.7 mm)$^{-1}$. Its major use is as a film material especially for packaging [1].

High-Density Polyethylene (HDPE)

HDPE is produced by the coordination polymerization of ethylene using Ziegler-Natta catalysts under low pressure or in Philips (chromium oxide on silica catalyst) and Standard Oil (reduced molybdate on alumina catalyst) processes under moderately low pressure. This polymerization gave almost linear polyethylene but frequently has about five methyl groups per 1,000 carbon

atoms deliberately introduced by copolymerization. The crystallinity is about 70–90 %; therefore, the density is high (about 0.96 g cm^{-3}) and the melting point is 120–135 °C. Appearances are translucent (or opaque), hard, and stiff. Typical HDPE exhibits a tensile modules of 1.0 GPa, a tensile strength of 30 MPa, an elongation at break of 500 %, and an Izod impact strength of 2–8 J (12.7 mm)$^{-1}$. Its main used is as a pipe, container, film and injection molding materials.

Linear Low-Density Polyethylene (LLDPE)

LLDPE exhibits similar properties to LDPE, but the preparation is similar to HDPE. LLDPE is produced by the copolymerization of ethylene with a few percent of a higher α-olefin comonomer (e.g., 1-butene, 1-hexene, and 1-octene) using Ziegler-Natta catalysts or the other coordination polymerization catalysts as described in HDPE [1]. The number of branches is 10–20 per 1,000 carbon atoms. The density is 0.92–0.94 g cm^{-3}, the crystallinity is 50–70 %, the melting point is 115–125 °C, and a tensile module is 270–530 MPa [3]. Single-site catalysts, well-designed metallocenes, gave excellent polymers with very narrow molecular weight distributions (MWDs) and comonomer distributions, which leads high strength and uniformity. Such polymers are called metallocene polyethylenes (mPE). Metallocene VLDPE and LLDPE are commercially produced using proprietary metallocene catalysts [5].

Ultra High Molecular Weight Polyethylene (UHMWPE)

UHMWPE is produced by Ziegler-Natta, metallocene, and FI (post-metallocene, Mitsui) catalysts. UHMWPE exhibits a long linear structure with very high molecular weight (>10^6), usually in the range of 2–6 million. The density (about 0.93 g cm^{-3}) is less than that of HDPE caused by the less crystallinity (about 50 %). The molecular structure results in one of the strongest materials

known for a given weight [6]. Various products are commercially available including fiber, sheets, very fine particles, rods, gears, and the other moldings. The impact strength, abrasion resistance, and essential inactivity of PE enable the medical use for tough biomaterials, e.g., artificial hip joints.

Uses

Polyethylene is widely used in our daily lives because of its chemical, biological, and electrical inactivity and toughness for its light weight. Major use of LDPE is films including bags, food packages protecting from many contaminations, agricultural products, wrapping films protecting industrial products against accidental damage during transport, and waterproof sheets for cooking, hygienic, and housing uses. In practical uses, polyethylene is used as a monolayer film or co-extruded with other materials such as a barrier material, e.g., poly(ethylene-*co*-vinyl alcohol) (PEVOH) shutting out gases. A thin coat of polyethylene on paper makes it resistant to wetting and makes it possible to use for liquid packaging of milk, juices, and other liquids. LDPE is used for the insulation of electricity cables. HDPE used molded materials including bottles, buckets, tanks, pipes, container, and so on. Polyethylene resists ordinary acids, alkaline, water, chemicals, and the other corrosive environments and, therefore, is used for shampoo, conditioner, cosmetic items, household cleaners, detergents, bleach, motor oil, coal oil, pesticides, herbicides, and many applications too numerous to mention [7].

Related Entries

▶ Polypropylene

References

1. Alger M (1997) Polymer science dictionary, 2nd edn. Chapman & Hall, London
2. Raff RAV, Allison JB (1956) Polyethylene. In: Mark H, Melville HW, Marvel CS, Whitby GS (eds) High polymers, vol 11. Interscience, New York
3. Masuda T, Makio H, Miyashita A (1997) Olefin polymerization by Ziegler-Natta catalysts. In: Kobayashi S (ed) Catalysis in precision polymerization. Wiley, Chichester
4. Kaminsky W, Sinn H (eds) (1988) Transition metals and organometallics as catalysts for olefin polymerization. Springer, Berlin
5. Vaughan A, Davis DS, Hagadorn JR (2012) Industrial catalysts for alkene polymerization. In: Coates GW, Sawamoto M (eds) Chain polymerization of vinyl monomers. Polymer science: a comprehensive reference, vol 3. Elsevier, Amsterdam, pp 657–672
6. Zohuri GH, Albahily K, Schwerdtfeger ED, Miller SA (2012) Metallocene alkene polymerization catalysts. In: Coates GW, Sawamoto M (eds) Chain polymerization of vinyl monomers. Polymer science: a comprehensive reference, vol 3. Elsevier, Amsterdam, pp 673–697
7. Demirors M (2011) The history of polyethylene. In: Strom ET, Rasmussen SC (eds) 100+ Years of plastics. Leo Baekeland and beyond, vol 1080, ACS symposium series., pp 115–145. doi:10.1021/bk-2011-1080.ch009

Polyfluorenes

Emil J. W. List-Kratochvil
NanoTecCenter Weiz Forschungsgesellschaft m.b.H., Weiz, Austria
Institute of Solid State Physics, Graz University of Technology, Graz, Austria

Definition

Polyfluorene homo- and copolymers, primarily synthesized by Suzuki- and Yamamoto-type aryl–aryl couplings, are an important class of conjugated polymers used in polymer light-emitting diodes, solar cells, and laser applications.

Introduction

Since the first report on electroluminescence from organic materials dated back to the 1960s [1], it was recognized that light-emitting small molecules [2] as well as light-emitting conjugated polymers [3] have enormous potential as active materials for large-area flat-panel displays, lighting, as well as laser applications [4].

Among different available chemical structures derived from the poly(*para*-phenylene) (PPP) motif, such as polyindenofluorenes PIF (2 of 3 aryl–aryl linkages are bridged) [5], poly (pentaphenylene)s (4 of 5 aryl–aryl linkages are bridged) [6], and ladder-type PPPs (LPPP) [7], highly emissive blue light-emitting polyfluorenes (PFs) have received particular attention during the last decades. Up to date more than 3,500 original research papers have been published dealing with the synthesis and characterization of PF-type polymers and their use in light-emitting and solar cell device applications.

First attempts to polymerize fluorene date back to as early as 1973 [8]. However, only after the first report on the synthesis of soluble poly (9,9-dialkylfluorenes) by Yoshino and co-workers in 1989 [9], different PFs and fluorene-based copolymers have been synthesized primarily based on Suzuki- and Yamamoto-type aryl–aryl couplings [10]. The photophysics and degradation of PF-type polymers have been intensively studied, and impressive improvements concerning color purity and device stability of PF and PIF-based devices have been made [11]. Spectroscopic and structural investigations revealed the complex interplay of the physical structure, the solid-state morphology, and the photophysics of polyfluorenes [12]. The PF-type homo- and copolymers have been successfully used as blue light-emitting conjugated polymer in polymer light-emitting diodes (PLEDs), solar cells, and laser applications.

Synthesis of PF-Type Polymers

Following the first synthesis of PFs via the oxidative coupling of 9,9-dialkylfluorene monomers with $FeCl_3$ as shown in Fig. 1, a group at Dow Chemicals showed an approach based on the Suzuki-type cross-coupling. This polycondensation requires two monomers with the functionality of the AA–BB type. 9,9-dialkyl-2,7-dibromofluorene and the corresponding 9,9-dialkylfluorene-2,7-diboronic esters have to be reacted in the presence of a palladium catalyst. This type of Suzuki coupling leads toward high molecular weight, soluble poly (9,9-dialkylfluorene-2,7-diyl)s [12] and enables the synthesis of strictly alternating copolymer. A second type of Suzuki cross-coupling is the reaction of one monomer of the AB type as shown in Fig. 2. This precursor material has to contain both a halide and a boronate. Independently, Nothofer and Scherf developed an alternate approach based on the Yamamoto-type homocoupling of 9,9-dialkyl-2,7-dibromofluorene as shown in Fig. 3 [13]. Both methods lead to high-quality PFs with a number
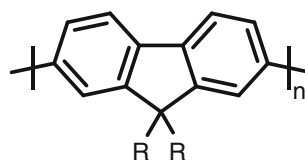
Polyfluorenes, Fig. 1 Structure of poly(9,9-dialkylfluorene-2,7-diyl) (PF)

Suzuki Coupling (AA-BB Type)
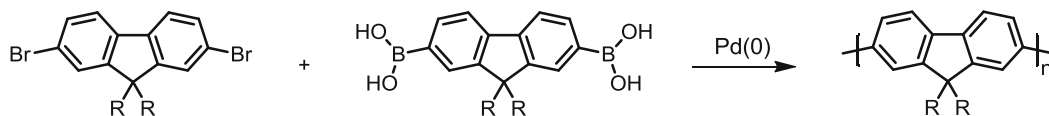
Suzuki Coupling (AB Type)

Polyfluorenes, Fig. 2 Synthesis of poly(9,9-dialkylfluorene-2,7-diyl) after two types of Suzuki coupling (*AA-BB type* and *AB type*)

Yamamoto Coupling

average molecular weight of up to 300,000, corresponding to a coupling of several hundreds of repeat units. In parallel, Müllen et al. have extended the pattern of bridged and non-bridged biphenyl units in PPP-type polymers by synthesizing PIF and poly(pentaphenylene)s [6, 14].
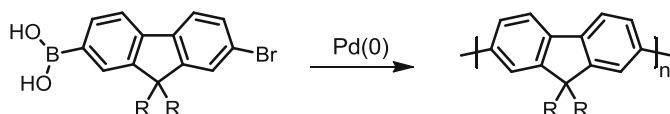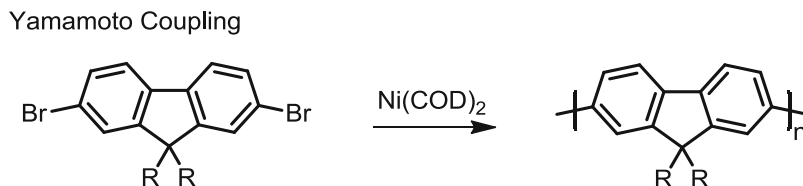
Aside from the emphasis on the synthesis of homopolymers, a variety of copolymers, mainly for device applications, containing additional hole and electron transport moieties either in the PF chain (including alternating copolymers) or by endcapping or side-chain substitution, have been made [15].

Despite the fact that in PF-type polymers one finds the optical bandgap of ca. 2.9 eV already developed for relatively short chain lengths of 5–6 repeat units reflecting a relatively short length of the effectively conjugated segments due to the weak interaction of the aromatic subunits, only polymers with a molecular weight >15,000 allow for processing into high-quality films from solution.

PFs exhibit a very rich variety of structures in the condensed state. In particular the substituents at the nine-position strongly influence the solid-state packing behavior. Today many derivatives with linear and branched alkyls as well as aryls including dendritic oligophenyl and spirobifluorene-type side chains exist. Moreover linear and branched poly(ethylene glycol) and ionic side chains making the polymers highly soluble in ethanol or water are known and used for PLED and sensor applications. In particular ethanol- or water-soluble PFs were used for realizing electron injection facilitating layers in multilayer PLED configurations processed from solution.

Different phases have been identified, including nematic liquid crystalline (LC) mesophases and crystalline phases including the so-called β-phase as found for linear n-octyl alkyls denoted as PFO or PF8 and a helical phase as found for

2-ethylhexyl resulting in the so-called PF2/6. Also nematic LC states have been found for PFs, which if quenched into a film, result in PLEDs with highly polarized light emission.

Photophysics

As shown in Fig. 4 PFs such as PF2/6, if spin cast from toluene, in thin films display an unstructured absorption with a maximum at 3.3 eV. The photoluminescence (PL) emission spectrum of such PFs shows a vibronic fine structure with an energetic spacing of ca. 180 meV (stretching vibration of the C=C–C=C structure of the polymer backbone) with the π^*–π transition at ca 2.9 eV yielding a deep blue emission. Dilute solutions using an apolar solvent show spectra very similar to that of the thin film only deviating by a bathochromic shift of ~20 meV for both absorption and emission. The PL quantum yield of PFs has been reported to be as high as 85 % in solution and 55 % in solid films with a typical total singlet exciton lifetime of 370 ps in solution and 170 ps in the solid state.

Structure and Morphology

As depicted in Fig. 5 compared to PFs such as PF2/6, which have branched alkyl chains, PFs with octyl–alkyl derivatives such as PFO display a unique packing behavior in condensed phase upon thermal treatment or in mixtures of polar and apolar solvents (chloroform/methanol) forming a so-called β-phase as compared to the to the regular, glassy (alpha-) phase. PFO in (chloroform/methanol) solutions of increasing methanol content shows an agglomeration of individual polymer chains. The agglomeration of single macromolecules is accompanied by the occurrence of a series of novel, redshifted absorption peaks at ca. 2.85, 3.04, and 3.22 eV.

P

Polyfluorenes,
Fig. 4 Absorption,
photoluminescence
emission, and
photoinduced absorption
spectrum of a typical PF2/6
polymer film (*full lines*) and
PF2/6 diluted in toluene
(*dashed line*)
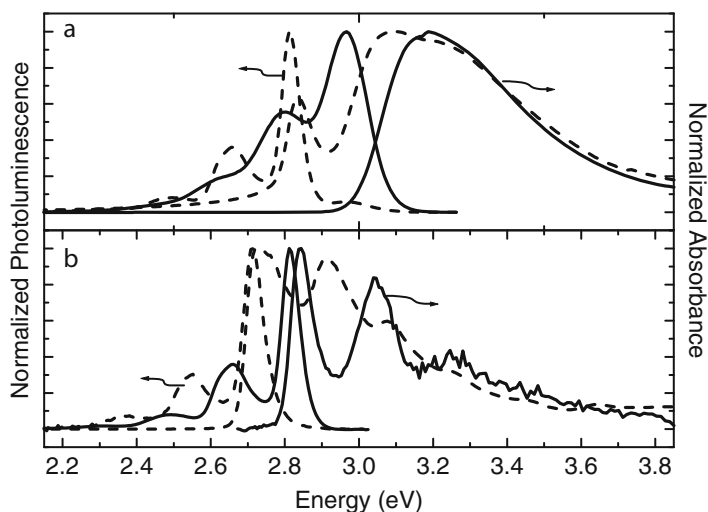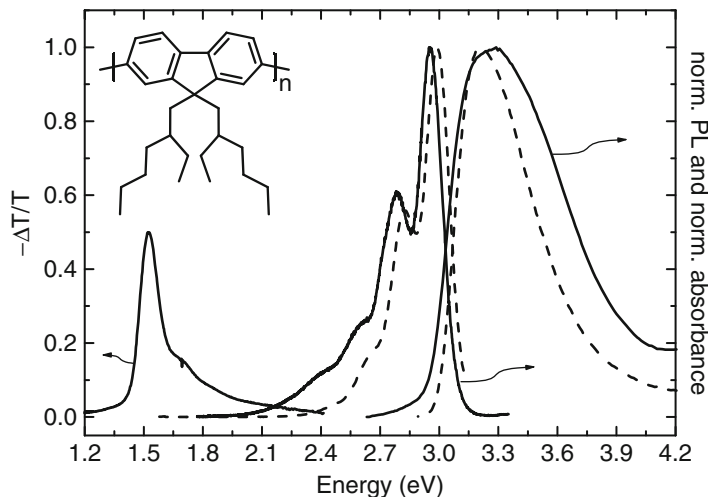
Polyfluorenes, Fig. 5 (**a**) Absorption and photoluminescence spectra of PFO in dilute solution (chloroform, *solid lines*) and after partial agglomeration (β-phase formation) in a chloroform/methanol mixture (v/v 75/25, *dashed lines*). (**b**) Absorption and photoluminescence spectra of the so-called β-phase of polyfluorene (*solid lines*, as derived from a numerical subtraction of the absorption and emission spectra in chloroform and in chloroform/methanol mixture, 75/25, resp., *solid lines*); for comparison the absorption and photoluminescence spectra of LPPP (R1: -hexyl, R2: -4-decylphenyl, R3: -methyl) are given (dilute solution, toluene, *dashed lines*) (Figure reproduced from Scherf and List [16])

The relative intensity of the β-phase-related bands increases for increasing the polar solvent content, while the intensity of the broad unstructured PF absorption decreases. Simultaneously the changes in absorption and the PL emission spectrum of PFO in chloroform/methanol mixtures reveal a series of novel emission bands at lower energies (2.81, 2.65, and 2.49 eV). Furthermore, the newly emerging redshifted absorption and emission bands of β-phase PFO possess, in contrast to "isolated" PF chains, a vibronic progression both in absorption and emission [16].

From a comparison with the absorption and emission properties of a fully planarized LPPP,

a clearer picture for the observations in the partly agglomerated (β-phase) and "isolated" PF sample can be derived. Both materials possess nearly identical spectral characteristics, which only differ in a slight redshift of ca. 100 meV of the LPPP spectra. From this it was concluded that the initially distorted backbone of PFs is flattened into a planarized conformation in the β-phase leading to a distinct redshift of the absorption and emission spectra by ca. 0.2 eV as well as the observation of a vibronic progression in the absorption spectrum.

The photoinduced absorption (PA) shows one dominant band with a maximum peaking at 1.54 eV, which is assigned to a transition from the 1^3B_u to a higher-lying m^3A_g triplet state. The energetic spacing between the ground state 1^1A_g and the lowest triplet state 1^3B_u was found to be 2.1 e V. This transition was also observed in phosphorescence from polymers containing residual catalyst or other impurities. Typically PF films do not exhibit a significant polaronic absorption band in steady state PA as a consequence of the rather low density of traps and the low energetic disorder of the bulk polymer, which is also reflected in the high mobility of charge carriers in PFs and the observation of a nondispersive transport. Furthermore the PA band has a remarkably low overlap with the PL emission, and PFs show relatively short-lived triplet states with a lifetime in the order of 2 ms in the solid state. These facts make PF the promising candidate for organic solid-state lasers since both observations drastically reduce quenching processes in the solid state [17].

Chemical Defects in PF Materials

The main reason preventing the ultimate breakthrough of PFs for blue light-emitting devices is absence of long-term stability. During device operation, residual oxygen can lead to photooxidative or thermal degradation and the formation of ketonic defect sites forming at the nine-position leading to low-energy emission bands around 530 nm (ca. 2.3 eV) and acting as electron trapping sites. In all different degradation experiments, which have been used in order to clarify the nature of the chemical defect, it being thermal stress experiments under elevated temperature, degradation under UV light, or the exposure to

a electron beam, a few common observations could be made.

The initial blue emission at 2.96 and 2.78 eV decreases significantly during treatment, and at the same time the broad, low-energy emission band around 2.3 eV evolves. Typically also the overall quantum yield of the sample is drastically lowered to 10 % of the original value. Simultaneously an IR feature at 1,720 cm^{-1} increases, which indicates that upon material degradation, chemical defects bearing ketonic groups are created.

Using model molecules for degraded polyfluorenes in the form of copolymers of 9,9-difarnesylfluorene and 9-fluorenone moieties, Scherf et al. have shown that such copolymers exhibit exactly the same properties as degraded polyfluorenes. From a series of spectroscopic experiments, it was found that the 9-fluorenone moieties forming upon degradation are acting as emissive sites giving rise to the 2.3 eV emission band, which is contrary to the earlier interpretation that excimer or aggregate formation is the primary source for the low-energy emission band in polyfluorene-type materials. This interpretation is in line with Lupton et al. using the fluorene/fluorenone model polymers to observe an on-chain fluorenone defect emission from single molecules in the absence of intermolecular interactions using single-molecule spectroscopy. Arylation of the nine-position can prevent the degradation process in PFs attaining long-term thermal and device stability. At this point it is worth noting that various peroxide species can also be formed in palladium-catalyzed Suzuki cross-coupling reactions in the presence of oxygen leading to similar effects at the end position of the polymer chain. In addition to this, the generation of peroxides in Suzuki cross-coupling reactions also paves a way to other chemical defects, among them especially hydroxy-terminated polyfluorenes [17].

PF Materials in PLED Applications

Among the PPP-based materials, different derivatives of highly emissive PFs have received particular attention as active emitters in polymer light-emitting diodes (PLEDs) due to their

P

extraordinary properties in device applications as originally demonstrated by Bradley [18]. PF-based PLEDs typically operate with an onset voltage at the optical bandgap at 2.9 eV with achieved device efficiencies as high as >8 cd/A. The electroluminescence spectrum of devices based on PF emitters is typically identical to the PL emission in the solid state with a maximum at 2.9 eV and the according vibronic shoulders at lower energy.

It has been demonstrated that using optimized synthetic strategies, one can achieve chemical stability of the PF-based emitter material and a high radiative quantum yield of the emissive unit yielding efficient and bright PLED devices with long lifetimes in the order of thousands of hours. Optimized PF-based PLEDs generally comprise additional hole and electron transport layers such as (N,N′-diphenyl-N,N′-(3-methylphenyl)-1,1′-biphenyl-4,4′-diamine (TPD) and 2-(4-biphenyl)-5-(4-tert-butylphenyl)-1,3,4-oxadiazole (PBD), combined with solution-deposited PF layers as blue emitter. Generally it has been shown that only by introducing additional transport layers can one achieve the required balanced charge carrier injection and an effective and balanced transport of electrons and holes toward the electro-optical active layer. Moreover a pinning of the emission zone to the center of the device, using heterojunctions with appropriate type II band level offset, to avoid quenching at either of the electrode interfaces has also been found to be rather favorable [19].

Related Entries

References

1. Helfrich W, Schneide WG (1965) Recombination radiation in anthracene crystals. Phys Rev Lett 14:229. doi:10.1103/Physrevlett.14.229

2. Tang CW, Vanslyke SA (1987) Organic electroluminescent diodes. Appl Phys Lett 51:913–915. doi:10.1063/1.98799 (Published online Epub Sep 21)

3. Burroughes JH, Jones CA, Friend RH (1988) New semiconductor-device physics in polymer diodes and transistors. Nature 335:137–141. doi:10.1038/335137a0 (Published online Epub Sep 8)

4. Müllen K, Scherf U (2006) Organic light-emitting devices: synthesis, properties, and applications. Wiley-VCH, Weinheim, p xvii, 410 p

5. Jacob J, Zhang JY, Grimsdale AC, Mullen K, Gaal M, List EJW (2003) Poly(tetraarylindenofluorene)s: new stable blue-emitting polymers. Macromolecules 36:8240–8245. doi:10.1021/ma034849m (Published online Epub Nov 4)

6. Jacob J, Sax S, Piok T, List EJW, Grimsdale AC, Mullen K (2004) Ladder-type pentaphenylenes and their polymers: efficient blue-light emitters and electron-accepting materials via a common intermediate. J Am Chem Soc 126:6987–6995. doi:10.1021/ja0398823 (Published online Epub Jun 9)

7. Scherf U, Mullen K (1995) The synthesis of ladder polymers. Synth Photosynth 123:1–40

8. Prey V, Schindlb H, Cmelka D (1973) Tests on polymerization of fluorene. Angew Makromol Chem 28:137–143. doi:10.1002/Apmc.1973.050280111

9. Fukuda M, Sawada K, Yoshino K (1989) Fusible conducting poly(9-Alkylfluorene) and poly(9,9-Dialkylfluorene) and their characteristics. Jpn J Appl Phys Part 2 Lett 28:L1433–L1435 (Published online Epub Aug)

10. Skotheim TA, Reynolds JR (2007) Handbook of conducting polymers. Conjugated polymers: processing and applications, 3rd edn. CRC Press, Boca Raton

11. List EJW, Guentner R, de Freitas PS, Scherf U (2002) The effect of keto defect sites on the emission properties of polyfluorene-type materials. Adv Mater 14:374–378. doi:10.1002/1521-4095(20020304)14:5<374::aid-adma374>3.0.co;2-u (Published online Epub Mar 4)

12. Winokur MJ, Slinker J, Huber DL (2003) Structure, photophysics, and the order-disorder transition to the beta phase in poly(9,9-(di-n,n-octyl)fluorene). Phys Rev B 67, 184106. doi:10.1103/Physrevb.67.184106 (Published online Epub May 1)

13. Miteva T, Meisel A, Knoll W, Nothofer HG, Scherf U, Muller DC, Meerholz K, Yasuda A, Neher D (2001) Improving the performance of polyfluorene-based organic light-emitting diodes via end-capping. Adv Mater 13:565. doi:10.1002/1521-4095(200104)13:8<565::Aid-Adma565>3.0.Co;2-W (Published online Epub Apr 18)

14. Grimsdale AC, Mullen K (2006) Polyphenylene-type emissive materials: poly(para-phenylene)s, polyfluorenes, and ladder polymers. Emiss Mater Nanomater 199:1–82. doi:10.1007/12_076

15. Leclerc M, Morin J-F (2010) Design and synthesis of conjugated polymers. Wiley-VCH, Weinheim, p xv, 363 p
16. Scherf U, List EJW (2002) Semiconducting polyfluorenes – towards reliable structure-property relationships. Adv Mater 14:477. doi:10.1002/1521-4095(20020404)14:7<477::aid-adma477>3.0.co;2-9 (Published online Epub Apr 4)
17. Scherf U, Neher D (eds) (2008) Polyfluorenes. Springer, Berlin/Heidelberg, p 332
18. Grice AW, Bradley DDC, Bernius MT, Inbasekaran M, Wu WW, Woo EP (1998) High brightness and efficiency blue light-emitting polymer diodes. Appl Phys Lett 73:629–631. doi:10.1063/1.121878 (Published online Epub Aug 3)
19. Tsujimura T (2011) OLED display fundamentals and applications. Wiley, Hoboken

Polyhedral Oligomeric Silsesquioxanes (POSS)

Maki Itoh
Dow Corning, Resins, Coatings, and Adhesives Product Development, Ichihara, Chiba, Japan

Synonyms

Cages; Oligosilsesquioxanes; Polysilsesquioxanes; Silicone resins: Silsesquioxanes

Definition

Among the M $[R_3SiO_{1/2}]$, D $[R_2SiO_{2/2}]$, T $[RSiO_{3/2}]$, and Q $[SiO_{4/2}]$ siloxane units, silicone resins mainly consist of T and Q units. The term "silsesquioxane" refers to silicone resins which consist only of T units (sesqui means 1.5 because in the T structure having three siloxane bonds, one oxygen atom is shared by the adjacent silicon atoms). Polyhedral oligomeric silsesquioxanes (POSS) are cage-like oligomer molecules of defined structures mainly consisting of cyclotri-, cyclotetra-, and cyclopenta-siloxane rings based on $^RT^3$ $[RSiO_{3/2}]$ unit for completely condensed cages in combination with $^RT^2$ $[RSi(OH)O_{2/2}]$ for incompletely condensed cages. Such cage structures are not just specific

to silsesquioxanes, but general silicone resins have more or less such structures.

Introduction

Polysiloxanes or silicones based on Si–O–Si bonding are classified into oils or elastomers that mainly consist of linear polymers from D unit $[R_2SiO_{2/2}]$ and silicone resins [1] in which the major building blocks are T $[RSiO_{3/2}]$ or Q $[SiO_{4/2}]$ units (see Fig. 1). Although being a network polymer, silicone resins are defined as solvent-soluble or solvent-meltable materials and are further cross-linked (cured) via the condensation of residual silanols or addition reaction (hydrosilylation) to be the final product form like coatings. In 1930, a researcher in Corning Glass Works dreamed of creating materials more thermally resistant than plastics yet having more flexibility than glass, thus hired an organic chemist, Frank Hyde. The history of silicones started by Hyde in this way developing silicone resins for electric insulation applications [2]. Their research merged with that at Melon Institute and with the scale-up production of chlorosilanes by Dow Chemical, from which Dow Corning was established and started commercial production of silicones in 1943. In the same era, Rochow at General Electric invented an economic method to produce methyl chlorosilanes known as direct process, followed by commercialization of silicones by General Electric in 1947 [3]. Current major silicone products use linear polydimethylsiloxanes, but the first product was silicone resins.

The term "silsesquioxane" refers to silicone resins which consist only of T units (sesqui means 1.5 because in the T structure, one silicon atom is bonded to 1.5 oxygen atoms as shared by the adjacent silicon atoms). Why silsesquioxane as one form of silicone resins is popular would be partly because the T structure, among the combination of M $[R_3SiO_{1/2}]$, D, T, and Q units, can form materials that can be defined as silicone resins by itself and partly because cage molecules of defined structures as shown in Fig. 2a-f are drawing attention [4–12]. These cage

structures are also called polyhedral oligomeric silsesquioxane (POSS). Although not being "sesqui," the class of structures by Q unit
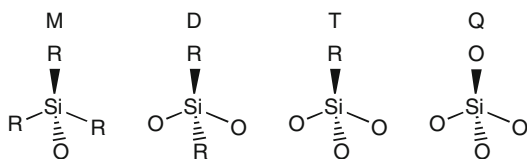
Polyhedral Oligomeric Silsesquioxanes (POSS), Fig. 1 Siloxane units

as shown in Fig. 2h is occasionally referred to silsesquioxanes [13]. This chapter refers to the formation of cage silsesquioxanes in polysilsesquioxanes, specific synthetic methods of cage silsesquioxanes, and examples of application to organic–inorganic hybrid materials as nanobuilding blocks. In the following sections in this chapter, literature may not be specifically indicated if the descriptions are included in refs. [4–13].

In this chapter for convenience, the abbreviations $^RT^0$, $^RT^1$, $^RT^2$, and $^RT^3$ are used to describe
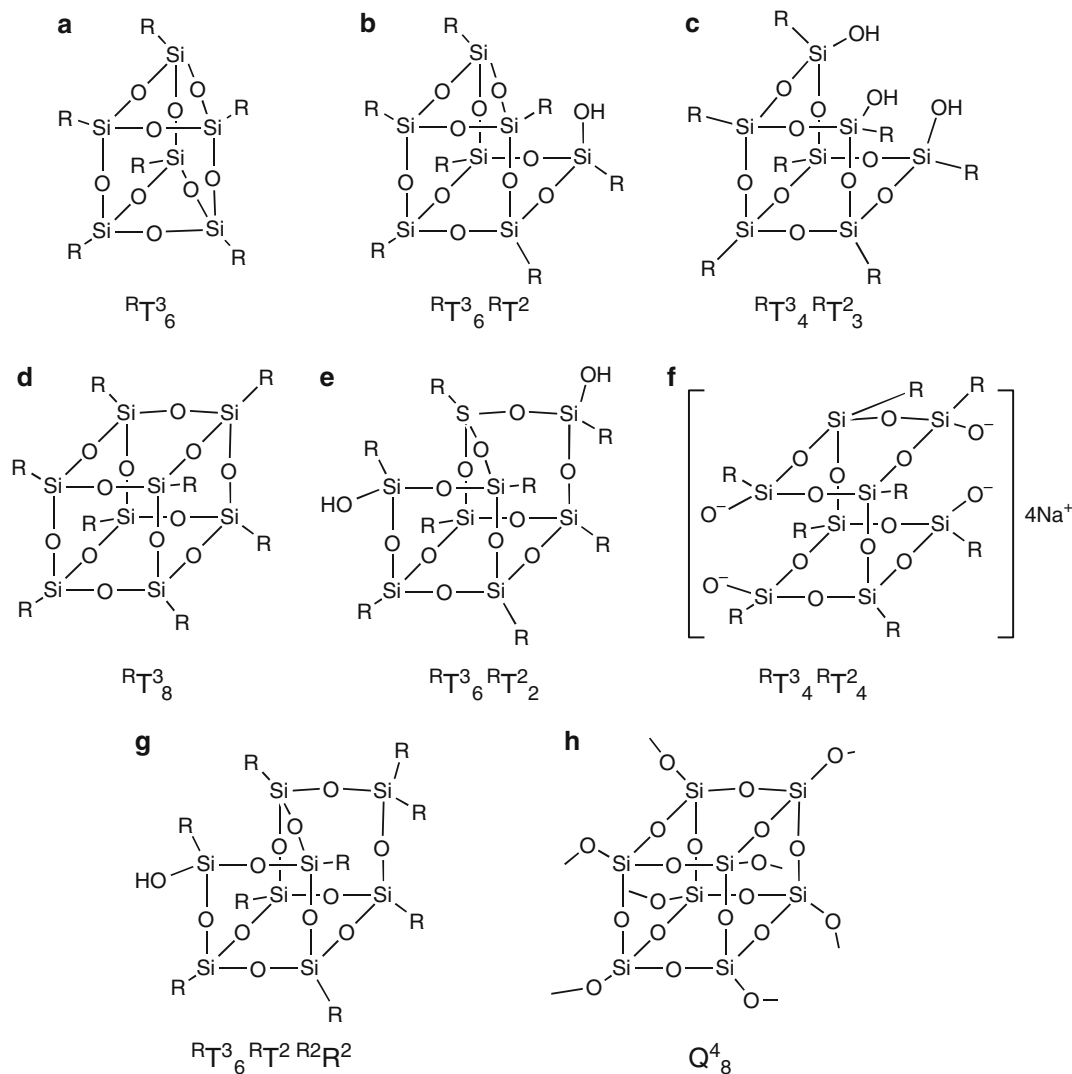
Polyhedral Oligomeric Silsesquioxanes (POSS), Fig. 2 Structure of silsesquioxanes or silicone resins (proposed structures included)

$RSi(OH)_3$, $RSi(OH)_2O_{1/2}$, $RSi(OH)O_{2/2}$, and $RSiO_{3/2}$, respectively (the superscript denotes the number of siloxane bonding and R is the substituent). Likewise, $^{RR'}D^0$, $^{RR'}D^1$, and $^{RR'}D^2$ denote $RR'Si(OH)_2$, $RR'Si(OH)O_{1/2}$, and $RR'SiO_{2/2}$ (R' is another substituent). In silicone chemistry, methyl substituent is usually omitted to be described. Ph denotes phenyl and Me is methyl.

Polysilsesquioxanes and Cage Molecules Therein

Silsesquioxanes are, as shown in Eq. 1, generally synthesized by hydrolytic polycondensation of the corresponding trichlorosilanes or trialkoxysilanes, i.e., $RSiCl_3$ or $RSi(OR'')_3$ where R'' is usually methyl or ethyl [1].

$$RSiX_3 \xrightarrow{H_2O} RSi(OH)_3 + 3HX \quad X = Cl, OR$$

$$\text{Hydrolyzate}$$

$$\xrightarrow{H^+ \text{ or } OH^-} RSiO_{3/2} + 3/2H_2O$$

$$\text{Silsesquioxane}$$

$$(1)$$

When chlorosilanes are used, the reaction is usually catalyzed by the hydrochloric acid formed. For alkoxysilanes, either an acid catalyst or a base catalyst is used. Equati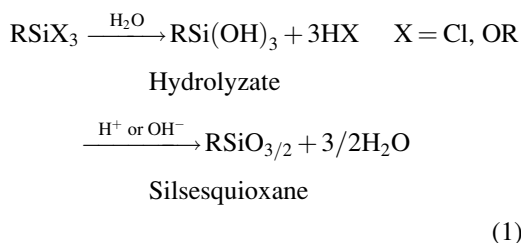on 1 shows the hydrolysis to form a trisilanol, followed by the polycondensation. In reality, however, the condensation starts before the completion of the hydrolysis. For instance, a reaction between $RSiCl_2OH$ and $RSiCl_3$ to form $RSiCl_2\text{-}O\text{-}SiRCl_2$ proceeds concurrently after hydrolysis of the first Si–Cl. At higher HCl concentration, the reaction rate of hydrolysis slows down, and the rate of condensation is accelerated; thus, more condensation reaction takes place before the completion of the hydrolysis as the hydrolysis proceeds. Reactions of alkoxysilanes are summarized in detail by Brinker and Scherer [14].

Hydrogen silsesquioxanes can be synthesized from $HSiCl_3$ using concentrated sulfuric acid and aromatic solvent. The presence of cubic octamer, $^HT^3_8$, is proven in polyhydrogensilsesquioxanes [15]. Itoh and coworkers identified the presence of cage molecules in polymethylsilsesquioxanes synthesized from methyltrichlorosilane in excess water under the acidic condition of hydrochloric acid [16]. Although the polymethylsilsesquioxane had an average molecular weight around 5,000, the resin contained a significant amount of low-molecular-weight species consisting of T^2 and T^3 units, ranging from $T^3_4T^2_3$ to $T^3_8T^2_2$, including many isomers with the sum of these molecules $\sim$8 wt%. One isomer of $T^3_6T^2_2$ was isolated of which structure was determined as that shown in Fig. 2e. These species appeared to consist mainly of cyclotetra- and cyclopenta-siloxane rings, but presence of strained cyclotrisiloxane rings also was suggested as exemplified in the structure shown in Fig. 2b (This structure was not determined by X-ray crystallography but one cannot draw a structure without a cyclotrisiloxane ring for a chemical formula of $T^3_6T^2$). In a more industrial type of methyl silicone resin consisting of methyl-T and dimethyl-D unit, a DT resin, species in which the T^2 units in the polymethylsilsesquioxane is replaced with D^2 [$Me_2SiO_{2/2}$] were found, e.g., $T^3_6 T^2D^2$, of which structure is exemplified in Fig. 2g. This suggests that general silicone resins consist of similar structures as silsesquioxanes.

Synthesis and Characteristics of POSS or Cage Silsesquioxane Molecules

The polymethylsilsesquioxane by Itoh and coworkers described in the previous section has the molecular formula of $T^2_{0.15} T^3_{0.85}$ [16]. While the degree of polymerization for this chemical formula from the monomer $CH_3Si(OH)_3$ is 95 %, Flory's random branching theory tells that the critical degree of polymerization for gelation (formation of infinite molecular weight insoluble network) for trifunctional monomer is 50 % [17]. Deviation from Flory's theory not to gel is due to the cyclization to form cyclotri- to penta-siloxanes, which results in the formation of POSS molecules. Formation of cage molecules is

essentially a spontaneous process. Hence, the effort for the synthesis of cage silsesquioxanes has been directed to find reaction conditions to provide these materials in high yields. The strategy could be to conduct the hydrolytic polycondensation in very dilute solution to promote intramolecular condensation at low temperature, e.g., room temperature with long reaction time. The cubic octamers (Fig. 2d) are the most famous among the POSS materials probably because the material can be recovered as precipitates by crystallization to be taken out of the reaction system, in addition to being relatively stable. Thus, synthesis of POSS was already reported in the 1950s mainly for cubic octamers. One example is that a ^{ph}-T^3_8 was obtained in 85 % yield using potassium hydroxide in dilute solution at room temperature. Various substituents, methyl, ethyl, n-propyl, n-butyl, n-hexyl, n-octyl, i-nonyl, vinyl, allyl, trifluoropropyl, cyclopentyl, phenyl, hydrido, etc., were reported for the completely condensed $^R T^3_n$ (n = 6, 8, 10).

By adding water to an acetone solution of cyclohexyltrichlorosilane and allowing to stand for 3 to 36 months, a mixture of $^R T^3_6$, $^R T^3_4 {}^R T^2_3$, and $^R T^3_6 {}^R T^2_2$ was obtained in 60–70 % yield. By several steps of solvent extraction, these materials were isolated, and the structures were determined as those in Fig. 2a, c, and e, respectively. In an effort to obtain such molecules in high yield in short time, stepwise dehydration reactions of the precursors were conducted. By hydrolyzing 1,1,2-trimethylpropyl- or t-butyltrichlorosilane in ether in the presence of aniline, the corresponding trisilanols, $RSi(OH)_3$, were obtained, and dimers, $(OH)_2RSi-O-SiR(OH)_2$, were able to be prepared by using ethanol, silica gel, and potassium hydroxide. By dehydration condensation of these precursors, the corresponding $^R T^3_6$ was obtained in 25 % and 41 % yields, respectively. By hydrolytic polycondensation of various triethoxysilanes using n-butyl-ammonium fluoride as the catalyst, $^{Ph} T^3_8$ and cyclohexyl- T^3_8 were obtained in 49 % and 95 % yields, respectively. $^{Ph} T^3_8$ was also obtained by reacting phenyltrimethoxysilane and 1.5 M equivalent of water in the presence of trimethylbenzylammonium hydroxide. A facile

synthesis of the incompletely condensed cages was reported by the decomposition of cyclohexyl-T^3_8. $^R T^3_6 {}^R T^2_2$ was obtained by the ring opening using trifluoromethanesulfonate, and $^R T^3_4 {}^R T^2_3$ was produced by tetraethyl ammonium hydroxide. Hydrolytic polycondensation of phenyltrimethoxysilane using sodium hydroxide afforded the sodium salty of $^{Ph} T^3_4 {}^{Ph} T^2_4$ known as a double-decker silsesquioxane as shown in Fig. 2f. It was reported that this compound was formed via the structure in Fig. 2c. When the isolated $T^3_6 T^2_2$ from the polymethylsilsesquioxane with the structure in Fig. 2e was exposed to the same acidic reaction condition as the hydrolytic condensation of methyltrichlorosilane, much of this material was consumed to form other isomers of $T^3_6 T^2_2$ as well as the cubic octamer [16]. In this way, siloxane bond rearrangement in acidic or basic condition is an important route to form POSS materials.

As examples for the POSS materials exhibiting characteristic features due to their shapes, encapsulation of fluoride ion or hydrogen in the silsesquioxane cage was reported. A wide variety of reports on the use of POSS materials in the field of catalyst like metal complexes can be found, partly as models for silica surface in heterogeneous catalysis and partly as homogenous catalysts of the POSS derivatives themselves.

Organic–Inorganic Hybrid Materials Using POSS

There are a few strategies to incorporate POSS into organic–inorganic hybrids as inorganic nano-building blocks. The first way is to use octa-functional-T^3_8. One example is to obtain liquid crystalline polymers by reacting $^H T^3_8$ and mesogens carrying vinyl groups via hydrosilylation. Another example of the use of $^H T^3_8$ is to react with a di-ene or di-yne monomer via hydrosilylation to form hybrid polymers. The second approach is functionalization onto the substituents. Octa(aminophenyl)silsesquioxane prepared through nitration of the phenyl group of $^{Ph} T^3_8$ can be further functionalized by the reaction between the amino group and an acid

Polyhedral Oligomeric Silsesquioxanes (POSS), Fig. 3 Preparation of monofunctional cubic octamer

R = cyclohexyl or cyclopentyl

R' =   **etc.**
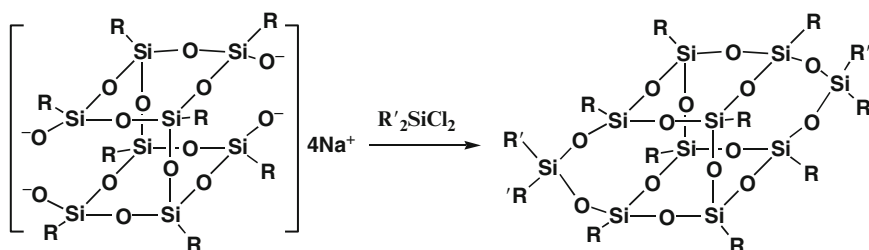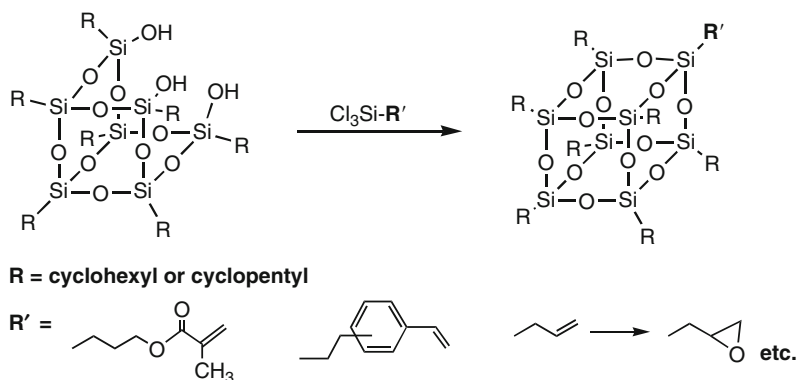
Polyhedral Oligomeric Silsesquioxanes (POSS), Fig. 4 Functionalization of the double-decker silsesquioxane

anhydride, etc. Bromination of the phenyl group is also a way to introduce functionality onto the phenyl group via low temperature catalytic coupling with para-substituted styrene, etc. The third method is to use the silanols in incompletely condensed cage compounds. Cyclohexyl-$T^3_6T^2_2$, Fig. 2e, can be reacted with dichlorosilanes, diaminosilanes, or polydimethylsiloxanes having these functionalities at the chain end to form copolymers with silsesquioxane molecules in the main chain. Reaction of cyclohexyl-$T^3_4T^2_3$, Fig. 2c, with R'SiCl$_3$ can introduce a functionality at one corner of a cubic octamer, such as methacryl, styryl, and epoxy as illustrated in Fig. 3, which can form organic polymers having POSS in the side chain. The side chain POSS can self-assemble into nanoscaled aggregates in selective solvents and form nanostructures in bulk. The sodium salt of the double-decker phenylsilsesquioxane, Fig. 2f, can be reacted with R'$_2$SiCl$_2$ to introduce functionalities to be copolymerized with organic monomers as shown in Fig. 4.

Cage Molecules Based on Q Unit

When the oxygen atoms at the corners of the cube in structure Fig. 2h are attached with eight trimethylsilyl groups, the material is one form of MQ-type resins [1] described as M_8Q_8. However, such structures do not appear to be formed spontaneously by hydrolytic condensation of the monomers like tetraethyl orthosilicate. The materials can be obtained as octasilicate anions (OSA) by the reaction of high-surface-area amorphous silica with R_4NOH, with $[R_4N^+]$ as the counter cation [13]. As an alternative silica source, rice hull ash is useful to provide OSAs in high yield in milder reaction conditions. OSAs are also good nano-building blocks since the anion can be easily reacted, for instance, with chlorosilanes for functionalization as exemplified in Fig. 5. By reacting with HMe$_2$SiCl, an OSA can form an octa-SiH-functional cubic octamer, which can be further functionalized or incorporated into hybrid materials by hydrosilylation in a similar manner as described above for $^HT^3_8$.
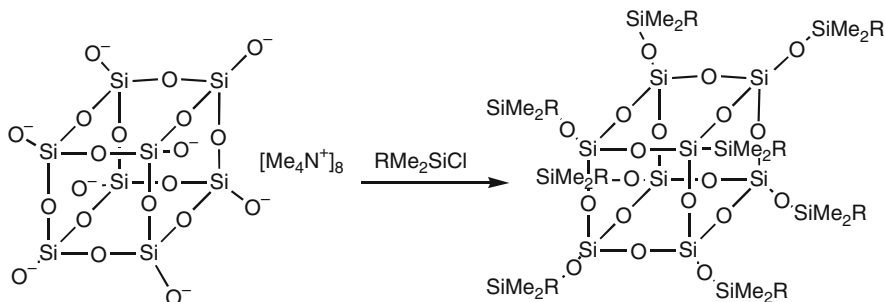
Polyhedral Oligomeric Silsesquioxanes (POSS), Fig. 5 Formation of functional Q_8

Summarizing Comments

Although (poly)silsesquioxanes are known for over 50 years, the use of cage silsesquioxanes as nano-building blocks for hybrid materials is more recent trend. Introduction of inorganic nature to organic polymers like improving thermal stability by hybridization could be attained by the incorporation of polysilsesquioxanes or silicone resins having molecular weight distributions. Being low-molecular-weight oligomers, POSS materials can be easily handled for functionalization and copolymerization, while high-molecular-weight polysilsesquioxanes may form insoluble gels during such processes. However, the use of POSS materials should be focused on obtaining specific properties taking advantage of their defined structures. Encapsulation of fluoride ion or hydrogen in the cage structure is one of such attributes. In the organic-POSS hybrid materials, self-assembly is an interesting feature. Most of the POSS materials synthesized or isolated to date are those with the number of silicon atoms around eight. New features may be found if larger molecules can be obtained in high yield. Including that, further exploration of the structure–property relationships of the POSS materials as well as those for the hybrid materials containing the cage silsesquioxanes would open up the possibility for producing materials of unmet properties.

Related Entries

▶ Inorganic Polymers: Overview
▶ Ladder-Type Polymers
▶ Layered Silicate-Based Rubber Nanocomposites
▶ Polysiloxanes

References

1. Baney RH, Itoh M, Sakakibara A, Suzuki T (1995) Silsesquioxanes. Chem Rev 95:1409–1430
2. Warrick EL (1990) Forty years of firsts. McGraw-Hill, New York
3. Ito K (ed) (1990) Silicone handbook. Nikkan Kogyo, Tokyo (in Japanese)
4. Voronkov MG, Lavrent'yev VI (1982) Polyhedral oligosilsesquioxanes and their homo derivatives. Top Curr Chem 102:199–236
5. Harrison PG (1997) Silicate cages: precursors to new materials. J Organ Chem 542:141–183
6. Unno M (1997) Silsesquioxanes – with focus on cage compounds. J Soc Silicon Chem Japan 8:16–22
7. Duchateau R (2002) Incompletely condensed silsesquioxanes: versatile tools in developing silica-supported olefin polymerization catalysts. Chem Rev 102:3525–3542
8. Chandrasekhar V, Boomishankar R, Nagendran S (2004) Recent development in the synthesis and structure of organosilanols. Chem Rev 104:5847–5010
9. (a) Kawakami Y (2007) Reactions of silicon compounds and development of functional materials based on the characteristics of compounds with silicon-containing bonds. 3. Structural control and functionalization of oligomeric silsesquioxanes (Part 1). Nippon Gomu Kyokaishi 80:317–324, (b) Kawakami Y (2007) Reactions of silicon compounds and development of functional materials based on the characteristics of compounds with silicon-containing bonds. 3. Structural control and functionalization of oligomeric silsesquioxanes (Part 2). Nippon Gomu Kyokaishi 80:356–359
10. Itoh M (2008) Cage silsesquioxanes. Mirai Zairyo 8(6):10–15

11. Cordes DB, Lickiss PD, Rataboul F (2010) Recent development in the chemistry of cubic polyhedral oligosilsesquioxanes. Chem Rev 110:2081–2173

12. Zhang W, Mueller AHE (2013) Architecture, self-assembly and properties of well-defined hybrid polymers based on polyhedral oligomeric silsesquioxane (POSS). Prog Polym Sci 38:1121–1162

13. Laine RM (2005) Nanobuilding blocks based on the $[OSiO_{1.5}]_x$ (x = 6, 8, 10) octasilsesquoxanes. J Mater Chem 15:3725–3744

14. Brinker CJ, Scherer GW (1990) Sol–gel science, the physics and chemistry of sol–gel processing. Academic, San Diego

15. Auner N, Bats JW, Katsoulis DE, Suto M, Tecklenburg RE, Zank GA (2000) Chemistry of hydrogen-octasilsesquioxane: preparation and characterization of octasilsesquioxane-containing polymers. Chem Mater 12:3402–3418

16. Itoh M, Suto M, Cook SD, Oka F, Auner N (2012) Characterization and Some Insights into the Reaction Chemistry of Polymethylsilsesquioxane or Methyl Silicone Resins. Int J Polym Sci, Special Issue on Silsesquioxanes–Recent Advancement and Novel Applications ID 526795

17. Nakahama S, Nose T, Akiyama S, Sanui K, Tsujita Y, Doi M, Horie K (1988) Essential polymer science (Japanese). Kodansha, Tokyo, p 61

Polyimide Synthesis

Mary Ann B. Meador and Stephanie L. Vivod
Materials and Structures Division, NASA Glenn
Research Center, Cleveland, OH, USA

Definition

Semi-aromatic or aromatic polymers consisting of imide rings typically fused to phenyls, resulting in high temperature stability and high glass transition temperatures.

Historical Background

Polyimides are an important class of step-growth polymers due to their high temperature stability, high glass transition temperature (T_g), and superior chemical resistance. Synthesis of aromatic polyimides was first reported in 1908. However, due to the lack of processability via melt polymerization, significant advances in polyimide synthesis and processing were not realized until the 1960s and 1970s by DuPont with the discovery of Kapton which is shown at the top of Fig. 1. This ignited an interest in polyimide research for scientific and commercial application by DuPont, the National Aeronautics and Space Administration, the Air Force labs, and others to accommodate the growing need for heat-resistant polymers that could be processed into useable parts [1]. Use temperatures as high as 300 °C are required for matrix resins for lightweight composites in aircraft engines, for example, making polyimides a choice material for such applications [2]. More recently, low dielectric constant combined with high temperature stability has allowed polyimides to be used as the insulating layer in microelectronics [3]. Other applications for high-temperature polyimides include high-performance adhesives [4], flexible substrate for sensor arrays for biomedical applications, and gas separation membranes [5, 6]. Polyimide membranes have high CO_2 permeability and CO_2/CH_4 selectivity combined with high temperature stability which makes them desirable for many industrial applications such as natural gas sweetening and biogas upgrading. Polyimides also have promise as membranes for high-temperature proton exchange membrane fuel cells [7]. More recently, porous polyimide aerogels have been fabricated that can be used as ultralow dielectric substrates (k = ~1.1) for antennas [8] or as high-temperature insulation materials for entry, descent, and landing applications [9].

Properties and Applications

Polyimides are very versatile materials. As previously mentioned, the most important properties of polyimides are high T_g and high temperature stability. Polyimides can withstand temperatures as high as 600 °C for short-term use. Long-term exposure especially in an oxidizing atmosphere can be up to about 300 °C. The most thermally stable polyimides contain aromatic backbone structures composed primarily of fused rings and rings directly linked by carbon-carbon

P

Polyimide Synthesis,
Fig. 1 Examples of
different polyimide
backbone structures

Kapton

More rigid backbone

More flexible backbones
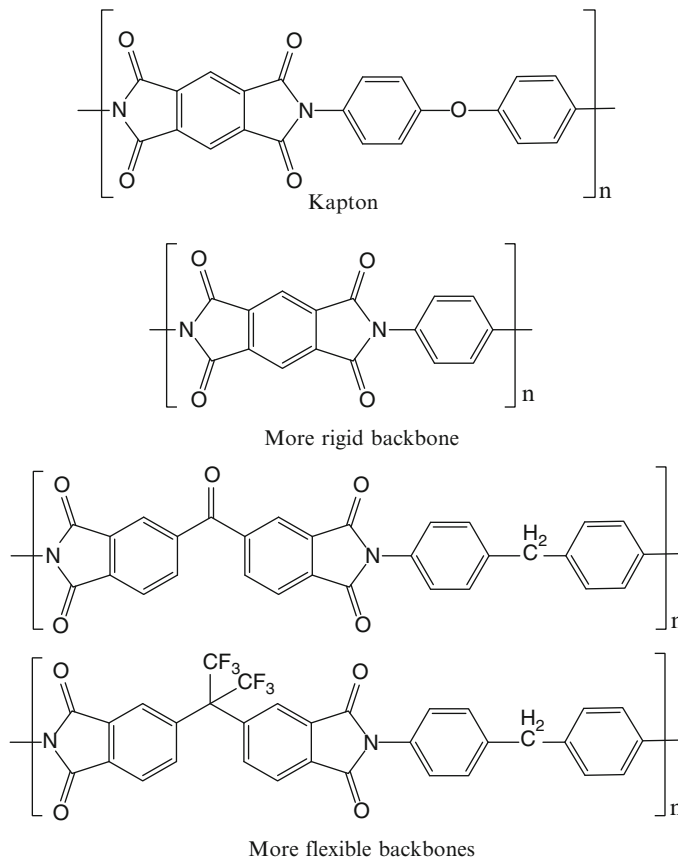
bonds as shown in Fig. 1, but the rigidity of the chains makes these formulations very difficult to process as well as brittle. Aliphatic or heteroatom links between aromatic rings, as well as aliphatic or aromatic side chains, some examples of which are shown in Fig. 1, make the polyimides easier to process and more flexible. However, there is a trade-off between processability, T_g, and thermal stability.

Polyimides have been employed in various applications in the microelectronics industry due to low dielectric properties, particularly as a planarization layer in forming multilevel interconnects used in high-performance integrated circuits [10]. Dielectric properties scale with density in polyimides. Hence, lower dielectric constants can be achieved either by increasing the free volume by use of larger side groups or by increasing porosity by fabricating into foams or aerogels. Adding functional groups increases the utility of polyimides. For example, the addition

of sulfonate groups to the polyimide backbone allows retention of water to conduct protons for fuel cell membranes, while the addition of fluorinated groups lowers water uptake for more moisture-resistant materials [11]. Addition of fluorinated groups, such as trifluoromethyls or hexafluoroisopropylidene groups, also improves solubility and processability by disrupting chain packing with less of a penalty in thermal properties.

The biomaterial industry has also seen an increase in use of polyimides due to characteristics such as chemical inertness as well as compatibility with device fabrication processes. In addition, polyimides exhibit excellent electrical, mechanical, and biologic compatibility for use in multiple implant applications, such as separation membranes, neural interfaces, cell adhesion substrates, and scaffolds for tissue regeneration [12]. A commonly employed method of fabrication involves adding a

biodegradable component such as poly(glycolic acid) (PGA) to polyimide to increase biocompatibility as well as structural integrity. Implants such as polyimide electrode devices are able to resist buckling by being coated with PGA prior to surgical insertion. The combination of the mechanical flexibility of polyimide and the mechanical rigidity of PGA below its T_g of 35 °C allows for a material that will remain firm upon insertion and then grow flexible and eventually biodegrade when exposed to body temperatures [13]. This type of technique has led to a growing interface between polyimides and biomedical applications using polyimide biocompatible materials for monofilament sutures, selective chemical delivery, as well as microelectrode devices for stimulation and recording of muscle and nerve signals [13].

Typical Synthesis

The synthesis of polyimides typically proceeds in a two-step reaction mechanism via melt or solution polymerization using aromatic diamines and aromatic tetracarboxylic dianhydrides. To illustrate, the synthesis of Kapton, a polyimide sold by DuPont and made from 4,4'-oxydianiline and pyromellitic dianhydride, is shown in Fig. 2. The first step is the formation of a soluble polymer precursor, polyamic acid (PAA), from the ring-opening reaction of the dianhydride with diamine, followed by intramolecular formation of imide from the condensation of polyamic acid. Each imide ring formed results in the evolution of one molecule of water. Formation of polyamic acid is typically prepared in dipolar aprotic solvent

P
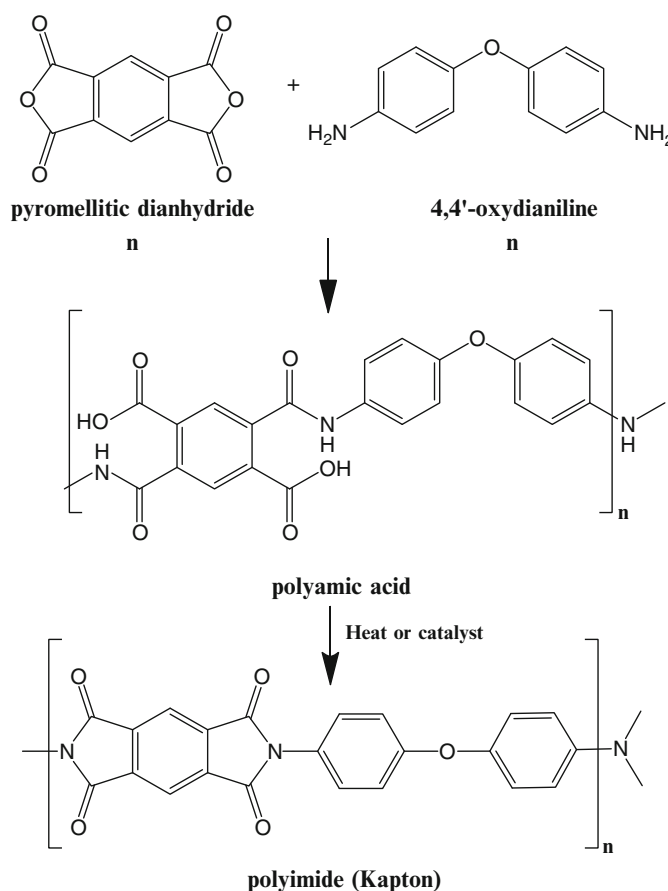
Polyimide Synthesis, Fig. 2 Typical synthesis of polyimide (Reprinted with permission from Ref. [20]. Copyright (1999) American Chemical Society)

such as *N*,*N*-dimethylformamide (DMF), *N*,*N*-dimethylacetamide (DMAc), *N*-methyl-2-pyrrolidone (NMP), or tetramethylurea (TMU) at room temperature by a nucleophilic substitution reaction of the carbonyl carbon of the anhydride with the amine. Although more difficult to remove and less thermally stable, dimethyl sulfoxide (DMSO) can also be used [14]. Imidization may also be carried out in solution, either by heating to temperatures >150 °C and removing evolved water via a Dean-Stark trap or at room temperature by use of base catalyst and a water scavenger, typically acetic anhydride. Depending on the backbone structure, polyimide solutions can be cast into films or spun into fibers. Alternatively, polyamic acid solutions can be cast into films and the solvent driven off before heating to >200 °C to effect imidization. In addition, dianhydride and diamine monomers can be ground together and the whole process (polyamic acid formation followed by imidization) can be carried out thermally by heating the mixture to >200 °C without use of solvent.

Polyimide matrix composites are typically made by applying the polyamic acid solution to fibers or fabric. Alternatively, resin transfer molding (RTM) can be used to introduce the polyimide into a fiber preform by melt flow. Typically, the polyimide is prepared as previously described and needs to be able to undergo a low viscosity flow in order to be fully incorporated into the fiber preform. Certain formulations of resin transfer moldable polyimide have been developed with low viscosity flow for just this purpose. Vacuum or a small amount of solvent can also be used to improve the flow of polymer into the preform. These techniques are referred to as vacuum-assisted RTM (VARTM) or solvent-assisted RTM (SARTM) [15].

A common method of analysis in determining chemical transformation is infrared spectroscopy. Characteristic absorption bands widely used to confirm the amic acid-imide transformation are seen at 1,720 cm^{-1} (C = O symmetrical stretching), 1,780 cm^{-1} (C = O asymmetrical stretching), 1,380 cm^{-1} (C-N stretching), and 725 cm^{-1} (C = O bending). Polyimide spectra will not exhibit absorption bands between 2,200 and 3,400 cm^{-1} typical of PAA, which implies the loss of *v* N-H, *v* O-H, and *v* C-H [16]. Other methods typically employed for characterization include nuclear magnetic resonance (NMR) spectroscopy, thermogravimetric analysis (TGA), differential scanning calorimetry (DSC), and dynamic mechanical measurement which provides curing and degradation data [17].

Addition Polyimides

An important class of polyimide for matrix resins for high-temperature composite applications is the so-called addition polyimides. For years aromatic polyimides only found application as films or coatings due to the difficult fabrication of copolymers formed by polycondensation melt processes. Thicker parts made strictly by polycondensation would result in voids due to the volatile condensation by-products becoming trapped in the matrix as it cured. In the 1970s a new class of thermosetting addition polyimides was developed in response to the need for improved processability and void free parts for composite applications [18]. Addition polyimides consist of short polymer chains (oligomers) endcapped with latent reactive groups. The most well-known example of this is the high-temperature resistant polymer, PMR-15, with norbornene endcaps [19]. As shown in Fig. 3, the end groups serve two purposes: to limit the molecular weight of the oligomer and to provide a site for cross-linking into a thermoset after imidization is complete [20]. This allows water evolved during imidization to escape from the part through the reactive endcaps before a final cure occurs at a higher temperature. Since the oligomers are relatively low molecular weight (1,500 for PMR-15), the resin undergoes flow before the final cross-linking step, resulting in good consolidation and low void content, even in thicker parts.

Also as shown in Fig. 3, PMR-15 introduced the concept of using methanol-soluble tetracarboxylic diester diacids in place of the dianhydrides. This allowed the monomers to be applied to fibers for composite fabrication using lower boiling alcohol solvents than typically
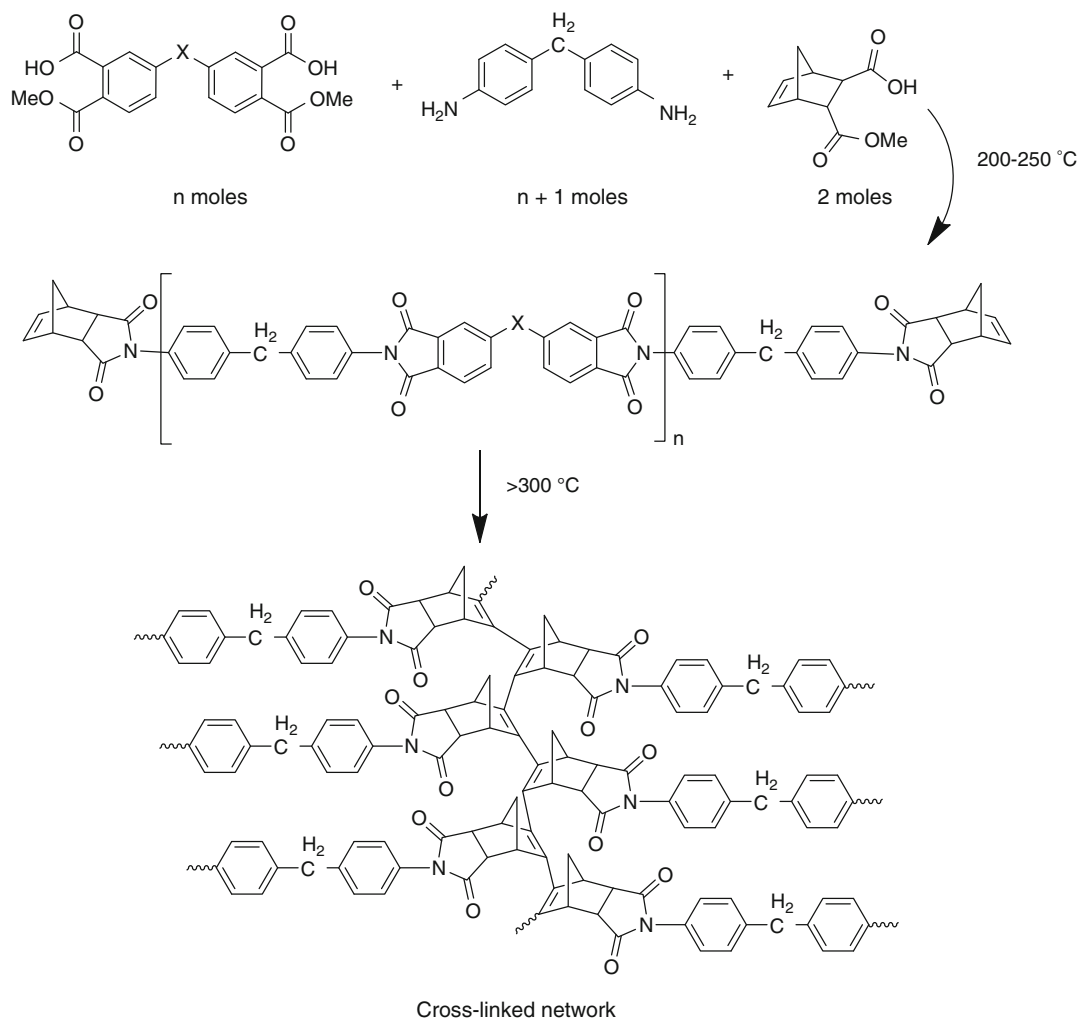
Polyimide Synthesis, Fig. 3 Synthesis of addition-type polyimide (PMR-15) through latent reactive end groups (Reprinted with permission from Ref. [19]. Copyright (1999) American Chemical Society)

needed to dissolve the polyimide monomers or polymers. Thus, this is the reason these are called PMR polyimides – PMR stands for "polymerization of monomeric reactants." The reaction still proceeds via the dianhydride which reforms from the diester diacid at elevated temperatures.

Because the norbornene endcap and the cross-link that forms are aliphatic, the amount of endcap does reduce the thermal stability. Hence, there is again a trade-off between processability (low molecular weight oligomers are favored) and thermal stability (which would improve with higher molecular weight oligomers between

the cross-links). Other latent reactive endcaps that have been used in polyimide thermoset resins include acetylenes, phenylacetylenes, cyclophanes, biphenylenes, and benzocyclobutenes as shown in Fig. 4, though norbornene is the most established commercially [2].

Materials synthesized by addition polymerization exhibit excellent thermomechanical properties and improved processability. However, due to the high level of cross-linking, they tend to be more brittle. Siloxane-containing oligomers or fluorinated backbone structures have been synthesized in attempts to overcome these

Polyimide Synthesis,
Fig. 4 Alternate latent
reactive endcaps for
addition polyimides

4-aminophenylacetylene

Phenylethynylphthalic anhydride

2-aminobenzocyclobutane

4-amino[2,2]-paracyclophane

2-aminobiphenylene
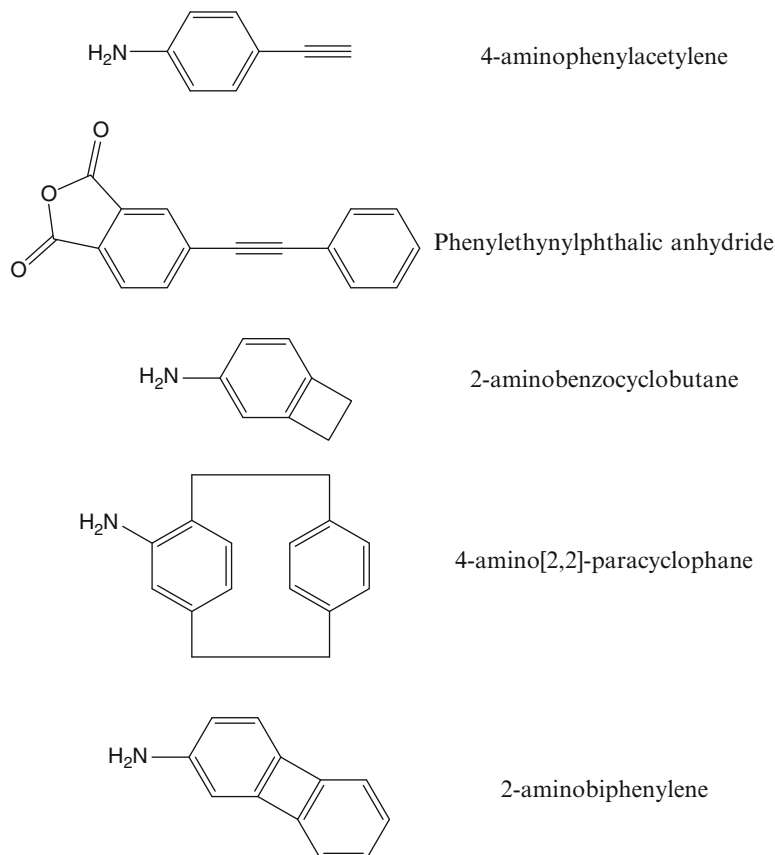
shortcomings by allowing for a higher degree of flexibility as depicted in Fig. 5 [21, 22].

Porous Polyimides

While it is important to reduce void content for polymer matrix composites to provide the best mechanical and thermal stability, many researchers have examined ways to introduce porosity into the polyimide to reduce dielectric constant. These approaches include foam formation, introduction of low-density fillers, use of thermally labile blocks, and incorporation of comonomers containing perfluoroalkyl groups and side chains [23]. The latter approach increases free volume in the polyimides. The lowest density polyimides as previously mentioned are made by forming polyimide gels from solution, followed by critical point drying to remove the liquid portion and produce

polyimide aerogels as shown in Fig. 6 [24]. In this approach, polyamic acid oligomers are fabricated by dissolving aromatic diamines and tetracarboxylic dianhydrides together at low solid content. Addition of cross-linker, typically tris (aminophenoxy)benzene or octa(aminophenyl) polysilsesquioxane, followed by base catalyst and acetic anhydride yields fully imidized gels typically in under an hour. The polyimide aerogels have densities ranging from 0.06 to 0.3 g/cm^3 which result in relative dielectric constants ranging from 1.08 to 1.3. The polyimide aerogels also have very low thermal conductivity similar to silica aerogels, combined with better strength properties similar to polymer foams, making them ideal insulation materials.

Main chain manipulation may have a significant effect on the polyimide properties; however, side group reactions have a much greater potential for variation of macromolecular structure. By incorporating large monomers or functionalizing
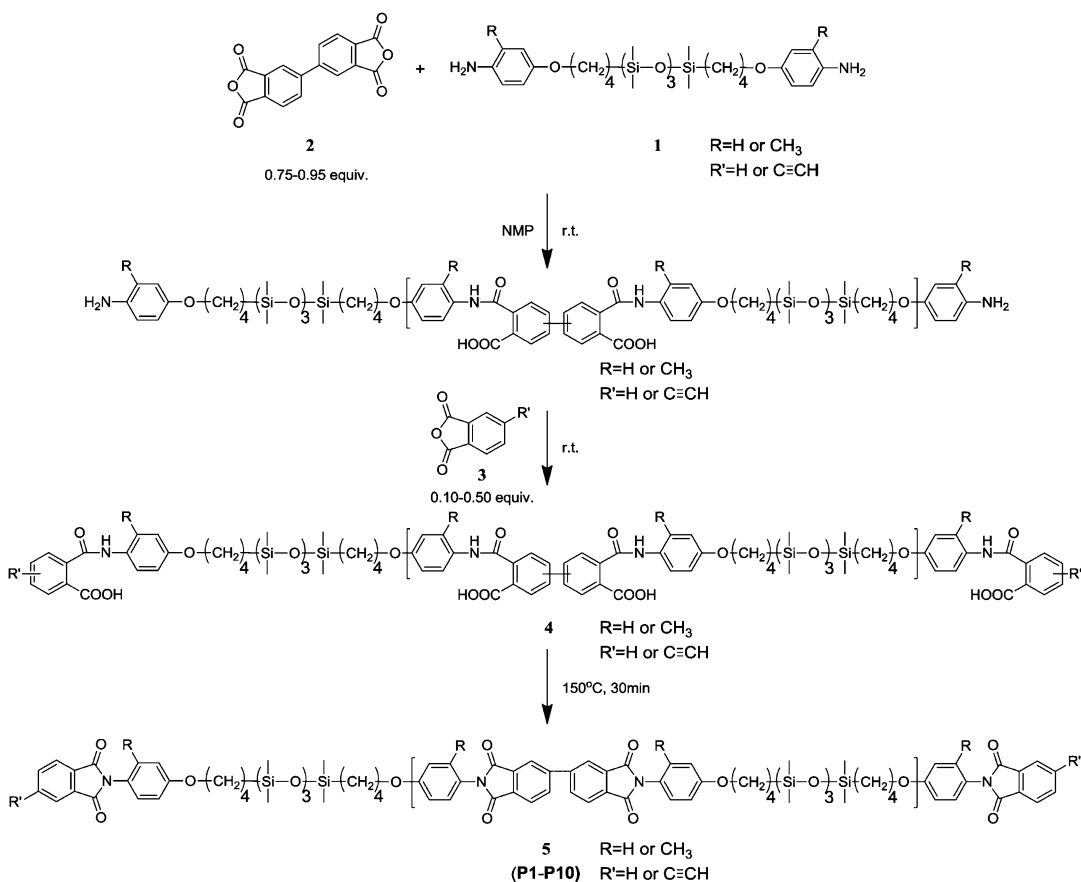
Polyimide Synthesis, Fig. 5 Siloxane-containing oligomers within polyimide matrix increase flexibility (Reprinted with permission Ref. [22]. Copyright (2013) American Chemical Society)

the backbone of the monomeric units, it is possible to create hyperbranched polymers for various self-assembled nanoporous structures. An example can be seen in Fig. 7 which varies large monomeric units of tris(4-aminophenyl)amine (TAPA) and hexafluoropropane dianhydride (6FDA) [25].

Atomic Oxygen-Resistant Polyimides

Atomic oxygen (AO), an elemental form of oxygen created by intense UV light exposure, is formed in lower Earth orbit (LEO) approximately 200–500 miles above Earth's surface. Oxygen in its single atomic form acts as an aggressively reactive agent which is a concern for spacecraft materials and satellites that may be subject to

surface erosion [26]. Atomic oxygen causes localized damage of polymeric materials resulting in mass loss and changes in optical, mechanical, electrical, and chemical properties. Degradation occurs by hydrogen abstraction which decomposes the polymer backbone into fragments of lower molecular weight oligomers [27].

High-temperature polyimide films can be tailored to have increased oxidative resistance by backbone manipulation of the polymer matrix. It has been shown that increasing thermal stability by increasing aromatic components in the linear chain and introducing –CF_3 groups will increase resistance to AO degradation [28]. Polyimides containing polyoligomeric silsesquioxane (POSS) units as side chains or in the backbone as seen in Fig. 8 show an increase in AO
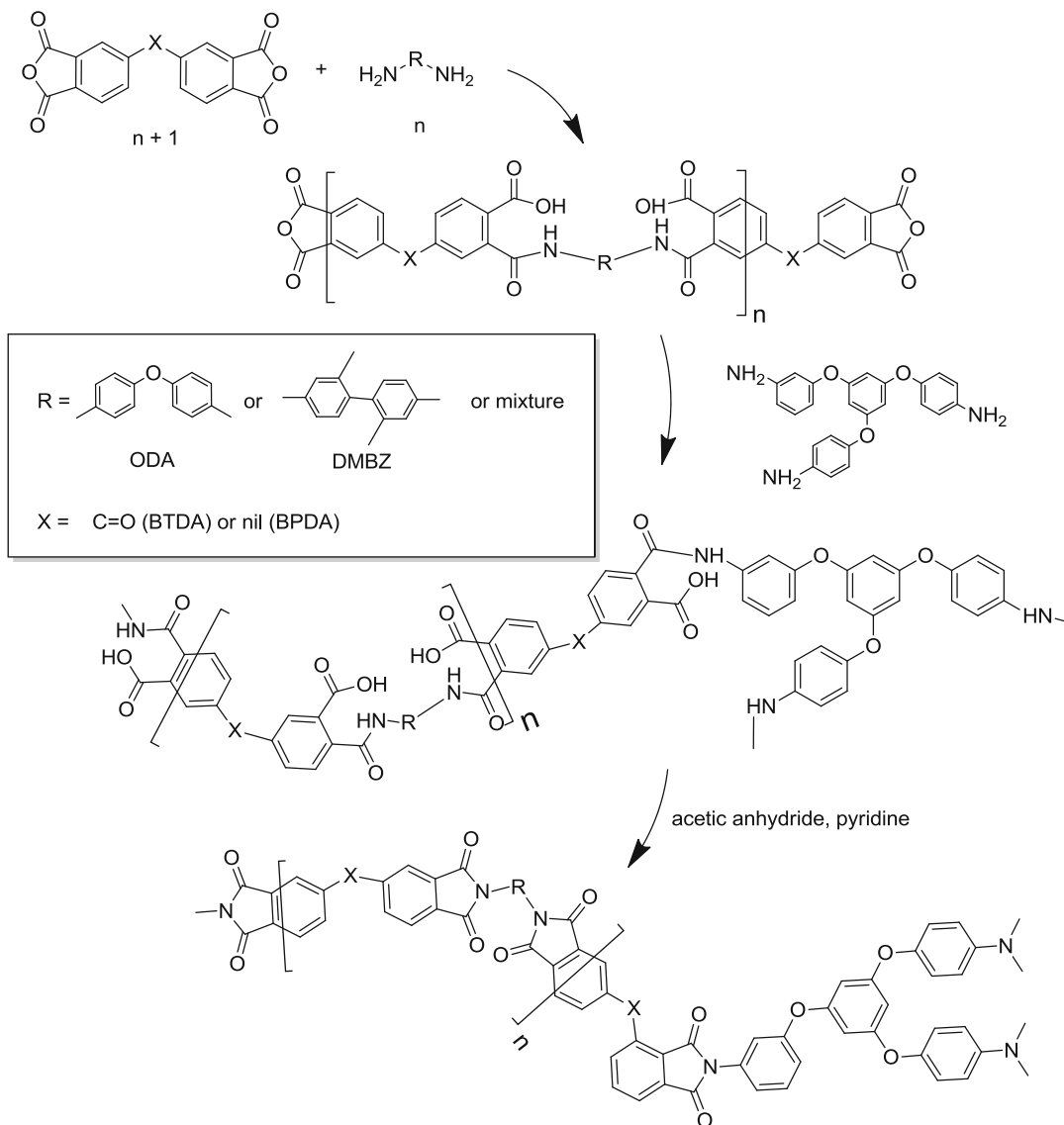
Polyimide Synthesis, Fig. 6 Cross-linked polyimide network formation from aromatic diamines, dianhydride, and aromatic triamine is the first step of polyimide aerogel fabrication (Reprinted with permission Ref. [24]. Copyright (2012) American Chemical Society)

resistance making them a promising material for satellite and other space structures in LEO [29].

Summary

Polyimides are a versatile class of polymers with wide-ranging application due to their relatively high thermal stability, combined with excellent mechanical properties, wear resistance, low thermal expansion, and inertness to solvents, low dielectric constant, low relative permittivity, radiation resistance, and good processability. Polyimides are produced as thin films for microelectronic and membrane applications, as matrix resins for high-performance composites, and as porous aerogels for use as electrical or thermal insulation, among other things. Polyimides can
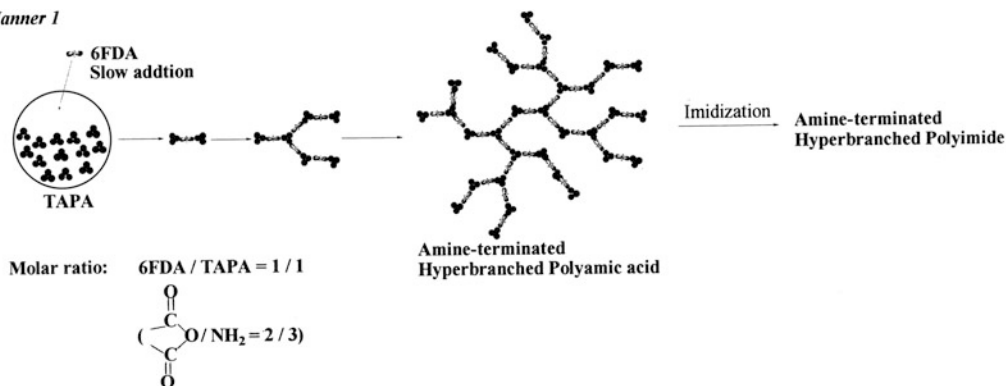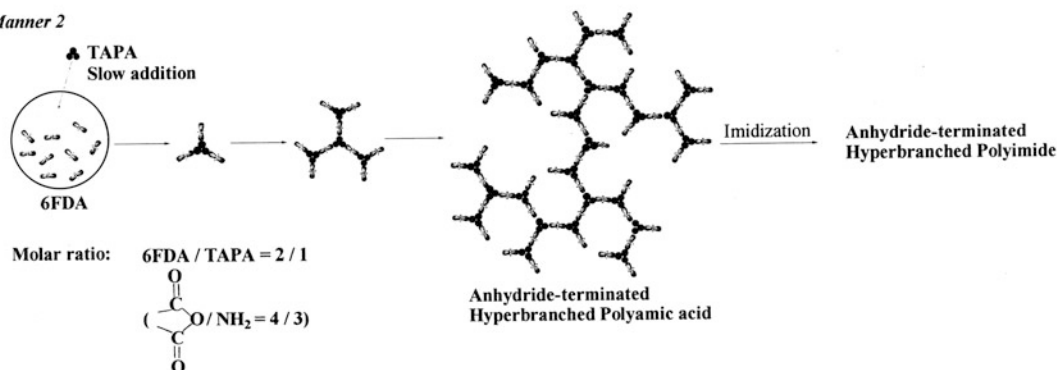
Polyimide Synthesis, Fig. 7 Depiction of various monomers used to create a hyperbranched porous polymer structure (Reprinted with permission Ref. [25]. Copyright (2000) American Chemical Society)
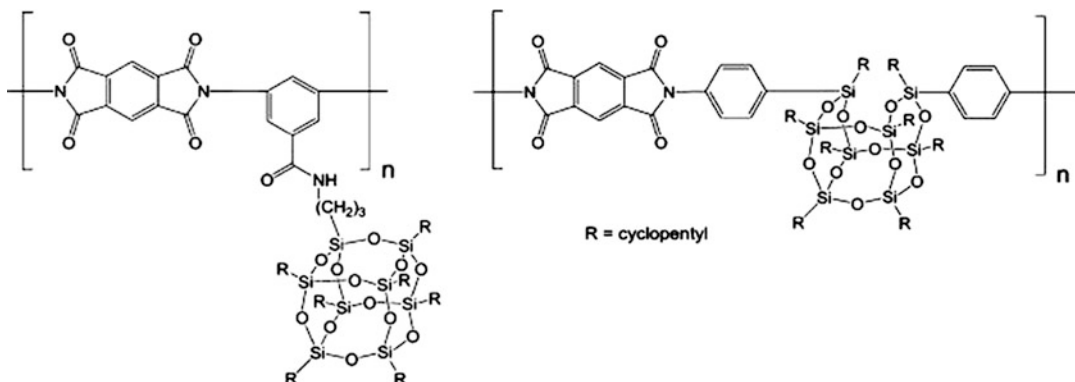
Polyimide Synthesis, Fig. 8 Polyimides containing polyoligomeric silsesquioxane (POSS) units as side chains or in the backbone show resistance to AO degradation (Reprinted with permission Ref. [29]. Copyright (2012) American Chemical Society)

be produced as thermoplastics or cross-linked into thermosetting materials. Polyimides have also found use as materials for biomedical devices, neural interface membranes, and tissue scaffolds. Tailoring the properties of polyimides for different applications is easily achieved through altering the backbone chemistry or adding side groups, recognizing that there is often a trade-off between thermal stability and other desired properties.

Related Entries

▶ Chain-Growth Condensation Polymerization
▶ Cross-Linked Polymer Synthesis
▶ Gas Separation Membranes
▶ Ladder-Type Polymers
▶ Nanofiltration Membranes
▶ Nanoporous Polymer Filters and Membranes, Selective Filters
▶ Polymers for Fuel Cells
▶ Telechelic Polymer: Preparation and Application

References

1. Critchley JP, Knight GJ, Wright WW (1983) Heat resistant polymers. Plenum Press, New York
2. Meador MA et al (1998) Recent advances in the development of processable high-temperature polymers. Annu Rev Mater Sci 28:599–630
3. Maier G et al (2001) Low dielectric constant polymers for microelectronics. Prog Polym Sci 26:3–65
4. Progar DJ, St. Clair TLJ (1994) Adhesion Sci Technol 8:67
5. Zhang Y, Sunarso J, Liu S, Wang R (2013) Current status and development of membranes for CO2/CH4 separation: a review. Int J Greenhouse Gas Contr 12:84–107
6. Sanders DF, Smith ZP, Guo R, Robeson LM, McGrath JE, Paul DR, Freeman BD (2013) Energy-efficient polymeric gas separation membranes for a sustainable future: a review. Polymer 54:4729–4761
7. Bose S, Kuila T, Nguyen TXH, Kim NH, Lau KT, Lee JH (2011) Polymer membranes for high temperature proton exchange membrane fuel cell: recent advances and challenges. Prog Polym Sci 36:813–843
8. Meador MAB, Wright S, Sandberg A, Nguyen BN, Van Keuls FW, Mueller CH, Rodriguez-Solis R, Miranda FA (2012) Low dielectric polyimide aerogels as substrates for lightweight patch antennas. ACS Appl Mater Interfaces 4:6346–6353
9. Aegerter M, Leventis N, Koebel MM (2011) Aerogels handbook. Springer, New York/Dordrecht/Heidelberg/London
10. Ghodssi R, Lin P (2011) MEMS materials and processes handbook. Springer, New York
11. Dhara MG, Banerjee S (2010) Fluorinated high performance polymers: poly(arylene ether)s and aromatic polyimides containing trifluoromethyl groups. Prog Polym Sci 35:1022–1077
12. Sun Y, Lacour SP, Brooks RA, Rushton N, Fawcett J, Cameron RE (2009) Assessment of the biocompatibility of photosensitive polyimide for implantable medical device use. J Biomed Mater Res 90A:648–655
13. Stieglitz T (2001) Flexible biomedical microdevices with double-sided electrode arrangements for neural applications. Sensors and Actuators A: Physical (2001) 90:203–211
14. Ghosh MK, Mittal KL (1996) Polyimides: fundamentals and applications. Plastics engineering. CRC Press, New York
15. Connell JW, Smith JG, Hergenrother PM (2003) High temperature transfer molding resins: laminate properties of PETI-298 and PETI-330. High Perform Polym 15:375–394
16. Santhana Gopala Krishnan P, Vora RH, Chung TS, Uchimura SI, Sasaki N (2004) Studies on ionic salt of polyamic acid and related compounds. J Polym Res 11:299–308
17. Androva NA, Bessonov MI, Laius LA, Rudakov AP (1970) Polyimides: a new class of thermally stable polymers. Prog Mater Sci Ser 7:13–57
18. Abajo J, Campo JG (1999) Processable aromatic polyimides. Adv Polym Sci 140:23–59
19. Serafini TT, Delvigs P, Lightsey GR (1972) Thermally stable polyimides from solutions of monomeric reactants. Appl Polym Sci 16:905–915
20. Meador MAB, Johnston CJ, Frimer AA, Gilinsky-Sharon P (1999) On the oxidative degradation of nadic end-capped polyimides. Macromolecules 32:5532–5538
21. Labana SS (1977) Chemistry and properties of crosslinked polymers. Academic, New York
22. Shoji Y, Ishige R, Higashihara T, Morikawa J, Hashimoto T, Takahara A, Watanabe A, Ueda M (2013) Cross-linked liquid crystalline polyimides with siloxane units: Their morphology and thermal diffusivity. Macromolecules 46:747–755
23. Hedrick JL et al (1999) Nanoporous polyimides. Adv Polym Sci 141:1–43
24. Meador MAB, Malow EJ, Silva R, Wright S, Quade D, Vivod SL, Guo H, Guo J, Cakmak M (2012) Mechanically strong, flexible polyimide aerogels cross-linked with aromatic triamine. ACS Appl Mater Interfaces 4:536–544
25. Fang J, Kita H, Okamoto K (2000) Hyperbranched polyimides for gas separation applications. 1. Synthesis and Characterization. Macromolecules 33:4639–4646
26. Hartmann-Thompson C (2011) Applications of polyhedral oligomeric silsesquioxanes. Springer, Dordrecht
27. Reddy MR, Srinivasamurthy N, Agrawal BL (1993) Atomic oxygen protective coatings for Kapton film: a review. Surf Coat Technol 58:1–17
28. Kutz M (2012) Handbook of environmental degradation of materials. Elsevier, Oxford, UK
29. Minton TK, Wright ME, Tomczak SJ, Marquez SA, Shen L, Brunsvold AL, Cooper R, Zhang J, Vij V, Guenthner AJ, Petteys BJ (2012) Atomic oxygen effects on POSS polyimides in low earth orbit. ACS Appl Mater Interfaces 4:492–502

Polyisocyanides, Polyisocyanates

Eiji Ihara
Department of Material Science and
Engineering, Graduate School of Science and
Engineering, Ehime University, Matsuyama,
Japan

Synonyms

Polyisocyanate: nylon-1; Polyisocyanide: poly
(alkyliminomethylene), Polyisonitrile

Definition

Polymers obtained by polymerization of mono-
mers having an isocyanide group (R–NC)
(polyisocyanide) and an isocyanate group
(R–N=C=O) (polyisocyanate).

General

Polyisocyanides and polyisocyanates are both
obtained by the polymerization of monomers
with a highly reactive functional group,
isocyanide and isocyanate, respectively, and the
polymerization utilizes the unique reactivity of
each functional group. Both monomers can
contain a variety of alkyl or aryl groups,
which should be located around the resulting
polymer main chains and strongly affect the
properties of the polymers. The most important
and common characteristic of polyisocyanides
and polyisocyanates is that their polymer
main chains tend to assume helical conforma-
tions, which should be either left or right
handed. It should be also mentioned here that
a variety of optically active polymers with
respect to the helical sense have been prepared
from both monomers, and various applications
have been attempted using the chiral
polymers [1, 2].

Polyisocyanides

General methods for preparing a variety of
isocyanides have been established and some
isocyanides are even commercially available. It
should be pointed out that low molecular weight
isocyanides have an extremely offensive smell
and, thus, must be prepared and handled in
a good hood. The isocyano group can be consid-
ered as either a zwitterionic species with a C–N
triple bond or a neutral species with a divalent
carbene (Fig. 1). As can be assumed from both
formulations, isocyanide is a highly reactive
functional group, particularly exhibiting high
reactivity with metal complexes. The most com-
mon method for the isocyanide polymerization is
transition metal-catalyzed polymerization using
some Ni and Pd complexes. In the propagation,
the terminal carbon atom in isocyanide is
transformed into an imine-carbon in
1,1-addition mode, and the resulting polymers
have the imine substituent (=N–R) on every
main chain carbon atom (Fig. 1). As a conse-
quence, polyisocyanides with a bulky substituent
are rigid rodlike polymers, whose once kineti-
cally produced helical conformations remain sta-
ble even in solution.

Nickel(II) complexes such as $NiCl_2 \cdot 6H_2O$
have been reported to be the most convenient
and efficient catalysts for polymerization of var-
ious isocyanides. In the Ni-catalyzed polymeri-
zation, four monomer molecules are coordinated
to a square-planar Ni center, and a nucleophilic
species such as amine employed as an additive
nucleophilically attacks one of the coordinated
monomers, giving an imino Ni species, whose
Ni-bound imine-carbon is also nucleophilic
enough to attack the adjacent coordinated mono-
mer successively. Because of the preorganization
of the monomers around the Ni center, the suc-
cessive insertion of the monomers into the imino
Ni growing chain end kinetically results in the
formation of either a right- or left-handed helical
conformation as shown in Fig. 2 (merry-go-round
mechanism). As a result, after the polymerization
the resulting polyisocyanide has a right- or left-
handed helical structure, which can be retained if

P

Polyisocyanides,
Polyisocyanates,
Fig. 1 Polymerization of
isocyanide
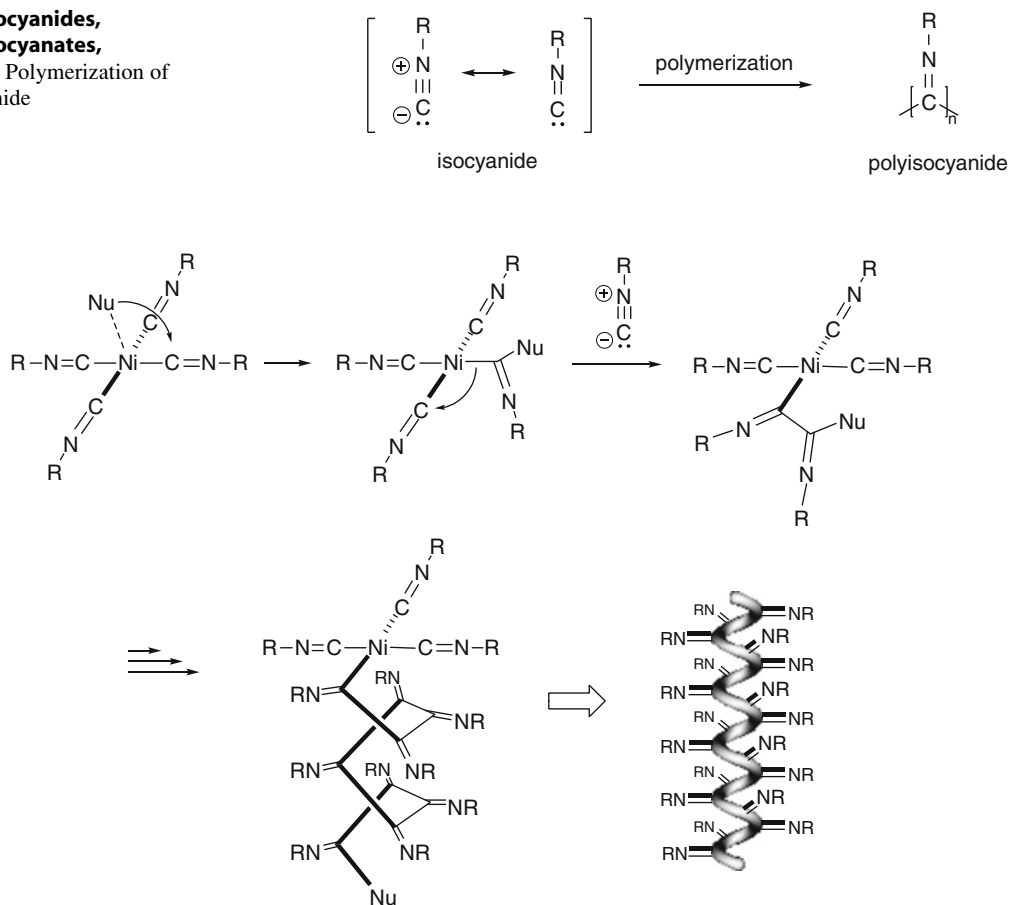
Polyisocyanides, Polyisocyanates, Fig. 2 "Merry-go-round mechanism" for polymerization of isocyanide

the helical conformation is stable enough not to be unfolded into a nonhelical conformation. Various studies with respect to the stability of the helical conformation have established that the helical conformation can be stable if the substituent has a certain degree of bulkiness. For example, poly(*tert*-butyl isocyanide) has a stable helical conformation even in solution, and a racemic mixture of the right- and left-handed helical polymers was separated into two enantiomers with each opposite helical sense by using chiral stationary phase for the separation (Fig. 3). On the other hand, because steric bulkiness of a phenyl group in poly(phenyl isocyanide) is not high enough for the helical conformation to be stable, the kinetically formed rigid-rod helical poly(phenyl isocyanide) via merry-go-round mechanism is transformed to a random-coil conformation after being kept in solution.

More importantly, although a racemic mixture of polymers with right- and left-handed helical conformations is kinetically obtained by the polymerization of isocyanide in the absence of any chiral factors, helix-sense-selective polymerization can be realized by using a chiral monomer (chiral bias) because the resulting right- and left-handed helical polyisocyanides should be diastereomers possessing different free energies. Accordingly, one of the helical senses exceeds the other in the resulting polymers, and the product possesses optical activity derived from the excess of one of the helical senses (Fig. 4).

For a representative example of the helix-sense-selective polymerization, an isocyanide monomer with an optically active short peptide
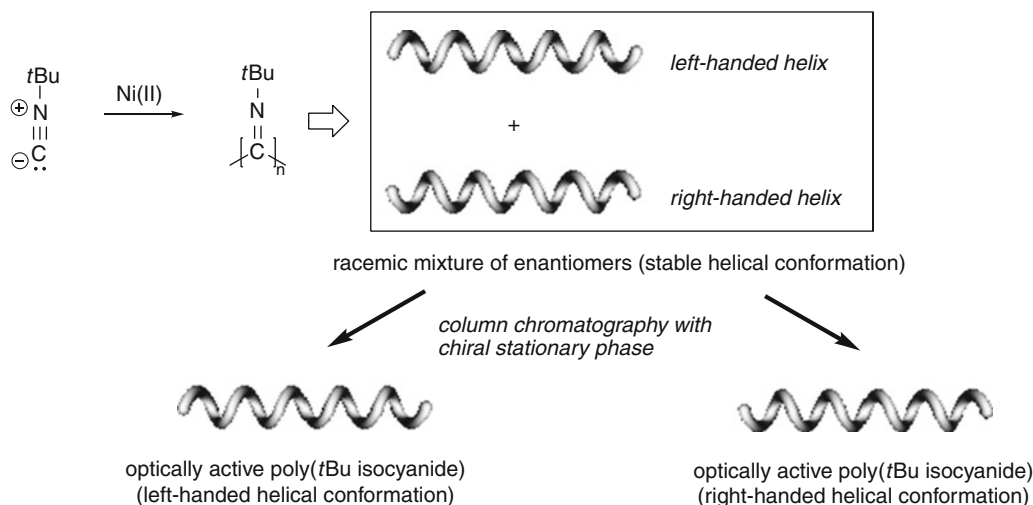
Polyisocyanides, Polyisocyanates, Fig. 3 Preparation of optically active poly(*tert*-butyl isocyanide)
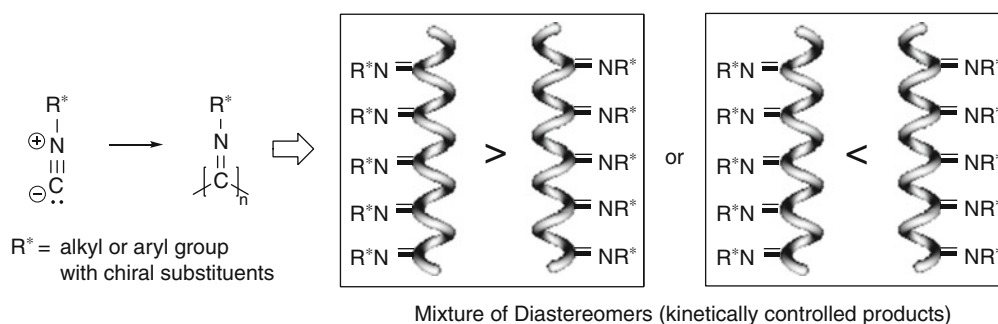
Polyisocyanides, Polyisocyanates, Fig. 4 Helix-sense-selective polymerization of isocyanide

chain has been polymerized to give a helical polymer ["poly(isocyanopeptide)"] with a predominant left-handed helical sense, where the intramolecular hydrogen-bonding networks among the peptide pendants contribute to stabilizing the kinetically formed one-handed helical conformation, although the peptide pendant is not bulky enough to stabilize the helical conformation with the steric constraint alone (Fig. 5). Because polyisocyanides generally assume 4/1 helix, where four repeating units constitute one cycle along the polymer backbone, the abovementioned hydrogen-bonding networks occur between n and n+4 repeating units, rendering the polymer main chain surrounded by four bundles of the peptide pendants along the polymer backbone. The stabilization of the 4/1 helical conformation via the intramolecular hydrogen bonds described above has been utilized to regularly align a variety of functional groups along the optically active helical polymer main chain. For example, functional chromophores such as porphyrin and perylene are introduced into monomers to investigate photophysical properties derived from the stacked alignment of the chromophores around the polymer backbone (Fig. 6). In particular, the perylene-containing polymers have been demonstrated to be effective as a component of photovoltaic cells. In addition, poly(isocyanopeptide)s bearing oligo(ethylene glycol) as a substituent can form artificial gels with similar physical properties as observed in biological polypeptide-derived gels because of their unique self-assembling nature.
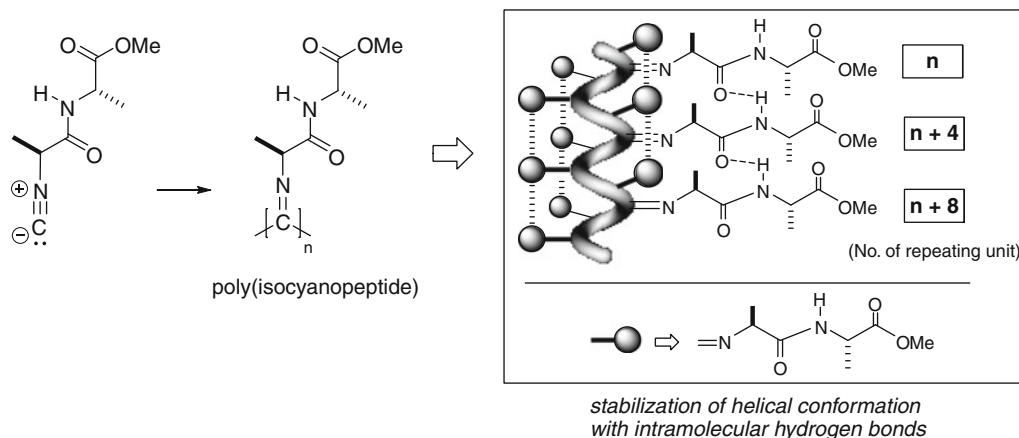
Polyisocyanides, Polyisocyanates, Fig. 5 Helix-sense-selective polymerization of isocyanopeptide
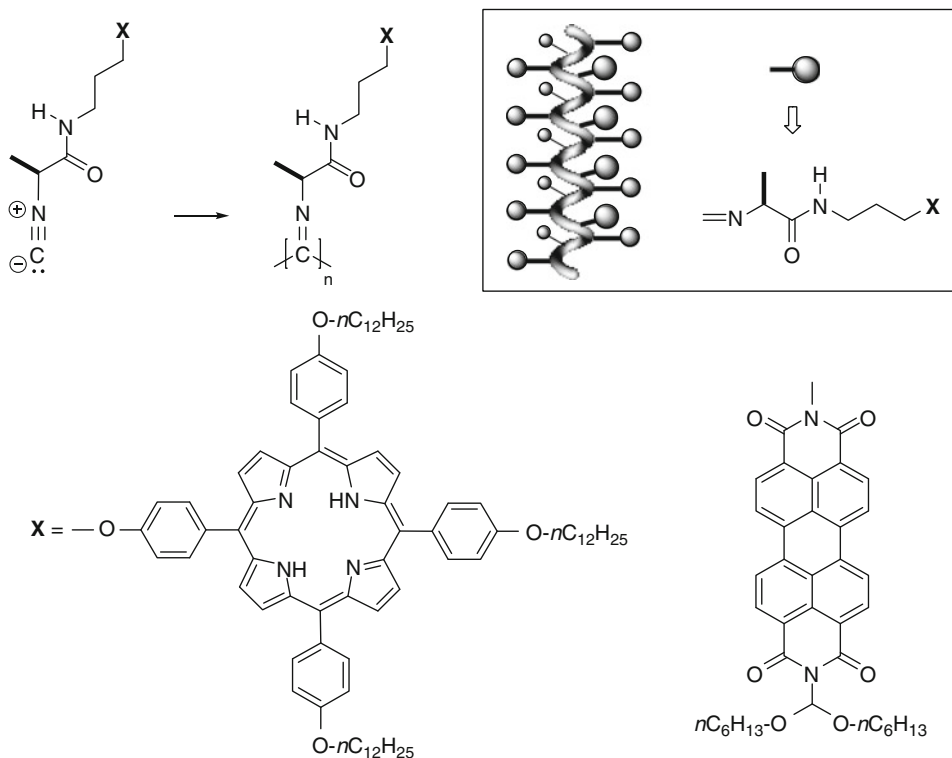
Polyisocyanides, Polyisocyanates, Fig. 6 Synthesis of left-handed helical polyisocyanides with functional chromophores

Interesting to note is that a stereogenic center separated from the polymer backbone via a rigid spacer can also affect the helical sense of the main chain, as demonstrated by the investigation of polyisocyanides shown in Fig. 7.

Syntheses of well-defined polyisocyanides with respect to molecular weight and molecular weight distribution (living polymerization) have been achieved by using some transition metal complexes (Fig. 8). [π-AllylNi(O₂CCF₃)]₂ is
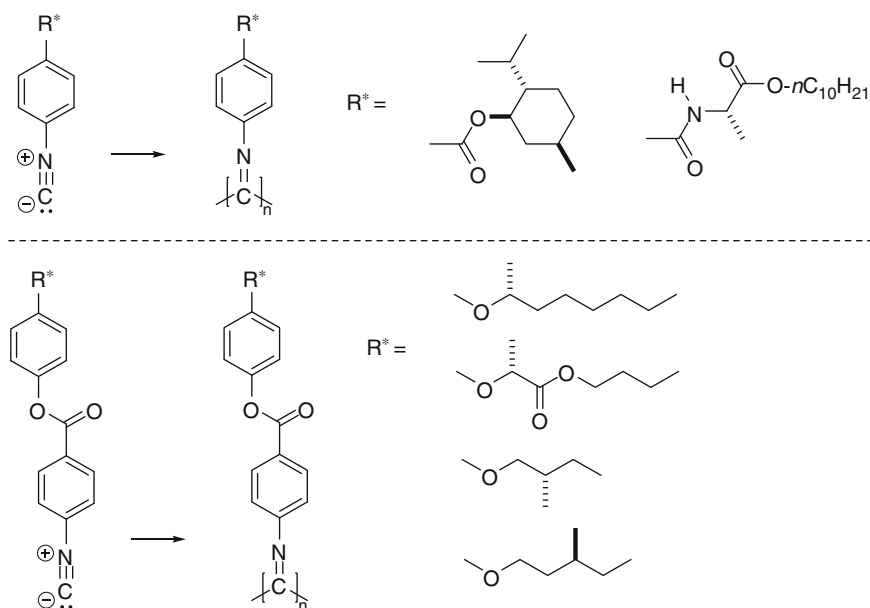
Polyisocyanides, Polyisocyanates, Fig. 7 Helix-sense-selective polymerization via chirality transfer through rigid spacer

Polyisocyanides, Polyisocyanates, Fig. 8 Initiators for living isocyanide polymerization

[π-allylNi(O$_2$CCF$_3$)]$_2$ Pt-Pd μ-ethynediyl complex   aryl-Rh complex

P
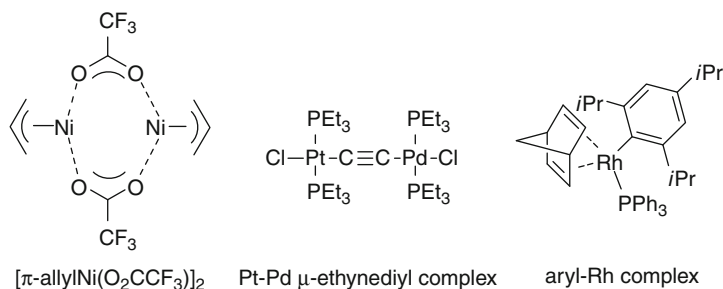
a representative example as an initiator for the living polymerization of alkyl isocyanides. Pt–Pd μ-ethynediyl complex can also be an efficient initiator for the living polymerization of aryl isocyanides. Interesting to note is that aryl isocyanide monomers insert into the Pd–C bond of the heterodinuclear complex and the propagating end derived therefrom, but the presence of the Pt moiety in the initiator is essential for the polymerization to occur from the complex. An aryl-rhodium complex has been reported to initiate the living polymerization of aryl isocyanides with bulky substituent on the aromatic ring. Along with the syntheses of polyisocyanides with narrow molecular weight distributions, preparation

of block copolymers of a variety of monomer combinations can be achieved by using these living polymerization initiators, contributing to application of polyisocyanides for functional polymeric materials.

A unique polymer synthesis has been realized by using Pd-initiated polymerization of 1,2-diisocyanobenzenes as monomers. As shown in Fig. 9, the successive insertion of the two adjacent isocyanides into Pd–C bond at the propagation chain end leads to the formation of 2,3-quinoxaline framework as a result of aromatization. Noteworthy is that the Pd-initiated polymerization proceeds in a living manner, affording polymers with narrow molecular weight distribution, and the propagating
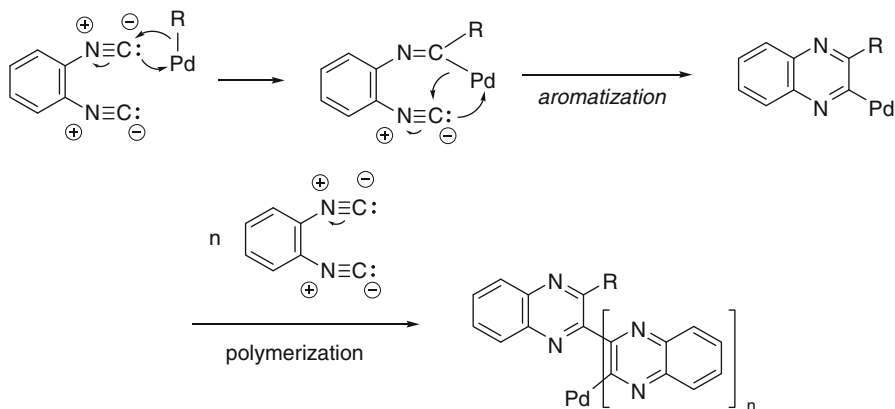
Polyisocyanides, Polyisocyanates, Fig. 9 Pd-initiated aromatizing polymerization of 1,2-diisocyanobenzene
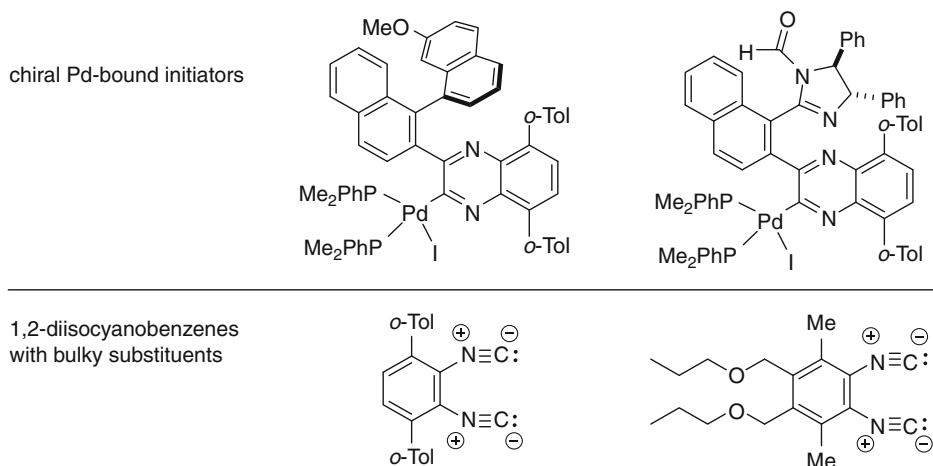
Polyisocyanides, Polyisocyanates, Fig. 10 Initiators and monomers for helix-sense-selective polymerization of 1,2-diisocyanobenzene

chain end containing quinoxalinyl-Pd moiety is stable even in the air and, thus, can be isolated in a form retaining the propagating ability. Furthermore, the resulting polymers can again assume a helical conformation if the substituents on the monomer are bulky enough, although the basic framework is totally different from those of aforementioned polyisocyanides obtained from monofunctional isocyanide monomers. The helical sense of the resulting helical polymers can be controlled by proper choice of Pd-containing initiators with some optically active ligands

(Fig. 10). Introduction of phosphine-containing 1,2-diisocyanobenzene as a comonomer in the helix-sense-selective polymerization gives one-handed helical polymers with metal-coordinating sites, which can be used as a polymeric catalyst for asymmetric reactions after ligation of some transition metals. Actually, the polymeric catalysts are effective as a catalyst for some asymmetric reactions because of the chiral environment of the metal-containing active site derived from the one-handed helical sense.

Polyisocyanates

Isocyanates can be polymerized by the reaction with nucleophilic reagents in a manner as shown in Fig. 11 to give polyisocyanate. The main chain structure solely consisting of *N*-substituted amide linkages can be regarded as nylon-1. Although the term "polyisocyanate" sometimes refers to low molecular weight compounds containing more than one isocyano group, this article deals with only polymers obtained from isocyanate monomers via transformation of their isocyano group. A variety of alkyl and aryl isocyanates can be prepared and some of them are commercially available. Because isocyanate is an inherently highly reactive functional group, the compounds should be handled and stored with considerable attention. The anionic polymerization can be initiated by nucleophiles such as sodium

cyanide (NaCN), but the control of the polymerization with respect to the molecular weight and molecular weight distribution is generally difficult basically because of the high tendency of the cyclic trimer formation as shown in Fig. 11. On the other hand, the initiators shown in Fig. 12 have been reported to be quite effective to inhibit the trimer formation, realizing living polymerization of isocyanates.

As well as the aforementioned polyisocyanides, polyisocyanates have been representative examples of helical polymers. However, in contrast to the polyisocyanides with bulky substituents, whose helical structure is rather stable with high inversion energy barrier, the barrier of the polyisocyanates is considerably lower, rendering the reversible helix inversion more feasible than those in polyisocyanides. Furthermore, the dynamic properties derived from the low inversion

Polyisocyanides, Polyisocyanates, Fig. 11 Polymerization and cyclic trimer formation of isocyanate
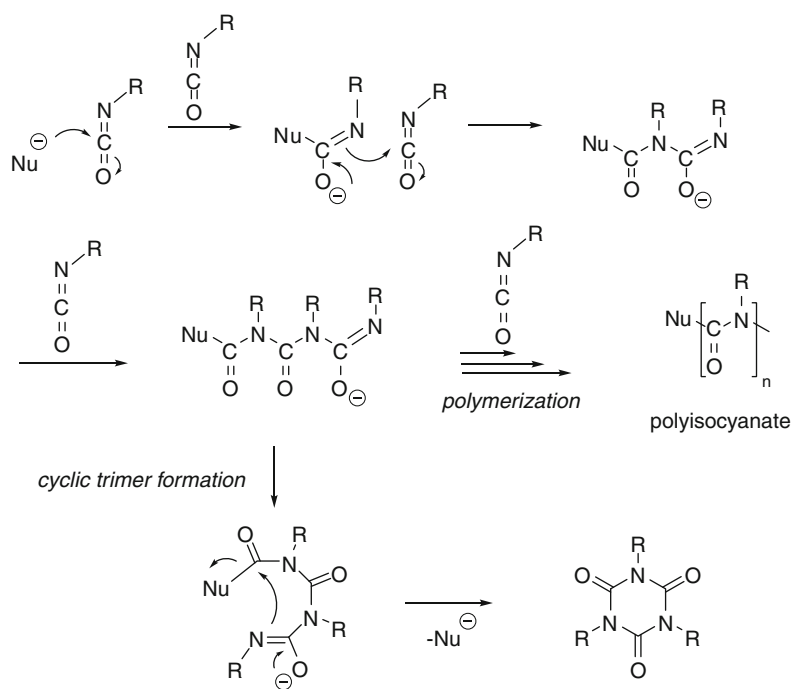
Polyisocyanides, Polyisocyanates, Fig. 12 Living polymerization initiators for isocyanates
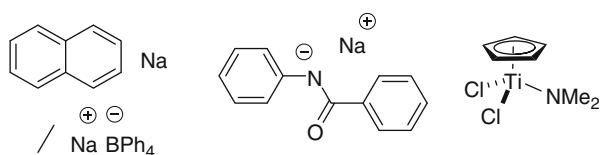
**Polyisocyanides,
Polyisocyanates,
Fig. 13** Dynamic helical
polymer with low inversion
barrier
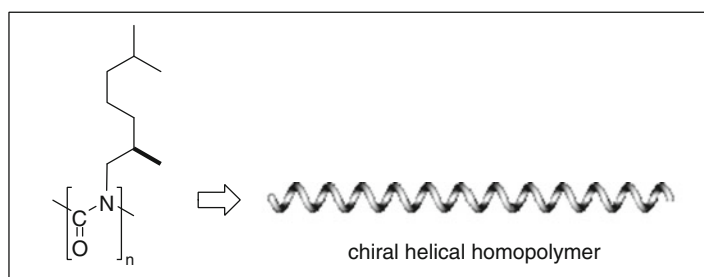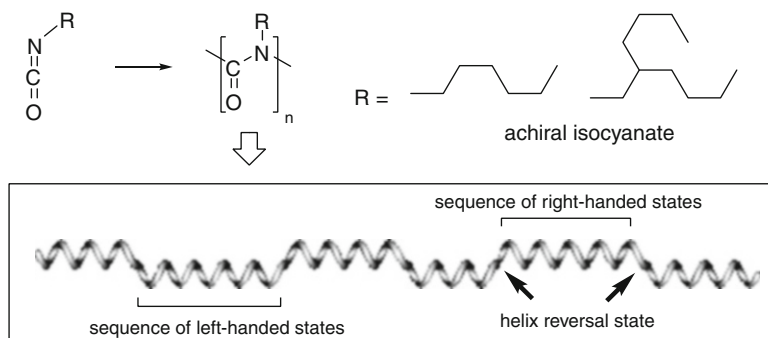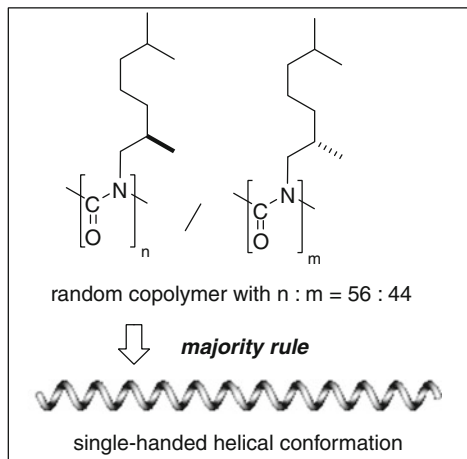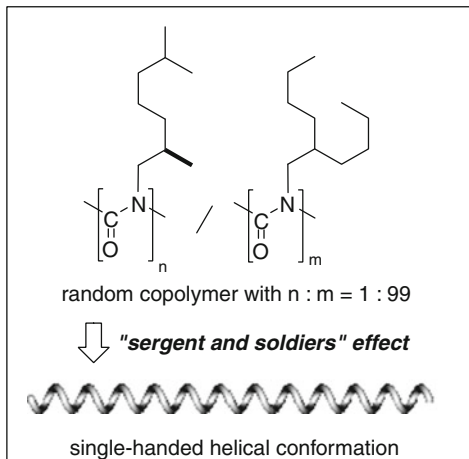
Polyisocyanides, Polyisocyanates, Fig. 14 Chiral amplification in polyisocyanate

barrier lead to some unique characteristics of polyisocyanates, which have been investigated in detail, and some important general principles have been established with respect to the conformation of dynamic helical polymers.

Because of the low barrier for the helical sense inversion, the helical sense of polyisocyanates should be determined thermodynamically. In the absence of any chiral factors in a monomer employed for the polymerization, the resulting polyisocyanate chain consists of an equal amount of left- and right-handed helical states (monomer units) separated by helix reversal state, which is energetically higher than those of two helical

states with respect to the free energy of each monomer unit (Fig. 13). On the other hand, when a chiral moiety is introduced to a monomer unit, the resulting helical polymer should be a diastereomer, and there should be energy difference between the right- and left-handed helical states in the polymer. It has been revealed that although the energy difference between the diastereomeric monomer units is rather low, the activation energy for the inversion of the monomer unit is so high that inversion state rarely exists in the polymer chain. Furthermore, the small energy difference per monomer unit can be significantly amplified in the polymer with high degree of polymerization, resulting in the predominance of one of the helical states in the polymer chain even in the presence of only a small amount of a chiral monomer unit. As a result, when a small amount of a chiral isocyanate is copolymerized with a large excess of an achiral isocyanate, the resulting copolymer has an excess of one-handed helical structure, which is called "sergeant and soldiers" effect. Likewise, when a mixture of enantiomers with one of them slightly exceeding the other is polymerized, the resulting polymer has predominantly a helical sense preferred by the major enantiomer ("majority rule") (Fig. 14).

The unique dynamic properties with respect to the helical sense have been attempted to be utilized for some applications. For example, because the helical sense of polyisocyanates could be sensitive to the external stimuli, the cis–trans isomerization of azobenzene unit incorporated into the monomer structure was used to control the helical sense by photoirradiation.

The important and useful characteristic of polyisocyanate is its stiff and helical polymer backbone, which makes it a representative example of rodlike polymers. In combination with the controllability of its anionic polymerization, reactivity of isocyanate monomers has provided a rare opportunity for preparing rod–coil block copolymers with block copolymerization with vinyl monomers such as styrene and 2-vinylpyridine. In particular, a series of block copolymers of *n*-hexylisocyanate and 2-vinylpyridine with a well-defined block sequence and block lengths have been prepared, and their unique properties based on the self-assembling of poly(*n*-hexylisocyanate) blocks have been extensively investigated.

Related Entries

▶ Asymmetric Polymerization
▶ Optical Resolution Materials

References

1. Cornelissen JJLM, Rowan AE, Nolte RJM, Sommerdijk NAJM (2001) Chiral architectures from macromolecular building blocks. Chem Rev 101:4039–4070
2. Yashima E, Maeda K, Iida H, Furusho Y, Nagai K (2009) Helical polymers: synthesis, structures, and functions. Chem Rev 109:6102–6211

Polymer Brushes

Yasuyuki Murase
Kao Corporation, Tokyo, Japan

Synonyms

Brushlike structure; Tethered polymer

Definition

Polymer brush is a layer where polymer chains are anchored by one end either through physisorption or by covalent bonding on the surface.

Introduction

Polymer brush is a layer at the solid-liquid (or liquid-liquid or air-liquid) interface, where polymer chains are anchored by one end to the solid (or liquid) surface [1]. Typical examples of polymer brushes are schematically drawn in Fig. 1. The significance of polymer brushes is
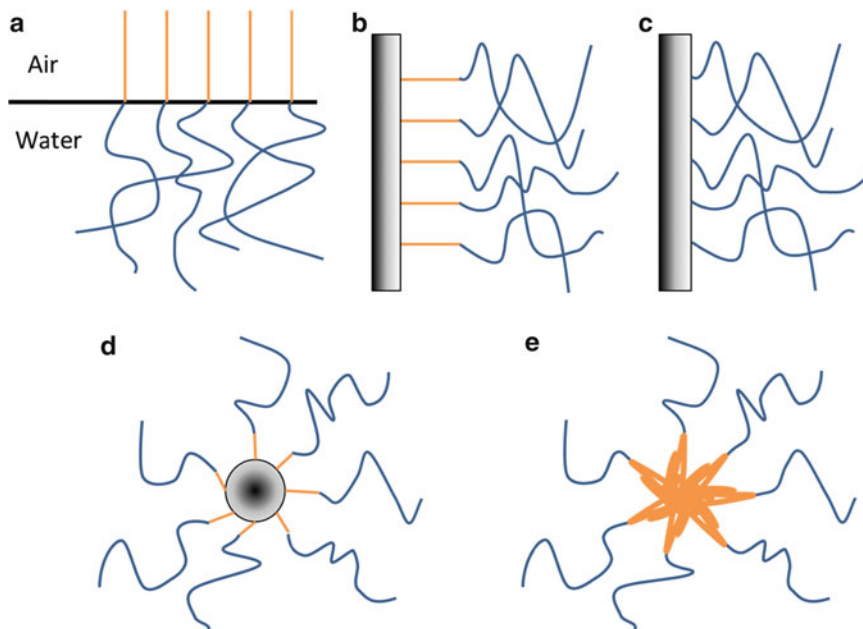
Polymer Brushes, Fig. 1 Polymer brushes in different forms: (**a**) monolayers at the air-water interfaces, (**b**) brush immobilized on a solid plate by the adsorption method, (**c**) brush immobilized on a solid plate by covalent bonding, (**d**) colloid particle covered by brush, (**e**) micelles

not limited to their fundamental aspects but extends to many technological applications.

Properties of the polymer brush are determined by both the layer thickness and the brush density. The structure of the polymer brushes is analyzed in terms of the constitution and conformation of polymer chains. When the polymer brushes interact with the surface of the other, when it interacts with each other, polymer brushes have demonstrated properties. For example, polymer brush controls the dispersibility of the fine particles, adsorption/separation and transport properties of the specific material, and tribological properties (such as friction and wear characteristics and lubricant).

Polymer brushes have been modeled by self-consistent method, scaling law, and computer simulation (such as molecular dynamics and Monte Carlo method). Polymer molecules within a brush in the good solvent are stretched away from the attachment surface as a result of the fact that they repel each other by excluded volume effect (steric repulsion) and osmotic pressure. Because the influence of the electrostatic effect is large in the osmotic pressure, it is necessary to consider separately polyelectrolyte brushes with electrostatic charge [2].

By applying a polymer brush on the material surface, it is possible to significantly change the properties of the material surface. For example, water repellency and wettability of the surface change just grow a polymer brush on the metal substrate or glass surface. The brushes are often characterized by the high density of grafted chains. The limited space then leads to a strong extension of the chains and unusual properties of the system. The significance of polymer brushes is not limited in fundamental aspects but extends to many technological applications. The increase of polymer brushes study is largely owing to the recent development in surface modification and characterization. Advanced technologies such as nanotechnology and microchemistry require well-defined surfaces with unique functions, and there is high expectation for polymer brushes because successful technological applications of polyelectrolytes were achieved and well known as smart gels. Cooperation of multidisciplinary

fields, preparation, and characterization are necessary for the further progress of studies and applications of polymer brushes [3–5].

Preparation

Sample preparation is important for pursuing the study on polymer brushes [2]. However, there are some difficulties in the preparation: (1) usually well-controlled solid state synthesis is difficult, and often it is obtained in nonuniform surfaces, and (2) the electrostatic repulsions, due to the charges of polyelectrolyte chains, are so strong especially in pure water that they do not allow the chains to build a dense brush. These difficulties are (at least) a part of the reasons for the situation that experiments on these charged brushes have been very scarce. In order to discuss the structure and interaction of the polymer brushes, thickness and density distribution controlled brush was used. So far three major approaches have been presented.

The first is the Langmuir-Blodgett method. This method uses amphiphiles as the hydrophilic group and prepares the brush at the air-water interface, which can be deposited onto a solid substrate. Certain organic molecules, which are usually amphiphiles bearing both of the hydrophilic (water-loving) and the hydrophobic (water-hating) group, will orient themselves at the air-water interface to minimize their free energy. The resulting surface film is one molecule in thickness and is called Langmuir film (or monolayer, monomolecular layer). They are transferable onto a solid surface, and the transferred film is called as Langmuir-Blodgett (LB) film. When they are spread on the aqueous phase, they form polymer brushes at the air-water interface, which can be transferred on hydrophobic substrates (Fig. 1a) [6].

The second is the adsorption method that again uses an amphiphilic type of compounds. The hydrophobic part can adsorb on a hydrophobic surface and anchor the hydrophilic group. Amphiphiles containing polyelectrolyte chains as the hydrophilic group associate in micelles when dissolved in water (Fig. 1e). Resulting micelles are coated by polyelectrolyte chains, which are regarded as polymer brushes at the liquid-liquid interface. From amphiphile solutions (or dispersions), the amphiphiles adsorb onto hydrophobic plates or colloidal particles to form the polymer brush (Fig. 1b, d). The advantage of the preparing brush layers by the adsorption method is its simple and easy operation. However, the brushes are less ordered, and it is difficult to prepare the brush in a well-controlled and well-defined structure. In the case of hydrophobic colloidal particles, moreover, they can flocculate even at modest salt concentrations, so the correct procedure for obtaining dispersed colloids must be sought by changing system parameters such as surface hydrophobicity, particle size, block composition, and solvent quality.

The third method uses covalent bonding and is divided into two categories: one is the case where the initiators are bound onto the solid surfaces and successive polymerization occurs in situ consuming monomer precursor dissolved in the solvent and another is the case where polymers are bound to the solid surfaces through the linker group that is on the one terminal of the polymer chain (Fig. 1c). In the third method, often polymers covalently bound to the solid surfaces are neutral and ionized afterwards. Preparation of stable, well-defined polymer brushes requires the covalent bonding for anchoring one end (end-grafting) of the polymers on a flat surface. The recent progress in the solid surface modification and functionalization has facilitated this approach [7, 8].

This approach is roughly divided into two types: (1) covalent attachment of preformed polymers to the solid surface via a terminal coupling group and (2) in situ polymerization of precursor monomers on solid surfaces (surface-initiated polymerization). Usually, polymers are synthesized or attached in the neutral form, and subsequently the ionization reaction takes place using ionization procedures such as the dissociation of the ionizable group (e.g., –COOH), the protonation, and the chemical modification (e.g., sulfonation reaction). A tethered polymer chain tries to maintain its random coil conformation in the solution; the chain density of resulting brush layers is somewhat low.

P

Polymer Brushes, Table 1 Preparation methods of polymer brushes

Preparation method	Characteristic
Monolayer and LB films	Well-defined brushes are prepared
	High chain densities are obtained
	It is less suitable for high-molecular weight polymer
Adsorbed brushes, micelles, and bilayers	Easy for preparation
	The brushes are not well defined
	Requires preparation of high salt concentrations or low curvature surfaces
Covalently end-grafted brushes	Stable, well-defined brushes are prepared
	Applicable for many kinds

In order to prepare denser brushes, we need to employ "in situ polymerization" (or "surface-initiated polymerization"). In case of "in situ polymerization," a key to the approach is to create suitable initiation sites on the surfaces of solid substrates. Recent progress in self-assembled monolayers (SAM) made it possible to prepare well-organized, surface-bound initiator layers [7, 8]. In situ polymerization method is rapidly progressing owing to the development of self-assembled monolayers particularly in the availability of anchoring groups (e.g., thiol for gold [7, 8]) and the initiators [9]. This will enable us to synthesize polymer brushes in wider variations of chemical structures on various substrates with controlled density and thickness [10].

Summaries are found in Table 1.

Characterization

Various characterization techniques are applicable for the study of the polymer brushes. An important structure of polymer brushes that should be well understood is the surface structure. This structure can be measured directly by scanning probe microscopy (SPM), scanning tunnel microscopy (STM), atomic force microscope (AFM), scanning electron microscope (SEM), and transmission electron microscope (TEM). Fourier transform infrared (FTIR) spectroscopy is most often employed for surface chemical information. The surface pressure-molecular area isotherm is a useful tool for studying the nanostructures at the air-water interface. Neutron and X-ray reflectivity measurement and ellipsometry are applicable to flat surfaces, whereas neutron scattering and dynamic light scattering are applicable to colloidal systems coated with polymer brushes. SFA and AFM measurements are a more direct method to determining surface thickness of polymer brushes, although attention should be paid to distinction between the double layer interaction due to the surface charges of the opposing polymer brushes and the steric component. Small amount of impurities can disturb the measurement; thus, the samples should be prepared with extensive cares without dust or impurity. For the reflectivity measurement, the data fitting based on a model is necessary, though sample preparations for them may be relatively easier than the SFA and AFM measurement. Moreover, combined two kinds of measurement methods are measured at the same time, and detailed researches are advanced.

For the details of characterization, it can be seen in Table 2.

SFA measurement has been proven useful in obtaining information about the concrete structures of polymer brushes. The measurement was employed to study interactions between monolayers of an anionic polyelectrolyte, poly (methacrylic acid), on mica [6]. The polymer brushes were prepared by depositing monolayers of the poly(methacrylic acid) amphiphile by the LB technique. The observed force was repulsive and was altered by ionization and structural changes of the polymer brushes at different pH values and NaBr concentrations. The majority of negative charges were insulated by counterions, resulting in saturation of repulsion at shorter distances. The thickness of the polyelectrolyte layer was determined from the force measurement.

Polymer Brushes, Table 2 Properties and methods of characterization

Properties or characterization	Method
Surface structure	Scanning probe microscopy (SPM)
	Scanning tunnel microscopy (STM)
	Atomic force microscope (AFM)
	Scanning electron microscope (SEM)
	Transmission electron microscope (TEM)
Surface chemical information	FTIR, contact angle measurement
Surface thickness	Surface force apparatus (SFA)
	Neutron scattering, neutron reflectivity
	X-ray reflectivity, dynamic light scattering (DLS), ellipsometry
Surface density	Neutron scattering, neutron reflectivity
	X-ray reflectivity, DLS, isotherm
Adsorption amount	Quartz-crystal microbalance (QCM)
Surface charge interaction	SFA, AFM, isotherm

When the carboxylic acid group was ionized by more than 10 %, the polyelectrolyte chain was extended to a length about six times greater than that of its hypercoiled [6].

Applications

Application of polymer brushes appeared only recently when various methods for covalently anchoring of the brush have become available. The first is to consider the brush as the single monolayer gel similar to hydrogels with expectations that the brush will exhibit a unique property of hydrogels. The small size of the brush structure should enhance changes associated with gel properties such as swelling and shrinkage, which are often slow processes in the large scale [11]. Poly (acrylic acid) (PAA) was grafted onto a porous glass filter in order to construct a pH-dependent system for the regulation of liquid permeation. The permeation rate was found, indeed, high at

low pH conditions, while it was low under high pH conditions. A possible explanation for this permeation profile is that at low pHs, protonated PAA chains shrink, thereby opening the pores of the filter, and that at high pHs, dissociated PAA chains are extended to cover the pores. The gating was regulated by the conformational change of poly (glutamic acid) that undergoes a helix-coil transition in response to pH.

The second is to employ them for the surface treatment and modification, which is important for nanotechnology. The wetting properties of surfaces are manipulated by patterning of covalently bound polyelectrolytes [12]. Combination of photolithographic techniques with surface-initiated polymerization provided continuous films in which there are discrete areas of hydrophilic and hydrophobic polymer brushes. Polyelectrolyte, poly(acrylic acid), domains exhibited the high wettability (small contact angle) to water, which can be controllable by external agents (e.g., by shifting pH). These systems may be useful in technological applications including photoresists, sensors, and microfluidic networks.

The preparation method of polymer brushes is developed; there are some researches of structure of particles with polymer brushes. Making a monolayer and taking the structure which is separated with a fixed distance is reported [13–15]. The particles with high-density brushes formed order structure at the air-water interface. The distance between contiguity particles became very large, and increasing with the molecular weight, because the graft chains were almost fully extended [13, 14]. Since this structure can be built on a substrate, making a pattern on a substrate in multiple research fields is expected [3–5, 16].

Related Entries

- ▶ Langmuir-Blodgett (LB) Film
- ▶ Proteins as Polymers and Polyelectrolytes
- ▶ Self-Assembled Monolayer
- ▶ Surfactant Assemblies (Micelles, Vesicles, Emulsions, Films, etc.), an Overview

P

References

1. Advincula RC, Brittain WJ, Caster KC, Rühe J (2004) Polymer brushes. Wiley-VCH, Weinheim
2. Kurihara K, Murase Y (2002) Polyelectrolyte brushes. In: Tripathy SK, Kumar J, Nalwa HS (eds) Handbook of polyelectrolytes and their applications. American Scientific, Los Angeles
3. Minko S (2006) Responsive polymer brushes. J Macromol Sci C Polym Rev 46:397–420
4. Azzaroni O (2012) Polymer brushes here, there, and everywhere: recent advances in their practical applications and emerging opportunities in multiple research fields. J Polym Sci A Polym Chem 50:3225–3258
5. Jiang H, Xu FJ (2013) Biomolecule-functionalized polymer brushes. Chem Soc Rev 42:3394–3426
6. Kurihara K, Kunitake T, Higashi N, Niwa M (1992) Surface forces between monolayers of anchored poly(methacrylic acid). Langmuir 8:2087–2089
7. Patel SS, Tirrell M (1989) Measurement of forces between surfaces in polymer fluids. Annu Rev Phys Chem 40:597–635
8. Jordan R, Ulman A, Kang JF, Rafailovich MH, Sokolov J (1999) Surface-initiated anionic polymerization of styrene by means of self-assembled monolayers. J Am Chem Soc 121:1016–1022
9. Edmondson S, Osborne VL, Huck WTS (2004) Polymer brushes via surface-initiated polymerizations. Chem Soc Rev 33:14–22
10. Matyjaszewski K, Davies TP (2002) Handbook of radical polymerization. Wiley-Interscience, New York
11. Ito Y, Park YS, Imanishi Y (1997) Visualization of critical pH-controlled gating of a porous membrane grafted with polyelectrolyte brushes. J Am Chem Soc 119:2739–2740
12. Husemann M, Morrison M, Benoit D, Frommer J, Mate CM, Hinsberg WD, Hedrick JL, Hawker CJ (2000) Manipulation of surface properties by patterning of covalently bound polymer brushes. J Am Chem Soc 122:1844–1845
13. Ohno K, Koh K, Tsujii Y, Fukuda T (2003) Fabrication of ordered arrays of gold nanoparticles coated with high-density polymer brushes. Angew Chem Int Ed 42:2751–2754
14. Goto A, Fukuda T (2004) Kinetics of living radical polymerization. Prog Polym Sci 29:329–385
15. Talingting MR, Ma Y, Simmons C, Webber SE (2000) Adsorption of cationic polymer micelles on polyelectrolyte-modified surfaces. Langmuir 16:862–865
16. Moro T, Takatori Y, Ishihara K, Konno T, Takigawa Y, Matsushita T, Chung U, Nakamura K, Kawaguchi H (2004) Surface grafting of artificial joints with a biocompatible polymer for preventing periprosthetic osteolysis. Nat Mater 3:829–836

Polymer Catalysts

Shinichi Itsuno
Department of Environmental and Life Sciences, Toyohashi University of Technology, Toyohashi, Japan

Synonyms

Polymer-immobilized catalysts; Polymer-supported catalysts

Definition

Polymer catalysts are polymers possessing catalytically active moieties. The catalytic moiety is usually attached to the side chain of synthetic polymers such as polystyrene. Polymer catalysts are used as catalysts for various kinds of organic synthesis. Cross-linked polymers are often employed as polymer support material due to their insolubility. Insoluble polymer catalysts can be easily separated from the reaction mixture and reused. Some of the catalysts are incorporated into the main chain of the polymer.

General Aspect of Polymer Catalysts

Chemical reactions in green chemical processes usually require the use of catalyst in order to accelerate them under mild reaction conditions. The catalysts must be separated from the reaction mixture when the reaction is completed. Hopefully they are recovered, regenerated, and reused. Most of the catalysts, however, cannot be easily recycled. When a molecule possessing catalytic activity is immobilized to a cross-linked polymer, the polymer catalyst can be easily separated from the reaction mixture by simple filtration. Linear polymer supports are also separable through precipitation processes. Since polymers are not volatile, the use of polymer catalysts can reduce the toxicity and the odor.

There are many applications of polymer catalysts in organic synthesis [1]. For example, many organometallic complexes have been used as catalysts for various reactions to show high selectivity and specificity. Since these complex catalysts are usually difficult to be recovered, the polymer immobilization technique is one of the important alternatives. In order to use these catalysts in organic solvents, organic polymers such as polystyrene are utilized as polymer supports for the catalysts. On the other hand, the use of water as a reaction medium is also important in greener organic synthesis in order to reduce the use of toxic organic solvents. Hydrophilic or amphiphilic polymers are utilized as support polymers in aqueous media. Moreover, in case that the polymer catalysts show sufficient turnover number and turnover frequency, such high performance polymer catalysts are applicable to the continuous flow system [2]. A reactant solution is introduced into the column packed with an insoluble polymer catalyst. The desired product is obtained continuously by using this system.

Not only the improvement of chemical processes by means of polymer catalysts, microenvironment within the polymer network sometimes influences the catalytic activity. In some cases, polymer catalysts show higher catalytic activities compared with the corresponding nonsupported catalysts in homogeneous solution. Since the polymer catalysts have such attractive features, it is useful to adopt them in many advanced organic synthesis.

Polymer Catalysts in Organic Synthesis

Typical examples of polymer catalysts used in organic synthesis involve poly(4-vinylpyridine) **1** in its basic form and sulfonated polystyrene **2** in its acid form, which act as catalysts in some base- and acid-catalyzed reactions, respectively. Transition metal catalysts have been also immobilized into cross-linked polymer. A typical polymer transition metal catalyst is polymer-supported triphenylphosphine-PdCl$_2$ **3**. Several types of palladium catalysts on polymer supports are now commercially available and used as
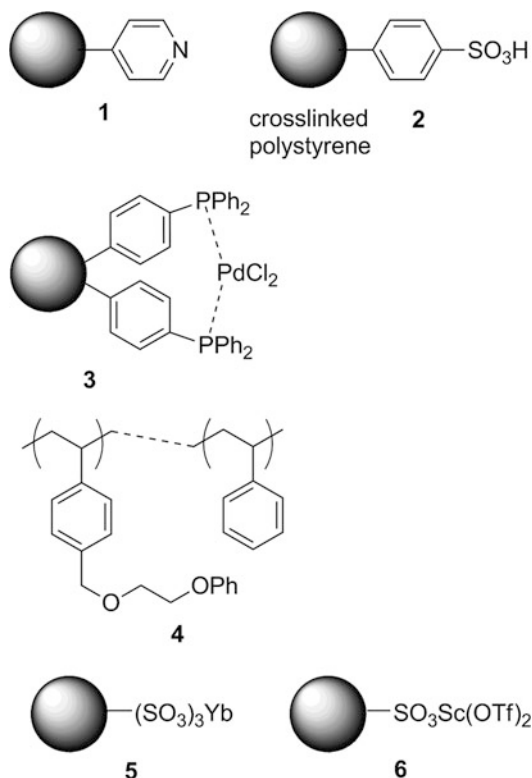
Polymer Catalysts, Fig. 1 Typical examples of polymer catalyst in organic synthesis

catalysts in various organic reactions including Suzuki-Miyaura, Mizoroki-Heck, Negishi, Stille, and Sonogashira coupling reactions. Another example is a microencapsulation of highly toxic Os species into polymer. Phenoxyethoxymethyl polystyrene **4** is used for the preparation of microencapsulated OsO$_4$, which is useful as a safer catalyst of dihydroxylation of olefins. Figure 1 shows typical examples of polymer catalyst used in organic synthesis.

Lewis acids work as important catalysts in various chemical transformations in organic synthesis. For example, both ytterbium (III) polystyrene sulfonate **5** and polymer-supported scandium (III) bis(trifluoromethanesulfonate) **6** are useful for various organic reactions such as acetal formation, aldol reaction, alkylation, aza-Diels-Alder reaction, and ring opening of epoxides. These polymer Lewis acid catalysts are commercially available. Many other Lewis acid catalysts immobilized to polystyrene resin

have also been developed [3]. They are easily separated from the reaction mixture after the reaction is completed. The polymer catalysts recovered from the reaction mixture are usually reused for the next reaction.

Polymer Catalysts in Asymmetric Synthesis

One of the most attractive applications of polymer catalysts in organic reactions is the asymmetric catalysis. Expensive chiral catalysts should be recovered and reused in the chemical process. Microenvironment constructed in chiral polymer catalyst may influence the stereoselectivity of reaction. Typical examples of polymer catalysts including chiral transition metals and chiral organocatalysts are summarized in this entry. A number of chiral polymer catalysts are prepared by pendant-type immobilization of chiral catalyst into the polymer side chain. For example, aromatic rings of polystyrene can be easily modified to attach chiral catalyst on its side chain. Alternatively, main-chain chiral polymers have been recently developed as chiral polymer catalysts for asymmetric synthesis. A chiral catalyst containing two functionalities has been incorporated into the polymer main chain during polymerization.

Polymer Catalysts Containing Chiral Transition Metal Complexes

Various polymer-immobilized chiral catalysts for enantioselective reactions have been developed [1]. Transition metal-chiral ligand complexes are one of the promising choices of the catalysts for their immobilization into polymer [2]. Among a variety of chiral transition metal catalysts, the following examples show some advantages of polymer catalysts.

Among the asymmetric hydrogenation catalysts developed for ketone reduction, complexes derived from chiral 1,2-diamines and $RuCl_2$/diphosphines provide one example of the most efficient catalysts. Various polymer catalysts containing the chiral Ru complex have been prepared and used for the asymmetric hydrogenation. Polystyrene (PSt)-immobilized chiral 1,2-diamine **7** and PEG-immobilized ones **8** are effectively used as chiral polymeric ligand of Ru catalyst [1].

Figure 2 demonstrates the polymer catalysts and their use in enantioselective hydrogenation of acetophenone **9**. Chiral Ru complex prepared from **7**, XylBINAP ((S)-(-)-2,2'-bis[di(3,5-xylyl) phosphino]-1,1'-binaphthyl), and $RuCl_2$ shows excellent catalytic activity in the asymmetric hydrogenation of aromatic ketones. These polymer catalysts can be recycled many times without any loss of their catalytic activity. Another interesting
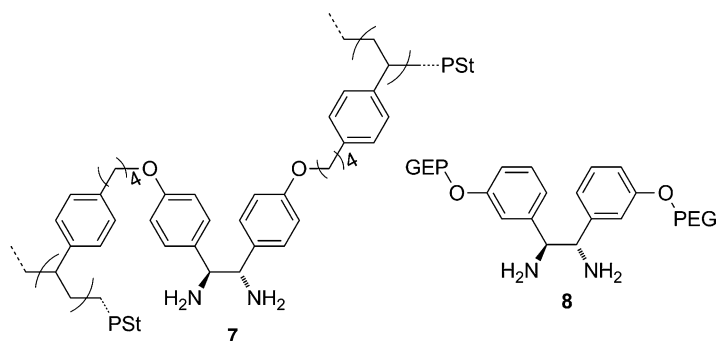
Polymer Catalysts, Fig. 2 Asymmetric hydrogenation of acetophenone with polymer-immobilized chiral diamine-Ru complex
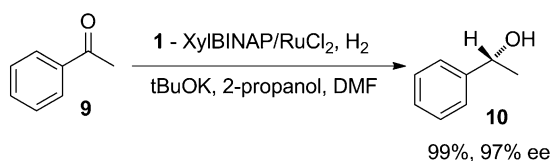
Polymer Catalysts,
Fig. 3 Asymmetric
hydrogenation of α-amide
ketone under DKR
condition
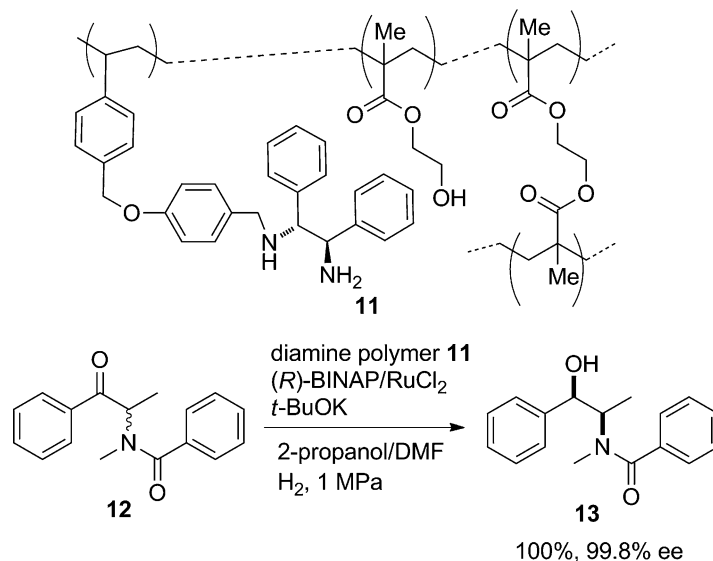
application of polymeric catalyst containing chiral 1,2-diamine ligand is the asymmetric hydrogenation under dynamic kinetic resolution (DKR) condition. By using the polymer catalyst prepared from polymer **11**, (*R*)-BINAP, and RuCl$_2$, asymmetric hydrogenation of α-(*N*-benzoyl-*N*-methylamino)propiophenone **12** through DKR is performed to yield *syn*-β-amide alcohol **7** exclusively with nearly perfect enantioselectivity (Fig. 3) [4]. The polymer catalyst shows higher stereoselectivity compared with the corresponding low-molecular-weight catalyst in homogeneous solution system. This example reveals that microenvironment created in the polymer network strongly influence the stereoselective performance of the catalyst. In polymer **11**, hydroxyethyl methacrylate unit and methacrylate cross-linkage provide a suitable microenvironment for the catalyst moiety.

A noticeable method of asymmetric reduction without hydrogen gas is asymmetric transfer hydrogenation, which is a promising catalytic method for the synthesis of chiral alcohols and amines. One of the powerful asymmetric catalysts for the enantioselective reduction of carbonyl and imine compounds under the transfer hydrogenation reaction condition is TsDPEN-transition metal complexes (TsDPEN = *p*-toluenesulfonyl-1,2-diphenylethylenediamine) developed by Noyori and Ikariya [5]. Lemaire et al. reported

the first example of immobilization of monosulfonylated 1,2-diphenylethylenediamine into cross-linked polystyrene [6]. In the enantioselective reduction of acetophenone, Lemaire's cross-linked polymer catalyst shows lower catalytic activity with 84 % ee. The corresponding original low-molecular-weight catalyst in solution system gives 94 % ee. Much improvement is realized when quaternary ammonium sulfonate structure is introduced into cross-linked polystyrene. The polymeric chiral ligand **17** is readily prepared by terpolymerization of **14**, **15**, and **16** (Fig. 4).

The polymer catalyst containing quaternary ammonium sulfonate gives the quantitative conversion with 98 % ee in the reduction of acetophenone [7]. This example shows that structural modification of support polymers is important and sometimes gives higher catalytic activity and stereoselectivity with the polymer catalyst. Another interesting approach to the polymeric catalyst is to use the microsphere as support polymer. Since the microspheres possess relatively large surface area, high catalyst loading is possible. Polymer microspheres functionalized with chiral TsDPEN ligand are prepared by precipitation polymerization [8]. Monodisperse, cross-linked poly(divinylbenzene) and poly(methacrylic acid-*co*-ethylene glycol dimethacrylate) microspheres

Polymer Catalysts,
Fig. 4 Asymmetric
transfer hydrogenation of
acetophenone in water
using polymer-
immobilized catalyst

Polymer Catalysts Containing Chiral Organocatalyst

Chiral organocatalyst is another important catalyst in asymmetric synthesis [13, 14]. In comparison with transition metal catalysts, organocatalysts are usually less active and so a relatively large amount of catalyst is required. In most cases, more than 10 mol % of the organocatalyst is needed to complete the reaction. Some of them are amphiphilic organic molecules such as quaternary ammonium salts, phosphonium salts, and oligo ethylene glycols. It is necessary to use amphiphilic organocatalyst, especially when the organic reactions proceed in aqueous phase. Since water

with (*R*,*R*)-TsDPEN moiety are successfully prepared by precipitation polymerization. The site of introduction of the (*R*,*R*)-TsDPEN moiety into polymer microspheres is controllable by changing the order of addition of the corresponding monomers. Not only polystyrene but also other polymer supports such as PEG [9], PE [10], and silica [11] are used [12].

is the ultimate green solvent, the use of water as a solvent or a reaction medium should always be considered [15]. A drawback in the use of these organocatalysts in aqueous system is the separation of the amphiphilic catalyst from the reaction mixture. The use of polymer organocatalysts is capable of avoiding this difficulty during the workup processes. Various polymer organocatalysts have been developed.

One of the typical applications of chiral quaternary ammonium salts as organocatalysts is asymmetric alkylation of glycine derivative **18** to give optically active amino acid **19** (Fig. 5). Chiral quaternary ammonium salts **20** having C_2 symmetry developed by Maruoka shows high level of catalytic activity with almost perfect enantioselectivity [16]. Another important chiral organocatalyst is derived from cinchona alkaloid **21** [17, 18]. These chiral organocatalysts not only are highly active and stereoselective in the asymmetric alkylation reactions but also are useful catalysts for other several types of asymmetric transformations [19]. Therefore, the polymer catalysts containing such catalyst structures have attracted much attention in asymmetric reaction.

Polymer Catalysts, Fig. 5 Asymmetric benzylation of glycine derivative **18** with polymer-immobilized chiral quaternary ammonium catalyst
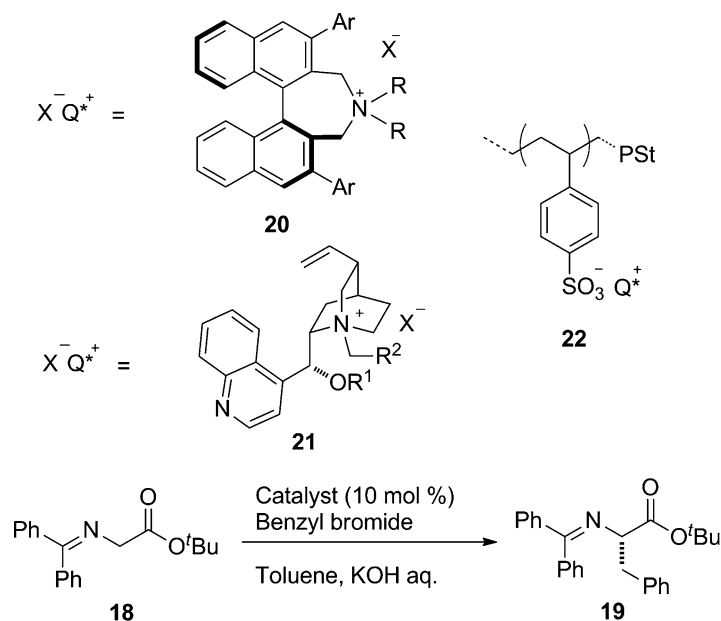
Many applications of cinchona alkaloid-based organocatalysts have been attached onto polymer to use as catalysts in asymmetric transformations. However, most of them end up with lowered enantioselectivity and reactivity mainly due to the immobilization into insoluble cross-linked polymers.

One successful example of the immobilization of chiral quaternary ammonium salts into cross-linked polymer is the use of ionic bond [20]. Chiral quaternary ammonium sulfonate **22** is a typical example of the ionic bonded immobilization. By using the ionic bonded immobilization of chiral quaternary ammonium salt, no extra chemical modification is required to attach the catalyst into polymer support. The polymer chiral organocatalyst can be easily separated from the reaction mixture and reused many times. The enantioselective reaction readily takes place in the presence of the polymer catalyst with higher enantioselectivity compared with the corresponding unsupported catalyst.

Since the ionic bond of quaternary ammonium sulfonate is sufficiently stable to be used as catalyst even in aqueous solution, a novel polymer chiral organocatalyst has been developed. Ion exchange reaction between disulfonate **23** and

bis(quaternary ammonium salt) **24** gives polymer **25** containing the ionic bonds in its main chain (Fig. 6). This is the first example of the ionic polymer synthesis. The hydrophilicity-hydrophobicity balance of the ionic polymers can be precisely controlled with the combination of the monomers. The use of the ionic polymer of well-controlled balance is sometimes critical to be a highly active catalyst. The chiral ionic polymers **25** have been efficiently used as chiral organocatalysts in asymmetric reactions. Chiral main-chain polymer organocatalyst **26** prepared from cinchona alkaloid shows excellent performance in the asymmetric alkylation reaction as shown in Fig. 6. Since the chiral ionic polymers are insoluble in both water and organic solvents, they can be easily recovered and reused.

A similar polymerization proceeds between disulfonic acid and chiral bis(imidazolidinone) [2]. Sulfonic acid reacts with secondary amine to form the stable salt. The obtained chiral polymers contain ionic bond on each repeating unit. The ionically bonded chiral polymer **27** is applicable to asymmetric Diels-Alder reaction of **28** and **29** to give the corresponding cyclic adduct **30** in high yield with high level of enantioselectivity (Fig. 7).

Polymer Catalysts, Fig. 6 Asymmetric benzylation of glycine derivative **18** with chiral ionic polymer catalyst
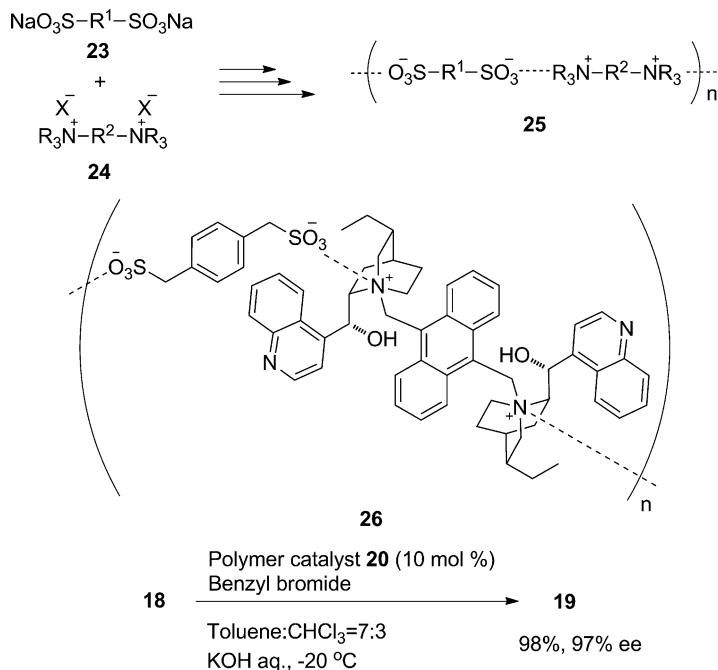
Polymer Catalysts, Fig. 7 Asymmetric Diels-Alder reaction with chiral ionic polymer **27**
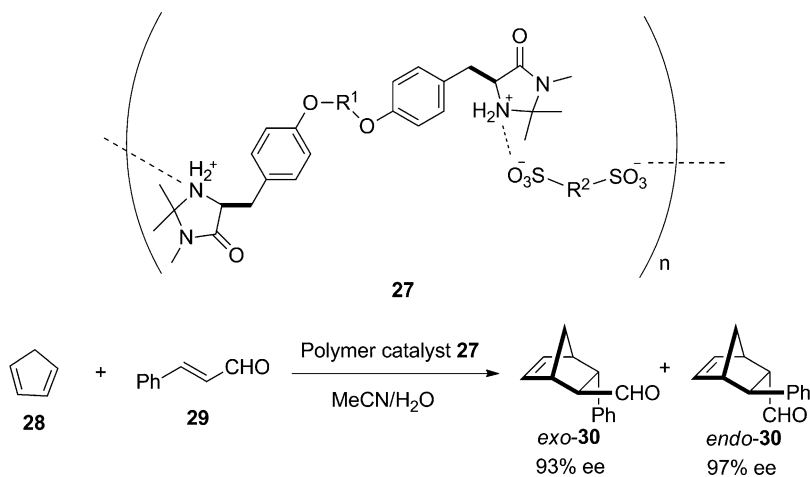
Summary

Various polymer catalysts have been developed and used in organic synthesis. Mainly due to the facility of their recovery and recycle uses, insoluble polymer-immobilized catalysts have been utilized. Recent significant progress in the chiral polymer catalysts provides novel strategies in the asymmetric synthesis. The chiral polymer catalysts have not only the advantage of recycle use but a great potential of higher performance in the stereoselective reactions. Main-chain chiral polymers give promising future applications in enzyme-like reactions.

Related Entries

▶ Polymer Reagents
▶ Supramolecular Catalysis

References

1. Ding K, Uozumi Y (eds) (2008) Handbook of asymmetric heterogeneous catalysis. Wiley-VCH, Weinheim
2. Itsuno S (ed) (2011) Polymeric chiral catalyst design and chiral polymer synthesis. Wiley, Hoboken
3. Itsuno S (2008) Polymer-supported metal lewis acids, Chapter 19. In: Yamamoto H, Ishihara K (eds) Acid catalysis in modern organic synthesis, vol 2. Wiley-VCH, Weinheim
4. Chiwara VI, Haraguchi N, Itsuno S (2009) Polymer-Immobilized Catalyst for Asymmetric Hydrogenation of Racemic α-(N-Benzoyl-N-methylamino) propiophenone. J Org Chem 74:1391–1393
5. Hashiguchi S, Fujita A, Takehara J, Ikariya T, Noyori R (1995) J Am Chem Soc 117:7562–7563
6. ter Halle R, Schultz E, Lemaire M (1997) Synlett 1257–1258
7. Arakawa Y, Haraguchi N, Itsuno S (2006) Tetrahedron Lett 47:3239–3243
8. Haraguchi N, Nishiyama A, Itsuno S (2010) J Polym Sci Part A Polym Chem 48:3340–3349
9. Li X, Chen W, Hems W, King F, Xiao J (2004) Tetrahedron Lett 45:951–953
10. Dimroth J, Schedler U, Keilitz J, Haag R, Schomacker R (2011) Adv Synth Catal 353:1335–1344
11. Xiao W, Jin R, Cheng T, Xia D, Yao H, Gao F, Deng B, Liu G (2012) A bifunctionalized organic-inorganic hybrid silica: synergistic effect enhances enantioselectivity. Chem Commun 48:11898–11900
12. El-Shehawy AA, Itsuno S (2005) Preparation of Immobilized Chiral Ligands onto Polymer Supports and Their Application to Asymmetric Synthesis. In: Bregg RK (ed) Current topics in polymer research, Chapter 1. Nova Science, New York, pp 1–69
13. Dalko PI (ed) (2007) Enantioselective organocatalysis. Wiley-VCH, Weinheim
14. Ooi T, Maruoka K (2007) Recent Advances in Asymmetric Phase-Transfer Catalysis Angew Chem Int E 46:4222–4266. Hashimoto T, Maruoka K (2007) Recent Development and Application of Chiral Phase-Transfer Catalysts Chem Rev 107:5656–5682
15. Kobayashi S (ed) (2012) Water in organic synthesis, science of synthesis. Thieme, Stuttgart
16. Aleman J, Cabrera S (2013) Chem Soc Rev 42:774–793
17. Song CE (ed) (2009) Cinchona alkaloids in synthesis & catalysis. Wiley-VCH, Weinheim
18. Marcelli T, Hiemstra H (2010) Cinchona Alkaloids in Asymmetric Organocatalysis, Synthesis 1229–1279
19. Maruoka K, Shirakawa S (2013) Recent Developments in Asymmetric Phase-Transfer Reactions. Angew Chem Int Ed 52:4312–4348
20. Itsuno S, Haraguchi N (2012) Supported organocatalysts, Chapter 2.3.5. In: Maruoka K (ed) Science of synthesis, asymmetric organocatalysis 2: bronsted base and acid catalysts, and additional topics. Thieme, Stuttgart

Polymer Colloids with Focus on Nonspherical Particles

Masayoshi Okubo
Graduate School of Engineering, Kobe University, Kobe, Japan

Synonyms

Anomalous particles; Anisotropic particles; Composite particles

Introduction

Polymer colloids cover very broad subjects, so this entry focuses on the nonspherical particles, which exhibit interesting and unique functionalities of application due to their shape. Such particles can be utilized to synthesize materials with unique crystal structures, light scattering properties, and external (e.g., shear field and electric field) field-responsive materials. Thus, control of particle shape is of practical importance for industrial applications. In general, polymer particles prepared by heterogeneous polymerization as typified by emulsion polymerization exhibit a spherical shape as a result of the minimization of the interfacial free energy. However, the preparation of nonspherical polymer particles has been described in many reports on the preparation of composite particles consisting of two kinds of polymers by seeded emulsion polymerization [1]. Most of them were prepared by chance and are reflected in their unique particle morphologies formed during the polymerizations, which are determined by the competition between thermodynamic and kinetic factors. For example, high viscosity inside the particles during seeded polymerization prevents the particles from attaining their thermodynamic equilibrium morphology, and consequently nonspherical particles with nonequilibrium morphology dominated by kinetic factors are obtained. Therefore, because the formation of nonspherical particles based on the kinetic control is strongly dependent of

polymerization conditions, the formation mechanisms are complex. The particle shapes (morphologies) are not only isotropic but also anisotropic.

On the other hand, several other approaches for the preparation of nonspherical particles have also been developed: microfluidic technique [2], deformation of spherical polymer particles by external force [3], the self-organized precipitation method [4], and release of a common good solvent from thermodynamically stable nonspherical polymer/solvent droplets [5].

Recent works on the preparation of micrometer-sized, unique nonspherical polymer particles mainly by seeded dispersion polymerization will be described as follows:

1. *Golf ball-like particles* [6]: Micrometer-sized, monodisperse "golf ball-like" compote polymer particles were prepared by seeded dispersion polymerization of *n*-butyl methacrylate (*n*-BMA) with PS/styrene-*co*-sodium styrene sulfonate (P(S-NaSS)) core-shell seed particles in the presence of dodecane droplets in a methanol/water (80/20, w/w) medium, followed by evaporation of the dodecane (Fig. 1). The dimples at the surface formed by the volume reduction of poly(*n*-BMA)/dodecane domains were deep when P(S-NaSS)

shell was thick, whereas when it was thin, the prepared particles had polyhedral shape.

2. *Snowman-like particles* [7]: Micrometer-sized, snowman-like particles were prepared by evaporation of toluene from PS/PMMA/toluene droplets dispersed in an aqueous solution of polyoxyethylene nonylphenyl ether (Emulgen 911) nonionic surfactant (0.33 wt%).
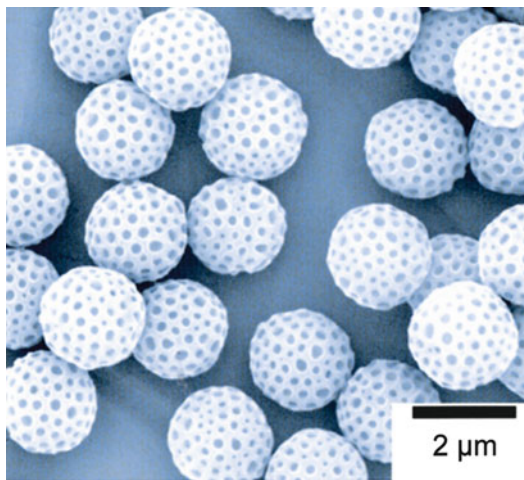
Polymer Colloids with Focus on Nonspherical Particles, Fig. 1 Golf ball-like PMMA/PS (2/1, w/w) composite particles prepared by seeded dispersion polymerization of styrene in a methanol/water (8/2, w/w) medium in the presence of decalin droplets

Polymer Colloids with Focus on Nonspherical Particles, Fig. 2 SEM photograph (**a**) of PS/PMMA (1/1, w/w) composite particles prepared by evaporation of toluene from polymers/toluene (1/12, w/w) droplets dispersed in 3.3 g/L-water Emulgen 911 aqueous solution and TEM photograph (**b**) of ultrathin cross section of RuO$_4$-stained composite particles
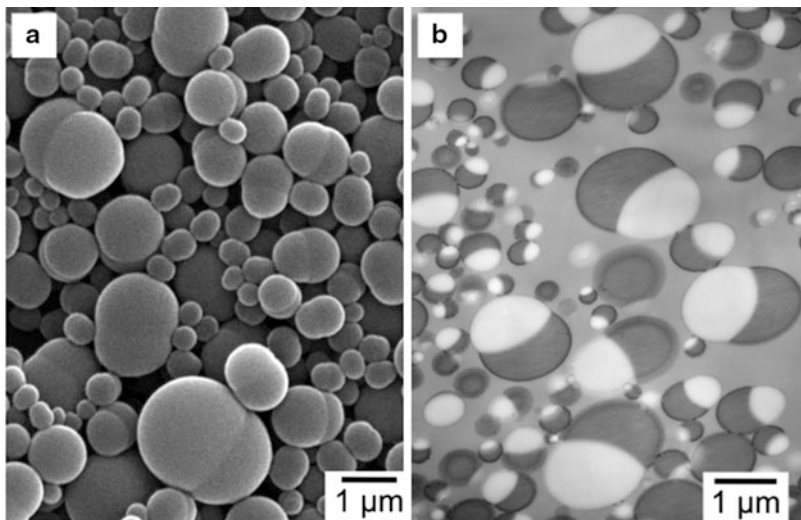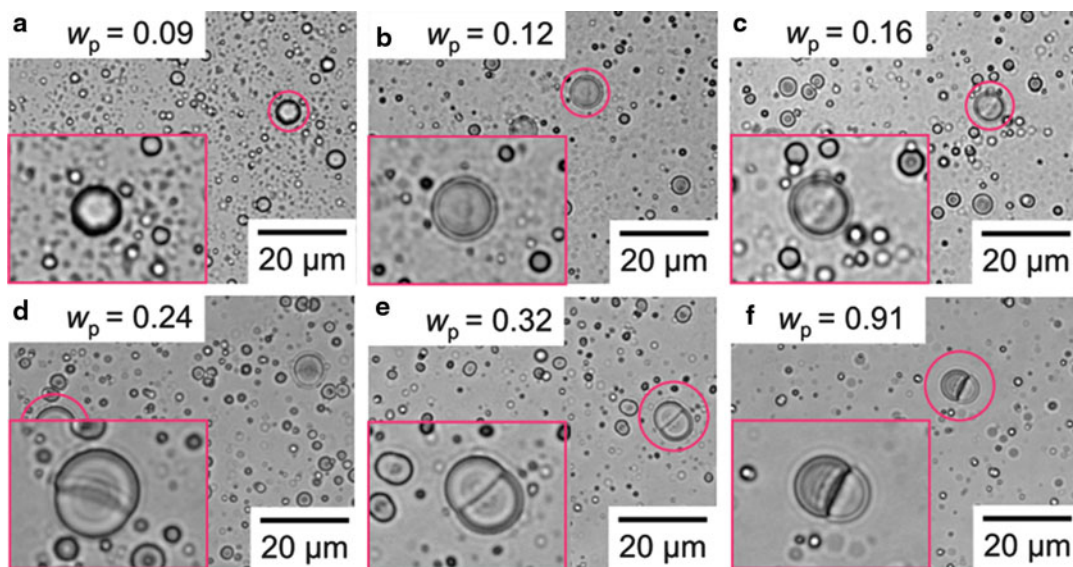
Polymer Colloids with Focus on Nonspherical Particles, Fig. 3 Optical micrographs of PS/PMMA/toluene droplets dispersed in 0.33 wt% Emulgen 911 aqueous solution in an uncovered glass vial after different storage times (h): (**a**) 0; (**b**) 4; (**c**) 6; (**d**) 8; (**e**) 9; (**f**) 13. Initial weight ratio of the droplets: 1/1/24. Numbers in the figure show the weight fraction of polymer (Wp) in the droplets

In the intermediate of toluene evaporation, where polymer concentration in droplets was still low (0.12–0.24 wt%) and polymer molecules can still move therein, the droplets changed from spherical to snowman-like at close to thermodynamic equilibrium. To our knowledge, there are no previous reports describing such unambiguous formation of solvent-swollen nonspherical composite polymer particles at thermodynamic equilibrium in the absence of cross-linking (Figs. 2 and 3).

When seeded emulsion polymerization of styrene with PS seed particles having cross-linked structures were carried out, similar submicron-sized, monodisperse snowman-like particles [8] were prepared [9], where they are called dicolloids and had anionic charges at one side of the surface and positive charges at the other side at an appropriate pH value. Similar snowman-like particles were prepared by seeded emulsion polymerization of styrene with cross-linked PS seed particles, of which surfaces had been previously
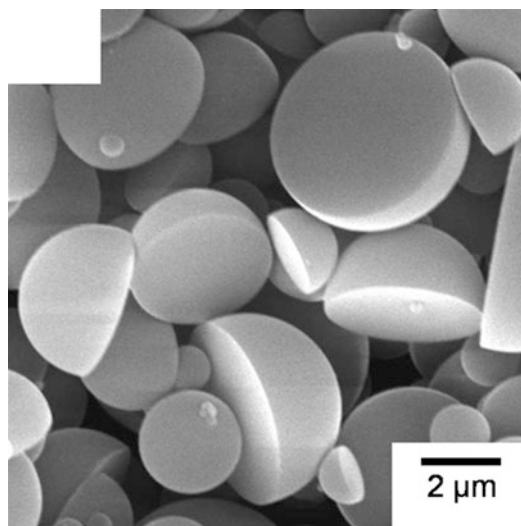
Polymer Colloids with Focus on Nonspherical Particles, Fig. 4 SEM photograph of hemispherical PS particles after rapid removal of HD with methanol from PS/HD particles having Janus structure prepared by slow evaporation of toluene from PS/HD/toluene (1/1/29, v/v/v) droplets dispersed in 0.33 wt% aqueous solution of Emulsion 931
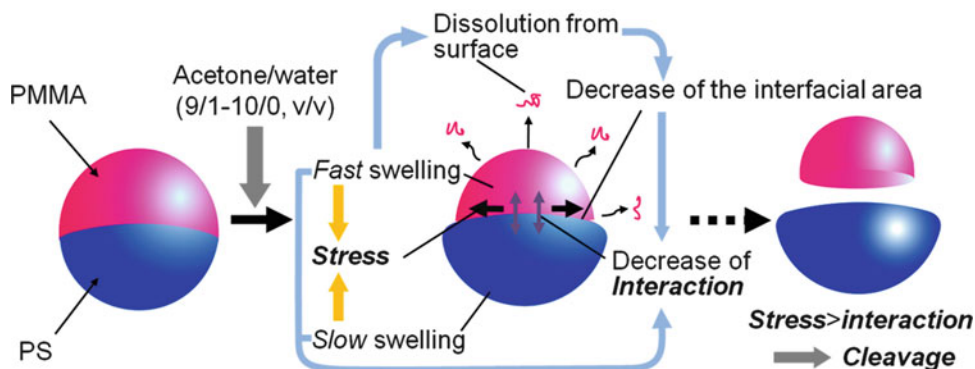
Polymer Colloids with Focus on Nonspherical Particles, Fig. 5 Schematic representation of the cleavage of Janus PMMA/PS composite particles by contacting with an acetone/water medium, resulting in two hemispherical particles
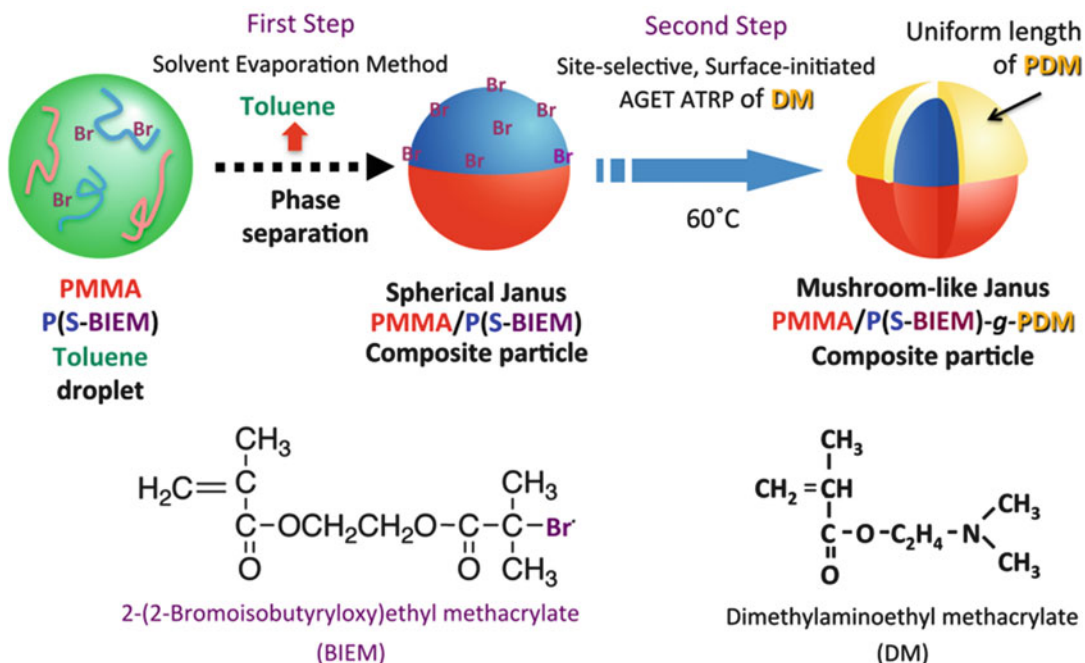
Polymer Colloids with Focus on Nonspherical Particles, Fig. 6 Schematic representation of the preparation of mushroom-like PMMA/P(S-BIEM)-*g*-PDM by site-selective surface initiated AGET ATRP

modified with a thin hydrophilic polymer layer [10].

Seeded polymerization of styrene or various methacrylic monomers with micron-sized, monodisperse, cross-linked PS seed particles gave snowman-like particles with different size balances of the head and body [11], where adsorption/absorption state of the monomer controlled the shape [12]. Kegel and coworkers reported that the absorption time greatly affected the shape [8].

3. *Hemispherical particles* [5, 13]: Micrometer-sized, monodisperse hemispherical and dimple PS particles were prepared by heating spherical PS particles at higher temperature than a glass transition temperature of the PS particles
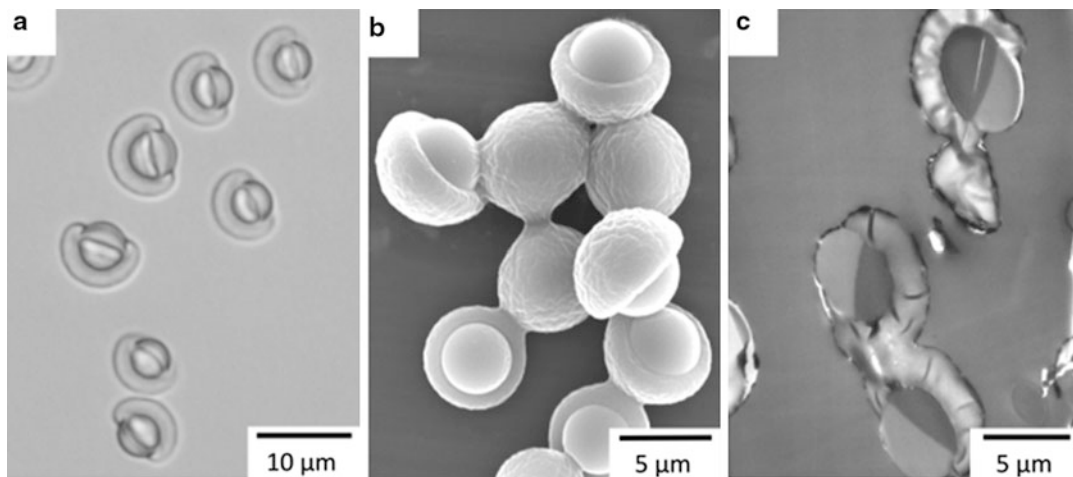
Polymer Colloids with Focus on Nonspherical Particles, Fig. 7 Optical micrograph and TEM photograph of mushroom-like PMMA/P(S-BIEM)-*g*-PDM particles and TEM photograph of ultrathin cross section of the RuO$_4$-stained particles
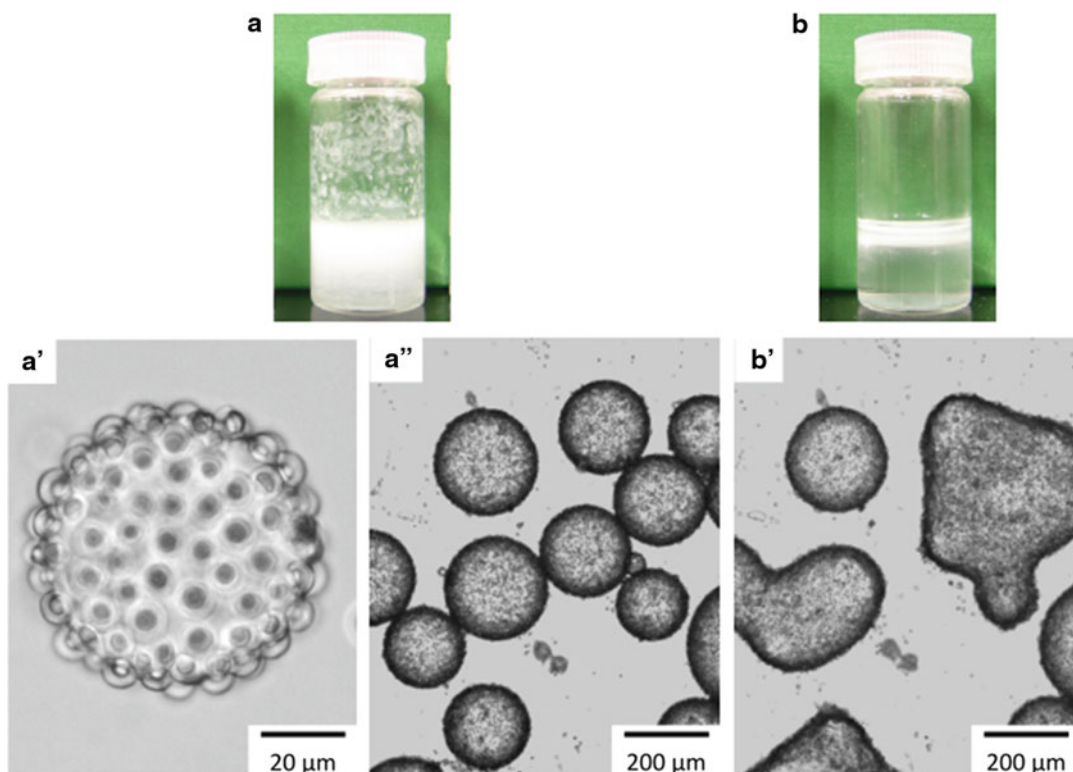
Polymer Colloids with Focus on Nonspherical Particles, Fig. 8 (**a**, **b**) Photographs of 1-octanol/water mixture after vigorous stirring in the presence of PMMA/P (S-BIEM)-*g*-PDM particles and (a′, a″, b′) optical micrographs of 1-octanol-in-water emulsion droplets stabilized by the Janus particles at pH 7.2 at (a, a′, a″) 25 °C and (b, b′) after rising to 60 °C. Both micrographs of (a″) and (b′) were on the same visual field
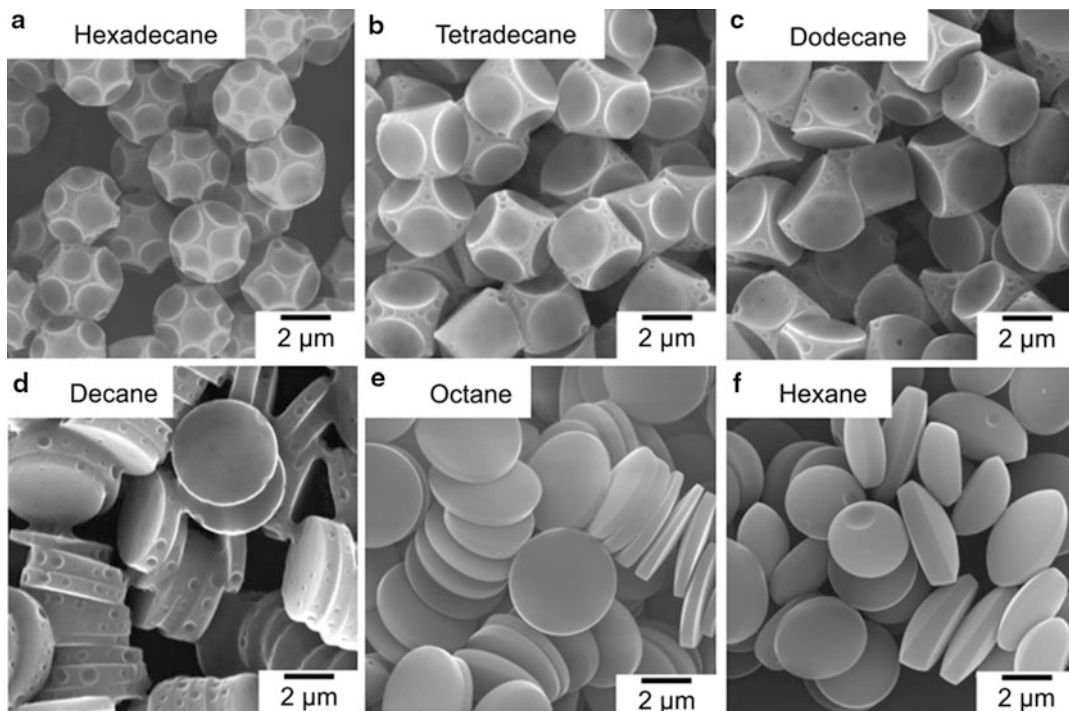
Polymer Colloids with Focus on Nonspherical Particles, Fig. 9 SEM photographs of PS particles after the extraction of PEHMA and hydrocarbon with 1-butanol from PS/PEHMA/hydrocarbon composite particles prepared by seeded dispersion polymerizations in methanol/water (80/20, w/w) medium in the presence of various kinds of saturated hydrocarbon: (**a**) hexadecane; (**b**) tetradecane; (**c**) dodecane; (**e**) octane; (**f**) hexane

dispersed in a methanol/water medium in the presence of decane droplets and subsequent cooling down to the room temperature [5]. The optimum conditions for the formation of the hemispherical and dimple particles including temperature, stirring rate, and composition of medium were demonstrated. Formation of the hemispherical and dimple particles was caused by absorption of decane into the PS particles during the heating process, phase separation (Janus structure) of PS/decane particles during the cooling process, and removal of the decane phase by evaporation. The size of the dimple depended on the amount of decane in the PS particles (Figs. 4 and 5).

Based on the knowledge obtained in the above experiment, hemispherical PS particles were prepared by slow evaporation of toluene (used common good solvent) from homogeneous PS/hexadecane (HD)/toluene droplets dispersed in

surfactant aqueous solutions at room temperature, followed by the rapid removal of HD from PS/HD particles with Janus structure [13c].

Similar micrometer-sized, hemispherical particles were prepared as a result of the cleavage of Janus polymethyl methacrylate (PMMA)/PS composite particles by dispersing into acetone/water (9/1–10/0, v/v) media or a THF/water (8/2 v/v) medium [13b]. The spherical composite particles having the Janus structure were prepared by the slow evaporation of toluene from homogenous PMMA/PS toluene droplets dispersed in an aqueous medium in advance.

4. *Mushroom-like particles* [14]: Many nonspherical polymer particles have been formed by chance, but we successfully prepared mushroom-like particles as planned shown in a schematic representation (Fig. 1) based on the concept of particle design (Fig. 6). The first step is macrophase
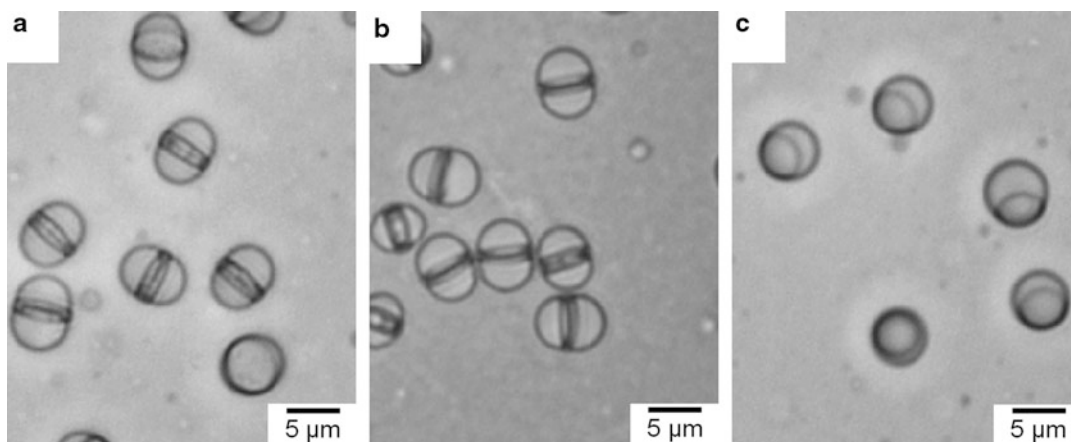
Polymer Colloids with Focus on Nonspherical Particles, Fig. 10 Optical microscope photographs of PS/PEHMA/decane composite particles prepared by seeded dispersion polymerizations in methanol/water (80/20, w/w) medium in the presence of decane droplets for 24 h (**a**) and 72 h (**b**) and those (**c**) after heat treatment of former particles (**a**) at 150 °C for 24 h

separation between PMMA and styrene-2-(2-bromoisobutyryloxy)ethyl methacrylate) copolymer (P(S-BIEM)) in toluene droplets induced by evaporation of toluene as a common good solvent, resulting in spherical PMMA/P(S-BIEM) Janus particles. Bromine atom is a highly active initiator site for activator generated by electron transfer for atom transfer radical polymerization (AGET ATRP) of 2-(dimethylamino)ethyl methacrylate (DM) at one side of the surface as the second step. For the preparation of the Janus, seed particles with almost the same interfacial area between each polymer phase and the aqueous medium were prepared using sodium dodecyl sulfate as surfactant. Because poly (DM) has lower critical solution temperature in water at about 34 °C and pKa at 6.8, the mushroom cap consisting of poly(DM) has temperature- and pH-responsive properties. Therefore, the mushroom-like PMMA/P (S-BIEM) Janus particles work as particulate surfactant for Pickering emulsion of 1-octanol-in-water, where the stabilization or destabilization could be controlled by changing the pH values and temperature [14]a (Fig. 7).

5. *Disclike and hamburger-like particles* [15]: Micrometer-sized, monodisperse "hamburger-like" particles were obtained by seeded dispersion polymerization of 2-ethylhexyl methacrylate (EHMA) with PS seed particles in the presence of decane in a methanol/water medium and resulted in disclike particles by the removal of poly(EHMA) and decane with 1-butanol. The hamburger-like morphology was maintained at 60 °C (above Tg of the particle) for at least 1 week in spite of less thermodynamic stability than hemispherical morphology [15]b (Figs. 8, 9, and 10).

Related Entries

▶ Miniemulsion Polymerization
▶ Pickering Emulsion Polymerization
▶ Smart Materials

References

1. Okubo M (1990) Control of particle morphology in emulsion polymerization. Makromol Chem Macromol Symp 35/36:307–325
2. Kim S-H, Abbaspourrad A, Weitz DA (2011) Amphiphilic crescent-moon-shaped microparticles formed by selective adsorption of colloids. J Am Chem Soc 133:5516–5524
3. Park BJ, Furst EM (2010) Fabrication of unusual asymmetric colloids at an oil-water interface. Langmuir 26:10406–10410

4. Tajima A, Higuchi T, Yabu H (2008) Hemispherical polymer nano-particles of polyisoprene-poly(methyl methacrylate) blend with core-shell structure. Colliods Surf A 313:332–334

5. Tanaka T, Komatsu Y, Fujibayashi T, Minami H, Okubo M (2010) A novel approach for preparation of dimple and hemispherical polystyrene particles. Langmuir 26(6):3848–3853

6. (a) Fujibayashi T, Komatsu Y, Konishi N, Yamori H, Okubo M (2008) Effect of polymer polarity on the shape of "golf ball-like" particles prepared by seeded dispersion polymerization. Ind Eng Chem Res 47:6445–6449; (b) Konishi N, Fujibayashi T, Tanaka T, Minami H, Okubo M (2010) Effects of properties of the surface layer of seed particles on the formation of golf ball-like polymer particles by seeded dispersion polymerization. Polym J 42(1):66–71

7. Saito N, Nakatsuru R, Kagari Y, Okubo M (2007) Formation of "snowmanlike" polystyrene/poly (methyl methacrylate)/toluene droplets dispersed in an aqueous solution of a nonionic surfactant at thermodynamic equilibrium. Langmuir 23:11506–11512

8. Kegel WK, Breed D, El-Aasser M, Pine DJ (2006) Formation of anisotropic polymer colloids by disparate relaxation times. Langmuir 22:7135–7136

9. Mock EB, Zukoski CF (2010) Emulsion polymerization routes to chemically anisotropic particles. Langmuir 26(17):13747–13750

10. Mock EB, Bruyn HD, Hawkett BS, Gilbert RG, Zukoski CF (2006) Synthesis of anisotropic nanoparticles by seeded emulsion polymerization. Langmuir 22:4037–4043

11. Okubo M, Wang Z, Yamashita T, Ise E, Minami H (2001) Morphology of micron-sized, monomer-adsorbed, cross-linked polymer particles having snowman shape prepared by the dynamic swelling method. J Polym Sci A Polym Chem 39:3106–3111

12. Okubo M, Wang Z, Ise E, Minami H (2001) Adsorption of styrene on micron-sized, monodisperse, cross-linked polymer particles in a snowman-shaped state by utilizing the dynamic swelling method. Colloid Polym Sci 279:976–982

13. (a) Yamagami T, Tanaka, T, Suzuki T, Okubo M (2013) Preparation of hemispherical polymer particles via phase separation induced by microsuspension polymerization. Colloid Polym Sci 291:71–76; (b) Yamashita N, Konishi N, Tanaka T, Okubo M (2012) Preparation of hemispherical polymer particles by cleavage of a Janus poly(methyl methacrylate)/polystreyne composite particle. Langmuir 28:12886–12892; (c) Tanaka T, Yamagami T, Nogami T, Minami H, Okubo M (2012) Preparation of hemispherical polystyrene particles utilizing the solvent evaporation method in aqueous dispersed systems. Polym J 44(11):1112–1116

14. (a) Tanaka T, Okayama M, Minami H, Okubo M (2010) Dual stimuli-responsive "mushroom-like" Janus polymer particles as particulate surfactants. Langmuir 26(14):11732–11736; (b) Tanaka T, Okayama M, Kitayama Y, Kagawa Y, Okubo M (2010) Preparation of "mushroom-like" Janus particles by site-selective surface-initiated atom transfer radical polymerization in aqueous dispersed systems. Langmuir 26(11):7843–7847

15. (a) Fujibayashi T, Okubo M (2007) Preparation and thermodynamic stability of micron-sized, monodisperse composite particles of disc-like shapes by seeded dispersion polymerization. Langmuir 23(15):7958–7962; (b) Fujibayashi T, Tanaka T, Minami H, Okubo M (2010) Thermodynamic and kinetic considerations on the morphological stability of "hamburger-like" composite polymer particles prepared by seeded dispersion polymerization. Colloid Polym Sci 288(8):879–886

Polymer Films for Packaging

Preetha Balakrishnan[1], Merin Sara Thomas[1,2], Laly A. Pothen[2,3], Sabu Thomas[1,4,6] and M. S. Sreekala[5]

[1]International and Inter University Centre for Nanoscience and Nanotechnology, Mahatma Gandhi University, Kottayam, Kerala, India
[2]Department of Chemistry, C.M.S. College, Kottayam, Kerala, India
[3]Department of Chemistry, Bishop Moore College, Mavelikara, Kerala, India
[4]School of Chemical Sciences, International and Interuniversity Centre for Nanoscience and Nanotechnology, Mahatma Gandhi University, Kottayam, Kerala, India
[5]Department of Chemistry, SreeSankara College Kalady, Enakulam, Kerala, India
[6]Universiti Teknologi MARA, Selongor, Shah Alam, Malaysia

Definition

Packaging is a concept in which the package, the product and the environment interact to extend the shelf-life, or to enhance the safety, while maintaining the quality of the product.

Introduction

Worldwide annual plastic production is estimated to surpass 300 million tons by 2015 [1]

representing trillions of dollars in terms of global economic returns. Petroleum resources are extensively used in producing these polymers, which leads to concerns in terms of both economic and environmental sustainability. Basic packaging materials, such as paper and paperboard, plastic, glass, metal, and a combination of materials of various chemical natures and physical structures, are used to fulfill the functions and requirements of packaged foods depending on their type. However, there has been an ever-increasing effort in the development of different kinds of packaging materials in order to enhance their effectiveness in keeping the food quality with improved convenience for processing and final use. Among the four basic packaging materials, petroleum-based plastic materials have been widely used since the middle of the twentieth century. It is mainly because they are cheap and convenient to use with good processing property, good aesthetic quality, and excellent physicochemical properties. More than 40 % of the plastics are used for packaging, and almost half of them are used for food packaging in the form of films, sheets, bottles, cups, tubs, trays, etc. After their useful life, it is desirable for the packaging materials to biodegrade in a reasonable time period without causing environmental problems. Though the synthetic plastic packaging materials have been widely used for the packaging of various types of food, they caused a serious environmental problem since they are not easily degraded in the environment after use. Not surprisingly, the environmental impact of packaging is frequently studied within the literature. However, there are several criteria which are to be fulfilled before applying it in the packaging field.

Polymers Used for Packaging Application

One of the major problems associated with petroleum-based plastic products is safe waste disposal. Even though they are very cheap and easy to process, the problems are very high at the stage of waste disposal. In this scenario, biodegradable polymers gain its importance.
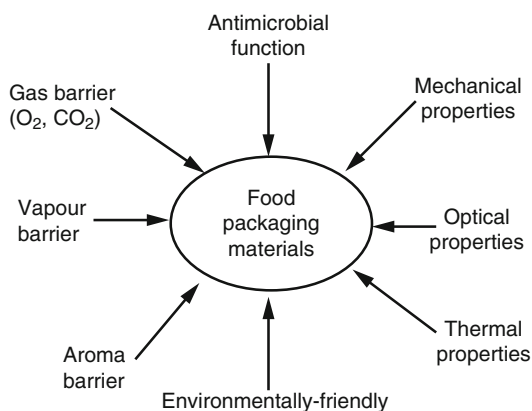
Polymer Films for Packaging, Fig. 1 General properties required for food packaging materials

Biopolymer-based packaging materials obtained from naturally derived renewable materials such as polysaccharides, proteins, and lipids have become the focus of worldwide attention in recent years. Such biopolymers offer favorable environmental advantages of recyclability and reutilization compared to conventional petroleum-based synthetic polymer. One of the major fields in which these packaging applications of biodegradable polymers can be applied is in food packaging industry [2]. The basic requirements for food packaging applications are shown in Fig. 1.

Polyethylene (LDPE, HDPE, LLDPE, VLDPE)

Polyethylene is the most common plastic produced in the world. It comes in a wide variety of physical properties. Polyethylene can be hard and rigid or soft and pliable. In the packaging industry, soft and pliable films are often used to package and store a large variety of products and even waste. Polyethylene offers the lowest softening point of the basic packaging plastics. The low cost of polyethylene production has encouraged producers to prefer its use over many other plastics. The lower softening point results in lower processing energy costs. There are three types of polyethylene commonly used in the packaging industry: high-density polyethylene (HDPE), low-density polyethylene (LDPE), and linear low-density polyethylene.

Polypropylene

Polypropylene is a clear glossy film with a high strength and puncture resistance. It has a moderate barrier to moisture, gases, and odors, which is not affected by changes in humidity. It is used in similar applications to LDPE. Oriented polypropylene is a clear glossy film with good optical properties and a high tensile strength and puncture resistance [3]. It has moderate permeability to gases and odors and a higher barrier to water vapor, which is not affected by changes in humidity. It is widely used to pack biscuits, snack foods, and dried foods.

PET

Poly(ethylene terephthalate) (PET) is one of the polymers most widely used in the packaging industry. However, it is highly desirable to enhance its barrier properties for applications, such as carbonated drinks and other rigid and flexible packaging applications. The nanocomposite route offers unique possibilities to enhance the properties of this material, provided that adequate thermally resistant and legislation-complying nanoadditives are used [4].

PLA

Several studies on poly lactic acid (PLA)-based packaging have shown that they could replace some of the conventional packaging for a number of food products. PLA may have packaging applications for a broader array of products [5] as modern and emerging production technologies lower its production costs. The production of PLA presents numerous advantages: (1) it can be obtained from a renewable agricultural source; (2) its production consumes quantities of carbon dioxide; (3) it provides significant energy savings; (4) it is recyclable and compostable; (5) it can help improve farm economies; and (6) the physical and mechanical properties can be manipulated through the polymer architecture.

Starch

Starch is a widely available and easy biodegradable natural resource. To produce a plastic-like starch-based film, high water content or plasticizers (glycerol, sorbitol) are necessary. These plasticized materials (application of thermal and mechanical energy) are called thermoplastic starch (TPS). Starch-based thermoplastic materials (e.g., blends of TPS with synthetic/biodegradable polymer components, like polycaprolactone, polyethylene-vinyl alcohol, and polyvinyl alcohol) have been successfully applied on the industrial level for foaming, film blowing, injection molding, blow molding, and extrusion applications.

Cellulosic Polymers

Different studies on cellulose-based films showed that they could be an alternative for packaging several food products. Popa and co-workers conducted different studies on cellulose-based films and showed that they could be an alternative for packaging several food products and stated that paper and board, based on cellulose, are the most widely used renewable packaging materials nowadays [6].

Polymer Nanocomposites for Packaging

Nanocomposites exhibit increased barrier properties, increased mechanical strength, and improved heat resistance compared to their neat polymers and conventional composites [7]. Incorporating nanofillers into polymer matrices will reduce the existing problems associated with polymers. Recently, several research groups started the preparation and characterization of various kinds of biodegradable polymer nanocomposites, i.e., bio-nanocomposites, showing properties suitable for a wide range of applications. Biodegradable natural and synthetic polymers have been filled with layered silicate in order to enhance their desirable properties while retaining their biodegradability in a comparatively economic way.

Nanofillers Used

Clay Nanoparticles

Layered silicates also known as nanoclays are most commonly utilized nanofillers in the synthesis of polymer-layered silicate nanocomposites. Among these layered silicates, phyllosilicates (2:1)

are extensively used in preparing clay-based nanocomposites. The crystal arrangement in the silicate layers is made up of two tetrahedrally coordinated atoms amalgamated to edge-shared octahedral sheets. The dispersibility of layered silicates into individual layers is governed by its own ability for surface modification via ion exchange reactions that can replace interlayer inorganic ions with organic cations. Renewable polyesters are mostly organophilic compounds, while the pristine silicate layers are miscible only with hydrophilic polymers. The silicate layers can be made miscible with hydrophobic polymer by introducing/exchanging interlayer cation galleries (Na^+, Ca^{2+}, etc.) of layered silicates with organic compounds [8].

Cellulose

The properties of the cellulose-based nanocomposites depend on the dimensions and consequent aspect ratios as well as mechanical and percolation effects. Researchers have been indicated that the tensile properties and transparency of the nanocomposites increase with the aspect ratio of the cellulose nanoparticles. However, Jiang et al. [9] showed that filler orientation and distribution play an important role in realizing the mean aspect ratio. Hence, the actual mechanical properties of the filled systems can differ by large extent when fillers do not follow a symmetric distribution and that those follow. Basically two types of nanoreinforcements can be obtained from cellulose – microfibrils and whiskers.

Carbon Nanotubes

In polymer nanocomposites, they have been utilized as high-performance functional fillers, which not only improved thermal/mechanical performance but also provided additional functionalities such as fire retardant, moisture resistance, electromagnetic shielding, and barrier performances. The field of polymer nanocomposites with carbon nanomaterial has been highly diversified; carbon nanotube (CNT)-based polymer composites have been widely explored in many aspects as described elsewhere [10].

Silica (SiO_2)

Silica nanoparticles ($nSiO_2$) have been reported to improve mechanical and/or barrier properties of several polymer matrices. Wu and co-workers observed that the addition of $nSiO_2$ into a polypropylene (PP) matrix improved tensile properties of the material – not only strength and modulus but also elongation.

Starch Nanocrystals

Kristo and et al. reported that the addition of starch nanocrystals (SNC) improved tensile strength and modulus of pullulan films, but decreased their elongation. The glass transition temperature (Tg) values shifted to higher temperatures with increasing SNC content, which was attributed to a restricted mobility of pullulan chains due to the formation of strong interactions between SNC as well as between filler and matrix [11].

Preparation

Polymer nanocomposites can be prepared by solution mixing, melt processing, and layer-by-layer (LbL) assembly.

Solution Mixing

Solution mixing is one of the most commonly used techniques for preparing nanofiller-reinforced polymer matrix composites. Solution mixing generally involves three major steps: dispersing filler in a suitable solvent, mixing with a polymer solution, and recovering the composite by precipitating or casting a film.

Melt Processing

Melt blending is a convenient method to produce CNT-based nanocomposites owing to its cost-effectiveness, fast production, and environmental benefits, being a solvent-free process. Melt blending uses high temperature and high shear forces to disperse nanofillers in a thermoplastic polymer matrix, using conventional equipment for industrial polymer processing.

Layer-by-Layer (LbL) Assembly Involving Clays

Layer-by-layer (LbL) self-assembly is a method by which a multilayer coating/film of

P

nanometer-thick layers can be made by sequential adsorption of oppositely charged polyelectrolytes on a solid support.

Characterization

Polymer nanocomposites exhibit markedly improved packaging properties due to the nanometer-size dispersion of nanofillers in the polymer matrix. These improvements include increased barrier properties, increased mechanical properties, and improved heat resistance.

Mechanical Properties

Formation of nanocomposite with nanoclays has shown pronounced improvement in the mechanical properties with several polymers such as polyethylene, polypropylene, nylon 6, poly(Ɛ-caprolactone), polyethylene terephthalate, etc., even with low filler loading. The improvement in the mechanical properties by the use of clay was first reported by Toyota Research Center [12]. When nanoclay was reinforced with nylon, it was found that the mechanical properties such as tensile strength, tensile modulus, and impact strength of the composite enhanced profoundly. The study on mechanical properties of polymer/clay nanocomposites revealed that the properties are dependent on filler content.

Barrier Properties

Polymer nanocomposites show excellent barrier properties against gases such as O_2, CO_2, etc., and water vapor. Generally, barrier properties obtained when nanofillers are dispersed within a polymer matrix are dependent on the free volume in material, the polymer chain segment mobility, and the size of diffusing molecules as well as on the dispersion level, the orientation, the amount of dispersed nanoparticles, the interfacial compatibility between nanocomposite elements, the presence of additional additives, etc.

The existence of clay nanoparticles in polymer nanocomposites increases the tortuosity of the diffusive path for a penetrant molecule (Fig. 2), thereby increasing the effective path length for diffusion and providing excellent barrier properties [13].
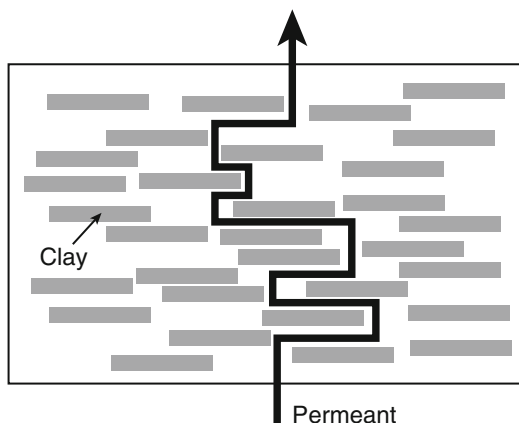
Polymer Films for Packaging, Fig. 2 The existence of clay nanoparticles in polymer nanocomposites

Biodegradation/Antimicrobial Properties

Biodegradability of bio-nanocomposites is one of the most interesting issues in the bio-nanocomposite materials. Biopolymers are widely used as matrix material in the field of packaging industry because of their biodegradability. It is expected that the biodegradability of the resulting nanocomposites should not be sacrificed after the formation of nanocomposites. For most biodegradable polymers, some of their physical properties need to be improved in order to fight with petroleum-based materials. The incorporation of antimicrobial compounds like silver nanoparticles [14] into food packaging materials has received considerable attention. Films with antimicrobial activity could help control the growth of pathogenic and spoilage microorganisms. An antimicrobial nanocomposite film is particularly desirable due to its acceptable structural integrity and barrier properties imparted by the nanocomposite matrix and the antimicrobial properties contributed by the natural antimicrobial agents impregnated within.

In order to fully exploit the properties of silver nanoparticles, they should be well dispersed on the surface of the polymer matrix without the formation of aggregates, which otherwise dramatically reduce the antimicrobial effect of silver. Moura et al. [15] developed cellulose-based bactericidal nanocomposites containing silver nanoparticles and studied the antibacterial activity by disk diffusion method. Different sizes of

nanoparticles were investigated to optimize the performance of the composites.

Applications

Nowadays, polymeric nanocomposite materials are widely used as packaging materials in food packaging, in electronic packaging, and in industrial packaging. Specific examples include packaging for processed meat, cheese, cereals, and dairy products, printer cartridge seals and medical container seals for blood collection tubes, and stoppers for medical containers and blood bags, baby pacifiers, and drinking water bottles.

The major use of polymer nanocomposites is in the field of food packaging. The use of protective coatings and suitable packaging by the food industry has become a topic of great interest because of their potentiality for increasing the shelf life of many food products [16, 17]. By means of the correct selection of materials and packaging technologies, it is possible to keep the product quality and freshness during the time required for its commercialization and consumption.

Currently, clay particles at the nanoscale are the most common commercial application of nanoparticles. The industrial applications of nanoclay in multilayer film packaging include beer bottles, carbonated drinks, and thermoformed containers. Nanoclays embedded in plastic bottles and nylon food films stiffen packaging and reduce gas permeability, keeping oxygen-sensitive foods fresher and extending shelf life. Bayer polymers have created a low-cost nanoclay composite interior coating for paperboard cartons to keep juice fresher.

Recycling of Plastic Packaging Materials

Presently, packaging materials have brought serious ecological problems while making considerable contributions to economic development. Plastics are the main packaging material, and the pollution caused by these materials after their use cannot be discarded [18]. This type of pollution is termed as "white pollution."

Recycling provides opportunities to reduce oil usage, carbon dioxide emissions, and the quantities of waste requiring disposal. This can be made into practice by mechanical recycling, by chemical recycling, and by organic recycling.

Mechanical recycling is a method by which waste materials are recycled into "new" (secondary) raw materials without changing the basic structure of the material in which the original polymer properties are being maintained or reconstituted. It is a well-established technology for the material recovery of conventional plastics (e.g., PP, poly ethylene (PE), PET, and PS). Its main advantage is that part of the resources consumed for the production of the plastic materials is not wasted, but preserved for a use in the same, similar, or different application. This technology of mechanical recycling is applicable to both bio-based conventional plastics and to most grades of biodegradable plastics.

Chemical recycling can be applied to mixed or soiled waste and can be converted to gaseous fuel or feedstock for chemical plant. Feedstock recycling technologies satisfy the general principle of material recovery, but are more costly than mechanical recycling. Gasification, hydrogenation, and pyrolysis are some of the methods used for chemical recycling.

Conclusion

Polymer nanocomposites as packaging materials in food packaging, in electronic packaging, and in industrial packaging have drawn attention in scientific community due to their versatile properties. Recently the attention in the packaging industry regarding the use of bioplastics has been shifting from compostable/biodegradable materials toward bio-based materials. Renewable resource-based biopolymers such as starch, cellulosic plastics, and corn-derived plastics such as PLA and polyhydroxyalkanoates (PHAs) are some of the most widely used biopolymers to produce nanocomposites for use of packaging applications. The incorporation of nanoparticles into the polymer system improves the mechanical and barrier properties of the materials. In addition

P

to the improvement in the mechanical and barrier properties, these nanostructures are responsible for providing active or smart properties to the packaging system such as anti-microbial activity. Recycling of these packaging materials also attained much interest because packaging materials have brought serious ecological problems.

References

1. Halden RU (2010) Plastics and health risks. Annu Rev Public Health 31:179–194
2. Rhim J-W, Park H-M, Ha C-S (2013) Bio-nanocomposites for food packaging applications. Prog Polym Sci 38:1629–1652
3. Lei J, Yang L, Zhan Y, Wang Y, Ye T, Li Y, Deng H, Li B (2014) Plasma treated polyethylene terephthalate/polypropylene films assembled with chitosan and various preservatives for antimicrobial food packaging. Colloids Surf B Biointerfaces 114:60–66
4. Bowditch TG (1997) Penetration of Polyvinyl Chloride and Polypropylene Packaging Films by Ephestia cautella (Lepidoptera: Pyralidae) and Plodia interpunctella (Lepidoptera: Pyralidae) Larvae, and Tribolium confusum (Coleoptera: Tenebrionidae). J Econ Entomol 90(4):1028–1101, ISSN 0022-0493
5. Gruber PR, O'Brien M (2002) Polylactides. "NatureWorksTMPLA". In: Doi Y, Steinbüchel A (eds) Biopolymers. Polyesters III. Applications and commercial products, 1st edn. Wiley-VCH, Weinheim, pp 235–250
6. Almenar E, Samsudin H, Auras R, Harte B, Rubino M (2008) Postharvest shelf life extension of blueberries using a biodegradable package. Food Chem 110(1):120–127
7. Popa M, Belc N (2007) Packaging. Food Safety 1:68e87
8. Makino Y, Hirata T (1997) Modified atmosphere packaging of fresh produce with a biodegradable laminate of chitosan-cellulose and polycaprolactone. Postharvest Biol Technol 10(3):247–254
9. Giannelis EP (1996) Polymer layered silicate nanocomposites. Adv Mater 8:29–35
10. Moniruzzaman M, Winey KI (2006) Polymer nanocomposites containing carbon nanotubes. Macromolecules 39:5194–5205
11. Kristo E, Biliaderis CG (2007) Physical properties of starch nanocrystal reinforced pullulan films. Carbohydr Polym 68:146–158
12. Kunz DA et al (2013) Clay-based nanocomposite coating for flexible optoelectronics applying commercial polymers. ACS Nano 7(5):4275–4280
13. Cabedo L, Gimenez E, Lagaron JM, Gavara R, Saura JJ (2004) Development of EVOH–kaolinite nanocomposites. Polymer 45(15):5233–5238
14. Fernández A, Soriano E, Hernández-Munoz P, Gavara R (2010) Migration of antimicrobial silver from composite of polylactide with silver zeolite. J Food Sci 75(3):E186–E193
15. de Moura MR, Mattoso LHC, Zucolotto V (2012) Development of cellulose-based bactericidal nanocomposites containing silver nanoparticles and their use as active food packaging. J Food Eng 109:520–524
16. Coles R, McDowell D, Kirwan MJ (2003) Food packaging technology. Blackwell, Oxford
17. Kirwan MJ, Strawbridge JW (2003) Plastics in food packaging. In: Coles R, McDowell D, Kirwan MJ (eds) Food packaging technology. Blackwell, Oxford, pp 174–240
18. Carvalho MT, Agante E, Durão F (2007) Recovery of PET from packaging plastics mixtures by wet shaking table. Waste Manage 27(12):1747–1754

Polymer Flocculants

Shinobu Kawaguchi and Shimpei Hasegawa
Polymeric Agents Research Department, Sanyo Chemical Industries, Ltd., Kyoto, Japan

Synonyms

Clarifying reagent; Flocculants; Flocculating polymers; Flocculating reagent; Polymeric flocculant

Definition

Polymer flocculants are water-soluble polymers which can form flocs from individual small particles in a suspension by adsorbing on particles and causing destabilization through bridging or charge neutralization.

Polymer flocculants are high molecular weight polymers and have hydrogen-bonding groups and/or ionic groups in the molecule.

Polymer flocculants promote the separation of particles from water to clean water.

Historical Background

Polymer flocculants have a collecting and precipitating function. Polymer flocculants tend to be used in water purification, because polymer flocculants can increase aggregates by gathering components of fine turbidity which cannot sink as it is in the wastewater and can enhance solid–liquid separation from a wastewater.

Natural polymer flocculants such as starch, sodium alginate, and gelatin had been used since the 1920s [1]. Aggregation performance of natural polymer flocculants is not the best because of their low molecular weight of several tens of thousands. At present, natural polymer flocculants have been replaced by synthetic polymer flocculants in the various applications and used only in applications such as food processing and water supply [2].

Synthetic polymer flocculants are relatively new compared to natural polymer counterparts. It was the first example that American Cyanamid Co. developed polyacrylamide industrially and applied it as a polymer flocculant in 1952. Synthetic polymer flocculants with higher molecular weight than that of natural polymer flocculants display a superior aggregation performance. In the early days of developments of synthetic polymer flocculants, nonionic- and anionic-type polymer flocculants that are capable of promoting separation of the suspension in the wastewater were developed. In the 1960s, the dehydration process of sludge from sewage treatment was demanded with the spread of sewerage. Consequently, cationic-type polymer flocculants which are quite effective in sludge dewatering were developed [3, 4]. However, as organic matter contents in the sludge increased, cationic-type polymer flocculants could not work effectively in sludge dewatering. Amphoteric-type polymer flocculants were also developed, which are highly effective in such kinds of sludge dewatering through the combination with inorganic flocculants [5].

Nature of Flocculation

The terms of coagulation and flocculation are often used to describe the whole process of aggregation. Coagulation is the process linked with destabilization interaction energy. Flocculation generally relates to the transport phase in which particles get in contact with each other as a result of relative motion.

Flocculation can occur only if some conditions are satisfied (type of polymer flocculants, additive amounts, stirring speed, and pH). The main task is to overcome the energy barrier. There are two principal paths. In the first, destabilization is promoted by reducing the energy barrier, which provides conditions in which van der Waals or other adhesive forces can dominate. Energy barrier reductions can be induced by reducing the spatial extent of the double-layer interaction energy or the surface potential as a result of changes in the surface chemistry. In the second, although a significant energy barrier exists, its kinetic effects can be avoided by mechanical bridging or by entrapment within a precipitate. In a practical sense, a combination of some destabilization mechanisms may also work [6].

Principle of Flocculation by Polymer Flocculants

Small amounts of polymer flocculants can increase aggregates of particles in wastewater. Two mechanisms of aggregation are known: charge neutralization (bridging via electrostatic patch interactions, electrostatic bridge based on point charges) and cross-linking adsorption (polymer bridging) [7].

In charge neutralization, two mechanisms have been supposed. One is bridging via electrostatic patch interaction model. Polymer flocculants having charge density interact with oppositely charged particles. The net residual charge of the polymer patch on one particle surface can attach to the bare part of an oppositely charged particle [8] (Fig. 1). The other is electrostatic bridging based on a point-
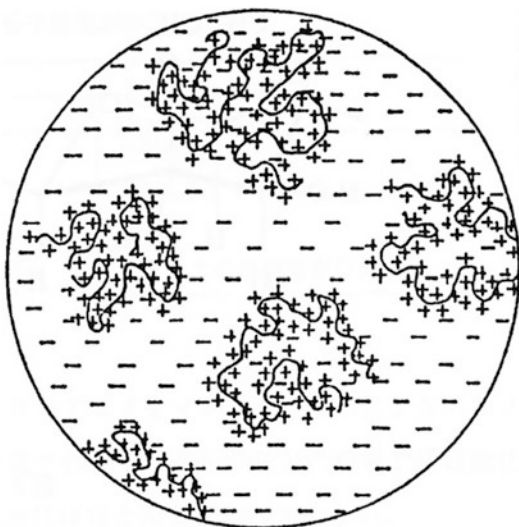
Polymer Flocculants, Fig. 1 Schematic view of adsorption of cationic polymer flocculants on a charged particle
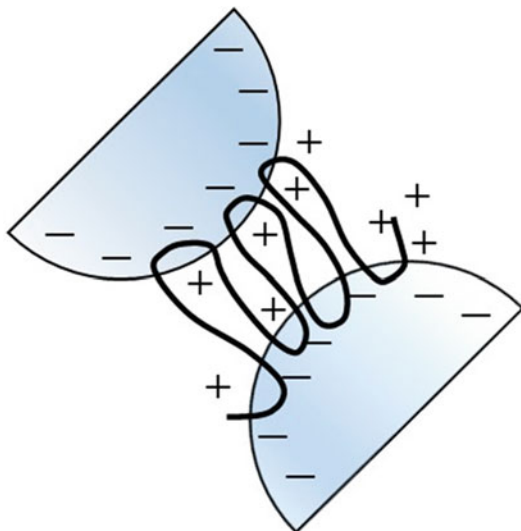
Polymer Flocculants, Fig. 3 Bridging flocculation with adsorbed polymer
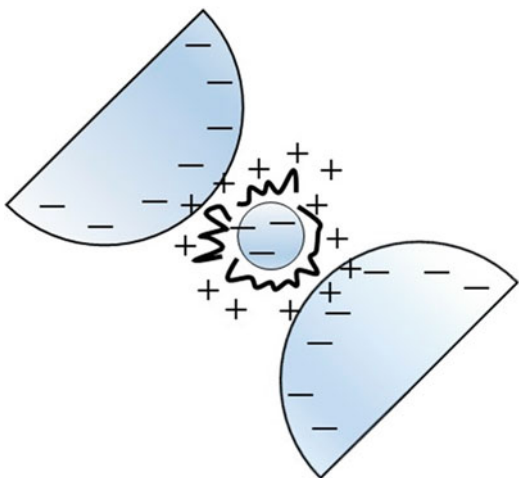
Polymer Flocculants, Fig. 2 Electrostatic bridge on point charges

charge model. A small particle covered with polymer flocculants combines opposite charged other particles through electrostatic bridging [9] (Fig. 2).

In cross-linking adsorption, the mechanism has been believed as described below. Polymer flocculants adsorb on one particle in a suspension and cross the distance over which repulsion forces effectively adsorb onto another. Adsorption is generally formed by coulombic electrostatic reactions or van der Waals attraction and

hydrophobic bonding interactions. Where the particle and polymer are of opposite charges, adsorption by electrostatic attraction will reduce the net charge on the particle and improve the prospects of destabilization as a result of reductions in the energy barrier. Because of the high molecular weight of polymer flocculants, extended loops and tails can form and increase the probability of attachment with other particles (Fig. 3).

The rate of aggregate growth is a key factor for flocculation. The aggregate growth rate depends both on the interparticle collision frequency and on whether collisions result in adhesion. If the collisions are caused by Brownian motion, the process is called perikinetic aggregation. In the case where collisions are brought about by bulk fluid motion, the term orthokinetic aggregation applies [10]. Perikinetic aggregation applies to particles smaller than about 1 μm. For larger particles, the orthokinetic process dominates.

In the case of perikinetic aggregation, the simple scenario is the case of a same size collection of particles at a concentration of n particles per unit volume. When a collision occurs, aggregation connects to a reduction in the primary particle concentration. This is expressed by:

$$dn/dt = -\alpha k_P n^2 \qquad (1)$$

$$k_P = 4kT/(3\mu) \qquad (2)$$

In which α is the collision efficiency factor, k_P is rate constant, k is the Boltzmann constant, T is the absolute temperature, and μ is the dynamic viscosity of the medium.

In the case of orthokinetic aggregation, the relative particle motion which results in a flux of particles toward another is determined by the local velocity gradient or strain rate $(\varepsilon/v)^{1/2}$, in which ε is the rate of energy dissipation per unit mass and v is the kinematic viscosity. In stirred reactors, this factor is often represented by velocity gradient G, although the former definition is more appropriate. In the early stages of flocculation growth, particle growth responds to G, this being in accord with the kinetic behavior. At later stages, the particle growth ceases with a limiting size whose magnitude depends on G, because aggregates are being broken as fast as they form. Hence, the aggregation rate can be explained by

$$dn/dt = -\alpha k_o n^2 + k_R n \qquad (3)$$

in which k_R is breakage rate constant.

And k_o is a rate constant specified by

$$k_o = (2/3)Gd^3 \qquad (4)$$

in which G is mean velocity gradient and d is identical particle diameter [7].

Classification of Polymer Flocculants

Polymer flocculants are widely used in water treatment, serving as a primary coagulant of more often used as a means of enhancing the floc strength of dewaterability. There are many kinds of polymers which have various molecular weight, charge type (nonionic, anionic, cationic, or amphoteric), and charge density (Fig. 4).
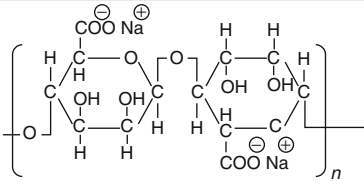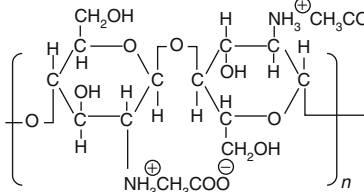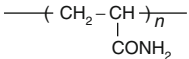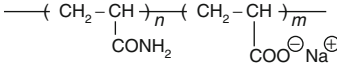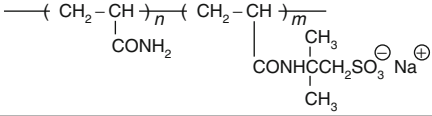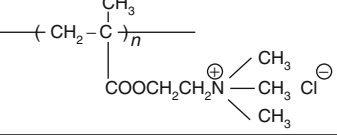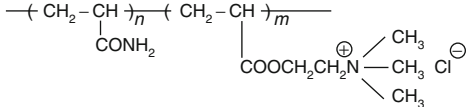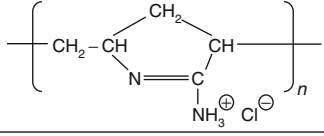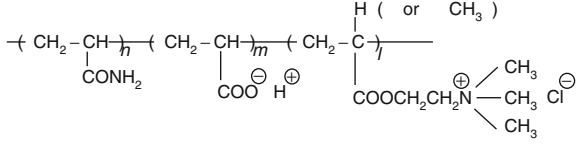
Polyacrylamide is a representative of nonionic polymer flocculants. Polyacrylamide can be easily synthesized as a high molecular weight polymer and has amide groups featuring hydrogen bonding which can effectively adsorb small particles in wastewater. Molecular weight is between several million and ten and several million. Because of their aggregation ability which is not dependent on pH, their aggregation effects are more efficient than anionic polymer flocculants in acid and neutral pH.

Representative anionic polymer flocculants are as follows: (1) partially hydrolyzed polyacrylamides, (2) copolymers of acrylamide and acryl acid soda, (3) copolymers of acrylamide and acrylamide-2-methyl-propan sulfonic soda (AMPS), and (4) poly(sodium acrylate). In general, anionic polymers with copolymer composition of 5–40 mol% sodium acrylate or hydrolyzed acrylamide with similar acid contents are mainly used. Owing to their high molecular weight of 10–20 million, anionic polymer flocculants can promote aggregation effectively at the amounts of several ppm for wastewater. The aggregation properties depend on pH, because the dissociation degree of anionic groups in the anionic polymer changes according to pH. Anionic polymer flocculants are usually used in neutral and basic conditions.

Representative cationic polymer flocculants include (1) copolymers of acrylamide and acryloyloxyethyl trimethylammonium chloride, (2) poly(methacryloxyethyl trimethylammonium chloride), and (3) polyamidine. Their molecular weight ranges from several million to less than 20 million. Cationic polymer flocculants are fully quaternized with methyl chloride and therefore positively charged over a wide pH range. They can especially neutralize for negatively charged particles in wastewater, and they can form aggregates which can be dehydrated easily [11].

Other representative cationic water-soluble polymers are as follows: polyethylenimine, poly(diallyldimethylammonium chloride), polyamine, and condensation polymers composed of epichlorohydrin and dimethyl amine or dicyandiamide. Since their molecular weights are usually lower than those of the cationic polymer flocculants described above, these cationic water-soluble polymers have only charge neutralization abilities. They do not have aggregation abilities and therefore are often called coagulant.

Type		Chemical Structure
Natural polymer flocculants	anion — alginate sodium	
	cation — chitosan (acetate salt)	
Synthetic polymer flocculants	non — polyacrylamide	
	anion — poly (acrylamide · acrylate sodium)	
	anion — poly (acrylamide · acrylamide -2-met -hylpropane sulfo -nate sodium)	
	cation — poly (dimethyl aminoet -hyl methacrylate methylchloride)	
	cation — poly (acrylamide · dimethyl aminoeth - hyl acrylate methylchloride)	
	cation — polyamidine (hydrochloride salt)	
	ampho-ion — poly (acrylamide · acryl acid · dimeth -yl aminoethyl (meth) acrylate methylchloride	

Polymer Flocculants, Fig. 4 Representative polymer flocculants

Representative amphoteric polymer flocculants are composed of methacryloxyethyl trimethylammonium chloride, acryloyloxyethyl trimethylammonium chloride, acrylamide, and acrylic acid. Amphoteric polymer flocculants have molecular weight of several million to less than 20 million and have cationic parts and anionic parts in the same polymer chain.

Any charge-type (nonionic, anionic, cationic, or amphoteric) synthetic polymer flocculants can be synthesized by radical polymerization method such as aqueous solution polymerization, emulsion polymerization, and reverse-phase suspension polymerization.

Natural polymer flocculants are typically sodium alginate, modified chitosan, and modified starch. Sodium alginate is used after alginic acid from kelp, seaweed, laver etc. is reacted with aqueous sodium hydroxide. Chitosan can be obtained by deacetylation of chitin from shrimp and crab. Starch is used as a water-soluble polymer after the process of heating in water or alkali treatment. Their molecular weight is several tens of thousands. Flocculation performances of natural polymer flocculants are not better than synthetic polymer flocculants because of their lower molecular weight than those of synthetic polymer flocculants. Natural polymer flocculants have attracted as a biodegradable polymer flocculants [12].

Flocculation Ability of Polymer Flocculants

Upon using a polymer flocculant, flocculation ability is affected by various factors. Flocculation ability is controlled by molecular weight, charge type, and charge density of polymer flocculants. Flocculation ability is affected by organic contents, pH, pulp density, temperature, and shear on the flocs. Flocculation ability is evaluated by polymer dosage, aggregation particle size, and so on [13–15].

Regarding polymer dosage, there is a suitable range for the amount. In a suitable dosage region, both adsorption and bridging act in a well-balanced manner, and therefore polymer flocculants can form flock. In contrast, flocculation does not proceed smoothly when the added amount is too small or excess. At the shortage of dosage, the flocs become small. At the excess of dosage, adsorption occurs in excess and bridging does not occur enough, and consequently there are dispersed states in the repulsion between particles.

The effect of molecular weight is described below. In the case of high molecular weight polymer, large size flocs can be formed upon suitable polymer dosage. However, excess amounts of polymer dosage result in the small size of flocs and the increase of nonadsorbed polymer. On the other hand, in the case of lower molecular weight polymer, the floc size cannot be controlled by polymer dosage, although the floc size is small and nonadsorbed polymer decreases.

Analytical Evaluation of Polymer Flocculants

For the characterization of polymer flocculants, evaluations of charge density and molecular weight are important.

Charge density of polymer flocculants is evaluated as colloid equivalent value (meq/g). Colloid equivalent value means mg equivalent number of ionic groups contained in 1 g polymer flocculants. In general, anionic groups take minus values and cationic groups plus values. Colloid equivalent value can be measured by titration method.

Molecular weight of polymer flocculants is generally evaluated by calculation based on correlation equation between intrinsic viscosity and molecular weight [16–18]. As a simple method, intrinsic viscosities are often substituted to Brookfield viscosity of polymer aqueous solution (mPa · s). Recently, according to the development of analytical apparatus, there is also an attempt to measure molecular weight by small-angle laser light-scattering analysis [19, 20]. For the case of polyacrylamide, molecular weight can be measured by GPC method in the molecular weight region of several million.

Example of Using Polymer Flocculants

Polymer flocculants are mainly used for cases such as clarification with sedimentation of wastewater and dewatering of sludge.

Clarification with sedimentation of wastewater by using polymer flocculants is described as
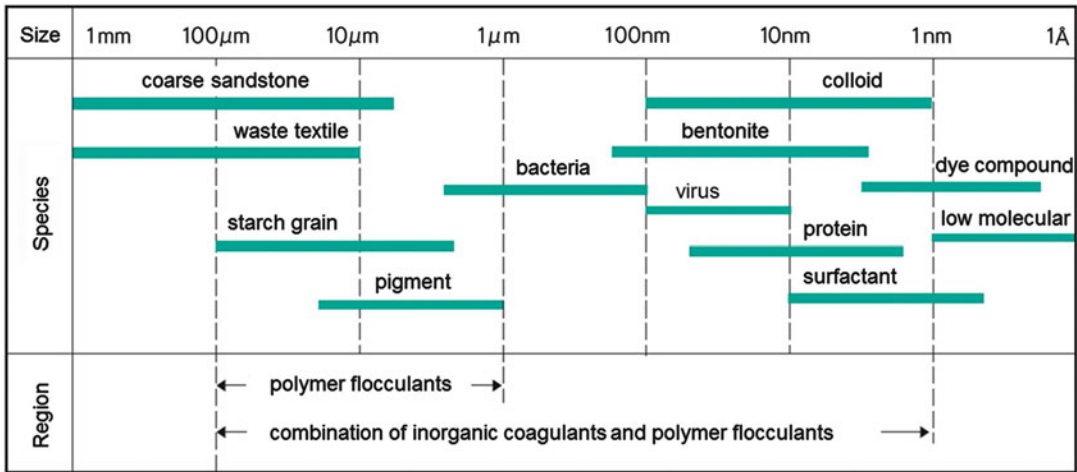
Polymer Flocculants, Fig. 5 Particle size vs usage region of polymer flocculants

following. Colloidal particles in wastewater are of various sizes. There is a lower limit to the particle size that can be flocculated with polymer flocculants alone, and therefore fine colloidal particles cannot be flocculated (Fig. 5). In general, wastewater treatments are executed by using combinations of polymer flocculants and inorganic coagulants. For inorganic coagulants, the molecular weight is small and the charge density is high, and therefore the effect of charge neutralization of the colloidal particles is strong. Although inorganic coagulants are suitable for collecting fine colloidal particles in wastewater, only small flocs can be obtained, and the sedimentation time of small flocs is longer than the time of large flocs. Addition of nonionic, anionic, or amphoteric polymer flocculants which possess high molecular weight and adsorption groups such as amide and carboxyl groups, followed by the addition of inorganic coagulants, can form large and strong flocs grown from small flocs through bridging. As a result, the use of combinations of polymer flocculants and inorganic coagulants can promote sedimentation. A typical concrete treatment process is as follows: (1) inorganic coagulants are added to wastewater or sludge and stirred, (2) pH is controlled at ca. eight, (3) polymer flocculants are added and stirred, (4) colloidal particles become flocs and precipitated, (5) precipitated flocs containing

large amounts of water are often dewatered and the volume is reduced. Flocculating sedimentation treatments are applied to purification of industrial sewage and also wastewater containing less soluble organic substances originating from mineral collecting, civil engineering work, etc.

Dewatering of sludge by using polymer flocculants is described as follows. In the case of industrial sewage and sewage water containing water-soluble organic substances, the purification process except for the removal of colloidal particles is generally performed through activated sludge treatment for the removal of soluble organic substances (Fig. 6). Activated sludge treatment is useful for the removal of organic substances by the growth of microorganisms. Large amounts of organic sludge are produced by activated sludge treatment because microorganisms and microorganism carcasses are increased. These sludges are composed of water and several % of solid contents, and so dewatering treatment of sludge is significant to reduce sludge volumes. Sludge cannot be dewatered enough without flocculants because solid contents of sludge bearing many anionic groups such as carboxyl groups have negative charges on their particle surfaces and are stably dispersed. Cationic polymer flocculants can promote to flocculate aggregates and dewater sludges. Cationic polymer flocculants bearing
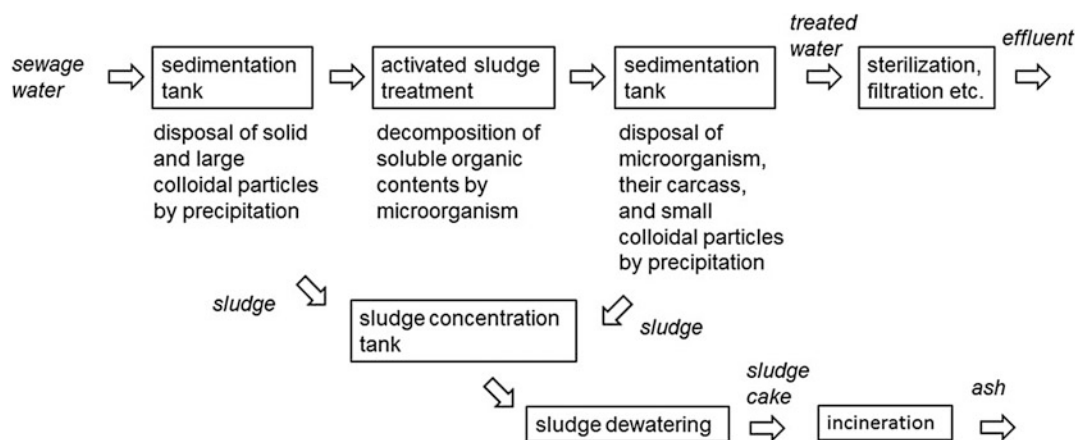
Polymer Flocculants, Fig. 6 Example of wastewater treatment process flowchart

cationic groups in polymer chains can neutralize negative charges on the surface of colloidal particles in sludge and can bridge between particles to form large and strong flocs for easily dewatering. Sludge containing flocs is dehydrated by sludge-dewatering equipment, separated to solids called sludge cake, and finally disposed by landfill, incineration, or compost. The water content of sludge cake after dewatering treatment is usually ca. 80 %, and the volume of sludge can be reduced to 1/10 the original volume of sludge. Polymer flocculants which are capable of reducing water content of sludge more than before are strongly requested in the treatment of dewatering sludge because of cost reduction. When cationic polymer flocculants cannot dewater enough in consequence of festering sludge, a combination of inorganic coagulants and amphoteric polymer flocculants is often applied. Although amphoteric polymer flocculants bearing both cationic groups and anionic groups in the same polymer chain show weaker charge neutralization abilities than cationic polymer flocculants do, amphoteric polymer flocculants are expected to form ion complexes with cationic and anionic groups to display strong bridge effects at appropriate pH states. Because of the above reasons, amphoteric polymer flocculants are added to sludge after inorganic coagulants are first added to sludge, and charge neutralization is reached. As a result, strong aggregates are formed and the water content can be reduced.

Summary

Polymer flocculants are water-soluble high molecular weight polymers and consist of various nonionic, anionic, cationic, or amphoteric polymers. Polymer flocculants can form effectively aggregates from individual small particles in a suspension by adsorbing on particles and causing destabilization through bridging or charge neutralization. Because of their unique ability of aggregation, polymer flocculants have been designed for application in the fields of various water treatments. Polymer flocculants are expected to play an important role as green materials to resolve the environmental water problems.

Related Entries

▶ Flory–Huggins Equation
▶ Free-Radical Addition Polymerization (Fundamental)
▶ Ion-Containing Polymer Synthesis
▶ Ion-Exchange Resins
▶ Monomers, Oligomers, Polymers, and Macromolecules (Overview)

References

1. Horiuchi T (2000) Functions and applications of water soluble polymers. CMC, Tokyo, p 49
2. Fang ZD, Jun L, Huan Y (2013) Mechanism study on flocculating organic pollutants by chitosan with different molecular in wastewater. Am J Eng Res 2:91–95
3. Noda M (1968) Class and mechanism of action of polymer flocculants. Koubunshi, Tokyo, p 404
4. Suzuki M (1972) Applications of polymer flocculants. Koubunshi, Tokyo, p 586
5. Kawaguchi S (2009) Flocculation and precipitation, vol 13, Performance chemicals series. Sanyo Chemical Industry Press, Kyoto, p 5
6. Dobiáš B (1993) Coagulation and flocculation : theory and applications, vol 47, Surfactant science series. CRC Press, New York
7. Bache DH, Gregory R (2007) Flocs in water treatment. IWA Publishing, London, pp 21–27
8. Yan YD, Biggs S (2004) The flocculation efficiency of polydisperse polymer flocculants. Int J Miner Process 73:161
9. Gregory J (1973) J Colloid Interface Sci 42:448
10. IUPAC (1997) Compendium of chemical terminology, 2nd edn. Blackwell, Oxford/Malden
11. Fan A, Somasundaran P (2000) A study of dual polymer flocculation. Colloids Surf A Physicochem Eng Asp 162:141–148
12. Brostow W, Singh RP (2009) Polymeric flocculants for wastewater and industrial effluent treatment. J Mater Educ 31:157–166
13. Chaiwong N, Nuntiya A (2008) Influence of pH, electrolytes and polymers on flocculation of kaolin particle. Chiang Mai J Sci 35:11–16
14. SNF Floerger Water soluble polymers. http://snf.com.au/downloads/Water_Soluble_Polymers_E.pdf
15. Tripathy T, De BR (2006) Flocculation: a new way to treat the waste water. J Phys Sci 10:93–127
16. Griebel T (1992) Molecular characterization of water-soluble, cationic polyelectrolytes. Macromol Chem 193:811–821
17. Griebel T (1991) Characterization of water-soluble, cationic polyelectrolytes as exemplified by poly(acrylamide-co-trimethylammonium ethylethacryate chloride) and the establishment of structure–property relationships. Colloid Polym Sci 269:113–120
18. Ogishima M et al (2002) Polymer flocculants user manual. Tokyo Metropolitan Sewerage Service Corporation, Tokyo, pp 111–117
19. Hecker R (2000) Flow field-flow fractionation of polyacrylamides: commercial flocculants. Sep Sci Technol 35(4):593–612
20. Leeman M (2007) Asymmetrical flow field-flow fractionation coupled with multi-angle light scattering and refractive index detections for characterization of ultra-high molar mass poly(acrylamide) flocculants. J Chromatogr A 1172:194–203
21. Niinae T (2006) Polymer flocculants, vol 436. Sanyo Chemical Industry News Press, Kyoto, pp 1–4. http://www.sanyo-chemical.co.jp/pr/pdf/pk61.pdf

Polymer Lasers and Optical Amplifiers

Dimali Amarasinghe Vithanage,
Graham A. Turnbull and Ifor D. W. Samuel
Organic Semiconductor Centre, SUPA, School of
Physics and Astronomy, University of
St. Andrews, St. Andrews, Fife, UK

Definition

A *polymer laser* is a laser that uses a polymer as the gain medium. A *polymer optical amplifier* is a device which amplifies an optical signal using a polymer as the gain medium.

Introduction

Lasers play an important role in everyday life such as in electronic devices, communication networks, and spectroscopy tools. Optical amplifiers increase the intensity of weak signals and are used to compensate propagation and splitting losses in optical communications. Most lasers are made from inorganic semiconductors (e.g., GaAs), doped glasses (e.g., Nd:YAG), or gases (e.g., argon) as the gain medium. However, lasers can also be made from organic molecules such as dyes and conjugated polymers. Organic laser dyes have been used in solutions to achieve laser action since the 1960s. There are two main types of polymer lasers: those that incorporate dyes into a polymer host matrix and those that use a conjugated polymer as the gain medium.

When dyes are doped in an inert polymer matrix, they can be configured as a solid-state dye laser with high gain and broadband emission. Emission across the visible and near infrared is possible by using the appropriate dye. The matrix can be a number of different materials, but the most commonly used are sol-gel and polymethyl methacrylate (PMMA).

Conjugated polymers are a type of organic semiconductor which have a structure of alternating single and double carbon bonds in the backbone. This chemical structure leads to novel semiconducting optoelectronic properties combined with some of the attractive properties of polymers such as simple fabrication and flexibility. This distinctive combination of properties has resulted in the successful development of optoelectronic devices such as organic light-emitting diodes (OLEDs), lasers, photovoltaic devices, and transistors made from conjugated polymers. Like laser dyes, they have strong visible emission, but they have the added benefit of exhibiting low concentration quenching, which allows them to have high fluorescence quantum yields (of up to 90 %) even in undiluted films. Their strong optical gain over a broad spectral range makes them attractive for compact-visible lasers and optical amplifiers.

Stimulated Emission

A laser consists of a gain medium in a resonator. The gain medium amplifies light which propagates backwards and forwards in the resonator and is amplified each time it passes through the gain medium. The amplification process is by stimulated emission where photons of the same frequency and direction as the stimulating photon are emitted. This leads to coherent emission in a beam with a narrow range of wavelengths. An optical amplifier operates in a similar way except that there is no resonator, so the light is amplified in a single pass. The first dye laser was demonstrated in solution by Lankard et al. in 1966 and in the solid state by Soffer and McFarland in 1967 [1]. The first conjugated polymer laser was demonstrated decades later by Moses in a solution of poly[2-methoxy-5-(2′-ethylhexyloxy)-p-phenylene vinylene] (MEH-PPV) in 1992 [2]. This was followed by Tessler et al. in 1996 with lasing in a solid-state polymer film, configured as a planar microcavity laser [3]. Currently all polymer lasers and optical amplifiers are excited using another light source – they are optically pumped. Nearly all polymer lasers have required another laser to power them, although the demonstration of plastic lasers pumped by a light-emitting diode is a significant step towards inexpensive miniature polymer lasers [4].

Stimulated Emission in Polymers

Some of the main families of conjugated polymers used for lasing are polyfluorenes, poly(phenylene vinylenes), and polythiophenes. Examples are shown in Fig. 1. Common dyes doped in polymer matrices include rhodamines, perylenes, pyromethanes, and coumarins. The π-π* transition is responsible for the absorption of photons that correspond to the energy gap between the highest occupied molecular orbital (HOMO) and the lowest unoccupied molecular orbital (LUMO) states. Emission stems from excited states as shown in Fig. 2 [5]. The absorption of light leads to a singlet excited state often referred to as a singlet exciton because it consists of a bound e-h pair. Electrons from the ground state S_0 are excited to higher vibronic levels of the S_1 electronic state, $S_{1,n}$ forming singlets which have the same electronic spin. From this point, the excitons go through fast vibronic cooling to the $S_{1,0}$ state. Emission occurs from the $S_{1,0}$ state to $S_{0,vib}$ followed by relaxation to $S_{0,0}$ after further cooling [5]. The materials have broadband emission spectra.

While the molecular energy states of conjugated polymers share many features with dyes, they exhibit less concentration quenching of the luminescence [6–8]. This is because the molecular structure in polymers is large and disordered and contains side chains resulting in less aggregation at high concentrations and so giving high photoluminescence (PL) efficiencies.

P
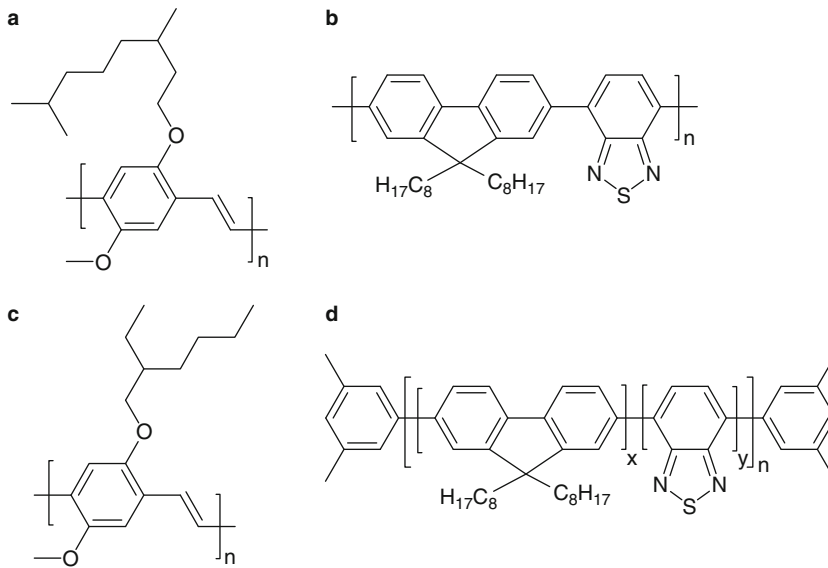
Polymer Lasers and Optical Amplifiers, Fig. 1 Chemical structures of some conjugated polymer materials used for lasers and amplifiers: (**a**) OC$_1$C$_{10}$-PPV, (**b**) F8BT, (**c**) MEH-PPV, and (**d**) ADS233YE
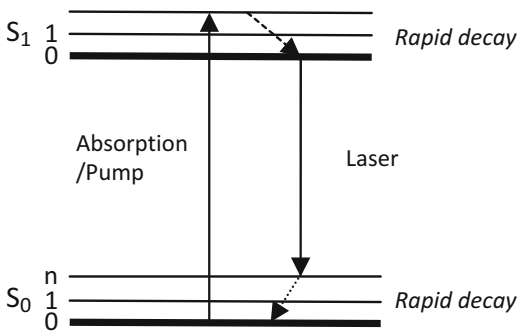
Polymer Lasers and Optical Amplifiers, Fig. 2 Schematic of energy levels of a dye molecule or conjugated polymer. The absorption of light excites an electron to form a vibrationally excited singlet state S$_{1n}$. Internal conversion through vibronic relaxation occurs to S$_{10}$. From there the singlet decays radiatively to a vibrationally excited level of the ground state S$_{0n}$ and finally undergoes vibronic relaxation to S$_{00}$. This represents a four-level laser system

This contrasts with the situation in dyes and rare earth ions, in which the efficiency drops significantly at high concentrations [6].

For lasing to occur, first there has to be *population inversion*. This occurs when the population density of excited molecules in the upper energy level (the S$_{1,0}$ state) is higher than that in at least one of the lower S$_{0,n}$ states. With population inversion obtained, an incident photon whose energy matches the gap between these singlet states will be more likely to interact with the larger excited state population to stimulate emission from S$_1$ to S$_0$ than be absorbed. In the stimulated emission process, the emitted photon has the same frequency, phase, and direction as the incident photons. The light that passes through the medium is amplified exponentially according to the equation [3, 9]:

$$I = I_0 \exp(g - \alpha)z$$

where I_0 is the initial intensity, g is the gain coefficient, α is the loss coefficient due to absorption and scattering, and z is the path length. The gain coefficient is defined as [6, 7, 9]:

$$g = \sigma N$$

where N is the population density of the S$_1$ state and σ is the stimulated emission cross section. The gain has to be stronger than the losses in the medium for the light to be amplified.

Optical amplification can be demonstrated using a pump probe configuration or amplified

spontaneous emission (ASE). A pump probe system has two beams which overlap spatially. Gain induced by the pump beam then amplifies the probe beam. ASE measurements are conducted by exciting the material and detecting the edge emission with a spectrometer. The pump fluence is gradually increased until spectral line narrowing is visible, which is the signature of ASE.

Dye-Doped Polymer Waveguide and Fiber Amplifiers

Solution dye amplifiers have been demonstrated with gains of up to 40 dB in 1 cm cuvettes [6, 9]. For practical applications, a solid-state structure is preferred and has been demonstrated in the form of waveguide structures [11] and fibers [12].

Solid-state dye-doped waveguide amplifiers have demonstrated gains of 26 dB with Rhodamine 6G mixed in PMMA. Fiber amplifiers have an advantage of being easy to couple with POF. Fibers of up to 1 m in length have demonstrated high gains of 33 and 25 dB using Rhodamine B [12] and Rhodamine 6G [13] doped in PMMA. The drive of using red emitters was to have emission wavelengths that are compatible with the transmission window of polymer optical fibers (POF).

Conjugated Polymer Amplifiers

Stimulated emission in conjugated polymers can be used to make optical amplifiers. Such amplifiers have been demonstrated both in solution and in thin-film waveguides. The first solution-based amplifiers were successfully demonstrated using OC_1C_{10}-PPV (a polymer closely related to MEH-PPV) and F8BT (shown in Fig. 1b) using a 1 cm quartz cuvette [6]. A gain of up to 40 dB was obtained with a very broad bandwidth of 50 Thz.

Following the successful demonstration of gain in solution, the conjugated polymer materials were investigated in a solid-state form as this would give a more practical, solvent-free device structure. The solid-state structures were a bigger challenge than the solution-based amplifiers as (1) the waveguides have to have high coupling efficiency and (2) the conjugated polymer films are amorphous making cleaving a problem as
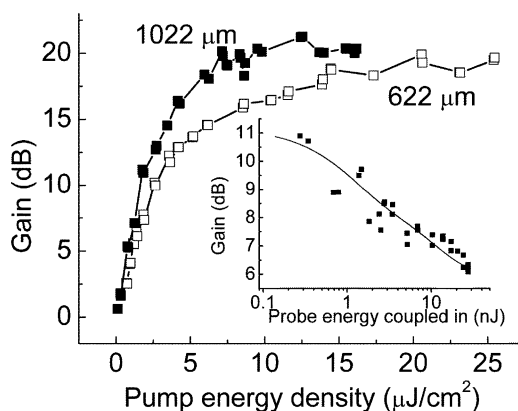
Polymer Lasers and Optical Amplifiers, Fig. 3 Gain dependence on pump energy density for a solid-state amplifier made from the conjugated polymer MEH-PPV. The figure shows amplification of a 630 nm signal wavelength for two waveguide lengths (622 and 1,022 μm). The inset shows variation of gain with signal energy for a waveguide length of 822 μm and pump energy density fixed at 2 μJ/cm^2. The solid line is a fit to gain saturation in a pulsed amplifier (Reprinted with permission [14])

they do not produce smooth clean edges required for edge coupling.

To overcome some of these challenges, the first solid-state-conjugated polymer amplifiers used gratings to couple the light into and out of the polymer. Solid-state amplifiers were started as slab waveguides which have then progressed to integrated amplifiers [11] discussed further in this article. The first conjugated polymer film used was a PPV derivative, MEH-PPV, which was demonstrated to give a gain of 21 dB in a 1 mm-length waveguide, as shown in Fig. 3 [14]. This was followed by various polyfluorene materials F8BT, Red-F, and ADS233YE with gains 18, 19, and 37 dB/mm [6, 11, 14]. This means that a weak signal can be amplified a hundred times or more by only 1 mm of material. The gain per mm is shown in Fig. 4 and is an order of magnitude higher than dye-doped amplifiers and several magnitudes higher than rare earth-doped amplifiers.

Polymer Lasers

To make a laser, one must combine an optical amplifier with a resonator. Often the resonator is a cavity. The resonator is an optical feedback

Polymer Lasers and Optical Amplifiers, Fig. 4 Upper panel shows gain demonstrated in solid-state amplifiers using semiconducting polymer waveguides (*open symbols*), dye-doped polymer waveguides (*half-filled squares*), fibers (*solid symbols*), and rare earth-doped polymer fibers (*crosses*) as a function of signal wavelength. The lower panel shows the gain obtained per 1 mm length of the waveguide or fiber used (Reprinted with permission [6])
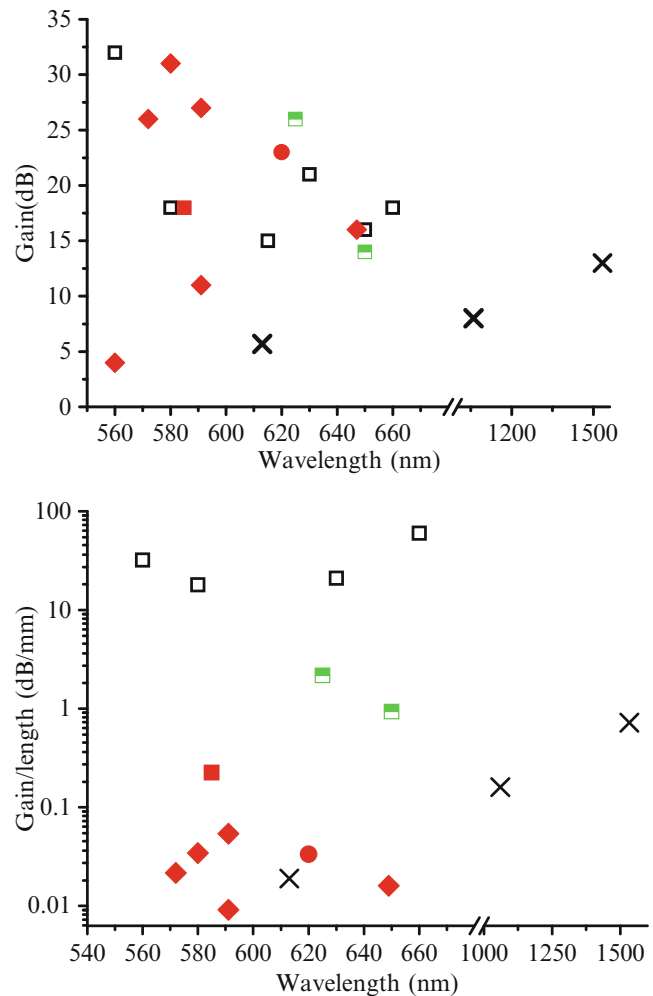
structure in which the light is made to travel back and forth through the gain medium. For laser oscillation to occur, the gain has to be higher than the losses through each round trip (the laser threshold condition). The resonant cavity defines the frequency of light (within the gain spectrum of the lasing material) for which there is constructive feedback.

Resonators for Polymer Lasers

The simple processing of polymers has enabled a wide range of resonators to be used in polymer lasers. The simplest conventional laser resonator consists of two mirrors placed on either end of the gain medium with one mirror partially reflecting to allow some of the light to escape as a laser

beam. Such resonators have been used for conjugated polymers in solutions and dye-doped fibers [15]. For thin-film polymer lasers however, a wider range of resonators have been used. A brief description of the operating principles of the most commonly used cavities is described here. For detailed information on further resonators, Samuel and Turnbull [10] and Chenais and Forget [16] are recommended.

The three most common laser resonators are distributed feedback lasers (DFB), microcavity lasers, and microring resonators, the structures of which are shown in Fig. 5. The most common resonator is the DFB resonator which uses a grating structure to reflect propagating modes in a waveguide [17]. These gratings are usually
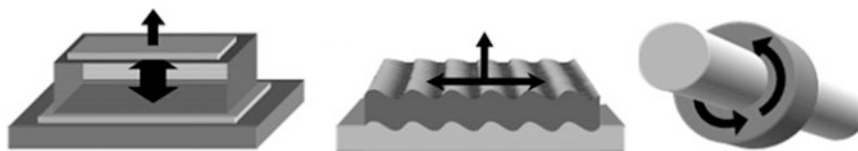
embedded into the substrate onto which the polymer film is spin coated. If the Bragg condition is satisfied, light will be coupled between counter-propagating waveguide modes, and an optical Bloch resonance will be supported by the structure. The Bragg condition is given by

$$m\lambda = 2n_{eff}\Lambda$$

where λ is the Bragg wavelength, Λ is the period of the grating, n_{eff} is the effective refractive index of the polymer waveguide, and m is the order of the diffraction. For a given grating, there is only a discrete set of wavelengths that will be diffracted from that grating and constructively interfere to produce the Bragg wave.

Second-order DFB lasers ($m = 2$) have been widely used for polymer lasers. These provide a surface emission of the laser light perpendicular to the polymer film and hence avoid the need for high-quality edge facets on the waveguide. Two-dimensional DFB lasers (photonic crystal lasers) have also been widely used for polymer lasers, giving feedback in multiple directions in the polymer film and improved control of the surface-emitted laser beam.

An alternative to using a grating structure is using end mirrors as with the microcavity resonator. The first microcavity-conjugated polymer laser was demonstrated by Tessler et al. in 1996 [3]. This consisted of a thin (100 nm thickness) polymer film sandwiched between one dielectric and one metal mirror. The design forms a linear cavity with one mirror being highly reflective and the second partially transmitting. The structure supports resonant modes for a discrete set of wavelengths, where the round-trip length of the cavity is equal to an integer number of wavelengths [10].

Compared to microcavity and distributed feedback lasers, microring resonators have a very different configuration, using cylindrical resonators which support whispering gallery modes propagating by total internal reflection (TIR) around the ring [10]. They are often composed of a polymer film deposited around a silica optical fiber or metal wire. The resonator is made by dipping the core into a polymer solution. An alternative processing method is to deposit the polymer on the inner surface of a microcapillary. The resulting emission is not in a well-defined direction, but uniformly in all directions perpendicular to the axis of the ring.

Electrical Pumping

The first organic lasers were optically excited by tabletop high-powered pulsed laser systems. Such configurations are bulky and expensive and are not well suited to practical applications. An electrically pumped laser system would be an attractive alternative, combining light weight and low cost, building on the great advances in organic LED technology using conjugated polymers. However, the demonstration of a polymer electrical injection laser has proven to be a very challenging task. There are several materials factors which have blocked progress in this area. Firstly, the drift mobilities in the conjugated polymers that exhibit high photoluminescence efficiency are usually very low, and so it is a challenge to achieve a sufficiently high density of singlet states in the gain medium under electrical injection. Under electrical injection a large population of triplet states is also formed. These may absorb in the emission band of the singlet states and suppress optical gain. There is also further substantial absorption from the injected electrons and holes which have not yet formed excitons.
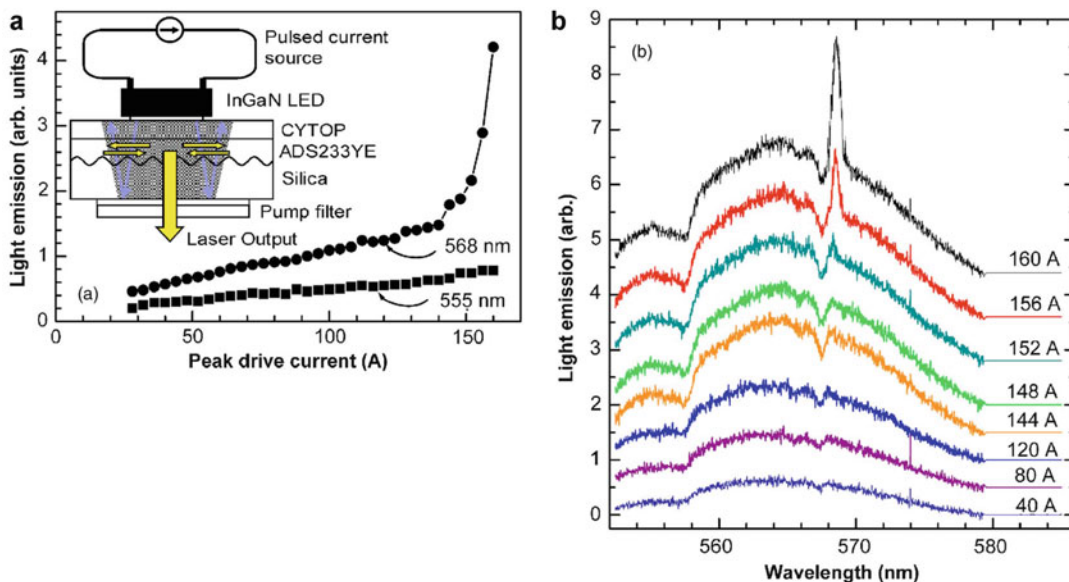
Polymer Lasers and Optical Amplifiers, Fig. 6 (**a**) Light emission at 568 and 555 nm as a function of peak drive current. Inset: Schematic diagram of the hybrid InGaN semiconducting polymer laser. (**b**) Surface emission spectra from the hybrid electrically pumped polymer laser for different drive currents (Reprinted with permission [4])

An alternative approach, which avoids these materials problems, is to use indirect electrical pumping, in which the electrical injection and population inversion are spatially separated. This indirect approach has been achieved using a distributed feedback polymer laser integrated on the emitting surface of an inorganic (InGaN) LED. Under a pulsed nanosecond drive in the LED, Yang et al. observed the onset of laser action in the polymer with a narrow line-width laser emission as shown in Fig. 6 [4]. While the polymer laser itself is still optically driven, this approach allows for a low-cost and easily integrated alternative to laser pump sources, achieving the main benefits anticipated of direct electrical drive.

Applications of Polymer Lasers and Amplifiers

Research and testing of these devices have been driven by spectroscopy and proof of principle in high-speed data communications networks. Their broadband tunability and simple processing made it possible to have a portable and single tunable optical source for spectroscopy. Applications of polymer lasers and amplifiers range from communications to explosive sensing with new applications being continuously explored. The research is at an early stage, but there is considerable interest.

Switching of Laser and Amplifiers

For ultrafast optical data communications networks, integrated circuits, and signal processing, an all-optical switch that is simple and cheap to manufacture on any surface is desirable. Such devices would be compatible with polymer optical fibers (POF) [15] which are a very promising alternative to twisted copper cables. POFs are a low-cost, light-weight, more flexible alternative, can be easily installed and spliced, and can be connected on-site to use in harsh inner-city environments in place of twisted copper cables or silica fibers. Switching of the gain in a polymer optical amplifier can be achieved by using an optical switch pulse that is resonant to a higher

Fig. 7 *Top*: Principle of switching. The energy level diagram shows how the input and switch pulses affect the probe pulse. (**a**) Amplification of probe light. (**b**) The switch pulse pushes excitons to a higher excited state and the resulting probe signal is not amplified. *Bottom*: Switching of a data stream shown in a pulse sequence. The output pulse sequence of the amplifier is modulated by a highly intense switch pulse (Reprinted with permission [7])
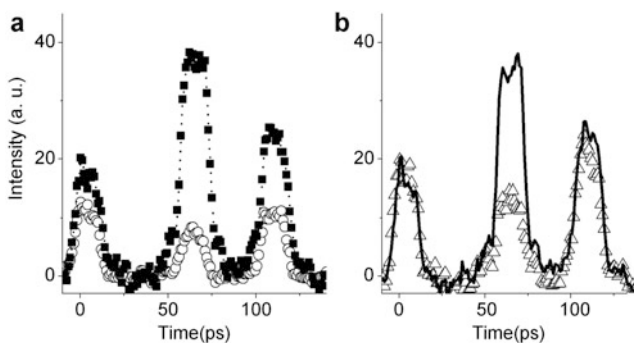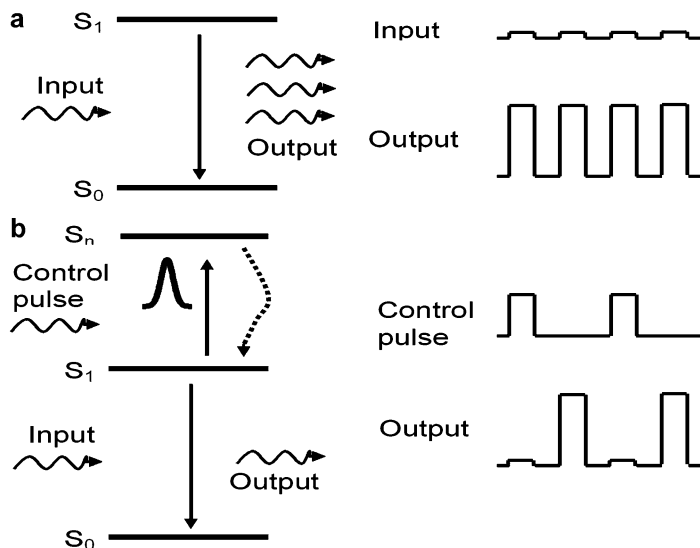
Polymer Lasers and Optical Amplifiers, Fig. 8 Amplification results for a spin-coated film of a fluorene-based copolymer. (**a**) Unamplified pulse sequence (*open symbols*) and amplified pulse sequence (*closed symbols*). (**b**) Amplified pulse sequence when switch pulse was applied (*open symbols*) and amplified pulse sequence after the switch pulse was applied (*solid line*) (Reprinted with permission [7])

excited state, S_n. The switch pulse is applied to temporally and spatially overlap the signal pulse that should be suppressed. The switch pulse further excites the excitons in the S_1 state to an upper excited state as illustrated in Fig. 7. This results in a reduced number of excitons to relax from the S_1 to the S_0 state, and therefore, the probe beam is no longer amplified. This method allows to wavelength convert the signal.

Switching of gain in a polymer amplifier was demonstrated using a polyfluorene-conjugated polymer with a switching rate of 500 GHz [18]. This was applied to suppress amplification of a single pulse in a sequence of amplified pulses. The amplification of the pulse was suppressed with 70 % efficiency, while the remaining amplified pulses were not affected as shown in Fig. 8. Switching of a laser was also demonstrated using the polyfluorene materials Red-F and F8BT [19, 20]. Laser wavelengths were in the visible region and the switching wavelength an IR pulse which corresponded to the data transmission window. Figure 9 shows the laser emission turned off.

Explosive Sensing

A promising emerging application for polymer lasers is the sensing of explosives. Due to

Fig. 9 Switching of laser
pulse at 692 nm. The
pumping and switching
wavelengths were 492 nm
and 1.28 μm. The pumping
and switching energies were
40 nJ and 2 μJ (Reprinted
with permission [7])
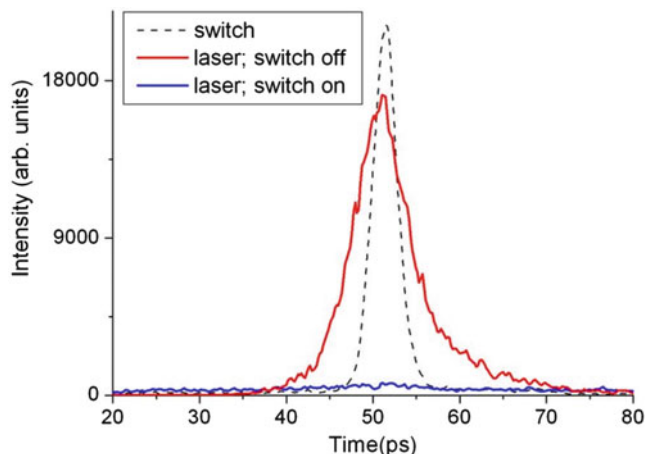
increased threats and security issues, there is
a need for highly sensitive detecting methods to
trace explosives. One approach to this problem is
to use luminescent polymer films and lasers as
sensors for nitro aromatic vapors.

Most explosives contain electron-deficient
compounds. In the presence of electron-rich-
conjugated polymers, an electron transfer occurs
from the LUMO of the conjugated polymer to the
LUMO of the explosive. The first polymer for
sensing explosives using fluorescence was dem-
onstrated in 1998 using the fluorescence of films
of phenyleneethynylene polymers with TNT
vapor. This has progressed onto the use of conju-
gated polymer lasers instead of fluorescence as it
improves the strength of the response which is
critical for detecting trace amounts within
extremely short times. The electron transfer pro-
cess reduces the population inversion for lasing
and suppresses the emission of the laser. The
laser emission can therefore be used as
a transducer to detect the presence of explosive
vapor [21, 22]. A demonstration of laser emission
suppression is shown in Fig. 10 [21] using the
organic materials PFO and polymer of intrinsic
microporosity (PIM-1).

Spectroscopy and Integrated Polymer Lasers and Amplifiers

Polymer lasers are apt spectroscopic sources due
to their broadband tunability and size. Lemmer
et al. have demonstrated conjugated polymer
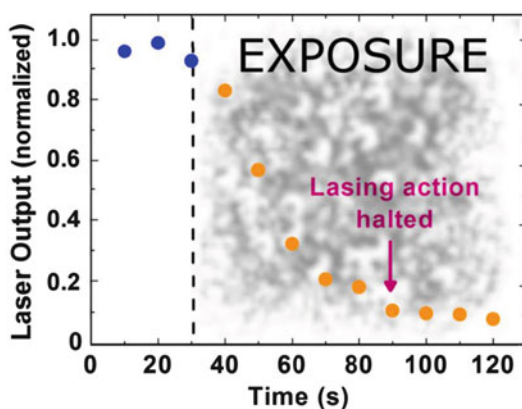
Polymer Lasers and Optical Amplifiers,
Fig. 10 PIM-1 laser emission dynamics during a 90 s
exposure when the laser is continuously excited at an energy
intensity of 346 μJ/cm^2 (Reprinted with permission [21])

DFB lasers with up to 19 nm tunability with
sufficiently low lasing threshold that they could
be pumped with a laser diode instead of a high-
powered laser system [23, 24]. They have also
demonstrated using an organic DFB laser as an
excitation source for Raman spectroscopy. In this
case the material was a dye doped in a small
molecule organic semiconductor.

Their broadband tunability combined with the
fact that organic material can be deposited on any
material surface means they can be integrated
into a single multifunctional device that is com-
pact, portable, and CMOS compatible. A bulky
device would need careful alignment or coupled

into waveguides which introduce more losses to the system. A lab-on-a-chip device would be a reliable alternative. The polymer can be simply added on to the chip at the final stage, once all processing work such as evaporation and etching are completed, thus having no adverse effect on the polymer material properties. Lab-on-a-chip systems using lasers or amplifiers have been demonstrated using dye-doped polymers. Such a device was demonstrated by Kristensen et al. [25] using a first-order DFB laser comprising of Rhodamine 6G doped in SU8 polymer. The laser was optically excited and the output was coupled into a curved polymer waveguide.

Conclusion

Polymer lasers and amplifiers are at an earlier stage of development than their inorganic counterparts. Nevertheless a range of important proof of principle demonstrations has shown their potential. There has been tremendous progress in reducing the size of the pump source. Indirect electrical pumping is a major advance, enabling simple compact lasers to be made. These can be expected in a range of applications of which spectroscopy and explosive detection are most advanced.

Related Entries

▶ Conducting Polymers
▶ Conjugated Polymer Synthesis
▶ Optical Absorption of Polymers
▶ Poly(arylene-vinylene)s
▶ Polyfluorenes
▶ Polymer Optical Fiber

References

1. Soffer BH, McFarland BB (1967) Continuously tunable, narrow-band organic dye lasers. Appl Phys Lett 10:266
2. Moses D (1992) High quantum efficiency luminescence from a conducting polymer in solution: A novel polymer laser dye. Appl Phys Lett 60:3215
3. Tessler N, Denton GJ, Friend RH (1996) Lasing from conjugated-polymer microcavities. Nature 382:695
4. Yang Y, Turnbull GA, Samuel IDW (2008) Hybrid optoelectronics: a polymer laser pumped by a nitride light-emitting diode. Appl Phys Lett 92:163306
5. Lakowicz JR (1999) Principles of fluorescence spectroscopy. Kluwer Academic Publishers, Springer, New York
6. Amarasinghe D, Ruseckas A, Turnbull GA, Samuel IDW (2009) Review on organic semiconductor optical amplifiers. Proc IEEE 97:106
7. Vithanage Chiranthika Dimali Amarasinghe (2008) Solid state optical conjugated polymer amplifier; with ultrafast gain switching
8. Calzado EM, Villalvilla JM, Boj PG, Quintana JA, Diaz-Garcia MA (2006) Concentration dependence of amplified spontaneous emission inorganic-based waveguides. Organ Electron 7:319
9. Ramon MC, Ariu M, Xia R, Bradley DDC, Marinelli MAR, Morgan CN, Penty RV, White IH (2005) A characterization of Rhodamine 640 for optical amplification: Collinear pump and signal gain properties in solutions, thin-film polymer dispersions, and waveguides. J Appl Phys 97:073517
10. Samuel IDW, Turnbull GA (2007) Organic semiconductor lasers. Chem Rev 107:1272
11. Grivas C, Pollnau M (2012) Organic solid-state integrated amplifiers and lasers. Laser Photon Rev 6(4):419–462
12. Tagaya A, Teramoto S, Nihei E, Sasaki K, Koike Y (1997) High-power and high-gain organic dye-doped polymer optical fiber amplifiers: novel techniques for preparation and spectral investigation. Appl Optics 36:572
13. Rajesh M, Sheeba M, Geetha K, Vallaban CPG, Radhakrishnan P, Nampoori VPN (2007) Fabrication and characterization of dye-doped polymer optical fiber as a light amplifier. Appl Optics 46:106
14. Amarasinghe D, Ruseckas A, Vasdekis AE, Goossens M, Turnbull GA, Samuel IDW (2006) Broadband solid state optical amplifier based on a semiconducting polymer. Appl Phys Lett 89:201119
15. Kuriki K, Kobayashi T, Imai N, Tamura T, Nishihara S, Nishizawa Y, Tagaya A, Koike Y, Okamoto Y (2000) High-efficiency organic dye-doped polymer optical fiber lasers. Appl Phys Lett 77:331
16. Chenais S, Forget S (2013) Organic solid-state lasers, Series in optical sciences. Springer, New York
17. Kogelnik H, Shank CV (1971) Stimulated emission in a periodic structure. Appl Phys Lett 18:153
18. Amarasinghe D, Ruseckas A, Vasdekis AE, Turnbull GA, Samuel IDW (2008) Picosecond gain switching of an organic semiconductor optical amplifier. Appl Phys Lett 92:083305
19. Perissinotto S, Lanzani G, Zavelani-Rossi M, Salerno M, Gigli G (2007) Ultrafast optical switching in distributed feedback polymer laser. Appl Phys Lett 91:291108
20. Xia R, Cheung C, Ruseckas A, Amarasinghe D, Samuel IDW, Bradley DDC (2007) Wavelength conversion from silica to polymer optical fibre communication

wavelengths via ultrafast optical gain switching in a distributed feedback polymer laser. Adv Mater 19:4054

21. Wang Y (2012) Low threshold organic semiconductor lasers, hybrid optoelectronics and applications as explosive sensors. Springer, London
22. Thomas SW III, Joly GD, Swager TM (2007) Chemical sensors based on amplifying fluorescent conjugated polymers. Chem Rev 107:1339–1386
23. Klinkhammer S, Liu X, Huska K, Shen Y, Vanderheiden S, Valouch S, Vannahme C, Bräse S, Mappes T, Lemmer U (2012) Continuously tunable solution-processed organic semiconductor DFB lasers pumped by laser diode. Opt Express 20:6357
24. Gather MC, Meerholz K, Danz N, Leosson K (2010) Net optical gain in a plasmonic waveguide embedded in a fluorescent polymer. Nat Photon 4:457–461
25. Christiansen MB, Schøler M, Kristensen A (2007) Integration of active and passive polymer optics. Opt Express 15:3931–3939

Polymer Optical Fiber

Yasuhiro Koike[1] and Kenji Makino[2]
[1]Keio Photonics Research Institute, Keio University, Science and Technology, Yokohama, Japan
[2]Graduate School of Science and Technology, Keio Photonics Research Institute, Keio University, Yokohama, Kanagawa, Japan

Synonyms

Plastic optical fiber; POF

Definition

Polymer optical fiber (POF) is basically composed of polymer core and cladding. The core has a refractive index higher than that of the cladding. When the incident light angle is larger than the critical angle determined by Snell's law, the light is confined to the core and travels long distance along the fiber.

Historical Background

The principle of light propagation through an optical fiber is simply explained as follows [1].

An optical fiber generally consists of two coaxial layers in cylindrical form. One is a core in the central part of the fiber. The other is a cladding in the peripheral part, which completely surrounds the core. Although the cladding is not required for light propagation in principle, the cladding plays important roles in practical use, such as protection of the core surface from imperfections and refractive index changes caused by physical contact or absorbing contaminants, and enhancement of the mechanical strength. The core has a refractive index slightly higher than that of the cladding. Therefore, when the incident angle of the light input to the core is greater than the critical angle determined by Snell's law, the input light is confined to the core region and propagates for long distances through the fiber because the light is repeatedly reflected back into the core region due to the total internal reflection at the interface between the core and cladding. The propagation of light along the fiber can be described in terms of electromagnetic waves called modes, which are a pattern of electromagnetic field distributions. The fiber can guide a certain discrete number of modes that must satisfy the electric and magnetic field boundary conditions at the core-cladding interface according to its material and structure, as well as the light wavelength.

Optical fibers can be commonly classified into two types: single-mode and multimode fibers [2]. As the names suggest, the single-mode fiber (SMF) allows only one propagating mode, while the multimode fiber (MMF) guides a large number of modes. Both the SMF and MMF are again divided into two classes: step index (SI) and graded index (GI) fibers. Moreover, optical fibers can be categorized by base materials: silica glass and polymer. Polymer optical fibers (POFs) consist of a polymer core and cladding. POFs are typically MMFs because POFs can have great advantages provided by the large core due to the high flexibility inherent to polymers. Figure 1 conceptually illustrates the refractive index profiles and ray trajectories in an SI SMF and SI and GI MMFs. Core sizes of typical optical fibers are shown in Fig. 2.
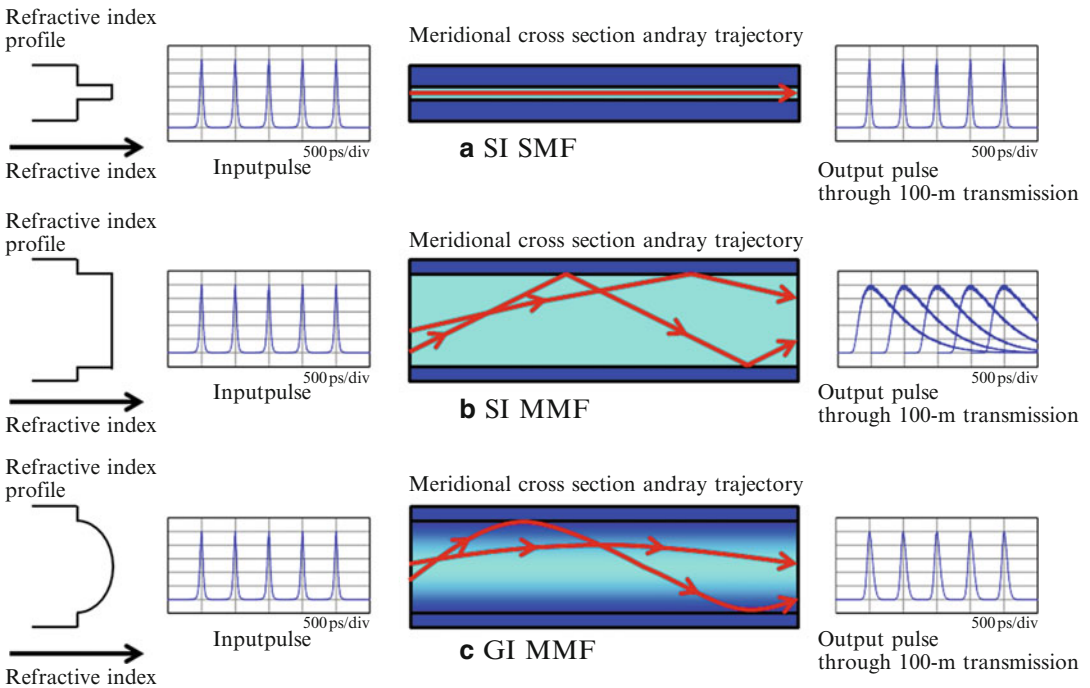
Polymer Optical Fiber, Fig. 1 Classification of optical fibers
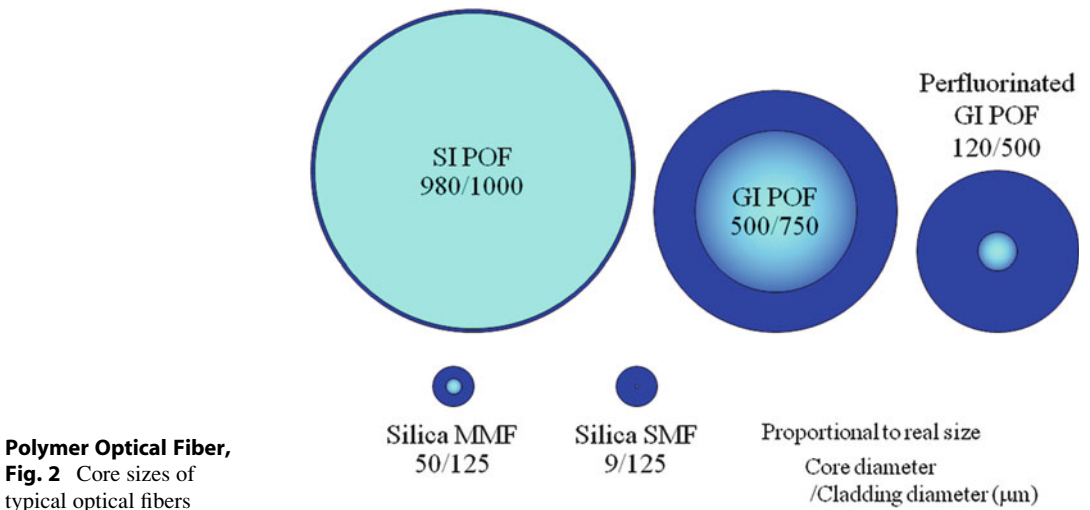
Polymer Optical Fiber, Fig. 2 Core sizes of typical optical fibers

Silica-based SMFs are widely used in long-haul communication systems such as undersea networks because silica fibers have extremely low attenuation due to the purified silica glass and extremely high bandwidth due to the absence of modal dispersion (described below) of SMFs in principle [3]. Recently, in addition to use in long-haul telecommunications, optical fibers have been required for data communications in local area networks (LANs) at homes, offices, hospitals, vehicles, and airplanes. As optical signal processing and transmission speed have increased with developments in information and communication technologies, metal wiring has

become a bottleneck for high-speed data transmission systems and large parallel processing computer systems. This is because the electrical wiring causes significant problems, including electromagnetic interference, high signal reflection, high power consumption, and heat generation [4]. Thus, optical networking is expected even in very short-reach networks. However, connecting SMFs requires accurate alignment using expensive and precise connectors because of the extremely small core diameters, below 10 μm, almost 1/10 that of the human hair. The connections of the SMFs lead to high installation costs, especially in LANs, where a lot of connections are expected [5]. Therefore, MMFs have been investigated to realize rough and cost-effective connections because of their relatively larger cores. Typical silica MMFs have core diameters of 50 or 62.5 μm larger than the SMFs. However, the core diameters of silica MMFs cannot be enlarged enough for rough and easy connection. Silica MMFs with larger core diameters are easily broken because silica glass is inherently brittle. In addition, silica MMFs were suffered from critical problems such as modal noise and unstable bandwidth performance.

POFs can have much larger core diameters, from hundreds of micrometers to nearly 1 mm. SI POFs with core diameters of almost 1 mm are commercially available. The large core diameters of SI POFs enable rough, easy, and cost-effective connection, and SI POFs are expected to be transmission media in LANs. However, as the required data rate becomes higher and higher, SI POFs cannot achieve reliable data transmission because of the low bandwidths induced by large modal dispersion. Modal dispersion can be briefly explained as follows. As shown in Fig. 1, different rays travel along their paths with different lengths, where each distinct ray can be thought of as a mode for simple interpretation. The lights travel at the same velocity along their optical paths because of the constant refractive index throughout the core region in SI POF. Consequently, even when the different modes are launched at the same time, the same velocity and different path lengths result in different propagation speeds along the fiber, thus leading to

pulse spread in time. The pulse broadening caused by modal dispersion seriously restricts the transmission speed of SI POF because overlaps of the broadened pulses induce intersymbol interferences and disturb correct signal detections, increasing the bit error rate [6]. In contrast, GI POFs have been investigated as transmission media in high-speed and short-reach networks [7]. GI POFs have a cylindrically symmetric refractive index profile that gradually decreases from the core axis to the core-cladding interface. The modal dispersion can be dramatically reduced by forming a near-parabolic refractive index profile in the core region of MMF, which allows much higher bandwidth (i.e., higher-speed data transmission) [8]. The ray confined to near the core axis, corresponding to a lower-order mode, travels a shorter geometrical length at a slower light velocity along the path because of the higher refractive index. The sinusoidal ray passing through near the core-cladding boundary, considered to be a higher-order mode, travels a longer geometrical length at a faster velocity along the path, particularly in the lower refractive index region far from the core axis. As a result, the output times from the fiber end of rays passing through the shorter geometrical length at the slower velocity and through the longer geometrical length at the faster velocity can be almost the same with the optimum refractive index profile. Thus, GI POFs can realize stable and reliable high-speed communication due to the high bandwidth. Moreover, GI POFs can have much larger core diameters due to the inherent flexibility of polymers. GI POFs allow rough connection and easy handling, which dramatically reduces the installation costs of networks, particularly in LANs [9]. Therefore, GI POFs are attracting a great deal of attention in consumer use because of their user-friendly characteristics.

Attenuation

Attenuation of fibers, or transmission loss, is the primary determinant of the maximum transmission distance of some optical communication systems without amplifiers or repeaters, as well

as the maximum output power from the light source and the minimum receiver sensitivity. Attenuation is basically caused by absorption, scattering, and radiation of optical power. Attenuation is defined as the ratio of input and output powers and is expressed by linearly adding the losses due to the individual components in units of dB [10]. Optical power decreases exponentially with distance as light travels along a fiber. Therefore, attenuation is discussed for a given fiber length and is typically described in dB/km:

$$\alpha = -\frac{10}{L}\log_{10}\left(\frac{P_{\text{out}}}{P_{\text{in}}}\right), \qquad (1)$$

$$\alpha = \alpha_a + \alpha_s + \alpha_r, \qquad (2)$$

where α is the total attenuation, P_{in} is the input optical power into the fiber, P_{out} is the output optical power from the fiber, L is the fiber length, and α_a, α_s, and α_r are the losses caused by absorption, scattering, and radiation, respectively. The extrinsic factors of fiber attenuation, such as contaminations, refractive index perturbations, chemical impurities, structural imperfections, and geometrical fluctuations, are not discussed here because the extrinsic attenuation strongly depends on the fabrication method. Thus, intrinsic absorption and scattering are explained in this section.

Absorption Loss

In general, materials absorb light at wavelengths corresponding to the resonance frequencies of the molecules. Intrinsic absorption losses in optical fibers primarily originate from electronic transitions in the ultraviolet wavelength region and molecular vibrations in the near-infrared (IR) wavelength region.

Absorption due to electronic transitions between the different energy levels within the materials is known as electronic transition absorption. This light absorption occurs when a photon excites an electron to a higher energy level. Electronic transition absorption peaks typically appear in the ultraviolet wavelength region. The optical loss caused by electronic transition absorption α_{et} obeys Urbach's empirical rule [11]:

$$\alpha_{\text{et}} = A\exp\left(\frac{B}{\lambda}\right), \qquad (3)$$

where λ is the wavelength of the light and A and B are inherent constants of the materials. These parameters have been empirically determined in poly(methyl methacrylate) (PMMA), polystyrene (PS), and polycarbonate (PC), which are typical polymers for POFs [12]. Figure 3 shows the calculated electronic transition absorption losses for PMMA, PS, and PC. The electronic transition absorption loss of PMMA is remarkably small in

Polymer Optical Fiber, Fig. 3 Calculated electronic transition absorption losses of PMMA, PS, and PC
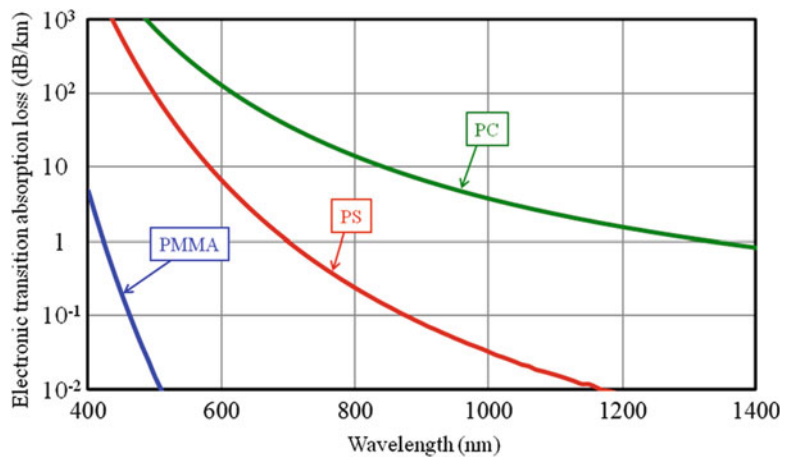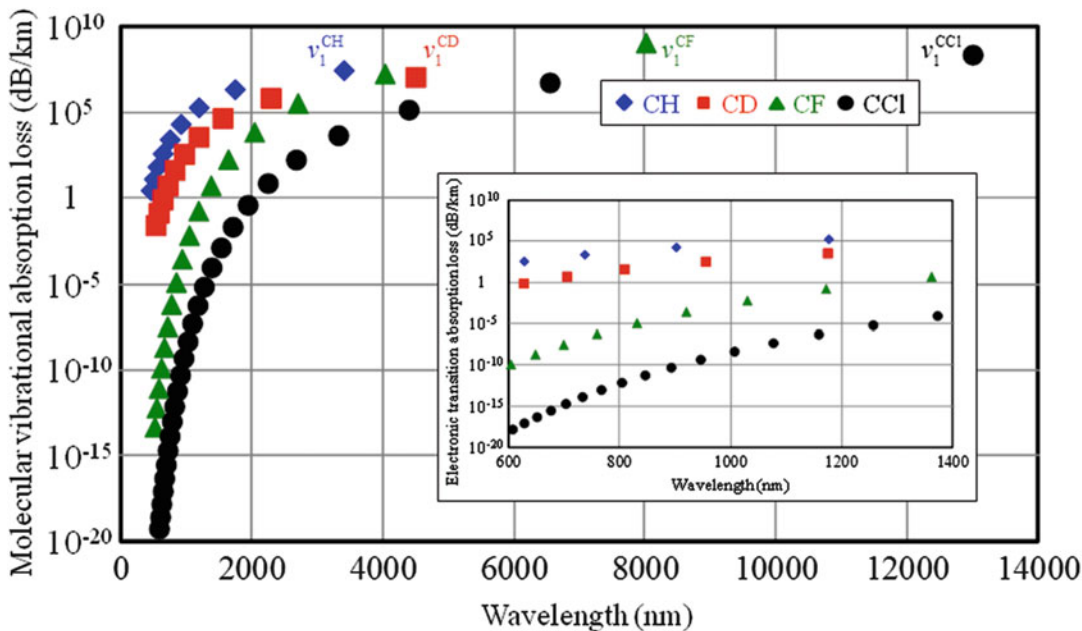
Polymer Optical Fiber, Fig. 4 Calculated absorption losses due to overtones of molecular vibrations of CH, CD, CF, and CCl bonds. Inset shows the magnified wavelength range of interest

the visible wavelength region, and negligible in POF applications, because the loss decreases exponentially with increasing wavelength. In contrast, PS and PC exhibit relatively large electronic transition absorption losses because of the transition from π to π* in the benzene rings.

Absorption in the wavelengths from the visible to near-IR regions is primarily caused by harmonics and the couplings of vibrations of chemical bonds. Vibrational absorptions of carbon-hydrogen (CH) bonds strongly affect the transmission losses of POFs in this wavelength region. The effect of vibrational absorptions of CH bonds can be reduced by replacing the hydrogen with a heavier atom X. The molecular vibrational absorption loss α_{mv} due to the overtone vibration of the CX bonds, based on the Morse potential and Lambert-Beer law, is described by

$$\alpha_{mv} = 3.2 \times 10^8 \frac{\rho}{M} N^{CX} \left(\frac{E_v^{CX}}{E_1^{CH}} \right), \qquad (4)$$

where ρ is the density, M is the molecular weight of the monomer, N^{CX} is the number of CX bonds in the monomer unit, v is the vibrational quantum

number, and E_v^{CX}/E_1^{CH} denotes the energy ratio of the v-th vibration of the CX bond to the fundamental vibration of the CH bond [13]. Figure 4 shows the calculated absorption losses caused by the overtones of molecular vibrations of various CX bonds, where the typical physical constants of PMMA were adopted, and these parameters were assumed to be unaffected by substituting deuterium (D), fluorine (F), and chlorine (Cl) for the hydrogen. The absorption intensities decrease by one order when increasing the v value by one. In addition, the fundamental vibration wavelengths shift to much longer wavelengths when heavier atoms are substituted for the hydrogen. Therefore, the effect of the vibrational absorption can be dramatically reduced and become negligible in the visible and IR regions by replacing the hydrogen with heavier atoms.

Scattering Loss

Scattering losses arise from refractive index variations caused by microscopic heterogeneous structures, such as fluctuations in material density or composition. Refractive index variations smaller than the wavelength induce Rayleigh

Polymer Optical Fiber,
Fig. 5 Calculated
scattering losses of PMMA,
PS, and PC
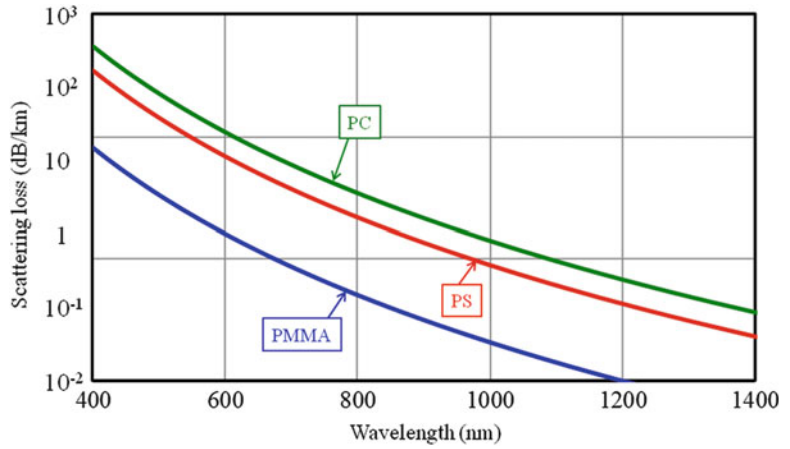
scattering. The optical power attenuation due to Rayleigh scattering α_{Rs} is described by

$$\alpha_{Rs} = 10\log(e)\frac{8\pi^3}{3\lambda^4}n^8 p_e^2 k_B T_f \beta_T, \qquad (5)$$

where n is the refractive index, p_e is the photoelastic coefficient, k_B is the Boltzmann constant, β_T is the isothermal compressibility of the material, and T_f is not the actual temperature of the material but the fictive temperature at which the density fluctuations are frozen. Scattering intensity is inversely proportional to the fourth power of the wavelength; hence, the Rayleigh scattering loss can be roughly estimated by [9]

$$\alpha_{Rs}(\lambda) = \alpha_{Rs}(\lambda_0)\left(\frac{\lambda_0}{\lambda}\right)^4. \qquad (6)$$

Thus, the scattering loss decreases dramatically with increasing wavelength. In addition, a lower refractive index or lower isothermal compressibility of a material also lead to lower scattering loss. The inevitable scattering loss has been experimentally analyzed, based on thermal fluctuation theory derived by Einstein [14], for PMMA, PS, and PC. Figure 5 shows the scattering losses of PMMA, PS, and PC calculated using Eq. 6. The scattering losses of PS and PC are much higher than that of PMMA because of the optical anisotropy of the benzene rings. The intrinsic scattering

loss of PMMA has only a slight influence on the total attenuation in the visible and near-IR wavelength regions, although extrinsic scattering strongly affects the transmission loss in practice.

Bandwidth

The bandwidth, or transmission capacity, of a fiber determines the maximum transmission data rate or the maximum transmission distance. Most optical fiber communication systems adopt pulse modulation. If an input pulse waveform can be detected without distortion at the other end of the fiber, except for the decrease in optical power, the maximum link length is limited by the fiber attenuation. However, in addition to the optical power attenuation, the output pulse is generally broader in time than the input pulse. This pulse broadening restricts the bandwidth of the fiber. The bandwidth is determined by the impulse response as follows [10]. Optical fibers are usually considered to be quasilinear systems, and thus the output pulse is described by

$$p_{out}(t) = h(t) * p_{in}(t). \qquad (7)$$

The output pulse $p_{out}(t)$ from the fiber can be calculated in the time domain through the convolution (denoted by *) of the input pulse $p_{in}(t)$ and the impulse response function $h(t)$ of the fiber. The Fourier transformation of Eq. 7 provides

a simple expression for the product in the frequency domain:

$$P_{\text{out}}(f) = H(f)P_{\text{in}}(f), \qquad (8)$$

where $H(f)$ is the power transfer function of the fiber at the baseband frequency f. The power transfer function defines the bandwidth of the optical fiber as the lowest frequency at which $H(f)$ is reduced to half the value of that at DC. The power transfer function is easily determined from the Fourier transform of the experimentally measured input and output pulses in the time domain or from the measurement of the output power from the fiber in the frequency domain from DC to the bandwidth frequency. A higher bandwidth means less pulse broadening and enables higher-speed data transmission. The bandwidth limitation also largely determines the maximum link length for a given data rate in some MMF systems. The pulse broadening, theoretically proportional to the fiber length, is primarily caused by two mechanisms of dispersion in POFs. One is intermodal dispersion; the other is intramodal dispersion. The rms width of the impulse response σ is calculated as

$$\sigma = \sqrt{\sigma_{\text{inter}}^2 + \sigma_{\text{intra}}^2}, \qquad (9)$$

where σ_{inter} and σ_{intra} are the rms widths of the pulse broadening induced by intermodal and intramodal dispersions, respectively. Another type of dispersion, called polarization mode dispersion, arises from the anisotropies of the structure and material, which result in slightly different propagation constants for the two orthogonal polarization modes. The effect of polarization mode dispersion usually can be ignored in MMFs. Therefore, this section explains the intermodal and intramodal dispersions and the bandwidths of POFs.

Intermodal Dispersion

Intermodal dispersion, or modal dispersion, can be briefly explained as follows (see also section "Historical Background"). When an optical pulse is input into a MMF, the optical power of the pulse is generally distributed to large number of the fiber modes. Different modes travel at different propagation speeds along the fiber; thus, different modes launched at the same time reach the output end of the fiber at different times. Therefore, the input pulse is broadened in time as it travels along the MMF.

This pulse-broadening effect, well known as modal dispersion, is significantly observed in SI MMF. The modal dispersion is generally a dominant factor of the pulse broadening in MMFs. However, the modal dispersion can be dramatically reduced by forming a near-parabolic graded refractive index profile in the core region of MMF. The refractive index distribution strongly affects the bandwidth of MMF. The optimization of the refractive index profile in GI MMFs is an important issue for reducing the modal dispersion. A power-law index profile approximation is a well-known method for analyzing the optimum profile of GI MMFs [3]. In the power-law profile approximation, the refractive index distribution of a GI MMF is described by

$$n(r) = \begin{cases} n_1 \left[1 - 2\Delta\left(\frac{r}{a}\right)^g \right]^{\frac{1}{2}} & \text{for} \quad 0 \leq r \leq a, \\ n_2 & \text{for} \quad r > a \end{cases}$$
$$(10)$$

where $n(r)$ is the refractive index as a function of radial distance r from the core center, n_1 and n_2 are the refractive indices of the core center and the cladding, respectively, and a is the core radius. The profile exponent g determines the shape of the refractive index profile, and Δ is the relative index difference, given by

$$\Delta = \frac{n_1^2 - n_2^2}{2n_1^2}. \qquad (11)$$

Equation 10 includes the SI profile when $g = \infty$.

An optimum profile exponent g_{opt}, which minimizes the modal dispersion and the difference in delay of all the modes and maximizes the bandwidth, is expressed as follows based on the analysis of Maxwell's equations:

$$g_{\text{opt}} = 2 + \varepsilon - \Delta \frac{(4 + \varepsilon)(3 + \varepsilon)}{5 + 2\varepsilon}, \qquad (12)$$

$$\varepsilon = -\frac{2n_1}{N_1} \frac{\lambda}{\Delta} \frac{d\Delta}{d\lambda}, \quad N_1 = n_1 - \lambda \frac{dn_1}{d\lambda}. \qquad (13)$$

Equation 12, in the absence of the wavelength dependence of the refractive index of a material, becomes the simple expression

$$g_{\text{opt}} = 2 - \frac{12}{5}\Delta. \qquad (14)$$

High bandwidth can be typically achieved when the profile exponent g is approximately 2.0. However, the refractive indices of materials generally depend on the wavelength, which induces profile dispersion.

Profile dispersion is caused by the wavelength dependence of the refractive index [3]. The profile dispersion p is given by

$$p = \frac{\lambda}{\Delta} \frac{d\Delta}{d\lambda}. \qquad (15)$$

The g_{opt} value depends on the relative index difference Δ, which is a function of the refractive indices of the core and the cladding. These refractive indices are determined by the wavelength and the dopant characteristics. If the polymer matrix and dopant have an identical wavelength dependence of the refractive index, the g_{opt} value obeys Eq. 14. However, the wavelength dependence of the refractive index of the dopant is generally different from that of the polymer matrix; hence, the shape of the refractive index profile depends on the wavelength. Therefore, even if the optimum refractive index profile is provided at a particular wavelength, this refractive index profile is different from the optimum profile at another wavelength. The profile dispersion also depends on the wavelength of the light signal. The effect of the profile dispersion can be compensated for by the refractive index profile by taking it into account, which is easily explained by Eqs. 12, 13, and 15. Thus, the g_{opt} value is shifted by the profile dispersion. Consequently, the intermodal dispersion can be minimized by the optimum refractive index profile by taking the profile dispersion into account. Then, intramodal dispersion becomes important for achieving high bandwidth. Additionally, SMFs exhibit even higher bandwidths than GI MMFs because the modal dispersion does not exist in principle; thus, intramodal dispersion seriously restricts the bandwidth of SMF [3].

Intramodal Dispersion

Intramodal dispersion, or chromatic dispersion, is the pulse widening caused by the finite spectral width of the light source. Intramodal dispersion comprises material and waveguide dispersions.

Material dispersion is induced by the wavelength dependence of the refractive index of the core material [10]. The group velocity of a given mode depends on the wavelength, and the output pulse is thus broadened in time, even when optical signals with different wavelengths travel along the same path. This effect is generally much smaller than the modal dispersion in MMFs; however, it is no longer negligible when the modal dispersion is sufficiently suppressed.

Waveguide dispersion arises from the wavelength dependence of the optical power distribution of a mode between the core and cladding. Light at shorter wavelengths is more completely confined to the core region, while light at longer wavelengths is more distributed in the cladding. Light at longer wavelengths has a greater portion in the cladding and thus travels at higher propagation speed because the refractive index of the cladding is lower than that of the core, i.e., the effective refractive index is lower.

Low Attenuation and High-Bandwidth Polymer Optical Fiber

The attenuations of the first reported SI and GI POFs were greater than 1,000 dB/km. The various analyses of the intrinsic factors of fiber attenuation described above revealed the theoretical limit of transmission loss and clarified that such high attenuations were not strongly affected by the intrinsic factors, but were mainly induced by the extrinsic factors, e.g., contaminations and

Polymer Optical Fiber,
Fig. 6 Measured
attenuation spectra of
PMMA-, PMMA-d8-, and
CYTOP-based GI POFs
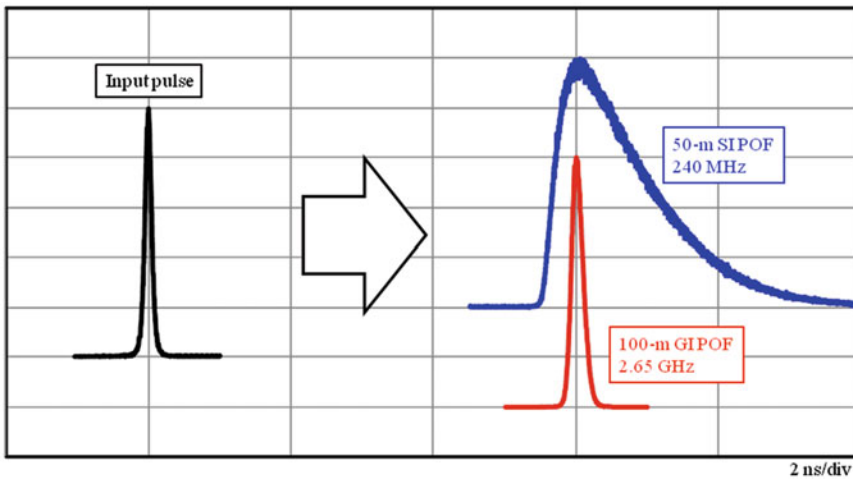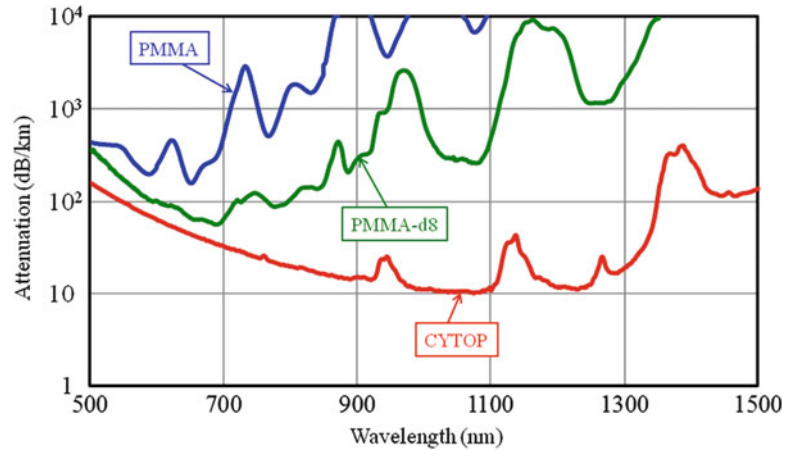
Polymer Optical Fiber, Fig. 7 Measured output pulse waveforms through 50-m SI and 100-m GI POFs under overfilled mode launch conditions

structural imperfections. There are various reports of further reductions in attenuation by substituting heavier atoms for the hydrogen [15]. Figure 6 shows the measured attenuation spectra of GI POFs based on PMMA, perdeuterated PMMA (PMMA-d8), and a perfluorinated polymer that is commercially available with a trade name of CYTOP. The remarkable reductions in the transmission losses of GI POFs were experimentally observed because of the substitution of the hydrogen. The CYTOP-based GI POF exhibited extremely low attenuation because of the low absorption loss due to the absence of the CH bond and the low scattering loss resulting from

the low refractive index as mentioned above, although the extrinsic factors were still not entirely eliminated.

Large number of modes, typically more than tens of thousands, can propagate in POFs because of the large cores. Therefore, decreasing the modal dispersion has been a key issue in POFs. The measured output pulses from PMMA-based 50-m SI and 100-m GI POFs under overfilled mode launch conditions are shown in Fig. 7. In the SI POF, the output pulse was significantly broadened compared with the input pulse, and the bandwidth was seriously restricted. The GI POF was proposed to improve the bandwidth

Polymer Optical Fiber, Fig. 8 Material dispersions of PMMA, CYTOP, and silica
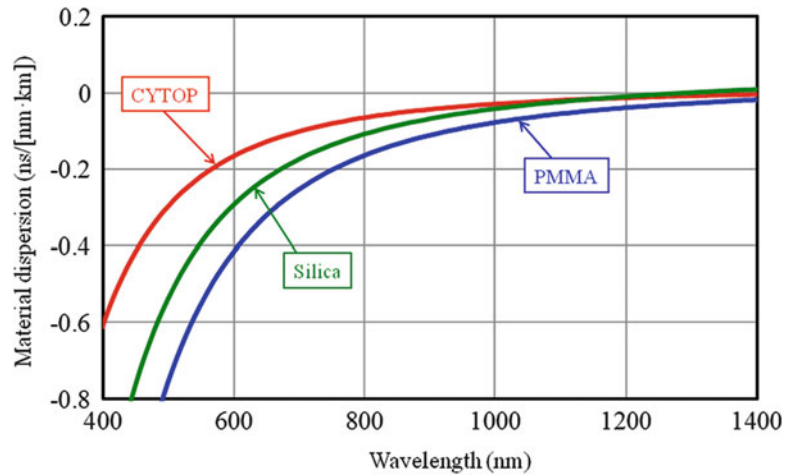
limitation induced by the large modal dispersion of the SI POF [7], and the refractive index profile can be precisely controlled for optimization [12]. The bandwidth of the GI POF was dramatically enhanced to be several GHz for 100 m by the precise control of the refractive index profile. This is the effect of the decrease in the modal dispersion primarily caused by the GI profile.

Further bandwidth improvement has been investigated using perfluorinated polymers [16]. Perfluorinated polymers have valuable characteristics of low material dispersions as well as low transmission losses. Figure 8 shows the material dispersions of PMMA, CYTOP, and silica calculated from the wavelength dependences of their refractive indices. CYTOP has a material dispersion much smaller than PMMA and even lower than silica, particularly in the wavelength region from the visible to near-IR, which means that CYTOP-based GI POFs with an optimum refractive index profile can realize a higher bandwidth than silica-based GI MMFs. The CYTOP-based GI POFs demonstrated 40 Gb/s and higher data transmissions over 100 m [17]. The material dispersion curve of CYTOP was insensitive to the wavelength, compared with silica and PMMA. Thus, the bandwidth of CYTOP-based GI POFs is also expected to be insensitive to the wavelength.

The wavelength dependences of the bandwidths of 100-m PMMA and CYTOP-based GI POFs and silica-based GI MMF were theoretically estimated from their material dispersions, as shown in Fig. 9, where the refractive index profiles of all the fibers were optimized at a wavelength of 850 nm and the rms spectral width of the light source was assumed to be 1.0 nm. The wavelength dependence of the optimum profile was small in CYTOP-based GI POFs, as mentioned above, because CYTOP has low material and profile dispersions. Therefore, the CYTOP-based GI POF can maintain high-bandwidth characteristics over a wider wavelength range compared with silica-based GI MMFs. Consequently, CYTOP-based GI POFs can utilize various light sources with larger varieties of wavelengths, and hence more channels are available in wavelength division multiplexing (WDM) systems, which indicates that CYTOP-based GI POFs can realize higher data rate communication systems.

Applications

Demand for optical fiber communications substituting for electrical wiring is rapidly increasing not only in long-haul networks but also in short-reach networks such as LANs and even interconnections. A bit rate greater than tens of Gb/s will be required in these networks. GI POFs are attracting a great deal of attention for intrabuilding and interconnection networks because of their high bandwidth, low bending loss, high flexibility, and large core, which allows

Polymer Optical Fiber, Fig. 9 Calculated bandwidths of PMMA- and CYTOP-based GI POFs and silica-based GI MMFs as a function of wavelength. Their refractive index profiles were optimized at a wavelength of 850 nm, and the rms spectral width of the light source was assumed to be 1 nm
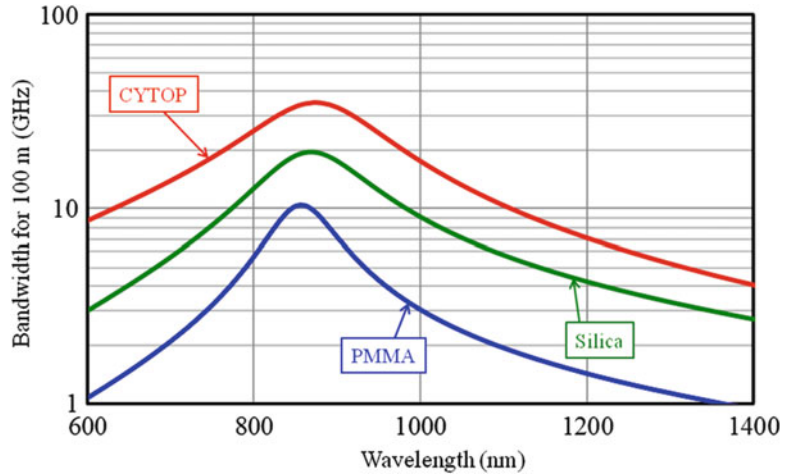
easy handling and rough connections and thus enables easy installation of a high-speed network at a low cost. In addition to the inherent flexibility, there is no fear of GI POFs causing human injury, even if the GI POF is broken and the fiber end is exposed. Silica fibers are easily broken by physical contact, and the broken pieces are dangerous because most broken silica glasses have sharp edges. This is a great advantage of GI POFs for consumer use. The GI POF is also expected to be used even in automotive or aircraft networks because the GI POF has no electromagnetic interference problems in principle and because the GI POF is lighter in weight than a metal cable, which leads to higher energy efficiency.

More realistic video image and more real-feeling face-to-face communication requires higher resolution, more natural color, and higher frame rates. Thus, higher and higher data rate transmission will become essential technology in the near future. A video transmission in the format of 8-K ultrahigh definition (8-K UHD) typically requires a data rate greater than 100 Gb/s, which means that more than ten conventional copper cables are required because the bandwidth of the copper cable is severely limited. A bundle of many copper cables induces significant problems in practical use because of the thick, stiff, and heavy cable and the space-consuming interface. In contrast, the high-bandwidth GI POF is thin, flexible, and lightweight, and the interface can be quite compact, even if several GI POFs are packed into a bundle. Thus, the GI POF allows easy handling and rough connections.

Another advantage of the GI POF is observed in radio over fiber (RoF), analog signal transmission. Analog signals cannot be transmitted correctly through the silica MMF because of some types of noise. Analog video signal has been transmitted through the GI POF and silica MMF with the same optical transceivers. The received video image through the silica MMF was too noisy to be watched and enjoyed. In contrast, the clear video image was observed through the GI POF.

These characteristics are great advantages of the GI POF for interconnection, mounting design, and consumer use. Low-loss and high-bandwidth GI POFs will accelerate a remarkable paradigm shift in network architecture and home appliances.

Related Entries

▶ Light Scattering of Polymer
▶ Optical Absorption of Polymers

References

1. Born M, Wolf E (1999) Principles of optics: electromagnetic theory of propagation, interference and diffraction of light, 7th edn. Cambridge University Press, Cambridge
2. Hecht J (2005) Understanding fiber optics, 5th edn. Prentice Hall, New Jersey, USA.

3. Olshansky R (1979) Propagation in glass optical waveguides. Rev Mod Phys 51:341–367. doi:10.1103/RevModPhys.51.341
4. Ball P (2012) Computer engineering: feeling the heat. Nature 492:174–176
5. Polishuk P (2006) Plastic optical fibers branch out. IEEE Commun Mag 44:140–148. doi:10.1109/MCOM.2006.1705991
6. Cunningham DG, Lane WG (1999) Gigabit ethernet networking. Macmillan Technical Publishing, Indianapolis
7. Koike Y (1991) High-bandwidth graded-index polymer optical fibre. Polymer 32:1737–1745. doi:10.1016/0032-3861(91)90356-n
8. Gloge D, Marcatili EAJ (1973) Multimode theory of graded-core fibers. Bell Syst Tech J 52:1563–1578
9. Zubia J, Arrue J (2001) Plastic optical fibers: an introduction to their technological processes and applications. Opt Fiber Technol 7:101–140. doi:10.1006/ofte.2000.0355
10. Keiser G (2010) Optical fiber communications, 4th edn. McGraw Hill, New York
11. Urbach F (1953) The long-wavelength edge of photographic sensitivity and of the electronic absorption of solids. Phys Rev 92:1324–1324
12. Kaminow IP, Li T, Willner AE (2013) Optical fiber telecommunications vi. Academic, Oxford
13. Groh W (1988) Overtone absorption in macromolecules for polymer optical fibers. Makromol Chem 189:2861–2874
14. Einstein A (1910) Theory of opalescence of homogenous liquids and liquid mixtures near critical conditions. Ann Phys 33:1275–1298
15. Tanio N, Koike Y (2000) What is the most transparent polymer? Polym J 32:43–50. doi:10.1295/polymj.32.43
16. Koike Y, Ishigure T (2006) High-bandwidth plastic optical fiber for fiber to the display. J Lightwave Technol 24:4541–4553. doi:10.1109/jlt.2006.885775
17. Decker PJ, Polley A, Kim JH, Ralph SE (2011) Statistical study of graded-index perfluorinated plastic optical fiber. J Lightwave Technol 29:305–315

Polymer Reagents

Kensuke Naka
Department of Chemistry and Materials Technology, Graduate School of Science and Technology, Kyoto Institute of Technology, Sakyo-ku/Kyoto, Japan

Synonyms

Polymer-supported reagents; Solid-supported reagents

Definition

Polymer reagents are those which possess reactive organic groups either covalently or ionically bonded to a macromolecular support and used in stoichiometric quantities to induce the chemical reaction of an added substrate.

What Is the Polymer Reagent?

In a polymer reagent, reactive organic groups are either covalently or ionically bonded to a macromolecular support and used in stoichiometric quantities to achieve the chemical reaction of an added substrate (Fig. 1) [1–3]. The use of polymer reagents as well as polymer catalysts can generally combine the benefits of solid-phase chemistry with the advantages of solution-phase synthesis. The polymer catalyst is a conventional catalytic species attached to a macromolecular support as described in the previous topic. Polymer catalysts are generally used in catalytic quantities relative to reaction substrates and can often be reused many times. On the other hand, the polymer reagents have been employed as stoichiometric reagents. After the chemical reaction using the reactive groups in the polymer reagents, resulting by-products remain attached to the insoluble polymer and can be removed by simple filtration instead of standard workup techniques. Some of these can be regenerated for repeated use.

Starting with the introduction of solid-phase peptide synthesis by Merrifield in 1963, insoluble supports such as low cross-linked polystyrene have been implemented in a wide range of synthetic methodologies. The use of polymer supports in organic synthesis has become common practice, especially following the rapid development of combinatory chemistry. The increasing demands in the drug discovery process have led to a shift in attention away from solid-supported organic chemistry toward liquid-phase parallel synthesis.

Despite the well-known advantage of insoluble supports, there are several shortcomings in the use of these resins due to the heterogeneous

P

Polymer Reagents, Fig. 1 Reaction of polymer reagents

nature of the reaction conditions. By replacing insoluble supports with soluble polymers, reagents and catalysts attached to the soluble polymers can have essentially the same reactivity as their low-molecular-weight counterparts. However, product purification is still facilitated through application of macromolecular properties. Therefore, the use of soluble polymer-supported reagents and catalysts has gained significant attention as an alternative to traditional solid-phase synthesis [4].

History

Merrifield first reported the concept of solid-phase peptide synthesis using heterogeneous chloromethylated polystyrene that was 2 % cross-linked by divinylbenzene (Merrifield resin) in 1963. Merrifield peptide synthesis is the most highly developed method of synthesis with solid supports. Every step of the synthesis is carried out in the same polymer. The basic steps are as follows (Fig. 2). Step (1) an *N*-protected amino acid is attached as an ester to a cross-linked polystyrene support. Step (2) the protecting group is removed. Step (3) an *N*-protected, activated amino acid is coupled to the amino group of the polymer-bound amino acid. Steps 2 and 3 are repeated with different amino acids to produce a desired peptide sequence. Step (4) the completed peptide is cleaved from the polymer, deprotected, and purified.

The key features of the Merrifield method that have led to its widespread use are as follows. At each stage of the synthesis, the polymer-bound peptide can be separated from all other components of the reaction mixture by filtration. This makes possible the use of a large excess of the soluble *N*-protected amino acid to drive each coupling step to high conversion. In addition, the method can be automated.

Advantage and Disadvantage

Most of the advantage and disadvantage of the polymer reagents are overlapped with those of polymer catalysts. The polymer-bound species, i.e., reagents, catalysts, products, or by-products, can be separated from the reaction mixture. Macroscopic solids and gels can usually be separated from liquids by simple filtration. Soluble polymers and colloids can be separated from low-molecular-weight compounds by ultrafiltration. Polymer-supported reagents are potentially adaptable to continuous flow processes, and features reduced toxicity and odor of supported species compared with low-molecular-weight species and chemical differences, such as prolonged activity or altered selectivity of a reagent, in supported form compared with its soluble analog. However, main disadvantages of supported reagents are (1) higher cost, (2) lower reactivity due to diffusional limitations, (3) greater difficulty of analysis of the structure of the supported species and of impurities, (4) inability to separate polymer-bound impurities, and (5) lesser stability of organic supports than of inorganic supports.

Considerable effort has been devoted to the modification of polymeric reagents to give chemoselectivities different from those of soluble reagents. These modifications often depend upon the reduced mobility of polymer-bound species compared with low-molecular-weight species. The regenerability and efficiency of polymer usage are most important with polymer-support reagents. Among the easily regenerated reagents are those based on ion exchange resins, which require only a treatment with an excess of the ionic reactant for regeneration. For example, the phosphine oxide by-products of Wittig reactions can be regenerated to phosphines as described below.

Preparation

The supports that Merrifield utilized for his early work in solid-phase peptide synthesis were based on 2 % divinylbenzene cross-linked polystyrenes which require solvent swelling for reagents to

Polymer Reagents,
Fig. 2 Basic steps of
Merrifield peptide
synthesis
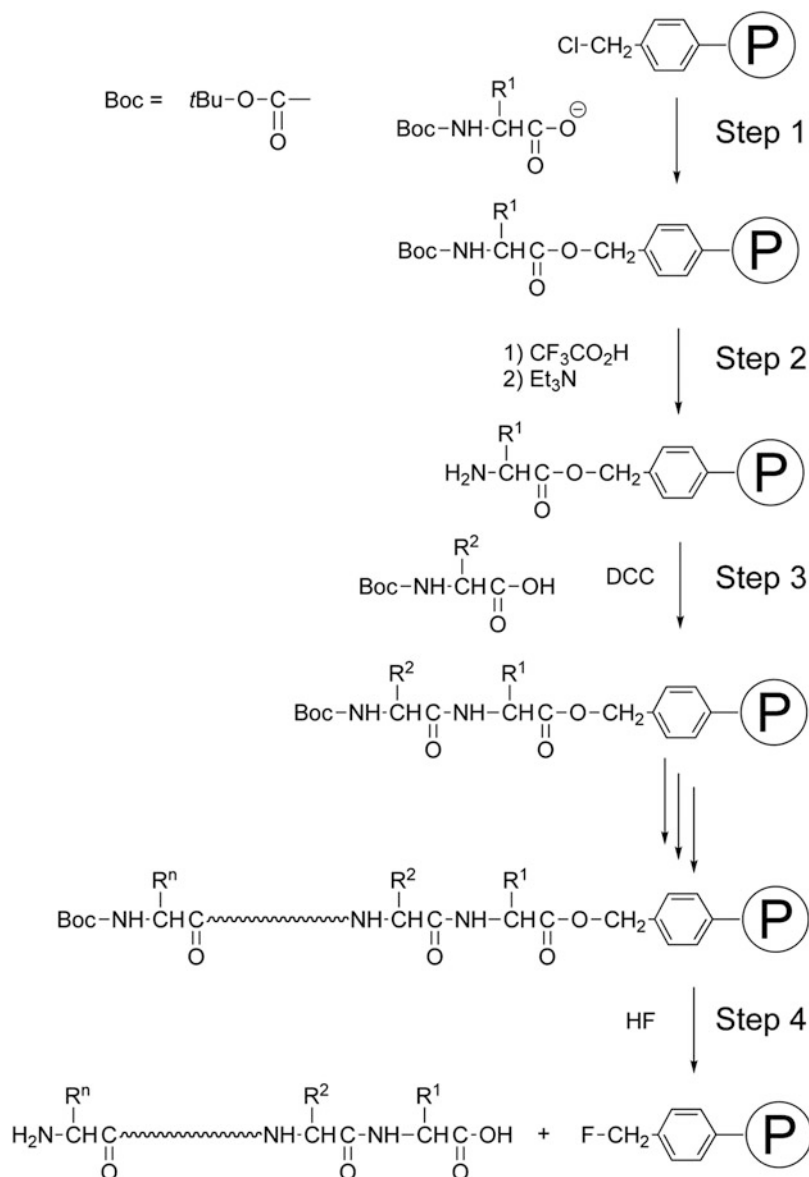
access internal functional groups. Polystyrene is still one of the most popular polymeric materials used due to its inexpensiveness, ready availability, mechanical robustness, chemical inertness, and facial functionalization. The polymer is most commonly prepared by copolymerization with reactive monomers such as chloromethylstyrene or bromomethylstyrene, thus ensuring an even site distribution of the functionalized sites within the polymer matrix. The resins of high quality are normally employed

and the desired functional groups introduced by using polymer reactions.

To improve the performance of polymer supports, many strategies have been developed. Macroporous ion exchange type resins based on polystyrene are also widely used. Cross-linkers other than divinylbenzene are possible to modulate the physical and chemical properties of the resins. Other polymers such as polyisobutylenes, polynorbornenes, poly(ethylene glycol)s, and polysiloxanes are also available [3].

Polymer Reagents,
Fig. 3 Wittig reaction by
use of an insoluble
polymeric phosphine
reagent
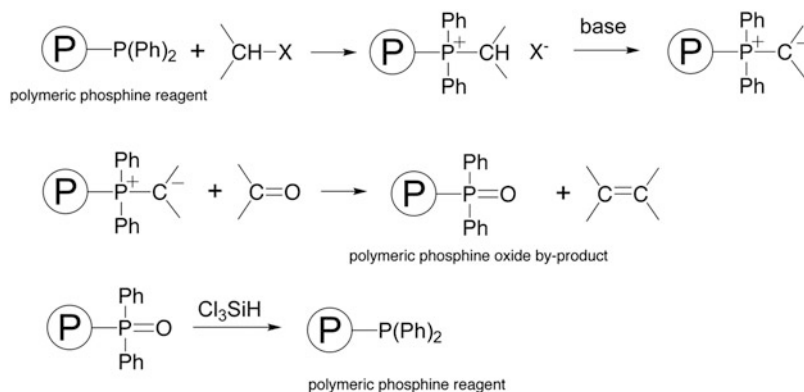
Examples

Several examples of the most useful and common polymer reagents in organic synthesis are briefly introduced.

In spite of the widespread application of the Wittig reaction to olefin synthesis, a principal disadvantage of this reaction is the difficulty of separating the main product from the by-product, triphenylphosphine oxide. However, by use of the insoluble polymeric phosphine reagent, the by-product remains attached to the polymer after the reaction and is readily separated from the desired product (Fig. 3). Moreover, the polymeric phosphine oxide by-product can be readily recycled and reused in further Wittig reactions.

Insoluble polymer-bound carbodiimide derivatives have been prepared and used as condensing agents in the synthesis of peptides. Polymeric carbodiimides have the advantage that the by-product, urea, remains attached to the polymer and can be readily converted back into the polymeric carbodiimide.

Polymer redox reagents were one of the earliest examples of polymeric reagents, because of the relative difficulty in the preparation of redox reagents and in working up of reaction mixtures. Important polymeric redox reagents are hydroquinone-quinone, thiol-disulfide, pyridine-dihydropyridine, polymeric dyes, and polymeric metal complex system.

Several functional polymers have been reported for use in the acylation and alkylation of different substrates. For example, an insoluble polymer containing the anhydride functional group was used for the conversion of an amine or alcohol to amide or ester. The insolubility of the resin-bound reagent can have the effect of isolating the reactive groups on the polymer from each other. The reactive carbanion derivative of a bound ester is first generated, and self-condensation with unreacted ester is inhibited by the rigid matrix. The production of these stable monoanions then allows reaction with acyl or alkyl halides to give selectively monoacetylated or monoalkylated products.

Related Entries

▶ Cross-Linked Polymer Synthesis
▶ Polymer Catalysts
▶ Polymeric Drugs
▶ Polystyrene (PSt)

References

1. Akelah A, Sherrington DC (1981) Application of functionalized polymers in organic synthesis. Chem Rev 81:557–587
2. Kraus MA, Patchornik A (1980) Polymeric reagents. J Polym Sci Macromol Rev 15:55–106. doi:10.1002/pol.1980.230150103
3. Lu J, Toy PH (2009) Organic polymer supports for synthesis and for reagent and catalyst immobilization. Chem Rev 109:815–838. doi:10.1021/cr8004444
4. Dickerson TJ, Reed NN, Janda KD (2002) Soluble polymers as scaffolds for recoverable catalysts and reagents. Chem Rev 102:3325–3344. doi:10.1021/cr010335e

Polymer Surfactant

Hideki Matsuoka
Department of Polymer Chemistry, Kyoto
University, Kyoto, Kyoto Prefecture, Japan

Synonyms

Amphiphilic polymer; Polymeric surfactant;
Polysoap

Definition

Polymers having a surface-active nature.

Introduction

"Surfactant" is a coinage from "surface-active
agent." The surfactant molecule consists of a
small, hydrophilic head group and a long, hydro-
phobic tail, whose shape is often compared to a
tadpole. The head is ionic or nonionic, and in
most cases the tail consists of hydrocarbons.
A surfactant is adsorbed at the air/water interface
when dissolved in water, which results in
decrease of surface tension of the solution and
foam formation. This nature is surface activity.
Surfactants form micelles in solution above the
critical micelle concentration (cmc). "Polymer
surfactant" is a surfactant that consists of polymer
both for head and tail groups (Fig. 1). They might

be a block copolymer or graft copolymer. The
polymer surfactant also forms micelles in solu-
tion above cmc. The polymer surfactant generally
has a much lower cmc than the low-molecular
weight surfactant, and its micelle (polymer
micelle) is very stable. The polymer micelle is
mostly a multimolecular micelle with some
aggregation number like the surfactant, but a
unimolecular micelle is possible when the hydro-
philic part is long enough. The polymer micelle is
attracting keen attention as a carrier in the drug
delivery system because of its high stability, suit-
able size, and lower cmc. Since not only the
hydrophobic tail but also the hydrophilic "head
group" is a polymer, a conformational change of
the hydrophilic head chain sometimes drastically
changes the micelle morphology, which can be
applied to stimuli-responsible self-assembling
systems.

Historical Background

It was in 1936 that H. Staudinger established the
existence of "polymer" as a high-molecular
weight molecule that consists of small "mono-
mers" connected by covalent bonds. The first
report on polymeric micelle might be that
in 1964 by Krause [1]. They prepared a
triblock copolymer of poly(methylmethacrylate)
(PMMA) and polystyrene (PS), i.e., PMMA-
b-PS-*b*-PMMA, and measured "molecular
weight" by light scattering in various solvents.
They observed an anomalously high molecular
weight for acetone and triethylbenzene as a
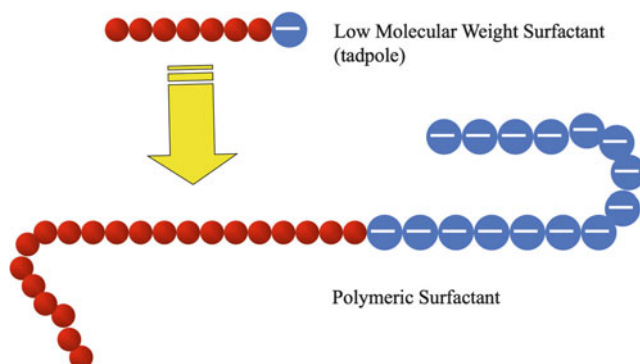
**Polymer Surfactant,
Fig. 1** Low-molecular
weight surfactant and
polymeric surfactant

Low Molecular Weight Surfactant
(tadpole)

Polymeric Surfactant

solvent, while normal molecular weight was found in butanone and toluene. Butanone and toluene are good solvents both for PMMA and PS. Acetone is a good solvent for PMMA but not for PS, and triethylbenzene is a good solvent for PS but not for PMMA. This nature results in micelle and revise-micelle formation, respectively. Recently, di- and triblock copolymers consisting of poly(ethylene oxide) (PEO) and poly(propylene oxide) (PPO), i.e., PEO-PPO and PEO-PPO-PEO, with various block lengths and block ratios have become commercially available, which has contributed to fundamental study and industrial applications of polymer micelle systems [2]. Very recently, in addition to the living ionic polymerization technique, development of living radical polymerization techniques, such as an atom transfer radical polymerization (ATRP) [3], nitroxyl radical-mediated polymerization (NMP) [4], and reversible addition fragmentation chain transfer (RAFT) [5] polymerization techniques, is utilized to prepare novel amphiphilic block copolymers with various combinations of hydrophilic and hydrophobic blocks with strictly controlled molecular weight and distribution.

Examples and Applications

The cmc of surfactants is often estimated by surface tension of the solution. The surface tension decreases with increasing surfactant concentration and then becomes constant. The concentration at the bending point is cmc. However, the bending point for polymeric surfactants is sometimes unclear [6] (Fig. 2). Its origin has not been clarified, but the first possibility is an impurity in the polymer substance since it is generally difficult to purify polymers compared to low-molecular weight surfactants. The second possibility is the molecular weight distribution of polymer surfactant. The synthesized polymer surfactants are not perfectly monodisperse but have a certain molecular weight distribution. Since the cmc, i.e., the bending point in surface tension, depends on molecular weight, the mixture of different molecular weight polymer surfactants gives an unclear bending point.
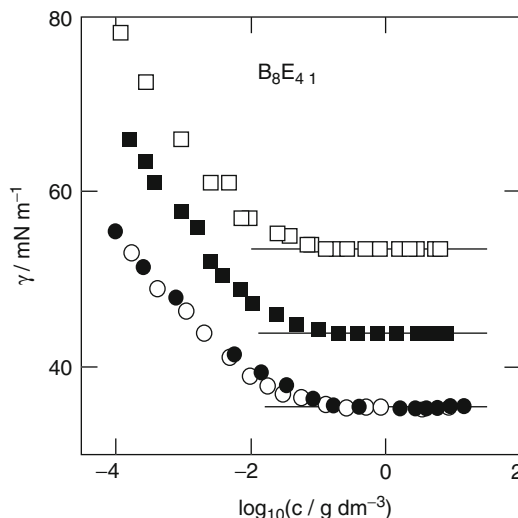
Polymer Surfactant, Fig. 2 Polymer concentration dependence of surface tension of Pluronic polymer in aqueous solution (Reprinted with permission from Ref. [6]. Copyright (1997) American Chemical Society)

Since the "head group" of the polymer surfactant is also a long polymer chain, its conformational change sometimes causes a drastic change of polymer micelle morphology. The micelle size and shape, and also the aggregation number of the micelle, follow the famous concept of the critical packing parameter by Israelachvili [7]. This behavior is the same as that of the low-molecular weight surfactant. The micelle size is governed by the balance of interfacial tension of the core/solvent interface and the steric repulsion between the head group chains. The micelle shape depends on the relative size and length of the head and tail groups: cone-like molecules like spherical micelle formation and cylindrical surfactants like lamellae or vesicle formation. For the ionic polymeric surfactant, whose head group is a polyelectrolyte, salt addition affects its conformation. Not only steric conformation but also inter- and intramolecular electrostatic repulsion of polyelectrolyte contributes to a change in packing parameter. In some cases, the shielding effect on electrostatic repulsion is dominant, and salt addition results in spherical polymer micelle transfer to rodlike micelles [8] (Fig. 3). However, in another case, such as a weakly ionic polyelectrolyte head
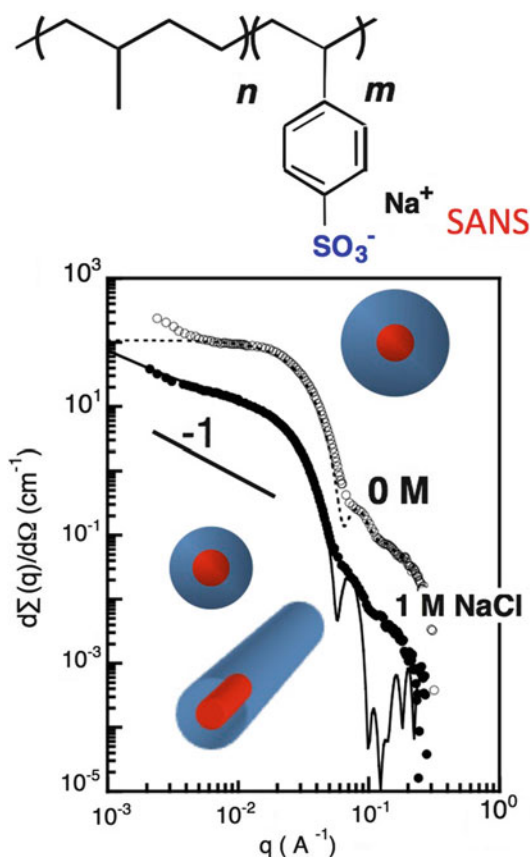
Polymer Surfactant, Fig. 3 Sphere to rod transition of ionic block copolymer in aqueous solution by salt addition. Small-angle neutron scattering (SANS) data (Reprinted with permission from Ref. [8]. Copyright (2007) American Chemical Society)

chain, the spherical polymer micelle changed to a smaller spherical micelle with smaller aggregation number due to the enhanced steric hindrance between head chains, which is shrunken by the electrostatic shielding effect of the added salt [9]. The dominant factor might depend on each system.

A famous application of polymer micelle is the drug carrier in the drug delivery system. Since PEO chain has high biocompatibility, Kataoka et al. prepared diblock copolymer systems of PEO with modified poly(amino acid) and applied it as a drug carrier. Quite interesting is the size effect they found [10]. The polymer micelle is optimum in size as a drug carrier; a smaller or larger micelle is inefficient as a carrier.

The advantage of polymer micelle in this system is the stability of the micelle, and addition of PEO for biocompatibility, and low cmc. Since the drug carrier solution is diluted in the circulation in the body, a low cmc is preferable.

An important factor for polymer micelle systems is the glass transition temperature (Tg) of the hydrophobic block chain. For example, Tg of PS is about 98 °C, which means PS in a glassy state at room temperature. Hence, the polymeric micelle having a PS hydrophobic core is also in a glassy state at room temperature [11]. In surfactant systems and also in most polymer surfactant systems, the micelle and unimer in solution are in dynamic equilibrium. The unimers (one-polymer chains) go into the micelle, but another unimer in the micelle comes out from the micelle into the solvent. Since this dynamic equilibrium cannot be established with the PS system, the polymer micelle with a PS core at room temperature is not in equilibrium. The size and shape can depend on how it was prepared. Since the PS core is glassy, no change in size or shape occurs even by salt addition [11]. To obtain micelle in equilibrium in such a case, a good solvent both for hydrophobic and hydrophilic blocks should be used. In this solvent, the polymer molecules are molecularly dissolved (micelle aggregate is not formed). Then, the solvent is changed to water (or preferable solvent) very slowly by dialysis, for example. This method is also used for drug carrier preparation [12]. If the drug itself is hydrophobic, the drug molecules are taken in the micelle core in dialysis process (Fig. 4).

The PEO chain is biocompatible and also thermosensitive. Many polymers have lower solubility at a higher temperature, and the most famous example is poly(N-isopropylacrylamide) (PNIPAm). PNIPAm is water soluble at room temperature, but it has a transition point at about 34 °C, and it becomes hydrophobic (water insoluble) above it. Its water solution changes from transparent to turbid at this transition temperature, called lower critical solution temperature (LCST). By using this kind of functional polymer, in other words stimuli-responsive polymers, stimuli-sensitive polymer micelle systems can be prepared. The block copolymer, consisting of an

P
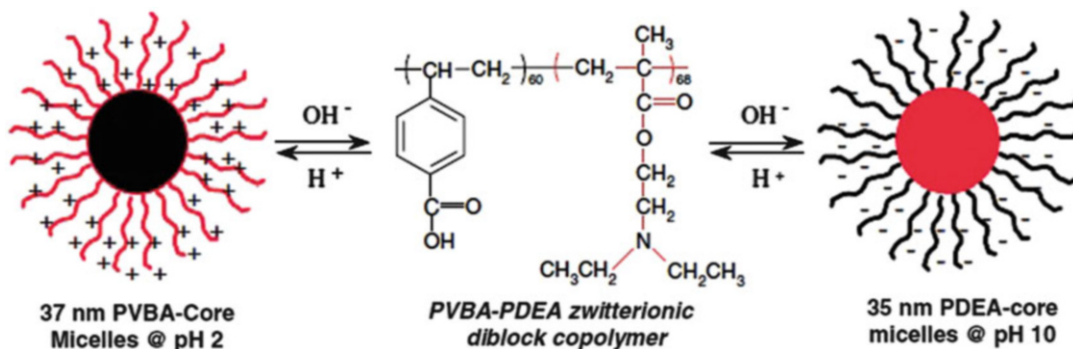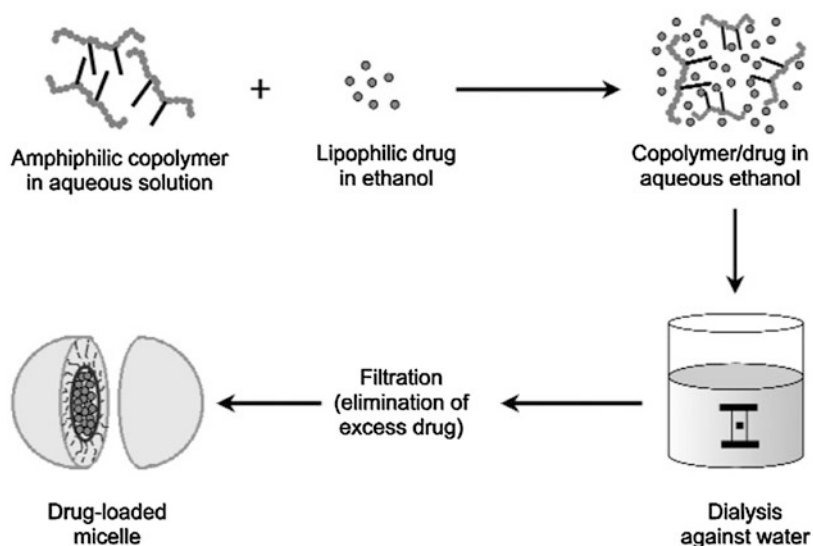
Polymer Surfactant, Fig. 5 pH-depended micelle/unimer/reverse micelle transition behavior of zwitterionic diblock copolymer (Reprinted from Ref. [16] Copyright (2006), with permission from Elsevier)

ionic block and PNIPAm block, can be molecularly dissolved in water at room temperature, but it forms a polymeric micelle above 34 °C which has a "hydrophobic" PNIPAm core [13]. Many kinds of stimuli-responsive units or polymers can be introduced into polymer micelle systems, such as salt concentration, pH, and light irradiation. A famous example is the "schizophrenic micelle" system developed by S. Armes group [14–16]. They introduced one or more stimuli-responsive units in polymeric surfactant molecules and prepared a system, which shows micelle/unimer/reversed micelle transition by stimuli. A micelle/unimer/reversed micelle

transition by only one parameter, i.e., pH, was also shown to be feasible [16] (Fig. 5). By tuning the block ratio of hydrophilic and hydrophobic block in addition to introducing the responsive unit, micelle/unimer/vesicle transition was shown to be possible by changing the pH and temperature [17] (Fig. 6). Needless to say, this kind of responsibility is quite useful for drug delivery application, since the drugs can be released at the target position in the body only.

A very unique property of "polymeric surfactant" was reported by Matsuoka et al. [13, 18]. The ionic amphiphilic diblock copolymers consist of a polyelectrolyte block and hydrophobic
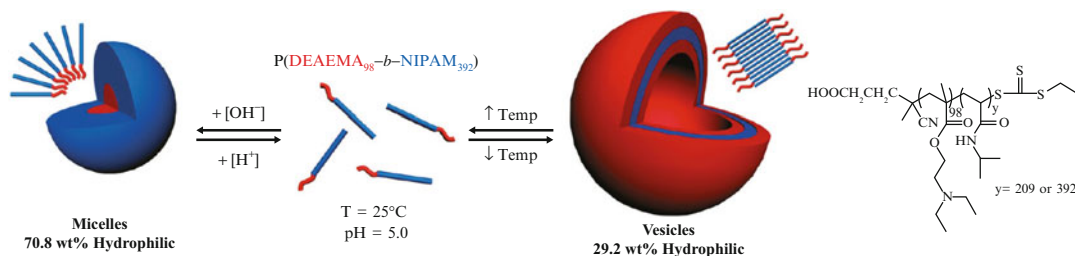
Polymer Surfactant, Fig. 6 pH- and temperature-responsive micelle/unimer/vesicle transition of diblock copolymer in solution (Reprinted with permission from Ref. [17] Copyright (2010) American Chemical Society)

block and become non-surface active, i.e., the surface tension of the solution does not decrease and foam formation is not observed either, while micelles are formed in solution due to its amphiphilic nature. This means that this polymer does not adsorb at the air/water interface; this property is called "non-surface activity." The origin of this very unique character is, in principle, a kind of polymer effect. Since the hydrophobic block is ionic, an electrostatic repulsion from the air/water interface due to an image charge effect is so strong that the polymers can hardly adsorb at the water surface. This effect destabilized the adsorbed state. On the other hand, a very stable polymer micelle is formed in the bulk solution. If this micelle state is more stable than the adsorbed state, which is destabilized by an image charge effect, the molecules do not adsorb at the air/water interface but form a micelle in solution, which is non-surface activity itself.

Polymeric surfactants are also useful as an emulsifier [19]. Graft-type polymeric surfactants are often commercially used as an emulsifier in the industrial field, such as cosmetics. Small surfactant molecules penetrate into the skin, but polymeric surfactants do not since they are large enough, which makes them safe in skin care. Polymeric surfactant micelle particles with polyelectrolyte corona can be applied to nano-reactor since the corona has a very high ion density. Gold nanoparticles can be efficiently synthesized in the ionic corona due to the high concentration of reactant, i.e., Au ions, which are concentrated in the corona as a counterion of the micelle [20].

Related Entries

▶ Block Copolymers
▶ Molecular Self-Organization
▶ Polymer Brushes
▶ Polymeric Micelles
▶ Rodlike Micelles
▶ Surfactant Assemblies (Micelles, Vesicles, Emulsions, Films, etc.), an Overview

References

1. Krause S (1964) Dilute solution properties of styrene-methyl methacrylate block copolymer. J Phys Chem 68(7):1948–1955
2. (a) Batrakova EV, Han H-Y, Miller DW, Kabanov AV (1998) 71. Effects of pluronic P85 unimers and micelles on drug permeability in polarized BBMEC and Caco-2 cells Pharm Res 15:1525–1532 (b) Foster B, Cosgrove T, Hammouda B (2009) Pluronic-Triblock Copolymer Systems and Their Interactions with Ibuprofen, Langmuir 25(12):6760–6766
3. Wang J-S, Matyjaszewski K (1995) Controlled living radical polymerization - atom-transfer radical polymerization in the presence of transition-metal complexes. J Am Chem Soc 117:5614–5615
4. Hawker CJ, Bosman AW, Harth E (2001) New polymer synthesis by nitroxide mediated living radical polymerizations. Chem Rev 101:3661–3688
5. Chiefari J, Chong YK, Ercole F, Krstina J, Jeffery J, Le TPT, Mayadunne RTA, Meijs GF, Moad CL, Moad G, Rizzardo E, Thang SH (1998) Living free-radical polymerization by reversible addition-fragmentation chain transfer: The RAFT process. Macromolecules 31(16):5559–5562
6. Yu G, Yang Z, Ameri M, Attwood D, Collett JH, Price C, Booth C (1997) Diblock copolymers of ethylene oxide and 1, 2-butylene oxide in aqueous solution. Effect of E-block-length distribution on

P

self-association properties. J Phys Chem B 101:4394–4401

7. Israelachvili JN (1991) Intermolecular and surface forces, 2nd edn. Academic, London/New York

8. Kaewsaiha P, Matsumoto K, Matsuoka H (2007) Sphere-to-rod transition of non-surface-active amphiphilic diblock copolymer micelles: A small-angle neutron scattering study. Langmuir 23:9162

9. Imae T (2001) Morphology and nanostructure of amphiphilic polymer micelles with fluorinated core and nonfluorinated corona. Kobunshi Ronbunshu 58(4):178–188 (in Japanese)

10. Cabral H, Matsumoto Y, Mizuno K, Chen Q, Murakami M, Kimura M, Terada Y, Kano MR, Miyazono K, Uesaka M, Nishiyama N, Kataoka K (2011) Accumulation of sub-100 nm polymeric micelles in poorly permeable tumours depends on size. Nat Nanotechnol 6:815–823

11. Matsuoka H, Maeda S, Kaewsaiha P, Matsumoto K (2004) Micellization of non-surface-active diblock copolymers in water. Special characteristics of poly(styrene)-block-poly(styrenesulfonate). Langmuir 20(18):7412–7421

12. Francis MF, Cristea M, Winnik FM (2004) Polymeric micelles for oral drug delivery: Why and how. Pure Appl Chem 76(7–8):1321–1335

13. Ghosh A, Yusa S, Matsuoka H, Saruwatari Y (2013) J Chem Biol Interface 1(1):41–48

14. Bütün V et al (1998) Unusual aggregation behavior of a novel tertiary amine methacrylate-based diblock copolymer: Formation of micelles and reverse micelles in aqueous solution. J Am Chem Soc 120:11818

15. Liiu SY, Billingham NC, Armes SP (2001) A schizophrenic water-soluble diblock copolymer. Angew Chem Int Eng 40:2328

16. Bütün V, Liu S, Weaver JVM, Bories-Azeau X, Cai Y, Armes SP (2006) A brief review of 'schizophrenic' block copolymers. React Funct Polym 66:157

17. Smith AE, Xu X, Kirkland-York SE, Savin DA, McCormick CL (2010) "Schizophrenic" Self-Assembly of Block Copolymers Synthesized via Aqueous RAFT Polymerization: From Micelles to Vesicles. Macromolecules 43(3):1210–1217

18. Matsuoka H, Chen H, Matsuomoto K (2012) Molecular weight dependence of non-surface activity for ionic amphiphilic diblock copolymers. Soft Matter 8(35):9140–9146

19. Rager T, Meyer WH, Wegner G, Mathauer K, Mächtle W, Schrof W, Urban D (1999) Block copolymer micelles as seed in emulsion polymerization. Macromol Chem Phys 200:1681

20. Sharma S, Ballauff M (2004) Cationic spherical polyelectrolyte brushes as nanoreactors for the generation of gold particles. Macromol Rapid Commun 25:547

Polymer Synthesis via Click Reactions

Haiqiang Wu[1], Jingzhi Sun[1], Anjun Qin[1,3] and Ben Zhong Tang[1,2,3]
[1]MOE Key Laboratory of Macromolecular Synthesis and Functionalization, Department of Polymer Science and Engineering, Zhejiang University, Hangzhou, China
[2]Department of Chemistry, Institute for Advanced Study, Institute of Molecular Functional Materials, The Hong Kong University of Science and Technology, Kowloon, Hong Kong, China
[3]Guangdong Innovative Research Team, State Key Laboratory of Luminescent Materials and Devices, South China University of Technology, Guangzhou, China

Synonyms

1,3-Dipolar polycycloaddition; Polytriazole

Definition

The polymer synthesis via click reactions refers to a kind of polymers that were synthesized by the reactions enjoying such advantages as high efficiency, mild reaction conditions, regioselectivity, and functional tolerance. The representative example is the polytriazoles synthesized by the azide-alkyne click reaction, i.e., azide-alkyne click polymerization (AACP).

Introduction

A chemist is born to create new artificial substances and useful processes using naturally occurring substances. In the polymer research field, the two most critical tasks are the exploration of new types of monomers and development of new polymerization reactions. Needless to
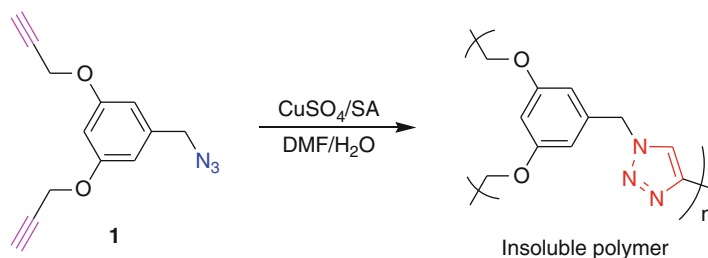
Polymer Synthesis via Click Reactions, Fig. 1 Attempted synthesis of hyperbranched polytriazole (*hb*-PTA) by Cu(I)-catalyzed click polymerization of 3,5-bis(propargyloxy)benzyl azide (**1**). *SA* ascorbic acid, *DMF N,N*-dimethylformamide

say, without effective polymerization routes being established, monomeric species cannot be converted to polymeric products. It is well known that most of the polymerizations, if not all, are developed from organic reactions of small molecules. The Cu(I)-catalyzed azide-alkyne cycloaddition (CuAAC), the most known click reaction and reported independently by Sharpless and Meldal in 2002, was a near-perfect and efficient reaction to produce solely 1,4-disubstituted 1,2,3-triazole derivatives [1, 2]. Thanks to its high efficiency and orthogonality, the click reaction has found wide applications in diverse areas including in polymer and material sciences [3–5]. With the efforts of polymer scientists paid, functional polytriazoles with linear and hyperbranched structures have been synthesized by such a powerful reaction, and in turn the azide-alkyne click polymerization was established.

Polytriazole Synthesis via Metal-Catalyzed AACP

Besides the application of the CuAAC in the post-functionalization of preformed polymers, the polymer scientists have tried to use it to directly synthesize polymers and foster it into a polymerization reaction, i.e., click polymerization [6]. Interestingly, the effort was first paid to synthesize hyperbranched polytriazoles (*hb*-PTAs) by the CuAAC. In 2004, Voit and coworkers tried to prepare *hb*-PTAs by the polymerization of 3,5-bis(propargyloxy)benzyl azide (**1**) mediated by $CuSO_4$ and sodium ascorbate (Fig. 1) [7]. Unfortunately, a rubbery substance precipitated

out from the reaction mixture, which was insoluble in organic solvents probably due to the cross-linking of the formed triazole rings with the copper species. Although imperfect, this work is the first attempt in the area of research on click polymerization. Subsequent experiments by others showed that the "standard recipe" for the CuAAC reaction is not suitable for the synthesis of processible *hb*-PTAs. The alternative approaches to provide soluble *hb*-PTAs are either using organo-soluble Cu(I) catalyst, such as $Cu(PPh_3)_3Br$, or minimizing the amount of water used in the aqueous mixtures [6].

While the CuAAC produces solely 1,4-disubstituted 1,2,3-triazole derivative, ruthenium complexes such as $Cp*Ru(PPh_3)_2Cl$ ($Cp* = 1,2,3,4,5$-pentamethylcyclopentadiene) could efficiently catalyze azide-alkyne click reaction to yield exclusively 1,5-disubstituted 1,2,3-triazole derivatives, which may exhibit different properties and thus provides a platform for investigating their structure–property relationships [8]. Attracted by these features, in 2008, Tang and coworkers reported the first example of $Cp*Ru(PPh_3)_2Cl$-catalyzed azide-alkyne click polymerization of diazides **2** and triyne **3**, from which 1,5-regioregular *hb*-P**4** with high molecular weights were produced in high yields under mild conditions in short time (Fig. 2) [9]. Furthermore, they found that $[Cp*RuCl_2]_n$, the precursor of $Cp*Ru(PPh_3)_2Cl$, was also effective in catalyzing the AACP, which will greatly popularize the application of Ru-catalyzed AACP.

P

Fig. 2 Synthesis of *hb*-P**4**
by Cp*Ru(PPh$_3$)$_2$Cl-
catalyzed click
polymerization of diazides
2 and triyne **3**
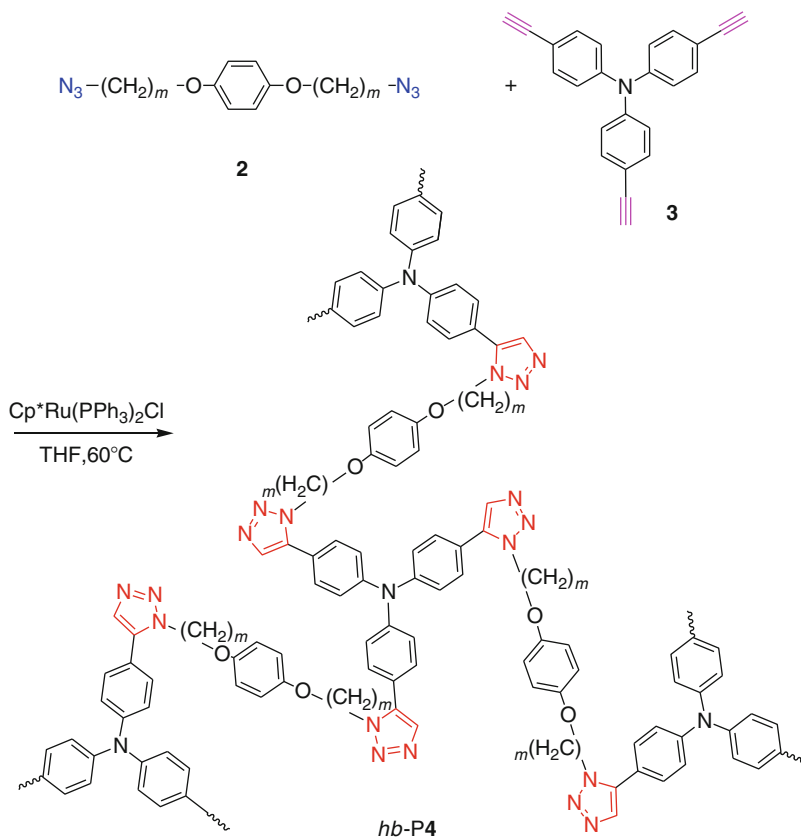
**Polymer Synthesis via
Click Reactions,**
Fig. 3 Synthetic route to
polytriazoles P**7** by the Cu
(I)-catalyzed azide-alkyne
click polymerization of
diazide **5** and diyne **6**
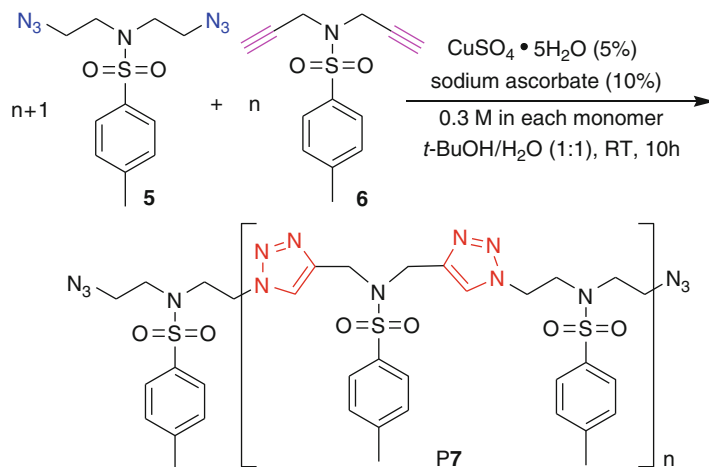
After Voit's attempt on *hb*-PTA synthesis, researchers commenced preparing linear PTAs using the click polymerization. The first report along the line was on the synthesis of nonconjugated PTAs. In 2004, Fokin, Finn, and coworkers carried out the polymerization using the bifunctional azides and alkynes as monomers and CuSO$_4$/sodium ascorbate as catalytic system in 1:1 *t*-BuOH/H$_2$O. The dimethyl sulfoxide-soluble PTAs were obtained (Fig. 3) [10]. From then on,

many efforts have been paid on the preparation of functional linear PTAs, which have been found to have wide applications in material and biological sciences.

In general, the Cu(I) sources were either generated in situ by the reduction of Cu (II) in the presence of reducing agents or the direct Cu(I) compounds or complexes. In 2013, Bowman and coworkers reported another Cu(I) generation approach [11]. The precursor of catalytic system was $CuCl_2$/1,1,4,7,7-pentamethyldiethylenetriamine (PMDETA), which could be reduced to Cu(I) species by visible light in the presence of a photoinitiator of bis(2,4,6-trimethylbenzoyl)-phenylphosphine oxide (Irgacure 819). Afterwards, they used this catalyst generation strategy to perform the AACP in bulk, and a highly cross-linked, high glass transition temperature polymer with extensive triazole linkages was obtained from multifunctional azide and alkyne monomers.

Polytriazole Synthesis via Metal-Free AACP

Although the Cu(I)- and Ru(II)-catalyzed AACPs are powerful in preparing functional PTAs with linear and hyperbranched structures, the complete removal of the metallic residues from the products after reaction is difficult. It is well known that the metallic residue is detrimental to the electronic and optical properties of polymeric materials and could cause cytotoxicity when used in biological field, which will greatly limit their applications in these areas.

To surmount this difficulty, Tang and coworkers successfully developed a metal-free click polymerization (MFCP) of activated alkyne of bis(aroylacetylene) and diazide under mild reaction conditions in 2006 [12]. Heating the mixtures of bis(aroylacetylene)s and diazides in polar solvents such as DMF/toluene at a moderate temperature of 100 °C readily produced poly(aroyltriazole)s (PATAs) with high molecular weights [number-averaged molecular weight (M_n) up to 13,350 with polydispersity (PDI) of 2.0] and regioregularities [fraction of 1,4-disubstituted 1,2,3-triazoles ($F_{1,4}$) in the PATAs up to 92 %] in high yields (up to 98 %) (Fig. 4). In addition, this MFCP propagated
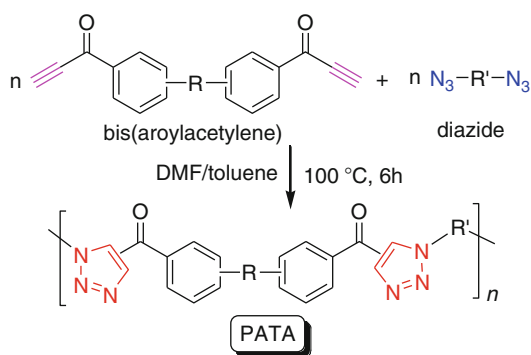
Polymer Synthesis via Click Reactions, Fig. 4 General synthetic route to PATAs by metal-free click polymerization of bis(aroylacetylene) and diazide monomers

smoothly without exclusion of moisture and oxygen, which has greatly simplified the experiment operation and is anticipated to widen its applications. When they reported their work in 2007, they formally defined this azide-alkyne polycycloaddition as "click polymerization" for the first time.

The preparation of aroylacetylenes, however, requires many reaction steps and involves the use of reactive reagent and toxic heavy metal oxidants under harsh reaction conditions. The propiolates, in which the triple bond is adjacent to an electron-withdrawing ester group, are structurally similar to aroylacetylenes and anticipated to be used as the monomer for MFCP. It is noteworthy that the propiolates could be readily synthesized from commercially available propiolic acid and aromatic or aliphatic diols via a one-step and one-pot esterification procedure under mild reaction conditions. Katritzky and coworkers reported the polymerization of propiolates and azides in 2007 [13]. They carried out the polymerization in bulk at elevated temperature but no regioselectivity was available. This polymerization remains silent until Qin, Tang, and coworkers reinvestigated systematically in 2011 [14]. They used the reaction conditions similar to those of the MFCP of aroylacetylene and azide and found that the results of polymerization of propiolates and azides are indeed quite similar. Poly(aroxycarbonyltriazole)s (PACTs) with high molecular weights (M_n up to 14,900 with PDI of 1.58) and

regioregularities ($F_{1,4}$ up to 90 %) could be obtained in excellent yields (up to 99 %) (Fig. 5).

Furthermore, inspired by the fact that the activated alkynes could undergo the MFCP with azide under mild reaction conditions, Qin, Tang, and coworkers designed and synthesized an activated azide of 4,4′-diazidoperfluorobenzophenone and used it to react with alkynes without the addition of metallic species [15]. The polymerization results showed that PTAs with high regioregularity ($F_{1,4}$ higher than 82 %) and satisfactory molecular weights (M_n up to 11,500 with PDI of 2.95) could be obtained in high yields (up to 95.1 %) (Fig. 6). These results are also similar to those of the MFCPs of activated alkynes and azides, suggesting that it is another type of MFCP.

Property of Synthesized Polytriazoles

Thanks to the functional tolerance of AACP, a wide variety of functional groups incorporated in the azide and alkyne monomers could be polymerized by this technique, which endows the produced PTAs with unique chemical and physical properties, such as photoluminescence, chemosensing, fluorescent imaging, photonic patterning, optical nonlinearity, photovoltaic effect, light refractivity, and biological activity. These functional properties have been well summarized by Tang and coworkers in 2010 and 2012 [16, 17].
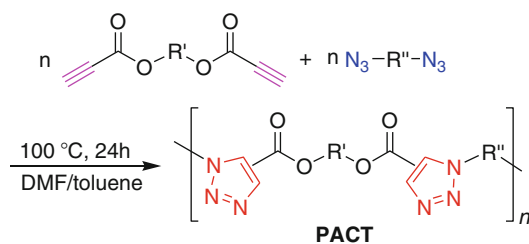
The recently reported application of AACP is to prepare self-healing hyperbranched PATAs [18]. As reported by Qin, Tang, and coworkers, the MFCP of bis(aroylacetylene)s and triazole readily furnished hyperbranched PATAs (hb-P14 and hb-P15) with high molecular weights (M_n up to 8,250 with PDI of 3.37) in excellent yields (up to 97.6 %) (Fig. 7).

These polymers are processable and have excellent film-forming ability. High-quality homogeneous films and sticks free from defects could be obtained by casting. Thanks to the remaining azide and aroylacetylene groups on the periphery of hb-PATAs, the cut halves of their films and sticks could be healed by stacking or pressing together at elevated temperature (Fig. 8). Furthermore, the self-healed materials show higher mechanical strength than their pristine films or sticks. Since they do not need the addition of other components and could be simply triggered by heating, such self-healing process is anticipated to be widely applied in diverse areas.

Perspective

The past decade has witnessed the rapid growth of AACPs, using which linear and hyperbranched PTAs with versatile functional properties were obtained. However, this area is still full of challenges and opportunities. Designing and

Polymer Synthesis via Click Reactions, Fig. 5 General synthetic route to PACTs by metal-free click polymerization of dipropiolate and diazide monomers

Polymer Synthesis via Click Reactions, Fig. 6 Synthetic route to polytriazoles P10 by metal-free click polymerization of activated diazide **8** and diynes **9**
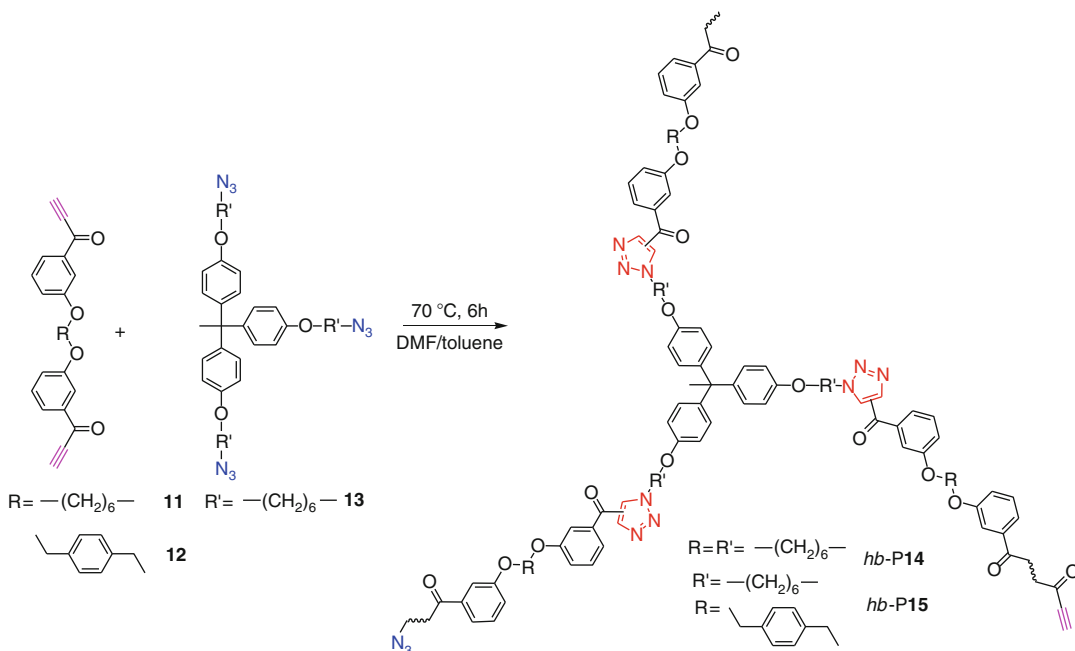
Polymer Synthesis via Click Reactions, Fig. 7 Synthesis of hyperbranched PATAs by metal-free click polymerization of bis(aroylacetylene)s (**11** and **12**) and diazide (**13**)

Polymer Synthesis via Click Reactions, Fig. 8 (**a**) The self-healing process of the *hb*-P**14** sticks and (**b**) the proposed mechanism of self-healing of polymer sticks
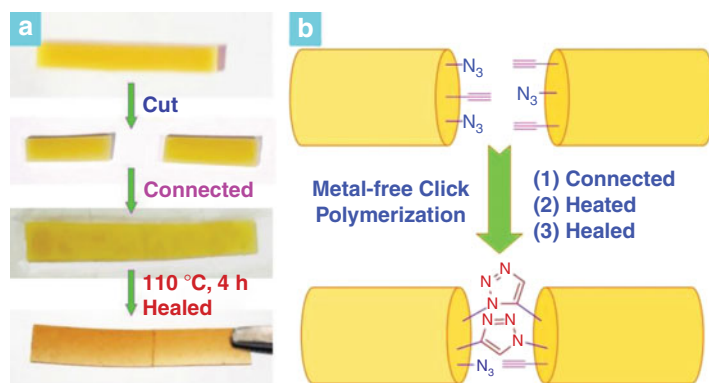
synthesizing functional azide and alkyne monomers, screening new catalysts with high efficiency and regiospecificity, establishing new types of click polymerization, and exploring unique property and novel applications will be the further directions and endeavors in this area. It is believed that the AACP will be eventually developed into a powerful and versatile tool for the syntheses of new polymers with well-defined molecular structures and advanced functional properties.

Related Entries

References

1. Rostovtsev VV, Green LG, Fokin VV, Sharpless KB (2002) A stepwise Huisgen cycloaddition process: copper(I)-catalyzed regioselective "ligation" of azides and terminal alkynes. Angew Chem Int Edit 41:2596–2599
2. Tornøe CW, Christensen C, Meldal M (2002) Peptidotriazoles on solid phase: [1,2,3]-triazoles by regiospecific copper(I)-catalyzed 1,3-dipolar cycloadditions of terminal alkynes to azides. J Org Chem 67:3057–3064
3. Meldal M, Tornøe CW (2008) Cu-catalyzed azide-alkyne cycloaddition. Chem Rev 108:2952–3015
4. Lahann J (2009) Click chemistry for biotechnology and materials science. Wiley, Chichester
5. Witczak ZJ, Bielski R (2013) Click chemistry in glycoscience: new developments and strategies. Wiley, Hoboken
6. Qin AJ, Lam JWY, Tang BZ (2010) Click polymerization. Chem Soc Rev 39:2522–2544
7. Scheel AJ, Komber H, Voit BI (2004) Novel hyperbranched poly(([1,2,3]-triazole)s derived from AB$_2$ monomers by a 1,3-dipolar cycloaddition. Macromol Rapid Commun 25:1175–1180
8. Zhang L, Chen XG, Xue P, Sung HHY, Williams ID, Sharpless KB, Fokin VV, Jia GC (2005) Ruthenium-catalyzed cycloaddition of alkynes and organic azides. J Am Chem Soc 127:15998–15999
9. Qin AJ, Lam JWY, Jim CKW, Zhang L, Yan JJ, Häussler M, Liu JZ, Dong YQ, Liang DH, Chen EQ, Jia GC, Tang BZ (2008) Hyperbranched polytriazoles: click polymerization, regioisomeric structure, light emission, and fluorescent patterning. Macromolecules 41:3808–3822
10. Diaz DD, Punna S, Holzer P, McPherson AK, Sharpless KB, Fokin VV, Finn MG (2005) Click chemistry in materials synthesis. 1. Adhesive polymers from copper-catalyzed azide-alkyne cycloaddition. J Polym Sci Part A Polym Chem 42:4392–4403
11. Gong T, Adzima BJ, Baker NH, Bowman CN (2013) Photopolymerization reactions using the photoinitiated copper (I)-catalyzed azide-alkyne cycloaddition (CuAAC) Reaction. Adv Mater 25:2024–2028
12. Qin AJ, Jim CKW, Lu WX, Lam JWY, Häussler M, Dong YQ, Sung HHY, Williams ID, Wong GKL, Tang BZ (2007) Click polymerization: facile synthesis of functional poly(aroyltriazole)s by metal-free, regioselective 1,3-dipolar polycycloaddition. Macromolecules 40:2308–2317
13. Katritzky AR, Meher NK, Hanci S, Gyanda R, Tala SR, Mathai S, Duran RS, Bernard S, Sabri F, Singh SK, Doskocz J, Ciaramitaro DA (2008) Preparation and characterization of 1,2,3-triazole-cured polymers from endcapped azides and alkynes. J Polym Sci Part A Polym Chem 46:238–256
14. Li HK, Wang J, Sun JZ, Hu RR, Qin AJ, Tang BZ (2012) Metal-free click polymerization of propiolates and azides: facile synthesis of functional poly (aroxycarbonyltriazole)s. Polym Chem 3:1075–1083
15. Wang Q, Li HK, Wei Q, Sun JZ, Wang J, Zhang XA, Qin AJ, Tang BZ (2012) Metal-free click polymerizations of activated azide and alkynes. Polym Chem 4:1396–1401
16. Qin AJ, Lam JWY, Tang BZ (2010) Click polymerization: progresses, challenges, and opportunities. Macromolecules 43:8693–8702
17. Li HK, Sun JZ, Qin AJ, Tang BZ (2012) Azide-alkyne click polymerization: an update. Chinese J Polym Sci 30:1–15
18. Wei Q, Wang J, Shen XY, Zhang XA, Sun JZ, Qin AJ, Tang BZ (2013) Self-healing hyperbranched poly (aroyltriazole)s. Sci Rep 3:1093

Polymer Vesicles

Ionel Adrian Dinu, Christoph Edlinger,
Evgeniia Konishcheva, Cornelia G. Palivan and
Wolfgang Meier
Department of Chemistry, University of Basel,
Basel, Switzerland

Synonyms

Artificial vesicles; Nanocompartments; Polymer hollow spheres; Polymersomes

Definition

Polymer vesicles, called polymersomes, are hollow spherical supramolecular assemblies composed of an aqueous cavity surrounded by a polymer membrane. Polymersomes are generated by self-assembly of amphiphilic copolymers in dilute solutions.

Introduction

In nature, compartmentalization plays a fundamental role in supporting life processes, such as metabolic reactions, transfer in/out of compounds, and signaling. In this respect cells represent essential compartments both in terms of complex processes taking place in situ and for

exchange of compounds through their lipidic membrane with embedded membrane proteins. The simplest model to mimic the cell membrane and its compartment topology is with lipid vesicles, liposomes. Favored for their structural analogy to cell membranes, biocompatibility, and biodegradability, liposomes were extensively studied as carriers for therapeutic or diagnostic purposes. However, the presence of membrane defects which induce mechanic instability of liposomes and undesired release of encapsulated compounds required new solutions for more stable compartments. Because the limitations of liposomes are not entirely solved by covering them with a polymer shell (e.g., using poly(ethylene glycol), PEG, in so-called PEGylation), synthetic analogues of liposomes were introduced. Compared to liposomes, polymersomes have higher mechanic stability, based on a thicker membrane (3–5 nm compared to 7–20 nm, respectively). In addition, their stability can be improved by cross-linking the polymer membrane [1]. Polymersomes can simultaneously encapsulate hydrophilic molecules in the aqueous cavity and hydrophobic molecules within the membrane (Fig. 1). In addition, specific molecules can be conjugated to the exterior surface to target the vesicles or to immobilize them on solid support [2].

Properties of polymer vesicles, such as size, stability, membrane thickness, flexibility, and permeability, are significantly influenced by the
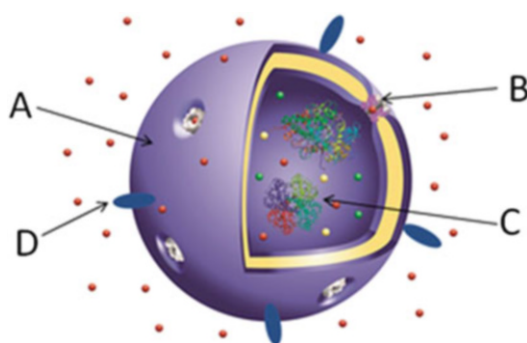
Polymer Vesicles, Fig. 1 Schematic representation of a polymersome (*A*) which can insert channel proteins or biopores within the membrane (*B*); can encapsulate proteins, enzymes, or mimics in the aqueous cavity (*C*); or can be functionalized on its surface (*D*)

chemical nature of the copolymers. By an appropriate selection of the copolymer's chemical composition, molecular weight, polydispersity, block length, and hydrophilic-to-hydrophobic ratio, the characteristics of the self-assembled assemblies, and in particular vesicles, can be individually tuned for each individual application. A particularly interesting strategy is to design vesicle membranes based on stimuli-responsive block copolymers because they induce dramatic changes of properties in the presence of the specific stimulus. Stimuli-responsive copolymers support development of vesicles able to change "on demand," with promising applications in nanomedicine. Polymersomes serve for encapsulation/entrapment of active molecules resulting in a variety of hybrid assemblies, such as drug delivery systems, carriers for contrast agents, nanoreactors, and artificial organelles [2].

Synthesis of Amphiphilic Block Copolymers

Amphiphilic block copolymers (AmBPs) consist of at least one hydrophilic and one hydrophobic block sequentially connected by covalent bonds. The resulting copolymer is composed of domains with opposite affinities for an aqueous solution. They self-assemble in solvents, which are selective only for one of the constituent blocks and can generate supramolecular assemblies with a wide variety of architectures, such as micelles, worms, tubes, or vesicles [3]. Depending on the composition, molecular weight, and relative length of the hydrophilic and hydrophobic blocks, it is possible to favor the formation of assemblies with a specific architecture or properties.

AmBPs are synthesized from a large variety of monomers following several synthetic routes: (i) a sequential controlled or living polymerization [4], (ii) a simple coupling reaction of homopolymers (by click chemistry) [5], and (iii) two consecutive polymerizations reactions, the first reaction serving to produce a preformed polymer used as macroinitiator for the second polymer reaction with a different mechanism than the first one [4].

(i) **Living polymerization** reactions (anionic and cationic) are frequently used to synthesize AmBPs [4], in which the reactions proceed in the absence of an irreversible chain transfer and chain termination. However, both living polymerization methods are significantly affected by the solvent nature and the presence of water and impurities and have limited applications for the synthesis of copolymers with functional groups as side chains. Therefore, in order to synthesize AmBPs with hydrophilic blocks having acidic or hydroxylic functional groups as side chains, protected monomers must be employed, which require deprotection after polymerization. Recent developments in controlled radical polymerization (CRP) methods provide a functional group side chain compatible route to synthesize AmBPs. These methods are less affected by the presence of impurities and provide conditions for a chain growth based on a rapid and dynamic equilibrium between dormant chains and propagating radicals [4]. Poly(*N*-(3-aminopropyl) methacrylamide hydrochloride)-*b*-poly (*N*-isopropylacrylamide) (PAMPA-*b*-PNIPAM), poly(styrene)-*b*-poly (L-isocyanoalanine (2-thiophen-3-yl-ethyl) amide) (PS-*b*-PIAT), and poly(acrylic acid)-*b*-polystyrene-*b*-poly(4-vinyl pyridine) (PAA-*b*-PS-*b*-P4VP) are examples of AmBPs synthesized by CRP methods [6–8]. When these synthetic methods are used to polymerize acidic monomers such as acrylic acid, protected monomers are necessary.

(ii) **Click chemistry methods** allow the synthesis of well-defined block copolymers with a wide variety of functional groups as side chains or end groups. The functional groups of AmBPs can be quantitatively and selectively modified by using relatively mild conditions without any side reactions. A variety of homopolymers can be coupled by click chemoselective reactions between their functional end groups such as (a) thiol-ene/thiol-yne additions; (b) thiol–disulfide exchange; (c) modification of epoxides,

anhydrides, oxazolines, and isocyanates by reaction with amines/alcohols/thiols; (d) Michael-type addition; (e) copper-catalyzed azide alkyne cycloaddition; (f) reaction of active esters with amines; (g) modification of ketones and aldehydes with amines/alkoxyamines/hydrazines; and (h) Diels–Alder reactions [5]. Click chemistry methods represent relatively safe and easy synthetic routes to create new AmBPs, to improve their interaction with specific molecules, and to bind specific molecules (proteins, enzymes, DNA) [2]. However, the use of click chemistry for synthesis of AmBPs is limited when the homopolymers have a different solubility in the selected solvent and does not allow for precise control of their molecular weight.

(iii) Polymerization method based on **two different consecutive polymerizations reactions**, where the first serves to produce a preformed polymer used as macroinitiator for the second reaction, is another method to design vesicle-forming AmBPs [4]. The end-group functionality of the macroinitiator can be achieved by in situ modification or by pretreatment of the prepolymer after the first polymerization. This method is used to produce symmetric triblock copolymers, such as poly(2-methyloxazoline)-*b*-poly(dimethylsil oxane)-*b*-poly(2-methyloxazoline) (PMOXA-*b*-PDMS-*b*-PMOXA) copolymers by starting from bifunctional macroinitiators [7].

Examples of AmBPs
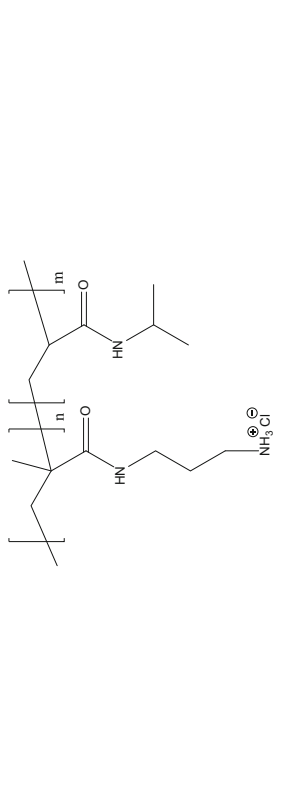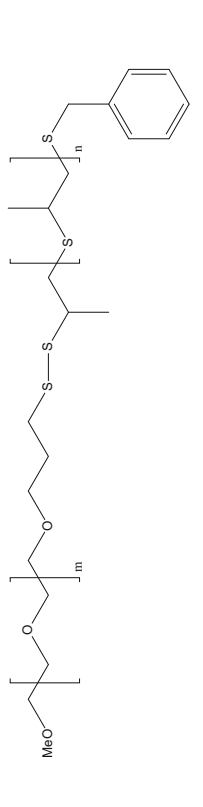
There are a large variety of vesicle-forming AmBPs with linear, branch, graft, star, or dendritic structure, relevant examples are included in Table 1 [6–8]. For example, polystyrene–poly (propylene imine) dendrimer is able to self-assemble and generate vesicles in aqueous solutions [6]. By selecting the nature of the constituent blocks, the resulting copolymer can possess special properties, such as biodegradability, biocompatibility, or stimuli responsiveness. Stimuli-responsive AmBPs generate "smart"

Polymer Vesicles, Table 1 Examples of vesicle-forming AmBPs

Copolymer	Structure	Properties	References
PMOXA-*b*-PDMS-*b*-PMOXA		Selective permeability and ability to incorporate membrane proteins	[3, 7]
PS-*b*-PIAT		Selective permeability	[3, 7]
PAA-*b*-PS-*b*-P4VP		pH-responsive	[6]
PB-*b*-PGA		pH-responsive	[6, 8]

(*continued*)

P

Polymer Vesicles, Table 1 (continued)

Copolymer	Structure	Properties	References
PAMPA-*b*-PNIPAM		Temperature responsive	[8]
PEG-SS-PPS		Sensitive to reducing environments	[6, 8]

vesicles, which release the encapsulated molecules "on demand," when the stimulus is present [6, 8]. Poly(butadiene)-*b*-poly(γ-L-glutamic acid) (PB-*b*-PGA) vesicles undergo reversible coil–helix transition in response to pH changes [6], while those based on PAMPA-*b*-PNIPAM are temperature responsive, and those based on poly (ethylene glycol)-SS-poly(propylene sulfide) (PEG-SS-PPS) are sensitive to reducing environments [8]. An interesting strategy to improve properties is achieved when synthetic blocks are coupled with natural ones, such as polypeptides, nucleic acids, or polysaccharides [9]. In this respect, poly(L-lysine)-*b*-poly(L-tyrosine) and poly(L-glutamic acid)-*b*-poly(propylene oxide)-*b*-poly(L-glutamic acid) are polypeptide-based copolymers, which form polymersomes [9].

Preparation of Polymer Vesicles

The driving force of the self-assembly process is the amphiphilic nature of the copolymers: the hydrophobic domain aggregates, to minimize its contact with water, while the hydrophilic domains become hydrated and stabilize the supramolecular assembly in solution.

In order to form vesicles (Fig. 2), an AmBP has to adapt to a conical shape supporting the formation of a curved membrane [10]. An appropriate balance of the hydrophobic and hydrophilic forces, resulting from a hydrophobic fraction of 10–35 wt% of the AmBP, favors polymersome formation, while other hydrophobic-to-hydrophilic ratios induce the formation of micelles, worms, or mixtures [1]. In addition, the solubility properties of AmBPs in water impose a specific route to generate supramolecular assemblies, in particular vesicles. For example, poor water soluble AmBPs are used to generate vesicles in aqueous media, in the presence of detergents, which stabilize the copolymers.

There are two main routes for vesicle formation: (i) dissolution of the AmBPs in water and (ii) dissolution of the AmBPs in a solvent and subsequent mixture with an excess of water.

(i) Dissolution of AmBPs in water serves as basis for three methods of polymersome preparation: **direct dissolution method**, **film rehydration method**, and **electroformation method**.

The easiest method for polymersome formation is the **direct dissolution method**, in which the polymer is directly mixed with an aqueous solution, and agitated (shaking, stirring, vortexing, or sonication) at a desired temperature, 3D assemblies are formed indicated by opaqueness in the solution. **Film rehydration method** for polymersome formation is based on a temporarily dissolution of the AmBPs in a solvent to produce a thin polymer film upon evaporation, followed by the hydration of the film. This method generates high polymer surface area for fast rehydration and more controlled conditions for vesicle formation than the direct dissolution method [10]. **Electroformation** method consists of hydration of the polymer film in the presence of an oscillating electric field, resulting in the

Polymer Vesicles, Fig. 2 Schematic representation of a polymersome generated by a triblock AmBP

hydrophilic hydrophobic hydrophilic
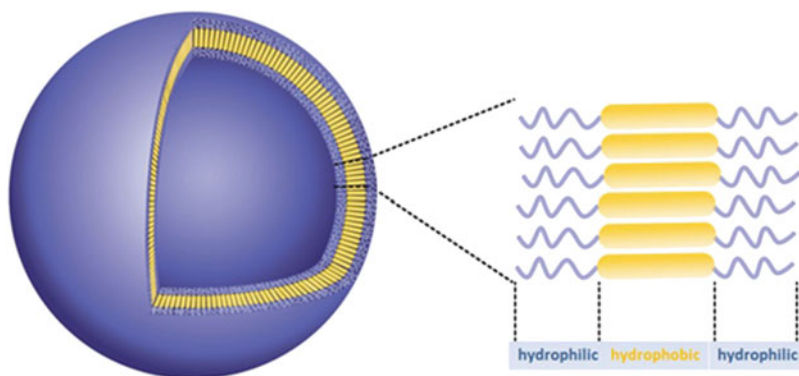
formation of vesicles with sizes in the μm range (giant vesicles).

(ii) Solvent-assisted preparation methods for polymersome formation are **kinetic trapping**, **thermodynamic trapping**, and **double emulsion**. They require a solvent capable of dissolving the polymer and which is miscible with water. These methods allow the use of a large variety of AmBPs but have drawbacks of the organic solvent being difficult to remove completely, interacting with the formed membrane, and denaturation of sensitive molecules such as proteins, enzymes, or siRNA [10, 11].

Kinetic trapping is a preparation method in which a polymer solution is injected into an excess of water, inducing a fast phase inversion. **Thermodynamic trapping** is a preparation method in which an excess of water is slowly added to the polymer solution, enabling the system to equilibrate [10]. A slightly different approach is the formation of **double emulsions** in which an aqueous solution containing the molecules intended to be encapsulated inside the vesicle is emulsified with a nonmiscible organic phase that contains the polymer. The oil phase is dispersed in a second aqueous medium by stirring or centrifugation, so that the solution is included into an oil drop, which serves for droplet formation, in a second aqueous phase. This method is used to create giant vesicles and offers the advantage of a very high encapsulation efficiency [11]. The removal of the remaining organic solvents is achieved through reduced pressure or, more efficiently, through dialysis.

The specificity of the preparation method influences the size of polymersomes and the encapsulation efficiency of the molecules in the aqueous cavity of the vesicles [2, 10]. Independent of the preparation method, the solutions containing polymersomes require to be "purified" by removing solvents, detergents, unencapsulated molecules, and other 3D assemblies, such as micelles, worms, or larger aggregates. The purification of the polymersome solution is usually achieved through size exclusion [10] or dialysis, the latter being better suited for solvent residues and detergents [12]. The control of the vesicle size and the removal of aggregates also represent an important step and are achieved by repeated extrusion through a filter [10] or by sonication [1].

Stability and Permeability of Polymer Vesicles

AmBPs self-assemble and form membranes that are thicker (10–25 nm thickness) than lipidic membranes (to 3–5 nm) [13] and are usually less permeable. The **stability** of polymersomes depends on the strength of the hydrophobic interactions between the hydrophobic segments inside the membrane. High temperature, the presence of solvents and detergents, or a broad size distribution of the AmBPs decreases the interactions, resulting in a lower mechanical stability of the membrane. A balance between the flexibility of the membrane, which allows an insertion of biomolecules without denaturation, and the stability of the membrane must be achieved [3]. The gelation of the aqueous content of vesicles by in situ polymerization is a method to increase the stability of the vesicles but has to be carefully considered when biomolecules are intended to be encapsulated inside the aqueous cavity in order to not affect their structure or biologic activity [13]. A more common approach for stabilization of vesicles is cross-linking of the membrane by polymerization of hydrophobic monomers inserted in the membrane. However, addition of monomers can affect the membrane, and the radical polymerization used for cross-linking can induce aggregation of vesicles [10]. The best way to stabilize vesicles is direct cross-linking of AmBPs, by polymerization of existing molecular groups, alkene groups, for example.

The **permeability** of vesicle membranes is important when transportation of molecules through the membrane is required, such as when polymersomes serve as compartments for the design of nanoreactors and artificial organelles. The vesicle membrane is rendered permeable by (i) using a specific chemical composition of AmBPs, (ii) chemical modification of the membrane, or (iii) insertion of channel

proteins. For example, PS-*b*-PIAT copolymers form porous membranes [13], while PMOXA-*b*-PDMS-*b*-PMOXA membranes, known as highly impermeable except to oxygen species, are permeabilized by an elegant method based on insertion of channel proteins [3]. Various channel proteins have been successfully inserted in PMOXA-*b*-PDMS-*b*-PMOXA membranes and supported a rapid transport of substrates into the membrane or products involved in in situ enzymatic reactions out of the membrane.

An alternative method to create defects in an impermeable membrane is based on the insertion of specific molecular groups that are degraded in particular conditions. Inserted hydrophilic photo-sensitizers on the surface of the vesicles disrupt the membrane upon irradiation [13]. The effect can be tuned by adjusting the concentration of the photosensitizer. Larger defects can be produced in the membrane of polymersomes by washing out domains of "sacrificial" AmBPs [10] or lipids [13], which are specially inserted for permeabilization of the membrane. These defects destabilize the membrane, and by carefully controlling the conditions, the vesicles preserve their overall spherical architecture. Also, the insertion of pH-sensitive groups (e.g., 2-(diethylamino)ethyl methacrylate) in the hydrophobic domain of the membrane induces a pH-dependent swelling, which destabilize the membrane and increase its permeability [13]. The pH responsiveness of one of the polymer domains can be used to completely disintegrate the membrane when an "on demand" release of the encapsulated compound is intended. Stimuli responsiveness of polymersome membrane represents a smart approach to release the encapsulated compounds in desired conditions provided by the presence of a specific, or combination of, stimulus (physical, chemical, enzymatic).

Functionalization of the Surface of Polymer Vesicles

When the intended use of polymersomes includes targeting approaches or immobilization on surfaces, it is necessary that their external surface contains **specific molecular** groups. The functionalization of polymersomes with exposed functional groups can be achieved either prior to vesicle formation by using AmBPs with the corresponding functional groups or by modification of the polymersomes via click chemistry. The two main risks regarding polymersome functionalization are unintended interactions of the functional groups and their deep insertion into the membrane due to hydrophobicity making them inaccessible [10, 14]. There are a large variety of possible functional groups and related reactions, which can be used to decorate a polymersome surface for each desired application. For example, a selective and robust reaction (in pH ranging from 4 to 12) is alkyne–azide cycloaddition, often regarded as the archetype of a click reaction. It has the advantage that the terminal bromine groups can be directly substituted by azides for AmBPs synthesized by ATRP [14].

Molecular recognition interactions, based on specific molecule pairs, as, for example, biotin/streptavidin or antigen–antibody, represent an elegant way to be used for targeting or immobilization of polymersomes [2, 3]. In order to specifically interact with the target cell, polymer vesicles are functionalized with specific molecules, such as RGD-peptides (integrin binding), folic acid [14], or polyguanylic acid [1].

Methods of Vesicle Characterization

3D supramolecular assemblies, and in particular polymersomes, are characterized by various scattering methods combined with microscopy methods (Fig. 3).

By measuring scattering properties of supramolecular assemblies, it is possible to establish their size, size distribution, morphology, and critical aggregation concentration. Light scattering method (LS) is applied when the size of assemblies, in particular vesicles, ranges from 100 nm up to several μm. In dynamic light scattering (DLS), fluctuations in the scattered light intensity on the microsecond time scale appear because of the diffusion of assemblies in a solution. Hydrodynamic radius of assemblies (R_h) is obtained by using Stokes–Einstein equation with an
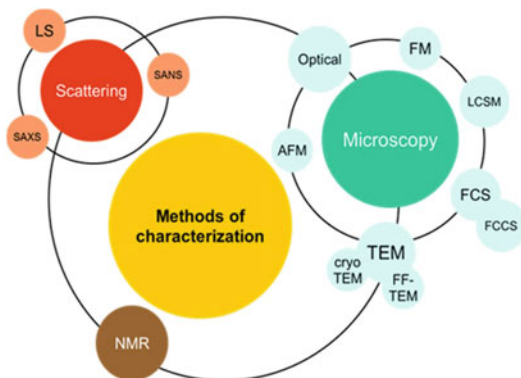
Polymer Vesicles, Fig. 3 The most commonly applied methods of characterization for polymer vesicles

angle-dependent apparent diffusion coefficient (D_{app}) and by extrapolation to zero concentration and zero momentum transfer [3]. Weight-average molecular weight (M_w), z-average radius of gyration (R_g), and the second viral coefficient (A_2) are evaluated from static light scattering experiment (SLS). A_2 gives information about particle–particle and particle–solvent interactions [3], while the ratio R_g/R_h, (ρ-parameter) indicates the morphology of the assembly. Theoretically, for thin vesicles $\rho = 1.0$, for homogeneous hard balls $\rho = 0.779$, and for polymers in extended conformations $\rho > 1$ [3]. The experimental values obtained for ρ-parameter allow identifying the formation of vesicles in a solution upon the self-assembly process. LS is a fast and precise technique but present [3].

Light scattering method is used in combination with the electrophoretic mobility of assemblies to obtain the zeta potential of vesicles [15]. In addition, stopped-flow spectroscopy serves to study the permeability of the vesicle membrane or the kinetics of vesicle formation [16].

If a solution contains assemblies with a size from few nm up to 100 nm, small-angle X-ray (SAXS), wide-angle X-ray (WAXS), or small-angle neutron (SANS) scattering methods can be applied to characterize them. SAXS is applied to very dilute solutions, where the distances between particles are much higher than their size, and allows the characterization of both polydisperse and monodisperse assemblies. For monodisperse assemblies, SAXS provide information

about their shape, aggregation number, and inner structure. However, monodispersity of the assemblies has to be proven by other methods [17]. SANS is a very useful tool for the investigation of the native structure of assemblies and interaction parameters. Unlike SAXS, SANS is very sensitive toward light elements and allows a more detailed investigation based on isotope labeling [17].

For direct visualization of supramolecular assemblies generated by self-assembly, in particular the formation of vesicles, various microscopy methods are used and the appropriate method selection depends on the assembly size or the structural details to be evaluated. Microscopy methods allow the estimation of morphology, size, and homogeneity of the supramolecular assemblies and represent a complementary proof of vesicle formation. In the case of giant vesicles with diameters above 1 µm, optical microscopy is a very simple and fast method that can be used to characterize them in solution. However, it has limited magnification, resolution, and contrast compared to electron microscopy [12, 15]. Polymersomes with sizes in the nanometer range are studied by electron microscopy. Transmission electron microscopy (TEM) provides a high-resolution (<1 nm) image of a specimen (Fig. 4). This technique is based on the interaction of a high-energy electron beam, which passes through the sample containing the assemblies. However, the high vacuum and the dried state of the sample, which are necessary for TEM, might affect the vesicles morphology in case of instable polymer membranes. Cryogenic TEM (cryo-TEM) serves for the investigation of vesicles in their natural hydrated state and enables the study of micellar polymorphism, spontaneous formation of vesicles, and their transition to lamellar or multilamellar structures [12].

Direct visualization of polymer vesicles with sizes large enough to be visualized by optical microscopy can be analyzed by fluorescence microscopy if the vesicle membrane is labeled with a fluorescent dye. This method has several advantages, such as high sensitivity, ability to distinguish specific nonfluorescent regions which are appropriately labeled, and the possibility of
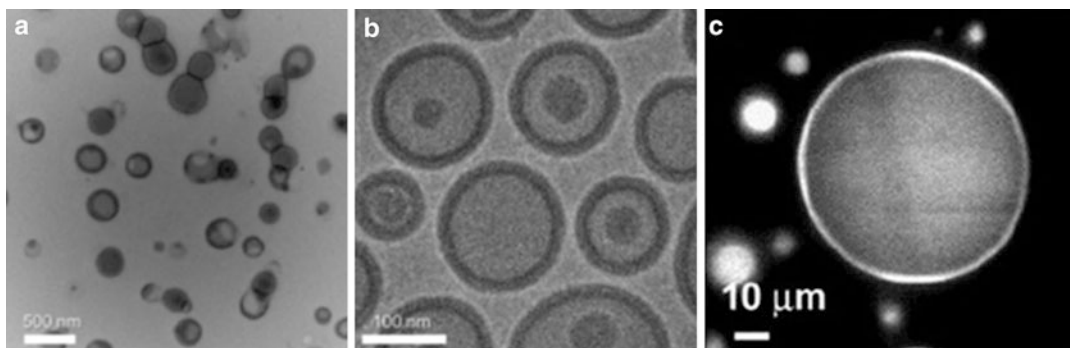
Polymer Vesicles, Fig. 4 Microscopy images of polymer vesicles. (**a**) TEM and (**b**) cryo-TEM images of PDMS-PMOXA-OH polymer vesicles, (**c**) LCSM micrograph of giant polymersomes of PEG-PLA in the presence of Nile red (Reprinted with permission from reference [12], Copyright 2005 Elsevier)

multiple labeling for visualization of individual molecules [12]. However, this technique has disadvantages of limited resolution (>0.2 μm), a decrease of the fluorescent intensity of dyes due to photo-bleaching, and the possible generation of reactive chemical species under illumination which promote a phototoxic effect [3].

A particular type of fluorescence microscopy is laser scanning confocal microscopy (LSCM), which allows obtaining images with a high resolution and contrast due to the reduction of the background fluorescence and an improved signal-to-noise ratio [12].

Fluorescence correlation spectroscopy (FCS) is based on a special fluctuation correlation approach, in which the laser-induced fluorescence of the excited fluorescent molecules that pass through a very small probe volume is auto-correlated in time to give information about the diffusion times of the molecules. The diffusion times, which are proportional to the R_H of the fluorescent molecules, provide information about interactions of the fluorescent molecules with larger target molecules, including formation of vesicles or encapsulation inside their cavity [18]. Fluorescence cross-correlation spectroscopy (FCCS) expands the FCS method by introducing two differently labeled particles, which provide a positive cross-correlation readout when bound to each other or located in the same carrier, thus diffusing through the confocal volume in a synchronized way. In contrast, the probability of simultaneous movement of freely diffusing fluorophores is so small that it can be neglected. The method is used for simultaneous characterization of vesicles and encapsulated compounds or for dynamic co-localization of different molecular in vesicles [19].

Scanning tunneling microscopy (STM) can be performed on conducting substrates and atomic force microscopy (AFM) on both conducting and nonconducting substrates to obtain images with a few Å resolution. These techniques have been applied to investigate polymer vesicles immobilized on a solid support [12].

Pulse gradient spin-echo NMR method (PGSE NMR) has been proposed to establish the size and size distribution of polymer vesicles and give information regarding the presence of interaction/aggregation phenomena [20].

Conclusion and Outlook

Polymer vesicles, as robust and straightforward produced compartments, can be modulated and easily control the sizes and assembly properties. Because of their diverse applications, polymer vesicles represent ideal candidates for applications in medicine, catalysis, environmental sciences, or food sciences. The large variety of AmBP supports the generation of polymer vesicles with a desired size, permeability, or responsivity. These assemblies can be advanced further through the combination of polymersomes with active compounds, such as enzymes, proteins, DNA, and mimics, in order to

design active systems, such as nanoreactors and artificial organelles. Polymersomes are necessary to shield the biomolecules and prevent their degradation by harmful environmental conditions to maintain the active component's specific activity, such the production of drugs, the detoxification of reactive oxygen species, and sensing of a specific molecule. These systems are gaining popularity today in various research fields and lead to the development new strategies for delivery of assemblies at a nanometer scale.

Related Entries

▶ Micelles and Vesicles
▶ Self-Assembly of Hyperbranched Polymers
▶ Stimuli-responsive Polymers

References

1. Discher DE, Ahmed F (2006) Polymersomes. Annu Rev Biomed Eng 8:323–341. doi:10.1146/annurev.bioeng.8.061505.095838
2. Najer A, Wu D, Vasquez D, Palivan CG, Meier W (2013) Polymer nanocompartments in broad-spectrum medical applications. Nanomedicine 8:425–447. doi:10.2217/nnm.13.11
3. Zhang X, Tanner P, Graff A, Palivan CG, Meier W (2012) Mimicking the cell membrane with block copolymer membranes. J Polym Sci Part A Polym Chem 50:2293–2318. doi:10.1002/pola.26000
4. Matyjaszewski K, Möller M (2012) Polymer science: a comprehensive reference. Elsevier, Amsterdam
5. Goldmann AS, Glassner M, Inglis AJ, Barner-Kowollik C (2013) Post-functionalization of polymers via orthogonal ligation chemistry. Macromol Rapid Commun 34:810–849. doi:10.1002/marc.201300017
6. LoPresti C, Lomas H, Massignani M, Smart T, Battaglia G (2009) Polymersomes: nature inspired nanometer sized compartments. J Mater Chem 19:3576–3590. doi:10.1039/B818869F
7. Renggli K, Baumann P, Langowska K, Onaca O, Bruns N, Meier W (2011) Selective and responsive nanoreactors. Adv Funct Mater 21:1241–1259. doi:10.1002/adfm.201001563
8. Cabane E, Zhang X, Langowska K, Palivan CG, Meier W (2012) Stimuli-responsive polymers and their applications in nanomedicine. Biointerphases 7:1–27. doi:10.1007/s13758-011-0009-3
9. Zhao L, Li N, Wang K, Shi C, Zhang L, Luan Y (2014) A review of polypeptide-based polymersomes. Biomaterials 35:1284–1301. doi:10.1016/j.biomaterials.2013.10.063

10. Edlinger C, Zhang X, Fischer-Onaca O, Palivan CG (2013) Polymer nanoreactors. In: Herman FM (ed) Encyclopedia of polymer science and technology, 4th edn. Wiley, New York
11. Marguet M, Bonduelle C, Lecommandoux S (2013) Multicompartmentalized polymeric systems: towards biomimetic cellular structure and function. Chem Soc Rev 42:512–529. doi:10.1039/C2CS35312A
12. Kita-Tokarczyk K, Grumelard J, Haefele T, Meier W (2005) Block copolymer vesicles-using concepts from polymer chemistry to mimic biomembranes. Polymer 46:3540–3563. doi:10.1016/j.polymer.2005.02.083
13. Le Meins JF, Sandre O, Lecommandoux S (2011) Recent trends in the tuning of polymersomes' membrane properties. Eur Phys J E 34:1–17. doi:10.1140/epje/i2011-11014-y
14. Lallana E, Sousa-Herves A, Fernandez-Trillo F, Riguera R, Fernandez-Megia E (2012) Click chemistry for drug delivery nanosystems. Pharm Res 29:1–34. doi:10.1007/s11095-011-0568-5
15. Lee JS, Feijen J (2012) Polymersomes for drug delivery: design, formation and characterization. J Controll Release 161:473–483. doi:10.1016/j.jconrel.2011.10.005
16. Tang CY, Zhao Y, Wang R, Hélix-Nielsen C, Fane AG (2013) Desalination by biomimetic aquaporin membranes: review of status and prospects. Desalination 308:34–40. doi:10.1016/j.desal.2012.07.007
17. Šegota S, Težak D (2006) Spontaneous formation of vesicles. Adv Colloid Interface Sci 121:51–75. doi:10.1016/j.cis.2006.01.002
18. Pramanik A, Rigler R (2001) FCS-analysis of ligand-receptor interactions in living cells. In: Rigler R, Elson ES (eds) Fluorescence correlation spectroscopy. Theory and applications. Springer series in chemical physics, vol 65. Springer, Heidelberg, pp 101–131
19. Bacia K, Kim SA, Schwille P (2006) Fluorescence cross-correlation spectroscopy in living cells. Nat Methods 3:83–89. doi:10.1038/nmeth822
20. Cozzolino S, Sanna MG, Valentini M (2008) Probing interactions by means of pulsed field gradient nuclear magnetic resonance spectroscopy. Magn Reson Chem 46:S16–S23. doi:10.1002/mrc.2345

Polymer-Based Sensors

Zachary C. Smith and Samuel W. Thomas III
Pearson Chemistry Laboratory, Department of Chemistry, Tufts University, Medford, MA, USA

Synonyms

Biosensor; Chemosensor
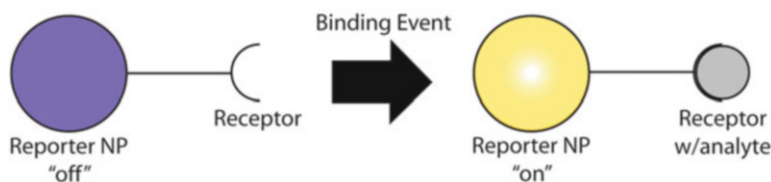
Polymer-Based Sensors, Fig. 1 An example of a general sensor design. This example uses non-covalent binding of a receptor with an analyte; analyte-sensor interactions can also include the making or breaking of covalent bonds

Definition

Polymer-based sensors are macromolecules that show a measureable change in a property in response to a stimulus in their environment, such as a particular molecule.

Introduction

Chemical and biological sensors work by interacting with analytes in their environment, which results in a change in an observable property to indicate the presence of a particular analyte. A general scheme for a sensor is illustrated in Fig. 1. The receptor interacts with an analyte through, for example, non-covalent binding or a chemical reaction. This event triggers a response in the reporter, which shows an observable physical change. This change is often in the optoelectronic properties of the sensor, such as its absorbance or emission of light or conductivity. Critical performance metrics for sensors are sensitivity, which indicates the smallest concentration that the sensor can detect, and selectivity, which is the extent to which a sensor can determine a particular analyte without interference from other components in the environment.

Chemical and biological sensors often have polymers as active components in their design. Polymers present a number of advantages to the design of sensors. Although every polymerization reaction has its own limitations with respect to, for example, functional group tolerance, polymerization reactions are highly modular. Different chemical structures are readily incorporated as pendant side chains on polymerizable moieties such as acrylates. Even if performing a polymerization reaction with a desired

side-chain structure is not possible, a variety of post-polymerization modification strategies using reactive polymer intermediates can yield the desired structure [1]. In addition, multiple chemical functionalities are often readily incorporated into polymeric structures by combining different monomers in the same polymerization reaction, including in the synthesis of polymers with well-defined architectures, such as block copolymers and gradient copolymers [2]. Finally, some polymer nanoparticle sensors have embedded small molecules that act as the reporter or receptor.

This entry focuses on nanoparticles consisting primarily of an organic polymer, in which the structure(s) of the polymer provides the receptor, the reporter, or both. Therefore, this entry does not include polymer nanoparticles where the polymer functions only as a structural component and not as the receptor or reporter. Polymer nanoparticles have sizes on the order of single digits to hundreds of nanometers. An important advantage of nanoparticles in sensing applications is their high surface area-to-volume ratio, which maximizes the receptor-environment interface. This approach also minimizes the amount of material required to perform a desired analysis, which can be important in biological applications due to any potential cytotoxicity.

Polymer Nanoparticle Properties and Design

Polymer nanoparticle sensors can be made of insulating polymers or conjugated polymers (Fig. 2). Insulating polymers consist of a polymer backbone that contains only single bonds. The polymer backbone of a conjugated polymer, however, comprises alternating double or triple bonds, which result in

Polymer-Based Sensors, Fig. 2 Examples of conjugated and insulating polymers used in polymer nanoparticles

Conjugated Polymers   **Insulating Polymers**

PPE

PAN

PFBT

PNIPA

PEDOT

PAA
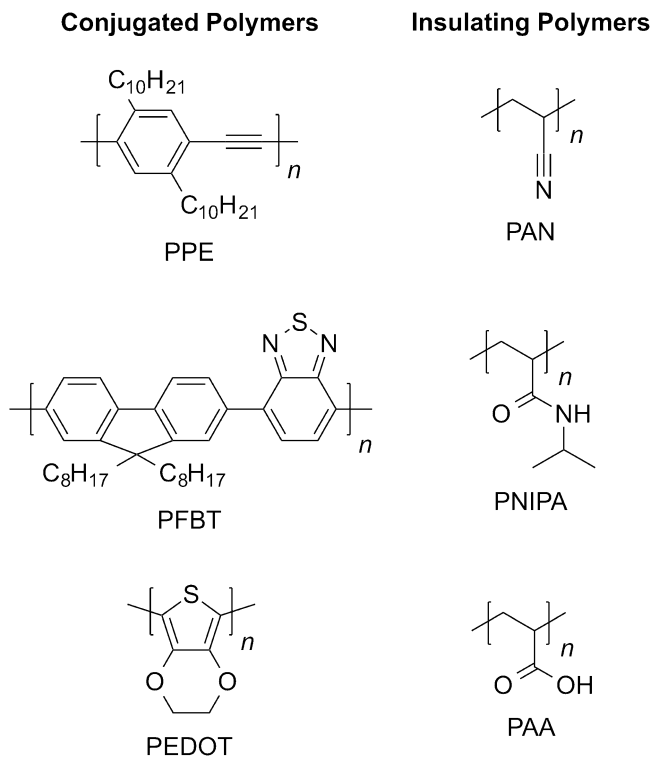
delocalization of electron density throughout the main chain of the polymer. This structural feature also allows many of these polymers to have conductivities that are larger in magnitude than nonconjugated polymers.

The physical properties of the polymers often dictate what type of detection method is used for the sensor. The innate conductivity of conjugated polymers makes them well suited for transistor-based detectors, which measure changes in conductivity. On the other hand, insulating polymers do not conduct electricity well enough to be used with these types of detectors. Another detection method measures changes in optical properties of the sensor. Both conjugated and insulating polymers can be amenable to this type of detection. Exciton and charge-carrier mobility of conjugated polymers can also result in large degrees of amplification, for example, of fluorescence quenching or energy transfer [3]. In addition, the main chains of conjugated polymers are chromophores, often resulting in materials that absorb and emit light efficiently.

Because of this feature, conjugated polymer nanoparticles (CPNs) have a high chromophore density [4]. Although these nanoparticles typically have a low quantum yield of fluorescence and a short fluorescence lifetime, they also often absorb light with large extinction coefficients in the visible range [5]. These features make CPNs attractive for sensing applications because the polymer backbone can provide structural support for the nanoparticle while also functioning as the reporter for the sensor. This dual purpose of structure and function is especially important since size is always a concern when working on the nanoscale.

In addition to the design of the main chains of polymers, the design of receptors on sensing materials, which are often pendant groups as polymer side chains, is also critical to their function. These receptors contain chemical groups that selectively bind to or react with specific analytes. The size and frequency of the side chain is an important consideration when designing polymer nanoparticles. If the side chain is too
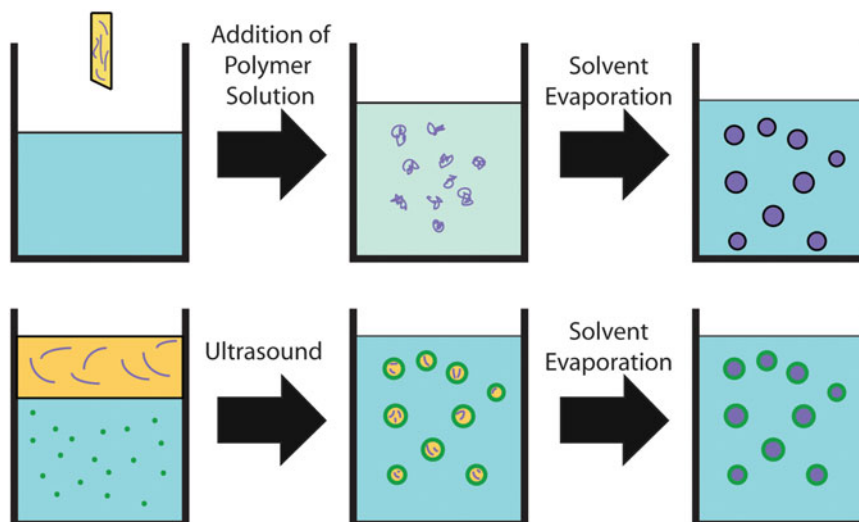
Polymer-Based Sensors, Fig. 3 Precipitation (*top*) and microemulsion (*bottom*) methods

large or if it is used too frequently along the polymer backbone, it can inhibit either the polymerization reaction or the aggregation and collapse of the polymer into a nanoparticle. One way to avoid this complication is to have the reporter added after the nanoparticle is formed through surface modification. This can be achieved by modifying functionality present on the polymer chains on the surface of the nanoparticles or encapsulating the nanoparticles in a readily modified material. This encapsulation is often done using silica because of its ubiquity and facile modification strategies [6]. However, any encapsulation has the inherent drawback of increasing the size of the nanoparticle. Most silica encapsulations add at least 2–5 nm to the diameter of the nanoparticle, although achieving uniform thin encapsulations is difficult when the coating is less than 5 nm [7].

Nanoparticle Fabrication

Polymer nanoparticles are typically made by one of two methods: precipitation or microemulsion. A cartoon illustrating the general procedures can be seen in Fig. 3. Generally, the precipitation method has lower yields than the microemulsion

method, but produces smaller nanoparticles. The precipitation method involves dissolving the polymer in a small amount of solvent. This solution is then quickly added to a poor solvent. The excess of poor solvent present causes the polymer to form solid precipitates. Several tactics facilitate making small nanoparticles: one method involves using the poor solvent in much larger volume and that the polymer solution is dilute. Studies have shown that the size of the resulting nanoparticles can be altered by modulating the concentration of the polymeric solution [8]. Another commonly used technique is to sonicate the solution during the mixing of polymer solution with the poor solvent. The ultrasonic treatment helps facilitate small particle formation by disrupting the interactions between individual polymer chains.

The microemulsion method involves creating nanospheres of hydrophobic solvent in an aqueous environment containing surfactant. One microemulsion technique involves carrying out the polymerization reaction inside the nanospheres, which utilizes a hydrophobic solvent, water, a surfactant, and the reagents necessary for the polymerization. These solvents and reagents can then be mixed, and the solution is then sonicated to form nanospheres that act as nanoscale

P

reactors for the many different types of polymerization used [9]. Recent work has shown that this approach can even be used for living radical polymerizations in aqueous dispersions [10]. The polymers then form within the confined spheres, making polymer nanoparticles in the process. An advantage of this approach is that the polydispersity of the polymer chains can be low, giving a relatively homogenous sample of nanoparticles [11]. The second microemulsion method utilizes a previously synthesized polymer dissolved in a hydrophobic solvent, water, and a surfactant. Upon formation of the nanospheres, the polymer chains are forced into a small spherical space where they aggregate. The solvent is then evaporated to form new polymer nanoparticles. Dynamic light scattering and transmission electron microscopy are generally useful techniques for characterizing the sizes of polymer nanoparticles.

Signal Transduction Methods and Examples

A number of transduction mechanisms for optical sensing with polymers exist. One type of sensor relies on photoinduced electron transfer (PET) [12] between the receptor and the reporter. Once the receptor binds or reacts with the analyte, there is a chemical change that alters the PET. This change in PET is usually seen as a change in emission intensity.

$$D \xrightarrow{h\upsilon} D^* \qquad (1)$$

$$D^* + A \xrightarrow{\text{Electron Transfer}} D^{+\cdot} + A^{-\cdot} \qquad (2)$$
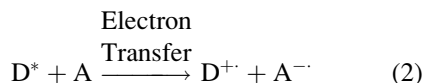
PET often occurs as a form of luminescence quenching that, once disrupted, allows for a large increase in fluorescence intensity. A good example of this pathway is a mercury (II) sensor that incorporated the luminescent metal terbium into a coordination polymer nanoparticle that utilized PET to quench the luminescence of terbium. However, the polymer was also able to coordinate mercury (II), which then disrupted the PET and allowed the terbium to emit (Fig. 4) [13].

Another type of sensing pathway relies on fluorescence resonance energy transfer (FRET), which differs from PET in that it is a form of energy transfer instead of electron transfer [12, 14].

$$D + A \xrightarrow{h\upsilon} D^* + A \xrightarrow{\text{Energy Transfer}} D + A^* \qquad (3)$$
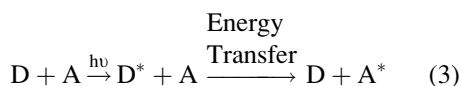
The excited donor (D*) transfers energy to the acceptor (A) through a nonradiative dipole-dipole interaction. A good example of this pathway can be seen in a polymer nanoparticle pH sensor (Fig. 5) [15]. The nanoparticle was made of poly (phenylene-ethynylene)/polystyrene blend which was covalently linked to the fluorescent dye fluorescein, the fluorescence intensity of which changes based on the pH of its environment.
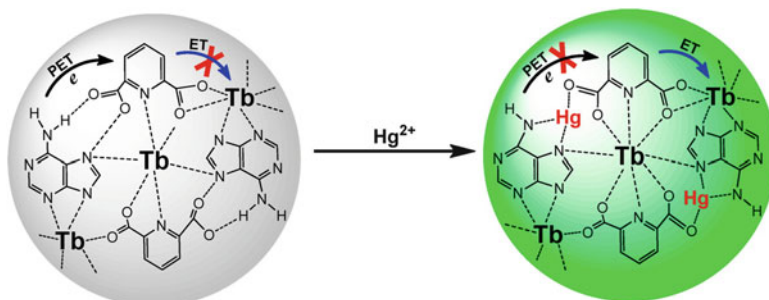
Polymer-Based Sensors, Fig. 4 Terbium-based polymer nanoparticle for detecting Hg^{2+} by PET mechanism (Reprinted with permission from Tan et al. [13]. Copyright (2012) American Chemical Society)

Polymer-Based Sensors, Fig. 5 FRET-based polymer nanoparticle pH sensor and fluorescence data (Adapted with permission from Chan et al. [15]. Copyright (2011) American Chemical Society)
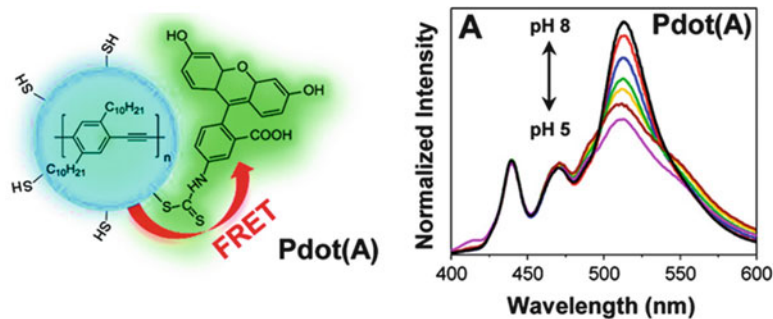
An interesting aspect of this sensor is that it is ratiometric, which indicates that there are two distinct signals that can be detected from the sensor, and that the ratio of intensity of these signals is the observable change the sensor relies upon. This property is useful because it is internally referenced, which makes it much easier to obtain quantitative data from the sensor. In this case, the fluorescein acts as the receptor and the reporter, while poly(phenylene-ethynylene) acts as a second, constant signal.

Biological Applications

Polymer nanoparticles are often used as sensors or probes to help study complex biological systems. One important characteristic is that the nanoparticles can be small, which is important in cells because it is desirable to have a probe that can pass easily from the body through the renal arteries [5]. Another reason why size is important is that the probe should not sterically disrupt the interaction that is being visualized. Encapsulating polymer nanoparticles in a more inert material, like silica, can decrease cytotoxicity and can allow further functionalization through surface modification. For biological applications it is important that the nanoparticles be water dispersible to prevent nanoparticle aggregation. Attaching hydrophilic side chains to typically hydrophobic conjugated polymers can lead to realization of this goal with CPNs. Another advantage of CPNs is that they can be used for two-photon fluorescence imaging [16], which can be used for real-time three-dimensional imaging of living tissue with a depth of 1 mm due to its use of near-infrared light which is absorbed less by biological tissues than visible light [17, 18]. The effectiveness of two-photon fluorescence imaging depends on the two-photon excitation cross section of the probe used, and if the two-photon excitation cross section is low, a much more powerful laser is needed. Conventional fluorescent dyes have a two-photon excitation cross section on the scale of 1,000 s of Goeppert-Mayer units (GM), while conjugated polymer nanoparticles have been shown to have two-photon excitation cross sections up to 200,000 GM [19].

Related Entries

▶ Biosensing Materials
▶ Chemical Sensor

References

1. Theato P, Klok H-A (2013) Functional polymers by post-polymerization modification. Concepts, guidelines and applications. Wiley-VCH, Weinheim
2. Davis KA, Matyjaszewski K (2002) Statistical, gradient, block, and graft copolymers by controlled/living radical polymerizations. Springer, Berlin
3. Thomas SW, Joly GD, Swager TM (2007) Chemical sensors based on amplifying fluorescent conjugated polymers. Chem Rev 107:1339–1386
4. Tian Z, Yu J, Wu C, Szymanski C, McNeill J (2010) Amplified energy transfer in conjugated polymer nanoparticle tags and sensors. Nanoscale 2:1999
5. Wu C, Chiu DT (2013) Highly fluorescent semiconducting polymer dots for biology and medicine. Angew Chem Int Edit 52:3086–3109
6. Vrignaud S, Benoit J-P, Saulnier P (2011) Strategies for the nanoencapsulation of hydrophilic molecules in polymer-based nanoparticles. Biomaterials 32:8593–8604

7. Zhang F, Lees E, Amin F, RiveraGil P, Yang F, Mulvaney P, Parak WJ (2011) Polymer-coated nanoparticles: a universal tool for biolabeling experiments. Small 7:3113–3127

8. Pecher J, Mecking S (2010) Nanoparticles of conjugated polymers. Chem Rev 110:6260–6279

9. Tian Z, Wu W, Li ADQ (2009) Photoswitchable fluorescent nanoparticles: preparation, properties and applications. Chem Phys Chem 10:2577–2591

10. Monteiro MJ, Cunningham MF (2012) Polymer nanoparticles via living radical polymerization in aqueous dispersions: design and applications. Macromolecules 45:4939–4957

11. Landfester K (2009) Miniemulsion polymerization and the structure of polymer and hybrid nanoparticles. Angew Chem Int Edit 48:4488–4507

12. Turro NJ, Ramamurthy V, Scaiano JC (2010) Modern molecular photochemistry of organic molecules. University Science Books, Sausalito

13. Tan H, Liu B, Chen Y (2012) Lanthanide coordination polymer nanoparticles for sensing of mercury (ii) by photoinduced electron transfer. ACS Nano 6:10505–10511

14. Lakowicz J (2006) Principles of fluorescence spectroscopy, 3rd edn. Springer, New York

15. Chan Y-H, Wu C, Ye F, Jin Y, Smith PB, Chiu DT (2011) Development of ultrabright semiconducting polymer dots for ratiometric pH sensing. Anal Chem 83:1448–1455

16. Wu C, Bull B, Szymanski C, Christensen K, McNeill J (2008) Multicolor conjugated polymer dots for biological fluorescence imaging. ACS Nano 2:2415–2423

17. Tuncel D, Demir HV (2010) Conjugated polymer nanoparticles. Nanoscale 2:484

18. Yao S, Belfield KD (2012) Two-photon fluorescent probes for bioimaging. Eur J Org Chem 2012:3199–3217

19. Wu C, Szymanski C, Cain Z, McNeill J (2007) Conjugated polymer dots for multiphoton fluorescence imaging. J Am Chem Soc 129:12904–12905

Polymeric Coatings to Fight Biofouling

Jens Friedrichs and Carsten Werner
Leibniz Institute of Polymer Research Dresden, Dresden, Germany

Synonyms

Antifouling coatings

Definition

Biofouling, the undesired accumulation of biomass on man-made surfaces, can be avoided by polymer-based surface coatings.

Biofouling

Biofouling – the accumulation and growth of communities of organisms on natural or artificial surfaces in contact with aerial or saline environments – can have severe negative consequences in a multitude of fields including industrial processes (e.g., food processing, textile, pulp and paper manufacturing) and medicine (e.g., nosocomial infections) and on seawater-contacting equipment (e.g., pipelines, cooling and filtration systems, fishing nets, ship hulls, and bridge pillars).

Biofilm Formation and Consequences of Biofouling

Biofouling is a complex process that, in most cases, can be described by a basic sequence of events. Firstly, the rapid adsorption of organic molecules (mainly proteins and polysaccharides) forms a conditioning film depending on the surface properties and the environmental conditions. This is quickly followed by the development of a microbial biofilm, which essentially involves (1) the attachment of bacteria cells (and diatoms), (2) the growth and multiplication of the attached cells, (3) the formation of mature colonies, and (4) cell detachment. In marine and freshwater environments, the microbial biofilms themselves influence the subsequent colonization with more complex organisms (e.g., algae spores and protozoa) by facilitating or inhibiting settlement. The final stage of fouling is characterized by the growth of macroalgae and the settlement and growth of larger marine invertebrates [1, 2].

Marine and freshwater biofouling is undesirable for many reasons. Microbial biofilms can cause local fluctuations in the concentration of various chemical species, such as oxygen and

metal ions, thus accelerating the corrosion of the metal substrata. The metabolic process or products (e.g., sulfides) may also be corrosive to steel surfaces. Biofouling can increase the roughness on ship hulls, resulting in a greater hydrodynamic drag. The resulting increases in fuel consumption and maintenance costs (such as dry dock cleaning, paint removal, and repainting) cost the US Navy alone more than one billion dollars per annum. In addition to economic losses, a serious threat associated with marine biofouling is the global, distributive spread of invasive species that endanger local biodiversity [3, 4].

The process of biofouling results from both physical and biochemical phenomena at material interfaces. The physical interactions are governed by factors such as electrostatic forces and water flow and lead to the formation of the conditioning biofilm and adsorption of microorganisms. The biochemically triggered phenomena include migration and secondary adhesion of microorganisms, the formation of biofilms, and the attachment and growth of macrofoulers. Whereas physical interactions are usually reversible, biochemical reactions are effectively irreversible. Thus, successful inhibition of the physical interactions could constrain the later biochemically controlled phenomena.

Biocides to Avoid Biofouling

Classical chemical strategies to reduce marine biofouling are based on the release of biocides. Some of the most successful paints used to protect marine vessels are based on tributyltin (TBT). In these types of paints, the biocide is embedded in a polymer matrix (such as vinyl and epoxy) that erodes in water. Consequently, when the coating is immersed in seawater, the TBT dissolves leaving a multiporous structure behind. Seawater then permeates into the film more deeply allowing more biocide to dissolve in the water. However, at some stage, the leached layer becomes less accessible to water, and the rate of TBT release falls below a minimum value required for antifouling. To circumvent this problem, a TBT-self-polishing copolymer (SPC)

technology was developed. TBT-SPC paints are based on acrylic polymers (usually methyl methacrylate) with TBT groups bound to the polymer backbone by an ester. This linkage is easily hydrolyzed in slightly alkaline environments such as seawater. This results in cleavage of the TBT portion from the copolymer releasing the biocides into the water. Once many TBT portions have been cleaved, the partially reacted, brittle, polymer backbone can be easily washed off by the moving seawater, which exposes a fresh coating surface [2].

Being highly effective, TBT was found to have a harmful impact on the environment because it accumulates in nontarget species causing malformations and other disorders. A global ban on the use of TBT is now in effect due to its negative ecological side effects. Similarly, the use of booster biocides (pesticides and herbicides), which are incorporated into cooperbased antifouling systems, is also under scrutiny due to their toxic effects on the environment. The environmental concerns associated with the use of leachable biocides have propelled efforts to develop nontoxic antifouling coatings [2].

A variety of non-biocidal antifouling methods have been developed including electric currents, acoustic vibrations, piezoelectric coatings, bubble curtains, ultraviolet radiation, magnetic fields, heating, and cryogenic treatments. All of these are either only effective in the short term, or species specific, or impractical to handle and apply [5].

Nontoxic, Polymer-Based Approaches to Fight Biofouling

In recent years, with advances in macromolecular synthesis and surface engineering techniques, polymer-based coatings have been designed and explored to resist the attachment of biofouling species (non-fouling surfaces) or allow for easy removal of adherent layers (foul-release surfaces). Settlement and adhesion of marine organisms on these polymer surfaces were shown to be affected by chemical, topographic, and biological cues. However, a set of basic physical and

chemical polymer properties were identified as necessary to produce an adhesion-resistant surface [6]:

- A flexible, linear backbone that introduces no undesirable interactions
- A sufficient number of surface-active groups, which are free to move to the surface and there impart a surface energy within a desired range
- A low elastic modulus
- A surface that is smooth at the molecular level to avoid infiltration of a biological adhesive leading to mechanical interlocking
- High molecular mobility in the backbone and surface-active side chains
- A thickness, which controls the fracture mechanics of the interface

Fouling-Release Coatings

Polymer-based coatings that fulfill many of the above given requirements are fouling-release (FR) coatings, which do not inhibit settlement but, instead, allow for easy removal of attached biofoulers. At present, commercially available, hydrophobic, FR coatings comprise two families of materials: fluoropolymers and silicones. Fluoropolymers provide nonporous, low surface free energy surfaces with good nonstick characteristics, while silicones improve the nonstick efficiency of fluoropolymers [7]. Polydimethylsiloxane (PDMS)-based FR coatings are mostly used because of their low surface energy and low micro-roughness. The silicone additives incorporated into PDMS coatings migrate to the coating surface and create a weakly bound surface layer that further enhances FR properties. FR coatings are primarily suitable for applications that feature high flow rates (fast traveling ships), and even then, fouling through slimes prevails, often necessitating underwater cleaning. This excludes them for use in many contexts, including static structures or aquaculture and slow-moving recreational and coastal commercial vessels. Furthermore, currently available foul-release coatings are relatively expensive, are easily damaged, and have poor mechanical properties [8].

Topography Effects

In addition to surface chemistry approaches, surface topography has also been shown to be effective in avoiding macrofouling on a larger scale. Settlement studies and field observations revealed that the attachment of a wide range of cells and organisms, including bacteria, algal spores, and invertebrate larvae, is sensitive to both the size and periodicity of the surface topography. It has been demonstrated that green algae spores are very selective in settlement behavior on engineered PDMS microtopographies such as the Sharklet AF™, which is a patterned PDMS surface inspired by shark skin. Various studies show that spores prefer to settle on surfaces that provide a topography with dimensions similar to the maximum width of the free-swimming spore body. Although the antifouling potential of microtopographical surfaces has been demonstrated beyond question, the underlying mechanisms responsible for reduced fouling remain largely unresolved.

Hydrophilic Coatings

Other polymer-based antifouling technologies rely on hydrophilic coatings. Demonstrating low polymer–water interfacial energy levels, these materials show resistance to protein adsorption and cell adhesion. Moreover, the related coatings exhibit low friction and are often considered to be superior to hydrophobic surfaces with respect to bacterial attachment and biofilm formation. In particular, polyethylene glycol (PEG) is a widely used, non-fouling polymer coating because it is nontoxic and considered biocompatible. PEG chains resist protein adsorption via two distinct effects: steric repulsion due to chain compression and a "barrier" created by structured water associated with the PEG chains. PEG has thus been used extensively for the preparation of non-fouling surfaces. In addition, it has been suggested that PEG chains can maintain the bioactivity of conjugated, bioactive molecules [9]. Therefore, many research groups have adopted PEG as a non-fouling spacer polymer for the immobilization of biomolecules

on surfaces. Different architectures of PEGylated surfaces – linear (brushes), branched (comblike polymers with PEGylated side chains), and hyperbranched (dendrimer) – have been shown to be effective. A recent advance in hydrophilic PEGylated coatings uses bio-inspired polymers prepared from methoxy-terminated PEG and the adhesive amino acid L-3,4-dihydroxy-phenylalaine.

Most PEG-modified surfaces are prepared using a "grafting to" strategy, which has the disadvantage that the grafting density is limited by steric restrictions and thus insufficient to achieve antifouling properties. Many researchers have therefore adopted "grafting from" strategies, such as surface-initiated, atom transfer, radical polymerization, for preparing polymer brushes with non-fouling properties. A fundamental disadvantage of PEG is its poor stability as the polymer readily undergoes oxidative degradation, especially at elevated temperatures. A range of bacteria can also metabolize PEG chains, primarily with the help of alcohol dehydrogenase enzymes. Long-term studies have repeatedly shown that PEG coatings fail to remain protein resistant over extended periods of time. Other hydrophilic, nonionic polymers were reported to be suitable coating materials for non-fouling surfaces, including dextran, polyacrylamide, poly(vinylpyrrolidone), or poly-2-methyl-2-oxazoline [10, 11].

Amphiphilic Surfaces

A recent trend in designing experimental coatings for antifouling purposes is to create surfaces with compositional (chemical) heterogeneity at the nanoscale through the thermodynamically driven phase segregation of polymer assemblies, followed by cross-linking in situ. For that purpose, amphiphilic copolymers are considered suitable as they consist of at least two constituents of different chemical nature, having both hydrophilic and hydrophobic components. The related coating designs may be based on blends of immiscible polymers or contrasting chemistries of block copolymers. The general aim is to combine the nonpolar, low surface energy, low modulus properties of hydrophobic components to reduce polar and hydrogen-bonding interactions with the bioadhesives used by fouling organisms with the protein repellence properties of the hydrophilic components. The resulting chemical "ambiguity," expressed in terms of amphiphilic nanodomains on the surface, may lower both entropic and enthalpic contributions to the adsorption proteins and glycoprotein bioadhesives. It was speculated that the protein resistance of nanopatterned, amphiphilic diblock copolymers results from the intrinsic high density of surface interfacial boundaries [12, 13].

Zwitterionic Surfaces

Inspired by the non-fouling properties of blood cells, polymers have also been studied as non-fouling surfaces that incorporate zwitterionic molecules, which are electrically neutral but carry positive and negative charges such as phosphatidylcholines. Zwitterionic materials deterred protein surface adsorption and were observed to be more stable than PEG-based coatings when trialed in marine applications. The zwitterionic structures on the surface create a strong, electrostatically induced hydration layer, contributing to superhydrophilic properties, with enhanced resistance to protein adsorption. The attachment of organisms was reported to be significantly reduced by weakened interactions between secreted bioadhesives from fouling organisms and the surface. Bioassays investigating such surfaces showed nearly complete inhibition of green algae spore settlement and reduced diatom attachment, as well as marked resistance to settlement of larger marine invertebrates [11, 12].

Hydrogels

Hydrogels (cross-linked polymer networks that swell in the presence of water) are especially interesting for non-fouling applications as they permit the combination of hydrophilic

characteristics with a tunable elastic modulus. As a prominent example, poly(hydroxyethyl methacrylate) hydrogels have been widely studied for the reduction of biofouling. However, without the addition of biocides, the coatings demonstrated rather poor antifouling properties. In other studies, a number of different hydrogels including alginate, chitosan, poly(vinyl alcohol), and agarose hydrogels were evaluated in laboratory tests with barnacles and marine bacteria. It was concluded that all tested hydrogels had lower settlement than polystyrene surfaces and that the differences between the gels were due to inherent chemical differences in the polymer network rather than the variation of modulus and hydrophilicity. Despite the promising results, fundamental challenges for the application of hydrogel-based coatings concern their long-term stability and mechanical properties [14].

Enzymes for Antifouling

An alternative approach to reducing adhesion of fouling organisms uses enzymes incorporated into coatings. Interest in the potential of enzymes as antifouling agents has been active for the past 20 years and is well represented in the patent literature [15]. The environmental and economical friendliness and the high substrate specificity of enzymes enable the generation of highly effective antibacterial surfaces, for example, for food packaging applications. More recently, enzymes have also been actively investigated and used as therapeutic agents to eliminate pathogenic biofilms in medicine. Major enzymatic antifouling mechanisms include:

- Cell lysis through the degradation of cell membrane components
- Degradation of compounds anchoring cells to the surface (1) of adhesives produced during settlement and anchorage and (2) of the extracellular matrix secreted by proliferating adhered organisms
- Disruption of intercellular communication (quorum sensing, i.e., bacterial cell–cell communication)

- Degradation of environmental substances (1) that are fundamental for the survival of the fouling organism or (2) generating antifouling compounds

Immobilized enzymes were reported to be active over a broader range of environmental conditions (pH, temperature) than free enzymes and characterized by a higher stability upon storage. Enzyme inhibition by substrates, reaction products, or any other components present in the environment may also be minimized through immobilization. The advantages associated with using immobilized enzymes for antifouling purposes include the localization of the enzyme where needed, i.e., at the coating–fouler interface, improving efficacy and the decrease of safety and environmental concerns because enzymes are confined to the coating surface and not released into the environment.

Enzyme immobilization methods described in the literature include adsorption, covalent bonding, cross-linking, graft copolymerization, and entrapment, and several different variations based on the combination of these methods have been developed. The increasing knowledge on the structure and catalytic mechanism of different enzymes increasingly allows for the application of molecular simulations for the rational development of immobilization methods [16]. Although physical adsorption and entrapment are the simplest methods for enzyme immobilization, these frequently result in enzyme leaching from the surface, low stability, and poor performance. Covalent immobilization typically yields systems with improved stability and with minimal enzyme leaching into the aqueous media. Covalent immobilization can be beneficial when envisaging applications in aqueous environments and when denaturing factors exist because the formation of multiple covalent bonds between the enzyme and carrier reduces conformational flexibility and thermal vibrations preventing enzyme denaturation and unfolding. A disadvantage associated with covalent binding is the chemical modification of the enzyme. Enzyme activity and stability can, however, be enhanced using site-directed immobilization schemes, which were reported to be

advantageous when compared with random immobilization strategies in several studies [17].

The number of investigations on the potential use of enzymes as antifouling agents has progressively increased over the past few years. Envisaging industrial applications, enzymes are economically viable and more advantageous than conventional biocides because they are currently available at affordable prices and are biodegradable.

As a recent example, a well-defined model system was developed to investigate the influence of immobilized subtilisin A on the adhesion of major marine foulers [18, 19]. The model system is based on reactive maleic anhydride (MA) copolymers covalently attached as nanometer-thick films to amino-functionalized surfaces. The system enables the covalent attachment of biomolecules through the high reactivity of the anhydride moieties toward primary amines [19]. By tuning the film preparation conditions and through the selection of the comonomer and molecular weight, the physicochemical properties of the MA copolymer films can be varied over a wide range. The use of reactive polymer surfaces with tunable physicochemical properties enabled investigation into the influence of the polymer substrate characteristics on the amount, activity, and antifouling properties of the immobilized enzyme [18, 19]. Purified subtilisin A was used to avoid spurious effects caused by stabilizers and preservatives usually present in commercial crude preparations. The immobilization of subtilisin A onto highly swelling, poly(ethylene-*alt*-maleic anhydride) copolymer films was found to be advantageous because it permitted higher enzyme loading and activity compared with enzyme immobilization onto the compact hydrophobic poly(octadecene-*alt*-maleic anhydride) copolymer films [19]. Studies evaluating the effects of immobilized subtilisin A on the initial steps of settlement and adhesion of marine bacteria, green algae spores, diatoms, and larger marine invertebrates revealed that the adhesion strength decreased in the presence of the active enzyme [18, 20]. In addition, a higher antifouling efficacy was observed for the immobilized enzyme when compared with similar amounts of free enzyme indicating the importance of enzyme localization at the cell–coating interface [18].

Related Entries

▶ Biobased Polymers

References

1. Hall-Stoodley L, Costerton JW, Stoodley P. Bacterial biofilms: from the natural environment to infectious diseases. Nat Rev Microbiol. 2004;2:95–108. doi:10.1038/nrmicro821
2. Yebra DM, Kiil S, Dam-Johansen K. Antifouling technology – past, present and future steps towards efficient and environmentally friendly antifouling coatings. Prog Org Coat. 2004;50:75–104. doi:10.1016/j.porgcoat.2003.06.001.
3. Callow ME, Callow JE. Marine biofouling: a sticky problem. Biologist (London). 2002;49:10–4.
4. Flemming H-C, Murthy PS, Venkatesan R, Cooksey KE. Marine and industrial biofouling. Berlin/Heidelberg: Springer; 2010.
5. Chambers LD, Stokes KR, Walsh FC, Wood RJK. Modern approaches to marine antifouling coatings. Surf Coat Technol. 2006;201:3642–52. doi:10.1016/j.surfcoat.2006.08.129.
6. Brady Jr RF. Properties which influence marine fouling resistance in polymers containing silicon and fluorine. Prog Org Coat. 1999;35:31–5. doi:10.1016/S0300-9440(99)00005-3.
7. Brady Jr RF. A fracture mechanical analysis of fouling release from nontoxic antifouling coatings. Prog Org Coat. 2001;43:188–92. doi:10.1016/S0300-9440(01)00180-1.
8. Buskens P, Wouters M, Rentrop C, Vroon Z. A brief review of environmentally benign antifouling and foul-release coatings for marine applications. J Coat Technol Res. 2013;10:29–36. doi:10.1007/s11998-012-9456-0.
9. Marconi W, Benvenuti F, Piozzi A. Covalent bonding of heparin to a vinyl copolymer for biomedical applications. Biomaterials. 1997;18:885–90.
10. Banerjee I, Pangule RC, Kane RS. Antifouling coatings: recent developments in the design of surfaces that prevent fouling by proteins, bacteria, and marine organisms. Adv Mater. 2011;23:690–718. doi:10.1002/adma.201001215.
11. Magin CM, Cooper SP, Brennan AB. Non-toxic antifouling strategies. Mater Today. 2010;13:36–44. doi:10.1016/S1369-7021(10)70058-4.
12. Krishnan S, Weinman CJ, Ober CK. Advances in polymers for anti-biofouling surfaces. J Mater Chem. 2008;18:3405. doi:10.1039/b801491d.

P

13. Grozea CM, Walker GC. Approaches in designing non-toxic polymer surfaces to deter marine biofouling. Soft Matter. 2009;5:4088–100. doi:10.1039/B910899H.

14. Magin CM, Finlay JA, Clay G, Callow ME, Callow JA, Brennan AB. Antifouling performance of cross-linked hydrogels: refinement of an attachment model. Biomacromolecules. 2011;12:915–22. doi:10.1021/bm101229v.

15. Terlizzi A, Fraschetti S, Gianguzza P, Faimali M, Boero F. Environmental impact of antifouling technologies: state of the art and perspectives. Aquat Conserv Mar Freshwat Ecosyst. 2001;11:311–7. doi:10.1002/aqc.459.

16. Hanefeld U, Gardossi L, Magner E. Understanding enzyme immobilisation. Chem Soc Rev. 2009;38:453. doi:10.1039/b711564b.

17. Cordeiro AL, Werner C. Enzymes for antifouling strategies. J Adhes Sci Technol. 2011;25:2317–44. doi:10.1163/016942411X574961.

18. Tasso M, Pettitt ME, Cordeiro AL, Callow ME, Callow JA, Werner C. Antifouling potential of Subtilisin A immobilized onto maleic anhydride copolymer thin films. Biofouling. 2009;25:505–16. doi:10.1080/08927010902930363.

19. Tasso M, Cordeiro AL, Salchert K, Werner C. Covalent immobilization of Subtilisin A onto thin films of maleic anhydride copolymers. Macromol Biosci. 2009;9:922–9. doi:10.1002/mabi.200900005.

20. Tasso M, Conlan SL, Clare AS, Werner C. Active enzyme nanocoatings affect settlement of balanus amphitrite barnacle cyprids. Adv Funct Mater. 2012;22:39–47.

Polymeric Drugs

Jiyuan Yang[1] and Jindřich Kopeček[1,2]
[1]Department of Pharmaceutics and Pharmaceutical Chemistry, University of Utah, Salt Lake City, UT, USA
[2]Department of Bioengineering, University of Utah, Salt Lake City, UT, USA

Synonyms

Macromolecular therapeutics; Polymer–drug conjugates; Polymeric nanomedicines

Definition

Nanosized water-soluble polymer (macromolecular) compounds with therapeutic activity; the major subgroup are polymer–drug conjugates.

Historical Background

Polymer compounds are widely used in medicine in many forms and combinations. This entry focuses on water-soluble polymers with biological activity and water-soluble polymer–drug conjugates. Water-soluble polymers may possess intrinsic biological activity that relates to their structure, molecular weight, charge density, charge distribution, conformation, and stability [1]. Macromolecules such as dextran, poly(N-vinylpyrrolidone), and hydroxyethyl starch have been used as blood plasma expanders to restore the blood volume following trauma or shock. Poly(2-vinylpyridine-N-oxide) has demonstrated activity against silicosis; its effect has been explained by the adsorption of the weakly basic polymer on the weakly acidic surface of silica. Polyelectrolytes stimulate interferon production in cells and living organisms. Stereochemistry has an impact on activity; isotactic poly(acrylic acid) possesses antiviral properties, whereas atactic poly(acrylic acid) does not [2].

A much wider use of water-soluble polymers has been to facilitate the delivery of drugs to diseased tissue by employing nanosized polymer–drug conjugates. The first polymer–drug conjugate has been prepared by Jatzkewitz who attached mescaline to polyvinylpyrrolidone via a glycylleucine spacer 60 years ago [3]. Mathé and coworkers pioneered conjugation of drugs to antibodies initiating targeted drug delivery [4]. The entry will focus on polymer–drug conjugates in general and polymer–anticancer drug conjugates in particular.

Biological Rationale

The major rationale for the use of water-soluble polymers as carriers of anticancer drugs is based on the mechanism of cell entry [5, 6]. Although the majority of low-molecular-weight drugs enter cells by diffusion across the plasma membrane, the entry of macromolecules is restricted to endocytosis. Macromolecules captured by this mechanism are usually channeled to the lysosomal compartment of the cell.
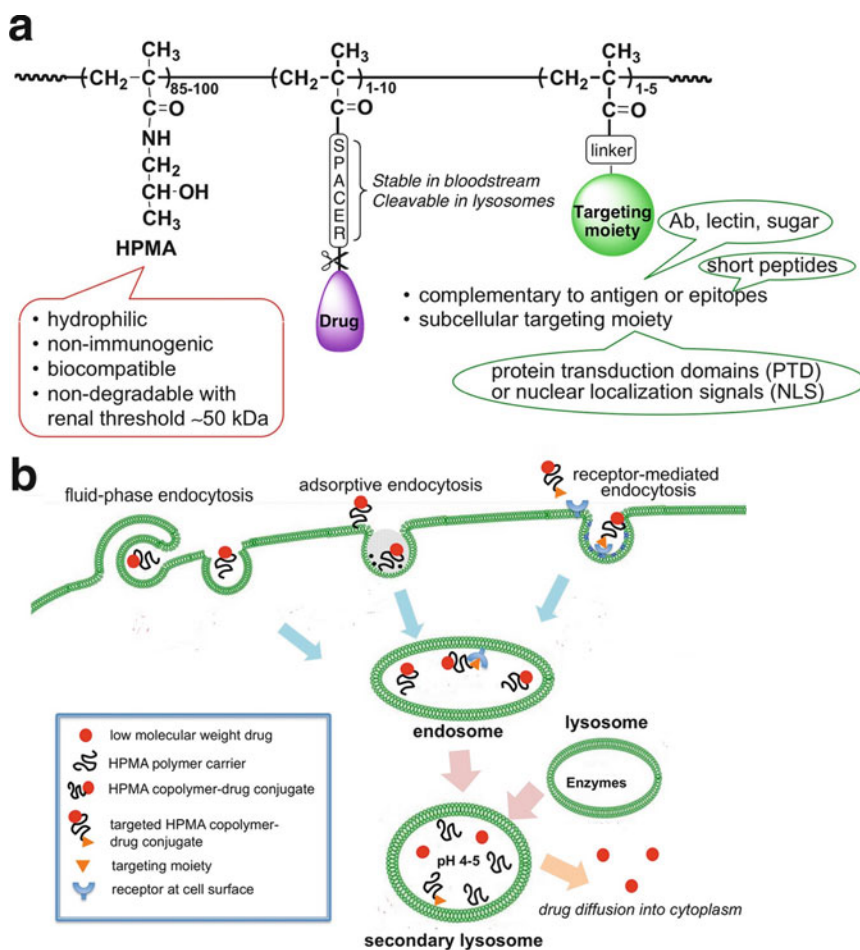
Polymeric Drugs, Fig. 1 (**a**) Typical structure of a targetable water-soluble polymer–drug conjugate. A drug is bound to the *N*-(2-hydroxypropyl) methacrylamide (*HPMA*) copolymer backbone via a spacer that is stable in the bloodstream but susceptible to enzymatically catalyzed hydrolysis in the lysosomal compartment of the cell. To achieve targeting a targeting moiety (antibody, antibody fragment, peptide, or saccharide) is attached to the backbone. Optionally, the conjugates contain a subcellular targeting moiety that directs the drug to a specific subcellular organelle. (**b**) Internalization of polymer–drug conjugates by endocytosis. The ultimate localization of the conjugate is the secondary lysosome

Targeting moieties, complementary to cell surface receptors, incorporated into the macromolecular structure render the macromolecule biorecognizable by a subset of (diseased) cells. This provides a mechanism to enhance the accumulation of drugs at target tissue. For efficiency, targetable polymer–drug conjugates should be biorecognizable at two levels: at the plasma membrane, eliciting selective recognition and internalization by a subset of target cells, and intracellularly, where lysosomal enzymes induce the release of drug from the carrier. The latter is a prerequisite for transport of the drug across the lysosomal membrane into the cytoplasm and translocation into the organelle decisive for biological activity (Fig. 1).

Design Principles

Polymer carriers need to be nontoxic and nonantigenic and possess a structure that provides drug attachment/release sites; they should be degradable or have a molecular weight below
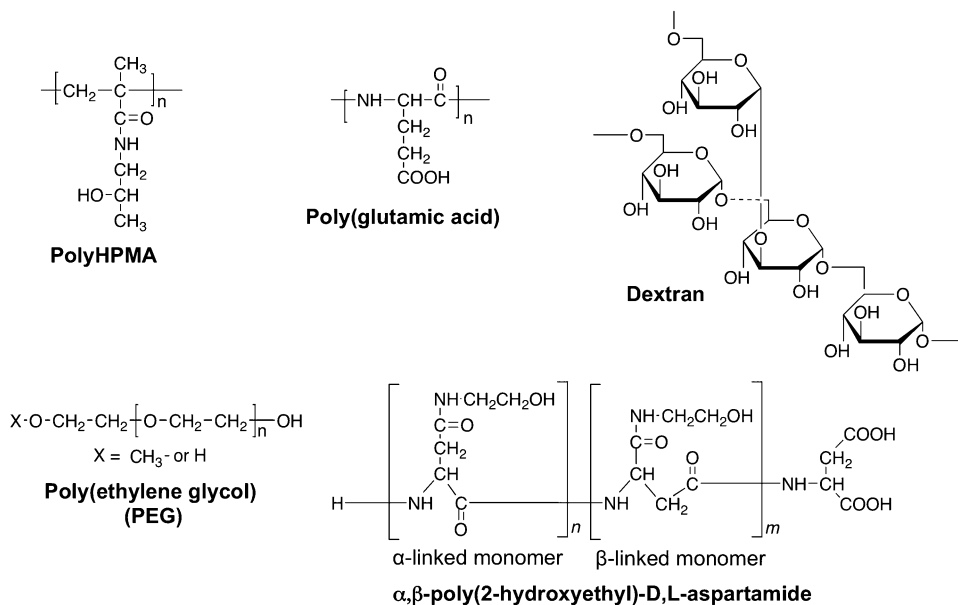
Polymeric Drugs, Fig. 2 Structures of representative polymer–drug carriers

the renal threshold (about 50 kDa for neutral hydrophilic random coils) to permit elimination via glomerular filtration. Frequently used carriers are poly[*N*-(2-hydroxypropyl)methacrylamide] (polyHPMA), poly(glutamic acid), poly(ethylene glycol) (PEG), dextran, and α,β-poly (2-hydroxyethyl)-D,L-aspartamide (Fig. 2).

Polymer–drug linkages need to be stable in the bloodstream and interstitial space but be susceptible to hydrolysis in the lysosomes. Due to a lower pH (∼5) in the lysosomes, the bond between drug and polymer might be degradable by chemical (Fig. 3a) or enzymatically catalyzed (Fig. 3b) hydrolysis. In conjugate A the drug (doxorubicin) is bound via a hydrazone bond that is stable at neutral pH (bloodstream) but hydrolyzes at acidic conditions (in late endosomes and lysosomes). There are numerous enzymes in the lysosomes, and the spacers connecting the polymer carrier and drug need to be designed to match the selected enzyme's active site. A frequently used spacer is the GFLG tetrapeptide; it fits into the active site of cathepsin B (Fig. 3b) [6].

Binding drugs to polymeric carriers generally results in a decrease of adverse effects, improved

pharmacokinetics, and modulation of the cell signaling and apoptotic pathways and has a potential to overcome multidrug resistance [6]. For example, doxorubicin (DOX) possesses serious cardiotoxicity; its maximum tolerated dose (MTD) in humans is 60–80 mg/m^2, whereas the MTD of HPMA copolymer–DOX conjugate in clinical trials was 320 mg/m^2 (in DOX equivalent) mainly due to less effective accumulation and endocytosis of macromolecules in heart tissue [7].

Active targeting. The incorporation of cancer cell-specific ligands, such as carbohydrates, lectins, antibodies, antibody fragments, and peptides, results in enhanced uptake of polymer–drug conjugates by cancer cells through cell surface biorecognition followed by receptor-mediated endocytosis [5, 6]. A comparison of the efficacy of an antibody-targeted and nontargeted conjugate is shown in Fig. 4. Human ovarian carcinoma OVCAR-3 xenografts were treated with OV-TL16 antibody (complementary to CD47)-targeted HPMA copolymer–drug (DOX and mesochlorin e$_6$ (Mce$_6$)) conjugates. Following the internalization of the conjugates into cancer cells, DOX will be released in the lysosomes
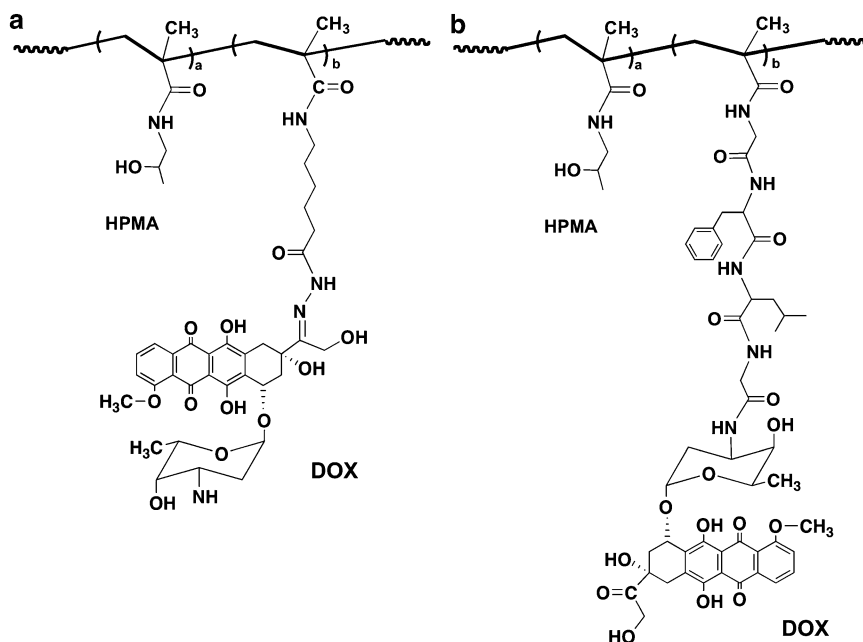
Polymeric Drugs, Fig. 3 Structure of the *HPMA* copolymer–doxorubicin (*DOX*) conjugates with different spacers. (**a**) Spacer hydrolytically cleavable in the endosomes/lysosomes; (**b**) spacer (Gly–Phe–Leu–Gly) cleavable by lysosomal enzyme cathepsin. (**b**) The amide bond originating in the terminal glycine is cleaved resulting in the release of (unmodified) drug (*DOX*)

P
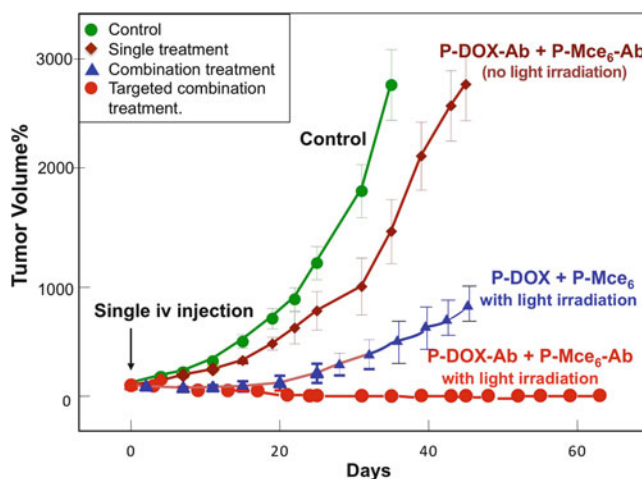
Polymeric Drugs, Fig. 4 Efficacy of combination chemotherapy and photodynamic therapy of human ovarian carcinoma OVCAR-3 xenografts in nude mice with nontargeted and OV-TL16 antibody-targeted conjugates. Therapeutic efficacy of a combination therapy of HPMA copolymer-bound mesochlorin e$_6$ (Mce$_6$) and doxorubicin (DOX) targeted with OV-TL16 antibodies was compared with nontargeted combination chemotherapy and photodynamic therapy and nontreated controls. Equivalent doses of targeted combination therapy enhanced the tumor-suppressive effect as compared to nontargeted combination therapy. Dose administered: 2.2 mg/kg DOX equivalent and 1.5 mg/kg Mce$_6$ equivalent. Irradiation for photodynamic therapy: 650 nm, 200 mW/cm^2, 18 h after administration (Adapted with permission from Ref. [8])

by cathepsin B-catalyzed hydrolysis, translocate into the cytoplasm, and ultimately enter nucleus where it will intercalate into DNA. Mce$_6$ is a photosensitizer that is not active without light. Following irradiation with light that matches its absorption spectrum, the photosensitizer is excited and transfers energy to molecular oxygen. The produced singlet oxygen is a very reactive species toxic to biological systems including cells.

Subcellular targeting. The activity of many drugs depends on their subcellular location; some drugs benefit from mitochondrial location and others from reaching the nucleus. Efforts are underway to evaluate conjugates that combine tumor and subcellular organelle targeting. For example, mitochondrial targeting can be achieved by exploiting the negative mitochondrial potential and use of positively charged triphenylphosphonium ions as mitochondrial targeting agents [9]. This concept may be used both in vitro and in vivo.

Passive targeting. The solid tumor vasculature is leaky and permits the extravasation of polymer–drug conjugates. The accumulation of polymers and polymer–drug conjugates in tumor tissue is molecular weight dependent. The higher the molecular weight, the higher the accumulation in the tumor with concomitant increase in therapeutic efficacy. This phenomenon, the enhanced permeability and retention (EPR) effect (Fig. 5a), is the predominant mechanism by which soluble macromolecular anticancer drugs exhibit their therapeutic effect on solid tumors. It is attributed to high vascular density of the tumor, increased permeability of tumor vessels, defective tumor vasculature, and malfunctioning or suppressed lymphatic drainage in the tumor interstitium [10].

Consequently, *molecular weight* (*Mw*) *and molecular weight distribution* are important factors in the design of effective polymer–drug conjugates. The renal threshold limits the molecular weight of the first generation (nondegradable) polymeric carriers to below 50 kDa; this lowers the retention time of the conjugate in the circulation resulting in suboptimal tumor accumulation with simultaneous decrease in pharmaceutical

efficiency. Higher-molecular-weight drug carriers with a nondegradable backbone deposit and accumulate in various organs, impairing biocompatibility. To overcome this dilemma, *backbone degradable*, *long-circulating polymer carriers* have been designed. These are high-molecular-weight, *linea*r polymeric carriers containing enzymatically degradable bonds in the (linear) polymer backbone (Fig. 5b) [11, 12]. Their synthesis was facilitated by recent developments in living radical polymerization and bioconjugation via click reactions. Compared with current polymer-based anticancer drug delivery systems, the distinct features of the new design (second-generation conjugates) are (a) longer intravascular half-life and higher accumulation in tumor tissue due to the EPR effect and (b) substantially augmented efficacy due to increased drug concentration in tumor tissue. The enhanced efficacy of the new backbone degradable HPMA copolymer–drug conjugates was demonstrated on ovarian cancer xenografts in mice [13, 14] and in a rat osteoporosis model [15]. A comparison of first-generation HPMA copolymer conjugates (P-GEM; containing nondegradable low-molecular-weight polymer backbones) with second-generation conjugates (diblock 2P-GEM and multiblock mP-GEM HPMA copolymer conjugates containing degradable bonds in the polymer backbone) is shown in Fig. 5c.

Clinical developments. Numerous water-soluble polymer–drug conjugates have been evaluated in clinical trials [16]: HPMA copolymer–DOX, galactosamine-targeted HPMA copolymer–DOX, HPMA copolymer–platinates, PEG–camptothecin, PEG-SN38, carboxymethyl dextran–exatecan (a camptothecin analog), cyclodextrin-based polymer–camptothecin, and poly(glutamic acid)-taxol. The poly(glutamic acid)-taxol conjugate was evaluated in Phase III clinical trials and the other conjugates in Phase I and/or Phase II clinical trials. When compared to corresponding low-molecular-weight drugs, clinical trials with polymer conjugates demonstrated decreased adverse effects, improved pharmacokinetics, improved patient compliance, and ease of drug administration [17, 18].
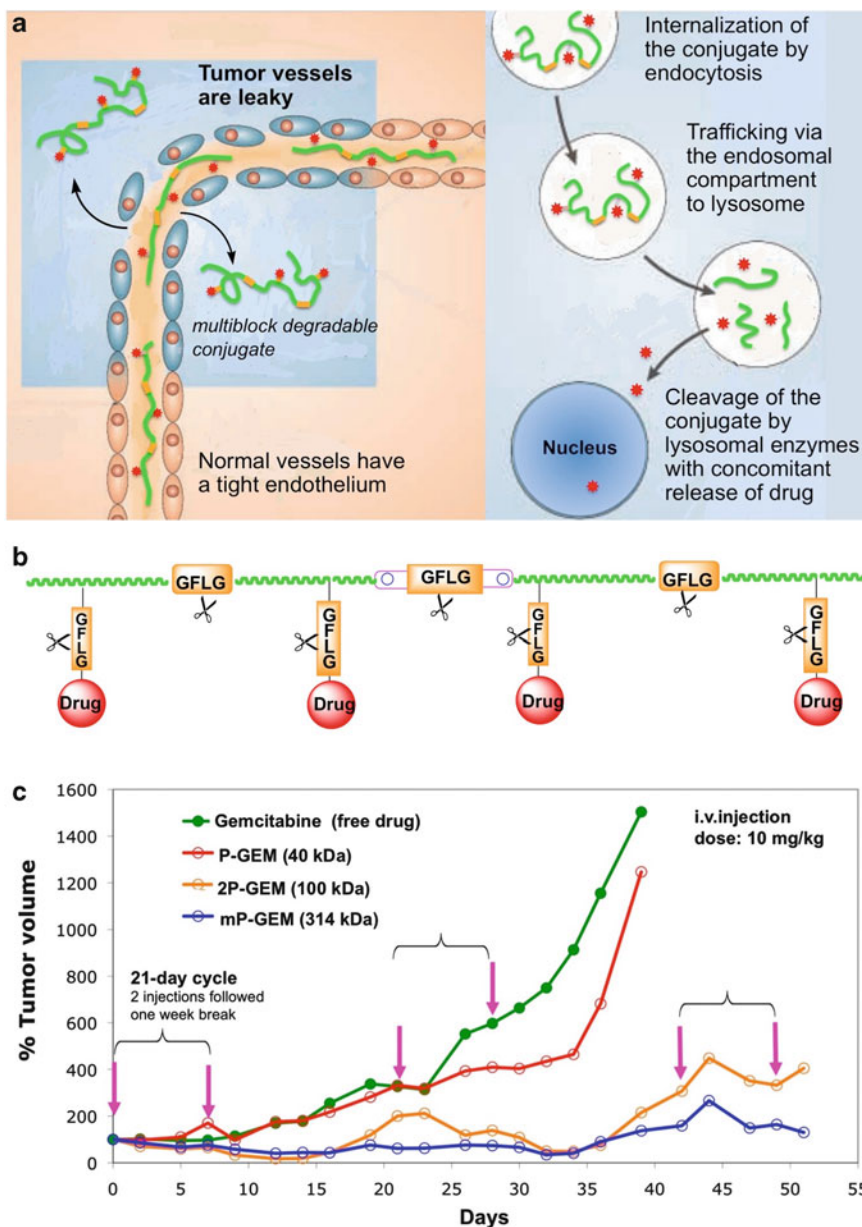
Polymeric Drugs, Fig. 5 Rationale for the design of long-circulating backbone degradable (second-generation) conjugates. (**a**) Schematic of the enhanced permeability and retention (EPR) effect. (**b**) Schematic structure of backbone degradable (second-generation) polymer–drug conjugates. (**c**) In vivo antitumor activity against A2780 human ovarian xenografts in nude mice. Comparison of backbone degradable long-circulating (second-generation) diblock HPMA copolymer–gemcitabine conjugate (2P-GEM) and multiblock HPMA copolymer–gemcitabine conjugate (mP-GEM) with low-molecular-weight (first-generation) HPMA copolymer–gemcitabine conjugate (P-GEM) (Unpublished data from Kopeček laboratory)

P
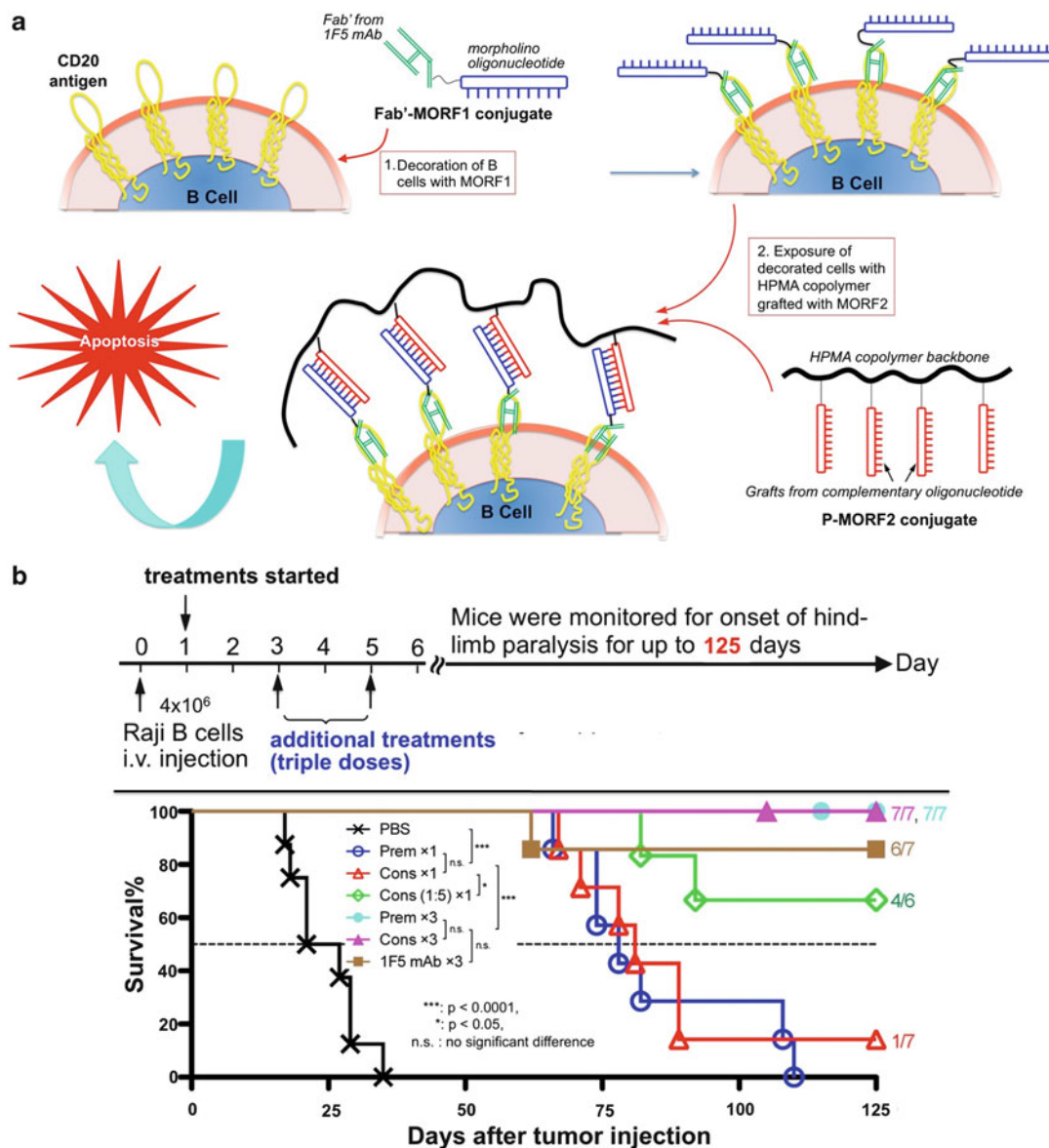
Polymeric Drugs, Fig. 6 Rationale of "drug-free polymer therapeutics." (**a**) Two nanoconjugates induce apoptosis of B cells by cross-linking of the CD20 antigens that is mediated by extracellular hybridization of complementary morpholino oligonucleotides (MORF1-MORF2). (**b**) Therapeutic efficacy of the nanomedicine against systemic lymphoma in SCID mice. Four million of Raji B cells were injected via tail vein on day 0; incidence of hind-limb paralysis or survival of mice was monitored until day 125. One-dose treatment on day 1; three-dose treatment on days 1, 3, and 5. PBS, mice injected with PBS ($n = 8$); Cons $\times 1$, consecutive treatment of Fab'-MORF1

and P-MORF2/v10, 1-dose ($n = 7$); Prem $\times 1$, premixture of Fab'-MORF1 and P-MORF2/v10, 1-dose ($n = 7$); Cons (1:5) $\times 1$, consecutive treatment, MORF1:MORF2 = 1:5, 1-dose ($n = 6$); Cons $\times 3$, 3 doses of consecutive treatment ($n = 7$); Prem $\times 3$, 3 doses of premixture ($n = 7$); 1F5mAb $\times 3$, three doses of 1F5mAb ($n = 7$). The paralysis-free survival of mice is presented in a Kaplan–Meier plot. Numbers of long-term survivors in each group are indicated (if any). Statistics: $p < 0.05$, ***$p < 0.0001$, n.s.: no significant difference (Adapted with permission from Ref. [20], Copyright 2014 American Chemical Society)

Example of a New Paradigm in Polymeric Drug Design

Recently, a new B-cell apoptosis induction system was proposed which avoids the use of low-molecular-weight drugs. The rationale is based on the observation that cross-linking of non-internalizing CD20 receptor on B-cell surface initiates apoptosis. The system is composed of a pair of complementary coiled-coil peptides or oligonucleotides, Fab' fragment of the 1F5 anti-CD20 antibody, and HPMA copolymer [19, 20]. One peptide or oligonucleotide is conjugated to the Fab' fragment, and the complementary one is conjugated in multiple grafts to polyHPMA. The exposure of CD20+ Raji B cells to Fab'–peptide1 or Fab'–oligonucleotide1 conjugate results in the decoration of the cell surface with multiple copies of peptide1 or oligonucleotide1 via antigen–antibody fragment biorecognition. Further exposure of the decorated cells to HPMA copolymer grafted with multiple copies of peptide2 or oligonucleotide2 produces dimerization on the cell surface. This second biorecognition event induces cross-linking of CD20 receptors and triggered apoptosis of B cells in vitro and in vivo. The morpholino oligonucleotide base system is depicted in Fig. 6.

Future Directions

There are two main approaches to advance the field of polymer drugs [17]: (a) improvements of the current design including design of conjugates for the treatment of noncancerous diseases, development of combination therapy with polymer–drug conjugates, identification of novel targeting strategies, improvement in subcellular targeting, and the perfection of backbone degradable, long-circulating polymer–drug conjugates and (b) the design of new paradigms in polymer therapeutics as shown above. Both approaches possess the potential to create more efficient conjugates. In addition, future developments will be greatly supported by results from advanced imaging techniques that permit noninvasive monitoring of the fate of conjugates in vivo. The level of our knowledge suggests that polymeric drugs will be widely used in the clinics within the next decade.

Related Entries

▶ Controlled Release
▶ Drug and Gene Delivery Using Hyperbranched Polymers
▶ Polymeric Micelles
▶ Stimuli-Responsive Bioconjugate

References

1. Kopeček J (1977) Soluble biomedical polymers. Polim Med 7:191–221
2. Mück KF, Rolly H, Burg K (1977) Herstellung und antivirale Wirksamkeit von Polyacrylsäure und Polymethacrylsäure. Makromol Chem 178:2773–2784
3. Jatzkewitz H (1955) Peptamin (glycyl-ʟ-leucyl-mescaline) bound to blood plasma expander (polyvinylpyrrolidone) as a new depot form of a biologically active primary amine (mescaline). Z Naturforsch 10b:27–31
4. Mathé G, Loc TB, Bernard J (1958) Effect sur la leucémie L1210 de la souris d'une combinaison par diazotation d'a méthoptérine et de γglobulines de hamsters porteurs de cette leucémie par hétérogreffe. Compte-rendus del'Académie des Sciences 3:1626–1628
5. Zhou Y, Kopeček J (2013) Biological rationale for the design of polymeric anti-cancer nanomedicines. J Drug Target 21:1–26
6. Kopeček J, Kopečková P (2010) HPMA copolymers: origins, early developments, present, and future. Adv Drug Deliv Rev 62:122–149
7. Vasey PA, Kaye SB, Morrison R, Twelves C, Wilson P, Duncan R et al (1999) Phase I clinical and pharmacokinetic study of PK1 [N-(2-hydroxypropyl) methacrylamide copolymer doxorubicin]: first member of a new class of chemotherapeutic agents – drug-polymer conjugates. Clin Cancer Res 5:83–94
8. Shiah JG, Sun Y, Kopečková P, Peterson CM, Straight RC, Kopeček J (2001) Combination chemotherapy and photodynamic therapy of targetable N-(2-hydroxypropyl)methacrylamide copolymer-doxorubicin/mesochlorin e₆-OV-TL 16 antibody immunoconjugates. J Control Release 74:249–253
9. Cuchelkar V, Kopečková P, Kopeček J (2008) Novel HPMA copolymer-bound constructs for combined tumor and mitochondrial targeting. Mol Pharm 5:696–709
10. Matsumura Y, Maeda H (1986) A new concept for macromolecular therapeutics in cancer therapy: Mechanism

P

of tumoritropic accumulation of proteins and the antitumor agent SMANCS. Cancer Res 46:6387–6392

11. Yang J, Luo K, Pan H, Kopečková P, Kopeček J (2011) Synthesis of biodegradable multiblock copolymers by click coupling of RAFT-generated heterotelechelic polyHPMA conjugates. React Funct Polym 71:294–302

12. Pan H, Yang J, Kopečková P, Kopeček J (2011) Backbone degradable multiblock N-(2-hydroxypropyl) methacrylamide copolymer conjugates via reversible addition-fragmentation chain transfer polymerization and thiol-ene coupling reaction. Biomacromolecules 12:247–252

13. Zhang R, Luo K, Yang J, Sima M, Sun Y, Janát-Amsbury MM, Kopeček J (2013) Synthesis and evaluation of a backbone biodegradable multiblock HPMA copolymer nanocarrier for the systemic delivery of paclitaxel. J Controll Release 166:66–74

14. Pan H, Sima M, Yang J, Kopeček J (2013) Synthesis of long-circulating backbone degradable HPMA copolymer-doxorubicin conjugates and evaluation of molecular weight dependent antitumor efficacy. Macromol Biosci 13:155–160

15. Pan H, Sima M, Miller SC, Kopečková P, Yang J, Kopeček J (2013) Promotion of bone formation in ovariectomized rats by high molecular weight backbone degradable HPMA copolymer – prostaglandin E$_1$ conjugate. Biomaterials 34:6528–6538

16. Li C, Wallace S (2008) Polymer-drug conjugates: recent advances in clinical oncology. Adv Drug Deliv Rev 60:886–898

17. Kopeček J (2010) Biomaterials and drug delivery: past, present, and future (perspective). Mol Pharm 7:922–925

18. Duncan R (2009) Development of HPMA copolymer-anticancer-drug carriers: clinical experience and lessons learned. Adv Drug Deliv Rev 61:1131–1148

19. Wu K, Yang J, Liu J, Kopeček J (2012) Coiled-coil based drug-free macromolecular therapeutics: in vivo efficacy. J Controll Release 157:126–131

20. Chu TW, Yang J, Zhang R, Sima M, Kopeček J (2014) Cell surface self-assembly of hybrid nanoconjugates via oligonucleotide hybridization induces apoptosis. ACS Nano 8:719–730

Polymeric Micelles

Nobuhiro Nishiyama and Hiroyasu Takemoto
Polymer Chemistry Division, Chemical Resources Laboratory, Tokyo Institute of Technology, Midori-ku, Yokohama, Japan

Synonyms

Block copolymer micelle; Polymer micelle; Polymeric micelle

Definition

Polymeric micelles are the core-shell-type nanoparticle formed through the self-assembly of block copolymers or graft copolymers in the selective solvents. Typical polymeric micelles have a spherical shape and the size is in the range of 10–100 nm. Compared with surfactant micelles, polymeric micelles show much higher thermodynamic and kinetic stabilities.

Introduction

Amphiphilic block copolymers and graft copolymers in the selective solvents spontaneously form supramolecular assemblies with spherical, cylindrical, and vesicular morphologies [1, 2]. The size and morphology of supramolecular assemblies critically depend on the chemical structures and compositions of the constituent block copolymers. Living polymerization is often applied for the synthesis of block copolymers with a narrow molecular weight distribution. Among such assemblies, spherical micelles with a characteristic core-shell structure are termed "polymeric micelles" (Fig. 1) and have been extensively studied so far. Polymeric micelles can be formed by various driving forces, such as hydrophobic interaction, π-π interaction, electrostatic interaction, and polymer-metal complex formation [3, 4]. Compared with surfactant micelles, polymeric micelles exhibit distinctive properties such as low critical micelle concentration (CMC), glass state (solid) core, and kinetic stability. Also, polymeric micelles are covered with a high density of shell-forming polymers, providing excellent colloidal stability and reduced interaction with other molecules. These properties of polymeric micelles allow their applications in various fields including biomedical applications [5]. Especially, the utility of polymeric micelles as drug vehicles has been widely accepted as described later.

Physicochemical Properties

Polymeric micelles typically have the core-shell structure in the size range of 10–100 nm.

Polymeric Micelles, Fig. 1 Formation of polymeric micelles through the self-assembly of precisely synthesized block copolymers
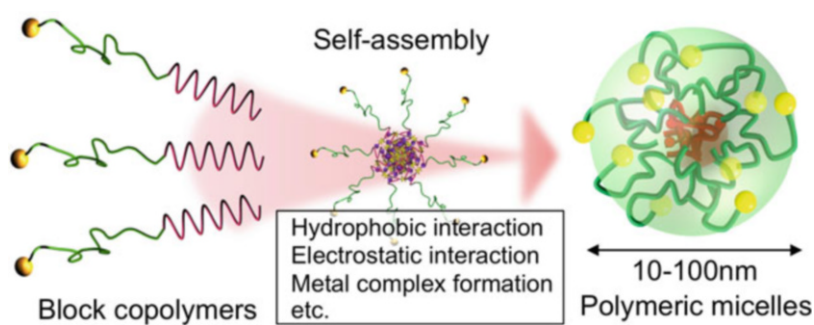
The driving force for micelle formation is the minimization of interfacial free energy of block copolymers with a large solubility difference. The shell-forming polymers are densely packed on the surface of polymeric micelles; therefore, the conformation of the shell-forming polymers is shifted from the "mushroom" structure to the extended, "brush"-like structure. The high surface coverage of the micelle with flexible polymers provides excellent colloidal stability regardless of their concentrations and media.

The physicochemical properties of polymeric micelles rely on several factors, including the properties of the core-forming segments such as hydrophobicity, the glass transition temperature (Tg), the degree of crystallinity, the secondary structure such as α-helix, and the length and ratio of each segment of block copolymers [3]. Also, the interaction between the core-forming segments and the loaded substances in the core affect the properties of polymeric micelles. For example, the complexation between platinum and polycarboxylate allows the formation of extremely stable polymeric micelles [3, 4]. Although individual polymers in the micelle are in dynamic equilibrium, polymeric micelles show high thermodynamic and kinetic stability. It is known that micelles have a critical micelle concentration (CMC) below which only unimers exist but above which both micelles and unimers are present. In general, polymeric micelles have a CMC value of 10^{-6}–10^{-7} M [6, 7], which is 1,000-fold lower than that of surfactant micelles (10^{-3}–10^{-4} M). Even when highly diluted below the CMC, polymeric micelles show slower dissociation into unimers (kinetic stability) due to the integrated molecular

effect and entangling of the micelle core-forming polymers [7].

As an example, the physicochemical property of polymeric micelles from poly(ethylene glycol)-*block*-poly(D,L-lactide) (PEG-*b*-PDLLA) copolymers is described [6]. PEG-*b*-PDLLA (Mw$_{PEG}$, 5,700; Mw$_{PDLLA}$, 5,400) were self-assembled into narrowly distributed micelles with 35 nm by dialysis or ultrasonication-aided dispersion method. Note that the Tg of PDLLA segment is 42 °C. At the temperature above Tg, the CMC increased with the temperature according to the equation, $\Delta G^0 \sim RT\ln(\text{CMC})$, where G^0 and R are the Gibbs standard free energy and the universal gas constant, respectively. This may be attributed to the temperature-dependent increase in the chain mobility of PDLLA segment in the micellar core. On the other hand, when the temperature is below Tg, the CMC was constant (6.0×10^{-7} M) regardless of the temperature. Furthermore, the polymer exchange rate between the micelles was accelerated by increasing the temperature from 25 °C to 40 °C. Thus, the characteristics of the core-forming polymers greatly affect the physicochemical property of polymeric micelles.

Biomedical Applications

Polymeric micelles have been receiving growing attentions in the biomedical fields, especially the application for drug delivery [8]. The paradigm of applying polymeric micelles for drug delivery was proposed by Ringsdorf in the early 1980s [9]. The utility of polymeric micelles as drug vehicles has been demonstrated in the late 1980s by

P

Kataoka [10] and Kabanov [11]. Polymeric micelles can encapsulate a variety of bioactive compounds such as hydrophobic substance, metal complexes, and nucleic acids, overcoming their poor solubility and degradation/inactivation. Easy and efficient drug loading without chemical modification is also advantageous in comparison with other drug vehicles. For example, hydrophobic drugs can be incorporated into polymeric micelles by the dialysis method or the oil in water (o/w) emulsion method, providing the loading capacity around 20 % [3]. On the other hand, the shell of hydrophilic polymers protects polymeric micelles from unwanted interaction with biological components. Note that poly(ethylene glycol) (PEG) is the most widely used as shell-forming polymers due to the flexibility with high degree of hydration, nontoxicity and less immunogenicity, and approval for intravenous administration by the Food and Drug Administration (FDA) [12]. After systemic administration, polymeric micelles can avoid the glomerular excretion in kidneys and recognition by reticuloendothelial system (RES) located in the liver, spleen, and lungs, achieving prolonged blood circulation with the half-life of several hours to 24 h (stealth property). Worth mentioning is that the high drug loading as aforementioned might not affect the biodistribution of polymeric micelles due to the segregated core-shell structure and compacted inner core. For the tumor targeting, the long-circulating micelles show preferential accumulation in solid tumors due to the leaky vasculature in the tumor tissue and impaired lymphatic drainage, which was termed the enhanced permeability and retention (EPR) effect proposed by Maeda and Matsumura [13]. As a result, polymeric micelles have been demonstrated to enhance the potency of antitumor agents in various tumor models [14, 15]. As an example, the plasma concentration and tissue distribution of polymeric micelles conjugating adriamycin (ADR) via an acid-labile linker are shown in Fig. 2. Micellar ADR showed prolonged circulation, achieving 15-fold greater than the area under the concentration curve (AUC) compared with free ADR. Owing to the EPR effect, micellar ADR showed significantly

higher tumor accumulation compared with free ADR ($AUC_{micelle}/AUC_{ADR} = 4.2$) (Fig. 2). Nevertheless, micellar ADR accumulated to a lesser extent in normal tissues including the heart, kidneys, and spleen, excepting some accumulation in liver due to its fenestrated endothelia in sinusoid (Fig. 2). As a result, micellar ADR exhibited approximately fourfold higher maximum tolerated dose and remarkably higher antitumor activity against several solid tumor models than free ADR. Currently, the micellar formulation conjugating an epimer of ADR, epirubicin, via an acid-labile linker (NC-6300/K-912 in Table 1) is under phase I clinical study. Table 1 summarizes micellar formulation of antitumor agents that are under the clinical study or have been approved for the clinical use.

Engineering and chemical modification of the constituent block copolymers allow the construction of more sophisticated drug nanocarriers: polymeric micelles with smart functionalities (Fig. 3) [17]. The introduction of targetable ligands such as antibody (fragments) and peptides onto the micellar surface enables targeting specific cells (function to reach desirable site in body). After reaching the target tissue, polymeric micelles can be endowed with the function to operate the cells, which comprises three multiple processes: (1) sensing (detecting specific environments such as pH, redox potential, and enzymatic reactions), (2) processing (modulating their properties and functions), and (3) operation (properly performing the desired tasks in a spatiotemporally controlled manner). This function is important for organelle-specific delivery of bioactive agents such as nucleic acids and photosensitizers. On the other hand, the integration of imaging components such as fluorescent probes, paramagnetic contrast agents, and radioactive substances can visualize the localization and functions of polymeric micelles (function to visualize). Such visible drug vehicles can be used for monitoring the disease progression and therapeutic response in a noninvasive manner. Furthermore, polymeric micelles can encapsulate sensitizers responding to external stimuli such
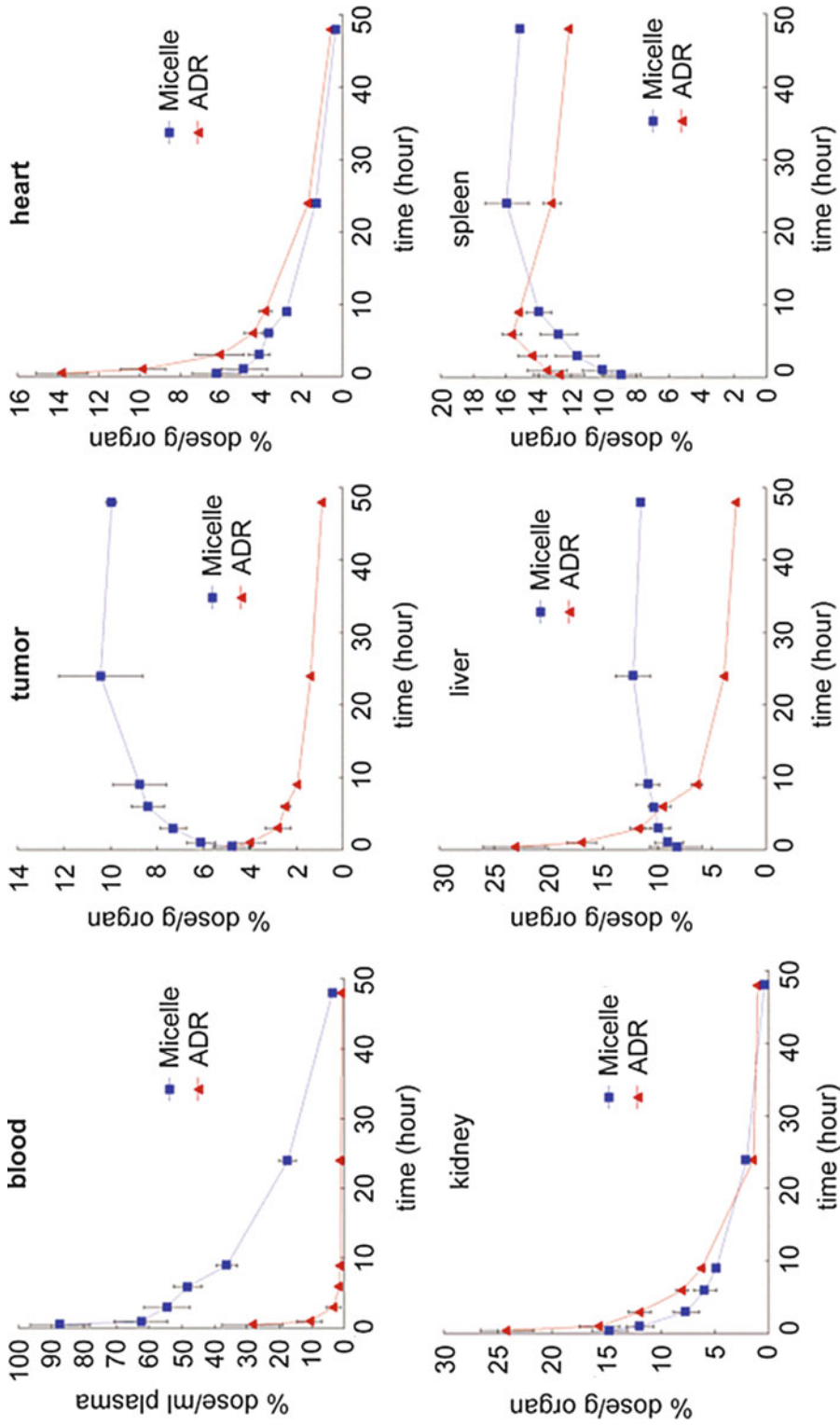
Polymeric Micelles, Fig. 2 Plasma concentration and tissue distribution of free adriamycin (*ADR*) and pH-sensitive ADR-loaded micelles (micelle) after systemic administration to CDF1 mice (*n* = 6) bearing murine colon adenocarcinoma C-26 (Reprinted from Ref. [16])

P

Polymeric Micelles, Table 1 Clinical status of polymeric micelles for cancer therapy

Identity	Drug	Type of carrier	Status
Genexol-PM	Paclitaxel	Polymeric micelle from PEG-*b*-poly(D,L-lactide)	Approved
NK105	Paclitaxel	PEG-*b*-polyaspartate modified with 4-phenyl-butanol	Phase III
NC-6004	Cisplatin	Polymer-metal complex micelle from PEG-*b*-poly(L-glutamic acid)	Phase III
NK012	SN-38	PEG-*b*-poly(L-glutamic acid)-drug conjugate	Phase II
NC-4016	DACHPt	Polymer-metal complex micelle from PEG-*b*-poly(L-glutamic acid)	Phase I
NC-6300/K-912	Epirubicin	PEG-*b*-polyaspartate-drug conjugate (pH sensitive)	Phase I
SP1049C	Doxorubicin	P-glycoprotein-targeting pluronic micelles	Phase II
CALAA-01	siRNA	PEGylated cyclodextrin-based cationic polymer	Phase I/II
BIND-014	Docetaxel	Polymeric micelle targeting prostate-specific membrane antigen	Phase I
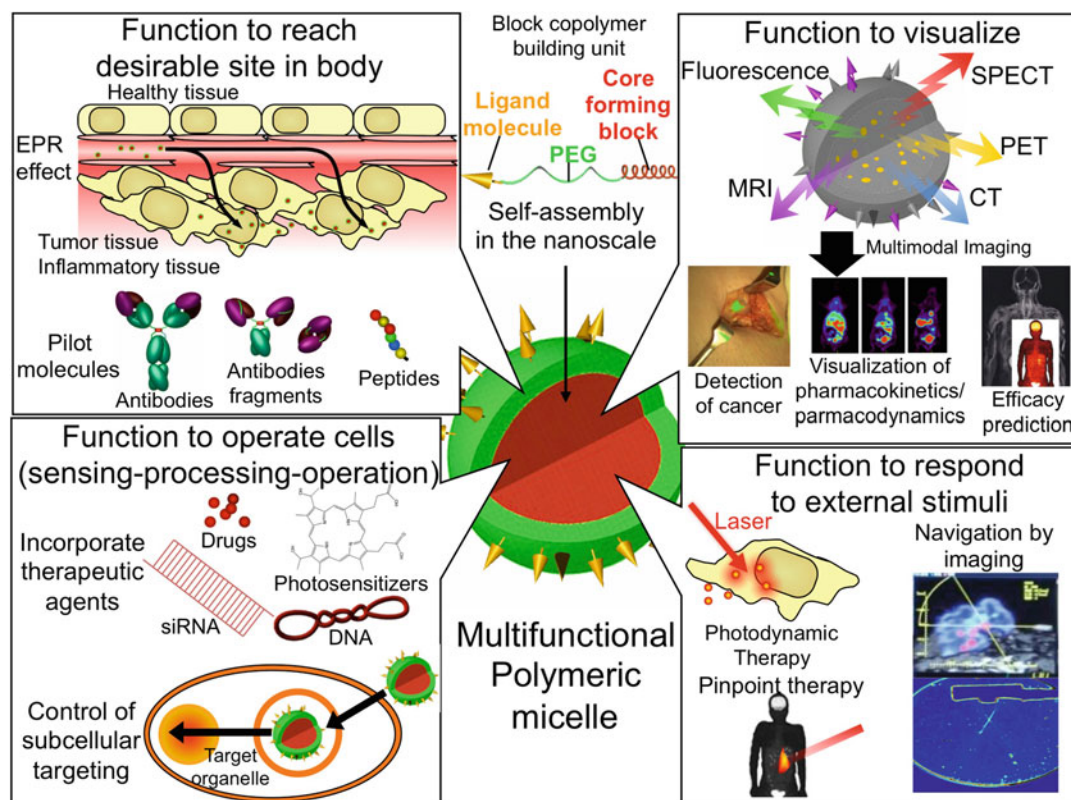
Polymeric Micelles, Fig. 3 Multifunctional polymeric micelles as a versatile platform for diagnosis and pinpoint therapy (Reprinted from Ref. [14])

as light, ultrasound, and neutron beam, achieving their specific accumulation in the target tissues or cells. The combination of medical devices and sensitizer delivery can achieve minimally invasive surgery (function to respond to external stimuli). Thus, multifunctional polymeric micelles are expected to realize effective but less toxic treatment against intractable diseases and improve the patients' quality of life (QOL).

Summary

Polymeric micelles are versatile nanoparticles, of which the size, morphology, and physicochemical properties can be controlled by the chemical structures of constituent block copolymers. Recent advances in precision chain polymerization including atom transfer radical polymerization (ATRP) and reversible addition-fragmentation chain-transfer (RAFT) polymerization allow the synthesis of various kinds of block copolymers with precise chain length and site-controlled functional groups. The finely engineered block copolymers are useful for the construction of polymeric micelles with smart functionalities such as the stimuli responsibility and specific molecule recognition ability. Such functional polymeric micelles have great potentials in biomedical applications. In particular, polymeric micelles can be a platform for molecular imaging and pinpoint drug delivery.

References

1. Zhang L, Eisenberg A (1995) Multiple morphologies of "crew-cut" aggregates of polystyrene-*b*-poly(acrylic acid) block copolymers. Science 268(5218):1728–1731

2. Discher DE, Eisenberg A (2002) Polymer vesicles. Science 297(5583):967–973

3. Nishiyama N, Kataoka K (2006) Nanostructured devices based on block copolymer assemblies for drug delivery: designing structures for enhanced drug function. Adv Polym Sci (Polymer Therapeutics II) 193:67–101

4. Nishiyama N, Kataoka K (2006) Current state, achievements, and future prospects of polymeric micelles as nanocarriers for drug and gene delivery. Pharmacol Ther 112(3):630–648

5. Owen SC, Chan DPY, Shoichet MS (2012) Polymeric micelle stability. Nano Today 7(1):53–65

6. Yamamoto Y, Yasugi K, Harada A, Nagasaki Y, Kataoka K (2002) Temperature-related change in the properties relevant to drug delivery of poly(ethylene glycol)-poly(D, L-lactide) block copolymer micelles in aqueous milieu. J Control Release 82(2–3):359–371

7. Yokoyama M, Sugiyama T, Okano T, Sakurai Y, Naito M, Kataoka K (1993) Analysis of micelle formation of an adriamycin-conjugated poly(ethylene glycol)-poly(aspartic acid) block copolymer by gel permeation chromatography. Pharm Res 10(6):895–899

8. Duncan R (2003) The dawning era of polymer therapeutics. Nat Rev Drug Discov 2(5):347–360

9. Hoerpel G, KlesseW, Ringsdorf H, Schmidt B (1982) Micelle-forming co- and block copolymers for sustained drug release. In: Proceedings of the IUPAC, international union of pure and applied chemistry, 28th macromolecular symposium. Inst Org Chem, Univ Mainz, Mainz Germany p 346

10. Yokoyama M, Miyauchi M, Yamada N, Okano T, Sakurai Y, Kataoka K, Inoue S (1990) Characterization and anticancer activity of the micelle-forming polymeric anticancer drug adriamycin-conjugated poly(ethylene glycol)-poly (aspartic acid) block copolymer. Cancer Res 50(6):1693–1700

11. Kabanov AV, Batrakova EV, Melik-Nubarov NS, Fedoseev NA, Dorodnich TY, Alakhov VY, Chekhonin VP, Nazarova IR, Kabanov VA (1992) A new class of drug carriers: micelles of poly (oxyethylene)-poly(oxypropylene) block copolymers as microcontainers for drug targeting from blood in brain. J Control Release 22(2):141–157

12. Harris JM (1992) Introduction to biotechnical and biomedical applications of poly(ethylene glycol), Chap 1. In: Harris JM (ed) Poly(ethylene glycol) chemistry: biotechnical and biomedical applications. Plenum, New York

13. Matsumura Y, Maeda H (1986) A new concept for macromolecular therapeutics in cancer chemotherapy: mechanism of tumoritropic accumulation of proteins and the antitumor agent smancs. Cancer Res 46(12):6387–6392

14. Cabral H, Matsumoto Y, Mizuno K, Chen Q, Murakami M, Kimura M, Terada Y, Kano MR, Miyazono K, Uesaka M, Nishiyama N, Kataoka K (2011) Accumulation of sub-100 nm polymeric micelles in poorly permeable tumours depends on size. Nat Nanotechnol 6(12):815–823

15. Cabral H, Murakami M, Hojo H, Terada Y, Kano MR, Chung U-I, Nishiyama N, Kataoka K (2013) Targeted therapy of spontaneous murine pancreatic tumors by polymeric micelles prolongs survival and prevents peritoneal metastasis. Proc Natl Acad Sci U S A 110(28):11397–11402

16. Bae Y, Nishiyama N, Fukushima S, Koyama H, Matsumura Y, Kataoka K (2005) Preparation and biological characterization of polymeric micelle drug carriers with intracellular pH-triggered drug release property: tumor permeability, controlled subcellular drug distribution, and enhanced in vivo antitumor efficacy. Bioconjugate Chem 16(1):122–130

17. Cabral H, Nishiyama N, Kataoka K (2011) Supramolecular nanodevices: from design validation to theranostic nanomedicine. Acc Chem Res 44(10):999–1008

P

Polymerization of Substituted Acetylenes

Toshio Masuda
Department of Polymer Materials, School of Material Science and Engineering, Shanghai University, Shanghai, China

Synonyms

Polymerization of acetylene derivatives

Definition

Polymerization is a group of reactions that provide high-molecular-weight polymers from usually low-molecular-weight monomers. Substituted acetylenes are acetylene derivatives which possess one or two groups on either or both sides of the acetylenic moiety. The polymerization of substituted acetylenes proceeds via the simultaneous cleavage of the triple bond and linkage formation between monomer molecules. The formed polymers possess alternating carbon–carbon double bonds along the main chain and various side groups and exhibit interesting photoelectronic properties based on the conjugated structure.

Introduction

The polymerization of acetylene and its derivatives in the presence of suitable transition-metal catalysts provides high-molecular-weight (MW) polymers (Fig. 1). The monomers include acetylene, mono- and disubstituted acetylenes, and α,ω-diynes. The polymers possess carbon–carbon alternating double bonds along the main chain and are expected to exhibit unique properties such as metallic conductivity based on the conjugated structure of the main chain. For more details of the polymerization and polymer properties of substituted acetylenes, the readers are encouraged to refer to monographs and review articles [1–3].

Natta and coworkers polymerized acetylene for the first time in 1958 by using a Ti-based catalyst. This polymerization proceeds by the insertion mechanism like the polymerization of olefins. Because of the lack of processability and stability, early studies on polyacetylenes were motivated only by theoretical and spectroscopic interests. In 1977, Shirakawa, Heeger, and MacDiamid discovered metallic conductivity of doped polyacetylene [4–6]. This discovery greatly stimulated polyacetylene chemistry, and now polyacetylene is recognized as one of the most important conjugated polymers. Many publications are now available about the chemistry and physics of polyacetylene itself.

The introduction of various side groups into polyacetylene has been attempted to change and/or improve its stability, solubility, processability, and functionalities. Early attempts led to the conclusion that only sterically unhindered monosubstituted acetylenes are polymerizable with Ziegler-type catalysts. Conventional ionic and radical initiators lack the ability to provide high-MW polymers from substituted acetylenes. The first successful polymerization of a substituted acetylene was achieved in 1974; group 6 transition metals were quite active for the polymerization of phenylacetylene (PA) to provide polymers with MWs over 10^4. Since then, promoted by the development of various effective transition-metal catalysts, a variety of polymers (called substituted polyacetylenes) have been successfully synthesized from substituted acetylenes. Acetylenic monomers that undergo polymerization with transition-metal catalysts cover a wide range from unsubstituted to mono- and disubstituted monomers and further α,ω-diynes as well as from hydrocarbon-based monomers to heteroatom-containing ones (Table 1). The synthesis of various substituted polyacetylenes orients the development of novel polymers displaying unique properties such as conductivity, nonlinear optical properties, magnetic properties, gas permeability, photo- and electroluminescent properties, and so on, which are not accessible with the corresponding vinyl polymers.

Polymerization of Substituted Acetylenes, Fig. 1 Polymerization of acetylenes

$$HC\equiv CH \longrightarrow \text{+}CH\text{=}CH\text{+}_n \quad (1)$$

$$HC\equiv CR \longrightarrow \text{+}CH\text{=}\underset{R}{C}\text{+}_n \quad (2)$$

$$RC\equiv CR' \longrightarrow \text{+}\underset{R}{C}\text{=}\underset{R'}{C}\text{+}_n \quad (3)$$

$$(4)$$
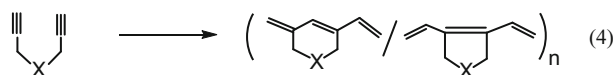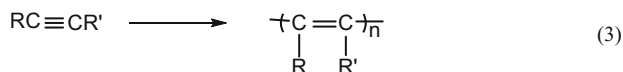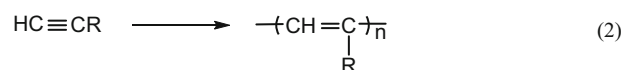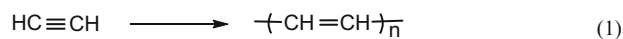
Polymerization of Substituted Acetylenes, Table 1 Examples of polymerizable acetylenic monomers

	Unsubstituted	Monosubstituted	Disubstituted	α,ω-Diyne
Hydrocarbon acetylenes	HC≡CH	HC ≡ C-n-Bu	MeC ≡ C-n-C_5H_{11}	
		HC ≡ C-t-Bu	MeC≡C-〈〉	
		HC≡C-〈〉	〈〉-C≡C-〈〉-t-Bu	Ph✕Ph
Heteroatom-containing acetylenes		HC ≡ C CO_2-n-Bu	Cl C=C-n-C_6H_{13}	EtO$_2$C CO$_2$Et
		HC≡C CH$_2$NHC-s-Bu* (‖O)	ClC≡C-〈〉	
		Me$_3$Si, HC≡C-〈〉	MeC ≡ CSiMe$_3$	Si Ph Ph
		CF$_3$, HC≡C-〈〉	〈〉-C≡C-〈〉-SiMe$_3$	

Table 2 lists transition-metal catalysts used for the polymerization of acetylenic monomers. It is noted that transition metals of various groups in the periodic table are useful. Typical metals in the catalysts include Ti, Nb, Ta, Mo, W, Fe, and Rh, although other metals such as Ru, Ir, Ni, and Pd have also been employed. The kind of monomers polymerizable with a particular catalyst is rather restricted; e.g., diphenylacetylenes are polymerizable only with Ta catalysts, while monosubstituted acetylenes with polar groups are polymerizable only with Rh catalysts. Hence it is important to recognize the characteristic of each catalyst. Two kinds of reaction mechanisms participate depending on the polymerization catalysts. One is the metathesis mechanism where the active species are metal carbenes, namely, species having a metal–carbon double bond, and the other is the insertion mechanism in which the active species are alkylmetals, namely, species having a metal–carbon single bond. The metathesis mechanism proceeds when Nb, Ta, Mo, and W catalysts are used, whereas the insertion mechanism holds with Ti, Fe, and Rh catalysts. The alternating

P

Polymerization of Substituted Acetylenes, Table 2 Typical catalysts for the polymerization of acetylenes

Group	4	5	6	8–10
Catalyst	Ti (O-n-Bu)$_4$ –Et$_3$Al	NbCl$_5$, TaCl$_5$	MoCl$_5$–n-Bu$_4$Sn, WCl$_6$–Ph$_4$Sn	Fe(acac)$_3$–Et$_3$Al
(Monomer[a])	(HC $\equiv$ CH)	(RC $\equiv$ CR′)	(HC $\equiv$ CR, RC $\equiv$ CR′)	(HC $\equiv$ CR)
		TaCl$_5$–n-Bu$_4$Sn	M(CO)$_6$–CCl$_4$–hν (M = Mo, W)	[(nbd)RhCl]$_2$
		(PhC $\equiv$ CC$_6$H$_4$-p-X)	(HC $\equiv$ CR, ClC $\equiv$ CR)	(HC $\equiv$ CPh, HC $\equiv$ CCO$_2$R)
			(RO)$_2$Mo(=NAr) = CH-t-Bu	(nbd)Rh$^+$BPh$_4^-$
			((HC $\equiv$ CCH$_2$)$_2$C(CO$_2$Et)$_2$)	(HC $\equiv$ CCH$_2$NHCOR)
Mechanism	Insertion	Metathesis	Metathesis	Insertion

[a]HC $\equiv$ CR and RC $\equiv$ CR′ denote mono- and disubstituted acetylenes, respectively

double bond structure is formed by both polymerization mechanisms, and so it is rather difficult to distinguish the polymerization mechanism from the polymer structure.

Polymerization of Acetylene and Its Derivatives

Polymerization of Acetylene

Polymerization of acetylene was first achieved by Natta and his coworkers using a Ti-based catalyst. At present, polyacetylene membrane can be directly obtained by the polymerization using Ti(O-n-Bu)$_4$–Et$_3$Al. This is called the Shirakawa method, which features high catalyst concentrations. Typical polymerization conditions are as follows: [Ti(O-n-Bu)$_4$] = 0.25 M, [Et$_3$Al] = 1.0 M in toluene, –78 °C, 500–600 mmHg acetylene pressure. Since the discovery of the metallic conductivity of doped polyacetylene in 1977, a tremendous amount of research has been done not only about polyacetylene but also about various conjugated polymers. In general, conjugated polymers intrinsically possess electric conductivity, and so they are called synthetic metals. Naarmann et al. have reported a method of preparing a highly conducting polyacetylene, in which the catalyst solution is aged in silicone oil at a temperature as high as 120 °C. Akagi et al. have synthesized helical polymers in chiral nematic liquid crystal media, which were prepared by adding chiral dopants to phenylcyclohexyl-based binary nematic liquid crystals, and observed very clear twisted fibrils of polyacetylene by scanning electron micrography.

Polymerization of Monosubstituted Acetylenes

Typical examples of the polymerization of monosubstituted acetylenes are shown in Table 3. Mo, W, and Rh catalysts, all of which involve transition metals, are particularly effective. Whereas Mo and W catalysts are sensitive to polar groups in the monomer, Rh catalysts are tolerant to such groups. In the same way, polar solvents can be used only with Rh catalysts and not with Mo and W catalysts. Another point is that Mo and W catalysts are effective to various sterically crowded monomers, while Rh catalysts are useful to rather restricted kinds of monomers including phenylacetylenes, alkyl propiolates, and N-propargylamides. In some cases, Fe and Pd complexes are also useful. It is noted that not only sterically unhindered monomers but also very crowded ones afford high-MW polymers with W and Mo catalysts. Typical monosubstituted acetylene monomers such as aliphatic acetylenes, ring-substituted phenylacetylenes, and other arylacetylenes are discussed below.

Aliphatic Acetylenes. Aliphatic terminal acetylenes with *prim*- and *sec*-alkyl groups provide orange to yellow, high-MW polymers when polymerized with iron alkanoate–organoaluminum catalysts. On the other hand, *tert*-alkylacetylenes, which are sterically very crowded, can be

Polymerization of Substituted Acetylenes, Table 3 Polymerization of monosubstituted acetylenes

Monomer	Catalyst	$\frac{MW}{10^3}$
(a) Monosubstituted hydrocarbon acetylenes/W, Mo catalysts		
HC ≡ C-n-Bu	WCl$_2$(OC$_6$H$_4$-o,o-Me$_2$)$_4$	170 (M_n)
HC ≡ C-t-Bu	MoCl$_5$	33 (M_n)
HC ≡ CPh	WCl$_6$–Ph$_4$Sn	15 (M_n)
HC ≡ CPh	W (CO)$_6$–CCl$_4$–hv	80 (M_n)
HC ≡ CC$_6$H$_2$-o, o-Me$_2$-p-t-Bu	W (CO)$_6$–CCl$_4$–hv	2,600 (M_w)
(b) Monosubstituted heteroatom-containing acetylenes/ W, Mo catalysts		
HC ≡ CCH(SiMe$_3$)-n-C$_5$H$_{11}$	MoCl$_5$–Et$_3$SiH	4500 (M_w)
HC ≡ CC$_6$H$_4$-o-SiMe$_3$	W (CO)$_6$–CCl$_4$–hv	3,400 (M_w)
HC ≡ CC$_6$H$_4$-o-GeMe$_3$	WCl$_6$	690 (M_w)
HC ≡ CC$_6$H$_4$-o-CF$_3$	W (CO)$_6$–CCl$_4$–hv	1,600 (M_w)
HC ≡ CC$_6$F$_4$-n-Bu	WCl$_6$–Ph$_4$Sn	220 (M_w)
HC ≡ C-α-thiophene	WCl$_6$–n-Bu$_4$Sn	20 (M_n)
HC ≡ CCH$_2$NH$_2$	Mo (OEt)$_5$–EtAlCl$_2$	insoluble
HC ≡ CCH$_2$Cl	MoCl$_5$	––
(c) Monosubstituted acetylenes/Rh, Pd catalysts		
HC ≡ CPh	RhCl$_3$–LiBH$_4$	5 (M_n)
HC ≡ CPh	(cod. RhCl)$_2$–NaOH	10 (M_w)
HC ≡ CPh	(nbd. RhCl)$_2$–Et$_3$N	1000 (M_w)
HC ≡ CH	(cod. RhCl)$_2$–NaOEt	insoluble
HC ≡ CC$_6$H$_4$-p-SiMe$_3$	(nbd.RhCl)$_2$	120 (M_w)
HC ≡ CCO$_2$-n-Bu	(nbd.RhCl)$_2$	84 (M_w)
HC ≡ CCH$_2$NHCH$_2$Ph	[Rh.cod. chel]$^+$X$^-$	4 (M_n)
HC ≡ CCH$_2$OH	PdCl$_2$	insoluble

polymerized by Mo and W catalysts, and the MW of the polymers reaches several 100,000.

Examples of the polymerizations of heteroatom-containing acetylenes have been increasing. The heteroatoms include Si, halogens, O, S, and N. In particular, Si and F endow the polymers with unique properties and functions, and they are unlikely to deactivate polymerization catalysts. Hence the synthesis of Si- and F-containing polyacetylenes has been examined particularly extensively. For instance, (trimethylsilyl)acetylene is polymerizable with W catalysts, but the product polymer is partly insoluble in any solvent. (Perfluoroalkyl)acetylenes yield white polymers soluble only in fluorine-containing solvents.

Recently, many monomers containing ether, ester, amide, carbamate, and sulfamide groups have successfully been polymerized by using Rh catalysts, mostly [(nbd)RhCl]$_2$ and (nbd) Rh$^+$BPh$_4^-$. While Rh catalysts are able to polymerize monomers having the OH group, the COOH group is known to terminate the Rh-catalyzed polymerization. Late transition metals such as Ru, Rh, and Pd are not oxophilic, and so they are useful as catalysts for the polymerization of highly polar monomers. If highly active Ru and Pd catalysts are developed, they will be very useful.

Phenylacetylene and Its Ring-Substituted Derivatives. The typical catalysts for the polymerization of phenylacetylene include W, Rh, and Fe catalysts. W catalysts produce an auburn polymer having trans-rich structure; WCl$_6$–Ph$_4$Sn is highly active, while W (CO)$_6$–CCl$_4$–hv is useful to achieve high MW (number-average MW: $M_n \sim 1 \times 10^5$). The polymerization by Rh catalysts proceeds in alcohols and amines to form a yellow polymer. A feature of Rh catalysts is high tolerance to polar groups, and hence, they are useful to polymerize various phenylacetylenes having polar groups (e.g., ether, ester, amine, carbazole, imine, nitrile, azobenzene, nitro groups) at para position, resulting in the formation of high-MW poly(phenylacetylenes). Another feature of Rh catalysts is that they give poly(phenylacetylene) whose MW reaches up to a few 100,000. When Fe(acac)$_3$–Et$_3$Al is used, the poly (phenylacetylene) formed is insoluble in any solvent and has the cis-cisoidal structure.

An interesting trend has been observed so far in the polymerization of ortho-substituted phenylacetylenes by W and Mo catalysts:

P

Phenylacetylene itself does not produce very high-MW polymer with W and Mo catalysts (MW $< 10^5$). On the other hand, phenylacetylenes having bulky CF_3 and Me_3Si groups at ortho position provide in high yields polymers whose weight-average MW (M_w) is as high as about one million (High MW around one million is usually determined by light scattering which provides the M_w value.). Thus, the steric effect of the ortho substituents greatly affects the polymerizability and the polymer MW of phenylacetylenes, while the electronic effect hardly influences them. For a similar steric reason, (*p-t*-butyl-*o,o*-dimethylphenyl)acetylene, an ortho-dimethyl-substituted phenylacetylene, also polymerizes into a high-MW polymer with W and Mo catalysts. Unlike W and Mo catalysts, Rh catalysts are not suited to ortho-substituted phenylacetylenes because Rh catalysts are rather sensitive to the steric effect.

Other Arylacetylenes. Various polymers have been prepared from monosubstituted acetylenes having condensed aromatic rings instead of phenyl group. Such condensed aromatic rings include naphthyl, anthryl phenanthryl, fluorenyl, pyrenyl, and so on. These monomers polymerize with W, Mo, and Rh catalysts, where the polymer yield usually decreases in the order of W, Mo, and Rh. The cis content of the polymers increases in the order of W < Mo < Rh, and the polymer solubility decreases in this order. Both 1- and 2-naphthylacetylens polymerize in high yields with W catalysts. 9-Anthrylacetylene polymerizes with W catalysts into a polymer insoluble in any solvents. However, if a long *n*-hexoxycarbonyl group is introduced at the 10 position, the formed polymer becomes soluble. This polymer has a dark purple color. 1- and 2-Anthrylacetylens are sterically less hindered, and the formed polymers are solvent soluble. These polymers having condensed aromatic rings are generally colored deeply (dark brown to dark purple) and show third-order nonlinear optical properties.

Polymerization of Disubstituted Acetylenes

In general, disubstituted acetylenes are sterically more crowded than their monosubstituted counterparts, and consequently, efficient catalysts for their polymerization are restricted virtually to group 5 and 6 transition-metal catalysts; Rh catalysts are not effective at all. Among disubstituted acetylenes, those with less steric hindrance polymerize with Mo and W catalysts and tend to give cyclotrimers with Nb and Ta catalysts. On the other hand, sterically crowded disubstituted acetylenes do not polymerize with Mo or W catalysts, but do polymerize with Nb and Ta catalysts. The polymers from disubstituted acetylenes having two identical groups or two groups of similar sizes are generally insoluble in any solvent. Most polymers from disubstituted acetylenes are colorless, though some aromatic polymers are colored yellow. Table 4 lists typical examples of the polymerization of disubstituted acetylenes.

Aliphatic, Monoaromatic, and Heteroatom-Containing Acetylenes. 2-Alkynes (e.g., 2-octyne), which are sterically not very crowded, polymerize with Mo catalysts to give polymers with MW over one million. For these monomers,

Polymerization of Substituted Acetylenes, Table 4 Polymerization of disubstituted acetylenes

Monomer	Catalyst	$\frac{M_w}{10^3}$
(a) Disubstituted acetylenes/W, Mo catalysts		
$MeC \equiv C$-*n*-Pr	$MoCl_5$	1,100
$ClC \equiv C$-*n*-C_6H_{13}	$MoCl_5$–*n*-Bu_4Sn	1,100
$ClC \equiv CPh$	$MoCl_5$–*n*-Bu_4Sn	690
$MeC \equiv CS$-*n*-Bu	$MoCl_5$–Ph_3SiH	180
$MeSC \equiv C$-*n*-C_6H_{13}	$MoCl_5$–Ph_3SiH	130
(b) Hydrocarbon acetylenes/Nb, Ta catalysts		
n-Pr-$C \equiv C$-*n*-Pr	$NbCl_5$	Insoluble
$PhC \equiv CMe$	$TaCl_5$–*n*-Bu_4Sn	1,500
$PhC \equiv C$-*n*-C_6H_{13}	$TaCl_5$–*n*-Bu_4Sn	1,100
$PhC \equiv CPh$	$TaCl_5$–*n*-Bu_4Sn	Insoluble
$PhC \equiv CC_6H_4$-*p-t*-Bu	$TaCl_5$–*n*-Bu_4Sn	3,600
$PhC \equiv CC_6H_4$-*p-n*-Bu	$TaCl_5$–*n*-Bu_4Sn	1,100
(c) Heteroatom-containing acetylenes/Nb, Ta catalysts		
$MeC \equiv CSiMe_3$	$TaCl_5$	730
$MeC \equiv CSiMe_3$	$NbCl_5$	220
$MeC \equiv CSiMe_3$	$TaCl_5$–Ph_3Bi	4,000
$MeC \equiv CGeMe_3$	$TaCl_5$	>100
$PhC \equiv CC_6H_4$-*p*-$SiMe_3$	$TaCl_5$–*n*-Bu_4Sn	2,200
$PhC \equiv CC_6H_4$-*p*-OPh	$TaCl_5$–*n*-Bu_4Sn	1,700

W and Nb catalysts are less active, and Ta catalysts yield only cyclotrimers. Symmetrical dialkylacetylenes (e.g., 4-octyne) are slightly more crowded, and consequently Nb, Ta, and W catalysts exhibit high activity, while Mo catalysts are not active. Since 1-phenyl-1-alkynes (e.g., 1-phenyl-1-propyne) exhibit even larger steric effects, Nb and Ta catalysts produce polymers having MW of 1×10^5–1×10^6. In contrast, W catalysts yield only oligomers of MW lower than 1×10^4, and Mo catalysts are inactive.

Regarding heteroatom-containing acetylenes, 1-trimethylsilyl-1-propyne (TMSP), sterically highly crowded Si-containing acetylene, polymerizes with Nb and Ta catalysts, but does not with Mo or W catalysts. The MW of the formed polymer is around one million, and still it is quite soluble in common solvents such as toluene and chloroform to give a free-standing membrane by solution casting. The MW of the polymer obtained with $TaCl_5$–Ph_3Bi reaches four million, which is among the highest for all the substituted polyacetylenes. 1-(Trimethylgermyl)-1-propyne polymerizes in a similar way to TMSP. Poly (TMSP) is famous as one of the most gas-permeable polymers [7, 8]. For reviews of substituted polyacetylenes as gas-permeable membranes, see references [9–12].

Cl-containing monomers afford high-MW polymers only with Mo catalysts. For instance, the polymerizations of 1-chloro-1-octyne and 1-chloro-2-phenylacetylene are catalyzed by $MoCl_5$–n-Bu_4Sn to give polymers whose MW exceeds 10^5. It appears that the electron-withdrawing chlorine atom plays some role in the inertness of these monomers to Nb, Ta, and W catalysts. Mo catalysts are uniquely effective in the polymerization of S-containing disubstituted acetylenes. Though there is a possibility that S as well as O in the monomer deactivates group 5 and 6 transition-metal catalysts, the basicity of S is weakened by the conjugation with the triple bond, resulting in the lower coordinating ability to the propagating species.

Diphenylacetylene and Its Derivatives. Diphenylacetylene itself forms a polymer in the presence of $TaCl_5$–n-Bu_4Sn. The formed polymer possesses a very high thermal stability, but is insoluble in any solvent. Regarding polymer solubility, there is a tendency that polyacetylenes having two identical alkyl groups in the repeat unit are insoluble in any solvents, whereas polyacetylenes having methyl and a long alkyl group are soluble in various solvents. By analogy, one can hypothesize that para- or meta-substituted diphenylacetylenes provide soluble polymers.

In fact, soluble, high-MW polymers can be obtained from many diphenylacetylenes having substituents. For instance, 1-phenyl-2-[(*p*-trimethylsilyl)phenyl]acetylene polymerizes with $TaCl_5$–cocatalyst in high yield. The polymer thus obtained is totally soluble in toluene and $CHCl_3$, and its MW is as high as about two million. In contrast, $TaCl_5$ alone and $NbCl_5$–cocatalyst are ineffective to this monomer unlike 1-(trimethylsilyl)-1-propyne. The diphenylacetylenes with m-Me_3Si, m-Me_3Ge, p-t-Bu, and p-n-Bu groups polymerize similarly, leading to totally soluble, high-MW polymers. Poly[1-phenyl-2-[(*p*-trimethylsilyl)phenyl]acetylene] is interesting as a gas separation membrane material because of high thermal stability and high gas permeability.

Since only Ta and Nb catalysts, which are not tolerant to polar groups, are available for the polymerization of disubstituted acetylenes, it is generally difficult to synthesize disubstituted acetylene polymers having highly polar substituents such as hydroxy group. The method of synthesizing poly[1-phenyl-2-(*p*-hydroxyphenyl) acetylene] has been developed; namely, this polymer is obtained by the polymerization of 1-phenyl-2-(*p*-siloxyphenyl)acetylene and the subsequent acid-catalyzed deprotection reaction.

Living and Stereospecific Polymerizations

Polymerization with Metal Halide-Based Metathesis Catalysts [13]. The general formula of metal halide-based living polymerization catalysts is expressed as MO_nCl_m–cocatalyst–ROH (M = Mo or W, n = 0 or 1, m = 5 or 4). The most important feature of these catalysts is easiness in preparation, while it is a weak point

Polymerization of Substituted Acetylenes, Table 5 Living polymerization of substituted acetylenes

Monomer	Catalyst[a]	$\frac{M_w}{M_n}$
$ClC \equiv C\text{-}n\text{-}C_6H_{13}$	**1**	1.13
$HC \equiv CC_6H_4\text{-}o\text{-}CF_3$	**1**	1.06
$HC \equiv CC_6H_4\text{-}o\text{-}SiMe_3$	**1**	1.07
$HC \equiv C\text{-}t\text{-}Bu^b$	**1**	1.12
$MeC \equiv CMe$	**2**	1.03
$(HC \equiv CCH_2)_2C(CO_2Et)_2$	**3**	~1.20
$HC \equiv CC_6H_4\text{-}o\text{-}SiMe_3$	**4**	1.05
$HC \equiv CPh^c$	**5**	1.05
$HC \equiv CPh^d$	**6**	1.12

a
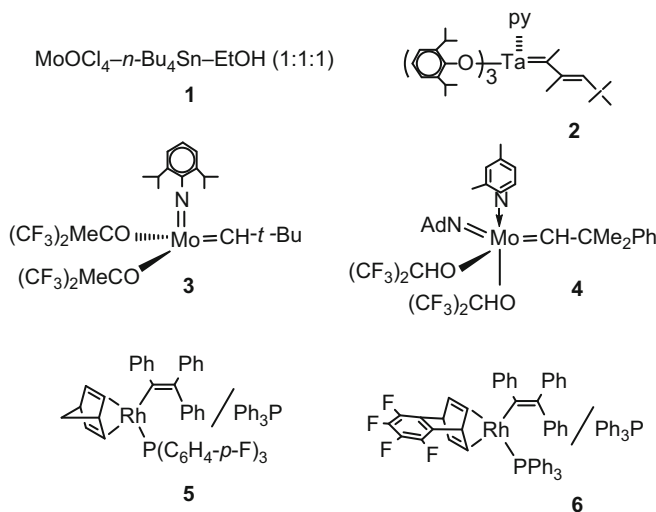
$bStereoregular$ (cis 97 %) living polymer formed
$cStereoregular$ (all-cis) living polymer (M_n 25,000) formed
$dStereoregular$ (all-cis) high-molecular-weight (M_n 401,000) living polymer formed

that the initiation efficiency of these catalysts is not quantitative. A typical living polymerization by metal halide-based catalysts has been achieved with 1-chloro-1-octyne as a monomer and using $MoOCl_4$–n-Bu_4Sn–EtOH (**1** in Table 5) as a catalyst. Specifically, poly(1-chloro-1-octyne) with narrow molecular weight distribution (MWD) ($M_w/M_n < 1.2$) is obtained, and the living nature is confirmed by the linear dependence of MW on monomer conversion and by the successful initiation of the polymerization of second-charged monomers with the living prepolymer.

The ternary $MoOCl_4$–n-Bu_4Sn–EtOH catalyst induces living polymerization of not only 1-choro-1-alkynes but also phenylacetylenes with bulky ortho substituents. The presence of bulky ortho substituents (e.g., CF_3, $SiMe_3$, $GeMe_3$, etc.) is essential to achieve excellent living polymerization, which is probably because ortho substituents are able to sterically preclude chain transfer and termination. Stereospecific living polymerization of *tert*-butylacetylene is possible with $MoOCl_4$–n-Bu_4Sn–EtOH, which gives a polymer with a narrow MWD. The nuclear magnetic resonance (NMR) spectrum of the formed polymer has shown that the cis content of main chain double bond reaches 97 % for poly(*tert*-butylacetylene) prepared at $-30\,°C$.

By the sequential living polymerization using the $MoOCl_4$–n-Bu_4Sn–EtOH catalyst, diblock

copolymers with very narrow MWD are selectively formed from any combinations of two monomers among 1-chloro-1-octyne, o-Me$_3$Si-phenylacetylene, and o-CF$_3$-phenylacetylene irrespective of the order of monomer addition. Further, this catalyst enables to produce ABC- and ABA-type triblock copolymers from these three monomers.

Polymerization with Single-Component Metal Carbene Catalysts [14]. A Ta carbene complex (**2** in Table 5) is the first example of single-component metathesis catalyst that induces the living polymerization of substituted acetylene, and the monomer used is 2-butyne. The initiation efficiency is quantitative, and the living end can be capped with aromatic aldehydes. Since polymers from symmetric acetylenes are generally insoluble, soluble poly(2-butyne) is accessible only when the degree of polymerization is suppressed below 200.

Mo carbene catalysts have been synthesized and proven to elegantly induce living cyclopolymerization of 1,6-heptadiynes. Mo carbenes ligated by bulky imido and alkoxy groups are effective (e.g., **3** in Table 5). The ability of the Mo carbenes to tolerate polar functional groups permits living polymerization of functionalized monomers containing ester, sulfonic ester, and siloxy groups. Endcapping of the polymers is readily accomplished using aromatic aldehydes including *p-N,N*-dimethylaminobenzaldehyde and *p*-cyanobenzaldehyde.

Ring-substituted phenylacetylenes have been adopted in the Mo carbene-initiated polymerization, leading to a finding that well-defined polymers are readily obtained with Mo carbenes ligated by less bulky alkoxy groups (e.g., **4** in Table 5). Like metal halide-induced living polymerizations, bulky ring substituents at the ortho position are required for controlled polymerization. The most characteristic point of the Mo carbene-catalyzed polymerization system is that all the steps including initiation and propagation can be readily monitored by an NMR technique thanks to the quantitative initiation.

Polymerization with Rh Catalysts. A vinylrhodium complex (**5** in Table 5) for the living polymerization of phenylacetylenes has been prepared, isolated, and fully characterized by X-ray analysis. Catalyst **5** polymerizes phenylacetylene and its para-substituted analogues to give living polymers (e.g., M_n 25 000; $M_w/M_n = 1.05$) with quantitative initiation efficiency. Living polymerization is also possible even in the presence of water. The isolation of **5** is not necessary, and the complex formed in situ by the reaction of [(nbd)RhCl]$_2$ with LiCPh $=$ CPh$_2$ and Ph$_3$P induces living polymerization in quantitative initiation efficiency. A remarkable feature of this polymerization system is the ability to introduce functional groups at the initiation terminal. For example, living poly(phenylacetylene) bearing a terminal hydroxyl group is readily obtained by the polymerization with a three-component catalyst, comprising [(nbd)RhCl]$_2$, LiCPh $=$ C(Ph)(C$_6$H$_4$-p-OSiCH$_3$-t-Bu), and Ph$_3$P, followed by the desilylation of the formed polymer. Polymerization of β-propiolactone with the terminal phenoxide anion of this polymer gives a new block copolymer of phenylacetylene with β-propiolactone.

Highly active Rh-based living polymerization catalysts have been developed, which enable the synthesis of poly(phenylacetylene) with high MW and narrow MWDs (e.g., $M_n = 195,000$, $M_w/M_n = 1.06$). For instance, a Rh-based ternary catalyst system composed of [(tfb)RhCl]$_2$ (tfb, tetrafluorobenzobarrelene), Ph$_2$C $=$ C(Ph)Li, and Ph$_3$P (1:5:10) induces the living polymerization of phenylacetylene with virtually 100 % initiation efficiency. Furthermore, a well-defined vinylrhodium complex [(tfb)Rh-{$-$C(Ph) $=$ CPh$_2$}(Ph$_3$P)] (**6** in Table 5) also polymerizes phenylacetylene in a living fashion with quantitative initiation efficiency in the presence of at least five equiv. of Ph$_3$P to Rh. The livingness of these polymerizations is confirmed by multistage polymerization, first-order linear plot, and effect of initial monomer concentration on MW and MWD, and their initiation efficiencies are practically quantitative. A salient feature of catalyst **6** is high activity even at a very low concentration ([M]$_0$/[Rh] $= 4000$, [Rh] $= 0.125$ mM) to quantitatively afford a high-MW polymer ($M_n = 401$ 000) having enough narrow MWD ($M_w/M_n = 1.12$). The formed polymer possesses highly stereoregular cis-transoidal main chain (cis content $= 99$ %).

P

Summary

The development of various transition-metal catalysts, including metathesis catalysts (W, Mo, Ta, and Nb) and Rh catalysts, has enabled the polymerizations of a variety of substituted acetylenes, i.e., aliphatic, aromatic, and heteroatom-containing monomers, and acetylene itself with respect to the kind of monomer and mono- and disubstituted acetylene derivatives with respect to the number of substituents. Typical polymerizable monosubstituted acetylenes include *tert*-butylacetylene, phenylacetylene, alkyl propiolates, *N*-propargylamides, etc. Sterically demanding *tert*-butylacetylene polymerizes with Mo and W catalysts; phenylacetylene with W, Mo, and Rh catalysts; and polar group-containing alkyl propiolates and *N*-propargylamides with Rh catalysts. Typical polymerizable disubstituted acetylenes include 1-chloro-1-octyne, 2-octyne, 1-phenyl-1-propyne, 1-(trimethylsilyl)-1-propyne, diphenylacetylenes, etc. Sterically rather uncrowded 1-chloro-1-octyne and 2-octyne polymerize effectively with Mo catalysts, 1-phenyl-1-propyne and 1-(trimethylsilyl)-1-propyne with Nb and Ta catalysts, and highly crowded diphenylacetylenes only with Ta catalysts. The polymers formed from these monomers possess high MWs and are composed of carbon–carbon alternating double bonds along the main chain and various side groups. They exhibit unique and interesting properties based on the conjugated structure, such as semiconductivity, photoluminescence, electroluminescence, electrochromism, and energy migration and transfer.

Related Entries

▶ Polyacetylenes

References

1. Sanda F, Masuda T, Shiotsuki M (2012) Alkyne Polymerization. In: Matyjaszewski K, Möller M (eds) Polymer science: a comprehensive reference, vol 3. Elsevier, Amsterdam, pp 875–954

2. Liu J, Lam JWY, Tang BZ (2009) Acetylenic polymers: syntheses, structures, and functions. Chem Rev 109:5799–5867

3. Masuda T, Sanda F, Shiotsuki M (2007) Polymerization of Acetylenes. In: Crabtree R, Mingos M (eds) Comprehensive organometallic chemistry III, vol 11. Elsevier, Oxford, pp 557–593, Chapter 16

4. Shirakawa H (2001) The discovery of polyacetylene film: the dawning of an era of conducting polymers. Angew Chem Int Ed 40:2574–2580

5. MacDiarmid AG (2001) Synthetic metals: a novel role for organic polymers. Angew Chem Int Ed 40:2581–2590

6. Heeger AJ (2001) Semiconducting and metallic polymers: the fourth generation of polymeric materials. Angew Chem Int Ed 40:2591–2611

7. Nagai K, Masuda T, Nakagawa T, Freeman BD, Pinnau I (2001) Poly[1-(trimethylsilyl)-1-propyne] and related polymers: synthesis, properties and functions. Prog Polym Sci 26:721–798

8. Masuda T, Nagai K (2006) In: Yampolskii Y, Pinnau I, Freeman BD (eds) Materials science of membranes. Wiley, Chichester, pp 231–250, Chapter 8

9. Yampolskii Yu (2012) Polymeric Gas Separation Membranes. Macromolecules 45:3298–3311

10. Nagai K, Lee Y-M, Masuda T (2007) Polymeric membranes for gas separation, water purificatioon and fuel cell technology. In: Matyjaszewsky K, Gnanou Y, Leibler L (eds) Macromolecular engineering. Wiley, Weinheim, pp 2451–2491, Part 4, Chapter 12

11. Aoki T, Kaneko T, Teraguchi M (2006) Synthesis of functional p-conjugated polymers from aromatic acetylenes. Polymer 47:4867–4892

12. Ulbricht M (2006) Advanced functional polymer membranes. Polymer 47:2217–2262

13. Masuda T, Sanda F (2003) Polymerization of substituted acetylenes. In: Grubbs RH (ed) Handbook of metathesis, vol 3. Wiley, Weinheim, pp 375–406, Chapter 3.11

14. Mayershofer MG, Nuyken O (2005) Living polymerization of substituted acetylenes. J Polym Sci Part A Polym Chem 43:5723–5743

Polymerization of α-Amino Acid *N*-Carboxy Anhydride

Hitoshi Kanazawa
Department of Industrial System, Faculty of Symbiotic Systems Science, Fukushima University, Fukushima, Japan

Abbreviations

Amino acid NCA, NCA	α-Amino acid *N*-carboxy anhydride

BLG NCA	γ-Benzyl-L-glutamate NCA
PBLG	Poly(γ-benzyl-L-glutamate)
PBLA	Poly(β-benzyl-L-aspartate)
ROP	Ring-opening polymerization
TCF	Trichloromethyl chloroformate
Cl content	Chlorine content
BuNH$_2$	*n*-Butylamine
MWD	Molecular weight distribution

Synonyms

4-Alkyl-1,3-oxazolidine−2,5-dione; Leuchs' anhydride; α-Amino acid *N*-carboxy anhydride: amino acid NCA; NCA

Definition

The polymerization of α-amino acid *N*-carboxy anhydrides (amino acid NCAs) is suitable for the synthesis of high molecular weight polypeptides with narrow molecular weight distribution. The polymerization is largely affected by the amino acid NCA purity and a moisture contamination in the reaction system. Amino acid NCAs are generally synthesized by the reaction of corresponding amino acids with phosgene or its derivatives.

Introduction

The first paper on the synthesis of glycine NCA was presented by Herman Leuchs in 1906 [1]. After about four decades, it was known that α-amino acid NCAs were useful monomers for the preparation of polypeptides. The polymerizations of NCAs were studied actively during the 1950s–1980s and used widely for the preparation of polypeptides with high molecular weight, at present [2]. The obtained oligo- or polypeptides are useful for simple models of proteins. The ring-opening polymerization of amino acid NCAs is generally initiated by bases and always accompanied by a release of CO_2. When a mixture of several kinds of amino acid NCAs is polymerized at once, random copolymers containing each amino acid residue are easily obtained.

The NCA polymerization initiated by bases or other initiators is generally considered a living polymerization, which is useful for the preparation of block polypeptides; when the complete polymerization of the first amino acid NCA is followed by the addition of the second NCA, the block polypeptide containing the two amino acid residues is obtained.

Amino Acids and Amino Acid NCAs

Amino acids are organic compounds having both amino and carboxyl groups, in a broad sense. In α-amino acids, they are attached to the first (α-) carbon atom; the generic formula is CHR(NH$_2$)COOH in most cases, where R is an organic substituent known as a "side chain." Amino acids have optical isomers, L-forms and D-forms. In particular, 20 kinds of L-forms of α-amino acids are important for protein components in the organism.

α-Amino acid *N*-carboxy anhydrides are 1,3-oxazolidine-2,5-dione (glycine NCA) and 4-alkyl-1,3-oxazolidine-2,5-diones and abbreviated as α-amino acid NCAs, Leuchs' anhydrides, or NCAs. L-Alanine and L-alanine NCA ((S)-4-methyl-1,3-oxazolidine-2,5-dione or (S)-4-methyl-2,5-oxazolidinedione) are given in Fig. 1. The term NCA is usually used to refer to α-amino acid NCA (although NCAs of β-amino acids, etc. are also possible). α-Amino acid NCA is abbreviated as amino acid NCA or NCA, hereafter. Amino acid NCA crystals are soluble in water very easily but converted to original amino acids, accompanying with a release of CO_2. When amino acid NCA crystals absorb moisture in air, their polymerization is initiated at the crystal surface.

**Polymerization of
α-Amino Acid *N*-Carboxy
Anhydride,**
Fig. 1 L-Alanine (*left*) and
L-alanine NCA (*right*)
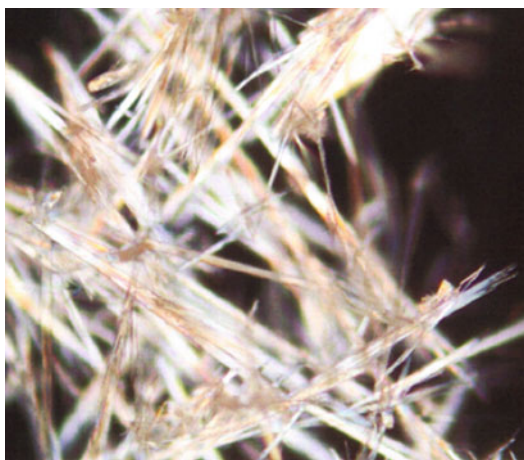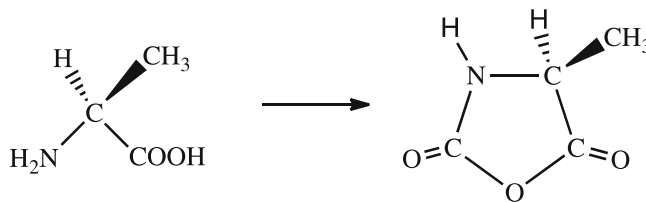
Polymerization of α-Amino Acid *N*-Carboxy Anhydride, Fig. 2 Photograph of BLG NCA crystals

Synthesis of Amino Acid NCAs

Amino acid NCAs are colorless and transparent crystals. Figure 2 gives a photograph of γ-benzyl-L-glutamate NCA (BLG NCA). They are prepared by the reaction of α-amino acids with phosgene or phosgene derivatives such as trichloromethyl chloroformate (TCF) and triphosgene (bis(trichloromethyl) carbonate) [3, 4] or the reaction with phosphorus tribromide [5, 6]. Triphosgene crystals are convenient because of the easy handling. The novel preparation method of some amino acid NCAs without phosgene derivatives was presented in a recent literature [7]. Synthesized amino acid NCA crystals are purified by the recrystallization in a mixture of solvent and precipitant. The recrystallization must be repeated about ten times in order to obtain extra-pure NCA crystals. The NCA purity should be determined by an exact analysis mentioned below. The NCA stored in a freezer should be purified just before use.

An Example of Preparation of Amino Acid NCAs

Finely ground γ-benzyl-L-glutamate (BLG) (10.0 g; 42.1 mmole) crystals are dispersed in tetrahydrofuran (THF: 200 ml) in a round-bottom flask. The suspension is heated at around 70 °C and stirred under reflux for 1 h. On the other hand, triphosgene crystals (4.60 g, 15.5 mmole) are dissolved in THF (200 ml) in another round-bottom flask, and the mixture is stirred for 1 h at 5–10 °C. The BLG suspension in THF is added to the triphosgene solution in THF in three steps, and the mixture is stirred for 2–5 h at 40–50 °C. When the reaction mixture becomes semitransparent, the reaction is almost finished. The reaction mixture is concentrated under reduced pressure until the volume becomes about 0–50 ml. When hexane (100–150 ml) is poured into the mixture, BLG NCA crystals precipitate at the bottom. After decanting the upper portion of the mixture, the mixture is dried under reduced pressure at 30–40 °C. Then, ethyl acetate (100 ml) is added in the flask to dissolve the NCA crystals. The solution is put in an Erlenmeyer flask, and hexane (200–300 ml) is added in it. BLG NCA crystals precipitate in the mixture. The yield is about 70 % at this stage. After the NCA crystals are collected by a glass filter, they are purified by the crystallization in ethyl acetate (solvent) and hexane (precipitant). These purification processes must be carried out in a dry box at low temperature. The recrystallization must be repeated several times until NCA crystals are purified as described below.

Other amino acid NCAs are prepared similarly to the above method. But, the yield of each amino acid NCA is different. For instance, the synthesis of glycine NCA using triphosgene gives a low yield.

Purification of Amino Acid NCAs

The polymerization of amino acid NCAs is extremely affected by the purity of the NCAs. However, it seems that most of the recent research papers do not describe the NCA purity. It was recommended in literatures that NCA crystals with Cl content less than 0.01 wt% should be used for the polymerization [8, 9]. This chloride content is a target value till now.

When amino acid NCAs are synthesized by phosgenation, several amino acid chlorides are formed as by-products [5]. Thus, the purity of amino acid NCAs is estimated by the Cl content, which has been determined by titration methods or elemental analysis. However, it is difficult to determine the Cl content below about 0.05 wt% by these methods. The titration methods give very low Cl content (sometimes, zero), even if the NCA contains chlorine over 0.1 wt%. An ion chromatography is an effective way for determining the exact Cl content as described below. The recrystallization must be repeated about ten times in order to obtain BLG NCA crystals with Cl content less than 0.01 wt%. The relation between the Cl content in BLG NCA crystals and the number of recrystallization is given in Fig. 3 [10].

In general, pure NCA crystals are transparent and noncolored. Colored NCA crystals must be more purified. Purified NCA crystals must be stored in a freezer at about −20 °C, being soaked
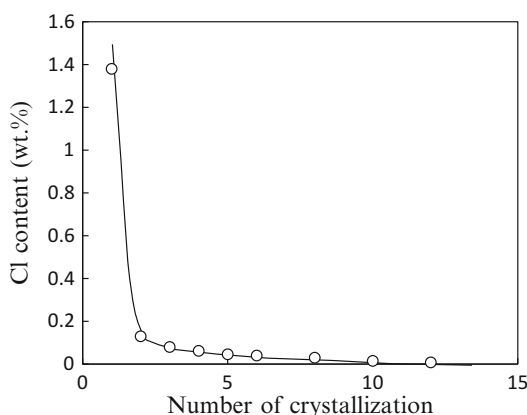
Polymerization of α-Amino Acid *N*-Carboxy Anhydride, Fig. 3 Relation between the number of crystallization (ethyl acetate/hexane) and Cl content in BLG NCA crystals

in a mixture of ethyl acetate and hexane in an Erlenmeyer flask. This flask containing the purified crystals is taken out from the freezer and is allowed to stand for a while until it is warmed to room temperature. The NCA crystals are filtered off, and the collected crystals are dissolved in warm ethyl acetate at 30–40 °C. The ethyl acetate solution of the purified to some extent becomes a little turbid, because the surface of well-purified NCA crystals is polymerized slightly by moisture in air during the purification process. The turbid material in the NCA solution in ethyl acetate must be removed by filtration, anytime. Conversely, if NCA crystals are not purified sufficiently, the solution in ethyl acetate becomes clear, suggesting that some impurities disturb the formation of the polymer on their surfaces. The NCA crystals must be always purified just before use for the polymerization. Sufficiently purified NCA crystals cannot be saved at a dry state even in a freezer because polymerization would spontaneously take place. If NCA crystals contain a lot of impurities and are not purified well, it is possible to store the dried crystals over P_2O_5. Such NCA crystals are stable and not polymerized by moisture in air. However, when such NCA crystals are used for polymerization, the results give many misunderstandings and resultant polypeptides may contain compounds harmful to the organisms. The importance is the accurate estimation of the purity of NCAs, as described below.

Determination of Purity of Amino Acid NCAs

An exact purity of NCA is determined by a combination of an oxygen flask combustion method and an ion chromatography. Dried NCA crystals (e.g., 0.1–0.2 g) are burned in an oxygen flask containing water (30 ml) according to a usual oxygen flask combustion technique. The Cl content in the aqueous solution is analyzed by a usual ion chromatography.

Polymerization

It is important to use amino acid NCAs with a high purity and avoid pre-polymerization before use.

The NCA polymerization is usually initiated by nucleophiles and bases. The bases are amines, pyridine, sodium methoxide, lithium bromide, sodium hydroxide, sodium borohydride, etc. The polymerization of amino acid NCAs initiated by bases has been extensively studied, and the reaction mechanisms are presented [2, 10–12]. In addition, metal salts and covalent metal compounds were used as initiators [2, 5].

There are three types of polymerizations: solution, precipitation-state (heterogeneous system), and solid-state polymerizations. In general, amino acid NCAs are easily soluble in normal organic solvents, but simple polypeptides such as polyglycine, poly(L-alanine), poly(L-valine), poly(L-leucine), and poly(L-phenylalanine) are not soluble in them. Therefore, the true solution polymerization of these amino acid NCAs is impossible. Thus, these NCAs are polymerized in a heterogeneous system, in which NCAs are soluble but growing polymers are precipitated. Thus, the polymerization occurs between dissolved NCAs and precipitated polymer.

The following matters are important for carrying out the polymerization of amino acid NCAs.

1. Using sufficiently purified amino acid NCA crystals; if the NCA crystals contain impurities to some extent, the initiators would be deactivated by the impurities.
2. Checking the purity of amino acid NCA crystals by an accurate analytical technique; if this process is not performed carefully, incorrect results would be obtained. All kinetic experiments should be made by using the NCAs which are just crystallized.
3. Avoiding the moisture contamination into amino acid NCA crystals, initiators, solvents, and reaction containers.
4. NCA crystals should be purified just before use; if NCA crystals coated with a slight amount of the preformed poly(amino acid) are used, the polymer can initiate the polymerization.

Solution Polymerization

NCAs of amino acid derivatives such as BLG, γ-alkyl-L-glutamate (ALG), β-benzyl-L-aspartate (BLA), β-alkyl-L-aspartate (ALA),

ε-carbobenzoxy- L-lysine, and L-sarcosine are polymerized in solutions of aprotic solvents, because the resulting polypeptides are soluble in them. Especially, the polymerization of BLG NCA has been researched widely to consider the polymerization mechanism, and the characterization methods of PBLG have been developed well.

Primary or tertiary amines are very useful for the initiation of the NCA polymerization. Polypeptides with broad MWD have been obtained in the amine-initiated NCA polymerization in many researches [8, 9, 13]. However, it is possible to obtain the polypeptides with narrow MWD when the polymerization is carried out by using sufficiently purified NCAs under strict conditions. The polymerization mechanisms initiated by a primary amine or a tertiary amine were investigated in the 1950s. The mechanisms have been studied thereafter. Several questions are mentioned, but no other mechanisms are presented at present.

The purity of amino acid NCAs is very important to practice the living polymerization of NCAs in solutions. Figure 4 shows the effect of the Cl content in BLG NCA crystals on the polymerization initiated by butylamine in dioxane [10]. When NCA crystals containing much
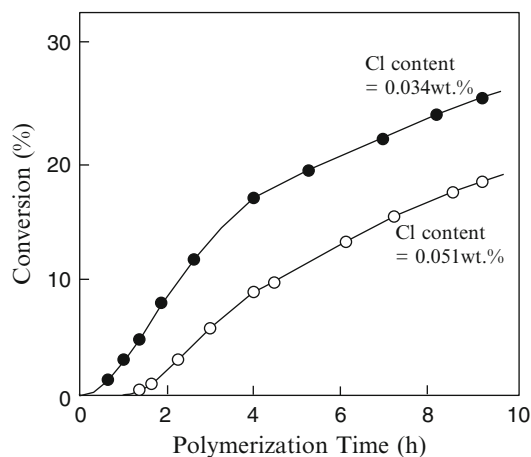
Polymerization of α-Amino Acid *N*-Carboxy Anhydride, Fig. 4 Polymerization of two BLG NCAs having different chlorine contents (*close circles*, 0.034 %, and *open circles*, 0.051 %), initiated by butylamine in dioxane. [NCA]/[I] = 200, temp. = 30 °C
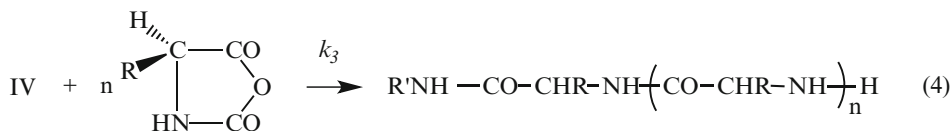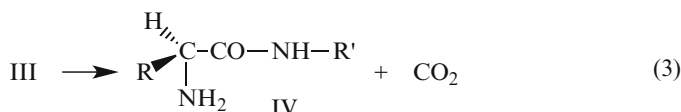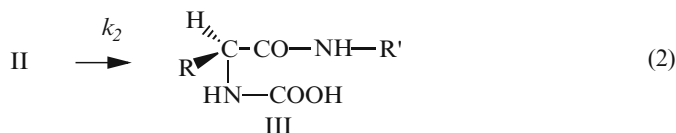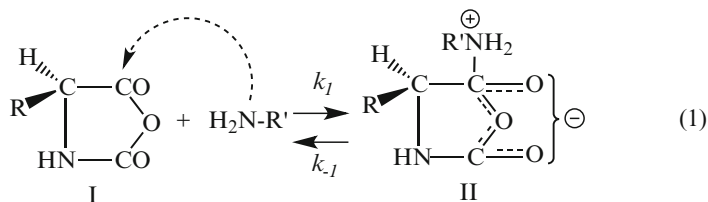
Polymerization of α-Amino Acid *N*-Carboxy Anhydride, Fig. 5 Nucleophilic addition mechanism for the polymerization of NCA

amount of impurities are used, the polymerization is not initiated for several days.

A Primary Amine Initiation: Nucleophilic Addition Mechanism

The polymerization of amino acid NCAs initiated by a primary amine such as butylamine, hexylamine, and benzylamine has been considered to follow "the nucleophilic addition mechanism." The mechanism is given in Fig. 5. A primary amine $R'NH_2$ attacks C5 of NCA I nucleophilically, and intermediate II is formed. Compound II gives compound III through ring opening. Compound III discharges CO_2 and gives compound IV which has an amino group. The amino group in IV attacks another NCA, and the resultant amine reacts with other NCAs one after another. The reaction of (1) is mostly considered as a rate-determining step. Because each amine initiator gives one polypeptide, the polymerization is considered as a kind of living polymerization; polypeptides with narrow MWD ($M_w/M_n \simeq$ 1.0) should be obtained. The initiation step (1) must be faster than the growing step (4).

The use of sterically unhindered primary aliphatic amines is preferable for this.

The solution polymerization of BLG NCA initiated by a primary amine has been investigated by many researchers, but poly(γ-benzyl-L-glutamate) (PBLG) with wide MWD was mostly obtained [8, 9, 11]. In order to explain these results, side reactions such as the attack to C2 by the terminal amine and the intramolecular cyclization of propagating polypeptides were considered to interfere with the formation of polypeptides with narrow MWD, and they are till now believed true [2, 6, 11, 12]. However, it was possible to obtain PBLG with very narrow MWD ($M_w/M_n \simeq$ 1.04) when the polymerization of well-purified BLG NCA was initiated by butylamine in the solution of dioxane, DMF, or dichloromethane, avoiding the pre-polymerization caused by moisture contamination [14]. However, the molecular weight of PBLG obtained in the solution polymerization initiated by a primary amine is limited up to around 40,000. In order to explain this upper limitation of the molecular weight, the following hypothesis was proposed. When PBLG molecules

grow to some extent, the basicity of the NH_2 end group becomes weak and the reactivity is decreased [15]. But this explanation is suspicious, because the solid-state polymerization of BLG NCA initiated by butylamine gave polypeptides having much higher molecular weight than the solution reaction, as described below. When the polymerization of BLG NCA proceeds to some extent in solutions, the growing PBLG molecules are known to make aggregations or gels in the solutions. It is considered that the NH_2 end groups are included in the aggregates and their reactivity would be lost.

Strong Base Initiator

Strong bases such as sodium methoxide and sodium hydroxide initiate the NCA polymerization similarly to primary amines. Because these bases are used as aqueous or methanol solutions, the solvents should initiate the NCA polymerization together with added initiators. Thus, the control of the polymerization by these initiators is difficult.

Activated Monomer Mechanism

The solution polymerization of amino acid NCAs initiated by tertiary amines such as pyridine and triethylamine (TEA) gives polypeptides with much higher molecular weight than that initiated by primary amines. The mechanism is called as "activated monomer mechanism" shown in Fig. 6 [11, 15]. At the beginning, a base draws out H at the N3 position of NCA I, and anion V and Base-H$^+$ are formed. Anion V attacks another NCA to form compound VI, which reacts with Base-H$^+$ and gives compound VII, accompanied with a release of CO_2. Compound VII reacts with another NCA anion V to form compound VIII as given in (8) similarly to the reaction (6). Compound VIII reacts with Base-H$^+$, releasing CO_2, and gives compound IX as shown in (9), similarly to (7). Compound IX continuously reacts with NCA anion V, and polypeptide chains grow as given in (10).

As *N*-substituted amino acid NCAs such as L-sarcosine NCA is not polymerized by tertiary amines, it is proved that the existence of the H atom at the N3 position of NCA is necessary for the polymer growing according to this mechanism [16]. It was reported that the NCA polymerizations initiated by tertiary amines produce polypeptides with high molecular weight and wide MWD [11, 15]. Such polypeptides have been obtained by many researchers, but these results cannot be explained by the mechanism given in Fig. 6. "High molecular weight" and "broad MWD" seem to be inconsistent with each other. The formation of polypeptides with broad MWD is mostly caused by multiple kinds of initiations, propagations, or terminations. However, polypeptides (PBLG) with high molecular weight and narrow MWD were obtained in the solution polymerization of BLG NCA initiated by TEA [14]. This fact suggests that the polymerization was made by only one initiation.

The activated monomer mechanism is not always believed true by all researchers, but alternative mechanisms are not proposed. The solid-state polymerization of BLG NCA initiated by TEA was not so reactive as compared with that initiated by a primary amine. This suggests that the initiation mechanisms by primary and tertiary amines are different from each other. The degree of polymerization ($\overline{DP}_n$) of obtained PBLG does not coincide with the molar ratio, [BLGNCA]/[TEA]. Further investigations are necessary for the clarification of the mechanism.

Some Organometallic Initiators

Organometallic complexes such as $[(Ph_3P)_2Ni$ (cyclooctadiene)], $[(CH_3)_3P)_4Co]$, etc. (general formula, $(L)_nM$; L = ligand, M = metal) were presented as initiators to give a living polymerization, which is useful for a well-defined block copolypeptide preparation [2, 12, 13]. However, the molecular weights of resultant polypeptides are not controlled well by the molar ratio, [NCA]/[metal]. Further investigations are expected to be made in extremely impurity-free environments using well-purified NCAs. On the other hand, rare earth metal complexes are presented as initiators to give polypeptides with
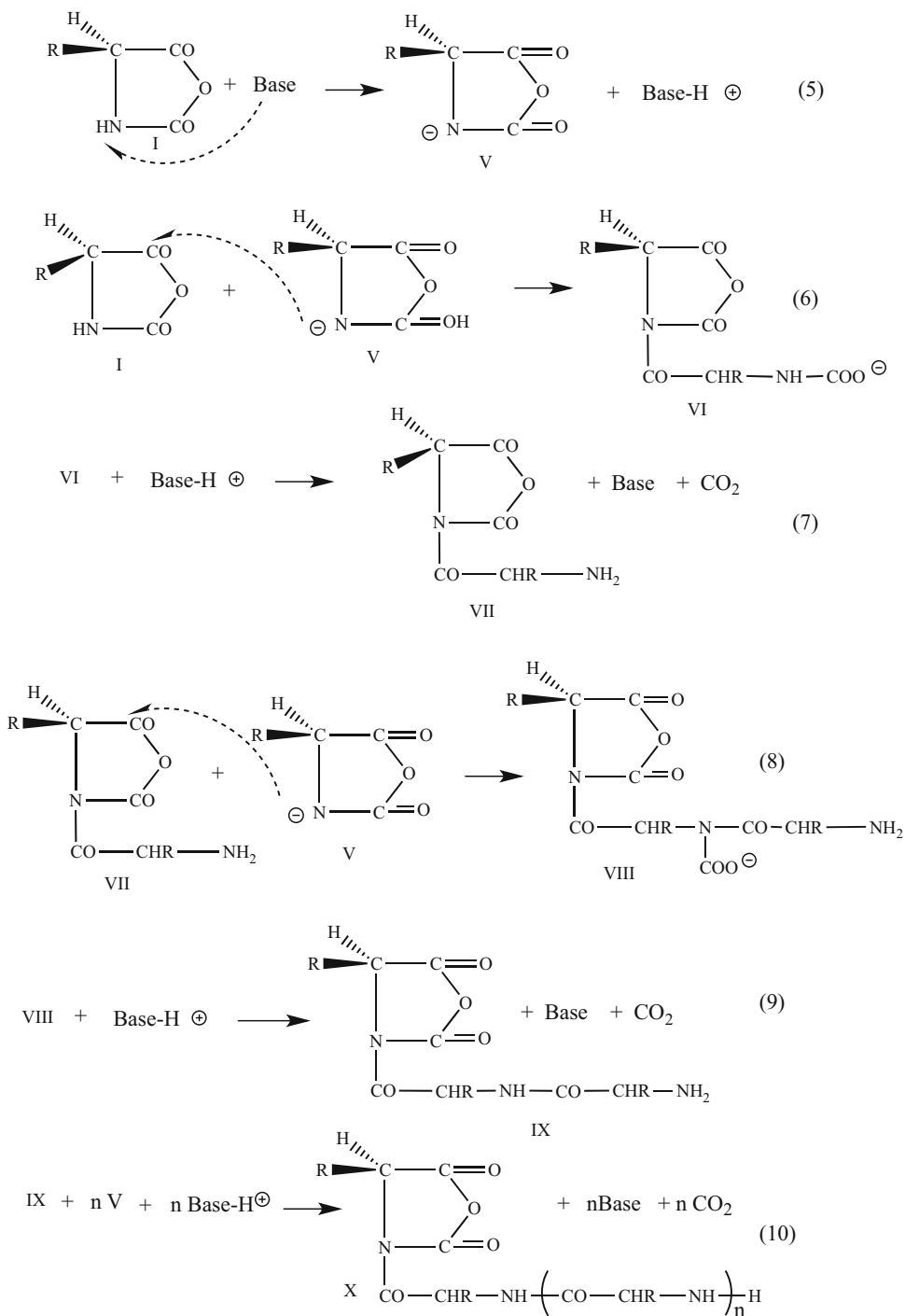
Polymerization of α-Amino Acid *N*-Carboxy Anhydride, Fig. 6   Activated monomer mechanism for the polymerization of NCA

narrow MWD [2]. It is said that the preparation and the use of both of these metal compounds require a considerable experience. In addition, the resultant polypeptides inevitably have metal elements at the molecular end. This might be sometimes a serious problem for using the polypeptides in organisms, as biopolymers.

Solid-State Polymerization of Amino Acid NCAs

When amino acid crystals are put in a nonpolar organic liquid such as hexane or heptane, which is a non-solvent for them, and then a primary amine is added into this mixture, the polymerization is initiated at the crystal surface. The polymerization of some NCA crystals proceeded to about 100 % conversion in the solid state (crystalline state) by increasing the reaction temperature to over 40–50 °C. While PBLG with the molecular weight of 40,000–50,000 is generally obtained in the solution polymerization initiated by a primary amine, the solid-state polymerization gives PBLG with the molecular weight over 130,000 and with the rather narrow MWD, ca. $M_w/M_n = 1.2$–1.5. This fact suggests that the reactivity of NH_2 end groups of growing polypeptides is not decreased even when the polymer molecules grow longer (see "Solution Polymerization"). This solid-state polymerization is available for every amino acid NCA whose corresponding polypeptide is not soluble in general organic solvents. Polyglycine, poly(L-alanine), poly(L-valine), poly(L-leucine), etc. can be obtained by the solid-state polymerization of each NCA initiated by *n*-butylamine. The solid-state reactivity of each amino acid NCA depends on its crystal structure, which affects also the structure of the resulting polypeptides [17]. Thus, the solid-state polymerization of amino acid NCAs is considered as a new-type topochemical polymerization. The solid-state polymerization should be carried out using well-purified NCA crystals, because the impurity effect is larger than that in the solution polymerization.

Polymerization of Racemic Amino Acid NCAs

When DL-amino acids (racemic amino acids) are reacted with phosgene, the corresponding DL-amino acid NCA crystals are not always synthesized. Although crystalline products are obtained, they are sometimes mixtures of L- and D-enantiomeric crystals and sometimes single crystals in which L- and D-amino acid NCA molecules are aligned regularly. For instance, when γ-benzyl-DL-glutamate is reacted with phosgene, a mixture of BLG and BDG NCA crystals is obtained. In general, the solution polymerization of the mixture of the D- and L-forms is not so reactive because of the steric hindrance in the reaction between the D- and L-forms. On the other hand, the crystal structure is very important for the solid-state polymerization of racemic amino acid NCAs. The crystal structure of DL-phenylalanine NCA prepared from racemic phenylalanine with phosgene is given in Fig. 7, where the hydrogen bonds are given by dashed lines [18, 19]. Therein, the solid-state polymerization initiated by n-butylamine was very reactive, probably caused by the suitable molecular alignment in the crystal structure.

Polymerization in the Precipitation State

Amino acid NCAs dissolve easily in acetonitrile, but the corresponding polypeptides are insoluble in it. When a primary amine is added into an amino acid NCA solution in acetonitrile, the polymerization is initiated and the resulting polypeptide precipitates soon. Further polymerization proceeds between the precipitated polymer and the dissolved NCAs, in a heterogeneous system. The reactivities of amino acid NCAs are very different from each other. This reaction is very convenient for almost all of amino acid NCAs. There are several references which report the high polymerizability of some amino acid NCAs in acetonitrile [20, 21]. However, when the polymerization of several well-purified NCA crystals was carried out in acetonitrile using n-butylamine initiator, avoiding strictly the moisture contamination into the polymerization system, the polymer conversion became very low [17, 22].

Determination of Molecular Weight and MWD of Polypeptides

The NCAs of γ- or β-esters of L-glutamic or L-aspartic acids are extensively used because the
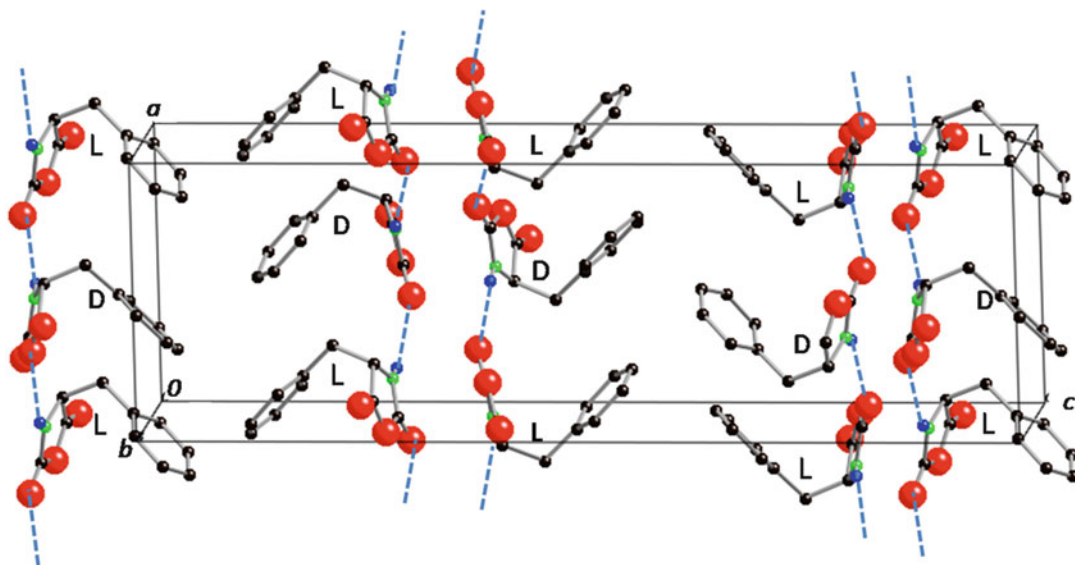
Polymerization of α-Amino Acid *N*-Carboxy Anhydride, Fig. 7   Crystal structure of DL-phenylalanine NCA

corresponding polypeptides are soluble in normal organic solvents. Especially, the polymerization of BLG NCA has been studied by many researchers because of the easy characterization of PBLG. A gel permeation chromatography (GPC) is useful for the estimation of the MWD of PBLG. Refractive index (RI), light scattering (LS), and viscosity detectors are used for the GPC. It is preferable to use these detectors at the same time. When only one of these detectors is used, it sometimes gives a misunderstanding that polypeptides with narrow MWDs are obtained.

Viscosity measurement and light-scattering methods in place of the GPC are useful for many kinds of polypeptides, because strong acid solvents such as dichloroacetic acid (DCA) and trifluoroacetic acid (TFA) are available. A mixture of DCA and methanesulfonic acid is used as a solvent for poly(L-phenylalanine). The GPC of polypeptide solutions in strong acids is impossible at present.

A MALDI-TOFMS (matrix-assisted laser desorption/ionization-time of flight mass spectrometry) is very often used for the measurement of molecular weight and MWD of polypeptides. But, several polypeptides seem to be decomposed in the course of the measurement, and only

polymer fragments are observed. Fundamentally, MALDI-TOFMS is an unsuitable tool to evaluate the average molecular weight and MWD of polydisperse polymers, because the easiness of ionization for the mass spectrometry is dependent on the molecular weight and the terminal groups. It is necessary that the GPC result coincides with the MALDI-TOFMS result.

Related Entries

▶ Precipitation Polymerization

References

1. Leuchs H (1906) Über die Glycin-carbonsaure. Ber Dtsch Chem Ges 39:857–861. doi:10.1002/cber.1906039013
2. Kricheldorf HR (2006) Polypeptides and 100 years of chemistry of α-amino acid *N*-carboxyanhydride. Angew Chem Int Ed 45:5752–5784. doi:10.1002/anie.200600693
3. Kanazawa H, Kawai T (1980) Polymerization of *N*-carboxy-amino acid anhydrides in the solid state. I. polymerizability of the various α-amino acid NCAs in the solid state. J Polym Sci Poly Chem Ed 18:629–642. doi:10.1002/pol.1980.170180222
4. Kanazawa H, Inada A, Kawana N (2006) Polymeri-sation of amino acid NCAs in acetonitrile and in the

solid state in hexane. Macromol Symp World Forum Adv Mater (Polychar-14) 242:104–112. doi:10.1002/masy.200651016

5. Kricheldorf HR (1987) α-Aminoacid-*N*-carboxy anhydrides and related heterocycles. Springer, Berlin

6. Kricheldorf HR, Lossow CV, Schwarz G (2005) Primary amine and solvent-induced polymerizations of L- or D, L-phenylalanine *N*-carboxyanhydride. Macromol Chem Phys 206:282–290. doi:10.1002/macp.200400417

7. Yamada S, Koga K, Endo T (2012) Useful synthesis method of polypeptides with well-defined structure by polymerization of activated urethane of α-amino acids. J Polym Sci Part A Polym Chem 50:2527–2532. doi:10.1002/pola.26052

8. Idelson M, Blout ER (1957) Polypeptides. XV. Infrared spectroscopy and the kinetics of the synthesis of polypeptides, primary amine initiated reactions. J Am Chem Soc 79:3948–3955. doi:10.1021/ja01572a002

9. Mitchell JC, Woodward AE, Doty P (1957) The polydispersity and configuration of low molecular weight poly-γ-benzyl-L-glutamates. J Am Chem Soc 79:3955–3960. doi:10.1021/ja01572a003

10. Kanazawa H, Inada A, Kawana N (2005) Influence of purity of *N*-carboxy amino acid anhydride crystals on their reactivity. Ningen Hattatsu Bunkagakurui Ronshu, Fukushima Daigaku 1:1–9

11. Sekiguchi H (1981) Mechanism of *N*-carboxy-α-amino acid anhydrides (NCA) polymerization. Pure Appl Chem 53:1689–1714

12. Cheng J, Deming T (2012) Synthesis of polypeptides by ring-opening polymerization of α-amino acid *N*-carboxyanhydrides. Top Curr Chem 310:1–26. doi:10.1007/128-2011-173

13. Deming T (1997) Transition metal-amine initiators for preparation of well-defined poly(γ-benzyl L-glutamate). J Am Chem Soc 119:2759–2760. doi:10.1021/ja962625w

14. Kanazawa H (2011) Reexamination of reactivity of *N*-carboxy amino acid anhydrides (41): preparation of polypeptides with monodispersed molecular weight distribution and molecular weight of over 200000. Annual conference of polymer science, Japan, Osaka, May 25

15. Imanishi Y (1972) Polymerization of α-amino acid anhydrides. Kobunshi 21:32–37. doi:10.1295/kobunshi.21.32

16. Bamford CH, Block H (1961) The initiation step in the polymerization of *N*-carboxy-α-amino-acid anhydrides. Part I. Catalysis by tertiary bases. J Chem Soc 4989–4991. doi:10.1039/JR9610004989

17. Kanazawa H (1998) Amino acid *N*-carboxy anhydrides with high polymerizability in the solid state. Mol Cryst Liq Cryst 313:205–210. doi:10.1080/10587259808044276

18. Kanazawa H, Ohashi Y (1996) Polymerization of *N*-carboxy anhydrides of L-and DL-valine, and L-and DL- phenylalanine in the solid state. Mol Cryst Liquid Cryst 277:45–54. doi:10.1080/10587259608046002

19. Kanazawa H, Uekusa H, Ohashi Y (1997) Structure of DL-phenyl alanine NCA, $C_{10}H_9NO$. Acta Crystallogr C53:1154–1156. doi:10.1107/ S010827019 7004010

20. Iwakura Y, Uno K, Oya M (1967) Polymerization of DL-alanine NCA and L-alanine NCA. J Polym Sci A-1(5):2867–2874. doi:10.1002/pol.1967.150051114

21. Oya M, Uno K, Iwakura Y (1968) Polymerization of α-amino acid *N*-carboxy anhydrides. III. Mechanism of polymerization of L- and DL-alanine NCA in acetonitrile. J Polym Sci A-1(6):2165–2177. doi:10.1002/pol.1968.150060813

22. Kanazawa H (2003) *N*-Carboxy-L-aspartic anhydride benzyl ester. Acta Crystallogr C59:O159–O161. doi:10.1107/S0108270103002567

Polymerization Reactions (Overview)

Koji Takagi
Department of Materials Science and Engineering, Graduate School of Engineering, Nagoya Institute of Technology, Nagoya, Japan

Synonyms

Polymer synthesis; Polymerization

Definition

Polymerization reactions mean the synthetic chemistry or methodology to prepare large molecular weight products (polymers) from small molecular weight substances (monomers).

Introduction

It is no wonder that a large number of polymers ranging from biological to non-biological materials very much contribute to us. Biological polymers are naturally occurring as exemplified by proteins, (deoxy)ribonucleic acids, and polysaccharides that form the basis of life. Biological polymers are highly important; however, this essay deals with non-biological synthetic polymers used for plastics, rubbers, fibers, and resins. These polymeric materials are indispensable for

the mankind living in the real world. For more than a century, new polymerization reactions have been developing as a technique for obtaining new (nano)materials [1]. From the mechanistic viewpoint, the polymerization reactions can be roughly divided into two types known as the chain-growth polymerization and step-growth polymerization. In the former polymerization process, polymers are generally produced by the successive addition of monomers to the chain end and the repeating unit is equivalent to the monomer. The chain-growth polymerization can therefore be called the addition polymerization. The chain-growth polymerization is further classified, based on the nature or structure of chain carrier usually at the polymer termini, into free radical, ionic, and coordination polymerization. Not only compounds bearing the carbon–carbon double bond called vinyl monomers but also those including the cyclic structure can polymerize via the ring-opening mechanism. These polymerization reactions are surveyed in the first part. On the other hand, in the step-growth polymerization, polymers are normally formed by the stepwise reaction of functional groups. Except for some special cases, monomers are consumed in the very early stage of the polymerization and the polymer molecular weight becomes large with increasing the reaction time. Linear polymers having functional groups such as ester and amide in the main chain are obtained from the stoichiometric amounts of bifunctional monomers. The step-growth polymerization reaction is further classified, based on the reaction mechanism, into condensation polymerization (or termed polycondensation) and polyaddition. These polymerization reactions are surveyed in the second part.

Free Radical Polymerization

The polymerization reaction where the chain carriers are carbon radicals with one unpaired electron is defined as free radical polymerization. The nomenclature "free radical" drives from the fact that the carbon radical bears no counterparts around them. Free radicals can be generated from the thermal and photochemical decomposition of unstable compounds called an initiator. The most heavily used initiators are organic peroxide [2] or azo compounds [3] containing the oxygen–oxygen (O—O) single bond and nitrogen–nitrogen (N=N) double bond, respectively. The application of external stimuli induces the homolytic cleavage to afford a radical species that is capable of reacting with the double bond of monomers (initiation). Radicals are also generated by the one-electron transfer reaction between the electron-rich compounds and electron-deficient ones, which is referred to as the redox system. The successive addition of monomers then takes place in a very short time giving rise to long polymer chains (propagation) [4]. The common monomer structures attacked by radicals are monosubstituted vinyl compounds $CH_2=CHX$ and 1,1-disubstituted derivatives $CH_2=CXY$. On the other hand, 1,2-disubstituted vinyl compounds $CHX=CHY$ hardly polymerize owing to the steric hindrance. Finally, two carbon radicals at the polymer termini react to annihilate each other to form one polymer chain (recombination) or two polymer chains (disproportionation), which corresponds to the termination of the polymerization reaction. Thus the concentration of radical species should be decreased to obtain high molecular weight polymers. The free radical is highly reactive, and the chain transfers to initiator, monomer, polymer, and solvent are possible side reactions to interrupt the formation of long polymer chain. Recently, controlled/living radical polymerizations were keenly investigated to afford well-defined polymer architecture [5].

Ionic Polymerization

The polymerization reaction where the chain carriers are ionic species is defined as ionic polymerization, and those carrying the carbenium ion and carbanion at the polymer termini are called cationic and anionic polymerizations, respectively. The biggest difference with the free radical polymerization is that counter ions are located

near the propagating end, with the formation of ion pair, during the polymerization reaction. The structure of ion pair depends on the dielectric constant of solvents, which influences the polymerization rate and stereo structure of resulting polymers. The solvent-separated ion pair is probable in highly polar solvents, while the contact ion pair is conceivable in less polar solvents. Monomers with the conjugated system that can stabilize the carbon radical by the resonance effect are possible candidates for the free radical polymerization, whereas the types of monomers susceptible to the ionic polymerization are closely related to the polarity factor [6]. Namely, monomers with the electron-donating substituent on the double bond form a stable carbenium ion, and their polymerizations proceed by the cationic mechanism. The representative monomers are isobutylene, styrene, and vinyl ethers [7]. Typical catalysts or initiators for the cationic polymerization are Lewis acids in combination with water, alcohol, and halides. Brönsted acids are also applicable, but the hydrogen halides tend to give the 1:1 adducts rather than polymers. In contrast to free radical polymerization, the termination reaction between two growing polymer chains in ionic polymerization does not occur essentially. Unimolecular side reactions such as the proton transfer to monomer and the β-proton abstraction from carbenium ion compete with the propagation, which makes the precision cationic polymerization difficult. But in many cases, quasiliving cationic polymerizations were reported by designing proper polymerization conditions [8]. As the electron-withdrawing substituent can stabilize carbanion, conjugated olefinic monomers bearing halide, ester, and nitrile groups can polymerize by the anionic mechanism. The representative monomers are vinylidene chloride, (meth)acrylic esters, and acrylonitrile [9]. Although styrene and 1,3-butadiene have no electron-withdrawing substituent on the double bond, they are also common monomers for the anionic polymerization due to the resonance stabilization of carbanion. The anionic polymerizations of these monomers are initiated by organometallic compounds, for example, organolithium and organomagnesium

reagents. For special monomers with the highly electrophilic character, water or moisture in air has enough activity to initiate the anionic polymerization. Of particular importance is that the anionic polymerizations of carefully purified monomers in the strictly dehydrated and deoxygenated media do not suffer from chain termination and transfer reactions. These polymerization systems are defined as living anionic polymerization [10, 11], which is useful for obtaining block copolymers by the sequential addition of two or more types of monomers.

Coordination Polymerization

In the early 1950s, the breakthrough in the polymerization of ethylene and propylene caused the dramatic change in the commercial production of polymers thereof. Ziegler found that the polymerization catalyst generated in situ from titanium tetrachloride with triethylaluminum enables the ambient-pressure polymerization of ethylene [12]. In contrast to branched polyethylene synthesized by the radical process at the high pressure and high temperature, linear high-density polyethylene (HDPE) can be obtained. Soon after the discovery of Ziegler, Natta succeeded in the polymerization of propylene by using the improved catalyst, which is prepared from titanium trichloride and diethylaluminum chloride [13]. The most important point is that the stereoregular polymerization occurs to give isotactic polypropylene having the high melting temperature. The Nobel Prize in chemistry was given for their outstanding contribution in the polymer science. Since the coordination of monomers to the vacant site of the metal complexes is essential for the propagation, these polymerizations are defined as coordination polymerization. The successive insertion of monomers between the transition metal and polymer chain is the propagating step of the polymerization reaction. So-called "Ziegler-Natta catalyst" is heterogeneous, and the polymerization surely proceeds at the surface of insoluble solid catalyst. On the other hand, various soluble single-site catalysts have been developed for the early and rate transition metal

complexes [14]. Zirconocene-based catalysts are effective for the stereoregular polymerization of propylene and styrene. Some palladium complexes can bring about the polymerization of not only hydrocarbon monomers but also polar monomers like acrylic esters.

Ring-Opening Polymerization

Many polymers are synthesized from monomers having the cyclic structures by the chain-growth mechanism. Since the addition followed by the ring opening of monomers constitutes the propagation step of polymerization, the corresponding reaction is defined as ring-opening polymerization. The typical monomers are lactone (ester), lactam (amide), cyclic ether, cyclic anhydride, and *N*-carboxyanhydride of amino acids [15]. The availability and polymerizability of cyclic monomers are strongly dependent on the ring size and the kind of hetero atom as the ring member, and the driving force of the reaction is the relief of ring strain. The ring-opening polymerization proceeds mostly by the cationic and anionic initiators to give industrially important polyesters, polyamides, polyethers, and polycarbonates. Namely, the ring-opening polymerizations of these monomers give polymers including hetero atoms in their main chains, which grant various physical properties to the polymer. The polymer with the similar repeating unit may be obtained by the condensation polymerization, while the ring-opening polymerization does not require the stoichiometric feed of a bifunctional monomer combination. The controls of molecular weight and molecular weight distribution are often possible under the optimized polymerization conditions. Cyclic monomers having the exocyclic double bond undergo the ring-opening polymerization by radical initiators [16]. In order to prevent the concurrent vinyl polymerization, the ring strain and the radical stabilizing group in the cyclic skeleton should be introduced. On the other hand, cyclic monomers having the endocyclic double bond polymerize by the transition metal catalysts in the ring-opening metathesis mechanism where the chain carrier is a metal carbene complex bearing the metal–carbon double bond [17]. Grubbs developed the first-generation ruthenium carbene complex and thereafter superior carbene complexes with the higher polymerization activity, and the functional group tolerability were investigated [18].

Condensation Polymerization (Polycondensation)

The polymerization reaction, in which low molecular weight compounds are eliminated by the reaction between functional groups, is defined as condensation polymerization. The most common reaction utilizes the chemistry of carbonyl groups in carboxylic acid and their derivatives (acid chloride, anhydride, ester, and so forth). Due to the electron negativity of the oxygen atom, many nucleophiles Y are susceptible to attack the carbonyl carbon in R–CO–X followed by the elimination of X as the leaving group to give R–CO–Y. The representative nucleophiles may be alcohol and amine. The reactivity of R–CO–X with Y is dependent on X and particularly Y. The direct reactions of carboxylic acids with alcohol and amine under harsh conditions (high temperature and high vacuum) provide polyesters and polyamides, respectively. One important example is the synthesis of poly (hexamethylene adipamide) (66-Nylon), where the hexamethylene diamine salt of adipic acid is heated over the melting temperature while evacuating the reaction mixture to remove water [19]. The stoichiometry of two functional groups is ensured by purifying the salt by recrystallization. The reactions of acid chloride and anhydride with amine take place under mild conditions (room temperature and ambient pressure) as a result of the high reactivity of carbonyl group. The polymerization of hexamethylene diamine dissolved in organic phase with adipic acid chloride in alkaline aqueous phase rapidly occurs at the oil/water interface known as the interfacial polycondensation [20]. The obtained 66-Nylon

P

can be pulled off as the fibrous form. Since the stoichiometry of two functional groups is established at the interface, high molecular weight polyamide can be obtained without strictly controlling the molar equivalence of monomers.

Polyaddition

When one functional group attacks another to make a new covalent bond without loss of any small molecules in the stepwise mechanism, the corresponding polymerization reaction is defined as polyaddition. Similar to the condensation polymerization, the nucleophilic addition of alcohol and amine may be the elementary step of the polyaddition. On the other hand, commonly used electrophiles include the vinyl group in acrylates and the carbonyl group in isocyanates. The successive additions of the $C=C$ double bond are well known as vinyl polymerization that is surveyed in the first part of this essay; however, this is not the necessary case. If the equimolar amount of diamine and diacrylate is heated, the Michael addition occurs to produce polymers bearing the amino and ester units in the main chain. Another popular example is the synthesis of polyurethane, where an equimolar amount of diol and diisocyanate is reacted in the presence of dibutyltin dilaurate as the catalyst. The free radical addition of dithiol toward olefinic double bond also proceeds in the polyaddition mechanism to give polymers bearing the sulfide unit in the main chain.

Related Entries

- ▶ Anionic Addition Polymerization (Fundamental)
- ▶ Anionic Ring-Opening Polymerization
- ▶ Cationic Addition Polymerization (Fundamental)
- ▶ Cationic Ring-Opening Polymerization
- ▶ Coordination Polymerization (Olefin and Diene)
- ▶ Coordination Polymerization (Styrene and Polar Vinyl Monomers)
- ▶ Free-Radical Addition Polymerization (Fundamental)
- ▶ Free-Radical Ring-Opening Polymerization
- ▶ Ring-Opening Metathesis Polymerization

References

1. Baekeland LH (1909) The synthesis, constitution, and uses of bakelite. J Ind Eng Chem 1:149–161
2. Mageli OL, Kolcynski JR (1968) Peroxy compounds. In: Mark HF, Gayload NG, Bikales NM (eds) Encyclopedia of polymer science and technology, vol 9. Wiley-Interscience, New York, pp 814–841
3. Zand R (1965) Azo catalyst. In: Mark HF, Gayload NG, Bikales NM (eds) Encyclopedia of polymer science and technology, vol 2. Wiley-Interscience, New York, pp 278–295
4. Price CC (1946) Mechanism of vinyl polymerizations. IX. Some factors affecting copolymerizations. J Polym Sci 1:83–89
5. Braunecker WA, Matyjaszewski K (2007) Controlled/living radical polymerization: futures, developments, and perspectives. Prog Polym Sci 32:93–146
6. Lenz RW (1967) Organic chemistry of synthetic high polymers. Wiley-Interscience, New York
7. Kennedy JP, Marechal E (1982) Carbocationic polymerization. Wiley, New York
8. Kennedy JP, Kelen T, Tudos F (1982) Quasiliving carbocationic polymerization. I.: classification of living polymerization in carbocationic systems. J Macromol Sci Chem A18:1189–1207
9. Hsieh HL, Farrar RC, Udipi K (1981) Anionic polymerization: some commercial applications. Chemtech 11:626–633
10. Henderson JF, Szwarc M (1968) The use of living polymers in the preparation of polymer structures and controlled architecture. Macromol Rev 3:317–401
11. Szwarc M (1968) Living polymers. In: Mark HF, Gaylord NG, Bikales NM (eds) Encyclopedia of polymer science and technology, vol 8. Wiley-Interscience, New York, pp 303–325
12. Ziegler K, Holzkamp E, Breil H, Martin H (1955) Polymerization of ethylene and other olefins. Angew Chem 67:426
13. Natta G, Pino P, Corradini P, Danusso F, Mantica E, Mazzanti G, Moranglio G (1955) Crystalline high polymers of α-olefins. J Am Chem Soc 77:1708–1710
14. Baugh L, Canich JAM (2010) Stereoselective polymerization with single-site catalysts. CRC Press, Florida
15. Brunelle DJ (1993) Ring-opening polymerization. Hanser Publishers, Munich
16. Endo T (2009) General mechanism in ring-opening polymerization. In: Dubois P, Coulembier O, Raquez JM (eds) Handbook of ring-opening polymerization. Wiley-VCH, Weinheim, pp 53–63
17. Scholl M, Ding S, Lee CW, Grubbs RH (1999) Synthesis and activity of a new generation of ruthenium-based olefin metathesis catalysts coordinated with

1,3-dimesityl-4,5-dihydroimidazol-2-ylidene ligands. Org Lett 1:953–956

18. Bielawski CW, Grubbs RH (2007) Living ring-opening metathesis polymerization. Prog Polym Sci 32:1–29

19. Palmer RJ (2001) Polyamides, plastics. Encyclopedia of polymer science and technology. Wiley, New York

20. Morgan PW (1965) Condensation polymers: by interfacial and solution methods. Wiley-Interscience, New York

Polymers for Charge Storage

Jennifer A. Irvin and Zachary W. Iszard
Department of Chemistry and Biochemistry,
Texas State University, San Marcos, TX, USA

Synonyms

Polymeric supercapacitors; Polymers for battery electrodes; Polymers for electrochemical capacitors; Polymers for energy storage

Definition

Polymers for charge storage: polymers that can be used to store energy for use in batteries or electrochemical capacitors.

Introduction

Current and emerging electronic devices have exacerbated the need for improvements in high-performance charge storage devices (CSDs). While traditional CSDs have relied on inorganic materials, such as metals and metal oxides [1], researchers are turning more and more to organic polymers for their charge storage ability [2]. Electroactive polymers (EAPs) rely on oxidation and reduction (redox) processes to store and release charge. These polymers can be used to store energy in batteries as well as in electrochemical capacitors. The advantages of EAPs in CSDs include high conductivity, mechanical

flexibility, chemical stability, raw material availability, ease of manufacturing, low cost, and reduced environmental impact [2]. There have been several recent reviews on the use of EAPs for charge storage applications [1–11].

Electroactive polymers, also known as inherently or intrinsically conductive polymers, consist of alternating double and single bonds. The removal of an electron (oxidation, also known as p-doping) results in a resonance-stabilized, positively charged polymer (Fig. 1). Conversely, the addition of an electron (reduction, also known as n-doping) results in a resonance-stabilized, negatively charged polymer (Fig. 1). The resonance delocalization of the resultant positive or negative charge results in conductivities as high as 10^4 S cm^{-1} [3], although values of 10^0 to 10^2 S cm^{-1} are more readily achievable. Both oxidation and reduction processes are theoretically reversible, so that the redox processes can be used repeatedly to store/release electrons. In practice, the reversibility of these processes depends on numerous factors, including polymer structure, device design, and solvent/electrolyte choice [2]. Redox processes in EAPs result in remarkable changes in properties of EAPs, including conductivity, color, volume, permeability, and reactivity. These redox-controllable properties have led to investigation of EAPs for use in a wide range of applications including electrochromics, sensors, actuators, and charge storage [3].

Polymers most commonly investigated for use in CSDs include polyacetylene (PAc), polythiophene (PT), poly(3,4-ethylene-dioxythiophene) (PEDOT), polypyrrole (PPy), polyaniline (PANI), poly-p-phenylene (PPP), and their derivatives (Fig. 2) [2, 4]. These and other polymers have found use in electrolytic capacitors, fuel cell catalyst support, secondary batteries, and electrochemical capacitors [4]. This entry is focused on the use of EAPs as the primary method of charge storage, e.g., in secondary batteries and electrochemical capacitors.

The configuration of EAP-based batteries and electrochemical capacitors is shown in Fig. 3. Both devices are comprised of charge collection plates, an anode, a cathode, an electrolyte, and an

P
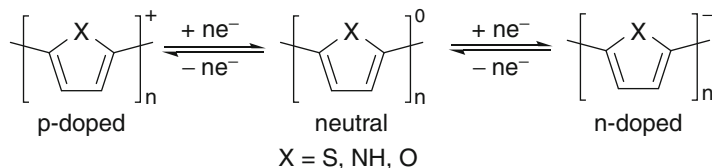
Polymers for Charge Storage, Fig. 1 Oxidation and reduction processes in EAPs such as the polyheterocycles shown here result in p-doped and n-doped polymers, respectively, and provide opportunity for charge storage
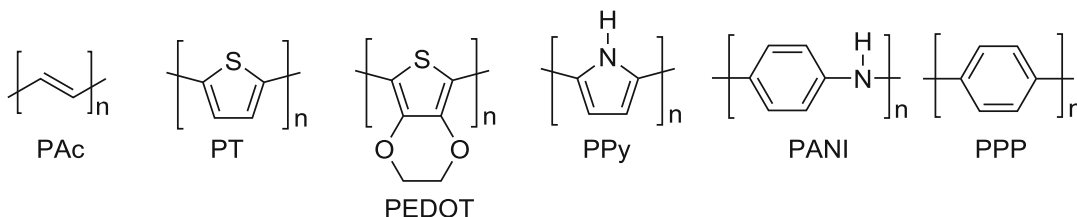
Polymers for Charge Storage, Fig. 2 Common EAPs investigated for use in charge storage devices include (from *left* to *right*) polyacetylene (*PAc*), polythiophene (*PT*), poly(3,4-ethylenedioxythiophene) (*PEDOT*), polypyrrole (*PPy*), polyaniline (*PANI*), poly-*p*-phenylene (*PPP*), and their derivatives
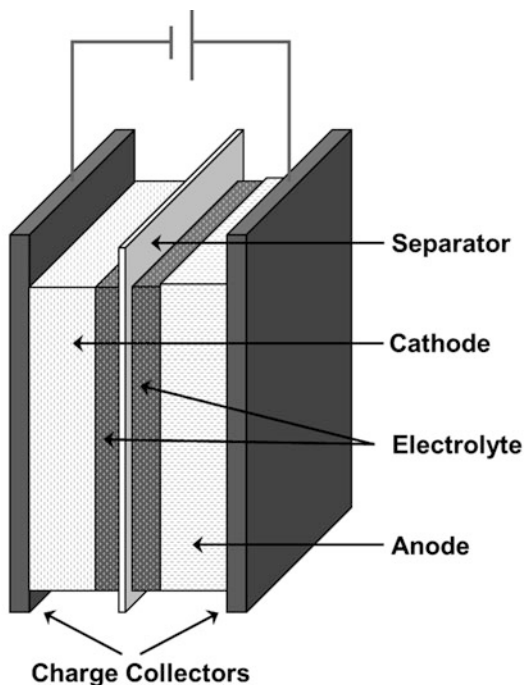
Polymers for Charge Storage, Fig. 3 Batteries and electrochemical capacitors share the same general components: charge collectors, an anode, a cathode, an electrolyte, and a physical separator

optional porous separator, which allows ion and electron flow across the device while preventing short circuits [2]. Charge collection plates are typically thin metal films. A wide range of separator materials has been investigated; suitable materials are electronically insulating, mechanically robust, chemically resistant, and readily wetted by electrolyte [12]. EAPs can be used as the anode and/or the cathode, either as films or as powders, with inorganic or carbonaceous materials often added for improved performance.

By convention, a battery electrode is characterized based on the electrochemical process (oxidation or reduction) that occurs during *discharging*. This is contrary to the terminology used in electrochemical capacitors, in which electrodes are characterized based on the electrochemical process (oxidation or reduction) that occurs during *charging* [13]. Thus an EAP that undergoes p-doping/reneutralization is considered to be the cathode when it is used as an electrode in an EAP-based battery, but it is considered to be the anode when it is used in an EAP-based electrochemical capacitor. This disparity has caused considerable confusion.

Polymers for Charge Storage, Fig. 4 Ragone plot comparing various power sources (Adapted with permission from Winter and Brodd [1]. Copyright 2004, American Chemical Society)
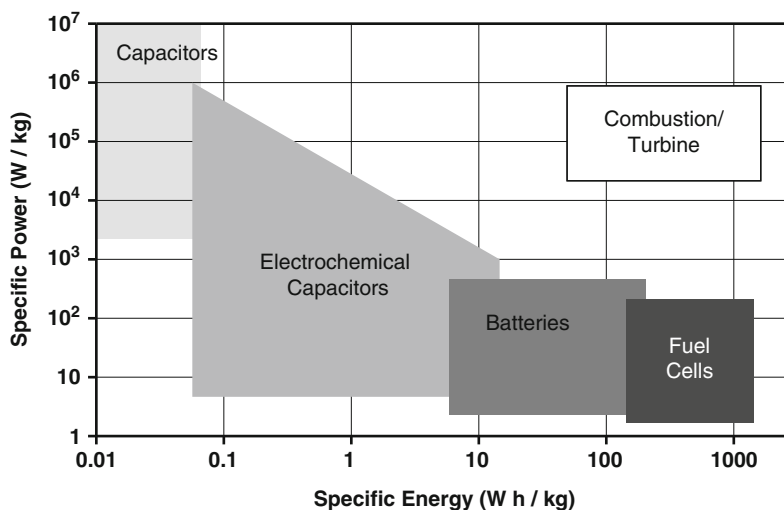
The effectiveness of CSDs is evaluated based on energy content and discharge rate. The energy content of a CSD can be related in terms of specific energy (also known as gravimetric energy density, measured in watt-hours per kilogram) and energy density (also known as volumetric energy density, measured in watt-hours per liter). Discharge rates of CSDs are measured in terms of specific power (also known as gravimetric power density, measured in Watts per kilogram) or power density (also known as volumetric power density, measured in Watts per liter). Ragone plots, in which specific power is plotted versus specific energy, are commonly used to characterize individual devices as well as to illustrate how the different types of charge storage devices compare. In Fig. 4, a Ragone plot reveals the differences between different types of devices: traditional capacitors store relatively little energy (i.e., have lower specific energy) compared to batteries, but batteries discharge much more slowly (i.e., have higher specific energy) than traditional capacitors [1]. Intermediate to these two technologies are the electrochemical capacitors (also known as supercapacitors).

In addition to energy content and discharge rate, there are several other useful parameters to consider when evaluating polymers for use in CSDs. Charge density (the amount of energy stored in the polymer, given as amp-hours per kilogram) and self-discharge rate (percentage loss in capacity per unit time) are also important considerations. Coulombic efficiency and voltage efficiency provide information about the percentage of total charge or voltage available. Cycle life – the number of cycles a device can be used before a certain percentage of capacity is lost – is an extremely important parameter for rechargeable devices. Finally, open-circuit voltage (OCV, the voltage loss across the device when no external current flows) and equivalent series resistance (ESR, the resistance the device exhibits to current flow) are important device parameters [2]. Additionally, electrochemical capacitors are evaluated based on their capacity (in Coulombs) and their specific capacitance (in Farads per gram or Farads per cubic centimeter).

Batteries

Background: Batteries can be primary (single use) or secondary (rechargeable); EAPs are used predominantly in secondary batteries due to the ease with which they can be repeatedly discharged and recharged [2]. EAPs can be used either as the anode or as the cathode in secondary batteries. A mixture of electronic and ionic

conductivity is observed using electrochemical impedance spectroscopy [2]. Likely applications of EAP batteries include portable consumer electronics (such as cellular telephones and hearing aids), military devices (such as GPS locators and night vision goggles), and electric vehicles (including commercial automobiles as well as unmanned aerial vehicles) [6]. For all of these applications, polymer research is focused primarily on increasing power densities relative to conventional lithium ion and metal hydride batteries.

While p-doped polymers can often undergo hundreds of thousands or even millions of charging/discharging processes with little loss in capacity, n-doped polymers usually undergo significant degradation in only a few cycles [2]. This degradation is usually attributed to the poor stability of carbanions formed during n-doping. For this reason, EAPs are typically used as the cathodes, while metals such as Li, Na, Mg, and Zn are used as the anodes [13]. Critical performance metrics for secondary batteries are charge densities in excess of 200 Ah kg^{-1}, outputs greater than 2 V, and a minimum of 500–1,000 charge–discharge cycles [7].

Electrolytes: Lithium salts, such as LiClO$_4$, LiAsF$_6$, LiBF$_4$, LiSO$_2$CF$_3$, LiN(SO$_2$CF$_3$)$_2$, and LiPF$_6$, are commonly used as battery electrolytes in solvents including water, propylene carbonate, ethylene carbonate, and ethers [14]. Battery electrolytes can be aqueous (in the case of PANI or PPy cathodes) or organic (in the case of PAc, PANI, PPy, PT, and PPP), with organic electrolytes needed when lithium anodes are used [2]. A thorough review of organic battery electrolytes is available [14]. Due to undesirable side reactions, batteries using aqueous electrolytes are generally limited to OCVs of 1–2 V, while organic electrolytes may allow OCVs in excess of 4 V. Ionic liquid electrolytes (organic salts that are liquid at room temperature) are a promising alternative shown to significantly enhance device stability [8].

Polyacetylene: Polyacetylene was extensively studied in early battery work, most often with lithium used as the anode. Charge density as high as 300 Ah kg^{-1} and specific energy as high as 175 Wh kg^{-1} were reported with OCV as high as 3.9 V, but poor stability and processing issues proved insurmountable [2, 7].

Polyaniline: Polyaniline is a promising alternative to polyacetylene, because PANI is a relatively stable polymer suitable for use in aqueous or organic batteries. Using a lithium anode and organic electrolyte, OCVs of 3.0 and 4.0 V can be achieved. Much lower OCVs (1.0–1.5 V) are achieved when using zinc anodes, but these allow the use of environmentally preferable aqueous acid electrolytes [2]. Charge densities reach 150 Ah kg^{-1}, and energy densities are as high as 350 Wh kg^{-1} [2]. The primary limitation of PANI batteries appears to be their cycling stability, which appears to be limited to 500 charge–discharge cycles [7]. Lithium–PANI batteries were marketed by Seiko–Bridgestone from 1987 until 1992, when sales were discontinued [15].

Polypyrrole: Polypyrrole cathodes can utilize aqueous or organic electrolytes; OCVs are generally between 3.0 and 4.0 V with organic electrolytes [13]. Charge densities up to 170 Ah kg^{-1} and energy densities up to 350 Wh kg^{-1} have been reported, with moderate improvements in performance seen when metal oxide or carbonaceous nanoparticles are added [2]. While the above performance is similar to PANI cathodes, cycle life of PPy cathodes is often significantly shorter, with less than 60 charge–discharge cycles attainable in many cases [7].

Polythiophene: Polythiophene and poly (3-alkylthiophene) cathodes have been extensively studied for use in secondary batteries, with organic electrolytes and lithium anodes used almost exclusively. Performance is somewhat less satisfactory than PANI and PPy; charge densities as high as 100 Ah kg^{-1}, energy densities as high as 325 Wh kg^{-1}, and OCVs as high as 4.2 V have been reported [2]. The composites of polythiophenes with carbonaceous or metal oxide nanoparticles are very promising, improving performance significantly [2, 13]. The cycle life of polythiophene cathodes is one driving force for continued research in these materials; hundreds or thousands of charge–discharge cycles are attainable in many cases [7]. Attempts to improve performance have largely focused on fused

thiophene derivatives; in addition to improved cathode performance, these polymers are also promising polymeric alternatives to battery anodes [2].

Poly(*p*-phenylene): Poly(*p*-phenylene) is not as highly electroactive as PANI, PPy, or PT, but it appears to be a reasonably good cathode material in alkali metal batteries. Its promising performance has been attributed to its crystallinity and resemblance to graphite [2]. When PPP is used as a cathode with lithium anodes, charge densities of 140 Ah kg^{-1} and energy densities of 300 Wh kg^{-1} have been reported; addition of carbonaceous nanoparticles improves performance slightly [2]. Research into PPP battery materials has not been as extensive as other EAP batteries. As with PT and PPy, the complete insolubility of PPP limits processing possibilities, but in contrast to PT and PPy, addition of solubilizing substituents to PPP significantly detracts from performance.

Future of EAP Batteries: While many of the polymers mentioned above are promising anode materials, improvements to cycle life are badly needed. It appears that modifications to electrolyte [8] and to electrode morphology [9] may provide the necessary improvements. Researchers are also working to improve stability of n-doped polymers; advances in this area could lead to EAP battery anodes and ultimately to lightweight, flexible, all-polymer batteries [2].

Electrochemical Capacitors

Background: There are two main types of capacitors. While double layer capacitors rely on electrostatic effects to store charge at a surface, electrochemical capacitors (also known as supercapacitors, ultracapacitors, or redox capacitors) use redox processes to chemically store charge. Electrochemical capacitors have traditionally used inorganic oxides (such as ruthenium oxide) or carbonaceous materials to store charge. Because the charge is stored on or near the surface of the particles, the capacity in these electrochemical capacitors is surface area limited; the maximum specific capacitance reported for a metal oxide electrochemical capacitor is

720 F g^{-1} (RuO$_2$), which is an order of magnitude higher than that reported for carbonaceous materials [2, 10, 11]. When electroactive polymers are used instead of metal oxides to store charge, the entire volume of the polymer should be available to store charge, with typical doping levels of one charge for every 2–5 repeat units [2, 7]. Additionally, EAPs are an attractive alternative to metal oxides due to EAPs' high charge densities and lower costs [6].

Electroactive polymer-based electrochemical capacitors (EPECs) have been studied extensively since the 1980s; Rudge and coworkers published an early review in which they characterized the different types of EPECs [16]. EPECs are described based on the type of polymer redox process occurring at each electrode [2, 16]. In a Type I EPEC, the same p-doping polymer is used on both electrodes, while in a Type II EPEC, different p-doping polymers are used at each electrode. A Type III EPEC uses one polymer that p-dopes at the anode and n-dopes at the cathode, and a Type IV EPEC uses a p-doping polymer at the anode and a different, n-doping polymer at the cathode. While Type I and II EPECs are typically quite stable with thousands to millions of cycles possible, Type III and IV EPECs are significantly less stable due to the relative instability of most n-doped polymers. However, Type III and IV EPECs are desirable due to their hypothetically much higher capacity, power density, energy density, and energy stored, as can be seen in Table 1 [2]. Most EPEC research has focused on the p-doping processes of polypyrrole, polythiophene, polyaniline, and their derivatives; research into n-doping polymers for use in Type III and Type IV EPECs has explored much more complex polymer structures in an attempt to stabilize the negative charges [2].

While critical performance metrics for batteries are well established, the same cannot be said for EPECs. In fact, performance results are not even reported consistently from research group to research group. The parameters that may or may not be reported include specific capacitance, charge density, energy density, output voltage, and cycle life; while some groups include only

Polymers for Charge Storage, Table 1 Hypothetical EPEC performance (of a 1 kg device containing 100 g EAP) [2]

EPEC type	Capacity (C)	Average current density (mA cm^{-2})	Average power density (W kg^{-1})	Energy stored (kJ kg^{-1})
I	7,500	0.50	125	1.9
II	11,250	0.75	280	4.2
III/IV	15,000	1.0	3,500	52

Polymers for Charge Storage, Fig. 5 Typical specific capacitances for different electrochemical capacitor materials (Adapted from Snook et al. [6], with permission from Elsevier)
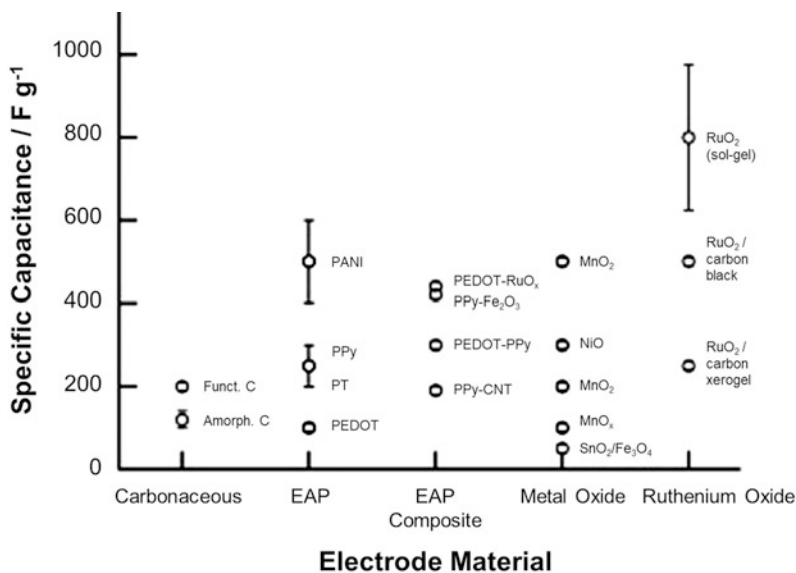
the mass of the active polymer in their calculations, others report the mass of the total device, leading to orders of magnitude difference in results [2, 6]! A need for standardization is certainly in order. One target that must be met in order to make EPECs a viable alternative to metal oxide electrochemical capacitors is a specific capacity higher than that of RuO_2 (720 F g^{-1}) [2]. Also, EPECs must be stable for a minimum of 1,000 cycles (though 100,000 cycles would be more desirable).

Electrolytes: The electrolytes commonly used in batteries may be used in EPECs, but additional electrolytes not suitable for batteries may be used with EPECs. Ammonium and tetraalkylammonium cations often replace the lithium cations used in batteries [10], and ionic liquid electrolytes have recently been shown to improve cycling stability [8]. Most EPECs utilize

organic solvents in their electrolyte formulations due to the increased output voltages, although aqueous electrolytes have been used in some cases [10].

EPEC Anodes: Polythiophenes, polypyrroles, polyanilines, and their derivatives have been extensively investigated for use as EPEC anodes. Typical specific capacitances for Type I EPECs prepared using these polymers can be seen in Fig. 5, along with the specific capacitances for carbonaceous, EAP-composite, and metal oxide electrodes. Note that, while PANI EPECs have much higher specific capacitances than other Type I EPECs or carbonaceous electrodes, they are still considerably lower than those of the best RuO_2 electrodes. Cycle life of EPECs is typically poor unless ionic liquid electrolytes are used [8].

EPEC Cathodes: Most of the n-doping polymers investigated for use in Type III and Type IV

EPECs are polythiophene derivatives. When electron-withdrawing groups are used pendant to the polymer backbone [16], electrodes are relatively stable but are poorly conductive in the n-doped state, so power densities are low [2, 6]. A more promising approach to enhancing the stability of n-doped polymers appears to be reducing bandgap, which increases intrinsic charge carrier densities and therefore increases stability in the n-doped state [2]. This approach often involves incorporation of conjugated nitrogen-containing heterocycles, which have high electron affinities. Enhanced stability (over 10,000 cycles) and reasonable energy and power densities were obtained using this strategy, and polymer morphology was found to have a significant impact on performance [17].

Composite Electrodes and Hybrid Devices: Combining an EAP with carbonaceous materials (including activated carbon, carbon nanotubes, and graphene) has been shown to significantly enhance specific power relative to double layer capacitors due to the lower equivalent series resistance [2], and stability and conductivity of the composite electrodes are improved over EAP electrodes. Unless the second component in the composite is RuO_2, specific capacitances are generally below 500 F g^{-1} [6]. One promising composite combines polypyrrole with iron oxide, yielding an inexpensive electrode with specific capacitance of 400 F g^{-1} [6]. Hybrid devices use a p-doping EAP as the anode in combination with a carbonaceous cathode. This relatively inexpensive approach eliminates instability issues associated with n-doping polymer-based cathodes and yields moderate specific capacitances (380 F g^{-1}) [2].

Future of EPECs: There are several good options for EPEC anodes based on polyaniline and polythiophene derivatives and composites; at current performance levels, these polymers will only be competitive with RuO_2 if cost and environmental impact significantly outweigh performance. In order to maximize stability, electrolytes must be carefully chosen. It appears that the highest potential to impact EPEC performance lies in the development of stable n-doping polymers for use as EPEC cathodes.

Conclusions

A wide variety of EAPs are promising for use as charge storage materials. The most reasonable use of these materials at present is as p-doping materials for battery cathodes or electrochemical capacitor anodes. Performance improvements are often possible by modification of electrolyte or morphology or by forming polymeric nanocomposites incorporating electroactive nanoparticles. Further developments are needed before n-doping EAPs can be used as battery anodes or electrochemical capacitor cathodes. Until stable n-doping EAPs are available, non-polymeric electrodes used in conjunction with stable p-doping EAPs are a reasonable alternative.

Related Entries

▶ Conducting Polymers
▶ Conjugated Polymer Synthesis
▶ Electroresponsive Polymer
▶ Polyaniline

References

1. Winter M, Brodd RJ (2004) What are batteries, fuel cells, and supercapacitors? Chem Rev 104(10):4245–4269. doi:10.1021/cr020730k
2. Irvin J, Irvin D, Stenger-Smith JD (2007) Electrically active polymers for use in batteries and supercapacitors. In: Skotheim T, Reynolds JR (eds) Conjugated polymers: processing and applications, 3rd edn, Handbook of conducting polymers. Taylor & Francis, Boca Raton
3. Zarras P, Irvin JA (2004) Electrically active polymers. In: Encyclopedia of polymer science and technology, 3rd edn. Wiley Interscience, New York
4. Holze R, Wu YP (2013) Intrinsically conducting polymers in electrochemical energy technology: trends and progress. Electrochim Acta. doi:10.1016/j.electacta.2013.08.100
5. Ramya R, Sivasubramanian R, Sangaranarayanan MV (2013) Conducting polymers-based electrochemical supercapacitors – progress and prospects. Electrochim Acta 101:109–129. doi:10.1016/j.electacta.2012.09.116
6. Snook GA, Kao P, Best AS (2011) Conducting-polymer-based supercapacitor devices and electrodes. J Power Sources 196:1–12. doi:10.1016/j.jpowsour.2010.06.084

P

7. Katz HE, Searson PC, Poehler TO (2010) Batteries and charge storage devices based on electronically conducting polymers. J Mater Res 25(8):1561–1574. doi:10.1557/JMR.2010.0201

8. Stenger-Smith JD, Irvin JA (2009) Ionic liquids for energy storage applications. Mater Matter 4(3):103–105, http://www.sigmaaldrich.com/technical-documents/articles/material-matters/ionic-liquids-for.html

9. Long JW, Dunn B, Rolison DR, White HS (2004) Three-dimensional battery architectures. Chem Rev 104(10):4463–4492. doi:10.1021/cr020740l

10. Kotz R, Carlen M (2000) Principles and applications of electrochemical capacitors. Electrochim Acta 45:2483–2498. doi:10.1016/S0013-4686(00)00354-6

11. Frackowiak E, Beguin F (2001) Carbon materials for the electrochemical storage of energy in capacitors. Carbon 39:937–950. doi:10.1016/S0008-6223(00)00183-4

12. Arora P, Zhang Z (2004) Battery separators. Chem Rev 104:4419–4462. doi:10.1021/cr020738u

13. Novak P, Muller K, Santhanam KSV, Haas O (1997) Electrochemically active polymers for rechargeable batteries. Chem Rev 97:207–281. doi:10.1021/cr941181o

14. Xu K (2004) Nonaqueous liquid electrolytes for lithium-based rechargeable batteries. Chem Rev 104(10):4303–4418. doi:10.1021/cr030203g

15. Kraft A (1997) Conducting polymers. In: Jones W (ed) Organic molecular solids: properties and applications. CRC Press, Boca Raton

16. Rudge A, Davey J, Raistrick I, Gottesfeld S, Ferraris JP (1994) Conducting polymers as active materials in electrochemical capacitors. J Power Sources 47:89–107. doi:10.1016/0378-7753(94)80053-7

17. Stenger-Smith JD, Lai WW, Irvin DJ, Yandek GR, Irvin JA (2012) Electroactive polymer-based electrochemical capacitors using poly(benzimidazobenzophenanthroline) and its pyridine derivative poly (4-aza-benzimidazobenzophenanthroline) as cathode materials with ionic liquid electrolyte. J Power Sources 220:236–242. doi:10.1016/j.jpowsour.2012.07.068

Polymers for Fuel Cells

David Aili, Jens Oluf Jensen and Qingfeng Li
Department of Energy Conversion and Storage, Proton Conductors Section, Technical University of Denmark, Lyngby, Denmark

Synonyms

Solid polymer electrolyte; Polymer electrolyte membrane

Definition

Ion conducting polymer based membranes are used as electrode separators in polymer electrolyte membrane fuel cells.

Introduction

During the last decades, fuel cells have received increasing attention for their potential to convert chemically bound energy directly into electrical energy with limited environmental impact. Of the different types of fuel cells, systems with polymer-based electrolytes are of special interest for certain applications due to their relatively simple and compact design and high power densities. On the fundamental level, they are further classified according to the nature of ionic-conducting species in the polymer-based electrolyte, i.e., acidic (proton conducting) or alkaline (hydroxide ion conducting) membranes. The type of electrolytes is of importance since it determines the electrochemistry at electrodes as well as the selection of materials for the system components and ultimately the operating conditions with respect to, e.g., temperature and humidification requirements. Many different types of fuels, such as hydrogen or methanol, have been considered depending on the type of fuel cell. Hydrogen can be easily oxidized to water and is the ideal fuel for such systems. Cells with acidic and alkaline electrolyte membranes are schematically illustrated in Fig. 1.

The requirements that the membrane has to fulfill are determined by the particular application and normally include high ionic conductivity, negligible electronic conductivity, low fuel and oxidant permeability, compatibility with other cell components, good mechanical strength, and long-term stability. Cost and environmental impact of manufacturing are also factors that need careful consideration.

The gas diffusion electrodes, usually made of a nonwoven carbon substrate with a layer of nanocrystalline platinum particles supported on high-surface-area carbon, are pressed directly to each side of the membrane to form an integral

Polymers for Fuel Cells, Fig. 1 Schematic illustration of fuel cells with acidic (*left*) and basic (*right*) polymer-based electrolytes

Anode: $H_2 \rightleftharpoons 2H^+ + 2e^-$
Cathode: $\frac{1}{2}O_2 + 2e^- + 2H^+ \rightleftharpoons H_2O$

Cell: $H_2 + \frac{1}{2}O_2 \rightleftharpoons H_2O$

Anode: $H_2 + 2OH^- \rightleftharpoons 2H_2O + 2e^-$
Cathode: $\frac{1}{2}O_2 + H_2O + 2e^- \rightleftharpoons 2OH^-$

Cell: $H_2 + \frac{1}{2}O_2 \rightleftharpoons H_2O$
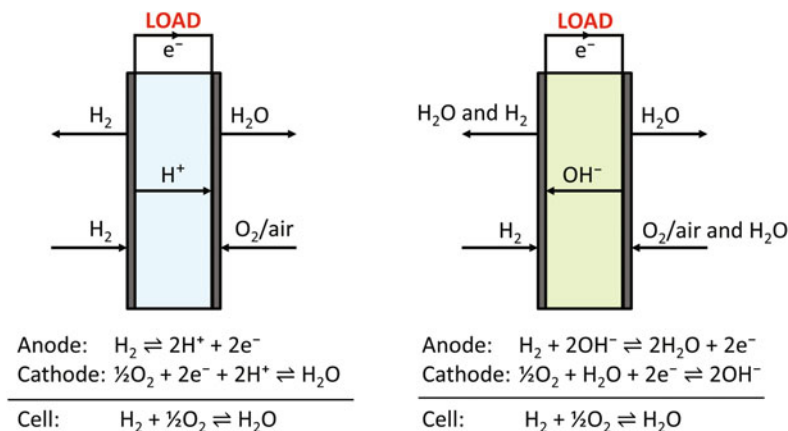
unit called a membrane electrode assembly (MEA). At the anode hydrogen is catalytically oxidized to release electrons that are passed through an external circuit to the cathode, producing the desired electrical work on the way. The reversible cell voltage for a fuel cell operated with hydrogen as fuel and oxygen as oxidant is 1.23 V under standard conditions, but due to the electrode irreversibility and gas permeation through the electrolyte, the practical cell voltage is significantly lower.

Types of Polymers and Scopes of This Entry

Polymer electrolyte membranes (PEM)s for fuel cells were first developed by Grubb and Niedrach [1] at General Electric (GE) in the earlier 1960s. The earliest membrane was based on a poly (phenolformaldehyde sulfonic acid) resin as prepared by condensation of phenolsulfonic acid and formaldehyde. This type of membrane was brittle, cracked when dried, and rapidly hydrolyzed. The first successful membrane was made of poly (styrenesulfonic acid) (PSSA), which showed a lifetime of about 200 h at 60 °C. By cross-linking styrene-divinylbenzene into an inert fluorocarbon matrix, the sulfonated polymer membranes exhibited acceptable strength in both the wet and the dry state. The membranes were used in several Gemini space missions in the 1960s. This type of membrane, however, suffers

from short lifetimes because of its limited oxidative stability. Breakthroughs were achieved with fluorinated polymers, which were adapted as membranes for fuel cells powering the Biosatellite mission in later 1960s and led to the renaissance of the polymer fuel cells from the 1980s [2].

This entry is started with a general description of perfluorinated as well as partially fluorinated polymers due to their historical and current importance. Aromatic polymers have been successfully explored in the last decades and are therefore described in some detail. To tailor the membrane properties and performance, composite membranes represent an effective approach. The newest development in this field is anion-conducting membranes, which is the last topic in the discussion. The status of the polymer membranes and their associated fuel cell technologies a thereafter discussed, followed by conclusive remarks.

Fluorinated Polymers

Poly(Perfluorosulfonic Acid)

After the pioneering work with membranes based on sulfonated polystyrene, the development of fuel cells with acidic polymer-based electrolytes was intensified in the late 1960s when the first poly(perfluorosulfonic acid) (PFSA) membranes were launched by DuPont under the trade name Nafion® [3]; see Fig. 2. The PFSA membranes
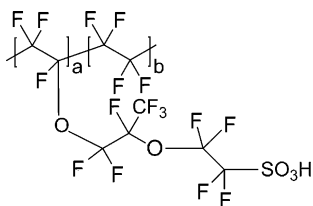
Polymers for Fuel Cells, Fig. 2 The chemical structure of Nafion®

comprise a group of cation-exchange materials that consist of a perfluorinated backbone with perfluorinated side chains containing terminal sulfonic acid groups. The development of fuel cell systems based on PFSA membranes has been further intensified during the last decades to a stage where the technology now has reached the commercial market.

The acidic side chain is the key to proton conduction, but the protons cannot just jump from one acidic site to another. The proton transport is facilitated by water molecules and the membrane must therefore be highly hydrated. During the hydration of PFSA membranes, the hydrophobic perfluorinated polymer backbones aggregate in regions with varying degrees of crystallinity providing the mechanical strength, whereas the hydrophilic acidic groups form water-filled percolating ionic domains with extreme local acidity providing pathways for proton conduction with water molecules as charge carriers [4]. However, several different models for the nano-morphology of PFSA membranes have been proposed mainly based on X-ray and neutron scattering techniques [5]. A schematic idealized illustration of the nanostructure of a hydrated PFSA membrane is depicted in Fig. 3.

Since the proton conduction in such materials is water mediated it is strongly dependent on the water content of the membrane, often normalized as the degree of hydration, λ, defined as the number of water molecules per sulfonic acid group. Under optimal conditions when the water content in the membrane is high ($\lambda > 15$) and at temperatures around 80 °C, the conductivity of PFSA membranes can reach above 0.1 S cm^{-1}, which allows for low ohmic losses in the fuel cell. The proton conductivity of PFSA materials at
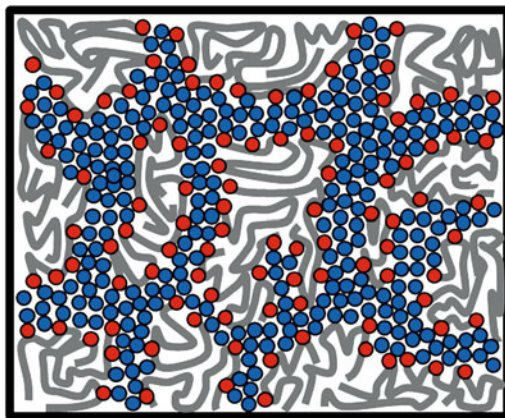
Polymers for Fuel Cells, Fig. 3 Two-dimensional schematic illustration of the percolation in a hydrated PFSA membrane. The *grey* strands represent the hydrophobic polymer backbones, while the *blue* and *red* circles represent water molecules and sulfonic acid groups, respectively

a certain degree of hydration generally increases with increasing concentration of sulfonic acid groups, often referred to as the ion-exchange capacity (IEC), defined as mmol acid equivalents per gram of polymer, or the equivalent weight (EW), defined as the average molecular weight of the polymer per mole sulfonic acid moieties. However, increasing the IEC or decreasing the EW results in enhanced water uptake, extensive volume swelling, and decreased mechanical strength. Ultimately it may lead to a complete dissolution of the membrane in water. Thus, a compromise between high IEC and good mechanical properties in the hydrated state has to be established, and typically for Nafion® membranes, the EW is around 1,100 g eq.$^{-1}$.

The poly(perfluorosulfonic acid)s are copolymers synthesized from tetrafluoroethylene (TFE) and a perfluorinated monomer containing the sulfonic acid functionality. The structure of the latter monomer can vary and determines the length of the sulfonic acid-terminated side chains, and the ratio between the two comonomers determines the equivalent weight of the resulting polymer. The synthetic strategy for Nafion® is schematically illustrated in Fig. 4.

Today, a wide range of different PFSA materials prepared by different synthetic approaches

Polymers for Fuel Cells, Fig. 4 Schematic illustration of the synthesis of Nafion®
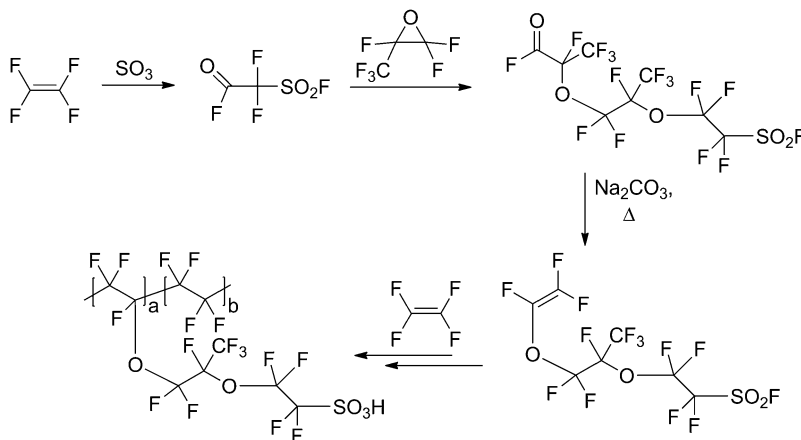
Polymers for Fuel Cells, Fig. 5 The chemical structure of Aquivion®

Polymers for Fuel Cells, Fig. 6 Chemical structure of radiation-grafted sulfonated polymers with ETFE (*left*) and PVDF (*right*) as base polymers
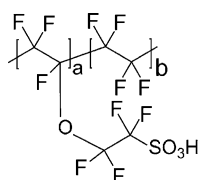
are available from various suppliers including Solvay Specialty Polymers (Aquivion®), 3 M™, Asahi Glass (Flemion®), Asahi Kasei (Aciplex®), and FuMA-Tech (fumion® F). The so-called short side chain PFSA materials, such as Aquivion® (Fig. 5), have been found to perform better in fuel cells than the conventional Nafion® membranes due to a favorable combination of low EW (790–900 g eq.$^{-1}$) and good dimensional stability.

PFSA materials are available commercially in the form of melt-extruded membranes and as dispersions in mixtures of water and low alcohols often used for electrode preparation and for membrane recasting. The recast membranes generally require annealing at elevated temperatures and pressures to develop the crystalline regions that provide the mechanical strength in the hydrated state. Recasting and annealing of PFSA membranes are preferably done using the neutral salt form of the polymer (e.g., sodium or potassium) to avoid partial decomposition and discoloration of the membranes at elevated temperatures in the dry state.

Partially Fluorinated Polymers

Radiation grafting is a versatile process offering the possibility to introduce acidic functionalities on activated sites in preformed polymer films. This technique has been implemented on a large number of different base materials of which some partially fluorinated polymers such as poly(ethylene-*alt*-tetrafluoroethylene) (ETFE) and polyvinylidene fluoride (PVDF), as schematically illustrated in Fig. 6, are among the more promising [6].

Radiation-grafted membranes can for example be produced using a roll-to-roll process in which the base film is irradiated to generate radicals and brought in contact with the monomer. Sulfonic acid functionalities can subsequently be introduced by employing a sulfonated monomer or through post-sulfonation of, e.g., styrene-grafted polymers. Employing radiation-grafted membranes based on ETFE, encouraging fuel cell test results have been demonstrated by

X = O, S
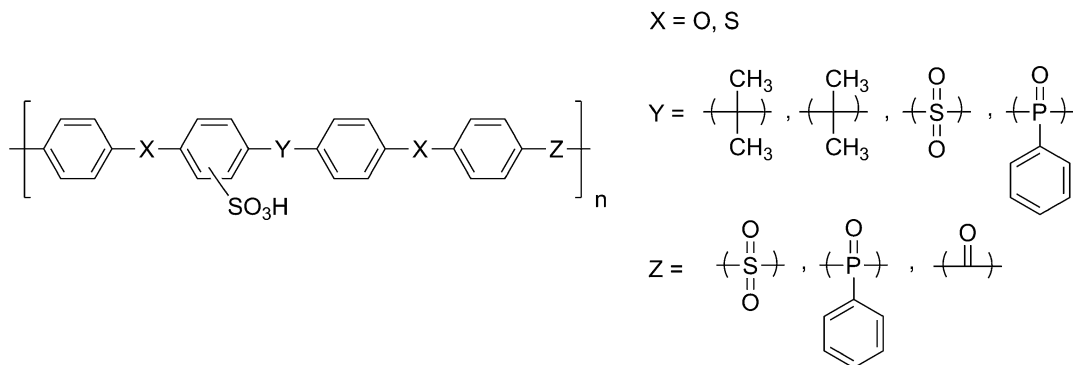
Polymers for Fuel Cells, Fig. 7 The chemical structure of a number of sulfonated polymers based on different poly (arylene ether)s

Ballard Power Systems showing performance comparable to that of Nafion®-based fuel cells.

Aromatic Polymers

Sulfonated Polymers

The development of novel cation-exchange materials based on alternative hydrocarbon polymers functionalized with pendant acidic groups is mainly motivated by a considerable potential cost reduction [7, 8]. The high chemical stability of the PFSA membranes is connected to the perfluorinated structure. Alternatively, stability can be provided by an aromatic structure. Chemically the C–F bonds have a bond strength of about 485 kJ mol^{-1}, the C–H bonds of the benzene ring of around 435 kJ mol^{-1}, and the aliphatic C–H bonds of typically about 350 kJ mol^{-1}. Just like for the PFSA materials or the partially fluorinated sulfonated polymers, the proton transport in such electrolyte systems is water mediated, which implies that careful control of the hydration characteristics is required. Among the more studied systems are sulfonic acid-functionalized aromatic homopolymers, statistical copolymers, block copolymers, and microblock copolymers such as poly(arylene ether)s, as exemplified schematically in Fig. 7.

The hydrophobicity of the polymer backbone and the acidity of the sulfonic acid groups in the non-perfluorinated materials are considerably lower than that of the PFSA polymers. One of the greatest challenges of this approach is thus to obtain a good hydrophobic/hydrophilic nanostructure in which protons can be effectively conducted [9]. This has been extensively addressed by investigating the structure-properties relationship of a large number of aromatic polymers and different structure derivatives with different sulfonation patterns and compositions of hydrophilic and hydrophobic blocks [10, 11].

The most common way to introduce sulfonic acid functionalities on the polymer backbones is through post-sulfonation by electrophilic aromatic sulfonation using sulfuric acid, oleum, chlorosulfonic acid, or sulfur trioxide complexes as reagents. However, this methodology is not regiospecific and gives limited control on the degree of sulfonation, which is of importance for the optimization of the hydrophilic/hydrophobic properties and thus the nanostructure and percolation during hydration. Alternatively sulfonated poly(arylene ether)s can be obtained by carrying out the polymerization from sulfonated monomers allowing for precise control of the degree of sulfonation and for introducing the sulfonic acid groups on electron-deficient positions in the aromatic backbone which cannot be sulfonated through electrophilic aromatic sulfonation. Commercially, sulfonated poly (arylene ether ketone)s are available in the form of membranes and as dispersions from, e.g., FuMA-Tech (fumion® P, K, and E). Compared with the PFSA materials which have

Polymers for Fuel Cells,
Fig. 8 Chemical structure
of *N*-sulfonated PBI (*top*),
zwitterionic sulfonated PBI
(*middle*), and a sulfonated
polyimide copolymer
(*bottom*)
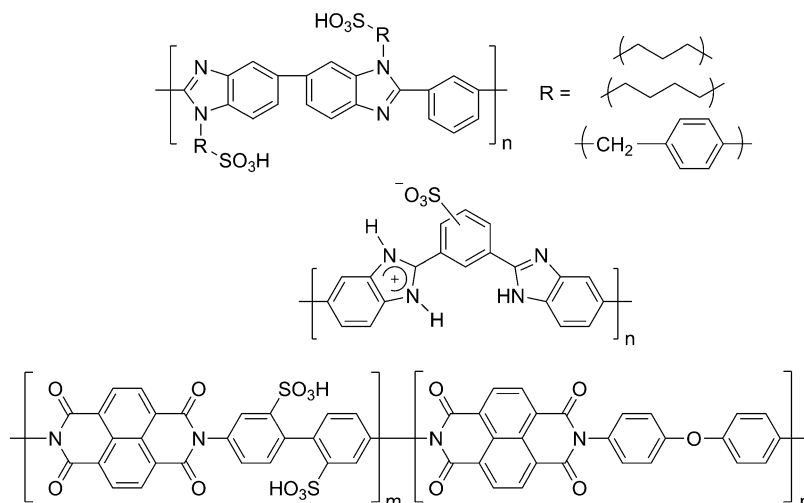
ion-exchange capacities typically around 0.9–1.0 meq g^{-1}, the ion-exchange capacity of the sulfonated poly(arylene ether)s is often considerably higher (2–5 meq g^{-1}) in order to obtain proton conductivity reaching above 0.01 S cm^{-1}.

Polybenzimidazoles are another family of aromatic engineering plastics that can be sulfonated to give materials with water-mediated proton conductivity [12]. Most work has been done on poly [2,2′-*m*-(phenylene)-5,5′-bibenzimidazole] (PBI) as shown in Fig. 8. PBI can be sulfonated through N-functionalization by treating the polymer with a strong non-nucleophilic base such as an alkali metal hydride and subsequently reacted with a sulfonated alkyl or aryl halide through a substitution reaction. Alternatively PBI can be sulfonated through doping with sulfuric acid or oleum after membrane casting followed by heat treatment at 450–600 °C for 30–120 s to give a zwitterionic polymer, also commonly referred to as stabilized PBI.

Other sulfonated aromatic polymers have been considered, such as sulfonated polyimide copolymers as schematically illustrated in Fig. 8 or sulfonated poly(phenylene oxide)s, poly(phenyl quinoxaline)s, and poly(phosphazene)s. A limited number of reports on polymers with protogenic moieties other than sulfonic acid, e.g., phosphinic acid, phosphonic acid, and sulfone imides, are also available in the literature.

Acid-Doped Polymers

From kinetic and system engineering points of view and with respect to the fuel impurity tolerance of the catalysts, it has been recognized that it would be strongly desirable to increase the fuel cell operating temperature to 120–200 °C [13]. This has triggered the development of polymer-based membrane materials in which the proton transport is not water mediated. One approach that was proposed nearly 20 years ago was to replace water as the proton solvent by phosphoric acid, which has good thermal stability and low vapor pressure at elevated temperatures and shows the highest intrinsic proton conductivity of any known species. A large number of phosphoric acid-imbibed membrane materials based on different polymers have been proposed throughout the years [8, 14–16]. However, membranes based on different structure derivatives in the polybenzimidazole family of materials and certain pyridine-containing aromatic polyethers (Fig. 9) are among the more promising and well-studied systems and selected as electrolytes for the high-temperature MEAs produced by, e.g., Danish Power Systems and Advent Technologies, respectively.

The common feature is that the polymers contain moieties with Brønsted base functionalities, making them hydrophilic in nature and giving them a high affinity for the doping acid. In such materials the protons are mainly conducted by

P
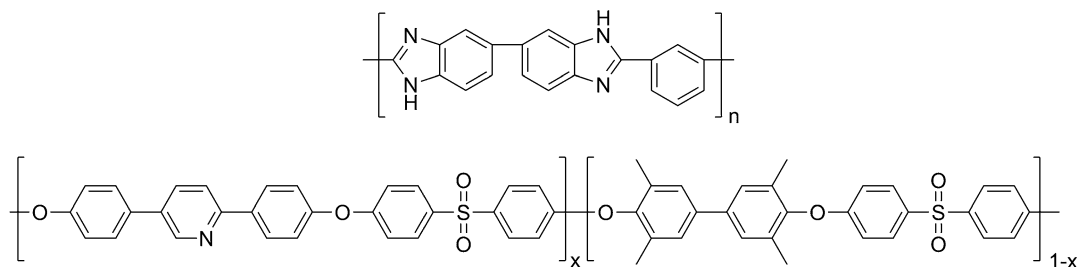
Polymers for Fuel Cells, Fig. 9 Chemical structure of poly(2,2′(*m*-phenylene)-5,5′bibenzimidazole) (*top*) and of a pyridine-containing aromatic poly(arylene ether sulfone) copolymer (*bottom*)

structural diffusion in a dynamic hydrogen bond network by the Grotthuss mechanism. Thus, no significant net movement of acid molecules occur which is a prerequisite for being able to avoid acid management systems. The proton conductivity of such materials is highly dependent on the acid content of the membrane, which in analogy with the degree of hydration for the cation-exchange membranes often is normalized as the acid doping level (ADL) defined as the number of phosphoric acid molecules per polymer repeat unit. At a given temperature and relative humidity, the proton conductivity generally increases with increasing acid content in the membrane. For example, for membranes in the polybenzimidazole family, the anhydrous proton conductivity at around 150 °C increases from about 0.03 to 0.09 S cm^{-1} when the ADL increases from about 6 to 11. The presence of small amounts of water in the phosphoric acid-doped polymer matrix considerably improves the proton transport which means that the conductivity is further increased by humidification. With an extreme ADL of above 30, the conductivity can reach above 0.2 S cm^{-1}, which is nearly half of that for pure phosphoric acid under similar conditions. However, due to the strong plasticizing effect of the acid dopant, an increasing ADL has a severe negative impact on the mechanical properties of the membrane. Thus, a compromise between proton conductivity and mechanical strength generally has to be made, and much effort has been devoted to improve the mechanical properties at high ADLs by, e.g., increasing the linear molecular weight of the polymer or through different cross-linking concepts. Another

approach that has been extensively investigated is binary PBI-based systems prepared by introducing a secondary sulfonic acid-functionalized polymeric component. In this type of acid-base blend membranes, ionic cross-links are developed between the two polymers to give a material with strong resistance to swelling in phosphoric acid as well as improved mechanical stability and sometimes improved chemical resistance.

The first synthetic route for PBI as reported in the early 1960s was based on a two-step procedure in which a pre-polymer was first prepared by heating an equimolar mixture of 3,3′-diaminobenzidine and diphenyl isophthalate at 270 °C for 1.5 h and subsequently further condensed at 360 °C for 1 h. Today, PBI is most often synthesized by homogeneous solution polymerization from equimolar mixtures of 3,3′-diaminobenzidine (freebase or tetrahydrochloride salt) with isophthalic acid or terephthalic acid in polyphosphoric acid (PPA) as the polycondensation solvent at 170–200 °C to give *m*PBI or *p*PBI, respectively, as shown in Fig. 10.

After cooling, the crude mixture is poured into water and the precipitated polymer is extensively washed with an aqueous base and water. After drying the polymer can be dissolved in a polar aprotic solvent (often with the addition of a small amount of LiCl as stabilizer) such as *N,N*-dimethylacetamide (DMAc), *N,N*-dimethylformamide (DMF), *N*-methyl-2-pyrrolidone (NMP), or dimethylsulfoxide (DMSO) from which membranes can be cast by solvent evaporation. After treatment in hot water in order to wash out eventual impurities,

Polymers for Fuel Cells,
Fig. 10 Synthetic route for
mPBI by homogeneous
solution polymerization
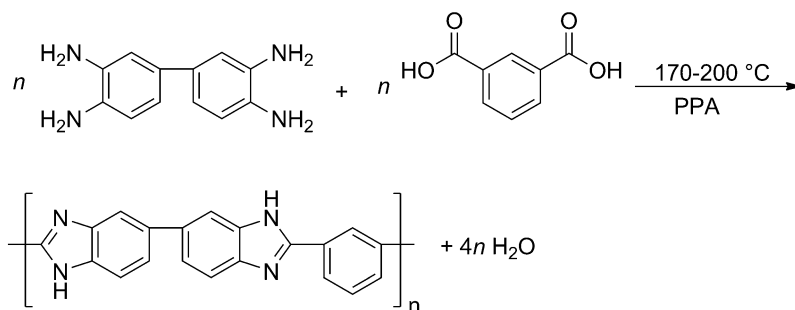
stabilizers, and solvent residuals, the membranes are imbibed with phosphoric acid in aqueous solutions of different concentrations at different temperatures and for different durations, which are the primary parameters to control the ADL. Alternatively the homogenous crude mixture can be tape cast directly followed by hydrolysis of the polyphosphoric acid in an atmosphere with carefully controlled temperature and humidity [17]. The polyphosphoric acid, which is a good solvent for PBI, is thus converted through hydrolysis into orthophosphoric acid in which the polymer is less soluble to form gel membranes with ADLs above 30.

Composite Systems

Regardless of which subtype of polymers used for the membrane electrolyte, much work has been devoted to the development of composite systems aiming at improving the physicochemical properties of the membranes and ultimately the *in situ* fuel cell performance [18]. The most widely studied secondary components are inorganic hygroscopic oxides such as silica, titania, zirconia, and alumina or bifunctional hygroscopic inorganic materials with intrinsic proton conductivity such as zirconium phosphates, heteropolyacids, or sulfonated silica or titania. For the sulfonated polymers, this has mainly targeted improved hydration characteristics and mechanical properties of the membranes allowing for operation at slightly elevated temperatures. For direct methanol fuel cells, the high methanol permeability through the sulfonated polymer membranes is causing voltage losses

and poor fuel utilization, but the permeation rate can be reduced by introducing a secondary component in the polymer matrix. Composite membranes with a secondary component for pure mechanical reinforcement, such as porous polytetrafluoroethylene-reinforced PFSA from Gore Fuel Cell Technologies, have proved promising with respect to both performance and fuel cell durability. Similarly, composite electrolyte systems with similar types of secondary components have been thoroughly investigated for acid-doped membranes for operation at elevated temperatures aiming at improving mechanical properties and reducing the proton transport resistance.

Polymers for Alkaline Fuel Cells

Even though the fuel cells based on cation-exchange polymers (especially PFSA) in general show superior performance in terms of power density, their widespread commercial competitiveness is constrained by their dependence on noble metals as catalyst materials. On the other hand, the alkaline fuel cell (AFC) using aqueous KOH as electrolyte (the first type of fuel cells used in NASA Apollo space programs in 1950s) can be constructed as a completely noble metal-free power system. One of the main drawbacks of the AFC is that the liquid KOH is very sensitive to the presence of CO_2 from either fuel or air, leading to precipitation of crystalline potassium carbonate and therefore blocking the porous electrode structure. In alkaline anion-exchange membranes, no mobile cations (e.g., K^+) are present, eliminating the formation of crystal

P
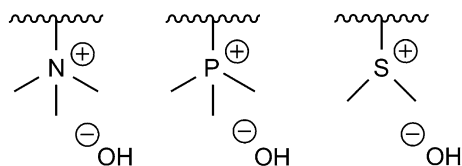
Polymers for Fuel Cells, Fig. 11 Chemical structure of ammonium, phosphonium, and sulfonium anion-exchange moieties

Polymers for Fuel Cells, Fig. 12 Chemical structure of a quaternary ammonium-functionalized poly(phenylene ether sulfone)

Polymers for Fuel Cells, Fig. 13 Chemical structure of polyethylene oxide (*left*), chitosan (*center*), and polyvinyl alcohol (*right*)

carbonates, though the carbonation still may result in decreased conductivity of the membrane. This has resulted in a dramatically increased interest in developing polymers for alkaline fuel cell electrolytes during the last few years [19]. Several different anion-exchange groups, as exemplified in Fig. 11, can be tethered to a polymer backbone to give anion-exchange polymers.

Quaternary ammonium-functionalized polymers have been known since the early 1960s, and in the membrane form they are widely used as anion conductors in different electrodialysis processes. In the hydroxide form they generally show stability limitations, and the principal degradation mechanism is directly connected to the pronounced nucleophilicity of the hydroxide ion. The use of a polymer backbone with good alkali resistance, such as members in the polysulfone family of materials, limits the rate of chain scission. However, the quaternary ammonium groups are prone to attack by the hydroxide ions causing different degradation and rearrangement reactions, and much effort is currently devoted to the development of polymers with anion-exchange moieties that are stable at high pH [20, 21]. Quaternary ammonium groups can be readily introduced onto aromatic polymers such as poly(arylene ether sulfone)s as shown in Fig. 12 through chloromethylation followed by amination with a tertiary alkyl or aryl amine to give the chloride salt of the ionomer, which subsequently can be converted into the hydroxide form by treatment with a dilute aqueous hydroxide salt solution.

In analogy with the cation-exchange materials, the hydroxide ion conductivity mechanism in anion-exchange membranes is water mediated and thus strongly dependent on the water content
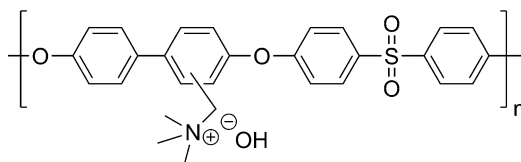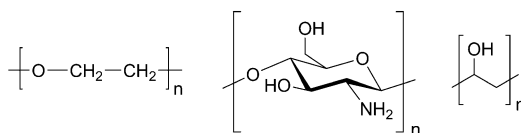
of the membrane. However, little is known about the morphology of anion-exchange membranes on the microscopic level and on the structure-conductivity relationship.

An alternative approach to obtain a polymer-based material with hydroxide ion conductivity is to imbibe a neutral polymer matrix with an aqueous hydroxide salt. Generally the polymers used for this purpose contain Brønsted base functionalities such as oxygen, nitrogen, or sulfur that interact with the cation of the hydroxide salt. The polymers in this class of materials, e.g., polyethylene oxide (PEO), chitosan, and polyvinyl alcohol (PVA) (Fig. 13), often referred to as ion-solvating polymers, are generally water soluble to some extent.

When imbibed with potassium hydroxide (KOH), the ion conductivity is strongly dependent on the concentration of the aqueous base in the membrane. The ion-solvating polymers are however known to exhibit stability limitations in the presence of hydroxide salts, and under normal fuel cell operating conditions, the ohmic resistance is gradually increased due to a continuous leaching of the dopant.

Fuel Cell Applications

For fuel cells the conductivity of the membrane has to be higher than about 10^{-2} S cm^{-1} to get reasonable *in situ* area-specific resistances of

0.1–0.3 Ω cm^2 with practical membrane thicknesses of 40–150 μm. As previously discussed, the proton transport through the membranes based on sulfonated polymers is water mediated which limits the fuel cell operating temperature to about 80 °C unless the system is pressurized to keep the membrane well hydrated. On the other hand, fuel cells based on phosphoric acid-doped membranes can operate under anhydrous conditions at temperatures up to at least 180 °C.

Due to the high capital cost of the polymer-based fuel cell technology, the long-term durability is, however, the most critical factor and lifetimes of many thousands of hours are normally required [22]. Many different degradation modes connected to different cell components simultaneously occur. The polymer-based electrolytes are exposed to harsh conditions during fuel cell operation, such as aggressive radicals, voltage gradients, and temperature and humidity cycling, which gradually damages the functionality of the membranes and may ultimately lead to cracks and pinholes. For the acid-doped membrane electrolytes, the acid loss can be fatal since it gradually increases the ohmic resistance in the cell. Depending on the operating conditions and how the end of life is defined, lifetimes ranging from a few thousands of hours up to 60,000 h have been reported for PFSA-based systems. Similarly, lifetimes exceeding 10,000 h have been reported for high-temperature PEMFCs based on phosphoric acid-doped membranes. Alkaline fuel cells based on anion-exchange membranes are still in an early development phase, and only a limited number of lifetime studies are available in the literature and lifetimes exceeding 100 h are rare. In general and irrespective of the type of membrane electrolyte, the longest lifetimes have been reported for fuel cells operating at a continuous and relatively low current load and at temperatures well below the maximum rated temperatures.

Conclusive Remarks

Fuel cells with polymer-based electrolytes represent an attractive approach to obtain compact fuel cell systems with high power density. A large number of polymers have been considered as base materials for the membranes. In membranes containing protogenic groups such as sulfonic acid moieties, the proton transport is water mediated which limits the operating temperature to about 80 °C. Among the polymer membranes of this subtype, poly(perfluorosulfonic acid) membranes are the most well-studied materials showing superior characteristics in terms of proton conductivity and chemical resistance. Sulfonated polymers based on partially fluorinated or aromatic polymers are also under active development as cheaper alternatives to the PFSA materials, but facing challenges with respect to the formation of pathways through which protons effectively can be conducted in the hydrated state. For fuel cells operating in the 100–200 °C range, phosphoric acid-imbibed membranes based on aromatic nitrogen heterocyclic polymers, especially in the polybenzimidazole and poly(arylene ether) families of materials, are of particular interest.

On one hand, an attractive approach which could potentially allow for a completely noble metal-free system is to use anion-exchange membranes as electrolytes in alkaline fuel cells. This concept is still in an early development phase and facing great challenges with respect to long-term durability. The proton exchange membrane fuel cell technology, on the other hand, has reached a certain degree of maturity. Research efforts are currently devoted to further improvement of the performance and durability and to reduction of the cost, for example through the development of new membranes and electrocatalysts, which is expected to dramatically improve the viability and competitiveness of the technology.

Related Entries

▶ Conducting Polymers

References

1. Grubb WT, Niedrach LW (1960) Batteries with solid ion-exchange membrane electrolytes. J Electrochem Soc 107:131–135

P

2. Prater K (1990) The renaissance of the solid polymer fuel cell. J Power Sources 29:239–250

3. Mauritz KA, Moore RB (2004) State of understanding of Nafion. Chem Rev 104:4535–4585

4. Hickner MA (2012) Water-mediated transport in ion-containing polymers. J Polym Sci Part B Polym Phys 50:9–20

5. Wu L, Zhang Z, Ran J, Zhou D, Li C, Xu T (2013) Advances in proton-exchange membranes for fuel cells: an overview on proton conductive channels (PCCs). Phys Chem Chem Phys 15:4870–4887

6. Gubler L, Gursel SA, Scherer GG (2005) Radiation grafted membranes for polymer electrolyte fuel cells. Fuel Cells 5:317–335

7. Hickner MA, Ghassemi H, Kim YS, Einsla BR, McGrath JE (2004) Alternative polymer systems for proton exchange membranes (PEMs). Chem Rev 104:4587–4611

8. Zhang H, Shen PK (2012) Advances in the high performance polymer electrolyte membranes for fuel cells. Chem Soc Rev 41:2382–2394

9. Kreuer KD (2001) On the development of proton conducting polymer membranes for hydrogen and methanol fuel cells. J Membr Sci 185:29–39

10. Park CH, Lee CH, Guiver MD, Lee YM (2011) Sulfonated hydrocarbon membranes for medium-temperature and low-humidity proton exchange membrane fuel cells (PEMFCs). Prog Polym Sci 36:1443–1498

11. Ariza MJ, Jones DJ, Rozière J (2002) Role of post-sulfonation thermal treatment in conducting and thermal properties of sulfuric acid sulfonated poly(benzimidazole) membranes. Desalination 147:183–189

12. Jones DJ, Rozière J (2001) Recent advances in the functionalisation of polybenzimidazole and polyetherketone for fuel cell applications. J Membr Sci 185:41–58

13. Li Q, He RH, Jensen JO, Bjerrum NJ (2003) Approaches and recent development of polymer electrolyte membranes for fuel cells operating above 100 °C. Chem Mater 15:4896–4915

14. Li Q, Jensen JO, Savinell RF, Bjerrum NJ (2009) High temperature proton exchange membranes based on polybenzimidazoles for fuel cells. Prog Polym Sci 34:449–477

15. Kallitsis JK, Geormezi M, Neophytides SG (2009) Polymer electrolyte membranes for high-temperature fuel cells based on aromatic polyethers bearing pyridine units. Polym Int 58:1226–1233

16. Asensio JA, Sánchez EM, Gómez-Romero P (2010) Proton-conducting membranes based on benzimidazole polymers for high-temperature PEM fuel cells. A chemical quest. Chem Soc Rev 39:3210–3239

17. Mader J, Xiao L, Schmidt TJ, Benicewicz BC (2008) Polybenzimidazole/acid complexes as high-temperature membranes. In: Scherer G (ed) Advances in polymer science, vol 216. Springer, Berlin/Heidelberg, pp 63–124

18. Herring AM (2006) Inorganic-polymer composite membranes for proton exchange membrane fuel cells. Polym Rev 46:245–296

19. Hickner MA, Herring AM, Coughlin EB (2013) Anion exchange membranes: current status and moving forward. J Polym Sci Part B Polym Phys 51:1727–1735

20. Merle G, Wessling M, Nijmeijer K (2011) Anion exchange membranes for alkaline fuel cells: a review. J Membr Sci 377:1–35

21. Couture G, Alaaeddine A, Boschet F, Ameduri B (2011) Polymeric materials as anion-exchange membranes for alkaline fuel cells. Prog Polym Sci 36:1521–1557

22. Borup R, Meyers J, Pivovar B, Kim YS, Mukundan R, Garland N, Myers D, Wilson M, Garzon F, Wood D, Zelenay P, More K, Stroh K, Zawodzinski T, Boncella J, McGrath JE, Inaba M, Miyatake K, Hori M, Ota K, Ogumi Z, Miyata S, Nishikata A, Siroma Z, Uchimoto Y, Yasuda K, Kimijima KI, Iwashita N (2007) Scientific aspects of polymer electrolyte fuel cell durability and degradation. Chem Rev 107:3904–3951

Polymers for Nonlinear Optics

Larry R. Dalton
Departments of Chemistry and Electrical Engineering, University of Washington, Seattle, WA, USA

Synonyms

Hybrid nonlinear optics; Organic nonlinear optics

Definition

Nonlinear optics refers to the nonlinear optical response (nonlinear changes in the index of refraction or absorption) arising from the interaction of quasi-delocalized electrons with applied electric fields. Nonlinear optical polymers are macromolecular materials with extended π-electron segments.

Principles

The interaction of applied electric fields (both electric fields of frequencies from dc (0 Hz)

to terahertz (THz) applied through electrode structures and the electric field component of electromagnetic radiation including radiation at infrared and optical frequencies) can result in the perturbation of the charge distribution of materials, including the electron distribution of conjugated π-electron containing macromolecular materials. The effect of such interaction on both the (molecular) dipole moment ($\mu_i(E)$) and the macroscopic induced polarization ($P_i(E)$) can be represented by a power series expansion in terms of the applied electric fields [1–8]:

$$\mu_i(E) = \mu_i(0) + \alpha_{ij}E_j + \beta_{ijk}E_jE_k + \gamma_{ijkl}E_jE_kE_l + \dots$$

$$P_i(E) = P_i(0) + \chi^{(1)}_{ij}E_j + \chi^{(2)}_{ijk}E_jE_k + \chi^{(3)}_{ijkl}E_jE_kE_l +$$

where $\mu_i(0)$ is the dipole moment of the ith molecule in the absence of applied electric fields, α_{ij} is the molecular polarizability, β_{ijk} is the molecular first hyperpolarizability, γ_{ijkl} is the molecular second hyperpolarizability, $P_i(0)$ is the macroscopic polarization in the absence of applied electric fields, $\chi^{(1)}_{ij}$ is the linear optical susceptibility, $\chi^{(2)}_{ijk}$ is the second-order nonlinear optical susceptibility, $\chi^{(3)}_{ijkl}$ is the third-order nonlinear optical susceptibility, and the indices i, j, k, l denote various components of the associated vectors and tensors. Note that each of the applied electric fields can, in general, be of the same or different frequencies. For weak electromagnetic fields, the electronic response of the material will be linear and can be described by absorption (the imaginary component of $\chi^{(1)}$) and the index of refraction (the real component of $\chi^{(1)}$) of the material. The index of refraction is defined as the ratio of the speed of light in vacuo divided to the speed of light in the material. The real and imaginary components of the linear susceptibility are related by the Kramers-Kronig relationship. When stronger fields are applied, the higher-order (nonlinear) terms of the above equations can no longer be ignored, and both second-order (β and $\chi^{(2)}$) and third-order (γ and $\chi^{(3)}$) effects can be observed and exploited for a variety of technological applications. There are many subtleties to the definition and discussion of nonlinear optical effects, and the reader is referred elsewhere for more detailed insight into nomenclature and computational conventions [1–9]. With this caveat, it can be noted that the second-order term in the above power series expansion can give rise to the linear electro-optic (EO or Pockels) effect, second harmonic generation (SHG) or frequency doubling, difference frequency generation (DFG), sum-frequency generation (SFG), optical rectification (OR), and optical parametric generation and oscillation (OPG and OPO). In like manner, the third-order term can give rise to the optical Kerr effect (OKE), degenerate four-wave mixing (DFWM) where the input and output frequencies are the same, third harmonic generation (THG) or frequency tripling, four-wave mixing (FWM) where the input and output frequencies are different, sum-frequency generation (SFG), and the quadratic electro-optic (QEO) effect. As with linear susceptibility, real (voltage-dependent index of refraction changes) and imaginary (nonlinear absorption) components exist for the second- and third-order nonlinear susceptibilities.

Technological Applications

Applications of second-order optical nonlinearity normally exploit the real component, while both real and imaginary components of third-order nonlinear optical activity are exploited. For example, the real component of $\chi^{(3)}$ is used for switching or modulation of an optical beam by application of a second intense (control) optical beam (the optical Kerr effect), while the imaginary component of $\chi^{(3)}$ is used for sensor protection exploiting reverse saturable absorption. Technological interest in π-electron organic macromolecular materials derives from several of their properties. First of all, conjugated π-electrons exhibit intrinsic femtosecond timescale response to time-varying electrical fields resulting in the potential for device bandwidths as high as tens of terahertz (THz).

Second, macromolecular organic nonlinear optical materials are amenable to a wide range of processing options including spin casting of thin films, vapor deposition of thin films, control of chromophore order (including acentric order) by electric field (including laser-assisted electric field) poling, sequential-synthesis/self-assembly of thin films, reactive ion etching, e-beam etching, laser lithography, and soft lithography techniques [6, 8, 10]. Conformal and flexible devices can be fabricated by lift-off techniques [11]. Organic macromolecular materials are also compatible with integration for a wide range of materials including metals, metal oxides, semiconductors, and a variety of other macromolecular materials. The relatively low dielectric constants of organic materials can be advantageous for sensor applications (e.g., detection of electromagnetic fields or phenomena that influence the index of refraction). A final substantial advantage of organic nonlinear optical materials is the potential for very large optical nonlinearities by design of the molecular components. Such design can also be used to control processability, optical loss, dielectric permittivity, thermal stability, and photostability [6, 7, 12].

Second-Order Nonlinear Optical Materials

The realization of nonzero second-order optical nonlinearity requires noncentrosymmetric symmetry at both the molecular and macroscopic material levels. Thus, many active second-order nonlinear optical materials are prepared from dipolar chromophores by incorporating the chromophores into macromolecular (dendrimer, polymer) matrices and electric field poling such materials near their glass transition temperature. Second-order nonlinear optical chromophores commonly consist of an electron-rich donor connected to an electron-deficient acceptor through a π-electron bridge. Figure 1 illustrates a chromophore based on common features including an amine donor, an isophorone (cyclohexylene)-protected polyene bridge, and a tricyanovinylfuran acceptor. Although many other donors, acceptors, and bridges have been explored, chromophores such as shown in Fig. 1 yield among the highest reported molecular first hyperpolarizabilities leading ultimately to material electro-optic activity 3–15 times higher than
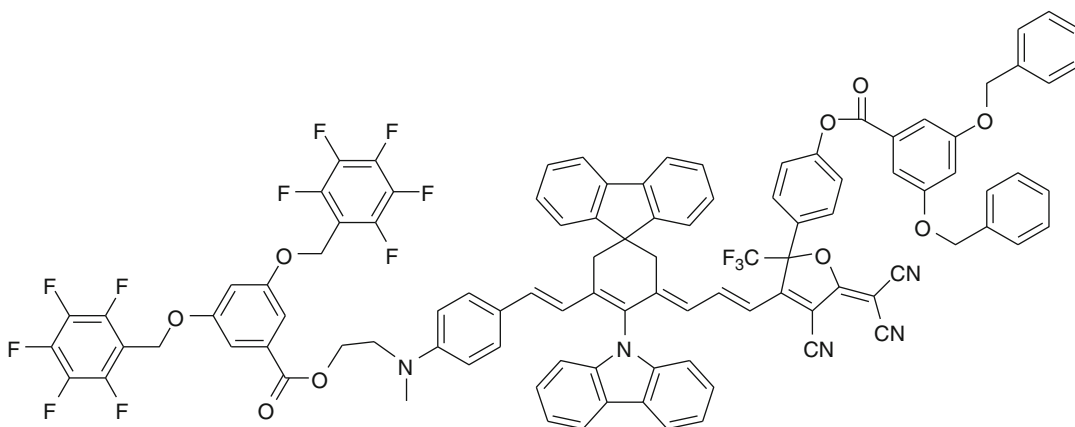
Polymers for Nonlinear Optics, Fig. 1 A representative second-order nonlinear optical chromophore is shown illustrating a core, which consists of an amine donor and tricyanovinylfuran (TCF-CF$_3$) acceptor connected by an isophorone-protected polyene bridge. Arene/perfluoroarene (quadrupolar interaction moieties – shown) or coumarin (dipolar interaction moieties – not shown) can be added to control

chromophore organization [6, 7] and processability [13]. The 2,5-positions of the cyclohexene (isophorone)-protected bridge can be modified to control chromophore association and organization preventing excitonic interactions and enhancing poling efficiency. The ends and waists of chromophores can be further modified for incorporation of chromophores into polymers and dendrimers and to incorporate moieties that permit cross-linking [12]

that of lithium niobate. Nonlinear optical behavior can be viewed as an applied electric field changing the mixing of neutral (as shown) and charge separated or zwitterionic (where the donor gives up an electron to the acceptor) limiting electronic structures in the ground state of the chromophore. Chromophores such as those illustrated in Fig. 1, where the neutral form dominates the ground state, are referred to as neutral ground state (NGS) chromophores, and a positive β value is observed for such chromophores. Chromophores where the charge-separated (zwitterionic, ZGS) form dominates the ground state are characterized by negative β values. The basic (core) chromophore structure of Fig. 1 can be modified with moieties that give rise to intermolecular dipolar and quadrupolar interactions that enhance poling efficiency and poling-induced electrooptic activity [6, 7]. Modification of the fundamental chromophore structure can also be used to inhibit unwanted excitonic interactions and the optical loss associated with such interactions. Modifications can also be used to introduce moieties permitting cross-linking (lattice hardening) by Diels-Alder chemistry [12].

Third-Order Nonlinear Optical Materials

Third-order nonlinear optical materials do not require noncentrosymmetric order but are also composed of chromophores containing donor, acceptor, and π-electron bridge regions. The symmetry is now quadrupolar rather than dipolar, e.g., donor-bridge-donor, acceptor-bridge-acceptor, donor-bridge-acceptor-bridge-donor, or acceptor-bridge-donor-bridge-acceptor. Third-order chromophores are often charged so that a counterion is required [14]. Third-order chromophores based on polyene bridges frequently yield negative γ values. Such chromophores can also yield real to imaginary γ ratios that are greater than 1, which are important for optical switching and control applications. Modifications of the third-order chromophores, including the 2,5-positions of the isophorone-protected polyene structure, can also be employed to control chromophore association and cross-linking.

Devices and Device Performance

One of the most common devices utilizing nonlinear optical materials is the Mach-Zehnder interferometer, which consists of Y branches at the input and output that split optical transmission in a waveguide into two arms at the input of the device and then recombine that transmission into a single arm at the output. An applied electric field is used to change the charge distribution (index of refraction) of the waveguide material in one arm of the Mach-Zehnder interferometer, and this, in turn, changes the interference of the two optical beams at the output of the device. This device is used to transduce electrical signals onto an optical transmission (using second-order materials) or to control and encode an optical beam with a signal carried on a second high-power optical beam (using third-order materials). The control signal is thus transduced onto the output as an amplitude modulation. The voltage required to produce full-wave modulation (a $180°$ phase shift in one arm) for Mach-Zehnder waveguides utilizing second-order nonlinear optical materials is

$$V_\pi = \lambda h / \left(n^3 r_{33} L \Gamma\right)$$

where λ is the optical wavelength, h is the separation of drive electrodes, n is the index of refraction, r_{33} is the principal element of the material electro-optic tensor, L is the length of the electrode (optical/electric field interaction length), and Γ is the optical/electric field modal overlap integral. For electrically poled polymer nonlinear optical materials, $r_{33} = N\beta_{zzz}(\varepsilon, \omega) < \cos^3\theta > g(\varepsilon, n)$ where N is the chromophore number density, $\beta_{zzz}(\varepsilon, \omega)$ is the principal element of the molecular first hyperpolarizability tensor, $<\cos^3\theta>$ is the acentric order parameter, and g (ε, n) is the modified Lorentz-Onsager factor. The parameters ε, ω, and n are, respectively, the dielectric permittivity, optical frequency, and index of refraction. Improvement of r_{33} permits shorter device lengths (L), which is important for high-density integration of electronics and photonics. Shorter device lengths also reduce optical

P

propagation loss and ultimately total optical insertion loss. In turn, r_{33} can be improved by improving N, $\beta_{zzz}(\varepsilon, \omega)$, and/or $<\cos^3\theta>$. Throughout the 1990s and to 2004, all-organic (organic cladding, organic nonlinear optical core, organic cladding) waveguide Mach-Zehnder devices were fabricated. Since 2004 most device research has focused on silicon-organic hybrid (SOH) devices fabricated by integrating organic electro-optic materials with silicon photonic (including slotted) waveguides [14–16]. Such devices benefit from the concentration of electromagnetic (optical) fields associated with the high index of refraction of silicon. For some second-order nonlinear optical applications (e.g., electro-optic modulators), waveguide devices as small as 1 mm in length have been driven by 0.5 V (180° phase shift with application of 0.5 V). For electronic digital signal transduction onto optical transmissions, SOH devices permit information processing with energy efficiency as low as 0.6 femtojoule (fJ)/bit. Modulation bandwidths in excess of 100 GHz and 100 Gbit/s have been demonstrated for analog and digital signals using second-order organic nonlinear optical materials [15]. Another application of second-order optical nonlinearity that has received considerable attention is terahertz (THz) generation and detection for THz imaging and spectroscopy. Bandwidths to 30 THz have been demonstrated. For third-order nonlinear optical materials, a 4 mm long silicon-organic hybrid (SOH) device yielded a nonlinearity coefficient of 10^{-5} W^{-1} km^{-1} and all-optical information processing (demultiplexing) at 170 Gbit/s [16]. Modulation bandwidths to tens of THz have been demonstrated. Second-order organic nonlinear optical materials have been used to fabricate Mach-Zehnder modulators, phase modulators, directional couplers, spatial light modulators, A/D converters, optical gyroscopes, high bandwidth/high stability oscillators, acoustic spectrum analyzers, reconfigurable optical add/drop multiplexers (ROADMs), phased array radar, and a variety of sensors as well as THz devices noted above. Third-order materials have largely been used to fabricate devices for sensor protection and optical modulation.

Commercialization

The commercialization of second-order nonlinear optical materials is relatively immature; however, companies such as GigOptix/Lumera, Omega Optics, Lightwave Logic, Soluxra, and Rainbow Photonics continue to pursue some research and development and commercialization. Research and development efforts exist at a number of larger corporations including Boeing and Intel. Lockheed-Martin has a long tradition of research involving organic electro-optics. Research is increasingly focused on SOH technology. Commercial electro-optics continues to be dominated by devices based on lithium niobate, although there is increasing interest in silicon modulators. There do not appear to be any current efforts to commercialize third-order organic nonlinear optical materials.

Related Entries

▶ Electroresponsive Polymer
▶ Low-Bandgap Polymers
▶ Molecular Self-Organization
▶ Nano-/Microfabrication
▶ Optical Absorption of Polymers
▶ Photonic Crystal
▶ Refractive Index
▶ Supramolecular Polymers (Coordination Bonds)

References

1. Ostroverkhova O (2013) Handbook of organic materials for optical and (opto)electronic devices: properties and applications. Woodhead, Cambridge, UK
2. Nalwa HS, Miyata S (1996) Nonlinear optics of organic molecules and polymers. CRC Press, Boca Raton
3. Dalton LR (2002) Nonlinear optical polymeric materials: from chromophore design to commercial applications. Adv Polym Sci 158:1–86
4. Herman W, Foulger S (2010) Organic thin films for photonics applications. ACS Symposium Series, Washington, DC
5. Sun SS, Dalton LR (2008) Introduction in organic opto-electronic materials. CRC Press, Boca Raton

6. Dalton LR, Sullivan PA, Bale BH (2010) Electric field poled organic electro-optic materials: state of the art and future prospects. Chem Rev 110:25–55. doi:10.1021/cr9000428

7. Dalton LR, Benight SJ, Johnson LE, Knorr DB Jr, Kosilkin I, Eichinger BE, Robinson BH, Jen A, Overney R (2011) Systematic nano-engineering of soft matter organic electro-optic materials. Chem Mater 23:430–445. doi:10.1021/cm102166

8. Chen A, Murphy E (2011) Broadband optical modulators: science, technology, and applications. Taylor & Francis, New York

9. Leuthoid J, Freude W, Brosi JM, Baets R, Dumon P, Biaggio I, Scimeca ML, Diederich F, Frank B, Koos C (2009) Silicon organic hybrid technology – a platform for practical nonlinear optics. Proc IEEE 97:1304–1316. doi:10.1109/JPROC.2009.2016849

10. Huang Y, Paloczi GT, Yariv A, Zhang C, Dalton LR (2004) Fabrication and replication of polymer integrated optical devices using electron-beam lithography and soft lithography. J Phys Chem B 108:8606–8613. doi10.1021/jp049724d

11. Song HC, Oh MC, Ahn SW, Steier WH, Fetterman HR, Zhang C (2003) Flexible low-voltage electro-optic polymer modulators. Appl Phys Lett 82:4432–4435. doi:10.1063/1.1586474

12. Shi Z, Luo J, Huang S, Polishak BM, Zhou XH, Liff S, Younkin TR, Block BA, Jen AKY (2011) Tuning the kinetics and energetics of Diels-Alder cycloaddition reactions to improve poling efficiency and thermal stability of high-temperature cross-linked electro-optic polymers. J Mater Chem 22:951–959. doi:10.1039/c1jm14254b

13. Knorr DB Jr, Benight SJ, Krajina B, Zhang C, Dalton LR, Overney RM (2012) Nanoscale phase analysis of molecular cooperativity and thermal transitions in dendritic nonlinear optical glasses. J Phys Chem B 116:13793–13805

14. Li Z, Liu Y, Kim H, Hales JM, Jang SH, Luo J, Baehr-Jones T, Hochberg M, Marder SR, Perry JW, Jen AKY (2012) High-optical-quality blends of anionic polymethine salts and polycarbonate with enhanced third-order non-linearities for silicon-organic hybrid devices. Adv Mater 24:OP326–OP340. doi:10.1002/adma.201202325

15. Korn D, Palmer R, Yu H, Schindler PC, Alloatti L, Baier M, Schmogrow R, Bogaerts W, Selvaraja SK, Lepage G, Pantouvaki M, Wouters JMD, Verheyen P, Van Campenhout J, Chen B, Baets R, Absil P, Dinu R, Koos C, Freude W, Leuthold J (2013) Silicon-organic hybrid (SOH) IQ modulator using the linear electro-optic effect for transmitting 16QAM at 112 Gbit/s. Opt Express 21:13219–13227. doi:10.1364/OE.21.013219

16. Koos C, Vorreau P, Vallaitis T, Dumon P, Bogaerts W, Baets R, Essembeson B, Biagglo I, Michinobu T, Diederich F, Freude W, Leuthold J (2009) All-optical high-speed signal processing with silicon-organic hybrid slot waveguides. Nat Photonics 3:216–219. doi:10.1038/nphoton.2009.25

Polymers for Organic Spintronics

Dali Sun and Z. Valy Vardeny
Department of Physics and Astronomy,
University of Utah, Salt Lake City, UT, USA

Synonyms

Organic spin valves; Spin pumping

Definitions

Polymers used in the field of *spintronics*, which include injection, control, manipulation, and detection of spin-polarized electrons.

Introduction

Organic materials are promising for spintronics applications mainly because of the expected long spin relaxation time of spin-polarized electrons [1]. Also the organic material flexibility, low cost production, and unlimited versatility of chemical synthesis make organic spintronics a promising alternative to conventional inorganic spintronics. Spin-polarized transport characterized by giant magnetoresistance (GMR) was first demonstrated in fabricated organic spin valves in 2004 [2], with potential spintronics applications in magnetic random access memory. This achievement has triggered plentiful of additional experiments using various organic spintronics devices, with the aim to demonstrate spin-aligned electron injection from metallic ferromagnet (FM) electrodes into organic semiconductors and control of electroluminescence intensity by external magnetic field [3]. *This entry reviews the state-of-the-art organic spintronics devices.*

The GMR concept may be readily demonstrated by analyzing one of the generic spintronics devices, namely, the organic spin valve (OSV) [2] (Fig. 1). The OSV device consists of a nonmagnetic spacer sandwiched between two FM materials

P
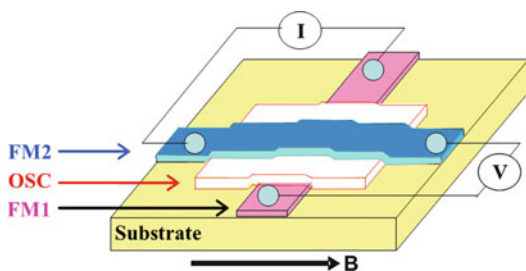
Polymers for Organic Spintronics, Fig. 1 The OSV architecture. FM1 and FM2 are ferromagnetic electrodes with different coercive fields. OSC is the organic semiconductor interlayer

(FM1 and FM2) [4, 5]. A charge electron or hole (carrier) injected from FM1 with the spin sense aligned parallel to the magnetization direction of FM2 experiences low resistance; this is the "parallel" alignment. In contrast, for the "antiparallel" configuration, where the injected carrier spin sense is aligned opposite to the FM2 magnetization direction, it experiences high resistance. The switch from low resistance to high resistance (and vice versa) is induced by sweeping an external magnetic field, B upward (and downward), and led to the original name of this device (Fig. 2a). In OSV devices the nonmagnetic spacer is a pristine organic semiconductor that may be a polymer; see Fig. 1 for the device operation.

The organic spacer in the OSV devices ought to preserve the spin polarization of the injected carrier for long distances, and thus the carrier's spin relaxation time should be long. Organic semiconductors are composed of light elements that have weak spin-orbit interaction; consequently they possess relatively long spin relaxation times [1]. Indeed, GMR has been measured in OSV devices based on small molecule and polymer spacers, both as thick films and thin tunnel junctions [2, 3, 5]. For example, by inserting a buffer layer of cobalt nanodots between the top FM electrode and organic spacer, 300 % GMR was observed in Alq$_3$-based OSV devices [6]. Although the hyperfine interaction (HFI) has been thought to play an important role in organic magnetotransport, only recently its important role in spintronics was demonstrated

by more direct experimental evidence [7]. For example, if the HFI constant, a, determines the spin-lattice relaxation time, T_{SL}, of the injected carriers, and consequently also their spin diffusion length in OSV devices, then the device performance may be enhanced simply by manipulating the nuclear spins of the organic spacer atoms. Moreover, the HFI may also play an important role in other organic magneto-electronic devices such as two-terminal devices and other spin response processes such as optically detected magnetic resonance in organic semiconductor films [7].

"Isotope Exchange" for Improving Organic Spin-Related Organic Devices

The role of the HFI in various organic spin-related or magneto-electronic devices and films was clearly demonstrated by replacing all strongly coupled hydrogen atoms (^{1}H, nuclear spin I = ½) in the organic π-conjugated polymer poly(dioctyloxy) phenyl vinylene (DOO-PPV) spacer (dubbed here H-polymer), with deuterium atoms (^{2}H, I = 1) (hereafter D-polymer) having much smaller a, namely, $a(D) = a(H)/6.5$ [7]; this replacement is known as isotope exchange. The injected spin-aligned carriers in magneto-electronic devices need to preserve their spin sense upon reaching the opposite electrode [5]. Since the charge (and spin) transport occurs in polymers mainly by diffusion [8], it is clear that the spin diffusion length, λ_S, would determine the device performance. Therefore, to improve the spin-related device "figure of merit," there is the need to optimize λ_S in the organic material interlayer. In reality λ_S is determined by the carrier diffusion constant, D and $T_{SL,}$ where $\lambda_S = (DT_{SL})^{1/2}$, and therefore longer T_{SL} leads to larger λ_S. This was in fact verified by the isotope exchange of DOO-PPV polymers [7].

The H- and D-polymer films were sandwiched between two FM electrodes with different coercive fields, B_c. These were LSMO and Co thin films, with low-temperature coercive fields $B_{c1} \approx$ 4 mT and $B_{c2} \approx 10$ mT, respectively, and nominal
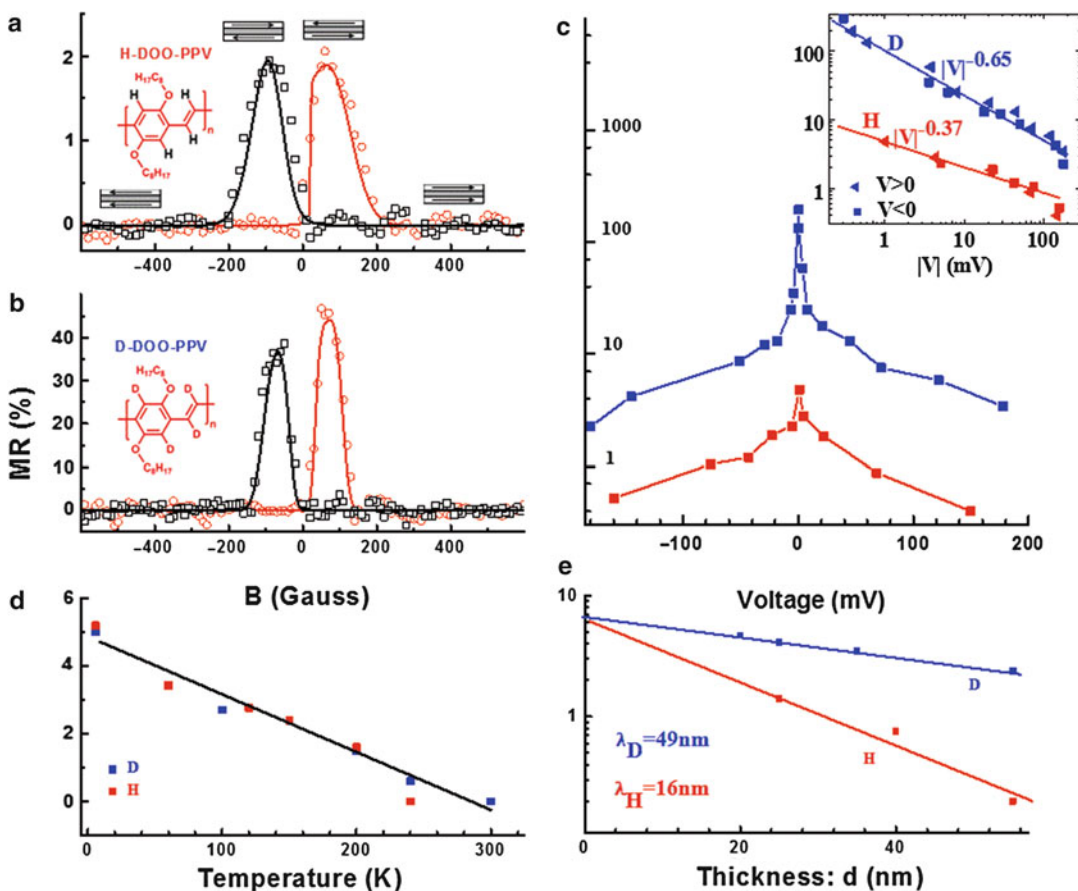
Polymers for Organic Spintronics, Fig. 2 *Isotope dependence of magnetoresistance (MR) in organic spin valves based on DOO-PPV polymers.* (**a**, **b**) MR loop of LSMO (200 nm)/DOO-PPV (25 nm)/Co (15 nm) spin-valve device measured at $T = 10$ K and $V = 10$ mV, based on (**a**) H- and (**b**) D-polymers. The polymer repeat units are shown in the corresponding *insets* in the panels. The *black* (*red*) curve denotes MR measurements made while decreasing (increasing) B. The nominal resistance is ~200 and ~170 kΩ, respectively, for the H- and D-polymer OSVs. The antiparallel (*AP*) and parallel (*P*) configurations of the FM magnetization orientations are shown in the *insets* at low and high B, respectively. The lines through the data points are simulations [7]. (**c**) The

maximum MR value (MR_{SV}) of OSV devices fabricated in a similar way to those shown in (**a**) and (**b**) (with $d = 35 \pm 5$ nm), as a function of the applied bias voltage, V, measured at $T = 10$ K; note the logarithmic y-scale. *Inset*: The same data plotted on a log-log scale showing the isotope-dependent power law behavior. (**d**) Normalized MR_{SV} of OSVs similar to those shown in (**a**–**c**) as a function of temperature, measured at $V = 80$ mV. (**e**) MR_{SV} of D- and H-polymer OSVs (similar to those shown in (**a**–**d**) of various experimentally determined thicknesses, d measured at $T = 10$ K and $V = 80$ mV). The lines are fits, where $MR_{SV}(d) = 6.7$ % $\exp(-d/\lambda_s)$, with spin diffusion lengths, $\lambda_s(D) = 49$ nm and $\lambda_s(H) = 16$ nm (Based on Ref. [7])

(literature) "spin injection polarization degree" $P_1 \approx 95$ % and P_2 of ~35 %. Since $B_{c1} \neq B_{c2}$, then it was possible [7] to switch the relative magnetization directions of the FM electrodes from parallel (P) to antiparallel (AP) alignment (and vice versa), upon sweeping the external magnetic field, B (Fig. 2a, b), where the device

resistance, R, is dependent on the relative magnetization orientations. When $R(AP) > R(P)$, the maximum MR value, $[\Delta R/R]_{max}$ (or MR_{SV}), is given by the ratio $[R(AP)–R(P)]/R(P)$ in %. According to a modified Jullière formula [9], MR_{SV} depends on the spin polarization of the FM electrodes P_1 and P_2 by the relation

P

$$\frac{\Delta R}{R}\Big|_{\max} = \frac{2P_1 P_2 \exp(-d/\lambda_S)}{1 - P_1 P_2 \exp(-d/\lambda_S)} \qquad (1)$$

In Eq. 1 d is the organic interlayer thickness. The MR(B) response in OSV was measured to register the MR_{SV} value in OSVs based on the two polymers at various bias voltages, V (Fig. 2d), and temperatures, T (Fig. 2e), using the same LSMO substrate [7]; this was possible since the LSMO substrate is relatively stable in air, and its spin injection properties were found to be robust.

Figure 2a, b shows representative MR(B) responses for two similar OSV devices ($d \sim 25$ nm) based on H- and D-polymers at $T = 10$ K and $V = 10$ mV [7]. As is clearly seen, the devices based on the D-polymer have *much larger* MR_{SV} values than those based on the H-polymer. This holds true for similar devices at all V, T, and d (Fig. 2c–e). The improved magnetic properties of OSVs based on the D-polymer may be explained using Eq. 1 by a larger λ_S. Indeed, the major difference between the injected spin ½ carriers in D- and H-polymers is their spin relaxation time, T_{SL}, which was shown to be much longer in the D-polymer using optically detected magnetic resonance experiments [7]. Fig. 2e shows the MR(B) response of OSV devices having various d but otherwise the same LSMO substrate, which were measured at the same temperature and bias voltage. From the exponential $MR_{max}(d)$ dependence, λ_S could be extracted. The obtained spin diffusion length values were $\lambda_S(D) = 49$ nm, whereas $\lambda_S(H) = 16$ nm [7], in excellent agreement with the increase in T_{SL} measured using optically detected magnetic resonance performed on the two polymers. Based on these results, it was concluded that the improved spin transport in the organic layer is the main advantage of the D-polymers to form more efficient OSVs. Thus, the use of *deuterated* organic semiconductors as the device interlayer, both as evaporated small molecules and spin-cast polymers, should substantially improve the OSV device figure of merit.

Spin OLEDs

Using D-DOOPPV as the organic spacer material in order to increase the spin diffusion length and LiF-covered Co film as the cathode in order to reduce the voltage needed for bipolar injection, a spin-OLED device was fabricated which showed ~1 % hysteretic MEL(B) response at low temperatures [10]. The operation of the spin OLED is determined not only by spin injection into and diffusion through the active organic interlayer but also by the dependence of the electroluminescence (EL) emission intensity on the electron and hole spin polarization. The EL emitted from the spin OLED, similar to that of an ordinary polymer-based OLED, results from the recombination of singlet excitons [11]. In turn, singlet excitons are generated from the injected spin ½ electrons and holes that are paired in a spin singlet configuration [10]. Therefore, the singlet exciton density, and consequently also the EL emission intensity, depends on the spin polarization of the injected carriers, resulting in magneto-EL (MEL) spin-valve effect. Furthermore, in some OLEDs where both EL emission and longer wavelength electro-phosphorescence emissions are substantial, the spin-OLED device might be used to modulate the device emission color.

One of the major obstacles in realizing a spin-OLED device is the bias voltage needed to generate EL emission [10]. Typical OSV response is limited to low bias voltage (<1 V), whereas for efficient EL emission much higher bias voltage is required (>10 V for Alq$_3$ based OSV) [2]. In fact, this is one of the main reasons why spin-OLED devices could not be realized until 2012, when Co/LiF FM electrode was used to reduce the bias voltage needed for "double injection" [10].

The structure of the successful spin-OLED device was in the form of *LSMO/D-DOOPPV (d)/LiF(d')/Co/Al*. The turn-on voltage V_o for substantial EL in the fabricated devices was $V_o \sim 3.5$ V, compared to $V_o \sim 10$ V on the same organic interlayer but without the LiF

layer. With this spin-OLED configuration, a maximum of 1 % change in MEL was obtained at low temperature [10]. This shows that deuterated polymers may serve as the active interlayer in spin OLEDs and other spin-related magneto-electronic devices, so the "isotope exchange" H with D is important for organic spintronics [12].

References

1. Naber WJM, Faez S, van der Wiel WG (2007) Organic spintronics. J Phys D Appl Phys 40:R205–R228
2. Xiong ZH, Wu D, Vardeny ZV, Shi J (2004) Giant magnetoresistance in organic spin-valves. Nature 427:821–824
3. Vardeny ZV (2010), Organic Spintronics, 1st ed, CRC Press, Boca Raton
4. Fert A (2008) Nobel lecture: origin, development, and future of spintronics. Rev Mod Phys 80:1517–1530
5. Dediu VA, Hueso LE, Bergenti I, Taliani C (2009) Spin routes in organic semiconductors. Nat Mater 8:707–716
6. Sun D, Yin L, Sun C, Guo H, Gai Z, Zhang X–G, Ward TZ, Cheng ZH, Shen J (2010) Giant magneto-resistance in organic spin-valves. Phys Rev Lett 104:236602
7. Nguyen TD, Hukic-Markosian G, Wang F, Wojcik L, Li XG, Ehrenfreund E, Vardeny ZV (2010) Isotope effect in spin response of π-conjugated polymer films and devices. Nat Mater 9:345–352
8. Horovitz G (2007) Organic thin film transistors. Semiconducting Polymers, Hadziioannou G, Malliaras GG (eds), Wiley, Weinheim, pp 531–567
9. Julliere M (1975) Tunneling between ferromagnetic films. Phys Lett A 54:225–226
10. Nguyen TD, Ehrenfreund E, Vardeny ZV (2012) Spin-polarized organic light emitting diode based on a novel bipolar spin-valve. Science 337:204–207
11. Malliaras GG, Friend RH (2005) An organic electronics primer. Phys Today 58:53. doi:10.1063/1.1995748
12. Nguyen TD, Basel TP, Pu Y-J, Li X-G, Ehrenfreund E, Vardeny ZV (2012) Isotope effect in the spin response of aluminum tris(8-hydroxyquinoline) based devices. Phys Rev B 85:245437

Polymers for Solar Cells

Luyao Lu and Luping Yu
Department of Chemistry and The James Franck Institute, The University of Chicago, Chicago, IL, USA

Synonyms

Acceptor; Bulk heterojunction; Conjugated polymers; Donor; Energy conversion; Low-bandgap polymers; Organic photovoltaics; Polymer solar cells

Definition

$$PCE = \frac{V_{oc} \times J_{sc} \times FF}{P_{in}},$$

where PCE is power conversion efficiency, V_{oc} is open circuit voltage, J_{sc} is short circuit current density, FF is fill factor, and P_{in} is input power (Fig. 1a).

Introduction

The total amount of solar radiation absorbed by the Earth is around 120,000 terawatts (TW) per year, which is 9,000 times more energy than the worldwide consumption in 1 year (13 TW) [1]. Thus it has been widely recognized that solar energy is the key to solving future energy crisis. Several approaches have been developed to utilize solar energy, such as solar fuels, solar thermal energy, and solar cells. Among those, solar cell is the most mature technology which converts solar energy directly into electricity. However, commercially available solar cells composed of crystalline silicon are not cost-effective and limit the application of this technology. To reduce the cost, extensive research efforts have been focused on developing

P

a

$$PCE = \frac{V_{oc} \times J_{sc} \times FF}{P_{in}}$$

$$FF = \frac{J_m \times V_m}{J_{sc} \times V_{oc}}$$

b
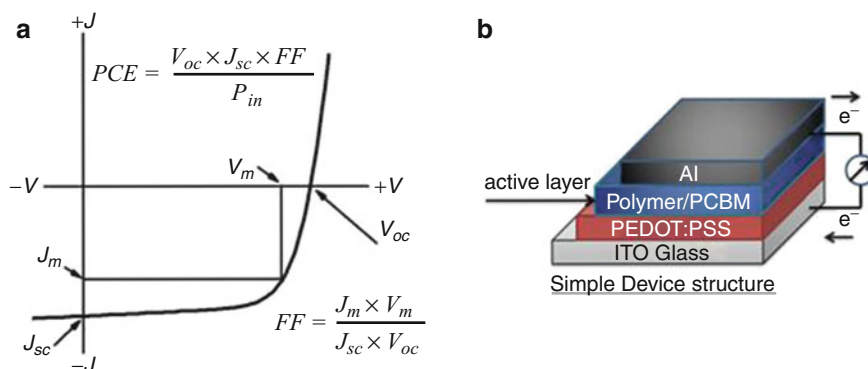
Polymers for Solar Cells, Fig. 1 (**a**) Typical current–voltage characteristics in a solar cell with illustration of important parameters: PCE is power conversion efficiency, V_{oc} is open circuit voltage, J_{sc} is short circuit current density, FF is fill factor, P_{in} is input power, V_m and J_m are the voltage and current at maximum power point. (**b**) Structure of polymer–fullerene BHJ solar cell

semiconducting organic polymer materials for solar cell application in the last decade [2, 3]. Organic solar cells exhibit the potential advantages in preparing lightweight, flexible devices through roll to roll solution process at a low cost. The state-of-the-art organic bulk heterojunction (BHJ) polymer solar cells composed of polymer donor and fullerene acceptor have recently reached power conversion efficiency (Fig. 1a) over 9 % in a single-junction structure [4] and over 10 % in tandem cells [5]. This entry discusses the development of the state-of-the-art polymers used for highly efficient organic solar cells.

Mechanism of Photovoltaic Effect in OPV Solar Cells and Required Design Rules for Polymer Solar Cells

The typical device structure of a polymer–fullerene solar cell is illustrated in Fig. 1b. ITO is transparent indium tin oxide and serves as anode; PEDOT:PSS is poly (3,4-ethylenedioxythiophene)-polystyrene sulfonate and works as anode buffer layer. Al is metal cathode. There are inverted solar cells with different architecture of devices. For example, MoO_3 could serve as anode buffer layer, and gold or silver works as anode, while TiO_2 plays the role of cathode buffer layer with ITO being the cathode in inverted solar cells [6]. The simplified

operation mechanism of the state-of-the-art polymer BHJ organic solar cells is shown in Fig. 2, which contains several steps. First of all, photogenerated excitons are formed after light absorption in the active layer materials; the excitons could then diffuse to the interface of donor and acceptor where charge-transfer takes place and results in the formation of a charge-transfer complex, driven by the offset of LUMO (lowest unoccupied molecular orbital) energy levels between donor and acceptor. Finally, the separated holes and electrons will be further dissociated thermally and move towards two electrodes and be collected.

In order to achieve a high power conversion efficient (PCE), each step mentioned above needs to be highly efficient and the whole process optimized synergistically. Current research efforts have identified that fullerene derivatives, such as [6,6]-phenyl-C61-butyric acid methyl ester ($PC_{60}BM$) or [6,6]-phenyl-C71-butyric acid methyl ester ($PC_{70}BM$), are very effective as electron acceptors in most of the polymer solar cells to date. The key bottleneck of materials is the organic or polymeric semiconductors as donor materials. After extensive research activities in the past years, the following design rules for the development of promising donor polymer materials can be extracted [7]:

1. Donor materials should exhibit high efficiency in light harvest and absorb most of the solar
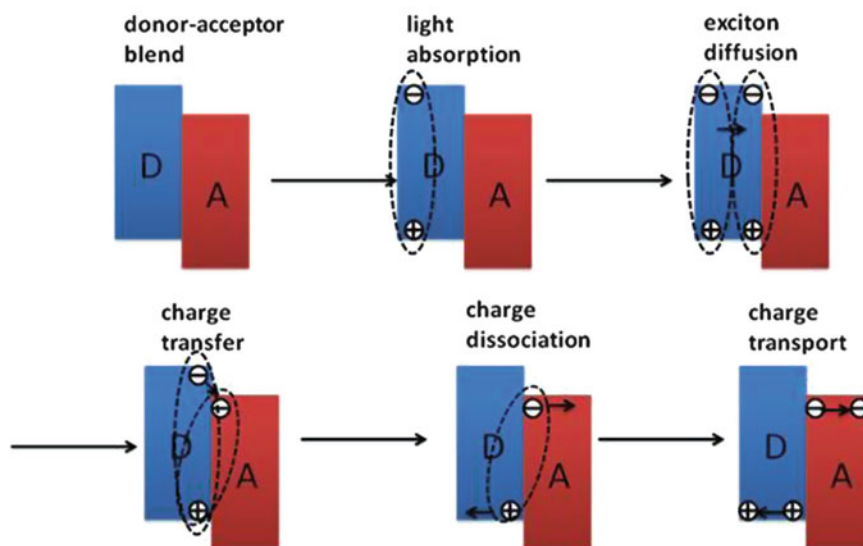
Polymers for Solar Cells, Fig. 2 Simplified operating mechanism of polymer (D)–fullerene (A) solar cells

energy in solar spectrum. The maximum density of solar photon flux is around 700 nm. The absorption of the donor materials must cover this region. Thus, it is crucial to develop low-bandgap polymers with high absorption coefficient in the red to near-infrared region for increased J_{sc}.

2. The LUMO energy level offset between donor and acceptor needs to be sufficient for exciton dissociation, and the minimum value is generally around 0.3–0.6 eV.

3. The V_{oc} of the device is known to be correlated to the difference between HOMO (highest occupied molecular orbital) energy level of the donor and LUMO energy level of the acceptor. Since PCE is proportional to the product of V_{oc} and J_{sc}, it is important to attain a balance between pursing a narrow bandgap donor for improved J_{sc} and a deep-lying HOMO energy level for improved V_{oc} while keeping enough driving force for charge dissociation.

4. The donor materials should exhibit high hole mobility (10^{-4} cm^2/Vs or higher) to facilitate hole transport in the active layer and reduce charge recombination after charge dissociation.

5. The donor polymers should exhibit good solubility in organic solvents like chlorobenzene and dichlorobenzene for solution processing. Good miscibility with PCBM is also required to form an interpenetrating nanoscale morphology in the BHJ active layer for efficient charge separation and transport.

Low-Bandgap Polymers for Polymer Solar Cells

Poly(3-Hexylthiophene) (P3HT)

P3HT is one of the most widely studied polymer materials for organic solar cells in the past several years. The molecular structure of P3HT and PCBM is shown in Fig. 3. The state-of-the-art PCEs of P3HT-based solar cells have reached 5 % in a single-junction cell with PCBM [8]. The PCE values of OPV solar cell based on P3HT can be further improved by using different fullerene derivatives [9]. Several key parameters which have large influences on the performance of P3HT-based solar cells such as regioregularity, molecular weight, and film morphology are discussed below.
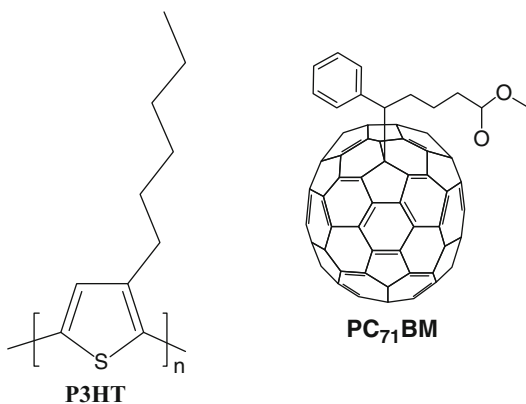
Polymers for Solar Cells, Fig. 3 Chemical structures of P3HT and PCBM

Regioregularity (RR) of P3HT is defined as the percentage of the monomers that adopt head to tail configuration. Increase in regioregularity of P3HT leads to threefold effects for pristine P3HT film: (1) redshift of the absorption of the film, (2) increase in solid-state absorption coefficient, and (3) enhanced crystallinity and facilitated charge transport. However, P3HT with RR values at 91 % could exhibit similar or even better PCE than those with RR values at 96 % [10]. Thus, maximizing RR values could not definitely lead to best performance for P3HT solar cells when PCBM is present simultaneously.

The molecular weight of P3HT also affects the absorption and transport properties significantly. It has been reported that P3HT with a molecular weight less than 10 kDa is unable to harvest photons and transport charges effectively [11]. Molecular weight strongly influences the molecular packing of P3HT backbone. High molecular weight results in high hole mobility and thus high photovoltaic performance to a certain point. Further increasing the molecular weight could cause distortion of the backbone due to tangled side chains and result in decreased charge transport and inferior PCEs.

The ideal morphology of BHJ solar cells is recognized as a bicontinuous interpenetrating network formed between donor and acceptor. To ensure a maximum interface area for exciton dissociation and charge transport, the domain sizes of both components should be around

10–20 nm, which is twice the exciton diffusion length (5–10 nm). Several methods have been used to control the morphology of P3HT:PCBM films, such as thermal annealing, solvent annealing, and the use of small amount of additives. These methods could be applied to other polymer:PCBM system as well.

Before thermal annealing, P3HT:PCBM active layer usually consists of different phases, both amorphous and semicrystalline with large phase separation. Thermal annealing could create crystalline domains from the amorphous phase with optimized sizes. The condition for thermal annealing will depend on the materials used, the ratio of the blend, and the solvents used.

The rate of evaporation of the solvents depends on the nature of the solvents used and has a huge effect on film morphology. Low boiling point solvents will lead to rapid evaporation and poor crystallization of P3HT since self-organization of P3HT occurs during the spin cast process when the solvents evaporate. The so-called solvent annealing is a technique that keeps the spin-casted films under a relatively long contact with the solvent vapor. This procedure would allow slow evaporation rate of the solvent during the preparation process and help to control the separation of domains and crystallization of the components, it has been proved to be an effective method to optimize the morphology of P3HT films.

The use of additives is a useful strategy to control the morphology of the composite films for highly efficient organic solar cells. Additives should have higher boiling point than the principal solvent and better solubility for PCBM than the donor polymers. Under this guidance, the morphology of the active layer could be controlled during the evaporation process since PCBM will precipitate out slower than donor materials.

Polythieno[3,4-b]-Thiophene/Benzodithiophene (PTB) Series Polymers

As discussed above, in order to achieve a high PCE, a synergistic approached is needed for material design and synthesis. Two strategies are developed to synthesize new polymers with

low energy bandgaps: (1) The first strategy is the donor–acceptor approach that combines both electron-rich and electron-deficient units into one polymer backbone via a cross-coupling reaction to tune the HOMO and LUMO energy levels of the resulting copolymers. The HOMO energy level of the copolymer is similar to the HOMO energy level of the electron-donating unit, while the LUMO energy level of the copolymer is close to the LUMO energy level of the electron-accepting unit. (2) The second strategy is the quinoidal structures. Certain monomers will prefer to exhibit quinoidal structures in delocalized states, leading to narrow energy bandgaps. A good example of the second strategy is the PTB series polymers developed in the Yu group [12–14]. The structures of PTB polymers are listed in Fig. 4. The polymer system is composed of benzodithiophene and thieno[3,4-b]thiophene (TT) units. The TT units are well known to exist in a certain degree of quinoidal structure. Indeed, these polymers exhibited almost ideal bandgap around 1.6–1.8 eV. The solar cell parameters of all PTB series polymers with $PC_{60}BM$ and $PC_{70}BM$ are summarized in Table 1. Particularly, by mixing PTB7 with $PC_{70}BM$, a PCE of 7.4 % was achieved, and this was the first polymer solar cell device which showed a PCE value higher than 7 %. Compared to P3HT, the absorption of PTB series polymers was extended to 700 nm due to the control of bandgap around 1.7 eV; this ensures efficient absorption of high energy photons in the solar spectrum. Solubility of the polymers and miscibility with PCBM could be controlled by introducing proper side chains to the polymer backbone. The extended π system in the benzodithiophene unit also enables good π–π stacking with a shorter distance between different polymer backbones and results in high hole mobilities. From the solar cell results of PTB series polymers, it is found that the alkoxy-substituted PTB3 shows deeper HOMO and LUMO energy levels compared with alkyl-substituted PTB2 and this leads to increase in V_{oc} from 0.60 to 0.72 eV. The introduction of fluorine atom in thienothiophene unit also helps to decrease the HOMO and LUMO energy levels and shows increased V_{oc} from 0.66 to 0.74 eV (from PTB5 to PTB4). More systematic studies of this system revealed the important role of dipolar change between excited state and ground state of repeating units on charge separation, thus the

PTB1: X=H, R_1= n-dodecyl, R_2= n-octyloxy;
PTB2: X=H, R_1= 2-ethylhexyl, R_2= n-octyloxy;
PTB3: X=H, R_1= 2-ethylhexyl, R_2= n-octyl;
PTB4: X=F, R_1= n-octyl, R_2= 2-ethylhexyloxy;
PTB5: X=H, R_1= n-octyl, R_2= 2-ethylhexyloxy;
PTB6: X=H, R_1= 2-butyloctyl, R_2= n-octyloxy;
PTB7: X=F, R_1= 2-ethylhexyl, R_2= 2-ethylhexyloxy

Polymers for Solar Cells, Fig. 4 Chemical structures of PTB series polymers

Polymers for Solar Cells, Table 1 Energy levels and solar cell parameters of PTB/PCBM solar cells

Polymer blend	E_{HOMO} (eV)	E_{LUMO} (eV)	J_{sc} (mA/cm^2)	V_{oc} (V)	FF (%)	PCE (%)
PTB1/PC_{60}BM	−4.90	−3.20	12.5	0.58	65.4	4.8
PTB1/PC_{70}BM			15.5	0.58	62.3	5.6
PTB2/PC_{60}BM	−4.94	−3.22	12.8	0.60	66.3	5.1
PTB3/PC_{60}BM	−5.04	−3.29	13.9	0.72	58.5	5.9
PTB4/PC_{60}BM	−5.12	−3.31	13.0	0.74	61.4	6.1
PTB4/PC_{70}BM			14.8	0.70	64.6	7.1
PTB5/PC_{60}BM	−5.01	−3.24	10.7	0.66	58.0	4.1
PTB6/PC_{60}BM	−5.01	−3.17	7.74	0.62	47.0	2.3
PTB7/PC_{60}BM	−5.15	−3.31	14.50	0.74	68.97	7.4

R$_1$=2-butyloctyl, R$_2$=2-butylhexyl

P1

P2

R$_1$=2-ethylhexyl, R$_2$=3-butylnonyl

P3

R$_1$=2-ethylhexyl

P4

R$_1$=2-ethylhexyl

P5

R$_1$=2-ethylhexyl

P6

R$_1$=2-ethylhexyl

P7
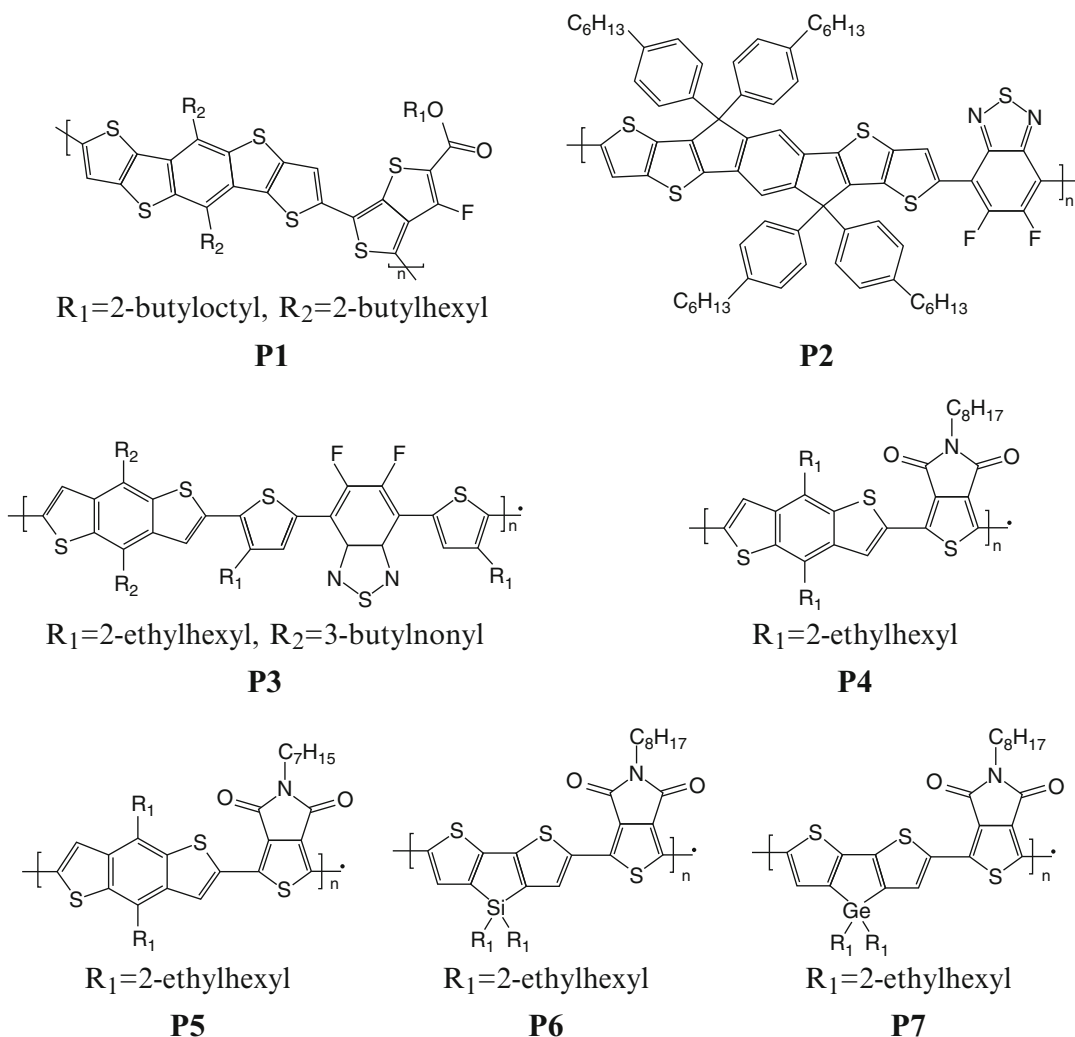
Polymers for Solar Cells, Fig. 5 Chemical structures of P1–P7

solar energy conversion efficiency [15, 16]. These polymer solar cells can be further optimized with formulation in device architecture.

Other State-of-the-Art Low-Bandgap Donor–Acceptor-Type Copolymers

In addition to PTB series polymers, many other low-bandgap polymers have been synthesized with the attempt to lower HOMO energy levels while maintaining enough driving force for charge dissociation. Several other highly efficient solar cell systems with PCE values larger than 7 % are summarized below. The structures of the polymer P1–P7 are listed in Fig. 5. For a better understanding, the donor unit of the copolymer is kept left in the structure, while the acceptor unit is kept right. The ladder-type polymer P1 composed of the 5-ring dithieno[2,3-d:2′,3′-d′]benzo[1,2-b:4,5-b′] dithiophene and benzodithiophene as the building blocks shows an extended π conjugated system compared to PTB series polymers, which helps to lower the positive charge density and exciton binding energy. By using proper side chains in the polymer to optimize the miscibility with

PC$_{70}$BM, a PCE of 7.6 % was achieved, with a V_{oc} at 0.89 V, a J_{sc} at 13.0 mA/cm^2, and a FF at 0.65 [17]. Another 7-ring ladder-type donor indacenodithieno[3,2-b]thiophene unit was copolymerized with 5,6-difluorobenzothiadiazole unit. The two F atoms on benzothiadiazole unit lower the HOMO energy level without changing the absorption properties. The long conjugated backbone ensures planarity and good hole mobility for polymer P2. A PCE of 7.03 is achieved without any additive or thermal annealing [18]. A similar acceptor unit with two alkylated thienyl units attached to 5,6-difluorobenzothiadiazole was copolymerized with benzodithiophene. The corresponding polymer P3 shows a high V_{oc} at 0.91 V, a J_{sc} at 12.9 mA/cm^2, and a FF at 0.61, resulting in a PCE of 7.2 % [19]. The low-bandgap polymer P4 based on benzodithiophene and thieno[3,4-c]pyrrole-4,6 dione unit gives a PCE at 7.5 % when mixed with PC$_{70}$BM. Further optimization is achieved by changing the linear side chains in the polymer backbone which impact the polymer self-assembling in thin films. A similar polymer P5 with N-C$_7$H$_{15}$ chain in thieno[3,4-c]pyrrole-4,6 dione unit leads to a PCE of 8.5 %, with a V_{oc} at 0.97 V, a J_{sc} at 12.6 mA/cm^2, and a FF at 0.70 [20]. The dithienosilole unit is also used to replace the benzodithiophene unit for high-performance solar cells. P6 is synthesized with a low-bandgap (1.73 eV) and deep HOMO energy level and gives a PCE of 7.3 %, with a V_{oc} at 0.88 V, a J_{sc} of 12.2 mA/cm^2, and a FF of 0.68 [21]. P6 could be further modified by introducing Ge atom to replace Si atom in the dithienosilole unit. Incorporation of Ge atom increases the HOMO energy level of 50 mV and extends the absorption to 735 nm. P7 yields an average PCE of 7.3 % when mixed with PC$_{70}$BM in an inverted solar cell structure [22].

Conclusion

Although the current state-of-the-art polymer solar cells have reached a promising performance with PCEs close to 10 %, real commercialization of this technique is still not ready yet. Further material development is still essential to achieve higher PCEs. The several design rules we mentioned above should be satisfied for the next generation of polymer solar cells, such as broad absorption of the polymer which covers the maximum solar spectra, high hole mobility, and appropriate energy level alignments with PCBM. In addition to that, long-term stability and large area device production of the solar cells are two important issues that need to be addressed.

Related Entries

▶ Charge-Transporting Polymers
▶ Ladder-Type Polymers
▶ Low-Bandgap Polymers
▶ Polymers for Transistors

References

1. Armaroli N, Balzani V (2007) The Future of energy supply: challenges and opportunities. Angew Chem Int Ed 46:52–66
2. Gunes S, Neugebauer H, Sariciftci NS (2007) Conjugated polymer-based organic solar cells. Chem Rev 107:1324–1338
3. Cheng YJ, Yang SH, Hsu CS (2009) Synthesis of conjugated polymers for organic solar cell applications. Chem Rev 109:5868–5923
4. He ZC, Zhong CM, Su SJ, Xu M, Wu HB, Cao Y (2012) Enhanced power-conversion efficiency in polymer solar cells using an inverted device structure. Nat Photonics 6:591–595
5. You JB, Dou LT, Yoshimura K, Kato T, Ohya K, Moriarty T, Emery K, Chen CC, Gao J, Li G, Yang Y (2013) A polymer tandem solar cell with 10.6% power conversion efficiency. Nat Commun 4:1446
6. Po R, Carbonera C, Bernardi A, Camaioni N (2011) The role of buffer layers in polymer solar cells. Energy Environ Sci 4:285–310
7. Dennler G, Scharber MC, Brabec CJ (2009) Polymer-Fullerene Bulk-Heterojunction solar cells. Adv Mater 21:1323–1338
8. Li G, Shrotriya V, Huang JS, Yao Y, Moriarty T, Emery K, Yang Y (2005) High-efficiency solution processable polymer photovoltaic cells by self-organization of polymer blends. Nat Mater 4:864–868
9. Zhao GJ, He YJ, Li YF (2010) 6.5% efficiency of polymer solar cells based on poly(3-hexylthiophene) and Indene-C60 Bisadduct by device optimization. Adv Mater 22:4355–4358

10. Sivula K, Luscombe CK, Thompson BC, Frechet JMJ (2006) Enhancing the thermal stability of polythiophene: Fullerene solar cells by decreasing effective polymer regioregularity. J Am Chem Soc 128:13988–13989

11. Schilinsky P, Asawapirom U, Scherf U, Biele M, Brabec CJ (2005) Influence of the molecular weight of Poly(3-hexylthiophene) on the performance of bulk heterojunction solar cells. Chem Mater 17:2175–2180

12. Liang YY, Feng DQ, Wu Y, Tsai ST, Li G, Ray C, Yu LP (2009) Highly efficient solar cell polymers developed via fine-tuning of structural and electronic properties. J Am Chem Soc 131:7792–7799

13. Liang YY, Xu Z, Xia JB, Tsai ST, Wu Y, Li G, Ray C, Yu LP (2010) For the bright future–bulk heterojunction polymer solar cells with power conversion efficiency of 7.4%. Adv Mater 22:E135–E138

14. Liang YY, Wu Y, Feng DQ, Tsai ST, Son HJ, Li G, Yu LP (2009) Development of new semiconducting polymers for high performance solar cells. J Am Chem Soc 131:56–57

15. Carsten B, Szarko JM, Son HJ, Wang W, Lu LY, He F, Rolczynski BS, Lou SJ, Chen LX, Yu LP (2011) Examining the effect of the dipole moment on charge separation in donor-acceptor polymers for organic photovoltaic applications. J Am Chem Soc 133:20468–20475

16. Carsten B, Szarko JM, Lu LY, Son HJ, He F, Botros YY, Chen LX, Yu LP (2012) Mediating solar cell performance by controlling the internal dipole change in organic photovoltaic polymers. Macromolecules 45:6390–6395

17. Son HJ, Lu LY, Chen W, Xu T, Zheng TY, Carsten B, Strzalka J, Darling SB, Chen LX, Yu LP (2013) Synthesis and photovoltaic effect in Dithieno[2,3-d:2′,3′-d′]Benzo[1,2-b:4,5-b′]dithiophene-based conjugated polymers. Adv Mater 25:838–843

18. Xu YX, Chueh CC, Yip HL, Ding FZ, Li YX, Li CZ, Li XS, Chen WC, Jen AKY (2012) Improved charge transport and absorption coefficient in Indacenodithieno[3,2-b]thiophene-based ladder-type polymer leading to highly efficient polymer solar cells. Adv Mater 24:6356–6361

19. Zhou HX, Yang LQ, Stuart AC, Price SC, Liu SB, You W (2011) Development of fluorinated Benzothiadiazole as a structural unit for a polymer solar cell of 7% efficiency. Angew Chem Int Ed 50:2995–2998

20. Cabanetos C, El Labban A, Bartelt JA, Douglas JD, Mateker WR, Frechet JMJ, McGehee MD, Beaujuge PM (2013) Linear side chains in Benzo[1,2-b:4,5-b′]dithiophene–Thieno[3,4-c]pyrrole-4,6-dione polymers direct self-assembly and solar cell performance. J Am Chem Soc 135:4656–4659

21. Chu TY, Lu JP, Beaupre S, Zhang YG, Pouliot JR, Wakim S, Zhou JY, Leclerc M, Li Z, Ding JF, Tao Y (2011) Bulk heterojunction solar cells using Thieno [3,4-c]pyrrole-4,6-dione and Dithieno[3,2-b:2′,3′-d] silole copolymer with a power conversion efficiency of 7.3%. J Am Chem Soc 133:4250–4253

22. Amb CM, Chen S, Graham KR, Subbiah J, Small CE, So F, Reynolds JR (2011) Dithienogermole as a fused electron donor in bulk heterojunction solar cells. J Am Chem Soc 133:10062–10065

Polymers for Transistors

Bob C. Schroeder and Iain McCulloch
Department of Chemistry and Centre for Plastic Electronics, Imperial College London, London, UK

Synonyms

Organic field-effect transistor; Organic semiconductor; Plastic electronics

Definition

Polymer: A polymer is a macromolecule with high molecular mass and composed of the repetition of structural units of significantly lower molecular weights. Polymers often possess very different chemical and physical properties compared to the smaller molecules they are composed of.

Transistor: A transistor is a semiconducting device that is used to switch and amplify electronic signals. The electric current flows between two electrodes, source and drain, and is controlled by an electric field applied to a third electrode, the gate.

Historical Background

The field-effect transistor principle was first patented in 1925 by Julius Edgar Lilienfeld, but it would take nearly another quarter of a century until the first working field-effect transistor (FET) based on a germanium crystal was built at Bell Laboratories in 1948 by William Shockley, John Bardeen, and Walter Brattain. Since its discovery,

the transistor has progressed immensely, and although the first devices were built out of scientific curiosity and for research purposes, electrical engineers quickly discovered their potential to switch and amplify electronic signals. Nowadays transistors are an essential building block of a -technology-based society, and none of the common electronic devices such as computers or cell phones would be possible without transistors.

Transistors are fabricated from semiconducting material, and historically inorganic semiconductors such as germanium and silicon have been used, while for some specialized applications semiconducting alloys such as gallium arsenide can be employed. Nevertheless, the production of electronic grade inorganic semiconductors is energy demanding with severe environmental hazards due to toxic by-products. Besides the costly production, inorganic semiconductors are often brittle and incompatible with flexible substrates, except if performance and material crystallinity are sacrificed in favor of substrate compatibility. Amorphous silicon (a-Si) is such an example and can be processed at low temperatures on plastic substrates, but its electron mobility of ~1 cm^2/Vs is significantly lower than that achieved with crystalline silicon (>50 cm^2/Vs). Organic semiconductors are a new class of materials that emerged during the last two decades, and they are addressing some drawbacks usually encountered with inorganic semiconductors. Organic materials can be cheaply processed from solution-based deposition techniques such as inkjet or roll-to-roll printing, which allows large area production and most importantly makes the processing on flexible substrates possible, thus opening the possibility for new application, such as flexible displays, smart fabrics, transparent electronics, etc. [1–3].

Device Architecture and Operating Principles

Organic field-effect transistors (OFET) use organic semiconductors in the device channel instead of inorganic silicon/germanium. The scope of organic semiconductors comprises both small molecule and polymer semiconductors, but this entry will focus exclusively on the applications of polymeric materials. Field-effect transistors are operated via the application of an electric field that causes the accumulation of charges at the dielectric/semiconductor interface, and the flow of those charges is controlled by the application of a potential between two electrodes, source and drain. There are four different OFET architectures (depicted in Fig. 1) to sandwich the

P
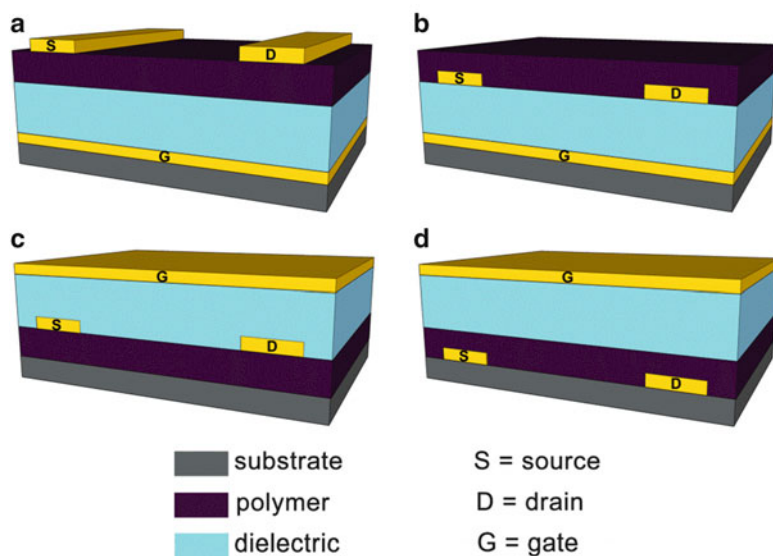
Polymers for Transistors, Fig. 1 Schematic representation of the different OFET architectures; (**a**) bottom-gate, top-contact, (**b**) bottom-gate, bottom-contact, (**c**) top-gate, top-contact, and (**d**) top-gate, bottom-contact
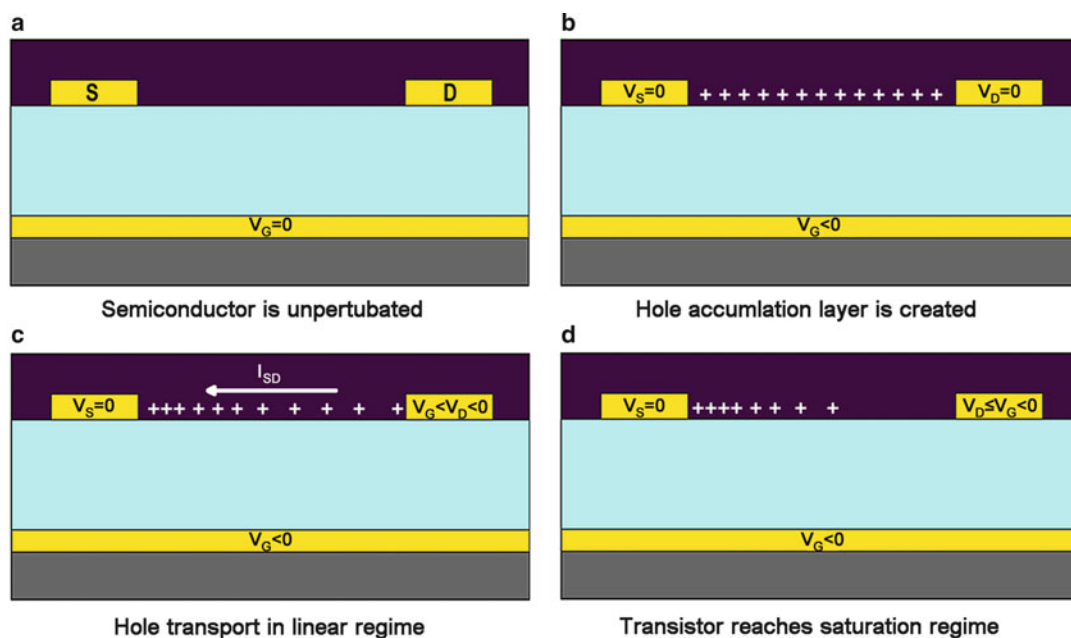
Polymers for Transistors, Fig. 2 Schematic representation of the hole transport in a bottom-gate, bottom-contact OFET at different gate (V_G) and drain voltages (V_D)

polymer semiconductor between the gate/dielectric and the electrodes. The kind of architecture used in device fabrication is rather important because it will have an influence not only on the complexity of the manufacturing process but ultimately also on the device performance and characteristics.

When the gate voltage (V_G) is set to zero, a negligible current flows between the source and the drain electrodes, and the transistor is in the "OFF" state (Fig. 2a). By applying a negative bias to the gate electrode, a hole accumulation layer is created at the p-type semiconductor/dielectric interface, but there is still no current (I_{SD}) across the channel (Fig. 2b). Only when a negative voltage is applied to the drain electrode (V_D) that a current starts to flow between source and drain electrodes, and the transistor is switched "ON" (Fig. 2c). As long as the V_D is less negative than the V_G, the transistor is in a linear regime, but once the V_D equals and exceeds the V_G, the transistor enters its saturation regime, and the channel "pinches off," which means that the

channel current (I_{SD}) saturates and becomes independent of the V_D (Fig. 2d).

Important transistor parameters, such as mobility (μ), threshold voltage (V_T), and on-off ratios (I_{on}/I_{off}), can be extracted from the transfer and output curves. Typical examples of such curves are shown in Fig. 3. One of the most important parameters of organic semiconductors is the charge carrier mobility, which is the relationship between the carrier speed in the semiconductor and the applied field. The mobility can be mathematically described as follows:

$$\mu(V_G) = \frac{\partial I_{SD}}{\partial V_G} \frac{L}{W C_i} \frac{1}{(V_G - V_T)}$$

where C_i is the capacitance per unit area of the gate dielectric, L is the length, and W is the width of the channel. In other words, the mobility depends on the conductivity, the device geometry, and the applied voltages. One has to be careful though when applying various models derived from inorganic semiconductor physics to organic semiconducting devices.
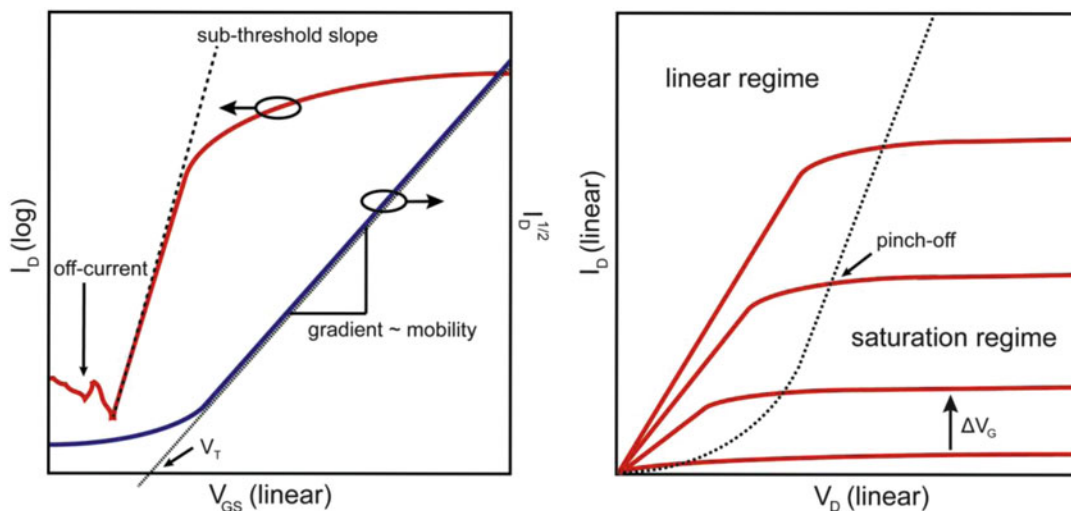
Polymers for Transistors, Fig. 3 Schematic showing typical transfer characteristics (*left*) and output curves (*right*) of an OFET. Some important transistor parameters such as threshold voltage (V_T), off-current, or pinch-off point are highlighted for clarity

Semiconducting Polymer Requirements [4]

Polymers are mainly composed of sp^3-hybridized carbon atoms, which are linked together by localized σ-bonds. These bonds assure the molecule's integrity, but the localized electrons within the bond cannot contribute to the electric conductivity without causing the molecule's breakup. Therefore purely σ-bonded polymers like polyethylene or polyvinyl chloride are extraordinary electric insulators.

Conjugated polymers on the other hand are mainly composed of sp^2-hybridized carbons. Contrary to the tetrahedral geometry of an sp^3-hybridized carbon, the sp^2 carbon possesses three sp^2 orbitals with a planar trigonal geometry and an out of plane p_z orbital, perpendicular to the plane containing the three sp^2 orbitals. While the electrons in the sp^2 orbitals can form σ-bonds, the electrons in the p_z orbitals are available to form π-bonds and to delocalize via conjugation over neighboring π-bonds, thus ensuring the electrical conductivity of π-conjugated polymers without causing the disintegration of the molecule.

The electron delocalization along the polymer backbone not only is responsible for the electric conductivity of the polymer but also defines the optical properties of the polymer. Both frontier energy levels, the highest occupied molecular orbital (HOMO) and the lowest unoccupied molecular orbital (LUMO), depend on the distance the π-electrons can delocalize over, the effective conjugation length. The effective conjugation length is the maximal overlap of p_z orbitals along the conjugated polymer backbone and depends besides many factors on the degree of polymerization [5]. Whereas a single thiophene unit shows discrete energy levels, the covalent coupling of several π-bonds leads to orbital interactions, which cause a splitting in the HOMO and LUMO energy levels [6]. With increasing conjugation length the difference between HOMO and LUMO energies narrows, until the system reaches saturation by forming continues band structures. The chain length from which this saturation is observed depends on the nature of the monomers, but usually a bandgap saturation is observed from 10 to 15 repeating units.

For OFET applications, the frontier energy levels play a very important role for various reasons. First the accessibility of either HOMO or LUMO defines the very nature of the

semiconductor, n-type or p-type. In the case where electrons can be injected into the LUMO, the semiconductor is said to be n-type, meaning that the charge carriers are electrons. On the other hand, if positive holes can be readily injected into the HOMO, the polymer is a p-type semiconductor, meaning that the charge carriers are holes. More recently a series of materials have emerged that allow both hole and electron injections into the corresponding orbitals; those materials are considered ambipolar and the charge carriers are either holes or electrons. A second important property dictated by the HOMO energy levels is the polymer stability under ambient conditions, which affects device lifetime and performance. It is generally accepted that a HOMO energy level below −4.9 eV is needed to prevent polymer oxidation in the presence of both oxygen and water. The frontier energy levels are intrinsic properties of the semiconducting material and can be engineered to meet certain criteria by molecular design of the polymer backbone [7].

Another important parameter to consider when designing semiconducting materials for OFET applications is the processability. In order to fully exploit the solution processability of polymer semiconductors, polymers should be soluble in a variety of organic solvents, in order to be formulated into inks with different viscosities and to accommodate a large variety of printing techniques. Solution viscosity is often controlled by either the concentration or the molecular weight of the polymer; the higher the molecular weight, the more viscous the resulting polymer formulation will be, but at the same time the overall solubility of the polymer decreases. To counterbalance this effect and to increase solubility, alkyl side chains of various length and nature can be attached to the conjugated polymer backbone [8, 9]. Besides the conjugated backbone, the choice of the proper alkyl side chain is essential to insure high performance in OFETs. Not only are the side chains responsible for the solubility and processability of the material, but they play a crucial role in the film-forming dynamics as well. The formation of a conducting channel at the semiconductor/dielectric interface is a prerequisite in order to operate a transistor, and therefore it is essential to gain control over the film-forming physics at this barrier. To ensure the formation of a continuous high-quality polymer film in which the conducting channel can form, the polymer backbone should adopt some kind of order. This can be achieved by the formation of well interconnected crystalline domains or by the formation of strong π-π interactions between adjacent polymer chains. For a long time, the formation of edge-on lamellar stacking was considered crucial to achieve high mobilities, but recent research indicates that this simplified idea is not entirely true and that it is nevertheless possible to achieve high carrier mobilities in more face-on materials where the length scale of ordering is also much smaller [10].

One way to achieve strong π-π interactions is to stiffen the polymer backbone and to minimize the torsion angle between the different monomer units. A large torsion angle between aromatic building blocks limits effective electron delocalization and not only leads to higher bandgap values due to a reduced conjugation length but also hinders the material to π-stack. Several synthetic methods, other than changing the aromatic building blocks, allow reducing the torsion angles in the conjugated polymer backbone. The regioregular placement of alkyl chains on a polythiophene polymer backbone, for example, has been found to reduce the steric hindrance between neighboring alkyl chains, thus allowing a more planar arrangement of the backbone. Fortunately the synthetic possibilities are not limited to alkyl chain chemistry; other possibilities to minimize torsional disorder along the polymer backbone are to bridge neighboring aromatic cores with covalent bonds and to introduce non-covalent interactions, such as hydrogen bonding, to render the rotation more difficult and less favorable [11, 12].

Thiophene-Based Polymers

Electron-rich polythiophenes were first synthesized in the early 1980s, but due to their poor solubility, chemists quickly shifted their interest to the much more soluble poly-3-alkylthiophenes (**P3ATs**).

Polymers for Transistors, Fig. 4 Possible regiochemistry for 3-alkylthiophenes; the *red arrows* highlight the σ-bonds along which significant torsional twist can be expected due to steric hindrance between alkyl chains
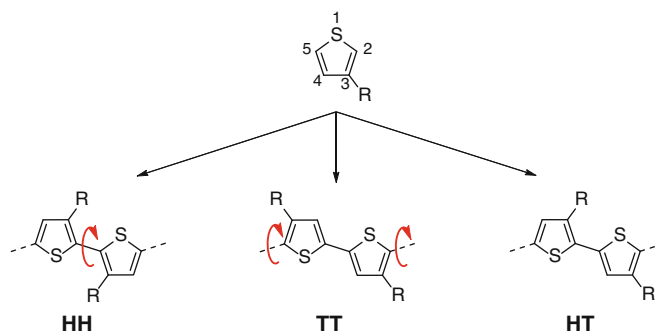
The facile synthesis and good solubility of alkylated polythiophenes are responsible for the popularity of these materials, and it is not surprising that to this date **P3AT**s are among the most studied semiconducting polymers [13]. Given the asymmetric nature of the 3-alkylthiophene monomer, one has to distinguish between three different coupling possibilities at the α-positions, summarized in Fig. 4. The introduction of "head-to-head" (**HH**) and "tail-to-tail" (**TT**) coupling into the polymer backbone can lead to significant backbone twisting and hinders π-π stacking. "Head-to-tail" (**HT**) coupling on the other hand prevents backbone twisting by minimizing steric hindrance between the alkyl side chains, which leads to a planar backbone and causes the polymer to self-organize into supramolecular structures.

In order to achieve high hole mobilities in poly (3-alkylthiophenes), it is essential to minimize miscouplings along the polymer chain, which in return allows the polymer to self-assemble into a lamellar structure [14]. This particular organization leads to very strong π-π interactions and large crystalline domains, hence enabling two-dimensional charge transport in the plane of the substrate. Lamellar order however is not the only criteria to be met to achieve high carrier mobilities in poly(3-alkylthiophenes); it is equally important to ensure good interconnectivity between the different crystalline domains. Low molecular weight poly(3-hexylthiophene) (**P3HT**) has been shown to be particularly sensitive to processing conditions and depending on the film morphology hole mobilities fluctuate between 10^{-5} and 10^{-3} cm²/Vs. High molecular

weight **P3HT** on the other hand was found to be less dependent on processing conditions, leading not only to higher but also to a narrower spread of hole mobilities between 0.01 and 0.1 cm²/Vs. Even though the low molecular weight **P3HT** is more crystalline than the higher molecular weight one, the lack of interconnectivity between the crystalline domains made the polymer extremely dependent on processing conditions and was identified as one of the limiting factors for hole mobilities [15]. Subsequently research groups tried to improve the hole mobilities of **P3HT** by substituting the hexyl side chains for longer linear (octyl and dodecyl) ones to improve crystallinity and interconnectivity, but no higher mobilities than for **P3HT** could be achieved. One of the possible reasons for this might be that in case of long alkyl side chains, the backbone crystallization has to compete with the side chain crystallization, which could lead to badly aligned crystalline domains and more grain boundaries, whose presence can be detrimental for charge transport. Even though **P3AT**s achieve decent hole mobilities in OFET devices, their extensive use as semiconductor is limited by their high-lying HOMO energy level around −4.8 eV. Due to the high-lying HOMO, **P3AT**s run the risk of electrochemical oxidation under ambient operating conditions, which would significantly lower the device lifetimes.

By decreasing the alkyl chain density on the polymer backbone, the HOMO energy level can be lowered compared to **P3HT**, which should increase the stability of the polymer towards oxidation, while maintaining the solution processability at the same time. One such example would

P
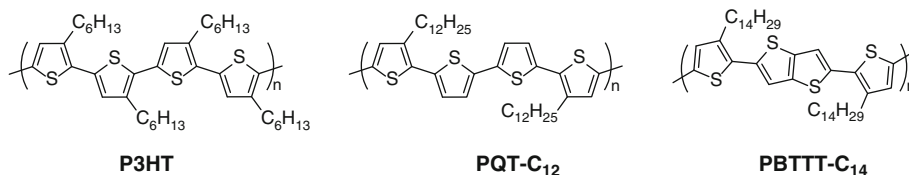
Polymers for Transistors, Fig. 5 Chemical structures of three of the most important thiophene-based semiconducting polymers

be polyquaterthiophene (**PQT-C₁₂**), which similar to **P3HT** self-assembles into highly ordered lamellar π-stacks (Fig. 5). In OFET devices, hole mobilities around 0.2 cm^2/Vs could be achieved after the **PQT-C₁₂** was annealed at 120–140 °C [16].

Another strategy to lower the HOMO energy level is to introduce more aromatic building blocks with higher aromatic resonance stabilization into the polymer backbone. McCulloch et al. synthesized **PBTTT**, a thiophene-based polymer that incorporates the aromatic and planar thieno[3,2-*b*]thiophene into the backbone [17]. The aromatic thienothiophene moiety in **PBTTT** has a larger resonance stabilization energy than the thiophene rings in **P3HT** and **PQT-C₁₂**, reflected in a reduced electron delocalization along the polymer backbone, and as a consequence lowers the HOMO energy level of **PBTTT** to −5.1 eV. Such a low HOMO level makes **PBTTT** less susceptible to oxidation by water or oxygen, which is a necessity to guarantee long-term device stability under ambient operating conditions. Additionally the lower alkyl chain density per unit length in the polymer backbone allows **PBTTT** to interdigitate with the alkyl chains of adjacent polymer chains in order to self-assemble into highly ordered three-dimensional crystalline domains oriented normal to the substrate. Furthermore, PBTTT is a liquid-crystalline polymer, which is an interesting physical property for semiconducting polymers because the crystalline-to-liquid-crystalline phase transition can be exploited during thermal annealing steps to reduce structural defects in crystalline domains without causing an isotropic melt of the material. Depending on the processing conditions, hole mobilities between 0.2 and 1.0 cm^2/Vs could be achieved with **PBTTT**.

All thiophene-based semiconducting polymers have a range of desirable features for transistor applications, notably their tendency to self-assemble and to form large highly ordered crystalline domains. The electron-rich character of thiophenes however limits their application areas because of their limited oxidative stability. A different approach is to copolymerize electron-rich donor units with more electron-poor accepting units. By alternating electron donating and withdrawing building blocks in the polymer backbone, the bond lengths are no longer evenly distributed along the backbone, which leads to a reduction of the bandgap due to orbital mixing. Furthermore the use of two different monomers allows chemists to combine various monomers together and to adjust the opto-electric properties of the polymers for specific applications. During the last decade, a plethora of monomers and polymers has been developed. To discuss each material separately is beyond the scope of this entry, and the focus will be put only on a small selection of classes of donor-acceptor polymers for transistor applications.

Cyclopentadithiophene (CPDT)- and Indacenodithiophene (IDT)-Based Polymers

One possibility to promote high mobility in polymer semiconductors is to fuse the coplanarity of the polymer backbone to minimize conformational, and thus energetic, disorder. Prominent approaches consist of bridging otherwise flexible π-conjugated systems with σ-bonds, thus creating rigid rodlike building blocks, which allow better electron delocalization, stronger

Fig. 6 Two examples of donor-acceptor polymers based on fused conjugated building blocks

CPDT-BT   **IDT-BT**
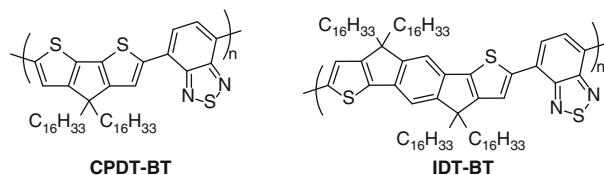
intermolecular interactions, and lower bandgaps. Two of the most prominent examples of this class of monomers are cyclopentadithiophene (**CPDT**) and indacenodithiophene (**IDT**); the chemical structures are depicted in Fig. 6. **CPDT** copolymerized with the benzo[*c*][1,2,5] thiadiazole (**BT**) was first introduced in 2006. Initial hole mobilities were rather low (1.5×10^{-2} cm^2/Vs) compared to polythiophene polymers; this was believed to be caused by the lack of macroscopic order in this new class of materials. After the substitution of the branched 2-ethylhexyl side chains on the **CPDT** unit for long linear hexadecyl chains, the hole mobility could be significantly increased to 0.17 cm^2/Vs even though no evidence could be found for long-range order in the polymer film [18]. Through careful optimization of processing conditions, the hole mobility of **CPDT-BT** could be gradually increased above unity, and more recently impressive carrier mobilities of 5.5 cm^2/Vs were reported for single fibers of **CPDT-BT** [19].

Zhang et al. elongated the **CPDT** motif even further by adding a benzene ring to the fused donor system [20]. The new indacenodithiophene (**IDT**) system has a planar and rigid structure, which should lower energetic disorder when incorporated into polymer backbones, thus promoting good carrier transport. When copolymerized with the electron-poor **BT** unit, a polymer is obtained which does not exhibit long-range order; however, hole mobilities in the range of 0.8–1.2 cm^2/Vs were obtained in BC-TG transistors. Because of its low-lying HOMO energy level (-5.4 eV), **IDT-BT** shows excellent ambient stability and the on-off currents remain nearly unchanged after the device was operated in air during 1,000 h. Detailed morphological studies on **IDT-BT** revealed the lack of long-range order and crystallinity that previously were considered requirements to achieve

high charge carrier mobilities in polymer semiconductors. At present it is believed that in the absence of macroscopic order, the charge transport along the polymer backbone is of utmost importance and that the rigid backbone of **IDT** polymers provides an optimal platform to allow high charge mobility in OFET devices [10].

Diketopyrrolopyrrole (DPP)-Based Ambipolar Polymers

Diketopyrrolopyrrole (**DPP**)-based structures were initially developed in the 1980s as high-performance dyes for industrial applications. With two electron-withdrawing lactam units, however, the planar **DPP** core is an excellent candidate to be used in donor-acceptor low-bandgap polymers [21, 22]. Initially, the **DPP** core was flanked with phenyl rings, but the increased backbone twist caused by steric hindrance between the phenyl and **DPP** units limited carrier mobilities to around 10^{-4} cm^2/Vs. A breakthrough for **DPP**-based polymers in OFET devices came with the introduction of thienyl flanking groups. Being smaller in size than benzene, the backbone twisting between the five-membered thiophene ring and the **DPP** chromophore could be significantly reduced. More recently crystal structures of **DPP** molecules revealed favorable H-bonding interactions (depicted in Fig. 7) between the β-hydrogen on the thiophene ring and the lactam oxygen on the **DPP** core. These attractive interactions further contribute to the planarization of the π-conjugated system. Once the torsional twist in **DPP**-based polymers was reduced, the carrier mobilities soared, as evidenced by comparing **DPPP-2T** and **DPPT-2T**. **DPPT-2T** has shown impressively high hole mobilities of ~1.6 cm^2/Vs, which is comparable to mobilities

P
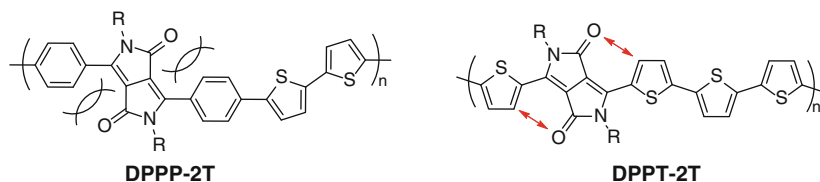
Polymers for Transistors, Fig. 7 Chemical structures of **DPPP-2 T** and **DPPT-2 T**; the sterical hindrance in **DPPP** and the H-bonding interactions in **DPPT** are shown for clarity
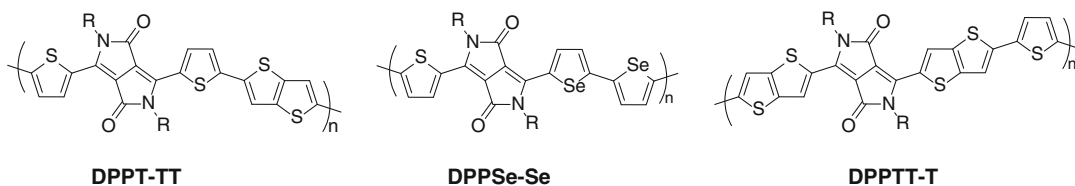
Polymers for Transistors, Fig. 8 Chemical structure of a selection of high-performing DPP-based donor-acceptor polymers

measured in amorphous silicon, whereas the hole mobility in **DPPP-2T** never exceeded 0.04 cm^2/Vs. Furthermore, the electron mobility of the phenyl **DPP** was negligible, whereas electron mobilities of 0.18 cm^2/Vs could be achieved with the thiophene counterpart. **DPP**-based polymers often show ambipolar characteristics, and it is speculated that this desirable feature is in relation with the strong electron-withdrawing carbonyl groups on the **DPP** chromophore, resulting in a delocalized and low-lying LUMO (lowest unoccupied molecular orbital) energy level on the one hand and the low-bandgap of **DPP** polymers, maintaining the HOMO energy level reasonably high, on the other hand. The combination of these two features allows the efficient injection of both holes and electrons into the polymer.

Due to the high performances achieved with **DPPT**-based polymers, the electron-deficient **DPP** core has stimulated the interest of the scientific community, and a large variety of derivatives have been synthesized since. Some of the most important and highest performing examples are presented in Fig. 8.

The polymerization of **DPPT** with thieno [3,2-*b*]thiophene (**TT**) leads to a further stiffening of the backbone compared to **DPPT-2T**. After high-temperature thermal annealing at

320 °C, balanced hole and electron mobilities exceeding 1 cm^2/Vs were achieved in BC-TG device architectures [23]. The higher annealing temperature had a much bigger effect on the electron mobility, which suggests that electron-trapping impurities are only evacuated from the semiconducting film at elevated temperatures. One way to modulate the n-type mobility is to lower the LUMO of the semiconductor, in order to be more accessible for reduction, thus facilitating electron injection. The substitution of the sulfur heteroatom in the thiophene ring for selenium has been found to be an efficient way of influencing the LUMO energy level because the nature of the heteroatom contributes significantly to the LUMO wave function. A selenophene-based **DPP** analogue was synthesized and introduced successfully into a polymer, **DPPSe-Se** [24]. Compared to the thiophene-based analogue, which showed unbalanced ambipolarity, balanced ambipolar characteristics with mobilities around 0.1 cm^2/Vs could be obtained with **DPPSe-Se** after modest thermal annealing. It is noteworthy that these balanced carrier mobilities were obtained in a BG-BC device architecture, which is more practical and easier to fabricate than the BC-TG one.

Bronstein and co-workers designed yet another DPP derivative by flanking the

Polymers for Transistors, Fig. 9 Chemical structures of two important rylene diimide-based n-type polymers

PDI-2T   NDI-2T
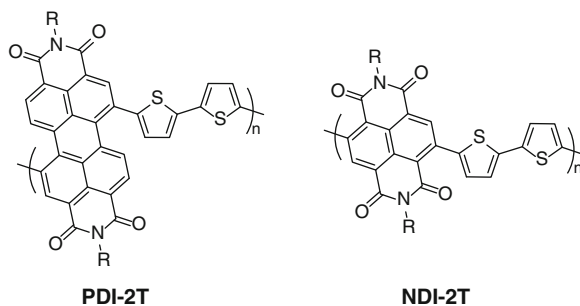
electron-deficient core with thieno[3,2-*b*]thiophene [25]. The elongated **TT** unit allows stiffening the conjugated backbone further and extends the HOMO wave function distribution along the polymer backbone. Copolymerized with thiophene, **DPPTT-T** achieved outstanding hole mobilities of up to 1.95 cm^2/Vs in TG-BC transistors without the need for high-temperature annealing. Interestingly, **DPPTT-T** exhibited no crystallinity or macroscopic order, which again supports the idea that backbone rigidity plays a very important role in order to achieve high carrier mobilities and can no longer be neglected when designing new semiconducting polymers.

n-Type Polymers Based on Rylene Diimides

Rylene diimides are a very valuable class of semiconducting materials often used in n-type channel transistors [26, 27]. Similar to the aforementioned **DPP** unit, rylene diimide systems contain two electron-withdrawing imide functionalities located on the periphery of naphthalene or larger derivatives. The chemical robustness of rylene derivatives and the strong electron-withdrawing imides make rylene diimides excellent candidates for stable n-type transistors.

In Fig. 9, two of the most prominent rylene-based polymers are depicted. As mentioned previously, the electron-withdrawing character of the four carbonyl groups on the rylene core lowers the LUMO significantly (−4 eV), which makes those materials suitable for charge injection from electrodes with high-lying work functions, such as gold. In addition the low-lying

HOMO levels of **PDI-2T** (−5.6 eV) and **NDI-2T** (−5.4 eV) should provide the materials with excellent stability towards ambient oxidation. Initial device performance did not quite demonstrate the high expectations, and electron mobilities in the range of 10^{-2} to 10^{-3} cm^2/Vs were measured for both polymers. However when operated in air, **NDI-2T** maintained its carrier mobility, while the **PDI-2T** mobility dropped by more than one order of magnitude. After optimization, the electron mobilities could be dramatically increased, and **NDI-2T** achieved electron mobilities of 0.85 cm^2/Vs under ambient operating conditions [28]. Contrary to **DPP**-based materials, it was not possible to achieve well-balanced ambipolar charge transport with rylene-based polymers, and to date the highest hole mobility achieved with **NDI-2T** is 0.1 cm^2/Vs. Rivnay and co-workers investigated the molecular packing of **NDI-2T**, and a similar microstructure to **IDT-BT** was observed with no evidence of a highly ordered microstructure [29]. Even though rylene diimide-containing polymers do not yet achieve the high and balanced ambipolar charge transport of **DPP**-based materials, their high oxidative stability makes them excellent candidates for air-stable OFETs with improved operating lifetimes.

Conclusion

With ongoing research, the field of semiconducting polymers is slowly shifting from highly ordered polymers such as **P3HT** or **PBTTT** to short contact donor-acceptor polymers. This new class of materials has been proven to be less

P

sensitive to processing conditions while still maintaining high carrier mobilities. In addition, the molecular design made it possible to specifically tailor polymers for either p- or n-type charge transport. All these new insights into structure–property relationships and the more sophisticated processing conditions make the fabrication of fully printed electronics, based on polymers, no longer wishful thinking but an achievable goal for the near future.

Related Entries

▶ Conducting Polymers
▶ Conjugated Polymer Synthesis
▶ Poly(thiophene)s

References

1. Arias AC et al (2010) Materials and applications for large area electronics: solution-based approaches. Chem Rev 110:3–24
2. Hamilton R et al (2010) Development of polymer semiconductors for field-effect transistor devices in displays. In: Franky So (ed) Organic electronics: materials, processing, devices and applications, CRC Press, Boca Raton, Fl, p 393
3. Klauk H (2006) Organic electronics, 1st edn. Wiley-VCH, Weinheim
4. Schroeder BC (2013) New thiophene based semiconducting materials for applications in plastic electronics. Department of Chemistry, Imperial College London, London
5. Skotheim A, Reynolds JR (2007) Handbook of conducting polymers, 3rd edn. CRC Press, Boca Raton/London
6. Chochos CL, Choulis SA (2011) How the structural deviations on the backbone of conjugated polymers influence their optoelectronic properties and photovoltaic performance. Prog Polym Sci 36(10):1326–1414
7. Mei J et al (2013) Integrated materials design of organic semiconductors for field-effect transistors. J Am Chem Soc 135(18):6724–6746
8. Lei T, Wang J-Y, Pei J (2014) Roles of flexible chains in organic semiconducting materials. Chem Mater 26(1):594–603
9. Mei J, Bao Z (2014) Side chain engineering in solution-processable conjugated polymers for organic solar cells and field-effect transistors. Chem Mater 26(1):604–615
10. Peet J et al (2009) The role of processing in the fabrication and optimization of plastic solar cells. Adv Mater 21(14–15):1521–1527
11. McCulloch I et al. (2012) Design of semiconducting indacenodithiophene polymers for high performance transistors and solar cells. Acc Chem Res 45(5):714–722
12. Yu C-Y et al (2009) Thiophene/phenylene/thiophene-based low-bandgap conjugated polymers for efficient Near-infrared photovoltaic applications. Chem Mater 21(14):3262–3269
13. Nielsen CB, McCulloch I (2013) Recent advances in transistor performance of polythiophenes. Progress Polym Sci 38(12):2053–2069
14. Osaka I, McCullough RD (2008) Advances in molecular design and synthesis of regioregular polythiophenes. Acc Chem Res 41:1202–1214
15. Kline R et al (2005) Dependence of regioregular poly (3-hexylthiophene) film morphology and field-effect mobility on molecular weight. Macromolecules 38:3312–3319
16. Ong BS et al (2004) High-performance semiconducting polythiophenes for organic thin-film transistors. J Am Chem Soc 126(11):3378–3379
17. McCulloch I et al (2009) Semiconducting thienothiophene copolymers: design, synthesis, morphology, and performance in thin-Film organic transistors. Adv Mater 21:1091–1109
18. Zhang M et al (2007) Field-effect transistors based on a benzothiadiazole–cyclopentadithiophene copolymer. J Am Chem Soc 129(12):3472–3473
19. Wang S et al (2012) Organic field-effect transistors based on highly ordered single polymer fibers. Adv Mater 24(3):417–420
20. Zhang WM et al (2010) Indacenodithiophene semiconducting polymers for high-performance, air-stable transistors. J Am Chem Soc 132(33):11437–11439
21. Nielsen CB, Turbiez M, McCulloch I (2013) Recent advances in the development of semiconducting DPP-containing polymers for transistor applications. Adv Mater 25(13):1859–1880
22. Li Y et al (2013) High mobility diketopyrrolopyrrole (DPP)-based organic semiconductor materials for organic thin film transistors and photovoltaics. Energy Environ Sci 6(6):1684–1710
23. Chen Z et al (2012) High-performance ambipolar diketopyrrolopyrrole-thieno[3,2-b]thiophene copolymer field-effect transistors with balanced hole and electron mobilities. Adv Mater 24(5):647–652
24. Kronemeijer AJ et al (2012) A selenophene-based low-bandgap donor–acceptor polymer leading to fast ambipolar logic. Adv Mater 24(12):1558–1565
25. Bronstein H et al (2011) Thieno[3,2-b]thiophene-diketopyrrolopyrrole-containing polymers for high-performance organic field-effect transistors and organic photovoltaic devices. J Am Chem Soc 133:3272–3275
26. Anthony JE et al (2010) n-type organic semiconductors in organic electronics. Adv Mater 22:3879–3892
27. Zhan X et al (2011) Rylene and related diimides for organic electronics. Adv Mater 23(2):268–284

28. Yan H, Chen Z, Zheng Y, Newman C, Quinn JR, Dötz F, Kastler M, Facchetti A (2009) A high-mobility electron-transporting polymer for printed transistors. Nature 457:679–686

29. Rivnay J et al (2010) Unconventional face-on texture and exceptional in-plane order of a high mobility n-type polymer. Adv Mater 22(39):4359–4363

Polymers from Plant Oils

Hiroshi Uyama
Department of Applied Chemistry, Graduate
School of Engineering, Osaka University, Suita,
Osaka, Japan

Synonyms

Plant oil-based polymers; Vegetable oil-based polymers

Definition

Polymers from plant oils are macromolecules obtained by using plant oils as starting materials. Acrylates and epoxides for cured polymers and polyols for polyurethanes are typical derivatives of plant oils, which can be used for various industrial applications.

Introduction

Worldwide potential demands for replacing petroleum-derived raw materials with renewable plant-based ones in production of polymeric materials are quite significant in the social and environmental viewpoints. The use of bioresources as starting substrates for polymeric materials would help halt greenhouse warming and contribute to global sustainability without the depletion of scarce fossil resources. Among bioresources, plant (vegetable) oils are expected as an ideal alternative chemical feedstock [1, 2]. Plant oils are one of the cheapest resources in abundance from various oilseeds. They are mainly used for food and feed, and about 15 % are converted into industrial products for various applications.

Plant oils are triglycerides, fatty acid esters of glycerol. Their composition (chain length and number of double bonds of fatty acids) depends on plant species (Table 1). The C=C double bonds of fatty acids can be used for polymerization; however, their reactivity is low owing to the internal olefin structure and the allylic structure is not suitable for radical polymerizations. Furthermore, the aliphatic chain of the products cannot provide sufficient rigidity and strength for some applications. An alkyd resin, a polyester modified by unsaturated fatty acid, is one of the oldest polymers based on plant oils [3]. The commercial production began in 1993 at General Electric. It is mainly used in the field of coatings and printing inks.

Various types of polymers from plant oils were reported [4–8]. For development of polymeric materials from plant oils, the modification of the C=C double bond into more reactive functional groups has been extensively studied. Oxidations, C–C bond-forming additions to the C=C double bond, and metathesis reactions are typical methods of the modification of plant oils.

Polymeric Materials from Epoxidized Plant Oils

Epoxidized plant oils, which are prepared from hydroperoxides, hydrogen peroxide, or molecular oxygen with different catalysts, were polymerized by using hardeners such as amines and acid anhydrides or thermally latent cationic catalysts. Epoxidized soybean oil (ESO) and epoxidized linseed oil (ELO) are commercially available as stabilizer for processing of poly(vinyl chloride). To improve properties of the polymers from epoxidized plant oils, various approaches have been investigated [9].

Silane coupling agents having reactive cyclic ether groups were used for preparation of bio-based nanocomposites (Fig. 1). The curing of epoxidized plant oils with 3-glycidoxypropyltrimethoxysilane (GPTMS) using thermally latent cationic catalyst

Polymers from Plant Oils, Table 1 Composition of fatty acids of typical plant oils

Fatty acid	Stearic (18:00)	Oleic (18:01)	Linoleic (18:02)	Linolenic (18:03)	Other
Soybean oil	2~7	20~35	50~57	3~8	5~13
Palm oil	3~7	37~50	7~11		36~51
Rapeseed oil	1~3	46~59	21~32	9~16	4~12
Sunflower oil	2~5	15~35	50~75	0~1	3~8
Linseed oil	2~5	20~35	5~20	30~58	4~12
Corn oil	2~5	25~45	40~60	0~3	7~14
Rise oil	1~3	35~50	25~40	0~1	11~24
Olive oil	1~3	70~85	4~12	0~1	8~19
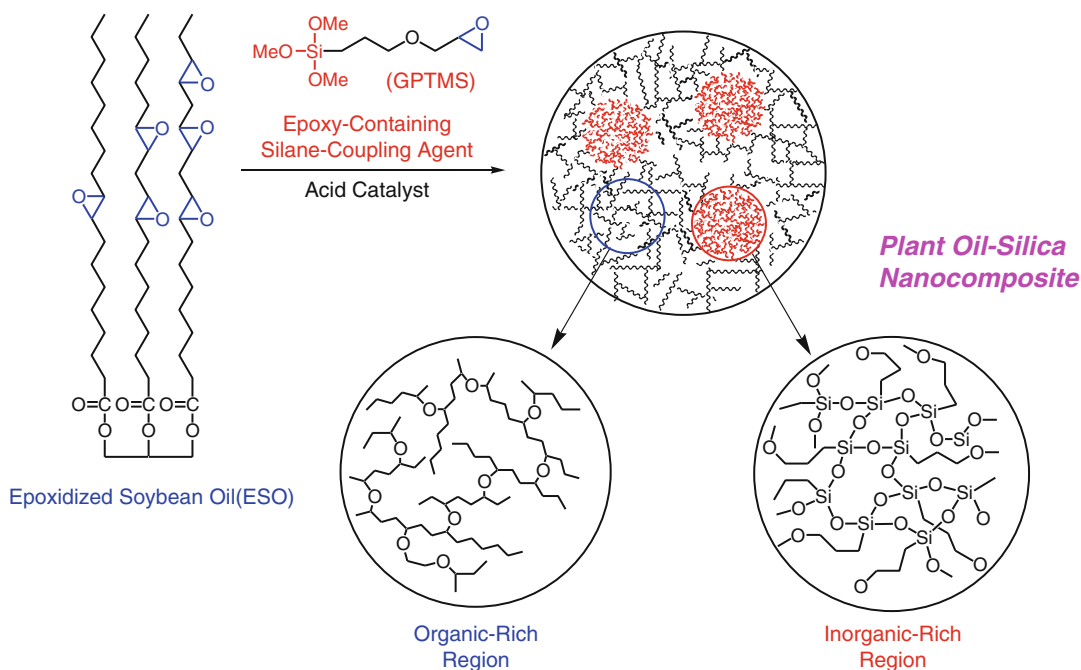
Polymers from Plant Oils, Fig. 1 Nanocomposite of silicone and plant oil-based polymer

produced transparent nanocomposites, in which both oxirane groups of epoxidized plant oils and GPTMS were copolymerized to produce an organic polymer matrix, simultaneously forming a silica network [1]. The nanocomposite showed excellent film properties; the hardness and mechanical strength were improved by incorporating the silica network into the organic polymer matrix and the good flexibility was observed. The dynamic viscoelasticity analysis showed reinforcement effect by the inorganic network.

Clays (montmorillonites) are one of the most popular additives for improvement of mechanical and thermal properties of polymers. ESO was subjected to intercalation into an organically modified clay, followed by an acid-catalyzed curing of the epoxy-containing triglyceride, leading to production of bio-based nanocomposites (Fig. 2). The dynamic viscoelasticity analysis exhibited the significant reinforcement effect by the addition of the clay. The composite showed improved barrier property for water vapor.

Polymers from Plant Oils,
Fig. 2 Nanocomposite of clay and plant oil-based polymer
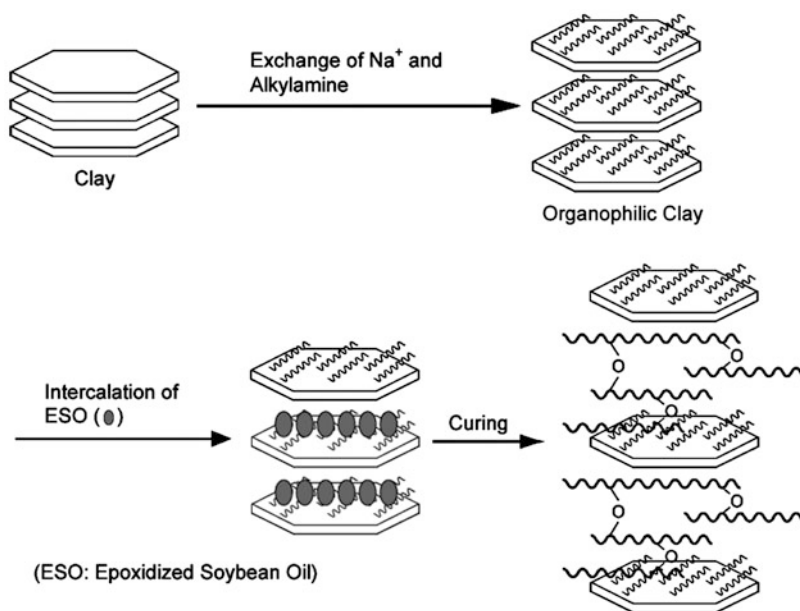
Cellulose is one of the most popular fillers for polymers. However, hydrophilic cellulose is often difficult to combine hydrophobic polymers in nanometer levels. Thus, porous materials or nonwoven mats of cellulose were used for preparation of composites of cellulose and oil polymers. It was reported that a biocomposite of the oil-based network polymer and cellulose fiber was prepared by the acid-catalyzed curing of ESO in the presence of the microfibrillated cellulose (MFC) sheet (nonwoven mat). The large improvement of mechanical and thermal properties of the ESO polymer was achieved by using MFC as filler. Ultrafine fibers of poly(lactic acid) obtained by electrospinning were also used for preparation of a biocomposite of polyESO. Plant oil-based elastomers were prepared by the curing of ESO in the presence of rosin derivatives. The brittle property of polyESO was significantly improved by these additives.

The products obtained from epoxidized plant oils and hardeners such as amines and acid anhydrides often showed improved properties in comparison with those of polymers by cationic curing of epoxidized plant oils. The curing with decamethylene diamine gave the bio-based elastomer. Crosslinking of epoxidized plant oils and diglycidyl ether of bisphenol F with an anhydride curing agent produced the bio-based polymer with high Izod impact strength and fracture toughness. ELO was crosslinked by a dimer acid from natural oils. The dimer acid has long alkane chains (C_{36}), which improved the mechanical properties of the polymer from ELO.

Epoxidized plant oils were easily converted to acylate plant oils by the reaction with acrylic acid. This acylate was subjected to the photopolymerization, yielding the crosslinked polymer. Additionally, thermosetting of the plant oil-based acrylate and conventional vinyl monomers afforded the crosslinked polymers. Epoxidized plant oil was partially modified by acrylic acid, which was used as comonomer for roof coating (Fig. 3); the residual epoxy group was slowly cured after the coating on roof. Click reaction was also used for curing of plant oils. Alkynated and azidated soybean oils were prepared from ESO, and these compounds were reacted by using copper as catalyst.

Vernonia oil, a naturally occurring epoxy-containing triglyceride, was used for preparation of bio-based crosslinked materials. This oil was cured by a cationic initiator in the presence of a copolymer of glycidyl methacrylate and styrene to give the crosslinked film with high-gloss surface.

P

Polymers from Plant Oils, Fig. 3 Molecular design of plant oil-based coating for roof
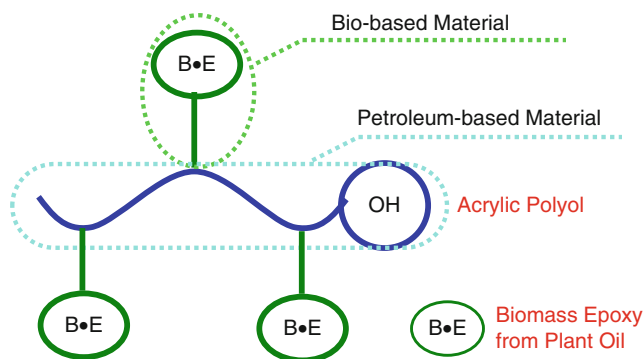
Polymers from Plant Oils, Fig. 4 Photo of castor oil-based polyurethane form
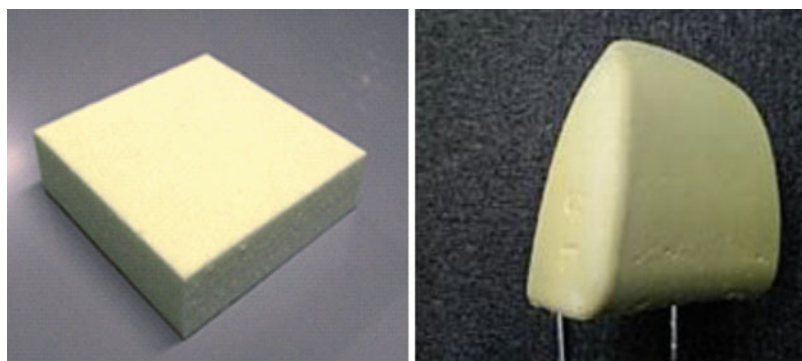
Polyols from Plant Oils

Polyols are essential substrates for polyurethane production. Castor oil and its derivatives as well as derivatives of soybean oil are commercially available as polyol for industrial applications of polyurethanes [10, 11].

Castor oil is mainly composed of ricinoleic acid bearing a secondary hydroxyl group and glycerol. Castor oil is produced primarily in India and classified as non-edible oil due to the nauseant properties. Various industrial applications of castor oil and its derivatives have been developed. Castor oil is used as polyol for polyurethanes, which have wide acceptance in automotive, building, and furniture industries. Sebacic acid and 11-aminoundecanoic acid are industrially produced by pyrolysis of castor oil (and the following derivatization). These compounds afford engineering bio-nylons (typically, nylon 610 and nylon 11) with good mechanical and thermal properties. Various polyesters were synthesized from ricinoleic acid and its derivatives for applications of coatings and biodegradable materials. Branched poly(lactic acid) was prepared by the polymerization of lactide in the presence of castor oil. The product was used as polyol for bio-based polyurethane form (Fig. 4).

Polyols based on various plant oils were developed. One synthetic route was the reaction of epoxidized plant oil with alcohol. Polyols from canola, mid-oleic sunflower, soybean, linseed, sunflower, and corn were prepared and used for the preparation of bio-based polyurethanes. Polyol from soybean is commercialized, which is prepared via transesterification with methanol and the subsequent formylation and hydrogenation.

Related Entries

References

1. Biermann U, Friedt W, Lang S, Lühs W, Machmüller G, Metzger JO, Rüsch gen Klaas M, Schäfer HJ, Schneider MP (2000) New syntheses with oils and fats as renewable raw materials for the chemical industry. Angew Chem Int Ed 39:2206–2224. doi:10.1002/1521-3773(20000703) 39:13<2206::AID-ANIE2206>3.0.CO;2-P

2. Biermann U, Bornscheuer U, Meier MAR, Metzger JO, Schäfer HJ (2011) Oils and fats as renewable raw materials in chemistry. Angew Chem Int Ed 50:3854. doi:10.1002/anie.201002767

3. Hofland A (2012) Alkyd resins: from down and out to alive and kicking. Prog Org Coat 73:274–282. doi:10.1016/j.porgcoat.2011.01.014

4. Khot SN, Lascala JJ, Can E, Morye SS, Williams GI, Palmese GR, Kusefoglu SH, Wool RP (2001) Development and application of triglyceride-based polymers and composites. J Appl Polym Sci 82:703–723. doi:10.1002/app.1897

5. Desroches M, Benyahya S, Besse V, Auvergne R, Boutevin B, Caillol S (2014) Synthesis of bio-based building blocks from vegetable oils: a platform chemicals approach. Lipid Technol 26:35–38. doi:10.1002/lite.201400014

6. Sharma V, Kundu PP (2008) Condensation polymers from natural oils. Prog Polym Sci 33:1199–1215. doi:10.1016/j.progpolymsci.2008.07. 004

7. Meier MAR, Metzger JO, Schubert US (2007) Plant oil renewable resources as green alternatives in polymer science. Chem Soc Rev 36:1788–1802. doi:10.1039/b703294c

8. Xia Y, Larock RC (2010) Vegetable oil-based polymeric materials: synthesis, properties, and applications. Green Chem 12:1893–1909. doi:10.1039/c0gc00264j

9. Tan SG, Chow WS (2010) Biobased epoxidized vegetable oils and its greener epoxy blends: a review. Polym Plast Technol Eng 49:1581–1590. doi:10.1080/03602559.2010.512338

10. Lligadas G, Ronda JC, Galia M, Cadiz V (2010) Plant oils as platform chemicals for polyurethane synthesis: current state-of-the-art. Biomacromol 11:2825–2835. doi:10.1021/bm100839x

11. Mutlu H, Meier MAR (2010) Castor oil as a renewable resource for the chemical industry. Eur J Lipid Sci Technol 112:10–30. doi:10.1002/ejlt.200900138

Polymers with Large Spin-Orbit Coupling

C. X. Sheng and Z. Valy Vardeny
Department of Physics and Astronomy, University of Utah, Salt Lake City, UT, USA

Synonyms

Organic spintronics; Phosphorescence

Definition

Polymers that have large spin-orbit coupling due to embedded heavy atoms and thus show strong phosphorescence.

Introduction

The dynamics of spin singlet and triplet excitons in π-conjugated polymers define their performance as optically active layer in organic light-emitting diodes (OLEDs) and organic photovoltaic (OPV) cells. As an example, if both triplet and singlet excitons can be used in OLEDs to convert electrical energy to electroluminescence (EL) emission, then the fraction of excitons that potentially can emit light may reach 100 % [1]. Similarly in OPV based on donor/acceptor (D–A) blends, the photogenerated singlet exciton in the polymer donor domains may recombine *before* reaching the D–A interface, because of its relatively short lifetime (~100 ps). In contrast, because of the much longer lifetime (~5 μs), triplet excitons could reach the D–A interface with larger probability and thus could potentially be the answer to this loss mechanism [2]. Therefore, both OLED and OPV technologies may substantially benefit from the proper use of the spin triplet states. Alas, because the spin-orbit coupling (SOC) in polymers is typically very weak (<5 Gauss), triplet excitons cannot be efficiently photogenerated via intersystem crossing (ISC) in most donor polymers for OPV enhancement and,

P

similarly, cannot efficiently emit light in OLEDs. The SOC however can be enhanced by embedding heavy atoms such as platinum (Pt) in the polymer backbone chains.

Recently a series of polymers and oligomers in which platinum (Pt) atoms are inserted in the organic polymer's building blocks have been synthesized [3, 4]. The Pt atom has large SOC and thus increases the effective SOC of the polymer chain. In fact, the Pt atoms may be inserted into the polymer chain with variable inter-Pt distance (i.e., between adjacent intrachain Pt atoms), and this tunes the effective SOC of the polymers [5, 6]. Such enhanced SOC, in turn, may increase the ISC rate from the singlet to the triplet manifold, which would make triplet excitons more viable for OPV applications. In addition, the enhanced SOC may also trigger substantive phosphorescence (PH) emission from the lowest triplet state [3–6], and thus the emission spectrum from such semiconductor polymers may contain both fluorescence (FL) and PH bands (Fig. 1). In fact, these two bands span the visible spectral range and therefore may potentially be used in designing "white" electroluminescence emission from the same polymer in OLEDs (dubbed

WOLED), with internal quantum efficiency approaching 100 % [7].

These beneficial triplet characteristic properties are the main reason that a variety of Pt-containing polymers have been synthesized and studied. Most of these studies however have been focused on the photophysics of the triplet excitons [3–6]. Importantly, the dynamics of the internal conversion and ISC processes have been only recently elucidated [6], and the metal-to-ligand charge transfer (*MLCT*) state, which has been studied extensively in organometal complexes, has been addressed in Pt-containing polymers. In a recent work [6], a broad arsenal of linear and nonlinear optical (NLO) spectroscopies has been applied to two Pt-containing polymers with different π-conjugated spacer unit length between the nearest intrachain Pt atoms, which controls the spin dynamics of excited states, namely, the timescales of the ISC process in this class of materials. It was found that the ISC time in these Pt-polymers is very short, of the order of 2 ps depending on the intrachain Pt-atom occurrence in the polymer chain. The ISC rate, in turn, also determines the relative strength of the respective FL and PH emission

Polymers with Large Spin-Orbit Coupling, Fig. 1 (**a**): Schematic structure of Pt-1 and Pt-3 polymers, where the spacer between adjacent Pt atoms varies from one to three benzene rings, respectively [6]. (**b**) The steady-state emission spectra of Pt-1 (*green*) and Pt-3 (*red*) polymer films; the absorption spectrum (*blue*) is also shown. Two emission bands are apparent, fluorescence (FL) at high energy and phosphorescence (PH) at low energy
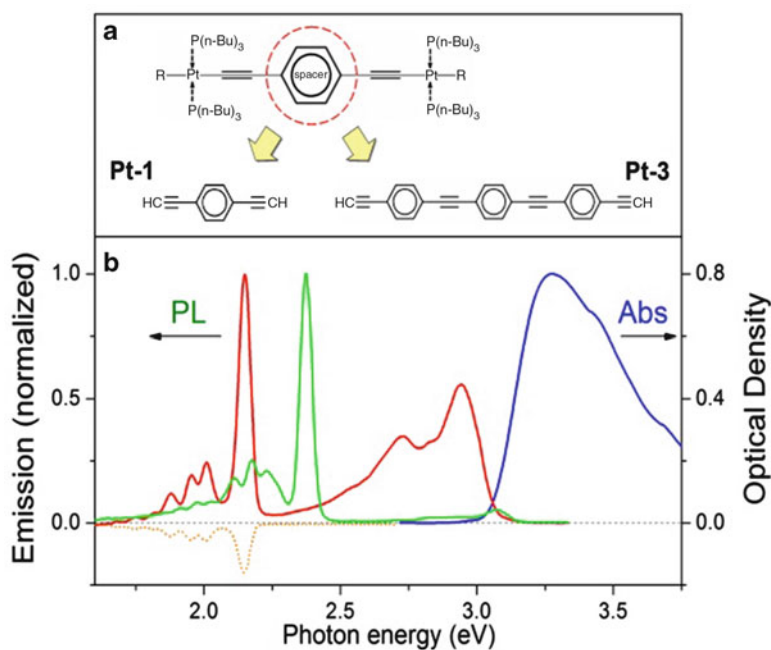
bands, and therefore, the emission color of the potential WOLED based on these polymers may be controlled by synthetic means mainly because the SOC in the polymers can be readily tuned.

Pt-Polymer Synthesis

Transition metals such as Pt are elements that have filled or partially filled d-orbitals and are found in a wide variety of oxidation states. Dative covalent bonds can be formed between central metal atoms and ligands, and the bonding geometry depends on the oxidation state of the metal [8, 9]. Pt(II) forms square planar complexes where the five degenerate d-orbitals of the metal ion have their degeneracy lifted by the Coulomb interactions with the ligand orbitals. It was found [10] that the conjugation could extend through the Pt atom, as a result of mixing between the frontier orbitals of the metal and the conjugated ligands. The extent of mixing depends on the overlap between the ligand and metal orbitals and thus may vary from ligand to ligand. Since Pt (II) takes a square planar configuration and forms stable bonds with ethynylenes, it is possible to synthesize organometallic polymers of the structure shown in Fig. 1 [11]. The two conjugated phosphine ligands allow for solubility, whereas the two conjugated ligands that consist of the ethynylene groups are bridged by a conjugated spacer, R, from the backbone of the polymer

(Fig. 2). A more elaborate scheme as well as alternative schemes that have been recently tried have led to the synthesis of Pt-3, where a spacer of three benzene rings was inserted between two adjacent Pt-polymers. This polymer shows both fluorescence (FL) and phosphorescence (PH) bands (Fig. 1) [6].

Polarization Properties of the Phosphorescence Emission Band

The triplet exciton is composed of three spin sublevels that can be reached by resonant absorption or are unequally populated in thermal equilibrium. These properties may polarize the PH emission band from the Pt-polymers. For example their strong SOC makes it possible to obtain circularly polarized PH emission if excited by circularly polarized excitation. Figure 1 illustrates that the Pt-polymers show two PL emission bands; these are FL with emission from the lowest singlet exciton and PH with emission from the lowest triplet excitons. The relative intensities and spectral positions of these two bands can be tuned by the spacer group between two adjacent intrachain Pt atoms. The FL band cannot be polarized because it originates from singlet excitons. In contrast, the PH band may be polarized if excited with circularly polarized light [12], especially under the influence of a strong magnetic field.

Polymers with Large Spin-Orbit Coupling, Fig. 2 An outline of the synthesis process of Pt-containing ethynylene monomers and polymers from organic ligands with spacer group, R
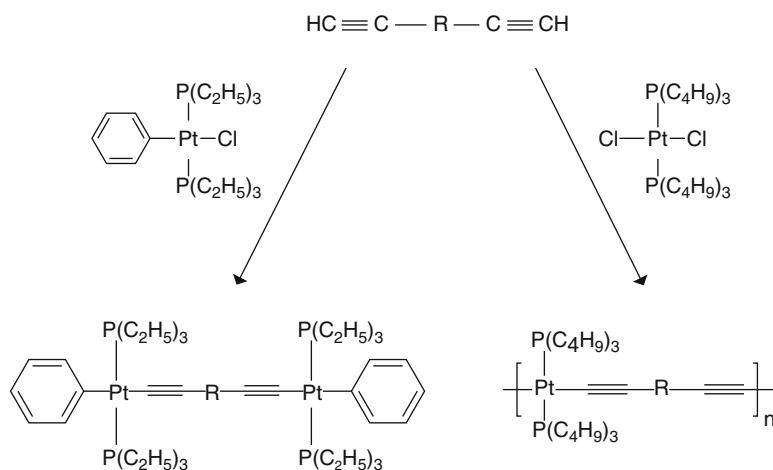
There are two methods by which spin-aligned triplet excitons may be photogenerated by circularly polarized optical absorption. The Pt-1 polymer is special because the order of the excited states is reversed, namely, the metal-to-ligand charge transfer (MLCT) state of the *d*-electrons of the Pt atoms lies *lower* than the π–π* singlet excited state [6]. In this case resonant excitation with circularly polarized light into the polymer absorption edge may preserve the spin sense and lead to circularly polarized PH emission. The second method is resonant excitation into the lowest lying triplet exciton using circularly polarized pump. Since the lowest triplet exciton in these polymers emits PH, the absorption into this state is also allowed. This was recently shown in Pt-1, where a weak absorption band was obtained at the 0–0 PH emission band, and the PH excitation spectrum showed a band at this photon energy [5].

In addition, there is another method to get circularly polarized PH emission without using circularly polarized pump excitation. Following excitation over the optical gap using unpolarized or linearly polarized light, triplet excitons are formed in the Pt-polymers in record time. Since the *spin relaxation time* in these polymers is much shorter that the *triplet lifetime*, then the triplet sublevel population reaches thermal equilibrium, where the three spin sublevels are populated by a Boltzmann distribution. Because the three spin sublevels possess different degree of emitting circularly polarized light, the thermal equilibrium reached at zero magnetic field may induce circularly polarized PH emission. In a strong magnetic field, the three spin sublevels are simply $m = 1, 0$, and -1, of which circularly polarized emission is, respectively, clockwise, linear, and anticlockwise. Under these conditions, the strength of the circularly polarized PH emission changes linearly of the magnetic field and then saturates at large field compared to the triplet zero-field splitting parameters.

In summary, because of the strong SOC of the Pt-polymers, the ISC rate is large, phosphorescence emission is substantive, and OLED based on these polymers may show white electroluminescence based on the two emission bands, namely, fluorescence (FL) and phosphorescence (PH) bands.

In addition circularly polarized emission peculiar to other π-conjugated polymers may be also obtained with the Pt-polymers.

Related Entries

► Conjugated Polymer Synthesis

References

1. Sun YR et al (2006) Management of singlet and triplet excitons for efficient white organic light-emitting devices. Nature 440:908–912
2. Dyer-Smith C et al (2010) Triplet formation in fullerene multi-adduct blends for organic solar cells and its influence on device performance. Adv Funct Mater 20:2701–2708
3. Wilson JS et al (2000) Triplet states in a series of Pt-containing ethynyleness. J Chem Phys 113:7627–7635
4. Wilson JS et al (2001) Spin-dependent exciton formation in π-conjugated compounds. Nature 413:828–831
5. Khachtryan B, Nguyen TD, Vardeny ZV, Ehrenfreund E (2012) Phosphorescence superradiance in a Pt-containing π-conjugated polymers. Phys Rev B 86:195203
6. Sheng C-X, Singh S, Gambetta A, Drori T, Tong M, Tretiak S, Vardeny ZV (2013) Ultrafast intersystem-crossing in platinum containing π-conjugated polymers with tunable spin-orbit coupling. Sci Rep 3:2653
7. Furuta PT, Deng L, Garon S, Thompson ME, Frechet JMJ (2004) Platinum-functionalized random copolymers for use in solution-processible, efficient, near-white organic light-emitting diodes. J Am Chem Soc 126:15388–15389
8. Springborg M, Albers RC (1996) Electronic structure of Pt in polyene. Phys Rev B 53:10626–10631
9. Johnson BFG, Kakkar AK, Khan MS, Lewis J, Dray AE, Friend RH, Wittmann F (1991) Synthesis and optical spectroscopy of platinum-metal-containing di- and tri-acetylenic polymers. J Mater Chem 1:485–486
10. Khaletskii A, Doklady M (1956) The chemistry of piazothiole (3,4-benzo-1,2,5-thiadiazole). Chemistry 106:31–34
11. Khan MS, Al-Mandhary MRA, Al-Suti MK, Raithby PR, Ahrens B, Male L, Friend RH, Kohler A, Wilson J (2003) Synthesis and characterization of new acetylide-functionalized aromatic and

hetero-aromatic ligands and their dinuclear platinum complexes. Dalton Trans 65–73

12. Vardeny ZV, Wei X (1998) Optical probes of photoexcitations in conducting polymers. In: Skotheim TA, Elsenbaumer RL, Reynolds J (eds) Handbook of conducting polymers, 2nd edn. Marcel Dekker, New York, pp 639–671

Polyphenylenes

A. Dieter Schlüter
Institute of Polymers, ETH Hoenggerberg,
Zürich, Switzerland

Synonyms

Aromatic polymers; Conjugated polymers; Rigid-rod polymers

Definition

The phenylene units in polyphenylenes (PP) are connected to one another through carbon-carbon single bonds resulting in linear polymers comprised of carbon and hydrogen atoms only (Fig. 1). No functional groups such as esters or amides are in between the phenylenes (or benzene-diyls) as is the case in the perhaps more common aromatic polyesters, polyamides, and the like. The hexagonal phenylene units can in principle be connected in 1,2-fashion (*ortho*), 1,3-fashion (*meta*), or 1,4-fashion (*para*) leading to the corresponding poly(*ortho-*, *meta-*, or *para*-phenylene)s. Mixtures thereof can also be realized like in the poly(*meta-para*-phenylene), **1**, shown in Fig. 1 [1]. By far the largest attention received the poly(*para*-phenylene)s (PPP), which is the reason why this article concentrates on them. Because of their straight main chain, parent PPP and its manifold laterally substituted derivatives such as the hexyl chain-decorated polymer **2** [2] are often viewed as prototype rigid-rod polymers. This suggests self-assembly (mesophase) behavior as a possible field of application. PPPs are also of interest because of the potential conjugation

between consecutive repeat units (RUs), the magnitude of which depends of the dihedral angle between consecutive phenylenes. This in turn depends on the substituents on the backbone and the conditions under which the polymer is investigated (e.g., solution or bulk). Sterically demanding substituents increase the dihedral angle and thus decrease conjugation, while clips between consecutive phenylene rings, forcing them into a coplanar conformation, can give rise to maximum conjugation. The conjugated nature of PPPs results in attractive optoelectronic properties which is nicely shown by the partially bridged polyfluorenes (**PF**) [3] and the completely bridged ladder-type structures such as **3** (see below) [4]. PPs are a special case of polyarylenes in which the RUs can in principal be any aromatic moiety including hetaromatics.

History

There are a number of early attempts towards synthesis of PPs with the three different linkage motifs. Three of them shall be discussed a bit further. Kovacic published a *direct* method in which benzene was polymerized with Friedel-Crafts catalysts under oxidative conditions [5]. While this chemistry was particularly easy to perform, the obtained products were insoluble and intractable and their structure was irregular. Ballard and his coworkers from the former ICI in England devised a precursor or *indirect* route to high molar mass PP but failed to obtain a product with one kind of linkage only (preferably 1,4). Rather 1,2-linkages also occurred to a sizeable degree. Later, Grubbs solved the issue of stereoregularity of the precursor polymer [6]. Yamamoto, finally, applied Kumada's transition metal-mediated cross-coupling chemistry in the presence of metallic magnesium mainly to 1,4-dihalobenzenes to arrive at parent PPP [7]. This resulted in the first structurally defined representative of the PP family with a specific 1,4-connectivity with, however, rather limited molar mass. The growing polymer chains early on "realize" their restricted conformational space and also their rigid-rod character and therefore precipitate out of solution already after about
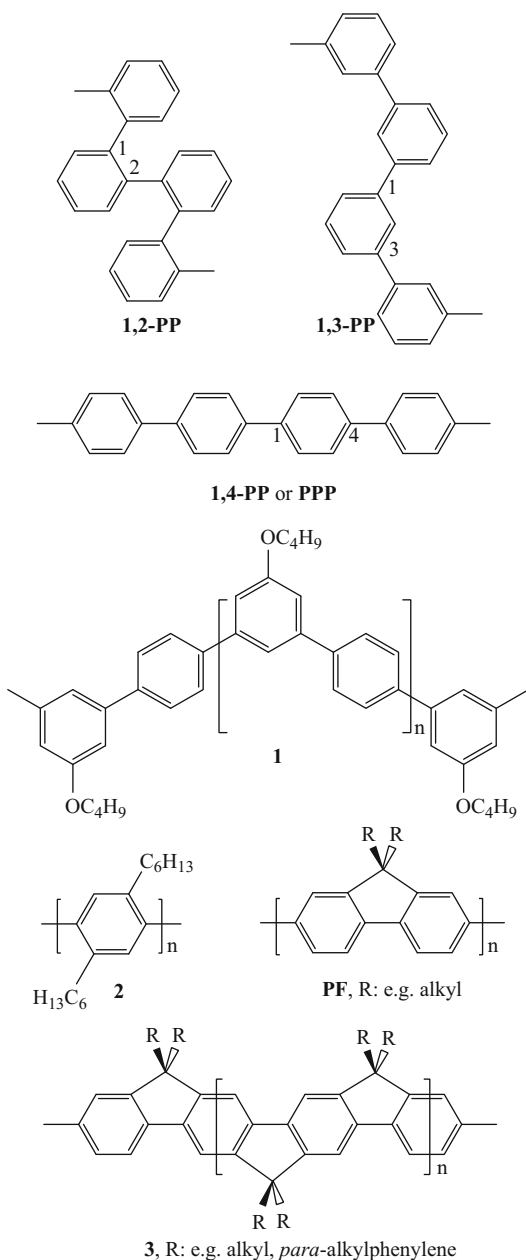
Polyphenylenes, Fig. 1 Chemical structures of PPs with 1,2-, 1,3-, and 1,4-connectivity and two particular PPs, one with two different connectivities, **1**; and another which is strictly 1,4-connected but is decorated with two flexible alkyl chains at every RU, **2**. Two important derivatives of PP, the polyfluorenes (**PF**) and the ladder polymers **3**, are also given

10–15 RUs. Nevertheless, because of its regioregularity this work is to be considered a milestone in PP synthesis. It should be noted that the Yamamoto route very much like Kovacic's method is a *direct* approach to PPs. As will be seen, the best method presently available also starts from benzene derivatives which are coupled to one another directly.

Conjugated polymers were a very hot topic in the 1980s when it was discovered that polyacetylene (PA) upon oxidation or reduction ("doping") turns into a highly electrically conducting material [8]. Doped PA shows metallike conductivity and normalized by weight can reach conductivities competitive to metallic copper. This discovery stimulated major efforts also into other hydrocarbon conjugated polymers. Interestingly, Kovacic PP exhibits the same main characteristics in terms of conductivity upon oxidation as PA despite its ill-defined chemical structure, although the conductivities are much lower. This was part of the motivation for what in retrospect can be considered the next important milestone in PPP synthesis: the application of the Nobel Prize-winning Suzuki-Miyaura cross-coupling (SMCC) [9] to bifunctional aromatic monomers carrying solubilizing flexible chains. This development took place in the late 1980s at the Max-Planck-Institute for Polymer Research in Mainz, Germany, and led to the first high molar mass, yet soluble and processable PPPs (next chapter) [10].

Synthesis

A good *direct* synthesis of PPPs needs to consider two key issues: the intrinsically low solubility of rigid rods and an as high as possible conversion per bond formation step. Otherwise high molar masses will not be accessible because either the growing polymer precipitates prematurely, which suppresses further growth, or Carothers equation [11] shows its power, and only short chains are produced because of the statistical nature of this step-growth polymerization. In the late 1980s, it was already known what to do to increase the

AA/BB approach

AA-Monomer   BB-Monomer

[cat] / Base

AB approach

AA-Monomer

[cat] / Base

AA/BB approach : Example

$(HO)_2B$ ... $B(OH)_2$ + Br ... Br → ...

C_6H_{13}

C_6H_{13}

3   **4**   **5**
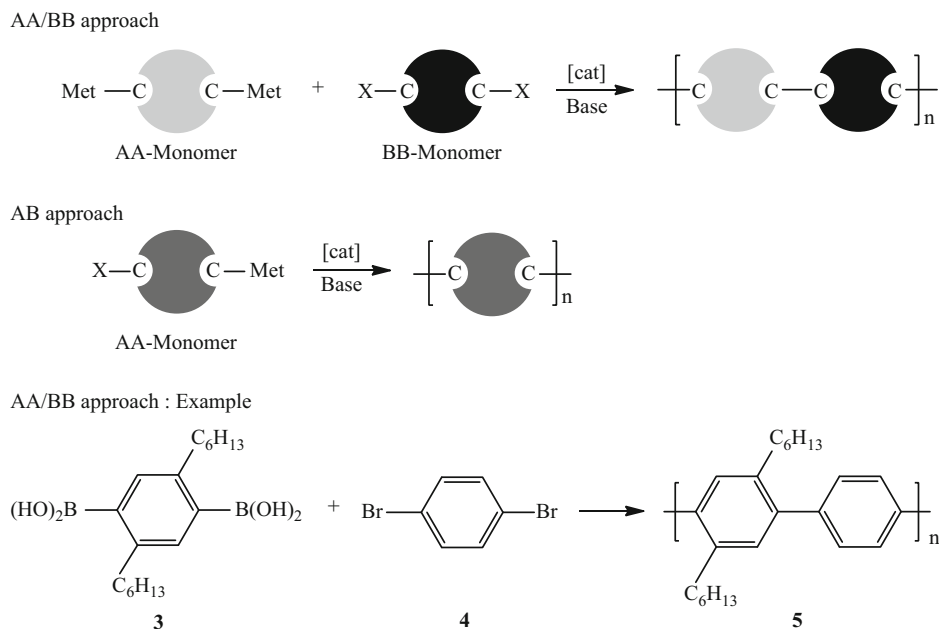
Polyphenylenes, Fig. 2 The two main synthetic approaches: the AA/BB case using two monomers with complementary functional groups and the AB case using one monomer only which carries the two complementary functional groups at the same time. For the AA/BB approach, a concrete example is also shown. Note the flexible hexyl chains that serve to mediate sufficient solubility both to keep the growing chain in solution and to obtain processable materials. *Met* metal cations such as Mg^{2+} and Zn^{2+} or boronic acids/boronic acid esters, *X* leaving groups such as halides and triflates, *[cat]* transition metal (0) complexes such as Pd

solubility of otherwise insoluble materials [12]: The attachment of flexible chains increases the entropy when going into solution, and at the same time disturbs the packing in the solid state disfavoring crystallization. Equipped with this knowledge and the then still recent SMCC of bromobenzene with benzene boronic acid to give biphenyl in a yield of 99 % (!) [13] made Rehahn et al. to try the chemistry shown in Fig. 2 [2]. They combined AA monomer **3** with BB monomer **4** and, in fact, obtained polymer **5** which turned out to be fully soluble (even) in chloroform at room temperature, an unheard of property of a rigid rod at that time. They also tried the AB approach with similar success. Because the catalyst used had commercial grade quality, the molar mass did not exceed 20–30 kDa at that time, which however was vastly improved by using highly pure Pd complexes instead. This discovery of what now is known as Suzuki polycondensation (SPC) [10] has led to hundreds of publications and countless patents. Even technical scale syntheses based on microreactor technology have been developed using this powerful polymerization.

Figure 2 does not specify the nature of the functional group in monomers (Met and X) in order to make clear that SPC is not the only transition metal-mediated cross-coupling polycondensation which can in principle be used. While X is always a leaving group such as bromide or chloride and triflate for all methods, the nature of the metal has also been varied and decides over how the method is called. In SPC it is always a boron-based group (boron is not a metal but rather a metalloid), whereby boronic acid pinacol ester is often applied for simplicity of purification of the monomers carrying this group. However, for example, Kumada, Negishi, and Stille chemistry where Mg, Zn, and Sn,

P

respectively, take the role of boron have also been employed. In most cases, SPC seems to be superior in terms of achievable molar mass. Extremely high molar masses in the range of a 10E6 Da have been claimed for this method in the patent literature [10]. Note that Yokozawa and Kiriy collected evidence that in certain cases SPC may proceed according to a chain-growth process [14, 15].

Applications

PPs in all their forms and variants found widespread applications [10]. They range from tough, amorphous (transparent) films, which are competitive to commercial polycarbonate [1], to blue emitters in polymer-based organic light-emitting diodes (OLEDs), where certain representatives even reached commercial relevance [16, 17]. A comprehensive and recent review on this rather important field of electroluminescence of PPs and related conjugated polymers is available in Ref. [18]. Particularly for the use of PPs (here PFs) in electro-optical devices, it was of crucial importance to master synthesis to the degree that defects are suppressed. Otherwise they can dominate the performance in a detrimental way [19]. PPPs and other conjugated polymers were also investigated for photonic applications, e.g., in semiconducting polymer lasers [20]. Finally their interesting lyotropic behavior leading to anisotropic micelles shall be mentioned as well as the fact that charged versions served as study objects for how rigid polyelectrolytes order themselves in solution, and a few studies dealt with aspects such as molecular reinforcement [10].

Related Entries

▶ Chain-Growth Condensation Polymerization
▶ Conducting Polymers
▶ Conjugated Polymer Synthesis
▶ Ladder-Type Polymers
▶ Polymerization Reactions (Overview)

References

1. Kandre R et al (2007) Suzuki polycondensation put to work: a tough poly(*meta*-phenylene) with a high glass-transition temperature. Angew Chem Int Ed 46:4956–4959. doi:10.1002/anie.200700966
2. Rehahn M, Schlüter AD, Wegner G (1990) Soluble poly(*para*-phenylene)s. Makromol Chem 191:1991–2003
3. Leclerc M (2001) Polyfluorenes: twenty years of progress. J Polym Sci Part A Polym Chem 39:2867–2873. doi:10.1002/pola.1266
4. Scherf U, Müllen K (1991) Polyarylenes and poly(arylenevinylene)s.7. A soluble ladder polymer via bridging of functionalized poly(*para*-phenylene)-precursors. Makromol Chem Rap Commun 12:489–497. doi:10.1002/marc.1991.030120806
5. Kovacic P, Jones MB (1991) Dehydro coupling of aromatic nuclei by catalyst-oxidant systems: poly(*p*-phenylene). Chem Rev 87:357–379
6. Gin DL, Conticello VP, Grubbs RH (1994) Stereoregular precursors to poly(p-phenylene) via transition-metal-catalyzed polymerization. 2. The effects of polymer stereoregularity and acid catalysts on precursor aromatization: a characterization study. J Am Chem Soc 116:10934–10947
7. Yamamoto T (2010) Organometallic polycondensation for conjugated polymers. In: Chujo Y (ed) Conjugated polymer synthesis: methods and reactions. Wiley-VCH, Weinheim
8. Chiang CK, Druy MA, Gan SC, Heeger AJ, Louis EJ, McDiarmid AG, Park YW, Shirakawa H (1978) Synthesis of highly conducting films of derivatives of polyacetylene, $(CH)_x$. J Am Chem Soc 100:1013–1015
9. Miyaura N, Suzuki A (1995) Palladium-catalyzed cross-coupling reactions of organoboron compounds. Chem Rev 95:2457–2483. doi:10.1021/cr00039a007
10. Sakamoto J et al (2009) Suzuki Polycondensation: Polyarylenes à la Carte. Macromol Rapid Commun 30:653–687. doi:10.1002/marc.200900063
11. Cowie JMG (1973) Polymers: chemistry and physics of modern materials. International Textbook Company, Aylesbury
12. Ballauff M (1989) Stiff-chain polymers – structure, phase-behavior, and properties. Angew Chem Int Ed Engl 28:253–267. doi:10.1002/anie.198902533
13. Miyaura N, Yanagi A, Suzuki A (1981) The palladium-catalyzed cross-coupling reaction of phenylboronic acid with haloarenes in the presence of bases. Synth Commun 11:513–519
14. Yokoyama A, Suzuki H, Kubota Y, Ohuchi K, Higashimura H, Yokozawa T (2007) Chain-growth polymerization for the synthesis of polyfluorene via Suzuki–Miyaura coupling reaction from an externally added initiator unit. J Am Chem Soc 129:7236–7237. doi:10.1021/ja070313v

15. Elmalem E, Kiriy A, Huck WTS (2011) Chain-growth Suzuki polymerization of n-type fluorene copolymers. Macromolecules 44:9057–9061

16. Scherf U, Neher D (2008) Polyfluorenes. Adv Polym Sci 212, Springer, Berlin/Heidelberg. doi:10.1007/978-3-540-68734-4

17. Grimsdale AC, Müllen K (2006) Polyphenylene-type emissive materials: poly(*para*-phenylene)s, polyfluorenes and ladder polymers. Adv Polym Sci 199:1–82. doi:10.1007/12_076

18. Grimsdale AC et al (2009) Synthesis of light-emitting conjugated polymers for applications in electroluminescent devices. Chem Rev 109:897–1091

19. Scherf U, List EJW (2002) Semiconducting polyfluorenes: towards reliable structure-property relationships. Adv Mater 14:477–487. doi:10.1002/1521-4095

20. Hide F, Diaz-Garcia MA, Schwartz BJ, Heeger AJ (1997) New developments in the photonic applications of conjugated polymers. Account Chem Res 30:430–436

Polypropylene

Yoshinori Takashima
Department of Macromolecular Science,
Graduate School of Science, Osaka University,
Machikaneyama, Toyonaka, Osaka, Japan

Synonyms

Polypropene; Poly(propene), PP

Definition

Polypropylene (PP), which is prepared by polymerization of propylene, forms transparent and translucent crystalline plastics, thermoplastic resins, and heat-resistant compounds. The polymer properties highly depend on the tacticities (isotactic, syndiotactic, and atactic).

Introduction

Polypropylene (PP) is one of commodity plastics (e.g., polyethylene, polystyrene, acrylonitrile butadiene styrene resin, polyvinyl chloride, and polymethyl methacrylate) (Fig. 1) [1, 2]. The history of polypropylene began in 1954 when German chemist Karl Rehn and Italian chemist Giulio Natta first polymerized propylene. PP is prepared with an organometallic olefin polymerization catalyst. A certain type of organometallic olefin polymerization catalysts with bulky ligands yields crystalline isotactic and syndiotactic PP. Atactic PP materials with amorphous structures, which are prepared by organometallic catalyst without stereoregularity capability, are used as additive molding agents because they have excellent solubility, adherence, printing capabilities, and gas barriers. Although the properties of atactic PP materials are similar to those of polyethylene (PE), PP has higher heat resistance and mechanical strength, improving the stretching property and resistance to fatigue. Isotactic and syndiotactic PP materials are used in films, sundry goods, automotive products, industrial products, and textiles. In addition, propylene is polymerized with olefin derivatives (e.g., ethylene, hexane, etc.) to produce an elastic propylene copolymer.

Chemical Structure and Physics

Tacticity (Stereoregularity)

Tacticity is an important concept to understand the relation between the chemical structure and physical properties. The orientation of each methyl group relative to the methyl groups in neighboring monomer units greatly influences the crystalline properties of PP. PP has an asymmetric carbon atom, which determines the absolute configuration of the polymer structure. This stereoregularity is called "tacticity." Isotactic, syndiotactic, and atactic structures of PP are prepared by coordination polymerization. In isotactic polymers, all the substituents are located on the same side of the polymer backbone. Specifically, the methyl groups of the PP side chain are oriented in the same direction. The absolute configuration of propylene units in isotactic PP is the same, whereas, in syndiotactic polymers the

P

Polypropylene,
Fig. 1 Chemical structure
of commodity plastics

Poly(ethylene)   Poly(propylene)   Poly(styrene)

Poly(vinyl chloride)

ABS resin
(Acrylonitrile-Styrene-Acrylate resin)

AS resin
(Acrylonitrile styrene resin)   Poly(methyl methacrylate)
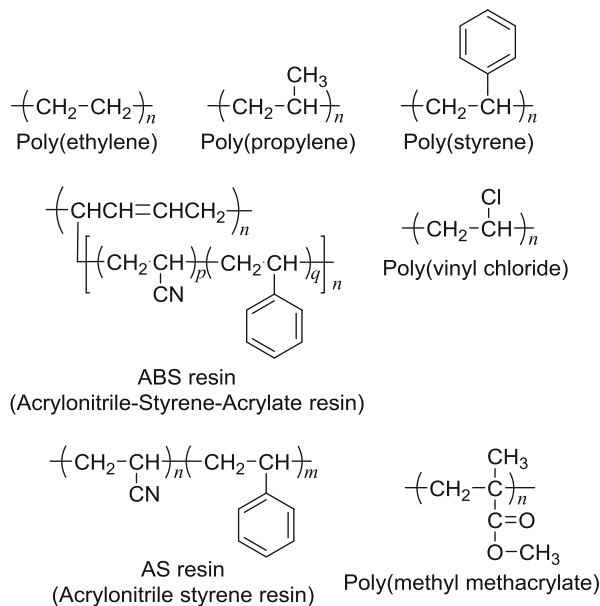
absolute configuration of the asymmetric carbon atom is alternatively arranged in along the chain. In atactic polymers, the substituent groups are arranged randomly along the chain (Fig. 2). The tacticity can be determined using ^{13}C-NMR (nuclear magnetic resonance) to analyze the meso (the same orientation of the methyl group in neighbor units) and racemo (opposite orientation of the methyl group in neighbor units) ratio along the chain. Ziegler–Natta catalysis produces isotactic PP, while radical polymerization yields atactic PP. Isotactic polymers are usually semicrystalline and often form a helix configuration.

Physical Properties

The physical properties of PP greatly differ in tacticity. Isotactic and syndiotactic PP is semicrystalline and forms a helix configuration. However, atactic PP does not form a crystalline structure. The crystal structure of isotactic PP forms a 3/1 helix, forming α (monoclinic system), β, γ, and smectic systems. The crystal structure of syndiotactic PP forms a 2/1 helix based on an orthorhombic system.

The melting point of PP varies in accordance with the tacticity. In particular, the melting point and glass-transition point of isotactic PP are 160–166 °C and ~20 °C, respectively, which depend on the molar fraction of the meso ratio. However, perfectly isotactic PP exhibit 176 °C and –10 °C, respectively. An increase in the ratio of the meso, diad, and triad of PP increases the melting point [3].

Chemical Properties

PP shows chemical resistance; it is not deteriorated by acid, base, hot water, oil, etc. On the other hand, PP without an antioxidant is relatively oxidized by oxygen in air. The generated third carbon radical reacts with oxygen to produce hydroperoxide, which deteriorates via a chain reaction. At a high temperature, PP is easily oxidized during the mold process. The main chain of PP deteriorates by UV light irradiation under sunlight. To improve the anti-weatherability, benzophenone, benzotriazole, and carbon black are added as UV absorbents.

Preparation of Polypropylene

Radical polymerization of propylene does not give high-molecular-weight PP because the hydrogen at the allyl position has a high reactivity. Moreover, PP prepared by radical polymerization forms an atactic polymer with a low molecular weight. The coordination polymerization plays an
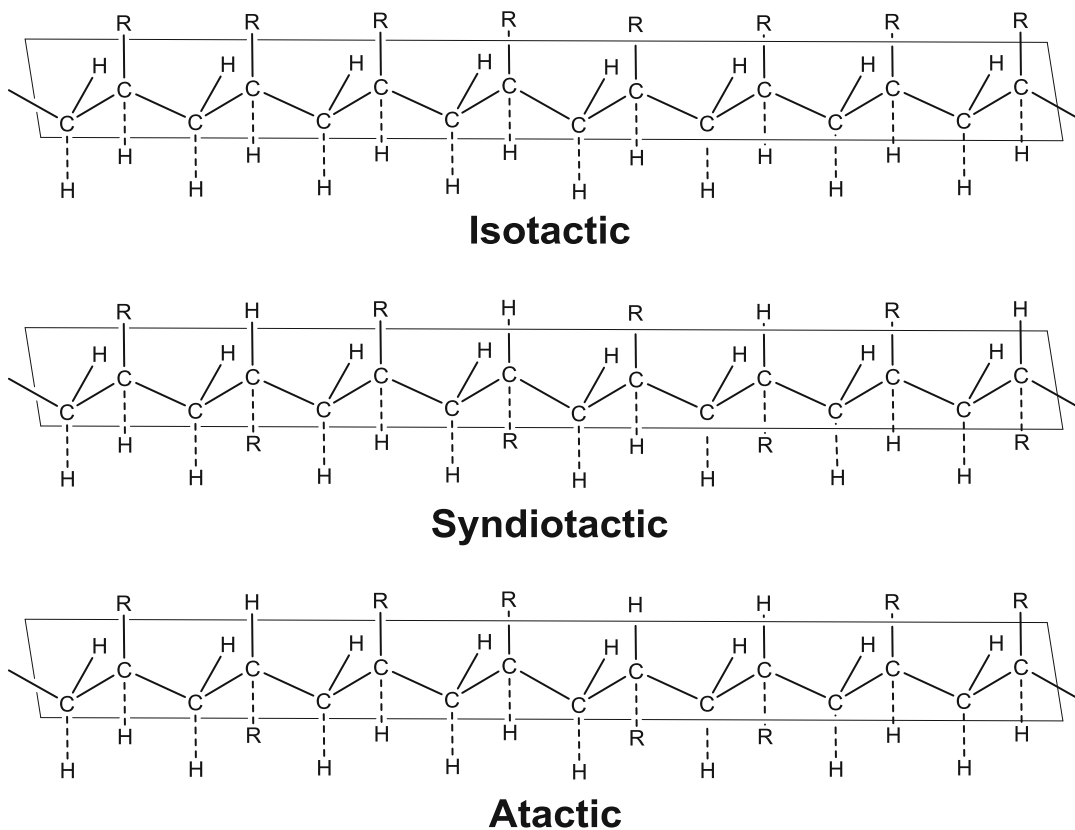
Polypropylene, Fig. 2 Tacticity of poly(propylene)

important role in realizing industrially useful iso-tactic and syndiotactic PP [3].

Polypropylene Prepared by the Ziegler–Natta Catalyst

In 1953, Karl Ziegler found an excellent polymer-ization catalyst for ethylene by mixing $TiCl_4$ and AlR_3 (trialkyl aluminum) [4]. The mixture forms $TiCl_3$, which is the real catalytic species. On the other hand, a mixed catalyst is unsuited for the polymerization of propylene to prepare higher atactic PP due to the multi-binding sites of the monomer. In 1954, Giulio Natta from Italy and Karl Rehn from Germany found that a mixture of $TiCl_3$ and AlR_2Cl (dialkyl aluminum) exhibits a high polymerization activity to produce isotactic PP [5]. A mixture of halides of transition metals to prepare polymers from α-olefins (1-alkenes) is called Ziegler–Natta catalysts. Early transition metals (e.g., titanium, chromium, vanadium, and

zirconium) are used as olefin polymerization catalysts, but these catalytic systems require the addition of organic derivatives of nontransition metals, particularly alkyl aluminum compounds as cocatalysts. Ziegler and Natta were awarded the Nobel Prize in Chemistry in 1963.

The Ziegler–Natta catalysts are categorized as either heterogeneous-supported catalysts or homo-geneous catalysts. $TiCl_4$ with terephthalic esters as a Lewis base-supported $MgCl_2$ shows a high poly-merization activity in heterogeneous-supported cat-alysts. The catalyst with phthalic ester as a Lewis base instead of a benzoic acid derivative exhibits a high polymerization activity (600–1,300 kg/g) and a high isotacticity (97 %) [6, 7].

Polypropylene Prepared by Metallocene Catalysts

Metallocene catalyst is one of the important poly-merization catalysts in the homogeneous olefin

P
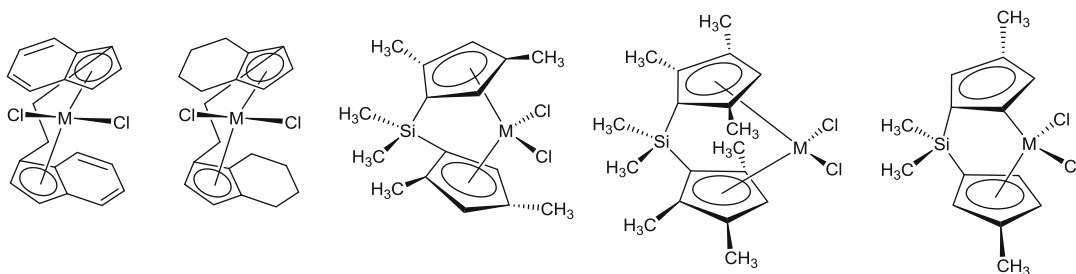
Polypropylene, Fig. 3 Typical examples of metallocene catalysts for propylene

Polypropylene, Fig. 4 Chemical structures of post-metallocene catalysts
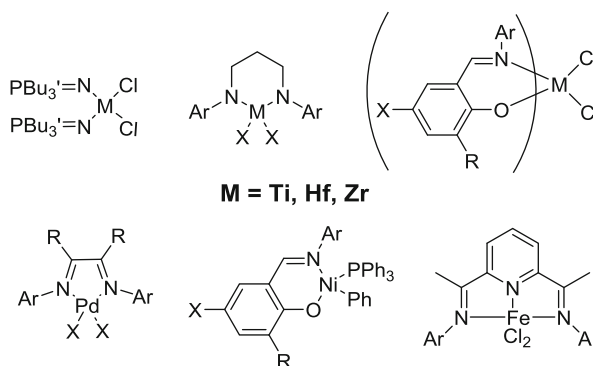
polymerization catalyst [8, 9]. A metallocene catalyst is composed of a metallocene consisting of two cyclopentadienyl anions (Cp, which is $C_5H_5^-$) bound to a transition metal center and methyl aluminoxane (MAO). Unlike heterogeneous catalysts, metallocene catalysts can easily control the tacticity of the resulting PP as a function of ligand designs [10]. Depending on the chemical structure of the ligand, the catalysts effectively provide isotactic [11, 12] and syndiotactic PP (Fig. 3). A typical cocatalyst is MAO, but borate derivatives and clay composites (e.g., montmorillonite) also show excellent cocatalyst abilities. The catalyst is referred to as a single-site catalyst due to having a single reactive point [12–14].

Polypropylene Prepared by Post-Metallocene Catalysts

In the late 1990s, high-activity olefin polymerization catalyst without the metallocene structure developed one after the other. Although Cp-type later transition metal complexes with iron (Fe), nickel (Ni), and palladium (Pd) do not show polymerization activity for ethylene and propylene, their complexes with a another certain type of ligand (e.g., diimine ligand, phenoxy imine ligand, bis(imino)pyridine ligand, etc.) show a high polymerization activity for these compounds. These nitrogen-based metal complexes are called "post-metallocene catalysts." Post-metallocene catalysts have bulky ligands to control the coordination of propylene. For example, a zirconium complex with a salicylimine ligand exhibits a high activity for propylene and high tacticity control for PP (Fig. 4). Although post-metallocene catalysts have received attention due to their excellent properties, more research is necessary before this technology can be practically used [15–18].

References

1. Karian HG (2003) Handbook of polypropylene and polypropylene composites, 2nd edn. Marcel Dekker, New York, Revised and expanded. [In: Plast Eng (New York, NY, U. S.), 2003; 67]. ISBN 0824740645

2. Pasquini N (ed) (2005) Polypropylene handbook, 2nd edn. Carl Hanser Verlag, Munich. ISBN 156990385-9

3. Bai F, Li F, Calhoun BH, Quirk RP, Cheng SZD (1998) Physical constants of polypropylene. In: Brandrup J, Immergut EH (eds) Polymer handbook, 4th edn. Wiley, New York

4. (a) Ziegler K, Gellert HG, Zosel K, Lehmkuhl W, Pfohl W (1955) Aluminum in organic chemistry. Preparation of aluminum alkyls and dialkylaluminum hydrides. Angew Chem 67:424. (b) Ziegler K, Holzkamp E, Breil H, Martin H (1955) The M. ovrddot.uhlheim low-pressure polyethylene process. Angew Chem 67:541–547

5. Natta G (1955) A new class of polymers from α-olefins having exceptional structural regularity. J Polym Sci 16:143–154

6. Kashiwa N (1980) Super active catalyst for olefin polymerization. Polym J (Tokyo) 12:603–608

7. Hoff R, Mathers RT (eds) (2010) Handbook of transition metal polymerization catalysts. Wiley, Hoboken. doi:10.1002/9780470504437. ISBN 9780470137987

8. Sinn H, Kaminsky W (1980) Ziegler-Natta catalysis. Adv Organomet Chem 18:99–149

9. Ewen JA (1984) Mechanisms of stereochemical control in propylene polymerizations with soluble Group 4B metallocene/methylalumoxane catalysts. J Am Chem Soc 106:6355–6364

10. Kaminsky W, Kulper K, Buschermohle M, Luker H (1988) Process for the preparation of polyolefins. US4769510, ACA1264399A1, DE3443087A1, EP0185918A2, EP0185918A3, EP0185918B1

11. Spaleck W, Antberg M, Rohrmann J, Winter A, Bachmann B, Kiprof P, Behm J, Herrmann WA (1992) High-molecular-weight polypropylene via mass-tailored zirconocene-type catalysts. Angew Chem 104:1373–1376 (See also (1992) Angew Chem Int Ed Engl 1331(1310):1347–1350)

12. Hill AF (2002) Organotransition metal chemistry. Royal Society of Chemistry, London. ISBN 0854046224

13. Kissn Y (ed) (2008) Alkene polymerization reactions with transition metal catalysts, vol 173. Elsevier, Amsterdam. ISBN 9780444532152

14. Alt HG, Koeppl A (2000) Effect of the nature of metallocene complexes of group IV metals on their performance in catalytic ethylene and propylene polymerization. Chem Rev (Washington, DC) 100:1205–1221

15. Kennedy JF, Turan N (1999) In: Stevens MP (ed) Polymer chemistry: an introduction, 3rd edn. Oxford University Press, New York. ISBN 0195124448

16. Ittel SD, Johnson LK, Brookhart M (2000) Late-metal catalysts for ethylene homo- and copolymerization. Chem Rev (Washington, DC) 100:1169–1203

17. Younkin TR, Connor EF, Henderson JI, Friedrich SK, Grubbs RH, Bansleben DA (2000) Neutral, single-component nickel(II) polyolefin catalysts that tolerate heteroatoms. Science (Washington, DC) 287;460–462

18. Giambastiani G, Campora J (eds) (2011) Olefin upgrading catalysis by nitrogen-based metal complexes II: state-of-the-art and perspectives. Springer, Dordrecht. ISBN:9789048138142, ISBN:9789400706958. [In: Catal Met Complexes, 2011; 36]

Polyrotaxanes (Conjugated)

Francesco Di Stasio[1], Sergio Brovelli[2],
Sophia C. Hayes[3] and Franco Cacialli[4]
[1]Istituto Italiano di Tecnologia, Genoa, Italy
[2]Dipartimento di Scienza dei Materiali,
Università degli Studi di Milano-Bicocca,
Milan, Italy
[3]Department of Chemistry, University of Cyprus,
Nicosia, Cyprus
[4]Department of Physics and Astronomy, and
London Centre for Nanotechnology, University
College London, London, UK

Synonyms

Cyclodextrins; Electroluminescence; Interchain interactions; Polarized emission; Thermal stability

Definition

Conjugated polyrotaxanes are supramolecular model materials for studying the photophysics of intermolecular interactions in organic semiconductors and their heterojunctions.

Optical Properties of Conjugated Polyrotaxanes: Control and Tuning of Intermolecular Interactions

Intermolecular interactions affect the chemical, biological, and physical properties of a huge variety of systems [1] such as protein folding [2], prion formation, and cellular organization [3],

P

as well as the rich photophysics of natural dyes and synthetic organic semiconductors [4, 5]. The underpinning science of such interactions is thus significantly relevant for the development of consumer electronics displays and other optoelectronics applications.

Control of excited states dimensionality in electronic and photonic materials is recognized as an effective tool for tailoring their photophysics. For example, since their discovery, conjugated polymers have been studied as model systems for one-dimensional (1D) semiconductors, but their physical properties in thin films and large molecular ensembles are dominated by three-dimensional (3D) effects due to significant intermolecular interactions. The presence of strong intermolecular interactions and the formation of excited states spreading over more than one molecular unit give rise to a redshift of the photoluminescence (PL) spectrum and a lower radiative rate [6]. This is due to either ground-state electronic interactions ("aggregates") or formation of excited-state dimers (or "excimers" within the language of molecular photophysics of aromatic compounds).

Conjugated polyrotaxanes [7–9] provide a remarkable model system for studying the influence of interchain interactions on the electronic dynamics of organic semiconductors [10]. Cyclodextrin insulation reduces the ubiquitous intermolecular interactions [11], which control their photophysics without affecting the electronic levels of the frontier orbitals by suppressing the tendency to form aggregates or weakly coupled excimers [12, 13] detrimental for luminescence efficiency and color purity [6]. While formation of interchain species is more likely in the solid state and in concentrated solutions, even in dilute aqueous solutions of aromatic unthreaded chains the photoluminescence decay displays long-lived components and is both non-exponential and strongly dependent on concentration. Concomitant with a redshifted time-integrated emission, these are optical signatures of interchain species. However, polyrotaxane photoluminescence decay dynamics are exponential and independent of concentration despite the incomplete shielding of the conjugated cores by the cyclodextrins [9, 14].

Furthermore, photophysical and electroluminescence studies of polyrotaxanes with increasing degree of threading (quantifiable by the so-called threading ratio, TR) show that progressive supramolecular encapsulation preserves the photophysics of the isolated chains without affecting solid films charge transport, thus yielding enhanced and blueshifted electroluminescence with respect to unthreaded conjugated polymers. Incorporation of luminescent polymers into cyclodextrin macrocycles also reduces energy transport rates and therefore exciton diffusion to quenching sites [15, 16] or redshift of the luminescence [17]. Such properties are all highly relevant to the development of conjugated semiconductors for optoelectronics applications. In addition, since cyclodextrin threading is achieved via hydrophobic binding, which requires water solubility, polyrotaxanes are functionalized via addition of polar groups and are thus also conjugated polyelectrolytes (CPE), which are being intensively investigated for a variety of biosensing applications.

As an illustrative example of the versatility of cyclodextrin encapsulation for achieving fine control of the optical properties of semiconducting organic polymers, both water-soluble (polyelectrolitic) and organic-soluble conjugated polyrotaxanes are going to be discussed (Fig. 1 shows different types of conjugated backbones together with the chemical structure of α-, β-, and γ-cyclodextrins).

Photophysics of Polyrotaxanes

Spectroscopic investigations of diluted solutions at different concentrations offer the most direct method to assess the consequences of threading on the formation and decay of interchain and intrachain excitonic species.

Time-integrated and time-resolved photoluminescence studies of diluted water solutions of PF.Li, PPP.Li, and PDV.Li (Fig. 1) and the same derivatives threaded with β-cyclodextrin macrocycles show that the polyrotaxanes PL spectrum and decay kinetic are independent from solution concentration. In fact, no spectral shift can be

Fig. 1 Chemical structures
of cyclodextrin-threaded
conjugated polyrotaxanes
with poly(4,4′-diphenylene
vinylene) (PDV.Li), poly
(para-phenylene) (PPP.Li),
and poly(fluorene) (PF.Li)
backbones with
naphthalene stoppers,
average degree of
polymerization: $n = 10$,
(Adapted from Ref. [7])
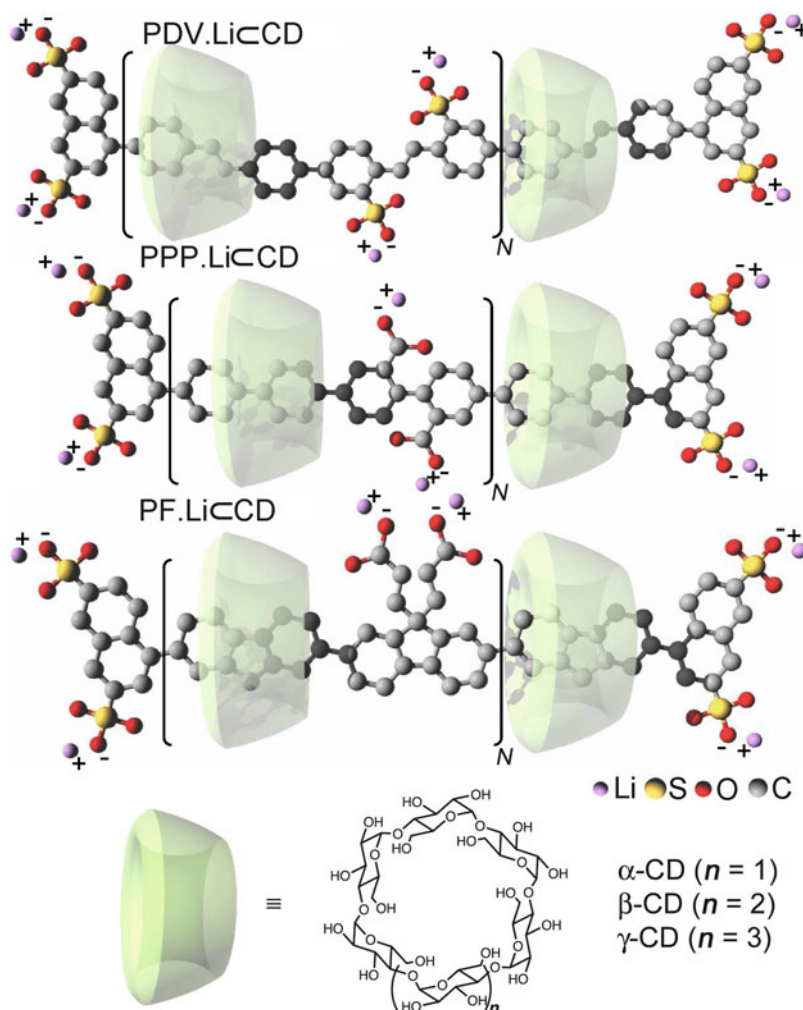
observed for the encapsulated system which shows remarkable single-exponential decay profiles for more than three decades even in high concentrated solutions. This is in contrast with the PL spectral behavior of the unthreaded polymer solutions, which evolve from matching the polyrotaxane emission in the most diluted case by displaying a progressive redshift and spectral broadening with increasing concentration [18].

Time-resolved PL measurements both spectrally resolved and at single wavelengths clearly show the suppression of intermolecular interactions. The PL kinetics at photon energies near the peak of the emission maximum for the polyrotaxanes show single-exponential decay kinetics independent of concentration, consistently with a monomolecular decay mechanism and a nearly complete suppression of aggregation. In comparison, the unthreaded material photophysics are instead strongly dependent on the solution concentration. The presence of two regimes in the emission decay confirms the coexistence of at least two emissive species with two different lifetimes: an intrachain exciton and a longer-lived emitting species. The single-exponential decay kinetics observed for the polyrotaxane is evidence that CD macrocycles largely prevent the formation of intermolecular excited states and ensure that the polyrotaxanes PL is dominated by intramolecular excitonic decay even at concentrations about three orders of magnitude higher than for the uninsulated analogues.

The clear prevalence of intramolecular de-excitation processes in polyrotaxane solutions, at the expense of interchain species formation, has a significant influence on the photoluminescence quantum yield. In fact, quantum efficiencies of polyrotaxane solutions are nearly concentration independent. This result is once again in contrast with what was observed for the unthreaded material solutions, whose PL quantum yields decrease with concentration. Furthermore, an overall increase in photoluminescence quantum yield is observed for polyrotaxanes compared to the unthreaded analogue.

Thermal Stability of Conjugated Polyrotaxane Conformation

Rotaxination imparts greater thermal stability to the polymer. Interestingly, the polymer is more susceptible to conformational fluctuations when it is unthreaded or at low TRs. The fingerprint region of the resonance Raman (RR) spectrum [19] of PDV.Li for progressive cyclodextrin encapsulation and increasing temperature shows a significant decrease in all the band intensities in the case of PDV.Li and PDV.Li$\subset\beta$- CD for threading ratio = 0.5 (TR) as the temperature increases from 25 °C to 40 °C and 55 °C. Interestingly, the drop in intensities observed for PDV.Li and PDV.Li$\subset\beta$- CD TR = 0.5 is not recovered upon cooling, suggesting that any changes that occur are nonreversible [19]. In contrast, no changes are observed in the spectra for the higher TR analogues, suggesting an increased stability conferred to the polymer by the β-cyclodextrin macrocycles. The results from the RR studies showed that any conformational changes with temperature involve torsional movement only between the adjacent phenyl rings (due to thermally induced aggregation) with no torsional changes at the vinylene group.

Oriented Films Incorporating Water-Soluble Conjugated Polyrotaxanes

Orientation of polyrotaxane chains can be induced via tensile drawing of a polyvinyl alcohol (PVA) matrix where the emitting polymer is dispersed. Steady-state and time-resolved photoluminescence measurements suggest that the polyrotaxane chains are mostly oriented along the stretching direction, giving rise to strong polarized emission.

To quantify the polarization resulting from the alignment of the polymeric chains, the PL polarization ratio (R) for all different excitation/detection configurations as shown in Fig. 2 has been calculated. In what follows, these will be indicated with the general notation $R_{xx/xy} = PL_{xx}/PL_{xy}$, $R_{xx/yy} = PL_{xx}/PL_{yy}$ where the first index represents the polarization of the excitation and the second one represents the polarization of the PL (parallel ∥ or perpendicular ⊥ to the stretching direction for stretch-oriented
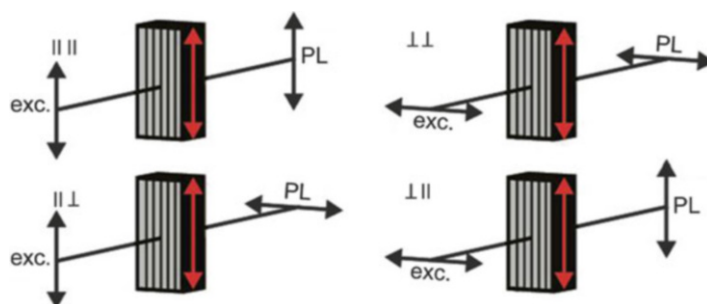
Polyrotaxanes (Conjugated), Fig. 2 Scheme of the four different configurations used to study the polarized photoluminescence. The *red arrow* represents the stretching direction for the oriented films and an arbitrary direction for unstretched films (Adapted from Ref. [20])
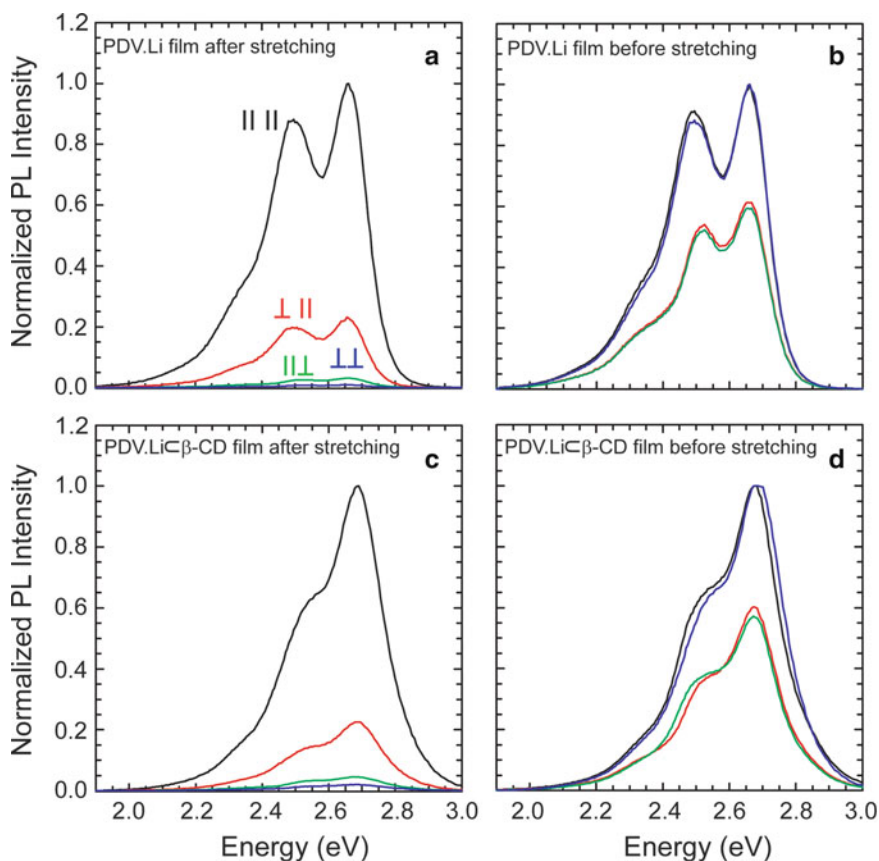
Polyrotaxanes (Conjugated), Fig. 3 PL spectra for stretched films (**a**, **c**) and unstretched films (**b**, **d**) with PDV.Li (**a**, **b**) or PDV.Li$\subset\beta$-CD (**c**, **d**). All spectra have been corrected for the overall system response and they were measured using a 3.3 eV laser diode as excitation source (Adapted from Ref. [20])

films and an arbitrary direction for unstretched films).

In Fig. 3, all PL spectra for the four different configurations are shown. The PL does not show any modification in spectral shapes upon stretching; in fact, the relative ratio between the vibronic peaks is maintained. The different polarization ratios (R) for all different configurations can be calculated. $R_{\|\|/\perp\perp}$ is ~51 for PDV.Li$\subset\beta$-CD and ~111 for PDV.Li (Fig. 3a, c). These values clearly demonstrate the high degree of chain alignment obtainable using a stretchable polymeric matrix such as PVA. Interestingly, this result also shows that the presence of the CDs partially hinders the alignment process. A tentative explanation is that CDs reduce the aspect ratio by increasing the thickness of the polymer chains impacting as well the

non-covalent interactions between the conjugated backbones and the PVA matrix.

The expected value of all these different ratios for a film with isotropic orientation is 1, since no differences in orientation are present and the emission of photons typically takes place from excited states not maintaining the initial polarization. For isotropic alignment or rapid exciton migration, $R_{\|\|/\|\perp} = R_{\|\|/\perp\|} = R_{\perp\perp/\|\perp} = R_{\perp\perp/\perp\|}$, which can be simplified in R⊥ to indicate the ratio of the luminescence from chromophores oriented parallel to the exciting laser and the PL from chromophores oriented perpendicular to the laser polarization. These results show that R⊥ ~ 1.75 for PDV.Li$\subset\beta$-CD and R⊥ ~ 1.60 for PDV.Li, higher values than expected. The higher value for the polyrotaxane film is due to the additional encapsulation provided by CDs [21]. However, R∥

has a value of 1 (as expected for random chromophore orientation) [22]. Once again, these results show that the presence of the CDs partially hinders the alignment of the conjugated backbone.

To investigate further the orientation of the conjugated strands induced by stretching of the PVA matrix, the time-resolved PL anisotropy $\gamma(t)$ at the PL peak value (~2.6 eV) for the configuration $\|\|/\perp$ were studied. Unstretched films show $\gamma(t = 0) \sim 0.36$ and $\gamma(t = 0) \sim 0.39$ for PDV.Li and PDV.Li$\subset\beta$-CD, respectively; both values are close to $\gamma(t = 0) = 0.4$ which is the maximum theoretical value for a randomly oriented ensemble of chromophores. This value corresponds to a rotation of the transition moment $\beta = 0°$; therefore, the absorption and emission moments of the conjugated chains are collinear [22]. Such a high level of PL anisotropy for randomly oriented chains is expected only for noninteracting chromophores [22], as for the polymers dispersed in the PVA matrix studied here. Stretched films instead show $\gamma(t) \sim 0.87$ and $\gamma(t) \sim 0.93$ for PDV.Li$\subset\beta$-CD and PDV.Li, respectively. In both systems, $\gamma(t)$ is constant for more than 6 ns, and since this value is approximately one order of magnitude longer than the intrachain exciton lifetime ($\tau \sim 870$ ps), negligible depolarization over this time regime can be assumed. Therefore, the data again imply that a high degree of orientation is obtained for both films, but the degree of orientation is slightly higher for PDV.Li than for PDV.Li$\subset\beta$-CD.

In summary, a high polarization ratio is obtained ($R_{\|\|/\perp\perp} = 111$ for PDV.Li) indicating that a high degree of orientation can be achieved. Supramolecularly encapsulated polymers can be employed to study the effect of intermolecular interaction on the emission anisotropy. Suppressed interchain interactions in polyrotaxanes combined with the PVA matrix result in slower depolarization of the emitted light which contributes to the overall PL anisotropy.

Optoelectronic Properties of Nonpolar Polyrotaxanes

Conjugated polyrotaxanes are typically prepared by the polymerization of an inclusion complex of the monomer, with concomitant end-capping. The formation of the inclusion complex is favored by hydrophobic interactions, and the polymerization is usually carried out in water [23], which requires the aromatic groups to carry water-solubilizing groups such as carboxylates or sulfonates. The resulting polyrotaxanes are polyanionic and are only processable from aqueous solution or from very polar organic solvents such as dimethyl sulfoxide, both due to the ionic water-solubilizing groups and due to the polar hydroxyl groups on the cyclodextrins. Ionic migration can facilitate the fabrication of high-efficiency devices with essentially balanced hole–electron populations (LECs or light-emitting electrochemical cells), but it can also be a source of device instability, providing a motivation for synthesizing neutral, nonionic polyrotaxanes, of similar structure to these polyelectrolytes.

It is however possible to post-process the ionic polyrotaxanes to achieve nonionic, lipophilic, organic-soluble polyrotaxanes by three different strategies involving alkylation, silylation, and esterification, as reported by Anderson and his group at Oxford [24]. This possibility offers significant new insight for the application in flexible white-light sources for displays and illumination, and it has attracted growing attention to polymer blends [25], since combination of materials with complementary emission spectra can result in extended coverage of the visible range. Specifically, the optical and electrical properties of polymer blends can be tuned via a careful design taking into account the relevant physical properties of the constituents. These include the energy of their frontier levels and thus their offsets at type II heterojunctions for either LED or PVD applications [26, 27], as well as their energy gap for engineering of the emission color. LEDs incorporating binary blends of polyfluorene derivatives have shown, for example, enhanced electroluminescence (EL) efficiency as a result of improved charge balance and optimized electron–hole recombination [28, 29].

Clearly, control of energy transfer between different chromophores of a blend [30] or even within a single polymer carrying different

groups [31] is crucial for control of the final emission color, and in particular for achieving white luminescence, since the close proximity of the constituents usually results in dominant emission from the lower gap material. Although phase separation of the polymers often occurs due to the small entropy of mixing of chemically different species, this takes place over several length scales, with the minimum size of "pure" domains being at least comparable to the Förster radius, still allowing significant and undesired transfer [30].

The use of organic-soluble polyrotaxanes [32], as at least one component of the blend, allows for achieving better control of energy transfer between the different polymeric species via control of the nanoscale interchain separation. Therefore, this approach can be used to obtain controlled suppression of ET between emissive species and to achieve white EL from binary blends of polyfluorene derivatives threaded into functionalized cyclodextrins. As illustrative examples, we mention here two different

polymer blends: a blue-emitting polyrotaxane, **PFBP.Me**⊂β- CD.THS blended with the green-emitting poly(9,9-dioctylfluorene-alt-benzothiadiazole) (**F8BT**) (blend "A"; see Fig. 4 for chemical structures), and a green-emitting fluorene-divinyl phenylene alternate copolymer encapsulated in functionalized β-cyclodextrins (**PFBV.Me**⊂β-CD.COPr) blended with a polyfluorene derivative, poly (9,9-dioctylfluorene-alt-N-(4-butylphenyl)-diphe-nylamine) (**TFB**) (blue emitter, blend "B", Fig. 5) [33].

Apart from the polyrotaxane used, these two polymer blends differ for the type of heterojunction that forms at the polymer-polymer interface, which is determined by the energy offset between the blend constituents. On the one hand, in blend "A", the energy offset between the frontier levels of **F8BT** and **PFBP.Me**⊂β- CD. THS is smaller than the exciton binding energy and no charge transfer complexes are formed. As a result, the emission spectrum of the mixture is the linear combination of the emission spectra of

Polyrotaxanes (Conjugated), Fig. 4 Blend "A". (**a**) Molecular structures of unthreaded benzylated **PFBP. Bn**, **F8BT**, and functionalized **PFBP.Me**⊂β-CD.THS polyrotaxane. (**b**) Energy diagram showing the position of the HOMO and LUMO levels for the isolated materials with no applied field and the work function of PEDOT: PSS (Adapted from Ref. [34])

Polyrotaxanes (Conjugated), Fig. 5 Blend "B". (**a**) Chemical structures of **PFBV.Me**⊂β-CD.COPr and **TFB**. The structure of the reference polymer (**PFBV**) is similar to that reported for the polyrotaxane but without the cyclodextrins (presented here as conical sheaths). **PFBV** consists of a non-threaded polyfluorene-*alt*-bivinylphenylene core with octyl chains functionalized fluorene units and terminated by phenyl groups. (**b**) Energy diagram showing the position of the HOMO and LUMO levels for the isolated materials with no applied field and the work function of PEDOT:PSS (Adapted from Ref. [33])

the individual polymers. On the other hand, the energy offset between the molecular orbitals of the constituents of blend "B" is comparable to the exciton binding energy which leads to the formation of exciplexes. The emission spectrum of the mixture is then due to the sum of the individual spectra and the additional feature due to the recombination of exciplexes. Both these systems are of obvious relevance to white emission for lighting applications.

Devices fabricated with blend "A" (see Fig. 4, ITO/PEDOT:PSS/polymer/Ca/Al) incorporate a ~200 nm thick film of either **PFBP.Me**⊂β-CD.THS:**F8BT** or **PFBP.Bn**:**F8BT** (80:20 w/w). For completeness, high-resolution PL maps of the active layers onto PEDOT:PSS/ ITO substrates by scanning near-field optical microscopy (SNOM) are shown in the inset of Fig. 6a.

The EL spectrum of **PFBP.Me**⊂ **CD.THS**: **F8BT** (80:20 w/w) devices shows the contributions of both polymers and is therefore characterized by the "Commission internationale de l'éclairage" (CIE) coordinates x = 0.282 and y = 0.336 which correspond to a "warm" white. This result is both remarkable and surprising, because one would still expect charge transport to occur preferentially through the uninsulated

F8BT rather than through the polyrotaxanes, also in view of the apparently percolating phase visible in the SNOM image in the inset of Fig. 6a. Instead, the presence of a blue emission clearly indicates that recombination is also occurring on the polyrotaxane, despite the strong insulation provided by the cyclodextrins. The implication is that the **F8BT** phase in rotaxinated blends is effectively below the percolation threshold [35].

In agreement with the EL spectra that show no percolation through F8BT-rich regions, the turn-on voltage of polyrotaxane:**F8BT**-based devices (~10 V at L = 0.01 cd/m²) is comparable to that of devices incorporating pure **PFBP.Me**⊂β- CD. THS [34]. Such values of turn-on voltages are still relatively high if compared to state-of-the-art LEDs and are obviously linked to the insulating nature of the functionalized cyclodextrins. In addition, the green emitter that gives the higher spectral contribution to the white emission benefits from the increase of the PL efficiency due to the supramolecular encapsulation. The EQE is 0.15 % (0.39 cd/A) which is encouraging, since it is one order of magnitude higher than that of LEDs based on the conventional blend (EQE ~ 0.01 %, 0.04 cd/A) and significantly higher than that obtained for devices based on
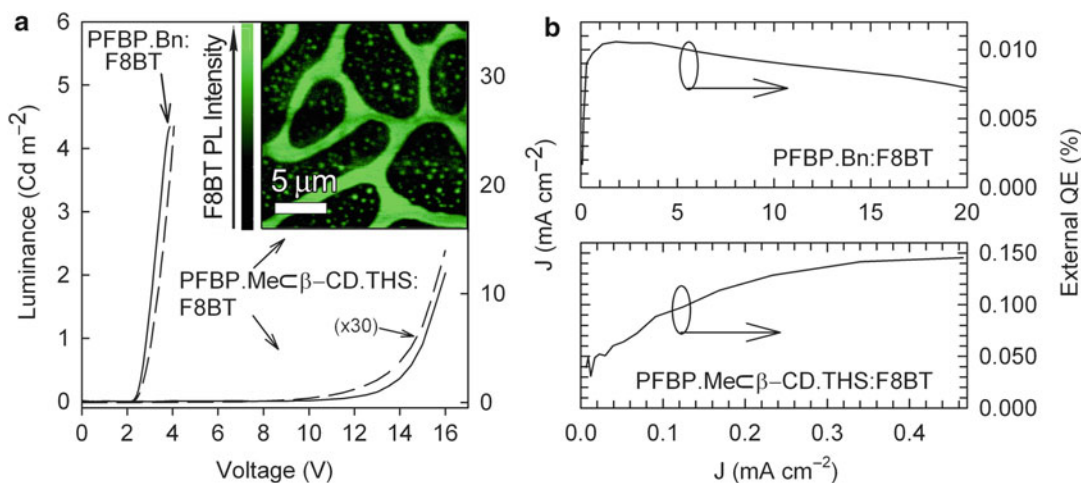
Polyrotaxanes (Conjugated), Fig. 6 (**a**) Current (*dashed line*) and luminance (*solid line*) versus voltage characteristics and (**b**) external quantum efficiency (*EQE %*) versus current density (*J*) characteristics of the devices. Inset of (**a**): SNOM image of CW intensity of **F8BT** emission (<2.4 eV) for **PFBP.Me**$\subset\beta$ -CD.THS**: F8BT** (8:2 w/w) blend excited at 2.67 eV (Adapted from Ref. [34])

pure rotaxanes [34]. The enhancement of EQE observed for the threaded blend with respect to the reference blend is in agreement with previous results for LEDs incorporating either ion-free [34] or electrolytic polyrotaxanes [8] and is explained by reduced aggregation in encapsulated systems, as also indicated by the higher PL efficiency and slower PL decay kinetics.

The use of an encapsulated blue emitter is not ideal in LEDs, since charge injection into the blue emitter is more difficult than in a green emitter, and the presence of the cyclodextrins further raises the EL turn-on voltage (~10 V) [36]. A possible strategy to circumvent this difficulty is the use of a "complementary" rotaxinated blend where the encapsulated compound is a green-emitting polyrotaxane and the blue emitter is instead a commercial unthreaded polymer.

The EL properties of a binary blend of the blue-emitting polyfluorene copolymer **TFB** and a green-emitting polyrotaxane are reported in Fig. 7 below, in which most of the 21 hydroxyl groups on each cyclodextrin unit have been converted to butanoate esters to reduce the hydrophilic character of the supramolecular assembly and thus ensure solubility in organic solvents.

The EL spectra of LEDs from both threaded and unthreaded blends (ITO/PEDOT:PSS/polymer/Ca/Al) display strong signs of emission from interchain states, as typically observed for type II polymer heterojunctions [28, 37]. The fact that EL and PL spectra are different in both single materials and in blends reflects the energy-selective nature of the charge transport process. In EL, the electronic levels of electroluminescent molecules play the dominant role, controlling the formation and recombination of excitons, so that the contribution of the blend components to the EL spectrum is different compared to what is observed upon photoexcitation. Furthermore, in type II systems, holes (electrons) are transported preferentially in the component with the highest (lowest) HOMO (LUMO) level. As a result, excitons are formed primarily at the polymer-polymer interface where the probability for exciplex formation is the highest. The EL spectrum of **PFBV.Me**$\subset\beta$-CD.COPr is blueshifted with respect to **PFBV**, which instead shows a featureless band. As a result of controlled ET and exciplex formation in the "rotaxinated blend" (20:80 **PFBV.Me**$\subset\beta$ -CD.COPr**:TFB** w/w), the EL spectrum is structured, and with a more pronounced blue component than the **PFBV**:**TFB**

P
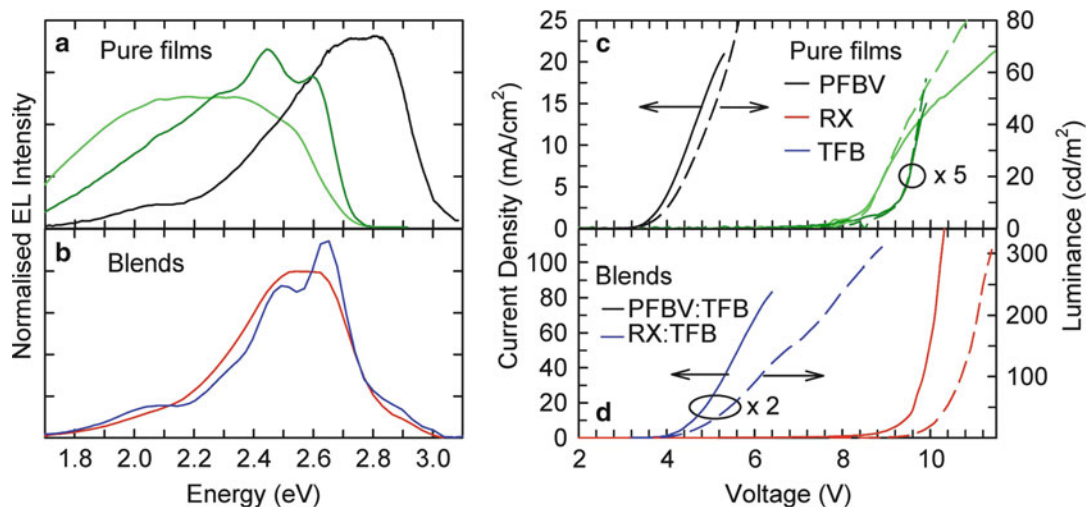
Polyrotaxanes (Conjugated), Fig. 7 Area-normalized EL spectra of ITO/PEDOT/polymer/Ca/Al devices incorporating active layers of (**a**) pure **PFBV**, **PFBV. Me**$\subset\beta$-CD.COPr and **TFB** and (**b**) their binary **TFB** blend (80 % w/w **TFB** fraction). (**c**) and (**d**) J-V-L of the very same LEDs as in (**a**) and (**b**) (the *color code* in (**a**) is the same as in (**c**)) (as for (**b**) and (**d**)) (Adapted from Ref. [33])

system, that results in an overall "cold" white light, corresponding to CIE color coordinates, $x = 0.26$ and $y = 0.33$. Figure 7c, d reports the current density-voltage-luminance characteristics of the LEDs in Fig. 7a, b. Importantly, the turn-on voltage for white EL is only 3.5 V, which is a factor of 3 lower than for the white-emitting LEDs incorporating blends of a blue-emitting polyrotaxane shown previously [36]. The EL external quantum efficiency is essentially comparable to the LEDs with the complementary blends, i.e., here a maximum EQE = 0.1 % for LEDs incorporating the rotaxane and its **TFB** blend (vs. 0.15 % in reference [36]) and EQE = 0.02 % for the **PFBV** blend was obtained (vs. 0.01 % in the complementary blend with the blue-emitting rotaxane) [36].

In summary, successful control of the energy transfer between polymeric species with resonant electronic transitions has been demonstrated by supramolecular encapsulation. Most importantly, the use of a green-emitting encapsulated polymer circumvents the difficulties encountered with a binary blend of a blue electroluminescent polyrotaxane and leads to drastically lowered turn-on voltage of white EL that can be achieved with only 20 % w/w of encapsulated moieties in the binary blend.

Conclusions

Conjugated polyrotaxanes powerfully demonstrate the versatility and far-reaching scope of macromolecular and supramolecular synthetic chemistry in producing structures that combine architectural elegance with useful properties, both for "real-world" applications and as an investigative "probe" to advance the understanding of the fundamental physical properties of soft condensed matter.

While the value of supramolecular chemistry has been amply recognized since the attribution of the Nobel Prize for Chemistry already in 1987, it is fascinating that this area still continues to produce a wealth of intellectual stimuli and powerful new knowledge to the present date.

Rotaxanes are a notable example in this context under a variety of aspects. First, they are threaded molecular wires acting as a remarkable class of model compounds that enable us to obtain a detailed, deep understanding of the influence of intermolecular interactions on the photophysics of conjugated semiconductors [7–9, 38].

In a second instance, conjugated polyrotaxanes are uniquely versatile, at a synthetic level, since

cores, end groups, and macrocycles can all be functionalized according to need or interest. The possibility of using electrolytic side chains, for example, affords the possibility of making non-phase-separated polymer blends with PEO, which are virtually immune from undesired phase separation phenomena and thereby enhance both PL and EL in LEC-like devices [39]. Similarly, the possibility of controlling the threading ratio adds an extra dimension to the space of parameters that can be tuned and fruitfully exploited for raising the efficiency or further tuning the emission color. Indeed, the possibility to swap the charged side chains for neutral ones and obtain organic-solvent-soluble threaded molecular wires solubilized also with the help of further functionalization of the cyclodextrin hydroxyls opens the way to significant new structures via combination with other organic-solvent-soluble materials [33, 34, 36]. Other intriguing possibilities derive from the scope for functionalization of the macrocycles with charge-transporting groups such as tri-aryl-amines, of the type found, for example, in state-of-the-art p-type semiconductors such as poly(9,9-dioctylfluorene-alt-*N*-(4-butylphenyl)-diphenylamine) (TFB) or poly((9,9- dioctyl-fluorene)-alt-bis-*N,N'*-(4-butylphenyl)-bis-*N,N'*-phenyl-1,4-phenylenediamine) (PFB).

Thirdly, by blending the organic-solvent-soluble materials mentioned above with other threaded and non-threaded luminescent materials, it is possible to achieve unprecedented results in terms of suppression of energy transfer (valuable to the fabrication of white-emitting LEDs) and suppressed polaron formation, so as to ensure broadband optical amplification and simultaneous multicolor lasing [33, 36, 40].

In conclusion, even if in terms of quantitative performance (e.g., external quantum efficiency of the LEDs, or their operational lifetime) this class of materials cannot quite compete with organic-solvent-soluble materials, these materials are providing a remarkably significant progress in the understanding of the fundamental properties of conjugated polymers and photophysics and there still is a tremendous scope for unleashing their potential in the years to come.

Related Entries

▶ Cyclodextrins-Based Supramolecular Polymers
▶ Supramolecular Polymers (Coordination Bonds)

References

1. Lehn JM (2004) Supramolecular chemistry: from molecular information towards self-organization and complex matter. Rep Prog Phys 67(3):249–265
2. Ansari A, Kuznetsov SV (2005) Is hairpin formation in single-stranded polynucleotide diffusion-controlled? J Phys Chem B 109(26):12982–12989
3. O'Shea P (2003) Intermolecular interactions with/within cell membranes and the trinity of membrane potentials: kinetics and imaging. Biochem Soc Trans 31:990–996
4. Gierschner J, Ehni M, Egelhaaf HJ, Milian Medina B, Beljonne D, Benmansour H, Bazan GC (2005) Solid-state optical properties of linear polyconjugated molecules: pi-stack contra herringbone. J Chem Phys 123(14):9
5. Poulsen L, Jazdzyk M, Communal JE, Sancho-Garcia JC, Mura A, Bongiovanni G, Beljonne D, Cornil J, Hanack M, Egelhaaf HJ, Gierschner J (2007) Three-dimensional energy transport in highly luminescent host-guest crystals: A quantitative experimental and theoretical study. J Am Chem Soc 129(27):8585–8593
6. Samuel IDW, Rumbles G, Collison CJ (1995) Efficient interchain photoluminescence in a high-electron-affinity conjugated polymer. Phys Rev B 52(16):11573–11576
7. Brovelli S, Cacialli F (2010) Optical and electroluminescent properties of conjugated polyrotaxanes. Small 6(24):2796–2820
8. Brovelli S, Latini G, Frampton MJ, McDonnell SO, Oddy FE, Fenwick O, Anderson HL, Cacialli F (2008) Tuning intrachain versus interchain photophysics via control of the threading ratio of conjugated polyrotaxanes. Nano Lett 8(12):4546–4551
9. Cacialli F, Wilson JS, Michels JJ, Daniel C, Silva C, Friend RH, Severin N, Samorì P, Rabe JP, O'Connell MJ, Taylor PN, Anderson HL (2002) Cyclodextrin-threaded conjugated polyrotaxanes as insulated molecular wires with reduced interstrand interactions. Nat Mater 1(3):160–164
10. Friend RH, Gymer RW, Holmes AB, Burroughes JH, Marks RN, Taliani C, Bradley DDC, Dos Santos DA, Bredas JL, Logdlund M, Salaneck WR (1999) Electroluminescence in conjugated polymers. Nature 397(6715):121–128
11. Schwartz BJ (2003) Conjugated polymers as molecular materials: How chain conformation and film morphology influence energy transfer and interchain interactions. Annu Rev Phys Chem 54:141–172

P

12. Jenekhe SA, Osaheni JA (1994) Excimers and exciplexes of conjugated polymers. Science 265(5173):765–768

13. Kim J, Swager TM (2001) Control of conformational and interpolymer effects in conjugated polymers. Nature 411(6841):1030–1034

14. Wilson JS, Frampton MJ, Michels JJ, Sardone L, Marletta G, Friend RH, Samori P, Anderson HL, Cacialli F (2005) Supramolecular complexes of conjugated polyelectrolytes with poly(ethylene oxide): Multifunctional luminescent semiconductors exhibiting electronic and ionic transport. Adv Mater 17(22):2659–2663

15. Michels JJ, O'Connell MJ, Taylor PN, Wilson JS, Cacialli F, Anderson HL (2003) Synthesis of conjugated polyrotaxanes. Chem Eur J 9(24):6167–6176

16. Chang MH, Frampton MJ, Anderson HL, Herz LM (2006) Photoexcitation dynamics in thin films of insulated molecular wires. Appl Phys Lett 89(23):3

17. Lim SF, Friend RH, Rees ID, Li J, Ma YG, Robinson K, Holmes AB, Hennebicq E, Beljonne D, Cacialli F (2005) Suppression of green emission in a new class of blue-emitting polyfluorene copolymers with twisted biphenyl moieties. Adv Funct Mater 15(6):981–988

18. Bourdakos KN, Dissanayake DMNM, Lutz T, Silva SRP, Curry RJ (2008) Highly efficient near-infrared hybrid organic-inorganic nanocrystal electroluminescence device. Appl Phys Lett 92(15):153311

19. Kasiouli S, Di Stasio F, McDonnell SO, Constantinides CP, Anderson HL, Cacialli F, Hayes SC (2013) Resonance raman investigation of β-cyclodextrin-encapsulated π-conjugated polymers. J Phys Chem B 117(18):5737–5747

20. Di Stasio F, Korniychuk P, Brovelli S, Uznanski P, McDonnell SO, Winroth G, Anderson HL, Tracz A, Cacialli F (2011) Highly polarized emission from oriented films incorporating water-soluble conjugated polymers in a polyvinyl alcohol matrix. Adv Mater 23(16):1855–1859

21. Chang MH, Frampton MJ, Anderson HL, Herz LM (2007) Intermolecular interaction effects on the ultrafast depolarization of the optical emission from conjugated polymers. Phys Rev Lett 98(2):4

22. Lakowicz JR (2006) Principles of fluorescence spectroscopy, 3rd edn. Springer, New York

23. Farcas A, Grigoras M (2003) Synthesis and characterization of a fully aromatic polyazomethine with rotaxane architecture. Polym Int 52(8):1315–1320

24. Frampton MJ, Claridge TDW, Latini G, Brovelli S, Cacialli F, Anderson HL (2008) Amylose-wrapped luminescent conjugated polymers. Chem Commun 24:2797–2799

25. Service RF (2005) Electronics: organic LEDs look forward to a bright, white future. Science 310(5755):1762–1763

26. Moons E (2002) Conjugated polymer blends: linking film morphology to performance of light emitting diodes and photodiodes. J Phys Condens Matter 14(47):12235–12260

27. Morteani AC, Sreearunothai P, Herz LM, Friend RH, Silva C (2004) Exciton regeneration at polymeric semiconductor heterojunctions. Phys Rev Lett 92:247402-1–247402-4

28. Morteani AC, Dhoot AS, Kim JS, Silva C, Greenham NC, Murphy C, Moons E, Ciná S, Burroughes JH, Friend RH (2003) Barrier-free electron–hole capture in polymer blend heterojunction light-emitting diodes. Adv Mater 15(20):1708–1712

29. Yim K-H, Zheng Z, Friend RH, Huck WTS, Kim J-S (2008) Surface-directed phase separation of conjugated polymer blends for efficient light-emitting diodes. Adv Funct Mater 18(19):2897–2904

30. Morgado J, Moons E, Friend RH, Cacialli F (2001) De-mixing of polyfluorene-based blends by contact with acetone: electro- and photo-luminescence probes. Adv Mater 13(11):810–814

31. Morgado J, Cacialli F, Friend RH, Iqbal R, Yahioglu G, Milgrom LR, Moratti SC, Holmes AB (2000) Tuning the red emission of a soluble poly(p-phenylene vinylene) upon grafting of porphyrin side groups. Chem Phys Lett 325(5–6):552–558

32. Frampton MJ, Anderson HL (2007) Insulated molecular wires. Angew Chem Int Edit 46(7):1028–1064

33. Brovelli S, Sforazzini G, Serri M, Winroth G, Suzuki K, Meinardi F, Anderson HL, Cacialli F (2012) Emission color trajectory and white electroluminescence through supramolecular control of energy transfer and exciplex formation in binary blends of conjugated polyrotaxanes. Adv Funct Mater 22(20):4284–4291

34. Frampton ML, Sforazzini G, Brovelli S, Latini G, Townsend E, Williams CC, Charas A, Zalewski L, Kaka NS, Sirish M, Parrott LJ, Wilson JS, Cacialli F, Anderson HL (2008) Synthesis and optoelectronic properties of nonpolar polyrotaxane insulated molecular wires with high Solubility in organic solvents. Adv Funct Mater 18(21):3367–3376

35. Stauffer D (1985) Introduction to percolation theory. Taylor and Francis, London, pp 87–100

36. Brovelli S, Meinardi F, Winroth G, Fenwick O, Sforazzini G, Frampton MJ, Zalewski L, Levitt JA, Marinello F, Schiavuta P, Suhling K, Anderson HL, Cacialli F (2010) White electroluminescence by supramolecular control of energy transfer in blends of organic-soluble encapsulated polyfluorenes. Adv Funct Mater 20(2):272–280

37. Morteani AC, Friend RH, Silva C (2006) Electronic processes at semiconductor polymer heterojunctions. In: Klaus M, Ullrich S (eds) Organic light emitting devices, Wiley-VCH. KGaA, Weinheim, pp 35–94

38. Petrozza A, Brovelli S, Michels JJ, Anderson HL, Friend RH, Silva C, Cacialli F (2008) Control of rapid formation of interchain excited states in sugar-threaded supramolecular wires. Adv Mater 20(17):3218–3223

39. Latini G, Winroth G, Brovelli S, McDonnell SO, Anderson HL, Mativetsky JM, Samori P, Cacialli

F (2010) Enhanced luminescence properties of highly threaded conjugated polyelectrolytes with potassium counter-ions upon blending with poly(ethylene oxide). J Appl Phys 107(12):124509

40. Brovelli S, Virgili T, Mroz MM, Sforazzini G, Paleari A, Anderson HL, Lanzani G, Cacialli F (2010) Ultra-broad optical amplification and two-colour amplified spontaneous emission in binary blends of insulated molecular wires. Adv Mater 22(33):3690–3694

Polyrotaxanes: Synthesis, Structure, and Chemical Properties

Hiroyasu Yamaguchi and Akira Harada
Department of Macromolecular Science,
Graduate School of Science, Osaka University,
Machikaneyama, Toyonaka, Osaka, Japan

Synonyms

Mechanically interlocked molecules

Definition

Polyrotaxanes are defined as molecular assemblies, in which many macrocycles are mechanically interlocked on a dumbbell-shaped molecule by bulky stoppers on its ends.

Introduction

Macrocycles rotate freely and translate on the axis in a dumbbell-shaped molecule in the rotaxane system. Since rotaxanes are one of the important components of molecular machines based on such structural features, rotaxanes have attracted increasing interest of researchers from nanotechnological aspects. The first artificial rotaxane was reported in 1967 [1]. Harrison et al. synthesized a [2]rotaxane (two in brackets indicates the number of components) by statistical reaction between a macrocycle and a dumbbell-shaped molecule. However, the yield of single reaction was very low. Harada et al. reported the first example of a polyrotaxane, in which a number of α-cyclodextrin (α-CD) molecules are interlocked on a poly(ethylene glycol) (PEG) chain by bulky stoppers [2]. Polyrotaxanes are paid much attention as smart soft materials with unique properties. A large number of examples of polyrotaxanes (Fig. 1) have been reported. These examples include various macrocycles, for example, cyclodextrins (CDs), crown ethers (CEs), cucurbiturils (CBs), cyclophanes (CPs), cyclobis(paraquat-*p*-phenylene), calix[*n*]arenes, and pillararenes (Fig. 2), and numerous types of axes depending on the macrocycles [3, 4].

CD Polyrotaxanes

Polyrotaxanes in which numerous α-CD molecules are threaded on a PEG chain have been prepared by mixing α-CD and PEG bis-amines with 2,4-dinitrofluorobenzene, which is sufficiently bulky to prevent α-CD from dethreading (Fig. 3) [2, 5, 6]. This is the first example of a polyrotaxane, named as a "molecular necklace." α-CD polyrotaxanes were used to construct a topological network architecture [7]. The intermolecular cross-linking reaction of CDs among polyrotaxanes allows a sliding motion of the network polymer chains. The swelling and the viscoelastic properties were found to be solvent dependent, reflecting the structural changes of the network [8]. A "molecular tube" was also prepared by the reaction of a CD polyrotaxane with epichlorohydrin dissolved in 10 % NaOH [9]. The molecular tube can accommodate I_3^- ions efficiently, whereas α-CD does not.

Anthracene groups are large enough to prevent dethreading of α- and β-CDs from an axle. A polyrotaxane with numerous β-CD molecules has been prepared by photodimerization of a 2-anthryl group in a precursor complex between β-CD and poly(propylene glycol) (PPG) with triphenylmethyl and 2-anthryl groups at each end of the PPG chain [10]. Polyrotaxanes containing γ-CD have been also prepared by photocyclodimerization of 9-anthryl groups at the ends of a polymer chain in the presence

P
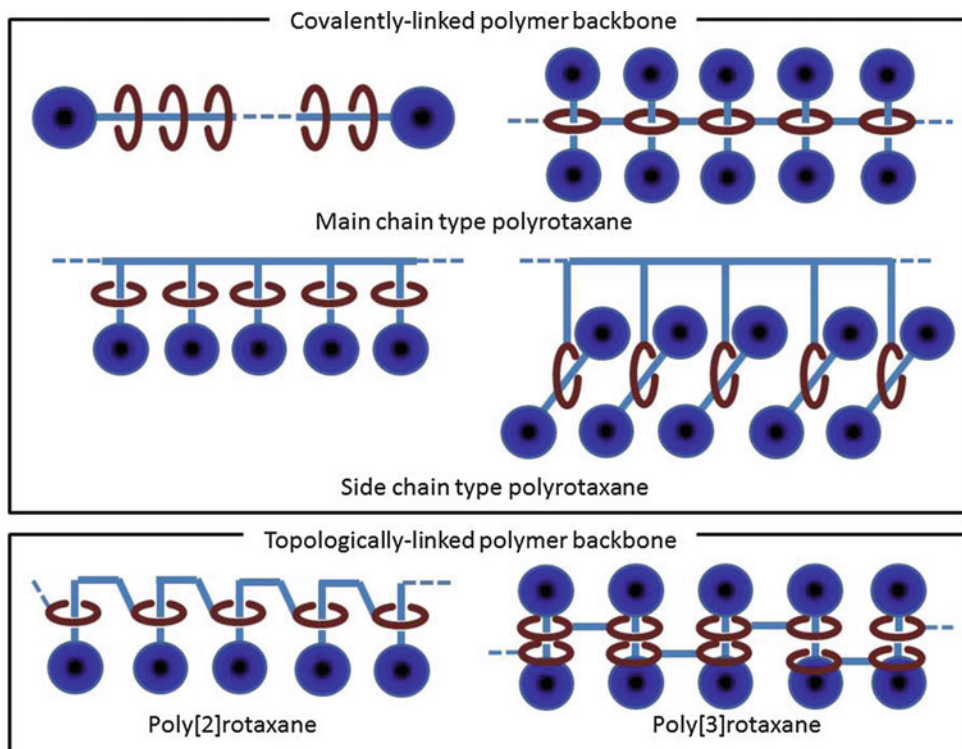
Polyrotaxanes: Synthesis, Structure, and Chemical Properties, Fig. 1   Various types of polyrotaxanes

of γ-CD. Wenz et al. obtained interlocked hetero-polyrotaxanes with β- and γ-CDs by photoirradiation to stilbene moiety in the polymer chain [11].

CE Polyrotaxanes

The hydrogen bonding interaction between a CE and a secondary ammonium salt is often used for the preparation of CE polyrotaxanes. The groups of Gibson, Stoddart, and Takata, respectively, actively synthesized a series of polyrotaxanes by utilizing CEs [12–14]. Polyrotaxanes of CEs with polyacrylonitrile, poly(methyl acrylate), poly (methyl methacrylate), and polystyrene were prepared via free radical polymerization [15]. Recently, dynamic covalent chemistry such as reversible imine formation, metal–ligand exchange, and olefin metathesis has been demonstrated as an effective tool for the preparation of various mechanically interlocked molecular

compounds [16]. Polyrotaxane networks were synthesized by using the reversible thiol–disulfide interchange reaction based on dynamic covalent chemistry [17]. Poly[2]rotaxanes and poly[3] rotaxanes were also synthesized by self-polycondensation of the [2]rotaxane monomer via the Sonogashira coupling reaction or by click polymerizations.

CB Polyrotaxanes

Cucurbit[n]urils (CB[n], n = 5–10) are a family of pumpkin-shaped macrocycles derived from glycoluril and formaldehyde. CB[6] forms complexes with protonated diaminoalkanes $^+NH_3(CH_2)_nNH_3^+$ (n = 4–7, K = 10^5–10^6 M^{-1} in aqueous formic acid). CB[7] binds methyl viologen (K = 2×10^5 M^{-1}) and ferrocene to give a 1:1 complex. CB[8] has a large cavity enough to simultaneously accommodate two aromatic guests with the size of (E)-diaminostilbene.
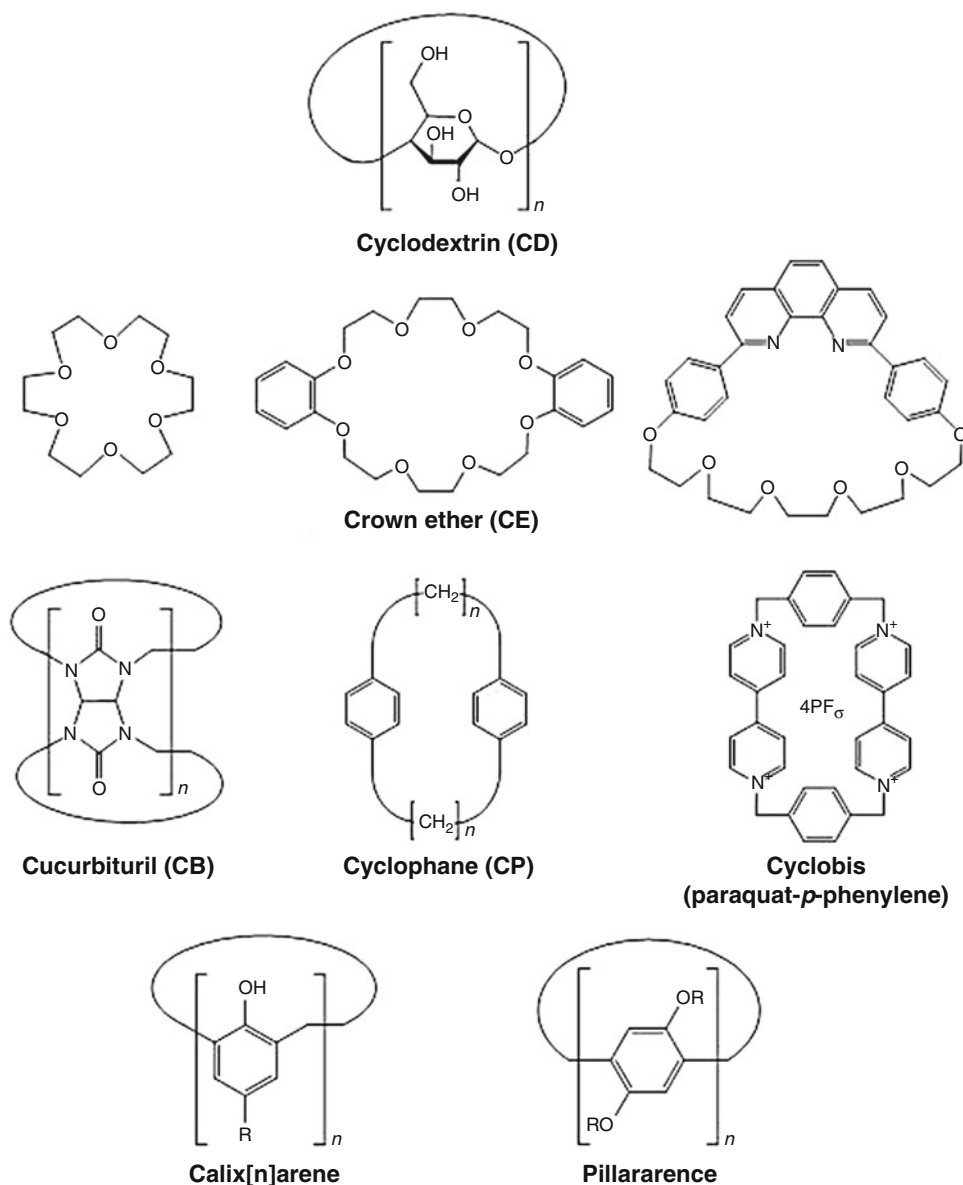
Polyrotaxanes: Synthesis, Structure, and Chemical Properties, Fig. 2 Structures of macrocycles

Kim et al. constructed a rotaxane containing CB and spermine as a thread by taking advantage of the strong tendency of CB to form inclusion complexes with aliphatic diammonium ions. They reported the x-ray crystal structure of a polyrotaxane containing CB molecules threaded on a one-dimensional (1D) coordination polymer in the solid state. Moreover, the 2D and 3D polyrotaxane networks were constructed [18].

Recently, Kim et al. reported a supramolecular fishing method for membrane proteins using the synthetic receptor–ligand pair, CB[7]-1-trimethylammonio methylferrocene [19]. Steinke et al. prepared a main-chain polyrotaxane in which polymerization and rotaxane formation simultaneously occur. They used catalytic 1,3-dipolar cycloaddition reactions for the preparation of polyrotaxanes (Fig. 4) [20].

**Polyrotaxanes:
Synthesis, Structure, and
Chemical Properties,
Fig. 3** Preparation of a CD
polyrotaxane
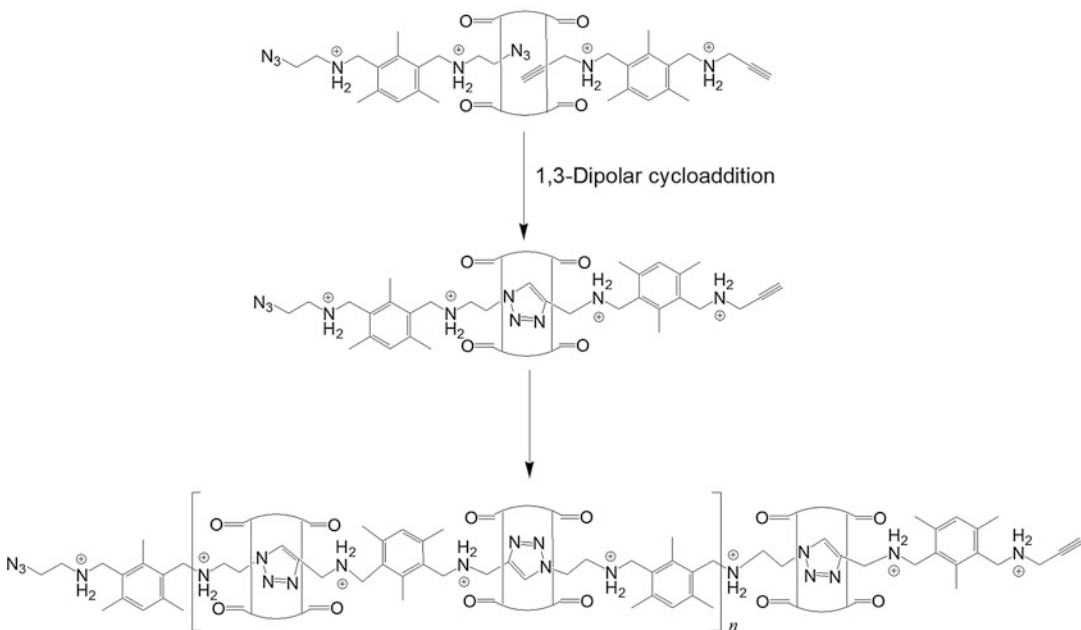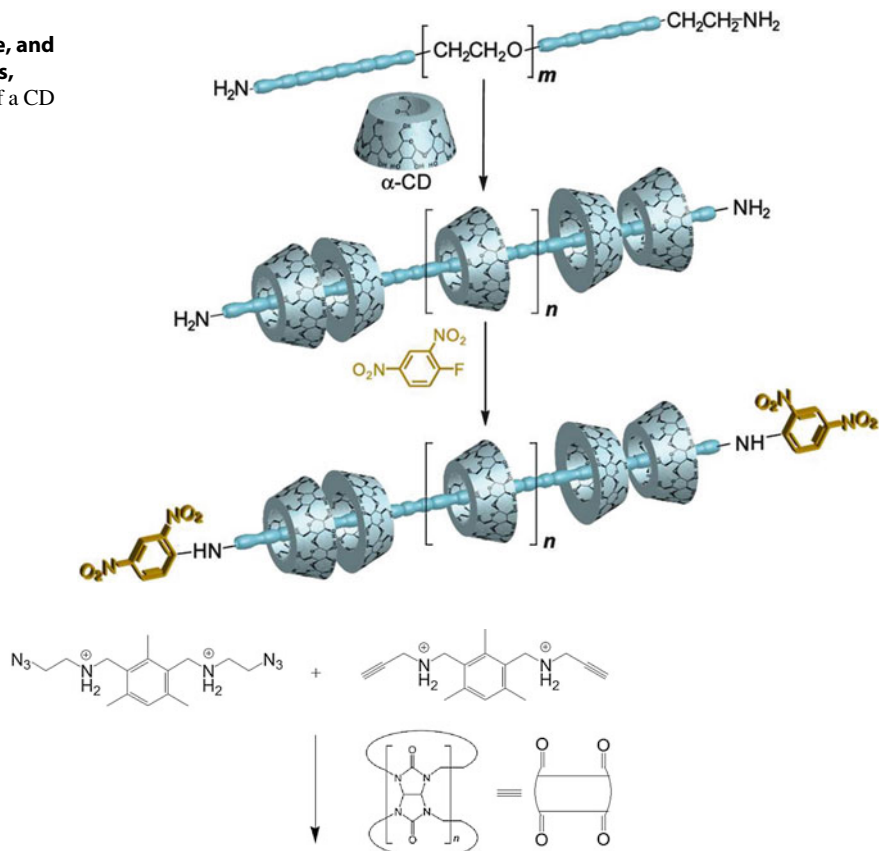
Polyrotaxanes: Synthesis, Structure, and Chemical Properties, Fig. 4 A polyrotaxane synthesized by catalytic 1,3-dipolar cycloaddition in the presence of CB[6]

Cyclophane/Cyclobisparaquat Polyrotaxanes

CPs form inclusion complexes with para-disubstituted aromatic compounds in aqueous solutions [21]. Some polyrotaxanes have been synthesized by using cyclobis(paraquat-phenylene) (a tetracationic CP) or flexible tetracationic macrocycle (a "Texas-sized" molecular box) [22]. Hydrogen bonding, π–π stacking, and charge–transfer interactions are efficient driving forces for these complex formations. The NMR signals of cyclobis(paraquat-phenylene) bound onto the polymer chain by threading can be distinguished from those moving freely in the solution. Recently, polyrotaxanes of CPs have been synthesized by the click chemistry approach as well as those of CDs, CEs, and CBs. Employing this approach, a lot of [n]rotaxanes have been prepared in a convergent and efficient manner [23].

Calixarene Polyrotaxanes

Although there are many reports on supramolecular formation between calixarenes and small molecules, only a few examples were reported on calixarene-based polyrotaxanes. A water-soluble, nanometer-scale metallo-capped polyrotaxane was prepared by the inclusion complexation of azocalixarenes with metallo-bridged CD dimers, displaying highly selective binding for Ca^{2+} [24]. A polyrotaxane was prepared by the polycondensation of p-tert-butylphenol with paraformaldehyde in the presence of PEGs [25].

Pillararene Polyrotaxanes

A polypseudorotaxane was synthesized from pillar[5]arene and viologen polymers (VP) [26]. The formation of the host–guest complex depended on the length of the linker between viologen moieties. Adamantyl moiety was found to be large enough to prevent the threading of pillar[5]arene. The formation of intermolecular hydrogen bonds between the OH moieties of pillar[5]arenes stabilized the structure. The polyrotaxane exhibited a thermally induced color change from yellow to violet. On heating, the intermolecular hydrogen bond became weakened, and the shuttling motion of pillar[5]arenes on the polymer axis was fast. Thus, efficient electron transfer from pillar[5]arenes to VP occurred, and the radical cation species were stabilized.

Metal Coordination Systems

Metal coordination chemistry can also be applied to immobilize the wheel components to the axial molecules. Metal ions are added to expand the rotaxane structures into the higher-ordered polyrotaxane frameworks as shown in CE and CB systems. Sauvage et al. showed that the use of transition metals as templating agents allowed strict control of the molecular assembly of the rotaxane precursors [27]. Polymetallorotaxanes can exhibit remarkably high conductivities when the redox potential of the metal matches the oxidation potential of the π system, thus leading to potential applications in chemoresistive sensors.

Related Entries

▸ Calixarenes-Based Supramolecular Polymers
▸ Crown Ethers-Based Supramolecular Polymers
▸ Cucurbiturils-Based Supramolecular Polymers
▸ Cyclodextrins-Based Supramolecular Polymers
▸ Dynamic Mechanical Properties
▸ Inclusion Polymerization
▸ Molecular Self-Organization
▸ Polycatenanes
▸ Polyrotaxanes (Conjugated)
▸ Supramolecular Network Polymers
▸ Supramolecular Polymers (Coordination Bonds)
▸ Supramolecular Polymers (Host-Guest Interactions)
▸ Topological Gels

References

1. Harrison IT, Harrison S (1967) Synthesis of a stable complex of a macrocycle and a threaded chain. J Am Chem Soc 89:5723–5724

2. Harada A, Kamachi M (1990) Complex formation between poly(ethylene glycol) and α-cyclodextrin. Macromolecules 23:2821–2823

3. Harada A, Hashidzume A, Yamaguchi H, Takashima Y (2009) Polymeric rotaxanes. Chem Rev 109:5974–6023

4. Arunachalam M, Gibson HW (2014) Recent developments in polypseudorotaxanes and polyrotaxanes. Prog Polym Sci. doi:10.1016/j.progpolymsci.2013.11.005

5. Harada A, Li J, Kamachi M (1992) The molecular necklace: a rotaxane containing many threaded α-cyclodextrins. Nature 356:325–327

6. Harada A, Li J, Kamachi M (1994) Preparation and characterization of a polyrotaxane consisting of monodisperse poly(ethylene glycol) and α-cyclodextrins. J Am Chem Soc 116:3192–3196

7. Okumura Y, Ito K (2001) The polyrotaxane gel: a topological gel by figure-of-eight cross-links. Adv Mater 13:485–487

8. Fleury G, Schlatter G, Brochon C, Hadziioannou G (2006) Unveiling the sliding motion in topological networks: influence of the swelling solvent on the relaxation dynamics. Adv Mater 18:2847–2851

9. Harada A, Li J, Kamachi M (1993) Synthesis of a tubular polymer from threaded cyclodextrins. Nature 364:516–518

10. Okada M, Harada A (2003) Poly(polyrotaxane): photoreactions of 9-anthracene-capped polyrotaxane. Macromolecules 36:9701–9703

11. Herrmann W, Schneider M, Wenz G (1997) Photochemical synthesis of polyrotaxanes from stilbene polymers and cyclodextrins. Angew Chem Int Ed Engl 36:2511–2514

12. Gibson HW, Liu S, Lecavalier P, Wu C, Shen YX (1995) Synthesis and preliminary characterization of some polyester rotaxanes. J Am Chem Soc 117:852–874

13. Rowan SJ, Stoddart JF (2002) Surrogate-stoppered [2]rotaxanes: a new route to larger interlocked architectures. Polym Adv Technol 13:777–787

14. Takata T (2006) Polyrotaxane and polyrotaxane network: supramolecular architectures based on the concept of dynamic covalent bond chemistry. Polym J 38:1–20

15. Gibson HW, Bryant WS, Lee S-H (2001) Polyrotaxanes by free-radical polymerization of acrylate and methacrylate monomers in the presence of a crown ether. J Polym Sci Part A Polym Chem 39:1978–1993

16. Fang L, Olson MA, Benitez D, Tkatchouk E, Goddard WA III, Stoddart JF (2010) Mechanically bonded macromolecules. Chem Soc Rev 39:17–29

17. Oku T, Furusho Y, Takata T (2004) A concept for recyclable cross-linked polymers: topologically networked polyrotaxane capable of undergoing reversible assembly and disassembly. Angew Chem Int Ed 43:966–969

18. Kim K (2002) Mechanically interlocked molecules incorporating cucurbituril and their supramolecular assemblies. Chem Soc Rev 31:96–107

19. Lee D-W, Park KM, Banerjee M, Ha SH, Lee T, Suh K, Paul S, Jung H, Kim J, Selvapalam N, Ryu SH, Kim K (2011) Supramolecular fishing for plasma membrane proteins using an ultrastable synthetic host–guest binding pair. Nat Chem 3:154–159

20. Tuncel D, Steinke JHG (1999) Catalytically self-threading polyrotaxanes. Chem Commun 35:1509–1510

21. Frampton MJ, Anderson HL (2007) Insulated molecular wires. Angew Chem Int Ed 46:1028–1064

22. Gong H-Y, Rambo BM, Karnas E, Lynch VM, Sessler JL (2010) A 'Texas-sized' molecular box that forms an anion-induced supramolecular necklace. Nat Chem 2:406–409

23. Aprahamian I, Miljanic OS, Dichtel WR, Isoda K, Yasuda T, Kato T, Stoddart JF (2007) Clicked interlocked molecules. Bull Chem Soc Jpn 80:1856–1869

24. Liu Y, Wang H, Zhang H-Y, Liang P (2004) A metallo-capped polyrotaxane containing calix[4]arenes and cyclodextrins and its highly selective binding for Ca^{2+}. Chem Commun 40:2266–2267

25. Yamagishi T-A, Kawahara A, Kita J, Hoshima M, Umehara A, Ishida S-I, Nakamoto Y (2001) In situ polycondensation of *p-tert*-butylphenol in the presence of poly(ethylene glycol)s for preparation of polyrotaxanes. Macromolecules 34:6565–6570

26. Ogoshi T, Kanai S, Fujinami S, Yamagishi T-A, Nakamoto Y (2008) *para*-Bridged symmetrical pillar[5]arenes: their Lewis acid catalyzed synthesis and host–guest property. J Am Chem Soc 130:5022–5023

27. Champin B, Mobian P, Sauvage J-P (2007) Transition metal complexes as molecular machine prototypes. Chem Soc Rev 36:358–366

Polysilanes

Michiya Fujiki
Graduate School of Materials Science, Nara Institute of Science and Technology, Ikoma-Nara, Japan

Synonyms

Amorphous silicon; Crystal silicon; Field-effect transistor; Light-emitting material; Oxidation; Semiconductor; Silane; Thermolysis

Definition

Polysilanes are the unique Si–Si bond nanomaterials and have unique properties and characteristics that are not simple analogues of organic polymers and nanomaterials. Optical bandgap is broadly tunable, ranging from near IR (1.1 eV) and UV (5 eV). The dimensionality of Si-Si nanomaterials is possible to transform between zero-, one-, two-, and three-dimensional structures by chemical, thermal, photochemical, and electrochemical processes.

Introduction

Polysilanes, i.e., Si-Si frameworks carrying various organic groups, are a rich family of attractive polymers and compounds with potential applications in chemistry, physics, and surface and nanomaterial science. Polysilanes have unique properties and inherent characteristics that are not analogous to organic polymers and compounds. This section outlines the historical background and recent advances in the production of Si nanomaterials using polysilanes and related Si–Si bond frameworks.

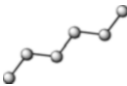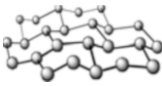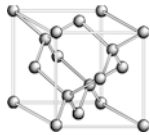## Hierarchy of the Si–Si Bond Family

The nature of the C–C bond leads to a rich variety of organic compounds that are thermally and kinetically stable in the presence of air and water. By referring to organic chemistry and the uniqueness of organosilanes, organosilicon chemists, and nanomaterials, scientists have designed and produced the corresponding organosilane analogues [1–3].

Si-Si frameworks are currently the most common fundamental source materials in microelectronics, optoelectronics, and photonics. Molecular silanes, including SiH_4, Si_2H_6, $HSiCl_3$, $SiCl_4$, and Me_2SiCl_2, are utilized in technology as Si sources to produce crystalline silicon (*c*-Si), polycrystalline silicon (*poly*-Si), amorphous silicon (*a*-Si:H), and silicon dioxide (SiO_2). Recently, Si–Si bond nanomaterials have been introduced that cover a broad range: (i) zero-dimensional (0-Dim) Si-Si frameworks, including nanocrystalline silicon (*nc*-Si) and silicon nanoparticles; (ii) one-dimensional (1-Dim) Si-Si frameworks, including chain-like polysilane and nanowires; (iii) two-dimensional (2-Dim) Si-Si frameworks, such as network-like polysilyne, Wöhler siloxene, and Si/SiO_2 superlattice; and (iv) three-dimensional (3-Dim) Si-Si frameworks, such as *c*-Si and *a*-Si:H (Table 1).

It has long been known that *c*-Si and *a*-Si:H, which are the most fundamental materials for microelectronics, are poor emitters in the UV-visible-near IR regions, with low quantum yields (Φ_F) of ~10^{-2} % at 300 K due to indirect electronic transitions with a narrow bandgap (1,127 nm, 1.1 eV). However, great efforts have been devoted to producing Si materials that are capable of efficiently emitting UV-visible light since the early reports of fairly efficient photoluminescence (PL) in the visible-near IR

Polysilanes, Table 1 Dimensionality of Si-Si frameworks and their optical bandgaps (E_g) in eV

0-Din	1-Din	2-Din	3-Din
SiH_4, $SiMe_4$			
Molecules	Chain–like	Sheet–like	Purely inorganics
E_g ~ 7 eV	E_g 2.9~4.1 eV	E_g 2.1~4.1 eV	E_g ~1.1 eV

region from *nc*-Si and porous Si (*por*-Si) in the 1990s. Several low-dimensional Si–Si bond frameworks have been theoretically and experimentally explored to date. When tailoring the UV-visible emission properties with a high Φ_F value, confining the photoexcited electron–hole pair (exciton) within the Bohr radius (r_B) of Si, which is on the order of ~5 nm, is of primary importance.

Wurtz-Type Reductive Polycondensation

In the early 1920s, Kipping, who is a father of organosilicon chemistry, reported an isolable Si-Si framework bearing phenyl groups prepared by the Wurtz-type polycondensation of diphenyl-dichlorosilane. Kipping attempted to produce tetraphenyldisilene by a Na reduction of diphenyl-dichlorosilane in benzene and toluene at reflux; he isolated soluble crystalline perphenylcyclosilanes $(Ph_2Si)_n$ ($n = 4$ and 6) and insoluble chain-like $(Ph_2Si)_n$. In 1949, Burkhard reported a similar insoluble, infusible white solid prepared by the Na reduction of dimethyldichlorosilane in benzene and toluene at reflux. This solid was characterized as poly(dimethylsilane). When these reactions were performed with Li in THF, perphenylcyclosilanes $(Ph_2Si)_n$ ($n = 4$–6) and permethylcyclosilanes $(Me_2Si)_n$ ($n = 6$) were isolated as the major products in excellent yields. These pioneering studies led to the versatile Wurtz-type condensation, which is useful in preparing families of organosilane molecules and polymers with a choice of substituents, solvent, some additives, and alkaline metals. The original Wurtz condensation required long reaction times and resulted in poor yields. To improve the yield and reduce the polymerization time, several modifications can be employed. For example, the use of a catalytic amount of crown ether and diglyme with Na metal readily afforded the corresponding chain-like polysilanes and network-like polysilynes under milder and safer conditions and in excellent yields [3, 4].

The disadvantages of the Wurtz condensation are its limitations in the use of organochlorosilanes, solvents, and additives, in that they may not contain any reactive functional groups, such as O–H, N–H, S–H, C=O, NO_2, C(=O)O, C≡N, C–Cl, C–Br, and C–I, except the C–O–C and C–F groups. Regardless of this limitation, the Wurtz-type reduction and its modifications are the most versatile methods for producing organosilicon compounds and materials.

This method is applicable to 0-Dim, 1-Dim, and 2-Dim Si nanomaterials.

Electrochemical Reduction

Electrochemical methods are among the safest, most environmentally friendly, and technically favorable processes for synthesizing Si nanomaterials (Fig. 1). The analogous electrochemical oxidation of thiophene, pyrrole, and aniline affords the corresponding polythiophene, polypyrrole, and polyaniline in the presence of an electrolyte at ambient temperature [3, 5].

In 1990, Canham found that photoluminescent *por*-Si can be formed by electrochemical corrosion when applied to a *p*-type *c*-Si wafer. Electrochemical reduction with alkaline earth metals (Mg and Mg-Cu) provides a milder coupling reaction with the corresponding organochlorosilane. Although the silanes that do not react with Mg are preferred, the electrochemical method is applicable to phenyl-containing
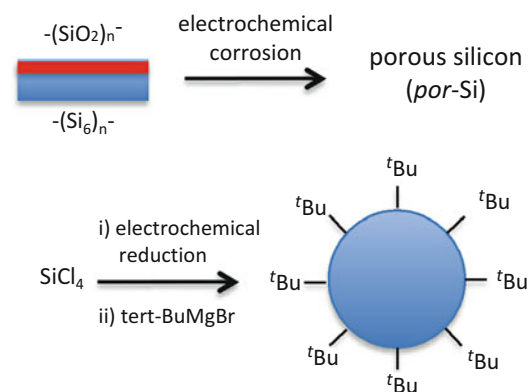
Polysilanes, Fig. 1 (*Top*) Electrochemical corrosion to prepare *por*-Si. (*Bottom*) Electrochemical reduction of SiCl_4, followed by in situ Grignard end-capping to prepare soluble Si nanoparticles

chlorosilane because Mg and Mg-Cu are not reactive when in contact with water and air.

In the 1990s, Shono et al. demonstrated the utility of electrochemical reduction with a Mg electrode to prepare dialkyldichlorosilanes in THF. Watanabe et al. applied the electrochemical method with the help of ultrasound to prepare soluble Si nanoparticles (nc-Si) capped with organic groups using tetrachlorosilane as the silicon source.

This method is applicable to 0-Dim and 1-Dim Si nanomaterials.

Ring-Opening Reactions from Precursors

Chain-like polysilane and block copolymers can be produced by ring-opening reactions of highly strained monocyclic and bicyclic compounds containing Si–Si bonds with the help of organolithium. For example, highly strained, masked disilene, initiated by an anionic catalyst, undergoes ring-opening polymerization. Although six-membered cyclosilanes such as $(Ph_2Si)_6$ and $(Me_2Si)_6$ are less sensitive to ring-opening reactions, smaller cyclosilanes such as $(R_2Si)_n$ (R = Ph, Me, H, n = 4 and 5), due to their inherent strain energy, are able to undergo ring-opening polymerization initiated by chemical reagents and thermolysis/photolysis. Well-defined cyclosilane derivatives are suitable as precursors for several polysilanes and organosilane compounds. Highly strained three-membered cyclosilanes, $(Ar_2Si)_3$, which have the ability to produce silylene Ar_2Si by photolysis and thermolysis, have been used to synthesize a rich family of compounds with Si=Si double bonds, including $Ar_2Si = SiAr_2$ (Ar = 2,4,6-trimethylphenyl and many substituted aromatics) [3, 6, 7].

This method is applicable to 0-Dim and 1-Dim Si nanomaterials.

Dehydrogenative Coupling with Organometallic Catalysts

Certain organohydrosilanes are used as silicon monomers for oxidative coupling reactions with organometallic catalysts including Zr, Ti, Hf, and Rh. Primary aryltrihydrosilanes such as $PhSiH_3$ give moderately higher molecular weight polymers than secondary diaryldihydrosilanes such as Ph_2SiH_2. Alkyltrihydrosilanes and dialkyldihydrosilanes, including n-octyl SiH_3 and di-n-octyl SiH_2, are used to produce the corresponding oligosilanes with the help of Wilkinson's catalyst, $(Ph_3P)_3RhCl$. More recently, Waterman et al. developed the selective synthesis of cyclic-10mers of PhHSi units from $PhSiH_3$ with an Ir complex [3, 8].

This method is applicable to 1-Dim Si nanomaterials.

Post-polymerization Toward Functionalization

Post-polymerization is applicable to a broad range of functionalization, as well as organic polymers. The most important issue in these reactions is the possibility of side reactions that break down the Si–Si bonds in Si-Si-based polymers and molecules. There is an inherent limitation: the functional groups that react with alkali and alkaline earth metals should be avoided [3].

This method is applicable to 1-Dim and 2-Dim Si nanomaterials.

De-intercalation of Calcium Silicide

As an alternative to these chemical reduction reactions, de-intercalation from Zintl phases under controlled hydrolysis at lower temperatures can produce the corresponding Si–Si-bonded solids (Fig. 2). Calcium silicide, $CaSi_2$, a typical Zintl phase, is produced by mixing Ca and Si with a small amount of Fe as a catalyst at high temperatures in a vacuum. Ionic solid $CaSi_2$, which has a high electrical conductivity and metallic behavior, is an ideal 2-Dim Si-Si framework structure. Negatively charged Si–Si-bonded nanosheets are regularly intercalated with positively charged Ca. The formal charges are $[(Si_6)^{2-}]_{1/3}//Ca^{2+}$. $CaSi_2$ looks like sila-graphene, comprised solely of Si–Si single bonds [3, 9].

P
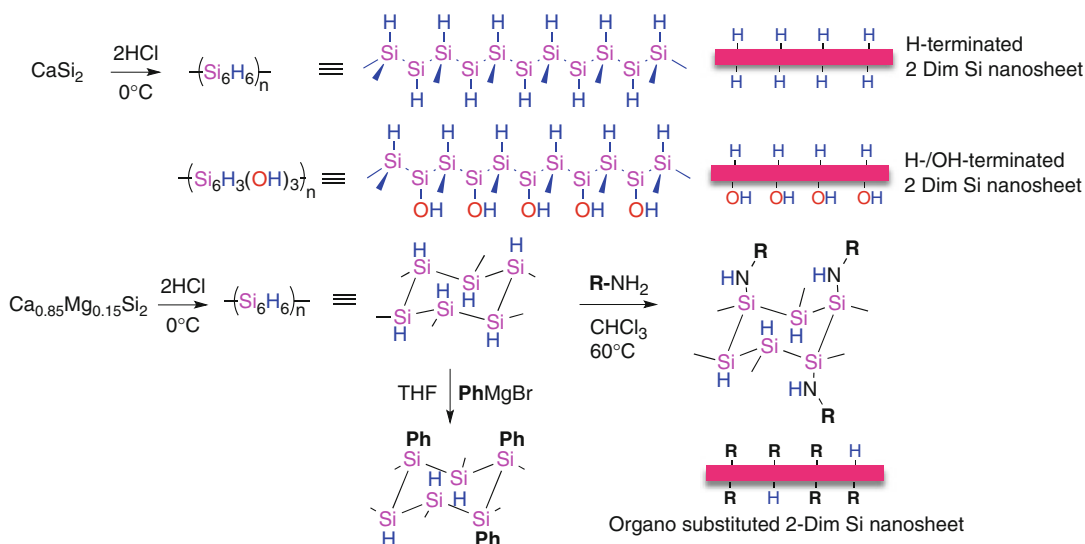
Polysilanes, Fig. 2 De-intercalation of CaSi$_2$ and its Mg alloy under controlled HCl treatment to prepare $(Si_6H_6)_n$ frameworks

By de-intercalating the Ca^{2+} from CaSi$_2$ with HCl, the Si layer opens the bandgap, thus leading to semiconducting properties that enable emission in the visible region. Recently, to produce monolayer 2-Dim Si-Si frameworks with H termini, the controlled hydrolysis of $(Ca_xMg_{1-x})Si_2$ followed by substitution with organic groups was successfully employed to give monolayer Si nanosheets carrying organic moieties that are readily soluble and/or dispersible in common organic solvents.

This method is applicable to 2-Dim Si nanomaterials.

Chemical Modification of Si–H Bonds at the *c*-Si Surface

Monolayers consisting of Si–H bonds at the *c*-Si surface may be chemically modified to introduce functional groups and provide great stability to water and air. The *c*-Si surface offers an ideal 2-Dim Si-framework: Si–Si-bonded nanosheets with puckered hexagonal lattices. Various functional groups have been successfully employed. A layer of Si–H bonds on *c*-Si can be formed by treatment with aqueous HF, followed by the removal of the SiO$_2$ layers from the bare *c*-Si [3, 10].

Microelectronic and photonic applications of *c*-Si inevitably use *c*-Si wafers with Si(100) and Si(111) orientations. However, when exposed to air, the surface layer of fresh *c*-Si rapidly forms ultrathin SiO$_2$ layers due to auto-oxidation. The native SiO$_2$, however, can be readily removed chemically with fluoride ions. The Si(111) surface is an ideal 2-Dim Si nanosheet with coagulated cyclohexasilane (polysilyne), $(Si_6H_6)_n$. The Si(100) surface is 1-Dim Si with trans-zigzag chain-like polysilane with H side groups, $(Si_2H_4)_n$, as shown in Fig. 3. These hydride surfaces on the *c*-Si wafers are alternative Si sources that are suited for surface-functionalized Si semiconductors, although hydride surfaces are insoluble and difficult to exfoliate in common organic solvents.

The hydrosilylation of unsaturated organic compounds, including C=C and C≡C bonds, is possible and may provide alkenyl and alkyl termination from Si-H-terminated *c*-Si surfaces (Fig. 4). The first hydrosilylation to hydride-passivated *c*-Si(111) surfaces was demonstrated two decades ago. Diacyl peroxide radical species allow the insertion of alkenes to Si-H groups at the surface to provide high-quality alkyl monolayers at 100 °C in 1 h. *n*-Octadecene can be used to introduce an *n*-octadecyl monolayer onto the
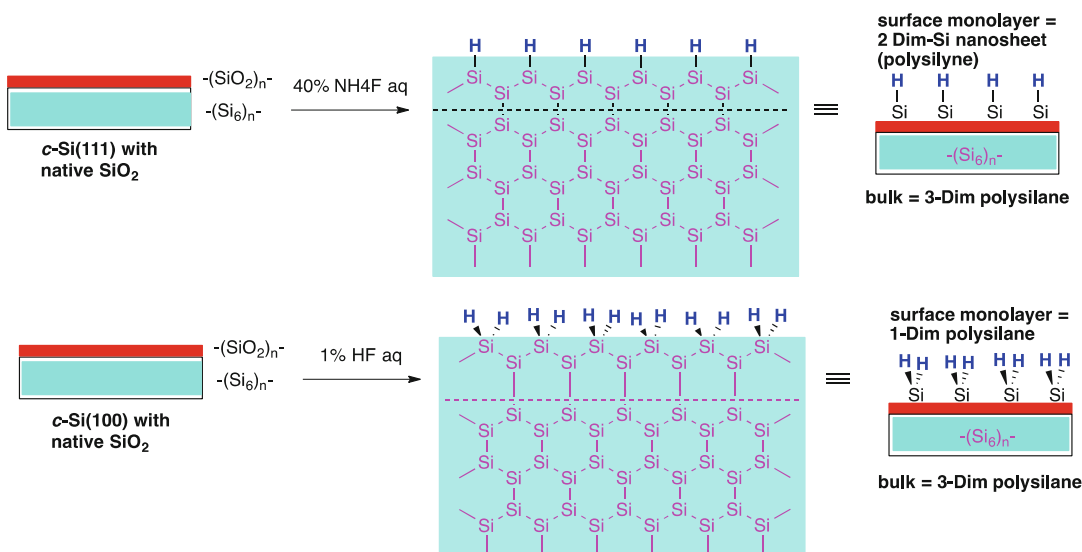
Polysilanes, Fig. 3 Schematic illustration of the two Si–H bonding states at the *c*-Si(111) and *c*-Si(100) surfaces

surface with a high degree of coverage in a dense-packed state with a tilt angle of ~30°. Surprisingly, the octadecene-modified *c*-Si surface possessed excellent chemical resistance toward air, aerated organic solvents, water, inorganic acids, aqueous ammonia, and fluoride ions. Several other surface functionalizations, with the help of such ordinary chemical reactions as C-H activation, ester hydrolysis, hydroboration, and grafting from polymerization, have been successfully demonstrated.

This method is applicable to 2-Dim Si nanomaterials.

Network-Like Polysilane (Polysilyne)

Chain-like polysilane is considered a soluble polymeric model of a 1-Dim silicon semiconductor. Little progress has been made toward the realization of 2-Dim Si-Si frameworks and ideal coagulated sila-graphene made of fused six-member rings (Fig. 5) [3, 11, 12].

Bianconi and Weidman reported for the first time the successful synthesis of *n*-hexylpolysilyne, which is a Si–Si-bonded polymer network and a soluble polymeric model of 2-Dim silicon and *a*-Si polymers, via the Wurtz condensation of

n-hexyltrichlorosilane with a liquid Na-K alloy and high-power ultrasonic waves (USW). Although this Na-K experiment with USW has disadvantages regarding safety, the resulting polysilyne features a collection of various micro-structures, and the polysilyne displays novel physical properties. Furukawa et al. developed a milder, safer synthesis of several polysilynes with alkyl and aralkyl groups using Na and a catalytic amount of crown ether in hot toluene. Jenneskens et al. used graphite-K in place of Na-K and Na-crown ether. Crown ether is not needed to produce fluoroalkyltrichlorosilane when fluoroalkylated polysilyne is reduced with Na in inert solvents.

Thermolysis

Crude solid *c*-Si is produced commercially by the thermolysis of highly corrosive and toxic $HSiCl_3$. Hydrogenated *a*-Si (*a*-Si:H) films are formed by the chemical vapor deposition (CVD) of highly flammable and explosive SiH_4 and Si_2H_6 with and without plasma-assisted external electromagnetic forces. Thus, *a*-Si:H is considered an insoluble highly cross-linked Si-Si framework with SiH and SiH_2 termini. By applying
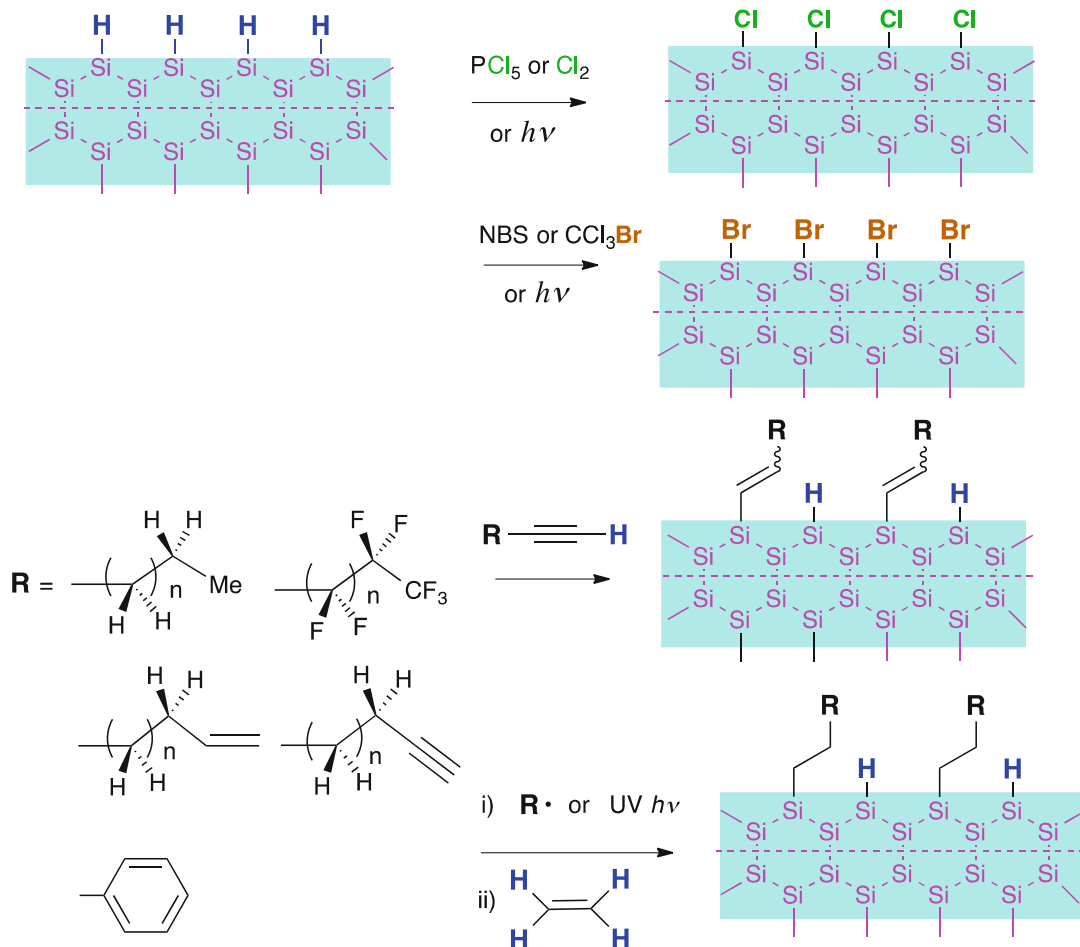
Polysilanes, Fig. 4 Surface chemical modifications of the Si–H bonds states at the *c*-Si(111) surface

a high-power Kr-F excimer laser to an *a*-Si:H film, polycrystalline silicon (*poly*-Si) films are formed due to the elimination of H atoms and thermal annealing. Higher temperatures at the surface of *a*-Si:H, typically above 500 °C, are required to eliminate the H atoms as H_2 gas. Because the Kr-F laser wavelength (248 nm) matches well with the Sis-Sis* transitions of *a*-Si:H and *poly*-Si, the elimination of H atoms occurs efficiently [3, 13–16].

As an alternative process to conventional thermal decomposition, CVD, and Kr-F laser-promoted H elimination, the flash thermolysis of soluble 2-Dim Si-Si frameworks, alkylpolysilyne, in a vacuum has been recently successfully employed. Unless they are under vacuum conditions, polysilanes and polysilyne may turn into

silicon carbide (SiC). The flash process, which means a rapid removal of volatile organic substances and H_2 gas, enables the facile control of the dimensions of the Si structure from 2-Dim to 3-Dim. The flash thermolysis of alkylpolysilyne in a vacuum above 500 °C leads to the formation of *poly*-Si with a minimal amount of SiH termini. However, the size of the crystals is limited to between several μm and several nm.

This method is applicable to 1-Dim and 2-Dim Si nanomaterials.

In 2006, Shimoda et al. demonstrated for the first time a solution-processable *poly*-Si thin film with high carrier mobilities by means of XeCl excimer laser pyrolysis of an *a*-Si film (Fig. 6). The film is obtained by a three-step pyrolysis of a parent polysilane, $(SiH_2)_n$, at 300–550 °C

Polysilanes, Fig. 5 Synthesis of organopolysilynes and organopolygermyne

n-butyl polysilyne

3,3,3-trifluropropyl polysilyne

n-butyl polygermine
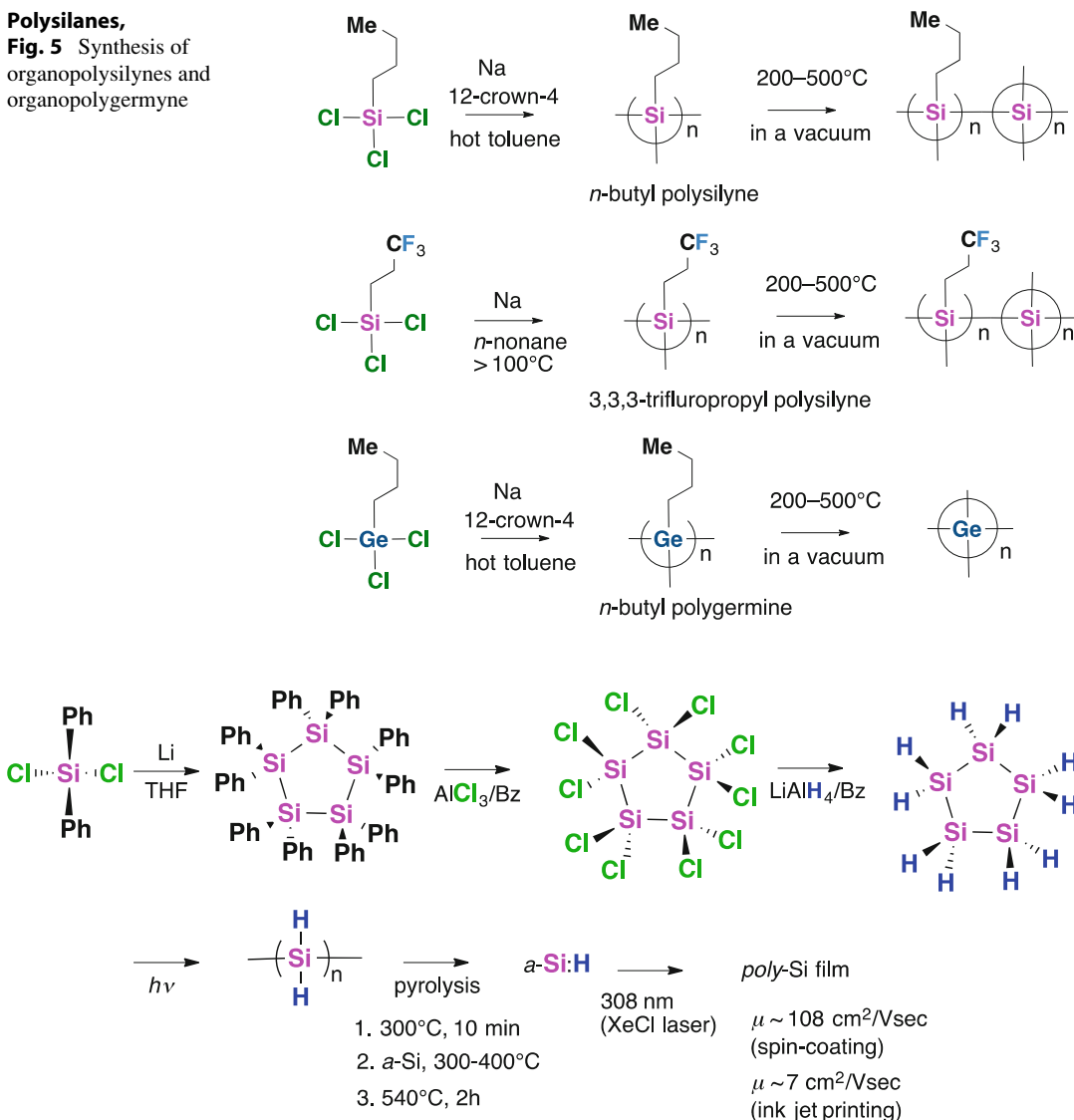
Polysilanes, Fig. 6 Synthetic route of a solution processable *poly*-Si film using diphenyldichlorosilane as a source material

in an O$_2$-free glove box. The hydrogenated polysilane is produced by a four-step synthesis, including a photolysis-induced ring-opening polymerization using diphenyldichlorosilane as a starting material.

Recently, several soluble alkylpolysilynes carrying *n*- and branched alkyl groups were successfully synthesized by the Wurtz reduction of the corresponding alkyltrichlorosilanes in the presence of crown ether as co-catalyst and

soluble polysilyne carrying trifluoroalkyl groups in the absence of crown ether (Fig. 5).

A soluble polysilyne bearing *n*-butyl group exhibits a green photoluminescence (PL) at 540 nm (2.3 eV). Its soluble Ge analogue, polygermyne bearing *n*-butyl groups, exhibits a red PL, peaking at 690 nm (1.8 eV) (Figs. 5 and 7). These polysilyne and polygermyne compounds gradually change to a colorless solid because of auto-oxidation within a few weeks
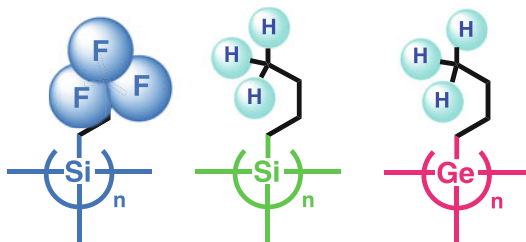
Polysilanes, Fig. 7 Schematic pictures of *n*-butylpolysilyne, 3,3,3-trifluoropropylpolysilynes, and *n*-butylpolygermyne with oxygen and water molecules

when the polymers are stored without special care. However, the polysilyne carrying the electron withdrawing 3,3,3-trifluoropropyl group is unique in that it emits blue (470 nm, 2.6 eV) in THF and UV light (338 nm, 3.7 eV) in *n*-octane. This marked PL solvatochromism is due to solvent polarity-induced switching in the intramolecular C-F/Si interactions.

Moreover, fluoroalkylated polysilyne remains unaffected by auto-oxidation due to intra- and intermolecular C-F/Si interactions between the electron donating Si-Si network and the 3,3,3-trifluoropropyl group. Thin films of trifluoropropylpolysilyne exhibit excellent resistance to air oxidation for at least 1 month. Trifluoropropylpolysilyne in a vacuum treated above 500 °C, however, exhibits no such air stability due to the loss of the trifluoropropyl group.

Because organopolysilynes are soluble model polymers of *a*-Si:H and "coagulated silagraphene," the further thermolysis of organopolysilynes and their photophysical properties under vacuum has received much attention. Recently, visible light emission from various soluble polysilynes at 460 nm (2.70 eV) and 740 nm (1.68 eV) at 77 K and room temperature was demonstrated by controlling the thermolysis temperature (200–500 °C) in a vacuum, resulting in multilayered Si nanosheets. When very weakly deep-red light-emitting Si nanoparticles produced by the thermolysis of *n*-butyl polysilyne at 500 °C were exposed to air, the PL switched abruptly to an intense blue (l = 430 nm) with a high Φ_F of 20–25 % at room temperature due to the alternation of the siloxene-like Si nanosheets.

Outlook

Currently, *c*-Si, *poly*-Si, and *a*-Si:H are the most archetypal semiconducting materials for microelectronics, optoelectronics, and photonics. By chemically controlling Si-Si frameworks, one can produce a broad range of Si nanomaterials: (i) 0-Dim Si (*nc*-Si and silicon nanoparticles), (ii) 1-Dim Si (chain-like polysilane and nanowires), (iii) 2-Dim Si (network-like polysilyne, Wöhler siloxene, and Si/SiO$_2$ superlattice), and (iv) 3-Dim Si (*c*-Si and *a*-Si:H). In recent years, solution processes for the fabrication of electronic and optoelectronic devices, as alternative methods to conventional vacuum and vapor phase deposition processes, have received much attention in a wide range of applications due to the many advantages of processing simplicity, reduced production costs, and safety of the chemical treatment. Particularly, the utilization of liquefied Si as a source of polymeric nanomaterials that are air stable, nontoxic, nonflammable, and nonexplosive is crucial in the envisaged applications of printed semiconductor devices for large-area flexible displays, solar cells, and thin-film transistors. Recent progress in this area has been greatly focused on organic semiconductors with *p*-conjugated polymers and molecules due to their processability. As discussed above, recent developments in several 2-Dim and pseudo 3-Dim Si nanomaterials may lead to promising Si nanomaterials that are solution-processable, wide- and mid-gap semiconductors, covering a wide range of optical bandgaps (1.1 eV (1,120 nm)–4.1 eV (300 nm)). With the help of a wide tunability of the bandgap, these Si nanomaterials may serve as printable inorganic inks for solar energy conversion devices, as well as photoluminescent and electroluminescent devices.

Related Entries

▶ Charge-Transporting Polymers
▶ Conducting Polymers
▶ Cross-Linked Polymer Synthesis

References

1. Brus L (1994) Luminescence of silicon materials: chains, sheets, nanocrystals, nanowires, microcrystals, and porous silicon. J Phys Chem 98:3575–3581. doi:10.1021/j100065a007

2. Yu PY, Cardona M (2005) Fundamentals of semiconductors: physics and materials properties, 3rd edn. Springer, Berlin, pp 345–426, Chapter 7

3. Fujiki M (2014) Si–Si bond polymers, oligomers, molecules, surface, and materials. In: Müllen K, Reynolds JR, Masuda T (eds) Conjugated polymers: a practical guide to synthesis. Royal Society of Chemistry, London

4. Miller RD, Michl J (1989) Polysilane high polymers. Chem Rev 89:1359–1410. doi:10.1021/cr00096a006

5. Cullis AG, Canham LT, Calcott PEJ (1997) The structural and luminescence properties of porous silicon. J Appl Phys 82:909–965. doi:doi.org/10.1063/1.366536

6. Cypryk M, Gupta Y, Matyjaszewski K (1991) Anionic ring-opening polymerization of 1,2,3,4-tetramethyl-1,2,3,4-tetraphenylcyclotetrasilane. J Am Chem Soc 113:1046–1047. doi:10.1021/ja00003a050

7. Iwamoto T, Kira M (2006) Progress in the chemistry of stable disilenes. Adv Organomet Chem 54:73–148. doi:doi.org/10.1016/S0065-3055(05)54003-6

8. Wetherby AE, Mucha NT, Waterman R (2012) High activity and selectivity for silane dehydrocoupling by an Iridium catalyst. ACS Catal 2:1404–1407. doi:10.1021/cs300186v

9. Okamoto H, Sugiyama Y, Nakano H (2011) Synthesis and modification of silicon nanosheets and other silicon nanomaterials. Chem Eur J 17:9864–9887. doi:10.1002/chem.201100641

10. Buriak JM (2002) Organometallic chemistry on silicon and germanium surfaces. Chem Rev 102:1271–1308. doi:10.1021/cr000064s

11. Bianconi PA, Weidman TW (1988) Poly (n-hexylsilyne): synthesis and properties of the first alkyl silicon [RSi]n network polymer. J Am Chem Soc 110:2342–2344. doi:10.1021/ja00215a077

12. Furukawa K, Fujino M, Matsumoto N (1990) Optical properties of silicon network polymers. Macromolecules 23:3423–3426. doi:10.1021/ma00216a006

13. Shimoda T, Matsuki Y, Furusawa M, Aoki T, Yudasaka I, Tanaka H, Iwasawa H, Wang D, Miyasaka M, Takeuchi Y (2006) Solution-processed silicon films and transistors. Nature 440:783–786. doi:10.1038/nature04613

14. Fujiki M, Kawamoto Y, Kato M, Fujimoto Y, Saito T, Hososhima S, Kwak G (2009) Full-visible-spectrum emitters from pyrolysis of soluble Si–Si bonded network polymers. Chem Mater 21:2459–2466. doi:10.1021/cm900567g

15. Fujiki M, Kato M, Kawamoto Y, Kwak G (2011) Green-and-red photoluminescence from Si–Si and Ge–Ge bonded network homopolymers and copolymers. Polym Chem 2:914–922. doi:10.1039/C0PY00345J

16. Fujiki M, Fujimoto Y, Saxena A, Kawabe T, Kwak G (2012) Air-stable poly(3,3,3-trifluoropropylsilyne) homo- and copolymers. Polym Chem 3:3256–3265. doi:10.1039/C2PY20508D

Polysiloxanes

Takahiro Gunji
Faculty of Science and Technology, Department of Pure and Applied Chemistry, Tokyo University of Science, Noda, Chiba, Japan

Definition

Polysiloxane is an inorganic polymer, which consists of siloxane bonding in the main chain [1]. "Inorganic polymer" is a polymer, which consists of non-carbon element or elements in the main chain. "Siloxane bonding" means the chemical bonding, which consists of silicon-oxygen-silicon catenation.

Polysiloxane is formed by a connection of many unit structures to be a high-molecular-weight compound. When the number of repeating unit is not so high, the compound is named as oligosiloxane. The number of repeating unit to define poly- and oligosiloxanes is unclear.

Structural Unit of Siloxanes

The main chain of siloxanes is composed of silicon and oxygen. Oxygen atom simply links two silicon

P

atoms to form siloxane bonding. Because silicon is an element located at 14 group and third period, silicon has four valence electrons. The general structure of silicon is explained as $Si(OSi)_n R_{4-n}$ where n is a numeral number 0, 1, 2, 3, or 4.

Monofunctional unit structure M, $SiR_3 O_{1/2}$, such as trimethylsiloxy $Si(CH_3)_3 O_{1/2}$ or triethoxysiloxy $Si(OCH_2CH_3)_3 O_{1/2}$ is important as a terminal group in polysiloxane. Difunctional unit structure D, $SiR_2 O_{2/2}$, such as dimethylsiloxy $Si(CH_3)_2 O_{2/2}$ or ethoxy(methyl)siloxy $Si(OCH_2CH_3)(CH_3)O_{2/2}$ is important as a structure in the main chain. Trifunctional unit structure T, $SiRO_{3/2}$, such as methylsilsesquioxy $Si(CH_3)O_{3/2}$ or ethoxysilsesquioxy $Si(OCH_2CH_3)O_{3/2}$ is utilized as a structure in the main chain to form a branching, cage, and ladder structure. Tetrafunctional unit structure Q, $SiO_{4/2}$, is used to form a branching. The name "Q" is originated from the "quarto" or "quasi" to distinguish from "tri."

Formation of Siloxane Bonding

Siloxane bonding is formed by several methods. The popular and simple technique is the hydrolytic polycondensation reaction of sila-functional compounds such as chlorosilanes, alkoxysilanes, acetoxysilanes, aminosilanes, isocyanatosilanes, etc. Polysiloxanes are synthesized by the hydrolysis of sila-functional compounds to form silanol and then condensation reaction between silanols or silanol and sila-functional moiety to form siloxane bonding. Non-hydrolytic condensation process is another choice by the reaction of acetoxysilanes with alkoxysilanes [2] or alkoxysilanes with chlorosilanes [3] to form siloxane bonding with the production of acetates or acetyl chloride. The third method is the oxidation of silicon-silicon bonding [4, 5]. This technique is effective when a precursor compound with a proper structure is synthesized. The fourth method is the oxidation of hydrosilyl group followed by the condensation reaction [6]. The fifth method is the extraction of siloxane skeleton from the natural silicate, which is useful for the preparation of oligosiloxanes such as disiloxanes, trisiloxanes, or cyclotrisiloxanes [7].

The rate for the formation of siloxane bonding is highly dependent on the reaction condition such as concentration of silanes, temperature, steric hindrance of functional group, and polarity of solvent. The hydrolysis and condensation is favored under high concentration of silanes, high temperature, low steric hindrance of the functional group, and low polarity of solvent. The condensation rate for the formation of siloxane bonding is controllable because the reaction rate of hydrolysis is higher than that of condensation reaction [8]. Namely, polysiloxanes with a highly regulated molecular weight and molecular weight distribution are produced by a careful control of the hydrolysis rate and the condensation rate.

The hydrolysis and condensation reaction of alkoxysilanes is often catalyzed by acid or base catalyst. Under acidic condition, silanol is formed by a series of reactions which consist of the protonation of oxygen atom in alkoxy group, the attack of water to the silicon atom, the elimination of alcohol, and the elimination of proton. Then, the protonated silanol or alkoxy group is attacked by silanol to form siloxane bonding with a production of water or alcohol, respectively. Linear-shaped polysiloxanes are formed by repeating these reactions. On the other hand, under basic condition, silanol is formed by the attack of hydroxide ion to the silicon atom and the elimination of alkoxy group. When di-, tri-, or tetrafunctional silane is subjected to the hydrolysis reaction, the attack of hydroxide ion to silanol is favored after the first attack of hydroxide ion to silicon atom to produce silanediol, silanetriol, or silanetetrol. These silane polyols are subjected to the three-dimensional condensation reaction randomly to form a silica gel. Generally, almost all of the alkoxysilanes in feed are subjected to the hydrolysis and condensation reaction to form silanol or siloxane bonding under acidic condition, while a mixture of silica gel and unreacted alkoxysilane is formed under basic condition [9].

Polydimethylsiloxane

Polydimethylsiloxane is one of the well-known polysiloxanes. Polydimethylsiloxanes, which are

denoted as $((CH_3)_2SiO)_n$, are named as silicones because this polymer is representative to be formed by the polymerization of silicoketone $(CH_3)_2Si = O$ as an imaginary compound.

Polydimethylsiloxanes are classified into two groups based on the catenation: cyclics and linears. Cyclics such as dimethylcyclotrisiloxane and dimethylcyclotetrasiloxane are the most stable dimethylsiloxanes.

Polydimethylsiloxanes are prepared by a complicated procedure such as hydrolysis of dichlorodimethylsilane and a following ring-opening polymerization of cyclics. Difunctional dimethylsilane such as dichloro(dimethyl)silane or dialkoxy(dimethyl)silane is subjected to the hydrolysis under acidic or basic conditions. Polydimethylsiloxane is prepared by a ring-opening polymerization of cyclics using a strong acid or a strong base, which breaks the siloxane bonding and stabilizes the terminal group of polymer chain. The polymerization is terminated by neutralization. This polymerization reaction is based on the equilibrium of cyclic and linear polysiloxane chains, because the depolymerization of linear polydimethylsiloxanes to cyclics takes place as a reversed reaction.

Polydimethylsiloxanes are known as a heat-resistant polymer. The fluidity is almost constant and no significant change is observed on heating and cooling process.

Side groups are easily changed by mixing other silane monomers in a desired ratio during the polymerization. Vinyl, hydrido, and chloromethyl groups are often introduced as a side chain. On the other hand, branching is introduced by mixing tri- or tetrafunctional silane to form DT resin or DQ resin.

Polysilsesquioxane

Polysilsesquioxanes are polysiloxanes with the formula of $(RSiO_{3/2})_n$. Polysilsesquioxanes, in other words, consisted of a repeating T or Q unit.

Polysilsesquioxanes are classified into three groups based on the catenation: cage, ladder, and amorphous. Cage and ladder polysilsesquioxanes have a highly regulated structure which is formed by a precise condensation of T or Q unit. The amorphous polysilsesquioxanes are formed by a random condensation of T or Q unit.

Cage polysilsesquioxanes are synthesized by a careful hydrolytic polycondensation of tri- or tetrafunctional silanes. Hidrido, alkyl, vinyl, aryl, alkoxy, and tetraalkylammoniumoxy groups are well-known side groups [10]. The synthetic procedure is varied depending on the side group. Octamer is the most stable isomers among the cage polysilsesquioxanes, which consisted of two cyclic tetramers in the face-to-face fashion. The octamers are denoted as T_8^R by describing the number of T unit as a subscript and the abbreviation of side-chain group as a superscript: T_8^H and T_8^{Me} denote the formulae $(HSiO_{3/2})_8$ and $(MeSiO_{3/2})_8$, respectively. If the octamers are synthesized from tetrafunctional silanes, they are denoted as Q_8^R such as Q_8^{Et} and Q_8^{TMA} for $((EtO)SiO_{3/2})_8$ and $((Me_4NO)SiO_{3/2})_8$, respectively. Other functional groups such as 3-methacryloxypropyl, 3-mercaptopropyl, or 3-methoxypropyl are easily synthesized by hydrosilylation of T_8^H with allyl compounds in the presence of platinum catalyst.

Ladder silsesquioxanes are synthesized by a reputation of careful reactions. The first ladder polysilsesquioxane was reported to be formed by a simple hydrolysis of trichloro(phenyl)silane followed by an equilibrium condensation in the presence of potassium hydroxide [11]. However, the product based on this procedure is doubtful whether it is a ladder-structured polysilsesquioxane or not. A real ladder polysilsesquioxanes are produced by a hydrolytic polycondensation of 3-aminopropyl(trimethoxy) silane under acidic condition to form $(Cl(H_3N (CH_2)_3SiO_{3/2})_n$ [12]. This compound is found to be twisted to form a rod-like structure, which is accumulated to form a hexagonal structure. Ladder oligosilsesquioxanes are synthesized by a careful condensation and separation of trifunctional silanes: isopropyl [13] and methyl [14] oligosilsesquioxanes are synthesized and characterized.

The amorphous polysilsesquioxanes are synthesized by a simple hydrolytic condensation of

P

tri- or tetrafunctional silane [15, 16]. The catenation of T or Q unit is not controlled to provide a randomly condensed product. The products are often gels because of the control-free condensation of silanetriol or silanetetrol. A soluble polysilsesquioxane is formed by a careful tandem reaction of hydrolysis and polycondensation by controlling the rates of hydrolysis and condensation.

Resins

MT resins are synthesized from mono- and trifunctional silanes. The main structure is composed of T unit. The degree of condensation is controlled by the reaction condition such as temperature, concentration, molar ratio of water to functional silanes, etc. The condensation of T unit is terminated by the reaction with M unit. The degree of condensation, molecular weight, and degree of branching are controlled by the molar ratio of M and T unit and reaction procedure.

MQ resins are synthesized from mono- and tetrafunctional silanes. The main structure is composed of Q unit, which is close to the structure of silica. The MQ resin becomes sticky and brittle by increasing the degree of condensation. M unit is added to terminate the residual silanol group in the resin. The silanes are fully hydrolyzed to diminish all functional groups in Q unit.

TQ resins are synthesized from tri- and tetrafunctional silanes. Because they have no terminal group in the resin, tri- and tetrafunctional silanes are fully hydrolyzed. Some special care should be given to avoid gelation.

References

1. Alemán J, Chadwick AV, He J, Hess M, Horie K, Jones RG, Kratochvíl P, Meisel I, Mita I, Moad G, Penczek S, Stepto RFT (2007) Definitions of terms relating to the structure and processing of sols, gels, networks, and inorganic-organic hybrid materials (IUPAC Recommendations 2007). Pure Appl Chem 79:1801

2. Shapatin AS, Markina RF, Zhinkin DY, Blekh LM, Sobolevskaya LV, Sobolevskii MV (1969) Polyorganosiloxanes. USSR SU 255575 19691028

3. Wakabayashi R, Sugiura Y, Shibue T, Kuroda K (2011) Practical conversion of chlorosilanes into alkoxysilanes without generating HCl. Angew Chem Int Ed 50:10708

4. Sakurai H, Kira M, Kumada M (1971) A new oxygen-insertion reaction into silicon-silicon bonds with tertiary amine oxides. Bull Chem Soc Jpn 44:1167

5. Tamao K, Kumada M, Takahashi T (1975) Oxidation of silicon-silicon and silicon-hydrogen bonds with molecular oxygen and bis(trimethylsilyl) peroxide. J Organomet Chem 94:367

6. Gunji T, Ueda N, Abe Y (2008) Syntheses of Linear Ethoxysiloxanes by the oxidative condensation of triethoxysilane. J Sol–gel Sci Tech 48:163

7. Goodwin GB, Kenney ME (1990) A new route to alkoxysilanes and alkoxysiloxanes of use for the preparation of ceramics by the sol-gel technique. Inorg Chem 29:1216

8. Assink RA, Kay BD (1988) Sol-gel kinetics. 2. Chemical speciation modeling. J Non-Cryst Solids 99:359

9. Brinker CJ, Scherer GW (1990) Sol–Gel science: the physics and chemistry of Sol–Gel processing. Academic, New York

10. Abe Y, Gunji T (2004) Oligo and polysiloxanes. Prog Polym Chem 29:149

11. Brown JF Jr, Vogt LH Jr, Katchman A, Eutance JW, Krantz KW (1960) Double chain polymers of phenylsilsesquioxane. J Am Chem Soc 82:6194

12. Kaneko Y, Iyi N, Matsumoto T, Kitamura K (2005) Synthesis of rodlike polysiloxane with hexagonal phase by sol–gel reaction of organotrialkoxysilane monomer containing two amino groups. Polymer 46:1828

13. Unno M, Suto A, Matsumoto H (2002) Pentacyclic laddersiloxane. J Am Chem Soc 124:1574

14. Suyama K, Gunji T, Arimitsu K, Abe Y (2006) Synthesis and structure of ladder oligosilsesquioxanes: tricyclic ladder oligomethylsilsesquioxanes. Organometallics 25:5587

15. Takamura N, Gunji T, Hatano H, Abe Y (1999) Preparation and properties of polysilsesquioxanes: polysilsesquioxanes and flexible thin films by acid-catalyzed controlled hydrolytic polycondensation of methyl- and vinyltrimethoxysilane. Polym J Sci Part A Polym Chem 37:1017

16. Gunji T, Hayashi Y, Komatsubara A, Arimitsu K, Abe Y (2012) Preparation and properties of flexible free-standing films via polyalkoxysiloxanes by acid-catalyzed controlled hydrolytic polycondensation of tetraethoxysilane and tetramethosyxilane. Appl Organomet Chem 26:32

Polystyrene (PSt)

Takaya Terashima
Department of Polymer Chemistry, Graduate
School of Engineering, Kyoto University, Kyoto,
Japan

Synonyms

Polystyrene; PS; Styrene polymer; Styrenic
polymer

Definition

Polymer obtained from addition polymerization
of styrene.

Introduction

Polystyrene is a polymer of styrene [–(CH$_2$CH
(C$_6$H$_5$))$_n$–], which is categorized as one of the
most popular thermoplastic resins including
high-density polyethylene, low-density polyeth-
ylene, polypropylene, and poly(vinyl chloride)
[1, 2]. Polystyrene was first discovered in distil-
lation of storax resin (a natural resin) in 1839 by
Eduard Simon (in Germany). The commercial
production of polystyrene as a synthetic resin
began in the 1930s (in 1931 by BASF, in 1938
by Dow). Various styrene-based polymers are
now manufactured as resin, form, and rubber all
over the world to be processed into materials and
goods essential for our daily life.

Polystyrene can be prepared by four kinds of
addition polymerization of styrene through differ-
ent active species and/or intermediates: via radical,
anionic, cationic, and coordination polymerization
(Fig. 1) [1]. The primary structure of polystyrene
(molecular weight, stereoregularity, etc.) is depen-
dent on polymerization systems to importantly
affect physical and mechanical properties. Free
radical polymerization is most widely used to com-
mercially produce atactic polystyrene with high
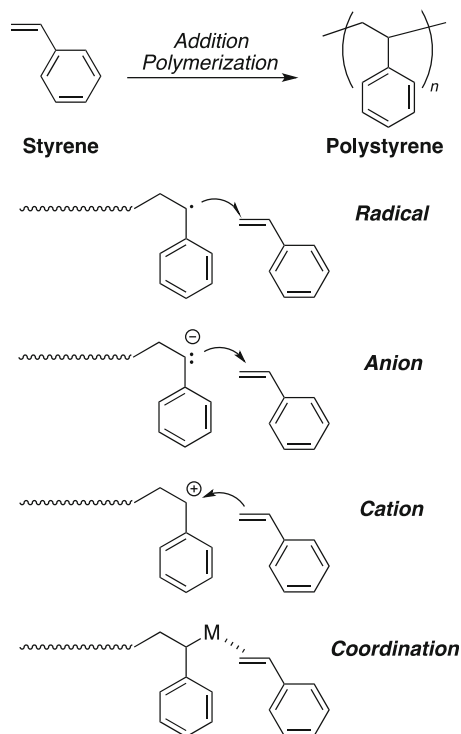
Polystyrene (PSt), Fig. 1 Synthesis of polystyrene via
addition polymerization of styrene

molecular weight (M_w = 200,000–300,000), i.e.,
general-purpose polystyrene (GPPS), which
results in an amorphous polymer with relatively
high glass transition temperature (T_g = ~100 °C)
owing to multiple but randomly oriented
(non-stereospecific) phenyl groups. Such polysty-
rene is thus hard and transparent solid at ambient
temperature to be processed into clear thermoplas-
tic products by extrusion or injection-molding
techniques at high temperature (180–260 °C).
However, atactic polystyrene involves low resis-
tance to impact (brittle), heat, and chemicals
(easily soluble in organic solvents). These points
are now successfully modified and improved by
the following strategies: copolymerization with
other monomers (e.g., acrylonitrile, butadiene)
and/or rubbers, blending with other polymers
(e.g., rubbers, elastomers), and precision control
of stereoregularity of polystyrene. For example,
syndiotactic polystyrene obtained from coordina-
tion polymerization is a crystalline polymer to

P

have robust mechanical properties and high heat and chemical resistance [3, 4].

This entry reviews "polystyrene" from polymerization chemistry of styrene and precision synthesis of polystyrene with well-controlled primary structure to general properties and applications of polystyrene-based materials.

Polymerization of Styrene

Addition Polymerization. Generally, addition polymerization (nonliving system) involves four reaction processes: initiation, propagation, termination, and chain transfer. Figure 2a shows typical reaction processes in free radical polymerization: (1) *initiation*, formation of active radical species (R•) from initiators (I) and subsequent addition of the radicals (R•) into monomers (M); (2) *propagation*, consecutive addition of

radical polymer terminals (P•) to monomers (M) to grow polymers (P•); (3) *termination*, coupling reaction (P–P) or disproportionation (P + P) of two growing polymers (P•); and (4) *chain transfer*, reaction of radical polymer terminals (P•) with chain transfer agents (A) including solvents, monomers, and polymers to give terminated polymers (P) and new active species (A•) that immediately initiate polymerization.

In such free radical polymerization of styrene, active species (R•: e.g., carbon radicals) are slowly and gradually generated from initiators (I) but immediately react with monomers (M) to grow polymers up to large molecular weight (P) until bimolecular termination and/or chain transfer reaction of the growing polymers. The reaction cycle competitively and successively proceeds during polymerization. As a result, number-average molecular weight (M_n) of polymers (polystyrene) becomes large even at the
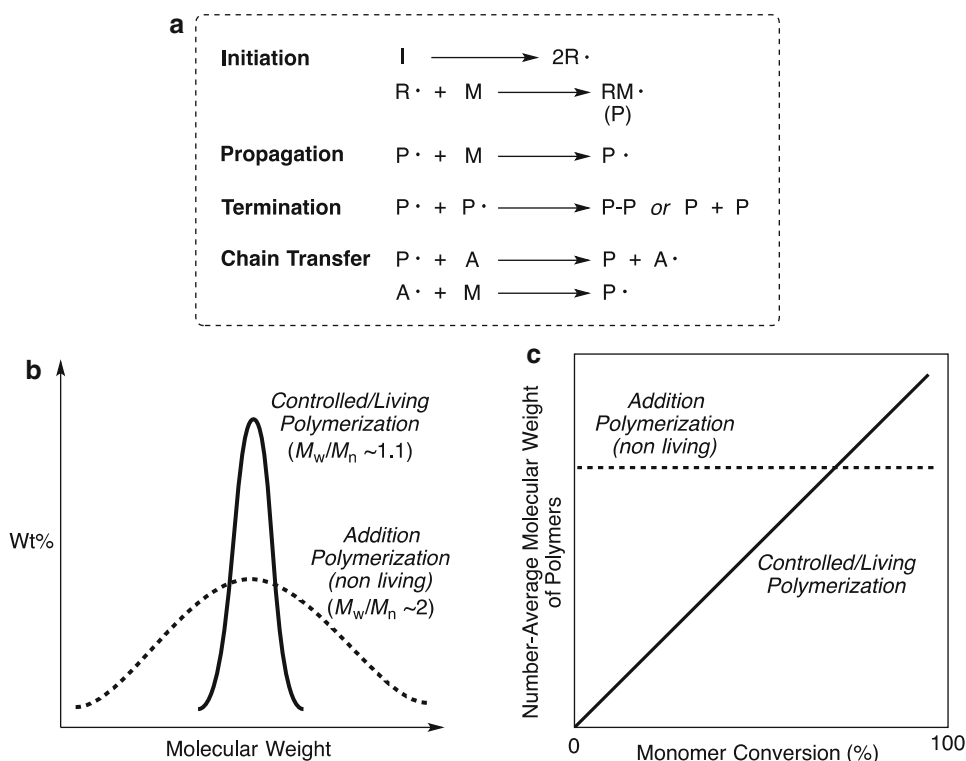
Polystyrene (PSt), Fig. 2 (**a**) Free radical addition polymerization of monomers. Effects of polymerization systems (nonliving vs. living/controlled) on (**b**) molecular

weight distribution and (**c**) number-average molecular weight of polymers as a function of monomer conversion

initial stage of polymerization to be almost kept constant independently of monomer conversion, while molecular weight distribution of polymers turns broad (M_w/M_n, ~2.0) (Fig. 2b, c: dash lines).

In contrast, controlled/living polymerization undergoes initiation and propagation without termination and chain transfer reaction in principle [5, 6]. Thus, if initiation homogeneously takes place much faster than propagation to grow polymers, number-average molecular weight of polymers linearly increases with monomer conversion, and molecular weight distribution becomes narrow (M_w/M_n, ~1.1) and ideally obeys Poisson distribution (Fig. 2b, c: solid lines). Molecular weight of polymers can be precisely controlled by tuning the molar feed ratio of monomers ([M]) to an initiator ([I]): $M_n = F$w (formula weight of M) × (conversion/100) × ([M]/[I]). Such living polymerization was

sensationally first discovered in anionic polymerization of styrene in 1956 by Michael Szwarc [6]. This opens precision polymer synthesis such as block copolymers, end-functional polymers, graft copolymers, and star polymers [5–7].

Four kinds of styrene polymerization systems (radical, anion, cation, coordination) respectively have advantages and disadvantages in efficiency, controllability, and accessibility. Figure 3 summarizes typical initiating/catalytic systems for styrene polymerization and the features of the products [1, 3, 4, 6–16].

Free Radical Polymerization. Free radical polymerization is most widely used to synthesize polystyrene [1, 2]. Thanks to the highly active but neutral growing species, radical polymerization has lots of attractive advantages: (1) efficient high yield synthesis (e.g., bulk polymerization), (2) no requirement of strict purification of

Polymerization			Initiating/Catalytic System	Molecular Weight	Tacticity	Properties
Radical	*Free*		Spontaneous Initiation	Broad Distribution ($M_w/M_n > 2$)		
			Radical Initiator (peroxide, azo compounds)			
	Living (Controlled)	MCLRP ATRP	Alkyl Halide / Metal Catalyst (Ru, Cu, Fe, Ni etc.)	Controlled Narrow Distribution ($M_w/M_n < 1.3$)	Atactic	Amorphous
		NMP	BPO / TEMPO Alkoxyamine			
		RAFT Polym.	Trithiocarbonate Dithiocarbamate			
Anionic	*Living*		Naphthalene / Alkyl Metal (K, Na, Li)	Controlled Quite Narrow Distribution ($M_w/M_n < 1.1$)	Atactic	Amorphous
			Alkyl Lithium (*n*-BuLi, *sec*-BuLi etc.)			
Cationic	*Free*		Strong Acid (HClO$_4$ etc.)	Low Broad Distribution ($M_w/M_n > 2$)	Atactic	Amorphous
			Proton Source / Lewis Acid (H$_2$O/AlCl$_3$, ROH/BF$_3$)			
	Living		1-phenylethyl chloride (PhEtCl) / SnCl$_4$ / *n*-Bu$_4$NCl	Controlled Narrow Distribution ($M_w/M_n \sim 1.1$)		
Coordination	*Stereospecific*		TiCl$_4$ / Al(CH$_2$CH$_3$)$_3$ (Ziegler-Natta Catalyst)	$M_w/M_n \sim 2$	Isotactic	Crystalline (T_m = ~230 ºC)
			Ti(η-C$_5$H$_5$)Cl$_3$ / MAO (Half-titanocene)		Syndiotactic	Crystalline (T_m = ~270 ºC)

Polystyrene (PSt), Fig. 3 Primary structure (molecular weight, tacticity) and properties of polystyrene obtained from addition polymerization (radical, anionic, cationic, and coordination polymerization) of styrene with typical initiating/catalytic systems. *MCLRP* metal-catalyzed living radical polymerization, *ATRP* atom transfer radical polymerization, *NMP* nitroxide-mediated radical polymerization, *RAFT polym.* reversible addition-fragmentation chain transfer polymerization

Polystyrene (PSt),
Fig. 4 Free radical
polymerization of styrene
with BPO

Initiation
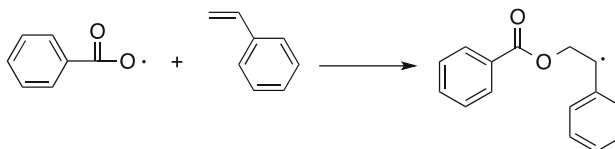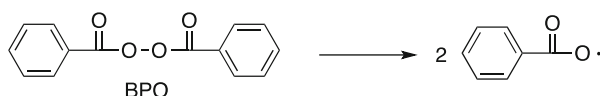
Propagation
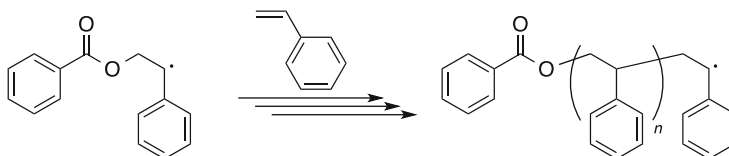
Termination
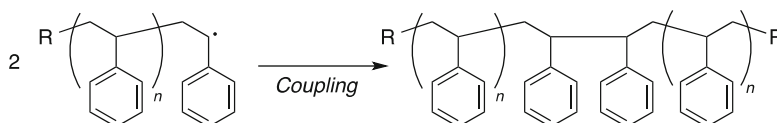
monomers and solvents, (3) efficient polymerization in water (i.e., dispersion or emulsion polymerization in water), and (4) direct polymerization of polar functional monomers and random copolymerization of various monomers, resulting in efficient modification of physical properties and functionalization.

Peroxide and azo compounds (e.g., benzoyl peroxide, BPO; 2,2′-azobisisobutyronitrile, AIBN) are often employed as initiators for styrene polymerization (Fig. 4). Typically, BPO is thermally decomposed via the homolytic cleavage of the oxygen-oxygen bond to gradually generate benzene carboxyl radicals that immediately initiate chain polymerization of styrene. The propagation is terminated by the coupling reaction of two polystyrene radicals. The final products have large molecular weight, broad molecular weight distribution (M_w/M_n ~2), and no specific stereoregularity (atactic).

Uniquely, spontaneous initiation without any external addition of radical initiators is also effective for styrene polymerization at over 100 °C (Fig. 5). However, the resulting products are slightly contaminated by styrene dimers and trimers (1–2 wt%) such as 1-phenyltetralin and

1,2-diphenylcyclobutane. Hence, the following two mechanisms for radical generation are proposed: (1) a reactive dimer (A–H), obtained from Diels-Alder dimerization of styrene, reacts with styrene (S) to give a dimer radical (A•) and a styrene radical (SH•) (Fig. 5a), and (2) two styrene molecules are transformed into 1,4-diradical (•S–S•) (Fig. 5b).

General-purpose polystyrene (GPPS), a typical example of polystyrene commercially produced via free radical polymerization, has weight-average molecular weight (M_w) of 200,000–300,000 [1]. In the industrial process, bulk polymerization of styrene via spontaneous initiation is often conducted at 100–170 °C, whereas the inevitable volatile dimers (Fig. 5) sometimes cause problems during extrusion and molding operation. Thus, radical initiators (e.g., peroxide) are also appropriately combined so as to suppress such oligomer formation, which further enhances polymerization rate to access polystyrene with desired molecular weight and yield. The selection of commercial manufacture processes among bulk, solution, suspension, precipitation, and emulsion polymerization is dependent on types (e.g., resin, form, lattice), features, and uses of products.
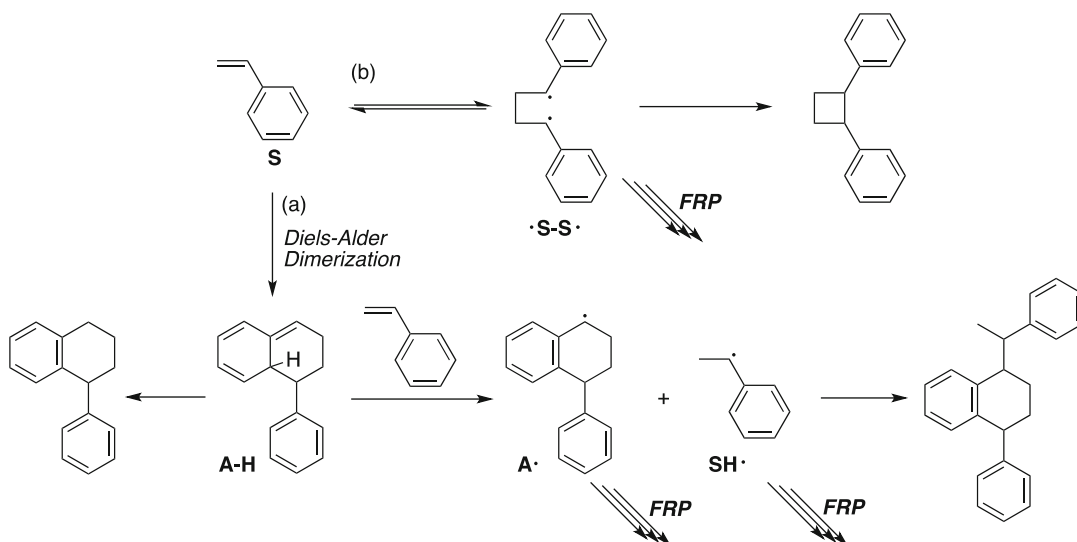
Polystyrene (PSt), Fig. 5 Spontaneous initiation in free radical polymerization (*FRP*) of styrene

Chain transfer reactions are effective for molecular weight control and terminal functionalization. Typically, carbon tetrachloride (CCl_4) induces multiple chain transfer in styrene polymerization to reduce molecular weight of the resulting polystyrene. Here, polystyrene radical (PS•) reacts with CCl_4 to give a chlorine-capped polystyrene (PS–Cl) and trichloromethane radical (CCl_3•); the CCl_3• immediately initiates polymerization, while the resulting polystyrene (CCl_3–PS•) again reacts with CCl_4 to form styrene oligomer (CCl_3–PS–Cl: named as telomer). Thiol derivatives (R–SH) carrying functional groups in turn lead to end-functional polystyrenes (R–S–PS–H).

The stable storage of styrene is important in commercial-scale operations [1]. Phenol/quinone and nitroxide derivatives work as inhibitors for radical polymerization. For example, 4-*tert*-butylcatechol of 10–50 ppm in the presence of oxygen effectively prevents styrene from unpredictable polymerization.

Radical Copolymerization. Copolymerization with other monomers is effective to modulate physical properties of polymers and functionalize polymers. In particular, radical copolymerization is applicable to broad ranges of monomers. Styrene can be copolymerized with various monomers including methyl methacrylate (MMA), methyl acrylate (MA), acrylonitrile (AN), butadiene (BD), *N*-butyl maleimide (BMI), maleic anhydride (MAh), vinyl chloride (VC), and vinyl acetate (VAc) (Fig. 6) [1, 17].

If the reactivity of growing polymer radicals relies on the structure of the terminal monomer unit, copolymerization of two monomers (M_1, M_2) is defined by four elementary kinetic steps (Eqs. 1, 2, 3, and 4 in Fig. 6). Monomer composition and sequence in copolymers are thus dependent on monomer reactivity ratios ($r_1 = k_{11}/k_{12}$, $r_2 = k_{22}/k_{21}$) that are based on the ratio of the rate constants in Eqs. 1, 2, 3, and 4. Typical examples are the following:

(a) $r_1 > 1$, $r_2 < 1$: M_1 is preferentially attacked by both M_1 radical (M_1•) and M_2 radical (M_2•) to give random copolymers with sequence and composition distribution. When $r_1 < 1$, $r_2 > 1$, the relationship between M_1 and M_2 is reversed. In the case of quite large r_1 ($\gg 1$), M_1-rich polymers (almost M_1 homopolymers) are obtained.

(b) $r_1 < 1$, $r_2 < 1$: M_1 is preferentially consumed by M_2• and M_2 is in turn done by M_1• to result in random copolymers with alternating-rich monomer sequence.

P

$$r_1 = \frac{k_{11}}{k_{12}} \qquad r_2 = \frac{k_{22}}{k_{21}}$$

Monomer Reactivity (M_1: S)

M_2	r_1	r_2	Polymer
MMA	0.52	0.46	
MA	0.75	0.18	
AN	0.33	0.17	*Random*
BD	0.78	1.3	
BMI	0.02	0.06	
MAh	0.04	0	*Alternating*
VC	17	0.02	
VAc	55	0.01	*S-Rich*
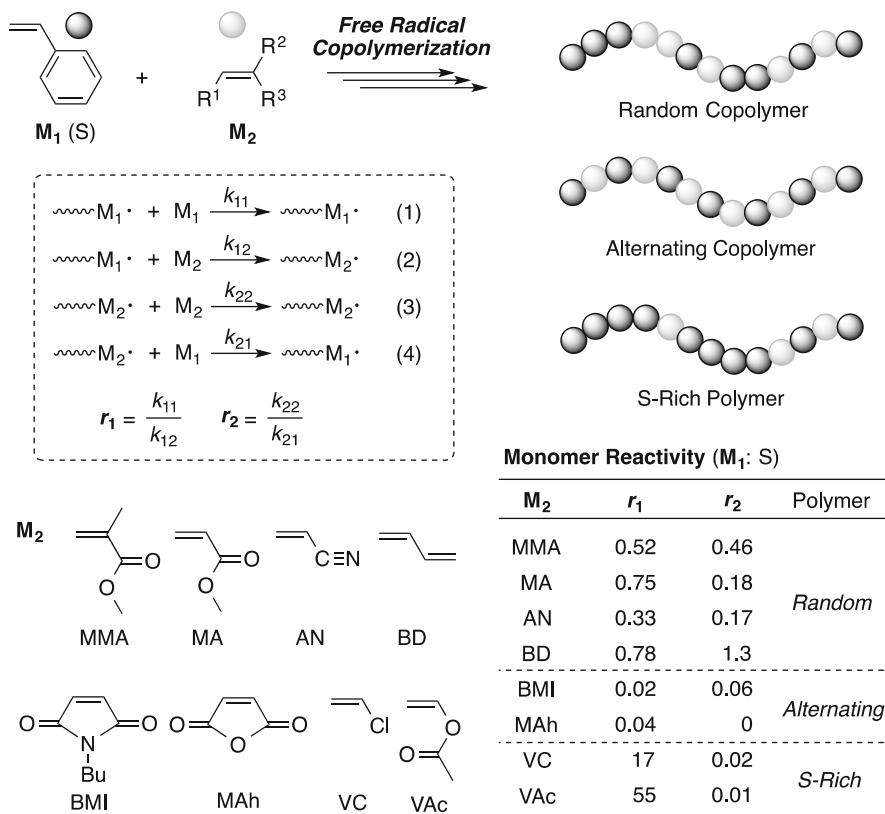
Polystyrene (PSt), Fig. 6 Free radical copolymerization of styrene (M_1: S) with other monomers (M_2): M_2 = methyl methacrylate (*MMA*), methyl acrylate (*MA*), acrylonitrile (*AN*), butadiene (*BD*), *N*-butyl maleimide (*BMI*), maleic anhydride (*MAh*), vinyl chloride (*VC*), and vinyl acetate (*VAc*)

(c) $r_1 \sim 0$, $r_2 \sim 0$: M_1 and M_2 have no homopolymerizability in this monomer combination to give alternating copolymers of M_1 and M_2.

Considering monomer reactivity ratios (r_1, r_2: Fig. 6) [17], copolymerization of styrene (M_1: S) with MMA, MA, AN, and BD (M_2) efficiently gives corresponding random copolymers. Actually, S/AN random copolymers are commercially produced via radical copolymerization as a thermoplastic SAN resin with heat and chemical resistance better than GPPS. Copolymerization of styrene with *N*-alkyl maleimide (e.g., BMI) or MAh yields alternating copolymers. Maleimide and MAh have 1,2-disubstituted, electron-withdrawing groups to be selectively attacked by electron-rich polystyrene radicals, while the resulting electron-poor radicals in turn selectively react with electron-rich styrene. Such unique reactivity of styrene and maleimide is now applied to the tailor-made design of sequence-regulated copolymers via direct addition of maleimide derivatives into living radical polymerization of styrene [18]. In contrast, copolymerization of styrene with VC or VAc provides styrene-rich copolymers or almost styrene homopolymers.

Living Anionic Polymerization. Anionic polymerization of styrene first opened "living polymerization" as a precision polymerization system. In conjunction with appropriate initiators under highly purified conditions, anionic polymerization of styrene proceeds only through initiation and propagation without any termination and chain transfer to provide polystyrene with precisely controlled primary structure (e.g., molecular weight with narrow distribution ($M_w/M_n < 1.1$), terminal structure) (Fig. 7) and
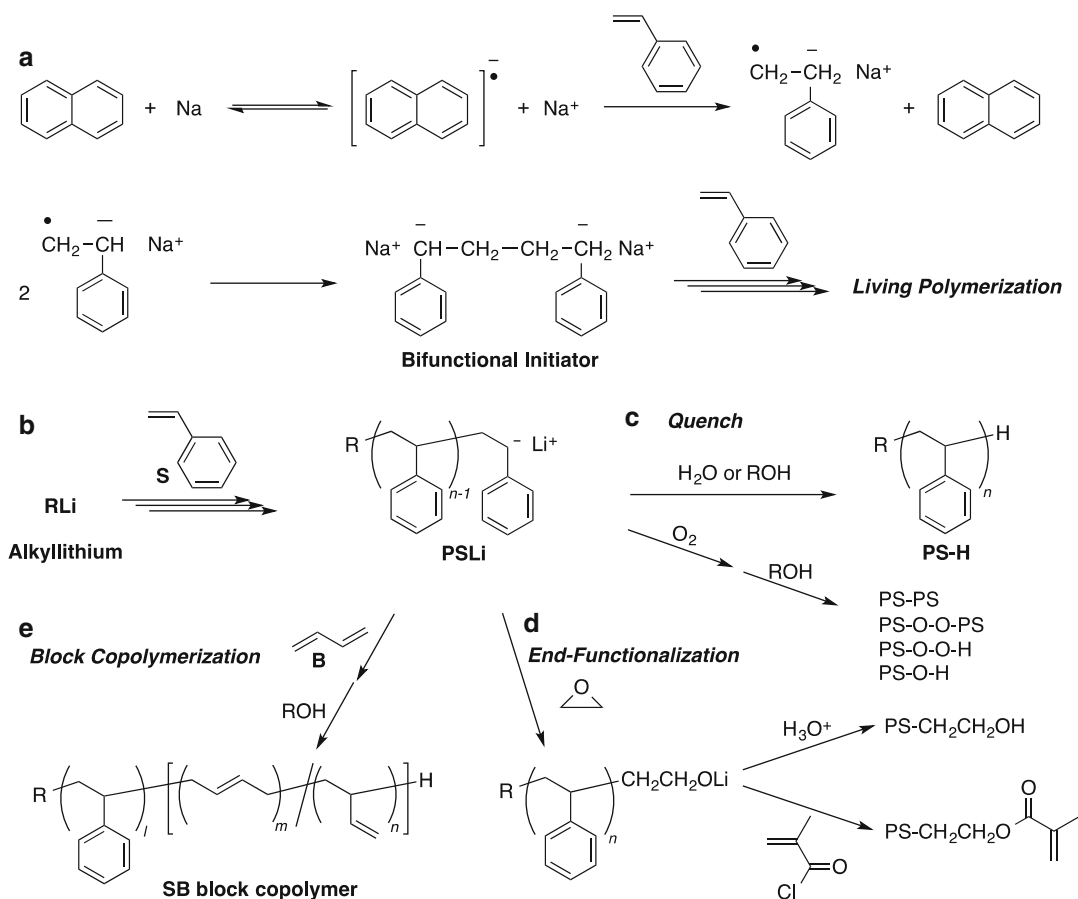
Polystyrene (PSt), Fig. 7 Living anionic polymerization of styrene (*S*) with (**a**) naphthalene/Na or (**b**) alkyllithium (*RLi*). (**c**) Quenching of PSLi with H_2O or ROH into PS–H. (**d**) End functionalization of PSLi with ethylene oxide. (**e**) Block copolymerization of butadiene (*B*) with PSLi into SB block copolymer

well-defined architecture (block, star, graft) [7]. The key is to remove oxygen and water from chemical reagents and reaction vessels.

The first living anionic polymerization of styrene by M. Szwarc was achieved with the initiating system of sodium metal with naphthalene in tetrahydrofuran (THF) (Fig. 7a) [6]. Here, sodium naphthalene (aromatic radical anion) induces electron transfer to styrene to give a styrene radical anion, which rapidly dimerizes to be a bifunctional initiator for styrene polymerization. Alkyl lithium including *n*-butyl lithium and *sec*-butyl lithium is also effective as an initiator (Fig. 7b) [7]. They are commercially available in solution to be readily utilized for polymerization.

Even after full consumption of styrene (S, conversion >99 %), polystyrene terminals are still "living" as benzyl anion structure (PSLi: red color). Thus, direct addition of degassed alcohol and water effectively quenches polystyryl lithium (PSLi) into proton-capped polystyrene (PS–H, Fig. 7c), whereas that of second monomers (e.g., butadiene) or reactive reagents into living PSLi solutions affords block copolymers and end-functional polymers (Fig. 7d, e). Styrene-butadiene-styrene triblock copolymers induce microphase separation to be thermoplastic elastomers. Removal of oxygen from chemicals and reactors is essential for both efficient polymerization of styrene and end transformation of PSLi; otherwise, oxygen as impurity

P

1) Arm-First: Multi-Functional Coupling Agents
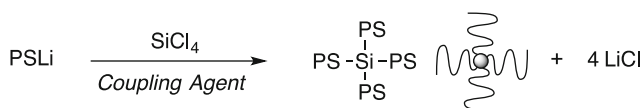
2) Arm-First: Arm Linking Reactions
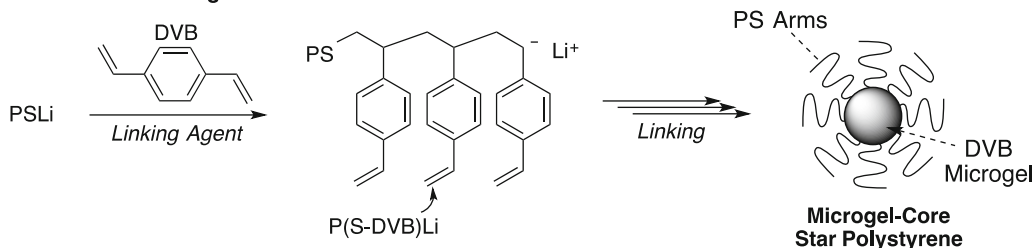
3) Core-First: Multi-Functional Microgel Initiators
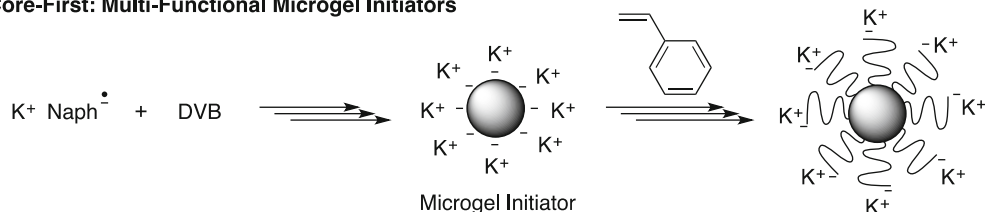
Polystyrene (PSt), Fig. 8 Synthesis of star polystyrenes via living anionic polymerization: (*1*) arm-first method with a multi-functional coupling agent (SiCl$_4$) with PSLi; (*2*) arm-first method via linking reaction of PSLi with a divinyl compound (*DVB* divinyl benzene); (*3*) core-first method from anionic polymerization of styrene from a multi-functional microgel initiator

provides a complex mixture of products including bimolecular termination (Fig. 7c).

Branched Polystyrene. Branched structures and unique three-dimensional architectures are designable via living anionic polymerization of styrene to give various well-defined star and graft polystyrenes [7]. For example, three kinds of methodologies have been developed for star polystyrenes: (1) arm-first method with multi-functional coupling agents, (2) arm-first method with bifunctional linking agents, and (3) core-first method with multi-functional microgel initiators (Fig. 8).

The first method is suitable for star polymers with precision arm numbers; for example, the coupling reaction of polystyrene lithium (PSLi) with tetrachlorosilane (SiCl$_4$) provides a four PS-arm star polymer. Crosslinking reaction of PSLi with divinyl benzene (DVB) gives microgel-core star polymers with multiple PS arms and large molecular weight, while the arm

number has distribution. A core-first method is also effective for microgel-core star polymers with multiple PS arms, whereas the molecular weight distribution is much larger than that by arm-first method.

Cationic Polymerization. Polystyrene is also obtained from cationic polymerization of styrene in conjunction with strong acids (e.g., HClO$_4$, CF$_3$SO$_3$H) and proton sources with Lewis acids [8]. However, the carbocation of growing terminals often induces chain transfer reaction via β-proton elimination and intra- or intermolecular Friedel-Crafts alkylation to aromatic rings. Hence, the synthesis of polystyrene with high molecular weight by cationic polymerization is difficult, compared with that by radical or anionic counterparts. However, since the possibility of living cationic polymerization of *p*-methoxystyrene (*p*MOS) was suggested [9], various initiating systems have been developed for vinyl ethers and styrene derivatives [8, 10].

Polystyrene (PSt),
Fig. 9 Isotactic
polystyrene and
syndiotactic polystyrene
obtained from coordination
polymerization of styrene
with TiCl$_4$/AlEt$_3$ and Ti
(η–C$_5$H$_5$)Cl$_3$/MAO,
respectively

TiCl$_4$ / AlEt$_3$
(Ziegler-Natta Catalyst)

Isotactic

Ti(η-C$_5$H$_5$)Cl$_3$ / MAO
(Half-titanocene)

Syndiotactic
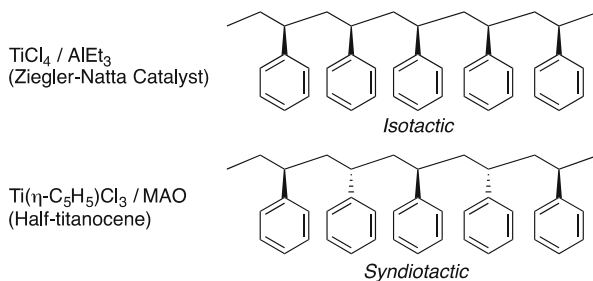
Now, well-controlled polystyrene can be also obtained from the initiating system of 1-phenylethyl chloride (PhEtCl, an adduct of HCl with styrene) and SnCl$_4$ in the presence of n–Bu$_4$Cl in CH$_2$Cl$_2$ at low temperature (−15 °C) [8].

Coordination Polymerization. Coordination polymerization with appropriate initiating systems often provides stereospecific polymers with crystalline properties. After the first discovery of a Ziegler-Natta catalyst for isotactic polypropylene, various catalytic systems were developed for stereospecific polymerization of olefins including styrene. A typical Ziegler-Natta catalyst (TiCl$_4$/AlEt$_3$) efficiently gives isotactic crystalline polystyrene (T_m = ~230 °C, T_g = ~100 °C) (Fig. 9) [1, 4]. More innovatively, Idemitsu Kosan (Co., Ltd.) successfully developed a half-titanocene catalyst [(η–C$_5$H$_5$)TiCl$_3$/methylaluminoxane] for syndiotactic crystalline polystyrene (M_w/M_n ~2, T_m = ~270 °C, T_g = ~100 °C) [3, 4]. Both isotactic polystyrene and syndiotactic counterpart are opaque in crystalline state, though atactic polystyrene is transparent in amorphous state. The crystallization rate for syndiotactic polystyrene is larger than that for isotactic counterpart. Owing to the high melting temperature and crystalline structure, syndiotactic polystyrene has heat and chemical resistance better than atactic polystyrene.

Living Radical Polymerization. Thanks to high functionality tolerance, living radical polymerization (LRP) allows us to directly synthesize well-controlled functional polymers with polar functional monomers even in polar solvents [11–16]. After the first proposal of a LRP system with iniferter in 1982 by Otsu, various LRP systems such as nitroxide-mediated radical polymerization (NMP) [14, 15], metal-catalyzed LRP (atom transfer radical polymerization: ATRP) [11–13], and reversible addition-fragmentation chain transfer (RAFT) polymerization [16], have been developed. They are applicable to preparation of well-controlled polystyrene (Fig. 10a). The key in LRP is to introduce covalent "dormant species" (~C–Y) that can be reversibly cleaved with physical (heat, light) or chemical (catalyst) stimuli to generate carbon radicals as "active species" for polymerization (~C• + •Y). The equilibrium shifts to dormant species to keep radical concentration low during polymerization, which effectively reduces bimolecular termination of growing polymer radicals to successfully induce controlled/living radical polymerization.

For example, styrene polymerization with BPO in the presence of 2,2,6,6-tetramethylpiperidine 1-oxyl (TEMPO) provides well-controlled polystyrene with narrow molecular weight distribution (Fig. 10b) [14, 15]. Here, a benzene carboxyl radical from BPO first reacts with styrene and the resulting radical is then capped with TEMPO to in-situ form an alkoxyamine initiator with carbon-oxygen bond. TEMPO is originally an inhibitor for radical polymerization, whereas the dormant carbon-oxygen bond of the initiator and polymer terminals is reversibly and homolytically cleaved by heat to give active carbon radicals for styrene polymerization. Pre-synthesized alkoxyamines are also useful as initiators for NMP of styrene. Recent advances in LRP systems afford tailor-made design of various styrene-based functional polymers with well-defined three-dimensional architectures.

P
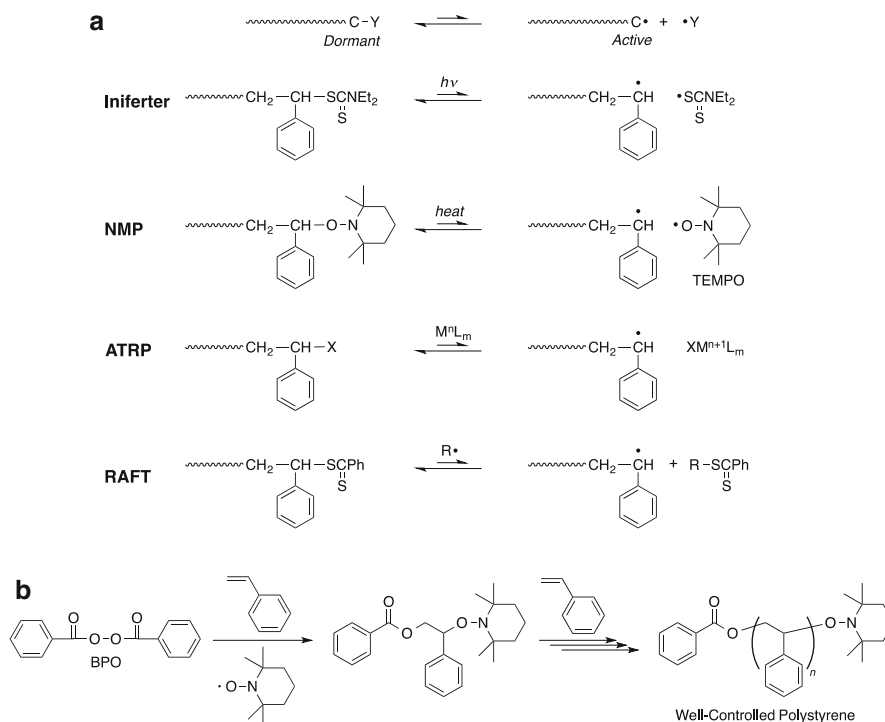
Polystyrene (PSt), Fig. 10 (**a**) Living/controlled radical polymerization of styrene: iniferter-mediated polymerization, nitroxide-mediated radical polymerization (*NMP*), metal-catalyzed living radical polymerization or atom transfer radical polymerization (*ATRP*), reversible addition-fragmentation chain transfer (*RAFT*) polymerization. (**b**) NMP of styrene with BPO and TEMPO
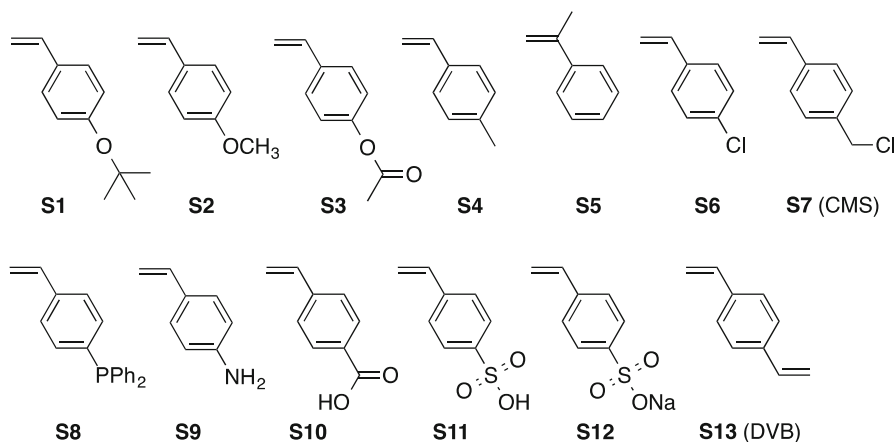
Polystyrene (PSt), Fig. 11 Styrene derivatives and functional styrenes

Styrene Derivatives. Lots of styrene derivatives are developed to modulate properties of polystyrene and design functional polymeric materials. Figure 11 illustrates commercially available styrene monomers with the following substituents: ether, ester, alkyl, halogen, phosphine, amine, carboxylic acid, sulfonic acid, sodium sulfonate, and olefin (**S1–S13**).

Owing to the high versatility and functionality tolerance, radical polymerization is applicable to all of the styrene derivatives (**S1**–**S13**). It should be noted that functional styrenes bearing carboxylic acid (**S10**), sulfonic acid (**S11**), and sodium sulfonate (**S12**) are directly polymerized in polar organic solvents (alcohols) or water. α-Methylstyrene (**S5**) has ceiling temperature at 61 °C in radical bulk polymerization; thus **S5** should be polymerized at low temperature to prepare poly(**S5**) with high molecular weight.

On the other hand, adaptability of ionic (anionic, cationic) polymerization depends on the substituents (functional groups) of styrene, because ionic growing terminals may react with the substituents. Styrene derivatives carrying ether (**S1**, 4-tertiarybutoxy; **S2**, *para*-metoxy), alkyl (**S4**, *para*-methyl; **S5**, α-methyl), halogen (**S6**, *para*-chloro), phosphine (**S8**, 4-diphenylphosphino), and olefin (**S13**, divinylbenzene; DVB) can be polymerized by anionic mechanism [7, 19], while styrenes bearing ester (**S3**, 4-acetoxy), halomethyl (**S7**, *para*-chloromethyl; CMS), amine (**S9**, 4-amino), and acidic groups and the salts (**S10**–**S12**) induce side reactions or no polymerization. Cationic polymerization is effective for styrenes bearing ether (**S1**, **S2**), alkyl (**S4**, **S5**), and halogen (**S6**, **S7**) substituents [8–10].

S1 and **S3** are typical protecting monomers for 4-hydroxystyrene; polymers of **S1** or **S3** are transformed with acid or base, respectively, into poly(4-hydroxystyrene). Owing to the reactive chloromethyl group, **S7** (CMS) is a versatile precursor for various styrene derivatives. In addition, **S7** is "inimer" that works as both initiator (chloromethyl group) and monomer (olefin) in metal-catalyzed LRP and ATRP, which efficiently gives hyperbranched polystyrene. A phosphine-bearing styrene (**S8**) is often employed as a ligand for polymer-supported metal catalysts [20]. So far, phosphine (**S8**)-bearing microgel star polymers (soluble) and polystyrene gels (insoluble) have been developed for active and recyclable catalysts for organic reactions. **S9**–**S12** are typical precursor monomers for polyelectrolytes. **S13** is a general linking agent to prepare crosslinked gels, microgels, and star polymers. Poly(styrene/DVB) gels are used as filler for size-exclusion chromatography.

Properties and Commercial Products of Polystyrene

Polystyrene and styrene copolymers are commercially manufactured as thermoplastic resin, form, and rubber/latex in large scale [1–3]. This section deals with commercial polystyrenes and styrene copolymers (Fig. 12), especially focusing on the production process, properties, and applications.

General-Purpose Polystyrene (GPPS). GPPS means a thermoplastic resin of linear atactic polystyrene with high molecular weight (M_w = 200,000–300,000) and glass transition temperature of about 100 °C. Such polystyrene is produced by radical polymerization in bulk, dispersion, or solution. The major process is now bulk polymerization in continuous stirred tank reactors or stratified agitated tower continuous plug flow reactors. Physical and mechanical properties of GPPS are summarized in Table 1, compared with those of other polystyrene resins.

Advantages of GPPS are given: good transparency; light (specific gravity, 1.05); high rigidity (tensile strength at yield, ~40 MPa; tensile elastic modulus, ~3,000 MPa); good moldability and processability (high thermal stability, high dimension accuracy, good colorability); excellent electric properties (high volume resistivity, $>1 \times 10^{16}$ Ω•cm; high electrical breakdown strength, ~20 kV/mm); and high chemical resistance to acid, base, and salt. GPPS is transformed into products via injection or extrusion molding techniques at high temperature (180–260 °C). The uses of GPPS typically include disposable cups, food containers, compact disk cases, and food packaging films.

However, GPPS has several drawbacks: low impact resistance (tensile elongation at rupture, 1–2 % (brittle); impact strength (notched Izod), ~20 J/m), low chemical resistance to organic solvents (soluble), and low heat resistance (continuous heat-resistant temperature, 70–90 °C). Such limited properties are improved via the following strategies.

P
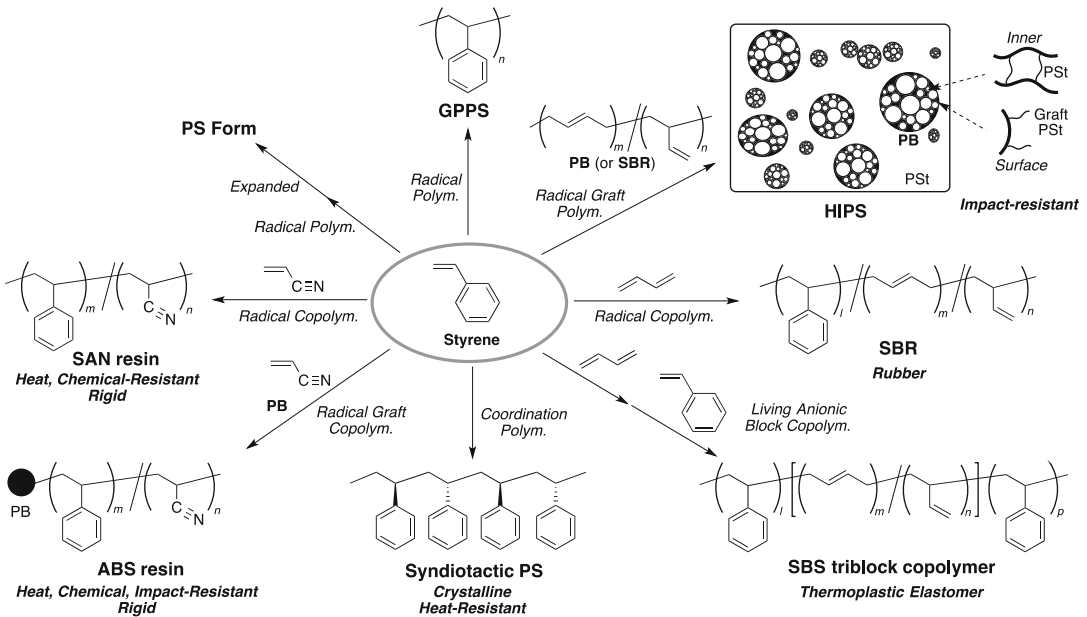
Polystyrene (PSt), Fig. 12 Commercially produced polystyrene (*PS*) and styrene-based copolymers: general-purpose polystyrene (*GPPS*), high-impact PS (*HIPS*), PS form; styrene-acrylonitrile (*SAN*) resin, styrene-acrylonitrile-butadiene (*ABS*) resin, syndiotactic PS; styrene-butadiene-styrene (*SBS*) triblock copolymer, styrene-butadiene rubber (*SBR*)

Polystyrene (PSt), Table 1 Physical and mechanical properties of injection-molded styrene polymers[a]

	Polystyrene (GPPS)	High-impact PS (HIPS)	SAN Copolymer[b]	ABS Copolymer[c]
CAS registry number	9003-53-6	9003-55-8	9003-54-7	9003-56-9
Specific gravity	1.05	1.05	1.08	1.04
Vicat softening point, °C	96	95	107	103
Tensile strength at yield, MPa	42	30	69	41
Tensile elastic modulus, MPa	3,200	2,100	3,800	2,100
Tensile elongation at rupture, %	1.8	15	3.5	20
Impact strength (notched Izod), J/m	21	130	21	270

[a]Ref. [1]
[b]Styrene-acrylonitrile copolymer: 24 w% acrylonitrile
[c]Acrylonitrile-butadiene-styrene copolymer

To improve "impact resistance": (1) blending soft rubbers (polybutadiene, styrene-butadiene copolymer) to rigid styrene (co)polymers via graft polymerization, leading to high-impact polystyrene (HIPS) and acrylonitrile-butadiene-styrene (ABS) copolymer, and (2) blending styrene-butadiene block copolymers to polystyrene.

To improve "chemical resistance": copolymerization of acrylonitrile with styrene to styrene-acrylonitrile (SAN) copolymer and ABS copolymer.

To improve "mechanical strength" and *"heat resistance"*: (1) copolymerization of acrylonitrile with styrene to SAN copolymer and (2) stereospecific coordination polymerization

of styrene to syndiotactic crystalline polystyrene.

Polystyrene Form. Polystyrene forms consist of the assembling structure of the multiple small polystyrene particles containing air. Note that the air volume fraction is 98 % (polystyrene, 2 %). Thus, polystyrene forms are light, impact-resistant, waterproof, and well moldable. The typical manufacture process is given. Formable styrene beads with the diameter of 0.3–2 mm are first prepared by suspension radical polymerization of styrene in the presence of blowing agents such as pentane or hexane. The styrene beads are then pre-expanded with steam at 100 °C. The pre-expanded beads are finally molded into products with steam at 110–120 °C. Tailor-made polystyrene forms are widely utilized for packaging, insulation, and building and construction materials.

High-Impact Polystyrene (HIPS) and Transparent Impact Polystyrene (TIPS). HIPS is a polymer alloy, in which rubber particles of polybutadiene (PB) or styrene-butadiene copolymer (styrene-butadiene rubber, SBR) are dispersed in continuous polystyrene layer. Because of the blended rubbers, HIPS is opaque but impact resistant (impact strength (notched Izod), ~130 (HIPS) > ~20 (GPPS) J/m) with high rigidity and good moldability. The production of HIPS undergoes bulk or dispersion radical polymerization of styrene in the presence of butadiene-based rubbers (PB or SBR). Via the in-situ polymerization, polystyrene is efficiently grafted on the rubber surfaces and placed as crosslinking units within the rubber particles, in which polystyrene radicals add to olefins of rubber chains and the resulting radicals further react with polystyrene radicals (coupling, graft-onto) or styrene (polymerization, graft-from). The morphology control of rubbers (particle size, size distribution, structure) by graft polymerization is particularly important to perform desired physical properties. The use is typically directed to office automation equipment (e.g., exteriors of copy, printer), home electronic products (e.g., air conditioner, television), toys, and food containers.

The opacity of HIPS is caused by the different refractive indices between polystyrene matrix and rubber particles. In contrast, transparent impact polystyrene (TIPS) can be also obtained from blending styrene-butadiene block copolymers of high styrene content (~75 wt%) into GPPS. The block copolymers induce microphase separation to form small butadiene rubber domains (<20 nm) in polystyrene matrix, which effectively suppresses the scattering of light.

Styrene-Butadiene Rubber (SBR) and Thermoplastic Elastomer. SBR is a random copolymer of styrene and butadiene, which is manufactured in the largest scales among synthetic rubbers (about 30 % in all synthetic rubbers). SBR is synthesized by emulsion polymerization of styrene and butadiene, where general SBR contains about 24 % of styrene. There are two kinds of SBRs: cold rubber and hot rubber. The former is prepared with redox initiating systems at relatively low temperature (5–10 °C), while the latter is obtained with peroxide or azo initiators at high temperature (40–50 °C). Most of SBR is cold rubber mainly employed for automobile tires, while hot rubber produced in small scale is used for adhesive. To express good elasticity for tires, cold rubber is blended with carbon black as stiffener and anti-aging agents for high durability, followed by the crosslinking with sulfur.

In contrast, styrene-butadiene-styrene (SBS) triblock copolymers become thermoplastic elastomers without any chemical crosslinking owing to the microphase separation between hard styrene segments and soft butadiene counterparts. The triblock copolymers are efficiently produced via living anionic block copolymerization of styrene with alkyllithium. Blending styrene-butadiene block copolymers with polystyrene gives transparent impact polystyrene (TIPS).

Styrene-Acrylonitrile (SAN) Resin. SAN resin is a random copolymer of styrene and acrylonitrile, which is manufactured in the largest volume scale among styrene copolymers by radical polymerization through bulk, dispersion, and emulsion processes. Copolymerization of styrene and acrylonitrile is often conducted at almost azeotropic composition (styrene-acrylonitrile = 76/24) so as to directly reflect the monomer composition to copolymers. Thanks

P

to acrylonitrile units, SAN copolymers have chemical and heat resistance better than GPPS, keeping as good transparency as GPPS. Thus, SAN resin is often employed for table equipment, home electronic products (e.g., electric fan, juicer), automobile parts, and miscellaneous goods (e.g., cosmetics cases, disposable lighter cases).

Acrylonitrile-Butadiene-Styrene (ABS) Resin. ABS resin is a polymer alloy of two phases, in which polybutadiene rubber particles are dispersed in rigid SAN copolymer matrix. As a result, ABS resin shows high impact resistance (impact strength (notched Izod), ~270 J/m) with high chemical and heat resistance, good surface gloss, and good formability. Though production of ABS resin first began by just blending polybutadiene particles into SAN copolymer matrix, the synthetic process has recently shifted to bulk or emulsion radical copolymerization of styrene and acrylonitrile in the presence of polybutadiene. Here, SAN copolymers are effectively grafted to polybutadiene particles via the addition of SAN copolymer radicals to olefins in polybutadiene (graft-onto), followed by the subsequent copolymerization of styrene and acrylonitrile (graft-from) and the coupling reaction with copolymer radicals (graft-onto). The impact strength of ABS resin can be controlled by the particle size of polybutadiene and the grafting efficiency of SAN copolymers; the particle size of 0.25–0.45 μm seems to be suitable for high impact resistance. ABS resin is thereby utilized for office automation equipment, automobile parts (exterior and interior), home electronic products (e.g., air conditioner, refrigerator, washing machine), and building components.

Syndiotactic Polystyrene. Syndiotactic, crystalline polystyrene was first successfully synthesized via coordination polymerization of styrene with a half-titanocene catalyst (e.g., $(\eta–C_5H_5)$ $TiCl_3$/methylaluminoxane) by Idemitsu Kosan Co., Ltd., and is now commercially produced as an engineering plastic [3]. Thanks to the crystallinity, syndiotactic polystyrene has heat resistance (continuous heat-resistant temperature, 130 °C), chemical resistance (especially for engine oil and gasoline for automobile), and

dimensional stability, better than atactic GPPS. Thus, syndiotactic polystyrene is applied to automotive electric components, home electronic products, and tableware.

References

1. Priddy DB (2014) Styrene polymers. In: Mark HF (ed) Encyclopedia of polymer science and technology, 4th edn. Wiley, Hoboken, pp 247–336
2. Scheirs J, Priddy DB (eds) (2003) Modern styrenic polymers: polystyrenes and styrenic copolymers. Wiley, West Sussex
3. Tomotsu N (2014) Syndiotactic polystyrene. In: Mark HF (ed) Encyclopedia of polymer science and technology, 4th edn. Wiley, Hoboken, pp 1–20
4. Ishihara N, Kuramoto M, Uoi M (1988) Stereospecific polymerization of styrene giving the syndiotactic polymer. Macromolecules 21:3356–3360
5. Webster OW (1991) Living polymerization methods. Science 251:887–893
6. Szwarc M (1956) Living polymers. Nature 178:1168–1169
7. Hsieh HL, Quirk RP (1996) Anionic polymerization: principles and practical applications. Marcel Dekker, New York
8. Matyjaszewski K (ed) (1996) Cationic polymerizations: mechanisms, synthesis, and applications. Marcel Dekker, New York
9. Higashimura T, Mitsuhashi M, Sawamoto M (1979) Synthesis of *p*-methoxystyrene-isobutyl vinyl ether block copolymers by living cationic polymerization with iodine. Macromolecules 12:178–182
10. Sawamoto M (1991) Modern cationic vinyl polymerization. Prog Polym Sci 16:111–172
11. Matyjaszewski K, Tsarevsky NV (2009) Nanostructured functional materials prepared by atom transfer radical polymerization. Nat Chem 1:276–288
12. Kamigaito M, Ando T, Sawamoto M (2001) Metal-catalyzed living radical polymerization. Chem Rev 101:3689–3746
13. Ouchi M, Terashima T, Sawamoto M (2009) Transition metal-catalyzed living radical polymerization: toward perfection in catalysis and precision polymer synthesis. Chem Rev 109:4963–5050
14. Georges MK, Veregin RPN, Kazmaier PM, Hamer GK (1993) Narrow molecular weight resins by a free radical polymerization process. Macromolecules 26:2987–2988
15. Hawker CJ, Bosman AW, Harth E (2001) New polymer synthesis by nitroxide mediated living radical polymerizations. Chem Rev 101:3661–3688
16. Moad G, Rizzardo E, Thang SH (2008) Radical addition-fragmentation chemistry in polymer synthesis. Polymer 49:1079–1131
17. Greenley RZ (1999) Free radical copolymerization reactivity ratios. In: Brandrup J, Immergut EH,

Grulke EA (eds) Polymer handbook, 4th edn. Wiley, New York, pp 181–308
18. Lutz J-F (2013) Writing on polymer chains. Acc Chem Res 46:2696–2705
19. Hirao A, Loykulnant S, Ishizone T (2002) Recent advance in living anionic polymerization of functional styrene derivatives. Prog Polym Sci 27:1399–1471
20. Terashima T (2014) Polymer microgels for catalysis. In: Mark HF (ed) Encyclopedia of polymer science and technology, 4th edn. Wiley, Hoboken, pp 1–31

Polyurethane Synthesis

Nigel Barksby[1], Jeffrey F. Dormish[2] and Karl W. Haider[1]
[1]Polyurethane Raw Materials, Bayer MaterialScience LLC, Pittsburgh, PA, USA
[2]Adhesive Raw Materials, Bayer MaterialScience LLC, Pittsburgh, PA, USA

Synonyms

Carbamate(s); Isocyanate- or polyisocyanate-based polymers; Polycarbamate(s); Urethane(s)

Definition

Polyurethanes are a versatile class of polymeric materials containing multiple carbamate functional groups in the polymer chain.

Introduction

Polyurethanes (PU) were first prepared in 1937 by Otto Bayer and include a wide range of modular-like structures with an extremely diverse range of properties. Polyurethanes are a unique class of thermoset and thermoplastic polymers that can display rigid or elastomeric behavior depending on their chemical and morphological structure. Detailed overviews of PU chemistry, properties, and applications have been described in several excellent monographs [1–5] and review articles [6].

Both cellular (foamed) and noncellular (solid) polyurethanes are commonly prepared, and these products can function in a broad array of industrial and consumer applications. The relevance of PU is evidenced by the 11.7 million tons of polyurethane raw materials that were produced globally in 2012 [7].

Reaction Chemistry Overview

Polyurethanes are typically made by the addition polymerization of di- or polyisocyanates with polynucleophiles (active hydrogen-containing moieties) to form a polymer backbone (Fig. 1).

These polynucleophiles can be polyhydroxyl or polyamino functional macromonomers (dubbed "polyols"), low molecular weight compounds ("chain extenders"), or mixtures of both. Depending on the functionality of the polyisocyanate and polyol components, thermoplastic or thermoset polymers can be prepared. *Note:* Diisocyanates and polyisocyanates are often referred to collectively as isocyanates, a convention that will also be used here. Polyurethane properties are largely determined by the chemical nature of the polymer building blocks, the stoichiometry of the isocyanate/hydroxyl (–OH) components, and the density, all of which can be varied to produce polymers with the desired property profile.

Building Blocks

Isocyanates
Diisocyanates and polyisocyanates can be represented as R-(NCO)$_n$, where $n \geq 2$. They are characterized by their functionality (n), the nature of the R group (aliphatic or aromatic), and their isocyanate content where:

$$\text{wt. \% NCO } = 4200/\text{NCO eq. wt.}$$

Many commonly used PU building blocks are diisocyanates having molecular weight below 300 g/mol. The most important aromatic diisocyanates are toluene diisocyanate (TDI), an
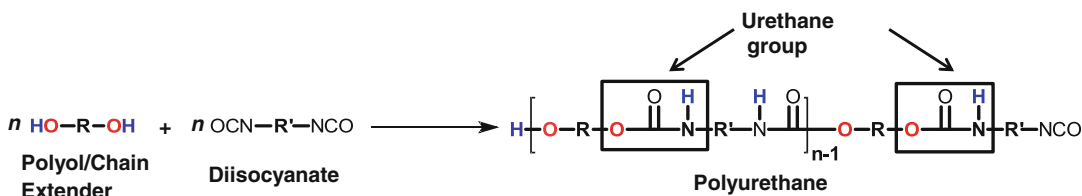
Polyurethane Synthesis, Fig. 1 Generic polyurethane structure
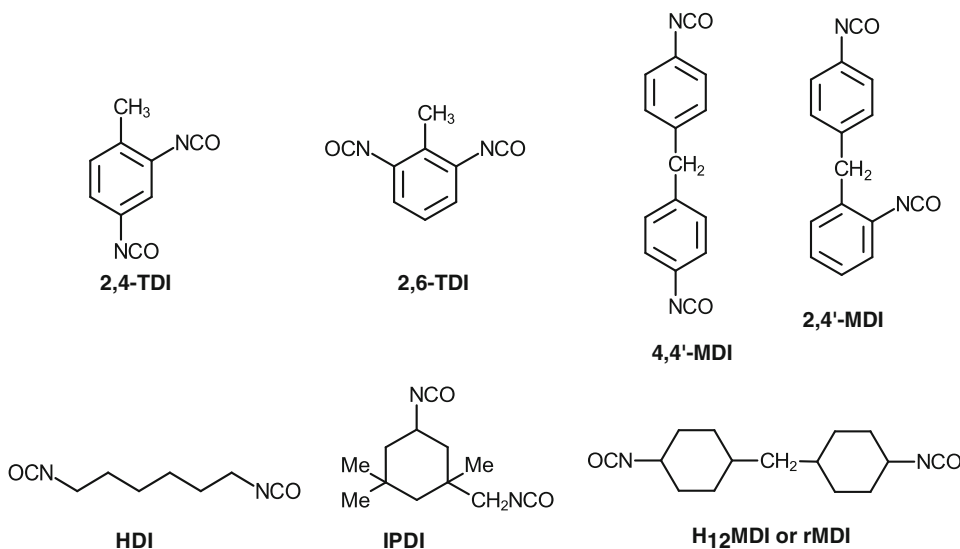
Polyurethane Synthesis, Fig. 2 Commonly used diisocyanates

isomer mixture of 2,4-TDI and 2,6-TDI, and methylene diphenyl diisocyanate (MDI) – a mixture of 4,4′-MDI and 2,4′-MDI isomers. Common aliphatic diisocyanates include hexamethylene diisocyanate (HDI), isophorone diisocyanate (IPDI), and hydrogenated MDI (H$_{12}$MDI) (see Fig. 2).

Isocyanate Manufacture

Diamine Phosgenation
Various routes to preparing isocyanates are known [1, 8, 9], and some examples are shown in Fig. 3. The most common route involves phosgenating diamines. Diamines are readily phosgenated in a nonreactive solvent such as chlorobenzene. The diamine (dissolved in solvent) is added to a concentrated solution of

phosgene to form a carbamyl chloride and an amine hydrochloride. The resultant mixture is then heated while feeding additional phosgene to form the diisocyanate. Excess phosgene and HCl are removed and the phosgene is recycled. For laboratory work, various phosgene substitutes including trichloromethyl chloroformate (diphosgene) and *bis*-(trichloromethyl) carbonate (triphosgene) are often used for easier handling.

Isocyanic Acid Addition to Electron-Rich Olefins
Some isocyanates can be produced by the reaction of diolefins such as *m*-divinylbenzene, with isocyanic acid; however, the isocyanic acid (HNCO) is unstable and must be generated in situ by pyrolysis of cyanuric acid. A modification of this process is the reaction of the diolefin with ethyl
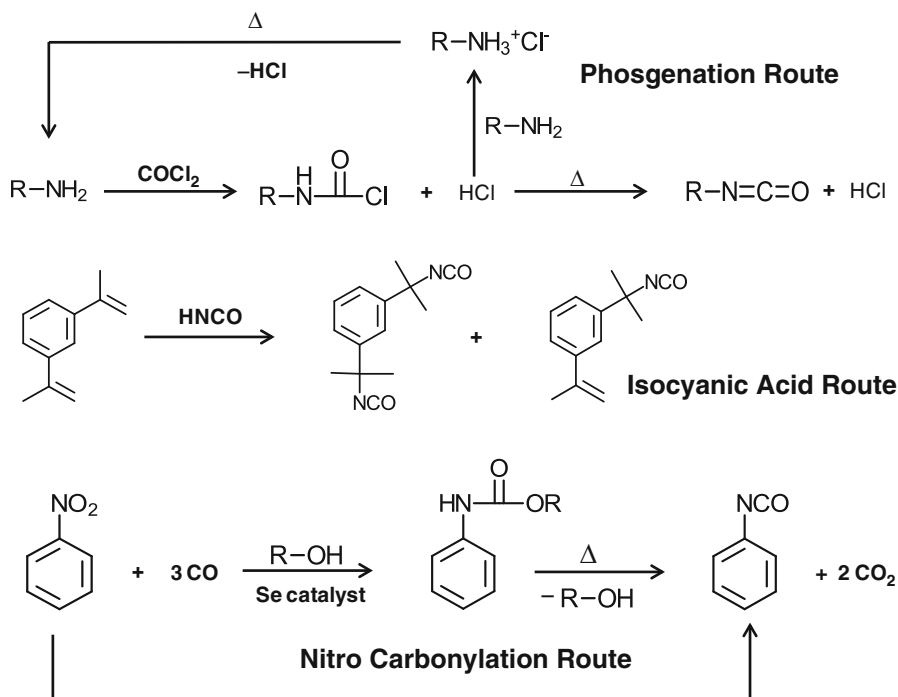
Polyurethane Synthesis, Fig. 3 Isocyanate synthesis routes

carbamate to give the biscarbamate, which is subsequently cleaved to give a mixture of the mono and diisocyanate.

Carbonylation of Nitro Compounds

In the 1960s, direct conversion of a nitro compound into an isocyanate using carbon monoxide was demonstrated. However, low isocyanate yields have limited its commercial potential. A modification is the reaction of a nitro compound with carbon monoxide in the presence of an alcohol using selenium or other noble metal catalyst. The presence of the alcohol leads to the formation of the corresponding urethane, which can be used to generate an isocyanate by thermolysis.

"Transesterification"/Thermolysis

Non-phosgene routes to the production of aliphatic diisocyanates are also known. In one method, a diamine precursor, in the presence of dibutyl carbonate, is reacted with urea and *n*-butanol with simultaneous removal of ammonia. Thermolysis of the resulting biscarbamate yields isophorone diisocyanate and a small amount of isocyanate monocarbamate.

Other well-known alternative non-phosgene methods are mainly of scientific interest (no commercial use). These include the Hofmann, Curtius, Schmidt, and Lossen rearrangements. More recently developed routes, including the reaction of di-tert-butyl dicarbonate with amines, nucleophilic substitution of alkyl halides, tosylates and similar compounds with metal cyanates, and cleavage of formamides and carbamates are reviewed in detail elsewhere [9].

Polyisocyanate and Modified Isocyanate Synthesis

In addition to the diisocyanates already described, higher functional polyisocyanates and modified diisocyanates (Fig. 4) are produced by various methods. A very common aromatic polyisocyanate, polymeric MDI (PMDI), is obtained by phosgenating the polynuclear oligoamines resulting from the condensation of aniline and formaldehyde.
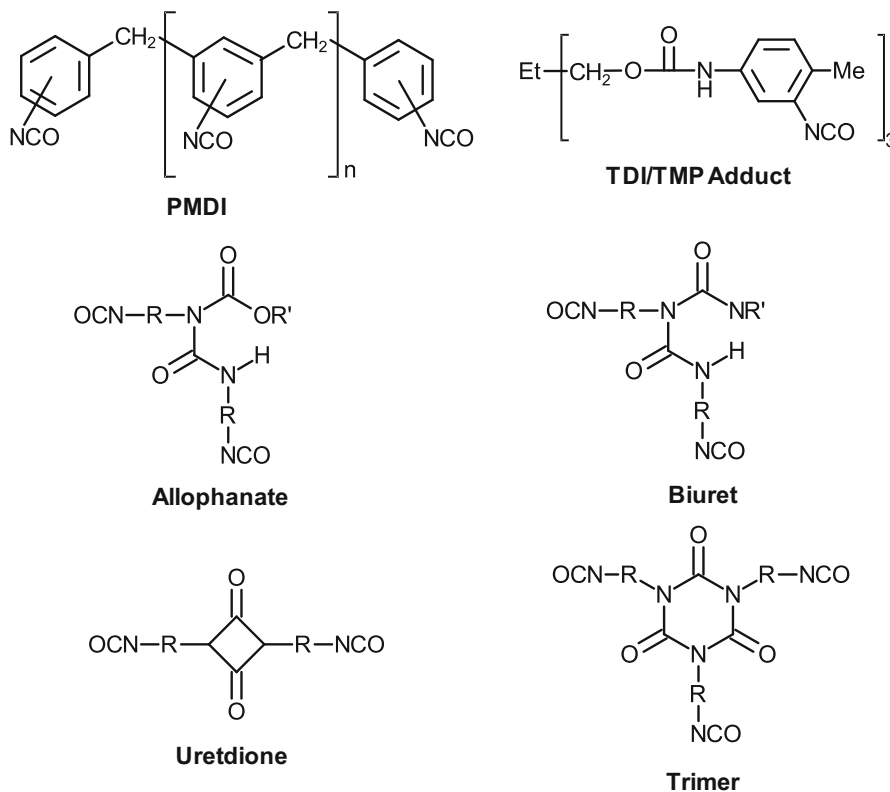
Polyurethane Synthesis, Fig. 4 Multifunctional polyisocyanates

Chemical derivatization or oligomerization of diisocyanates to generate polyisocyanate or modified isocyanates is also common (Fig. 4). For example, reaction of the triol trimethylolpropane (TMP) with difunctional TDI results in an isomeric mixture that contains mostly a urethane-modified trifunctional isocyanate (TDI/TMP Adduct), as well as small amounts of higher homologues. Modified isocyanates can also be generated by secondary reaction of isocyanates with urethane groups to form allophanates or with urea groups to form biurets. Dimerization of isocyanates to uretdiones (UD) or trimerization to isocyanurates (trimer) is also well established. These compounds can be synthesized in situ during the polyaddition reaction using suitable catalysts or produced specifically for use as building blocks in two-component reactions (common with PU coatings).

Polyol Structures

Polyol is the general term for a hydroxyl functional macromonomer, which is often used as a PU building block. Polyols can be represented as $R-(OH)_n$, where $n \geq 2$ and R represents a homo- or heteropolymeric unit having molecular weight typically ranging from ~400 to 15,000 g/mol. Polyols are characterized by their functionality (n); the polymeric backbone unit, R; and their hydroxyl number (OH #), where:

$$OH\# = 56,100/\ OH\ eq.\ wt.$$

Common backbone functional groups include polyether (most commonly polyoxyethylene, polyoxypropylene, and polyoxytetramethylene), polyester, polybutadiene, polycarbonate, polysiloxane, or polyacrylic. Examples of some of the more commonly used polyols are shown in Fig. 5.
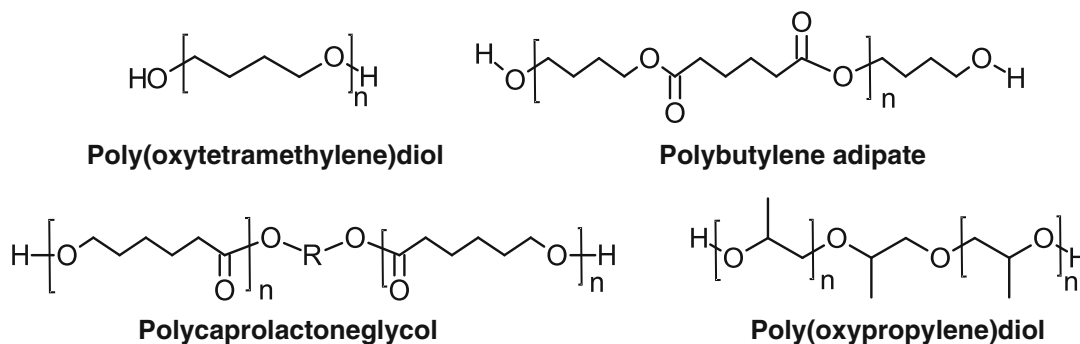
Polyurethane Synthesis, Fig. 5 Representative polyol structures

Polyurethane Synthesis, Fig. 6 Polyether polyol block copolymer synthesis
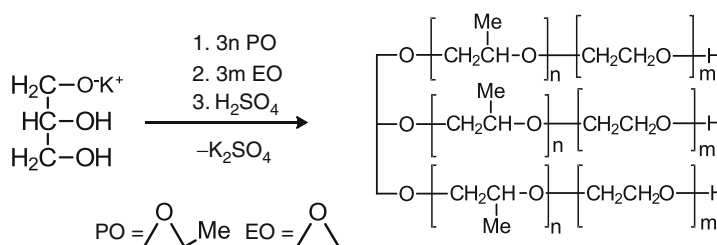
Polyol selection is dictated by the desired polyurethane characteristic (hydrolysis resistance, solvent resistance, UV resistance, etc.). Low molecular weight di-, tri-, and higher functional materials may be used as chain extenders or cross-linkers depending on their functionality. Higher molecular weight polyols, together with isocyanates, are key raw materials for polyurethane manufacture.

Polyether Polyol Synthesis
Polyalkylene oxide polyether polyols are the most important group of polyols used in polyurethanes and account for almost 80 % of the total polyol production. The general formula of this class of polyols can be represented by H$\cdot$(OR)$_m$OH, where R represents an alkyl group.

Polyether polyols of this type are prepared by ring opening polymerization of alkylene oxides such as ethylene oxide (EO), propylene oxide (PO), and butylene oxide (BO) in the presence of a starter molecule such as water, glycerin, or a higher functionality initiator. Basic catalysts like potassium hydroxide have long been, and continue to be, used to catalyze these polymerizations. However, a well-known side reaction of base catalyzed polymerization of PO is isomerization to allyl alcohol, which results in monofunctional by-products that serve as chain terminators in PU synthesis reactions. Specialized catalysts, often double metal cyanides (DMC), can be used to minimize this side reaction.

Block copolymers of propylene oxide and ethylene oxide are commonly used in polyurethanes, and specific characteristics can be obtained by adjusting the size and position of EO blocks within the polyether. These block copolymers are prepared by sequential addition of PO, followed by EO (Fig. 6). Alternatively the EO and PO can be added simultaneously, to produce random copolymers.

Polyester Polyol Synthesis
Polyester polyols are synthesized by the polycondensation reaction of dicarboxylic acids (or derivatives such as anhydrides) with polyglycols (Fig. 7). The mechanism is an equilibrium reaction and is shifted toward polyester formation through the removal of water from the reaction mixture. Formation of high molecular weight hydroxyl-terminated polyols is achieved
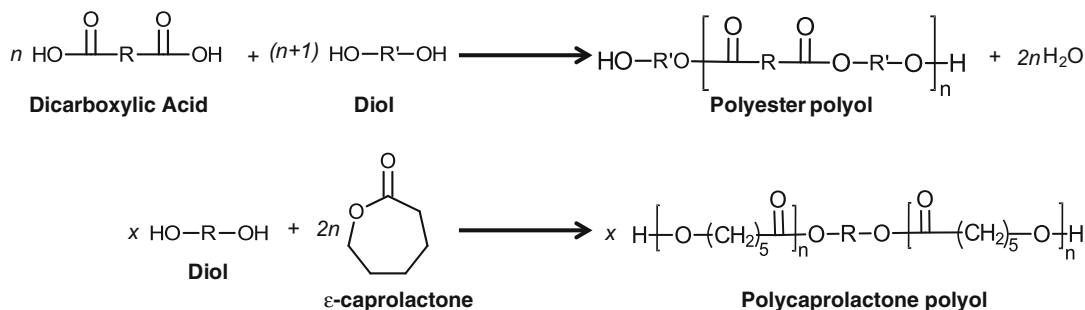
Polyurethane Synthesis, Fig. 7 Polyester polyol synthesis

by using a stoichiometric excess of glycol. The resulting polyol can be either primary or secondary hydroxy terminated depending on the type of glycol used. Polyurethanes based on polyester polyols are degraded by hydrolysis of the ester linkages; hydrolysis rates can be reduced through the addition of additives such as polycarbodiimides.

Polycaprolactone Polyol Synthesis
Polycaprolactone (PCL) polyols are a type of polyester polyol synthesized by the ring opening of ε-caprolactone (Fig. 7). Starter molecules are usually di- or trifunctional alcohols such as ethylene glycol, glycerin, or trimethylolpropane. Ring opening is normally catalyzed by organometallics to provide appropriate production rates.

Polycarbonate Polyols
Polycarbonate polyols can be prepared by reaction of diols with phosgene, but the current preferred process involves a transesterification type reaction of a diol with diphenylcarbonate. One of the more established polycarbonate polyols is based on hexamethylene diol. More recently, routes to produce polycarbonate or polycarbonate polyether polyols from copolymerization of ethylene or propylene oxide and CO_2 have been developed. These polyols (Fig. 8) have the benefit of using CO_2 as a monomer, which is attractive both from a cost and environmental perspective. Compared with the conventional polyether polyols, these materials have higher viscosity, which increases with CO_2 incorporation.
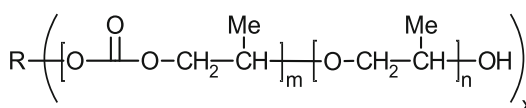
Polyurethane Synthesis, Fig. 8 Polycarbonate polyether polyol

Chain Extenders
In addition to the polyols mentioned above, various chain extenders are also used as the isocyanate reactive component. Chain extenders are low MW materials with two or more isocyanate reactive groups that are incorporated into the polyurethane main chain during synthesis. Most chain extenders are diols, triols, diamines, or alkanolamines with a MW of <400 g/mol. Examples of frequently used chain extenders include ethylene glycol, 1,4-butanediol, hydroquinone *bis* (*beta*-hydroxyethyl) ether, trimethylol propane, ethylene diamine, methylene *bis*-*o*-chloroaniline (MOCA), diethyl toluene diamine (DETDA), isophorone diamine, and diethanolamine.

Commonly Used Additives in Polyurethanes
With respect to PU synthesis, blowing agents, surfactants, and catalysts play a particularly important role. Blowing agents are used to produce cellular materials and can be classified as either physical or chemical. In physical blowing agents, the heat of the polymerization reaction is used to volatilize liquid blowing agents to generate gasses, which expand during polymerization to generate a cellular polymer network. Chemical

blowing agents involve reaction of the blowing agent (typically water) with the isocyanate during the polymerization to generate a gaseous blowing agent (typically CO_2). In either case, these gasses may remain within the cellular network in closed-cell foams or escape the network in open-cell foams. Blowing agent choice is influenced by performance (particularly low thermal conductivity for insulating foams) as well as its safety and impact on the environment – particularly ozone depletion and global warming potential (ODP and GWP, respectively). The most commonly used physical blowing agents are hydrocarbons (HC), hydrofluorocarbons (HFCs), hydrochlorofluorocarbons (HCFCs) (being phased out), and carbon dioxide. Commercial introduction of the first hydrofluorolefin (HFO) blowing agent, which is attractive due to its low GWP and zero ODP, is underway. Water remains the most commonly used chemical blowing agent.

Surfactants are important components used to reduce surface tension, emulsify incompatible ingredients, and promote bubble nucleation and stabilization in cellular materials. These surfactants are most commonly block copolymers of polydimethylsiloxanes (PDMS) and polyalkylene oxides (typically polyethylene or polypropylene oxides).

Catalysts are often used to accelerate the reaction rate of polynucleophiles with isocyanate groups or to promote trimerization of the isocyanate group to form cross-linked polymers. The most commonly used catalysts are tertiary amines and organometallics (often tin based). An important consideration with catalysts is their relative catalytic effect on the rate of reaction of isocyanates with hydroxyl groups versus their reaction with water. Tertiary amines, which more selectively promote the reaction with water, are known as "blow catalysts," while the organometallics are "gel catalysts," i.e., generally more selective for the reaction of isocyanates with alcohol groups. Combinations of blow and gel catalysts are often used to provide the desired reaction profile.

Other additives such as fillers, antioxidants, light stabilizers, flame retardants, pigments, and plasticizers are used to achieve the desired properties and environmental durability. The appropriate selection of these additives is highly application specific.

Isocyanate-Based Polymerization Routes

Polyurethanes are typically made by the addition polymerization of di- or polyisocyanates with polynucleophiles to produce polyurethanes and related compounds. Reactions between isocyanates and hydroxyl or amino functional groups produce, in addition to urethanes and ureas, a related family of compounds including allophanates and biurets, which result from subsequent reaction of the nascent polyurethane or polyurea active N-H group, with an additional isocyanate group. As a result, these functional groups are often incorporated into polyurethane structures.

The reaction of isocyanates with active hydrogen-containing compounds is driven by the relatively high enthalpy of formation of isocyanates. The primary polymerization reaction, that of an alcohol or amine with an isocyanate, is highly exothermic, with typical enthalpy of reaction of about 20–25 kcal/mol. Given this strong thermodynamic driving force, high molecular weight polyurethanes are readily produced, provided component stoichiometry (e.g., ratio of equivalents of isocyanate/hydroxyl) is properly maintained.

In these urethane-forming and related reactions, the isocyanate reacts as an electrophile, where the active hydrogen-containing component (e.g., alcohol, amine, urethane, urea) acts as the nucleophile. This reactivity can be attributed to the reduced electron density at the carbon of the NCO group, due to the effect of the adjacent electronegative oxygen and nitrogen atoms. Consistent with this, electron withdrawing groups adjacent to the isocyanate functional group lead to increased reactivity of the isocyanate, while electron donating groups retard reactivity. Therefore, aromatic isocyanates (R-NCO, where R is an aryl group) are more reactive than aliphatic isocyanates where R is an alkyl group. Steric hindrance at either the

P

isocyanate or nucleophile can dramatically reduce reactivity.

The nature of the nucleophile also has a strong influence on reactivity. Table 1 shows the relative reactivity of various active hydrogen-containing compounds with an isocyanate.

About two thirds of polyurethane raw materials (polyisocyanates and polyols) are used in the production of cellular polyurethanes [7]. The key reaction used to generate these cellular materials is that of the diisocyanate and water. This "blow" reaction first forms an unstable carbamic acid, which quickly decomposes into an amine and carbon dioxide. The amine reacts with additional isocyanate producing a urea group with the in situ generated carbon dioxide functioning as a blowing agent (Fig. 9). Thus these water-blown foams

contain mixtures of urethane and urea linkages; however, as the majority of the starting intermediates are hydroxyl terminated, the materials are generally referred to as polyurethane foams. Auxiliary blowing agents (ABA) can also be incorporated as necessary for further density reduction.

"One-Shot" PU Synthesis

In the "one-shot" process, all reactive components are combined in a single polymerization step. Advantages of this method include the possibility of low temperature processing and ease of handling of low viscosity components. This method is often practiced for the synthesis of rigid and flexible polyurethane foams and some elastomers. Although conceptually the simplest processing method, in some instances (e.g., cast elastomers), significant shrinkage and inhomogeneity often result due to the highly exothermic reaction. Also, compatibility of the polar polyol/chain extender components with the nonpolar isocyanates can be an issue.

"Prepolymer" Synthesis of PU

In the "prepolymer method," polyol and polyisocyanate are first combined (stoichiometric excess of isocyanate groups) and allowed to react to form an NCO-terminated prepolymer. Many prepolymers are storage stable and commercially available. In a second step, the chain extender and isocyanate-terminated prepolymer are combined and allowed to react to form the polyurethane. This approach has the advantage of lower levels of monomeric isocyanate, lower temperature rise during cure, and improved compatibility of the components compared with the "one-shot" method. Disadvantages compared with the "one-shot" method may include high prepolymer viscosity and high mix ratios (prepolymer/chain

Polyurethane Synthesis, Table 1 Relative reactivity of active hydrogen-containing compounds with isocyanate group [10, 11]

Active hydrogen-containing compound	Representative structure	Approximate relative reaction rate[a]
Primary aliphatic amine	R-NH$_2$	1×10^3
Secondary aliphatic amine	(R$_2$N)-H	$2–5 \times 10^2$
Primary aromatic amine	Ar-NH$_2$	2–3
Primary hydroxyl	RCH$_2$-OH	1
Water	HOH	1
Carboxylic acid	RCOOH	4×10^{-1}
Secondary hydroxyl	R$_2$CH-OH	3×10^{-1}
Ureas	R-NH-CO-NH-R	1.5×10^{-1}
Tertiary hydroxyl	R$_3$C-OH	5×10^{-3}
Urethane	R-NH-CO-OR	3×10^{-3}
Phenol	AR-OH	3×10^{-3}
Amide	RCO-NH$_2$	1×10^{-3}

[a]Uncatalyzed reaction at 25 °C

Polyurethane Synthesis, Fig. 9 Formation of polyurea and CO$_2$ blowing agent from reaction of isocyanate and water

extender (up to 15:1)), which can cause issues with mixing and metering.

"Quasi-prepolymer" PU Synthesis

The "quasi-prepolymer" method is a hybrid of the "one-shot" and "prepolymer" methods. "Quasi prepolymers," where a portion of the polyol component has been pre-reacted with the polyisocyanate component, are combined with a mixture of polyol and low molecular weight chain extender. This is often a good compromise offering some advantages of the "prepolymer" and "one-shot" methods.

Synthesis of Aqueous Polyurethane Dispersions (PUD)

Polyurethane dispersions (PUDs) are high molecular weight polyurethanes based primarily on aliphatic isocyanates, with a backbone composed of polyether, polyester, or polycarbonate polyols. They have a particle size in the range of 50–300 μm.

Stable dispersions are achieved by incorporating hydrophilic groups into the backbone of the polymer. The hydrophilic groups may be anionic (carboxylate, sulfonate) or nonionic (ethylene oxide-based monols); in some cases, cationic stabilization is employed. Early dispersion technology required the use of solvents such as N-methyl-2-pyrrolidone (NMP) to produce a stable dispersion, and these solvents remained in the final product. Technology has now been developed that yields dispersions without cosolvent.

There are primarily two methods currently used in production. The prepolymer process involves making an isocyanate-terminated prepolymer containing a carboxylate or sulfonate group. This hydrophilic prepolymer is then dispersed in water using high shear forces. NMP may be added to the prepolymer to facilitate the dispersing step. The final molecular weight is achieved through reaction of the remaining isocyanate groups with a chain extender, often a diamine or hydrazine. The second, more recent process is the acetone process illustrated in Fig. 10. The prepolymer is made from the polyisocyanate and the polyol of choice. This prepolymer is then dissolved in acetone and
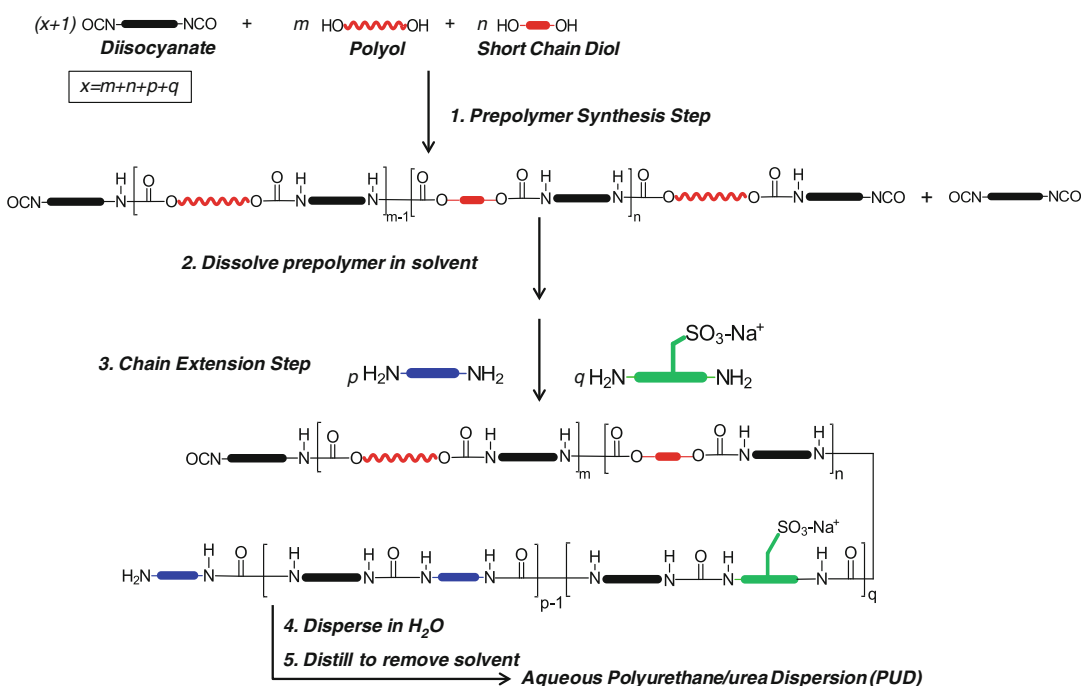
Polyurethane Synthesis, Fig. 10 Polyurethane dispersion (PUD) synthesis

dispersed in water containing a diamino sulfonate group and other diamines to generate the high molecular weight polyurethane. The acetone is subsequently distilled off to yield a stable solvent-free dispersion.

The heat resistance and hydrolytic stability is improved by cross-linking the dispersion with water-dispersible polyisocyanates, which are made by incorporating a nonionic or an anionic group of the type described above into the isocyanate. Cross-linkers are typically used in the range of 5–7 % based on the weight of the dispersion.

Polyurethane Morphology

Many polyurethanes have a phase-separated morphology, with domains of "hard blocks" made up of interchain hydrogen-bonded (H-bonded) urethane linkages dispersed in flexible polyol-based "soft blocks." This structure is depicted schematically in Fig. 11. These relatively weak non-covalent H-bonds form thermally reversible cross-links to provide mechanical reinforcement and a restoring force when the material is strained. In linear PU, these non-covalent H-bonds represent the only cross-linking present and may impart the materials with property profiles (mechanical properties/solvent resistance) comparable to thermoset, covalently cross-linked polymers.

Non-isocyanate-Based Synthetic Routes

In addition to routes based on isocyanate monomers, there are a number of synthetic routes to PU that do not employ polyisocyanate functional monomers as starting materials. The motivation
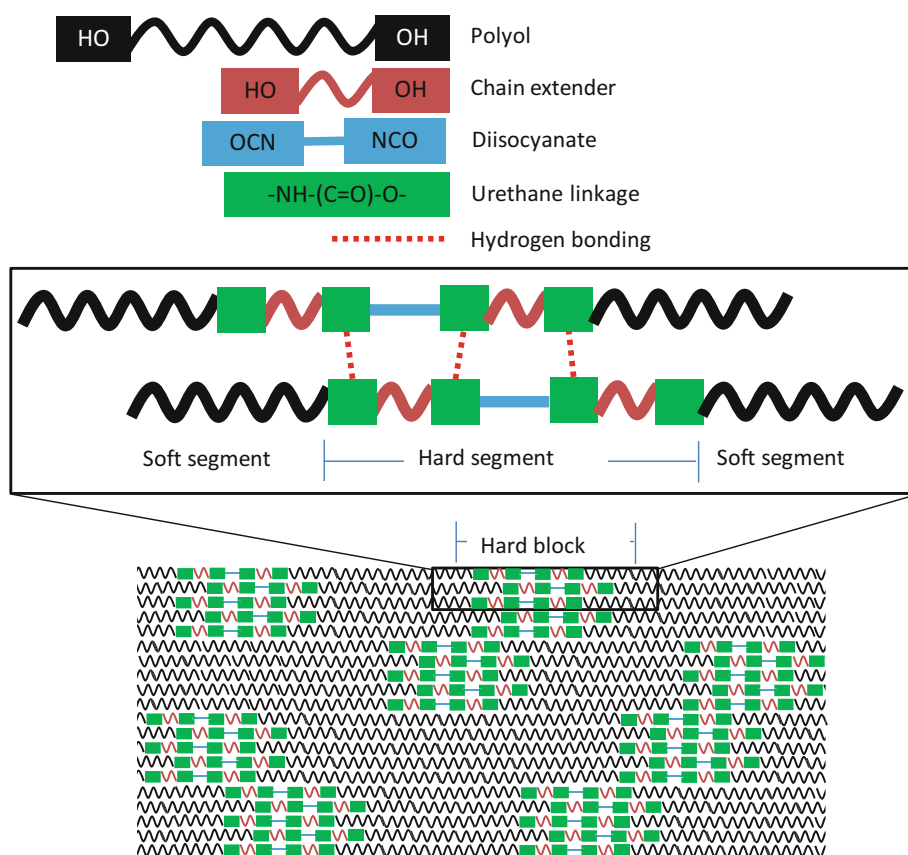
Polyurethane Synthesis, Fig. 11 Schematic of phase-separated PU illustrating soft and hard blocks

Polyurethane Synthesis, Fig. 12 Blocked isocyanate chemistry
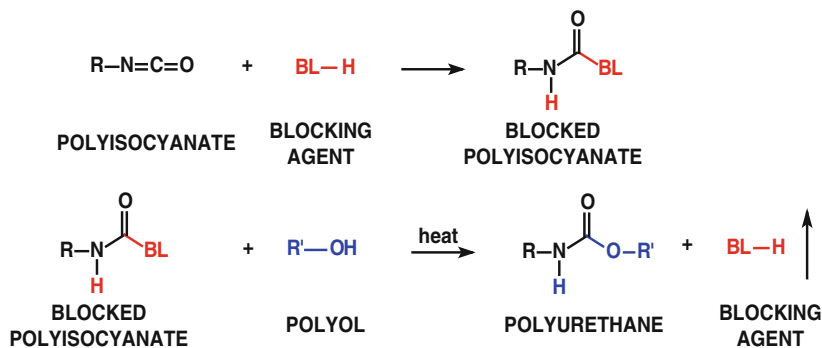
for identifying these alternative routes is driven by several factors, chief among them the desire to avoid the need for specialized equipment for safely handling phosgene or isocyanate-containing monomers. Strictly speaking, isocyanate-free or non-isocyanate-based routes include any synthetic pathway where the components combined by the user for the polymerization step do not include an isocyanate group-containing monomer as a reactive component. Cases where a monomer is derived from an isocyanate-containing compound (e.g., blocked isocyanate routes) or liberates a free isocyanate group during the synthesis (e.g., amino alcohol route) are included as non-isocyanate routes by this definition. With the exception of blocked isocyanate routes, the isocyanate-free routes are generally not practiced widely commercially but are used primarily for research and development purposes.

Blocked Isocyanate Routes

Blocked isocyanate chemistry is a unique synthetic path used to prepare one-component coatings that cure at elevated temperatures. These modified isocyanates are made by reaction of an isocyanate with a blocking agent. One-component formulations based on mixtures of blocked isocyanates and polyether polyols are stable at room temperature but cure at elevated temperature with release of the blocking agent (Fig. 12). The curing temperature is influenced by both the isocyanate and the type of blocking agent used. Reduced curing temperatures are possible with the use of a tin catalyst.

Polyurethane Synthesis, Table 2 Deblocking temperature of isophorone diisocyanate blocked with various blocking agents

Blocking agent	Deblocking temperature (°C)	
	Without catalyst	With 1 % DBTL[a]
ε-CAP	175	163
MEKO	156	137
DMP	158	112
DIPA	136	115

[a]Dibutyl tin dilaurate catalyst

Typical blocking agents include ε-caprolactam (ε-CAP), methyl ethyl ketoxime (MEKO), 3,5-dimethylpyrazole (DMP), and diisopropyl amine (DIPA). The range of deblocking temperatures with and without a tin catalyst is shown in Table 2. The base isocyanate in these examples is an IPDI trimer.

Additional Non-isocyanate-Based Synthetic Routes

Various $\alpha,\omega-$aminoalcohols have been used to prepare polyurethanes by selective reaction of the amine group with di-t-butyl tricarbonate to produce in situ (after decomposition of the intermediate) the corresponding α-hydroxy-ω-isocyanate. This intermediate then polymerizes to the corresponding polyurethane. (Fig. 13). This strategy for homopolymerization of the hydroxyl-containing isocyanate is necessary because selective phosgenation of the amine group of α,ω-aminoalcohols to prepare the requisite α-hydroxy-ω-isocyanate compounds cannot be achieved due to the competing reaction of the alcohol group with phosgene.

P
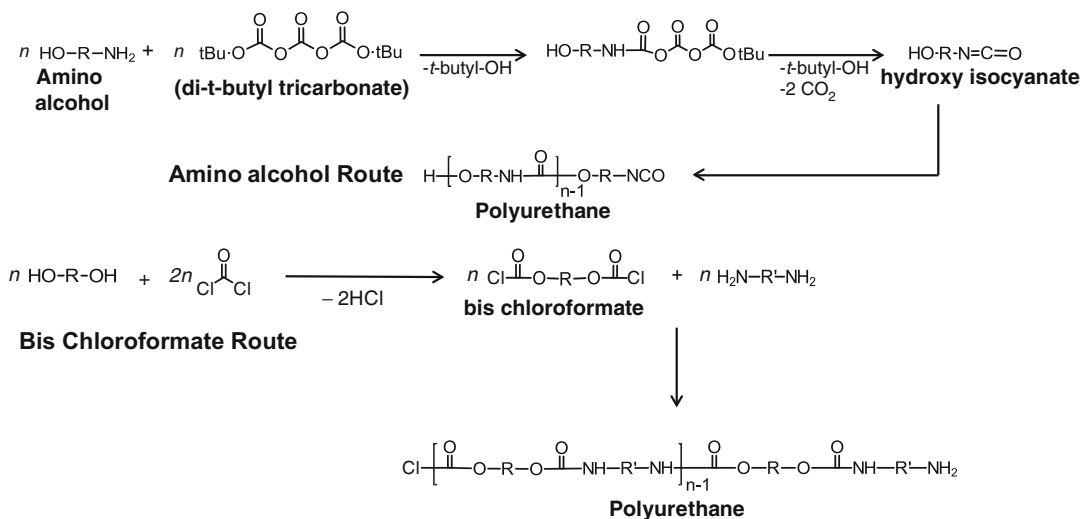
Polyurethane Synthesis, Fig. 13 Non-isocyanate-based routes to PU

Perhaps the most well known of the NCO-free routes to polyurethanes is the *bis* chloroformate route, which employs the same raw materials as the more conventional isocyanate-based route (phosgene, polyols, and polyamines). However, rather than phosgenating the polyamine to produce a reactive polyisocyanate, phosgene is first combined with the polyol component to form a *bis* (chloroformate), which is subsequently polymerized to the polyurethane by reaction with the diamine (Fig. 13). In a related route, a bisphenyl carbonate replaces the *bis* (chloroformate) as the comonomer which reacts with the diamine.

Reaction of bisphenyl carbamates with polyhydroxyl functional materials also results in polyurethanes. Here, rather than "activating" the alcohol to produce a monomer which reacts with the diamine as in the *bis* chloroformate route, the diamine is first "activated" by reaction with diphenyl- or dimethylcarbonate. The resulting bisphenyl or bismethyl carbamate reacts via condensation polymerization with the polyol component. Removal of the reaction by-product (e.g., phenol or methanol) may be used to drive the equilibrium to produce high molecular weight polyurethanes.

Other isocyanate-free routes to PU include: the polyaddition of bifunctional cyclic carbonates with diamines to produce hydroxyl functional urethanes, polycondensation of ethylene carbonate, diamines and diols, ring opening polymerization of cyclic urethanes, and the copolymerization of substituted aziridines with CO_2. Detailed descriptions of these and other non-isocyanate-based routes to polyurethanes have recently been discussed in detail in excellent review articles [9, 12].

Summary and Recent Trends in Polyurethane Synthesis

Although very mature products, application and product innovation in PU continues. Today's need for simple, energy-efficient processing with fast cycle times, coupled with demands for improved health, safety, and environmental impact, continues to drive developments.

For example, in PU raw materials and processing, work continues to develop catalysts that give optimized cure profiles tailored for specific applications. Renewable raw materials are being evaluated, particularly for polyester polyol components (diacids and diols) and chain extenders (diols). A new class of polycarbonate polyether-based polyols is emerging. These

building blocks, based on copolymers of CO_2 and alkylene oxides, incorporate a new low-cost environmentally attractive comonomer for polyol production.

Driving PU product developments are ever higher demands on insulation performance, which are being addressed through control of cell size and structure, and demand for new fire retardant strategies. Additionally, next generation rigid insulation systems are being developed to accommodate novel blowing agent chemistries, which continue to evolve toward more environmentally friendly materials. Broader use of polyurethane matrices in fiber-reinforced composites is also emerging.

Related Entries

References

1. Oertel G (1993) Polyurethane handbook, 2nd edn. Hanser, Munich
2. Randall D, Lee S (2002) The polyurethane book. Wiley, New York
3. Adam N et al (2005) Polyurethanes. In: Ullmann's encyclopedia of industrial chemistry. Wiley-VHC, Weinheim, pp 546–604
4. Avar G, Meier-Westhues U, Casselmann H, Achten D (2012) Polyurethanes. In: Matyjaszewski MK (ed) Polymer science: a comprehensive reference, vol 10. Elsevier BV, Amsterdam, pp 411–441
5. Meier-Westhues U (2007) Polyurethanes coatings, adhesives and sealants. Vincentz Network GmbH & Co., Hannover
6. Engels HW, Pirkl HG, Albers R, Albach RW, Krause J, Hoffmann A, Casselmann H, Dormish J (2013) Polyurethanes: versatile materials and sustainable problem solvers for today's challenges. Angew Chem Int Ed 52:9422–9441. doi:10.1002/anie.201302766
7. The Chemical Industry Education Centre (2014) The essential chemical industry online – Polyurethanes. University of York, York. http://www.essentialchem-icalindustry.org/polymers/polyurethane. Accessed 4 May 2014
8. Ulrich H (1996) Chemistry and technology of isocyanates. Wiley, Chichester
9. Kreye O, Mutlu H, Meier M (2013) Sustainable routes to polyurethane precursors. Green Chem 15:1431–1455. doi:10.1039/c3gc40440d
10. Herrington R, Hock K (1998) Flexible polyurethane foams, 2nd edn. The Dow Chem Co., Midland, Michigan
11. Ionescu M (2005) Chemistry and technology of polyols for polyurethanes. Rapra Technology Limited, Shawbury
12. Hahn C, Keul H, Moeller M (2012) Hydroxyl-functional polyurethanes and polyesters; synthesis, properties and potential biomedical application. Polym Int 61:1048–1060. doi:10.1002/pi.4242

POM (Polyoxymethylenes), Polyacetals

Tamotsu Hashimoto and Toshikazu Sakaguchi
Department of Materials Science and Engineering, Graduate School of Engineering, University of Fukui, Bunkyo, Fukui, Japan

Synonyms

Acetal; Acetal polymer; Acetal resin; Polyformaldehyde

Definition

Polyoxymethylenes are commercially available engineering thermoplastics used in precision parts requiring high mechanical strength, stiffness, toughness in the wide range of temperature and environment.

POM (Polyoxymethylenes)

Polyoxymethylenes (POM) (Eq. 1), sometimes called acetal polymer or acetal resins, are highly crystalline thermoplastic materials exhibiting a broad array of useful properties including high mechanical strength, stiffness, and toughness in the wide range of temperature and environment [1–5].

P

**POM
(Polyoxymethylenes),
Polyacetals,
Fig. 1** Dipole moments in
a 9/5 helical and a planer
zigzag conformations
of POM

a 9/5 helix

b planar zigzag
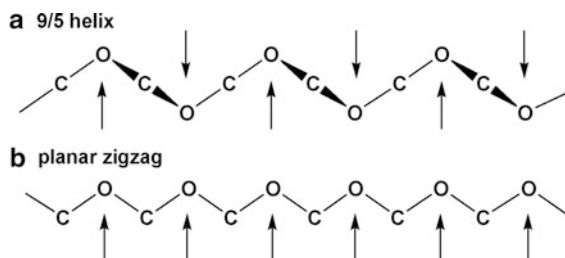
In many practical applications, POM have replaced metals in a variety of precision parts because of balanced properties as engineering plastics. POM are the first commercial engineering plastic, and they still play an important role in our life. A huge amount of POM is currently manufactured by many companies, and further new high-performance POM are developed.

$$\left(\!-CH_2O-\!\right)_n \qquad (1)$$
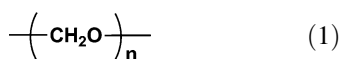
Historical Part in Industry

Although POM have been known since the study by Staudinger in the early 1920s [6], the POM was not a useful material because it was lacking in sufficient thermal stability. In the early 1960s, two types of POM were first commercialized: Delrin®, an acetal homopolymer introduced by Du Pont in 1960 [7], and Celcon®, an acetal copolymer introduced by Celanese (now Hoechst Celanese) in 1961 [8]. Both acetal homopolymer and acetal copolymer consist primarily of oxymethylene repeating units based on formaldehyde or trioxane (cyclic trimer of formaldehyde), but they differ in the mode of polymerization from which they are derived, in main chain structure, in end-group structure, in degree of crystallinity and melting point of crystallites, and hence in some of properties. Subsequently, BASF, Polyplastics, Asahi Chemical, and Mitsubishi Gas Chemical have commercialized acetal resins. Asahi Chemical manufactures acetal block copolymer as well as acetal homo- and copolymers [5].

Today, their production processes are producing about 600,000 metric tons of POM worldwide.

Polymerizations for POM Production

Formaldehyde is inherently highly reactive monomer toward ionic chain polymerization, that is, anionic and cationic polymerizations [9]. Polymers obtained by both the polymerizations have the structure of polyacetal chain of alternating carbon and oxygen atoms. Acetal homopolymers are manufactured by anionic polymerization of aldehyde, in which a suitable catalyst anion adds to the carbonyl carbon of formaldehyde to form an alkoxide propagating species. Amines, ammonium salts, organometallic compounds, and metal chelates can be used as anionic catalysts. Onium salts like ammonium salts (e.g., $R_3NH^+OH^-$; R = alkyl) are commonly used for industrial production (Eq. 2). It is necessary to polymerize highly purified and anhydrous formaldehyde, because water and other protonic impurities cause chain transfer reactions to limit polymer molecular weight. A chain transfer reaction of the growing end with water is shown (Eq. 3). A protonic compound such as methanol is sometimes added as a chain transfer agent for the purpose of controlling polymer molecular weight.

$$R_3NH^+\,OH^- \;+\; CH_2{=}O \;\longrightarrow\; HOCH_2O^-\,R_3NH^+$$

$$CH_2{=}O$$

$$\xrightarrow{\qquad} \quad HO\!\left(\!-CH_2O-\!\right)_n\!CH_2O^-\,R_3NH^+$$

$$(2)$$

$$HO-(CH_2O)_n-CH_2O^- \; R_3NH^+ \quad + \quad H_2O \quad \longrightarrow$$

$$HO-(CH_2O)_n-CH_2OH \quad\quad + \quad R_3NH^+ \; OH^-$$

$$(3)$$

Acetal copolymers are manufactured by cationic ring-opening copolymerization of trioxane as a main monomer and cyclic ether, most commonly ethylene oxide or 1,3-dioxolane, as a comonomer. Commercial acetal copolymers are estimated to contain 0.1 to 15 mol% of the cyclic ether. Lewis acids and protonic acids can be used as cationic catalysts. Typical catalysts for the copolymerization are boron trifluoride (BF_3) and its ether complexes (e.g., BF_3OEt_2). The electrophilic portion of the catalysts adds to the monomers to form the growing cations to form a random copolymer containing long sequence of oxymethylene units separated by an oxyethylene unit (Eq. 4). Acetal block copolymers are manufactured by the anionic polymerization of formaldehyde via controlled chain transfer with the polymer having an active hydrogen atom in the terminal groups [R(X)-OH; R = alkyl chain; X = oxyalkylene chain] [5].

$$(4)$$

Stabilization of POM via End-Group Transformation

The polymers obtained from the polymerization system normally have hemiacetal end groups ($-CH_2-O-CH_2-OH$), which are thermally unstable. The polymer chain easily causes depolymerization to form monomeric formaldehyde under heating. Therefore, the terminal hemiacetal groups should be converted into thermally stable end groups. This is accomplished for acetal homopolymers by treating the terminal hemiacetal groups with acetic anhydride to form thermally stable acetate end groups (Eq. 5). Such end-capped POM can be obtained directly by adding acetic anhydride as a chain transfer agent in anionic polymerization.

$$(5)$$

In a polymer chain of acetal copolymers, thermally stable oxyethylene units ($-CH_2-CH_2-O-$) are occasionally present. Controlled thermal treatment of acetal copolymers removes the unstable hemiacetal end groups until the stable oxyethylene-based unit ($-CH_2-CH_2-OH$) is reached as a terminal (Eq. 6). In addition, the hydroxyethyl terminal groups ($-CH_2-CH_2-OH$) are alkali resistant so that acetal copolymers are stable to highly alkaline environments. Note that the terminal acetate groups of acetal homopolymers are sensitive to alkaline regents.

$$(6)$$

The terminal acetate groups of acetal homopolymers and the terminal oxyethylene groups of acetal copolymers can be decomposed by the exposure to acidic substances, oxygen, high temperature, etc. If once the polymer chain scission occurs, it triggers the depolymerization. In the case of homopolymers, the depolymerization causes a significant decrease of polymer molecular weights. On the other hand, the

depolymerization ceases when the next oxyethylene-based unit becomes polymer end group for acetal copolymers. To prevent the chain scission, some stabilizers are commonly incorporated into the polymer melts. Phenolic compounds such as 4,4′-butylidenebis (6-*tert*-butyl-3-methylphenol) are used to suppress thermal-oxidative decomposition. To prevent acidolytic decomposition, alkaline-earth metal salts and nitrogen-containing compounds such as calcium carbonate and dicyanodiamide, respectively, can be used as an acid trapping agent.

Structure

The chains of POM have a 9/5 helical conformation rather than a planer zigzag conformation like polyethylene, as shown in Fig. 1. The COC chain segments have a dipole moment, which is stabilized in 9/5 helix because the dipoles are located alternately in the polymer chain (Fig. 1a). In contrast, the COC segments in a planer zigzag conformation have a strong parallel dipole moment (Fig. 1b). In 9/5 helix, the repeat distance is 1.739 nm, the COC bond angle 112 °, and the OCO bond angle 111°. The helical chains bend at approximately 10 nm length to form lamellar structures. The well-regulated lamellar structures and the strong interaction between lamellar crystals bring to the mechanical strength of POM.

Properties

POM are highly crystalline thermoplastic resins. The reported degrees of crystallinity are about 70 % for acetal homopolymers and about 60 % for acetal copolymers at room temperature. This crystallinity imparts good surface lubricity, hardness, and chemical resistance, but limits adhesion ability of the surface. The melting points of the POM crystallites are about 175 °C for acetal homopolymers and about 165 °C for acetal copolymers. The number-average molecular weights of commercialized POM are
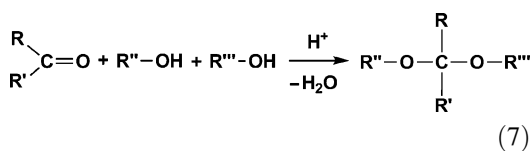
20,000–80,000, and the polydispersity ratios (weight-average molecular weight/number-average molecular weight) range from 2.0 to 3.0. The glass transition temperatures of POM are observed to be about −60 °C in the dynamic viscoelastic test, but its simple and regular structure induces tightly packed crystals with high melting temperature. Because of its higher degree of crystallinity, acetal homopolymer has higher level of mechanical properties such as tensile strength, flexural strength, impact resistance, and hardness than acetal copolymer. On the other hand, the copolymer has greater elongation in the tensile test and better retention of properties in long-term aging in some environments. POM has found a wide variety of applications in the automotive, industrial, plumbing, appliance, and other fields where their strength properties, hardness, lubricity, and wear resistance can be used to maximum advantage.

Acetal homopolymers and copolymers are very stable toward numerous chemicals. Their mechanical properties are hardly affected by continuous contact with conventional organic solvents such as alcohols, esters, ethers, and hydrocarbons as well as common fuels. Additionally, acetal polymers swell only slightly in contact with water and organic solvents. These properties are also important for the use of construction materials.

Polyacetals

In a basic organic chemistry, aldehyde and ketones react with alcohols in the presence of an acid catalyst to yield acetals [R''-O-C(R)(R′)-O-R‴] (Eq. 7). Acetals are commonly employed as a protecting group for aldehydes and ketones, because the acetal linkages [$-O$-C(R)(R′)-O-] are stable to bases, reducing agents, and various nucleophiles but easily converted into the corresponding carbonyl compounds [O = C(R)(R′)] and alcohols [R''-OH and R‴-OH] via degradation of acetal linkages by treatment with aqueous acids. Hydrolysis rates under acidic conditions increased in the order R''-O-CH$_2$-O-R‴ < R''-O-CH(R′)-O-R‴ < R''-O-C(R)(R′)-O-R‴ as would be expected for the stability of a

carbocation intermediate [10]. Commercially manufactured polyacetals are polyoxymethylenes (POM) $[-(CH_2O)_n-$; their acetal linkages are $-O-CH_2-O-$, thus the most stable to acid] obtained by polymerization based on formaldehyde or trioxane monomers and are widely used as engineering plastics (see above). In contrast, there are many examples of the synthesis of polyacetals with a variety structures. Depending on their main chain and side chain structures, they exhibit different properties and different acid-induced degradability.

$$R'' - O - \overset{\overset{\displaystyle R}{|}}{\underset{\underset{\displaystyle R'}{|}}{C}} - O - R''' + HO - X - OH \xrightarrow[-R''-OH, -R'''-OH]{H^+}$$

$$\left(O - \overset{\overset{\displaystyle R}{|}}{\underset{\underset{\displaystyle R'}{|}}{C}} - O - X \right)_n \tag{9}$$

$$CH_2{=}CH{-}O{-}X{-}O{-}CH{=}CH_2 + HO{-}X'{-}OH \xrightarrow{H^+}$$

$$\left(O - \overset{\overset{\displaystyle CH_3}{|}}{CH} - O - X - O - \overset{\overset{\displaystyle CH_3}{|}}{CH} - O - X' \right)_n \tag{10}$$

$$CH_2{=}CH{-}O{-}X{-}OH \xrightarrow{H^+} \left(O - \overset{\overset{\displaystyle CH_3}{|}}{CH} - O - X \right)_n \tag{11}$$

$$\overset{\displaystyle R}{\underset{\displaystyle R'}{}}\!\!\!C{=}O + R''{-}OH + R'''{-}OH \xrightarrow[-H_2O]{H^+} R'' - O - \overset{\overset{\displaystyle R}{|}}{\underset{\underset{\displaystyle R'}{|}}{C}} - O - R''' \tag{7}$$

Synthesis of Polyacetals With Various Routes

Polyacetals were primarily synthesized by polycondensation of aldehydes and diols (Eq. 8) [11]. In the polycondensation method, by-product water should be removed from the reaction mixture to obtain high-molecular-weight polymers. The acetal exchange reaction of acetals with diols can be used to prepare polyacetals via a similar stepwise polycondensation process, where by-products are alcohols (Eq. 9) [12]. As an entirely different and more straightforward route, polyaddition of divinyl ethers and diols (Eq. 10) [13] and self-polyaddition of vinyl ethers with a hydroxyl group (Eq. 11) [14, 15] are effective, where the acid-catalyzed addition reaction between a vinyl ether group and a hydroxyl group of these monomers produces polyacetals in the stepwise manner without the elimination of a small molecule.
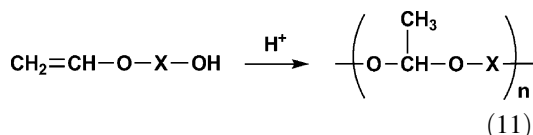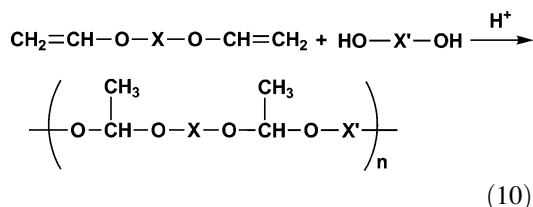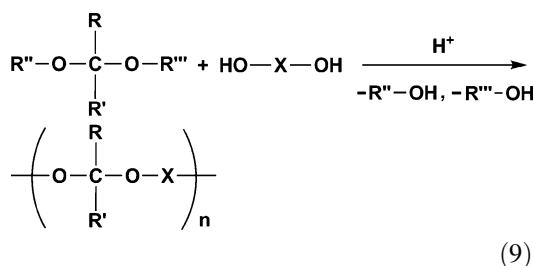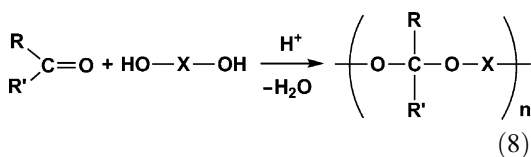
Polyacetals as Degradable Polymers

Chemistry of polyacetals provides polymer materials with suitable degradability for some purposes. One example involves the development of environmentally friendly, chemically recyclable commodity polymers with polyacetal segments. Acetal linkage-incorporated polyurethanes [16] and epoxy resins [17] undergo smooth degradation to produce raw materials for chemical recycling. Another example is directed toward the development of synthetic biomaterials for tissue engineering and drug delivery applications [18].

Related Entries

▶ Polyethers

References

1. Persak KJ, Fleming RA (1986) The history of acetal homopolymer. In: Seymour RB, Kirshenbaum GS (eds) High performance polymers: their origin and development. Elsevier, New York, pp 105–114

$$\overset{\displaystyle R}{\underset{\displaystyle R'}{}}\!\!\!C{=}O + HO{-}X{-}OH \xrightarrow[-H_2O]{H^+} \left(O - \overset{\overset{\displaystyle R}{|}}{\underset{\underset{\displaystyle R'}{|}}{C}} - O - X \right)_n \tag{8}$$

P

2. Dolce TJ, McAndrew FB (1986) Acetal copolymer, a historical perspective. In: Seymour RB, Kirshenbaum GS (eds) High performance polymers: their origin and development. Elsevier, New York, pp 115–124

3. Serle AG (1985) Acetals. In: Margolis JM (ed) Engineering thermoplastics, properties and applications. Marcel Dekker, New York, pp 151–175

4. Forschirm A, McAndrew FB (1996) Acetal resins. In: Salamone JC (ed) Polymeric materials encyclopedia, vol 1. CRC Press, New York, pp 6–11

5. Masamoto J (1993) Modern polyacetals. Prog Polym Sci 18:1–84

6. Staudinger H (1920) Uber polymerisation. Ber dtsch Chem Ges A/B 53:1073–1085

7. MacDonald RN (1956) Polyoxymethylens. US Patent 2,768,994

8. Walling CT, Brown F, Bartz KW (1962) Copolymers. US Patent 3,027,352

9. Vogl O (2000) Addition polymers of aldehydes. J Polym Sci Part A: Polym Chem 38:2293–2299

10. Smith MB, March J (1992) March's advanced organic chemistry, reactions, mechanisms, and structure, 5th edn. Wiley-Interscience, New York, pp 465–468

11. Ofstead EA (1990) Polyacetals. In: Kroschwitz JI (ed) Concise encyclopedia of polymer science and engineering. Wiley-Interscience, New York, p 746

12. Hefferman MJ, Murthy N (2005) Polyketal nanoparticles: a new pH-sensitive biodegradable drug delivery vehicle. Bioconjug Chem 16:1340–1342

13. Heller J, Penhale DWH, Helwing RF (1980) Preparation of polyacetals by the reaction of divinyl ethers and polyols. J Polym Sci Polym Lett Ed 18:293–297

14. Zhang H, Ruckenstein E (2000) Self-polyaddition of hydroxyalkyl vinyl ethers. J Polym Sci Part A Polym Chem 38:3751–3760

15. Hashimoto T, Ishizuka K, Umehara A, Kodaira T (2002) Synthesis of polyacetals with various main-chain structures by the self-polyaddition of vinyl ethers with a hydroxyl function. J Polym Sci Part A Polym Chem 40:4053–4064

16. Hashimoto T, Umehara A, Urushisaki M, Kodaira T (2004) Synthesis of a new degradable polyurethane elastomer containing polyacetal soft segments. J Polym Sci Part A Polym Chem 42:2766–2773

17. Hashimoto T, Meiji H, Urushisaki M, Sakaguchi T, Kawabe K, Tsuchida C, Kondo K (2012) Degradable and chemically recyclable epoxy resins containing acetal linkages: synthesis, properties, and application for carbon fiber-reinforced plastics. J Polym Sci Part A Polym Chem 50:3674–3681

18. Falco EE, Patel M, Fisher JP (2008) Recent developments in cyclic acetal biomaterials for tissue engineering applications. Pharm Res 25:2348–2356

Precipitation Polymerization

Dongwei Zhang and Xinlin Yang
Key Laboratory of Functional Polymer Materials, Ministry of Education, Institute of Polymer Chemistry, Collaborative Innovation Center of Chemical Science and Engineering, Nankai University, Tianjin, China

Synonyms

Cross-linked polymer synthesis; Dispersion polymerization; Emulsion polymerization

Definition

Precipitation polymerization takes place via radical initiation of the monomers/cross-linkers in a homogeneous system followed by propagation through a chain addition mechanism resulting in precipitation of the polymer network in a poor solvent (poorer than a θ solvent) leading to polymer particles with a narrow size distribution produced in the absence of any stabilizer or surfactant.

Introduction

Polymer microspheres refer to particles containing polymer components with diameters in the order of submicron to tens of microns and with spherical shape. These nano- or microspheres have many unique characteristics: (i) small size and volume for each particle; (ii) large specific surface area useful for adsorption phenomena, chemical reactions, and light-scattering studies; (iii) high diffusibility and mobility through the medium by gravity, electrical field, and Brownian motions; (iv) stable dispersions due to the following forces, electrostatic repulsive forces, van der Waal's attractive forces, and steric repulsive forces among the particles; (v) uniformity of the

size distribution; and (vi) variation of diameter, surface chemistry, composition, surface texture, and morphology easily possible. Polymer micro- and nanospheres/capsules with internal structures have found wide applications in both traditional and modern technologies, including as biosensors, tissue regeneration, chromatography, water treatment, casting additives, controlled release reservoirs, biomedical devices, colloidal crystals, supporting materials for recoverable catalyst, and super-hydrophobic/hydrophilic materials.

The polymer microspheres can be prepared by two approaches: (a) physical methods, such as emulsification, coacervation, and spray-drying, and (b) chemical techniques, like heterogeneous polymerization. Usually, the polymer particles produced via the physical process have a broad distribution in size. The polymer microspheres having different size ranges and monodispersity can be synthesized by various polymerization techniques, including emulsion polymerization, soap-free emulsion polymerization, dispersion polymerization, suspension polymerization, activated swelling polymerization, seeded polymerization, precipitation polymerization, and distillation precipitation polymerization. Among them, suspension, emulsion, and dispersion polymerizations as traditional heterogeneous techniques have played important roles in industrial production. The suspension polymerization involves well-dispersed liquid monomer droplets in an aqueous system with a steric stabilizer and vigorous stirring to yield the polymer particles as a dispersed solid phase. It is very difficult to control the size uniformity of the polymer particles because such an approach is influenced by a dynamic process control. Steric stabilizers like poly(N-vinylpyrrolidone) (PVP) should be utilized to stabilize the polymer microspheres and prevent them from coagulation.

Emulsion polymerization starts in micelles and further occurs in the colloidal latex particles stabilized by (micelle forming) surfactants. Later in the process the surfactant molecules also supply electrostatic stabilization. This process utilizes usually water-soluble initiators and is most suitable for water-insoluble monomers. For both these processes, the complete removal of the surfactant or stabilizer from the resultant polymer particles is very difficult and can lead to problems in some applications.

Fundamental Aspects

Among the diverse heterogeneous polymerization techniques, precipitation polymerization is unique for the synthesis of polymer micro-/nanospheres with uniform size and shape, and the resulting polymer microspheres are free of any added surfactant or stabilizer. This technique starts as a homogeneous mixture of the monomer(s), initiator, and optional solvents. The polymer microspheres are formed via polymerization of the monomers/cross-linkers and precipitate out from the homogeneous solution. During the polymerization, the growing polymer chains phase-separate from the continuous medium by enthalpic precipitation or entropic precipitation, in those cases where cross-linking prevents the polymer and solvent from mixing [1]. In poor solvents, precipitation polymerization normally produces micrometer-sized polymer particles. While in good solvents, precipitation polymerization produces turbid macroscopic gels, largely dependent on the original monomer concentration [2]. Initially the technique did not attract much attention due to the difficulty in controlling the polymer particle uniformly. Recently, Stöver et al. reported the precipitation polymerization for the synthesis of monodisperse cross-linked polydivinylbenzene (PDVB) microspheres [3] and core-shell polymer microspheres [4]. Furthermore, Stöver did quantitative compositional mapping of these polymer particles by soft X-ray spectroscopy [5]. Distillation precipitation polymerization has been developed as a powerful and facile technique for the synthesis of monodisperse polymer microspheres with various functional groups, core-shell polymer microspheres, inorganic/polymer core-shell composite/hybrid microspheres, and multilayer structured microspheres [6, 7]. In distillation precipitation polymerization the solvent is partially distilled out during the polymerization. The main difference between the normal precipitation

polymerization and distillation precipitation is the agitation of the polymerization system. Precipitation polymerization is performed by rolling the reaction system on a shaking-bed or a rotary-evaporator equipment in the lab. Distillation precipitation polymerization is carried out via distilling part of the solvent out of the polymer nano-/microspheres in order not to bump. Photo-initiated precipitation polymerization has been subsequently developed for the synthesis of monodisperse PDVB particles [8]. More recently, "living" radical polymerizations have been utilized for the synthesis of molecularly imprinted polymer microspheres via the combination of precipitation polymerization and "living" radical polymerization, such as atom transfer radical polymerization (ATRP) [9], reversible addition-fragmentation transfer (RAFT) polymerization [10], and iniferter-induced "living" radical polymerization (ILRP) [11]. A general introduction to the different categories of precipitation polymerization and the underlying mechanisms has been well summarized by a review [12].

Examples and Applications

For precipitation polymerization of the hydrophobic monomers, low monomer loadings (usually as low as 5 vol%), a suitable covalent cross-linker, and a near θ reaction condition (solvent, temperature) are necessary to form narrow or monodisperse polymer microspheres. The formation of microgels, microspheres, space-filling gels, and coagulum as a function of cross-linking degree and solvency of the medium has been reported for precipitation polymerization of poly(divinylbenzene-*co*-methylstyrene) (P(DVB-*co*-MSt)) [13], poly(divinylbenzene-*co*-maleic anhydride) (P(DVB-*co*-MAn)) [14], and poly (methacrylic acid-*co*-(ethyleneglycol) methyl ether methacrylate-*co*-ethylene dimethacrylate) (PMAA-*co*-EGDMA-*co*-EDMA)) [15]. All these results indicate that the solvent for precipitation polymerization has a remarkable influence on the morphology of the resultant polymer network. As a result, acetonitrile as the solvent in many cases

meets the solvency conditions for the formation of narrow or monodisperse polymer particles via (distillation) precipitation polymerization with various polarities, including PDVB (nonpolar) [3, 6], poly(ethyleneglycol dimethacrylate) (PEGDMA, medium polarity) [16], and poly(*N*, *N'*-methylene diacrylamide) (PMBAAm, strong polarity) [17].

The formation process of the polymer particles via precipitation polymerization consists of two stages: nucleation and growth [18]. Nucleation likely starts by aggregation of soluble oligomers to form swollen microgels, which subsequently desolvate and collapse to form the nuclei. The particle growth during precipitation polymerization of DVB in acetonitrile occurred via an entropic precipitation polymerization manner as shown in Fig. 1, in which the soluble monomers and oligomeric species are captured from the solution through the reaction with the residual vinyl groups on the surface of PDVB microspheres due to the steric hindrance of PDVB network. The polymer particles are stabilized by an auto-steric effect of the transient surface gel layer under a swollen state during the growth of the PDVB microspheres. The growth mechanism of PEGDMA microspheres by distillation precipitation polymerization in acetonitrile is much similar to that of PDVB microspheres, in which the surface vinyl groups captured the newly formed oligomers and EGDMA monomers to enlarge the PEGDMA particles [16].

The versatility of control of morphology and properties of the polymer nanostructures has drawn much attention as an interdisciplinary subject in the past several decades. Among them, raspberry-like and bilayer nanostructures have aroused keen interest among many researches owing to their controlled hierarchical structures and properties as well as wide potential application (e.g., in glass covers for solar cells, artificial super-hydrophobicity, improved wettability of gradient surfaces, as nano-reactor, and for pesticide applications). The morphology of the resultant poly(ethyleneglycol dimethacrylate-*co*-methacrylic acid)/polydivinylbenzene (P(EGDMA-*co*-MAA)/PDVB nanocapsules formed through
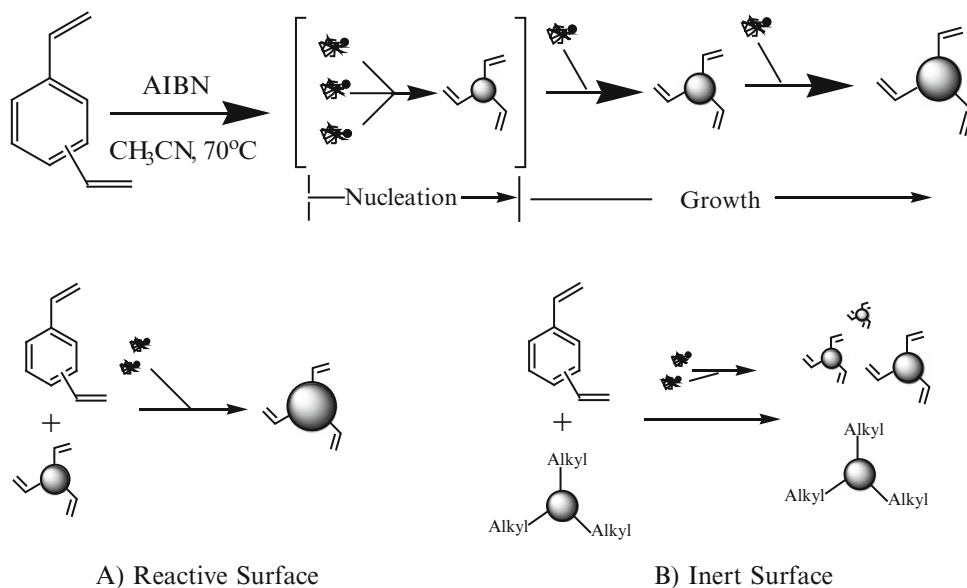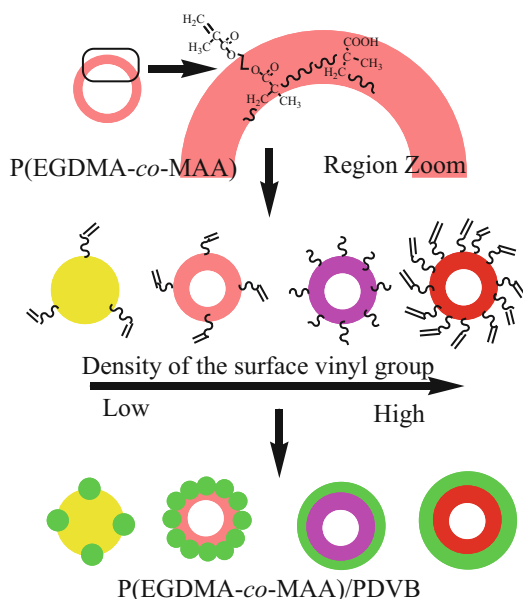
Precipitation Polymerization, Fig. 1 Growth mechanism of polydivinylbenzene microspheres for precipitation polymerization via surface vinyl group-capture process [18]

in situ precipitation polymerization of DVB in the presence of P(EGDMA-*co*-MAA) nanocapsules as templates was controlled by the density of the residual surface vinyl groups of the P(EGDMA-*co*-MAA) nanocapsules, which was dependent on the cross-linking degree (EGDMA) for the distillation precipitation copolymerization of EGDMA and MAA [19]. The formation mechanism of P(EGDMA-*co*-MAA)/PDVB nanocapsules with different morphologies is illustrated in Fig. 2. The density of the surface vinyl groups on the P(EGDMA-*co*-MAA) nanocapsule templates plays a vital role for precipitation polymerization of DVB to produce randomly distributed PDVB domains over P(EGDMA-*co*-MAA) templates, raspberry-like P(EGDMA-*co*-MAA)/PDVB hybrid nanocapsules, and bilayer structure nanocapsules, which depends on the various capture ability of DVB monomers and oligomers during the precipitation polymerization with different density of the surface vinyl groups of P(EGDMA-*co*-MAA) templates.

The hydrophilic polymer microspheres with uniform size are essential for drug delivery system (DDS) because the distribution of the

microspheres in the body and the interaction with biological cells are greatly affected by the particle size. Amphiphilic copolymer containing carboxylic acid group with different architectures have been prepared for their utilization in emulsion polymerization and for the investigation of their unique rheological behavior. Monodisperse hydrophilic polymer microspheres with functional groups, such as aldehyde, imide, and amide, have been obtained via a radiation precipitation polymerization without stirring in the absence of any stabilizer or catalyst [20]. It is important to control the morphologies of the resultant polymers containing hydrophilic comonomers. However, it is difficult to prepare the hydrophilic polymer microspheres with uniform shape via precipitation polymerization. Monodisperse hydrophilic polymer microspheres with spherical shape ranging from 160 nm to 1.52 μm and carboxyl groups have been prepared by distillation precipitation copolymerization of (meth)acrylic acid with either EGDMA or DVB cross-linker in presence of 2-azobisisobutyronitrile (AIBN) as initiator in neat acetonitrile without stirring [21]. The results indicated that the loading of carboxyl groups in

the resultant P(DVB-*co*-AA) microspheres was much lower than the AA fraction in comonomer feed, especially with AA fraction lower than 0.90, which may be originated from the higher reactivity of PDVB cross-linker comparing to that of AA during distillation precipitation polymerization. The loading capacity of the carboxyl groups on the surface of the hydrophilic polymer

Precipitation Polymerization, Fig. 2 Formation mechanism of the P(EGDMA-*co*-MAA)/PDVB nanocapsules with various morphologies controlled by the density of the surface vinyl group [19]

microspheres can be varied between 0.2 and 10.0 mmol/g via altering the feed of (M)AA and the cross-linker.

Monodisperse poly(methacrylic acid) (PMAA) microspheres have been prepared by distillation precipitation polymerization of MAA in acetonitrile with AIBN as initiator in absence of any cross-linker [22]. Monodisperse PMAA microspheres with spherical shape and smooth surface have been synthesized with diameters ranging from 60 to 290 nm below the glass transition temperature of PMAA ($T_g = 185\ °C$) in the absence of any surfactant or stabilizer. During the polymerization, the PMAA is still in a glass state for the possible formation of monodisperse polymer nanospheres, not a viscous network as a coagulum. The residual MAA monomer can be adsorbed on the PMAA nuclei by hydrogen-bonding interaction, which provides the incorporated reactive vinyl groups on the particle surface for the further growth of the PMAA particles as shown in Fig. 3a. The particle growth may be proceeding through the capture of the soluble oligomers or residual MAA monomers by the adsorbed vinyl groups on the surface during the polymerization via a reactive and entropic capture mechanism. On the other hand, the initiator may react with the monomer in solution to form oligomeric radicals throughout the polymerization. When the oligomers grow larger than the critical chain length, these oligomers will precipitate from the homogeneous reaction
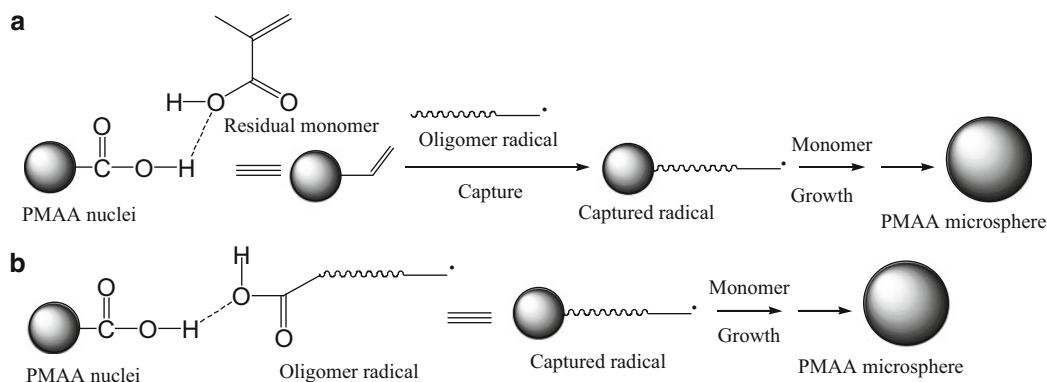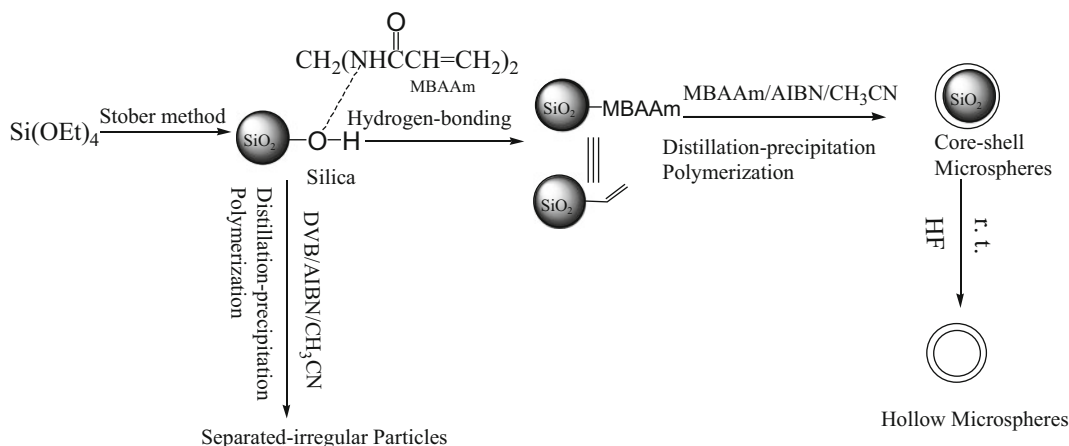

Precipitation Polymerization, Fig. 3 Growth mechanism of poly(methacrylic acid) microspheres by distillation precipitation polymerization via hydrogen-bonding capture process [22]

system and are captured by the original PMAA seeds and the carboxylic acid units on the oligomer radical, which was illustrated in Fig. 3b. In other words, the polymerization is initiated in the homogeneous medium, which is much similar to the typical solution polymerization.

The combination of the properties of inorganic and organic building blocks within a single material has attracted rapidly expanding interest for material scientists because of the possibility to combine the various functional groups of organic components with the advantages of thermally stable and robust inorganic substrates. These inorganic/polymer core-shell composite/hybrid particles can exhibit novel and excellent properties, such as mechanical, chemical, electrical, rheological, magnetic, optical, and catalytic, by varying the compositions, dimensions, and structures of the core and shell. These hybrid polymer particles might find applications as drug delivery system, in diagnostics, coatings, and catalysis. Monodisperse silica/PMBAAm core-shell composite microspheres have been prepared by distillation precipitation polymerization of MBAAm in the presence of silica nanogels as templates without formation of separate pure polymer particles. The thickness of the PMBAAm shell is controlled through the feed of MBAAm monomer [23]. The encapsulation of PMBAAm onto the silica cores is driven by the hydrogen-bonding interaction between the polar hydroxyl group and the amide unit of PMBAAm species during the polymerization to incorporate the reactive vinyl groups on the surface of inorganic template, as shown in Fig. 4. Then the adsorbed vinyl groups on the surface of silica nanospheres capture the MBAAm monomers and newly formed oligomers from the reaction system for the uniform encapsulation of PMBAAm for the formation of silica/PMBAAm core-shell composite microspheres. These surface radicals act as the reactive loci for the further polymerization to enlarge polymer particles, which are stabilized by the steric effect and the electrostatic repulsion.

Silica nanoparticles, which can be conveniently prepared by the hydrolysis of organic silicates via a sol-gel process, have wide applications in many fields including cosmetics, printing, and electronic industries. However, these nanoparticles tend to coagulate due to their high surface energy and polycondensation of their surface groups. Therefore, it is necessary to prevent coagulation by using silica/polymer hybrid core-shell hybrid particles where the modification of surface properties originates from the polymer component. Monodisperse 3-(methacryloxy) propyl trimethoxysilane (MPS)-modified silica nanospheres are prepared from the hydrolysis of siloxane tetraethyl orthosilicate (TEOS) via a sol-gel process having active hydroxyl groups with the successive coating of MPS to

Precipitation Polymerization, Fig. 4 Preparation and mechanism for the formation of silica/PMBAAm composite materials [23]
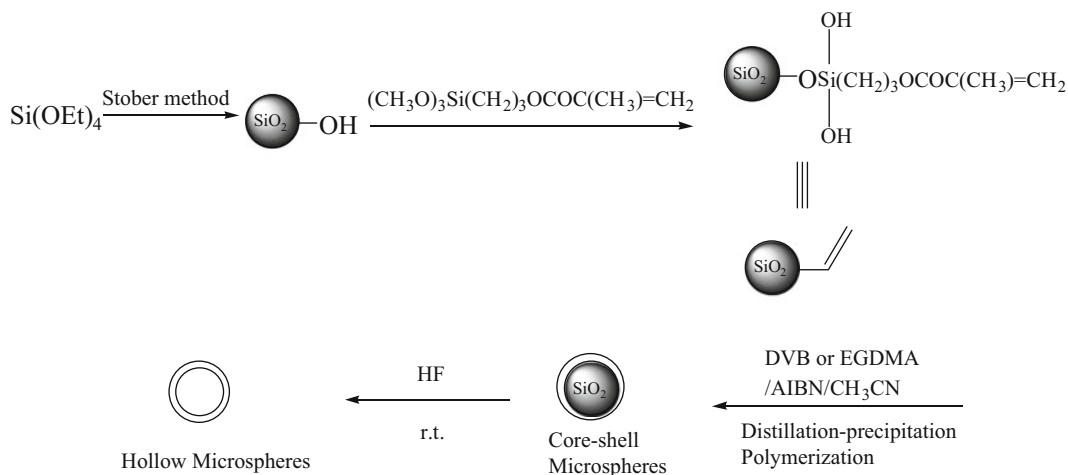
Precipitation Polymerization, Fig. 5 Preparation of silica/polymer core-shell hybrid microspheres and the corresponding hollow polymer microspheres [24]

incorporate the reactive vinyl groups on the surface. Monodisperse silica/PDVB and silica/PEGDMA core-shell hybrid microspheres have been prepared by distillation precipitation polymerization of DVB and EGDMA in the presence of MPS-modified silica nanospheres as templates, during which the polymer shell is coated over the surface of inorganic seeds via a vinyl capture growth mechanism as shown in Fig. 5 [24]. In such a way, the polar surface of inorganic silica nanospheres with reactive hydroxyl groups has been successfully transferred to the nonpolar PDVB and weak-polar PEGDMA shell with hydrophilicity.

Hollow polymer microspheres (nanocapsules) have been an interesting research topic due to their wide applications, including the encapsulation of drugs and enzymes for controlled release, fillers, pigments, catalysts, adsorption materials for sound, and the enhanced water retention and stable dynamic water behavior for proton exchange membrane fuel cell (PEMFC). The hollow polymer microspheres with different functional groups, such as chloromethyl, pyridyl, carboxyl, hydroxyl, amide, and ester, as well as with responsive properties, have been synthesized via the selective removal of the linear PMAA or silica core from the corresponding PMAA/polymer or silica/polymer core-shell microspheres, which can be facilely

prepared by a two-stage distillation precipitation polymerization.

Superparamagnetic nanoparticles have been extensively pursued for bio-separation, magnetic catalytic carrier, drug delivery, and magnetic resonance imaging (MRI). Although there have been many significant developments in the synthesis of magnetic nanoparticles, maintaining the stability of these nanospheres for a long time without agglomeration or precipitation is an important issue. Much effort has been devoted to modify the surface properties of magnetite, as the hydrophobic surface limits applications. Coating a functional polymer shell onto the magnetite cores could solve these problems, which not only protect the core from damaging environments such as oxygen, acids, and bases but also render the nanoparticles biocompatible, stable, water dispersible, and with desired functionalities. The magnetite nanospheres contain some carboxyl groups on their surface via introduction of sodium citrate to the magnetite synthetic system for their stabilization. The synergic hydrogen-bonding interaction between carboxyl groups and ester groups is strong enough to make the magnetite capture monomer or oligomer onto its surface during the distillation precipitation polymerization of EGDMA [25]. In such a way, the hydrogen-bonding interaction plays a key role

Precipitation Polymerization, Fig. 6 The process and mechanism for synthesis of Fe₃O₄/PEGDMA core-shell microspheres via distillation precipitation polymerization [25]
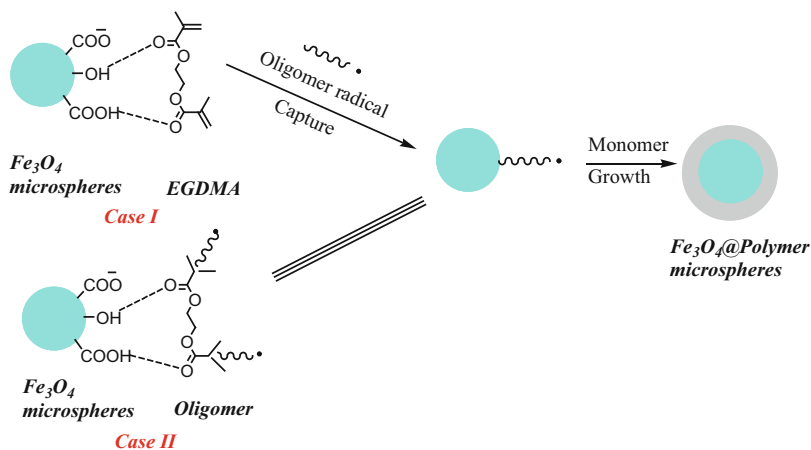
as the driving force during the encapsulation of PEGDMA on magnetite cores with initial incorporation of the reactive vinyl group or radical. The process and mechanism for the synthesis of Fe₃O₄/PEGDMA core-shell microspheres is presented in Fig. 6. In case I, the adsorbed vinyl groups on the surface of magnetite nanospheres via the hydrogen-bonding interaction between the ester groups of EGDMA monomer and the carboxyl groups of the sodium citrate stabilizer as well as the hydroxyl groups of magnetite capture the newly formed oligomer radicals for the encapsulation of PEGDMA to produce magnetite/PEGDMA core-shell composite particles. In case II, the adsorbed radicals via the hydrogen-bonding interaction, which is formed by the reaction between the initiator and EGDMA monomers in the solution, react with the EGDMA monomers from the solution to enlarge the PEGDMA shell layer. Both cases occur simultaneously during the whole distillation precipitation polymerization.

Based on the understanding of the mechanism for the synthesis of silica/polymer and magnetite/polymer microsphere, various inorganic/polymer core-shell hybrid microspheres have been prepared by distillation precipitation polymerization in the presence of different inorganic particles as seeds, including titania, zirconium oxide, ellipsoidal hematite, tin oxide, etc. These hierarchical multilayer core-shell microspheres have been of considerable interest with their thermal,

plasmonic, optical, rheological, and catalytic properties, which would be facilely obtained by tuning the size, monodispersity, building blocks, composition, and morphology. The interaction between the hierarchical layers with various composition and thickness provides unique characteristics comparing to the homogeneous microspheres.

Science and technology of polymer microspheres and their applications have been developed rapidly during the last decade because of the era demands for fine-particle materials, mesoscopic science, nanotechnology, etc., which all concern the polymer microspheres and colloids. There are many novel polymer colloids having a chance to be utilized, such as colloidal crystals, which include polymer microspheres with different functional groups and various structures, hollow polymer particles, unsymmetric particles, composite/hybrid particles, etc. The especially noteworthy fields will be the mechanism for the formation of monodisperse polymer microsphere, design and control of the definite morphology and structure of the fine polymer particles, and the further application of intelligent polymer microspheres, control of the soft aggregation, and ordered assembly of polymer colloids.

Related Entries

▶ Encapsulation with Conventional Emulsion Polymerization

References

1. Sosnowski S, Gadzinowski M, Slomkowski S (1996) Poly(L, L-lactide) microspheres by ring-opening polymerization. Macromolecules 29:4556–4564
2. Antonietti M, Bremser W, Schmidt M (1990) Microgels: model polymers for the crosslinked state. Macromolecules 23:3796–3805
3. Li K, Stöver HDH (1993) Synthesis of monodisperse poly (divinylbenzene) microspheres. J Polym Sci Polym Chem Ed 31:3257–3263
4. Koprinarov I, Hitchcock AP, Li WH, Heng YM, Stöver HDH (2001) Quantitative compositional mapping of core–shell polymer microspheres by soft X-ray spectromicroscopy. Macromolecules 34:4424
5. Li WH, Stöver HDH (2000) Monodisperse cross-linked core–shell polymer microspheres by precipitation polymerization. Macromolecules 33:4354–4360
6. Bai F, Yang XL, Huang WQ (2004) Synthesis of narrow or mono-disperse poly(divinylbenzene) microspheres by distillation-precipitation polymerization. Macromolecules 37:9746–9752
7. Yang XL (2009) Distillation precipitation polymerization as a powerful and facile technique for the synthesis of monodisperse polymer microspheres and their application, Chapter 8. In: Research Signpost (ed) Recent research developments in applied polymer science, vol 4. Research Signpost, Trivandrum, pp 209–268
8. Lime F, Irgum K (2007) Monodisperse polymeric particles by photoinitiated precipitation polymerization. Macromolecules 40:1962–1968
9. Zu BY, Pan GQ, Guo XZ, Zhang Y, Zhang HQ (2009) Preparation of molecularly imprinted polymer microspheres via atom transfer radical precipitation polymerization. J Polym Sci Polym Chem Ed 47:3257–3270
10. Pan GQ, Zhang Y, Ma Y, Li CX, Zhang HQ (2011) Efficient one-pot synthesis of water-compatible molecularly imprinted polymer microspheres by facile RAFT precipitation polymerization. Angew Chem Int Ed 40:11731–11734
11. Li JY, Zu BY, Zhang Y, Guo XZ, Zhang HQ (2010) -One-pot synthesis of surface-functionalized molecularly imprinted polymer microspheres by iniferter-induced "living" radical precipitation polymerization. J Polym Sci Polym Chem Ed 48:3217–3228
12. Li GL, Möhwald H, Shchukim DG (2013) Precipitation polymerization for fabrication of complex core–shell hybrid particles and hollow structures. Chem Soc Rev 42:3628
13. Downey JS, Mclsacc G, Frank RS, Stöver HDH (2001) Poly(divinylbenzene) microspheres as an intermediate morphology between microgel, macrogel, and coagulum in cross-linking precipitation polymerization. Macromolecules 34:4534–4541
14. Frank RS, Downey JS, Yu K, Stöver HDH (2002) Poly(divinylbenzene-alt-maleic anhydride) microgels: Intermediates to microspheres and macrogels in cross-linking copolymerization. Macromolecules 35:2728–2735
15. Goh ECC, Stöver HDH (2002) Cross-linked poly (methacrylic acid-co-poly(ethylene oxide) methyl ether methacrylate) microspheres and microgels prepared by precipitation polymerization: a morphology study. Macromolecules 35:9983–9989
16. Bai F, Yang XL, Huang WQ (2006) Preparation of narrow or monodisperse poly(ethyleneglycol dimethacrylate) microspheres by distillation-precipitation polymerization. Eur Polym J 42:2088–2097
17. Liu GY, Yang XL, Wang YM (2007) Preparation of monodisperse hydrophilic polymer microspheres with N,N'-methylenebisacrylamide as crosslinker by distillation precipitation polymerization. Polym Int 56:905–913
18. Downey JS, Frank RS, Li WH, Stöver HDH (1999) Growth mechanism of poly(divinylbenzene) microspheres in precipitation polymerization. Macromolecules 32:2838–2844
19. Feng HL, Yan EW, Zhang J, Yang XL, Li CX (2013) A controlled morphology of polymeric nanocapsules via the density of surface vinyl group for the precipitation polymerization. Polymer 54:4511–4520
20. Naka Y, Yamamoto Y (1992) Preparation of microspheres by radiation-induced polymerization. II. Mechanism of microsphere growth. J Polym Sci Polym Chem Ed 30:1287–1298
21. Bai F, Yang XL, Li R, Huang B, Huang WQ (2006) Monodisperse hydrophilic polymer microspheres having carboxyl acid group by distillation precipitation-polymerization. Polymer 47:5775–5784
22. Bai F, Huang B, Yang XL, Huang WQ (2007) Preparation of monodisperse poly(methacrylic acid) microspheres by distillation precipitation polymerization. Eur Polym J 43:3923–3932
23. Liu GY, Yang XL, Wang YM (2007) Synthesis of silica/poly(N,N'-Methylenebisacrylamide) core-shell composite materials by distillation-precipitation polymerization. Polymer 48:4385–4392
24. Liu GY, Zhang H, Yang XL, Wang YM (2007) Facile synthesis of monodisperse silica/polymer hybrid microspheres and hollow polymer microspheres. Polymer 48:5896–5904
25. Liu B, Zhang W, Yang FK, Feng HL, Yang XL (2011) A facile method for synthesis of Fe_3O_4@polymer microspheres and their application as magnetic support for loading metal nanoparticles. J Phys Chem C 115:15875–17884

Proteins as Polymers and Polyelectrolytes

Shigeru Kunugi
Department of Biomolecular Engineering, Kyoto
Institute of Technology, Kyoto, Japan

Abbreviations

a.a.   amino acids
LbL   layer-by-layer

Definition

pI isoelectric point.

Polymeric Molecule

Proteins consist of amino acids conjugated by peptide bonds, which is a type of amide bond formed from a carboxyl group and an amino group in α-amino acids (except for one case). This special type of amide bond is called as a peptide bond and the large molecules (polymers) thus obtained are polypeptides.

A polypeptide is, as with synthetic polyamides, basically a condensation polymer and fundamentally a single and liner polymer. One or more polypeptides form proteins, and in many cases, several (single) proteins form an assembled molecule: a polymeric protein. Each component protein is called a subunit, and a protein having only one subunit is a single-subunit protein.

Proteins perform a wide variety of functions in living organisms, and the size or length of a polypeptide also varies widely. The largest (longest) single protein known is Titin (connectin: contributing to the passive stiffness of the muscle), which has a molecular size around 30,000 amino acid residues and three million Da. Although this depends on the definition of a "protein," the smallest protein is composed of 20 amino acids (TRP-cage) or less.

Natural proteins are composed of 20 kinds of amino acid; 19 are α-amino acids and one is an imino acid. Except for the simplest one (glycine), 19 amino acids are chiral and all are usually L-forms. In the polypeptide chain of a protein, these amino acids are in a queue, and the order of this sequence is crucial. This designated sequence determines the function of a protein, and it is encoded within the gene, as a sequence of deoxy-nucleotides in DNA. Typically, this sequence of amino acids controls the structure of the protein and thus its function. The a.a. sequence in a polypeptide is called as the primary structure. Proteins form their unique and hierarchical 3-D structures, derived from this a.a. sequence. The secondary structures are mainly formed through interactions (van der Waals, hydrogen bonding etc.) between the backbone chains of a peptide and are less influenced by the characteristics of the side chains. The interactions among the side chains lead to the formation of a complex 3-D structure, which is called the tertiary structure. Inter-peptide chain interaction produces further higher-order structures, such as polymeric proteins (quaternary structure). Even in the cases of fibrous and linear proteins, such as keratin and collagen, the interactions among different polypeptide chains are crucial in forming the final and functional structures.

In the words of polymer science, proteins and polypeptides are condensation, linear, hetero-chiral, chiral, sequential, and structural polymers.

The rapid development of molecular biology has now elucidated the a.a. sequences of many proteins. Furthermore, the 3-D structures of many proteins can be obtained by X-ray crystallography. As for the sequential polymerization of amino acids in vitro, the so-called solid-phase synthesis of polypeptides, originally developed by Merrifield, now provides an easy and quick tool, after many years of expert-oriented liquid-phase methods. Today, polypeptides with over 100 a.a. can be synthesized by this solid-phase method.

The most salient question is now on the relationship between the a.a. sequence and the

P

(uniquely) formed 3-D structures of proteins. There have been a number of challenges on this matter over the past three decades [1–4].

Among many methods, there are several approaches based on polymer statics. In other words, proteins and polypeptides are only special cases of polymers in general from this point of view. The 3-D structures of proteins to perform their physiological functions (functional structures) are highly dependent on the environmental conditions, such as temperature, pressure, pH, and the concentration of additives including nonaqueous solvents. In physical reality, they translate into thermal motion, interaction valance, hydration, dielectric constant, solubility, etc. Both the thermal phase changes of synthetic polymers and the thermal denaturation of proteins can also be treated by the theories of polymer statics [5–7].

Polyelectrolytes

Among the 20 amino acids comprising proteins, there are several ionizable amino acids. They carry ionizable groups in their side chains: two are acids (Asp, Glu) and three are bases (Arg, Lyz, His). The terminals of a polypeptide chain are also ionizable as ammonium (aminium) cations and carboxylate anions. This means that polypeptides will usually bear anions and/or cations in these molecules and have the polyelectrolyte characteristics. Most of them carry both types of charge and are classified as polyampholite.

Many of these ionizable groups are weak acids/bases, and the total charges in a protein molecule can be changed in response to the environmental hydronium ion concentration (pH). Furthermore, the content of the charged groups (species and number) is different in each individual protein. Thus, proteins show very characteristic behaviors in response to the solution pH. This is another and very important characteristic of proteins. For most proteins, there is a pH value of solution where the net charge of the whole protein molecule becomes zero, since the week acids lose the anionic character in excess

acids and the weak bases lose their cationic character under excess basic conditions. This value is known as the isoelectric point (pI).

For example, some pI standards for electrophoretic analysis are available commercially. Among them, the low pI sample is often pepsinogen and the high pI standard is cytochrome c. The pI of the former is lower than three and that of the latter is higher than ten. Pepsinogen is a precursor of pepsin enzyme and pepsin loses 44 a.a. from this precursor. Thus, the net charge increases around +7, and its pI drops well below three. Lysozyme is known as a more basic protein, and its pI is higher than 11. When the surface charge density in neutral pH solutions of these two proteins and myoglobin (pI ≈ 7) are compared, pepsin shows mostly red color (negative charge: polyanion) and lysozyme shows blue color (positive charge: polycation), whereas myoglobin is in patches, as illustrated in Fig. 1.

The overall net charges of proteins are very important in the isolation and purification processes of the proteins. For example, the solubility of proteins becomes the lowest under conditions of pH ≈ pI, near where the proteins are usually crystallized.

Ion-exchange chromatography (or ion chromatography) is a useful tool for protein purification, in which protein solutions are eluted through ion-exchange chromatography column [8]. When a charged protein sample is eluted through the column, a protein that carries the charge opposite to the column matrix will be bound, whereas a protein with the same or no charge will pass through the column. By changing the pH of the eluent, the target protein will be released from the column. This is actually an application of the overall polyelectrolyte nature of proteins.

Among the electrophoretic methodologies, capillary gel electrophoresis directly exploits the polyelectrolyte character of the proteins [9, 10]. The separation of proteins depends on the overall charges and the sizes (ionic radii) of the protein molecules, as well as their electroosmotic flow. By changing the pH value or the ionic strength of the supporting liquid phase, the protein mixture is separated and ionized. This technique is mainly used for the analysis of protein-based pharmaceuticals and quality controls.
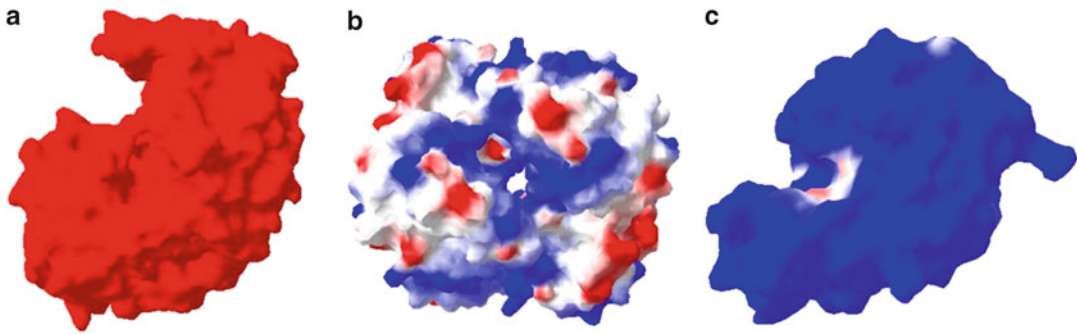
Proteins as Polymers and Polyelectrolytes, Fig. 1 Surface charge distribution of bovine pepsin (**a**: PDB 5PEP), human myoglobin (**b**: 4HHB), and hen egg lysozyme (**c**: 1LYZ), under neutral conditions. Drawn by using Swiss PDB Viewer

Another unique electrophoretic method is isoelectric focusing [10]. This technique also utilizes the polyelectrolyte (polyampholyte) nature of proteins, but, more precisely, it separates protein mixtures on the basis of their pI values. If charge-carrying proteins are subjected into an electrophoretic gel with a pH gradient and then an electric field is applied, they migrate toward the oppositely charged electrode. However, at the pH zone equal to their pI values, they will stop moving. Depending on each characteristic pI, pH zone at which the sample stops is different for different proteins, and hence they can be separated.

Electrostatic interactions often support the stabilization and formation of protein-protein complexes, either thermodynamically or kinetically. However, as seen in Fig. 1, the charges are not always distributed evenly over the whole protein molecule, but some parts have opposite charges. In some cases, even though the net charge of a protein molecule is of one type, the opposite type of charge in a specific site of the protein plays a critical role in structure formation and/or function performance. Furthermore, several examples have been found in polymeric proteins where the inter-subunit surfaces have the opposite charges and the first driving force of complex formation is electrostatic interaction.

Interactions between Proteins and Proteins with Non-protein Polyelectrolytes

The polyelectrolyte nature of a protein can generate various kinds of interactions with nonprotein polyelectrolytes. Biopolymers such as polynucleic acids and ionized polysaccharides are considered to be natural polyelectrolytes [11–13]. A very basic example is the interaction of DNA with histone protein. DNA carries negative charges due to their phosphate linkages and can be considered as a semiflexible polyanion. Histone is a positively charged protein, and a core histone is composed of eight subunits. DNA and histone interact, besides other various forces, by electrostatic interactions between the DNA phosphates and the arginine/lysine residues of the histone as a kind of polyelectrolyte complex. Histones are acetylated and deacetylated at their lysine residues. An acetylation removes positive charges and weakens the histone-DNA interaction to relax the chromatin, thus activating transcriptional activity. A deacetylation restores the cationic charges and the packed (condensed) form.

In ribosomes, electrostatic interactions between the numerous arginine and lysine residues of ribosomal proteins and the phosphate groups of the RNA backbone also mediate many protein-RNA contacts to stabilize inter-domain interactions, which are necessary to maintain the structural integrity of the ribosome subunit, together with a variety of other interactions.

Polysaccharides often carry ionic charges, and oppositely charged proteins interact with these ionic polysaccharides. Ionic, especially sulfated, polysaccharides bind proteins through electrostatic interactions between the sugar anionic groups and the cationic sites of the proteins, in
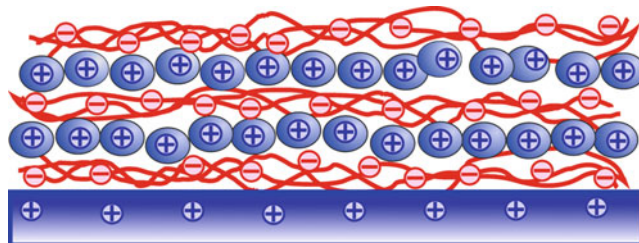
Proteins as Polymers and Polyelectrolytes, Fig. 2 Schematic representation of LbL formation with cationic proteins (*blue circles*) and anionic polyelectrolytes (*red strings*) on a positively charged matrix. Five layers are shown and the number of charges is not stoichiometric

addition to the highly specific sequences. For example, heparin, a highly sulfated polysaccharide located on the cell surface, interacts with various extracellular matrix proteins to control proteolysis, modulate the angiogenesis and metastasis of tumors, and oligomerize cell growth factors, etc.

There are many proteins included in biological membranes. Nonspecific electrostatic interactions work as a driving force for the association of peripheral proteins with membranes, since biological membranes usually carry charges on their surfaces [14]. These electrostatic interactions not only contribute to membrane association but also affect the subcellular targeting, control membrane binding, and affect the organization of proteins and lipids at the membrane surfaces.

Recently, interactions between proteins and synthetic polyelectrolytes have been the focus of research again. The attractive interactions between proteins and polyelectrolytes are widespread, from free polyelectrolyte chains to polyelectrolytes grafted onto surfaces, such as polyelectrolyte brushes and polymer networks. The main hypothesis is that polyelectrolyte chains work as multivalent counterions for the localized opposite charges on the protein surfaces. This kind of interaction has various applications: separations, delivery, and wound repair. The related fields are biosensing, tissue engineering, and pharmacology. One example is a layer-by-layer (LbL) assembled thin film, produced through the alternating adsorption of complementary multivalent species onto a substrate via electrostatic interactions (Fig. 2).

Hydrogen bonding or other secondary interactions are also utilized. This method can control the composition of materials at the nanometer level [15–19].

Related Entries

▶ Biomembrane as a Soft Matter
▶ Conjugated Polyelectrolytes
▶ Ion-Exchange Resins
▶ Nano-/Microfabrication
▶ Structures in Ion-Containing Polymers

References

1. Robson B, Vaithilingam A (2008) Protein folding revisited. In: Conn PM (ed) Molecular biology of protein folding, part B, vol 84, Progress in molecular biology and translational science. Elsevier B.V, Amsterdam, pp 161–202
2. Sharma V, Kaila VRI, Annila A (2009) Protein folding as an evolutionary process. Physica A 388:851–862. doi:10.1016/j.physa.2008.12.004
3. Naganathan AN (2012) Coarse-grained models of protein folding as detailed tools to connect with experiments. Wiley Interdiscip Rev Comput Mol Sci 3:504–514. doi:10.1002/wcms.1133
4. Rizzuti B, Daggett V (2013) Protein folding and stability: a Prague cemetery. In: Neira JL (ed) Archives biochemistry biophysics, vol 531. Elsevier B.V, Amsterdam, pp 128–135. doi:10.1016/j.abb.2013.02.001
5. Dill KA (1999) Polymer principles and protein folding. Protein Sci 8:1166–1180
6. Zhou HX (2004) Polymer models of protein stability, folding, and interactions. Biochemistry 43:2141–2154. doi:10.1021/bi036269n

7. Hsu H-P, Grassberger P (2011) A review of Monte Carlo simulations of polymers with PERM. J Stat Phys 144:597–637. doi:10.1007/s10955-011-0268-x

8. Jungbauer A, Hahn R (2009) Ion-exchange chromatography. In: Burgess RR, Deutscher MP (eds) Guide to protein purification, 2nd edn. Methods in enzymology, vol 463. Academic, Boston, pp 349–371. doi:10.1016/S0076-6879(09)63022-6

9. Zhu Z, Lu JJ, Liu S (2012) Protein separation by capillary gel electrophoresis: a. Anal Chim Acta 709:21–31. doi:10.1016/j.aca.2011.10.022

10. Righetti PG, Sebastiano R, Citterio A (2013) Capillary electrophoresis and isoelectric focusing in peptide and protein analysis. Proteomics 133:25–340. doi:10.1002/pmic.201200378

11. Korolev N, Vorontsova OV, Nordenskiold L (2007) Physicochemical analysis of electrostatic foundation for DNA-protein interactions in chromatin transformations. Prog Biophys Mol Biol 95:23–49. doi:10.1016/j.pbiomolbio.2006.11.003

12. Wong GCL, Pollack L (2010) Electrostatics of strongly charged biological polymers: ion-mediated interactions and self-organization in nucleic acids and proteins. In: Leone SR, Cremer PS, Groves JT, et al (eds) The annual review of physical chemistry, vol 61. Annual Reviews, Palo Alto, pp 171–189. doi:10.1146/annurev.physchem.58.032806.104436

13. Kovensky J (2009) Sulfated oligosaccharides: new targets for drug development? Curr Med Chem 16:2338–2344

14. Mulgrew-Nesbitt A, Diraviyam K, Wang J et al (2006) The role of electrostatics in protein-membrane interactions. BBA-Mol Cell Biol Lipids 1761:812–826. doi:10.1016/j.bbalip.2006.07.002

15. Perico A, Ciferri A (2009) The supramolecular association of polyelectrolytes to complementary charged surfactants and protein assemblies. Chemistry 22:6312–6320. doi:10.1002/chem.200900637

16. Ariga K, Ji Q, Hill JP (2010) Enzyme-encapsulated layer-by-layer assemblies: current status and challenges toward ultimate nanodevices. In: Caruso F (ed) Modern techniques for nano- and microreactors/-reactions, vol 229, Advances in polymer science. Springer, Berlin, pp 51–87. doi:10.1007/12_2009_42

17. Hammond PT (2012) Building biomedical materials layer-by-layer. Mater Today 15:196–206

18. Becker AL, Henzler K, Welsch N, Ballauff M, Borisov O (2012) Proteins and polyelectrolytes: a charged relationship. Curr Opin Colloid Interface Sci 17:90–96. doi:10.1016/j.cocis.2011.10.001

19. Kayitmazer AB, Seeman D, Minsky BB, Dubin PL, Xu YS (2013) Protein-polyelectrolyte interactions. Soft Matter 9:2553–2583. doi:10.1039/c2sm27002a

Pullulan

Yoshiro Tahara and Kazunari Akiyoshi
Department of Polymer Chemistry, Graduate School of Engineering and ERATO Bio-Nanotransporter Project, Japan Science and Technology Agency (JST), Kyoto University, Nishikyo-ku, Kyoto, Japan

Synonyms

Glucose-based polymer; Polysaccharide

Definition

Pullulan is a glucose-based polysaccharide, repeating units of which are described as $\alpha(1 \rightarrow 4)$Glu-$\alpha(1 \rightarrow 4)$Glu-$\alpha(1 \rightarrow 6)$Glu.

Structure and Basic Properties

Pullulan is one of the most well-known and extensively studied glucose-unit polysaccharides. Dry pullulan is a white-to-off-white, tasteless, odorless powder that is easy to dissolve in water at 25 °C. In contrast with other glucose-based polysaccharides such as cellulose, amylose, or dextran, pullulan has unique regularly repeating units described as $\alpha(1 \rightarrow 4)$Glu-$\alpha(1 \rightarrow 4)$Glu-$\alpha(1 \rightarrow 6)$Glu (Fig. 1). In other words, the repeating unit of pullulan is $\alpha(1 \rightarrow 6)$-linked maltotriose, which is an $\alpha(1 \rightarrow 4)$-linked glucose trimer. This regular alternation of $\alpha(1 \rightarrow 4)$ and $\alpha(1 \rightarrow 6)$ bonds produces the high solubility and unique chain flexibility of pullulan in water. Using NMR spectroscopy, it was shown that the $\alpha(1 \rightarrow 6)$-linked glucose residues in pullulan have higher motional freedom than $\alpha(1 \rightarrow 4)$-linked glucose residues, which have a primary hydroxyl group in the C6 position. The conformational properties of these glucose units of pullulan lie between those of amylose and dextran. The many structural analyses of pullulan that have been performed using Fourier transform

Pullulan,
Fig. 1 Structural comparison of glucose-based polysaccharides (cellulose, amylose, dextran, and pullulan)


Cellulose, β(1→4)Glu

Amylose, α(1→4)Glu

Dextran, α(1→6)Glu

Pullulan, α(1→4)Glu-α(1→4)Glu-α(1→6)Glu

Maltotriose
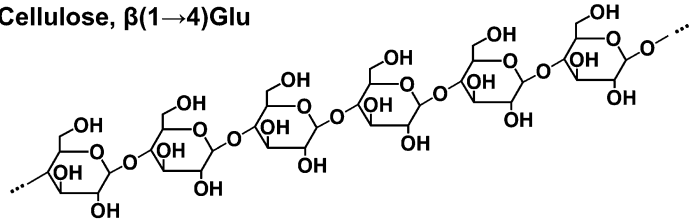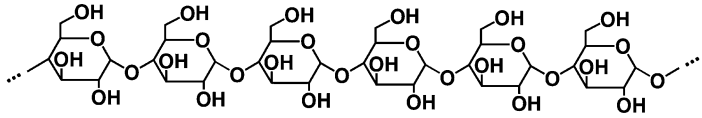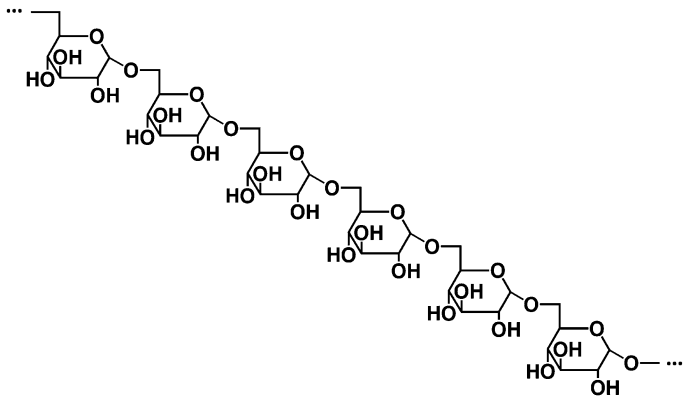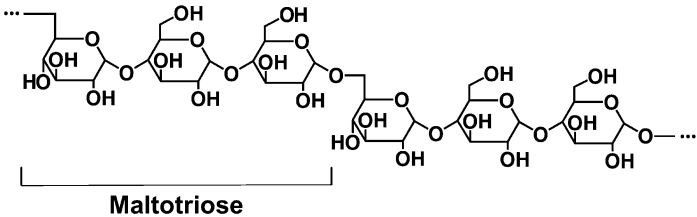
infrared spectroscopy, Raman spectroscopy, circular dichroism spectroscopy, and computer simulation studies have indicated that pullulan has a considerable mechanical strength and hydrodynamic properties [1].

Historical Background and Biological Production

In 1938, Bauer was the first to observe the production of a polysaccharide in *Aureobasidium pullulans*, a ubiquitous black yeast-like fungus. In the late 1950s, this novel polysaccharide was isolated from culture broths of *Aureobasidium pullulans* and was named as "pullulan." The basic structure of pullulan was resolved in the 1960s; it was shown that pullulan consists of α(1 → 6)-linked polymers formed from maltotriose subunits. The Hayashibara Company (Okayama, Japan) optimized the fermentation medium and growth conditions of *Aureobasidium pullulans* to produce pullulan, which has a particular molecular weight, and
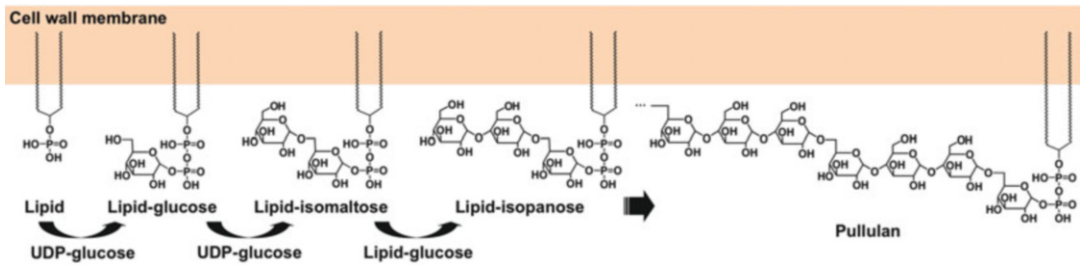
Pullulan, Fig. 2 Biosynthesis of pullulan at the cell wall membrane of *Aureobasidium pullulans*
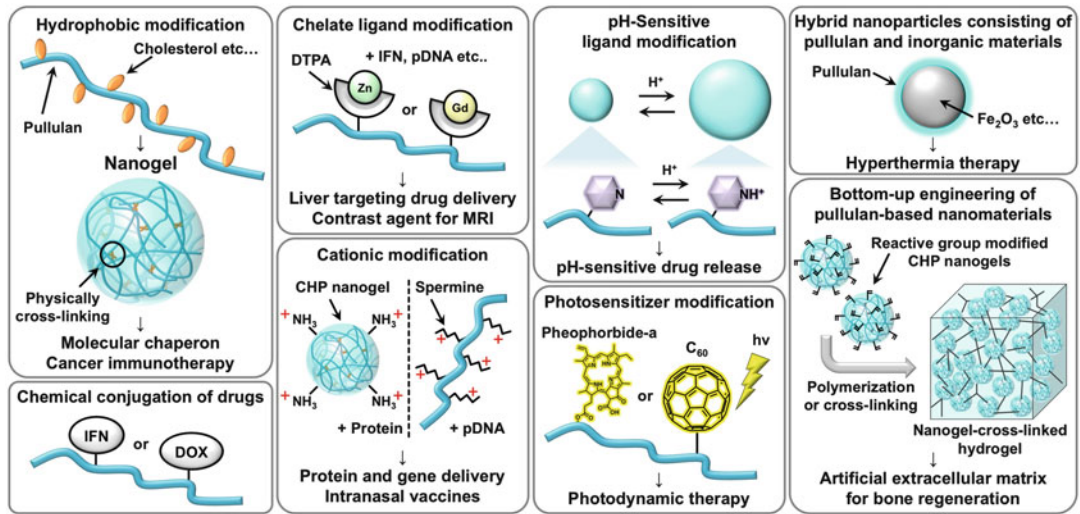
Pullulan, Fig. 3 Pullulan-based nanomaterials

P

started the commercial production of pullulan in 1976 [2].

Aureobasidium pullulans synthesizes pullulan intracellularly at the cell wall membrane, and the pullulan is then secreted out to the cell surface to form a loose, slimy layer. Uridine diphosphate (UDP)-glucose is an important pullulan precursor. First, lipid-linked pyrophosphate-glucose (lipid-glucose) is prepared from UDP-glucose using pyrophosphorylase. Subsequently, lipid-linked pyrophosphate-isomaltose (lipid-isomaltose) is produced via the transfer of glucose residues from the UDP-glucose. The lipid-isomaltose then reacts with lipid-glucose to yield lipid-linked pyrophosphate-isopanose (lipid-isopanose). Finally, isopanosyl residues are polymerized into pullulan chains (Fig. 2) [3].

Applications: Pullulan-Based Nanomaterials

Hydrophobic Modification

Various pullulan-based nanomaterials have been developed in recent decades, and the efficacy of these materials has been demonstrated in a variety of high-impact applications (Fig. 3). Some of the most notable of these materials are nanogels, which are nanometer-sized gels (approximately 0.1–100 nm). Recently, nanogels have been prepared using various polymers and methods [4]. Nanogels were first reported in the 1990s, when they were produced using cholesterol-modified pullulan [5], and the term "nanogel" was officially defined by the International Union for Pure and Applied

Chemistry (IUPAC) [6]. Pullulan-based nanogels have been used in medical and pharmaceutical research fields for applications such as drug delivery and tissue engineering [7]. The medical and pharmaceutical fields represent some of the most active areas for pullulan-based nanomaterials, and we concentrate on these areas in this section.

In 1993, Akiyoshi et al. prepared cholesterol-bearing pullulan (CHP) and demonstrated that the cholesterol group of CHP provided physically cross-linking points through hydrophobic interactions in water, and CHP formed stable and monodisperse nanogels with a diameter of less than 50 nm in water [5]. In comparison with polymeric micro/nanospheres, nanogels can contain a large amount of water and can incorporate bioactive drugs such as proteins and nucleonic acids within the nanoscale polymer networks. Motivated by reports of the successful use of CHP to form physically cross-linked nanogels, Akiyoshi and his coworkers prepared various types of pullulan-based nanogels. For example, pullulan was modified using alkyl chain, photoresponsive spiropyran, and thermoresponsive poly(2-isopropyl-2-oxazoline). Additionally, amine or double bond-modified CHP was prepared for cationic material and bottom-up engineering, respectively, as described below in detail. In other examples, siloxane-modified CHP was prepared for inorganic cross-linking, Arg-Gly-Asp peptide-modified CHP was prepared for integrin-mediated protein delivery, imidazole-modified CHP was prepared for metal-coordinative cross-linking, and vitamin B6-modified pullulan was prepared for protein cross-linking. Pullulan-based nanogels have also been reported from other groups, including deoxycholic acid-modified pullulan, poly (L-lactide)-grafted pullulan, and alkyl chain-modified hydroxyethyl/vinyl methacrylate pullulan [8].

One of the most attractive characteristics of CHP nanogels is the molecular chaperone function; specifically, CHP nanogels can spontaneously trap proteins in the nanoscale hydrogel matrix. For example, CHP nanogels formed complexes with various proteins such as insulin,

bovine serum albumin, α-chymotrypsin, myoglobin, and cytochrome c through hydrophobic interactions [7, 8]. In most cases, the nanogel-protein complexes showed high colloidal stability. In nature, molecular chaperones selectively entrap denatured proteins or their intermediates via macromolecular host-guest interactions—primarily, hydrophobic interactions—and prevent irreversible aggregation. With the aid of ATP and another co-chaperone, the host chaperone releases the refolded protein. CHP nanogels have been reported to act as artificial molecular chaperones. CHP nanogels can trap heat/chemically denatured proteins, suppress the irreversible aggregation of denatured proteins, significantly increase the colloidal and thermal stability of proteins, and release proteins via the addition of β-cyclodextrin, which dissociates the complexation of CHP nanogels with proteins because the cholesteryl group is a suitable guest for β-cyclodextrin. Because of these properties, CHP nanogels are regarded as artificial molecular chaperones. The chaperone-like activity of CHP nanogels for the refolding of acid-denatured green fluorescent protein is comparable with that of the native chaperone. This nanogel system is also effective for renaturation of the inclusion body of a recombinant protein belonging to the serine protease family. Additionally, CHP nanogels interact with amyloid β-protein, and the resulting complexes significantly reduce the toxicity of amyloid β-protein in both primary cortical cultures and microglial cell cultures [7, 8].

The molecular chaperone function of CHP nanogels has led to breakthroughs in drug delivery systems, especially for protein or peptide delivery. Cancer immunotherapy is one of the most well-studied examples [9, 10]. The complexes of CHP nanogels with cancer antigen proteins can trigger an unprecedented immune response, making them useful in cancer immunotherapy. Clinical trials of CHP-antigen complexes as multifunctional cancer vaccines (activation of both CD8+ killer T cells and CD4+ helper T cells) were initiated in 2004. The hydrophobic antigen proteins were complexed by a CHP nanogel, without aggregation, and were effectively internalized into antigen-presenting cells such as dendritic or

macrophage cells in vivo. A preliminary phase I clinical trial demonstrated the effects of the nanogel system, especially for the treatment of esophageal cancer. In other studies, CHP nanogels containing HER2 protein antigen, a cancer-related gene product, were subcutaneously injected into mice with cholangiocarcinoma and antitumor killer T cells, and antibody-producing helper T cells were efficiently induced. Moreover, CHP nanogels have been found to be effective as controlled-release carriers of interleukin-12 for the cytokine immunotherapy of cancer [8].

Chemical Conjugation of Drugs

In 1996, Tabata and his research group demonstrated the liver targeting of interferon (IFN) in vivo, facilitated by the high affinity of pullulan to the liver or asialoglycoprotein receptors. IFN was chemically conjugated with pullulan (IFN-pullulan) using a cyanuric chloride method. After intravenous injection of the IFN-pullulan into mice, the liver accumulation of IFN was significantly increased for the IFN-pullulan, whereas the gastrointestinal and carcass distribution was reduced compared with free IFN and a physical mixture of free IFN and pullulan. The accumulation was observed even 24 h after injection, indicating that the pullulan conjugation was essential to enhance the liver accumulation of IFN [11].

In 2011, a pullulan-based doxorubicin (DOX) conjugation with folic acid, which is a targeting agent for several tumor cells, was prepared (DOX-folate-pullulan). In vitro studies showed that these polymers formed particles approximately 100–150 nm in size. At pH 5.5, they released DOX at a higher rate than at pH 7.4 or in plasma. After 72 h of incubation, the IC_{50} values of tumor cells that were overexpressing the folic acid receptor using the DOX-folate-pullulan were lower than those of non-expressing cells, whereas the IC_{50} values were same for the over- and non-expressing cells when free DOX or DOX-pullulan without folic acid were used [12].

Chelate Ligand Modification

Tabata et al. continued to report liver-targeting approaches using pullulan modified with chelate ligands. Diethylenetriamine pentaacetic acid (DTPA), a metal-chelating residue, was introduced to pullulan (DTPA-pullulan), and IFN-β [13] was coordinately conjugated with DTPA-pullulan in the presence of zinc ions in water. This non-covalent approach to the modification of IFN with pullulan decreased the loss of drug activity. IFN-DTPA-pullulan enhanced the delivery of IFN to the liver and induced oligoadenylate synthetase activity in the liver to a greater extent than free IFN. Furthermore, zinc ion-mediated delivery using pullulan was applied to the liver-targeting delivery of plasmid DNA (pDNA) [14]. After intravenous administration, the DTPA-pullulan conjugation of pDNA with zinc ions enhanced the in vivo gene expression of liver to a greater extent compared with free pDNA, and the gene expression lasted for over 12 days after injection. These studies suggested that zinc ion-mediated protein/DNA delivery using chelate ligand-modified pullulan was a promising method for targeting delivery to the liver.

In 2011, Na and coworkers prepared gadolinium-conjugated DTPA-pullulan (Gd-DTPA-pullulan) as a hepatocyte-specific contrast agent for magnetic resonance imaging (MRI). The Gd-DTPA-pullulan showed greater contrast enhancement in orthotopic rat hepatocarcinoma compared with a commercially available agent, and the contrast effects lasted up to 24 h. After in vivo administration, the Gd-DTPA-pullulan displayed a discriminative MR contrast on the regenerative and malignant hepatic nodules that were sequentially observed during the progress of cirrhotic hepatocarcinoma [15].

Cationic Modification

The intracellular delivery of exogenous biomacromolecules remains a topic of growing interest in bioscience and medical applications. Efficient intracellular protein/gene delivery has been reported using cationic-modified pullulan-based nanomaterials. Akiyoshi and coworkers introduced ethylenediamine into CHP to form positively charged CHP nanogels [16, 17]. The cationic CHP nanogels strongly interacted with various proteins to form stable nanogel-protein complexes, which were efficiently introduced

P

into cells. One advantage of nanogels is that they can form colloidally stable complexes with proteins several tens of nanometers in size, where the complexes are suitable for effective intracellular uptake. In addition, cationic CHP nanogels were reported as effective carriers of intranasal vaccines. Mucosal vaccines are expected to represent a new generation of vaccines that can prevent pathogenic infections. For example, a complex consisting of a cationic CHP nanogel with a nontoxic subunit of *Clostridium botulinum* type A neurotoxin (BoHc/A) adhered continuously to the nasal epithelium, and BoHc/A was effectively taken up by the mucosal dendritic cells after the release from the cationic CHP nanogel [18].

Pullulan-based carriers for gene delivery have been developed recently. Tabata and his research group prepared conjugates of pullulan with spermine, a natural polyamine. Pullulan-spermine increased the transfection of pDNA into cells and greatly reduced the cytotoxicity compared with Lipofectamine 2000, a commercially available cationic lipid. This gene delivery system was applied to bone marrow-derived mesenchymal stem cells, and the genetic modification of stem cells was successfully achieved [19].

pH-Sensitive Ligand Modification

The development of pH-sensitive drug carriers that respond to the local acidic pH conditions around diseased tissues such as tumors is important. Na and coworkers reported a pH-sensitive ligand-modified pullulan, namely, pullulan acetate (PA). The acetylation of the pullulan increased the hydrophobicity and resulted in pH-sensitive swelling behavior. In a later study, sulfadimethoxine (SDM) was introduced into PA. SDM is an antibacterial agent that shows reversible solubility at approximately physiological pH values. The SDM-PA formed nanoparticles with a mean diameter of <70 nm at pH 7.4; the diameter increased under low-pH conditions. The release rate of Adriamycin was significantly higher at pH 6.8 than at pH 7.4. The cell viability of a breast tumor cell incubated with Adriamycin-loaded SDM-PA was lower at pH 6.8 than at pH 7.4, while the cell viabilities were the same at different pH values when free

Adriamycin and unloaded SDM-PA were used; this suggested that the SDM-PA showed pH-sensitive drug release behavior [20]. Another approach for the creation of pH-sensitive carriers was developed using histidine. Deoxycholic acid and histidine were substituted into pullulan, and DOX was loaded into the resulting materials. The pH-dependent size increase and cytotoxicity were observed to be similar to those of SDM-PA [21]. In other applications, PA was conjugated with vitamin H (biotin). Biotin performs as a growth promoter at the cellular level, and it is present at higher concentrations in cancerous tumors, compared with normal tissue; this suggests that the cell surface receptors for biotin could be overexpressed on tumor cells. To investigate this hypothesis, biotin was modified with PA to form nanoparticles (BPAs); the BPAs were strongly adsorbed on HepG2 cells, indicating that HepG2 cells have biotin receptors, and targeted delivery is available using this approach [22].

Photosensitizer Modification

Na and coworkers prepared photosensitizer (PS)- and folate-modified pullulan [23]. In an early study, folic acid-modified pullulan (folate-pullulan) containing DOX was reported to form nanogels. These nanogels delivered DOX to the cells in vitro. In a subsequent study, PS (pheophorbide-a) was conjugated to folate-pullulan via a degradable ester bond to form PS-folate-pullulan nanogels. Although photodynamic therapies have been studied intensively for the treatment of tumors and non-oncological disorders, some difficulties remain with the use of free PS; such difficulties include water insolubility and phototoxicity. While the PS-folate-pullulan nanogels showed photoactive properties in organic solvents, these properties were suppressed in PBS, owing to the self-quenching of the PS moieties, and the quenching of the PS in the nanogels was restored via incubation with esterase or HeLa cancer cells. These results suggested that the PS-folate-pullulan nanogels were internalized in cancer cells via folate receptor-mediated endocytosis and disintegrated by various enzymes in the lysosome, leading to the restoration of the photoactivity. These results

suggested that self-quenching PS-folate-pullulan nanogels could be used to design photodynamic therapies with minimal unfavorable phototoxicity.

Tabata and his research group chemically modified pullulan with fullerene (C_{60}), which generates reactive oxygen species in a high yield under exposure of weak visible light and acts as a potential photosensitizer for photodynamic therapies [24]. The C_{60}-pullulan conjugates had a high binding affinity for HepG2 cells with asialoglycoprotein receptors; in contrast, they showed a low binding affinity to HeLa cells without the receptors. Following the intravenous injection of C_{60}-pullulan conjugates into mice carrying subcutaneous tumors of HepG2 cells, significantly stronger photodynamic effects were observed in the tumors. It was concluded that the pullulan conjugation gave C_{60} a targeting ability toward HepG2 cells, resulting in enhanced photodynamic tumor therapy effects.

Hybrid Nanoparticles Consisting of Pullulan and Inorganic Materials

Magnetic nanoparticles consisting of metal ions have been recognized as a promising tool for the site-specific delivery of drugs and diagnostic agents. However, most magnetic nanoparticles are easily destroyed or cleared from circulation, owing to the hydrophobicity and high cytotoxicity. Gupta et al. reported that the surface modification of superparamagnetic iron oxide nanoparticles with pullulan increased cell viability and adhesion. In addition, pullulan-coated nanoparticles and uncoated nanoparticles were internalized into cells via different mechanisms, suggesting that pullulan-coated magnetic particles could be useful for medical imaging [25]. In another study, magnetic nanoparticles were coated with PA. Results from saturation magnetization measurements and cytotoxicity assays indicated that the nanoparticles were superparamagnetic and exhibited no significant cytotoxicity. Furthermore, the nanoparticles had superior hyperthermic effects on tumor cells in vitro under magnetic field induction,

suggesting that the nanoparticles had great potential as magnetic hyperthermia mediators [26].

CHP was also used to prepare hybrid nanoparticles with inorganic materials using a nanogel-template technique. For example, calcium phosphate was mixed with CHP nanogels or nanogel-absorbed liposomes and then precipitated by slowly increasing the pH. The resulting particles were used as biocompatible drug carriers with controlled-release properties [27]. Hybrid nanoparticles consisting of CHP and iron oxide were produced using a simple procedure in which iron chlorides formed iron nanoparticles; this occurred after heating and the addition of an alkali solution to the reactive sites produced by the CHP nanogels. The resulting hybrid nanoparticles had a narrow, nanometer-sized distribution and high colloidal stability in water. These nanoparticles are currently being applied as contrast agents for MRI and as magnetic hyperthermia therapy materials [28].

Bottom-Up Engineering of Pullulan-Based Nanomaterials

The effective control and design of the cross-linking and nano-domains in macroscale hydrogels are important focuses of research. Akiyoshi and coworkers developed a bottom-up method to form gel materials, using pullulan-based nanogels as the building blocks [8]. In a first study, CHP nanogels were reported to form macrogels at a relatively high concentration. Subsequently, CHP was modified with the functional groups, and macrogels or semi-micrometer-sized particles were prepared via the polymerization or cross-linking of CHP nanogels. For example, CHP was modified with methacryloyl and acryloyl groups.2-Methacryloyloxyethylphosphorylcholine, N-isopropylacrylamide, and polyethylene glycol with four branched terminal thiol groups (PEGSH) were used as co-monomers or as cross-linkers. CHP nanogels have great potential as molecular chaperones and protein delivery carriers. Therefore, macrogels containing CHP

P

nanogels can perform as functional materials in biotechnological and biomedical applications. In particular, CHP nanogel-cross-linked macrogels consisting of acryloyl-substituted CHP and PEGSH were used as an artificial extracellular matrix for the controlled release of protein pharmaceuticals in regenerative medicine [29]. Effective guided bone regeneration or successful bone formation was induced in vivo by CHP nanogel-cross-linked macrogels loaded with bone morphogenetic proteins or fibroblast growth factors. These findings suggested that efficient tissue regeneration was successfully achieved using biodegradable CHP nanogel-cross-linked hydrogels by precisely controlling the release of multiple cytokines and hormones.

Related Entries

▶ Dendrimers and Hyperbranched Polymers in Medicine
▶ Drug and Gene Delivery Using Hyperbranched Polymers
▶ Self-Assembly of Hyperbranched Polymers
▶ Supramolecular Hydrogels

References

1. Singh RS, Saini GK, Kennedy JF (2008) Pullulan: microbial sources, production and applications. Carbohydr Polym 73:515–531
2. Prajapati VD, Jani GK, Khanda SM (2013) Pullulan: an exopolysaccharide and its various applications. Carbohydr Polym 95:540–549
3. Cheng KC, Demirci A, Catchmark JM (2011) Pullulan: biosynthesis, production, and applications. Appl Microbiol Biotechnol 92:29–44
4. Kabanov AV, Vinogradov SV (2009) Nanogels as pharmaceutical carriers: finite networks of infinite capabilities. Angew Chem Int Ed Engl 48:5418–5429
5. Akiyoshi K, Deguchi S, Moriguchi N, Yamaguchi S, Sunamoto J (1993) Self-aggregates of hydrophobized polysaccharides in water. Formation and characteristics of nanoparticles. Macromolecules 26:3062–3068
6. Alemán J, Chadwick AV, He J, Hess M, Horie K, Jones RG, Kratochvíl P, Meisel I, Mita I, Moad G, Penczek S, Stepto RFT (2007) Definitions of terms relating to the structure and processing of sols, gels, networks, and inorganic–organic hybrid materials (IUPAC recommendations 2007). Pure Appl Chem 79:1801–1829
7. Sasaki Y, Akiyoshi K (2010) Nanogel engineering for new nanobiomaterials: from chaperoning engineering to biomedical applications. Chem Rec 10:366–376
8. Sasaki Y, Akiyoshi K (2012) Nanogel engineering by associating polymers for biomedical applications. In: Hydrogel micro and nanoparticles. Wiley-VCH Verlag GmbH & Co. KGaA, Weinheim, pp 187–208
9. Ikuta Y, Katayama N, Wang L, Okugawa T, Takahashi Y, Schmitt M, Gu X, Watanabe M, Akiyoshi K, Nakamura H, Kuribayashi K, Sunamoto J, Shiku H (2002) Presentation of a major histocompatibility complex class 1-binding peptide by monocyte-derived dendritic cells incorporating hydrophobized polysaccharide-truncated HER2 protein complex: implications for a polyvalent immuno-cell therapy. Blood 99:3717–3724
10. Uenaka A, Wada H, Isobe M, Saika T, Tsuji K, Sato E, Sato S, Noguchi Y, Kawabata R, Yasuda Y, Doki Y, Kumon H, Iwatsuki K, Shiku H, Monden M, Jungbluth AA, Ritter G, Murphy R, Hoffman E, Old LJ, Nakayama E (2007) T cell immunomonitoring and tumor responses in patients immunized with a complex of cholesterol-bearing hydrophobized pullulan (CHP) and NY-ESO-1 protein. Cancer Immun 7:9
11. Xi K, Tabata Y, Uno K, Yoshimoto M, Kishida T, Sokawa Y, Ikada Y (1996) Liver targeting of interferon through pullulan conjugation. Pharm Res 13:1846–1850
12. Scomparin A, Salmaso S, Bersani S, Satchi-Fainaro R, Caliceti P (2011) Novel folated and non-folated pullulan bioconjugates for anticancer drug delivery. Eur J Pharm Sci 42:547–558
13. Suginoshita Y, Tabata Y, Matsumura T, Toda Y, Nabeshima M, Moriyasu F, Ikada Y, Chiba T (2002) Liver targeting of human interferon-β with pullulan based on metal coordination. J Control Release 83:75–88
14. Hosseinkhani H, Aoyama T, Ogawa O, Tabata Y (2002) Liver targeting of plasmid DNA by pullulan conjugation based on metal coordination. J Control Release 83:287–302
15. Yim H, Yang SG, Jeon YS, Park IS, Kim M, Lee DH, Bae YH, Na K (2011) The performance of gadolinium diethylene triamine pentaacetate-pullulan hepatocyte-specific T1 contrast agent for MR-I. Biomaterials 32:5187–5194
16. Hasegawa U, Nomura SM, Kaul SC, Hirano T, Akiyoshi K (2005) Nanogel-quantum dot hybrid nanoparticles for live cell imaging. Biochem Biophys Res Commun 331:917–921
17. Ayame H, Morimoto N, Akiyoshi K (2008) Self-assembled cationic nanogels for intracellular protein delivery. Bioconjug Chem 19:882–890
18. Nochi T, Yuki Y, Takahashi H, Sawada S, Mejima M, Kohda T, Harada N, Kong IG, Sato A, Kataoka N,

Tokuhara D, Kurokawa S, Takahashi Y, Tsukada H, Kozaki S, Akiyoshi K, Kiyono H (2010) Nanogel antigenic protein-delivery system for adjuvant-free intranasal vaccines. Nat Mater 9:572–578

19. Thakor DK, Teng YD, Obata H, Nagane K, Saito S, Tabata Y (2011) Nontoxic genetic engineering of mesenchymal stem cells using serum-compatible pullulan-spermine/DNA anioplexes. Tissue Eng Part C Methods 17:131–144

20. Na K, Lee KH, Bae YH (2004) pH-sensitivity and pH-dependent interior structural change of self-assembled hydrogel nanoparticles of pullulan acetate/oligo-sulfonamide conjugate. J Control Release 97:513–525

21. Na K, Lee ES, Bae YH (2007) Self-organized nanogels responding to tumor extracellular pH: pH-dependent drug release and in vitro cytotoxicity against MCF-7 cells. Bioconjug Chem 18:1568–1574

22. Na K, Bum Lee T, Park KH, Shin EK, Lee YB, Choi HK (2003) Self-assembled nanoparticles of hydrophobically-modified polysaccharide bearing vitamin H as a targeted anti-cancer drug delivery system. Eur J Pharm Sci 18:165–173

23. Bae BC, Na K (2012) Development of polymeric cargo for delivery of photosensitizer in photodynamic therapy. Int J Photoenergy 2012:1–14

24. Liu J, Tabata Y (2010) Photodynamic therapy of fullerene modified with pullulan on hepatoma cells. J Drug Target 18:602–610

25. Gupta AK, Gupta M (2005) Cytotoxicity suppression and cellular uptake enhancement of surface modified magnetic nanoparticles. Biomaterials 26:1565–1573

26. Gao F, Cai Y, Zhou J, Xie X, Ouyang W, Zhang Y, Wang X, Zhang X, Wang X, Zhao L, Tang J (2010) Pullulan acetate coated magnetite nanoparticles for hyper-thermia: preparation, characterization and in vitro experiments. Nano Res 3:23–31

27. Sugawara A, Yamane S, Akiyoshi K (2006) Nanogel-templated mineralization: polymer-calcium phosphate hybrid nanomaterials. Macromol Rapid Commun 27:441–446

28. Katagiri K, Ohta K, Koumoto K, Kurosu K, Sasaki Y, Akiyoshi K (2013) Templated nucleation of hybrid iron oxide nanoparticles on polysaccharide nanogels. Colloid Polym Sci 291:1375–1380

29. Fujioka-Kobayashi M, Ota MS, Shimoda A, Nakahama K, Akiyoshi K, Miyamoto Y, Iseki S (2012) Cholesteryl group- and acryloyl group-bearing pullulan nanogel to deliver BMP2 and FGF18 for bone tissue engineering. Biomaterials 33:7613–7620

P